IMAGE-GUIDED THERAPIES FOR PROSTATE AND KIDNEY CANCERS

EDITORS: Rafael Sanchez-Salas and Mihir Desai

A Joint SIU-ICUD International Consultation

Melbourne, Australia, October 15–18, 2015

Co-sponsored by
SIU (Société Internationale d'Urologie)
ICUD (International Consultation on Urological Diseases)

www.siu-urology.org

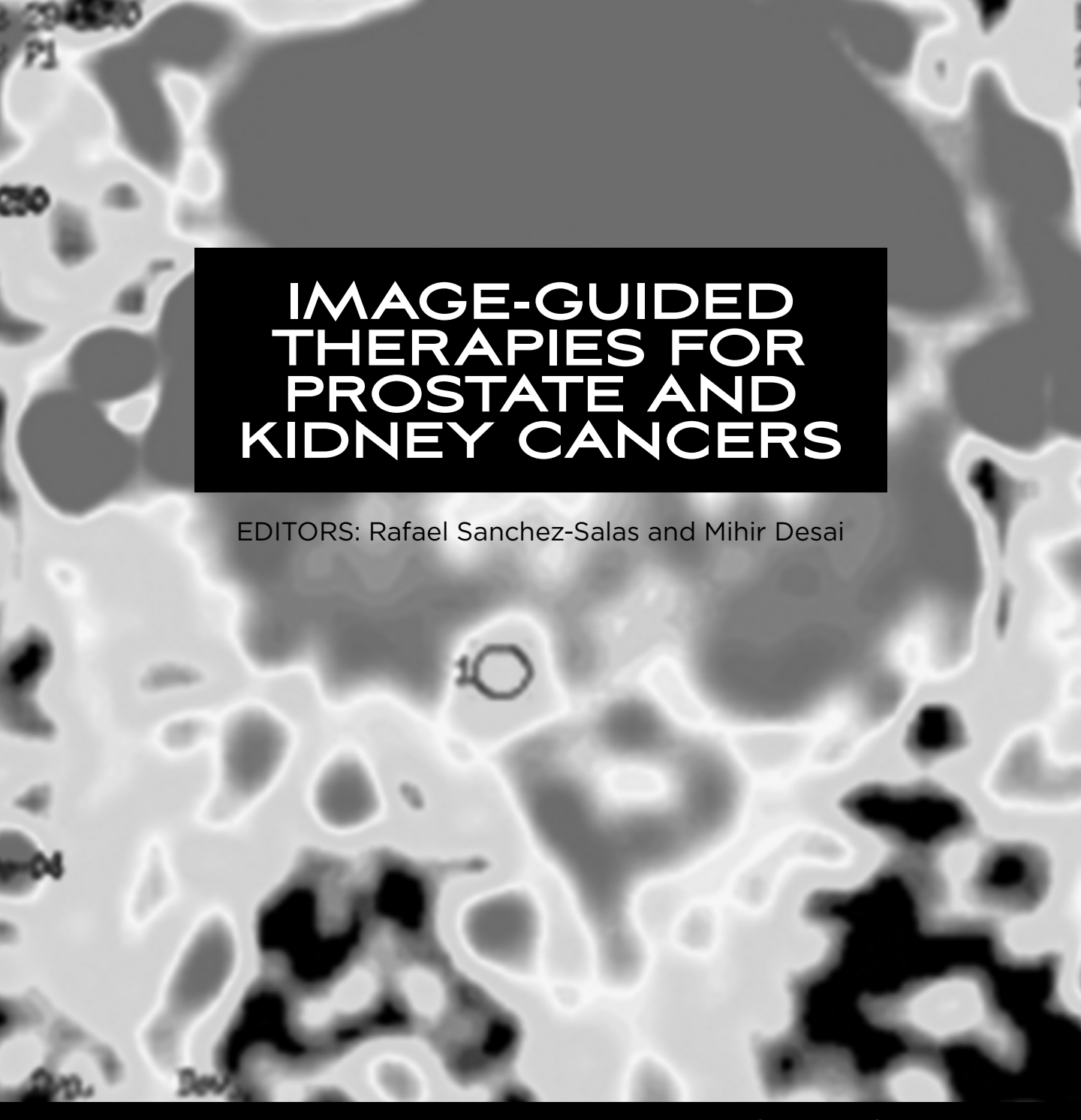

IMAGE-GUIDED THERAPIES FOR PROSTATE AND KIDNEY CANCERS

EDITORS: Rafael Sanchez-Salas and Mihir Desai

A Joint SIU-ICUD International Consultation

Melbourne, Australia, October 15–18, 2015

Co-sponsored by
SIU (Société Internationale d'Urologie)
ICUD (International Consultation on Urological Diseases)

Image-Guided Therapies for Prostate and Kidney Cancers
A Joint SIU-ICUD International Consultation

Editors
Rafael Sanchez-Salas and Mihir Desai

Published by the Société Internationale d'Urologie (SIU)

For information and orders:
SIU Central Office
1155 Robert-Bourassa Blvd.
Suite 1012
Montréal, Québec
Canada H3B 3A7
T: +1 514 875-5665
F: +1 514 875-0205
E: communications@siu-urology.org
W: www.siu-urology.org

Coordination: SIU Communications Office
Managing Editor: Christine Albino
Medical Copyediting and Proofreading: Namita Kumar, Stephanie MacLean, Areti Malapetsas, Stephanie Minelga, Cody Patton, Jamal Rahal
Layout and Design: SAM Design, Montréal, Canada

Acknowledgment: SIU would like to thank Dr. Jochen Walz for providing the imaging scan used on the book cover.

ISBN: 978-0-9877465-9-7

Table of Contents

COMMITTEE 7

COMMITTEE 9

Abbreviations Used in the Text

124I	iodine-124
α/β ratio	alpha-beta ratio
3D	three-dimensional
3T-MRI	3 Tesla magnetic resonance imaging
3DVP	3D assessment of volume preservation
5-ARIs	5-alpha-reductase inhibitors
A2M	alpha 2-macroglobulin
aCGH	array comparative genomic hybridization
ACR	American College of Radiology
ACT	alpha 1-antichymotrypsin
ADC	apparent diffusion coefficient
ADT	androgen deprivation therapy
AE	adverse event
AFMS	anterior fibromuscular stroma
AFS	anterior fibromuscular stroma
AKI	acute kidney injury
AMACR	alpha-methylacyl coenzyme A racemase
AML	angiomyolipoma
ANNA	artificial neural network analysis
API	alpha 1-protease inhibitor
AQP	aquaporin
AS	active surveillance
ASA	American Society of Anesthesiologists
ASPS	alveolar soft part sarcoma
ASTRO	American Society for Radiation Oncology
AUA	American Urological Association
AUC	area under the curve
BAP1	BRCA-1 associated protein-1
BCR	biochemical recurrence

BED	biologically effective dose
BFSR	biochemical-free survival rate
BHD	Birt-Hogg-Dubé
BI-RADS	Breast Imaging-Reporting and Data System
BMI	body mass index
bNED	biochemical no evidence of disease
BOLD	blood oxygenation level dependant
BPH	benign prostatic hyperplasia
BPSA	benign prostate-specific antigen
BRFS	biochemical relapse-free survival
Bx	biopsy
C-TRUS	computerized supported transrectal ultrasound
CA	cryoablation
CAD	computer-aided diagnosis
CAIX	carbonic anhydrase IX
CAPRA	Cancer of the Prostate Risk Assessment
CAR	computer-assisted reporting
CCI	Charlson Comorbidity Index
ccpRCC	clear cell papillary renal cell carcinoma
Ccr	creatinine clearance rate
ccRCC	clear cell renal cell carcinoma
CECT	contrast-enhanced computed tomography
CE-T1	Contrast-enhanced T1
CEUS	contrast-enhanced ultrasound
CG	Cockcroft-Gault
cG250	girentuximab
CGA	Comprehensive Geriatric Assessment
CGH	comparative genomic hybridization
CI	Concordance Index
CI	Confidence interval
CK5/6	cytokeratin
CK-Pan	wide spectrum cytokeratins
CKD	chronic kidney disease

CKD-EPI	Chronic Kidney Disease Epidemiology Collaboration
CNB	core needle biopsy
CO2	carbon dioxide
COLD	Cryo On-Line Database
cPSA	complexed form of prostate-specific antigen
CSC	clinically significant cancer
CSM	cancer- specific mortality
CSPCa	clinically significant prostate cancer
CSS	cancer-specific survival
CT	computed tomography
CUDI	contrast ultrasound dispersion imaging
CysC	cystatin C
CW	continuous wave
CZ	central zone
DAP	diameter axial polar
DC	direct current
DCE	dynamic contrast-enhanced
DCE-MR	dynamic contrast-enhanced magnetic resonance
DCE-MRI	dynamic contrast-enhanced magnetic resonance imaging
DCE-US	dynamic contrast-enhanced ultrasound
DFS	disease-free survival
DICOM	Digital Imaging and Communications in Medicine
DIL	dominant intraprostatic lesion
DLSI	dynamic light scattering imaging
DMSA	dimercaptosuccinic acid
DNA	deoxyribonucleic acid
DR	detection rate
DRE	digital rectal examination
DRS	Decisional Regret Scale
DTPA	diethylenetriaminepentaacetic acid
DW	diffusion-weighted
DW-MRI	diffusion-weighted magnetic resonance imaging
DWI	diffusion-weighted imaging

EAU	European Association of Urology
EBRT	external beam radiotherapy/radiation therapy
ECE	extracapsular extension
ECG	electrocardiogram
ECOG	Eastern Cooperative Oncology Group
EDRN	Early Detection Research Network
EDTA	ethylenediaminetetraacetic acid
EDV	end-diastolic blood flow velocity
eGFR	estimated glomerular filtration rate
EM	electromagnetic
EMA	epithelial membrane antigen
EORTC	European Organisation for Research and Treatment of Cancer
EPIC	Expanded Prostate Cancer Index Composite
ERC	endorectal coil
ERG	ETS-related gene
ERSPC	European Randomized Study of Screening for Prostate Cancer study
ESR	electron spin resonance
ESUR	European Society of Urogenital Radiology
FACT	Functional Assessment of Cancer Therapy
FDA	Food and Drug Administration
FDG	fludeoxyglucose
FH	fumarate hydratase
fINM	fluorescent intravital microscopy
FISH	fluorescent in situ hybridization
FITC-dextran	fluorescein isothiocyanate-dextran
FLA	focal laser ablation
FLT	fluorothymidine
FNA	fine-needle aspiration
FNAB	fine-needle aspiration biopsies
fPSA	free prostate-specific antigen
FSE	fast spin echo
FSH	focal salvage high-intensity focused ultrasound

FT	focal treatment
G	gauge
GFR	glomerular filtration rate
GOR	Grade of Recommendation
GRE	gradient echo
GS	Gleason score
HDR	high-dose rate
H&E	hematoxylin and eosin
HGPCa	high-grade prostate cancer
HGPIN	high-grade prostatic intraepithelial neoplasia
HIF	hypoxia-inducible factor
HIF-1α	hypoxia-inducible factor 1-alpha
HIFU	high-intensity focused ultrasound
hK2	human kallikrein 2
hK	human kallikrein
HLRCC	hereditary leiomyomatosis and renal cell carcinoma
HOCT	hybrid oncocytic/chromophobe tumours
HPRCC	hereditary papillary renal cell carcinoma
HRCCS	hereditary renal cell carcinoma syndrome
HS	histoscanning
HSH	hemi-salvage high-intensity focused ultrasound
Hsp27	heat shock protein 27
HT	hormone therapy
HU	Hounsfield unit
ICC	intraclass correlation coefficient
ICUD	International Consultation on Urological Diseases
IGRT	image-guided external beam radiotherapy
IHC	immunohistochemistry
IIEF	International Index of Erectile Function
IMRT	intensity-modulated radiotherapy
iPSA	intact prostate-specific antigen
IPSS	International Prostate Symptom Score
IQR	interquartile range

IRE	irreversible electroporation
ISUP	International Society of Urological Pathology
IT	information technology
IV	intravenous
K	lysine
KDM5C	lysine-specific demethylase 5C
KDIGO	Kidney Disease: Improving Global Outcomes
KT	knowledge transfer
LA	laparoscopic ablation
LCA	laparoscopic cryoablation
LDI	light density index
LDR	low dose rate
LDRB	low dose rate brachytherapy
LEDC	Low-energy direct current
LHRH	luteinizing hormone releasing hormone
LITT	laser interstitial thermotherapy
LOE	Level of Evidence
LPN	laparoscopic partial nephrectomy
LRFA	laparoscopic radiofrequency ablation
LUTS	lower urinary tract symptoms
MAG3	mercaptoacetyltriglycine
MDCT	multidetector computed tomography
MDRD	Modification of Diet in Renal Disease
medRCC	medullary renal cell carcinoma
MFS	metastasis-free survival
MFSR	metastasis-free survival rate
MIB1	methylation-inhibited binding protein 1
miRNA	microribonucleic acid
MIS	minimally invasive surgery
MiT	micropthalmia transcription factor
mp	multiparametric
mp-MRI	multiparametric magnetic resonance imaging
mp-US	multiparametric ultrasound

MR	magnetic resonance
mRCC	metastatic renal cell carcinoma
MRI	magnetic resonance imaging
MRI-TBx	MRI-targeted biopsy
mRNA	messenger ribonucleic acid
MRS	magnetic resonance spectroscopy
MRSI	magnetic resonance spectroscopic/spectroscopy imaging
mtDNA	mitochondrial deoxyribonucleic acid
mTHPC	m-tetrahydroxyphenylchlorin
mTOR	mechanistic target of rapamycin
MTSC	mucinous tubular and spindle cell carcinomas
MTT	mean transit time
MVD	microvessel density
MW	microwave
MWA	microwave ablation
NADH	nicotinamide adenine dinucleotide
NCCN	National Comprehensive Cancer Network
NePhRO	scoring system made up of the (Ne)arness to collecting system, (Ph)ysical location of the tumor in the kidney, (R)adius of the tumor, and (O)rganization of the tumor
NGAL	neutrophil gelatinase-associated lipocalin
NICE	National Institute for Health and Care Excellence
NPV	negative predictive value
NR	not reported
NS	nephrometry score
NSS	nephron-sparing surgery
NVB	neurovascular bundle
OAR	organs at risk
OCT	optimal cutting temperature
OPN	open partial nephrectomy
OR	odds ratio
OS	overall survival
PA	percutaneous ablation
PACE	Preoperative Assessment of Cancer in the Elderly

PACS	picture archiving and communication systems
PADUA	preoperative aspects and dimensions used for an anatomical score
PAP	prostatic acid phosphatase
PBRM1	polybromo 1
PBx	prostate biopsy
PC	PADUA classification
PCa	prostate cancer
PCA	percutaneous cryoablation
PCA3	prostate cancer gene 3
PCNA	proliferative cell nuclear antigen
PCOS	Prostate Cancer Outcomes Study
PDGFR	platelet-derived growth factor receptor
PDS	power Doppler sonography
PDT	photodynamic therapy
PFS	progression-free survival
PELICAN	Project to Eliminate Lethal Prostate Cancer study
PET	positron emission tomography
PET/CT	positron emission tomography with computed tomography
PFVP	percent functional volume preservation
PHI	Prostate Health Index
PHS	prostate histoscanning
PI	primary intervention
PIN	prostatic intraepithelial neoplasia
PI-RADS	Prostate Imaging Reporting and Data System
PIVOT	Prostate Cancer Intervention Versus Observation Trial
PLCO	Prostate, Lung, Colorectal, and Ovarian trial
PLIN2	perilipin 2
PN	partial nephrectomy
PNET	primitive neuroectodermal tumor
PPV	positive predictive value
PRCC	papillary renal cell carcinoma
PRF	proton resonance frequency
PRFA	percutaneous radiofrequency ablation

PRIAS	Prostate Cancer Research International Active Surveillance study
PRISMA	Preferred Reporting Items for Systematic Reviews and Meta-Analyses
PROMIS	PROstate MRI Imaging Study
proPSA	proenzyme PSA
PSA	prostate-specific antigen
PSAD	prostate-specific antigen density
PSADT	prostate-specific antigen doubling time
PSAV	prostate-specific antigen velocity
PSMA	prostate-specific membrane antigen
pT	pathological stage
PTEN	phosphatase and tensin homologue
PZ	peripheral zone
QOL	quality of life
RAPN	robot-assisted partial nephrectomy
RE	reversible electroporation
REDEEM	REduction by Dutasteride of clinical progression Events in Expectant Management study
R.E.N.A.L.	(R)adius (tumour size as maximal diameter), (E)xophytic/endophytic properties of the tumour, (N)earness of tumour deepest portion to the collecting system or sinus, (A)nterior (a)/posterior (p) descriptor and the (L)ocation relative to the polar line
RCC	renal cell carcinoma
RCN	renal cortical neoplasm
RCT	randomized controlled trial
RF	radiofrequency
RFA	radiofrequency ablation
RFS	recurrence-free survival
RI	resistive index
RIS	radiology information system
RITA	radiofrequency interstitial tissue ablation
RMB	renal mass biopsy
RN	radical nephrectomy
RNA	ribonucleic acid

ROC	receiver operating characteristic
ROI	region of interest
RON	renal oncocytic tumour
ROS	reactive oxygen species
RP	radical prostatectomy
RPN	robotic partial nephrectomy
RPPA	reverse-phase protein array
RR	relative risk
RRP	radical retropubic prostatectomy
RT	radiotherapy
RT-PCR	reverse transcription polymerase chain reaction
RTB	renal tumour biopsy
RVS	real-time virtual sonography
SABR	stereotactic ablative radiation therapy
SARR	surgical approach renal ranking
SAVP	surgeon assessment of volume preservation
SB	systematic biopsies
SBRT	stereotactic body radiotherapy
SCT	sickle cell trait
SDH	succinate dehydrogenase
SE	spin echo
SEER	Surveillance, Epidemiology, and End Results
SETD2	SET domain containing 2
SHIM	Sexual Health Inventory for Men
SIR	Society of Interventional Radiology
SNR	signal-to-noise ratio
Sp	specimen
SPCG	Scandinavian Prostate Cancer Group
SPCG-4	Scandinavian Prostate Cancer Group Number 4 trial
SPECT/CT	combined functional imaging with single-photon emission computed tomography (SPECT) with the anatomic imaging of computed tomography (CT)
SPOP	speckle-type POZ protein
SR	structured report

SRM	small renal mass
SRS	stereotactic radiosurgery
SWOG	South Western Oncology Group
SV	seminal vesicle
SVI	seminal vesicle invasion
SW	shear wave
SWE	shear wave elastography
T	Tesla
T1W	T1-weighted
T2W	T2-weighted
TB	targeted biopsies
TBx	targeted biopsy
TC	tubulocystic carcinoma
TCC	transitional cell carcinoma
TCM®	Tissue Change Monitoring software
TEAE	treatment emergent adverse events
TFE3	transcription factor 3
TIC	time–intensity curve
TMB	template-guided mapping biopsy
TMT	targeted molecular therapy
TNM	tumor-node-metastasis
TP53	tumour protein 53
TTMB	transperineal template-guided mapping biopsy
tPSA	total prostate-specific antigen
TR	repetition time
TRCC	translocation renal cell carcinoma
TRUS	transrectal ultrasound
TSC	tuberous sclerosis complex
TSG	tumor suppressor gene
TTF-1	thyroid transcription factor 1
TULSA	transurethral ultrasound therapy
TURP	transurethral resection of prostate
TZ	transitional zone

UC	ulcerative colitis
UCA	ultrasound contrast agent
UCLA-PCI-SF	University of California, Los Angeles Prostate Cancer Index Short Form
uPSA	ultrasensitive prostate-specific antigen
URF	Urethrorectal fistula
US	ultrasound
UTE	ultrashort echo time
UTI	urinary tract infection
VAS	visual analog score
VEGF	vascular endothelial growth factor
VEGF-A	vascular endothelial growth factor A
VEGFR	vascular endothelial growth factor receptor
VHL	von Hippel-Lindau
VHLD	von Hippel-Lindau disease
V-MAT	volumetric-modulated arc therapy
VOA	vascular occluding agents
VTP	vascular targeted photodynamic therapy
WHO	World Health Organization
WiR	wash-in rate
WWD	weighted mean difference
WW	watchful waiting

Preface

Rafael Sanchez-Salas
France

Mihir Desai
United States

The worldwide adoption of the term *focal therapy* represents a paradigm shift, from the days when the objective of cancer therapy was to cure at all costs to a more recent rationalized approach that takes into account important variables such as comorbidities, quality of life, and avoidance of complications.

This particularized and more rational treatment for both prostate and renal carcinomas was introduced and refined following great developments in medical imaging. The aim of this Consultation was to clearly state the role of image-guided ablative techniques for the treatment of prostate and renal cancers.

The quest for an effective and less aggressive treatment for prostate and renal tumours is not new. On the prostate side, we have witnessed an enormous evolution, from open surgery to classic and robotic-assisted laparoscopic techniques that have completely changed the evaluation of outcomes in prostate cancer. This, in turn, produced a positive impact on the morbidity and quality of life results of the surgical intervention. Radiotherapy has also evolved to remain efficacious in controlling cancer, with less associated collateral damage.

In kidney cancer, the wave of improvements has been similar. From the original open procedures offered to patients in the past, we have moved forward to controlling the cancer using safe, reliable, minimally invasive nephron-sparing renal surgery.

Simultaneously, we have become aware of the indolent nature of some kidney and prostate tumours that can eventually undergo active surveillance based on a patient's particular characteristics. Furthermore, several needle-based ablative techniques have been coined that effectively treat tumours in a less invasive fashion.

Today, the cancer diagnostic and treatment pathways for both prostate and renal carcinomas feature different therapeutic options, from active surveillance to more radical interventions, like surgery. Focal therapy represents a middle-ground treatment option. It should be strongly supported by high-quality imaging, cutting-edge radiological technology, and above all, radiologists with dedicated experience in urology who are able to reliably obtain adequate information from imaging. That is, tumours are to be identified and biopsied with imaging, and the ablative treatment and follow-up strategy to be supported by these techniques.

Urology has always been a technologically bound surgical specialty. As the imaging tools have become of the utmost importance in the diagnosis and treatment of urological malignancies, the urologist's role remains that of the cornerstone of the multispecialty team involved in the assessment of the disease.

This Consultation represents a unique effort from a large international faculty, working in nine committees, as part of the SIU-ICUD on Image-Guided Therapies for Prostate and Renal Carcinomas held in Melbourne, Australia in October 2015, chaired by Mihir Desai and Rafael Sanchez-Salas. Each chapter consists of the report of one committee, and the book was completed based on the scientific report of the Consultation Scientific Committee, which consists of the chairs of the Consultation together with the chairs of all the committees.

The scientific report will be submitted separately for publication in the *World Journal of Urology*. The report from the Consultation Scientific Committee not only reflects the importance of imaging in urological oncology, but also reflects other important elements, such as the evolution of oncological staging and the essential role of pathology in the diagnostic and treatment pathways.

This project attempts to add a valuable piece of information on the subject of image-guided therapies for prostate and renal tumours through the academic philosophy of the previous International Consultation on Urological Diseases initiated and promoted by Dr. Paul Abrams since 1993.

Introduction

Rafael Sanchez-Salas
France

Mihir Desai
United States

This consultation summarizes a state-of-the-art literature review and its recommendations on various aspects of image-guided therapy for prostate and renal cancers—truly a "hot-topic" in the world of urology.

On behalf of the International Consultation on Urological Diseases (ICUD), and its steering committee representing the major urological associations in the world (EAU, SIU, AUA, UAA, CAU, ICS), it is a great pleasure to thank the chairmen and committee members of each of the nine chapters for their hard work in producing this impressive update on this exciting and rapidly evolving field. As co-chairmen, we would like to express our immense gratitude to the SIU leadership for entrusting us with this important project. We would like to especially acknowledge the wise guidance and solid contribution that Paul Abrams provided us on every step of the planning and execution of the consultation.

Urology has been at the forefront of adopting sophisticated cutting-edge technology in the diagnosis and treatment of various conditions. With the increasing detection of early stage cancers, image-guided ablative therapies—both needle-based and extracorporeal—are likely to play an increasing role in the management of prostate and kidney cancers.

We constructed this consultation by defining specific clinical questions or scenarios, such as goals of initial evaluation, diagnosis and imaging, available ablation energies and, surveillance and treatment of recurrence. This consultation explores a relevant yet controversial topic in urology and will hopefully contribute to its further expansion and refinement. Our consultation follows on a tradition that was first set in 1996 and includes a broad area of expertise such as urology, pathology and radiology. In this regard, we would like to thank the radiology and pathology chairs and committee members that went over and beyond in creating this comprehensive document. After creating a committee for each of the 9 chapters, the chairs presented a summary of their exhaustive review during the 35th Congress of the Société Internationale d'Urologie in Melbourne, Australia, from October 15th to 18th, 2015. We recorded the discussion and comments during these sessions and the final manuscripts were created accordingly.

Last but not the least, none of this would be possible without the incredible SIU team of Christine Albino, Anna Johansen and Valerie Guillet. Their hard-work and patience have been critical to the successful execution of this project.

Evidence-Based Medicine Overview of the Main Steps for Developing and Grading Guideline Recommendations

P. Abrams, S. Khoury, A. Grant

Introduction

The International Consultation on Urological Diseases (ICUD) is a non-governmental organization registered with the World Health Organisation (WHO). In the last ten years, consultations have been organized on BPH, prostate cancer, urinary stone disease, nosocomial infections, erectile dysfunction and urinary incontinence. These consultations have looked at published evidence and produced recommendations at four levels: highly recommended, recommended, optional and not recommended. This method has been useful but the ICUD believes that there should be more explicit statements of the levels of evidence that generate the subsequent grades of recommendations.

The Agency for Health Care Policy and Research (AHCPR) have used specified evidence levels to justify recommendations for the investigation and treatment of a variety of conditions. The Oxford Centre for Evidence-Based Medicine have produced a widely accepted adaptation of the work of AHCPR. (June 5th 2001, www.cebm.net).

The ICUD has examined the Oxford guidelines and discussed with the Oxford group their applicability to the consultations organized by ICUD. It is highly desirable that the recommendations made by the consultations follow an accepted grading system supported by explicit levels of evidence.

The ICUD proposes that future consultations should use a modified version of the Oxford system which can be directly "mapped" onto the Oxford system.

1. First Step

Define the specific questions or statements that the recommendations are supposed to address.

2. Second Step

Analyze and rate (level of evidence) the relevant papers published in the literature.

The analysis of the literature is an important step in preparing recommendations and their guarantee of quality.

2.1 What papers should be included in the analysis?

- Papers published, or accepted for publication in the peer-reviewed issues of journals.
- The committee should do its best to search for papers accepted for publication by the peer-reviewed journals in the relevant field but not yet published.
- Abstracts published in peer-reviewed journals should be identified. If of sufficient interest, the author(s) should be asked for full details of methodology and results. The relevant committee members can then "peer review" the data, and if the data confirms the details in the abstract, then that abstract may be included, with an explanatory footnote. This is a complex issue – it may actually increase publication bias as "uninteresting" abstracts commonly do not progress to full publication.
- Papers published in non-peer-reviewed supplements will not be included. An exhaustive list should be obtained through:
  - I. The major databases covering the last ten years (e.g. Medline, Embase, Cochrane Library, Biosis, Science Citation Index).
  - II. The table of contents of the major journals of urology and other relevant journals, for the last three months, to take into account the possible delay in the indexation of the published papers in the databases.

It is expected that the highly experienced and expert committee members provide additional assurance that no important study would be missed using this review process.

2.2 How are papers analyzed?

Papers published in peer-reviewed journals have differing quality and level of evidence. Each committee will rate the included papers according to levels of evidence (see below).

The level (strength) of evidence provided by an individual study depends on the ability of the study design to minimize the possibility of bias and to maximize attribution.

It is influenced by:

The type of study, whose hierarchy is outlined below:

- Systematic reviews and meta-analysis of randomized controlled trials
- Randomized controlled trials
- Non-randomized cohort studies
- Case-control studies
- Case series
- Expert opinion

How well the study was designed and carried out

Failure to give due attention to key aspects of study methodology increases the risk of bias or confounding factors, and thus reduces the study's reliability.

The use of **standard checklists** is recommended to insure that all relevant aspects are considered and that a consistent approach is used in the methodological assessment of the evidence.

The objective of the checklist is to give a quality rating for individual studies.

How well the study was reported

The ICUD has adopted the CONSORT statement and its widely accepted checklist. The CONSORT statement and the checklist are available at www.consort-statement.org.

2.3 How are papers rated?

Papers are rated following a level of evidence scale.

ICUD has modified the Oxford Centre for Evidence-Based Medicine levels of evidence.

The levels of evidence scales vary between types of studies (i.e. therapy, diagnosis, differential diagnosis/ symptom prevalence study) the Oxford Centre for Evidence-Based Medicine Website: www.cebm.net.

3. Third Step: Synthesis of the Evidence

After the selection of the papers and the rating of the level of evidence of each study, the next step is to compile a summary of the individual studies and the overall direction of the evidence in an **Evidence Table**.

4. Fourth Step: Considered Judgment (Integration of Individual Clinical Expertise)

Having completed a rigorous and objective synthesis of the evidence base, the committee must then make a judgment as to the grade of the recommendation on the basis of this evidence. This requires the exercise of judgment based on clinical experience as well as knowledge of the evidence and the methods used to generate it. Evidence-based medicine requires the integration of individual clinical expertise with the best available external clinical evidence from systematic research. Without the former, practice quickly becomes tyrannized by evidence, for even excellent external evidence may be inapplicable to, or inappropriate for, an individual patient. On the other hand, without current best evidence, practice quickly becomes out of date. Although it is not practical to lay our "rules" for exercising judgment, guideline development groups are asked to consider the evidence in terms of quantity, quality, and consistency, as well as applicability, generalizability and clinical impact.

5. Fifth Step: Final Grading

The grading of the recommendation is intended to strike an appropriate balance between incorporating the complexity of type and quality of the evidence, and maintaining clarity for guideline users.

The recommendations for grading follow the Oxford Centre for Evidence-Based Medicine. The levels of evidence shown below have again been modified in the light of previous consultations. There are now four levels of evidence instead of five.

The grades of recommendation have not been reduced and a "no recommendation possible" grade has been added.

6. Levels of Evidence and Grades of Recommendation for Therapeutic Interventions

All interventions should be judged by the body of evidence for their efficacy, tolerability, safety, clinical effectiveness and cost-effectiveness. It is accepted that, at present, little data exists on cost-effectiveness for most interventions.

6.1 Levels of evidence

Firstly, it should be stated that any level of evidence may be positive (the therapy works) or negative (the therapy doesn't work). A level of evidence is given to each individual study.

Level of Evidence	Criteria
I	▪ Incorporates Oxford 1a, 1b ▪ Usually involves: ▪ meta-analysis of trials (randomized controlled trials [RCTs]) or, ▪ a good-quality RCT or, ▪ "all or none" studies in which treatment is not an option (e.g. in vesicovaginal fistula)
II	▪ Incorporates Oxford 2a, 2b and 2c ▪ Includes: ▪ ***low-quality RCT*** (e.g. <80% follow-up), ▪ ***meta-analysis*** (with homogeneity) of ***good-quality prospective cohort studies*** ▪ May include a single group when individuals who develop the condition are compared with others from within the original cohort group. ▪ There can be parallel cohorts, where those with the condition in the first group are compared with those in the second group
III	▪ Incorporates Oxford 3a, 3b and 4 ▪ Includes: ▪ ***good-quality retrospective case-control studies***, where a group of patients who have a condition are matched appropriately (e.g. for age, sex, etc.) with control individuals who do not have the condition ▪ ***good-quality case series,*** where a complete group of patients, all with the same condition, disease or therapeutic intervention, are described without a comparison control group
IV	▪ Incorporates Oxford 4 ▪ Includes ***expert opinion***, where the opinion is based not on evidence but on "first principles" (e.g. physiological or anatomical) or bench research. ▪ The ***Delphi process*** can be used to give expert opinion greater authority: ▪ involves a series of questions posed to a panel ▪ answers are collected into a series of "options" ▪ these "options" are serially ranked; if a 75% agreement is reached, then a Delphi consensus statement can be made

6.2 Grades of recommendation

The ICUD will use the four grades from the Oxford system. As with levels of evidence, the grades of evidence may apply either positively (procedure is recommended) or negatively (procedure is not recommended). Where there is disparity of evidence, for example if there were three well-conducted RCTs indicating that Drug A was superior to placebo, but one RCT whose results show no difference, then there has to be an individual judgment as to the grade of recommendation given and the rationale explained.

Grade A recommendation usually depends on consistent level I evidence and often means that the recommendation is effectively mandatory and placed within a clinical-care pathway. However, there will be occasions where excellent evidence (level I) does not lead to a Grade A recommendation, for example, if the therapy is prohibitively expensive, dangerous or unethical. Grade A recommendation can follow from Level II evidence. However, a Grade A recommendation needs a greater body of evidence if based on anything except Level I evidence.

Grade B recommendation usually depends on consistent level 2/3 studies, or "majority evidence" from RCTs.

Grade C recommendation usually depends on level 4 studies or "majority evidence" from level 2/3 studies or Delphi processed expert opinion.

Grade D "No recommendation possible" would be used where the evidence is inadequate or conflicting and when expert opinion is delivered without a formal analytical process, such as by Delphi.

7. Levels of Evidence and Grades of Recommendation for Methods of Assessment and Investigation

From initial discussions with the Oxford group, it is clear that application of levels of evidence/grades of recommendation for diagnostic techniques is much more complex than for interventions. The ICUD recommends that, as a minimum, any test should be subjected to three questions:

1. Does the test have good technical performance? For example, do three aliquots of the same urine sample give the same result when subjected to dipstick testing?
2. Does the test have good diagnostic performance, ideally against a "gold standard" measure?
3. Does the test have good therapeutic performance, that is, does the use of the test alter clinical management? Does the use of the test improve outcome?

For the third component (therapeutic performance) the same approach can be used as for section 6.

8. Levels of Evidence and Grades of Recommendation for Basic Science and Epidemiology Studies

The proposed ICUD system does not easily fit into these areas of science. Further research needs to be carried out in order to develop explicit levels of evidence that can lead to recommendations as to the soundness of data in these important aspects of medicine.

Conclusion

The ICUD believes that its consultations should follow the ICUD system of levels of evidence and grades of recommendation, where possible. This system can be mapped to the Oxford system.

There are aspects to the ICUD system that require further research and development, particularly diagnostic performance and cost-effectiveness, and also factors such as patient preference.

Summary of the International Consultation on Urological Disease Modified Oxford Centre for Evidence-Based Medicine Grading System for Guideline Recommendations

Levels of Evidence	Description
I	Meta-analysis of RCTs or high-quality RCT
II	Low-quality RCT or good-quality prospective cohort study
III	Good-quality retrospective case-control study or cohort study
IV	Expert opinion

Abbreviation: RCT=randomized controlled trial

Summary of the International Consultation on Urological Disease Modified Oxford Centre for Evidence-Based Medicine Grading System for Guideline Recommendations

Grades of Recommendation	Description
A	Usually consistent with level I evidence
B	Consistent level II or III evidence or "majority evidence" from RCTs
C	Level IV evidence or "majority evidence" from level II or III studies
D	No recommendation possible because of inadequate or conflicting evidence

RCT=randomized controlled trial

Scientific Committees

CONSULTATION CHAIR

Rafael Sanchez-Salas
France

CONSULTATION CHAIR

Mihir Desai
United States

COMMITTEE 1 Diagnosis of Prostate Cancer and Selection for Focal Therapy

CHAIR

Jochen Walz
France

Jochen Walz, France

CO-CHAIR

Rafael Sanchez-Salas, France

MEMBERS

Fernando Bianco, United States

Alberto Bossi, France

Ernesto Cordeiro, Argentina

Roman Ganzer, Germany

Massimo Lazzeri, Italy

Guillaume Ploussard, France

Jose Rubio, Spain

Arjun Sivaraman, France

Chi-hang Yee, China

COMMITTEE 2-I Imaging in Localized Prostate Cancer: I. Multiparametric Ultrasound

CHAIR

Eric Barret
France

Eric Barret, France

CO-CHAIR

Olivier Rouvière, France

MEMBERS

Jean Michel Correas, France

Jean de la Rosette, The Netherlands

Tim Idzenga, The Netherlands

Petr Macek, Czech Republic

Olivier Hélénon, France

Arnoud Postema, The Netherlands

Arjun Sivaraman, France

Hessel Wijkstra, The Netherlands

COMMITTEE 2-II

Imaging in Localized Prostate Cancer: II. Multiparametric Magnetic Resonance Imaging

CHAIR

Eric Barret
France

Eric Barret, France

CO-CHAIR

Olivier Rouvière, France

MEMBERS

Flavio Barchetti, Italy

Joyce G. R. Bomers, The Netherlands

Peter L. Choyke, United States

Matthieu Durand, United States

Jurgen Fütterer, The Netherlands

Christian G. Overduin, The Netherlands

Valeria Panebianco, Italy

Philippe Puech, France

Ardeshir R. Rastinehad, United States

Raphaele Renard-Penna, France

Giovanni Rosi, Italy

Ash K. Tewari, United States

Sarah Toledano-Massiah, France

Ismail Baris Turkbey, United States

COMMITTEE 2-III

Imaging in Localized Prostate Cancer: III. Role of Molecular Imaging Techniques

CHAIR

Eric Barret
France

Eric Barret, France

CO-CHAIR

Olivier Rouvière, France

MEMBERS

Hedvig Hricak, United States

Herbert Alberto Vargas, United States

Andreas Wibmer, United States

COMMITTEE 3 Prostatic Biopsies: Available Techniques and Approaches

CHAIRS

Badrinath R. Konety
United States

Osamu Ukimura
United States

Badrinath R. Konety, United States

Osamu Ukimura, United States

MEMBERS

Ahmed El-Shater Bosaily, United Kingdom

Jurgen Fütterer, The Netherlands

Arvin K. George, United States

Mahir Maruf, United States

Neil Mendhiratta, United States

Caroline M. Moore, United Kingdom

Peter A. Pinto, United States

Ardeshir R. Rastinehad, United States

Samir S. Taneja, United States

Arnauld Villers, France

Christopher Warlick, United States

COMMITTEE 4 Available Ablation Energies To Treat Prostate Cancer

CHAIR

Jean de la Rosette
The Netherlands

Jean de la Rosette, The Netherlands

CO-CHAIR

Jonathan Coleman, United States

MEMBERS

Martijn de Bruin, The Netherlands

Sébastien Crouzet, France

José Luis Domínguez-Escrig, Spain

Theo de Reijke, The Netherlands

Scott Eggener, United States

Sangeet Ghai, Canada

Aaron Katz, United States

György Kovacs, Germany

Sascha Pahernik, Germany

Bradley Pieters, The Netherlands

John Varkarakis, Greece

COMMITTEE 5 Surveillance After Focal Therapy

CHAIR

Thomas J. Polascik
United States

Thomas J. Polascik, United States

CO-CHAIR

Mahul Amin, United States

MEMBERS

Sangeet Ghai, Canada

Rafael E. Jimenez, United States

James Kench, Australia

Laurence Klotz, Canada

Rodolfo Montironi, Italy

Satoru Muto, Japan

Ardeshir R. Rastinehad, United States

Kae Jack Tay, United States

Baris Turkbey, United States

Arnauld Villers, France

COMMITTEE 6 Goals for Evaluation and Diagnosis of the Small Renal Mass

CHAIRS

Fernando P. Secin
Argentina

Fernando P. Secin, Argentina

CO-CHAIR

Robert Uzzo, United States

MEMBERS

Paul Cairns, United States

Paul Crispen, United States

Ithaar Derweesh, United States

Chaitanya Divgi, United States

Darrel Drachenberg, Canada

Vinay Duddalwar, United States

John Eisenbrey, United States

Ethan Halpern, United States

William Huang, United States

Stella Kang, United States

Brian Lane, United States

Marc Smaldone, United States

Edouard Trabulsi, United States

COMMITTEE 7 — Renal Tumour Biopsy: Indications, Technique, Safety, Accuracy/ Results, Pathologic Reporting and Impact on Treatment Decision Making

CHAIR

Michael A.S. Jewett
Canada

Michael A.S. Jewett, Canada

CO-CHAIR

Mahul B. Amin, United States

MEMBERS

Antonio Finelli, Canada

Xuesong Li, China

Mesut Remzi, Austria

Otto Van Delden, The Netherlands

Alessandro Volpe, Italy

Pathology Section

Andrew J Evans, Canada

Maurizio Colecchia, Italy

Naoto Kuroda, Japan

Victor E. Reuter, United States

Ondrej Hes, Czech Republic

David Grignon, United States

Isabela Werneck da Cunha, Brazil

COMMITTEE 8 Available Ablation Energies to Treat Small Renal Masses

CHAIR

Maria Pilar Laguna
The Netherlands

Maria Pilar Laguna, The Netherlands

CO-CHAIR

Jochen Walz, France

MEMBERS

Thomas Atwell, United States

Riccardo Autorino, United States

Andrea Cestari, Italy

Jeffrey Gahan, United States

Tobias Klatte, Austria

Krijn van Lienden, The Netherlands

Dogu Teber, Germany

Peter GK Wagstaff, The Netherlands

Patricia J Zondervan, The Netherlands

COMMITTEE 9 Follow-up Evaluation After Focal Ablation of Renal Masses

CHAIR

Jaime Landman, United States

Jaime Landman
United States

CO-CHAIR

Vinay Duddalwar, United States

MEMBERS

Mahul B. Amin, United States

Manju Aron, United States

Jeffrey Cadeddu, United States

Heidi Coy, United States

Chandana Lall, United States

Kari Nelson, United States

Zhamshid Okhunov, United States

Steve Raman, United States

Pheroze Tamboli, United States

C1

Diagnosis of Prostate Cancer and Selection for Focal Therapy

CHAIR

Jochen Walz, France

CO-CHAIR

Rafael Sanchez-Salas, France

MEMBERS

Fernando Bianco, United States
Alberto Bossi, France
Ernesto Cordeiro, Argentina
Roman Ganzer, Germany
Massimo Lazzeri, Italy
Guillaume Ploussard, France
Jose Rubio, Spain
Arjun Sivaraman, France
Chi-hang Yee, China

CONTENTS

Diagnosis of Prostate Cancer and Selection for Focal Therapy

1.1 Introduction

One of the key aspects of focal therapy is selection of the right patient with the right cancer characteristics that will allow satisfying treatment results. For patient selection, several tools could be used to estimate cancer volume, extension, and aggressiveness. One of these tools is the biomarker prostate-specific antigen (PSA), which is associated with advanced disease in univariate analysis but loses its significance to estimate disease aggressiveness when adjusted for age, Gleason grade, and stage. Prostate-specific antigen velocity >2 ng/mL/year is associated with a shorter time to prostate cancer death, high Gleason score (GS), and advanced pathology. Prostate-specific antigen used to be associated with cancer volume in older studies, but lost this ability recently due to screening or early detection strategies. Despite this, each increase per unit (ng/mL) of PSA increases the cancer volume by 0.322 cc. None of the currently available studies specifically explored PSA as a tool for patient selection for focal therapy. Based on consensus meetings, PSA levels <15 ng/mL are accepted as a selection criterion for focal therapy. Another biomarker is prostate cancer gene 3 (PCA3), where several cutoffs (25–30–39) allow for differentiating GS ≥7 from GS <7. Another cutoff (35) allows for estimating cancer volume >0.5 cc, and mean values are different between patients with unifocal (48) versus multifocal disease (88). Proenzyme PSA (proPSA) is yet another biomarker, where the Prostate Health Index (PHI) provides the highest area under the curve (AUC) for differentiating GS ≥7 from GS <7. Moreover, PHI significantly increases the predictive accuracy of models predicting cancer volume <0.5 cc. Proenzyme PSA and its derivate are significantly higher in T3 disease. Similarly to PSA, PCA3 and proPSA were not specifically evaluated for their use for patient selection for focal therapy. No clear recommendations can be given.

The ideal patient characteristics for focal therapy are based on consensus meetings. Patients should have a life expectancy of >10 years and not <5 years. Exclusion of individual patients should be based on good clinical judgment, being mindful of all comorbidities, and performance status. The ideal cancer characteristics for focal therapy are also based on consensus meetings. Initially, focal therapy was applied to prostate cancers with GS of 3+3. Currently, it is accepted for treating GS 3+4 prostate cancers. Multifocality is the main limitation of focal therapy; of note, 80% of secondary lesions are of low volume (<0.5 cc). Based on consensus meetings, all lesions with GS 3+3 ≥5-mm core length, GS 3+4 ≥5-mm core length, and any GS 4+3 should be treated. It is unclear whether all GS 3+4 ≤3-mm core length should be treated. Bilateral disease should not preclude focal therapy. The main aim of focal therapy is the treatment of the index lesion. This index lesion can be localized by either biopsy strategies or imaging. The hypothesis behind the index lesion is that such an index lesion is, in background of multifocal prostate cancer, the dominant lesion that will influence biological behaviour of the disease, clinical course, and eventually lethality. It is also the largest-volume lesion that is likely to harbour the highest Gleason grade, both being strong prognostic factors. The index lesion is also the large-volume lesion where the most lethal clone may inhabit its vicinity. It is of note that currently no direct evidence is available to support this hypothesis. Some studies show that metastasis derives from a single tumour clone (the index lesion); others show that metastasis derives from different cell clones. More research is necessary to understand the clonal origin of prostate cancer metastasis as well as to understand the risk for progression of nonsignificant lesions to high-grade lesions over time. No clear recommendations regarding the ideal patient and cancer characteristics for selection could be given.

Localized prostate cancer can be managed with several options where the currently available standards are active surveillance (AS), radical prostatectomy (RP), and radiotherapy (RT). Regarding active surveillance, it is clear that a candidate for active surveillance does not need any treatment due to low-risk characteristics and/or high comorbidities, and therefore focal therapy should not be an alternative in these patients. Radical prostatectomy and radiotherapy are indicated in intermediate-risk and high-risk prostate cancer patients. In the intermediate-risk patients, focal therapy could be considered as an alternative for these two standards. High grades of recommendation could be given for all three standard treatment options. No true comparison to focal therapy is available so far.

1.2 Role of Biomarkers in the Diagnosis of Prostate Cancer

1.2.1 Prostate-specific antigen (PSA)

Since the discovery of prostate-specific antigen (PSA) in late 1970s,[1] it has been a notable marker in prostate cancer. Being a protein product of human kallikrein gene *KLK3* on chromosome 19, it is released in zymogen form from the prostatic epithelium and is found in seminal fluid as well as in serum. The expression of KLK3 is induced by androgens, and the activation of PSA is a multi-step enzymatic process. While PSA circulates in both bound and unbound forms, most PSA is complexed to the antiproteases alpha 1-antichymotrypsin (ACT), alpha 2-macroglobulin and alpha 1-protease inhibitor (API).[2] Up to 70% of PSA that enters the serum is bound to these proteins, and the majority of PSA is found to be complexed with ACT, which remains detectable with immunological assays.

The unbound free PSA is inactive and without proteolytic activity. Together with the bound PSA in the serum, a total PSA level in serum is a function of prostate pathology, and it also varies with age, race, and prostate volume. Prostate cancer cells do not make more PSA than normal prostatic tissue. On the contrary, prostate cancer cells make less PSA than normal prostatic tissue.[3] Prostate cancer is histologically characterized by loss of the basal cell layer, derangement of the basal lamina, diminished epithelial polarity, and lack of connection of the glandular acini.[4] The elevated serum PSA levels in prostate cancer patients are postulated to be the result of disruption of the cellular architecture within the prostate gland.[5] When the barrier afforded by the basement membranes is breached, it can result in a leak of PSA into intercellular compartments, which are drained by lymphatic vessels into the circulation. While such postulation is common, the exact molecular mechanism by which PSA level is increased in prostate cancer patients remains unclear.[4]

1.2.1.1 Role of PSA in estimating cancer aggressiveness

By the mid-1980s, Stamey *et al.* showed that PSA was more sensitive than prostatic acid phosphatase (PAP) in the detection of prostatic cancer, and was likely to be more useful in monitoring responses and recurrence after therapy.[5] In the same study, it was demonstrated that PSA appeared to increase with advancing clinical stage. Since then, effort has been made to use PSA to estimate cancer aggressiveness. The Scandinavian Prostate Cancer Group (SPCG) attempted to identify the small proportion of patients who are destined to develop lethal prostate cancer by using PSA levels.[6] By using PSA

monitoring data from the watchful waiting arm of the SPCG Number 4 (SPCG-4) trial,[7] the role of PSA in predicting a fatal outcome, namely metastases or death, was studied. The cohort included 267 men diagnosed with early localized prostate cancer between 1989 and 1999, with PSA value of <50 ng/mL. Upon log-linear regression, PSA level at baseline was statistically significantly associated with lethal prostate cancer in the age-adjusted analysis (relative risk [RR], 1.24; 95% confidence interval [CI], 1.00–1.54; p=0.05). However, PSA has lost its statistical significance after adjusting for all other covariates of age, Gleason score (GS), and tumour stage (RR, 1.17; 95% CI, 0.95–1.45; p=0.15). Similar results were shown by Pinsky *et al.*[8] Data from the Prostate, Lung, Colorectal, and Ovarian (PLCO) Cancer Screening Trial were analyzed. Prostate-specific antigen levels of a group of men who were diagnosed with prostate cancer and who previously had undergone multiple screening tests in the PLCO Cancer Screening Trial were studied in association with the final prostatectomy pathological stage. It was found that PSA was associated with advanced pathological stage in univariate analysis. However, such association disappeared when the analysis controlled for clinical stage and biopsy GS. Tseng *et al.* from The Johns Hopkins Hospital also failed to demonstrate PSA levels being associated with disease progression on multivariate analysis.[9] Thus, other perspectives have been employed to increase the predictive value of PSA as a means to assess prostate cancer aggressiveness.

Prostate-specific antigen dynamics has been proposed as an alternative. Carter *et al.* introduced the concept of PSA velocity (PSAV) in 1992, which was defined as the annual rate of increase in serum PSA value.[10] Their initial analysis worked on the data of 54 men in the Baltimore Longitudinal Study of Aging. The authors found that PSAV was significantly greater in those who were subsequently diagnosed with prostate cancer than in those who would develop benign prostatic hyperplasia (BPH). Indeed, the rate of rise in PSA levels before prostate cancer treatment was noted to be correlated with prostate cancer outcome in some studies. D'Amico *et al.*[11] investigated 1,095 men with localized prostate cancer, and found that an annual PSAV of >2.0 ng/mL was associated with a significantly shorter time to death from prostate cancer and death from any cause compared with an annual PSAV of ≤2.0 ng/mL. Such correlation was independent of PSA level and biopsy GS. Furthermore, the same study suggested that a higher PSAV would be more likely to imply a higher GS as well as a more advanced pathological stage. While these findings were generated from patients of RP, a similar observation was noted from patients of external radiation therapy.[12] It may imply that the dynamics of the early PSA change may reflect the biological behaviour of the tumour. A high PSAV at the beginning of a newly diagnosed prostate cancer case may characterize a lethal tumour that warrants intensive treatment. On the other hand, a low PSAV may indicate a slowly progressing disease that may not require any radical local therapy.[6]

Various other studies on pretreatment PSAV for predicting disease aggressiveness have been published, with mixed results. Eighty-two patients who underwent radical retropubic prostatectomy (RRP) had PSAV documented by Thiel *et al.*[13] In men with pathologically organ-confined disease, PSAV was 1.12 ng/mL/year, while that with non-organ-confined cases was 1.88 ng/mL/year. However, there was no statistically significant relationship between PSAV and final pathological stage. In a log-linear model, Fall *et al.* found that PSAV was associated with the development of lethal prostate cancer.[6] In spite of this, the authors found that in the receiver operating characteristic (ROC) analysis, the accuracy of classifying the disease as either indolent or destined to progress was low, regardless of the cutoff point chosen for PSAV. Similarly, Pinsky *et al.* reported that PSAV was not predictive for advanced

pathological stage when the analysis was controlled for biopsy GS and clinical stage.[8] In an analysis by Memorial Sloan-Kettering Cancer Center, O'Brien *et al.* investigated the usefulness of pretreatment PSAV as well as PSA doubling time (PSADT) in predicting the outcome of prostate cancer treatment.

Twenty-two published definitions of PSA dynamics were analyzed, and the cohort included 2,938 patients before going for RP. While PSADT and PSAV presented a higher predictive accuracy for biochemical recurrence and metastasis over PSA alone, the improvements in predictive accuracy were small. The authors concluded that there was yet to be any justification for adopting PSA dynamics in predicting treatment outcome for prostate cancer. This conclusion was consistent with the finding from a systematic review published by the same group of authors.[15] Potential reasons for such lack of accuracy in the performance of PSA dynamics, especially with respect to PSAV, may be accounted for by the long observation period needed to obtain a valid calculation of PSAV that is not disturbed by considerable short-term fluctuations. This may not be easy to achieve in clinical practice.

Apart from PSAV, PSA density has also been studied to assess its association with prostate cancer aggressiveness. Kundu *et al.* tested such association with a screened and an unscreened cohort of patients with clinically localized prostate cancer treated with RP.[17] The analysis of 1,662 patients revealed a significant trend for worsening clinicopathological prognostic features as PSA density increased. Increasing from a PSA density of 0.1 ng/mL/cc to 0.19 ng/mL/cc and beyond, there was a decreasing chance of patients having an organ-confined disease with clear surgical margins, and an increasing chance of patients having a Gleason sum greater than 7. Despite such positive finding, the need for transrectal ultrasound and its associated inter-examiner variability may have deterred PSA density from gaining wide acceptance in the risk assessment of prostate cancer.

1.2.1.2 Role of PSA in estimating cancer volume

In the classical study published by Stamey *et al.* in 1987, multivariate regression was performed to assess the factors correlated with pretreatment PSA levels.[5] Variables taken into account in the analysis included cancer volume, prostate weight, seminal-vesicle invasion, GS, age, hyperplastic tissue in BPH, and capsular invasion. The results showed that the log of cancer volume was the best predictor for the log of PSA (regression coefficient, 0.59; $p<0.001$). In light of such strong relationship between PSA level and cancer volume, the authors investigated the usefulness of the pretreatment PSA level to predict cancer volume, and demonstrated a positive result ($t=5.9$; $p<0.001$). Similarly, Blackwell *et al.*, published in 1994, reported that median serum PSA level was significantly different between cancers that were organ confined, those that had capsular perforation or seminal vesicle invasion, and those with positive lymph node ($p<0.001$).[18] Bivariate analysis also showed that there was a positive correlation of PSA level with cancer volume ($r=0.56$; $p<0.001$), and multivariate analysis showed that cancer volume was the major contributor to serum PSA level.

However, in another report by Stamey *et al.* in 2002, the authors showed that there were serious limitations in the relationship between serum PSA level and prostate cancer volume.[19] From the analysis of 875 men who underwent RP between 1984 and 1997, the Pearson correlation between cancer volume and pre-operative PSA level was weak (Pearson correlation $R2=0.27$), and was driven by large cancers with PSA level greater than 22 ng/mL. These findings led the authors to conclude that the relationship between prostate cancer and serum PSA was tenuous at best, especially with serum PSA

less than 10 ng/mL and perhaps even less than 22 ng/mL. A subsequent report from the same centre on 1,317 consecutive radical prostatectomies over 20 years suggested that serum PSA was related to prostate cancer in their early series.[20] However, the data from their last 5 years of RP demonstrated that serum PSA has only been related to BPH. Such phenomenon was attributed to aggressive prostate cancer screening and earlier detection. Other authors have also reported similar findings on the relationship between serum PSA levels and tumour volume.[21]

While it is a common observation that the relationship between serum PSA and tumour volume decreased from early treatment years to recent years, Ochiai *et al.* demonstrated that the association remained at a significant level.[22] From the prostatectomy database of the M. D. Anderson Cancer Center, the authors randomly selected 200 men from 1991 to 1994 (early group) and 200 men from 2000 to 2003 (recent group). A significant relationship was observed between log PSA level and log tumour volume (r=0.486; $p<0.001$, and r=0.237; $p<0.01$) in both the early and recent groups. Multiple regression analyses revealed that in the recent group, log non-cancerous prostate tissue volume had the most significant association with log PSA level, whereas in the early group, log tumour volume had the most significant association. In another report on this subject with the same time frame, Kato *et al.* found similar positive correlations.[23] Analyses of 735 prostatectomy patients from 1997 to 2002 revealed that there were positive correlations between serum PSA levels and tumour volume and the relative tumour volume as a percentage. The authors further suggested that for each ng/mL unit increment of serum PSA, there was a 0.302 cc increase in total tumour volume and a 0.7% increase in relative tumour volume. From their data, total tumour volume could be calculated using the formula Volume (cc) = 3.476 + 0.302 x PSA (ng/mL).

Some factors have been suggested to affect the relationship between PSA levels and the tumour itself. Stamey *et al.* reported 3 cases of transition zone cancers from 7 to 86 cc in volume.[24] These tumours from transition zones presented a clinical syndrome of a highly elevated PSA level, BPH on digital rectal examination, a non-diagnostic transrectal ultrasound, and frequently negative transrectal or perineal needle biopsies. Such observation accounted for some cases with an extraordinarily high serum PSA level and organ-confined cancer at prostatectomy. One postulation was that central tumours have more neighbouring epithelial tissue than peripheral ones.[25]

The factor of obesity has also been looked into for its impact on PSA operating characteristics for the diagnosis and prognostication of prostate cancer. Data from Bañez *et al.* showed that in men undergoing RP, a higher body mass index (BMI) was associated with a higher plasma volume.[26] Hemodilution might therefore be responsible for the lower serum PSA concentrations among obese men with prostate cancer. As a result, there had been concerns that the PSA level might be less effective for predicting the outcomes in men with obesity. A later publication from the same group concluded that although hemodilution existed, it was unlikely to affect the ability of pretreatment PSA to predict the pathological features, including Gleason scores, positive surgical margins, extracapsular extension, and seminal vesicle invasion.[27] Further evaluation on the relationship between BMI, PSA, and tumour volume by Mitchell *et al.* concluded that pretreatment PSA correlated significantly with the tumour volume, and no significant correlation was found between BMI and pre-operative PSA level.[28] On multivariate analysis, controlling for BMI, the pretreatment PSA level remained a significant predictor for the tumour volume.

1.2.1.3 Role of PSA in selecting patients for focal therapy

Focal therapy was first reported in 2002 by Onik *et al.*, who proposed the idea of nerve-sparing cryotherapy.[29] Such an idea stemmed from the concept of nerve-sparing RP, in an attempt to increase the potency rate after cryotherapy. In the pilot study reported by Onik *et al.*, patients were selected based on their biopsy results showing a unilateral tumour as well as the patient's potency status. Prostate-specific antigen level, biopsy Gleason scores, and clinical stage were not taken into account in patient selection. The same selection criteria of an organ-confined, unilateral tumour without PSA consideration were also adopted by Bahn *et al.* in their early series of cryotherapy.[30] Those authors reported a biochemical disease–free status, according to the American Society for Radiation Oncology (ASTRO) definition, by 92.8% at a mean follow-up of 70 months. A negative biopsy rate of 96.0% was observed.

After the introduction of extensive transperineal three-dimensional template mapping biopsies to improve the diagnostic localization of cancer foci and focal therapy ablation templates, Onik *et al.* updated the results of their focal therapy series in 2007.[31] In the updated series, PSA was taken into account not as an inclusion/exclusion criterion, but as a means of determining the extent of tissue ablation. In such context, PSA greater than 10 ng/mL would call for greater tissue ablation because of the increased risk for recurrence.

In general, before 2010, patients with "low-risk" prostate cancer were considered to be candidates for focal therapy. There is a broad agreement between clinicians that by definition of "low-risk", it means parameters of PSA less than 10 ng/mL, GS less than 7, and clinical stage less than T2b. The inclusion criterion of PSA less than 10 ng/mL for focal therapy was supported by the Task Force panel in 2008[32] and the panel of multidisciplinary experts in a consensus workshop on focal therapy in 2010.[33] Besides PSA levels, the Task Force panel also included a PSA density of less than 0.15 ng/mL/g as an inclusion criterion,[32] considering it to be helpful in controlling for the prostate volume.

Multifocality and heterogeneity are usually observed in prostate cancer, but Liu *et al.* demonstrated that despite common genomic heterogeneity in primary cancers, most metastatic cancers arise from a single precursor cancer cell.[34] Previous studies had also demonstrated that only index tumour volume, but not total tumour volume, was found to be an independent predictor for progression.[35,36] There is increasing evidence that the natural history of the disease is ultimately driven by the largest and most undifferentiated focus within the prostate, i.e., the index lesion.[37] This concept of index lesion made an impact on the approach in selecting the appropriate candidates for focal therapy. Changing from previously only including patients with low-risk disease, the approach of more and more experts is now accepting the idea of focal therapy being proposed to patients with intermediate-risk disease. Trials have expanded to include patients with a PSA level of 15 ng/mL or less.[38]

In a report from a consensus meeting on focal therapy in 2014, the panel of experts agreed with a high level of consensus that focal therapy should be recommended for intermediate-risk patients.[39] This implied the inclusion of patients with PSA 10–20 ng/mL. The panel also agreed on the use of focal therapy in low-risk patients, i.e., PSA less than 10 ng/mL. However, such agreement was reached with a lower level of consensus. Such a change in focal therapy inclusion criteria reflected the growing confidence in the technique and promising medium-term follow-up results. Within similar recommendations, in the criteria for focal therapy proposed by Marien *et al.*, PSA 3–10 ng/mL or

10–20 ng/mL was put forward.[40] In an international multidisciplinary consensus meeting on focal therapy trial design, PSA less than 15 ng/mL was recommended as an inclusion criterion.[41] For PSA more than 15 ng/mL, it was advised that patients should be counselled with caution.

Brachytherapy is a therapy that requires different patient selection. Langley *et al.* published the selection criteria for focal therapy with low-dose rate seed implants.[42] In their recommendation, PSA less than or equal to 15 ng/mL was proposed.

1.2.1.4 Future research priorities for PSA

Despite PSA still being a common factor to be considered in assessing tumour volume, tumour aggressiveness, and plausibility of treatment options, there are certain limitations and uncertainties. Some aggressive prostate cancers do not demonstrate a rapid rise of total PSA.[43] Furthermore, the effect of previous BPH treatment, e.g., 5-alpha-reductase inhibitors (5-ARIs), on PSA kinetics for tumour progression remains mostly unpredictable. Keetch *et al.* reported that finasteride appeared to lower total and percent-free PSA (free PSA, or fPSA) levels equally in men with BPH and did not appear to change the ratio of free-to-total serum PSA.[44] While free PSA to total serum PSA level has been used to assess the risk for prostate cancer in patients with PSA level less than 10 ng/mL,[45] there has not been much investigation on its role in the pathological prediction for tumour characteristics. In the analysis of 581 men who underwent RP, Graefen *et al.* did not detect any statistically significant association between free PSA and organ-confined status or posttreatment PSA outcome.[46] On the contrary, Shariat *et al.* found that pre-operative free PSA was associated with adverse pathological features, biochemical progression, and features of aggressive disease progression in patients with total PSA level less than 10 ng/mL.[47] One report by Larsen *et al.* looked into the predictive ability of free PSA.[48] The authors demonstrated that free PSA was strongly associated with prostate cancer risk, and free PSA below the median value 20% had a 2.4-fold increased risk for aggressive prostate cancer within 14 years, compared with men with more than 20% free PSA. Further studies are needed to define the role of free PSA in the estimation of tumour characteristics, and furthermore, its relationship to patient selection and treatment failure with respect to focal therapy.

In the process of finding an appropriate biomarker for the diagnosis of prostate cancer, it is more and more apparent that it takes a panel of markers rather than just a single one to achieve better specificity and sensitivity. The same may be applied to finding an appropriate test for estimating tumour characteristics, in order to select the best candidate for focal therapy. A biomarker may reflect disruption of a biochemical pathway by a particular mechanism. Given the complexity of the molecular abnormalities associated with prostate cancer, it is likely that more than a single marker is needed to accurately classify tumours into distinct prognostic categories.

There are three molecular forms of free PSA in the serum, each contributing to roughly one-third of free PSA, namely proPSA, benign PSA (BPSA), and intact PSA (iPSA).[50] Studies have shown that not only a higher level of proPSA is associated with a higher risk for prostate cancer,[49] but also that elevated proPSA-to–free PSA ratios have been associated with aggressive pathological features and decreased biochemical disease–free survival after prostatectomy.[50] Prostate Health Index adopts a mathematical formula that improves the clinical diagnostic performance of PSA by combining the results of three automated blood tests (total PSA, free PSA, and [-2]proPSA).[51] Such mathematical formula was also found to be applicable to assessing tumour aggressiveness. The risk of detecting a clinically aggressive

cancer was shown to be increased in men with higher PHI readings.[52] Furthermore, the PHI value was suggested to correlate with tumour volume.[53] Apart from PHI, there are other panels of biomarkers used for prostate cancer screening. The use of assays for several kallikreins in combination is an example—specifically, these include a panel of four kallikrein markers: free PSA, single-chain iPSA, total PSA, and human kallikrein-related peptidase-2 (hk2).[54] All these are potential panels of biomarkers for cancer profiling, indicating the tumour volume and behaviour. More data is needed to verify their values in the context of focal therapy for prostate cancer.

1.2.1.5 Level of evidence and grade of recommendation

Role of PSA in estimating cancer aggressiveness

No studies available that specifically use PSA to estimate cancer aggressiveness in the setting of focal therapy. Outside of this context, the data summarizes as:
Level of evidence: 3b
Grade of recommendation: D

Role of PSA in estimating cancer volume

No studies available that specifically use PSA to estimate cancer volume in the setting of focal therapy. Outside of this context, the data summarizes as:
Level of evidence: 3b
Grade of recommendation: D

Role of PSA in selecting patients for focal therapy

No studies available that systematically evaluate PSA to select patients for focal therapy. Outside of this context, the data summarizes as:
Level of evidence: 3a
Grade of recommendation: C

1.2.2 Prostate cancer gene 3 (PCA3)

1.2.2.1 Introduction

Following the recommendations of the Oxford Centre for Evidence-Based Medicine, which are accepted by the International Consultation on Urological Diseases (ICUD),[55] we define as first step the specific statement to address in this document: the role of PCA3 as a biomarker of prostate cancer (PCa) in a focal treatment strategy. For that purpose, we analyze and rate the relevant papers published in the literature in the major databases covering the last 10 years.

For a diagnostic test such as PCA3, the ICUD recommends, that, as a minimum, it should be subjected to three questions: a) Does the test have good technical performance, for example, do three aliquots of the same urine sample give the same result when subjected to testing?; b) Does the test have good diagnostic performance, ideally against a "gold standard" measure?; and c) Does the test have good therapeutic performance, that is, does the use of the test alter clinical management, and does the use of the test improve outcome?

Focusing on focal treatment (FT), we adapt these objectives regarding PCA3 as a biomarker in PCa diagnosis in answering these four questions:

- **What is the role of the biomarker in estimating cancer aggressiveness?** This will be answered by finding out the relation of PCA3 to the Gleason score, both at biopsy (Bx) tissue and specimen (Sp) tissue, pathological stage (pT) and extracapsular extension at Sp, and validation as a marker for indolent versus significant PCa in both Bx and Sp.
- **What is the role of the biomarker in estimating cancer volume?** This will be analyzed by focusing on the number of affected cores at Bx and tumour volume at Sp.
- **What might be the role of the biomarker in selecting patients for focal therapy?** This will be answered by assessing PCA3 in relation to multifocality and multi-parametric magnetic resonance imaging (mpMRI) data.
- **What are future research priorities?** This will be answered by analyzing a combination of PCA3 and mpMRI strategies.

1.2.2.2 Material and methods

Electronic searches of the word "PCA3" in papers in English or Spanish at MEDLINE, the Cochrane Database of Systematic Reviews, and the National Institute for Health and Care Excellence (NICE) websites (all accessed 1st of June 2015) with no time frame limits. Papers offering any relevant data to those previously presented were considered. This included randomized and quasi-randomized trials, non-randomized cohort studies, case-controlled studies, longitudinal studies, and case series or reports. Those papers considered for inclusion were assessed for quality where relevant, in terms of sequence generation, allocation concealment, blinding, handling of incomplete data, selective reporting, and freedom from other biases. A level of evidence **[LOE]** was then assigned to all included studies according to the ICUD-modified version of the Oxford Centre for Evidence-Based Medicine system.[55] Where quality was considered to be poor, the LOE was reduced accordingly. Recommendations (graded A–D) were made on the basis of consistent or "majority evidence" identified.

1.2.2.3 Results

Using the term "PCA3", 320 published papers were found; 231 ie, were discharged due to title or abstract, repeated series, not related to topic, or focused on molecular biology. Eighty-nine were selected for full paper analysis and after a second triage, 56 were discharged due to the same reasons. Finally, 36 were fully analyzed as valid papers related to PCA3 and its role in focal treatment strategies.

1.2.2.4 Technical performance and analytical validity

The analytical validity of PCA3 has been recently reviewed by the NICE Guidelines, finding no gold standard for analytical validity that could be used as a reference standard in the studies. The authors found that the limited evidence on analytical validity often lacked detailed information, which made formal quality assessment difficult, but uncertainty in the precision of the PCA3 assay at a lower cutoff point was pointed out.

It has been recommended to obtain the urine after digital rectal examination (DRE), as urine taken by micturition or catheterization gives similar but always slightly lower informative rates.[56,57] The variability of PCA3 scores on repeated measures confirmed the risk class for about 80% of patients; of the remaining 20% of patients, the risk class was upgraded in two-thirds and downgraded in

one-third.[58] In other studies, accuracy varied from 90% to 118% for PCA3.[56,59] Knowing that as in every biomarker, PCA3 is most informative when taken as a continuous variable, all these data should alert clinicians to use with caution those PCA3 scores that are near the given cutoff points, as suggested by different authors in order to differentiate indolent and significant prostate cancers.[60]

Another aspect to be taken into account when analyzing the PCA3 literature is the source of the sample, as most of the published results have been performed with whole urine following a commercially available test (PROGENSA®, Gen Probe, San Diego, USA), but urine sediments have also been used. The advantage of urine sediments over a whole urine sample may be that clinical data can be correlated to all the cells and cell fragments that were present in the collected urine, but the whole urine technically simplifies the procedure. These different sources have been argued to explain different prognostic results.[61]

1.2.2.5 Role of PCA3 in estimating cancer aggressiveness

Prostate cancer gene 3 has been analyzed separately in initial and repeated Bx, but the focus in this chapter is to analyze its prognostic role in both as a potential informative marker of PCa aggressiveness. In **Table 1-1**, the reader can take a quick look at the statistically significant relations of PCA3 to different variables related to PCa prognosis in both Bx and RP specimens.

A European, multicentre study showed that the PCA3 score was significantly higher in men with biopsy high-grade prostate cancer (HGPCa; GS ≥7).[62] Different cutoffs have been proposed to differentiate between GS ≤7 or >7; 28.1 versus 45.3,[63] 31.8 versus 49.5,[64] and 40 versus 72.[62] Related to PCA3 statistics to diagnose HGPCa, it has been published that a cutoff of 25 PCA3 has an AUC of 0.638, with a sensitivity of 76.5 (95% CI, 60.0–87.6) and a specificity of 51.6 (95% CI, 46.9–6.3).[65]

Regarding Gleason score and FT, an interesting issue is to know how many HGPCa we miss within a screening strategy if PCA3 is used. In a prospective, randomized study where patients were all biopsied if PCA3 was ≥35 and randomized 1:1 to Bx or observation if PCA3 was <35, the authors found 3% of Gleason PCa ≥7 based on usual PSA kinetics as criteria for Bx at 10.1 months of follow-up.[66] Other authors showed that at a PCA3 cutoff of 20, missed HGPCa was 2%, and none was significant PCa.[62] Different researchers propose a cutoff of 39, showing that no PCa with a GS higher than 4+3 was missed.[67] But the most powerful value of a biomarker is when it demonstrates improvement of a basal nomogram based in clinicopathological variables. Hansen *et al.* constructed such a nomogram which included PCA3;[68] when it was applied at probability thresholds ≤30%, only a few patients with HGPCa (≤2%) would be missed while avoiding up to 55% of unnecessary biopsies, and this nomogram has been externally validated in three series,[69–71] showing ≤6% of missed HGPCa while avoiding up to 48% of unnecessary biopsies.[69]

TABLE 1-1 Statistically significant relation between PCA3 and PCa aggressiveness*

Reference	n	T	Biopsy information				Radical prostatectomy specimen information					
			No/% affected cores	GS	MF	Ind/ Sig	TV	GS	pT	MF	Ins	Sg
Whitman *et al.*[75]	72	Sp					+		+			
Nakanishi *et al.*[72]	57/96	I/Sp	-	-			+	+	-		+	
Hessels *et al.*[61]	330/70	A/Sp		-		-	-	-	-		-	-
Liss *et al.*[57]	100	Sp						-	-			
Vlaeminck-Guillem *et al.*[88]	102	Sp					+	-	-	+		
Auprich *et al.*[76]	305	Sp					+	-	-		+	-
de la Taille *et al.*[62]	516	I	+	+		+						
Ploussard *et al.*[79]	106	Sp					+	+	+		+	+
van Poppel *et al.*[60]	348/175	A/Sp	+	+		+		+				
Durand *et al.*[74]	160	Sp	+	+			+	+/-	+/-			
Pepe *et al.*[77]	38	Sp					+		+		+	+
Cornu *et al.*[89]	291	I	+	+								
Augustin *et al.*[73]	127	Sp					-	-	-			-
Chevli *et al.*[90]	3,073	I		+								
Ferro *et al.*[78]	78	Sp					+	+	+			
Cantiello *et al.*[91]	156	Sp					+	-	+			+

*Empty scoring means that issue was not available, + means that this particular variable showed statistically significant differences related to PCA3 values; - means that this particular variable was analyzed but showed no statistically significant relation to PCA3 values; +/- means that this particular variable showed statistically significant differences at the univariate analysis but not in the multivariate one.

Abbreviations: %, percentage; A, all; ECE, extracapsular extension; GS, Gleason score; Ind/Sig, indolent versus significant prostate cancer (different criteria used); I, initial biopsy; MF, multifocality; pT, pathological stage; R, repeated biopsy; Sg, pathologically significant tumour; Sp, radical prostatectomy specimen; T, used tissue for analysis; TV, tumour volume.

Prostate cancer aggressiveness is finally summarized labelling it as an indolent or a significant cancer on biopsy, and this is crucial for choosing between FT or active surveillance (AS). Prostate cancer gene 3 values have been related to this, with median values of 31 versus 57.[62] Haese *et al.* also reported significant differences in the median PCA3 scores for indolent versus significant cancers (21 vs. 42).[63] In other series, the median/average PCA3 score in men with low-volume/low-grade cancer and significant cancer was 17.8/24.5 and 42.4/56.5, respectively.[72] Grouping different data in the literature, the median PCA3 score was ~20 (range, 18–32) in men with indolent PCa and ~50 (range, 42– 57) in men with significant PCa.

When PCA3 was analyzed in RP series, results were also controversial regarding its prognostic role, as is shown in **Table 1-1**.[60,61,72–75] In the largest series, the addition of PCA3 to multivariable intermediate- and high-risk PCa models did not improve prediction, but the authors observed that at lower values of PCA3, it was associated with low-volume tumours and insignificant PCa at the Sp.[76] The addition of PCA3 resulted in an improved multivariable AUC ranging from +3.0% to 3.9%, with the highest predictive AUC obtained (0.922) for the detection of insignificant PCa at the Sp, using a PCA3 cutoff threshold of 24 combined with Gleason score at the Bx and percentage of positive cores.[76] Other authors have confirmed these results in shorter series.[72,77] This could be important when facing a patient with a low-risk tumour, as a low PCA3 is an additive tool that could help the patient to initially choose an AS program instead of FT, or a patient with an intermediate-risk tumour, where a low PCA3 could help the patient to choose an FT instead of radical treatment, taken together with the rest of clinicopathological and magnetic resonance imaging (MRI) information in both scenarios.

1.2.2.6 Role of PCA3 in estimating cancer volume

Cancer volume is capital to planning FT; its calculation can be clinically induced by taking into account the number of affected cores or its percentage related to the obtained cores. Prostate cancer gene 3 has been related to a percentage >33% versus ≤33% positive biopsy cores, with a median PCA3 score of 78 and 39, respectively.[62] When tumour volume is calculated in RP specimens by different methods, its relation to PCA3 shows controversial results, as shown in **Table 1-1**, but there are more series confirming a relation between higher PCA3 values and higher tumour volume (**Table 1-1**). Durand *et al.* showed in a multicentric French study on 160 RP specimens that a PCA3 score of >35 was an independent predictor in a multivariate analysis for tumour volume >0.5 mL (odds ratio [OR], 2.7; p=0.04),[74] confirming similar results in other series.[72,75,77,78] Others have also shown a relation of PCA3 to the dominant tumour volume, what can be additionally important within an FT strategy, but it has not been compared with mpMRI analyzing RP specimens.[72]

In a series analyzing only low-risk PCa, the authors identified the value of 25 as predictive for a tumour volume <0.5 cm^3 that bore witness to insignificant disease. The risk of having a cancer ≥0.5 cm^3 and significant PCa was increased by three fold in men with a PCA3 score of ≥25 compared with men with a PCA3 score of <25 with most AS biopsy criteria used; this data might help the clinician to recommend AS instead of FT in doubtful cases with normal mpMRI.[79]

1.2.2.7 Role of PCA 3 in selecting patients for focal therapy

Radical prostatectomy specimens show the "truth" about PCa characteristics. Extrapolation of their data when examined by pathologists experienced with prostate disease and blinded to PCA3 score results tells us the relation of this biomarker to multifocality and its complementarity to mpMRI results. In a case series study, Vlaeminck-Guillem *et al.* found that patients with multifocal disease had a significantly higher mean PCA3 score than patients with unifocal disease (88 vs. 46), pointing out in their multivariate analysis that multifocality was an independent factor influencing PCA3 score.[80] In the context of FT, the finding that PCA3 score can predict multifocality at surgery potentially is quite interesting. Whether it could be used to help decide on FT remains to be determined in larger studies.

More important is the combination of any new biomarker with mpMRI in order to optimize FT strategies and to establish their complementarity. Sciarra *et al.* showed in a study in repeat Bx where patients were randomized to standard Bx or Bx following an mpMRI, that the use of mpMRI for indicating sites suitable for re-biopsy can significantly improve the sensitivity of the PCA3 test in the diagnosis of PCa, but no significant difference (p=0.089) in the predictive value of the PCA3 score was found with respect to distinguishing PCa cases on the basis of the GS ≤ 7 (3+4) versus ≥ 7 (4+3).[81] Leyten *et al.* showed in a retrospective study of their patients with PCA3 and mpMRI in their diagnoses process that patients with a suspicious region for PCa on mpMRI had a significantly higher PCA3 score than patients with no suspicious region (median, 54 vs. 29; p= 0.002), but nearly all patients (23/25 patients) with PCA3 scores <35 and prostate cancer upon biopsy had a suspicious region for prostate cancer upon mpMRI.[82] In other series analyzing PCA3 and mpMRI in 106 low-risk PCa patients at biopsy, both factors were independently predictive for significant disease at the RP specimen, but only a suspected T3 disease on mpMRI was significantly predictive for a pT3 disease in RP specimen (OR, 5.3; p=0.020).[79]

This issue is actually under research in controlled trials, but two Italian publications analyzing the combined approach in a repeat Bx scenario led the NICE Guidelines to publish that if mpMRI is included in initial PCa characterization, biomarkers such as PCA3 or PHI do not have noticeable impact on outcomes. Firstly, Busetto *et al.* showed that the base model AUC was improved up to 0.742 (95% CI, 0.664–0.821) with the addition of PCA3, but the best discrimination (AUC, 0.808; 95% CI, 0.742–0.874) was obtained using the full model (base clinical model plus mpMRI and PCA3) or just the base clinical model plus mpMRI, with an AUC of 0.781 (95% CI, 0.664–0.821).[83] Secondly, Porpiglia *et al.* confirmed this hypothesis in the repeat Bx scenario, showing in their multivariate logistic regression analysis in the full model that only mpMRI was a significant independent predictor for PCa diagnosis. Prostate cancer gene 3 was an independent predictor only in the absence of mpMRI.[84]

These unicentric studies have to be taken as hypothesis generating, due to the selection bias, participation of specialized uro-radiologists, different mpMRI devices and software solutions, and generalization questioned due to the same reasons and known mpMRI irregular availability and bad homogenization. The role of PCA3 and the complementarity of PCA3 with mpMRI must be evaluated in prospective studies—not only in the repeat Bx scenario but also in the initial Bx one for the characterization of PCA3 within AS or FT protocols. The sensitivity, specificity, positive predictive value (PPV), negative protective value (NPV), and cutoff value of PCA3 that will give an optimal balance between sensitivity and specificity to predict MRI outcome should be evaluated prospectively, and all this information is awaiting ongoing protocols such as PROstate MRI Imaging Study (PROMIS; ClinicalTrials.gov number NCT01292291) to shed some light on this point and finally optimize AS and FT protocols.

1.2.2.8 Future research priorities for PCA3

1. Analytical validity should be refined, mostly if the biomarker is stressed to guide AS or FT protocols.
2. Prospective studies focusing on the combination and complementarity between PCA3 and mpMRI are urgently needed, as availability and easy interpretation are qualities of the biomarker that should be stressed in

well-done clinical and prospective studies to determine whether it is useful to select which patients need an initial mpMRI. This is a research field for which it is desirable to optimize mpMRI use if possible.

3. Analysis of the clinical utility of PCA3 pathways to evaluate how the addition of PCA3 might affect patient outcomes, including long-term outcomes such as mortality and morbidity from PCa treated by different approaches (AS, FT, RP, etc.).
4. Combination of PCA3 with the TMPRSS2:ERG fusion gene has shown in many series better prognostic value,[85–87] and the combination test needs to be prospectively tested in FT strategies.

1.2.2.9 Conclusions

In summary, the main potential sources of bias in the included studies relating different scenarios where PCA3 has been tested are patient selection and lack of reported details on the intervention test, comparators, and biopsies. No meta-analyses were carried out because of the heterogeneity in the included studies.

As the reader can intuitively think, PCA3 has been linked to PCa aggressiveness, but the evidence for that is weak and controversial, as most of it comes from retrospective case series [**LOE 3b]** with a grade of recommendation **[GOR]** of **B** following ICUD recommendations.[55] The association between PCA3 score and PCa aggressiveness needs further evaluation in controlled studies to confirm the utility in selecting men with clinically insignificant PCa. While this biomarker has been translated into an FT strategy characterization, it should be clear that it has not been analyzed in its outcomes, and that all the information is extrapolated from series of RP and with diagnostic purposes, so there is a clear lack of information on this issue. Additionally, the combination of PCA3 with a diagnosis pathway including mpMRI is not fully analyzed in the literature **[LOE 3b, GOR B]**, and it should be further and prospectively investigated with the intention to select patients for initial mpMRI if possible, as generalization of mpMRI before the initial Bx is not possible at the moment in many countries and there still lack of standardization. Once PCa has been diagnosed, it is clearly evident that an mpMRI is needed for planning FT or other treatments, but it seems that PCA3 could be less useful at this point.

1.2.2.10 Level of evidence and grade of recommendation

Role of PCA3 in estimating cancer aggressiveness

No studies available that specifically use PCA3 to estimate cancer aggressiveness in the setting of focal therapy. Outside of this context, the data summarizes as:

Level of evidence: 3b

Grade of recommendation: D

Role of PCA3 in estimating cancer volume

No studies available that specifically use PCA3 to estimate cancer volume in the setting of focal therapy. Outside of this context, the data summarizes as:

Level of evidence: 3b

Grade of recommendation: D

Role of PCA3 in selecting patients for focal therapy

No studies available that systematically evaluate PCA3 to select patients for focal therapy. Outside of this context, the data summarizes as:

Level of evidence: 4

Grade of recommendation: D

1.2.3 Proenzyme PSA (proPSA)

1.2.3.1 Abstract

Prostate-specific antigen is recognized as an organ-specific marker, with low specificity and sensitivity in discriminating prostate cancer from benign conditions, such as prostatic hyperplasia or chronic prostatitis. [-2]proPSA (p2PSA), a precursor of PSA, and two of its derivatives, namely p2PSA/fPSA (%p2PSA), and the Beckman Coulter Prostate Health Index (PHI), have been investigated as new markers to accurately detect PCa. Several papers have addressed the clinical validity and utility of p2PSA and its derivatives for early diagnosis of PCa. Those studies suggest that p2PSA is the most cancer-specific form of PSA, as it is preferentially expressed in PCa tissue and significantly elevated in serum of men with PCa. [-2]proPSA, %p2PSA, and PHI measurements improve the specificity of the available tests (PSA and derivatives) in detecting PCa, avoiding unnecessary biopsies. When investigators selected PHI, its levels appeared to correlate with more aggressive diseases. At pathological assessment, PHI correlates with the PCa volume and would be indicative of low-volume cancer, which could be treated by focal therapy. The p2PSA and PHI tools were considered as prognostic and predictive for biochemical recurrence.

1.2.3.2 Introduction

Since the late 1980s, the diagnosis and follow-up of prostate cancer have relied on the use of PSA, a blood laboratory measurement that was shown to be associated with pathological diagnosis of cancer and had both diagnostic and prognostic clinical validity and utility. In 1986, the US Food and Drug Administration (FDA) approved the test to monitor those men already diagnosed with cancer, and in 1994 it went further, authorizing the test to help detect cancer in men aged 50 years or older. Over time, PSA has provided significant advancements in diagnosis and prognosis of PCa, although it was counterbalanced by its low sensitivity and specificity.[92] Prostate-specific antigen levels are indeed affected by biologic variability, which may be related to differences in androgen levels, prostate manipulation or ejaculation, or benign conditions.[93] Prostate-specific antigen clinical availability led to a frenzied hunt for the tumour, but its indiscriminate use allowed critics of the testing, once regarded as heretics, to gain credibility. In 2004, the World Health Organization (WHO) arranged an international consultation to assess new markers recognizing the limitation of PSA testing,[94] and recently, PSA has been thrust into public spotlight after several publications showed the risk for overdiagnosis and overtreatment, especially of low-risk PCa that would not have affected the longevity or the quality of life had PSA testing not been performed. Such shortcomings led urologists to investigate some isoforms of PSA, p2PSA first, and to develop novel algorithms for the diagnosis of PCa.

1.2.3.3 [-2]proPSA biology and PHI

Prostate-specific antigen is an androgen-regulated chymotrypsin-like serine protease that is part of the family of proteases known as kallikreins, encoded by a cluster of genes located on human chromosome 19q13.4,[95,96] and it is also known as human kallikrein (hK) 3. It is produced in high levels

within the prostatic ductal and acinar epithelium, with a 17-amino acid leader sequence (preproPSA) that is cleaved cotranslationally to generate an inactive 244-amino acid precursor protein (proPSA), with seven additional amino acids compared with mature PSA.[95,97,98] Generally, proPSA is normally secreted from the prostate luminal epithelial cells, and after its release into the lumen, the pro-leader part is removed and converted to its active form by the effect of hK 2 and hK 4, which have a trypsin-like activity and are expressed predominantly by prostate secretory epithelium.[99] Cleavage of the N-terminal seven amino acids from proPSA generates the active enzyme (PSA), which has a mass of 33 kDa. Normally the enzymatically active PSA is confined to the prostate gland by a tight and orderly prostatic glandular architecture, and only a few PSA molecules leak into the circulation, and PSA serum concentration is a million-fold lower than that in the seminal plasma (0.5–5 g/L).[100] The measurable serum total PSA (tPSA) comprises either a complexed form (cPSA, 70–90%), bound by protease inhibitors (primarily alpha1-antichymotrypsin) and a non-complexed form (free PSA [fPSA]).[101] Recently, fPSA was discovered to exist in at least three molecular forms: proPSA, benign PSA (BPSA), and inactive intact PSA (iPSA), covering approximately 33%, 28%, and 39% of fPSA, respectively.[49,102] Benign PSA is a degraded form of PSA that is identical to the native, mature PSA with 237 amino acids, but contains two internal peptide bond cleavages at Lys182 and Lys145. Immunohistochemical studies have shown that BPSA is expressed preferentially in the transitional zone of the prostate and is associated with pathological BPH.[103] Intact PSA is similar to native PSA, but is inactive due to structural or conformational changes. The partial removal of the leader sequence of the preproPSA leads to other truncated forms of proPSA. Thus, theoretically, seven isoforms of proPSA should exist, although only [-1], [-2], [-4], [-5], and [-7]proPSA have been found; there is still no evidence of [-3] and [-6]proPSA. All these forms of proPSA are enzymatically inactive, but they might play a role in cancer detection, especially [-2]proPSA.[104] Notably, *in vitro* experiments have shown that the p2PSA form cannot be activated by either hK2 or trypsin.[105] Once it is formed, p2PSA is resistant to activation into the mature PSA form, and consequently could be the most reliable test for cancer detection. Mikolajczyk *et al.*,[106] using a monoclonal antibody recognizing p2PSA, found increased staining in the secretions from malignant prostate glands. In particular, p2PSA is differentially elevated in peripheral gland cancer tissue; conversely, transition zone tissue contains little or no proPSA. Mikolajczyk *et al.* found that p2PSA was specifically higher in patients with PCa. Analyzing a small number of patients with biopsy positive for PCa and tPSA of between 6 and 24 ng/mL, those authors found that p2PSA comprised a high fraction of the fPSA (25–95%), which was greater than in patients with a negative biopsy. However, the molecular basis for the proPSA elevation in PCa is uncertain, although decreased cleavage by hK 2 could be the cause.[106]

1.2.3.4 Role of proPSA in estimating cancer aggressiveness

1.2.3.4.1 [-2]proPSA

Sokoll *et al.* were the first to study the role of p2PSA in the early detection of PCa.[107] Their study involved archival serum from 119 men (31 PCa, 88 non-cancer), obtained before biopsy and in the tPSA range of 2.5–4.0 ng/mL. The serum levels of the tPSA, fPSA, proPSA isoforms ([-2], [-4], and [-7]proPSA) and the proPSA/fPSA ratio were analyzed: PSA and %fPSA values were similar between the non-cancer and PCa groups, but %proPSA was relatively higher in the PCa group (50.1 ± 4.4%) compared with the non-cancer group (35.5 ± 6.7%; p=0.07). The AUC for %proPSA was 0.688 compared with 0.567 for %fPSA. At a fixed sensitivity of 75%, the specificity was significantly greater for %proPSA, at 59%, compared with %fPSA, at 33% (p<0.0001).[107] In a follow-up study of the same group, on multivariate logistic regression analyses, at a fixed sensitivity of 90%, the combination

of proPSA ([-2], [-4], and [-7]proPSA) with tPSA and %fPSA showed significantly higher specificity (44%) for early prostate cancer detection than did the individual variables (13%, 23%, and 33%, respectively).[108]

Catalona *et al.* confirmed these results in a later study analyzing serum specimens from 1,091 ie, patients (635 benign, 456 cancer) who underwent prostatic biopsies.[50] In men with a PSA of 2–4 ng/mL, at a threshold of 1.8%, %proPSA detected 90% of cancers including 100% (16/16) of extracapsular tumours and 96.6% (28/29) of tumours with Gleason scores ≥7, avoiding 19% of unnecessary biopsies. This is the first evidence of the potential correlation between p2PSA and cancer aggressiveness.

In 2004, Mikolajczyk *et al.* retrospectively evaluated the serum samples of 380 men (238 cancer, 142 non-cancer) with tPSA of 4–10 ng/mL.[109] In agreement with previous studies, %proPSA ([-2], [-4], [-5], and [-7]) had a higher AUC than did %p2PSA, fPSA, and complexed PSA (AUC of 0.69, 0.64, 0.63, and 0.57, respectively). In men with %fPSA >25%, %p2PSA had the highest accuracy (AUC, 0.77). At a threshold of 2.5, %p2PSA had a sensitivity of 90%, and 36% of prostate biopsies could be avoided. However, in patients with %fPSA <15%, at 90% sensitivity, %proPSA had a higher accuracy (AUC, 0.703; specificity, 36%) than %p2PSA (AUC, 0.669; specificity, 21%).

Further studies identified p2PSA as the more cancer-specific PSA isoform. Sokoll *et al.* evaluated the relationship between p2PSA and PCa, using serum samples of 123 men (51% PCa, 49% non-cancer) enrolled in the Early Detection Research Network (EDRN) study.[110] Overall, the %fPSA was significantly lower, while p2PSA and %p2PSA were higher in PCa patients. Also, in the PSA range of 2–10 ng/mL, p2PSA and %p2PSA continued to be significantly associated with PCa: %p2PSA AUC was 0.73, compared with 0.53 for %fPSA. Later, the same authors investigated the potential correlation between p2PSA and PCa aggressiveness, and found that %p2PSA performed significantly better than %fPSA at lower (2–4 ng/mL) PSA levels.[111]

Stephan *et al.* studied 475 patients (264 PCa, 211 non-cancer) with tPSA 2–10 ng/mL, showing that the multivariable model including %p2PSA, %fPSA, tPSA, and age (but not prostate volume) reached the highest AUC (0.84) and specificity (53.1%) compared with tPSA (22.7%), %fPSA (45.5%), and %p2PSA (41.7%) alone at fixed sensitivity (90%).[112]

[-2]proPSA level changes over time were suggested to be a potential predictor for PCa development and aggressiveness. In 2012, Rhodes *et al.* reported that p2PSA increased with advancing age and prostate volume; however, the greatest p2PSA level changes were seen in men who subsequently developed PCa (+8.1%/year) compared with those who did not (+3.5%/year) after a median follow-up of 7 years.[113] The same group found a different racial expression of p2PSA. The baseline p2PSA levels in black men were slightly higher than those in white men (median, 6.3 vs. 5.6 pg/mL, respectively) and more interestingly, white men (from the Olmsted County Study of Urinary Symptoms and Health Status among Men cohort) with higher baseline p2PSA levels had an almost eight-fold higher risk for subsequent PCa diagnosis (hazard ratio [HR], 7.8; 95% CI, 2.2–27.8). Thus, baseline p2PSA and p2PSA changes over time might be useful predictors for PCa development and aggressiveness.[114]

1.2.3.4.2 PHI

[-2]proPSA (p2PSA) appears, however, to have the highest predictive accuracy for aggressive cancer when it is associated with other variables. Beckman Coulter Inc. developed a mathematical algorithm, defined as: (p2PSA/fPSA) · √tPSA, and named it Prostate Health Index (PHI).

Le *et al.* evaluated the predictive ability of PHI in a prospective PCa screening setting.[115] The study involved 2,034 men undergoing PCa screening: 322 patients were advised to undergo prostate biopsy for elevated PSA level (>2.5 ng/mL) and/or suspicious DRE, but only 74 patients received a prostate biopsy; of these, 63 had a tPSA level of 4–10 ng/mL and a normal DRE. Prostate Health Index had the highest predictive ability (AUC, 0.77), followed by %p2PSA (AUC, 0.76) and %fPSA (AUC, 0.68), while tPSA alone lacked in sensitivity and specificity in the 2.5–10 ng/mL range (AUC, 0.50). At a sensitivity of 88.5%, PHI and %p2PSA outperformed %fPSA or tPSA (specificity, 64.9 and 48.6 vs. 40.5 and 24.3%, respectively).

Jansen *et al.* retrospectively evaluated serum samples of 405 patients enrolled in the Rotterdam arm of the European Randomized Study of Screening for Prostate Cancer (ERSPC) and 351 samples from Innsbruck Medical University.[116] The authors found significantly higher PCa predictive value and specificity for PHI and %p2PSA. Unfortunately, they had limited additional value in identifying aggressive PCa (GS, ≥7).

In a multicentre, double-blind, case-controlled clinical trial to validate PHI in the 2.0–10.0 ng/mL PSA range, with about 1,372 men enrolled in eight medical centres from October 2003 to June 2009, PHI was found to have the greatest PCa predictive accuracy (AUC, 0.703) compared with %fPSA (AUC, 0.648), fPSA (AUC, 0.615), p2PSA (AUC, 0.557), or tPSA (AUC, 0.525), directly correlating with GS (p=0.013), with an AUC of 0.724 for GS ≥4+3 disease.[51] Moreover, men with PHI >55.0 had a 52% likelihood of being diagnosed with PCa on biopsy compared with 26% of men with PHI <25.0. In particular, compared with PHI <25.0, the relative risk for PCa detection was 1.6-, 3.0-, and 4.7-fold higher at PHI 25.0–34.9, 35.0–54.9, and ≥55.0, respectively. At a PHI cutoff of 21.3, GS was ≥7 in 25% of missed cancers, thus the authors suggested a careful surveillance. The same group recently published two other studies. In one involving 892 men from a prospective, multicentre study undergoing prostate biopsy, the AUC for PHI (0.704) was significantly higher than that for %fPSA (0.649; p=0.005) and tPSA (0.527; p<0.001) in men with PSA 1.6–7.8 ng/mL WHO calibration (corresponding to 2–10 ng/mL Hybritech calibration).[117] Higher PHI values were associated with higher PCa risk and GS. In the second study, Loeb *et al.* confirmed that PHI may distinguish men at highest risk for clinically significant cancer.[118] The authors investigated, by a multicentre prospective trial, 658 men aged 50 years or older with tPSA ranging from 4 to 10 ng/mL and normal DRE. Focusing on significant PCa, PHI had the highest AUC for GS ≥7 (AUCs, PHI 0.707; %fPSA 0.661; p2PSA 0.558; PSA 0.551). Furthermore, the authors found that at the 90% sensitivity, using a cutoff for PHI of 28.6, 30.1% of patients could have been spared an unnecessary biopsy for benign disease or insignificant prostate cancer compared with 21.7% using %fPSA.

Similar results were reported in Europe by Guazzoni *et al.*[119] In 2011, the authors conducted an observational prospective study of 268 consecutive men with PSA 2–10 ng/mL and normal DRE who were undergoing prostate biopsy. %p2PSA and PHI were the strongest predictors for positive prostatic biopsy outcome. Prostate Health Index and %p2PSA improved the accuracy of a base multivariate

model (including tPSA, fPSA, prostate volume, and age) by 11% and 10%, respectively (p<0.001). Similarly, in patients with tPSA 4–10 ng/mL, the inclusion of PHI and %p2PSA significantly increased multivariate predictive accuracy from 72% to 83% (+11%) in both models (p<0.001). Lazzeri *et al.* extended and confirmed the data in a clinical cohort of men with previous negative biopsies, but persistent suspicion of PCa.[120] %p2PSA and PHI were the most accurate predictors for disease. In multivariable logistic regression models, %p2PSA and PHI achieved independent predictor status, and significantly increased the accuracy of multivariable models by 8% to 11% (p≤0.034). At a PHI cutoff of 28.8, 116 (52.25%) biopsies could have been avoided, missing PCa in 6 patients, but none with a Gleason score ≥7, demonstrating a real clinical utility.

Lazzeri *et al.* validated previous results in an observational, prospective, multicentre, European cohort (PROMEtheuS Project).[121] This study involved 646 patients from five European countries with tPSA 2–10 ng/mL who were subjected to initial prostate biopsy for suspected PCa. [-2]proPSA, %p2PSA, and PHI significantly increased the accuracy of the base multivariable model by 6.4%, 5.6%, and 6.4%, respectively (p<0.001). At 90% sensitivity, the PHI cutoff of 27.6 could avoid 100 (15.5%) biopsies, missing 26 (9.8%) cancers (23 with GS 6, 3 with GS 3+4).

Stephan *et al.* presented a European, multicentre study involving 1,362 patients with tPSA 1.6–8.0 ng/mL (668 PCa, 694 non-cancer), where the serum concentrations of tPSA and fPSA were both calibrated against a WHO reference material.[122] %p2PSA and PHI were significantly higher in all PCa subcohorts (positive initial or repeat biopsy result or negative DRE) (p<0.0001) compared with patients without PCa. Prostate Health Index had the largest AUC (0.74) and provided significantly better clinical performance for predicting PCa compared with %p2PSA (AUC, 0.72; p=0.018), p2PSA (AUC, 0.63; p<0.0001), %fPSA (AUC, 0.61), or tPSA (AUC, 0.56). Significantly higher PHI was observed for patients with Gleason score ≥7 (PHI, 60) compared with Gleason score <7 (PHI, 53; p=0.0018), confirming its relationship with PCa aggressiveness.

Recently, Boegemann *et al.* presented a multicentre study showing that %p2PSA and PHI have a superior diagnostic performance for detecting prostate cancer in young men (<65 years) with a tPSA range of 1.6–8.0 ng/mL compared with tPSA and %fPSA at initial and repeat biopsy and for predicting significant prostate cancer.[123] Those results are very similar to ones by Fossati *et al.* published some months before.[124] In 238 patients, who were aged <60 years, PCa was found in 67 subjects (28.1%) and, on univariate analysis, %p2PSA (AUC, 0.704) and PHI (AUC, 0.7) were the most accurate predictors, and these significantly outperformed tPSA (AUC, 0.549), fPSA (AUC, 0.511), and %fPSA (AUC, 0.557) in the prediction of PCa at biopsy (p≤0.001). In multivariate logistic regression models, %p2PSA and PHI achieved independent predictor status and significantly increased the accuracy of multivariate models by 6.3% and 7.6%, respectively (p≤0.05).

Two recent Asian studies confirmed previous results in another population setting. Ito *et al.* reported data of 239 consecutive men with a tPSA of 2.0–10.0 ng/mL who were undergoing prostate biopsy.[125] When PHI was used as a biopsy indicator and sensitivity was fixed at 95%, unnecessary biopsies could be avoided in 28% of men. Accordingly, Ng *et al.* retrospectively analyzed archived serum samples from 230 Asian patients more than 50 years of age who had undergone their first prostate

biopsy with PSA 4–10 ng/mL and a negative DRE. Prostate Health Index was the best predictor for the prostate biopsy results.[126] At a sensitivity of 90%, the use of PHI could have avoided unnecessary biopsies in 104 (45.2%) patients.

Finally, Lughezzani *et al.* developed and validated in more than 729 patients a PHI-based nomogram to predict PCa at extended prostate biopsy. Including PHI in a multivariable logistic regression model, based on patient age, prostate volume, DRE, and biopsy history significantly increased predictive accuracy by 7% from 0.73 to 0.80 ($p<0.001$).[127] Decision-curve analysis showed that using the PHI-based nomogram resulted in the highest net benefit for detecting clinically significant prostate cancer. This nomogram was also externally validated in a recent, multicentre, European study.[128]

Overall, studies to date suggest that %p2PSA and PHI are more accurate than standard reference tests in predicting clinically significant prostate cancer at initial and repeat biopsy.

1.2.3.5 Role of proPSA in estimating cancer volume

Guazzoni *et al.* investigated the relationship between p2PSA and its derivatives, namely %p2PSA, PHI, and PCa characteristics at final pathology in a contemporary population of patients treated with RP for clinically localized PCa.[129] The authors conducted an observational, prospective study of 350 consecutive men diagnosed with clinically localized PCa who underwent RP. Pre-operative %p2PSA and PHI were significantly higher in patients with pT3 disease, pathological GS ≥7, and those with GS upgrading ($p<0.001$). These results showed that %p2PSA and PHI are related to both PCa volume and aggressiveness.

In the PSA era, mean tumour volume is drastically decreased, and evidence suggests that smaller tumours are less aggressive and less frequently associated with progression.[130] Although the volume threshold for clinically significant PCa is still controversial, data from autopsy series, cystoprostatectomy, and RP series support the concept that the 0.5–mL threshold volume with no GS of 4 or 5 can be used for the definition of clinically insignificant tumours.

Guazzoni *et al.* found that PHI, but not %p2PSA, significantly increases the predictive accuracy of a basic model including patient age, tPSA, fPSA, f/tPSA, clinical stage, and biopsy Gleason sum for tumour volume <0.5 mL.[129] In Guazzoni's series, only 15% of patients with a PCa volume <0.5 mL had Gleason sum 7 disease (no one GS >7), indicating that PHI, as a biomarker, could be a subject of interest and discussion in further studies. Fossati *et al.* used the PROMETHEUS database to validate the hypothesis that p2PSA, %p2PSA, and PHI might correlate with pathologic cancer features and be able to discriminate indolent from aggressive phenotypes in a large prospectively collected, multicentre, European, contemporary cohort of patients who underwent RP for clinically localized PCa.[131] The authors reported that median pre-operative p2PSA (17.6 vs. 12.4 pg/mL), %p2PSA (2.52 vs. 2.02), and PHI (64.9 vs. 42.9) were significantly higher in patients with pT3 disease and pathologic GS ≥7, compared with patients without adverse pathologic characteristics (all $p<0.0001$). Unfortunately, Fossati and coworkers did not evaluate the tumour volume as a pathologic outcome because these data were not available for three of the six institutions involved in the study.

Heidegger *et al.* found that p2PSA values were highly different (p<0.001) between GS ≥8 and GS ≤7 already 3 years before diagnosis, and that pre-operative p2PSA values were significantly higher in men with ≥pT3a compared with ≤pT2c PCa up to 4 years before diagnosis (p <0.01).[132] [-2]proPSA was shown to have a high PPV concerning GS ≥8 and GS ≤7, as well as extraprostatic extension.

1.2.3.6 Role of proPSA in selecting patients for focal therapy

Currently, there is a wide debate about the role of new tools for defining candidates for focal therapy. No overall consensus exists in defining the ideal candidate for primary focal therapy, despite a number of consensus statements from a number of groups. This reflects different schools of thought with respect to the role of focal therapy in the current spectra of disease risk.[133] In 2007, the International Task Force on Prostate Cancer and the Focal Lesion Paradigm proposed very conservative clinical and biopsy criteria for selecting focal therapy patients and the PSA cutoff was <10 ng/mL.[132] Other consensus groups have attempted to introduce greater flexibility in these criteria by essentially allowing intermediate- and some higher-risk prostate cancers, setting the PSA cutoff higher than 10 ng/mL.[134] Unfortunately, no one considered p2PSA and PHI as selection criteria for patient candidates for focal therapy.

Some papers dealt with the role of p2PSA and PHI in patient selection for active surveillance. Makarov *et al.* found that the ratio p2PSA/%fPSA in serum was significantly higher at diagnosis in men developing unfavourable biopsies (0.87 ± 0.44) compared with those with favourable biopsies (0.65 ± 0.36; p=0.02).[135] Moreover, p2PSA/%fPSA (HR, 2.53; p=0.02) was significantly associated with unfavourable biopsy in Kaplan-Meier and Cox analyses. Tosoian *et al.* reported data from 167 men scheduled in a single-institution AS program.[136] Risk for biopsy reclassification was significantly associated with lower %fPSA (p=0.002), and higher %p2PSA (p<0.0001) and PHI (p<0.0001) at baseline. Finally, Hirama *et al.* evaluated the predictive impact of baseline p2PSA and related indices on the pathological reclassification at 1 year in 67 patients enrolled over 134 candidates for AS.[137] %p2PSA and PHI at baseline were significantly different between the reclassification and non-reclassification groups (2.44 vs. 1.88, p=0.003; 60.3 vs. 47.8, p=0.01; respectively). By multivariate logistic regression analysis, baseline %p2PSA and PHI (both p=0.008) were the only independent predictive factors for pathological upgrade at 1 year during AS.

New biomarkers could be used in the follow-up after focal therapies. Although PSA outcomes are accepted as a valid outcome in standard therapies, the clinical utility of PSA kinetics in tissue preservation is yet to be determined. Unfortunately, no PSA or p2PSA and PHI outcome measures have been validated in focal therapy yet.

1.2.3.7 Future research priorities for proPSA

An ideal biomarker for PCa should be able to hold as much information as possible for the target disease. It means that an ideal biomarker should be able to discriminate men with or without PCa, discriminate men with indolent from men with clinically significant PCa, and it should guide the treatment. Furthermore, a biomarker should assist physicians in defining prognosis and in following up patients. In other words, a biomarker for PCa should live with the patient throughout his life.

Lughezzani *et al.* tested the hypothesis that pre-operative PHI levels could help to predict early biochemical recurrence (BCR) in men after RP.[138] In 313 patients treated by RP for clinically localized prostate cancer at a single institution between 2010 and 2011, the authors found that the 2-year BCR-free survival rate was 92.5% in the overall population and 96.7% in patients with organ-confined disease. The most significant PHI cutoff value for discriminating between patients with and without BCR was 82. In this interim analysis of a study, whose final data are expected within the next year, the 2-year BCR-free survival rate was 97.7% in patients with a pre-operative PHI level <82 relative to 69.7% in patients with a PHI level ≥82 (log-rank test $p<0.001$). In multivariable Cox regression analyses, PHI level emerged as an independent predictor for BCR in both the pre-operative and post-operative settings, and was more accurate than several established BCR predictors.

Recently, two different papers, by Tilki *et al.* and Kang *et al.*, addressed the role of ultrasensitive PSA (uPSA) for early detection of BCR after radical prostatectomy for localized PCa.[139,140] In their systematic review, Tilki and coworkers concluded that uPSA might be useful in the early diagnosis of PCa recurrence after radical prostatectomy. Unfortunately, its specificity was poor, the PPVs were low, and no ideal cutoff could be established. Furthermore, those authors failed to find evidence that earlier detection of recurrence translates into clinical utility. On the contrary, Kang and colleagues revealed that a first post-operative uPSA of 0.03 ng/mL or greater was the optimal threshold to identify recurrence. They performed a multivariate analysis, which confirmed that only a first post-operative ultrasensitive value of 0.03 ng/mL or greater showed the highest risk (HR, 8.5; $p<0.0001$) and identified BCR with greater sensitivity than undetectable first conventional PSA (70% vs. 46%). The median lead-time advantage was 18 months over the conventional definition of PSA 0.2 ng/mL or greater. Those two papers open a new horizon about the role of biomarkers in the diagnosis and management of BCR after RP.

The sensitivity for detecting BCR, which remains the main surrogate for disclosing a treatment failure, is directly related to the sensitivity of the PSA assay. The historical detection limit of commercial first-generation PSA assays ranged from 0.3 to 0.5 ng/mL, but the new generation of uPSA is able to reach a detection limit of 0.001 ng/mL, which has been shown to detect BCR months to years earlier when compared with conventional assays. Nevertheless, the uPSA test is not yet incorporated in clinical practice, as acceptable performance characteristics have not been defined.

One of the main clinical issues to address remains the post-treatment follow-up in men who receive radical treatment for localized PCa in order to identify either patients in whom the therapy failed requiring adjuvant/salvage treatments or patients with BCR who are not at risk for clinical progression. Although RP offers a high overall cancer control rate, even in appropriately selected men, up to a third of men undergoing RP will experience failure manifested by a rising serum PSA without clinical or radiological evidence of disease.[141] The natural clinical course of patients with BCR is highly variable, as some patients may experience rapid clinical progression to local and systemic disease, while in others it may pose no threat to their health. Pound *et al.* found that the 5-year risk for clinical progression in men with BCR ranged from 27% to 60%; clinical progression-free BCR might reflect the recurrence of indolent prostate cancer, incorrect pathological evaluation, or a PSA being produced by benign prostate tissue, which was left behind after RP (benign positive surgical margin).[142,143] Prostatic cancer–specific mortality at 15 years was shown to be equivalent in men with or without BRC.[144] As not all men with PSA failure develop clinically evident local or distant

recurrence, not all patients with clinical progression die of prostate cancer, and some men would receive radiotherapy unnecessarily. Furthermore, as radiotherapy is associated with well-recognized toxicity, a quandary emerges regarding the role of traditional and ultrasensitive PSA in determining the need for secondary adjuvant therapy and identifying clinically significant BCR. There is a need, or priority, for additional tests to increase the probability of detecting clinically significant recurrent PCa at an early stage in order to offer an accurate secondary therapy, reduce the side effects of late treatments, and avoid unnecessary secondary therapy.

As p2PSA is normally expressed in pg/mL, it could be more sensitive and accurate than tPSA and uPSA for detecting early BCR in patients after RP and might guide adjuvant treatments, avoiding unnecessary secondary treatments. In a preliminary study published as a congress abstract, Ceriotti *et al.* found that by assessing the Limit of Detection (LoD) for p2PSA using sera from patients with proven recurrent PCa after RP, the analyzer is able to detect reliably p2PSA starting from a concentration of as low as 0.8 pg/mL, and this concentration might be considered the cutoff sufficient to detect and monitor biochemical recurrence of PCa.[370] Recently, also in a published congress abstract, Lazzeri investigated the hypothesis that p2PSA is more sensitive than total PSA for early detection of BCR after RP for localized PCa. The study was an observational, ongoing, prospective, cohort study in a contemporary cohort of 134 consecutive patients with localized PCa (pT2-3/N0), who had undergone RP.[371] After a median follow-up of 22 months, 22 (16.5%) patients showed BCR; 18 of 22 had p2PSA ≥0.8 pg/mL. Five patients showed a contemporary increase of PSA and p2PSA, and 13 developed p2PSA >0.8 pg/mL before BCR. The mean lead-time advantage was 11.5 months over the conventional definition of PSA BCR.

The goal of recent research has been to improve the laboratory assay sensitivity in order to decrease the follow-up time necessary to either pronounce a patient free of disease with reasonable certainty or introduce an adjuvant therapy as early as possible. With the introduction of uPSA, several attempts to identify earlier those patients who will develop BCR have been made. [-2]proPSA (normally expressed in pg/mL) might be a valid tool for defining early BCR, and it might be introduced in clinical practice to identify patients who have BCR, earlier than other current laboratory assays can do. Use of p2PSA might be a useful tool for either evaluating the potential advantages of early treatment [hormone therapy (HT) or radiotherapy (RT)] for patients at very high risk for BCR after RP or for ruling out patients in whom adjuvant therapy would result unnecessary. Finally, a correlation between post-operative p2PSA and specific pathological outcomes (i.e., positive surgical margins [R1] after RP) might help clinicians in the decision-making process.

1.2.3.8 Conclusion

[-2]proPSA and PHI are simple, non-invasive blood tests which have been shown to be more accurate than PSA in detecting prostate cancer and reducing unnecessary biopsies in men with tPSA values from 2–10 ng/mL. Several authors have found that higher PHI values are associated with increased probability of clinically significant (aggressive) prostate cancer. A correlation with the pathological and clinical outcome was found by different authors, and preliminary results suggest a role for p2PSA for follow-up after PCa treatment.

1.2.3.9 Level of evidence and grade of recommendation

Role of proPSA in estimating cancer aggressiveness

No studies available that specifically use proPSA to estimate cancer aggressiveness in the setting of focal therapy. Outside of this context, the data summarizes as:
Level of evidence: 3b
Grade of recommendation: D

Role of proPSA in estimating cancer volume

No studies available that specifically use proPSA to estimate cancer volume in the setting of focal therapy. Outside of this context, the data summarizes as:
Level of evidence: 3b
Grade of recommendation: D

Role of proPSA in selecting patients for focal therapy

No studies available that systematically evaluate proPSA to select patients for focal therapy. Outside of this context, the data summarizes as:
Level of evidence: 4
Grade of recommendation: D

1.3 Selection for Focal Therapy

1.3.1 The ideal patient characteristics

1.3.1.1 Introduction

In light of the continuous development and refinement of diagnostic and therapeutic approaches for focal therapy, appropriate patient selection becomes an issue of paramount importance. Currently, no international consensus exists for defining the ideal candidate for focal therapy despite various statements published in the literature. Recommendations for patient selection are mainly based on recently published papers by expert consensus panels. However, these recommendations have not been validated so far due to lack of oncologic long-term follow-up data of focal therapy studies. It is therefore important to emphasize that the majority of current recommendations of numerous national and international expert panels are based on level five evidence **[LOE 5]**. This chapter will summarize the current status for patient selection criteria, focussing on life expectancy, risk factors, comorbidity, and sexual activity.

1.3.1.2 Life expectancy

In May 2013, a consensus meeting by 13 focal therapy experts was held during the 6th International Symposium on Focal Therapy and Imaging in Prostate and Kidney Cancer.[41] The panel discussion followed multiple rounds of questionnaires based on the Delphi approach that were processed by 48 experts in the field from Europe, United States, and Asia. The primary goal of the panel was to define an international multidisciplinary consensus on trial design in focal therapy for prostate cancer. The panel concluded that patients should have a life expectancy of >10 years to be included in focal therapy trials.

Four years earlier, in 2009, an expert panel conducted by de la Rosette came to comparable results that patients eligible for focal therapy should have a life expectancy of 10 or more years.[33]

Results of another consensus meeting of 15 experts were published by Donaldson *et al.* in 2015.[39] The panel's conclusion concerning life expectancy differed slightly, saying that age is not a primary determinant of focal therapy. However, the experts considered that there is uncertainty in patients younger than 40 years of age and in those older than 80 years of age. Focal therapy would be best suited in patients with a life expectancy of >10 years, and it should not be offered to patients with life expectancy of less than 5 years.

1.3.1.3 Comorbidity

Only very few statements on comorbidity in patients eligible for focal therapy can be found in the literature. Patient selection based on comorbidity was discussed by two expert panels:[39,41]

In the 2013 consensus meeting by van den Bos *et al.*, no specific statement on exclusion criteria based on comorbidity can be found. The group concluded that "exclusion of individual patients should be based on good clinical judgment, being mindful of all comorbidities and performance status (e.g., heart disease, concurrent cancers)." Renal insufficiency as well as a history of chronic prostatitis were not considered to be exclusion criteria.[41]

The 2014 consensus panel by Donaldson *et al.* gives more specific recommendations. It is considered that patients with a WHO performance status of 0 or 1 are suitable candidates for focal treatment, but patients with a WHO performance status of 3 or 4 should not be offered focal therapy. There is uncertainty however in patients with a performance status of 2.[39]

1.3.1.4 Risk factors

Over the last years, there has been a paradigm shift to expand the inclusion criteria for patients for focal therapy. Due to lack of early oncologic results, focal therapy was considered primarily as an alternative to active surveillance. Based on growing evidence of satisfying early oncologic results, it is considered more and more as an alternative to radical prostatectomy.

In 2007, an international multidisciplinary expert group (International Task Force on Prostate Cancer and the Focal Lesion Paradigm) performed a literature review on the rationale and concerns about focal therapy and proposed study design parameters.[145] The group took a conservative approach to patient risk criteria and recommended focal therapy exclusively to patients with very low–risk disease based on cancer criteria as an alternative to active surveillance. According to the 2010 consensus group by de la Rosette *et al.*, focal therapy should be offered to patients with low-risk disease as an alternative to active surveillance, but the panelists extended their inclusion criteria to patients with a non-dominant Gleason score 4 pattern found on template biopsy. Patients with a dominant Gleason pattern 4 found on standard biopsy were to be excluded. Only patients with clinical stage not higher than T2a, N0, M0 were considered suitable.[33] This is foiled by other experts saying, "any man with localized prostate cancer suitable for curative therapy should be regarded as suitable for some form of focal therapeutic intervention."[146] According to the 2014 consensus on focal therapy trial design by van den Bos *et al.*, patients with clinical stage T2a, PSA of <15 ng/mL, and GS not higher than 3+4=7 were considered eligible in focal therapy studies.[41]

Donaldson *et al.* put more focus on patient risk classification. A high level of consensus was reached to include patients with intermediate-risk prostate cancer according to the National Comprehensive Cancer Network (NCCN) classification.[147] A shift from low to intermediate risk was justified by promising medium-term follow-up results from recent studies.[38,148] A low level of consensus was achieved for low-risk patients. In patients with well-characterized low-risk disease, focal treatment is considered as overtreatment. These patients are better served with active surveillance.[39] In 2011, the Transatlantic Consensus Group on active surveillance and focal therapy for prostate cancer proposed different trial designs in the assessment of focal therapy for prostate cancer. Among them they proposed phase 3 studies of low- to high-risk patients comparing focal therapy with radical whole-gland treatment with the outcome of freedom from metastasis.[149] However, up to now, no such prospective study has been initiated.

In a recent review by Valerio *et al.* summarizing 25 studies of focal therapy in the primary setting, a total of 1,109 (56%) patients were low risk, 704 (36%) were intermediate, and 164 (8%) were high risk. In 13 series, there were no risk categories available.[150]

1.3.1.5 Sexual activity

Despite the fact that preserving sexual function is one of the key goals to achieve with focal therapy in prostate cancer, only few comments on pre-treatment sexual function can be found in the current literature. Only the 2013 consensus by van den Bos *et al.* gives the statement that significant erectile dysfunction and urinary incontinence are not exclusion criteria for focal therapy.[41]

1.3.1.6 Conclusion

One of the main aspects of focal therapy in prostate cancer is appropriate patient selection. Current recommendations are mainly adopted from recent papers of expert panel meetings. This chapter illustrates that current expert panel recommendations are heterogeneous in several aspects. Only future studies with long-term follow-up will have the potential to clarify ideal patient characteristics and to help separate patients suitable for active surveillance from those that are best served with focal therapy or even radical treatment.

1.3.1.7 Level of evidence and grade of recommendation

The ideal patient characteristics

Life expectancy: No studies available that systematically evaluate life expectancy in the selection of patients for focal therapy.
Level of evidence: 4
Grade of recommendation: C

Comorbidities: No studies available that systematically evaluate comorbidities in the selection of patients for focal therapy.
Level of evidence: 4
Grade of recommendation: C

Risk factors: No studies available that systematically evaluate risk factors in the selection of patients for focal therapy.
Level of evidence: 4
Grade of recommendation: C

Sexual activity: No studies available that systematically evaluate sexual activity in the selection of patients for focal therapy.
Level of evidence: 4
Grade of recommendation: C

1.3.2 The ideal cancer characteristics

1.3.2.1 Abstract

A comprehensive literature review was performed to establish selection criteria for focal therapy as a treatment alternative for localized prostate cancer. Recent data have demonstrated a significant pathologic stage migration toward early-stage disease. The cancer volume of the clinically significant tumour (index lesion) has been proposed as a driving force of PCa progression, and therefore should be identified and treated at an early stage, whereas most of secondary lesions appear to be non-clinically significant to the patient. Clinical stage, baseline PSA, pre-operative extensive transperineal three-dimensional (3D)–template-guided mapping biopsies (TMBs), along with multi-parametric MRI (mpMRI), with precise mapping of the spatial distribution of PCa within the prostate remain important selection criteria for FT. Current understanding of the tumour biology of early-stage disease has led to the pre-operative identification of unifocal lesions. However, the detection of unilateral lesions seems to be a more feasible option with subsequent hemiablative treatment of the prostate.

1.3.2.2 Introduction

Current screening strategies have led to earlier diagnosis of PCa at lower clinical stages, lower grades, and smaller volumes—ultimately, to less-aggressive PCa.[151] As a result, men with localized PCa and physicians who advise them face a difficult therapeutic dilemma: surveillance versus radical whole-gland therapy—namely, the anxiety associated with delayed treatment, and consequent overtreatment of clinically insignificant tumours in combination with the significant morbidity of established therapies, respectively.[152] The advent of novel FT modalities may shed light on the dilemma and could fill the gap between these two poles, by providing new treatment alternatives for those patients. A wide variety of ablative methods have been introduced and applied in recent years as FT modalities with which cancer foci can be eradicated within the prostate gland, thus greatly reducing the associated side effects of radical treatment. Although FT is not yet the standard for organ-confined PCa, its therapeutic potential is highly promising.[153] To date, the consensus definition states that FT is "any approach able to preserve part of the prostatic tissue, whether by targeted ablation, hemiablation, and zonal 'hockey stick' ablation."[41,150] The ultimate goal of FT is to achieve "trifecta" outcomes: cancer control, fewer complications, and preservation of genitourinary function, along with maintenance of quality of life (QOL). Across the international literature, it has been suggested that FT may achieve this ambitious goal in selected patients. However, the complex challenge of patient selection remains.

1.3.2.3 Selection for focal therapy

The largest challenge of implementing FT in clinical practice remains candidate selection. In selecting candidates for focal ablative therapy, the urologist must primarily consider the goal of therapy. Based on this, appropriate methods for risk stratification and disease mapping should be used. The method of treatment is then selected, based on the mapping strategy.[154] Such strategy relies heavily on the ability to identify disease location with great accuracy. The better the mapping ability, the more focal the therapy can be. Theoretically, precise destruction of a lesion would necessitate image guidance or accurate disease localization by mapping template biopsy. In this context, in order to improve the diagnostic localization of cancer foci and FT ablation templates, extensive transperineal 3D-TMBs were proposed as a solution to the undersampling of standard transrectal ultrasound of the prostate (TRUS)-guided biopsies and the consequent possibility of undertreatment.[155,156] This biopsy method allows for systematic sampling of the entire gland by applying the same transperineal grid used for brachytherapy seed placement, and has led experts to define 3D-TMB as the gold standard for patient selection for FT.[157,158] In addition, during the last decade, mpMRI has been extensively developed—and revolutionized PCa detection. In fact, it has allowed not only detection but also characterization of PCa. The addition of diffusion-weighted images and dynamic contrast-enhanced (DCE) images to standard anatomical T2 images permits functional assessment of the prostatic tissue. Thus, fusion of mpMRI images with real-time TRUS ones (MRI/TRUS fusion guided) has led to targeted biopsies with higher accuracy in identifying and quantifying intracapsular clinically significant tumour foci.[159]

In this context, destruction of the dominant tumour foci may be adequate to alter the clinical course of PCa; the smaller, low-volume, low-grade satellite tumours that go undetected (organ-confined cancer <0.5 mL, no Gleason grade 4 or 5 component) should have no impact on the clinical course of the PCa that remains.[37,160,161] The conceptual paradigm of FT directed to the index lesion or dominant focus is potentially further validated by observations that among men with metastatic PCa, all metastatic sites are typically derived from one genotypic clonal cell population.[162,163] This observation is highly suggestive of the potential efficacy of FT broadly directed to the correct dominant tumour focus. Therefore, it is essential that such an approach relies on the identification of the dominant focus through biopsy and imaging.

There has been an evolution of the concept of FT that strictly correlates with the improvement of cancer detection and characterization. In the beginning of the 1990s, FT was associated with whole-gland treatment of localized PCa. In the 2000s, FT is aimed at treating unilateral disease with hemiablation and/or targeted ablation techniques, focusing on ablating just the index lesion(s), namely the largest and most undifferentiated cancer foci. This reflects the constant evolving nature of FT and how it can impact patient selection.[164] However, to date, overall consensus for defining the ideal candidate for primary FT constitutes a difficult task, despite several consensus statements. Indeed, during the first consensus conference on FT, experts recognized the constantly evolving nature of FT and how it can impact patient selection. Across this chapter, we aim to describe the ideal candidate for FT by presenting the evolution of the concept of FT and its impact on patient selection criteria.

1.3.2.4 Ideal cancer grade

In 2007, the International Task Force on Prostate Cancer and the Focal Lesion Paradigm first proposed very conservative criteria for selecting patients, essentially deeming FT an alternative to active surveillance in very low–risk disease.[145] These criteria were PSA level <10 ng/mL, the absence of Gleason grade 4 and 5, the use of extended biopsy schemes, and very restricted biopsy criteria, including maximum length of cancer in each core of 7 mm and maximum percentage of total cores with cancer of 33% (**Table 1-2**).

TABLE 1-2 International Task Force on Prostate Cancer and the Focal Lesion Paradigm: Proposed clinical, biopsy, and imaging criteria for focal therapy patient selection.[145]

		Reference
Clinical	Clinical stage T1 or T2A	Zelefsky *et al.*[363]
	PSA <10 ng/mL	D'Amico *et al.*[11]
	PSA density <0.15 ng/mL/mL	Goto *et al.*[180]
	PSA velocity <2 ng/mL yearly in the year prior to diagnosis	D'Amico *et al.*[11]
Biopsy	Minimum of 12 cores	Graefen *et al.*[364]
	No Gleason score 4 or 5	Zelefsky *et al.*[363]
	Maximum percentage of cancer in each core (e.g., 20%)	Tsuzuki *et al.*[365]
	Maximum length of cancer in each core (e.g., 7 mm)	Naya *et al.*[366]
	Maximum percentage of total cores with cancer (e.g., 33%)	Kestin *et al.*[367]
Imaging	Single lesion with a maximum size (e.g., 12 mm)	
	Maximum length of capsular contact (e.g., 10 mm)	
	No evidence of extraprostatic extension or seminal vesicle invasion	

PSA, prostate-specific antigen.

In 2009, a second consensus meeting was held with the objective of eradicating all measurable disease and reducing treatment-related side effects.[33] The second panel considered the presence of Gleason pattern 4 disease as non-exclusionary, based upon the observation that many men with low-risk features on biopsy are found to have non-dominant Gleason 4 disease at radical prostatectomy, with very little impact on the clinical course. In addition, the panel agreed to using a template-guided approach as the standard to qualify a patient for FT. Also, overall agreement was reached on the use of (MRI/TRUS fusion-guided) techniques for tumour localization whenever possible at expert centres (**Table 1-3**).

In recent years, other consecutive consensus groups have attempted to introduce greater flexibility in these criteria by essentially allowing intermediate-risk and some higher-risk PCa, effectively deeming FT an alternative strategy for those men who would normally be advised to have radical therapy.[42,149]

The shift in the indication of FT regarding risk strata over time, from low-risk patients to now treating intermediate- and even high-risk patients, is likely due in part to the growing confidence gained through the years in the technique and the promising medium-term follow-up results.[39]

TABLE 1-3 International Workshop on Focal Therapy and Imaging in Prostate & Kidney Cancer Consensus Panel.[33]

1. Candidates for focal therapy should ideally undergo transperineal template mapping biopsies, although a state-of-the-art multifunctional MRI with TRUS biopsy at expert centres may be acceptable.
2. Candidates for focal therapy should have a life expectancy of 10 or more years.
3. Patients with previous prostate surgery should be counselled with caution.
4. Patients with previous radiotherapy to the prostate or pelvis should not be treated until more data are available, although the panel accepts that focal salvage therapy may be a possibility in the future.
5. The effects of focal therapy on men with lower urinary tract symptoms are not well known. These men should be counselled with caution.
6. There will be specific attributes that are more related to the energy source than to focal therapy in general. Issues such as prostate size, presence of prostatic calcification, cysts, TUR cavity, access to rectum, and concurrent inflammation of rectal mucosa may need to be taken into consideration when selecting the optimal therapy.
7. Focal therapy should be limited to patients of low to moderate risk.
8. Focal therapy should be limited to men with clinical T2a or less N0M0 disease.
9. Focal therapy should be limited to men with radiologic ≤T2b N0M0 disease.
10. Defining the topography of the cancer is important. Disease that is predominantly apical or anterior in deposition may be technically difficult to manage with existing treatment modalities.
11. The long-term effects of focal therapy on potency/erectile functions are not known. Men should be counselled in this regard before therapy.

Abbreviations: MRI, magnetic resonance imaging; TRUS, transrectal ultrasound of the prostate; TUR, transurethral resection.

The concept of the index lesion and its impact on the prognosis of PCa have thus led to the development of a novel approach in selecting the candidates. If once FT was proposed for mainly patients with low-risk disease, current consensus meetings are expanding inclusion criteria to intermediate-risk patients.[33] Ongoing trials are also expanding criteria to include patients with a PSA value of up to 15 ng/mL, Gleason score of up to 4+3, and clinical stage of up to T2, and targeting unifocal as well as multifocal disease.[38]

1.3.2.5 Ideal cancer volume

Regarding the ideal prostate cancer volume to be treated and acknowledging that some energy sources have limitations in their ability to treat some anatomic regions—e.g., high-intensity focused ultrasound (HIFU) is limited to treating anterior lesions in small prostates only[165]—while others do not, it was agreed that prostate cancer volume should not be a primary determinant of eligibility for focal therapy.

However, the ideal cancer volume to be treated poses a more complex scenario. Historically, the threshold for clinically significant disease, capable of metastatic progression, has been set at 0.5 mL, with some Gleason grade component ≤4.[166] It has been shown that in >80% of patients with an index lesion of cancer, the aggregate volume of secondary tumours is <0.5 mL. As most metastatic cancers originate from a single clonal cancer cell, it would be reasonable and effective to identify and target this potentially lethal lesion with FT.[167] Thus, selective treatment of clinically significant disease, with acceptance of residual, insignificant disease may serve as a meaningful treatment paradigm.[167]

Recent consensus meetings did not agree on a maximum tumour volume beyond which FT is deemed not suitable. However, they highlighted other factors that need to be considered, including the size of the prostate, the grade of the lesion, and the boundaries and morphologic characteristics of the lesion.[39]

1.3.2.6 Multifocality

The concept of multifocality has generally been regarded as a major limitation in the rationale for FT in PCa. Several areas of evidence suggest that multifocality is not necessarily a limiting factor for tissue preservation. In fact, there has been increasing debate and gradual acceptance that not all tumours in the prostate behave similarly.[168] There is strong evidence that the vast majority of metastases find their origin in the same prostate cancer cell clone, derived from the same lesion, called the index lesion.[34,37] Histopathological features of the index lesion predict the clinical behaviour of the entire gland despite multiple synchronous tumours in >90% of patients. While PCa is typically multifocal with clonal heterogeneity of prostate cancer within the gland, not all tumours within a single gland have the potential for lethality.[34,37]

The index-lesion concept proposes that it is only the dominant lesion which drives the natural history of the disease.[160,161] In this context, only some lesions are clinically significant and may have an impact on the patient's health, whereas others are clinically insignificant. Thus, men who have only clinically insignificant disease have little to no chance of disease progression within their lifetime, and some have proposed they would have no certain benefit to being treated with active therapies.[168,169]

Current trials have differed in the approach to ablative strategies. Most investigators aim to treat all known areas of cancer in a hemiablative fashion for unilateral-confirmed disease, while others have deliberately allowed for ablation of the index lesion alone even when multifocal disease is found.[150]

The most recent consensus panel agreed that it was acceptable not to treat lesions of Gleason grade 3+3 up to a maximum cancer core length of 5 mm. In addition, the panel agreed that it is not acceptable to leave untreated lesions with Gleason grade 3+4 with a maximum cancer core length of 5 mm or any 4+3 disease of any length. However, the panel did not reach consensus on whether lesions with Gleason grade 3+4 with a maximum cancer core length of 3 mm could be left untreated.[39]

1.3.2.7 Unilateral/bilateral disease

Patients with unifocal, unilateral, or low-volume PCa are most suitable for FT; however, a great challenge persists in identifying patients with multifocal, clinically significant cancer foci who require aggressive whole-gland therapy from those with clinically insignificant focal cancers who may benefit from organ-sparing treatment. In this context, during the last consensus meetings, no agreement was reached about whether FT should be targeted to all lesions, but the panel agreed that multifocal cancer should not preclude FT.[39] Ultimately, the limiting factor for FT should be the clinical risk stratification, not the laterality of the cancer.[170]

Currently, most ongoing trials aim to treat all known areas of cancer, although a few aim to treat the index or clinically significant lesions, with surveillance of untreated insignificant lesions.[150]

1.3.2.8 Future research

Focal therapy is gaining interest as a potential treatment for localized PCa. In this rapidly evolving field, there is a need for robust trial designs to evaluate tissue-preserving strategies, so that clinically meaningful outcomes can be presented to physicians and their patients. It is essential to inform, counsel, and present the available data to patients on FT efficacy, its potential benefits and risks, as well as the chance of salvage strategies in case of treatment failure, highlighting the experimental nature of the technique. Ultimately, the patient's preference should have a decisive role in treatment choice.

However, successful adoption of FT relies on optimal patient selection. In this context, further research on imaging and pre-treatment prognostic indicators is necessary, stressing the need for an interdisciplinary scientific collaboration. Advances in imaging technology will allow for the precise and accurate identification, targeting, and eradication of PCa foci.

In addition, incorporation of molecular biology in the selection of PCa patients might be a step forward on the FT path. Development of molecular markers for aggressiveness of individual PCa foci will predict with better accuracy the disease's natural history.[171,172] Proteomic studies are now underway and are expected to identify new prognostic markers.[173,174]

1.3.2.9 Conclusions

Ongoing and future research on FT should be standardized and be part of clinical trials. Only well-constructed clinical trials with long-term follow-up comparing different management strategies for localized PCa will be able to provide all the necessary data to define the position of FT within the urological armamentarium.

1.3.2.10 Level of evidence and grade of recommendation

The ideal cancer characteristics

Ideal cancer grade: No studies available that systematically evaluate cancer grade in the selection of patients for focal therapy.
Level of evidence: 4
Grade of recommendation: C

Ideal cancer volume: No studies available that systematically evaluate cancer volume in the selection of patients for focal therapy.
Level of evidence: 4
Grade of recommendation: C

Multifocality: No studies available that systematically evaluate multifocality in the selection of patients for focal therapy.
Level of evidence: 4
Grade of recommendation: C

Unilateral/bilateral disease: No studies available that systematically evaluate unilateral/bilateral disease in the selection of patients for focal therapy.
Level of evidence: 4
Grade of recommendation: C

1.3.3 Defining the index lesion

1.3.3.1 Introduction

Prostate cancer is one of the major health care problems affecting men. With an estimated incidence of more than 2 million new cases likely to be diagnosed in United States every year, PCa is the most common solid-organ cancer affecting men, and one of the leading causes for cancer-related mortality.[175] The routine use of PSA screening for PCa is often debated, and several countries have adopted various screening strategies. Both formal and informal screening have resulted in a marked increase in PCa detection.[176] Long-term studies have demonstrated a significant downward stage migration associated with this sharp increase in PCa diagnosis.[177,178] The long, indolent natural history makes PCa treatment often perplexing. A proportion of newly diagnosed PCa patients harbour "insignificant disease", and are more likely to live with the cancer without any significant disease progression and health risks. They can be managed with "active surveillance", and any radical treatment is likely to be an "overtreatment".[179–182] However, inaccurate risk stratification into active surveillance can increase risk for potentially missing the window of opportunity for active treatment and cure. At the other end of spectrum, there is a group of patients who will definitely benefit from radical treatment—surgery or radiotherapy. The downside of radical treatment is the associated complications, which are noted even in experienced centres worldwide.[183–186] The transition point between the aforementioned two groups is ill defined, and this is further complicated by the inaccurate prostate imaging and biopsy systems.

Focal therapy is an alternative treatment option that is based on complete ablation of tumour within the prostate, with preservation of normal parenchyma and better preservation of genitourinary functions.[33,187–189] The improved functional outcomes following focal therapy, irrespective of the energy employed, is evident from the published literature. In the wide PCa disease spectrum, the role of focal therapy continues to evolve. In spite of PCa being predominantly a multicentric disease, it is postulated that a specific dominant (large volume) index lesion dictates the biological behaviour of the cancer and subsequent lethality of the disease.[37] The core principle of focal therapy is to accurately define, identify, and focally ablate the index lesion. In this review, we will focus on recent advances in the understanding of the index lesion for prostate cancer, and on the identification methods, controversies, and future direction for research.

1.3.3.2 Methods

An extensive review of the scientific literature concerning Index lesion for prostate cancer was performed. Articles were included that met the criteria set by the International Consultation on Urological Diseases (ICUD), and were classified by level of evidence using the Oxford Centre for Evidence-Based Medicine criteria adapted from the work of the Agency for Health Care Policy and Research as modified for use in previous ICUD projects.

1.3.3.3 Rationale

Multifocality is not a novel phenomenon in solid-organ cancers. Though traditionally multifocal cancers have warranted radical treatment of the affected organ, a better understanding of the cancer biology can permit the focal treatment of only the lethal component, hence preserving the remaining normal tissues and preventing inadvertent injury to the surrounding vital structures. Villers *et al.* from Stanford University evaluated 3 mm–cut sections of 234 radical prostatectomy specimens and

demonstrated the presence of multifocality in PCa with a dominant lesion and additional secondary tumours with normal intervening tissue, hence dismissing the earlier belief of the diffuse nature of prostate cancer.[190] In PCa, the cancer volume and Gleason score had been shown to be significant prognostic factors for cancer-specific survival. D'Amico *et al.* had demonstrated that the percentage of cancer in the biopsy cores was a significant predictor for biochemical recurrence and prostate cancer–specific mortality in patients undergoing radical prostatectomy/radiotherapy.[37,191,192] In a retrospective review of 535 patients who had undergone radical prostatectomy from the Shared Equal Access Regional Cancer Hospital database, Freedland *et al.* demonstrated that the percentage of positive cores and Gleason score from the dominant side of the prostate cancer were better independent predictors and risk stratification tools for PSA recurrence.[193] Cancer volume as an important prognostic indicator is also evident from its incorporation into several predictive nomograms. Similarly, several landmark articles and predictive tools had demonstrated the powerful prognostic importance of primary Gleason score at diagnosis. Tollefson *et al.* demonstrated in 1,688 patients followed up to 10 years that presence of primary Gleason 4 disease adversely affected the biochemical disease–free survival, cancer-specific survival, and systematic recurrence.[194] The Physicians' Health Study and Health Professionals Follow-Up Study reported a 3-fold increase in PCa mortality in patients with primary Gleason 4 cancer compared with Gleason 3 disease. To this date, the Gleason grade remains the single most significant factor in predicting PCa outcomes.[195]

The concept of index lesion is firmly based on the postulate that in a background of multiple cancers within the prostate, the largest lesion is most likely to harbour the lethal clone with the highest Gleason grade and also influences the lethality and metastatic potential of the disease. The congruous location of the large volume and highest Gleason grade had been demonstrated by several authors. Karavitakis *et al.* examined 100 consecutive radical prostatectomy specimens and identified 270 cancerous lesions. Of 170 satellite, secondary lesions identified, 87% were low volume (<0.5 cc) and 99.4% were lower grade (Gleason score 6 or less). Even in specimens with more than 2 cancer foci (25%), none were associated with aggressive disease.[161] Arora *et al.* studied 115 radical prostatectomy specimens between 2000 and 2001 and demonstrated that in a multifocal prostate cancer, the highest grade of Gleason cancer was located within the index lesion in 97% of specimens.[196] Similarly, Wise *et al.* analyzed 3 mm–cut sections of 486 RP specimens from 1992 to 1996 and found unifocal lesions in 17% of the specimens. Among the multifocal lesions, a mean of 2.9 secondary lesions was found with a mean volume of 0.63 cc. The progression-free survival was closely associated with index lesion volume, and the secondary lesion characteristics did not influence the outcome.[197] Another interesting observation by Ohori *et al.* is that in 1,832 RP specimens examined, 92% of the extracapsular extension arose from the index lesion.[369] Moreover, the incidence of unifocal disease reported in the literature is 13–67% and unilateral cancer is 13–63%.

The multifocal tumours within the prostate can be monoclonal or polyclonal. The monoclonal hypothesis states that the transforming event leading to neoplasia originates in one particular cell and spreads by intraprostatic metastasis, while polyclonality arises from a field effect to a common inciting stimulus with several cells undergoing different transforming pathways. Most of the genetic analyses of multicentric prostate cancer suggest a varying pattern of allelic losses on chromosomes, indicating clonal diversity. But monoclonality cannot be ruled out completely, as clonal divergence can result after intraprostatic spread.[198–200] However, in the Project to Eliminate Lethal Prostate Cancer (PELICAN study), Liu *et al.* analyzed 94 metastatic deposits from 30 men who had died from prostate

cancer. Copy number analysis and high-resolution genome-wide single-nucleotide polymorphism were used to demonstrate that metastatic deposits had a monoclonal origin. However, the authors did not trace the anatomic location of the lethal clone within the prostate.[34] These results are in conjunction with the single-locus genetic study evaluating the role of TMPRSS2-ETS in advanced PCa.[201] In spite of tumour heterogeneity in primary cancers, the metastatic clones arose from a single source.

The proof that we currently have represents scrambled pieces of evidence supporting the concept of index lesion, and future research will eventually help to connect the dots. In the present era, researchers strongly doubt "If Gleason 6 cancers are real cancers?",[202] and it is possible that the present-day index lesion of multifocal disease may be the sole, unifocal cancerous lesion of the future.

1.3.3.4 Definition

Index lesion in the background multifocal prostate cancer represents the dominant lesion that will influence the biological behaviour of the disease, which dictates the clinical course and eventual lethality of the cancer. The present evidence suggests that the largest-volume lesion with a multifocal disease is likely to harbour the highest Gleason cancer, both of which are strong prognostic factors in prostate cancer outcome. It is plausible that the most lethal clone that defines the disease progression may inhabit within or in the vicinity of these large-volume lesions but currently we do not have direct evidence.

1.3.3.5 Identification

One of the most challenging points in the history of prostate cancer diagnosis is the accurate identification and characterization of the disease. Over the past decade, tremendous improvement in prostate imaging and guided-biopsy techniques have improved the efficiency of cancer detection. Precise identification of the index lesion involves two crucial processes—imaging and biopsy. These are mutually exclusive, but often complementary processes that can be detrimental in the localization of the index lesion and eventual success of focal therapy.

1.3.3.5.1 Imaging

Multi-parametric magnetic resonance imaging (mpMRI) technology has made significant progress in the past decade and has effectively shifted from being a staging tool to being the most efficient imaging modality for prostate cancer. The high soft-tissue contrast, high resolution, and ability to incorporate functional imaging have enabled mpMRI to overcome several limitations in prostate cancer imaging. Currently, standard mpMRI includes T2-weighted images with diffusion- and perfusion-weighted sequences. Multi-parametric MRI has been demonstrated to detect high-grade and large cancers with high degree of accuracy than other available imaging techniques. Better understanding of MRI principles has resulted in better use of functional sequences to differentiate between low- and intermediate-risk disease. Futterer *et al.* performed a systematic review of the published literature to evaluate the clinical efficiency of mpMRI in identifying clinically significant cancers. The authors identified 12 mpMRI studies and demonstrated an accuracy, sensitivity, and specificity of 44–87%, 58–96%, and 23–87%, respectively, for detecting clinically significant cancers. The diagnosis was confirmed with various biopsy techniques, and heterogeneous definitions were used for defining clinical significance. The most interesting outcome of this analysis was the negative predictive value of the mpMRI, which ranged from between 63% and 98%.[203] Turkbey *et al.* evaluated 135 patients with PCa with mpMRI and subsequent RP and demonstrated excellent correlation between MRI

index tumour volumes and final histopathology.[204] Recently, Tan *et al.* examined 122 PCa patients who underwent mpMRI compared with whole-mount histopathology from RP specimens. Of 285 cancer foci, MRI detected 46.7% and missed 53.3% of the lesions, but with a higher sensitivity for detecting foci more than 1 cm (81.1% vs. 18.9%), GS of 7 or greater (72.7% vs. 27.3%), and index lesions (80.3% vs. 20.8%).[205] One of the limitations of MRI is the possibility of missing high-grade cancers, which varies from 5% to 20% in several centres. Improvement in MRI overall quality, reporting, and experience appears to improve cancer detection by radiologists. Several other promising ultrasound-based imaging adjuncts such as histoscanning, elastography, and contrast-enhanced ultrasound can complement MRI in equivocal cases.[206]

1.3.3.5.2 Biopsy

Conventional, 12-core, bi-sextant biopsy has the inherent limitation of being random, non-targeted, and dependent on chance to hit or miss the index lesion. Hence, we often face the dual challenge of false-negative biopsies and mischaracterization of cancer at biopsy. This results in inappropriate risk stratification, cancer progression during active surveillance, and the finding of insignificant cancer with radical prostatectomy. The success of focal therapy requires precise cancer information from the index lesion as well as reliable biopsy negativity to rule out significant cancers in multiple locations. Several advanced biopsy strategies are often employed to ensure accurate cancer localization.

Template-guided transperineal biopsies

For careful selection of men for focal therapy, transperineal template-guided mapping biopsy (TTMB) offers superior information on the index lesion and can be considered as a gold-standard biopsy technique.[158] The accuracy of TTMB for ruling in or ruling out cancers of ≥0.2 mL or ≥0.5 mL, respectively, is as high as 90–95%.[207] It provides three-dimensional orientation and location of the index lesion, which may be of significant importance for targeted focal therapy. Moreover, TTMB-detected cancers can be classified as significant or insignificant with an accuracy of 95%. Other advantages offered by TTMB are better sampling of the prostate, including the anterior zones with cores oriented along the cranio-caudal direction of the prostate, and reduced infectious complications. The limitations of routine use of TTMB are the need for regional anesthesia, large number of biopsy cores needed to be evaluated per patient, and the increased cost involved. With the routine use of mpMRI, the number of cores can be safely reduced to perform targeted biopsies.[158] Kasivisvanathan *et al.* performed combined transperineal template-guided mapping and MRI suspicious lesions–targeted biopsies in 182 men and demonstrated that detection of clinically significant cancers with transperineal MRI-targeted biopsies was similar to TTMB, with significant reduction in the detection of insignificant cancers.[208] In the present era of mpMRI, transperineal MRI-guided biopsies may offer cancer detection rates close to TTMB.[156]

Image guided–targeted biopsies

Improved imaging characteristics and cancer detection of mpMRI can guide targeted prostate biopsies. Three types of MRI-targeted biopsies exist in clinical practice—cognitive, software fusion, and in-bore techniques. Targeting can be performed through the transperineal or transrectal route. Magnetic resonance imaging–targeted biopsies are promising biopsy strategies that can provide accurate cancer characterization compared with conventional TRUS-guided biopsies. A systematic review of comparison of MRI-ultrasound (MRI-US) software fusion biopsies with standard TRUS biopsies was performed by Schoots *et al.* and Valerio *et al.* The authors demonstrated that the overall cancer

detection rates of targeted and TRUS biopsies were similar. However, MRI-targeted biopsies detected more clinically significant cancer with fewer biopsy cores.[209,210] As mentioned in the previous section, currently we do not have evidence to suggest that transperineal targeting is superior to transrectal-targeted biopsies.

Other ultrasound-based imaging technologies have been shown to provide target for guided biopsies—elastography, histoscanning, and contrast-enhanced ultrasound.[206] The promising results of these novel strategies are in various stages of research, and the exact clinical application will be clear in the future.

1.3.3.6 Controversies

The concept of index lesion has several unanswered questions that can be interpreted as either controversies or missing links in our current understanding.

Several authors have demonstrated the clonal origin of metastatic deposits from non-index lesions. Gburek *et al.* evaluated 12 PCa patients with lymph-node metastasis and showed that the chromosomal abnormalities with the metastatic deposits correspond to only 42% of the index cancers. The fact that chromosomal abnormalities matched the non-index cases is of particular concern.[211,212] Haffner *et al.* elegantly reconstructed the evolutionary pathway of metastatic deposit in a single patient several years after RP. The clone responsible for the metastases had chromosomal alterations in speckle-type POZ protein (SPOP), phosphatase and tensin homologue (PTEN), and tumour protein 53 (TP53). Interestingly, the clonal source localized to a single, small (2.2 mm × 1.3 mm) lesion composed solely of Gleason pattern 3 tumour glands within a large volume of high-grade disease.[213] Whether these anecdotal findings represent a rarer phenomenon or a common event needs to be verified.

The natural history of non-index lesions after successful ablation of index cancer is largely unknown, especially in a younger patient who will have a significant life span after therapy.[36] The multifocality hypothesis suggests a field change in the whole prostatic parenchyma, with certain clonal alterations being lethal. Though focal ablation effectively ablates the index lesion, the remaining parenchyma is being continuously exposed to the original inciting stimulus (androgen). The frequency of *de novo* high-grade cancer in the residual parenchyma or disease progression in secondary foci cannot be currently predicted.

1.3.3.7 Future research

Focal therapy is a promising treatment alternative that is based on the principle of index lesion, and future research in this field should aim at strengthening this concept. Field change and clonal diversity can be over a wide spectrum. The particular inciting stimulus that can cause lethal clone transformation at one foci might produce similar effects of varying degrees in multiple foci. Index lesions may represent the visible large tumour, and there may be many foci of microscopic lethal clone transformations. Researchers should actively look for genetic markers that can indicate the presence of multifocal lethal clones. These markers may eventually be a tool for stratifying the degree of field change within the prostate, and integrating such genetic markers may eventually improve the

patient selection for focal therapy. Moreover, larger studies should confirm the localization of the lethal clone within the index lesion. Uniform protocol and reporting of follow-up for focal therapy will eventually describe the fate of non-index lesions within the residual prostate.

1.3.3.8 Level of evidence and grade of recommendation

The topic of the index lesion is of importance for focal therapy of prostate cancer, but is of strategic or theoretical importance only. Therefore, no level of evidence is applicable and no recommendation can be given.

Level of evidence: Not Applicable
Grade of recommendation: Not Applicable

1.4 Alternatives to Focal Therapy

1.4.1 Active surveillance

1.4.1.1 Abstract

1.4.1.1.1 Objective

We present a summary of the Societé Internationale D'Urologie (SIU)–ICUD (SIU-ICUD) Joint Consultation on active surveillance recommendations in prostate cancer.

1.4.1.1.2 Materials and Methods

We performed a systematic review of the literature in July 2015 according to Preferred Reporting Items for Systematic Reviews and Meta-Analyses (PRISMA) guidelines. Primary endpoint was oncologic outcome (treatment-free survival, and disease-specific and all-cause mortality). Only 18 articles met the selection criteria, representing nine prospective or large retrospective cohort studies. For secondary endpoints, a comprehensive review was performed.

1.4.1.1.3 Results

Low-risk PCa patients who are amenable to AS usually are at least identified on clinical stage (T1-T2), Gleason score 6 on biopsy, and PSA level <10 ng/mL. Expanding active surveillance to intermediate-risk patients might be proposed in men with comorbidity and/or a short life expectancy. Magnetic resonance imaging–targeted biopsies reduce the risk for initial reclassification. Monitoring depends on regular clinical examination and PSA tests, and on control biopsies at variable intervals. Early confirmatory biopsy is optional. Progression to Gleason score 7 cancer on re-biopsy was the most widely used criterion for active treatment. The use of PSA kinetics and tumour volume increases, as triggers for active intervention are debatable. The active treatment rate ranged from 12% to 42.5%. The probability of a patient remaining on AS at 5 years ranged from 59% to 67%. No prostate cancer death was reported at 5-year follow-up. The 10-year overall survival rate varied from 80% to 98% among series. The main limitations were the absence of long-term follow-up and the lack of RCTs comparing AS with immediate active treatment.

1.4.1.1.4 Conclusion

Active surveillance with definitive treatment in the case of progression is safe and demonstrates favourable oncologic outcomes in low-risk prostate cancer patients. Randomized controlled trials are awaited to definitively provide the highest level of evidence. A standardized evidence-based protocol for patient selection and monitoring cannot be strictly recommended due to strong discrepancies between series. Future patient selection should be based on a multivariable approach for risk stratification incorporating not only widely used clinical and biopsy features, but also MRI findings and potential prognostic biomarkers.

1.4.1.2 Introduction

Management of low-risk PCa patients has thoroughly evolved over the last decades. Prostate cancer screening harms in terms of overdiagnosis and overtreatment, which have modified the PCa treatment paradigm. Randomized controlled trials of observation versus radical treatment have demonstrated that immediate active treatment could be a safe management option in low-risk PCa patients.[214,215] Active surveillance entails a strategy by which selected men are managed expectantly with the intention to apply potentially curative treatment in the case of signs of progression. This active management implies a close monitoring of patients during follow-up, and thereby is quite different from pure observation or watchful waiting. To date, AS is widely used for and integrated into various international guidelines.[216,217] Population-based studies have confirmed an increase in noncurative initial management in patients with low-risk PCa.[218] However, although some randomized trials are ongoing, no results from any controlled study are yet available to compare immediate treatment with active surveillance.[219,220]

1.4.1.3 Materials and Methods

We performed a systematic review of the literature up to July 2015 using the PubMed, Web of Science, and Embase databases according to the PRISMA guidelines. The search results were restricted to the English language with a 10-year limit. Keywords used were “active surveillance”, “watchful waiting”, “conservative management”, “expectant management”, “observation”, and “prostate cancer”. Additional references were identified from the reference list of each article. The study selection process is shown in the PRISMA diagram (**Figure 1-1**).

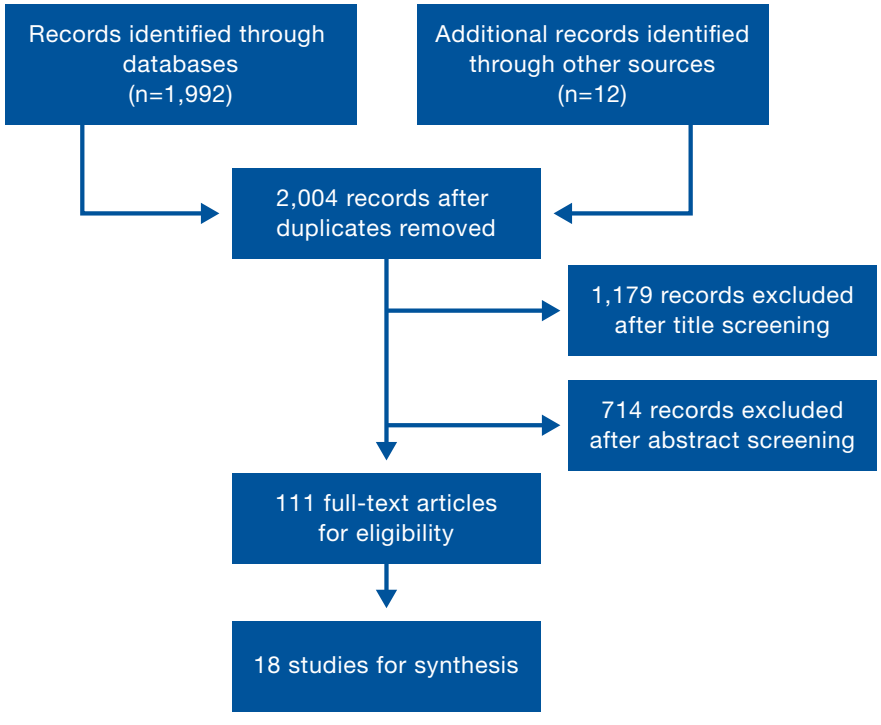

FIGURE 1-1
Preferred Reporting Items for Systematic Reviews and Meta-Analyses (PRISMA) Flowchart for Primary Endpoint (oncologic outcomes).

Primary endpoints were oncologic outcomes, defined as treatment-free survival, disease-specific mortality, and all-cause mortality. For such endpoints, systematic reviews, meta-analysis of RCTs, RCTs, and prospective non-randomized cohort studies were selected. The initial search resulted in 2,004 citations after removal of duplicates. After initial title screening, 825 references remained. After removal for not meeting inclusion criteria, full-text screening for the remaining 111 references was performed. Only 18 articles met the selection criteria, representing nine prospective or large retrospective cohort studies. For secondary endpoints, we performed a comprehensive review including preferentially recent articles and systematic reviews.

The evidence available was analyzed using the SIU-corrected Oxford method of assigning the levels of evidence, and summary recommendations based on these levels of evidence were graded and summarized in a dedicated table.[55]

1.4.1.4 Results

1.4.1.4.1 Criteria used for selection and deferred intervention

Patient selection for AS is of great importance, and is aimed at reducing overtreatment without missing aggressive disease. Low-risk PCa patients who are amenable to AS usually are at least identified on well-identified prognostic parameters: clinical stage, Gleason score at biopsy, and PSA level. The most common clinical data used to define low-risk PCa are a GS ≤6, PSA ≤10 ng/mL, and a clinical stage T1c-T2 disease, described by d'Amico *et al.*[221] However, published AS series used different criteria largely based on centre experiences and preferences, with no hard data (**Table 1-4**). The first criteria for insignificant/low-risk PCa were described by Epstein in 1994, updated in 2004, and used as AS selection criteria in some AS protocols.[181,222–224] Nevertheless, this definition is debatable.[225] Moreover, the use of stringent criteria for AS inclusion limit the number of patients offered surveillance. Thus, various series applied larger criteria.[225,226] In addition, some series enrolled men with more restrictive criteria, taking into account PSA density PSAD, PSA/prostate volume),[222,227] number of positive cores,[222,223,227–229] and maximal percent of involvement in any core[223,229,230] in order to reduce the risks for misclassification and progression. Given these discrepancies, no strict AS selection criteria for low-risk PCa can be recommended. After AS initiation, monitoring mainly depended on clinical examination and PSA tests every 3 to 6 months, and on control biopsies at variable intervals. Early confirmatory biopsy within the first 3 months after the diagnosis is optional. Most protocols recommended the first re-biopsy within the first 18 months. The subsequent interval varied from an annual to a 3-year one. Defining the ideal triggers for intervention remains difficult due to the absence of both long-term follow-up and identification of factors predictive for cancer-specific mortality. The definition of progression varied among AS series (**Table 1-4**). All AS series considered the presence of a Gleason score 7 cancer on biopsy as a strict criterion for progression. Discrepancies existed among studies regarding the increases of Gleason score 6 tumour volume or the PSA kinetics as a criterion for progression. Comparisons between series are difficult given that the progression-free survival highly depends on the criteria used to define progression and/or deferred treatment. The 3-year pathological progression rate was 48% in the observation arm of the REduction by Dutasteride of clinical progression Events in Expectant Management (REDEEM) trial.[230] The Johns Hopkins University series has demonstrated that the rate of biopsy reclassification was 8.9 per 100 person-years of follow-up when taking into account all biopsy reclassification and PSA kinetics, but only 4.0 per 100 person-years when considering the Gleason score upgrading.[222]

The use of PSA kinetics as a trigger for active intervention is debatable and not systematically assessed in AS protocols.[10] Prostate-specific antigen doubling time (PSADT) has been suggested as a trigger for deferred treatment, as men with a PSADT <3 years had an 8.5-fold increased risk for PSA progression after definitive treatment compared with men with longer PSADT.[227] Prostate-specific antigen velocity has been suggested to be more predictive for progression than PSADT.[228,231] Nevertheless, the University of Toronto protocol withdrew this factor as a criterion for intervention in 2009 given the lack of predictive value for outcomes.[226] Moreover, findings from the University of California, San Francisco (UCSF) and the Johns Hopkins University cohorts did not show any correlation between PSADT and biopsy progression or adverse pathology in radical prostatectomy specimens.[232,233] In series taking into account PSA kinetics as a trigger for intervention, active treatment was decided because of biopsy progression/reclassification in 30–79% of cases and because of PSA kinetics (doubling time, velocity) in 18–44% of cases.

TABLE 1-4 Active Surveillance Protocols and Follow-Up in Selected Articles

	N	Centre	Entry criteria	Monitoring	Progression	Follow-Up
University of Toronto	993	Single	GS 6 and PSA <10 OR GS 3+4 and PSA <20 and LE <10 y	DRE+PSA/3 mo 2 y then/6 mo Biopsy within 1 y then/3 – 4 y	PSADT <3 y (until 2009) Biopsy upgrading Clinical progression	6.4 y (0.2–19.8)
UCSF	321	Single	T1-T2 PSA <10 GS 6 <33% cores	DRE+PSA/3–6 mo Biopsy /1 – 2 y	PSAV >0.75 Biopsy upgrading	3.6 y
PRIAS	2494	Multicentre	T1/T2 PSA <10 PSAD <0.2 GS 6 1 or 2 cores	DRE+PSA/3 mo 2 y then /6 mo Biopsy 1 y – 4 y – 7 y	PSADT <3y Biopsy upgrading Biopsy progression	1.6 y
Göteborg	341	Single	T1 GS 6 PSA <10*	DRE+PSA/3 – 6 mo Biopsy within 3 y	PSA Biopsy upgrading Biopsy progression	6.0 y
Beaumont Hospital	80	Single	T1 GS 6 PSA <10 1 or 2 unilateral cores <50%/core	DRE+PSA/3 mo – 1 y then/4 mo – 2 y then/6 mo MRI within 6 mo Biopsy 1 y – 3 y – 6 y	PSADT <3y Biopsy upgrading Biopsy progression Clinical progression	3.1 y
University of Miami	230	Single	T1-T2 GS 6 PSA <10 1 or 2 cores <20%/core	DRE+PSA/3 – 4 mo – 2 y then/6 mo Biopsy within 1 y then/1 y	Biopsy upgrading Biopsy progression	2.7 y
Royal Marsden Hospital	471	Single	T1-T2 PSA <15 <50% cores GS 6 OR GS 3+4 if >65 y	DRE+PSA/3 mo – 1 y then/4 mo – 1 y then/6 mo Biopsy 1 y – 3 y – 5 y	PSAV >1 Biopsy upgrading Biopsy progression	5.7 y
Johns Hopkins University	769	Single	T1 PSAD <0.15 GS 6 1 or 2 cores <50%/core	DRE+PSA/6mo Biopsy/1 y	Biopsy upgrading Biopsy progression	2.7 y

*For the majority of the cohort (92 intermediate-risk PCa and 6 high-risk PCa patients also included).

Abbreviations: PRIAS, Prostate Cancer Research International Active Surveillance study; REDEEM, REduction by Dutasteride of clinical progression Events in Expectant Management study; UCSF, University of California, San Francisco.

GS, Gleason score; DRE, digital rectal examination; LE, life expectancy; mo, months; PSA, prostate-specific antigen; PSAD, PSA density; PSADT, PSA doubling time; PSAV, PSA velocity; y, years; /, every.

continued on **page 46**

TABLE 1-4 Active Surveillance Protocols and Follow-Up in Selected Articles, *Cont'd*

	N	Centre	Entry criteria	Monitoring	Progression	Follow-Up
REDEEM	155	Multicentre	T1-T2 GS 6 PSA <11 1–3 cores <50%/core	PSA/3 mo – 1 y then /6 mo DRE 18 mo – 3 y Biopsy 18 mo – 3 y	Biopsy upgrading Biopsy progression	2.7 y

*For the majority of the cohort (92 intermediate-risk PCa and 6 high-risk PCa patients also included).

Abbreviations: PRIAS, Prostate Cancer Research International Active Surveillance study; REDEEM, REduction by Dutasteride of clinical progression Events in Expectant Management study; UCSF, University of California, San Francisco.

GS, Gleason score; DRE, digital rectal examination; LE, life expectancy; mo, months; PSA, prostate-specific antigen; PSAD, PSA density; PSADT, PSA doubling time; PSAV, PSA velocity; y, years; /, every.

1.4.1.4.2 Treatment-free survival, disease-specific mortality, and all-cause mortality

Only 18 articles met the selection criteria, representing nine prospective or large retrospective cohort studies (**Table 1-5**).[150,222,223,226–230,234–245] All these series were uni- or multicentre cohorts. The paper by Fleshner *et al.* reported results from one observation arm derived from an RCT.[230] Large retrospective series were also analyzed (but not included in the evidence synthesis) and confirmed findings from prospective protocols.[243,244,246] Overall, 5,854 men have been followed by AS. Median follow-up after AS initiation varied from 1.6 to 6.4 years. The largest study was the multicentre Prostate Cancer Research International Active Surveillance (PRIAS) study enrolling 2,495 patients in 17 countries. The longest follow-up has been reported in the University of Toronto study.[226] Median follow-up from the first biopsy was 6.4 years. Overall, 993 patients were included, and 844 were alive at analysis time. Of 149 deaths, only 15 were attributable to prostate cancer. The 10- and 15-year overall survival rates were 80% and 62%, respectively. The actuarial cancer-specific survival rates were 98.1% and 94.3%, respectively. The cumulative hazard ratio for nonprostate-to-prostate cancer mortality was 9.2:1. Metastasis disease occurred in 28 patients (2.8%), and median time to metastasis was 7.3 years. Twenty-seven percent of patients underwent intervention. The 5-, 10-, and 15-year treatment-survival rates were 75.7%, 63.5%, and 55%, respectively. In other AS protocols, the active treatment rate ranged from 12% to 42.5%. The probability of a patient remaining on AS at 5 years ranged from 59% to 67%.[222,229] Median time to active treatment ranged from 1.2 to 3 years.[222,227,240] Loeb *et al.* recently published a 5-year, nationwide, follow-up study involving 1,729 low-risk to intermediate-risk PCa men choosing active surveillance in Sweden.[247] Sixty-four percent of men remained on AS after 5 years, in line with rates published in prospective cohorts. In all cohorts, no prostate cancer death was reported at 5-year follow-up. The 10-year overall survival rate varied from 80% to 98% among series. Overall, oncologic outcomes were comparable between series, despite differences between cohorts in patient selection and monitoring.

1.4.1.4.3 Outcomes from control biopsy and deferred radical treatment

One major limitation of AS is that a significant proportion of low-risk PCa patients harbours a more aggressive disease. Radical prostatectomy series in men with low-risk PCa eligible for AS according to very low–risk criteria have shown a rate of approximately 20–35% of higher-grade and/or non-organ-confined disease at final pathology.[248,249] Findings from immediate re-biopsies before AS inclusion also demonstrated a non-negligible rate of reclassification due to biopsy sampling error.[250–252]

Control biopsies during AS monitoring showed a consistent rate of 25–35% of biopsy reclassification due to GS upgrading or volume increase.[222,223,227,230,253,254] This rate was stable between the first and the second re-biopsy assessment.[228,230,253] In the University of Toronto series, the overall rate of GS upgrading over time was 31%.[255] The University of Miami series, which used the strictest selection criteria, reported the lowest rate of biopsy reclassification (4%).[240] The repeat biopsy data from the Royal Marsden Hospital protocol demonstrated a 12% rate of adverse pathology. However, a GS 3+4 was not considered as a biopsy progression criterion.[228]

TABLE 1-5 Repeat Biopsy and Oncologic Outcomes in Selected Articles

	Active treatment rate	CSS	OS	Intervention reasons	Lost to follow-up
University of Toronto	27%	10 y: 98.1%	10 y: 80%	PSADT 44% Upgrading 35% Patient 6% Upstaging 5%	2.5%
UCSF	24%	100%	10 y: 98%	PSAV 31% Upgrading 39.5% Patient 29%	NR
PRIAS	21.1%	100%	4 y: 86.5%	PSADT 21% Upgrading 41% Patient 9% Upstaging 38%	1.7%
Göteborg	36.9%	5 y: 100%	10 y: 81.1%	PSA 27.7% Upgrading/ staging 47.5% Patient 5%	NR
Beaumont Hospital	42.5%	100%	NR	PSA 18% Upgrading/ staging 68% MRI progression 12%	NR
University of Miami	14%	NR	NR	NR	NR
Royal Marsden Hospital	31.4%	8 y: 98%	8 y: 91%	PSAV 40.9% Upgrading/ staging 30% Patient 29%	NR
Johns Hopkins University	33.2%	100%	98.2%	Upgrading 45.1% Upstaging 54.9%	10.7%
REDEEM	12.2%	NR	NR	NR	NR

Abbreviations: PRIAS, Prostate Cancer Research International Active Surveillance study; REDEEM, REduction by Dutasteride of clinical progression Events in Expectant Management study; UCSF, University of California, San Francisco.

CSS, cancer-specific survival; OS, overall survival; PSA, prostate-specific antigen; PSADT, PSA doubling time; PSAV, PSA velocity; NR, not reported; y, years.

It's worthy to note that many cases of progression are likely better described as disease reclassification, especially during the early periods of AS. Indeed, a recent conditional survival analysis from Johns Hopkins University highlighted that the risk for reclassification significantly decreased with time beyond 2 years due to misclassification at diagnosis.[256] Does delayed radical prostatectomy after an initial surveillance lead to poorer oncologic outcomes compared with immediate prostatectomy? Radical prostatectomy results in men initially followed on AS showed organ-confined and favourable GS in a majority of cases. The rate of GS 7 or more and/or non-organ-confined PCa at final pathology after deferred radical prostatectomy ranged from 38% to 71%.[228,240,257,258] Analysis from the final pathology in 167 men included in the PRIAS study demonstrated a pT3-4 and/or GS 4+3 disease in 30% of cases.[257] There is no strong data available to compare oncologic outcomes between low-risk PCa men undergoing immediate or delayed radical prostatectomy.[259] Matched comparisons have suggested that the rate of adverse pathology did not differ between immediate and delayed radical prostatectomy patients.[260–262] However, such an assessment in prospective low-risk PCa management trials is needed. The impact of lifestyle intervention and dietary modification on AS outcomes remains unclear.[263,264] A high-quality RCT demonstrated a benefit for daily dutasteride in men undergoing AS in terms of disease reclassification after 3 years of follow-up (HR, 0.62; 95% CI, 0.43–0.89; p=0.009).[230] However, no difference between groups in survival rates has been reported and follow-up was short. Attention should be paid regarding the possible increased risk for high-grade PCa by 5-alpha-reductase inhibitor (5-ARI) use (US FDA issued a drug safety communication in 2011).[367]

1.4.1.4.4 Low-risk PCa selection improvement

MRI-targeted biopsies

Many studies have assessed the use of MRI in AS cohorts, although none considered MRI findings as inclusion or deferred treatment criteria.[265,266] The University of California, San Francisco (UCSF) and Royal Marsden Hospital AS cohorts were the first to retrospectively assess the role of MRI as a selection and monitoring tool.[267,268] Whereas the "visible" parameter of the lesion in T2-weighted imaging is not enough to better select low-risk PCa patients, multi-parametric imaging analysis, including contrast enhancement and diffusion-weighted sequences, seems to improve clinically significant PCa detection.[268–270] At diagnosis, the main role of MRI should be to guide targeted biopsies on suspicious lesions, and thereby, to reduce the risk for initial misclassification. In a recent systematic review of the literature, Schoots *et al.* showed that MRI-targeted biopsies or radical prostatectomy histopathology in MRI-positive cases resulted in reclassification in 30–50% of cases.[265] Most studies evaluating the correlation between MRI-targeted biopsies, adverse pathology at repeat biopsies, and progression supported the impact of MRI at diagnosis and during follow-up.[267,269–274] In a recent prospective series of 72 patients on AS, MRI-targeted biopsy was 6-fold more likely to yield a GS 7 or more cancer compared with standard biopsies.[271] Hu *et al.* evaluated MRI grading in relation to reclassification and found a significant risk for unfavourable disease at re-biopsy in the case of lesions classified as 4 or 5 by MRI.[273] Regarding the role of MRI as a monitoring tool, to date no strong data support the use of MRI in place of repeat biopsy for detecting progression. To summarize, MRI may be of great interest in AS, both as a reclassification and monitoring tool. Nevertheless, the level of evidence is limited by the relatively small number of studies and clear lack of standardization.[265] It remains unclear whether MRI should be done on all patients. Prospective studies are critically needed.

Biopsy characteristics

The overall tumour burden in diagnosis biopsy has proven to be predictive for disease progression or the probability of remaining on AS.[275] Thus, detailed biopsy parameters may be helpful in stratifying patients at very low risk and at low risk.[266,276–279] The use of stringent biopsy criteria for AS inclusion has reduced the risk for misclassification, but also limited the number of patients offered surveillance. The sampling error might reduce the risk of missing an aggressive component. The 12-core extended scheme was the recommended biopsy protocol used in most AS series. Some authors have suggested that the risk for initial reclassification might be reduced by the use of more extended biopsy schemes, of template transperineal biopsies, and of transition zone cores.[250,280–283] Nevertheless, no prospective comparison has been performed.

Clinical factors: age, race, obesity, familial history

Some studies showed a correlation between age and unfavourable disease.[284] Thus, age has been assessed for predicting AS progression.[226,227,230,285] Older patients may have poorer oncologic outcomes with surveillance.[286] However, results remain debatable, and differences could be explained by higher all-cause mortality in the elderly. The median age of men in the University of Toronto series was higher than that in the other series.[226] No strong difference in terms of cancer-specific survival was established. However, the all-cause mortality was superior in that series.

Obesity and race have also been suggested as risk factors for reclassification.[287–290] Data regarding familial history are limited.[291] To improve patient selection, nomograms have been developed incorporating all the potential risk factors for reclassification or progression.[292,293] External and/or prospective validation is necessary before routine clinical use.

Biomarkers: PCA3, PSA derivatives, genomic scores

Future efforts are also focused on the development of new biomarkers that can improve PCa aggressiveness prediction and provide independent prognostic value, in addition to current parameters such as Gleason score.[266,275] Prostate-specific antigen derivatives such as %fPSA, [-2]proPSA, and the combined PHI tests demonstrated correlations with unfavourable pathology.[91] In the prospective cohort from Johns Hopkins University, these PSA derivatives have been associated with biopsy reclassification and upgrading.[136,294] Baseline and longitudinal values of %fPSA, [-2]proPSA, and PHI tests were assessed. These findings have been confirmed in a Japanese, prospective, 1-year, follow-up study.[137]

Urinary biomarkers such as PCA3 and TMPRSS2:ERG scores may help in predicting high-grade disease. Prostate cancer gene 3 score has demonstrated to be predictive for insignificant, low-volume, and low-grade PCa.[76,79] Nevertheless, PCA3 score had proven poor discrimination for predicting progression and biopsy reclassification in a prospective AS cohort.[295] In another retrospective AS series, both PCA3 and TMPRSS2:ERG scores were significantly associated with higher-volume disease.[296] Median PCA3 and TMPRSS2:ERG scores increased incrementally with the number of positive cores at re-biopsy. However, no multivariable analysis has proven their independent value in addition to clinicopathological parameters. Few studies have investigated potential tissue markers.[294,297] From a prospectively maintained database including 265 patients followed on AS, Berg *et al.* showed that ERG positivity was a significant predictor for overall AS progression in multivariable analysis.[297]

Genomic scores have been evaluated in biopsy and radical prostatectomy cohorts. No data is available in AS cohorts to draw any strong conclusion regarding the clinical utility of genomic scores. Single-nucleotide polymorphisms in PCa risk have been assessed in the Royal Marsden Hospital AS cohort.[291] No relationship between the calculated genetic risk scores and adverse histology or time to treatment was reported.

1.4.1.4.5 Expanding AS to intermediate-risk PCa

The safety of expanding AS to intermediate-risk PCa patients is debatable. Evidence supports the heterogeneity of the intermediate-risk group as defined by d'Amico *et al.* Recent studies in men undergoing radical treatment such as radical prostatectomy, brachytherapy, or external beam radiotherapy have suggested that men with low-risk and favourable intermediate-risk PCa have similarly low estimates of biochemical recurrence–free and PCa-specific–free survival.[298–300] Intermediate-risk PCa patients defined by a PSA >10 ng/mL and/or a Gleason score 3+4, provided they were older than 65 years or had a life expectancy <10 years, have been included in both the University of Toronto and Royal Marsden Hospital AS cohorts with favourable oncologic outcomes.[226,228] Data from intermediate-risk PCa men (based on the Cancer of the Prostate Risk Assessment [CAPRA] score) included in the UCSF cohort were analyzed in a separate article.[238] The overall rate of active treatment (32%) as well as the upgrading rate at re-biopsies (30–35%) did not differ from those for low-risk PCa patients. Progression-free survival was 60% at 4 years. Nevertheless, the upstaging rate at final pathology in men undergoing delayed radical prostatectomy was higher in the intermediate-risk cohort: 50% versus 28%. van den Bergh *et al.* published similar oncologic outcomes in a cohort of 50 Gleason score 7 screen–detected PCa.[301] In a 5-year, Swedish, nationwide, follow-up study, the 5-year probability of discontinuing AS was 41% in intermediate-risk PCa patients compared with 34% in both very low–risk and low-risk PCa men.[247] Outcomes of patients with screen-detected localized prostate cancer (European Randomized Study of Screening for Prostate Cancer [ERSPC] trial) who initially elected to withhold radical treatment showed that the 10-year PCa-specific survival rates were comparable for low- and intermediate-risk patients, whereas overall survival rates (79.0% vs. 64.5%; p=0.003) were significantly different.[302]

Advances in imaging and prognostic biomarker development are awaited to better distinguish the ideal subgroup of intermediate-risk PCa men harbouring favourable disease given the large heterogeneity of widely used d'Amico risk groups.

1.4.1.5 Conclusions

Level 1 evidence is still lacking to confirm the safety of active surveillance as compared to immediate active treatment (**Table 1-6**). Thus, some of the evidence for such an approach comes from trials assessing radical treatment with observation. Large prospective cohorts demonstrated safe and favourable oncologic outcomes in low-risk PCa patients while waiting results from ongoing RCTs. Active treatment is recommended in the case of disease progression. A standardized evidence-based protocol for patient selection and monitoring cannot be recommended. Expanding active surveillance to intermediate-risk patients might be proposed in men with comorbidity and/or a short life expectancy. Future patient selection should be based on a multivariable approach for risk stratification incorporating not only widely used clinical and biopsy features, but also MRI findings and potential prognostic biomarkers.

TABLE 1-6 Level of Evidence and Grade of Recommendation

	Level of Evidence	Grade of Recommendation
Active surveillance is a recommended management option in low-risk PCa patients.	2	B
Eligibility for AS is based on clinical parameters, PSA-based criteria, and 12-core biopsy features.	2	B
Active surveillance might be an option in intermediate-risk PCa men, especially in those with comorbidity and/or a short life expectancy.	3	C
Deferred radical treatment after initial AS management does not lead to worse oncologic results than immediate treatment.	3	C
Monitoring is based on regular clinical examination, and PSA tests, every 3–6 months.	2	B
Control biopsy is scheduled within the first 18 months.	2	B
Progression is defined by Gleason score 7 or more on control biopsies.	2	B
Progression may be defined by significant increases of Gleason score 6, volume, and/or by PSA kinetics (PSADT, PSAV).	3	C
Active treatment is recommended in the case of progression.	2	B
Biomarkers may help in AS selection.	4	C
Magnetic resonance imaging plus targeted biopsies reduces the risk for reclassification at diagnosis.	3	B
Magnetic resonance imaging may help in AS monitoring.	4	C
Daily dutasteride reduces the risk for short-term disease reclassification.	2	B

Abbreviations: AS, active surveillance; PCa, prostate cancer; PSA, prostate-specific antigen; PSADT, PSA doubling time; PSAV, PSA velocity.

1.4.2 Prostatectomy

1.4.2.1 Abstract

1.4.2.1.1 Objective

Provide a summary of the SIU-ICUD Joint Consultation on Focal Therapy on the current indications for definitive treatment by means of radical prostatectomy.

1.4.2.1.2 Materials and Methods

Given the pervasive nature of cancer, traditional teaching would and should focus on the fundamental outcome measure: all-cause and cancer-specific survival. However, such a narrow view would be both irrelevant and unfair for newly diagnosed prostate cancer patients and for individualized or tailored cancer management. Furthermore, we can strongly argue that a vision of "prostate cancer" survival often triggers decision making on the profound bias elicited by fear of death, which triggers focusing on the second word "cancer" while completely overlooking the first word "prostate". For this work, we focused on a rather holistic outcome: quality of life coupled with all-cause survival, and how surgery could impact outcomes positively. Such a paradigm settles cancer-specific survival in a more certain probability realm of how much you are willing to lose in life span by living the way you want to live, decreasing the odds of regret. We dwell on secondary outcomes from intervention in the path of cancer survival. To meet our goal, a systematic review of the prostate cancer literature was conducted in September 2015 following PRISMA guidelines. From an initial denominator of 957 references, 115 met selection criteria, 78 of these represented clinical trials, and 37 came from robust series. We then focused on the primary outcomes: overall and cancer survival, functional outcomes, and regret; 53 references fulfilled this work.

1.4.2.1.3 Results

Men aged <65 years with PSA levels >10 ng/mL and a life expectancy of 10 years or more are the ones best suited for radical prostatectomy, as this modality offers substantial benefits in all-cause and cancer-specific survival. Prostate cancer treatment–naïve men 70 years or older are the least likely to benefit from radical prostatectomy, as the surgery would have minimal impact on survival and a deleterious effect on functional outcomes. In addition, there is little role for surgery for men harbouring low-risk disease. The most well-structured studies are consistent on adverse event rates for urinary and sexual dysfunction problems in 22% and 40–50% of patients, respectively, after radical surgery. The rate of regret of radical prostatectomy is significant at 10–25%. Regret is associated with adverse urinary and sexual function outcomes and does not improve over time. Robotic radical prostatectomy has become the approach of choice, because of QOL improvements in the short run (blood loss, risks of transfusion, pain, catheter times, and post-operative recovery). The robotic approach has led to several randomized trials evaluating several aspects of the technique, and has generated level 1b evidence for short-term continence outcomes—a 73% (0 or 1 pad per day) rate for men 13 to 15 weeks after robotic radical prostatectomy. Long-term oncologic control with the robotic approach appears to be equivalent, but there are no randomized controlled data like for open radical prostatectomy. The rate of regret for both procedures is statistically equivalent.

1.4.2.1.4 Conclusion

By end of 2015, there is level 1 evidence pointing for sound counselling of radical prostatectomy. The best candidates are patients aged <65 years and with a PSA >10 ng/mL. Surgery should not be the first option for any man aged >70 years with low-risk disease. The paradox of improved survival for younger-aged men and less probability of deleterious QOL (urinary and sexual function) outcomes, other than lack of ejaculation, sets it as the preferred choice for younger men. However, the number needed to treat (NNT) associated with regret after radical prostatectomy ranges from between 4 and 8. That is unacceptable and must be addressed pre-operatively to set expectations right. The robotic approach as the means for this treatment modality is being investigated in numerous clinical trials, providing encouraging results for this procedure. The penetration in and adoption of focal therapy for different types of patients will change the eligibility spectrum for radical prostatectomy, but unlike its empirical past, radical prostatectomy is the standard of care for specific set of patients until a newly emerging modality surpasses it.

1.4.2.2 Introduction

This century has already proven transcendent for radical prostatectomy:

1. It confronted its quackery history with level 1 evidence showing when and for whom this operation may be necessary.
2. It ended the relevance of decades-long debates between perineal ("original prostatectomy approach") and retropubic open RP.
3. Notwithstanding the emergence and marketing-driven exponential surge and criticism of robotic RP, the procedure is serving a new wave of clinical trials evaluating aspects of the surgical technique and critical outcomes.

To date, only one evidence-based, multi-institutional trial assessed the transcendent urinary function outcome after robotic RP, changing the paradigm of prostate cancer management, as answers to the formidable screening and treatment in RCTs highlighted the slow progressive natural history of prostate cancer. In this final aspect, the deleterious impact of surgery (open or robotic) on QOL was not a surprise; however, the limited impact of RP on all-cause survival was. In this century, the generosity of knowledge derived by copious research performed all over the world does not end there. Innovations in information technology (IT) continue to provide for unprecedented speed in knowledge exchange and dissemination of research results, contributing to an enhanced understanding of this prevalent disease.

The tremendous incremental impact of imaging technology, specifically the emergence of multiparametric MRI (mpMRI), of the prostate has created a powerful tool to walk that line between active surveillance and radical surgery.[303] Accurate mpMRI should provide "GPS-like information" on the prostate. This comes at a critical time when overtreatment takes the main stage, fueled by evidence-based data that points failure to fulfill our *primum non nocere* duty when managing prostate cancer in a significant number of newly diagnosed men.

The objective of this work is clear: to provide a complete and current perspective on focal therapy, a novel likely transcendent management option for prostate cancer patients. Its role will be propelled by this newly found—albeit imperfect[304]—GPS-like knowledge from mp-MRI fusion biopsy that shall continue to improve.[303,304] But as of now, it's good enough to serve as a gateway for focal management of prostate cancer. We strongly believe that this management strategy will achieve the *primum non nocere* intent, if not forever, for a significant time, and moreover, it will differentiate prostate cancers by their phenotype by challenging cancers to prove their aggressiveness. Our duty will be to produce factual research, demoting speculation and educating oncologists and their patients regarding who is best suited for focal therapy. A humble reflection from the evidence generated by the RP versus observation randomized trials leads us to recognize that we overestimated the positive impact of surgery for men with prostate cancer—at best, the magnitude is much smaller than previously thought. The worst outcome we can foresee in men treated with focal therapy is to experience progression and loss of life because the opted management choice was the wrong one. Invariably this will happen; but time and structured research shall render answers to minimize or eliminate such tragedies. In the meantime, this work aims to deliver evidence-based answers to the following questions:

1. Who is likely to be at risk for significant changes in QOL from RP for a real benefit in survival?
2. What are the evidence-based functional outcomes after RP?
3. Regret after RP—how common is it, and what influences this undesirable event?
4. Candidates for RP in the focal therapy era—how, and why yes or no?

1.4.2.3 Materials and methods

A systematic review of the prostate cancer literature was conducted in September 2015 following the directions for this work based on PRISMA guidelines.[305] We queried PubMed (pubmed.com), and restricted the information to English-written papers and excluded reviews. The ensuing elements *prostate cancer randomized clinical trial or multi-institutional series AND radical prostatectomy* were required for all searches. We then added *AND followed by* any of the following*: Robotic, Robotic-assisted, RALP, RARP, complications, adverse events, incontinence, erections, erectile dysfunction, impotence, strictures, regret, trifecta, recurrence, biochemical failure, salvage, metastasis, cancer survival, survival and outcomes.*

Our PRISMA search workflow was as follows. From an initial search of 957 citations, we filtered out 63 non-English papers, and were left with 876 articles. From these, we excluded 160 reviews, 10 systematic reviews, 2 practice guidelines, and 9 personal communications. Of the 695 references that remained, 551 were clinical trials, 16 meta-analyses, and 99 series. For 193 of these, a free full text was available. We then crossed the 695 references to the individual eligible terms, removed duplicates, and ended up with 115 studies that met the selection criteria, of which 74 were clinical trials and 37 were series. Free full text was available for 28 of these references. We then focused on the primary outcomes overall and cancer survival, functional outcomes, and regret, and obtained 53 references that fulfilled these criteria.

1.4.2.4 Results

1.4.2.4.1 Oncologic outcomes of radical prostatectomy

Radical prostatectomy has been one of those entropic procedures that has fascinated the urological field.[142,144,214,215,221,306–311] Indeed, it is a rich source for debate fed by a wealth of perspectives on its derived outcomes, its impact on the natural history of the disease, its indications, its sequence as part of treatment and, importantly, on how it should be conducted. Most would agree that bias has served as its fundamental source of entropy and like many things in life, how you tell a story can be more captivating than the story itself. Hard randomized data that compares treatment arms or management approaches was elusive. In fact, it took a century of data (100 years!) from the initial series presented and published by Hugh H. Young.[312] treating 10 men with the perineal approach to the initial results from the non-PSA era—Scandinavian Prostate Cancer Group Number 4 (SPCG-4)[308,313] trial that compared RP with watchful waiting (WW)—and then another decade for the results of the PSA era—Prostate Cancer Intervention Versus Observation Trial (PIVOT).[215] Yes, there were randomized trials, specifically a short golden period upon the emergence of luteinizing hormone releasing hormone (LHRH) analogues.[314–318] These prompted interest and the question of what role, if any, neoadjuvant hormonal therapy (NHT) had before RP. Most studies evaluated the impact of 3 months of castrating NHT prior to RP.[314–318] Of these, the one reported by Yee *et al.* portents the longest median follow-up (interquartile range [IQR]; range) for PSA progression–free patients of 8.0 years (5.2–10.7; 0.1–15.3).[318] The 7-year freedom from PSA progression was 80% and 78% for NHT+RP and RP alone, respectively. These rates changed little at 10 years, with 25 patients still at risk. The authors reported 14 deaths, but only one from prostate cancer.[318] The 5-year follow-up report from the multi-institutional (14-centre) RCT evaluating the question in clinical T2bN0M0 as reported by Soloway *et al.* revealed that despite notorious differences in positive margins rates—14% vs. 47% for NHT+RP vs. RP alone—the 5-year freedom from PSA recurrence was 65% and 68%, respectively.[317] Patients with negative margins in the NHT+RP arm recurred at twice the rates in the RP-alone arm (33% vs. 17%, respectively), indicating an artifact effect of NHT on margin status.[317] Perhaps the most provoking trial results came from the South Western Oncology Group (SWOG 9109) on 55 (T3-4N0M0) patients, where 4 months of NHT shrunk disease, as 56% had disease confined to the gland pathologically, and offered 10-year progression-free survival and overall survival rates of 40% and 68%, respectively.[314]

Freedom from progression

The approval by the FDA in the United States in 1986 for use of the biomarker PSA for monitoring treatment success after RP led to a paradigm transformation for the management of prostate cancer. Surgery was the natural and optimal source for management, as the PSA response rendered a black or white answer—no greys. Either a patient had an undetectable PSA level or a detectable one. Given the lack of randomized data, the initial reports came from either large academic series, surgeon series, or both.[142,144,307] In addition, the emergence of laparoscopy and specifically robotic surgery transformed the way RP was conducted. This transformation into the robotic approach was propelled by reports with low-quality evidence associated with robotic RP.[319] Nonetheless, numerous clinical trials are emerging, and early results suggest oncologic equivalency in terms of freedom from PSA progression.[320]

However, we encounter many common confounders when measuring the freedom from PSA progression outcome. Among them, and beside the ever-present selection bias, two specific ones are worth discussing. First, how was freedom from PSA progression defined? In other words, what was the PSA cutoff point? Second, how to interpret rates of metastatic disease, such that they could represent two different disease states depending on androgen deprivation therapy (ADT). The first question was elegantly addressed by Amling *et al.*[321] These researchers addressed the question straight on, and compared multiple definitions, for example a single PSA greater than 0.4 ng/mL, or greater than 0.2 ng/mL, or a PSA greater than 0.2 ng/mL and rising, or consecutive rises from nadir, etc. They found that the most prevalent definition of a PSA greater than 0.4 ng/mL was the most specific one and was consistent with further PSA elevations and disease progression.[321] However, as the standardization of the PSA test improved, Stephenson *et al.* showed that a contemporary PSA rise over 0.2 ng/mL was just as specific and indicated quite well disease progression.[311] In addition, the impact of PSA doubling time (PSADT) as described by D'Amico *et al.* led working groups to address what is the clinical way to follow potential PSA elevations so that both biochemical failure and accurate predictive PSADT are obtained.[322,323] Currently, any patient who is found to have a PSA >0.1 ng/mL should have it repeated at 4 and 8 weeks to both corroborate such elevation and allow for PSADT.[323] The second question about rate of metastatic disease is more elusive, given the fact that most patients with post-RP PSA elevations are treated and not observed. This is clearly exemplified by data from SPCG-4, revealing a 26% cumulative incidence of distant metastases at 18 years of follow-up.[214] However, the cumulative incidence for post-RP ADT was 43%.[214] Thus, most long-term series have not reported the non-castrate metastatic rates due to the competing event nature of secondary treatments, which frequently incorporates ADT; by the time metastatic lesions are seen, the patients' prostate cancer is on a castrate-resistant state.[214] Notwithstanding the analysis on a select group of patients (33%) of the universe of men with elevated PSA after RP in their series, Pound *et al.* first described the natural course of the disease for men observed after a post-RP PSA elevation and found that it took a median time of 7 years in the cohort of 304 men to develop non-castrate metastatic disease.[142] The median survival was 5 years; however, that was way before the new armamentarium of effective drugs and chemotherapy became available to men with castrate-resistant prostate cancer.

Cancer-specific survival and overall survival

A lot of light has been shed on these fundamentally critical outcomes by the results from both randomized trials comparing RP with watchful waiting (WW) or observation: SPCG-4 and PIVOT.[7,214,215,308,324]

The initial results from the SPCG-4 were reported by Holmberg *et al.* in 2002.[308] A total of 695 men were randomized to WW (n=348) or RP (n=347). The initial report carried a median follow-up of 6 years with no overall survival differences. However, significant differences in cancer-specific mortality rates between arms, 8.9% and 4.6% for WW and RP men, respectively (p=0.02), were seen for men who expired from prostate cancer.[308] Over the ensuing years, critical updates were provided from this trial comparing men accrued before the PSA era—reported PSA levels were performed on bank serum. At a median follow-up of 10.8 years, 294 death events had been registered, and it became clear that the driver for prostate cancer and overall survival differences was age at the time of RP.[325] **Figure 1-2** shows the split of the curves that correspond to a relative improvement of 50% and 41% in prostate cancer–specific survival and overall survival, respectively, for men <65 years at the time of RP.[325] Moreover, after 23 years of follow-up, 447 (64%) deaths events were encountered.[214] The benefit

of surgery with respect to death from prostate cancer continued to be largest for men <65 years of age at the time of surgery (RR, 0.45), as well as in those with D'Amico intermediate-risk prostate cancer—**Figure 1-3**.[214,221] The cancer outcomes derived from the PIVOT trial were described by Wilt *et al.*[215] At a median follow-up of 10 years, 171 of 364 men (47%) assigned to RP died, comparable to 183 of 367 (50%) assigned to observation (HR, 0.88; p=0.22). Importantly, this trial conducted in the PSA era demonstrated that overall and prostate cancer–specific survival did not differ among arms by age, race, coexisting conditions, self-reported performance status, or cancer histologic features.[215] However, RP was associated with overall and cancer-specific survival by the pre-operative PSA levels (**Figure 1-4**), and there was a trend for those with intermediate-risk disease; the latter validated findings from the SPCG-4 trial.[214,215,221] Reporting on a large multi-institutional series of 11,521 patients treated with RP at one of four premiere academic centres from 1987 to 2005, Eggener *et al.* observed 15-year prostate cancer–specific mortality rates for pathological Gleason score <6, 3+4, 4+3, and 8–10 of 0.2% to 1.2%, 4.2% to 6.5%, 6.6% to 11%, and 26% to 37%, respectively.307 These investigators noted that poorly differentiated cancer and seminal vesicle invasion were the prime determinants of prostate cancer–specific mortality after RP. Importantly, only 3 of 9,557 patients with organ-confined, pathological Gleason score 6 or less cancer died of prostate cancer.[307]

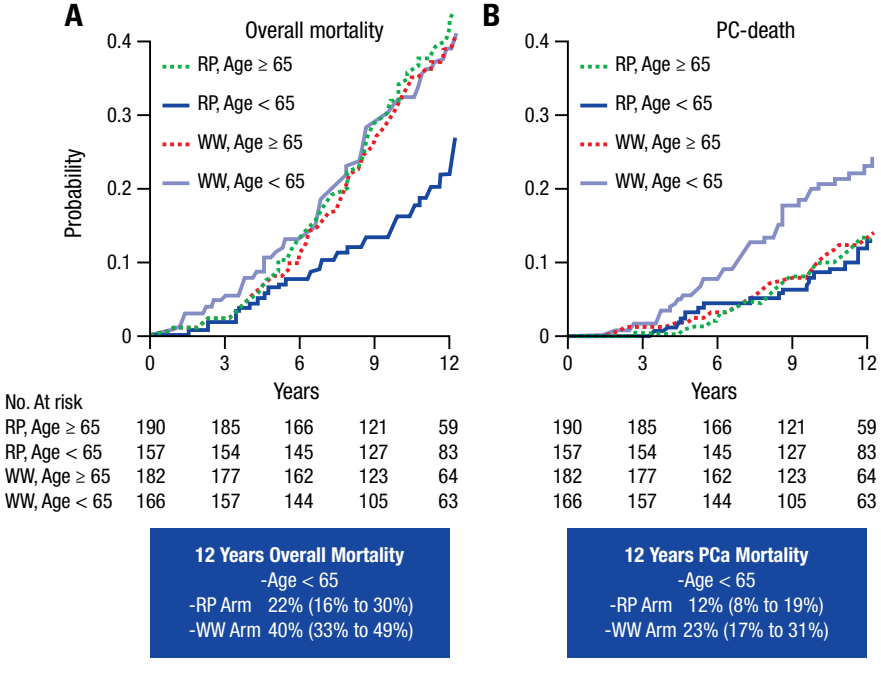

FIGURE 1-2
Cumulative incidence of death from any cause and death from prostate cancer by age group in the SPCG-4 trial.[325]

From: J Natl Cancer Inst. 2008;100:1144-1154. Radical Prostatectomy Versus Watchful Waiting in Localized Prostate Cancer: the Scandinavian Prostate Cancer Group-4 Randomized Trial. Bill-Axelson A, Holmberg L, Filén F, et al. By permission of Oxford University Press.

PCa, prostate cancer; RP, radical prostatectomy; SPCG-4, Scandinavian Prostate Cancer Group Study 4; WW, watchful waiting.

FIGURE 1-3
Stacked cumulative incidence of death from any cause, death from prostate cancer, and the development of metastasis, according to study group, age, and risk group in the SPCG-4 trial.

From: N Engl J Med. 2014;370:932, Bill-Axelson A, Holmberg L, Garmo H, et al. Radical Prostatectomy or Watchful Waiting in Early Prostate Cancer. Copyright © (2016) Massachusetts Medical Society. Reprinted with permission from Massachusetts Medical Society.

SPCG-4, Scandinavian Prostate Cancer Group Study 4.

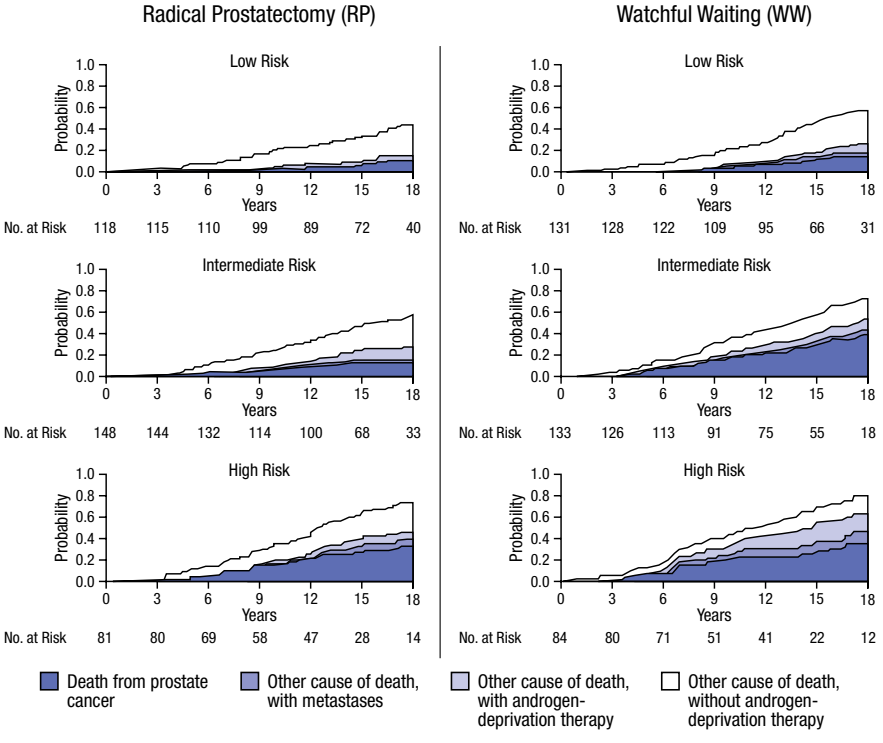

FIGURE 1-4
All-cause mortality and prostate cancer mortality for PSA >10 ng/mL in the PIVOT trial.[215] From: *N Engl J Med.* 2012;367:203, Wilt TJ, Brawer MK, Jones KM, *et al.* Radical Prostatectomy versus Observation for Localized Prostate Cancer.

Copyright © (2016) Massachusetts Medical Society. Reprinted with permission from Massachusetts Medical Society.

PSA, prostate-specific antigen; PIVOT, Prostate Cancer Intervention versus Observation Trial.

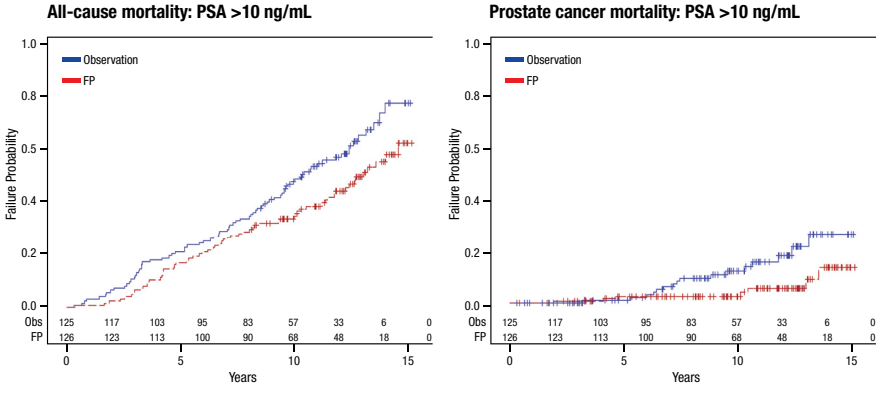

1.4.2.4.2 Quality of life and regret after radical prostatectomy

A natural question for an individual surviving prostate cancer due to RP is how good is my life going to be? Unfortunately, there are no easy answers.[326–330] Radical prostatectomy is a formidable procedure with many competing outcome events, and while cancer control is certainly the fundamental one, urinary function is a close second, and for many sexual function is as critical as life itself.[309,310,331] The so-called Trifecta outcome (cancer free, continent, and potent) is a challenging one, intertwined

by biology, surgical art, cancer knowledge, and the patient's own psychological and functional characteristics.[144] While the surgeon confronts a punctual situation in time—what is there at the time of RP, the patient continues with the motion propelled by the diagnosis of prostate cancer.[142,214,310] As his status as a survivor cements, so does his confidence, and other life elements influence and reinforce his persona. Notwithstanding the lack of evidence yet marketable exuberant data associated with the beginnings of robotic RP, there is good news, and notable research is underway addressing QOL–robotic RP technique outcomes.[319,328,332–339] Moreover, robotic RP is the most prevalent type of RP performed in Western Europe and North America. We can say with confidence that if a robot exists in a given hospital, then RP will be conducted in this fashion for the vast majority of patients. There are several trials now published addressing some of the critical elements that may affect functional outcomes after robotic RP. Outcomes reported by these RCTs include urinary continence, type of catheterization, erectile function, anastomosis techniques, patient positioning, and eye pressures.[320,328,332–340] Slowly but consistently, robust cohorts of patients randomized to robotic RP are growing with a far greater enthusiasm as compared to the prior century. Thus, with long-term follow-up, we would certainly have specific answers in the not-so-distant future. As for now, there is ample evidence that robotic RP provides improved outcomes over the short term in terms of post-operative pain, blood loss, risk for transfusion, and overall convalescence.[320,332,335,336,338,340] As there are plenty of reviews on those outcomes, we won't dwell on them in this chapter. Herein, we'll dwell on the functional elements of Trifecta outcomes (urinary and sexual function) and on the psychological impact of RP as measured by regret.

Urinary function and continence

Since 2008, four clinical trials have evaluated urinary continence after robotic RP,[332,335,338,340,341] one which has served as the first level 1 evidence [**LOE 1**] trial evaluating continence outcomes after robotic RP. This is a phase 4, multicentre, double-blind RCT evaluated solifenacin succinate versus placebo on urinary continence after robotic RP. This comprehensive investigation by Bianco *et al.* reported that upon catheter removal, patients were provided a wireless personal digital assistant (PDA) device to monitor urinary function and continence on a daily basis.[332] Altogether, 1,086 patients were screened and 640 were randomized. There were no statistical differences for urinary function and continence outcomes among treatment arms. This RCT trial showed that 73% of men achieved cumulatively "social continence of 0 or 1 pad" (**Figure 1-5**) 14 weeks after robotic RP, and no bladder neck contractures were seen during this short but critical period of follow-up.[332] Three additional studies addressed the association between robotic RP surgical technique and continence in terms of anterior and posterior periprostatic tissues reconstruction and posterior rhabdosphincter reconstruction.[335,338,340] All three RCTs showed no impact on continence outcomes derived from periprostatic tissue reconstruction among the combined 317 randomized patients.[335,338,340] These results are in line with those observed by Sanda and collaborators that measured outcomes—using the Expanded Prostate Cancer Index Composite (EPIC) questionnaire—reported by 1,201 patients and 625 spouses or partners at multiple centres.[310,342] In the study, about 30% of the 603 patients treated with robotic RP experienced urinary problems 3 months after RP. That percentage decreased to 7% at 1 and 2 years after RP, with the caveat that 24% and 20% of patients, respectively, still used pads. Urethral strictures—bladder neck contracture—contributed to poor urinary function in 5% of patients.[310]

FIGURE 1-5
Patient self-reported continence recovery after robotic RP using a personal assistant device.[332]

PDA, personal digital assistant.

Bianco, F. J., Albala, D. M., Belkoff, L. H. et al. A randomized, double-blind, solifenacin succinate versu placebo control, phase 4, multicenter study evaluating urinary continence after robotic assisted radical prostatectomy. J Urol. 2015;193:1305-10.

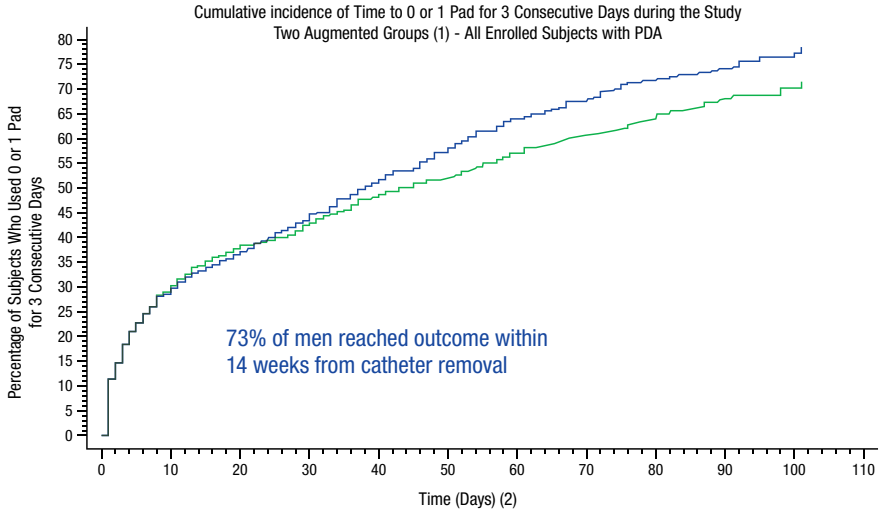

Sexual function

Physician-based reporting versus patient reporting was a premise for the Prostate Cancer Outcomes Study (PCOS), a population-based cohort registry based in six geographical areas of the United States.[343] Sexual function outcomes among 1,291 men was portrayed by Stanford *et al.*[344] Pre-surgical sexual function was described as a moderate/big problem by 17% of respondents. However, patient responses at 6-, 12-, and 24-month assessments showed sexual function as a moderate/big problem for 61%, 52%, and 42% of the cohort, respectively.[344] The post-RP decline in sexual function was seen across all levels: interest, frequency of sexual activity, and quality and firmness of erections. The impact was quite remarkable for men aged 60–74 years, as 80% reported erections firm enough for intercourse before RP, but only 12% and 17% reported firm erections, 12 and 24 months after surgery, respectively.[344] Such noteworthy results were completely validated by Sanda *et al.*[310] In this comprehensive study, compelling answers from patients and wives showed that 59%, 50%, and 43% of the RP cohort characterized sexual function as a moderate/big problem at 6, 12, and 24 months after RP, respectively.[310] These findings call for reflection, as 88% reported good sexual function at baseline and 44% attributed distress to the impact of surgery on sexual function. Furthermore, while nerve-sparing RP was associated with better recovery of sexual QOL than non-nerve-sparing RP, this impacted fewer than 20% of RP patients at the 24-month post-operative benchmark.[310] Finally, not so stringently controlled, patient-derived sexual function outcomes were reported by the PIVOT and SPCG-4 trials. The results were awfully similar—an 80% erectile dysfunction 1 to 2 years after RP in patients who participated in either landmark trial.[215,313,345]

Regret

Regret has been defined as "the emotion we experience when realizing or imagining that our current situation may have been better, if only we had decided differently". As discussed, long-term cancer survival is common for men with localized disease treated with RP. When death does occur, it is more often due to causes other than prostate cancer.[142,144,214,307] While results are encouraging, the situation demands that difficult decisions be taken at the onset by the patient and his treatment team when considering a definitive option such as RP or surveillance. In our view, focal therapy

will come to fill that large grey space. Hopefully then, when definitive options are chosen, patients will experience less regret. Regret has a close relation with the "Trifecta" outcome, as this ruefulness in the case of RP is associated with impaired urinary and sexual function. Cancer recurrence adds despair for patients who dwell on regret from QOL "sacrifices" that resulted from previous management decisions.[144,326,329,346,347] Patients may also regret the decision-making process toward a particular treatment option. That said, any plausible action will generate a reaction, and outcomes will never be perfect, thus regret exists and will exist for any given surgical procedure, especially when an undesirable outcome event happens: expectedly or unexpectedly. Outcome regret relates to regret due to an outcome of a decision, whereas decisional regret involves the way the decision was reached.[327,330,348] Of these two, the latter is easier to explain and discuss with patients. Decisional regret is related to many psychological factors, most of which are in the patient's psyche, personality, and QOL of his life. This is relevant, as research has shown that educating a person about regret prior to his decision can lead to anticipated compunction, which exerts a powerful behavioral influence, and yields more realistic expectations, and, as an example, encouraged participation in cancer screening and organ donation programs.[348,349] The measurement of regret among prostate cancer patients has been reported and validated. Various scales have been used and reviewed.[348] The most commonly used scales are the Decisional Regret Scale (DRS), and the simplified two questions regret scale designed by Clark *at al.*[326,327,347] Traditionally, regret assessment in RP patients came from protocols evaluating regret among treatments (external beam radiation, brachytherapy, ADT, and RP). Using either method, RP regret has ranged from between 12% and 27%.[326,328,329,345,350] The majority of these investigations evaluated surgery as a treatment arm among others. In most investigations, there were associations between regret and post-RP impairments in urinary and sexual function. Even though these outcomes may improve over the initial years of surgery, regret is greatly exacerbated by cancer progression or recurrence. Thus, regret rates don't decline significantly over time. Nguyen *et al.* explored regret in a large registry of 790 patients, where 410 received open RP. The overall regret rate for surgical respondents of this cross-sectional assessment was 15%; main factors associated with regret were affected sexual function, younger age, and cardiovascular comorbidity.[329] In a large prospective series, regret with robotic RP was estimated with the Clark questionnaire, administered a median of 15 months after surgery, where 703 (74%) men responded.[350] Overall, 12% of patients expressed regret toward their surgery. Key factors associated with increased decisional regret included post-operative incontinence and erectile dysfunction. Analysis of urinary continence by use of pads (0, 1, or 2 or more pads per day) showed incremental regret differences. Patients who required a daily safety pad were significantly more regretful of their decision to undergo surgery than patients who were completely dry. Furthermore, increased pad use led to higher levels of regret ($p<0.001$). Other independent factors associated with regret were impotence and experiencing a perioperative adverse event, associated with a 20% regret rate.[350] Two large series have been published addressing the question of regret among patients undergoing either open or robotic RP. In the study from Schroeck *et al.*, regret was evaluated in the early phases of a robotic program using the DRS scale sent to 953 patients from the Duke Longitudinal Urologic Surgery Patient Outcome Series.[351] This cross-sectional assessment of 1,327 patients carried a response rate of 61% among the groups. In total, 15% versus 24% of open RP and robotic RP, respectively, expressed decisional regret. There were no significant differences among surgical groups, but an association between regret and the EPIC questionnaire was seen, as lower scores in every EPIC domain, with the exception of the sexual domain, were observed for those indicating regret.[342,351] A better-structured and protocoled series using the DRS was conducted on 334 patients by Davison *et al.*[328] Patients underwent either open or

robotic RP, and 58% responded to 6- and 12-month assessments. Observed regret rates of 14% and 10% were noted for open RP and robotic RP patients, respectively (p=0.6). There was also a significant association between lower urinary and sexual EPIC scores and regret (p<0.01 for all).[328]

1.4.2.4.3 Best candidates for RP

Traditional teaching had it that any man with clinically localized prostate cancer with a 10-year life expectancy was a great candidate for RP. This is clearly not the case, as shown by the results of randomized trials. Taking the SPCG-4 trial data into consideration, Vickers *et al.* performed an individualized estimation of the benefit of RP.[324] As reported, by age of 65 years, the absolute 10-year risk reduction in prostate cancer mortality attributable to RP ranged from 4.5% to 17.2% for low- versus high-risk patients, respectively. Furthermore, little to no expected survival benefit accompanied men >70 years of age who had RP.[324] In addition, we ought to consider the following:

1. Provocative information from PIVOT showing a non-statistical difference yet eye-captivating 15% increase in mortality among men randomly assigned to RP versus observation.[215]
2. Only 3 of 9,557 patients with organ-confined, pathological Gleason score ≤6 cancer died of prostate cancer in the experience from four large academic centres; plus a 5% cancer mortality rate seen in patients with Gleason 3+4—the most common score seen in biopsy Gleason 6-upgraded patients.[307]

Taking all this data into consideration, we venture to suggest the following:

I. Definitive candidates for RP—expect most survival benefit—any N0M0 man:

- <55 years of age with acceptable comorbidities
- <65 years of age and PSA >10 ng/mL
- <70 years of age, acceptable comorbidities, who failed focal therapy
- <70 years of age, acceptable comorbidities, PSA <4 ng/mL, who failed radiation therapy, whole-gland cryotherapy, or high-intensity focused ultrasound (HIFU)

II. Good candidates for RP—with probable survival benefit and low regret—any N0M0 man:

- Impotent <65 years of age with acceptable comorbidities
- <65 years of age with PSA <10 ng/mL
- 55 to 65 years of age with high-volume low-risk cancers, acceptable comorbidities, and preferably impotent
- <70 years of age with intermediate- or high-risk cancers, acceptable comorbidities
- <70 years of age, acceptable comorbidities, PSA of between 4 and 10 ng/mL, who failed radiation therapy, whole-gland cryotherapy, or HIFU
- <75 years of age, acceptable comorbidities, PSA >10 ng/mL, who failed focal therapy, radiation therapy, whole-gland cryotherapy, or HIFU

III. Not good candidates—harm most likely, no survival benefit—any N0M0 man:

- >65 years of age with low-risk prostate cancer
- >70 years of age with treatment-naïve prostate cancer

1.4.2.5

Level of evidence and grade of recommendation for radical prostatectomy (from EAU prostate cancer guidelines):[368]

Recommendations	LOE	GOR
Patients who are suitable for AS and radiotherapy must have these options discussed with them.	4	A*
In patients with low- and intermediate-risk PCa and a life expectancy >10 years, RP should be offered.	1b	A
Nerve-sparing surgery may be attempted in pre-operatively potent patients with low risk for extracapsular disease (T1c, GS <7, and PSA <10 ng/mL, or refer to Partin tables/ nomograms).	2b	B
Multi-parametric MRI may help in deciding when to perform nerve-sparing procedures in intermediate- and high-risk disease.	2b	B
In patients with high-risk localized PCa and a life expectancy of >10 years, RP should be offered in a multimodality setting.	2a	A
In selected patients with locally advanced (cT3a) PCa and a life expectancy >10 years, RP may be offered in a multimodality setting.	2b	B
In highly selected patients with locally advanced PCa (cT3b-T4 N0 or any T N1), RP may be offered in a multimodality setting.	3	C

A* Upgraded following panel consensus.

Abbreviations: AS, active surveillance; EAU, European Association of Urology; GOR, grade of recommendation; GS, Gleason score; LOE, level of evidence; MRI, magnetic resonance imaging; PCa, prostate cancer; PSA, prostate-specific antigen; RP, radical prostatectomy.

1.4.3 Radiotherapy

1.4.3.1 Introduction

Radiotherapy (alone or associated with androgen deprivation therapy [ADT]) is an established treatment option for patients diagnosed with prostate cancer belonging to all risk groups.[153] So said, convincing experimental and clinical data have been published in recent years clearly demonstrating that high doses are needed in order to optimize clinical and biochemical outcomes when irradiating men with prostate cancer.[352–354] It is widely accepted that a dose-response relationship exists for prostate cancer, and conformal and intensity modulated external beam radiotherapy (EBRT) techniques have been developed to achieve an effective dose escalation and to allow a better sparing of radiosensitive dose-limiting adjacent normal structures such as the rectum and bladder. Feasibility dose-finding studies have been performed showing that total doses of about 85 Gy may be delivered to the whole prostate by EBRT with acceptable toxicities, but higher doses to the entire gland are today not considered achievable due to the dose constraints to the surrounding organs at risk. On the other hand, Cellini *et al.* and Pucar *et al.* have both elegantly shown that clinically detected local recurrences after EBRT (+/- ADT) usually occur in the primary tumour location within the prostate, and these conclusions corroborate histopathologic findings observed in patients undergoing salvage radical prostatectomy for intraprostatic local recurrence after EBRT.[355,356] Therefore, strong arguments exist to develop focal irradiation strategies that, from one side, will have a reduced impact on EBRT toxicity and, on the other side, will better concentrate the dose where needed. Any hope to correctly and safely perform a focal irradiation with EBRT rests on the parallel implementation of a sophisticated technology for RT dose delivery. Image-guidance strategies for image-guided EBRT (IGRT) both based on the implant of intraprostatic markers and/or the availability of real-time, online, Cone-beam computed tomography (CT) imaging for daily patient setup, should be performed and intensity modulated radiotherapy (IMRT) beams should be used. In this respect, stereotactic body radiotherapy (SBRT) seems nowadays to be the best available technology in order to better cope with these requirements.

1.4.3.2 External beam radiotherapy (EBRT) and focal treatment of prostate cancer

In general terms, two strategies may be envisaged when considering focal external beam irradiation. (a) A "pure" focal EBRT, where the tumouricidal dose is delivered only in an extremely focused way to the prostate subvolume deemed the clinically relevant one (i.e., the dominant intraprostatic lesion [DIL]), and where virtually the rest of the gland is not irradiated at all. (b) A "boost" strategy, where the whole gland is irradiated to a reasonably sufficient dose to eradicate all subclinical foci of the disease, and the DIL is simultaneously or subsequently irradiated to a higher-than-conventional dose. Clearly, the "pure" focal strategy should be probably indicated for patients in the low- to intermediate-risk group, while the "boost" one may also be proposed to patients in the high-risk group. Any data that has ever been published on "pure" focal EBRT should only be considered as a theoretical approach, at least within the frame of an EBRT technique. On the contrary, after the publication of a couple of purely technically oriented papers, the "partial boost" strategy has been challenged in quite a number of phase 2 trials, and has even been compared to the classical whole-gland approach in a recently closed phase 3 trial. van Lin *et al.*[357] demonstrated the theoretical feasibility of integrating two functional prostate magnetic resonance imaging techniques (dynamic contrast-enhanced MRI [DCE-MRI] and spectroscopy) into the treatment planning process for EBRT for the definition

and potential irradiation of a DIL to a high-dose intraprostatic boost. For a small group of 5 prostate cancer patients, a DIL-IMRT plan was calculated consisting of a whole prostate EBRT dose of 70 Gy and a DIL-boost of up to 90 Gy and compared to a classical IMRT plan of 78 Gy to the whole prostate. The tumour control probability and the rectal-wall normal tissue complication probability were theoretically derived for the two sets of data, and a decrease in the rectal-wall complication probability was observed for the DIL-IMRT plan without compromising the tumour control probability. This concept was studied in a much larger cohort of patients by Fonteyne *et al.*[358] Magnetic resonance imaging supplemented with spectroscopy (magnetic resonance spectroscopy [MRS]) maps were obtained and used in order to define (if feasible) a DIL in 230 prostate cancer patients. Interestingly, a DIL was revealed by MRI and/or MRS in 118 of 230 patients, and this made it possible to increase the dose into this volume to a minimum of 77 Gy as compared to 70 Gy to the rest of the prostate, without increasing the overall toxicity of the treatment. Several authors have subsequently published phase 2 pilot studies mainly devoted to definitively confirming the technically feasibility of the "partial boost" strategy. The research has been focused in two directions: (1) first of all, in establishing the most reliable tool in detecting the DIL to better guide the delivery of ultra-high RT doses with teams proposing multi-parametric MRI, F-choline positron emission tomography (PET), spectroscopy-MRI, or a combination of these, and (2) in identifying the best EBRT technique (IMRT, tomotherapy, SBRT, volumetric-modulated arc therapy [V-MAT], etc.) to deliver the dose as planned.[359–361] It is certainly worthwhile mentioning that the randomized phase 3 trial NCT01168479 (FLAME-trial) has successfully been completed with the recent inclusion of the last patient.[362] In the study, 566 intermediate- to high-risk prostate cancer patients have been randomized to a standard-dose EBRT of 77 Gy in 22 fractions (control arm) and to a study arm in which an integrated micro-boost of 95 Gy is delivered to a DCE-CT and MRI-defined DIL.

1.4.3.3 Conclusions

It seems unlikely that EBRT may play a major role in the setting of "pure" focal management of (low-risk) prostate cancer; other technologies appear to have a better selectivity if the treatment of (only) a subvolume of the prostatic gland is clinically indicated, and brachytherapy (both low and high dose rate) is certainly one of those. On the other hand, when a "boost" of dose on the DIL is envisaged, EBRT has proven effective, at least theoretically, to achieve a focussed dose distribution to ultra-high dose, while irradiating to a standard dose the rest of the prostatic gland without any increased toxicity. Results of an ongoing, phase 3, randomized clinical trial are awaited in order to prove the efficacy of such a strategy in the clinical setting.

1.4.3.4 Level of evidence and grade of recommendation for radiotherapy (from the EAU Prostate Cancer Guidelines):[368]

Recommendations	LOE	GOR
Patients who are suitable for AS and surgery must have these options discussed with them.	4	A
External beam radiotherapy should be offered in all risk groups of non-metastatic PCa.	2a	A
In low-risk PCa, the total dose should be 74–78 Gy.	1a	A
In patients with low-risk PCa, without a previous TURP and with a good IPSS and a prostate volume <50 mL, LDR brachytherapy is a treatment option.	2a	A
In intermediate-risk PCa, a total dose should be 76–78 Gy, in combination with short-term ADT (4–6 months) is recommended.	1b	A
In patients with high-risk localized PCa, a total dose of 76–78 Gy, in combination with long-term ADT (2–3 years) is recommended.	1b	A
In patients with locally advanced cN0 PCa, radiotherapy must be given in combination with long-term ADT (2–3 years).	1a	A
Intensity modulated radiotherapy is the recommended modality for definitive treatment of PCa by EBRT.	2a	A
In patients with cN+ PCa, pelvic external irradiation can be given in combination with immediate long-term ADT.	2b	B

Abbreviations: ADT, androgen deprivation therapy; AS, active surveillance; EBRT, external beam radiotherapy; EAU, European Association of Urology; GOR, grade of recommendation; IPSS, International Prostate Symptom Score; LDR, low-dose rate; LOE, level of evidence; PCa, prostate cancer; PSA, prostate-specific antigen; RP, radical prostatectomy; TURP, transurethral resection of the prostate.

1.5 References

1. Rao AR, Motiwala HG, Karim OM. The discovery of prostate-specific antigen. *BJU Int.* 2008;101(1):5–10.
2. Christensson A, Laurell CB, Lilja H. Enzymatic activity of prostate-specific antigen and its reactions with extracellular serine proteinase inhibitors. *Eur J Biochem.* 1990;194(3):755–763.
3. Meng FJ, Shan A, Jin L, *et al.* The expression of a variant prostate-specific antigen in human prostate. *Cancer Epidemiol Biomarkers Prev.* 2002;11(3):305–309.
4. Hong SK. Kallikreins as biomarkers for prostate cancer. *BioMed Res Int.* 2014;2014:526341.
5. Stamey TA, Yang N, Hay AR, *et al.* Prostate-specific antigen as a serum marker for adenocarcinoma of the prostate. *N Engl J Med.* 1987;317(15):909–916.
6. Fall K, Garmo H, Andrén O, *et al.* Prostate-specific antigen levels as a predictor of lethal prostate cancer. *J Natl Cancer Inst.* 2007;99(7):526–532.
7. Bill-Axelson A, Holmberg L, Ruutu M, *et al.* Radical prostatectomy versus watchful waiting in early prostate cancer. *N Engl J Med.* 2005;352(19):1977–1984.
8. Pinsky PF, Andriole G, Crawford ED, *et al.* Prostate-specific antigen velocity and prostate cancer gleason grade and stage. *Cancer.* 2007;109(8):1689–1695.
9. Tseng KS, Landis P, Epstein JI, *et al.* Risk stratification of men choosing surveillance for low risk prostate cancer. *J Urol.* 2010;183(5):1779–1785.
10. Carter HB, Pearson JD, Metter EJ, *et al.* Longitudinal evaluation of prostate-specific antigen levels in men with and without prostate disease. *JAMA.* 1992;267(16):2215–2220.
11. D'Amico AV, Chen MH, Roehl KA, *et al.* Preoperative PSA velocity and the risk of death from prostate cancer after radical prostatectomy. *N Engl J Med.* 2004;351(2):125–135.
12. D'Amico AV, Renshaw AA, Sussman B, *et al.* Pretreatment PSA velocity and risk of death from prostate cancer following external beam radiation therapy. *JAMA.* 2005;294(4):440–447.
13. Thiel R, Pearson JD, Epstein JI, *et al.* Role of prostate-specific antigen velocity in prediction of final pathologic stage in men with localized prostate cancer. *Urology.* 1997;49(5):716–720.
14. O'Brien MF, Cronin AM, Fearn PA, *et al.* Pretreatment prostate-specific antigen (PSA) velocity and doubling time are associated with outcome but neither improves prediction of outcome beyond pretreatment PSA alone in patients treated with radical prostatectomy. *J Clin Oncol.* 2009;27(22):3591–3597.
15. Vickers AJ, Savage C, O'Brien MF, *et al.* Systematic review of pretreatment prostate-specific antigen velocity and doubling time as predictors for prostate cancer. *J Clin Oncol.* 2009;27(3):398–403.
16. Shariat SF, Semjonow A, Lilja H, *et al.* Tumor markers in prostate cancer I: blood-based markers. *Acta Oncol.* 2011;50(suppl 1):61–75.
17. Kundu SD, Roehl KA, Yu X, *et al.* Prostate specific antigen density correlates with features of prostate cancer aggressiveness. *J Urol.* 2007;177(2):505–509.
18. Blackwell KL, Bostwick DG, Myers RP, *et al.* Combining prostate specific antigen with cancer and gland volume to predict more reliably pathological stage: the influence of prostate specific antigen cancer density. *J Urol.* 1994;151(6):1565–1570.
19. Stamey TA, Johnstone IM, McNeal JE, *et al.* Preoperative serum prostate specific antigen levels between 2 and 22 ng./ml. correlate poorly with post-radical prostatectomy cancer morphology: prostate specific antigen cure rates appear constant between 2 and 9 ng./ml. *J Urol.* 2002;167(1):103–111.
20. Stamey TA, Caldwell M, McNeal JE, *et al.* The prostate specific antigen era in the United States is over for prostate cancer: what happened in the last 20 years? *J Urol.* 2004;1724(Pt 1):1297–1301.
21. Loghin A, Preda O, Bacarea V, *et al.* Predictive preoperatory variables of the prostate tumor volume. *Rom J Morphol Embryol.* 2011;52(1 suppl):363–368.

22. Ochiai A, Troncoso P, Babaian RJ. The relationship between serum prostate specific antigen level and tumor volume persists in the current era. *J Urol.* 2007;177(3):903–906.

23. Kato RB, Srougi V, Salvadori FA, *et al.* Pretreatment tumor volume estimation based on total serum psa in patients with localized prostate cancer. *Clinics (Sao Paulo).* 2008;63(6):759–762.

24. Stamey TA, Dietrick DD, Issa MM. Large, organ confined, impalpable transition zone prostate cancer: association with metastatic levels of prostate specific antigen. *J Urol.* 1993;149(3):510–515.

25. Pejcic T, Hadzi-Djokic J, Topuzovic C, *et al.* [The analysis of some factors that influence on serum PSA level in localized prostate cancer patients: mathematical model.] [Article in Serbian] *Acta Chir Iugosl.* 2011;58(1):81–87.

26. Bañez LL, Hamilton RJ, Partin AW, *et al.* Obesity-related plasma hemodilution and PSA concentration among men with prostate cancer. *JAMA.* 2007;298(19):2275–2280.

27. Bañez LL, Sun L, Trock BJ, *et al.* Body mass index and prostate specific antigen as predictors of adverse pathology and biochemical recurrence after prostatectomy. *J Urol.* 2009;182(2):491–496; discussion 496–498.

28. Mitchell CR, Umbreit EC, Rangel LJ, *et al.* Does body mass index "dilute" the predictive property of prostate-specific antigen for tumor volume at radical prostatectomy? *Urology.* 2011;78(4):868–872.

29. Onik G, Narayan P, Vaughan D, *et al.* Focal "nerve-sparing" cryosurgery for treatment of primary prostate cancer: a new approach to preserving potency. *Urology.* 2002;60(1):109–114.

30. Bahn DK, Silverman P, Lee F Sr., *et al.* Focal prostate cryoablation: initial results show cancer control and potency preservation. *J Endourol.* 2006;20(9):688–692.

31. Onik G, Vaughan D, Lotenfoe R, *et al.* "Male lumpectomy": focal therapy for prostate cancer using cryoablation. *Urology.* 2007;70(6 Suppl):16–21.

32. Sartor AO, Hricak H, Wheeler TM, *et al.* Evaluating localized prostate cancer and identifying candidates for focal therapy. *Urology.* 2008;72(6 Suppl):S12–24.

33. de la Rosette J, Ahmed H, Barentsz J, *et al.* Focal therapy in prostate cancer-report from a consensus panel. *J Endourol.* 2010;24(5):775–780.

34. Liu W, Laitinen S, Khan S, *et al.* Copy number analysis indicates monoclonal origin of lethal metastatic prostate cancer. *Nat Med.* 2009;15(5):559–565.

35. Stamey TA, McNeal JM, Wise AM, *et al.* Secondary cancers in the prostate do not determine PSA biochemical failure in untreated men undergoing radical retropubic prostatectomy. *Eur Urol.* 2001;39(Suppl 4):22–23.

36. Noguchi M, Stamey TA, McNeal JE, *et al.* Prognostic factors for multifocal prostate cancer in radical prostatectomy specimens: lack of significance of secondary cancers. *J Urol.* 2003;170(2 Pt 1):459–463.

37. Ahmed HU. The index lesion and the origin of prostate cancer. *N Engl J Med.* 2009;361(17):1704–1706.

38. Ahmed HU, Hindley RG, Dickinson L, *et al.* Focal therapy for localised unifocal and multifocal prostate cancer: a prospective development study. *Lancet Oncol.* 2012;13(6):622–632.

39. Donaldson IA, Alonzi R, Barratt D, *et al.* Focal therapy: patients, interventions, and outcomes--a report from a consensus meeting. *Eur Urol.* 2015;67(4):771–777.

40. Marien A, Gill I, Ukimura O, *et al.* Target ablation--image-guided therapy in prostate cancer. *Urol Oncol.* 2014;32(6):912–923.

41. van den Bos W, Muller BG, Ahmed H, *et al.* Focal therapy in prostate cancer: international multidisciplinary consensus on trial design. *Eur Urol.* 2014;65(6):1078–1083.

42. Langley S, Ahmed HU, Al-Qaisieh B, *et al.* Report of a consensus meeting on focal low dose rate brachytherapy for prostate cancer. *BJU Int.* 2012;109(Suppl 1):7–16.

43. Boniol M, Autier P, Perrin P, *et al.* Variation of prostate-specific antigen value in men and risk of high-grade prostate cancer: analysis of the Prostate, Lung, Colorectal, and Ovarian Cancer Screening Trial Study. *Urology.* 2015;85(5):1117–1122.

44. Keetch DW, Andriole GL, Ratliff TL, *et al.* Comparison of percent free prostate-specific antigen levels in men with benign prostatic hyperplasia treated with finasteride, terazosin, or watchful waiting. *Urology.* 1997;50(6):901–905.

45. Roddam AW, Duffy MJ, Hamdy FC, *et al.* Use of prostate-specific antigen (PSA) isoforms for the detection of prostate cancer in men with a PSA level of 2-10 ng/ml: systematic review and meta-analysis. *Eur Urol.* 2005;48(3):386–399; discussion 398–399.

46. Graefen M, Karakiewicz PI, Cagiannos I, *et al.* Percent free prostate specific antigen is not an independent predictor of organ confinement or prostate specific antigen recurrence in unscreened patients with localized prostate cancer treated with radical prostatectomy. *J Urol.* 2002;167(3):1306–1309.

47. Shariat SF, Abdel-Aziz KF, Roehrborn CG, *et al.* Pre-operative percent free PSA predicts clinical outcomes in patients treated with radical prostatectomy with total PSA levels below 10 ng/ml. *Eur Urol.* 2006;49(2):293–302.

48. Larsen SB, Brasso K, Iversen P, *et al.* Baseline prostate-specific antigen measurements and subsequent prostate cancer risk in the Danish Diet, Cancer and Health cohort. *Eur J Cancer.* 2013;49(14):3041–3048.

49. Mikolajczyk SD, Marks LS, Partin AW, *et al.* Free prostate-specific antigen in serum is becoming more complex. *Urology.* 2002;59(6):797–802.

50. Catalona WJ, Bartsch G, Rittenhouse HG, *et al.* Serum pro-prostate specific antigen preferentially detects aggressive prostate cancers in men with 2 to 4 ng/ml prostate specific antigen. *J Urol.* 2004;171(6 Pt 1):2239–2244.

51. Catalona WJ, Partin AW, Sanda MG, *et al.* A multicenter study of [-2]pro-prostate specific antigen combined with prostate specific antigen and free prostate specific antigen for prostate cancer detection in the 2.0 to 10.0 ng/ml prostate specific antigen range. *J Urol.* 2011;185(5):1650–1655.

52. Catalona WJ, Bartsch G, Rittenhouse HG, *et al.* Serum pro prostate specific antigen improves cancer detection compared to free and complexed prostate specific antigen in men with prostate specific antigen 2 to 4 ng/ml. *J Urol.* 2003;170(6 Pt 1):2181–2185.

53. Bryant RJ, Lilja H. Emerging PSA-based tests to improve screening. *Urol Clin North Am.* 2014;41(2):267–276.

54. Gupta A, Roobol MJ, Savage CJ, *et al.* A four-kallikrein panel for the prediction of repeat prostate biopsy: data from the European Randomized Study of Prostate Cancer screening in Rotterdam, Netherlands. *Br J Cancer.* 2010;103(5):708–714.

55. Abrams P, Khoury S. International Consultation on Urological Diseases: evidence-based medicine overview of the main steps for developing and grading guideline recommendations. *Neurourol Urodyn.* 2010;29(1):116–118.

56. Sokoll LJ, Ellis W, Lange P, *et al.* A multicenter evaluation of the PCA3 molecular urine test: pre-analytical effects, analytical performance, and diagnostic accuracy. *Clin Chim Acta.* 2008;389(1–2):1–6.

57. Liss MA, Santos R, Osann K, *et al.* PCA3 molecular urine assay for prostate cancer: association with pathologic features and impact of collection protocols. *World J Urol.* 2011;29(5):683–688.

58. De Luca S, Passera R, Cappia S, *et al.* Fluctuation in prostate cancer gene 3 (PCA3) score in men undergoing first or repeat prostate biopsies. *BJU Int.* 2014;114(6b):E56–61.

59. Groskopf J, Aubin SM, Deras IL, *et al.* APTIMA PCA3 molecular urine test: development of a method to aid in the diagnosis of prostate cancer. *Clin Chem.* 2006;52(6):1089–1095.

60. van Poppel H, Haese A, Graefen M, *et al.* The relationship between Prostate CAncer gene 3 (PCA3) and prostate cancer significance. *BJU Int.* 2011;109(3):360–366.

61. Hessels D, van Gils MP, van Hooij O, *et al.* Predictive value of PCA3 in urinary sediments in determining clinico-pathological characteristics of prostate cancer. *Prostate.* 2010;70(1):10–16.

62. de la Taille A, Irani J, Graefen M, *et al.* Clinical evaluation of the PCA3 assay in guiding initial biopsy decisions. *J Urol.* 2011;185(6):2119–2125.

63. Haese A, de la Taille A, van Poppel H, *et al.* Clinical utility of the PCA3 urine assay in European men scheduled for repeat biopsy. *Eur Urol.* 2008;54(5):1081–1088.

64. Aubin SM, Reid J, Sarno MJ, *et al.* PCA3 molecular urine test for predicting repeat prostate biopsy outcome in populations at risk: validation in the placebo arm of the dutasteride REDUCE trial. *J Urol.* 2010;184(5):1947–1952.

65. Gittelman MC, Hertzman B, Bailen J, *et al.* PCA3 molecular urine test as a predictor of repeat prostate biopsy outcome in men with previous negative biopsies: a prospective multicenter clinical study. *J Urol.* 2013;190(1):64–69.

66. Rubio-Briones J, Casanova J, Dumont R, *et al.* Optimizing prostate cancer screening; prospective randomized controlled study of the role of PSA and PCA3 testing in a sequential manner in an opportunistic screening program. *Actas Urol Esp.* 2014;38(4):217–223.

67. De Luca S, Passera R, Bollito E, *et al.* Biopsy and radical prostatectomy pathological patterns influence Prostate cancer gene 3 (PCA3) score. Anticancer Res. 2013;33(10):4657–4662.

68. Hansen J, Auprich M, Ahyai SA, *et al.* Initial prostate biopsy: development and internal validation of a biopsy-specific nomogram based on the prostate cancer antigen 3 assay. *Eur Urol.* 2013;63(2):201–209.

69. Ruffion A, Devonec M, Champetier D, *et al.* PCA3 and PCA3-based nomograms improve diagnostic accuracy in patients undergoing first prostate biopsy. *Int J Mol Sci.* 2013;14(9):17767–17780.

70. Nygard Y, Haukaas SA, Eide GE, *et al.* Prostate cancer antigen-3 (PCA3) and PCA3-based nomograms in the diagnosis of prostate cancer: an external validation of Hansen's nomogram on a Norwegian cohort. *Scand J Urol.* 2015;49(1):8–15.

71. Rubio-Briones J B, Esteban LM, Casanova J, *et al.* Optimizing the clinical utility of PCA3 to diagnose prostate cancer in initial prostate biopsy. Choosing thresholds in a proposed nomogram. *BMC Cancer.* 2015;15:633.

72. Nakanishi H, Groskopf J, Fritsche HA, *et al.* PCA3 molecular urine assay correlates with prostate cancer tumor volume: implication in selecting candidates for active surveillance. *J Urol.* 2008;179(5):1804–1809; discussion 1809–1810.

73. Augustin H, Mayrhofer K, Pummer K, *et al.* Relationship between prostate cancer gene 3 (PCA3) and characteristics of tumor aggressiveness. *Prostate.* 2013;73(2):203–210.

74. Durand X, Xylinas E, Radulescu C, *et al.* The value of urinary prostate cancer gene 3 (PCA3) scores in predicting pathological features at radical prostatectomy. *BJU Int.* 2012;110(1):43–49.

75. Whitman EJ, Groskopf J, Ali A, *et al.* PCA3 score before radical prostatectomy predicts extracapsular extension and tumor volume. *J Urol.* 2008;180(5):1975–1978; discussion 1978–1979.

76. Auprich M, Chun FK, Ward JF, *et al.* Critical assessment of preoperative urinary prostate cancer antigen 3 on the accuracy of prostate cancer staging. *Eur Urol.* 2011;59(1):96–105.

77. Pepe P, Fraggetta F, Galia A, *et al.* Is PCA3 score useful in preoperative staging of a single microfocus of prostate cancer diagnosed at saturation biopsy? *Urol Int.* 2012;89(2):143–147.

78. Ferro M, Lucarelli G, Bruzzese D, *et al.* Improving the prediction of pathologic outcomes in patients undergoing radical prostatectomy: the value of prostate cancer antigen 3 (PCA3), prostate health index (phi) and sarcosine. *Anticancer Res.* 2015;35(2):1017–1023.

79. Ploussard G, Durand X, Xylinas E, *et al.* Prostate cancer antigen 3 score accurately predicts tumour volume and might help in selecting prostate cancer patients for active surveillance. *Eur Urol.* 2011;59(3):422–429.

80. Vlaeminck-Guillem V, Devonec M, Colombel M, *et al.* Urinary PCA3 score predicts prostate cancer multifocality. *J Urol.* 2011;185(4):1234–1239.

81. Sciarra A, Panebianco V, Cattarino S, *et al.* Multiparametric magnetic resonance imaging of the prostate can improve the predictive value of the urinary prostate cancer antigen 3 test in patients with elevated prostate-specific antigen levels and a previous negative biopsy. *BJU Int.* 2012;110(11):1661–1665.

82. Leyten GH, Wierenga EA, Sedelaar JP, *et al.* Value of PCA3 to predict biopsy outcome and its potential role in selecting patients for multiparametric MRI. *Int J Mol Sci.* 2013;14(6):11347–11355.

83. Busetto GM, De Berardinis E, Sciarra A, *et al.* Prostate cancer gene 3 and multiparametric magnetic resonance can reduce unnecessary biopsies: decision curve analysis to evaluate predictive models. *Urology.* 2013;82(6):1355–1360.

84. Porpiglia F, Russo F, Manfredi M, *et al.* The roles of multiparametric magnetic resonance imaging, PCA3 and prostate health index-which is the best predictor of prostate cancer after a negative biopsy? *J Urol.* 2014;192(1):60–66.

85. Tomlins SA, Aubin SM, Siddiqui J, *et al.* Urine TMPRSS2:ERG fusion transcript stratifies prostate cancer risk in men with elevated serum PSA. *Sci Transl Med.* 2011;3(94):94ra72.

86. Leyten GH, Hessels D, Jannink SA, *et al.* Prospective multicentre evaluation of PCA3 and TMPRSS2-ERG gene fusions as diagnostic and prognostic urinary biomarkers for prostate cancer. *Eur Urol.* 2014;65(3):534–542.

87. Chan SW, Nguyen PN, Violette P, *et al.* Early detection of clinically significant prostate cancer at diagnosis: a prospective study using a novel panel of TMPRSS2:ETS fusion gene markers. *Cancer Med.* 2013;2(1):63–75.

88. Vlaeminck-Guillem V, Bandel M, Cottancin M, *et al.* Chronic prostatitis does not influence urinary PCA3 score. *Prostate.* 2011;72(5):549–554.

89. Cornu JN, Cancel-Tassin G, Egrot C, *et al.* Urine TMPRSS2:ERG fusion transcript integrated with PCA3 score, genotyping, and biological features are correlated to the results of prostatic biopsies in men at risk of prostate cancer. *Prostate.* 2013;73(3):242–249.

90. Chevli KK, Duff M, Walter P, *et al.* Urinary PCA3 as a predictor of prostate cancer in a cohort of 3,073 men undergoing initial prostate biopsy. *J Urol.* 2014;191(6):1743–1748.

91. Cantiello F, Russo GI, Cicione A, *et al.* PHI and PCA3 improve the prognostic performance of PRIAS and Epstein criteria in predicting insignificant prostate cancer in men eligible for active surveillance. *World J Urol.* 2016;34(4)485–493.

92. Thompson IM, Pauler DK, Goodman PJ, *et al.* Prevalence of prostate cancer among men with a prostate-specific antigen level < or =4.0 ng per milliliter. *N Engl J Med.* 2004;350(22):2239–2246.

93. Roehrborn CG, Pickens GJ, Carmody T 3rd. Variability of repeated serum prostate-specific antigen (PSA) measurements within less than 90 days in a well-defined patient population. *Urology.* 1996;47(1):59–66.

94. Stenman UH, Abrahamsson PA, Aus G, *et al.* Prognostic value of serum markers for prostate cancer. *Scan J Urol Nephrol Suppl.* 2005;(216):64–81.

95. Kumar A, Mikolajczyk SD, Goel AS, *et al.* Expression of pro form of prostate-specific antigen by mammalian cells and its conversion to mature, active form by human kallikrein 2. *Cancer Res.* 1997;57(15):3111–3114.

96. Clements J, Hooper J, Dong Y, *et al.* The expanded human kallikrein (KLK) gene family: genomic organisation, tissue-specific expression and potential functions. *Biol Chem.* 2001;382(1):5–14.

97. Lovgren J, Rajakoski K, Karp M, *et al.* Activation of the zymogen form of prostate-specific antigen by human glandular kallikrein 2. *Biochem Biophys Res Commun.* 1997;238(2):549–555.

98. Takayama TK, Fujikawa K, Davie EW. Characterization of the precursor of prostate-specific antigen. Activation by trypsin and by human glandular kallikrein. *J Biol Chem.* 1997;272(34):21582–21588.

99. Takayama TK, McMullen BA, Nelson PS, *et al.* Characterization of hK4 (prostase), a prostate-specific serine protease: activation of the precursor of prostate specific antigen (pro-PSA) and single-chain urokinase-type plasminogen activator and degradation of prostatic acid phosphatase. *Biochemistry.* 2001;40(50):15341–15348.

100. Lilja H, Christensson A, Dahlen U, *et al.* Prostate-specific antigen in serum occurs predominantly in complex with alpha 1-antichymotrypsin. *Clin Chem.* 1991;37(9):1618–1625.

101. Stenman UH, Leinonen J, Alfthan H, *et al.* A complex between prostate-specific antigen and alpha 1-antichymotrypsin is the major form of prostate-specific antigen in serum of patients with prostatic cancer: assay of the complex improves clinical sensitivity for cancer. *Cancer Res.* 1991;51(1):222–226.

102. Mikolajczyk SD, Rittenhouse HG. Pro PSA: a more cancer specific form of prostate specific antigen for the early detection of prostate cancer. *Keio J Med.* 2003;52(2):86–91.

103. Mikolajczyk SD, Millar LS, Wang TJ, *et al.* "BPSA," a specific molecular form of free prostate-specific antigen, is found predominantly in the transition zone of patients with nodular benign prostatic hyperplasia. *Urology.* 2000;55(1):41–45.

104. Mikolajczyk SD, Grauer LS, Millar LS, *et al.* A precursor form of PSA (pPSA) is a component of the free PSA in prostate cancer serum. *Urology.* 1997;50(5):710–714.

105. Mikolajczyk SD, Marker KM, Millar LS, *et al.* A truncated precursor form of prostate-specific antigen is a more specific serum marker of prostate cancer. *Cancer Res.* 2001;61(18):6958–6963.

106. Mikolajczyk SD, Millar LS, Wang TJ, *et al.* A precursor form of prostate-specific antigen is more highly elevated in prostate cancer compared with benign transition zone prostate tissue. *Cancer Res.* 2000;60(3):756–759.

107. Sokoll LJ, Chan DW, Mikolajczyk SD, *et al.* Proenzyme psa for the early detection of prostate cancer in the 2.5-4.0 ng/ml total psa range: preliminary analysis. *Urology.* 2003;61(2):274–276.

108. Khan MA, Partin AW, Rittenhouse HG, *et al.* Evaluation of proprostate specific antigen for early detection of prostate cancer in men with a total prostate specific antigen range of 4.0 to 10.0 ng/ml. *J Urol.* 2003;170(3):723–726.

109. Mikolajczyk SD, Catalona WJ, Evans CL, *et al.* Proenzyme forms of prostate-specific antigen in serum improve the detection of prostate cancer. *Clin Chem.* 2004;50(6):1017.

110. Sokoll LJ, Wang Y, Feng Z, *et al.* [-2]proenzyme prostate specific antigen for prostate cancer detection: a national cancer institute early detection research network validation study. *J Urol.* 2008;180(2):539–543; discussion 543.

111. Sokoll LJ, Sanda MG, Feng Z, *et al.* A prospective, multicenter, National Cancer Institute Early Detection Research Network study of [-2]proPSA: improving prostate cancer detection and correlating with cancer aggressiveness. *Cancer Epidemiol Biomarkers Prev.* 2010;19(5):1193–1200.

112. Stephan C, Kahrs AM, Cammann H, *et al.* A [-2]proPSA-based artificial neural network significantly improves differentiation between prostate cancer and benign prostatic diseases. *Prostate.* 2009;69(2):198–207.

113. Rhodes T, Jacobson DJ, McGree ME, *et al.* Longitudinal changes of benign prostate-specific antigen and [-2]proprostate-specific antigen in seven years in a community-based sample of men. *Urology.* 2012;79(3):655–661.

114. Rhodes T, Jacobson DJ, McGree ME, *et al.* Distribution and associations of [-2]proenzyme-prostate specific antigen in community dwelling black and white men. *J Urol.* 2012;187(1):92–96.

115. Le BV, Griffin CR, Loeb S, *et al.* [-2]Proenzyme prostate specific antigen is more accurate than total and free prostate specific antigen in differentiating prostate cancer from benign disease in a prospective prostate cancer screening study. *J Urol.* 2010;183(4):1355–1359.

116. Jansen FH, van Schaik RH, Kurstjens J, *et al.* Prostate-specific antigen (PSA) isoform p2PSA in combination with total PSA and free PSA improves diagnostic accuracy in prostate cancer detection. *Eur Urol.* 2010;57(6):921–927.

117. Loeb S, Sokoll LJ, Broyles DL, *et al.* Prospective multicenter evaluation of the Beckman Coulter Prostate Health Index using WHO calibration. *J Urol.* 2013;189(5):1702–1706.

118. Loeb S, Sanda MG, Broyles DL, *et al.* The prostate health index selectively identifies clinically significant prostate cancer. *J Urol.* 2015;193(4):1163–1169.

119. Guazzoni G, Nava L, Lazzeri M, *et al.* Prostate-specific antigen (PSA) isoform p2PSA significantly improves the prediction of prostate cancer at initial extended prostate biopsies in patients with total PSA between 2.0 and 10 ng/ml: results of a prospective study in a clinical setting. *Eur Urol.* 2011;60(2):214–222.

120. Lazzeri M, Briganti A, Scattoni V, *et al.* Serum index test %[-2]proPSA and Prostate Health Index are more accurate than prostate specific antigen and %fPSA in predicting a positive repeat prostate biopsy. *J Urol.* 2012;188(4):1137–1143.

121. Lazzeri M, Haese A, de la Taille A, *et al.* Serum isoform [-2]proPSA derivatives significantly improve prediction of prostate cancer at initial biopsy in a total PSA range of 2-10 ng/ml: a multicentric European study. *Eur Urol.* 2013;63(6):986–994.

122. Stephan C, Vincendeau S, Houlgatte A, *et al.* Multicenter evaluation of [-2]proprostate-specific antigen and the prostate health index for detecting prostate cancer. *Clin Chem.* 2013;59(1):306–314.

123. Boegemann M, Stephan C, Cammann H, *et al.* The percentage of prostate-specific antigen (PSA) isoform [-2]proPSA and the Prostate Health Index improve the diagnostic accuracy for clinically relevant prostate cancer at initial and repeat biopsy compared with total PSA and percentage free PSA in men aged </=65 years. *BJU Int.* 2016;117(1):72–79.

124. Fossati N, Lazzeri M, Haese A, *et al.* Clinical performance of serum isoform [-2]proPSA (p2PSA), and its derivatives %p2PSA and the Prostate Health Index, in men aged <60 years: results from a multicentric European study. *BJU Int.* 2015;115(6):913–920.

125. Ito K, Miyakubo M, Sekine Y, *et al.* Diagnostic significance of [-2]pro-PSA and prostate dimension-adjusted PSA-related indices in men with total PSA in the 2.0-10.0 ng/mL range. *World J Urol.* 2013;31(2):305–311.

126. Ng CF, Chiu PK, Lam NY, *et al.* The Prostate Health Index in predicting initial prostate biopsy outcomes in Asian men with prostate-specific antigen levels of 4-10 ng/mL. *Int Urol Nephrol.* 2014;46(4):711–717.

127. Lughezzani G, Lazzeri M, Larcher A, *et al.* Development and internal validation of a Prostate Health Index based nomogram for predicting prostate cancer at extended biopsy. *J Urol.* 2012;188(4):1144–1150.

128. Lughezzani G, Lazzeri M, Haese A, *et al.* Multicenter European external validation of a prostate health index-based nomogram for predicting prostate cancer at extended biopsy. *Eur Urol.* 2014;66(5):906–912.

129. Guazzoni G, Lazzeri M, Nava L, *et al.* Preoperative prostate-specific antigen isoform p2PSA and its derivatives, %p2PSA and prostate health index, predict pathologic outcomes in patients undergoing radical prostatectomy for prostate cancer. *Eur Urol.* 2012;61(3):455–466.

130. Mouraviev V, Villers A, Bostwick DG, *et al.* Understanding the pathological features of focality, grade and tumour volume of early-stage prostate cancer as a foundation for parenchyma-sparing prostate cancer therapies: active surveillance and focal targeted therapy. *BJU Int.* 2011;108(7):1074–1085.

131. Fossati N, Buffi NM, Haese A, *et al.* Preoperative prostate-specific antigen isoform p2PSA and its derivatives, %p2PSA and Prostate Health Index, predict pathologic outcomes in patients undergoing radical prostatectomy for prostate cancer: results from a multicentric European prospective study. *Eur Urol.* 2015;68(1):132–138.

132. Heidegger I, Klocker H, Steiner E, *et al.* [-2]proPSA is an early marker for prostate cancer aggressiveness. *Prostate Cancer Prostatic Dis.* 2014;17(1):70–74.

133. Lazzeri M, Guazzoni G. Focal therapy meets prostate cancer. *Lancet.* 2010;376(9746):1036–1037.

134. Bostwick DG, Waters DJ, Farley ER, *et al.* Group consensus reports from the Consensus Conference on Focal Treatment of Prostatic Carcinoma, Celebration, Florida, February 24, 2006. *Urology.* 2007;70(6 Suppl):42–44.

135. Makarov DV, Isharwal S, Sokoll LJ, *et al.* Pro-prostate-specific antigen measurements in serum and tissue are associated with treatment necessity among men enrolled in expectant management for prostate cancer. *Clin Cancer Res.* 2009;15(23):7316–7321.

136. Tosoian JJ, Loeb S, Feng Z, *et al.* Association of [-2]proPSA with biopsy reclassification during active surveillance for prostate cancer. *J Urol.* 2012;188(4):1131–1136.

137. Hirama H, Sugimoto M, Ito K, *et al.* The impact of baseline [-2]proPSA-related indices on the prediction of pathological reclassification at 1 year during active surveillance for low-risk prostate cancer: the Japanese multicenter study cohort. *J Cancer Res Clin Oncol.* 2014;140(2):257–263.

138. Lughezzani G, Lazzeri M, Buffi NM, *et al.* Preoperative prostate health index is an independent predictor of early biochemical recurrence after radical prostatectomy: results from a prospective single-center study. *Urol Oncol.* 2015;33(8):337 e7– e14.

139. Tilki D, Kim SI, Hu B, *et al.* Ultrasensitive prostate specific antigen and its role after radical prostatectomy: a systematic review. *J Urol.* 2015;193(5):1525–1531.

140. Kang JJ, Reiter RE, Steinberg ML, *et al.* Ultrasensitive prostate specific antigen after prostatectomy reliably identifies patients requiring postoperative radiotherapy. *J Urol.* 2015;193(5):1532–1538.

141. Roehl KA, Han M, Ramos CG, *et al.* Cancer progression and survival rates following anatomical radical retropubic prostatectomy in 3,478 consecutive patients: long-term results. *J Urol.* 2004;172(3):910–914.

142. Pound CR, Partin AW, Eisenberger MA, *et al.* Natural history of progression after PSA elevation following radical prostatectomy. *JAMA.* 1999;281(17):1591–1597.

143. Djavan B, Milani S, Fong YK. Benign positive margins after radical prostatectomy means a poor prognosis--pro. *Urology.* 2005;65(2):218–220.

144. Bianco FJ, Jr., Scardino PT, Eastham JA. Radical prostatectomy: long-term cancer control and recovery of sexual and urinary function ("trifecta"). *Urology.* 2005;66(5 Suppl):83–94.

145. Eggener SE, Scardino PT, Carroll PR, *et al.* Focal therapy for localized prostate cancer: a critical appraisal of rationale and modalities. *J Urol.* 2007;178(6):2260–2267.

146. Ahmed HU, Emberton M. Is focal therapy the future for prostate cancer? *Future Oncol.* 2010;6(2):261–268.

147. Mohler JL, Armstrong AJ, Bahnson RR, *et al.* Prostate cancer, Version 3.2012: featured updates to the NCCN guidelines. *J Natl Compr Canc Netw.* 2012;10(9):1081–1087.

148. Bahn D, de Castro Abreu AL, Gill IS, *et al.* Focal cryotherapy for clinically unilateral, low-intermediate risk prostate cancer in 73 men with a median follow-up of 3.7 years. *Eur Urol.* 2012;62(1):55–63.

149. Ahmed HU, Akin O, Coleman JA, *et al.* Transatlantic Consensus Group on active surveillance and focal therapy for prostate cancer. *BJU Int.* 2012;109(11):1636–1647.

150. Valerio M, Ahmed HU, Emberton M, *et al.* The role of focal therapy in the management of localised prostate cancer: a systematic review. *Eur Urol.* 2014;66(4):732–751.

151. Klotz L, Emberton M. Management of low risk prostate cancer: active surveillance and focal therapy. *Curr Opin Urol.* 2014;24(3):270–279.

152. Gravas S, de Reijke T. Is focal therapy an alternative to active surveillance? *J Endourol*. 2010;24(5):855–860.

153. Heidenreich A, Bastian PJ, Bellmunt J, *et al*. EAU guidelines on prostate cancer. part 1: screening, diagnosis, and local treatment with curative intent-update 2013. *Eur Urol*. 2014;65(1):124–137.

154. Taneja SS, Mason M. Candidate selection for prostate cancer focal therapy. *J Endourol*. 2010;24(5):835–841.

155. Singh PB, Anele C, Dalton E, *et al*. Prostate cancer tumour features on template prostate-mapping biopsies: implications for focal therapy. *Eur Urol*. 2014;66(1):12–19.

156. Valerio M, Anele C, Freeman A, *et al*. Identifying the index lesion with template prostate mapping biopsies. *J Urol*. 2015;193(4):1185–1190.

157. Onik G, Barzell W. Transperineal 3D mapping biopsy of the prostate: an essential tool in selecting patients for focal prostate cancer therapy. *Urol Oncol*. 2008;26(5):506–510.

158. Sivaraman A, Sanchez-Salas R, Barret E, *et al*. Transperineal template-guided mapping biopsy of the prostate. *Int J Urol*. 2015;22(2):146–151.

159. Muller BG, Futterer JJ, Gupta RT, *et al*. The role of magnetic resonance imaging (MRI) in focal therapy for prostate cancer: recommendations from a consensus panel. *BJU Int*. 2014;113(2):218–227.

160. Bott SR, Ahmed HU, Hindley RG, *et al*. The index lesion and focal therapy: an analysis of the pathological characteristics of prostate cancer. *BJU Int*. 2010;106(11):1607–1611.

161. Karavitakis M, Winkler M, Abel P, *et al*. Histological characteristics of the index lesion in whole-mount radical prostatectomy specimens: implications for focal therapy. *Prostate Cancer Prostatic Dis*. 2011;14(1):46–52.

162. Cheng L, Song SY, Pretlow TG, *et al*. Evidence of independent origin of multiple tumors from patients with prostate cancer. *J Natl Cancer Inst*. 1998;90(3):233–237.

163. Andreoiu M, Cheng L. Multifocal prostate cancer: biologic, prognostic, and therapeutic implications. *Hum Pathol*. 2010;41(6):781–793.

164. Passoni NM, Polascik TJ. How to select the right patients for focal therapy of prostate cancer? *Curr Opin Urol*. 2014;24(3):203–208.

165. Feijoo ER, Sivaraman A, Barret E, *et al*. Focal high-intensity focused ultrasound targeted hemiablation for unilateral prostate cancer: a prospective evaluation of oncologic and functional outcomes. *Eur Urol*. 2016;69(2):214–220.

166. Villers A, Lemaitre L, Haffner J, *et al*. Current status of MRI for the diagnosis, staging and prognosis of prostate cancer: implications for focal therapy and active surveillance. *Curr Opin Urol*. 2009;19(3):274–282.

167. Ahmed HU. Introduction--targeting the lesion, not the organ. *Urol Oncol*. 2014;32(6):901–902.

168. Algaba F, Montironi R. Impact of prostate cancer multifocality on its biology and treatment. *J Endourol*. 2010;24(5):799–804.

169. Algaba F. [Pathological consideration of indolent and clinically non-significant prostate cancer definition]. [Article in Spanish] *Arch Esp Urol*. 2014;67(5):393–399.

170. Tareen B, Godoy G, Sankin A, *et al*. Laterality alone should not drive selection of candidates for hemi-ablative focal therapy. *J Urol*. 2009;181(3):1082–1089; discussion 1089–1090.

171. Artibani W. Landmarks in prostate cancer diagnosis: the biomarkers. *BJU Int*. 2012;110 Suppl 1:8–13.

172. Shariat SF, Canto EI, Kattan MW, *et al*. Beyond prostate-specific antigen: new serologic biomarkers for improved diagnosis and management of prostate cancer. *Rev Urol*. 2004;6(2):58–72.

173. Rantalainen M, Cloarec O, Beckonert O, *et al*. Statistically integrated metabonomic-proteomic studies on a human prostate cancer xenograft model in mice. *J Proteom Res*. 2006;5(10):2642–2655.

174. Jiang FN, He HC, Zhang YQ, *et al*. An integrative proteomics and interaction network-based classifier for prostate cancer diagnosis. *PLoS One*. 2013;8(5):e63941.

175. DeSantis CE, Lin CC, Mariotto AB, *et al*. Cancer treatment and survivorship statistics, 2014. *CA Cancer J Clin*. 2014;64(4):252–271.

176. Ilic D, Neuberger MM, Djulbegovic M, *et al*. Screening for prostate cancer. *Cochrane Database Syst Rev*. 2013;1:CD004720.

177. Etzioni R, Tsodikov A, Mariotto A, *et al.* Quantifying the role of PSA screening in the US prostate cancer mortality decline. *Cancer Causes Control*. 2008;19(2):175–181.

178. Hernández J, Thompson IM. Prostate-specific antigen: a review of the validation of the most commonly used cancer biomarker. *Cancer*. 2004;101(5):894–904.

179. Wolters T, Roobol MJ, van Leeuwen PJ, *et al.* A critical analysis of the tumor volume threshold for clinically insignificant prostate cancer using a data set of a randomized screening trial. *J Urol*. 2011;185(1):121–125.

180. Goto Y, Ohori M, Arakawa A, *et al.* Distinguishing clinically important from unimportant prostate cancers before treatment: value of systematic biopsies. *J Urol*. 1996;156(3):1059–1063.

181. Epstein JI, Walsh PC, Carmichael M, *et al.* Pathologic and clinical findings to predict tumor extent of nonpalpable (stage T1c) prostate cancer. *JAMA*. 1994;271(5):368–374.

182. Stamey TA, Freiha FS, McNeal JE, *et al.* Localized prostate cancer. Relationship of tumor volume to clinical significance for treatment of prostate cancer. *Cancer*. 1993;71(3 Suppl):933–938.

183. Ficarra V, Novara G, Rosen RC, *et al.* Systematic review and meta-analysis of studies reporting urinary continence recovery after robot-assisted radical prostatectomy. *Eur Urol.* 2012;62(3):405–417.

184. Ficarra V, Novara G, Ahlering TE, *et al.* Systematic review and meta-analysis of studies reporting potency rates after robot-assisted radical prostatectomy. *Eur Urol.* 2012;62(3):418–430.

185. Resnick MJ, Koyama T, Fan KH, *et al.* Long-term functional outcomes after treatment for localized prostate cancer. *N Engl J Med.* 2013;368(5):436–445.

186. Sheets NC, Goldin GH, Meyer AM, *et al.* Intensity-modulated radiation therapy, proton therapy, or conformal radiation therapy and morbidity and disease control in localized prostate cancer. *JAMA*. 2012;307(15):1611–1620.

187. Ahmed HU, Pendse D, Illing R, *et al.* Will focal therapy become a standard of care for men with localized prostate cancer? *Nat Clin Pract Oncol.* 2007;4(11):632–642.

188. Lindner U, Trachtenberg J, Lawrentschuk N. Focal therapy in prostate cancer: modalities, findings and future considerations. *Nat Rev Urol.* 2010;7(10):562–571.

189. Eggener S, Salomon G, Scardino PT, *et al.* Focal therapy for prostate cancer: possibilities and limitations. *Eur Urol.* 2010;58(1):57–64.

190. Villers A, McNeal JE, Freiha FS, *et al.* Multiple cancers in the prostate. Morphologic features of clinically recognized versus incidental tumors. *Cancer.* 1992;70(9):2313–2318.

191. D'Amico AV, Whittington R, Malkowicz SB, *et al.* Clinical utility of percent-positive prostate biopsies in predicting biochemical outcome after radical prostatectomy or external-beam radiation therapy for patients with clinically localized prostate cancer. *Mol Urol.* 2000;4(3):171–175; discussion 177.

192. D'Amico AV, Whittington R, Malkowicz SB, *et al.* Clinical utility of the percentage of positive prostate biopsies in defining biochemical outcome after radical prostatectomy for patients with clinically localized prostate cancer. *J Clin Oncol.* 2000;18(6):1164–1172.

193. Freedland SJ, Aronson WJ, Terris MK, *et al.* The percentage of prostate needle biopsy cores with carcinoma from the more involved side of the biopsy as a predictor of prostate specific antigen recurrence after radical prostatectomy: results from the Shared Equal Access Regional Cancer Hospital (SEARCH) database. *Cancer.* 2003;98(11):2344–2350.

194. Tollefson MK, Leibovich BC, Slezak JM, *et al.* Long-term prognostic significance of primary Gleason pattern in patients with Gleason score 7 prostate cancer: impact on prostate cancer specific survival. *J Urol*. 2006;175(2):547–551.

195. Stark JR, Perner S, Stampfer MJ, *et al.* Gleason score and lethal prostate cancer: does 3 + 4 = 4 + 3? *J Clin Oncol.* 2009;27(21):3459–3464.

196. Arora R, Koch MO, Eble JN, *et al.* Heterogeneity of Gleason grade in multifocal adenocarcinoma of the prostate. *Cancer.* 2004;100(11):2362–2366.

197. Wise AM, Stamey TA, McNeal JE, *et al.* Morphologic and clinical significance of multifocal prostate cancers in radical prostatectomy specimens. *Urology.* 2002;60(2):264–269.

198. Bostwick DG, Shan A, Qian J, *et al.* Independent origin of multiple foci of prostatic intraepithelial neoplasia: comparison with matched foci of prostate carcinoma. *Cancer.* 1998;83(9):1995–2002.

199. Hugel A, Wernert N. Loss of heterozygosity (LOH), malignancy grade and clonality in microdissected prostate cancer. *Br J Cancer.* 1999;79(3–4):551–557.

200. Jones TD, Wang M, Eble JN, *et al.* Molecular evidence supporting field effect in urothelial carcinogenesis. *Clin Cancer Res.* 2005;11(18):6512–6519.

201. Mehra R, Tomlins SA, Yu J, *et al.* Characterization of TMPRSS2-ETS gene aberrations in androgen-independent metastatic prostate cancer. *Cancer Res.* 2008;68(10):3584–3590.

202. Kulac I, Haffner MC, Yegnasubramanian S, *et al.* Should Gleason 6 be labeled as cancer? *Curr Opin Urol.* 2015;25(3):238–245.

203. Futterer JJ, Briganti A, De Visschere P, *et al.* Can clinically significant prostate cancer be detected with multiparametric magnetic resonance imaging? A systematic review of the literature. *Eur Urol.* 2015;68(6):1045–1053.

204. Turkbey B, Mani H, Aras O, *et al.* Correlation of magnetic resonance imaging tumor volume with histopathology. *J Urol.* 2012;188(4):1157–1163.

205. Tan N, Margolis DJ, Lu DY, *et al.* Characteristics of detected and missed prostate cancer foci on 3-T multiparametric MRI using an endorectal coil correlated with whole-mount thin-section histopathology. *AJR Am J Roentgenol.* 2015;205(1):W87–92.

206. Postema A, Mischi M, de la Rosette J, *et al.* Multiparametric ultrasound in the detection of prostate cancer: a systematic review. *World J Urol.* 2015;33(11):1651–1659.

207. Ahmed HU, Hu Y, Carter T, *et al.* Characterizing clinically significant prostate cancer using template prostate mapping biopsy. *J Urol.* 2011;186(2):458–464.

208. Kasivisvanathan V, Dufour R, Moore CM, *et al.* Transperineal magnetic resonance image targeted prostate biopsy versus transperineal template prostate biopsy in the detection of clinically significant prostate cancer. *J Urol.* 2013;189(3):860–866.

209. Schoots IG, Roobol MJ, Nieboer D, *et al.* Magnetic resonance imaging-targeted biopsy may enhance the diagnostic accuracy of significant prostate cancer detection compared to standard transrectal ultrasound-guided biopsy: a systematic review and meta-analysis. *Eur Urol.* 2015;68(3):438–450.

210. Valerio M, Donaldson I, Emberton M, *et al.* Detection of clinically significant prostate cancer using magnetic resonance imaging-ultrasound fusion targeted biopsy: a systematic review. *Eur Urol.* 2015;68(1):8–19.

211. Gburek BM, Kollmorgen TA, Qian J, *et al.* Chromosomal anomalies in stage D1 prostate adenocarcinoma primary tumors and lymph node metastases detected by fluorescence in situ hybridization. *J Urol.* 1997;157(1):223–227.

212. Qian J, Bostwick DG, Takahashi S, *et al.* Chromosomal anomalies in prostatic intraepithelial neoplasia and carcinoma detected by fluorescence in situ hybridization. *Cancer Res.* 1995;55(22):5408–5414.

213. Haffner MC, Mosbruger T, Esopi DM, *et al.* Tracking the clonal origin of lethal prostate cancer. *J Clin Invest.* 2013;123(11):4918–4922.

214. Bill-Axelson A, Holmberg L, Garmo H, *et al.* Radical prostatectomy or watchful waiting in early prostate cancer. *N Engl J Med.* 2014;370(10):932–942.

215. Wilt TJ, Brawer MK, Jones KM, *et al.* Radical prostatectomy versus observation for localized prostate cancer. *N Engl J Med.* 2012;367(3):203–213.

216. Morash C, Tey R, Agbassi C, *et al.* Active surveillance for the management of localized prostate cancer: guideline recommendations. *Can Urol Assoc J.* 2015;9(5–6):171–178.

217. Heidenreich A, Bastian PJ, Bellmunt J, *et al.* EAU guidelines on prostate cancer. part 1: screening, diagnosis, and local treatment with curative intent-update 2013. *Eur Urol.* 2014;65(1):124–137.

218. Weiner AB, Patel SG, Etzioni R, *et al.* National trends in the management of low and intermediate risk prostate cancer in the United States. *J Urol.* 2015;193(1):95–102.

219. Bratt O, Carlsson S, Holmberg E, *et al.* The Study of Active Monitoring in Sweden (SAMS): a randomized study comparing two different follow-up schedules for active surveillance of low-risk prostate cancer. *Scan J Urol.* 2013;47(5):347–355.

220. Lane JA, Donovan JL, Davis M, *et al.* Active monitoring, radical prostatectomy, or radiotherapy for localised prostate cancer: study design and diagnostic and baseline results of the ProtecT randomised phase 3 trial. *Lancet Oncol.* 2014;15(10):1109–1118.

221. D'Amico AV, Whittington R, Malkowicz SB, *et al.* Biochemical outcome after radical prostatectomy, external beam radiation therapy, or interstitial radiation therapy for clinically localized prostate cancer. *JAMA.* 1998;280(11):969–974.

222. Tosoian JJ, Trock BJ, Landis P, *et al.* Active surveillance program for prostate cancer: an update of the Johns Hopkins experience. *J Clin Oncol.* 2011;29(16):2185–2190.

223. Forde JC, Daly PJ, White S, *et al.* A single centre experience of active surveillance as management strategy for low-risk prostate cancer in Ireland. *Ir J Med Sci.* 2014;183(3):377–382.

224. Bastian PJ, Mangold LA, Epstein JI, *et al.* Characteristics of insignificant clinical T1c prostate tumors. A contemporary analysis. *Cancer.* 2004;101(9):2001–2005.

225. Ploussard G, Epstein JI, Montironi R, *et al.* The contemporary concept of significant versus insignificant prostate cancer. *Eur Urol.* 2011;60(2):291–303.

226. Klotz L, Vesprini D, Sethukavalan P, *et al.* Long-term follow-up of a large active surveillance cohort of patients with prostate cancer. *J Clin Oncol.* 2015;33(3):272–277.

227. Bul M, Zhu X, Valdagni R, *et al.* Active surveillance for low-risk prostate cancer worldwide: the PRIAS study. *Eur Urol.* 2013;63(4):597–603.

228. Selvadurai ED, Singhera M, Thomas K, *et al.* Medium-term outcomes of active surveillance for localised prostate cancer. *Eur Urol.* 2013;64(6):981–987.

229. Dall'Era MA, Konety BR, Cowan JE, *et al.* Active surveillance for the management of prostate cancer in a contemporary cohort. *Cancer.* 2008;112(12):2664–2670.

230. Fleshner NE, Lucia MS, Egerdie B, *et al.* Dutasteride in localised prostate cancer management: the REDEEM randomised, double-blind, placebo-controlled trial. *Lancet.* 2012;379(9821):1103–1111.

231. Iremashvili V, Manoharan M, Lokeshwar SD, *et al.* Comprehensive analysis of post-diagnostic prostate-specific antigen kinetics as predictor of a prostate cancer progression in active surveillance patients. *BJU Int.* 2013;111(3):396–403.

232. Whitson JM, Porten SP, Hilton JF, *et al.* The relationship between prostate specific antigen change and biopsy progression in patients on active surveillance for prostate cancer. *J Urol.* 2011;185(5):1656–1660.

233. Ross AE, Loeb S, Landis P, *et al.* Prostate-specific antigen kinetics during follow-up are an unreliable trigger for intervention in a prostate cancer surveillance program. *J Clin Oncol.* 2010;28(17):2810–2816.

234. Hardie C, Parker C, Norman A, *et al.* Early outcomes of active surveillance for localized prostate cancer. *BJU Int.* 2005;95(7):956–960.

235. van As NJ, Norman AR, Thomas K, *et al.* Predicting the probability of deferred radical treatment for localised prostate cancer managed by active surveillance. *Eur Urol.* 2008;54(6):1297–1305.

236. van den Bergh RC, Vasarainen H, van der Poel HG, et al. Short-term outcomes of the prospective multicentre 'Prostate Cancer Research International: Active Surveillance' study. BJU Int. 2010;105(7):956–962.

237. Carter HB, Kettermann A, Warlick C, *et al.* Expectant management of prostate cancer with curative intent: an update of the Johns Hopkins experience. *J Urol.* 2007;178(6):2359–2364; discussion 2364–2365.

238. Cooperberg MR, Cowan JE, Hilton JF, *et al.* Outcomes of active surveillance for men with intermediate-risk prostate cancer. *J Clin Oncol.* 2011;29(2):228–234.

239. Godtman RA, Holmberg E, Khatami A, *et al.* Outcome following active surveillance of men with screen-detected prostate cancer. Results from the Goteborg randomised population-based prostate cancer screening trial. *Eur Urol.* 2013;63(1):101–107.

240. Soloway MS, Soloway CT, Eldefrawy A, *et al.* Careful selection and close monitoring of low-risk prostate cancer patients on active surveillance minimizes the need for treatment. *Eur Urol.* 2010;58(6):831–835.

241. van den Bergh RC, Roemeling S, Roobol MJ, *et al.* Outcomes of men with screen-detected prostate cancer eligible for active surveillance who were managed expectantly. *Eur Urol.* 2009;55(1):1–8.

242. van den Bergh RC, Roemeling S, Roobol MJ, *et al.* Prospective validation of active surveillance in prostate cancer: the PRIAS study. *Eur Urol.* 2007;52(6):1560–1563.

243. Eggener SE, Mueller A, Berglund RK, *et al.* A multi-institutional evaluation of active surveillance for low risk prostate cancer. *J Urol.* 2009;181(4):1635–1641; discussion 1641.

244. Eggener SE, Mueller A, Berglund RK, *et al.* A multi-institutional evaluation of active surveillance for low risk prostate cancer. *J Urol.* 2013;189(1 Suppl):S19–25; discussion S25.

245. Soloway MS, Soloway CT, Williams S, *et al.* Active surveillance; a reasonable management alternative for patients with prostate cancer: the Miami experience. *BJU Int.* 2008;101(2):165–169.

246. Preston MA, Feldman AS, Coen JJ, *et al.* Active surveillance for low-risk prostate cancer: need for intervention and survival at 10 years. *Urol Oncol.* 2015;33(9):383.e9–16.

247. Loeb S, Folkvaljon Y, Makarov DV, *et al.* Five-year nationwide follow-up study of active surveillance for prostate cancer. *Eur Urol.* 2015;67(2):233–238.

248. El Hajj A, Ploussard G, de la Taille A, *et al.* Patient selection and pathological outcomes using currently available active surveillance criteria. *BJU Int.* 2013;112(4):471–477.

249. Suardi N, Capitanio U, Chun FK, *et al.* Currently used criteria for active surveillance in men with low-risk prostate cancer: an analysis of pathologic features. *Cancer.* 2008;113(8):2068–2072.

250. Abouassaly R, Lane BR, Jones JS. Staging saturation biopsy in patients with prostate cancer on active surveillance protocol. *Urology.* 2008;71(4):573–577.

251. Adamy A, Yee DS, Matsushita K, *et al.* Role of prostate specific antigen and immediate confirmatory biopsy in predicting progression during active surveillance for low risk prostate cancer. *J Urol.* 2011;185(2):477–482.

252. Berglund RK, Masterson TA, Vora KC, *et al.* Pathological upgrading and up staging with immediate repeat biopsy in patients eligible for active surveillance. *J Urol.* 2008;180(5):1964–1967; discussion 1967–1968.

253. Porten SP, Whitson JM, Cowan JE, *et al.* Changes in prostate cancer grade on serial biopsy in men undergoing active surveillance. *J Clin Oncol.* 2011;29(20):2795–2800.

254. Porten SP, Whitson JM, Cowan JE, *et al.* Changes in cancer volume in serial biopsies of men on active surveillance for early stage prostate cancer. *J Urol.* 2011;186(5):1825–1829.

255. Jain S, Loblaw A, Vesprini D, *et al.* Gleason upgrading with time in a large prostate cancer active surveillance cohort. *J Urol.* 2015;194(1):79–84.

256. Alam R, Carter HB, Landis P, *et al.* Conditional probability of reclassification in an active surveillance program for prostate cancer. *J Urol.* 2015;193(6):1950–1955.

257. Bul M, Zhu X, Rannikko A, *et al.* Radical prostatectomy for low-risk prostate cancer following initial active surveillance: results from a prospective observational study. *Eur Urol.* 2012;62(2):195–200.

258. Ha YS, Yu J, Patel N, *et al.* Pathologic findings in patients who underwent robot-assisted radical prostatectomy following active surveillance: a prospective study in a single center. *Minerva Urol Nefrol.* 2015;67(1):1–9.

259. van den Bergh RC, Albertsen PC, Bangma CH, *et al.* Timing of curative treatment for prostate cancer: a systematic review. *Eur Urol.* 2013;64(2):204–215.

260. Filippou P, Welty CJ, Cowan JE, *et al.* Immediate versus delayed radical prostatectomy: updated outcomes following active surveillance of prostate cancer. *Eur Urol.* 2015;68(3):458–463.

261. van den Bergh RC, Steyerberg EW, Khatami A, *et al.* Is delayed radical prostatectomy in men with low-risk screen-detected prostate cancer associated with a higher risk of unfavorable outcomes? *Cancer.* 2010;116(5):1281–1290.

262. Warlick C, Trock BJ, Landis P, *et al.* Delayed versus immediate surgical intervention and prostate cancer outcome. *J Natl Cancer Inst.* 2006;98(5):355–357.

263. Ornish D, Lin J, Chan JM, *et al.* Effect of comprehensive lifestyle changes on telomerase activity and telomere length in men with biopsy-proven low-risk prostate cancer: 5-year follow-up of a descriptive pilot study. *Lancet Oncol.* 2013;14(11):1112–1120.

264. Parsons JK, Pierce JP, Mohler J, *et al.* A randomized trial of diet in men with early stage prostate cancer on active surveillance: rationale and design of the Men's Eating and Living (MEAL) Study (CALGB 70807 [Alliance]). *Contemp Clin Trials.* 2014;38(2):198–203.

265. Schoots IG, Petrides N, Giganti F, *et al.* Magnetic resonance imaging in active surveillance of prostate cancer: a systematic review. *Eur Urol.* 2015;67(4):627–636.

266. van den Bergh RC, Ahmed HU, Bangma CH, *et al.* Novel tools to improve patient selection and monitoring on active surveillance for low-risk prostate cancer: a systematic review. *Eur Urol.* 2014;65(6):1023–1031.

267. Fradet V, Kurhanewicz J, Cowan JE, *et al.* Prostate cancer managed with active surveillance: role of anatomic MR imaging and MR spectroscopic imaging. *Radiology.* 2010;256(1):176–183.

268. van As NJ, de Souza NM, Riches SF, *et al.* A study of diffusion-weighted magnetic resonance imaging in men with untreated localised prostate cancer on active surveillance. *Eur Urol.* 2009;56(6):981–987.

269. Margel D, Yap SA, Lawrentschuk N, *et al.* Impact of multiparametric endorectal coil prostate magnetic resonance imaging on disease reclassification among active surveillance candidates: a prospective cohort study. *J Urol.* 2012;187(4):1247–1252.

270. Vasarainen H, Lahdensuo K, Savolainen R, *et al.* Diffusion-weighted magnetic resonance imaging in prostate cancer patients on active surveillance one year after diagnosis and before repeat biopsy. *Scand J Urol.* 2013;47(6):456–461.

271. Da Rosa MR, Milot L, Sugar L, *et al.* A prospective comparison of MRI-US fused targeted biopsy versus systematic ultrasound-guided biopsy for detecting clinically significant prostate cancer in patients on active surveillance. *J Magn Reson Imaging.* 2015;41(1):220–225.

272. Hoeks CM, Somford DM, van Oort IM, *et al.* Value of 3-T multiparametric magnetic resonance imaging and magnetic resonance-guided biopsy for early risk restratification in active surveillance of low-risk prostate cancer: a prospective multicenter cohort study. *Invest Radiol.* 2014;49(3):165–172.

273. Hu JC, Chang E, Natarajan S, *et al.* Targeted prostate biopsy in select men for active surveillance: do the Epstein criteria still apply? *J Urol.* 2014;192(2):385–390.

274. Marliere F, Puech P, Benkirane A, *et al.* The role of MRI-targeted and confirmatory biopsies for cancer upstaging at selection in patients considered for active surveillance for clinically low-risk prostate cancer. *World J Urol.* 2014;32(4):951–958.

275. Loeb S, Bruinsma SM, Nicholson J, *et al.* Active surveillance for prostate cancer: a systematic review of clinicopathologic variables and biomarkers for risk stratification. *Eur Urol.* 2015;67(4):619–626.

276. Bul M, van den Bergh RC, Rannikko A, *et al.* Predictors of unfavourable repeat biopsy results in men participating in a prospective active surveillance program. *Eur Urol.* 2012;61(2):370–377.

277. Iremashvili V, Soloway MS, Rosenberg DL, *et al.* Clinical and demographic characteristics associated with prostate cancer progression in patients on active surveillance. *J Urol.* 2012;187(5):1594–1599.

278. Ploussard G, de la Taille A, Terry S, *et al.* Detailed biopsy pathologic features as predictive factors for initial reclassification in prostate cancer patients eligible for active surveillance. *Urol Oncol.* 2013;31(7):1060–1066.

279. Shappley WV 3rd, Kenfield SA, Kasperzyk JL, *et al.* Prospective study of determinants and outcomes of deferred treatment or watchful waiting among men with prostate cancer in a nationwide cohort. *J Clin Oncol.* 2009;27(30):4980–4985.

280. Merrick GS, Delatore A, Butler WM, *et al.* Transperineal template-guided mapping biopsy identifies pathologic differences between very-low-risk and low-risk prostate cancer: implications for active surveillance. *Am J Clin Oncol.* 2014 Jul 25. [Epub ahead of print]

281. Ploussard G, Xylinas E, Salomon L, *et al.* The role of biopsy core number in selecting prostate cancer patients for active surveillance. *Eur Urol.* 2009;56(6):891–898.

282. Thompson JE, Hayen A, Landau A, *et al.* Medium-term oncological outcomes for extended vs saturation biopsy and transrectal vs transperineal biopsy in active surveillance for prostate cancer. *BJU Int.* 2015;115(6):884–891.

283. Wong LM, Toi A, Van der Kwast T, *et al.* Regular transition zone biopsy during active surveillance for prostate cancer may improve detection of pathological progression. *J Urol.* 2014;192(4):1088–1093.

284. Suardi N, Gallina A, Capitanio U, *et al.* Age-adjusted validation of the most stringent criteria for active surveillance in low-risk prostate cancer patients. *Cancer.* 2012;118(4):973–980.

285. Anderson CB, Sternberg IA, Karen-Paz G, *et al.* Age is associated with upgrading at confirmatory biopsy among men with prostate cancer treated with active surveillance. *J Urol.* 2015;194(6):1607–1611.

286. Margel D, Nandy I, Wilson TH, *et al.* Predictors of pathological progression among men with localized prostate cancer undergoing active surveillance: a sub-analysis of the REDEEM study. *J Urol.* 2013;190(6):2039–2045.

287. Bhindi B, Kulkarni GS, Finelli A, *et al.* Obesity is associated with risk of progression for low-risk prostate cancers managed expectantly. *Eur Urol.* 2014;66(5):841–848.

288. Cohn JA, Dangle PP, Wang CE, *et al.* The prognostic significance of perineural invasion and race in men considering active surveillance. *BJU Int.* 2014;114(1):75–80.

289. Jalloh M, Myers F, Cowan JE, *et al.* Racial variation in prostate cancer upgrading and upstaging among men with low-risk clinical characteristics. *Eur Urol.* 2015;67(3):451–457.

290. Ploussard G, de la Taille A, Bayoud Y, *et al.* The risk of upstaged disease increases with body mass index in low-risk prostate cancer patients eligible for active surveillance. *Eur Urol.* 2012;61(2):356–362.

291. Goh CL, Saunders EJ, Leongamornlert DA, *et al.* Clinical implications of family history of prostate cancer and genetic risk single nucleotide polymorphism (SNP) profiles in an active surveillance cohort. *BJU Int.* 2013;112(5):666–673.

292. Ankerst DP, Xia J, Thompson IM, *et al.* Precision medicine in active surveillance for prostate cancer: development of the canary-early detection research network active surveillance biopsy risk calculator. *Eur Urol.* 2015;68(6):1083–1088.

293. Iremashvili V, Burdick-Will J, Soloway MS. Improving risk stratification in patients with prostate cancer managed by active surveillance: a nomogram predicting the risk of biopsy progression. *BJU Int.* 2013;112(1):39–44.

294. Isharwal S, Makarov DV, Carter HB, *et al.* DNA content in the diagnostic biopsy for benign-adjacent and cancer-tissue areas predicts the need for treatment in men with T1c prostate cancer undergoing surveillance in an expectant management programme. *BJU Int.* 2010;105(3):329–333.

295. Tosoian JJ, Loeb S, Kettermann A, *et al.* Accuracy of PCA3 measurement in predicting short-term biopsy progression in an active surveillance program. *J Urol.* 2010;183(2):534–538.

296. Lin DW, Newcomb LF, Brown EC, *et al.* Urinary TMPRSS2:ERG and PCA3 in an active surveillance cohort: results from a baseline analysis in the Canary Prostate Active Surveillance Study. *Clin Cancer Res.* 2013;19(9):2442–2450.

297. Berg KD, Vainer B, Thomsen FB, *et al.* ERG protein expression in diagnostic specimens is associated with increased risk of progression during active surveillance for prostate cancer. *Eur Urol.* 2014;66(5):851–860.

298. Ploussard G, Isbarn H, Briganti A, *et al.* Can we expand active surveillance criteria to include biopsy Gleason 3+4 prostate cancer? A multi-institutional study of 2,323 patients. *Urol Oncol.* 2015;33(2):71.e1–9.

299. Raldow AC, Zhang D, Chen MH, *et al.* Risk group and death from prostate cancer: implications for active surveillance in men with favorable intermediate-risk prostate cancer. *JAMA Oncol.* 2015;1(3):334–340.

300. Zumsteg ZS, Spratt DE, Pei I, *et al.* A new risk classification system for therapeutic decision making with intermediate-risk prostate cancer patients undergoing dose-escalated external-beam radiation therapy. *Eur Urol.* 2013;64(6):895–902.

301. van den Bergh RC, Roemeling S, Roobol MJ, *et al.* Gleason score 7 screen-detected prostate cancers initially managed expectantly: outcomes in 50 men. *BJU Int.* 2009;103(11):1472–1477.

302. Bul M, van den Bergh RC, Zhu X, *et al.* Outcomes of initially expectantly managed patients with low or intermediate risk screen-detected localized prostate cancer. *BJU Int.* 2012;110(11):1672–1677.

303. Kirkham AP, Haslam P, Keanie JY, *et al.* Prostate MRI: who, when, and how? Report from a UK consensus meeting. *Clin Radiol.* 2013;68(10):1016–1023.

304. Siddiqui MM, Rais-Bahrami S, Turkbey B, *et al.* Comparison of MR/ultrasound fusion-guided biopsy with ultrasound-guided biopsy for the diagnosis of prostate cancer. *JAMA.* 2015;313(4):390–397.

305. Liberati A, Altman DG, Tetzlaff J, *et al.* The PRISMA statement for reporting systematic reviews and meta-analyses of studies that evaluate health care interventions: explanation and elaboration. *Ann Intern Med.* 2009;151(4):W65–94.

306. Young HH. The early diagnosis and radical cure of carcinoma of the prostate. Being a study of 40 cases and presentation of a radical operation which was carried out in four cases. 1905. *J Urol.* 2002;167(2 Pt 2):939–946; discussion 947.

307. Eggener SE, Scardino PT, Walsh PC, *et al.* Predicting 15-year prostate cancer specific mortality after radical prostatectomy. *J Urol.* 2011;185(3):869–875.

308. Holmberg L, Bill-Axelson A, Helgesen F, *et al.* A randomized trial comparing radical prostatectomy with watchful waiting in early prostate cancer. *N Engl J Med.* 2002;347(11):781–789.

309. Miller DC, Sanda MG, Dunn RL, *et al.* Long-term outcomes among localized prostate cancer survivors: health-related quality-of-life changes after radical prostatectomy, external radiation, and brachytherapy. *J Clin Oncol.* 2005;23(12):2772–2780.

310. Sanda MG, Dunn RL, Michalski J, *et al.* Quality of life and satisfaction with outcome among prostate-cancer survivors. *N Engl J Med.* 2008;358(12):1250–1261.

311. Stephenson AJ, Kattan MW, Eastham JA, *et al.* Defining biochemical recurrence of prostate cancer after radical prostatectomy: a proposal for a standardized definition. *J Clin Oncol.* 2006;24(24):3973–3978.

312. Young HH. The early diagnosis and radical cure of carcinoma of the prostate. Being a study of 40 cases and presentation of a radical operation which was carried out in four cases. 1905. *J Urol.* 2002;168(3):914–921.

313. Steineck G, Helgesen F, Adolfsson J, *et al.* Quality of life after radical prostatectomy or watchful waiting. *N Engl J Med.* 2002;347(11):790–796.

314. Berglund RK, Tangen CM, Powell IJ, *et al.* Ten-year follow-up of neoadjuvant therapy with goserelin acetate and flutamide before radical prostatectomy for clinical T3 and T4 prostate cancer: update on Southwest Oncology Group Study 9109. *Urology.* 2012;79(3):633–637.

315. Gleave ME, Goldenberg SL, Chin JL, *et al.* Randomized comparative study of 3 versus 8-month neoadjuvant hormonal therapy before radical prostatectomy: biochemical and pathological effects. *J Urol.* 2001;166(2):500–506; discussion 506–507.

316. Goldenberg SL, Klotz LH, Srigley J, *et al.* Randomized, prospective, controlled study comparing radical prostatectomy alone and neoadjuvant androgen withdrawal in the treatment of localized prostate cancer. Canadian Urologic Oncology Group. *J Urol.* 1996;156(3):873–877.

317. Soloway MS, Pareek K, Sharifi R, *et al.* Neoadjuvant androgen ablation before radical prostatectomy in cT2bNxMo prostate cancer: 5-year results. *J Urol.* 2002;167(1):112–116.

318. Yee DS, Lowrance WT, Eastham JA, *et al.* Long-term follow-up of 3-month neoadjuvant hormone therapy before radical prostatectomy in a randomized trial. *BJU Int.* 2010;105(2):185–190.

319. Kang DC, Hardee MJ, Fesperman SF, *et al.* Low quality of evidence for robot-assisted laparoscopic prostatectomy: results of a systematic review of the published literature. *Eur Urol.* 2010;57(6):930–937.

320. Di Pierro GB, Baumeister P, Stucki P, *et al.* A prospective trial comparing consecutive series of open retropubic and robot-assisted laparoscopic radical prostatectomy in a centre with a limited caseload. *Eur Urol.* 2011;59(1):1–6.

321. Amling CL, Bergstralh EJ, Blute ML, *et al.* Defining prostate specific antigen progression after radical prostatectomy: what is the most appropriate cut point? *J Urol.* 2001;165(4):1146–1151.

322. D'Amico AV, Moul JW, Carroll PR, *et al.* Surrogate end point for prostate cancer-specific mortality after radical prostatectomy or radiation therapy. *J Natl Cancer Inst.* 2003;95(18):1376–1383.

323. Arlen PM, Bianco F, Dahut WL, *et al.* Prostate Specific Antigen Working Group guidelines on prostate specific antigen doubling time. *J Urol.* 2008;179(6):2181–2185; discussion 2185–2186.

324. Vickers A, Bennette C, Steineck G, *et al.* Individualized estimation of the benefit of radical prostatectomy from the Scandinavian Prostate Cancer Group randomized trial. *Eur Urol.* 2012;62(2):204–209.

325. Bill-Axelson A, Holmberg L, Filen F, *et al.* Radical prostatectomy versus watchful waiting in localized prostate cancer: the Scandinavian prostate cancer group-4 randomized trial. *J Natl Cancer Inst.* 2008;100(16):1144–1154.

326. Brehaut JC, O'Connor AM, Wood TJ, *et al.* Validation of a decision regret scale. *Med Decis Making.* 2003;23(4):281–292.

327. Clark JA, Wray N, Brody B, *et al.* Dimensions of quality of life expressed by men treated for metastatic prostate cancer. *Soc Sci Med.* 1997;45(8):1299–1309.

328. Davison BJ, Matthew A, Gardner AM. Prospective comparison of the impact of robotic-assisted laparoscopic radical prostatectomy versus open radical prostatectomy on health-related quality of life and decision regret. *Can Urol Assoc J.* 2014;8(1–2):E68–72.

329. Nguyen PL, Chen MH, Hoffman KE, *et al.* Cardiovascular comorbidity and treatment regret in men with recurrent prostate cancer. *BJU Int.* 2012;110(2):201–205.

330. O'Carroll RE, Steele RJ, Libby G, *et al.* Anticipated regret to increase uptake of colorectal cancer screening in Scotland (ARTICS): study protocol for a randomised controlled trial. *BMC Public Health.* 2013;13:849.

331. Harden JK, Sanda MG, Wei JT, *et al.* Partners' long-term appraisal of their caregiving experience, marital satisfaction, sexual satisfaction, and quality of life 2 years after prostate cancer treatment. *Cancer Nurs.* 2013;36(2):104–113.

332. Bianco FJ, Albala DM, Belkoff LH, *et al.* A randomized, double-blind, solifenacin succinate versus placebo control, phase 4, multicenter study evaluating urinary continence after robotic assisted radical prostatectomy. *J Urol.* 2015;193(4):1305–1310.

333. Alemozaffar M, Sanda M, Yecies D, *et al.* Benchmarks for operative outcomes of robotic and open radical prostatectomy: results from the Health Professionals Follow-up Study. *Eur Urol.* 2015;67(3):432–438.

334. Brock G, Montorsi F, Costa P, *et al.* Effect of tadalafil once daily on penile length loss and morning erections in patients after bilateral nerve-sparing radical prostatectomy: results from a randomized controlled trial. *Urology.* 2015;85(5):1090–1096.

335. Menon M, Muhletaler F, Campos M, *et al.* Assessment of early continence after reconstruction of the periprostatic tissues in patients undergoing computer assisted (robotic) prostatectomy: results of a 2 group parallel randomized controlled trial. *J Urol.* 2008;180(3):1018–1023.

336. Prasad SM, Large MC, Patel AR, *et al.* Early removal of urethral catheter with suprapubic tube drainage versus urethral catheter drainage alone after robot-assisted laparoscopic radical prostatectomy. *J Urol.* 2014;192(1):89–95.

337. Raz O, Boesel TW, Arianayagam M, *et al.* The effect of the modified Z trendelenburg position on intraocular pressure during robotic assisted laparoscopic radical prostatectomy: a randomized, controlled study. *J Urol.* 2015;193(4):1213–1219.

338. Sutherland DE, Linder B, Guzman AM, *et al.* Posterior rhabdosphincter reconstruction during robotic assisted radical prostatectomy: results from a phase II randomized clinical trial. *J Urol.* 2011;185(4):1262–1267.

339. Yoo YC, Kim NY, Shin S, *et al.* The intraocular pressure under deep versus moderate neuromuscular blockade during low-pressure robot assisted laparoscopic radical prostatectomy in a randomized trial. *PLoS One.* 2015;10(8):e0135412.

340. Joshi N, de Blok W, van Muilekom E, *et al.* Impact of posterior musculofascial reconstruction on early continence after robot-assisted laparoscopic radical prostatectomy: results of a prospective parallel group trial. *Eur Urol.* 2010;58(1):84–89.

341. Takenaka A, Tewari A, Hara R, *et al.* Pelvic autonomic nerve mapping around the prostate by intraoperative electrical stimulation with simultaneous measurement of intracavernous and intraurethral pressure. *J Urol.* 2007;177(1):225–229; discussion 229.

342. Wei JT, Dunn RL, Litwin MS, *et al.* Development and validation of the expanded prostate cancer index composite (EPIC) for comprehensive assessment of health-related quality of life in men with prostate cancer. *Urology.* 2000;56(6):899–905.

343. Potosky AL, Harlan LC, Stanford JL, *et al.* Prostate cancer practice patterns and quality of life: the Prostate Cancer Outcomes Study. *J Natl Cancer Inst.* 1999;91(20):1719–1724.

344. Stanford JL, Feng Z, Hamilton AS, *et al.* Urinary and sexual function after radical prostatectomy for clinically localized prostate cancer: the Prostate Cancer Outcomes Study. *JAMA.* 2000;283(3):354–360.

345. Johansson E, Steineck G, Holmberg L, *et al.* Long-term quality-of-life outcomes after radical prostatectomy or watchful waiting: the Scandinavian Prostate Cancer Group-4 randomised trial. *Lancet Oncol.* 2011;12(9):891–899.

346. Polascik TJ, Walsh PC. Radical retropubic prostatectomy: the influence of accessory pudendal arteries on the recovery of sexual function. *J Urol.* 1995;154(1):150–152.

347. Clark JA, Wray NP, Ashton CM. Living with treatment decisions: regrets and quality of life among men treated for metastatic prostate cancer. *J Clin Oncol.* 2001;19:72–80.

348. Joseph-Williams N, Edwards A, Elwyn G. The importance and complexity of regret in the measurement of 'good' decisions: a systematic review and a content analysis of existing assessment instruments. *Health Expect.* 2011;14(1):59–83.

349. Li S, Zhou K, Sun Y, *et al.* Anticipated regret, risk perception, or both: which is most likely responsible for our intention to gamble? *J Gambl Stud.* 2010;26(1):105–116.

350. Lavery HJ, Levinson AW, Hobbs AR, *et al.* Baseline functional status may predict decisional regret following robotic prostatectomy. *J Urol.* 2012;188(6):2213–2218.

351. Schroeck FR, Krupski TL, Sun L, *et al.* Satisfaction and regret after open retropubic or robot-assisted laparoscopic radical prostatectomy. *Eur Urol.* 2008;54(4):785–793.

352. Cahlon O, Zelefsky MJ, Shippy A, *et al.* Ultra-high dose (86.4 Gy) IMRT for localized prostate cancer: toxicity and biochemical outcomes. *Int J Radiat Oncol Biol Phys.* 2008;71(2):330–337.

353. Dearnaley DP, Sydes MR, Graham JD, *et al.* Escalated-dose versus standard-dose conformal radiotherapy in prostate cancer: first results from the MRC RT01 randomised controlled trial. *Lancet Oncol.* 2007;8(6):475–487.

354. Peeters ST, Heemsbergen WD, Koper PC, *et al.* Dose-response in radiotherapy for localized prostate cancer: results of the Dutch multicenter randomized phase III trial comparing 68 Gy of radiotherapy with 78 Gy. *J Clin Oncol.* 2006;24(13):1990–1996.

355. Cellini N, Morganti AG, Mattiucci GC, *et al.* Analysis of intraprostatic failures in patients treated with hormonal therapy and radiotherapy: implications for conformal therapy planning. *Int J Radiat Oncol Biol Phys.* 2002;53(3):595–599.

356. Pucar D, Hricak H, Shukla-Dave A, *et al.* Clinically significant prostate cancer local recurrence after radiation therapy occurs at the site of primary tumor: magnetic resonance imaging and step-section pathology evidence. *Int J Radiat Oncol Biol Phys.* 2007;69(1):62–69.

357. van Lin EN, Futterer JJ, Heijmink SW, *et al.* IMRT boost dose planning on dominant intraprostatic lesions: gold marker-based three-dimensional fusion of CT with dynamic contrast-enhanced and 1H-spectroscopic MRI. *Int J Radiat Oncol Biol Phys.* 2006;65(1):291–303.

358. Fonteyne V, Villeirs G, Speleers B, *et al.* Intensity-modulated radiotherapy as primary therapy for prostate cancer: report on acute toxicity after dose escalation with simultaneous integrated boost to intraprostatic lesion. *Int J Radiat Oncol Biol Phys.* 2008;72(3):799–807.

359. Kuang Y, Wu L, Hirata E, *et al.* Volumetric modulated arc therapy planning for primary prostate cancer with selective intraprostatic boost determined by 18F-choline PET/CT. *Int J Radiat Oncol Biol Phys.* 2015;91(5):1017–1025.

360. Miralbell R, Molla M, Rouzaud M, *et al.* Hypofractionated boost to the dominant tumor region with intensity modulated stereotactic radiotherapy for prostate cancer: a sequential dose escalation pilot study. *Int J Radiat Oncol Biol Phys.* 2010;78(1):50–57.

361. Riches SF, Payne GS, Desouza NM, *et al.* Effect on therapeutic ratio of planning a boosted radiotherapy dose to the dominant intraprostatic tumour lesion within the prostate based on multifunctional MR parameters. *Br J Radiol.* 2014;87(1037):20130813.

362. Lips IM, van der Heide UA, Haustermans K, *et al.* Single blind randomized phase III trial to investigate the benefit of a focal lesion ablative microboost in prostate cancer (FLAME-trial): study protocol for a randomized controlled trial. *Trials.* 2011;12:255.

363. Zelefsky MJ, Ben-Porat L, Scher HI, *et al.* Outcome predictors for the increasing PSA state after definitive external-beam radiotherapy for prostate cancer. *J Clin Oncol.* 2005;23(4):826–831.

364. Graefen M, Ohori M, Karakiewicz PI, *et al.* Assessment of the enhancement in predictive accuracy provided by systematic biopsy in predicting outcome for clinically localized prostate cancer. *J Urol.* 2004;171(1):200–203.

365. Tsuzuki T, Hernandez DJ, Aydin H, *et al.* Prediction of extraprostatic extension in the neurovascular bundle based on prostate needle biopsy pathology, serum prostate specific antigen and digital rectal examination. *J Urol.* 2005;173(2):450–453.

366. Naya Y, Slaton JW, Troncoso P, *et al.* Tumor length and location of cancer on biopsy predict for side specific extraprostatic cancer extension. *J Urol.* 2004;171(3):1093–1097.

367. Kestin LL, Goldstein NS, Vicini FA, *et al.* Percentage of positive biopsy cores as predictor of clinical outcome in prostate cancer treated with radiotherapy. *J Urol.* 2002;168(5):1994–1999.

368. FDA Drug Safety Communication: 5-alpha reductase inhibitors (5-ARIs) may increase the risk of a more serious form of prostate cancer. Available: http://www.fda.gov/Drugs/DrugSafety/ucm258314.htm; Accessed March 12, 2016.

369. European Association of Urology (EAU) guidelines for prostate cancer. Available: http://uroweb.org/wp-content/uploads/EAU-Guidelines-Prostate-Cancer-2015-v2.pdf; Accessed March 12, 2016.

370. Ohori M, Eastham J, Koh H, *et al.* Is focal therapy reasonable in patients with early stage prostate cancer (CaP)—an analysis of radical prostatectomy (RP) specimens [abstract 1574]. *J Urol.* 2006;75:507.

371. Ceriotti F, Pontillo M, Lazzeri M, *et al.* Prostate cancer: Biomarkers: Definition of the Limit of Detection (LoD) for serum isoform [-2]proPSA in patients with recurrent prostate cancer after radical prostatectomy: An analytic study 28th Annual EAU Congress 2013; Milan, Italy. Abstract 855.

372. Lazzeri M, Lughezzani G, Abrate A, *et al.* Sensitivity of [-2]proPSA as an ultrasensitive PSA surrogate for the prediction of early biochemical recurrence after radical prostatectomy: an observational cohort study. AUA Annual Meeting 2015; New Orleans, LA. Abstract MP6-07.

C2-I

Imaging in Localized Prostate Cancer:
I. Multiparametric Ultrasound

CHAIR

Eric Barret, France

CO-CHAIR

Olivier Rouvière, France

MEMBERS

Jean Michel Correas, France
Jean de la Rosette, The Netherlands
Tim Idzenga, The Netherlands
Petr Macek, Czech Republic
Olivier Hélénon, France
Arnoud Postema, The Netherlands
Arjun Sivaraman, France
Hessel Wijkstra, The Netherlands

CONTENTS

Imaging in Localized Prostate Cancer:
I. Multiparametric Ultrasound

I-2.1 Introduction

The introduction of transrectal ultrasound (TRUS) for prostate imaging in the 1980s occupies an important landmark in prostate imaging.[1] The TRUS system offers excellent visualization of the prostate, guidance for biopsy, and treatment options like focal therapy using various energy sources. It is widely available, fast, low cost, and usually performed by urologists with or without local anesthesia, with minimal inter-observer variability. The evolving treatment trends in prostate cancer (PCa) management demands the most accurate cancer imaging information, but the overall performance of TRUS in PCa cancer localization and staging is disappointing.[2] Though cross-sectional imaging like magnetic resonance imaging (MRI) provides superior cancer information,[3] several investigators have attempted to add imaging adjuncts to the conventional grey-scale TRUS technology to improve the overall performance and, hence, the term "multiparametric ultrasound" (mp-US).[4] In this section, we publish an extensive review of the scientific literature concerning modalities in prostate ultrasound.

I-2.2 Technical Aspects of TRUS

I-2.2.1 Basic concepts of TRUS

The introduction of reliable imaging of the prostate has improved diagnosis and enabled PCa localization. Transrectal ultrasound was the first imaging modality used to aid in the diagnosis of PCa.

FIGURE 2.I-1

A Chair device with a rectal probe for TRUS imaging of the prostate.

B The first 3.5 MHz transducer on a rotating probe.

C B-scan of the prostate with a malignancy (indicated by the arrow) using a 3.5 MHz transducer.

With reprint permission from: Resnick MI. J Ultrasound Med. 2003;22(9): 869-877.

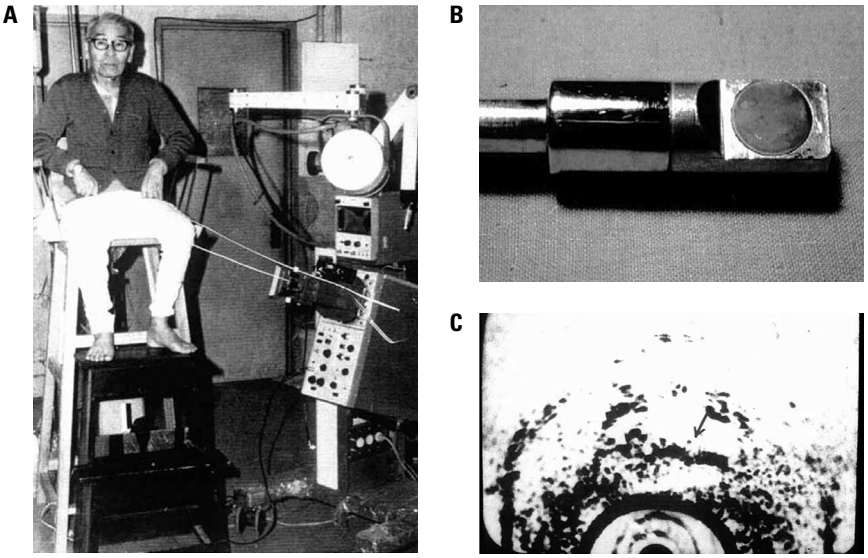

Transrectal ultrasound is still the most commonly used imaging modality. The ultrasound equipment is mobile and readily available, as opposed to alternative methods such as MRI and computed tomography (CT). Initially, in 1957, TRUS was described as a technology to assess rectal pathology.[5,6] Takahashi and Ouchi used TRUS to evaluate the prostate for the first time in 1963.[7] At that time, TRUS was still at the beginning of its development, and the image quality was not yet suitable for clinical interpretation. It was in 1968 that Watanabe *et al.* produced the first clinically applicable images of the prostate obtained with TRUS.[8,9] They used a chair device and transrectal radial probe with a 3.5 MHz transducer covered with a water-filled balloon (**Figure 2.I-1**).

This first endocavity ultrasound probe consisted of an ultrasound receiver mounted at 90° from the long axis of the probe. A 360° motor-driven sweep was made to provide highly reproducible static sonograms. In the following decades, ultrasound technology became more refined and, among other things, the frequency of the probes increased. With the earlier scanners, the majority of the investigators were convinced that cancers appeared as hyperechoic on the sonogram.[10] In the mid-80s, the frequency of the transducers increased to 5 MHz and then up to 7 MHz. These higher frequencies reduced the penetration depth but resulted in a higher level of detail and a better delineation of the architecture of the prostate. These transducers also demonstrated that tumours are generally hypoechoic.[11] This opened the door to localizing tumours in the prostate.

When used in conjunction with prostate needle biopsy, the detection rate (DR) of PCa dramatically exceeded that obtained in historical series of screening by digital rectal examination (DRE). In 1987, the first report was published on the application of TRUS in transrectal biopsy.[12]

With improved ultrasound imaging technology, TRUS became more and more the standard technique to guide the needle in performing a core biopsy of the prostate. From the first electronically rotated 1D transducer by Watanabe *et al.*, 2D ultrasound transducers were developed. These evolved via bi-plane and tri-plane transducers toward transducers that made three-dimensional (3D) imaging of the prostate possible. The currently state-of-the-art TRUS probes are 3 to 10 MHz handheld probes with a 4D (3D+t) imaging capability. For taking prostate biopsies using TRUS, the transrectal probes can be fitted with an adapter through which the biopsy needle is guided. Nowadays, when there is a suspicion of PCa based on DRE and prostate-specific antigen (PSA), ultrasound-guided biopsies typically follow.

I-2.2.1.1 TRUS probe

The first ultrasound probe that was used in 1967 by Watanabe *et al.* for TRUS imaging can be considered as a side-fire probe.[5] This probe consisted of one transducer mounted at an angle of 90° with respect to the long axis. Nowadays, TRUS probes consist of an array of elements that can each transmit ultrasound pulses and receive the echoes from the tissue. This array of elements can be oriented at 90° on the long axis (side-fire; see **Figure 2.I-2A** for an example) or at 0° on the long axis (end-fire; see **Figure 2.I-2B** for an example). One application for TRUS transducers is guiding the needle that is used to take prostate biopsies. In this procedure, there is a tendency to favour the end-fire probe over the side-fire probe.[13,14] The hypothesis of the authors was that the curved array at the tip of the end-fire probe allows more control and flexibility in manoeuvering the biopsy needle to the intended biopsy location.

FIGURE 2.I-2
A Side-fire TRUS probe.
B End-fire TRUS probe.

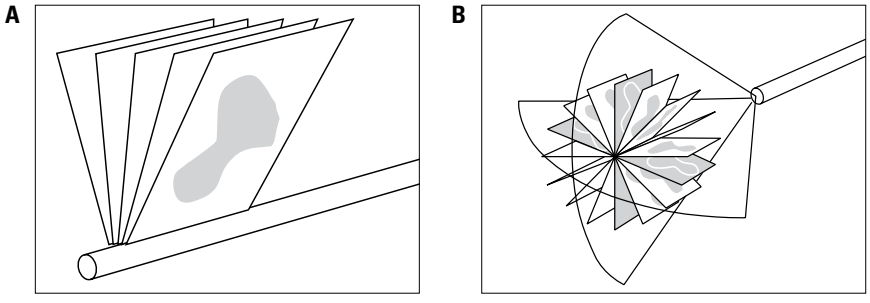

I-2.2.2 Diagnosing prostate cancer using grey-scale TRUS

The conventional techniques for diagnosing PCa are based on grey-scale TRUS. With the early transducers, the tumours were identified by their hyperechogenicity. With the higher frequency transducer, most peripheral zone (PZ) tumours came up as hypoechoic.[1] Prostate cancer may appear as hypoechoic on the sonogram because the stroma is replaced by infiltrating glandular tumour elements, but lesions can also appear as iso- or hyperechoic. Larger lesions usually turn up on the ultrasound image as hypoechoic. Shinohara *et al.* compared TRUS scans from 70 patients with the whole-mount histological section.[15] They found that 60% of the tumours were hypoechoic, and 30% were isoechoic and therefore difficult to distinguish from the surrounding tissue. On the other hand, TRUS could not only be used to diagnose and localize PCa, but also to determine the stage of the tumour. Rifkin *et al.* evaluated 51 histologically confirmed PCas.[16] They found that the Gleason score (GS) of the tumour correlated with the echogenicity of the lesions on the sonogram, whereas isoechoic lesions were associated with anaplastic, high-grade tumours.

Diagnosing and staging of PCa based on grey-scale TRUS images turned out to be not as straightforward. To improve the diagnosing and staging, several techniques have been developed.

I-2.2.2.1 Colour Doppler ultrasound imaging

In 1989, colour Doppler TRUS entered the armamentarium of PCa detection techniques.[17] Doppler imaging was based on quantifying the vasculature in the prostate to detect and localize prostate tumours based on the development of neovessels around the tumour (angiogenesis). Colour Doppler gave information on the direction and velocity of red blood cells, thereby identifying the vasculature in the prostate gland.

FIGURE 2.I-3
Example of Power Doppler Images for a 70-Year-Old Man Who Had cT1c Cancer With GS 6 on Image-Blind Systematic Biopsy at an Outside Facility

TRUS identified a hypoechoic lesion in the left base, suspicious for involvement of the left seminal vesicle (SV). TRUS-guided targeted staging biopsies revealed a GS of 7 (3+4).

With reprint permission from: Ukimura et al. BJU Int. 2013;111(8): E354-364.

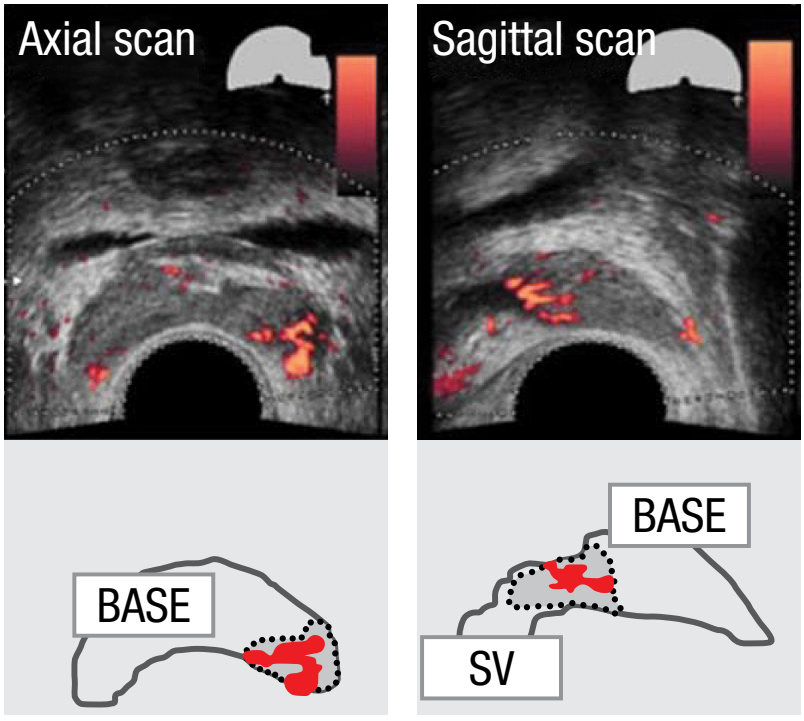

In 1995, power Doppler was introduced. This modality has the advantage over colour Doppler of being angle independent and, therefore, it could increase the useable dynamic range of the Doppler image, i.e. identify smaller vessels (an example is presented in **Figure 2.I-3**). Halpern *et al.*[18] compared grey-scale ultrasound, colour Doppler, and power Doppler in the detection of PCa and found no additional value of power Doppler over colour Doppler. They concluded that grey-scale and Doppler ultrasound did not reveal PCa with sufficient accuracy to avoid systemic biopsies. In 1997, Doppler imaging was enhanced with the use of contrast agents, which increased the contrast of blood with respect to the surrounding tissue.[19] With this study of a small group of 15 patients, the researchers concluded that contrast-enhanced ultrasonography promises to be a useful technique for better imaging of prostatic blood flow and might allow for a more accurate identification of malignant lesions.

I-2.2.2.1.1 Clinical performance of colour Doppler imaging

Sauvain *et al.* investigated the value of transrectal power Doppler sonography (PDS) in the detection of low-risk PCa.[20] In a study of 413 patients, 243 (59%) of these patients had a PSA level <10 ng/mL without a palpable lesion; of the 243 patients, 106 patients presented a cancer (cT1c). Fifty-eight of these 106 patients also had an abnormal PDS. With an abnormal PDS, the probability of having a positive biopsy is 57%, and the probability of having a significant cancer is 30%. In the population of 243 patients with a PSA level <10 ng/mL, the authors found a 45% sensitivity and a 74% specificity for PDS in diagnosing low-risk cancers.

Tsai *et al.* measured parameters such as the end-diastolic (blood flow) velocity (EDV) and the resistive index (RI) at each neurovascular bundle site.[21] These parameters were derived from the Doppler spectral waveform. In a group of 292 patients who also received systemic biopsies, EDV and RI

showed comparable diagnostic performance (area under the curve [AUC]=0.687 and 0.657, respectively), which was less than that of the PSA level (AUC=0.812). Among patients with a PSA level <20 ng/mL, the diagnostic performance of EDV and RI was comparable to that of PSA. At a cut-off value of 4.5 mL/second, EDV showed a 65.5% sensitivity and 66.7% specificity. The sensitivity and specificity of RI was 71.5% and 60.3%, respectively, at a cut-off of 0.71. The researchers concluded that the Doppler spectral parameters were not suitable for the detection of PCa in patients with a PSA level <10 ng/mL, but might help in diagnosing PCa in patients with PSA levels between 10 and 20 ng/mL.

I-2.2.3 Staging prostate cancer using grey-scale TRUS

Accurate clinical staging of PCa is of major importance in selecting the proper therapy for patients. For the staging of PCa, the Tumour Node Metastasis (TNM) classification is used. Several criteria have been proposed for the staging of PCa. The initial criterion was that of the overall shape and symmetry of the prostate. However, irregularities in shape and symmetry can also be attributed to benign prostatic hyperplasia (BPH) nodules. An increase in anterior-posterior diameter could be characteristic of PCa. This usually occurs with tumours of large volume, and in these cases staging is less relevant. When staging of PCa is relevant, TRUS mainly focuses on the distinction between tumours that are confined within the prostate (T1 and T2) and tumours that extend outside the prostate capsule (T3). In the case of a T3 grade tumour, there is also the distinction between extracapsular extension (ECE) and seminal vesicle invasion (SVI) that determines whether the tumour is of grade T3a or T3b. Observations on TRUS imaging like bulging, thickening, irregularity interruption, and asymmetrical contour have all been associated with capsular invasion. To identify SVI, some criteria have also been proposed. Asymmetry and hypoechoic regions within the SVs are suspicious indications of tumour extension.

Several studies have been performed to assess the accuracy of grey-scale TRUS in staging PCa. In one of the first preliminary studies, Peeling *et al.* identified the prostate capsule on TRUS images of 58 out of the 60 men who were included.[22] An ultrasound diagnosis of PCa was made in 32 out of the 33 men with proven disease, and they detected non-integrity only in the prostate capsule of 17 men with proven cancer. Many following studies compared the diagnostic performance of grey-scale TRUS with that of a DRE and/or MRI.

Vapnek *et al.* compared 64 patients' diagnostic performance of radiographic staging (MRI and/or TRUS) and DRE with histopathology after radical prostatectomy (RP).[23] The staging accuracies for MRI (67%) and TRUS (63%) were better than for DRE (42%), although MRI and TRUS suffered from understaging (22% and 31%, respectively). In the evaluation of ECE, TRUS performed better than MRI in terms of positive predictive value (PPV) (81% vs. 77%), but the negative predictive value (NPV) was disappointing (58% versus 56%). In the evaluation of SVI, both radiographic techniques performed poorly in terms of PPV (50% versus 40%), but excellently in terms of NPV (90% versus 96%).

In a multicentre trial, Smith *et al.* assessed the performance of DRE and TRUS prospectively in 263 patients.[24] Histological evidence of ECE and seminal vesical invasion was found in 231 and 52 patients, respectively. The areas under the receiver operating characteristics curve (ROC) for detection of ECE were 0.69 for TRUS and 0.72 for DRE. For detection of SVI, the areas under the

ROC curve were 0.74 and 0.69. In both cases, the results from TRUS and DRE were not significantly different. Their conclusion was that TRUS offered no unique or superior information compared with DRE in staging the local extent of PCa.

Ohori *et al.* investigated TRUS as a technique to identify ECE in comparison with DRE. The results from the two approaches were not significantly different but, by combining DRE and TRUS, they found a PPV of 79% and a sensitivity of 91%.[25]

Other favourable results have been published by Shinohara *et al.* They found in a retrospective study that the maximum diameter of the tumour as measured by TRUS correlated linearly with histology. Opposite results in terms of favourability have been published by Rorvik *et al.*; they reported an overall sensitivity of 68% and a specificity of 63% for TRUS in staging PCa.[26] Rifkin *et al.* compared the results from TRUS and MRI in staging PCa. From the total of 230 patients who were included in the study, TRUS staged 46% correctly, whereas MRI staged 57% correctly.[27] Finally, two studies presented results on the accuracy of TRUS in depicting ECE and SVI. In a population of 620 patients, Eisenberg *et al.* found an area under the ROC curve of 0.77.[28] In a similar population of 101 patients, Jung *et al.* found an area under the ROC curve of 0.81.[29]

A few studies focused on the detection of specific tumour grades using grey-scale TRUS. Ohori *et al.* assessed impalpable PCas defined as T1c and whether the visibility of these tumours on ultrasound is associated with different pathological features and/or prognoses, as compared with nonvisible impalpable tumours.[30] In 323 patients, the clinical stage was defined as impalpable cancer regardless of TRUS, as detected by needle biopsy. They found no difference in pathological features and progression between cancers that were visible and nonvisible on TRUS. Therefore, they concluded that in staging impalpable PCas, TRUS has no additional value. Similar results were reported by Augustin *et al.*[31] Hsu *et al.*, on the other hand, studied the detection of clinical unilateral T3a PCas.[32] A total of 267 patients underwent a DRE and TRUS prior to an RP, and the results were compared with pathology. In approximately 25% of the patients, the cancer was overstaged by DRE and/or TRUS, but the combination of DRE and TRUS gave the best results in staging T3a PCa: sensitivity 71%, specificity 41%, PPV 50%, and NPV 63%. Colombo *et al.* compared preoperative TRUS with pathology results after RP in 114 patients.[33] In 68% of the RP specimens, organ-confined cancer was correctly found by TRUS, and ECE was correctly identified in 32%. The staging performance of TRUS for organ-confined cancers (stage T1-2) was as follows: sensitivity 66%, specificity 33%, and PPV 56%. For advanced cancers (stage T3a/b/c), it was: sensitivity 33%, specificity 68%, and PPV 46%.

Since organ-confined PCas and those that display ECE and/or seminal vesicular invasion require a different treatment, it is important to stage PCas prior to treatment. The performance of grey-scale TRUS in staging PCa is still sub-optimal, and the combination with DRE does not provide much improvement in staging performance.

In general, it can be concluded that TRUS is a relatively good method for detection and diagnosis of PCa, and is more accurate than DRE. TRUS can be considered suitable for guiding the prostate biopsy needle. However, accurate localization of PCa would make targeted biopsies possible. Accurate localization of PCa also aids tremendously in selecting the right focal therapy for the patients. For staging purposes, TRUS is not the most suitable technique.

I-2.3 Contrast-Enhanced Ultrasound

Contrast-enhanced ultrasound (CEUS) targets the altered vascularization exhibited by various malignancies, including PCa. Through the process of tumour angiogenesis, prostatic tumours match increased vascularization to their metabolic needs. Without angiogenesis, prostate tumours cannot progress from small dormant lesions to clinically significant disease.[34] Various aspects of this altered blood supply are targeted by CEUS imaging techniques: higher perfusion of the malignant tissues, altered blood flow patterns caused by the abnormal structure of the microvasculature, and even the characteristic expression of molecules within the vasculature of prostate tumours. By exploiting these differences between malignant and benign prostate tissue, CEUS helps the observer detect, target, and monitor PCa.

I-2.3.1 Ultrasound contrast agents

In CEUS, an ultrasound contrast agent (UCA) is used to visualize or quantify blood flow. The first UCAs were unencapsulated air bubbles (first generation) and air bubbles with albumin or galactose shells (second generation). The current, third-generation UCAs are micro bubbles filled with perfluorocarbon gasses and use phospholipid, albumin, or polymer shells. Commonly used agents are SonoVue® by Bracco Suisse S.A., Definity® by Lantheus Medical Imaging, and Sonazoid™ by GE Healthcare. The use of heavier gasses and optimized shells have stabilized the bubbles, allowing prolonged in vivo half-lives, which are currently around 6 minutes.[35]

The micro bubbles have a diameter similar to that of red blood cells, in the range of 2 to 8 μm. Their small size enables the micro bubbles to pass through the microvasculature. The micro bubbles do not pass the vascular endothelium, and therefore remain in the intravascular compartment. Despite their size, micro bubbles are highly echogenic, and modern ultrasound scanners can detect a single micro bubble passing through the microvasculature.[36] The UCA is typically administered as a bolus injection just prior to TRUS imaging of the prostate or as a continuous intravenous catheter infusion during imaging.

Ultrasound contrast agents are safe. Adverse reactions are rare and UCAs are not nephrotoxic, as opposed to many radiographic contrast agents. The main cause of serious adverse events are anaphylactic shock, with an estimated incidence of 1 in 10,000.[37] The safety of using UCAs in patients with severe cardiopulmonary compromise has been questioned, although recent reports show that the use of UCAs in those patients is not accompanied with higher mortality.[38] Contraindications for UCA

use related to cardiopulmonary disease are regularly updated; it is advisable to check up-to-date listings of contraindications before UCA use and to keep epinephrine, or other medication to counter anaphylactic shock, at hand.

I-2.3.2 Contrast-enhanced Doppler imaging

The first use of UCAs in PCa imaging was in combination with the Doppler techniques. Doppler imaging in PCa is based on detecting the increased neovascularization associated with prostate tumours. Neovascularization starts with the formation of very small micro vessels in which blood flow is slow and hard to detect. With a continuous infusion of a UCA, a large number of highly echogenic scatterers are added to the bloodstream, increasing the sensitivity of the Doppler techniques to detect blood flow in small, low-flow vessels.[39]

In 2001, Sedelaar *et al.* showed that microvessel density (MVD) associated with PCa presence and prognosis is 1.93 times higher in areas that showed enhancement with contrast-enhanced power Doppler, compared to areas that showed no enhancement.[34,40] Through 3D contrast-enhanced power Doppler scanning, they were able to find 86% of tumours in a cohort of 70 patients scheduled for RP.[41] Various studies have compared the DRs of systematic biopsies with contrast-enhanced Doppler or contrast-enhanced power Doppler-targeted biopsies. The per-core DR is higher for the targeted biopsies. However, the PPV for an enhancing lesion is low. Furthermore, too many tumours are detected only by systematic biopsy to recommend omitting systematic biopsies.[42-44] One drawback of Doppler ultrasound is that it uses relatively high-energy ultrasound pulses, which causes premature bursting of the micro bubbles as they move into the imaging field.[45]

I-2.3.3 Dynamic contrast-enhanced ultrasound imaging

To overcome the aforementioned limitations of contrast-enhanced Doppler imaging, new low-energy scanning techniques have been developed that exploit the physical characteristics of the micro bubbles. When micro bubbles are insonified at frequencies commonly used in prostate TRUS, they start to oscillate non-linearly. The magnitude of the oscillating response depends on the stiffness of the shell and the relation between the size of micro bubble and the scanning frequency used. The non-linear oscillations produce reflected signals that are fractional multiples (harmonics) of the insonification frequency. These non-linear reflections can be detected and separated from the generally linear reflections of the tissues, enabling contrast-specific imaging, the key feature of harmonic, or dynamic contrast-enhanced ultrasound (DCE-US).[46] Three common techniques to separate contrast reflections from tissue reflections are pulse inversion, power modulation, and contrast pulse sequencing. Modern ultrasound scanners allow split-screen depiction of the grey-scale images and the contrast-specific images simultaneously to enable navigation through the prostate. The combination of contrast-specific imaging and the ability to detect single micro bubbles flowing through microvasculature allows visualization of blood flow patterns on both the macro- and microvascular scales.

During interpretation of DCE-US images, several features are associated with malignancy: asymmetrical rapid inflow, enhancing foci crossing the zonal borders, increased focal enhancement, and asymmetry of the intraprostatic vessels.[47] Asymmetrical rapid inflow is the most important distinguishing feature and can be best assessed after the injection of a UCA bolus while imaging one plane at a time. Alternatively, a flash-replenishment technique has been used in which all in-field micro bubbles are destroyed by a strong ultrasound pulse and the inflow of new micro bubbles is assessed thereafter.[48,49]

I-2.3.3.1 Clinical performance of DCE-US

Only limited data are available that evaluate the performance of DCE-US compared to RP specimens. Early studies by Halpern *et al.*[49] and Matsumoto *et al.*[50] achieved sensitivities of 42% and 41% in their cohorts of 12 and 50 patients, respectively. Because no tumour-negative regions were included in their analysis, specificity cannot be calculated from their data. Sano *et al.*[51] scanned 13 patients before prostatectomy and were able to detect 10 tumours with an average diameter of 18.7 mm using DCE-US, but missed the smaller tumours with an average diameter of 5.9 mm. Seitz *et al.*[47] performed DCE-US in 30 patients scheduled for prostatectomy and 5 patients scheduled for cysto-prostatectomy, with the observer blinded to whether PCa had previously been detected or not. The per-patient sensitivity and specificity, PPV, and NPV were 71%, 50%, 92%, and 13%, respectively. The varying results reported by the few small studies that compare DCE-US imaging with RP specimens call for larger well-designed trials with standardized and up-to-date imaging protocols. Xie *et al.*[52] correlated systematic biopsy results with DCE-US imaging in 150 patients and reported a per-biopsy site sensitivity, specificity, PPV, and NPV of 73%, 87%, 66%, and 90%. Zhao *et al.*[53] attained a sensitivity of 79% and a specificity of 86% for DCE-US correlated to systematic biopsy results in their cohort of 65 patients. Additionally, they performed targeted biopsies to help characterize both false negatives and false positives, and found that BPH and acute or chronic inflammation were associated with false positives. False negatives were mostly encountered in people with low serum PSA, normal DRE, low cancer volume, and moderately differentiated to well-differentiated tumours. Halpern *et al.*[54] compared the DRs of up to 6 DCE-US targeted cores and 12 core systematic biopsy results in 272 patients. Their data show a higher per-core DR for the targeted biopsies (16.4% vs. 8.5%); however, the per-patient DR was lower for the targeted cores than for the systematic biopsies (26% vs. 39%). Although biopsy studies almost universally show an added benefit of adding DCE-US–targeted biopsies to systematic biopsies, too many significant PCas are being missed by current targeted biopsy techniques to justify taking only the targeted biopsies.[55] Because the signs of malignancy displayed by DCE-US are often subtle, there is a considerable learning curve and user dependency associated with interpretation of the DCE-US imaging.

I-2.3.3.2 Quantification of DCE-US

FIGURE 2.I-4
Contrast Enhanced Ultrasound Imaging of Prostate Cancer

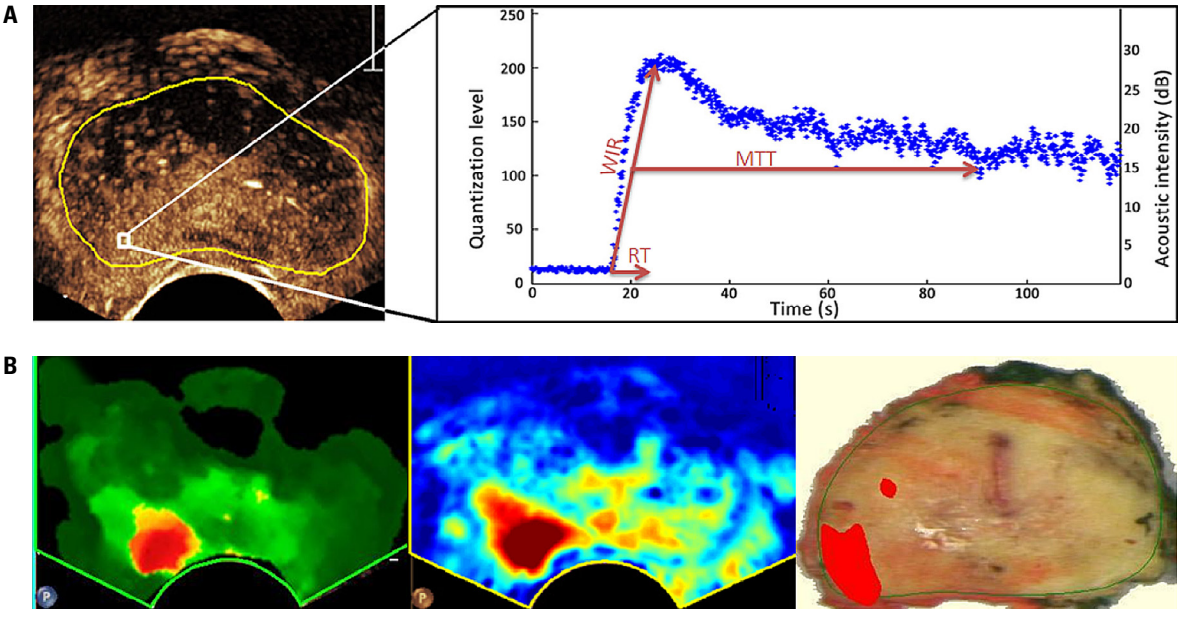

A Example of a time-intensity curve (TIC) for a given pixel.

B Left: Example of a probability map (red indicates a high suspicion) generated by dedicated software under the development of Bracco Suisse S.A. that analyzes the dispersion of wash-in rates (WiRs) among neighbouring pixels. Middle: Contrast ultrasound dispersion imaging map indicating a region of similarly shaped TICs, suspicious for PCa presence (marked red). Right: Histopathological examination of the same plane confirmed PCa presence in the right PZ (marked red).

Image taken from: Postema A, Idzenga T, Mischi M, et al. Ultrasound modalities and quantification: developments of multiparametric ultrasonography, a new modality to detect, localize and target prostatic tumors. Curr Opin Urol. 2015;25(3):191–197.

To reduce the user dependency associated with DCE-US interpretation and to enable detection of differences in blood-flow patterns too subtle for human interpretation, quantification techniques are being developed. Quantification techniques in DCE-US use algorithms to extract blood flow parameters from the recorded DCE-US images. The basis of these quantification techniques is the assessment of the enhancement of different regions over time, as the UCA spreads through the prostate. These time–intensity curves (TICs) for individual pixels or regions of interest are plotted and, from these TICs, various blood flow–related parameters can be extracted, such as WiR, rise time (RT), and mean transit time (MTT), which is the time between the 50% levels of the wash-in and wash-out phase of the TICs (**Figure 2.I-4**). Quantification software under development by Bracco Suisse S.A. can be used in various organs, including the liver and the mammary glands, and has been used in the prostate with promising results.[56] Using a prototype of this software package, Jung *et al.*[57] analyzed the DCE-US recordings of 20 men scheduled for RP. In 30 out of the 34 tumours, early enhancement could be detected using the software analysis, resulting in a sensitivity, specificity, PPV, and NPV of 88%, 100%, 90%, and 60%. The other parameters that were examined, MTT and RT, performed less well, detecting 29 and 25 tumours, respectively.

The current version of the software package enables the generation of maps of various perfusion parameters, as well as probability maps for tumour presence. Calculating the likelihood of tumour presence within a region is based on the statistical analysis of the histograms of WiRs in a small area around each pixel. Statistical parameters, such as the standard deviation and the mode, are calculated from these histograms, and the probability of tumour presence is calculated based on these parameters.

Postema *et al.*[58] used this current version of the software to predict systematic biopsy outcomes in 82 patients. With the use of the probability maps, 36.9% of biopsy locations were identified as suspicious and 63.1% as benign; 7.7% were false negatives. Only 3.5% of the biopsy locations were classified as benign while their corresponding biopsy showed PCa with a GS ≥7 and a per-core tumour involvement of ≥10%.

Other strategies for detecting prostate using DCE-US quantification exist. Mischi *et al.* focus on the dispersion kinetics of the UCA as it moves through the prostate, rather than perfusion parameters.[59] They hypothesize that the characteristics of the angiogenic vessels have unpredictable effects on perfusion on the microvascular level. The increased MVD associated with prostatic tumours and the presence of arteriovenous shunts promotes increased perfusion. Conversely, the increased tortuosity of the angiogenic vessels, the aberrant endothelial lining, and the higher interstitial pressure caused by leakiness of the capillaries have a diminutive effect on perfusion. The irregular structure of the angiogenic microvasculature in prostatic tumours is less efficient and therefore causes predictably lower dispersion of the UCA bolus throughout the prostate. Discrimination between benign and malignant tissue based on perfusion may therefore be less powerful than discrimination-based UCA dispersion kinetics. Their method is based on the observation that low UCA dispersion within a region of the prostate is associated with more similarly shaped TICs within that region. The study group has been refining their method of classifying regions as benign or malignant by using various measures for TIC similarity, including coherence and correlation, and attained an AUC of 0.88 in a dataset of 43 DCE-US recordings from 24 patients from two centres.[60]

I-2.3.4 Future of contrast-enhanced ultrasound

Several technical developments are expected to have a big impact on the field of CEUS in PCa imaging. Firstly, there are advances in the development of the micro bubbles. The ability to detect micro bubbles and separate UCA reflections from tissue reflections will likely improve from UCAs consisting of more uniformly sized micro bubbles.[46] Another development is the use of micro bubbles for molecular imaging. The results of the first clinical trials in humans with the molecularly targeted UCA BR55 are expected in the near future. These micro bubbles carry a heterodimer peptide targeting the vascular endothelial growth factor receptor 2, which is overexpressed in the neovasculature of many cancer types, including prostate, breast, ovarian, and pancreatic cancers. Other molecular targets are in the pre-clinical phase of development. Molecular imaging may play a major role in PCa imaging, as it could aid in early detection and characterization of PCa tumours, as well as molecular profiling of PCas.[61]

Another development is the recent advent of 4D (3D volumes over time) ultrasound scanners with contrast-ready endorectal probes, which will allow assessment of UCA flow throughout the prostate after the infusion of a single UCA bolus. Current 2D scanners allow in- and outflow recording in only one plane at a time, making scanning the entire prostate a costly and time-consuming process. Because blood flow through the prostate is fundamentally a 3D phenomenon, quantification techniques employing both perfusion and dispersion-based models to assess altered blood flow will likely be potentiated by 4D datasets. Secondly, the possibilities to combine imaging techniques and the interest in doing so are taking flight. Three-dimensional tumour probability maps derived from quantification of 4D DCE-US imaging could be fused with real-time grey-scale TRUS to facilitate targeted biopsy procedures. Dynamic contrast-enhanced ultrasound can be combined with other ultrasound modalities such as shear wave (SW) elastography and C-TRUS, forming what is called "multiparametric ultrasound." By effectively combining different imaging modalities that target different characteristics of PCa, superior discrimination between malignant and benign tissue should be possible.[4]

I-2.4 Real-Time Elastography

The increased stiffness of the prostate harbouring PCa compared to the normal prostate is a feature that has been used for decades for the detection of PCa using DRE.[62] However, DRE is facing many limitations, including subjectivity, inter-observer variability,[63] and limited accuracy for staging disease and locating the different foci,[64] which are two factors mandatory for planning primary therapy. An imaging technique able to map tissue elasticity could therefore be useful in detecting and locating cancer areas within the prostate. Up until recently, conventional imaging techniques did not provide any information about the elastic properties of organs. However, the elasticity (or, equivalently, the stiffness) of tissues in the body changes as disease progresses over several months and/or decades, depending on the speed of progression. Prostate cancer tissue becomes stiffer than the surrounding healthy prostate tissue due to several changes; there is an increase in cellular density and in microvascularization, destroying the glandular architecture[65] and triggering wound repair. This process is characterized by stromal reaction[65,66] and collagen deposition surrounding the cancer.[67] This deposition of collagen also significantly increases with increasing Gleason grade,[68,69] and is linked to a significant reduction in the acinar area in the PCa stroma. All these changes contribute to the increased stiffness of tissue affected by PCa.[70]

Several studies focused on ex vivo samples, mainly due to the engineering challenges of deploying mechanical devices to measure stiffness in vivo. In the late 1990s, Krouskop *et al.*[71] started to assess the mechanical properties of the prostate tissue. A significant difference between normal and cancerous prostate tissue stiffness was demonstrated.[72-74] Moreover, the increase in tissue stiffness was correlated to the aggressiveness of the disease, as evaluated with the GS,[74] and to the disease severity.[72] This fact is an important finding, as elasticity could help differentiating clinically significant cancer from insignificant disease. Benign prostatic hyperplasia nodules can often induce false positive diagnosis when using DRE and/or TRUS imaging, revealing the presence of prostate nodules at B-mode imaging. Young moduli of BPH versus cancerous tissues nodules are significantly different.[70,72]

Despite the limitations of ex vivo studies, these encouraging results, together with the wide use of TRUS for guiding systematic biopsy, prompted the development of an ultrasound-based elasticity imaging.

I-2.4.1 Prostate elastography techniques and normal pattern

Several ultrasound-based methods were developed in the past years in order to measure in vivo prostate tissue elasticities and provide an elasticity map. They improve both prostate lesion characterization and PCa detection; in particular, this approach can be extremely useful for prostate lesions, disclosing lesions on the elasticity map that are not visible in conventional TRUS imaging (iso-echogenic lesions) or other imaging modalities such as MRI. In fact, it is important to understand that iso-echogenic lesions can be detected with prostate elastography, as the displayed information does not rely on backscattered signals. Elastography may therefore have two major indications: to provide additional information for the characterization of prostate lesions and to improve the detection of PCas.

Two concepts are currently used for ultrasound elastography: the analysis of the strain or deformation of a tissue created by a mechanical force (static elastography or strain elastography), and the analysis of the propagation speed of an SW, which is linked to tissue elasticity.

I-2.4.1.1 Strain elastography

I-2.4.1.1.1 Techniques

Because soft tissues tend to exhibit higher strain (deformation) than stiffer areas when compression is applied, the strain is linked to the stiffness represented by the Young's modulus E by the following equation, where σ is the stress applied to the tissue and ε is the resulting strain:

$$E = \sigma / \varepsilon$$

Static or strain elastography is based on the analysis of the deformation in a sub-region (boxed area) triggered by an external stress (obtained by tissue compression generated by the transducer) or internal stress (generated by the patient's breathing or heart motion). The stress is supposed to be uniform in space and intensity. For prostate elastography, the external stress is applied on the patient's rectal wall, adjacent to the prostate PZ, by using the endocavity end-fire transducer as a compression device. A water-filled balloon placed between the imaging probe and the rectal wall can be used to improve the homogeneity of the deformation.[73] A speckle comparison, before and after compression, yields a colour map of local tissue deformation or strain called elastogram. The stiffness is estimated by visualizing the differences in strain between adjacent regions. Therefore, no quantitative elasticity analysis is available. The stiffness colour scale is automatically distributed from the lowest to the highest strain found in the stiffness box. Thus, the display depends upon the range of stiffness found in the box. This is why the size and position of the stiffness box may induce artifactual variation of the displayed strain; the stiffness box should cover the entire gland and the surrounding tissues. Only qualitative images are provided to the clinician, and semi-quantitative information can be derived by measuring strain ratio between two regions of interest (usually one considered normal in terms

of stiffness and one considered abnormal). The strain for each pixel is colour coded (or grey-scale coded) and displayed as an overlay on the B-mode image. Several years ago, this technique became available on endocavity probes to allow prostate scanning.

I-2.4.1.1.2 Acquisition and interpretation

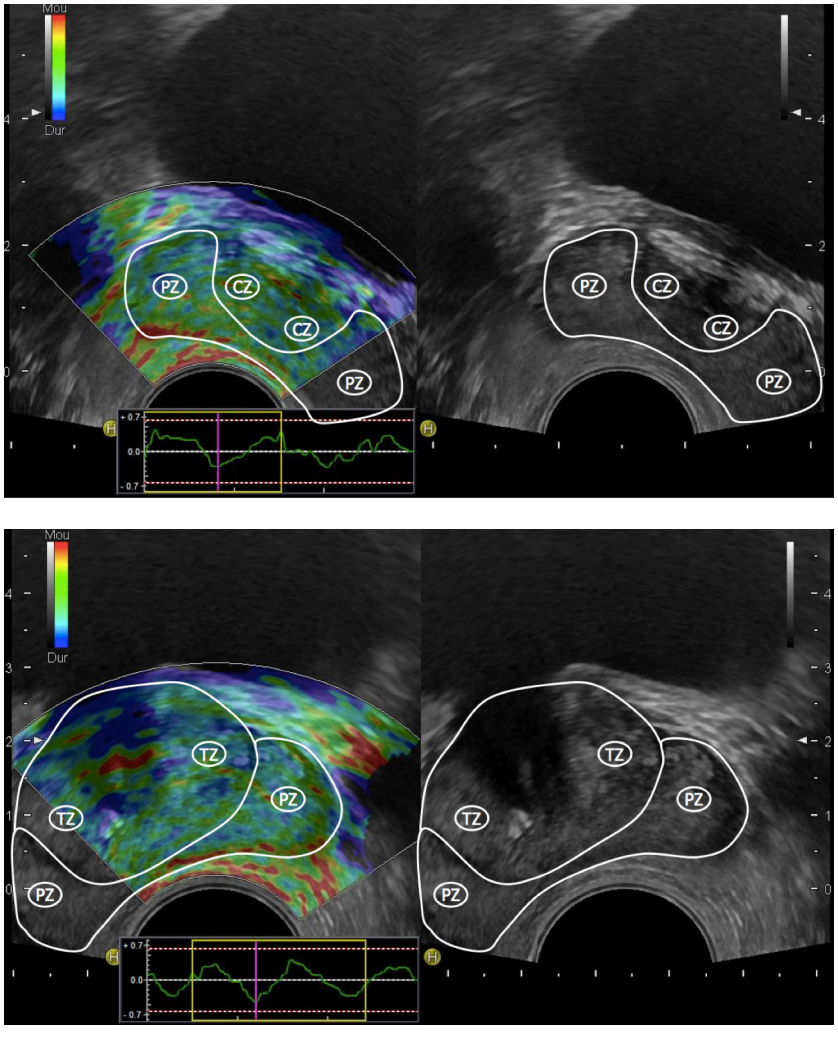

FIGURE 2.I-5
Prostate Strain Elastography: Typical Distribution of Elasticity Pattern in a 60-Year-Old Patient With Moderate BPH

A Transverse view at the base of the prostate, with right lateral rotation of the transducer. The PZ is coded with green and red colours due to soft to intermediate tissue stiffness. Some blue colours are seen at the edges of the gland, corresponding to non-deformation artifacts. At the most upper and anterior part of the gland, it is difficult to separate the central zone (CZ) from the anterior fibromuscular stroma (AFS). The pericapsular elastic border is coded in red (soft) and can be seen posteriorly.

B Transverse view at the junction between the prostate base and mid-gland, with left lateral rotation of the transducer. The PZ appears larger, with the same elasticity pattern. Some blue colours are seen anteriorly and laterally, corresponding to non-deformation artifacts. Transition zone (TZ) exhibits a more heterogeneous pattern due to BPH development. The pericapsular elastic border is coded in red (soft) and can be seen posteriorly.

Continued next page.

FIGURE 2.I-5, CONT'D

C Transverse view at the apex of the prostate, with left lateral rotation of the transducer. The PZ is mainly coded in green due to intermediate elasticity. The pericapsular elastic border is coded in red (soft) and can be seen anteriorly. Note the heterogeneous pattern of the urethra with peripheral ring-shaped lines.

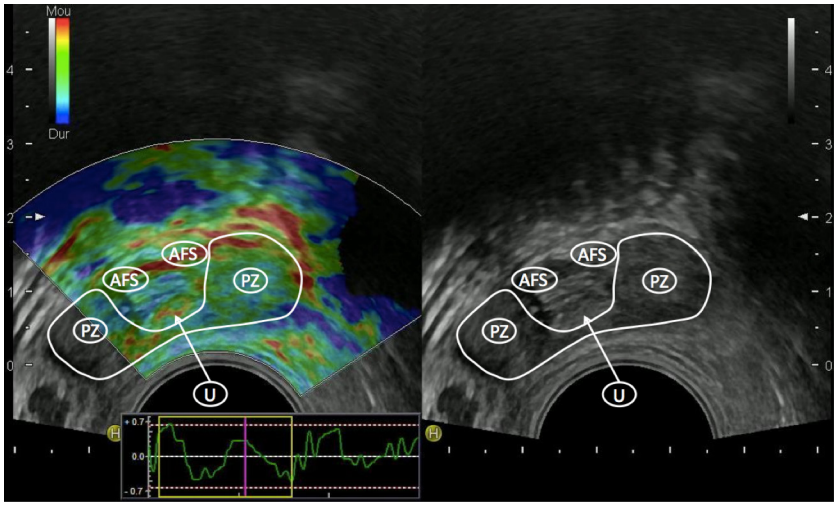

FIGURE 2.I-6
Prostate Strain Elastography of a 68-Year-Old Man With Biopsy-Proven Diffuse Prostate Cancer GS 7

This diagnosis was typically difficult and was initially missed by the MRI study. However, the elasticity pattern revealed the presence of abnormal stiff areas, coded in blue, distributed all over the peripheral and TZs. This pattern was very stable with the compression and decompression cycles.

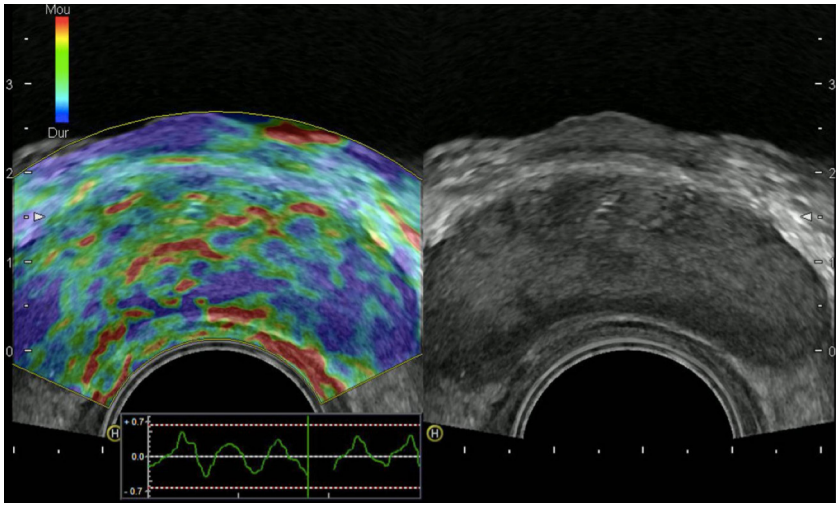

Prostate strain elastography is conducted after a complete B-mode and colour Doppler examination conducted in the transverse and sagittal planes, in order to measure prostate volume, identify suspicious areas in the peripheral gland (mostly hypoechoic and sometimes hypervascular), and analyze the periprostatic space (including the SVs). Strain elastography mode is activated, and each suspicious focal lesion detected during B-mode imaging is analyzed using slight compression–decompression cycles induced by the transrectal probe, while the patient is lying in a left lateral position. The entire gland can also be studied for detection of stiff areas, typically in the transverse plane. The quality index allows controls to ensure appropriate speed and pressure.

Stiff tissues exhibit a reduced strain colour coded in blue, while soft tissues have an increased strain coded in red. Hypoechoic lesions coded in blue are highly suspected to be malignant. The normal strain elastography pattern of the PZ is of intermediate elasticity (**Figure 2.I-5**), while the inner gland

(mostly the transitional zone) shows more heterogeneity and exhibits an increasing stiffness with growing age and volume (**Figure 2.I-5b**).[74] Hypoechoic lesions coded in blue are highly suspicious to be malignant (**Figure 2.I-6**).

I-2.4.1.2 SW elastography

I-2.4.1.2.1 Techniques

A

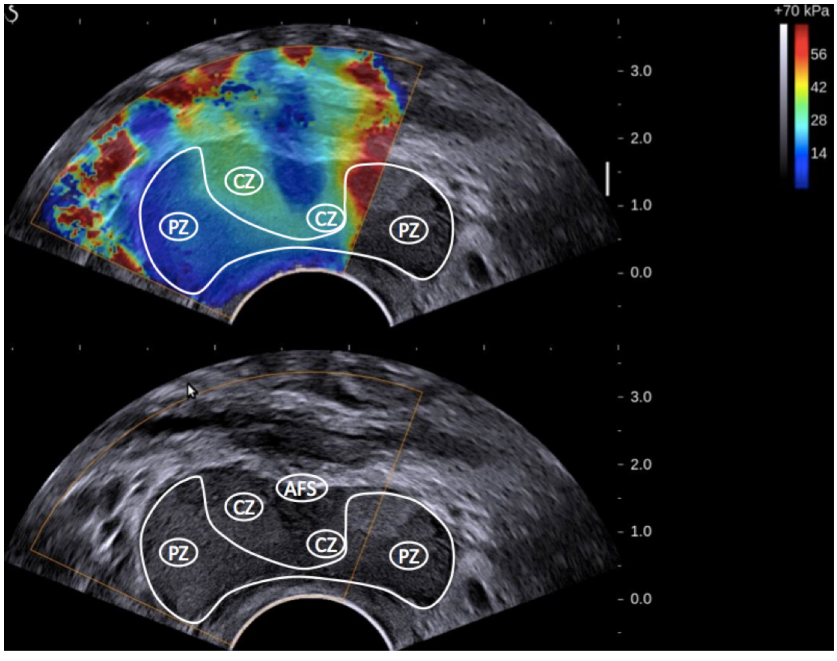

FIGURE 2.I-7
Prostate SW Elastography: Typical Distribution of Elasticity Pattern in a 35-Year-Old Patient With Minimal BPH, From Base (Fig. 2.I-7a) to Apex (Fig. 2.I-7d)

A Transverse view at the base of the prostate. The PZ is homogeneously soft and, thus, is coded with blue colours. The mean stiffness values are typically below 20 kilo Pascal (kPa). The CZ remains rather homogeneous due to minimal development of BPH, and appears slightly stiffer, with mean values ranging from 20 to 30 kPa. Shear wave elastography (SWE) improves the delineation of the two zones. The AFS is easily identified. Note that the space in between the rectal wall and the posterior PZ is coded in blue, reflecting the minimal pressure induced by the endocavity transducer.

Continued next page.

FIGURE 2.I-7, CONT'D

B Transverse view at the junction between the prostate base and mid-gland. The PZ appears larger and remains homogeneous, with typical soft pattern and mean stiffness values below 20 kPa. The CZ is still visible posteriorly rather homogeneous, due to minimal development of BPH, and appears slightly stiffer, with mean values ranging from 20 to 30 kPa. Because of some pressure induced by the transducer on the prostate, the posterior limit between the PZ and the CZ is not well seen at SWE. The TZ appears more heterogeneous due to BPH development.

C Transverse view at prostate mid-gland. The PZ exhibits the same homogeneous soft pattern, with mean stiffness values below 20 kPa. The TZ appears heterogeneous due to BPH development, and some anterior nodules not seen at B-mode imaging are displayed at SWE, with mean stiffness values of 30 to 50 kPa. Due to limited anterior penetration of SWE, the anterior fibromuscular stroma is not colour coded.

Continued next page.

B

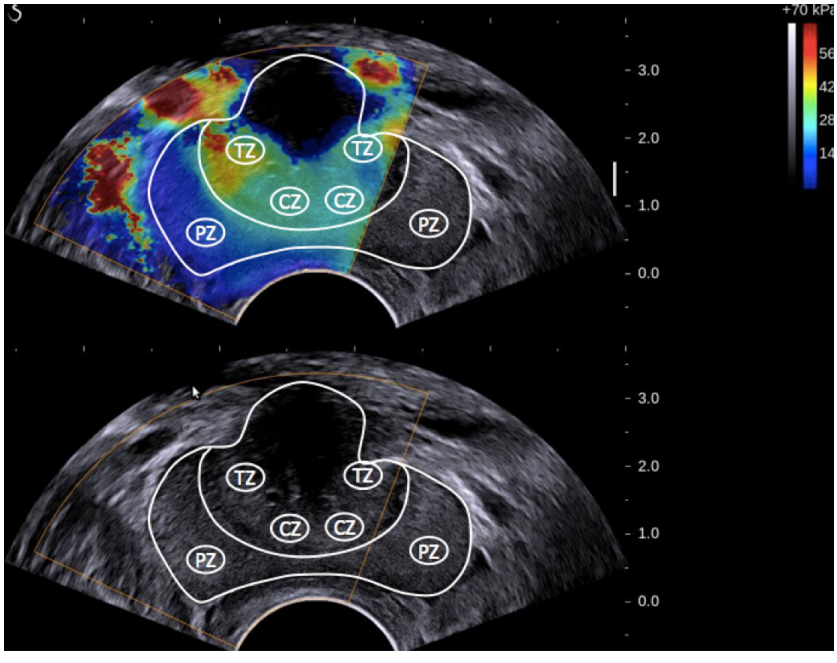

C

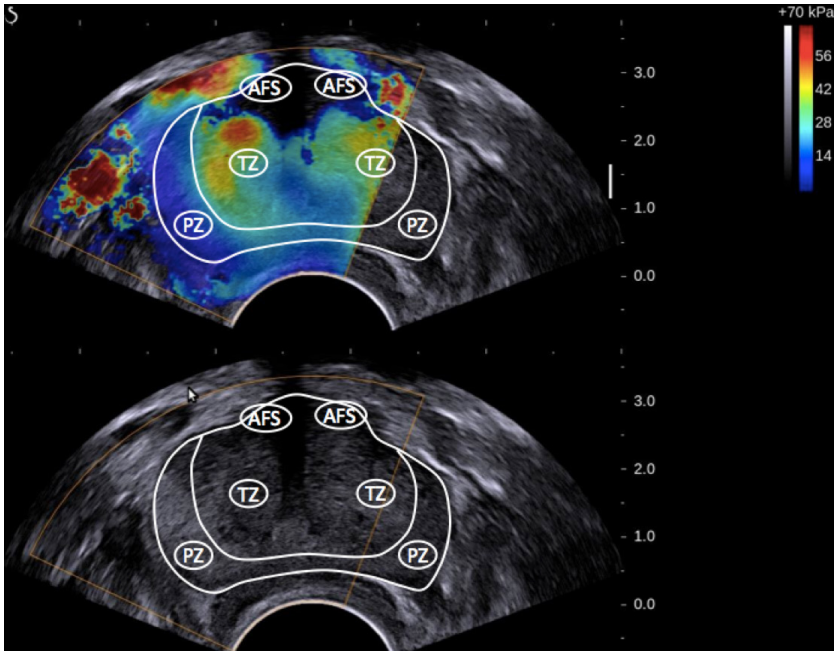

FIGURE 2.I-7, CONT'D

D Transverse view at prostate apex. The PZ exhibits the same homogeneous soft pattern, with mean stiffness values below 20 kPa. The TZ appears heterogeneous due to BPH development, and some anterior nodules not seen at B-mode imaging are displayed at SWE, with mean stiffness values of 30 to 50 kPa. The AFS is not colour coded.

Continued next page.

D

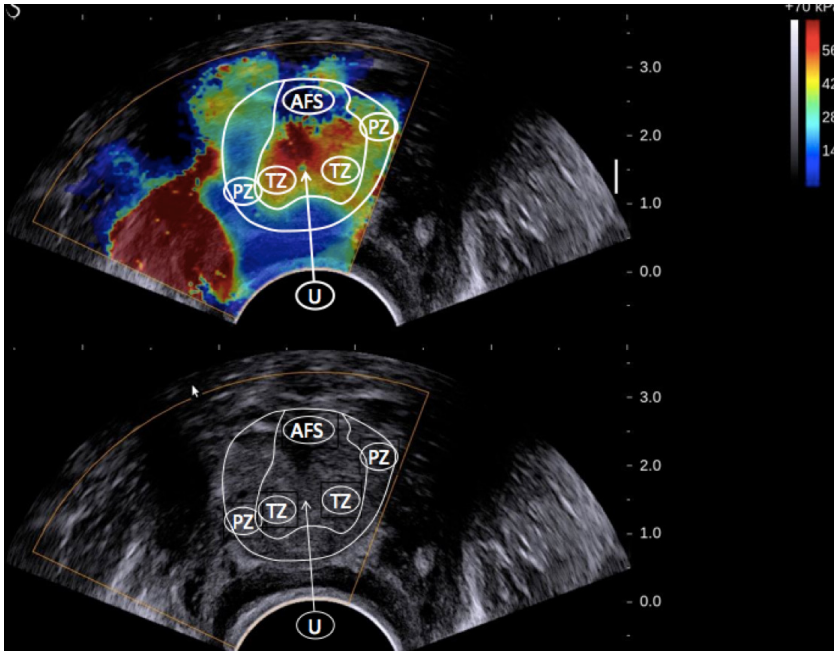

Unlike strain elastography, shear wave elastography (SWE) requires no compression of the rectal wall to produce elastograms. This technique is based on the measurement of SW velocity propagating through the tissues.[75] It belongs to the field of multi-wave imaging, as it combines two different waves: one (SW) that provides stiffness information and another (ultrasonic wave) that captures the propagation of the SW. Thanks to the combination of these two waves, SWE provides a dynamic quantitative map of soft tissues' visco-elastic properties in quasi real time. Mean elasticities are averaged from a region of interest (ROI) and can be displayed in kilo Pascal (kPa) or in metres per second (if SW velocities are displayed). Shear wave elastography's basic principle relies on two successive steps. First, an SW is remotely induced by the endocavity probe through the rectal wall in the prostate using the acoustic radiation force of a focused ultrasonic beam. Second, the SW propagation is captured by imaging the prostate with the endocavity probe. The shear modulus (i.e. stiffness) is derived by measuring the SW propagation velocity. The SW speed (in metres/second [m/s]) or the Young's modulus (in kPa) is colour coded for each pixel and displayed as an overlay on the image in B-mode (**Figure 2.I-7**).

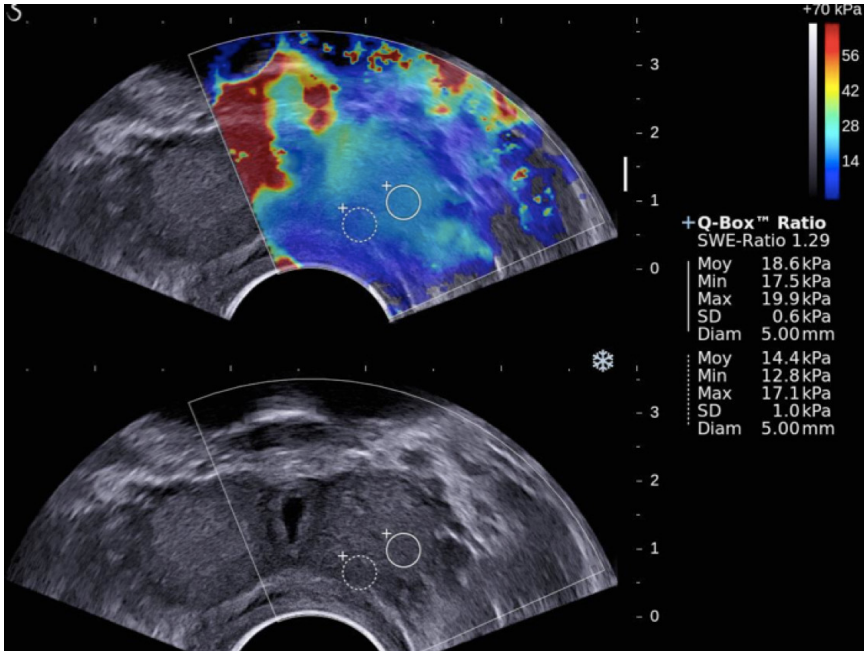

FIGURE 2.I-8
Prostate SWE Allows Quantitative Measurements of Tissue Stiffness Using ROI

The mean stiffness value is displayed for each ROI, and the minimal, maximal, and standard deviation values are calculated. When two ROIs are used to compare stiffness, the SWE elasticity ratio is calculated. This is a true ratio between mean elasticity values. For prostate SWE, the typical scale of displayed elasticity values is set to 50 to 70 kPa. Note that the posterior periprostatic space is colour coded in blue due to minimal pressure of the endocavity transducer.

Stiff tissues are colour coded in red, while soft tissues appear in blue. The elasticity values (mean, standard deviation, min, and max) are then calculated for each ROI (**Figure 2.I-8**). The ratio between the mean values of two ROIs placed in a suspicious region and in the adjacent normal PZ can be calculated (**Figure 2.I-8**). This technology became available on end-fire endocavity transducers only recently, which explains the limited number of published papers.

I-2.4.1.2.2 Acquisition and interpretation

Prostate SWE is also conducted after a complete evaluation of the prostate using B-mode and colour Doppler imaging in a patient lying in a left lateral position. Shear wave elastography mode is activated, and each suspicious focal lesion is analyzed, avoiding any pressure on the transducer. Optimized settings should include maximized penetration and an appropriate elasticity scale (70 to 90 kPa). The entire gland can also be scanned for detection of stiff areas in the transverse plane. The SWE box is enlarged to the maximum in order to cover half of the gland on a transverse plane. Thus, each side of the prostate is scanned separately and images are recorded from base to apex in two separate cineloops. For each plane, the transducer is maintained in a steady position during 3 to 4 seconds, until stabilization of the signals. Hypoechoic lesions coded in red are highly suspected to be malignant. The digital cineloop can be reviewed and ROI can be positioned on suspicious areas detected either at B-mode or during the SWE detection scan, even during the review process. The elasticity values (mean, standard deviation, min, and max) are then calculated for each ROI.

In young patients without prostatic disorder, the peripheral and central zones are coded in blue with a very homogeneous pattern (with the stiffness value ranging from 15 to 25 kPa), while the transitional zone exhibit stiffness below 30 kPa (**Figure 2.I-7**). With the development of benign prostate hypertrophy, the PZ remains soft, with a very homogeneous colour-encoding in blue (soft tissue), while the TZ become heterogeneous and hard (red colour), with a heterogeneous colour pattern and elasticity values ranging from 30 to 180 kPa[76] (**Figure 2.I-7**).

FIGURE 2.I-9

The Typical Pattern of Prostate Cancer at SWE and Its Role for Targeted Biopsy in a 70-Year-Old Man With Normal DRE and PSA Values at 4.9 ng/mL (3.5 ng/mL 2 Years Before)

A Prostate TRUS revealed a moderate increase of prostate volume at 40 mL and a single hypoechogenic nodule at B-mode imaging, with some vascularity detected with power Doppler energy. The nodule was located close to the apex at the anterior PZ (arrows) and was measured (maximal diameter 13 mm, volume 0.8 mL).

B Immediately prior to the biopsy procedure, SWE demonstrated a strong increase in stiffness at 47 kPa, with the adjacent normal PZ stiffness measured at 16 kPa (stiffness ratio: 2.9). At SWE, the stiffness was heterogeneous, and the stiffest area was posterior and internal.

Continued next page.

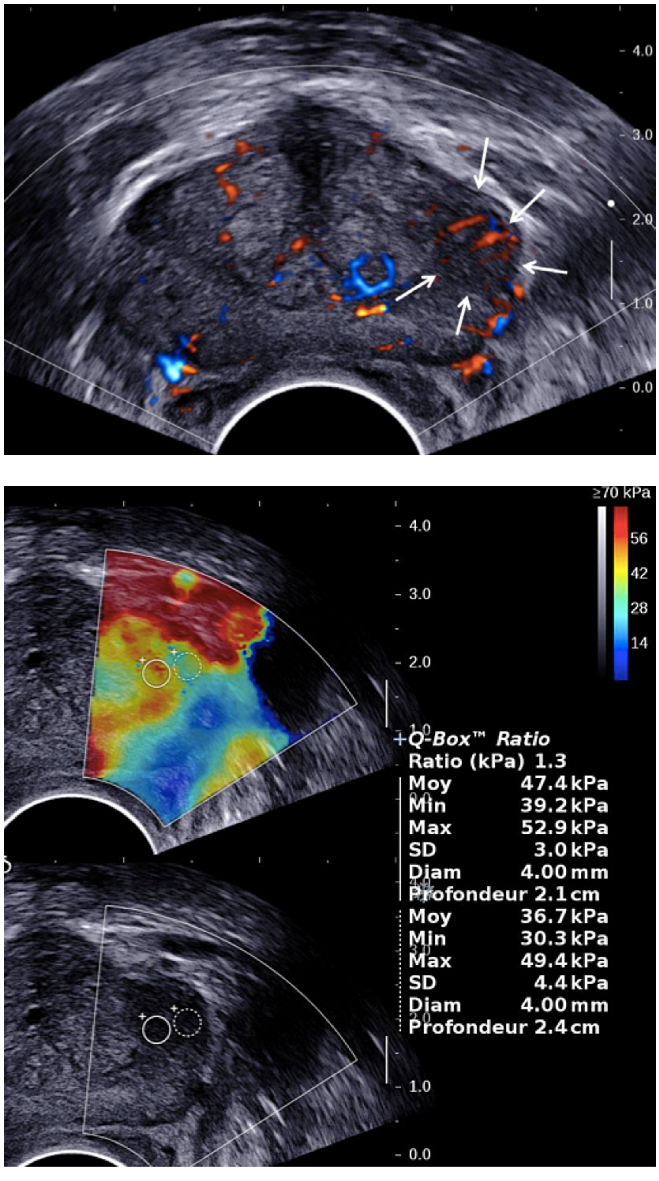

FIGURE 2.I-9, CONT'D

C-D The SWE sweep was performed from base to apex for detection of an additional target isoechogenic lesion at right apex (10 mm in size), with a mean stiffness of 52 kPa. The stiffer area was in contact with the urethra, surrounding it laterally and posteriorly. The targeted biopsies (3 per nodule) confirmed the diagnosis of prostatic adenocarcinoma GS 7 (3+4) for each nodule. For the first nodule detected at the left apex, the cancer length was 15 mm of the 32 mm taken by the 3 core biopsies (ratio: 47%). For the second nodule detected at SWE, the cancer length was 24 mm of the 34 mm taken by the 3 core biopsies (ratio: 71%). The MRI study did confirm the presence of these two nodules without any additional lesion. But systematic biopsies revealed significant PCa (GS 7) at mid-gland on the right and left sides.

C

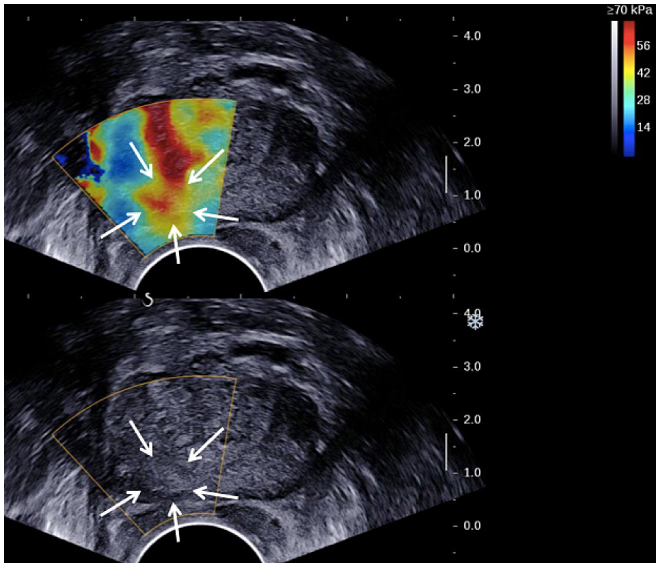

D

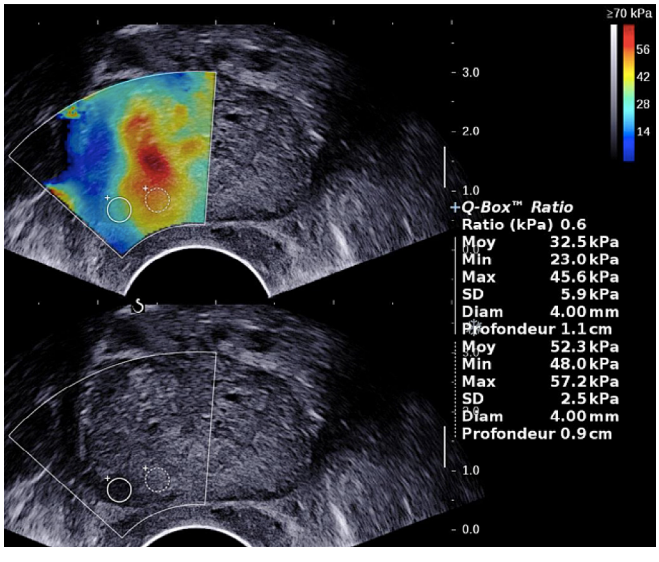

Shear wave elastography reproducibility has been studied in a single paper and showed an excellent overall intra-observer reproducibility (intraclass correlation coefficient=0.876), with minimal impact of ROI location, prostate volume, and clinical variables (intraclass correlation coefficient=0.826–0.917).[150] The real-time capability of SWE allows one to sweep through the whole gland and to perform detection of stiff foci that are not always displayed in the B-mode image (**Figure 2.I-9**). Prostate cancers usually appear as stiffer areas than the surrounding tissue.

I-2.4.2 Literature review

Several studies attest the value of both strain and SWE, as shown in **Table 2.I-1**, **Table 2.I-2**, and **Table 2.I-3**. Three different applications can be identified: first, characterization of an abnormal area detected at B-mode imaging, colour Doppler US, or even previous MRI examination; second, detection of a lesion not seen with any previous imaging technique; and, third, biopsy targeting. Prostate elastography requires specific training; the learning curve may be longer for strain elastography due to the variability of pressure applied with the transducer. Some of the discrepancies in the literature arise from the poorer performance of earliest implementations, and more up-to-date systems seem to be easier to use and seem to provide more consistent results. However, most US manufacturers are also developing SWE techniques and should be extending their use to the endocavity transducers.

I-2.4.2.1 Elastography performance compared with RP

Since systematic biopsies can miss significant PCa, many studies[73,76-88] have been conducted using RP as the gold standard to assess the overall accuracy of strain elastography for PCa diagnosis. A comparison with RP specimens allows for the exact localization, volume, histological type, and extracapsular extension of PCa lesions. Investigators scanning this group of patients might be biased, knowing that RP is scheduled.

TABLE 2.I-1 Summary of Elastography Studies Prior to RP Assessing Diagnostic Performance per Patient and per Core

Reference	Year	Technique	Patients	PCa #	Se (%)	Spe (%)	PPV (%)	NPV (%)	Acc (%)
Pallwein *et al.*[77]	2007	Strain	16	35	87	92	80	95	92
Tsutsumi *et al.*[78]	2007	Strain	51	77	82	60	-	-	-
Sumura *et al.*[79]	2007	Strain	17	-	74	88	-	-	-
Salomon *et al.*[80]	2008	Strain	109	451	75	77	88	59	76
Tsutsumi *et al.*[73]	2010	Strain	55	115	73	89	81	84	83
Walz *et al.*[81]	2011	Strain	28	88	73	79	67	83	77
Walz *et al.*[82]	2011	Strain	32	-	72	81	67	85	-
Brock *et al.*[83]	2011	Strain	229	894	66	72	81	53	68
Junker *et al.*[84]	2012	Strain	39	48	83	-	-	-	-
Pelzer *et al.*[85]	2013	Strain	50	-	-	-	-	-	-
Brock *et al.*[86]	2013	Strain	86	56	49	74	78	51	62
Junker *et al.*[87]	2014	Strain	39	61	67	-	-	-	-
Zhu *et al.*[88]	2014	Strain	56	-	67	89	-	-	83
Boehm *et al.*[76]	2015	SWE	60	60	81	69	67	82	74

Abbreviations: PCa #: prostate cancer lesion number. Se: sensitivity. Spe: specificity. PPV: positive predictive value. NPV: negative predictive value. Acc: accuracy.

The most important studies are summarized in **Table 2.I-1**. In 2011, Brock *et al.* conducted the largest study on strain elastography, including a total of 229 patients with biopsy-proven PCa prospectively screened for cancer-suspicious areas and extra-capsular extension using grey-scale ultrasound and strain elastography.[86] Among the 1,374 sectors evaluated, pathology reported the presence of cancer in 894 (62%) patients and extra-capsular extension in 47 patients. Strain elastography correctly detected 594 (66%) cancer-suspicious lesions, and grey-scale ultrasound correctly detected 215 (24%) cancer-suspicious lesions. Strain elastography sensitivity and specificity were 66% and 72%, respectively (**Table 2.I-1**), compared to 24% and 90%, respectively, for grey-scale ultrasound. Elastography identified the largest side-specific tumour focus in 68% of patients. Extra-capsular extension was identified with a sensitivity of 38% and specificity of 96% using strain elastography, compared to 15% and 97%, respectively, using grey-scale ultrasound. Most studies reported a significant improvement in PCa identification (**Table 2.I-1**); indeed, Zhang *et al.*[89] performed a meta-analysis using seven published studies,[76,79-82,84,90] which included a total of 508 patients, to assess the diagnostic performance of strain elastography using RP as the gold standard. They established that the pooled sensitivity and specificity were 72% (95% confidence interval: 70%–74%) and 76% (74%–78%), respectively. They concluded that strain elastography imaging has high accuracy in the detection of PCa. Several studies[73,80,85,88,89] also showed that PCa DRs using strain elastography are dependent on tumour size, tumour volume, localization, histological type, and extra-capsular extension. Strain elastography was found to be more sensitive in detecting PCa lesions with higher GSs, with large volumes, with extra-capsular extension, and located in the PZ and the apical part.

Boehm *et al.*[76] studied the capability of SWE to localize PCa lesions prior to RP, and also assessed the elasticity threshold for cancer foci detection. They showed that SWE allows the identification of cancer foci based on tissue stiffness differences, and that reliable cutoffs can be established, allowing examiner-independent localization of PCa foci.

In recent years, the concept of focal therapy has gained more and more interest.[91] The limitations of focal therapy for PCa are the multifocal nature of the disease, as well as the problem of correct identification and localization of the PCa lesions by prostate biopsy and/or imaging.[92] The goal of focal therapy is to treat this index lesion only. Walz *et al.*[82] evaluated the ability of strain elastography to identify the PCa index lesion, and they observed a low sensitivity of 59%, whereas systematic biopsies had a sensitivity of 68%. They concluded that if focal therapy had been based on strain elastography alone, only 60% of all patients would have received satisfactory treatment of the index lesion, whereas 40% of the patients would have been undertreated. However, they also noticed that combining biopsy data with strain elastography would have increased the sensitivity to 85%.

I-2.4.2.2 Elastography diagnosis performance compared to systematic biopsies

TABLE 2.I-2 Summary of Elastography (Strain and SWE) Studies Prior to Systematic Biopsy Assessing Diagnostic Performance per Patients and per Core

Reference	Year	Technique	N	PCa #	Per Patient in %					Core #	Per Core in %				
					Se	Spe	PPV	NPV	Acc		Se	Spe	PPV	NPV	Acc
Konig *et al.*[100]	2005	Strain	404	151	84	-	-	-	-	906	51	67	49	68	61
Pallwein *et al.*[101]	2008	Strain	492	125	89	72	62	91	77	2,952	69	89	51	95	87
Kamoi *et al.*[102]	2008	Strain	107	40	68	81	68	81	76	940	75	77	88	59	76
Miyagawa *et al.*[93]	2009	Strain	311	95	73	-	-	-	-	1,539	50	53	22	81	53
Brock *et al.*[103]	2012	Strain	178	91	51	-	-	-	-	1,068	61	68	32	89	68
Barr *et al.*[94]	2012	SWE	53	26	100	-	-	-	-	318	96	96	69	99	96
Ahmad *et al.*[97]	2013	SWE	50	33	-	-	-	-	-	626	92	89	95	83	91
Woo *et al.*[95]	2015	SWE	97	26	-	-	-	-	-	1,058	43	81	13	95	70
Correas *et al.*[96]	2015	SWE	184	68	93	63	59	94	74	-	96	85	48	99	85
Boehm *et al.*[98]	2015	SWE	95	38	95	67	49	90	58	-	-	-	-	-	-

Abbreviations: PCa #: prostate cancer lesion number; Se: sensitivity; Spe: specificity; PPV: positive predictive value; NPV: negative predictive value; Acc: accuracy.

Table 2.I-2 summarizes the studies assessing the diagnostic performance of elastography compared with randomized biopsies. Strain elastography studies reported average to good diagnostic performance, while SWE reported better diagnostic performance; accuracies, sensitivities, and NPVs ranged from 61% to 87 % and 70% to 96%, 50% to 75%, and 92% to 96% (except for Woo *et al.*), and 59% to 95% and 83% to 99%, respectively, for strain elastography and SWE. These improvements can be attributed to the higher reproducibility of SWE and its quantitative nature. Miyagawa *et al.*[93] performed a per-core histology analysis and compared the results with strain elastography data on 311 patients. Among the 1,528 (65%) acquisitions that could be analyzed, 805 cores were found negative and 733 were found positive. Of the 733 positive examinations, only 158 were associated with positive biopsies, leaving 575 elastography-positive acquisitions with negative biopsy, of which 424 (74%) images were considered to show prostatic hyperplasia.

TABLE 2.I-3 Summary SWE Stiffness Mean and Standard Deviation Findings for Benign (All, Normal Tissues, Inflammation, PIN), and Malignant Tissues (For All and GS 6, 7, 8, and 9 Lesions) for Each SWE Study When Available

Reference	Year	N	PCa #	Benign Tissue*				*p*	Malignant Tissue†				
				All	Norm	Infla	PIN		All	GS 6	GS 7	GS 8	GS 9
Barr *et al.*[94]	2012	53	26	22±12	-	-	-	0.0001	58±21	-	-	-	-
Ahmad *et al.*[97]	2013	50	33	75±47	-	-	83±39	0.0001	134±58	95±29	163±63	113±20	-
Woo *et al.*[95]	2015	97	26	33±18	32±17	46±38	26±11	0.002	55±46	33±19	55±49	57±40	88±64
Correas *et al.*[96]	2015	184	68	21±6	-	-	-	<0.0001	60±20	45±7	60±20	70±29	125±29
Boehm *et al.*[98]	2015	95	38	42±20	-	-	-	<0.0001	88±40	-	-	-	-

Abbreviations: Norm: normal; Infla: inflammation; PIN: prostatic intraepithelial neoplasia.
* For Barr *et al.* and Correas *et al.*, GS 6 lesions were considered PCa.
† For Boem *et al.*, Ahmad *et al.*, and Woo *et al.*, GS 6 lesions were considered as non-cancerous lesions.

SWE is a more recent technique, and fewer papers can be found in the literature (**Table 2.I-3**). In all studies, Young's modulus values of PCa were statistically significantly higher when compared with Young's modulus values (**Table 2.I-3**) of benign lesions ($p<0.002$ in all studies). Barr *et al.*[94] showed that the Young modulus value differences between benign lesions were all statistically non-significant: benign versus atypia ($p=0.818$), benign versus acute inflammation ($p=0.606$), benign versus chronic inflammation ($p=0.0509$), and acute inflammation versus chronic inflammation ($p=0.096$), while Woo *et al.*[95] showed significant difference between normal prostate tissue and chronic inflammation ($p=0.021$). Two studies showed a statistically significant linear trend of SWE elasticity with GS (Spearman's rank correlation coefficient equal $\rho=0.343$ in Woo *et al.*[95] and $\rho=0.282$ in Correas *et al.*,[96] both with $p<0.001$). In addition, aggressive PCa exhibited statistically significantly higher tissue stiffness ($p<0.01$ in all studies) than indolent PCa in several studies.[95-97] Boehm *et al.*[76] reported that false-positive results or false-negative results were observed in the anterior and TZ of the prostate gland. In the largest study, by Correas *et al.*,[96] which included 184 patients, sensitivity, specificity, PPV, and NPV were found to be at 97%, 70%, 70%, and 97%, respectively, for a 35 kPa cut-off for diagnosing PCa with GS ≥6. This threshold is very similar to the one found in the Barr *et al.*[94] study, which was 37 kPa. However, it is lower than the ones found in the Ahmad *et al.*,[97] Woo *et al.*,[95] and Boehm *et al.*[76] studies, which were 70 kPa, 43 kPa, and 50 kPa, respectively. In these latter studies, GS 6 lesions were considered as non-cancerous lesions in the statistical analysis. This consideration also explains why, in the Ahmad *et al.*[97] and Boehm *et al.*[76] studies, overall malignant and overall benign tissue mean elasticity values were higher than in Barr *et al.*[94] and Correas *et al.*[96] (**Table 2.I-3**).

I-2.4.2.3 Elastography targeted biopsy DR compared with DR of systematic biopsies

TABLE 2.I-4 DR per Patient and per Core of Elastography (Strain and SWE) With Systematic Biopsies (SB), Targeted Biopsies (TB), and SB+TB

Reference	Year	Technique	N	Study Design	# SB	# TB	DR per Patient %			DR per Core %		
							SB	TB	SB+TB	SB	TB	SB+TB
Konig *et al.*[100]	2005	Strain	404	SB+TB	10	≤4	-	31	37	-	-	-
Pallwein *et al.*[99]	2007	Strain	230	SB+TB	10	≤5	25	30	35	6	13	8
Nelson *et al.*[104]	2007	Strain	137	SB+TB	8	≤4	40	24	44	12	20	14
Kamoi *et al.*[105]	2008	Strain	107	SB+TB	10	≤4	31	29	37	15	55	19
Aigner *et al.*[106]	2010	Strain	94	SB+TB	10	≤5	19	21	28	5	24	8
Kapoor *et al.*[107]	2011	Strain	15	SB+TB	10	≤4	67	73	73	37	67	43
Ganzer *et al.*[108]	2012	Strain	139	SB+TB	10	≤4	47	32	53	11	22	14
Brock *et al.*[103]	2012	Strain	353	Mixed	10	≤10	39	51	45	-	-	-
Zhang *et al.*[109]	2012	Strain	148	SB+TB	12	≤4	-	41	44	14	76	19
Taverna *et al.*[110]	2013	Strain	102	SB	13	-	32	1	33	-	-	-
Salomon *et al.*[111]	2014	Strain	1024	SB+TB	10	≤4	39	29	46	-	-	-
Nygård *et al.*[112]	2014	Strain	127	SB+TB	10–12	≤4	48	24	50	18	28	20
Boehm *et al.*[98]	2015	SWE	95	SB+TB	6–18	≤3	36	28	40	9	11	9

Abbreviations: N: number of patients; SB: systematic biopsies; TB: targeted biopsies.

The clinical utility of elastography-targeted biopsies has been widely studied in recent years (**Table 2.I-4**). To assess the performance of elastography-targeted biopsies, most of the studies are comparing the current standard of systematic 10 to 12 core biopsy schemes with image-targeted biopsies and/or with the combination of both systematic and image-targeted biopsies. When looking at the overall DRs, all studies showed an increase over the systematic biopsy scheme, when systematic and targeted biopsies were combined. This increase in per patient and per core DRs varied between 1% to 10 % and 2% to 6%, respectively (**Table 2.I-4**).

Only one study (Boehm *et al.*[98]) was performed with SWE and showed that patients with suspicious SWE findings are at a 6.4-fold higher risk to harbor a clinically significant PCa, and that SWE-targeted biopsies increased the per-patient DR by 4%.

All SWE-targeted and strain-targeted biopsy studies showed an increase in DR. However, most studies also reported that a non-negligible number of patients with clinically significant PCa[55,98] can be missed performing only elastography-targeted biopsies. Therefore, elastography-targeted biopsy cores should be performed in combination with systematic biopsies.

I-2.4.3 Prostate elastography limitations

FIGURE 2.I-10
Prostate Elastography: Pitfalls and Limits

A Strain elastography: lack of signals on the elastogram seen at the right base of the gland due to limited contact between the transducer and the rectal wall (arrow).

B SWE: increased stiffness due to massive calcifications of the transitional zone.

C Prostate SWE: Large benign prostatic hypertrophy with penetration issues. There is no mapping of elasticities below 3 cm in the anterior part of the prostate.

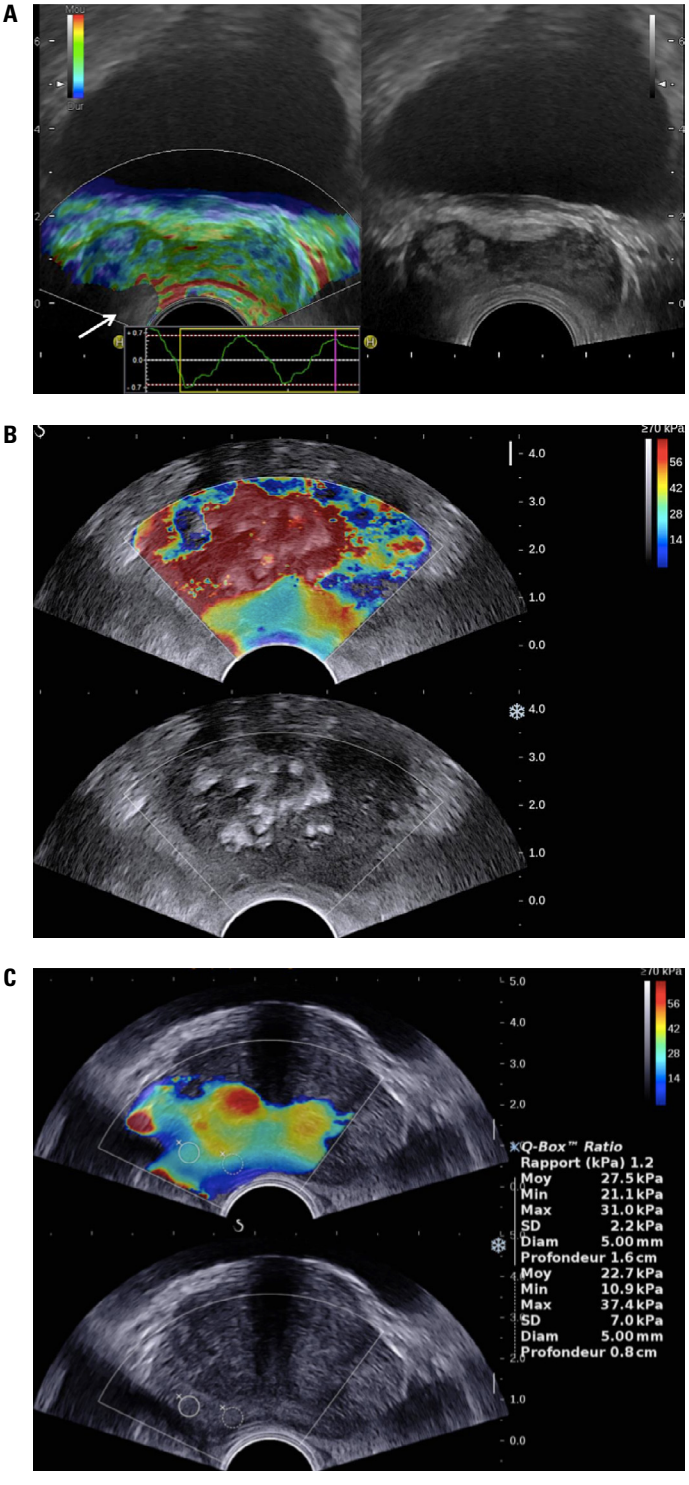

Prostate strain elastography is facing some challenges, such as the lack of uniform compression over the entire gland, the operator dependency, and the requirement of significant training in order to improve reproducibility and limit artifacts. The inter-observer agreement in detecting cancer can demonstrate a moderate agreement between readers, as demonstrated by low kappa values.[93] One of the most limiting factors is the difficulty in mastering the technique required to obtain appropriate strain elastograms. Even in experienced hands, up to 32% of strain elastographic acquisitions can be judged to be unevaluable due to technical problems, such as slippage of the compression plane.[78,93] The mismatch between the pre- and post-compression planes results in wrong estimation of the tissue elasticity, but this artifact can be reduced with training and balloon interposition. Prostatic hyperplasia is responsible for most of the false positive elastography evaluation.[93] Stiff areas can also result from inflammatory prostate disease and can be detected in up to 40% of the patients without detected cancer.[99] Compression of the prostate from the rectum may prevent transmission of sufficient deformation through the entire prostate, and more specifically the anterior region. It should be noted that compression applied to the posterior region of the prostate is different from that applied to the anterior region (due to depth). Also, the compression applied at the base is different than that applied in the apex (due to the different angulation of the end-fire probe) and therefore lack of signal on the elastogram may also appear (**Figure 2.I-10a**). This may affect the strain elastography DRs, which were reported to be lower at the anterior part of the prostate compared to that of posterior regions, and also lower in the prostate base compared to that of the apical regions, as shown by several studies.[73,84,87,100]

Prostate SWE is also facing some challenges. When a stiff area is encountered, the operator should release any pressure on the rectum to be sure that the stiffer pattern does not result from excessive pressure on the end-fire transducer; however, some pressure cannot be avoided when scanning the apex as the transducer is reclined, or when scanning large hypertrophic prostate that protrudes in the rectal lumen. In case of excessive pressure, the PZ sitting just against the transducer appears stiff. Shear wave elastography has other limitations, such as slow frame rate, small SWE box, image stabilization, and penetration issues. In the presence of macro-calcifications, the elasticity values are increased (**Figure 2.I-10b**). The SW pulse penetrates 3 to 4 cm. In a large prostate, this may not penetrate deep enough to measure the anterior zone of the large prostate[76,95] (**Figure 2.I-10c**).

Both SWE and strain elastography techniques also suffer from the same intrinsic limitations: not all cancers are stiff, and not all stiff lesions are cancers (particularly in the presence of calcifications and fibrous changes). This is why the analysis of the B-mode pattern of the stiff areas remains mandatory.

I-2.4.4 Future perspective

Prostate elastography (strain and/or SW) should become an additional US modality for routine prostate examination and biopsy procedures, in order to target suspicious areas and increase prostate biopsy DR. Shear wave elastography provides quantitative values of prostate tissue stiffness and reliable elasticity cut-offs, and an operator-independent real-time localization of PCa foci. The major advantage of the SW technology remains the shorter learning curve and the lack of variability, as the deformation of the prostate does not depend upon the operator skills but is produced by the ultrasound beam itself. Shear wave elastography will also enable the development of 3D prostate

elastography with multiplanar reconstruction, and MRI fusion to volumetric US, including elastography. These new modalities should include guiding capabilities in order to target biopsies to the most suspicious areas. The improvements in PCa detection are mandatory for the development of focal therapy.

I-2.5 Histoscanning

HistoScanning™ (HS) is an ultrasound-based computer-assisted technology for tissue characteristic differentiation. The technology was developed by Advanced Medical Diagnostics, in Belgium. Histoscanning is based on the utilization of one part of the back-scattered ultrasound waves—so-called native radiofrequency (RF) data. These data are different from the imaging information. Raw data are processed by three tissue characterization algorithms.[113] This is aimed to distinguish between benign and malignant tissue in solid organs. The use of histoscanning for PCa diagnosis was initially described in 2008.[114]

I-2.5.1 Techniques

FIGURE 2.I-11
Transrectal Probe Attached to a Magnetic Rotation Holder During Data Acquisition

Picture taken from video. Source: Dr P. Macek, Department of Urology, General University Hospital and First Medical Faculty of Charles University in Prague, Czech Republic.

FIGURE 2.I-12
An Example of Histoscanning Analysis With a 3D Prostate Model

The histoscanning analysis, together with colour highlighted suspicious areas, and the corresponding three-plane views can be used for scrolling through the prostate, in order to achieve an appropriate spatial distribution of lesions.

Source: Dr P. Macek, Department of Urology, General University Hospital and First Medical Faculty of Charles University in Prague, Czech Republic.

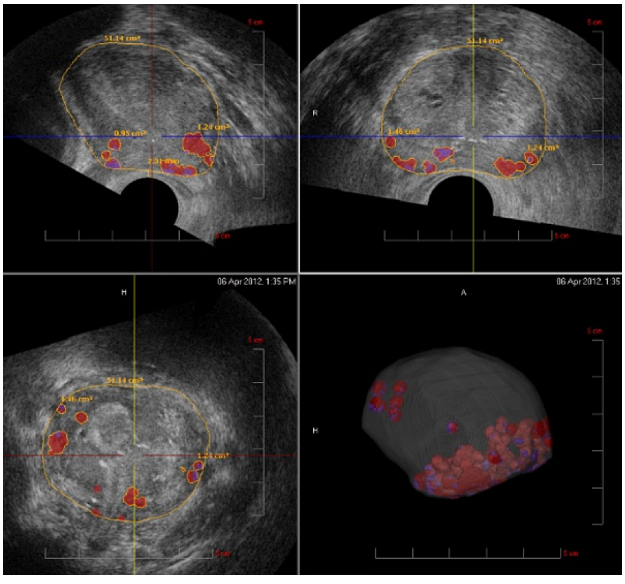

The system for prostate histoscanning (PHS) consists of the ultrasound system with transrectal probe and an attached dedicated computer workstation with processing software. So far, only BK Medical UK ultrasound scanners are approved for histoscanning.

The ultrasound probe is magnetically attached to a rotation holder (**Figure 2.I-11**), which is driven by the ultrasound machine. The patient's position for PHS is on his side or in the lithotomy position. The magnetic rotation holder can be handheld or attached to a metallic arm. During acquisition, the holder rotates so it moves the attached probe, which is scanning the prostate in a sagittal view from right to left by 179°, scanning one frame each 0.2°. Data are transferred to the workstation, where all frames are automatically combined and create a 3D model of the prostate and its vicinity. The operator then marks the borders of the prostate in the three planes, and the machine creates a 3D prostate model—the volume of interest. The volume of interest is then analyzed by the software, which highlights suspicious areas with colours (**Figure 2.I-12**). Data acquisition and processing usually take a few minutes, with more time needed for larger prostates. The minimum volume of tissue that is individually characterized is 0.04 mL.[115] Usually, regions equal to or greater than 0.1 mL are automatically marked as lesions of interest. Manual fine adjustment of the regions/lesions can be done as well. Therefore, unlike other ultrasound techniques, HS is non-real–time imaging. This allows cognitive lesion guidance or a dedicated biopsy software module (Histoscanning™ True Targeting [TT]) to help with navigation.

I-2.5.2 Detection rate and localization

Initial papers on PHS reported promising results of PCa detection with PHS-guided biopsies, with a RP specimen used as a reference standard.[114,116,117] Initial reports by Braeckman *et al.* found a 100% concordance in displaying multifocality and laterality[114] and, later, 100% sensitivity and 82% specificity for the diagnosis of PCa lesions of 0.5 mL and higher within the prostate.[116]

The sensitivity and specificity of 92% and 72%, respectively, for lesions of 0.2 mL within six regions (sextants) of the prostate were reported later.[114] However, these studies included small patient cohorts, and it is difficult to transpose the results into everyday practice.

Similar results for PCa detection within the six regions with 94% sensitivity and 80% specificity were reached by Nunez-Mora *et al.*, but also in patients with prior detected PCa.[118]

Schiffmann *et al.*, in the biopsy setting, found a sensitivity of 60.9% and specificity of 50.6% for lesions >0.2 mL, and 40.1% and 73.3%, respectively, for lesions >0.5 mL based on an analysis of 1,188 sextants (198 patients).[119]

Macek *et al.*, in the previously biopsy-confirmed PCa population prior RP, published a sensitivity of 60%, specificity of 66%, with an AUC of 0.63 for lesions ≥0.1 mL using a 12-sectors model,[120] which is also much lower compared to the initial enthusiastic report.

In 2013, Hamann *et al.* published HS-guided transperineal and transrectal prostate biopsy results. Transperineal HS-guided prostate biopsy has similar performance to systematic transrectal biopsy. But for HS-guidance only, 82.1% of cancers were detected with a maximum of 9 cores taken transperineally, and 53.6% of cancers were detected using the targeted transrectal approach.[115]

Recently, Hamann *et al.* published a paper comparing HS-navigated both transperineal and transrectal prostate biopsy supplemented by a standardized 14-core systematic transrectal prostate biopsy. They noted no difference in overall DR (sensitivity: 37.2%, specificity: 85.6%), but with HS-guidance, a smaller number of analyzed regions had to be targeted.[121]

Another interesting thing comes up when evaluating a correlation/reliability to predict the total tumour volume. Typically, a comparison between the HS tumour volume and RP specimen was used. Again, initial reports (13 patients) of Braeckman indicated very strong and reliable correlation ($r=0.98$, $p<0.001$).[114] Later, a slightly lower correlation was published by Simmons *et al.* (similar group composition, but with 27 patients) with $r=0.72$.[117]

Recent reports by Javed and Schiffman were the complete opposite, with $r=-0.065$ (24 patients) and $r=-0.008$ ($p=0.9$, 148 patients), respectively.[122,123]

The ability to predict ECE was tested by Javed *et al.* on 24 patients. This resulted in 100% sensitivity, but 23.5% specificity, which is therefore completely unusable.[123]

Salomon *et al.* reported that PHS may be helpful in the estimation of the probability of positive surgical margins, reporting that a presence of a 0.2-mL lesion in the lateroposterior part of the prostate resulted in a 3.7-times greater probability of the positive surgical margines.[124] However, reliability was not specifically addressed.

Similarly, the possibility of seminal vesical invasion was assessed by Schiffmann *et al.* in 131 patients (262 SVs), where, for a tumour volume of 0.2 mL or greater, the sensitivity was 61.5% and the specificity was 24.2%. The PPV was only 12.4% and the NPV was 78.3%.[125]

Until recently, HS could have been used only for cognitive guidance for transrectal biopsy, but a software modification named True Targeting (Prostate Histoscanning™ TT) was introduced by the manufacturer. This new tool was used by Sivaraman *et al.* to compare HS-guided biopsy with systematic biopsy. They found that HS-guided biopsy yielded a lower DR with target cores, 26%, versus 44% from systematic cores, and also with lower cancer length per core as detected by targeted biopsy.[126]

I-2.5.3 Limitations

It is important to notice that there are inconsistencies in the types of transrectal probes used for HS studies. It is another problem that we currently have with assessment: why we achieve such inconsistent HS results. Another reason may be the necessary experience using TRUS, as additional knowledge and skills are needed in order to perform good transrectal HS analysis. It is estimated that approximately 80 cases of PHS need to be performed in order to overcome the learning curve and improve results.[115] For optimal results, data acquisition is the key point of histoscanning analysis.

I-2.5.4 Summary

The real benefits of PHS for image-guided therapy are currently theoretical, because the large inconsistencies in the published data do not allow firm conclusion on the definitive usefulness of PHS. However, until more information is available, only experimental use of PHS with appropriate patient counselling is warranted, and omission of systematic biopsies in favour of HS-guided biopsy is not advisable.

I-2.6 Newer Ultrasound-Based Technologies

I-2.6.1 C-TRUS

Computerized ultrasound is one of the quantification modalities that uses the static TRUS images to identify cancer-suspicious areas by employing pre-defined computerized algorithms. Loch *et al.* developed this computer-based technology to improve the detection rate of PCa over the conventional grey-scale imaging modalities.[127] The algorithms for PCa were developed using artificial neural network analysis (ANNA) of the TRUS images, and the five pre-defined algorithms are used in the C-TRUS evaluation of the prostate.[128,129] The procedure requires initial bi-planar imaging of the prostate with conventional TRUS, and the recorded digital images are further analyzed by an integrated computer software to produce trans-axial images 5 mm apart from apex to base. Each of these images are analyzed with the five pre-defined algorithms to identify suspicious areas for cancer. These are highlighted with red areas superimposed on the original static TRUS images. The C-TRUS algorithms are independent of the grey-scale of the images and, hence, the grey level of the lesion does not influence the cancer detection.[130] Moreover, C-TRUS technology offers a tertiary health care

centre the flexibility of transferring the original static images via Internet to a higher referral unit, where they can undergo computer analysis. The suspicious areas can be marked and sent back for guided biopsies.[131]

The first study evaluated 289 slices whole-mount RP specimens from 61 patients, and found that ANNA correctly classified 99% and 79% of the pathologically proven benign and malignant areas, respectively.[129,130] In a clinical series of 132 patients with prior negative biopsy (median two biopsy series), C-TRUS targeted biopsies alone detected cancer in 50% of the patients.[130] In another series of 75 biopsy-naïve patients, C-TRUS–directed biopsies (6 target cores only) detected cancer in 31 patients (41%). However, repeat systematic TRUS biopsy rates are still awaited for comparison.[131] Walz *et al.* compared the preoperative C-TRUS images in 28 patients who underwent RP and found that the suspicious areas detected by C-TRUS had a sensitivity, specificity, PPV, and NPV of 83%, 64%, 80%, and 68%, respectively, for PCa.[132] Recently, Strunk *et al.* performed a combination of multiparametric MRI and C-TRUS in 20 patients with suspicion of PCa, and demonstrated that the combination of multiparametric MRI and C-TRUS had higher cancer detection than MRI alone. The DRs of C-TRUS in this study were 58% and could confirm those of the primary C-TRUS studies.[133]

I-2.6.2 3-D USG

Three-dimensional organ reconstruction of 2D ultrasound images has widespread clinical application in several fields. Similarly, 3D reconstruction of the prostate using the conventional 2D TRUS images was performed and analyzed for cancer detection and staging.[134] Simultaneous imaging of the prostate in the axial and the sagittal planes, followed by a computer reconstruction, provides a coronal as well as a 3D image. A special endocavity TRUS probe will be required to plot 3D images.[135] Early enthusiasm for 3D ultrasound did not translate to improved cancer detection over 2D images. The sensitivity and specificity for PCa detection using 2D ultrasound were 74% and 52%, and for 3D ultrasound they were 85% and 41%, respectively. However, 3D TRUS missed several significant hypoechoic lesions.[136] Mitterberger *et al.* evaluated the clinical performance of 3D for loco-regional staging in 180 patients diagnosed with PCa and planned for RP. 3D-TRUS had 84% sensitivity, 96% specificity, 94% PPV, 91% NPV, and an overall accuracy of 92% for identifying extra-capsular extension.[137] Currently, 3D-TRUS is not routinely employed for cancer detection or staging, since the cross-sectional imaging provides superior information.

However, with the advent of MRI-US fusion biopsy, 3D TRUS–based biopsy tracking systems are being employed to track the biopsy pathway.[138] The biopsy tracking system is further employed in re-biopsies, MRI fusion biopsy, and focal therapy.[139] 3D-TRUS is also routinely employed for treatment planning for brachytherapy and focal therapy like high-intensity focal ultrasound.

I-2.6.3 TRUS spectroscopy

TRUS spectroscopy is a quantification ultrasound modality that applies power spectrum analysis techniques to analyze the RF signals that are backscattered from the ultrasound techniques.[140] The pattern of the reflected RF signals is processed to determine the bi-acoustic properties of the micro-architecture of the prostatic tissue that produced the reflection. Inter-observer and instrument setting variability can be eliminated by using normalized frequency-dependent preset ultrasound data for

specific tissue characteristics. Ultrasound-based spectroscopy had shown to be capable of differentiating benign and malignant tissues at an experimental setting in non-urological cancers.[141-145] Lizzi *et al.* established the framework of power-spectrum analysis in tissue characterizations based on tissue acoustic properties. They further demonstrated that this model can be implemented to effectively differentiate various normal tissues like retina, liver, and prostate and also pathological tissues like metastatic deposits, intravascular plaques, etc.[146-148]

Recently, Sadeghi-Naini *et al.* performed TRUS spectroscopy in 15 patients undergoing RP, and correlated the findings with the final histopathology. The TRUS images spanning the whole prostate with 5 mm slices were generated with RF signals/spectroscopy marking the abnormal areas. Subsequently, the patients underwent RP after 2 weeks, and the whole-mount specimens were analyzed and correlated for cancer location. The authors demonstrated excellent correlation of the TRUS spectroscopy–estimated cancer extent with the RP specimen.[149]

I-2.7 Recommendations

Clinical experience with these newer US-based modalities for PCa detection is very limited, and hence no formal recommendations can be made for routine clinical use. These modalities should be further evaluated under a research model for better understanding of their clinical efficacy. (**Level of Evidence: 2B**)

I-2.8 Conclusion

Multiparametric ultrasound technologies have great potential and clinical utility in PCa detection. Some technologies reviewed in the article are predominantly at the research level, with limited clinical experience. Future research should aim at evaluating these US-based modalities in combinations to create a hybrid protocol that can make PCa detection easier, reliable, and reproducible.

I-2.9 References

1. Lee F, Torp-Pedersen ST, Siders DB, *et al.* Transrectal ultrasound in the diagnosis and staging of prostatic carcinoma. *Radiology.* 1989;170(3 Pt 1):609–615.
2. Yu KK, Hricak H. Imaging prostate cancer. *Radiol Clin North Am.* 2000;38:59–85.
3. Fütterer JJ, Briganti A, De Visschere P, *et al.* Can clinically significant prostate cancer be detected with multiparametric magnetic resonance imaging? A systematic review of the literature. *Eur Urol.* 2015;68(6):1045–1053.
4. Postema A, Mischi M, de la Rosette J, *et al.* Multiparametric ultrasound in the detection of prostate cancer: a systematic review. *World J Urol.* 2015;33(11):1651–1659.
5. Wild J, and Reid J. Progress in techniques of soft tissue examination by 15 megacycle pulsed ultrasound. In: Ultrasound in Biology and Medicine. Elizabeth Kelly (Ed) Washington, D.C.: *American Institute of Biological Sciences, Publication No. 3.*, 1957, pp. 30-45.
6. Smith J. Transrectal ultrasonography for the early detection and staging of prostate cancer. *J Clin Ultrasound.* 1996;24(8):455–461.
7. Takahashi H, Ouchi T. The ultrasonic diagnosis in the field of urology. *Proc Jpn Soc Ultrason Med.* 1963;3:7.
8. Watanabe H, Kato H, Kato T, *et al.* [Diagnostic application of ultrasonotomography to the prostate] [Article in Japanese]. *Nihon Hinyokika Gakkai Zasshi.* 1968;59(4):273–279.
9. Watanabe H, Igari D, Tanahasi Y, *et al.* Development and application of new equipment for transrectal ultrasonography. *J Clin Ultrasound.* 1974;2(2):91–98.
10. Rifkin M, Kurtz A, Choi H, *et al.* Endoscopic ultrasonic evaluation of the prostate using a transrectal probe: prospective evaluation and acoustic characterization. *Radiology.* 1983;149(1):265–271.
11. Lee F, McLeary R, Kumasaka G, *et al.* Transrectal ultrasound in the diagnosis of prostate cancer: location, echogenicity, histopathology, and staging. *Prostate.* 1985;7(2):117–129.
12. Weaver R, Noble M, Weigel J. Correlation of ultrasound guided and digitally directed transrectal biopsies of palpable prostatic abnormalities. *J Urol.* 1991;145(3):516–518.
13. Paul R, Korzinek C, Necknig U, *et al.* Influence of transrectal ultrasound probe on prostate cancer detection in transrectal ultrasound-guided sextant biopsy of prostate. *Urology.* 2004;64(3):532–536.
14. Ching C, Moussa A, Li J, *et al.* Does transrectal ultrasound probe configuration really matter? End fire versus side fire probe prostate cancer detection rates. *J Urology.* 2009;181(5):2077–2083.
15. Shinohara K, Wheeler T, Scardino P. The appearance of prostate cancer on transrectal ultrasonography: correlation of imaging and pathological examinations. *J Urol.* 1989;142(1):76–82.
16. Rifkin M, McGlynn E, Choi H. Echogenicity of prostate cancer correlated with histologic grade and stromal fibrosis: endorectal US studies. *Radiology.* 1989;170(2):549–552.
17. Fornage B. Transrectal duplex sonography of prostatic carcinoma: preliminary experience [abstract]. *Radiology.* 1989;173(P):81.
18. Halpern E, Strup S. Using gray-scale and color and power Doppler sonography to detect prostatic cancer. *AJR Am J Roentgenol.* 2000;174(3):623–627.
19. Ragde H, Kenny G, Murphy G, *et al.* Transrectal ultrasound microbubble contrast angiography of the prostate. Prostate. 1997;32(4):279–283.
20. Sauvain J, Sauvain E, Rohmer P, *et al.* Value of transrectal power Doppler sonography in the detection of low-risk prostate cancers. *Diagn Interv Imaging.* 2013;94(1):60–67.
21. Tsai Y, Jou Y, Chen C, *et al.* Doppler spectral waveform parameters at neurovascular bundle vessels in patients with prostate biopsy. *J Endourol.* 2014;28(3):364–370.
22. Peeling W, Griffiths G, Evans K, *et al.* Diagnosis and staging of prostatic cancer by transrectal ultrasonography. A preliminary study. *Br J Urol.* 1979;51(6):565–569.

23. Vapnek J, Hricak H, Shinohara K, *et al.* Staging accuracy of magnetic resonance imaging versus transrectal ultrasound in stages A and B prostatic cancer. *Urol Int.* 1994;53(4):191–195.

24. Smith J, Scardino P, Resnick M, *et al.* Transrectal ultrasound versus digital rectal examination for the staging of carcinoma of the prostate: results of a prospective, multi-institutional trial. *J Urol.* 1997;157(3):902–906.

25. Ohori M, Egawa S, Shinohara K, *et al.* Detection of microscopic extracapsular extension prior to radical prostatectomy for clinically localized prostate cancer. *Br J Urol.* 1994;74(1):72–79.

26. Rørvik J, Halvorsen O, Servoll E, *et al.* Transrectal ultrasonography to assess local extent of prostatic cancer before radical prostatectomy. *Br J Urol.* 1994;73(1):65–69.

27. Rifkin M, Zerhouni E, Gatsonis C, *et al.* Comparison of magnetic resonance imaging and ultrasonography in staging early prostate cancer. *N Engl J Med.* 1990;323(10):621–626.

28. Eisenberg M, Cowan J, Davies B, *et al.* The importance of tumor palpability and transrectal ultrasonographic appearance in the contemporary clinical staging of prostate cancer. *Urol Oncol.* 2011;29(2):171–176.

29. Jung A, Coakley F, Shinohara K, *et al.* Local staging of prostate cancer: comparative accuracy of T2-weighted endorectal MR imaging and transrectal ultrasound. *Clin Imaging.* 2012;36(5):547–552.

30. Ohori M, Kattan M, Utsunomiya T, *et al.* Do impalpable stage T1c prostate cancers visible on ultrasound differ from those not visible? *J Urol.* 2003;169(3):964–968.

31. Augustin H, Graefen M, Palisaar J, *et al.* Prognostic significance of visible lesions on transrectal ultrasound in impalpable prostate cancers: implications for staging. *J Clin Oncol.* 2003;21(15):2860–2868.

32. Hsu C, Joniau S, Oyen R, *et al.* Detection of clinical unilateral T3a prostate cancer - by digital rectal examination or transrectal ultrasonography? *BJU Int.* 2006;98(5):982–985.

33. Colombo T, Schips L, Augustin H, *et al.* Value of transrectal ultrasound in preoperative staging of prostate cancer. *Minerva Urol Nefrol.* 1999;51(1):1–4.

34. Russo G, Mischi M, Scheepens W, *et al.* Angiogenesis in prostate cancer: onset, progression and imaging. *BJU Int.* 2012;110(11 Pt C):E794–E808.

35. Schneider M. Characteristics of SonoVue™ *Echocardiography.* 1999;16(7 Pt 2):743–746.

36. Postema A, Idzenga T, Mischi M, *et al.* Ultrasound modalities and quantification: developments of multiparametric ultrasonography, a new modality to detect, localize and target prostatic tumors. *Curr Opin Urol.* 2015;25(3):191–197.

37. Wilson SR, Burns PN. Microbubble-enhanced US in body imaging: what role? *Radiology.* 2010;257(1):24–39.

38. Main M, Hibberd M, Ryan A, *et al.* Acute mortality in critically ill patients undergoing echocardiography with or without an ultrasound contrast agent. *JACC Cardiovasc Imaging.* 2014;7(1):40–48.

39. Smeenge M, Mischi M, Laguna Pes M, *et al.* Novel contrast-enhanced ultrasound imaging in prostate cancer. *World J Urol.* 2011;29(5):581–587.

40. Sedelaar J, van Leenders G, Hulsbergen-van de Kaa C, *et al.* Microvessel density: correlation between contrast ultrasonography and histology of prostate cancer. *Eur Urol.* 2001;40(3):285–293.

41. Sedelaar J, van Leenders G, Goossen T, *et al.* Value of contrast ultrasonography in the detection of significant prostate cancer: correlation with radical prostatectomy specimens. *Prostate.* 2002;53(3):246–253.

42. Mitterberger M, Aigner F, Horninger W, *et al.* Comparative efficiency of contrast-enhanced colour Doppler ultrasound targeted versus systematic biopsy for prostate cancer detection. *Eur Radiol.* 2010;20(12):2791–2796.

43. Taverna G, Morandi G, Seveso M, *et al.* Colour Doppler and microbubble contrast agent ultrasonography do not improve cancer detection rate in transrectal systematic prostate biopsy sampling. *BJU Int.* 2011;108(11):1723–1727.

44. Frauscher F, Klauser A, Volgger H, *et al.* Comparison of contrast enhanced color Doppler targeted biopsy with conventional systematic biopsy: impact on prostate cancer detection. *J Urol.* 2002;167(4):1648–1652.

45. Wink M, Frauscher F, Cosgrove D, *et al.* Contrast-enhanced ultrasound and prostate cancer; a multicentre European research coordination project. *Eur Urol.* 2008;54(5):982–992.

46. Tang M, Mulvana H, Gauthier T, *et al.* Quantitative contrast-enhanced ultrasound imaging: a review of sources of variability. *Interface Focus.* 2011;1(4):520–539.

47. Seitz M, Gratzke C, Schlenker B, *et al.* Contrast-enhanced transrectal ultrasound (CE-TRUS) with cadence-contrast pulse sequence (CPS) technology for the identification of prostate cancer. *Urol Oncol.* 2011;29(3):295–301.

48. Linden R, Trabulsi E, Forsberg F, *et al.* Contrast enhanced ultrasound flash replenishment method for directed prostate biopsies. *J Urol.* 2007;178(6):2354–2358.

49. Halpern E, McCue P, Aksnes A, *et al.* Contrast-enhanced US of the prostate with Sonazoid: comparison with whole-mount prostatectomy specimens in 12 patients. *Radiology.* 2002;222(2):361–366.

50. Matsumoto K, Nakagawa K, Hashiguchi A, *et al.* Contrast-enhanced ultrasonography of the prostate with Sonazoid. *Jpn J Clin Oncol.* 2010;40(11):1099–1104.

51. Sano F, Terao H, Kawahara T, *et al.* Contrast-enhanced ultrasonography of the prostate: various imaging findings that indicate prostate cancer. *BJU Int.* 2011;107(9):1404–1410.

52. Xie S, Li H, Du J, *et al.* Contrast-enhanced ultrasonography with contrast-tuned imaging technology for the detection of prostate cancer: comparison with conventional ultrasonography. *BJU Int.* 2012;109(11):1620–1626.

53. Zhao H, Xia C, Yin H, *et al.* The value and limitations of contrast-enhanced transrectal ultrasonography for the detection of prostate cancer. *Eur J Radiol.* 2013;82(11):e641–e647.

54. Halpern E, Gomella L, Forsberg F, *et al.* Contrast enhanced transrectal ultrasound for the detection of prostate cancer: a randomized, double-blind trial of dutasteride pretreatment. *J Urol.* 2012;188(5):1739–1745.

55. Van Hove A, Savoie P, Maurin C, *et al.* Comparison of image-guided targeted biopsies versus systematic randomized biopsies in the detection of prostate cancer: a systematic literature review of well-designed studies. *World J Urol.* 2014;32(4):847–858.

56. Tranquart F, Mercier L, Frinking P, *et al.* Perfusion quantification in contrast-enhanced ultrasound (CEUS)--ready for research projects and routine clinical use. *Ultraschall Med.* 2012;33 Suppl 1:S31–S38.

57. Jung E, Wiggermann P, Greis C, *et al.* First results of endocavity evaluation of the microvascularization of malignant prostate tumors using contrast enhanced ultrasound (CEUS) including perfusion analysis: first results. *Clin Hemorheol Microcirc.* 2012;52(2–4):167–177.

58. Postema A, Frinking P, Smeenge M, *et al.* Dynamic contrast-enhanced ultrasound parametric imaging for the detection of prostate cancer. *BJU Int.* 2016;117(4):598-603.

59. Mischi M, Kuenen M, Wijkstra H. Angiogenesis imaging by spatiotemporal analysis of ultrasound contrast agent dispersion kinetics. *IEEE Trans Ultrason Ferroelectr Freq Control.* 2012;59(4):621–629.

60. Mischi M, Kuenen M, Beerlage H, *et al.* Prostate cancer localization by contrast-ultrasound-dispersion imaging: results from a pilot study. *Eur Urol* Suppl. 2014;13(1):e1054.

61. Abou-Elkacem L, Bachawal S, Willmann J. Ultrasound molecular imaging: moving toward clinical translation. *Eur J Radiol.* 2015;84(9):1685–1693.

62. Zhai L, Madden J, Foo WC, *et al.* Characterizing stiffness of human prostates using acoustic radiation force. *Ultrason Imaging.* 2010;32(4):201–213.

63. Smith DS, Catalona WJ. Interexaminer variability of digital rectal examination in detecting prostate cancer. *Urology.* 1995;45(1):70–74.

64. Baumgart LA, Gerling GJ, Bass EJ. Characterizing the range of simulated prostate abnormalities palpable by digital rectal examination. *Cancer Epidemiol.* 2010;34(1):79–84.

65. Dvorak HF. Tumors: wounds that do not heal: similarities between tumor stroma generation and wound healing. *N Engl J Med.* 1986;315(26):1650–1659.

66. Tuxhorn JA, Ayala GE, Rowley DR. Reactive stroma in prostate cancer progression. *J Urol.* 2001;166(6):2472–2483.

67. Tuxhorn JA, Ayala GE, Smith MJ, *et al.* Reactive stroma in human prostate cancer: induction of myofibroblast phenotype and extracellular matrix remodeling. *Clin Cancer Res.* 2002;8(9):2912–2923.

68. Burns-Cox N, Avery NC, Gingell JC, *et al.* Changes in collagen metabolism in prostate cancer: a host response that may alter progression. *J Urol.* 2001;166(5):1698–1701.

69. Zhang Y, Nojima S, Nakayama H, *et al.* Characteristics of normal stromal components and their correlation with cancer occurrence in human prostate. *Oncol Rep.* 2003;10(1):207–211.

70. Phipps S, Yang TH, Habib FK, *et al.* Measurement of tissue mechanical characteristics to distinguish between benign and malignant prostatic disease. *Urology.* 2005;66(2):447–450.

71. Krouskop TA, Wheeler TM, Kallel F, *et al.* Elastic moduli of breast and prostate tissues under compression. *Ultrason Imaging.* 1998;20(4):260–274.

72. Carson WC, Gerling GJ, Krupski TL, *et al.* Material characterization of ex vivo prostate tissue via spherical indentation in the clinic. *Med Eng Phys.* 2011;33(3):302–309.

73. Tsutsumi M, Miyagawa T, Matsumura T, *et al.* Real-time balloon inflation elastography for prostate cancer detection and initial evaluation of clinicopathologic analysis. *AJR Am J Roentgenol.* 2010;194(6):471–476.

74. Goddi A, Sacchi A, Magistretti G, *et al.* Transrectal real-time elastography of the prostate: normal patterns. *J Ultrasound.* 2011;14(4):220–232.

75. Bercoff J, Tanter M, Fink M. Supersonic shear imaging: a new technique for soft tissue elasticity mapping. *IEEE Trans Ultrason Ferroelectr Freq Control.* 2004;51(4):396–409.

76. Boehm K, Salomon G, Beyer B, *et al.* Shear wave elastography for localization of prostate cancer lesions and assessment of elasticity thresholds: implications for targeted biopsies and active surveillance protocols. *J Urol.* 2015;193(3):794–800.

77. Pallwein L, Mitterberger M, Struve P, *et al.* Real-time elastography for detecting prostate cancer: preliminary experience. *BJU Int.* 2007;100(1):42–46.

78. Tsutsumi M, Miyagawa T, Matsumura T, *et al.* The impact of real-time tissue elasticity imaging (elastography) on the detection of prostate cancer: clinicopathological analysis. Int *J Clin Oncol.* 2007;12(4):250–255.

79. Sumura M, Shigeno K, Hyuga T, *et al.* Initial evaluation of prostate cancer with real-time elastography based on step-section pathologic analysis after radical prostatectomy: a preliminary study. *Int J Urol.* 2007;14(9):811–816.

80. Salomon G, Kollerman J, Thederan I, *et al.* Evaluation of prostate cancer detection with ultrasound real-time elastography: a comparison with step section pathological analysis after radical prostatectomy. *Eur Urol.* 2008;54(6):1354–1362.

81. Walz J, Marcy M, Maubon T, *et al.* [Real time elastography in the diagnosis of prostate cancer: comparison of preoperative imaging and histology after radical prostatectomy] [Article in French]. *Prog Urol.* 2011;21(13):925–931.

82. Walz J, Marcy M, Pianna JT, *et al.* Identification of the prostate cancer index lesion by real-time elastography: considerations for focal therapy of prostate cancer. *World J Urol.* 2011;29(5):589–594.

83. Brock M, von Bodman C, Sommerer F, *et al.* Comparison of real-time elastography with grey-scale ultrasonography for detection of organ-confined prostate cancer and extra capsular extension: a prospective analysis using whole mount sections after radical prostatectomy. *BJU Int.* 2011;108(8 Pt 2):E217–E222.

84. Junker D, Schafer G, Aigner F, *et al.* Potentials and limitations of real-time elastography for prostate cancer detection: a whole-mount step section analysis. *Scientific World Journal.* 2012;2012:193213.

85. Pelzer AE, Heinzelbecker J, Weiss C, *et al.* Real-time sonoelastography compared to magnetic resonance imaging using four different modalities at 3.0 T in the detection of prostate cancer: strength and weaknesses. *Eur J Radiol.* 2013;82(5):814–821.

86. Brock M, Eggert T, Palisaar RJ, *et al.* Multiparametric ultrasound of the prostate: adding contrast enhanced ultrasound to real-time elastography to detect histopathologically confirmed cancer. *J Urol.* 2013;189(1):93–98.

87. Junker D, Schafer G, Kobel C, *et al.* Comparison of real-time elastography and multiparametric MRI for prostate cancer detection: a whole-mount step-section analysis. *AJR Am J Roentgenol.* 2014;202(3):W263–W269.

88. Zhu Y, Chen Y, Qi T, *et al.* Prostate cancer detection with real-time elastography using a bi-plane transducer: comparison with step section radical prostatectomy pathology. *World J Urol.* 2014;32(2):329–333.

89. Zhang B, Ma X, Zhan W, *et al.* Real-time elastography in the diagnosis of patients suspected of having prostate cancer: a meta-analysis. *Ultrasound Med Biol.* 2014;40(7):1400–1407.

90. Pallwein L, Mitterberger M, Gradl J, *et al.* Value of contrast-enhanced ultrasound and elastography in imaging of prostate cancer. *Curr Opin Urol.* 2007;17(1):39–47.

91. Ward JF. Contemporary outcomes of focal therapy in prostate cancer: what do we know so far. *World J Urol.* 2010;28(5):593–597.

92. Ahmed HU. The index lesion and the origin of prostate cancer. *N Engl J Med.* 2009;361(17):1704–1706.

93. Miyagawa T, Tsutsumi M, Matsumura T, *et al.* Real-time elastography for the diagnosis of prostate cancer: evaluation of elastographic moving images. *Jpn J Clin Oncol.* 2009;39(6):394–398.

94. Barr RG, Memo R, Schaub CR. Shear wave ultrasound elastography of the prostate: initial results. *Ultrasound Q.* 2012;28(1):13–20.

95. Woo S, Kim SY, Cho JY, *et al.* Shear wave elastography for detection of prostate cancer: a preliminary study. *Korean J Radiol.* 2014;15(3):346–355.

96. Correas JM, Tissier AM, Khairoune A, *et al.* Prostate cancer: diagnostic performance of real-time shear-wave elastography. *Radiology.* 2015;275(1):280–289.

97. Ahmad S, Cao R, Varghese T, *et al.* Transrectal quantitative shear wave elastography in the detection and characterisation of prostate cancer. *Surg Endosc.* 2013;27(9):3280–3287.

98. Boehm K, Budaus L, Tennstedt P, *et al.* Prediction of significant prostate cancer at prostate biopsy and per core detection rate of targeted and systematic biopsies using real-time shear wave elastography. *Urol Int.* 2015;95(2):189–196.

99. Pallwein L, Mitterberger M, Struve P, *et al.* Comparison of sonoelastography guided biopsy with systematic biopsy: impact on prostate cancer detection. *Eur Radiol.* 2007;17(9):2278–2285.

100. Konig K, Scheipers U, Pesavento A, *et al.* Initial experiences with real-time elastography guided biopsies of the prostate. *J Urol.* 2005;174(1):115–117.

101. Pallwein L, Mitterberger M, Pinggera G, *et al.* Sonoelastography of the prostate: comparison with systematic biopsy findings in 492 patients. *Eur J Radiol.* 2008;65(2):304–310.

102. Kamoi K, Okihara K, Ochiai A, *et al.* The utility of transrectal real-time elastography in the diagnosis of prostate cancer. *Ultrasound Med Biol.* 2008;34(7):1025–1032.

103. Brock M, von Bodman C, Palisaar RJ, *et al.* The impact of real-time elastography guiding a systematic prostate biopsy to improve cancer detection rate: a prospective study of 353 patients. *J Urol.* 2012;187(6):2039–2043.

104. Nelson ED, Slotoroff CB, Gomella LG, *et al.* Targeted biopsy of the prostate: the impact of color Doppler imaging and elastography on prostate cancer detection and Gleason score. *Urology.* 2007;70(6):1136–1140.

105. Kamoi K, Okihara K, Ochiai A, *et al.* The utility of transrectal real-time elastography in the diagnosis of prostate cancer. *Ultrasound Med Biol.* 2008;34(7):1025–1032.

106. Aigner F, Pallwein L, Junker D, *et al.* Value of real-time elastography targeted biopsy for prostate cancer detection in men with prostate specific antigen 1.25 ng/ml or greater and 4.00 ng/ml or less. *J Urol.* 2010;184(3):913–917.

107. Kapoor A, Mahajan G, Sidhu BS. Real-time elastography in the detection of prostate cancer in patients with raised PSA level. *Ultrasound Med Biol.* 2011;37(9):1374–1381.

108. Ganzer R, Brandtner A, Wieland WF, *et al.* Prospective blinded comparison of real-time sonoelastography targeted versus randomised biopsy of the prostate in the primary and re-biopsy setting. *World J Urol.* 2012;30(2):219–223.

109. Zhang Y, Tang J, Li YM, *et al.* The contribution of strain patterns in characterization of prostate peripheral zone lesions at transrectal ultrasonography. *Acta Radiol.* 2012;53(1):119–126.

110. Taverna G, Magnoni P, Giusti G, *et al.* Impact of real-time elastography versus systematic prostate biopsy method on cancer detection rate in men with a serum prostate-specific antigen between 2.5 and 10 ng/mL. *ISRN Oncol.* 2013;2013:584672.

111. Salomon G, Drews N, Autier P, *et al.* Incremental detection rate of prostate cancer by real-time elastography targeted biopsies in combination with a conventional 10-core biopsy in 1024 consecutive patients. *BJU Int.* 2014;113(4):548–553.

112. Nygard Y, Haukaas SA, Halvorsen OJ, *et al.* A positive real-time elastography is an independent marker for detection of high-risk prostate cancers in the primary biopsy setting. *BJU Int.* 2014;113(5b):E90–E97.

113. Govindaraju SK, Ahmed HU, Sahu M, *et al.* Tissue characterisation in prostate cancer using a novel ultrasound approach. *Br J Med Surg Urol.* 2008;1(3):98–106.

114. Braeckman J, Autier P, Garbar C, *et al.* Computer-aided ultrasonography (HistoScanning): a novel technology for locating and characterizing prostate cancer. *BJU Int.* 2008;101(3):293–298.

115. Hamann MF, Hamann C, Schenk E, *et al.* Computer-aided (HistoScanning) biopsies versus conventional transrectal ultrasound-guided prostate biopsies: do targeted biopsy schemes improve the cancer detection rate? *Urology.* 2013;81(2):370–375.

116. Braeckman J, Autier P, Soviany C, *et al.* The accuracy of transrectal ultrasonography supplemented with computer-aided ultrasonography for detecting small prostate cancers. *BJU Int.* 2008;102(11):1560–1565.

117. Simmons L, Autier P, Zat'ura F, *et al.* Detection, localisation and characterisation of prostate cancer by Prostate HistoScanning™. *BJU Int.* 2012;110(1):28–35.

118. Nunez-Mora C, Garcia-Mediero JM, Patino P, *et al.* Utility of Histoscanning™ prior to prostate biopsy for the diagnosis of prostate adenocarcinoma. [Article in English, Spanish] *Actas Urol Esp.* 2013;37(6):342–346.

119. Schiffmann J, Tennstedt P, Fischer J, *et al.* Does HistoScanning™ predict positive results in prostate biopsy? A retrospective analysis of 1,188 sextants of the prostate. *World J Urol.* 2014;32(4):925–930.

120. Macek P, Barret E, Sanchez-Salas R, *et al.* Prostate histoscanning in clinically localized biopsy proven prostate cancer: an accuracy study. *J Endourol.* 2014;28(3):371–376.

121. Hamann MF, Hamann C, Olzem D, *et al.* [Value of perineal HistoScanning template-guided prostate biopsy] [Article in German]. *Urologe A.* 2015;54(11):1596–1601.

122. Schiffmann J, Fischer J, Tennstedt P, *et al.* Comparison of prostate cancer volume measured by HistoScanning and final histopathological results. *World J Urol.* 2014;32(4):939–944.

123. Javed S, Chadwick E, Edwards AA, *et al.* Does prostate HistoScanning play a role in detecting prostate cancer in routine clinical practice? Results from three independent studies. *BJU Int.* 2014;114(4):541–548.

124. Salomon G, Spethmann J, Beckmann A, *et al.* Accuracy of HistoScanning for the prediction of a negative surgical margin in patients undergoing radical prostatectomy. *BJU Int.* 2013;111(1):60–66.

125. Schiffmann J, Beyer B, Fischer J, *et al.* Histoscanning has low sensitivity and specificity for seminal vesicle invasion. *Urology.* 2014;84(5):1168–1171.

126. Sivaraman A, Sanchez-Salas R, Barret E, *et al.* Prostate histoscanning true targeting guided prostate biopsy: initial clinical experience. *World J Urol.* 2015;33(10):1475–1479.

127. Loch T. Computerized transrectal ultrasound (C-TRUS) of the prostate: detection of cancer in patients with multiple negative systematic random biopsies. *World J Urol.* 2007;25(4):375–380.

128. Loch T, Leuschner I, Genberg C, *et al.* Artificial neural network analysis (ANNA) of prostatic transrectal ultrasound. *Prostate.* 1999;39(3):198–204.

129. Loch T, Leuschner I, Genberg C, *et al.* [Improvement of transrectal ultrasound. Artificial neural network analysis (ANNA) in detection and staging of prostatic carcinoma] [Article in German]. *Urologe A.* 2000;39(4):341–347.

130. Loch T, Gettys T, Cochran JS, *et al.* Computer-aided image analysis in transrectal ultrasound of the prostate. *World J Urol.* 1990;8(3):150–153.

131. Grabski B, Baeurle L, Loch A, *et al.* Computerized transrectal ultrasound of the prostate in a multicenter setup (C-TRUS-MS): detection of cancer after multiple negative systematic random and in primary biopsies. *World J Urol.* 2011;29(5):573–579.

132. Walz J, Loch T, Salomon G, *et al.* [Imaging of the prostate] [Article in German]. *Urologe A.* 2013;52(4):490–496.

133. Strunk T, Decker G, Willinek W, *et al.* Combination of C-TRUS with multiparametric MRI: potential for improving detection of prostate cancer. *World J Urol.* 2014;32(2):335–339.

134. Bogers HA, Sedelaar JP, Beerlage HP, *et al.* Contrast-enhanced three-dimensional power Doppler angiography of the human prostate: correlation with biopsy outcome. *Urology.* 1999;54(1):97–104.

135. Tong S, Downey DB, Cardinal HN, *et al.* A three-dimensional ultrasound prostate imaging system. *Ultrasound Med Biol.* 1996;22(6):735–746.

136. Sedelaar JP, van Leenders GJ, Hulsbergen-van de Kaa CA, *et al.* Microvessel density: correlation between contrast ultrasonography and histology of prostate cancer. *Eur Urol.* 2001;40(3):285–293.

137. Mitterberger M, Pinggera G-M, Pallwein L, *et al.* The value of three-dimensional transrectal ultrasonography in staging prostate cancer. *BJU Int.* 2007;100(1):47–50.

138. Baco E, Rud E, Ukimura O, *et al.* Effect of targeted biopsy guided by elastic image fusion of MRI with 3D-TRUS on diagnosis of anterior prostate cancer. *Urol Oncol.* 2014;32(8):1300–1307.

139. Baco E, Ukimura O, Rud E, *et al.* Magnetic resonance imaging–transectal ultrasound image-fusion biopsies accurately characterize the index tumor: correlation with step-sectioned radical prostatectomy specimens in 135 patients. *Eur Urol.* 2015;67(4):787–794.

140. Feleppa EF, Fair WR, Tsai H, *et al.* Progress in two-dimensional and three-dimensional ultrasonic tissue-type imaging of the prostate based on spectrum analysis and nonlinear classifiers. *Mol Urol.* 1999;3(3):303–310.

141. Sadeghi-Naini A, Papanicolau N, Falou O, *et al.* Quantitative ultrasound evaluation of tumor cell death response in locally advanced breast cancer patients receiving chemotherapy. *Clin Cancer Res.* 2013;19(8):2163–2174.

142. Sadeghi-Naini A, Falou O, Czarnota GJ. Quantitative ultrasound spectral parametric maps: early surrogates of cancer treatment response. *Conf Proc IEEE Eng Med Biol Soc.* 2012;2012:2672–5.

143. Sadeghi-Naini A, Falou O, Czarnota GJ. Quantitative ultrasound visualization of cell death: emerging clinical applications for detection of cancer treatment response. *Conf Proc IEEE Eng Med Biol Soc.* 2012;2012:1125–8.

144. Sadeghi-Naini A, Falou O, Tadayyon H, *et al.* Conventional frequency ultrasonic biomarkers of cancer treatment response in vivo. *Transl Oncol.* 2013;6(3):234–243.

145. Sadeghi-Naini A, Sannachi L, Pritchard K, *et al.* Early prediction of therapy responses and outcomes in breast cancer patients using quantitative ultrasound spectral texture. *Oncotarget.* 2014;5(11):3497–3511.

146. Lizzi FL, Astor M, Liu T, *et al.* Ultrasonic spectrum analysis for tissue assays and therapy evaluation. *Int J Imaging Syst Technol.* 1997;8(1):3–10.

147. Lizzi FL, Greenebaum M, Feleppa EJ, *et al.* Theoretical framework for spectrum analysis in ultrasonic tissue characterization. *J Acoust Soc Am.* 1983;73(4):1366–1373.

148. Lizzi FL, Astor M, Feleppa EJ, *et al.* Statistical framework for ultrasonic spectral parameter imaging. *Ultrasound Med Biol.* 1997;23(9):1371–1382.

149. Sadeghi-Naini A, Sofroni E, Papanicolau N, *et al.* Quantitative ultrasound spectroscopic imaging for characterization of disease extent in prostate cancer patients. *Transl Oncol.* 2015;8(1):25–34.

150. Woo S, Kim SY, Lee MS, *et al.* Shear wave elastography assessment in the prostate: an intraobserver reproducibility study. *Clin Imaging.* 2015; 39(3):484-487.

C2-II

Imaging in Localized Prostate Cancer:
II. Multiparametric Magnetic Resonance Imaging

CHAIR

Eric Barret, France

CO-CHAIR

Olivier Rouvière, France

MEMBERS

Flavio Barchetti, Italy

Joyce G. R. Bomers, The Netherlands

Peter L. Choyke, United States

Matthieu Durand, United States

Jurgen Fütterer, The Netherlands

Christian G. Overduin, The Netherlands

Valeria Panebianco, Italy

Philippe Puech, France

Ardeshir R. Rastinehad, United States

Raphaele Renard-Penna, France

Giovanni Rosi, Italy

Ash K. Tewari, United States

Sarah Toledano-Massiah, France

Ismail Baris Turkbey, United States

CONTENTS

Imaging in Localized Prostate Cancer:
II. Multiparametric Magnetic Resonance Imaging

II-2.1 Introduction

Prostate cancer (PCa) imaging is a rapidly evolving and fascinating field. Prostate cancer is indeed an exception in oncology: because no imaging technique has shown its ability to clearly distinguish PCa from benign tissue, it is still diagnosed by random biopsies and treatment decisions are, eventually, based on the results of a random sampling of the gland. However, dramatic improvements in prostate magnetic resonance imaging (MRI) during the last decade will probably change this paradigm. It may be too soon, but one can foresee a close future where imaging will be used to diagnose PCa, and evaluate its size and perhaps its aggressiveness, in order to make rational management decisions. In the meantime, some questions remain partially unanswered: is multiparametric MRI (mpMRI) good enough to accurately depict the size, volume, and aggressiveness of PCa foci? What exact role can it play in candidates to prostate biopsy, in active surveillance (AS), or in patients with biochemical failure after primary treatment? Is image-guided focal treatment reasonable or not? Is inter-reader variability too large to recommend widespread use of prostate MRI?

This section will review recent evidence on all these issues.

II-2.2 Optimizing Imaging Protocols for Localized PCa

Over the past few years, mpMRI has become highly integrated into the diagnostic workup of patients at risk for PCa, as evidenced by the results that have emerged from sites around the world. However, despite its growing use, mpMRI is not always performed in a uniform manner, and it is important that standardized imaging guidelines be produced so that patients get the best diagnostic value from the scan that they undergo.

In 2012, the European Society of Urogenital Radiology (ESUR) produced an initial guideline, which set forth the minimal and optimal requirements for mpMRI of the prostate. The guideline proposed three distinct protocols: detection, staging, and node-bone evaluation.[1] This guideline not only provided advice on optimizing technical aspects of mpMRI of the prostate, but it also proposed a standardized method of evaluating mpMRI of the prostate, known as the Prostate Imaging and Reporting and Data System (PI-RADS). The emergence of PI-RADS led to a need for tailoring the mpMRI protocol according to patient characteristics, clinical questions, treatment options, and available MRI equipment. In 2015, the American College of Radiology (ACR) and ESUR jointly released a second version of PI-RADS (PI-RADS v2) in which additional suggestions regarding technique were made.[2] This harmonization, based on the use of a standard PI-RADS score, should facilitate communication of radiologists' findings to the referring physicians and should improve the use of mpMRI data.

Multiparametric MRI is a powerful imaging technique for detecting and staging PCa. However, a major obstacle is that there is currently no consensus regarding what constitutes an optimal mpMRI protocol for a given magnet type and patient population. Differences in opinion are related to variability in the strength of magnets (1.5Tesla [T] vs 3T), use of coils (endorectal coil [ERC] versus surface coils), individual imaging parameters (e.g. b-value used in diffusion-weighted imaging [DWI]), and patient population (screened or unscreened). A recent survey by the ACR including 36 academic centres revealed a diversity of approaches to the performance of prostate mpMRI, including 9 (25%) sites that use 1.5T with an ERC, 6 sites (17%) that use 1.5T without an ERC, 11 sites (31%) that use 3T without ERC, and 10 sites (28%) that use 3T with an ERC. Thus, there was broad diversity regarding field strength and use of ERC. More agreement was found regarding the choice of pulse sequences. All centres reported using T1-weighted (T1W) and T2-weighted (T2W) MRI in their protocols, 95% of them used diffusion-weighted MRI (DW MRI), and 82% used dynamic contrast-enhanced MRI (DCE MRI) routinely in their practice. Thus, mpMRI protocols tend to be non-uniform, even among academic centres.[2] Moreover, it is likely that even more differences would become apparent if this survey had been more detailed regarding parameters employed in the generation of scans. In an era of personalized medicine, tailoring the mpMRI protocol to the clinical needs, MRI equipment, and reimbursement policies is the only practical approach. In light of recent developments, this section provides updates on the minimal and optimal requirements of the two basic mpMRI protocols: Detection and Staging.

II-2.2.1 Detection protocol

TABLE 2.II-1 Detection and Staging Protocol Options Based on Magnet Systems and Coil Choices

Indication	Magnet system	Endorectal coil	Pulse sequences		
			T2W MRI	DW MRI	DCE MRI
Dectection	1.5T	Needed>optional	+	+	+
	3T	Optional>needed	+	+	+/–
Staging	1.5T	Needed	+	+	+
	3T	Needed>optional	+	+	+

Abbreviations: MRI: magnetic resonance imaging; T2W MRI: T2-weighted MRI; DW MRI: diffusion-weighted MRI; DCE MRI: dynamic contrast-enhanced MRI

FIGURE 2.II-1
53-Year-Old Man With a Prostate-Specific Antigen (PSA)=8 ng/mL and Gleason 3+3 Cancer (at transrectal ultrasound [TRUS]-Guided Systemic Biopsy)

The patient had a brain aneurysm clip, which was only 1.5T compatible. Multiparametric MRI obtained with 12-channel phased array surface coil at 1.5T including axial T2W MRI (**A**), apparent diffusion coefficient (ADC) map of MRI (**B**), DCE MRI (**C**) shows a lesion in the left mid-peripheral zone (PZ) (arrows). The patient underwent radical prostatectomy (RP), and histopathology revealed Gleason 3+4 tumour.

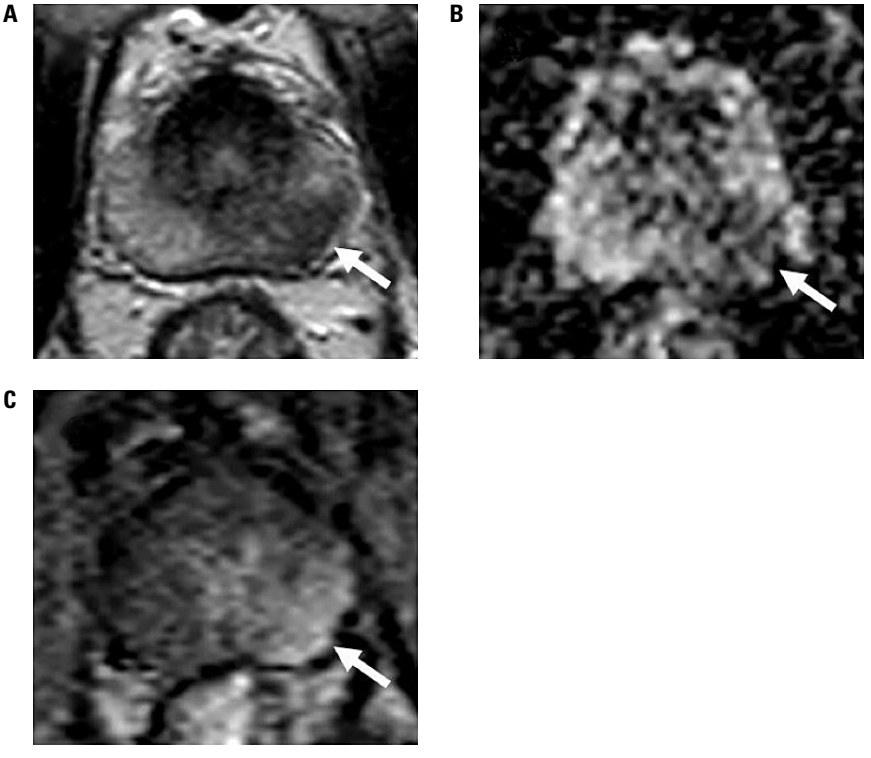

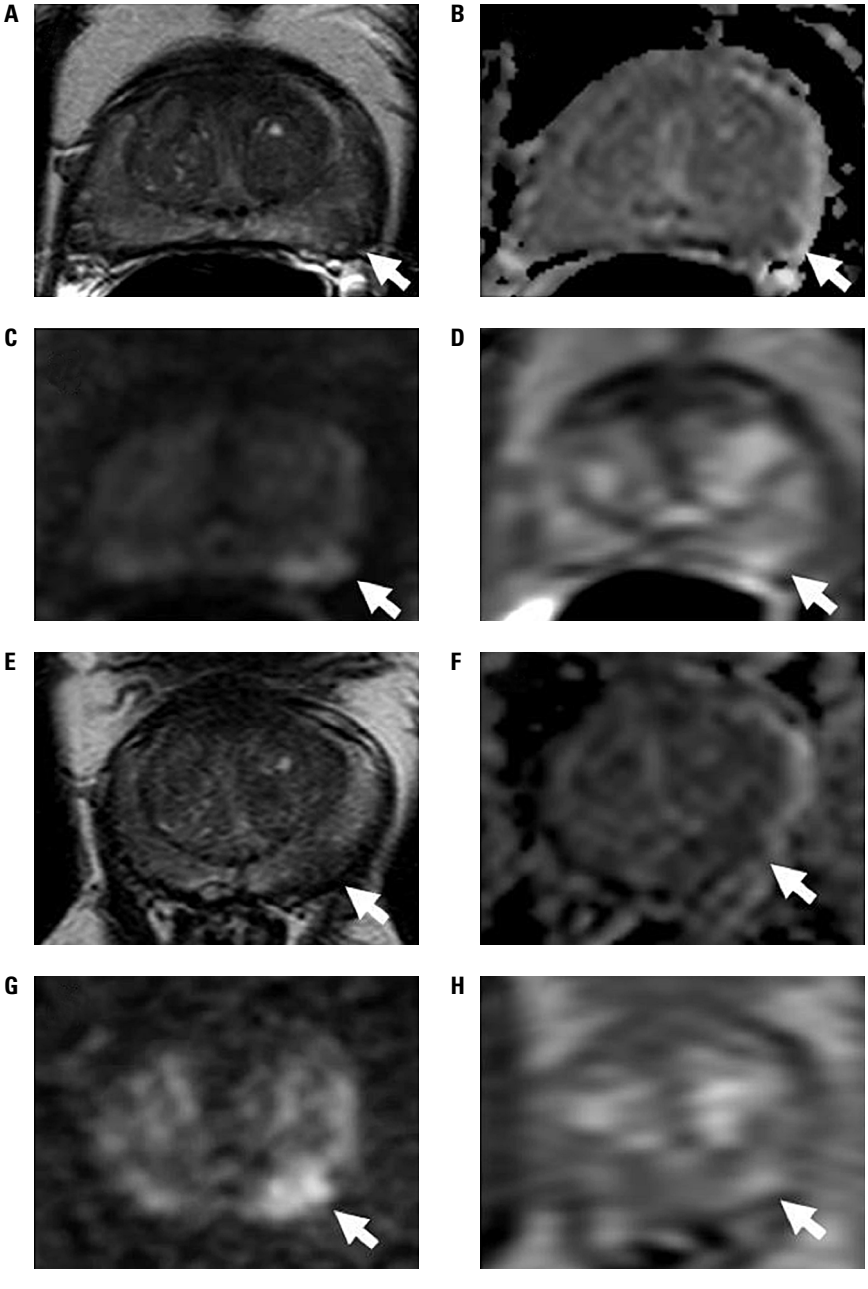

FIGURE 2.II-2
63-Year-Old Man With a PSA=4.7 ng/mL

Multiparametric MRI obtained with combined use of an endorectal coil including axial T2W MRI (**A**), ADC map of DW MRI (**B**), b value = 2,000s/mm^2 DW MRI (**C**), and DCE MRI (**D**) shows a lesion in the left mid-PZ zone (arrows). The same patient underwent an mpMRI with 32-channel phased array surface coil a year after the initial mpMRI, which again localizes the same lesion on axial T2W MRI (**E**), ADC map of DW MRI (**F**), b value = 1,500s/mm^2 DW MRI (**G**), DCE MRI (**H**) (arrows). The lesion was biopsied via TRUS/MRI fusion guidance and found to include Gleason 3+3 PCa.

For lesion detection, the magnet field strength can be either 1.5T or 3T. However, 3T systems provide much higher signal-to-noise ratio (SNR) compared to 1.5T systems, and this extra signal can be used to improve resolution, speed of acquisition, and diffusion imaging. However, an optimized protocol at either 1.5T or 3T can be sufficient to detect lesions without using an ERC, depending on the technical features of the MRI (**Figure 2.II-1**). For older 1.5T systems, image quality can be lacking and, to some extent, this can be mitigated by using an ERC. One study that used state of the art scanners compared non-ERC 3T scans to ERC 3T scans and showed no difference for lesion detection.[3] However, Turkbey

et al. recently showed better sensitivity (76% versus 45%) and positive predictive value (PPV) (80% versus 64%) for mpMRI consisting of T2W MRI plus DW MRI with an ERC, although almost all the additional lesions detected were considered not clinically significant. Therefore, it is possible that the smaller lesions detectable with an ERC actually do not improve the performance of MRI but, rather, increase the detection of inconsequential tumours.[4] Therefore, depending on the MR unit used, mpMRI can be successfully performed at 1.5T without an ERC. However, for most scanners, 3T field strength is desirable and generally does not require an ERC, although sensitivity may be further improved by using an ERC (**Table 2.II-1** and **Figure 2.II-2**).

TABLE 2.II-2 Basic Multiparamertic MRI Pulse Sequence Parameters and Technical Specifications (Adapted from McDonald *et al.* [7] and Puech *et al.* [21])

Pulse Sequence	Technical Specifications
T2W MRI	▪ 2D or 3D tri-plane (axial, coronal, sagittal) ▪ Fast-spin-echo (FSE) or turbo-spin-echo (TSE) ▪ Slice thickness: 3 mm, no gap ▪ FOV: generally 12–20 cm to encompass the entire prostate gland and seminal vesicles ▪ In plane resolution: ≤0.7 mm (phase) x ≤0.4 mm (frequency)
DW MRI	▪ TE: ≤90 msec; TR : >3000 msec ▪ Slice thickness: ≤4 mm, no gap ▪ FOV: 16–22 cm ▪ In plane resolution: ≤2.5 mm phase and frequency ▪ For ADC maps, if only two b-values can be acquired due to time or scanner constraints, it is preferred that the lowest b-value should be set at 50–100 sec/mm^2 and the highest should be 800–1000 sec/mm^2. ▪ High b-value images (>1400 sec/mm^2)
DCE MRI	▪ TR/TE: <100 msec/<5 msec ▪ Slice thickness: 3 mm, no gap ▪ FOV: encompass the entire prostate gland and seminal vesicles ▪ In plane resolution: ≤2 mm x ≤2 mm ▪ Temporal resolution: ≤15 sec (<7 sec is preferred) ▪ Total observation rate: >2 min ▪ Dose: 0.1 mmol/kg standard GBCA or equivalent high relaxivity GBCA ▪ Injection rate: 2–3 cc/sec

Abbreviations: 2D: two-dimensional; 3D: three dimensional; FSE: fast-spin echo; TSE: turbo-spin-echo; FOV: field of view; TE: echo time; TR: repetition time; ADC: apparent diffusion coefficient; GBCA, gadolinium-based contrast agent

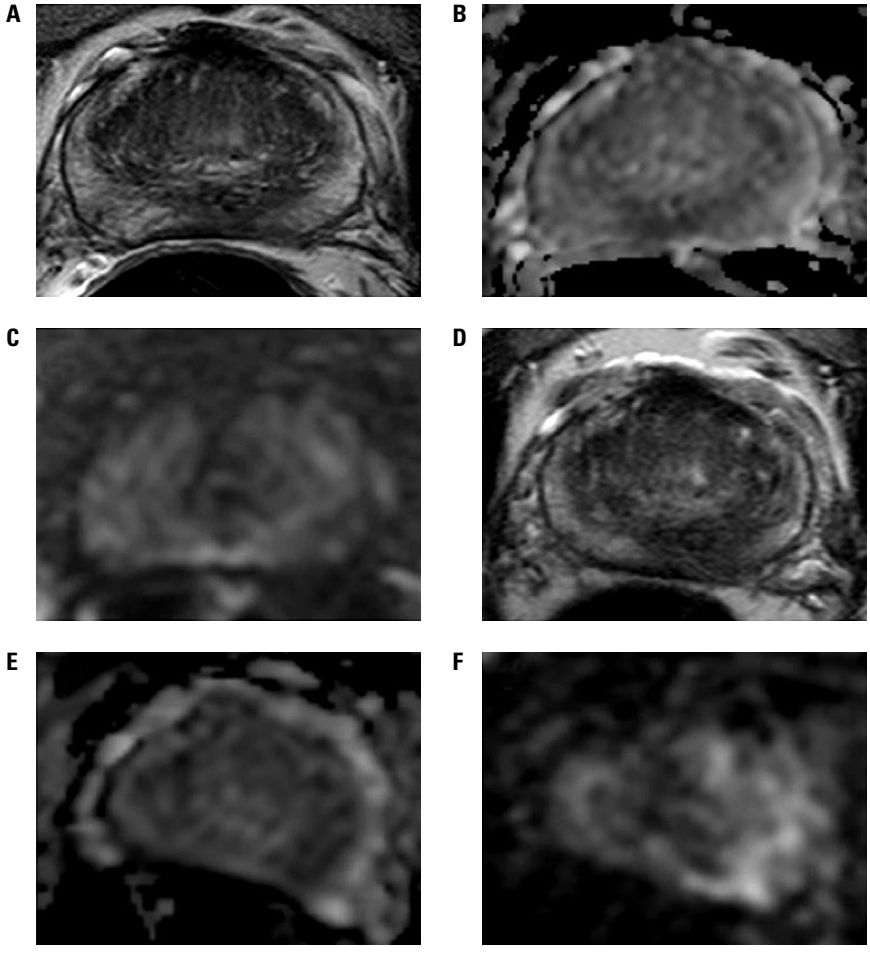

FIGURE 2.II-3
59-Year-Old Man With a PSA=3 ng/mL

Multiparametric MRI obtained with combined use of an endorectal coil including axial T2W MRI (**A**), ADC map of DW MRI (**B**), b value= 2,000 s/mm^2 DW MRI (**C**) shows no lesion in the prostate. The same patient underwent an mpMRI with 32-channel phased array surface coil a year after the initial mpMRI. Axial T2W MRI (**D**) again shows no lesion; however, ADC map of DW MRI (**E**) and b value = 1,500 s/mm^2 DW MRI (**F**) are limited due to rectal gas-related distortion and artifacts.

The pulse sequences that can be included in a detection protocol include an axial T1W MRI (for depiction of biopsy-related hemorrhage if the pre-imaging biopsy date is sooner than 8 weeks), triplane T2W MRI, transverse DW MRI (ADC maps and b value ≥1,400 s/mm^2 DW MRI), and transverse DCE MRI (**Table 2.II-2**). MR spectroscopy is no longer considered necessary for satisfactory mpMRI scanning and has been relegated to the research setting. T2W and DW MRI are considered mandatory sequences and form the basis of the PI-RADS v2 standard. Although DCE MRI's role is limited based on PI-RADS v2 guidelines, it is still considered a useful adjunct, particularly in challenging scenarios (e.g. when the tumour is in the anterior stroma or central zone) and in further evaluation of indeterminate lesions in the PZ.[5,6] Amongst all the mpMRI pulse sequences, DCE MRI is a relatively more invasive technique, since it includes a bolus injection of gadolinium-based contrast media (GBCA), which entails a low risk of inducing nephrogenic systemic fibrosis in patients with severe kidney failure, especially those on dialysis. Moreover, a recent paper reported that intravenous gadolinium exposure can be associated with neuronal tissue deposition, even in patients with normal kidney function.[7] Patients should be carefully evaluated for their renal function before initiating a plan of GBCA for DCE MRI. One important challenge with DW MRI when the ERC is not used is the presence of rectal gas and the generation of susceptibility and distortion artifacts, which can

potentially limit lesion detection. However, proper preparation of the patient, including having them expel gas prior to the study or by inserting small intrarectal air tubes in the rectum to decompress the gas, can be quite helpful in reducing this problem (**Figure 2.II-3**).

Ultimately, the ideal detection protocol depends on the individual needs of a medical centre. Cost, speed, and patient discomfort all have to be considered and will have different emphases for different situations. Certainly there has been a trend toward relatively simpler scan methods (obtained at 1.5T or 3T with no ERC) and shorter scans (limited to T2W MRI and DW MRI, with optional DCE MRI if needed). As MR technology improves, this trend will no doubt continue. However, the diversity of deployed MR scanner types and generations makes it difficult to provide one universal standardized acquisition protocol applicable to all centres and, thus, there is currently no world-wide accepted consensus regarding acquisitions of mpMRI of the prostate.

II-2.2.2 Staging protocol

Accurate local staging has, as its goal, the delineation of extracapsular extension (ECE) (i.e. stage T2 versus T3 disease), identification of seminal vesicle (SV) invasion, and identification of regional adenopathy and/or bone metastases. Currently, mpMRI is the most promising method for local staging prior to treatment, although it has limitations in sensitivity. It is widely accepted that mpMRI obtained with combined use of ERC and surface coils at 3T is needed to improve spatial resolution sufficiently so that capsular invasion can be detected.[8] However, an mpMRI protocol without ERC at 3T can nevertheless be useful for staging, although it is likely to be less sensitive than a scan obtained with an ERC. The evaluation of the prostatic capsular invasion requires very high spatial resolution and high image quality. The principle features of ECE are either overt/direct findings (direct extension visible on T2W images) or secondary features (capsular bulge, irregularity, broad capsular base, etc.) that are strongly associated with ECE. Studies suggest that the use of an ERC is helpful in detecting ECE with greater reliability.[9] Multiparametric MRI at 1.5T without an ERC is generally considered inadequate for staging.[10] However, Park *et al.* reported that mpMRI with ERC at 1.5T had comparable accuracy in local staging compared to no ERC mpMRI at 3T (70% versus 72% for with ERC versus without ERC protocols, respectively).[11] Recently, several studies comparing ERC versus no ERC at 3T for staging found the use of ERC to provide better image quality and accuracy for tumour localization when compared to body array coils. In 46 men who underwent prostatectomy, the area under the receiver operating characteristic curve (AUC) for localization of PCa was significantly increased from 0.62 to 0.68 ($p<0.001$) with ERC. ERC MRI significantly increased the AUCs for staging, and sensitivity for detection of locally advanced disease by experienced readers was increased from 7% (1 of 15) to a range of 73% (11 of 15) to 80% (12 of 15) ($p<0.05$), whereas a high specificity of 97% (30 of 31) to 100% (31 of 31) was maintained.[12] Seminal vesicle invasion is less sensitive to the need for an ERC and can be detected with either ERC or non-ERC mpMRI protocols, especially if the SVs are well distended.

The critical pulse sequences for optimizing a staging mpMRI protocol are again the axial T1W MRI (for depiction of biopsy-related hemorrhage), the triplane T2W MRI, the DW MRI (ADC maps and high b-value DW MRI), and DCE MRI. This multiparametric (MP) approach not only enables staging but also aids in predicting the aggressiveness of the lesions, especially when all sequences are positive, which implies a clinically significant PCa.[13] Moreover, DCE MRI is useful for SV invasion,

as enhancement of an SV mass is highly suggestive of metastases.[14] Although MR spectroscopy imaging (MRSI) has been in use for over a decade, its utility has decreased gradually since its value for cancer detection and staging is limited by the requirement of a large voxel size.[15] Moreover, it requires longer scan times, on-site physicists, and additional data processing, which limits enthusiasm for its use. Indeed, PI-RADS v2 suggests that MRSI is strictly a research option and is not mandatory[16] (**Table 2.II-2**).

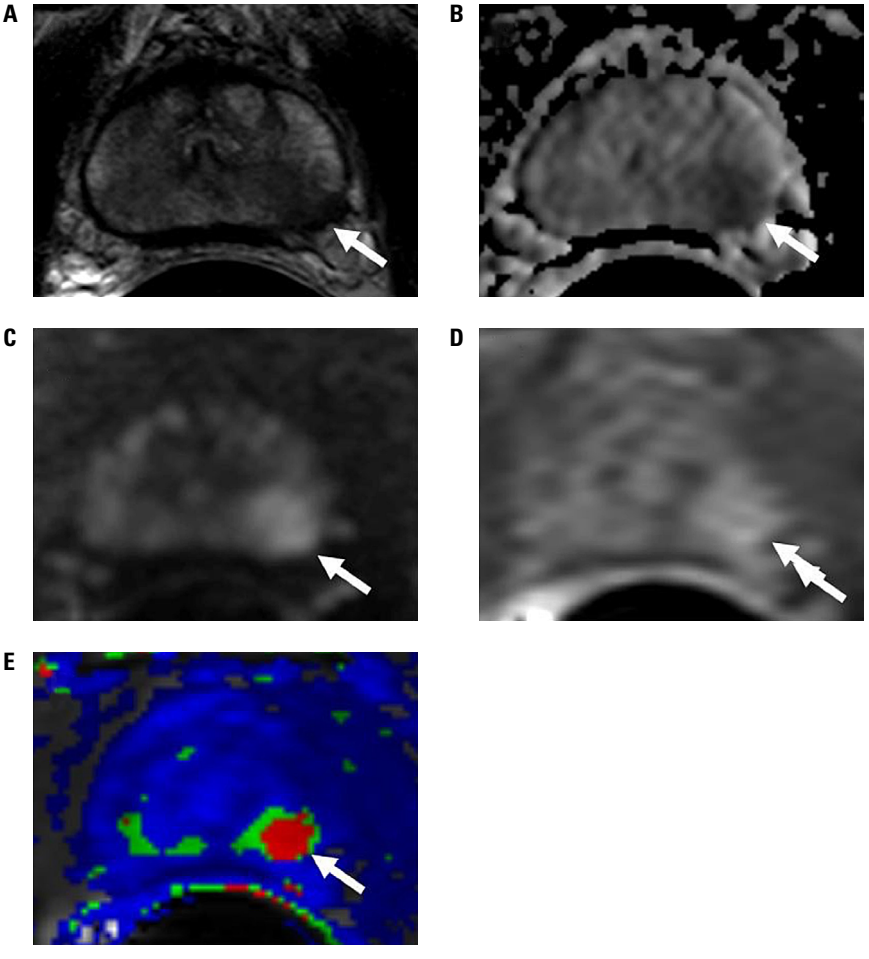

FIGURE 2.II-4
56-Year-Old Man With a PSA=8.15 ng/mL

Multiparametric MRI obtained with combined use of an endorectal coil including axial T2W MRI (**A**), ADC map of DW MRI (**B**), b value = 2,000 s/mm^2 DW MRI (**C**), DCE MRI (**D**), and K^{trans} map derived from DCE MRI (**E**) show a lesion in the left apical, mid-PZ (arrows). The patient underwent an RP.

An ideal staging protocol should provide the best possible spatial resolution for depiction of ECE while providing adequate coverage for detecting SV invasion; moreover, it should provide reliable information about tumour biology. Such goals can be achieved at 3T system with an ERC. However, this is an expensive technique for universal application (**Figure 2.II-4**). Additionally, use of ERC may be uncomfortable for the patients and can possibly result in patient non-compliance. Thus, the search continues for a comfortable yet accurate method of assessing ECE on mpMRI (**Table 2.II-1**).

II-2.3 Multiparametric-MRI Reporting and Scoring

The reported mpMRI accuracy for detecting clinically significant PCa varies greatly from one publication to another. Indeed, mpMRI accuracy depends on the cancer itself (non-nodular, low volume, low-grade cancers are supposedly harder to distinguish), on the technical protocol used for image acquisition (1.5T or 3T magnet, high-resolution coil or not, full or truncated sequences protocol, etc.), and on the reader's ability to find significant images in the images dataset, and to locate, describe, and quantify the likelihood of malignancy in their findings. Also, there are numerous ways those findings can be reported to the requesting physician.

Consequently, in an effort to harmonize practices, several professional societies, like the European Society of Radiology,[17] later joined with the ACR,[18] have published guidelines describing how to perform, interpret, and report prostate mpMRI. These guidelines include technical recommendations on how to perform the examination properly, how to localize and describe a suspicious image on all MRI sequences using an unified terminology (T2W imaging, DW imaging, DCE imaging, MR spectroscopy, and local staging), and how to summarize its likelihood of malignancy on a standardized Likert-like five-point scale called PI-RADS. The guidelines also describe how to communicate these findings to the requesting physician in a satisfactory manner.

Recently, a consensus team has published recommendations for the optimal use and reporting of prostate mpMRI in the specific context of focal therapy.[19]

II-2.3.1 Scoring systems used for prostate mpMRI interpretation

The first step of the interpretation process is to detect foci suspicious for clinically significant PCa within the gland. This requires a knowledge of PCa's natural history, gland anatomy and radioanatomy, and cancerous and benign tissue semiology. Reading has to be performed methodically. In a recent paper,[20] we encouraged a systematic and independent review of each of the three main compartments of the gland: the PZ, the transition zone (TZ), and the anterior fibromuscular stroma (AFMS), because each one has a slightly different semiology. Such analysis allows faster reading and review of the entire gland, without omission. This task is easier when the MP protocol is respected, because DCE imaging allows quick detection of foci of increased vascularization that usually match with cancer in the PZ, or foci of cancer difficult to detect on T2W or DW imaging. It has been demonstrated that simplified protocols, including only T2W and DW imaging, could yield, under certain conditions, similar detection rates, but most expert centres still use DCE imaging.

Once a significant image is detected, the second step is to provide an estimate of its malignancy. This classification can be qualitative or quantitative (i.e. with a score). Classifications are always based on semiology criteria that can be numerous (up to 14 per lesion), subjective, sequence specific, and complicated by multiples exceptions (size, location, etc.).[20-22] Thus, the main complaint of urologists is the subjectivity, complexity, and low reproducibility of mpMRI interpretation.[23,24]

II-2.3.1.1 PI-RADS

In an effort to harmonize practices, and following a consensus conference,[25] ESUR published professional recommendations in 2012.[1]

They introduced the PI-RADS scoring system to help classify mpMRI lesions. PI-RADS is a five-point, Likert-like scale designed to score each of the MP sequences, ranging from the lowest (1) to the highest (5) degree of suspicion for malignancy. **Table 2.II-3** summarizes the five main PI-RADS assessment categories.

TABLE 2.II-3 PI-RADS Assessment Categories

PI-RADS	Suspicion of clinically significant PCa	Full meaning of the PI-RADS score	Short explanation of the PI-RADS score
1	Very low	Clinically significant cancer is highly unlikely to be present	Not suspicious
2	Low	Clinically significant cancer is unlikely to be present	Slightly suspicious
3	Intermediate	The presence of clinically significant cancer is equivocal	Equivocal
4	High	Clinically significant cancer is likely to be present	Suspicious
5	Very high	Clinically significant cancer is highly likely to be present	Highly suspicious

A score of 1 out of 5, depicting completely normal PZ (bright and homogeneous on T2W images, without restriction or enhancement) or TZ tissue, has a high likelihood of being benign. Conversely, a score of 5 out of 5, depicting a typical cancer (PZ nodule with deep, low intensity on T2W images, with deep restriction and early enhancement at DCE), has the highest likelihood of being a clinically significant cancer. But, in practice, the majority of benign areas of tissue show some abnormalities (scars, normal enhancement, etc.), accounting for the majority of 2 out of 5 scores. The majority of clinically significant cancers show discordant semiology, with either atypical DW imaging, DCE imaging, or non-nodular appearance, accounting for the majority of 4 out of 5 scores. Remaining lesions (scoring 3 out of 5 = equivocal) show moderate signal changes and/or atypical morphology, and can either be malignant or benign. Version 1 of PI-RADS (PI-RADS v1) did not clearly define if the "final" PI-RADS of a suspicious image had to be a sum of 3 or 4 scores (ranging from 3–15 or 4–20 points), an average (ranging from 1–5), or a decision-support system to let the radiologist allocate the definitive score subjectively, with knowledge of additional criteria PI-RADS doesn't take into account (clinical information, lesion size, etc.).

TABLE 2.II-4 Semiology Criteria Used for Scoring PZ or TZ Lesions on the T2-Weighted Images in the 2015 PI-RADS v2 Scoring System

Series score	PZ	TZ
1	Uniform hyperintense signal intensity (normal)	Homogeneous intermediate signal intensity (normal)
2	Linear or wedge-shaped hypointensity or diffuse mild hypointensity, usually indistinct margin	Circumscribed hypointense or heterogeneous encapsulated nodule(s) (BPH)
3	Heterogeneous signal intensity or non-circumscribed, rounded, moderate hypointensity Includes others that do not qualify as 2, 4, or 5	Heterogeneous signal intensity with obscured margins Includes others that do not qualify as 2, 4, or 5
4	Circumscribed, homogenous moderate hypointense focus/mass confined to prostate and <1.5 cm in greatest dimension	Lenticular or non-circumscribed, homogeneous, moderately hypointense, and <1.5 cm in greatest dimension
5	Same as 4 but ≥1.5 cm in greatest dimension or definite extraprostatic extension/invasive behaviour	Same as 4, but ≥1.5 cm in greatest dimension or definite extraprostatic extension/invasive behaviour

Abbreviations: PZ: peripheral zone; TZ: transition zone; BPH: benign prostatic hyperplasia

TABLE 2.II-5 Semiology Criteria Used for Scoring PZ and TZ Lesions on the DWI Series in the 2015 PI-RADS v2 Scoring System

	PZ or TZ
Series score	DWI
1	No abnormality (i.e. normal) on ADC and high b-value DWI
2	Indistinct hypointense on ADC
3	Focal mildly/moderately hypointense on ADC and isointense/mildly hyperintense on high b-value DWI
4	Focal markedly hypointense on ADC and markedly hyperintense on high b-value DWI; <1.5 cm in greatest dimension
5	Same as 4, but ≥1.5 cm in greatest dimension or definite extraprostatic extension/invasive behaviour

Abbreviations: PZ: peripheral zone; TZ: transition zone; ADC: apparent diffusion coefficient; DWI: diffusion-weighted imaging

TABLE 2.II-6 Semiology Criteria Used for Scoring PZ and TZ Lesions on the DCE T1W Series in the 2015 PI-RADS v2 Scoring System

Series score	PZ or TZ DCE
Negative (–)	No early enhancement, or diffuse enhancement not corresponding to a focal finding on T2W and/or DW imaging or focal enhancement corresponding to a lesion demonstrating features of BPH on T2W imaging
Positive (+)	Focal AND earlier than or contemporaneously with enhancement of adjacent normal prostatic tissues AND corresponds to suspicious finding on T2W and/or DW imaging

Note that series score does not range from 1 to 5 like in other sequences, but only "positive" or "negative".
Abbreviations: PZ: peripheral zone; TZ: transition zone; DCE: dynamic contrast-enhanced; T2W: T2-weighted; DW: diffusion-weighted; BPH: benign prostatic hyperplasia

An updated version of PI-RADS (PI-RADS v2) was published in 2015. It clarifies how to assign an individual score to the most common MR series (T2W, DW, and DCE MRI), how to describe the findings using a glossary of terms, and, finally, how to build the final five-point scaled PI-RADS v2 score of the lesion, using a detailed scoring algorithm.[18]

Tables 2.II-4, **2.II-5**, and **2.II-6** reproduce the semiology criteria used in each MP sequence to assign a sub-score to the T2W, DW, and DCE pulse sequences used for calculation of the final PI-RADS v2 score.

PI-RADS v2 introduces dominant sequences depending on the location of the image in the gland, and uses DCE imaging at its lowest level, as opposed to the first version, which required calculation and assessment of enhancement curves with a dedicated software tool. Thus, DWI is supposed to be the dominant sequence for PZ images, with a minor contribution of DCE imaging, whereas in TZ, T2W imaging is dominant, completed by DW imaging. T2W imaging has no influence on the score in PZ, and DCE has no influence on the score in TZ, whereas in PZ, DCE is used to make the final decision and add the likelihood of malignancy to score 3 images at DW imaging. In other words, for image characterization, PI-RADS v2 ignores DCE information in TZ, and ignores T2W information in PZ.

TABLE 2.II-7 PI-RADS v2 Scoring Calculation Algorithm for PZ or TZ, Depending on the Scores of DWI, T2W, and DCE Imaging

PZ			
DW imaging (dominant)	**T2 (not used)**	**DCE (discriminant)**	**PI-RADS v2**
1	Any	Any	1
2	Any	Any	2
3	Any	Negative	3
		Positive	4
4	Any	Any	4
5	Any	Any	5

TZ			
T2W imaging (dominant)	**DCE (not used)**	**DW imaging (discriminant)**	**PI-RADS v2**
1	Any	Any	1
2	Any	Any	2
3	Any	≤4	3
		5	4
4	Any	Any	4
5	Any	Any	5

"Any" means the score can range from 1 to 5 for the T2W series, and negative or positive for the DCE series
Abbreviations: PZ: peripheral zone; DW: diffusion-weighted; DCE: dynamic contrast-enhanced; PI-RADS v2: Prostate Imaging and Reporting and Data System version 2; TZ: transition zone; T2W: T2-weighted

Table 2.II-7 reproduces the PI-RADS v2 scoring algorithm for suspicious PZ and TZ images at mpMRI, based on the scores of the series described in **Tables 2.II-2**, **2.II-3**, and **2.II-4**.

It should be noted that this new version states that PI-RADS score assessment should be strictly based on objective mpMRI findings, and to not incorporate factors such as the PSA, digital rectal examination (DRE), or other clinical information. Additionally, PI-RADS v2 specifies the target objective of the scoring: to provide a likelihood of malignancy for clinically significant cancer (defined as Gleason score [GS] ≥7 and/or volume ≥0.5 cc and/or extraprostatic extension).

Advanced imaging techniques, such as MRSI, which was included in PI-RADS v1, diffusion tensor imaging, fractional ADC, intravoxel incoherent motion imaging, blood oxygenation level dependant (BOLD) imaging, and MR-positron emission tomography (PET) are not included in the tools used for PI-RADS v2 scoring.

II-2.3.1.2 Other scoring techniques

Other scoring techniques have been published in the literature prior to PI-RADS:[22,23,26-29] the simpler and most widespread is the Likert scale. It is PI-RADS's ancestor. Apart from being defined as a five-point scale, Likert scales have a few common points with PI-RADS:

1. In the literature, there is no standardized or public list of criteria used for Likert scales' calculation. The Likert score is usually the graduated overall impression of the reader about a significant mpMRI image, based on a cognitive synthesis of the appearance of the lesion on all sequences. This is the reason why some authors call it a subjective score, in comparison with PI-RADS, which is an objective score based on criteria that can be opposed and verified on each sequence.
2. There is usually no lexicon or atlas available to describe abnormalities on T2W, DCE, or DW images, whereas there is one in PI-RADS helping readers to use the same terms.
3. Likert scales were used in variable forms to quantify either the suspicion for cancer or clinically significant cancer (with multiple definitions in the literature) and, until recently, authors sometimes did not specify this important detail in their works.[25]

TABLE 2.II-8 Semiology Signs Evoking Different Degrees of Likelihood of Malignancy in PZ or TZ

Likelihood of malignancy	PZ	TZ	AFMS
Signs highly suspicious of malignancy	▪ Consistent findings of marked low intensity T2 focus, marked restriction at DWI, and early enhancement at DCE ▪ Low-intensity T2 nodule, with convex borders, and high contrast with surrounding tissue in PZ	▪ Consistent findings of marked low-intensity T2 focus, marked restriction at DWI, and early enhancement at DCE	▪ Any early enhancement, even weak
Signs suspicious of malignancy	▪ Low-intensity T2 area, preferably with triangular shape, in an otherwise normal, high T2 intensity PZ ▪ Deep diffusion restriction (<0.9 mm^2/s), without nodular shape ▪ Earlier enhancement than surrounding tissue at DCE, contrasting with the rest of the PZ	▪ TZ nodule invading the PZ or the AFMS ▪ Ill-defined nodule, breaking the symmetry of the adenoma ▪ Nodule or area with very homogeneous signal ("charcoal sign") ▪ Nodule without peripheral low T2 rim ▪ Lesion located in the anterior and/or inferior halves of the gland ▪ Low or moderately low intense T2 area (similar to that of the rectum wall) ▪ Low-intensity T2 area visible on the high b raw DWI image (b >1,500), but not on DCE	▪ Isointense T2 area (usually, normal signal of the AFMS is very low, similar to that of the obturator muscles). Different intensity is suspicious

continued on **page 149**

TABLE 2.II-8 Semiology Signs Evoking Different Degrees of Likelihood of Malignancy in PZ or TZ, *Cont'd*

Likelihood of malignancy	PZ	TZ	AFMS
Non-specific signs	▪ Posterolateral location, instead of medial	▪ Earlier enhancement than surrounding tissue at DCE, contrasting with the rest of the TZ (not specific)	▪ Irregular shape ▪ Nodular shape ▪ Late enhancement (>3 min)
Signs suggestive of a probably benign lesion	▪ Non-nodular band image abnormality, rather perpendicular to the prostate surface	▪ Lesion located in the posterior half of the TZ ▪ Rimmed aspect of the nodule	—
Signs suggestive of benign image	▪ Low T2 intensity symmetric areas surrounding the ejaculatory ducts, with or without abnormality at DCE, and without abnormality at DWI ▪ Deep low T2 intensity nodular-like images between PZ and TZ at the base, tending to be lateral (this is central zone: the horseshoe sign)	▪ Lesion with high-intensity spots within it on T2W or diffusion-weighted images ▪ Very deep, low T2 intensity (similar to that of periprostatic muscles)	▪ No enhancement at all (triangular dark shape in the late DCE series)

These signs are not quantified. Assignment of a five-point scaled Likert score based on these findings depends on the lesion's topography and readers' synthesis of all signs.
Abbreviations: PZ: peripheral zone; TZ: transition zone; AFMS: anterior fibromuscular stroma; DWI: diffusion-weighted imaging; DCE: dynamic contrast-enhanced

In **Table 2.II-8**, we reproduce the criteria used to subjectively grade a lesion on a Likert scale.[20] Some of the criteria are missing in the current PI-RADS. This may explain why, depending on the criteria used for assessing suspicious images, one score may perform better than another.

II-2.3.1.3 Objective or subjective?

Use of PI-RADS scoring should strictly fit the semiology criteria described in the standard (for T2W, DW, and DCE imaging), and the final score's calculation should strictly comply with PI-RADS v2's algorithm description in PZ or TZ. Thus, a true PI-RADS score should be completely objective, reproducible, and enforceable.

Nevertheless, in routine practice, some lesions appear either more or less suspicious than their score predicts (AFMS lesion, lesion having high contrast with the rest of the gland, lesion with specific topography, lesion having grown between two examinations, etc.). Additionally, numerous tools such as specific post-processing algorithms (for T2W, DW, DCE, and MRSI), computer-aided diagnosis (CAD) results, or additional pulse sequences may provide useful information that is not implemented at the moment in the PI-RADS standard.

In these cases, the reader's impression can be different than what the PI-RADS score predicts, and there is a reason to complement the objective PI-RADS score with additional, more subjective findings. DCE enhancement of an image located in some parts of the TZ (e.g. the AFMS) may be very suggestive of malignancy, although this information had to be ignored to build a PI-RADS v2 score. In such cases of discrepancy, we encourage this addition, but without using two different scores for the same lesion (e.g. "lesion with an objective PI-RADS v2 score of 4/5, but highly suspicious due to its location" or "lesion with an objective PI-RADS v2 score of 5/5, but not suspicious due to the context of prostatitis and presence of numerous similar images in the gland" or "lesion with an objective PI-RADS v2 score of 3/5, but not suspicious due to its appearance in spectroscopic imaging").

Readers may prefer to avoid use of PI-RADS scoring when they believe it cannot apply, or does not translate their findings with enough accuracy (systematic use of MRSI, other sequences, etc.). In this case, we encourage using a similar five-point Likert scale, and expressing it this way in the report (e.g. "highly suspicious image with a subjective score of 5/5 in the left PZ (z08p)"), without mention of the "PI-RADS" acronym in the report.

II-2.3.1.4 PI-RADS accuracy and limitations

Several studies have demonstrated the accuracy of PI-RADS v1 in the classification of suspicious images,[22,30,31] and moderate to good inter-reader agreement. For instance, Renard-Penna *et al.* showed in 2015 that for a summed score of 9 points or greater, PI-RADS v1 sensitivity was 86.6%, specificity was 82.4%, PPV was 52.4%, negative predictive value (NPV) was 96.5%, and accuracy was 83.2%. Respective data for a subjective Likert scale scores of 3 or greater were 93.8%, 73.6%, 44.3%, 98.1%, and 73.3% in this prospective two-centre study that included 118 patients.[32] In another series of 215 patients, Vachée *et al.* observed respective AUCs of 0.8 and 0.74 in PZ for subjective Likert and objective PI-RADS v1, respectively, and 0.87 and 0.82 in TZ, respectively, with statistically significant differences in both cases. Other studies have shown different results, with slightly lower accuracies of objective PI-RADS v1 scoring versus subjective Likert-like scoring techniques,[22,33,34] suggesting that PI-RADS v1 criteria did not completely reflect all the components of an expert's judgment, or did not include significant criteria described in other scoring systems (e.g. size of the lesion, anterior or inferior location of TZ cancers, posterolateral location of PZ cancers, specific AFMS cancers, etc.).[20,29]

Two studies suggest that the PI-RADS score could be used as a triage test for selecting patients with suspicious images requiring target biopsies or, conversely, to defer biopsy procedure, depending on high (4 and 5 out of 5) or low (1 or 2 out of 5) PI-RADS scores, respectively.[32,35]

PI-RADS scoring has a few limitations:

a. A large proportion of significant MRI images remain equivocal (score of 3 out of 5) and cannot clearly be classified. Strict application of semiology criteria could overcome this drawback,[30] such as use of CAD either using atlases, computerized decision systems, automatic analysis,[36-42] new MRI sequences,[43,44] biomarkers,[45] or new post-processing algorithms that may be included in future versions of PI-RADS.
b. PI-RADS is to be used for assessing the likelihood that an image is a clinically significant cancer on untreated glands. In other words, it should not be used for describing images suspicious of recurrence after radiation beam external therapy, brachytherapy,

cryotherapy, or other focal treatments. Nor can it be used to describe focal abnormalities detected in patients with biological recurrence after prostatectomy.

c. One of the main limitations of existing scoring systems is that they have not undergone reliability assessment or multicentric prospective validation. Thanks to PI-RADS, such a large-scale prospective evaluation has become possible. This step has been taken by numerous studies dedicated to the validation of PI-RADS v1 reproducibility and accuracy (which we will discuss below). But PI-RADS v2 introduced a completely new scoring algorithm that will make teams unable to capitalize on previous works and require new studies to validate robustness, reproducibility, and accuracy of PI-RADS v2. To date, there is no reliable indication whether PI-RADS performs better than other scoring systems for the identification of clinically significant cancer.

We believe that PI-RADS is an evolving score, and will progressively be optimized in its next versions, just like the Breast Imaging-Reporting and Data System (BI-RADS) is regularly updated for breast cancer assessment. For instance, a lesion size of 15 mm is used to distinguish PI-RADS 4 versus PI-RADS 5 lesions. This threshold may vary in the next versions.

Therefore, it is important that all mentions of PI-RADS must specify its version (e.g. "PI-RADS v1," "PI-RADS v2"). Also, PI-RADS v2 makes no use of T2W MRI information in PZ and no use of DCE MRI information in TZ, which also may evolve in the next versions.

II-2.3.2 Scoring outcome

Physicians using mpMRI appreciate a five-point scale for assessing the likelihood of malignancy of the lesions radiologists describe. They understand that some images are not easy to characterize, or do not have typical appearance, and deserve an intermediate, equivocal score (3 out of 5). However, when an action on a suspicious lesion is necessary (target biopsy, focal therapy planning, special attention at time of surgery), they would rather have a binary scale stating whether the image is significantly suspicious or does not require attention. Thus, in most studies, the PI-RADS scale is dichotomized to "not suspicious" and "suspicious," with scores 1 and 2 considered as not suspicious and scores 3 to 5 as suspicious, even though score 3 lesions might be negative for cancer. This dichotomy is especially important for the calculation of PI-RADS accuracy for the detection of cancer (i.e. AUC), and is linked to the definition of what this score provides suspicion for (definition of clinically significant cancer).

In a few recent papers, some authors have found that PI-RADS/Likert lesions with scores of 3 out of 5 and positive for cancer corresponded to low-grade microfoci or cancers of low aggressiveness. Consequently, they proposed a different dichotomy (1 to 3 for "not suspicious" and only 4 and 5 for "suspicious"). This attitude has to be further studied, and may change the way radiologists score lesions, because today, for most radiologists, a lesion of score 3 out of 5 is supposedly significant.

This shows that radiologists performing mpMRI and assessing suspicious images need to:

- Use a standardized, and as objective as possible scoring system (PI-RADS), in order to ensure optimal reproducibility and inter-disciplinary communication
- Specify which version of the score is used
- Clearly know what this version of the score is designed for (e.g. assessing likelihood of malignancy of mpMRI images for clinically significant prostate cancer), in order to understand its accuracy and limitations
- Understand the outcome of the scoring
- Keep ability to report non-standard information (new sequences, CAD, etc.) that may improve lesions characterization
- Share this knowledge with requesting physicians (urologists, etc.), to avoid improper use of the score and potential drifts

II-2.3.3 Building standardized reports

A radiology report is a transcription of the radiologist's findings on images into an intelligible text. It contains a description of the images, followed by a conclusion that includes the radiologists's clinical impression on the entire data. It is primarily designed to answer the referring physician's clinical question. It will be read by other physicians and by the patient. Thus, its content has to be as objective as possible. Thus, a report is a reflection of the radiologist's responsibility to both the physicians and the patient.

There is great variability in the way mpMRI is reported (conventional free-text, semi-structured report, description of lesions with or without suspicion score, use of PI-RADS or a different score, addition or not of schematic prostate map or key images, etc.).[20,46-52]

ESUR guidelines include a dedicated section describing key elements for the reporting of this examination.[1] The primary objective of this approach is to harmonize practices in Europe, but thanks to a virtuous circle,[53] structured reporting allows wider promotion of guidelines, quicker adoption in radiology and urology, and, in the case of PI-RADS, an extension outside Europe and into the rest of the world.[18] The recent ACR/ESUR joint work on PI-RADS v2 includes a detailed glossary of terms, in an additional effort to harmonize the terminology.[18]

Key points of prostate mpMRI reporting are summarized in the 2015 PI-RADS v2 standard document:[18]

- To simplify and standardize the terminology and contents of radiology reports
- To facilitate the use of MRI for targeting biopsy
- To enable data collection and outcome monitoring
- To educate radiologists on prostate MRI reporting and to reduce variability in interpretations
- To enhance communication with the referring clinician

II-2.3.3.1 Standardization of content and terminology

Multiparametric MRI interpretation is built on the combination of multiple semiology criteria, whose basic enumeration on a scoring sheet, without explanation or medical analysis that takes into account semiology subtleties or clinical context, would have no sense. Most criteria need comprehensive

explanation or precision (e.g. PI-RADS v1 T2W criteria of score 3 "Intermediate appearances not in categories 1/2 or 4/5," or PI-RADS v2 ECE score 5 criteria "Bulges capsule of prostate") to be truly useful for the referring physician (urologist, radiation therapist, etc.).[1,18]

Prostate MRI reports should include all relevant information to allow use of mpMRI data under all circumstances (consultation with the patient, patient himself, multidisciplinary meeting, further comparison, follow-up, double reading, etc.) and easy data collection or comparison. Therefore, according to most authors, its format has to be structured, and its content needs to use a standardized and understandable terminology.

FIGURE 2.II-5
Sample Prostate mpMRI Report, Including Clinical Indication, Protocol, Findings, and Conclusion Paragraphs

Continued next page.

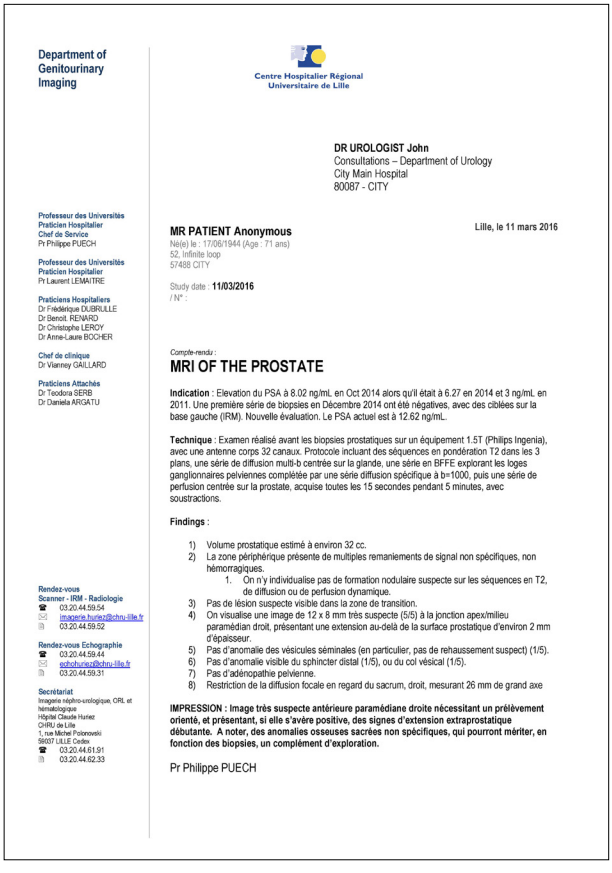

Department of Genitourinary Imaging

Centre Hospitalier Régional Universitaire de Lille

DR UROLOGIST John
Consultations – Department of Urology
City Main Hospital
80087 - CITY

Professeur des Universités
Praticien Hospitalier
Chef de Service
Pr Philippe PUECH

Professeur des Universités
Praticien Hospitalier
Pr Laurent LEMAITRE

Praticiens Hospitaliers
Dr Frédérique DUBRULLE
Dr Benoît. RENARD
Dr Christophe LEROY
Dr Anne-Laure BOCHER

Chef de clinique
Dr Vianney GAILLARD

Praticiens Attachés
Dr Teodora SERB
Dr Daniela ARGATU

Lille, le 11 mars 2016

MR PATIENT Anonymous
Né(e) le : 17/06/1944 (Age : 71 ans)
52, Infinite loop
57488 CITY

Study date : **11/03/2016**
/ N° :

Compte-rendu :

MRI OF THE PROSTATE

Indication : Elevation du PSA à 8.02 ng/mL en Oct 2014 alors qu'il était à 6.27 en 2014 et 3 ng/mL en 2011. Une première série de biopsies en Décembre 2014 ont été négatives, avec des ciblées sur la base gauche (IRM). Nouvelle évaluation. Le PSA actuel est à 12.62 ng/mL.

Technique : Examen réalisé avant les biopsies prostatiques sur un équipement 1.5T (Philips Ingenia), avec une antenne corps 32 canaux. Protocole incluant des séquences en pondération T2 dans les 3 plans, une série de diffusion multi-b centrée sur la glande, une série en BFFE explorant les loges ganglionnaires pelviennes complétée par une série diffusion spécifique à b=1000, puis une série de perfusion centrée sur la prostate, acquise toutes les 15 secondes pendant 5 minutes, avec soustractions.

Findings :

1) Volume prostatique estimé à environ 32 cc.
2) La zone périphérique présente de multiples remaniements de signal non spécifiques, non hémorragiques.
    1. On n'y individualise pas de formation nodulaire suspecte sur les séquences en T2, de diffusion ou de perfusion dynamique.
3) Pas de lésion suspecte visible dans la zone de transition.
4) On visualise une image de 12 x 8 mm très suspecte (5/5) à la jonction apex/milieu paramédian droit, présentant une extension au-delà de la surface prostatique d'environ 2 mm d'épaisseur.
5) Pas d'anomalie des vésicules séminales (en particulier, pas de rehaussement suspect) (1/5).
6) Pas d'anomalie visible du sphincter distal (1/5), ou du col vésical (1/5).
7) Pas d'adénopathie pelvienne.
8) Restriction de la diffusion focale en regard du sacrum, droit, mesurant 26 mm de grand axe

IMPRESSION : Image très suspecte antérieure paramédiane droite nécessitant un prélèvement orienté, et présentant, si elle s'avère positive, des signes d'extension extraprostatique débutante. A noter, des anomalies osseuses sacrées non spécifiques, qui pourront mériter, en fonction des biopsies, un complément d'exploration.

Pr Philippe PUECH

Rendez-vous
Scanner - IRM - Radiologie
☎ 03.20.44.59.54
✉ imagerie.hurez@chru-lille.fr
🖷 03.20.44.59.52

Rendez-vous Echographie
☎ 03.20.44.59.44
✉ echohurez@chru-lille.fr
🖷 03.20.44.59.31

Secrétariat
Imagerie néphro-urologique, ORL et hématologique
Hôpital Claude Huriez
CHRU de Lille
1, rue Michel Polonovski
59037 LILLE Cedex
☎ 03.20.44.61.91
🖷 03.20.44.62.33

FIGURE 2.II-5, CONT'D
Sample Prostate mpMRI Report, Including Clinical Indication, Protocol, Findings, and Conclusion Paragraphs

The second page is a standardized prostate map representing the most suspicious images using a coloured PI-RADS v1 scale. The third page includes key images of the lesion.

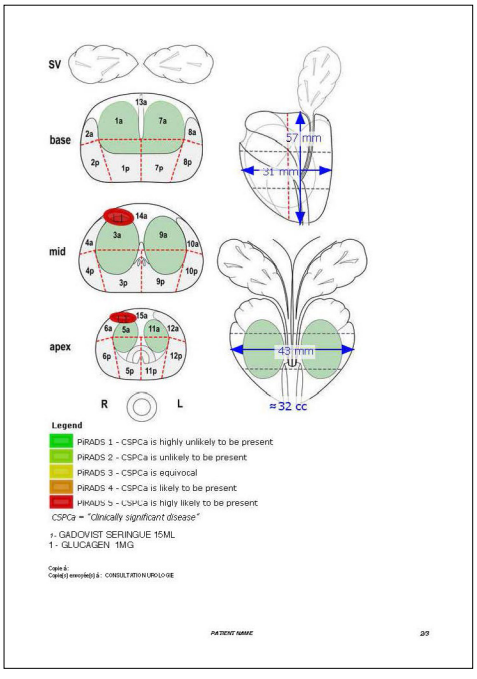

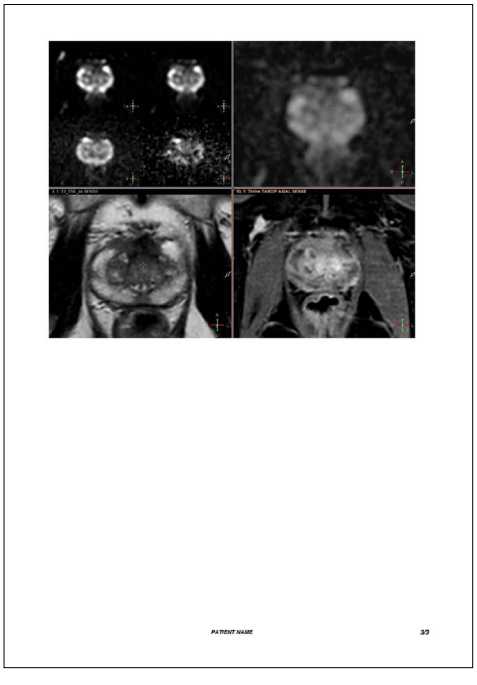

Structured reports (SRs), in comparison to free-text reports, allow easier data collection. Structured reports can be built using a text editing software (e.g. Microsoft Word) template, allowing pre-filling, use of checkboxes, use of lists, and even manual drawing. **Figure 2.II-5** shows a typical prostate mpMRI SR built by a radiologist at the time of interpretation using a word-processor template. These

templates allow faster editing of the report and immediate drawing of suspicious images onscreen. However, they suffer some drawbacks: they are time consuming, they are not usually connected to the picture archiving and communication system (PACS; directly to images) because they are stored in the radiology information system (RIS), and, as the text is stored into a word-processing document, the data are not easily collectable. Use of dedicated tools (discussed below) eventually linked to a database manager is faster and easier, but requires additional software, investment, and training.

Regardless of the form, we describe the framework and fundamental content of a standardized prostate mpMRI report in **Table 2.II-9**[54] (found at the end of this chapter).

II-2.3.3.2 Versioning

Due to the fact that two (and certainly more in the future) versions of PI-RADS are available, radiologists and urologists need to know the latest version of the standard, and radiologists must use the most recent version available. Also, the question of the version becomes important when PI-RADS is mentioned, and such mention in any report should either always be followed by the version number (e.g. PI-RADS v2), or used with an appendix at the end of the report stating which version is implicitely used when the term "PI-RADS" is mentioned.

II-2.3.3.3 Report appendixes

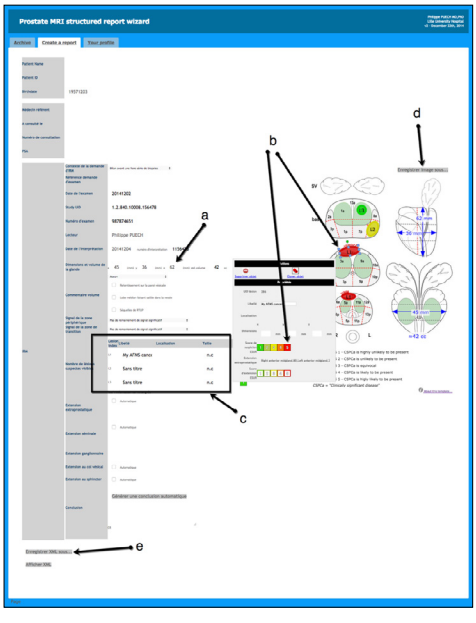

FIGURE 2.II-6
Sample Prostate mpMRI Report, Including Clinical Indication, Protocol, Findings, and Conclusion Paragraphs

The second page is a standardized prostate map representing the most suspicious images using a coloured PI-RADS v1 scale. The third page includes key images of the lesion.

In addition to the SR, a copy of a standardized prostate map, as described in current guidelines,[1] with manual or electronic drawing of lesions (**Figure 2.II-6**),[54] position, and size relative to the schematic gland should be included. Key images for the index lesion should also be included in the final report, to help physicians localize and recognize the most suspicious lesions.[20,47,49,55,56] Lesions having a suspicion of ECE should clearly have margins outside the contours of the schematic prostate slice.[56]

It is unclear whether a 16-, 27-,[26] or 39-[18] sector prostate map is optimal for the localization of lesions; however, all schematic representations of the prostate divide the gland in 3 cranio-caudal sections (base, mid-gland, and apex) with similar functionality.[1,17,18,20,26,47,56]

II-2.3.3.4 Computer-assisted reporting tools

Silveira *et al.* have demonstrated an improvement of prostate mpMRI report quality by using a structured template and informatics tools to generate the report automatically.[52] Recently, many so-called computer-assisted reporting (CAR) tools, designed to help radiologists build the SR, have been developed.[52,56-58] Some of them (web-based, software, free, or bound to equipment, etc.) can retrieve basic information (patient data, acquisition protocol, etc.) from existing data, and allow:

- Rapid and manual drawing of suspicious images on a standardized prostate map directly on the screen
- Reporting of the standard PI-RADS score (sometimes with assistance)
- Easy data collection (all data can be exported to an XML document, and exploited later)
- Sharing (by email, electronic transmission, etc.)

They are promising additions to RIS, or prostate-specific databases, and allow better compliance of SR to the standard.

II-2.3.3.5 Facilitating the use of MRI for target biopsies or focal therapy

Standardized SRs, especially when they include a prostate map and reference key images, are very helpful for target biopsies or focal therapy treatment planning. The SR cannot replace a face-to-face meeting between the radiologist and the physician who will perform the procedure, but can be a valuable addition to it. The SR will make physicians sure of what they target and will have to monitor.

Although it is still prospective, it is likely that, in the very near future, radiologists will be able to draw lesions in 3D, save them in a standard format (Digital Imaging and Communications in Medicine [DICOM]), and transmit these data on overlay on the MR-ultrasound (US) fusion biopsy systems, focal therapy (high-intensity focused ultrasound [HIFU], etc.), or surgery devices to guide surgeons during their procedures.

II-2.3.3.6 Data collection, outcome monitoring

Structured reports will take full benefit of dedicated software to enable a link between input data and automatic filling of a specific prostate oncology database.

Such databases allow better patient follow-up, key image collection, rapid image comparison, and data collection (clinic, PSA, pathology, etc.) in a single record, focused on prostate disease. This is especially important when following a patient's history at times of diagnosis, biopsy, treatment, and follow-up. In patients under AS, this kind of database helps radiologists identify images requiring special attention.

Databases also allow powerful searches, tracking of activity, strong support during multidisciplinary meetings, and teaching.

II-2.3.3.7 Education in radiology and reduction of variability in interpretation

Educating radiologists on prostate imaging can be divided into several steps, including initial education during their curriculum or continuing medical education (CME), training in image reading, an intermediate phase requiring double reading, and then a fully autonomous phase regularly updated by CME. Initial training has to be performed on various clinical presentations (typical PZ, TZ, or AFMS cancers, prostatitis, multifocal lesions, recurrences after prostatectomy or other therapy, etc.).[54]

Databases allow fast and easy identification and then collection of teaching cases that can serve as an up-to-date and living tool for radiology teaching.

Oncological databases, especially if dedicated to PCa and mpMRI management, allow linking to CAR tools (see above) to help fill the database, link to interpretation aids (glossaries of terms, standard terms, etc.), and grouping, in a single record, of several interpretations of the same data (double-reading). All these elements tend to reduce the variability in interpretation, as well as to harmonize practices among radiologists.

II-2.3.3.8 Enhancing communication with clinicians

The radiology report is the element of communication between the radiologist and the other clinicians. It has been shown that referring physicians prefer SRs, and that SRs are evidence of the reader's training and knowledge in the domain.[59] It is clear that SRs, especially if they follow an international standard and include a prostate map of significant images, are a major enhancement for the communication between radiologists and clinicians.

Such SRs should be accessible after a brief delay (1–4 days), remotely (via an electronic form) to avoid traditional postal mail delays. A clear mention of the version of PI-RADS used (see section 2.3.3.2 Versioning) should be made. A mention of the reader's certification might also be useful.

Additionally, a link to the image dataset should be made available, in order to make images easily reviewable either through PACS or remote access. Some electronic reporting systems allow access to key images by clicking on the suspicious image on the scoring sheet.

Access to the report and images should be possible with all the same functionalities, under all circumstances (consultation, office, operating room, multidisciplinary meeting room, etc.).

II-2.4 Prostate Biopsy and MRI

The ideal biopsy strategy would be to optimize the detection of clinically significant PCa and minimize the detection of low-grade, low-volume disease. To develop such a biopsy strategy, an individualized patient risk approach could be accomplished using pre-biopsy MRI. The role of prostate MRI has transformed over the last decade. Its utility has evolved from the evaluation of extra-prostatic extension to assisting in clinical patient management at all levels of care. Pre-biopsy MRI aids in PCa identification, localization, characterization of aggressiveness, and estimation of volume and contour. While the number of studies assessing the value of pre-MRI leading to image-targeted

biopsy is still limited, it has been demonstrated that MRI/TRUS-guided biopsy improves the yield of significant PCa detection rate in patients and reduces the number of insignificant PCa diagnosed in biopsy-naïve patients. This contributes to the accumulating evidence favouring MRI/TRUS-guided biopsy from image-blinded standard TRUS biopsy to a personalized biopsy strategy according to several determinants, including pre-biopsy MRI. However, because of underlying methodological pitfalls of current studies, the comparison of MRI/TRUS-guided biopsy with TRUS biopsy and the impact of pre-biopsy MRI need to be regarded with caution.

II-2.4.1 Advantages of MRI before first or repeat biopsy

To date, more and more clinicians are incorporating mpMRI in the workup of patients with a suspicion of PCa before biopsy. While questions and concerns remain open regarding MRI, performing pre-biopsy MRI has rapidly attracted interest among practicing urologists, due to several benefits. Efforts have been made to introduce evolving MRI to potentially visualize all clinically significant PCa.[25] Advantages of MRI before any biopsy would be supported by the rationale that sampling through the centre of the lesion yields more tissue, allowing more accurate characterization for pathologic examination,[60] which might reduce the risk of missing or misinterpreting a relevant lesion at prostate biopsy.[61]

The use of pre-biopsy MRI allows accurate PCa localization[62] before sampling, offering the opportunity to target a lesion. Prostate biopsy is still performed blinded for several reasons, including the lack of tools to localize PCa. Therefore, the prospect of localizing PCa prior to biopsy has led to the potential of the MRI-guided targeted biopsy approach, using cognitive- or software-based fusion of prostate MRI with real-time US images. This addresses many of the limitations of the standard TRUS-guided biopsy, aiming to improve detection of significant PCa while potentially reducing unnecessary biopsy of insignificant or absent PCa.[63,64] The data available to date have demonstrated an advantage of MRI-targeted biopsy with regard to the higher detection rate of significant PCa using fewer cores[65] than random (not targeted) systematic template-based sampling of the whole prostate by TRUS guidance.

Furthermore, the visualization of PCa using MRI provides precise 3D localization of the tumour before biopsy, which could have an impact on the per-lesion–based diagnostic approach. Knowing the location of MRI-derived targets could influence the urologist's decision making regarding biopsy techniques. To overcome difficult accessibility to certain areas of the prostate, changing the technical approach prior to doing biopsy could improve the chance for significant PCa detection. Localizing the lesion before biopsy cannot compensate for all issues associated with accessibility, but may allow some physicians to alter their approach with the goal of improving prostate sampling. For instance, the prostate's anterior location translates to limited access due to the inability of the current TRUS-biopsy platform to perform successful biopsy through the rectum wall to reach the suspicious area. In the setting of detection of prostate anterior tumours by pre-biopsy MRI, a primary transperineal approach could be performed to improve prostate sampling.[66]

Pre-biopsy MRI provides the opportunity for individualized patient risk stratification. Pre-biopsy MRI could be helpful in predicting the aggressiveness of tumours.[67] The definition of clinically significant PCa takes into account the volume of the tumour and the presence of a Gleason grade of

4 or 5. Currently, PSA, DRE, and TRUS-biopsy are used to stratify a patient's risk. One major limitation is the sampling error associated with the biopsy, which has been reported to under-grade up to 40% of patients after RP.[68] MRI could be an additional and helpful tool for grading lesions based on complementary information on water diffusion (DW MRI), metabolism (MR spectroscopy), and vascularity (DCE MRI). MRI-targeted biopsy can enhance the determination of aggressiveness via improved sampling of tumours within the prostate. Franiel *et al.*[69] investigated whether mpMRI is helpful in differentiating low-grade (GS ≤6) and high-grade (GS ≥7) PCa. Utilizing DCE kinetic models, low-grade PCa had significantly higher mean blood volume (1.76% vs 1.64%, p=0.039), longer mean transit time (6.39 s vs 3.25 s, p<0.001), and lower mean permeability (2.57 min [–1] versus 3.86 min [–1], p=0.011) than high-grade PCa. These features, achieved by using 1.5-T mpMRI, could be used to properly assess tumour aggressiveness and better manage the patient. Also, MR spectroscopy has shown promise in assessing a tumour's aggressiveness by revealing an increasing choline+creatinine/citrate ratio in high-grade tumours.[70] The comparison was established from statistical models, based on clinical features (DRE, PSA, biopsy, etc.), developed to predict indolent PCa. The AUC ranged up to 0.79, suggesting good accuracy. Ultimately, it was found that adding MR spectroscopy to MRI increases the predictive accuracy, improving the AUC from 0.803 (MRI model) to 0.854 (MRI+MR spectroscopy model). Villeirs *et al.*[71] have also investigated the ability of 1.5-T MR spectroscopy to predict high-grade PCa (GS ≥4+3) prior to biopsy. This study enrolled 356 men with a rising PSA. The follow-up was short (mean 21.3 months), and 220 patients had PCa confirmed by positive biopsy (41 high grade and 179 low grade). Results revealed a significant ability to eliminate high-grade PCa with an NPV of 98.4%. The rate of false positive findings was 7.3% in the 136 cancer-free men. However, despite these good results, MR spectroscopy is limited by its long scanning time and the need for post-processing. To date, among the other MR pulse sequences, DW MRI has demonstrated the best potential for characterizing PCa aggressiveness. Many publications have established a correlation between the high cellularity usually associated with high-grade PCa and low ADC values.[72]

MRI before biopsy could also assist in tumour staging by assessing tumour volume and contour, which may be crucial in planning the number of cores needed, as well as any subsequent focal therapy in localized PCa. Digital rectal examination and standard biopsy tend to underestimate the final PCa volume at RP in 20% of cases. The incremental value of MRI and MR spectroscopy to the staging nomograms for predicting organ-confined PCa has been assessed in a retrospective study.[73] This results in significant incremental value (p<0.02) to the nomograms in the overall study population. The contribution of MRI findings was significant in all risk groups, but was greatest in the intermediate- and high-risk groups (p<0.01 for both). Accuracy in the prediction of organ-confined PCa with MRI was higher when MR spectroscopy was used, but the difference was not significant. However, recent results suggest that MRI could also underestimate the PCa volume. In a correlation study by Le Nobin[74] performing a 3D co-registration methodology between pathology and MRI, PCa volume was likely to be underestimated by MRI, especially for high Gleason grades (≥4/5). Therefore, a much larger volume should be considered for biopsy to warrant detection.

Another advantage of pre-biopsy MRI is that it avoids post-hemorrhage artifact that restrain accuracy for PCa detection. Hemorrhage is responsible for the hyperintense signal on T1W images and hypointense signal on T2W images that may mimic PCa and decrease the MRI PPV. To circumvent this, a time delay of 6 to 8 weeks[75] has usually been required between biopsy and MRI to minimize

these artifacts. This is a long period and, even if respected, some lesions are still visible as hypersignals on T1W images, resulting in false positives on T2W MRI. MRI prior to biopsy could be an option to avoid such a bias.

II-2.4.2 Can MRI aid subsequent prostate biopsy and improve cancer detection?

Blinded conventional TRUS-biopsy misses 25% to 30% of PCa cases, both in biopsy-naïve patients and in patients with prior negative biopsy. The historical likelihood of missing significant PCa due to sampling error with sextant prostate biopsy strategy led to the introduction of new diagnostic approaches, for example the increase in the number of cores from 6 to 12.[76] Nomograms or genomic tests can also predict the individual risk of having PCa on subsequent biopsy. However, none of the approaches overcome the inherent limitation of undersampling using the traditional TRUS-biopsy approach. The introduction of MRI may improve PCa detection by directly targeting suspicious areas. However, conflicting results have been published so far. For instance, a recent randomized controlled trial (RCT) done by Baco *et al.*[77] compared two methods (12-core random TRUS biopsy versus 2-core MRI-targeted biopsy plus 12-core TRUS-biopsy) and reported no difference in diagnosing clinically significant PCa (defined as maximum cancer length ≥5 mm in Gleason 6 cancers or any Gleason ≥7 cancer). Conversely, in the systematic review by Moore *et al.*,[78] PCa was detected in 30% of targeted cores (375 out of 1,252) versus 7% of systematic cores (368 out of 5,441). On a per-patient basis, the cancer detection rate was 36% (526 of 1,442) for standard biopsy and 48% (650 of 1,345) for targeted biopsy.

A recent meta-analysis by Schoots *et al.* including 16 studies did not find any significant difference in overall PCa detection by TRUS-biopsy and MRI-targeted biopsy (sensitivity of 0.81 [95% confidence interval (CI), 0.70–0.88] vs 0.85 [95% CI, 0.80–0.89]). MRI-targeted biopsy and TRUS-biopsy missed the diagnosis of PCa in 15% and 19% of cases, respectively. However, MRI-targeted biopsy had a higher detection rate of clinically significant cancer (sensitivity of 0.91 [95% CI, 0.87–0.94] vs 0.76 [95% CI, 0.64–0.84]) and a lower detection rate of insignificant PCa (sensitivity of 0.44 [95% CI, 0.26–0.64] vs 0.83 [95% CI, 0.77–0.87]).[79] Therefore, MRI-targeted biopsy may not only improve the detection of clinically significant cancer, it may also diminish subsequent overtreatment by reduction of indolent PCa detection (over-diagnosis).[80] This was further confirmed by a randomized trial recently published by Panebianco *et al.*[81]

MRI may be particularly helpful in patients with persistently elevated serum PSA after a prior negative prostate biopsy.[82] MRI-targeted biopsy improved the detection of PCa compared to the standard scheme biopsies.[83] In a prospective study of 180 patients with prior negative biopsy, overall PCa detection was higher at second biopsy in the group with pre-biopsy MRI than in the one with standard TRUS-guided biopsy (45.5% versus 24.4%, respectively, p=0.01).[84] According to the recent systematic review by Schoots *et al.*, overall PCa detection in patients with prior negative biopsy was better with MRI-targeted biopsy than TRUS-biopsy, with a relative sensitivity of 1.62 (95% CI, 1.02–2.57). In addition, the improvement in the detection of significant PCa due to MRI-targeted biopsy was better in patients with prior negative biopsy than in biopsy-naïve patients (relative sensitivity 1.54, 95% CI,

1.05–2.57, and 1.10, 95% CI, 1.00–1.22, respectively). The reduced detection of insignificant PCa was, however, lower in patients with prior negative biopsy (relative sensitivity 0.51, 95% CI, 0.25–1.04, and 0.82, 95% CI, 0.03–21.4, respectively).

MRI-targeted biopsy can be performed using multiple techniques of fusion between MRI and US images, each bringing its own benefits and disadvantages. One prospective RCT comparing TRUS-biopsy plus MRI-targeted biopsy with visual guidance (MRI-visual-targeted biopsy) and TRUS-biopsy alone in biopsy-naïve men did not show any significant difference in overall PCa and significant PCa detection (64% [34 of 53] vs 57% [34 of 60]; 7.5% difference [95% CI, −10 to 25], p=0.5, and 55% [29 of 53] vs 45% [27 of 60]; 9.7% difference [95% CI, −8.5 to 27], p=0.8) respectively).[85] In the meta-analysis of Shoots *et al.*, MRI-visual-targeted biopsy did not show either a significant improvement compared to TRUS-biopsy (relative sensitivity 1.03, 95% CI, 0.91–1.16). Importantly, MRI-visual-targeted biopsy did not demonstrate inferior outcomes to targeted biopsy using US/MR fusion (MRI-fusion-targeted biopsy) in detecting overall and significant PCa, which is in accordance with Puech *et al.*[29] and Wysock *et al.*,[86] who reported no differences between those two techniques. Noteworthy is the fact that the MRI-fusion-targeted biopsy and MRI-in-bore-targeted biopsy improved significant PCa detection compared to TRUS-biopsy (relative sensitivity 1.29, 95% CI, 1.16–1.43, and 1.26, 95% CI, 1.08–1.46, respectively). In other words, evidence suggests that MRI-targeted biopsy, using fusion software or performed directly in bore, may benefit the diagnosis of significant PCa and may reduce the diagnosis of insignificant PCa in patients with a clinical suspicion of PCa, as compared to the standard TRUS biopsy. To our knowledge, only one recent systematic review[87] has been done so far to compare the benefits of the PCa detection rate of the multiple MRI-fusion-biopsy platforms available. To date, different platforms are Food and Drug Administration (FDA)-approved and mostly have strengthens and weaknesses that, in the end, didn't affect the benefit of doing pre-biopsy MRI in PCa detection in patients. Due to the limited number patients included in the study, heterogeneous study populations, and lack of consensus on significant PCa, Gayet *et al.* concluded that the general use of this technique in PCa diagnosis workup, whatever the platforms, should only be performed after critical consideration, even if the value of pre-MRI biopsy and targeted biopsy has been substantiated in patients with prior negative biopsy.

II-2.4.3 Can MRI prevent an unwanted biopsy?

Under certain circumstances, MRI could help rule out patients with persistently high PSA and prior negative biopsy. High PSA with negative biopsies presents a dilemma as to when testing can be discontinued. Established strategies for managing such patients without using MRI include a repeat biopsy scheme (10–12 cores), saturation/template biopsy (>12 cores), continued PSA monitoring, or other serum and urine markers. None of these strategies are satisfactory. The first two are invasive and may still miss significant cancer, while the third option does not address the necessary steps to take if the PSA continues to rise. The fourth, other serum and urine markers, have all demonstrated low sensitivity. A non-invasive imaging modality with a biomarker would constitute a major breakthrough in PCa diagnostics to rule out such patients for invasive biopsy monitoring in case of a negative biopsy result. MRI can then be used as a triage test in the population with persistently elevated or rising PSA levels to select patients who can avoid unnecessary subsequent prostate biopsy. Studies have shown that an MRI in patients with one set of negative biopsies and rising PSA levels is better than a repeat TRUS biopsy. In a screening population of 92 patients, Comet-Batlle *et al.* demonstrated

80% sensitivity, 76.1% specificity, 55.6% PPV, 91.1% NPV, and 77.2% accuracy for MRI, as compared to 85% NPV for a negative octant biopsy for PCa.[88] As a result, an MRI showing no evidence of disease in a patient with a marginally raised PSA and negative prior biopsy would seem to offer a similar level of reassurance as two sets of prostate biopsies reporting no cancer detected.

MRI could also at least defer prostate biopsy in the absence of any suspicion for PCa in MRI. Indeed, given the high sensitivity of MRI in detecting significant lesions, a negative MRI may prevent subsequent untargeted biopsy to detect low-risk disease. This approach is supported by a number of studies, including the series by Rouse *et al.*[89] that reported only 4% of significant PCa was missed by deferring biopsy on the basis of MRI findings.

However, MRI still cannot be used as a single surrogate for biopsy, and is not likely to be suited as a stand-alone test for diagnosing PCa. MRI has still missed one in six high-grade PCa: failure to identify 16% of men with high-grade PCa (GS ≥7) in a prospective study of 1,044 men with elevated PSA, among whom 241 had no suspicious lesions on MRI. Importantly, looking at the results of systematic mapping TRUS-biopsy, 75 patients who had no sign of disease on MRI (31%) were found to have a GS ≥6. This translated into an NPV of MRI for GS ≥6 and GS >7 (high-grade) of 53% and 84%, respectively. In addition, fusion MRI-targeted biopsy can't circumvent this lack of detection, based on the recent RCT published by Baco *et al.*, which reported a false-negative rate for clinically significant cancers of 13% more than that published by Moore *et al.*[78]

After all, one can argue that MRI is still better than the NPV of TRUS-biopsy with a cancer detection rate of 20% to 24% following initial TRUS-biopsy, no matter the technical approach (saturation or 12-core biopsy).[90,91] As a result, there is clearly going to be a trade-off. Using MRI is more accurate than image-blinded needle biopsy for identifying GS 7 or higher lesions, and it avoids diagnosing many insignificant PCa. However, using MRI alone risks missing a rather significant number of clinically important PCa. In conclusion, men with high PSA without any prior biopsy should consider traditional 12-core needle biopsy even if an MRI appears normal. For the time being, we cannot rely on MRI alone to completely eliminate the use of the conventional 12-core biopsy in biopsy-naïve patients with an abnormal PSA level.

II-2.4.4 Is routine pre-biopsy MRI cost effective?

To our knowledge, there has been no formal cost-effectiveness study on a large cohort and across various health care systems regarding the use of mpMRI before prostate biopsy. One European study from 2013 suggested that the costs of prostate MRI-in-bore-targeted biopsy is similar to those of the standard approach.[92] On first impression, this cost-effectiveness analysis provided a strong economic case for adopting the strategy based on MRI with an incremental cost-effectiveness ratio at just 323€ per quality-adjusted life year. However, this study has been criticized due to certain assumptions and uncertainties in the model structure and input data of this study. Moreover, the costs associated with treating the complications of TRUS-biopsy were not included in the model.

Given the fact that approximately 50% of patients with an elevated PSA and a negative prostate biopsy will undergo a second prostate biopsy,[91] mpMRI could be cost-effective if it could avoid prostate biopsy due to its high NPV. But to date, we don't know how many patients would safely avoid those biopsies based on negative MRI findings.

II-2.5 The Role of mpMRI in Active Surveillance

Low-grade prostate cancers have an indolent course and are characterized by a very slow growth rate. Active surveillance is an accepted treatment alternative for low-risk disease and is currently included in international guidelines (National Comprehensive Cancer Network [NCCN], European Association of Urology [EAU]) for clinical practice. Active surveillance offers the advantage of careful monitoring and early intervention for disease progression, thereby avoiding unnecessary overtreatment with the inherent side effects of radical treatment (prostatectomy or radiation therapy).[93]

During an AS program, low-grade prostate cancers are serially monitored for signs of disease progression. Prostate-specific antigen testing and DRE are administered periodically, along with a repeat biopsy of the prostate at one year and then at specific intervals thereafter. Active radical treatment is offered at the earliest indication of disease progression.[94]

The strategy of AS provides similar disease-free outcomes as compared to immediate treatment in this subset of patients and also reduces the overtreatment risks.[95]

Long-term studies have shown that around 35% of patients in AS switch to active treatment due to disease progression, most of which is noted in the first year, indicating the possibility of misclassification in the initial biopsy. The criteria employed for inclusion in AS protocols vary greatly from one protocol to another.[96] The majority of them, however, include criteria such as GS of 6 (3+3), PSA value <10 ng/mL, no presence of Gleason grade 4 or 5, tumour volume <0.5 cm^3, and no evidence of extra-prostatic disease at DRE. More recently, a subset of patients with Gleason 3+4 disease, with a very small volume of Gleason 4, have also been considered eligible for AS by some authors.[97]

Prostate biopsy is an essential component of AS. Biopsy findings depict the grade and the volume of cancer, and only patients who present with a low grade (Gleason pattern ≤3) and minimal cancer volume (≤2 positive biopsy cores, and/or ≤50% cancer involvement in individual cores) are candidates for AS if their clinical stage is ≤T2 and PSA levels are low (usually <10 ng/mL). Biopsies are systematically repeated during the follow-up to limit sampling errors and, rarely, to assess true progression to a higher grade and/or larger cancer volume. The histological findings of the first re-biopsy after diagnosis are generally the major cause for withdrawal from AS programs, because of PCa reclassification.

However, prostate biopsy is an invasive procedure that is associated with complications, and the cumulative risk of complications increases over multiple biopsies. In particular, in men with PCa on AS, the number of previous biopsies increases the risk of infectious complications (p=0.04).[98]

II-2.5.1 Rationale and capabilities of mpMRI

Multiparametric MRI is currently the most established imaging modality for significant PCa diagnosis. By using both anatomical and functional sequences like DW MRI, DCE MRI, and MR spectroscopy, mpMRI is able to provide important information about the location, shape, and aggressiveness of the lesion. Multiparametric proved to be an excellent modality to guide targeted biopsies for significant cancer detection, with sensitivity and specificity of 98% and 100%, respectively.[26] Several studies have documented reliable correlations between GS and apparent diffusion coefficient values obtained on DW MRI.[99,100] PCa is known as a typical multifocal neoplasm, and each focus may present a different aggressiveness and different GS. We found that tumour size and grade were important predictors of tumour detection and, in spite of PCa being multifocal, mpMRI can detect the most aggressive focus of cancer.[101] Multiparametric MRI also helps in determining the position and dimensions of each suspicious focus, in particular in the anterior portion of the gland where DRE and TRUS have low diagnostic accuracy.[102]

Additionally, mpMRI has been shown to have an NPV for clinically significant cancer (60%–95%). Patients with visible lesions on mpMRI tripled the risk of overall cancer progression.[103] Furthermore, patients with low-grade PCa (PSA <10 ng/mL and Gleason 6) in AS and a negative mpMRI have only a 3.5% probability to be reclassified into intermediate or high-risk disease.[104] It is commonly considered that larger lesions harbour more aggressive cancers. With the introduction of mpMRI into clinical practice, this notion is challenged. The largest lesion may not always correspond to the most aggressive site and, moreover, within a large neoplastic lesion, there may be areas of different histological differentiation with different degrees of aggressiveness.[105]

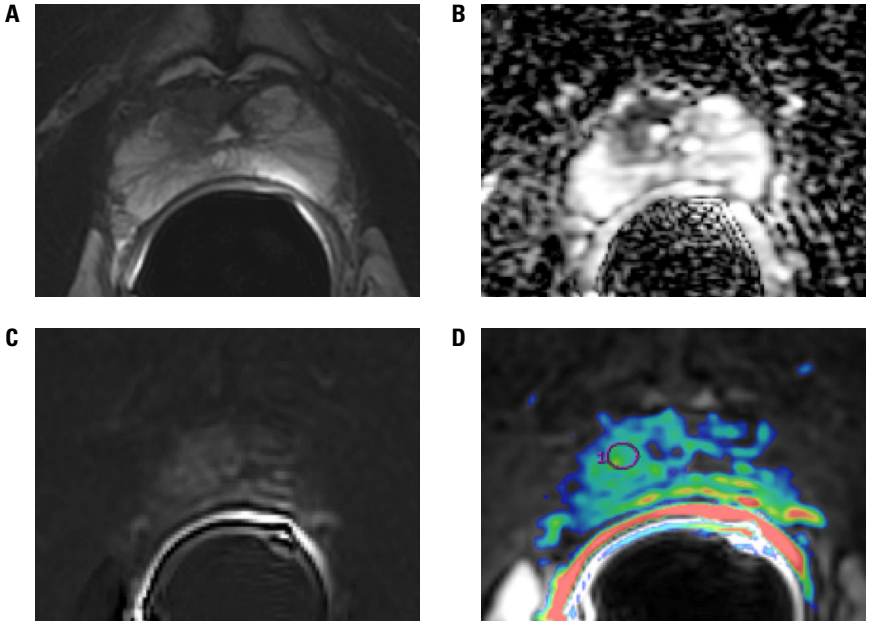

FIGURE 2.II-7

(**A**) 57-year-old patient, PSA 3.8 ng/mL, biopsy positive for focus of adenocarcinoma <20%, GS score 6 (3+3), and eligible for enrollment in an AS program. PSA increase after 8 months (4.3 ng/mL). The patient underwent mpMRI and therefore was excluded from the program. Axial T2W FSE image showing an area of marked hypointensity in the right anterior horn of PZ.

(**B**) ADC map with b-value of 0, 500, 1,000, and 3,000 mm^2/sec showing a significant area of restricted water diffusivity corresponding to the area highlighted in T2.

(**C**) Axial perfusion gradient-echo T1W.

(**D**) Perfusion colour map showing an area of mild enhancement in right anterior PZ; according to PI-RADS score (v2), overall score is 4.

The sequence that showed the highest performance in evaluating disease progression is DW MRI and, hence, best lends itself to an AS program. During the initial diagnosis, DWI is able to contribute significantly to identify the index lesion and hence provides appropriate target for the biopsy.[106] High-grade PCa usually has higher cellularity than healthy tissue, corresponding to a decreased ADC value. Similar to the clinical-pathologic eligibility criteria, mpMRI criteria have also been introduced according to PI-RADS v2 score. In fact, a PI-RADS score of 1 and/or 2 is consistent with the very low and low probability to have clinically significant cancer. In other words, prostate cancers missed at mpMRI are very small lesions (<0.5 cc) with low GS (≤6 [3+3]) that are suitable for AS. Although the use of mpMRI is not yet consolidated in the AS monitoring protocol, undoubtedly it can be a very useful tool that can detect early disease and monitor tumour progression. For example, a yearly mpMRI examination could be suggested to monitor patients in AS, and a switch of PI-RADS 1 or 2 to a higher score could be suggested as a reliable criterion to stop AS and switch to active treatment. With the presence of PI-RADS 3, an indeterminate pattern, the patient can go to the follow-up or to the biopsy based on the kinetics of PSA. With a PI-RADS score of 4 or 5, lesions are considered for targeted-biopsy. The diagnostic accuracy of mpMRI actually reaches considerable sensitivity and

specificity values of 91% and 95%, respectively, for larger lesions, and gets down to 44% for small, low-grade lesions <0.5 cm^3. For these reasons, it was proposed to perform MRI examination prior to performing a prostate biopsy, in order to target the biopsy to the index lesion or to avoid unnecessary biopsy. The role of the prostate biopsy in the context of an AS program is to register and confirm the progression of the disease suggested during the course of follow-up by the serum PSA levels, and its derivatives (PSA density, PSA velocity), or DRE. The fundamental weakness of TRUS-guided prostate biopsy, in whatever way it is carried out, is the lack of precision in the execution. The well-known limits are represented by the risk of sampling areas of healthy tissue, or neoplastic areas of lower grade than others.[107] Generally, the enrollment in the AS program has been done with random biopsies (performing no more than 12–14 random biopsies). Multiparametric MRI, if performed as a first-line examination, is able to depict each neoplastic or suspected area, and hence to follow them within an AS program.[81] It is able to quickly highlight even the smallest changes in the size, shape, extension, and cellularity, even after a minimal increase in PSA value (velocity and density). Recent studies confirm that in patients with increasing PSA values, AS can be reliably interrupted and switched to active treatment on the basis of MRI findings.[108] Though still controversial and not universally accepted, these findings confer the importance of mpMRI to follow up the course of AS (**Figure 2.II-7**). Negative mpMRI, despite the clinical suspicion of disease progression, can avoid making a prostate biopsy random. If there is clinical suspicion of disease progression, mpMRI is able to indicate which lesions present modifications to the parameters, in order to schedule a targeted biopsy. Today, it is not possible to switch from AS to active treatment based only on the mpMRI, and proven histology of disease progression is still necessary to switch to the subsequent treatment plans.[109]

II-2.5.2 Multiparametric MRI in active surveillance: indications and timing

Multiparametric MRI can assist in the appropriate classification of the patient into an AS program when it is performed as a first-line investigation in biopsy-naïve patients with suspicion of PCa (total PSA, PSA density, PSA velocity, family history). Subsequently, it can aid in more accurate follow-up of the index lesions, which is the most dominant lesion and more likely to influence the biological behaviour of the cancer. It can also accurately image the anterior zone tumours that may be missed at random biopsy.

Based on a very high NPV, mpMRI could miss some very small (<0.5 cc), low-risk (GS 6) lesions that would have been under AS if detected. This means that a patient with low-grade disease and a negative MRI has a high degree of confidence to remain in the AS program. Multiparametric MRI can detect early disease progression and re-classify the disease based on volume control and lesion characteristics (ADC mapping, onset of capsular infiltration), and can consequently trigger early active treatment.

We propose the following timing in AS protocols:

- Once a year in cases of PI-RADS score 1 and 2 tumours at first examination and no biopsy, and
- Every 8 months in cases of PI-RADS score 3 tumours. The biopsy is indicated only in case the index lesion changed at MRI (in terms of volume, ADC, etc.).

II-2.6 The Role of mpMRI in Focal Therapy

Focal therapy is a strategy by which the overtreatment burden of the current PCa pathway could be reduced.[110] However, only 13% to 33% of the patients have a unifocal PCa lesion and are eligible for focal therapy.[111] Consistent with the index lesion theory, even more patients would be suitable.[112]

Imaging is an important tool to select, guide, and follow patients who are eligible and undergoing focal therapy. During treatment, clinicians should be certain that the targeted tumour is being totally ablated and that, outside the targeted area, no significant tumour resides.[113] In the follow-up period, recurrences or residual tumour should be clearly recognized on imaging. Currently, in most institutions, MRI is being used to select patients for focal therapy and for image-guided targeted sampling, as well as a follow-up tool.

II-2.6.1 MRI for patient selection

A recently convened expert panel of urologists, radiologists, and basic researchers concluded that mpMRI is an important component of patient selection for focal therapy.[19]

There are different varieties of focal treatments modalities described in the literature: hemiablation, (i.e. treatment of the tumour affected lateralized hemisphere of the prostate), hockey stick ablation (i.e. hemiablation of the prostate plus one half of the contralateral hemisphere), and targeted focal therapy (i.e. only the tumour itself is treated). These approaches depend on the location and extent of the intraprostatic tumour, as well as the GS. In the selection of candidates for focal therapy, a combination of mpMRI and template-guided mapping biopsy provides a high NPV in the detection of lobes with significant cancer.[114]

For focal therapy, merely localizing and determining the aggressiveness of the PCa is not enough. Determining PCa volume and contours is of paramount importance for targeting focal therapy. Thus far, few studies have evaluated tumour volume estimation.[115-117] Tumour volume is underestimated by DW MRI, especially for GS (≥7) and high suspicion score 4/5 lesions.[74] T2-weighted MRI showed less underestimation of the actual tumour volume. Thus, a much larger region of the gland that is directly visualized on MRI warrants ablation to be confident of full tumour destruction. It seems that this discrepancy in boundary may be most significant at the non-capsular side of the lesion, given the tendency for tumours to originate close to the capsule and exhibit centripetal growth within the gland.[118] These findings have key implications in planning and performing focal therapy procedures, and would suggest the use of a security margin to be confident of full tumour destruction in view of the larger histological volume.[119]

II-2.6.2 Monitoring of focal therapy with MRI

Multiparametric MRI provides two key advantages for an effective focal treatment over other imaging modalities:

- First, its excellent soft tissue contrast and multi-planar imaging capabilities allow for clear visualization and localization of the tumour and for accurate (thermal) probe placement into the lesion. At this moment, mpMRI is the most sensitive and specific imaging technique for localizing PCa[120] and is already used to target the tumour during focal laser ablation,[121,122] cryoablation,[123] HIFU,[124] and low-dose rate and high-dose rate (HDR) prostate brachytherapy.[125-127]
- Second, MR thermometry can be used to non-invasively monitor and control the ablation in real-time by measuring the spatial distribution of tissue temperature during thermal ablation therapy. This is important to estimate boundaries of irreversible tissue necrosis such that damage to adjacent critical structures as the neurovascular bundle, the urethra, and the rectal wall can be minimized. The latter is important to circumvent cryoablation-induced recto-urethral fistula.[128] Nevertheless, temperature monitoring of a critical structure can be done by the insertion of thermosensors adjacent to the ablation area. However, this is invasive and information is provided from a single point.

Ideally, MR thermometry should provide high spatial and temporal resolution in three different directions to precisely monitor the temperature distribution within the targeted tissue. However, improving both comes at the cost of signal-to-noise reduction and increased temperature uncertainty. For this reason, a comparative assessment should be made to achieve the optimal compromise for a specific situation. MR image-guided laser ablation and MR image-guided focused US are, for example, relatively fast thermal ablation techniques and, therefore, a high temporal resolution is essential. Recent studies reporting on MR-guided focal laser ablation used a single slice with a spatial resolution of 0.8 x 0.8 x 5.0 mm or 1.2 x 2.5 x 5.0 mm and repeated every 5 seconds,[121,129,130] or five parallel slices with a spatial resolution of 1.0 x 1.0 x 3.0 mm, repeated every 6 seconds[131] to monitor the ablation process. However, without knowing the SNR and temperature accuracy, it is hard to estimate which sequence is optimal for monitoring MR-guided thermal ablation. Chopra *et al.* showed that using MR thermometry while applying trans-urethral MR-guided focused US allowed for stable temperature measurements achieved with a standard deviation of approximately ±1°C.[132]

With the currently available clinical MR sequences, MR temperature mapping is unfortunately not possible during MR image-guided cryoablation. When the tissue freezes, the free water is taken up into ice crystals, causing an extreme decrease of T2 relaxation time and, therefore, a loss of signal.[133] Despite the fact that the temperature gradient within the ice ball is not measurable with MR temperature mapping, MRI allows an excellent depiction of the ice-tissue boundary, with the ice ball presenting as a sharply delineated signal void on all conventional pulse sequences.[134] Next to this, the hyperintense rim observed surrounding the ice ball in fast T1W MRI corresponded to cooled but non-frozen temperatures induced proximal to the frozen zone.[135] Nevertheless, investigators have reported that the volume of the ice ball does not match the volume of tissue necrosis.[136] As a consequence, attention should be paid to the size and location of the lesion that needs to be ablated, and a safety margin of a few millimetres should be applied.

During MR image-guided cryoablation, the ice ball grows relatively slowly. For this reason, an acquisition time of 2 to 3 minutes between scans would typically be regarded as sufficient.[137] However, in situations where ablation is performed close to critical structures, faster imaging may be required to avoid unwanted tissue damage. Feedback on temperatures within the ice ball would be desirable in order to assess whether a sufficiently cold end temperature is achieved throughout the entire target lesion. However, an effective non-invasive approach for this is still needed. Several recent studies have demonstrated measurable MR signal from within the frozen tissue using ultrashort echo time (UTE) imaging, which may hold potential for MR thermometry.[138,139] Wansapura et al. investigated MR thermometry of frozen tissue using UTE signal intensity and R2* and demonstrated the feasibility of in vivo MR temperature maps during cryoablation in a canine experiment.[139] In another study by Kaye et al., it was determined that, within the cryogenic temperature range, the relation with temperature of both these MR parameters appeared consistent between different tissue types.[140] Nevertheless, further work into the accuracy and consistency of this approach is still required before this technique can be applied clinically.

In general, the benefits of performing focal therapy under MRI guidance (i.e. the accuracy during probe placement or the option of temperature mapping during the procedure) should be considered carefully against the disadvantages. These disadvantages include the need for special MR-compatible materials, a limited amount of space during the procedure for the patient and physician, the limited time available in MR scanners, and increased costs. Nevertheless, MR systems are increasingly being adjusted to allow interventional MR systems. New systems with wider and shorter bores are being developed to provide more space for the patient and the physician as well.

Another way to overcome the accessibility problem and to increase the speed of the procedure is to perform part of the procedure with the help of an MR-compatible robot. Several robots for transrectal or transperineal needle placement and low dose rate (LDR) seed implantation have been described in the literature, and the results of these studies are promising.[141-144] Alternatively, probes can be placed outside the MRI scanner room with the help of MR-TRUS fusion guidance. Real-time acquired TRUS images are fused with earlier acquired MR images of the prostate. In this way, focal therapy probes, for example cryoneedles or a laser fibre, can be inserted transperineally into the lesion. Afterward, the patients can be transferred to the MRI room to confirm accurate placement of the probe(s) and undergo real-time monitoring of the treatment with MR thermometry.

MRI can be used to assess the ablation size and validate the completeness of the focal therapy covering the target lesion. A few studies evaluated the ability of MRI to accurately determine the ablation volume. Larson *et al.* found a strong correlation (r=0.92) between MR volumetric assessment of damage and hematoxylin and eosin (H&E) assessment of damage when using different forms of minimally invasive treatment modalities to create intraprostatic lesions.[145] Linder *et al.* evaluated the effects of focal laser ablation on PCa tissue and the accuracy of MRI in determining ablated lesion volume by comparing the whole-mount histology and MRI in four patients who underwent focal laser ablation followed by RP.[146] Ablated areas were characterized by homogeneous coagulation necrosis. The MRI-calculated ablated volume correlated well with histopathology. T1W post-gadolinium MRI is able to determine the ablation accurately and can be used to assess treatment extent.

II-2.6.3 Follow-up with MRI

To date, there is little evidence about imaging in the follow-up after focal therapy of the prostate. In patients with a clinical suspicion of local PCa recurrence after definitive treatment, T2W MRI can detect a lobulated hyperintense mass in the RP fossa, but is less successful after focal therapies such as laser ablation, irreversible electroporation, focal brachytherapy, high-intensity focused US, photodynamic therapy, or cryosurgery. The addition of functional MRI techniques such as DWI and DCE MRI has shown promise to increase the overall imaging performance in the detection of local recurrence or residual disease.[147]

II-2.6.3.1 T2W MRI

The morphological changes in the prostate after irradiation include inflammation, glandular atrophy, fibrosis, and prostatic shrinkage.[148,149] These result in diffusely decreased signal intensity of the prostatic tissue and loss of the normal zonal anatomy, causing difficulty in distinguishing recurrence from irradiated normal tissue.[150,151] Reported sensitivities (26%–44%) and specificities (64%–86%) of T2W MRI for detection of local tumour recurrence have therefore been rather low, and many authors have recommended the use of additional techniques, like DW MRI and DCE MRI.[152-154]

FIGURE 2.II-8
Diagnostic MRI of a 55-year-old-male with a PSA of 18.2 ng/mL after external radiotherapy (**A-D**).

(**A**) Axial T2W MR image at the mid-level of the prostate. Post-radiotherapy effects are visible within the prostate. The PZ has similar signal intensity as the TZ.

(**B**) K^{trans} map at the same level as (**A**) demonstrates pathologic enhancement in the left peripheral (T=tumour) zone (arrow).

(**C** and **D**) ADC map and high b-value imaging demonstrate restriction in the same area as in (**B**). High b-value image demonstrates high signal intensity in the same area as in (**B** and **C**).

Focal cryoablation was performed and the PSA dropped to 1.5 ng/mL after 30 months (**E-H**).

(**E**) Cryoablation effects (arrows) are visible on T2W MRI; however, local recurrence or residual disease are difficult to depict.

(**F**) Contrast-enhanced MRI does not demonstrate abnormal enhancement.

(**G** and **H**) ADC map and high b-value imaging does not show any ADC reduction or high signal intensity on the high b-value.

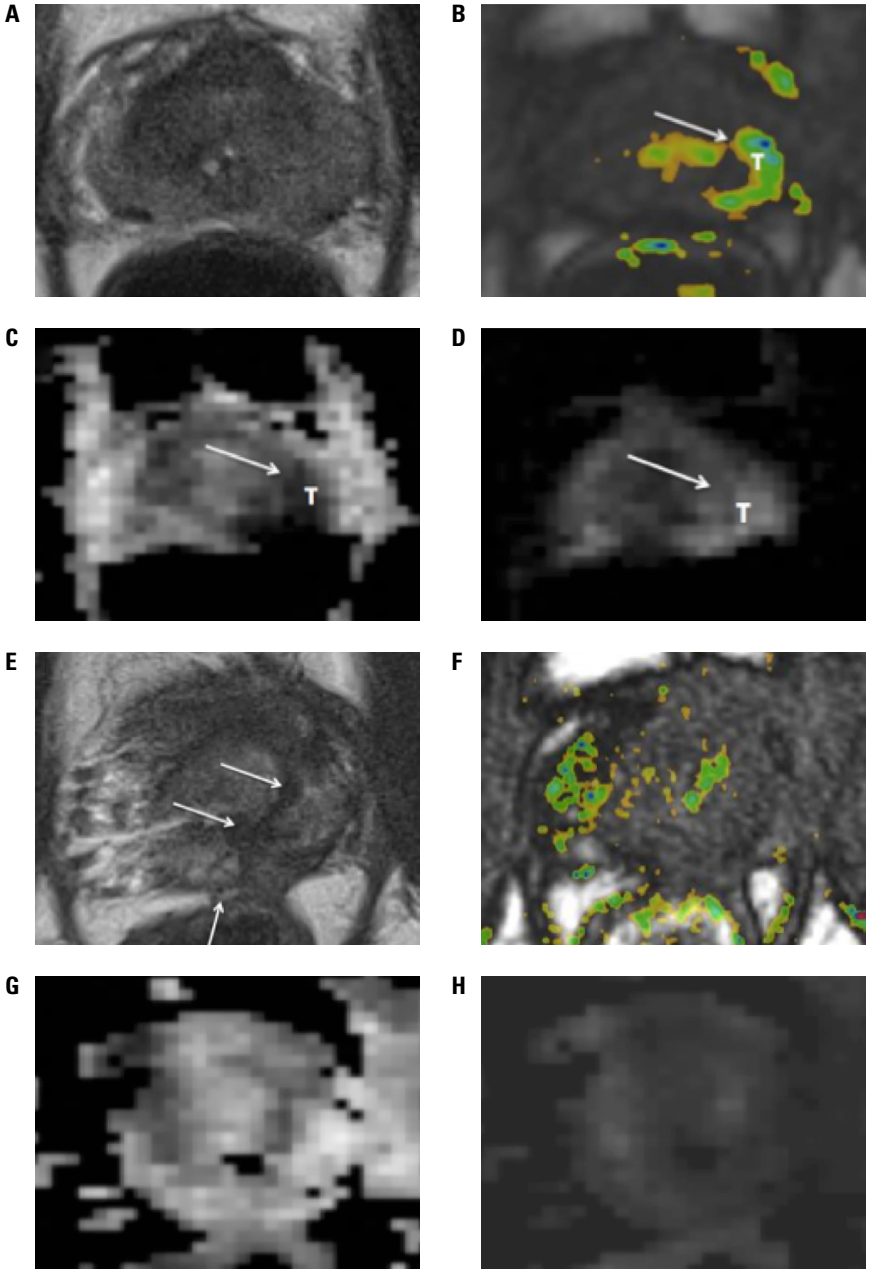

In thermal ablation, tissue heating induces coagulative necrosis in the target area, which becomes completely devascularized and surrounded by inflammation and edema.[155-157] MR images taken within days of high-intensity focused US may show a significant increase of the prostate volume, presumably due to transient edema, with slightly hyperintense areas on T1W images, most likely representing interstitial hemorrhage, and a central hypointense and ill-defined lesion on T2W images.[158] Similar findings are seen after photodynamic therapy. T2 heterogeneous signals are seen that are related to the edema and ischemic modifications induced by phototherapy.[159]

After 3 to 5 months, the prostate shrinks and the parenchyma becomes diffusely hypointense and ill-defined, with loss of the normal zonal anatomy on T2W images.[158,160] This MRI appearance of HIFU and laser ablation–induced changes is identical to those associated with cryotherapy (which induces cell death by hypothermic coagulation necrosis, direct cellular toxicity due to disruption of the cell membrane by formation of ice ball crystals and gene-regulated cell death) (**Figure 2.II-8**).[161] At 6 months after photodynamic therapy, important changes of the prostate shape and signal are found. Small areas of residual necrosis may still be present in the treated lobe, corresponding to coagulation necrosis.[159] Although residual or recurrent PCa has been reported to be somewhat more hypointense than the surrounding tissue, it remains difficult to correctly discriminate both entities with anatomical T2W MRI alone.[160,162,163] The addition of contrast-enhanced MRI or DWI may demonstrate local recurrence or residual disease after focal treatment.

II-2.6.3.2 Diffusion weighted MRI

FIGURE 2.II-9
Diagnostic MRI of a 57-year-old-male with a PSA of 13.7 ng/mL after external radiotherapy. Patient has an MR-targeted biopsy-proven local recurrence with a GS of 4+5 in the left lateral horn and TZ.

(**A**) T2-weighted MR image demonstrates a large bulky lesion (T) in the left peripheral and TZs, with increased and early enhancement (**B**). The ADC map (**C**) and high b-value imaging (**D**) shows restriction in this area, which is suspicious for recurrent disease.

Focal cryoablation was performed and the PSA dropped to almost 0.1 ng/mL; however, it progressively increased after 9 months up to 3.1 ng/mL.

(**E**) Cryoablation effects (arrows) are visible on T2W MRI; however, local recurrence or residual disease are difficult to depict.

(**F**) Contrast-enhanced MRI demonstrates abnormal enhancement in the anterior TZ.

(**G** and **H**) ADC map and high b-value imaging shows ADC reduction and high signal intensity on the high b-value in the same location. The mpMRI demonstrated a recurrence in the base of the prostate, which was proven with histology.

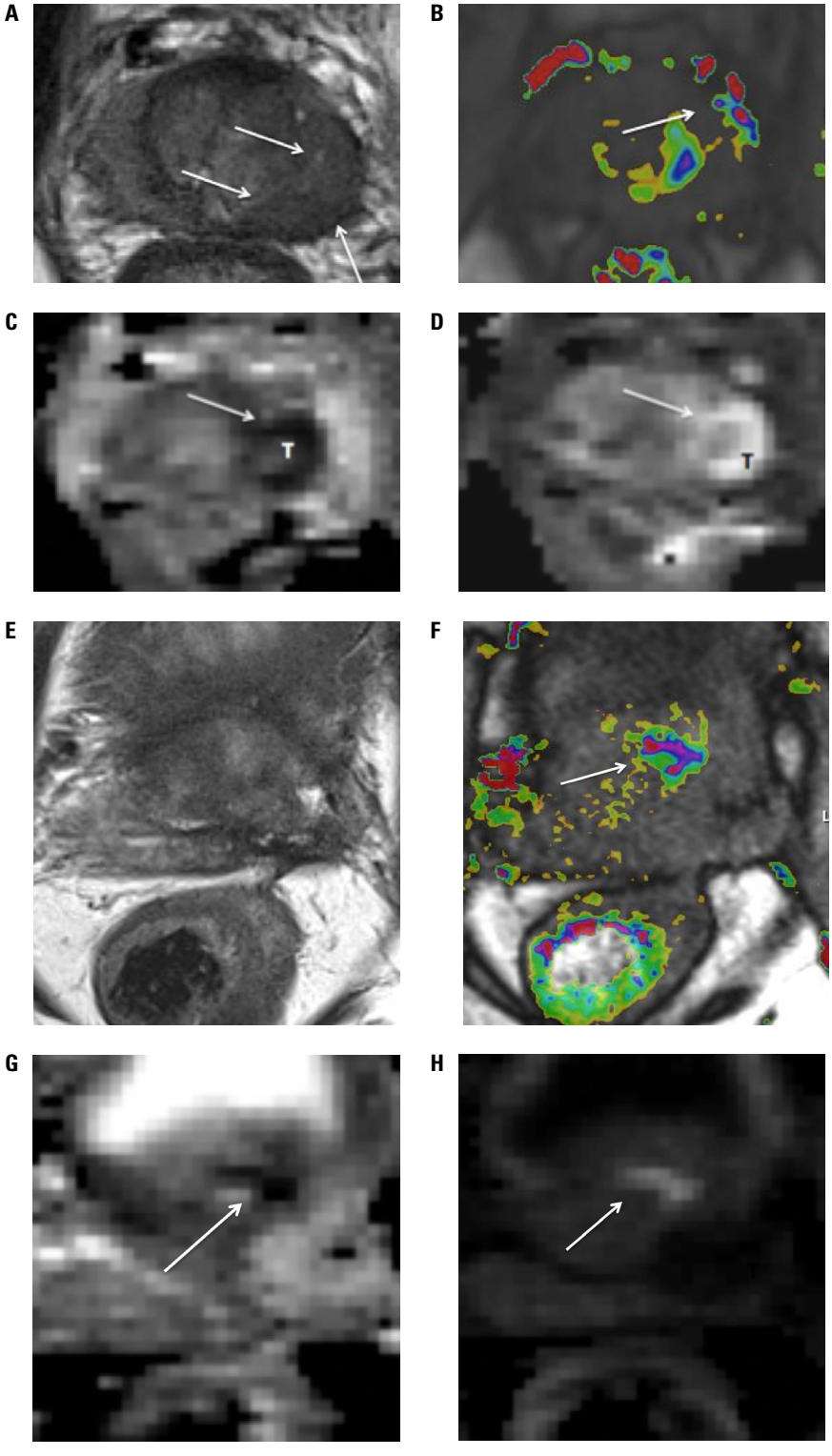

There is building evidence that DW MRI is able to detect local recurrence after RP. Kim *et al.* used the latter technique to predict recurrence after radiation therapy on 3T MR scanner without the use of an endorectal coil, and found that recurrent PCa had lower ADC values than the surrounding irradiated benign tissue, yielding a sensitivity and specificity of 49% and 93%, respectively.[154] The combination of T2W MRI and DW MRI was significantly more sensitive than anatomical MRI alone for the prediction of local recurrence after radiation therapy. After thermal ablation, on the other hand, both residual or recurrent tumour, fibrosis, and residual benign prostatic hypertrophic nodules may show lower ADC (**Figure 2.II-9**), compromising the use of DW MRI to differentiate benign from malignant changes.[155]

II-2.6.3.3 Dynamic contrast-enhanced MRI

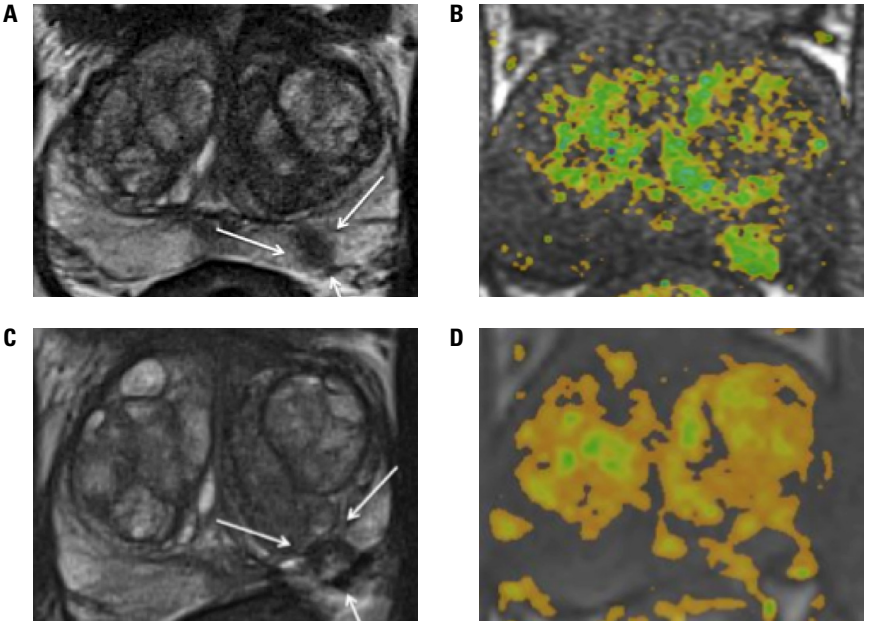

FIGURE 2.II-10
A 64-Year-Old Male With Unifocal Area of Gleason 3+4 PCa in the Left PZ

(**A**) T2-weighted MR image shows that the tumour has lower signal intensity than the PZ (arrows).

(**B**) The DCE MRI shows early enhancement.

(**C**) Patient underwent MRI-guided laser ablation and the follow-up MRI demonstrated only some rim enhancement (**D**), without evidence of residual disease.

Directly after thermal ablation (i.e. laser ablation and high-intensity focused US), the devascularized volume is initially depicted as a non-enhancing area surrounded by an enhancing rim on contrast-enhanced MR images.[155,156] Similar findings can be found after radiofrequency ablation. In non-thermal focal therapy techniques like irreversible electroporation, similar findings can be seen as with thermal energy techniques.[164] Consequently, detection of residual cancer foci at that time is limited (even with DCE MRI), both because of their small size and the difficulty to distinguish them from the inflammatory rim enhancement.[156] One to 6 months after focal therapy, the devascularized zone and peripheral rim enhancement progressively disappear in a centripetal manner as coagulation necrosis is replaced by fibrous scar tissue (**Figure 2.II-10**). This creates more favourable conditions for distinguishing residual or recurrent cancers using DCE MRI. Recurrences or residual disease are usually early enhancing and hypervascular, while post-high intensity focused US fibrosis is rather homogeneous, poorly enhancing, and hypovascular, with the exception of residual benign prostatic hypertrophic nodules, which can also be hypervascular and thus mimic tumour progression or recurrence.[155,156]

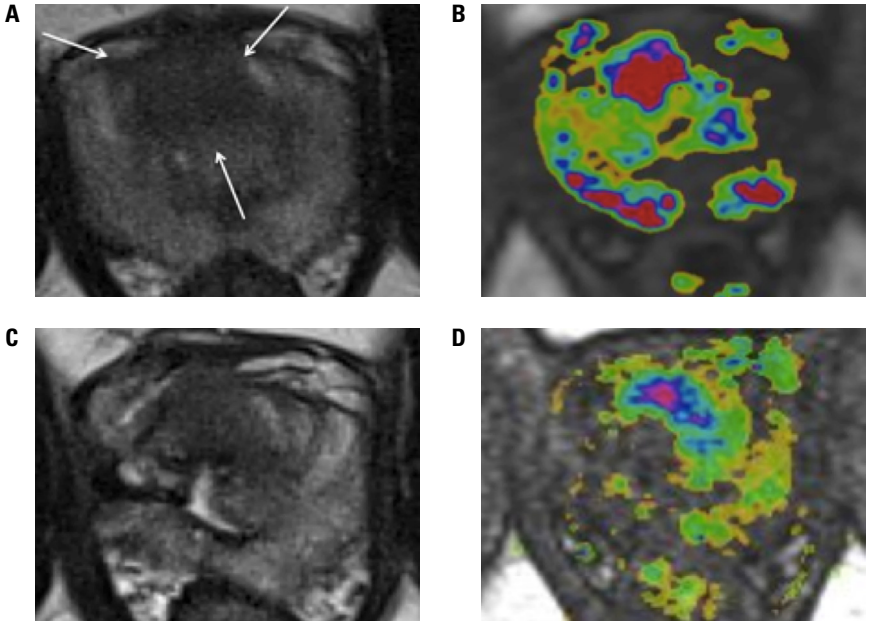

FIGURE 2.II-11
57-year-old male with an area of Gleason 3+3 PCa (PSA 16.6) in the anterior part of the TZ.

(**A**) T2-weighted MR image shows that the tumour has lower signal intensity than the TZ (arrows).

(**B**) The DCE MRI shows early enhancement in the same area as in (Figure 2.II-11A).

(**C**) Patient underwent HIFU, and the follow-up MRI demonstrated residual disease on T2W MRI and early enhancement (**D**).

One study compared mpMRI with anatomical T2W MRI. DCE MRI with T2W MRI in combination with DWI showed similar accuracy values (71%–73%), with a somewhat higher sensitivity of DCE MRI (80%–87% versus 63%–70%) at the cost of a lower specificity (63%–68% versus 74%–78%).[155] A more recent study was performed in 2012, in which 26 patients underwent both DCE MRI and targeted biopsy of the prostate after whole-gland high intensity focused US treatment. Sensitivity ranged between 73% and 87% among three readers, whereas specificity ranged between 73% and 82%[165] (**Figure 2.II-11**). These results were comparable with pre-biopsy prostate-specific antigen levels.

Moreover, using simple visual diagnostic criteria for DCE MRI, instead of quantitative parameters, was sufficient to increase the biopsy yield of MRI-guided biopsies versus routine biopsy in the detection of recurrent cancer after HIFU ablation.[156] After cryosurgery, contrast-enhanced MRI is not accurate in the prediction of treatment success because non-enhancement is variably consistent with complete cell death, and enhancement cannot differentiate between residual benign tissue and PCa recurrence.[161,166]

II-2.7 The Role of mpMRI in Detecting Local Recurrences After Treatment

The clinical suspicion of local recurrence of PCa after treatment is based on the onset of biochemical relapse, i.e. of the increase of the PSA level above a certain threshold.

With the increasing rate of success of early salvage therapy, the diagnosis of local tumour recurrence at the earliest possible stage has become pertinent. The goal of imaging in biochemical relapse after treatment is to detect local and/or metastatic recurrence. Technical improvements of prostatic MRI and, in particular, the development of MP and functional imaging now allow early detection of local recurrence after radical treatments (RP, radiation therapy) or focal therapy, HIFU, cryosurgery, and photodynamic therapy.

II-2.7.1 Local recurrence after RP

There is no indication for systematic imaging after RP, aside from biochemical relapse (two consecutive PSA values above 0.2 ng/mL) or suspicion of clinical recurrence (e.g. in case of abnormal findings in the prostate bed at DRE). When confronted with a clinical or biochemical suspicion of recurrence, the aim of imaging is to identify patients with a local recurrence eligible for external radiotherapy salvage treatment or alternative techniques such as HIFU or cryotherapy. Defining precise location of recurrence allows for identifying the target volume of radiotherapy, and therefore adapting irradiation in order to increase efficiency, all the while reducing the risk of side effects.

II-2.7.1.1 T2-weighted MRI

FIGURE 2.II-12
Local Recurrence After RP

Transverse T2W (**A**) and T1W (**B**) images after gadolinium injection: nodular hypointense thickening in front of the urethra-vesical anastomosis (**A**). Intense enhancement at the early arterial phase (**B**).

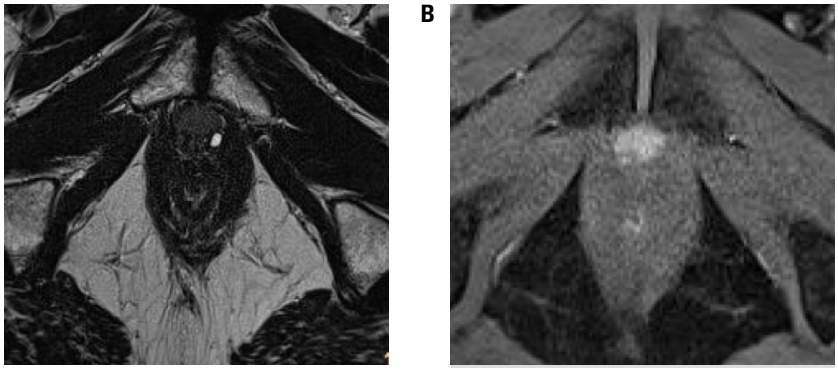

The recent development of functional MRI techniques has provided promising results for accurate detection and characterization of small recurrent PCa. Moreover, mpMRI after RP is a very useful tool to discriminate locoregional relapse from residual glandular healthy tissue, scar/fibrosis, and granulation tissue, and gives an idea of the aggressiveness of nodule recurrence by means of ADC values. The presence, on T2W images, of a lobulated nodular-like or mass-like soft tissue thickening in the prostatectomy bed that appear slightly hyperintense compared to pelvic muscles should be considered to be strongly suggestive of local recurrence (**Figure 2.II-12A**). Recurrences after RP

have been found anywhere along the surgical cavity. The most common site of postoperative local recurrence is the urethrovesical anastomosis around the bladder neck and the membranous urethra (40%–55%).[167] Other common sites of local recurrence are retro-vesical (between the urinary bladder and rectum), within SV remnants, and at the anterior or lateral surgical margins of the prostatectomy bed (around levator ani muscles).[168] Scar tissue appears hypointense on T2W images and in most cases is distinguishable from local recurrence.

II-2.7.1.2 DCE and DW MRI

DCE MRI is based on repetitive image acquisition before and during the passage of an IV-injected bolus of contrast agent (gadolinium). It has become the key element for differentiating local recurrence from postoperative changes (e.g. fibrosis). Recurrent tumours tend to enhance faster and more avidly after gadolinium administration in the early arterial phase, followed by a plateau or washout during the venous phase, while postoperative fibrosis tends to show either no enhancement or mild enhancement in the venous phase.[167,169] DCE MRI has been reported to increase diagnostic sensitivity from 48% to 88% and specificity from 52% to 100% compared with T2W MRI alone[176] (**Figure 2.II-12A** and **B**), and allows the detection of recurrent tumours measuring more than 5 mm, for a PSA level of less than 2 ng/mL, with an NPV of 95%.[170] Cirillo *et al.* studied 72 patients after RP. T2W MRI showed a sensitivity, specificity, and accuracy of, respectively, 61.4%, 82.1%, and 69.4% versus 84.1%, 89.3%, and 86.1% for DCE MRI.[167] However, in this study, recurrent tumours measured more than 15 mm for a PSA value of 1.23±1.3 ng/mL. In a recent study by Panebianco *et al.*, the combination of T2W and DCE imaging lead to a sensitivity and specificity value of, respectively, 98% and 94% in the detection of a local tumour recurrence for an average PSA value of 1.3 ng/mL (0.5–1.7 ng/mL) and an average lesion size of 5±0.6 mm (4–8 mm).[171]

DW MRI is also informative, especially with the use of high b-values (from 1,000 s/mm^2 and up to 3,000 s/mm^2) at 3T. However, they are often difficult to interpret because of artifacts due to digestive movements. The combination of DW and T2W MRI has a lower sensitivity and specificity rate than the combination of T2W and DCE MRI, due to a better spatial resolution of the latter.[171]

On the basis of these studies, dynamic contrast-enhanced imaging can be considered as the most reliable MRI technique for the detection of local PCa recurrence after RP.

II-2.7.2 Local recurrence after external beam radiation therapy

There is no indication for systematic imaging after external beam radiation therapy (EBRT), aside from biochemical or clinical relapse. The biochemical relapse is defined according to the Phoenix criteria (rise of the PSA level of more than 2 ng/mL above the nadir). Magnetic resonance imaging is the technique of choice to identify and localize recurrent PCa. The precise detection and localization of local tumour recurrence is of utmost importance for several purposes:

- For targeted TRUS-guided biopsy of suspicious areas: Thus, reducing the false-negative rate associated with systematic biopsies, and furthermore leading to a higher detection rate of recurrent PCa with a minimum number of biopsy cores compared to TRUS-guided systemic biopsies

- For appropriate treatment selection and planning (salvage therapy by surgery or focal therapy using HIFU or cryotherapy)

II-2.7.2.1 T2W MRI

After EBRT, the prostate appears decreased in volume and diffusely hypointense on T2W images, with a loss of zonal anatomy. The SVs also appear globally hypointense.

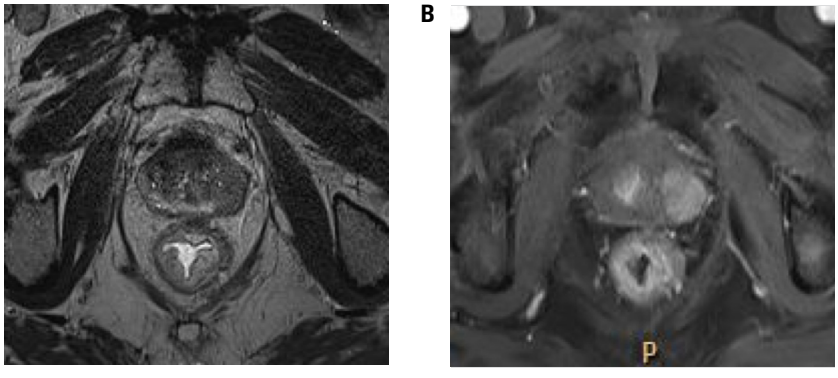

FIGURE 2.II-13
Imaging Findings After EBRT, Local Recurrence

T2-weighted images (**A**), T1W images after gadolinium enhancement (**B**). The prostate gland appears globally hypointense, with loss of zonal anatomy. Hypointense soft tissue thickening in the left part of the PZ with a mass-like effect on the capsula (**A**) and intense nodular enhancement after gadolinium injection (**B**).

Recurrences are most commonly located in the original tumour site.[172] T2W MRI alone is of a limited diagnostic accuracy because the recurrent tumour and the normal surrounding parenchyma both appear hypointense. Cancer can be detected under such circumstances if its signal intensity is lower than adjacent prostate tissue, and if it appears nodular or with a mass-like effect (**Figure 2.II-13A**). However, since treated cancer after radiotherapy has lower signal intensity than normal prostate tissue after radiotherapy, not only is it difficult to detect recurrent cancer, but it is even more difficult to distinguish it from treated tumour. The effects of EBRT on the T2W appearance of adjacent anatomical structures include increased bladder and/or rectal wall thickness, thickening of the perirectal fascia, and increased signal intensity of the pelvic sidewall musculature.

II-2.7.2.2 DCE and DW MRI

A considerable number of studies have explored the potential of functional techniques to improve the MRI assessment of local recurrent PCa after definitive EBRT, T2W MRI being of limited diagnostic accuracy.

After EBRT, recurrent tissue appears as hypervascular early enhancing homogeneous nodule, with an early washout, whereas in fibrosis the enhancement is homogeneous, slow, and less intense (**Figure 2.II-13B** and **C**).[153]

Rouviere *et al.*[153] compared T2W and DCE MRI in 22 patients, using biopsy results as the reference standard (PSA level range: 1.01–21 ng/mL). DCE MRI showed a statistically significant higher sensitivity than T2W imaging (0.70–0.74 versus 0.26–0.44), while the specificity of the two techniques was similar (0.73–0.85 versus 0.64–0.86). Furthermore, the inter-observer agreement was greater for DCE MRI (kappa=0.63–0.70) than for the T2W MRI (kappa=0.18–0.39).

However, Donati *et al.* showed that mpMRI composed of T2W, DW, and DCE imaging had greater accuracy in the detection of recurrent PCa after radiotherapy than T2W imaging alone, with no additional benefit if DCE imaging was added to T2W imaging and DW imaging. Moreover, T2W and DW imaging also yielded higher inter-reader agreement than any other combination tested (kappa=0.17–0.20 for T2W imaging alone, kappa=0.55–0.63 for T2W and DW imaging, kappa=0.32–0.34 for T2W and DCE imaging, and kappa=0.49–0.58 for T2W, DW, and DCE imaging).[173]

Morgan *et al.* compared MRI and transrectal prostate biopsy findings in 24 patients with rising PSA. The combination of T2W and DW imaging had a sensitivity and specificity of, respectively, 94% and 75% for detecting local tumour recurrence larger than 0.4 cm^2 within the prostate.[174] Furthermore, Kim *et al.*, in a preliminary experiment, found that for predicting locally recurrent PCa after EBRT, the use of combined T2W and DW imaging showed a better diagnostic performance compared to T2W imaging alone. Indeed, a significantly greater AUC was determined for combined T2W and DW imaging (0.879, $p<0.01$) as compared to T2W imaging alone (0.612).[175]

Therefore, according to these data, in the detection of locally recurrent PCa in patients who underwent EBRT, the combination of T2W and DW MRI appears to be the optimal approach.

Imaging findings in recurrent disease

Brachytherapy induces a decrease in volume of the prostate gland and SVs, as does EBRT. The prostate gland appears globally hypointense on T2W images, with loss of zonal anatomy. The capsule appears irregular, and the SV appears hypointense on T2W images, as well. Brachytherapy seeds can be seen on all sequences, but more particularly during DCE imaging. Tamada *et al.* evaluated the utility of mpMRI in detecting recurrent PCa after HDR brachytherapy. The sensitivity, specificity, and accuracy of each MRI pulse sequence in the detection of recurrent tumour were respectively 27%, 99%, and 87% for T2W MRI; 50%, 98%, and 90% for DCE MRI; and 68%, 95%, and 91% for DW MRI. The sensitivity of DW MRI in detecting recurrent tumour was significantly higher than that of T2W MRI ($p=0.004$). Multiparametric MRI achieved the highest sensitivity (77%) but with slightly decreased specificity (92%). These results indicate that an mpMRI protocol that includes DW MRI provides a sensitive method to detect local recurrence after HDR brachytherapy.[176]

II-2.7.3 Imaging after androgen deprivation therapy

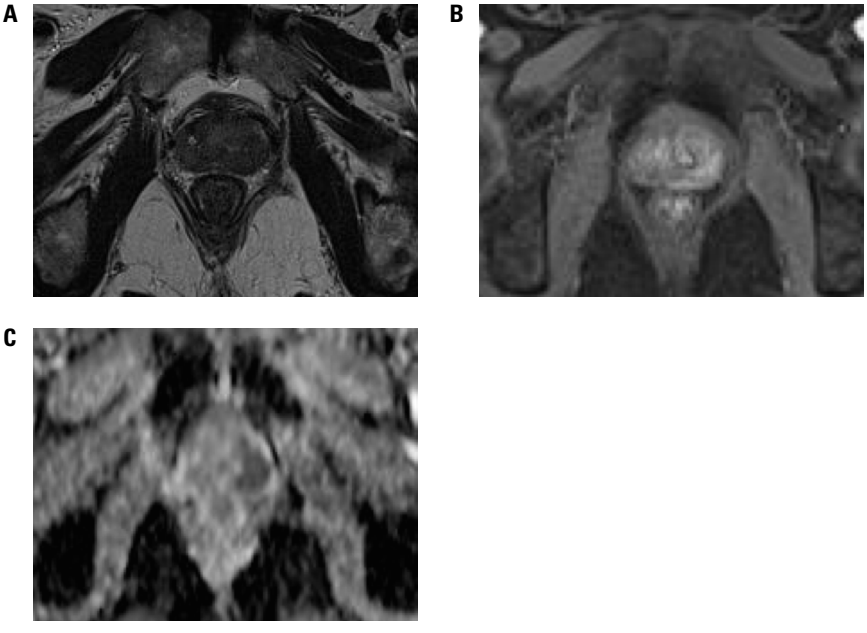

FIGURE 2.II-14
Imaging After Androgen Deprivation Therapy

Hypointense left-sided nodule on T2 weighted images, distinguishable in spite of a global decrease in signal intensity of the prostate gland due to therapy (**A**). Intense nodular enhancement at an early arterial phase on T1W images after gadolinium injection (**B**), corresponding dark nodular area on the ADC map consistent with restricted diffusion (**C**).

The morphological changes depend on the type and duration of androgen deprivation therapy. Changes are minimal or absent for short-term hormonal therapies. After long-term hormonal therapies, changes are major with a global decrease in volume of the prostate gland, more markedly in the peripheral prostate than in the transitional zone, and estimated at about 33.5±19.6%, mainly due to volume reduction in the PZ.[177] Changes also include a decrease in signal intensity on T2W images of the entire prostate gland, as well as SVs. The imaging features of the treated prostate and of PCa recurrence after androgen deprivation therapy may be similar to those after EBRT (decreased volume, decreased signal intensity on T2W images, loss of zonal differentiation); however, EBRT-induced changes in adjacent structures are absent. In some cases, recurrent cancer can be detected on morphological T2W images, but more often there is a lack of contrast between the low signal intensity of the recurrent tumour and the peripheral prostate, leading to overestimation of tumour volume and extra-prostatic extension. In spite of a decrease in capillary permeability in tumour tissue, DCE and DW MRI seem essential in detecting recurrent lesions[177] (**Figure 2.II-14A** to **C**).

II-2.7.4 Imaging after high-intensity focused US

High-intensity focused ablation causes coagulation necrosis in the targeted tissue by converting mechanical energy into heat and generating a cavitation effect. After HIFU, the PSA value decreases rapidly, with a nadir reached within 6 months.

There is currently no consensual definition of biochemical relapse after HIFU. As a result, most authors use the Phoenix criteria. Systematic biopsies are recommended 3 to 6 months after treatment and in case of a rise in PSA level, but they lack sensitivity to detect small recurrences.

Imaging may be requested:

- At an **early stage**, within 3 to 10 days of the treatment to assess the location and extent of tissue damage
- **6 months** after treatment and thereafter in case of a rise of the PSA value, for detection of recurrence, and pre-biopsy and preoperative mapping for a potential salvage therapy[156]

Early imaging (3 to 10 days after therapy)

FIGURE 2.II-15
Imaging Findings After HIFU at an Early Stage (10 Days After Therapy)

Dynamic contrast-enhanced T1W sequence. The treated area appears as a hypointense (non-enhanced) devascularized zone surrounded by a peripheral rim of enhancement.

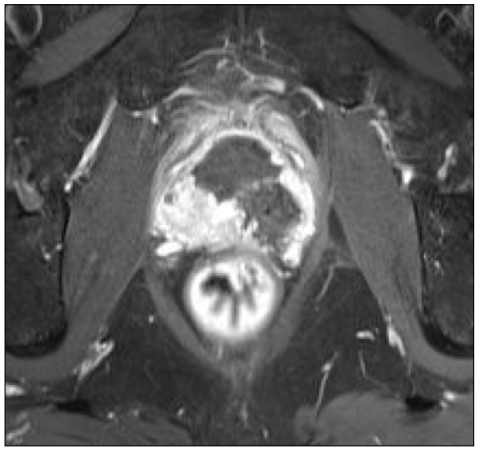

MR images obtained within days after HIFU ablation show a significant increase in prostate volume, presumably due to transient edema, with slightly hyperintense areas on T1W images, most likely representing interstitial hemorrhage. On fat-saturated gadolinium-enhanced non-dynamic T1W images, the treated area appears as a hypointense (unenhanced) devascularized zone (corresponding to the central core of coagulation necrosis) surrounded by a peripheral rim of enhancement (corresponding to inflammation and edema) (**Figure 2.II-15**). MRI allows determining whether the target has been treated. It provides information on the extent of tissue damage, and estimates the untreated parenchymal volume. The proportion of enhancing tissue on the initial post-treatment MRI is predictive of the gland volume at 6 months and of the PSA level nadir. Persisting enhancing prostatic tissue usually occurs at the periphery of the gland and is particularly common at the apex and the transitional zone.[178]

Late (>6 months) imaging findings: detecting recurrent disease

FIGURE 2.II-16
Imaging Findings 6 Months After HIFU, Recurrent Disease

Small residual prostate with no visible recurrence on T2W images (**A**). Dynamic contrast-enhanced T1W image (**B**) shows intense nodular enhancement in the right apex mid-gland with a corresponding dark area on the ADC map consistent with restricted diffusion (**C**).

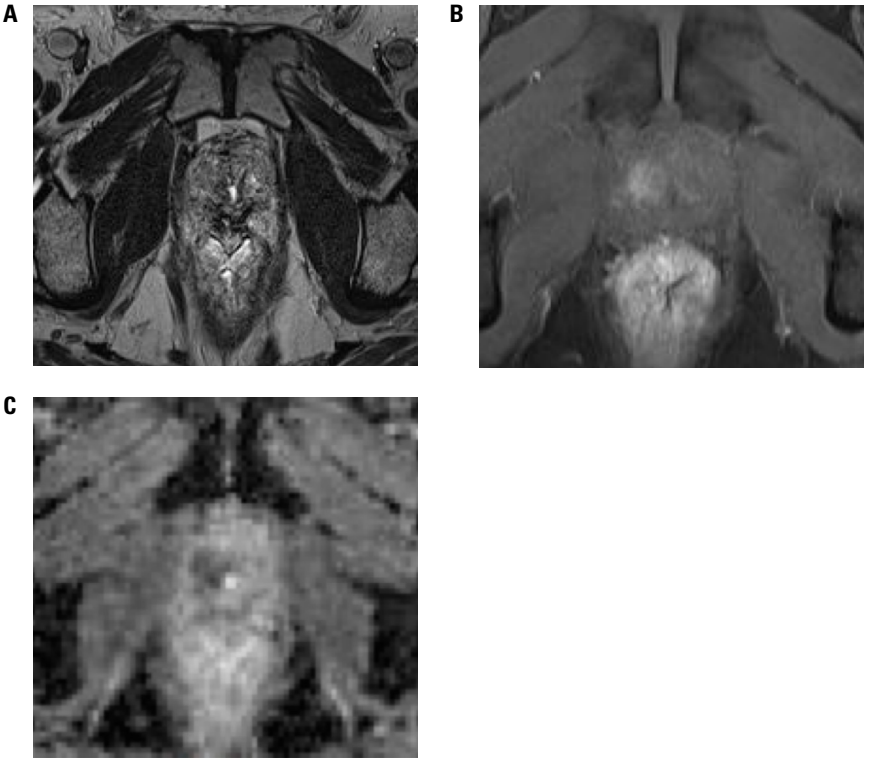

Morphological T2W images show a decrease in volume of more than 45% of the prostate gland[178,179] (**Figure 2.II-16A** and **B**). Kirkham *et al.*[178] showed that, at 6 months, there is a median volume reduction of 61% of the prostate gland. Kirkham *et al.* also concluded that the volume of prostate tissue enhancing on the initial post-treatment image correlated well with the PSA nadir and with the volume at 6 months. This volume loss is correlated with the completeness of gland coverage during treatment (subtotal, ablation of half of the gland, focal ablation). The prostate parenchyma is heterogeneously and diffusely hypointense on T2W images, with a loss of normal zonal anatomy, which makes it difficult to detect tumour recurrence. A cavity in continuity with the urethra may occur (as it does after transurethral resection of the prostate). The SVs have generally low signal intensity on T2W images. The peripheral enhancement rim has resolved, and is replaced by fibrosis and thickening of the prostate capsule. Furthermore, there is a thickening of the anterior rectal wall contiguously with the posterior prostatic capsule.

Although residual and recurrent malignant tumours of the prostate have been reported to have a lower signal intensity than the surrounding fibrosis, it remains difficult to correctly discriminate the two entities with anatomical T2W MRI alone. Therefore, it is essential to combine T2W MRI with DCE MRI and DW MRI to differentiate residual/recurrent cancers (which are usually hypervascular) from post-HIFU fibrosis (which is rather homogeneous and hypovascular).

DCE imaging is more sensitive in detecting recurrence than DW imaging after HIFU. Recurrent tumour tissue enhances quickly and intensely, whereas enhancement in fibrosis is slow and less intense. The combination of T2W and DCE MRI helps in guiding biopsies and thus sensitizing the detection of locally recurrent cancer in patients with biochemical relapse.[156] Furthermore, Kim *et al.* found, in 27 patients with biochemical relapse after HIFU ablation, that DCE MRI was significantly more sensitive (80%–87% versus 63%–70%) and less specific (63%–68% versus 74%–78%) than the combination T2W and DW MRI for detecting recurrent cancer.[155]

II-2.7.5 Imaging after cryotherapy

Local recurrences are mainly diagnosed by random prostate biopsy. Ultrasound accuracy is poor, as well as T2W MRI. In the same way as for HIFU ablation, DCE MRI, DW MRI, and spectroscopy allow for the detection of recurrence, help to guide biopsies, and thus help to select patients for a new session of HIFU or cryotherapy.[162,180]

II-2.8 Conclusion

A large body of literature suggests that mpMRI has become a reliable tool for assessing the presence and size of aggressive cancer in the prostate. Nonetheless, we must proceed with caution before recommending its widespread use; two major issues remain to be clarified. The first one is the NPV of mpMRI. Is it good enough to recommend skipping random biopsies in MR-negative parts of the prostate? Current literature sends mixed signals about this question, and there is no doubt that it will be the scope of intensive research during the next couple of years. The second problem concerns the standardization of prostate MRI interpretation. Recent initiatives have been made by the international radiological community to define a standardized way to interpret MR images. This raises the hope that the good results obtained with prostate MRI by specialized academic groups will be soon reproduced in less-experienced centres.

Only then will it be possible to define rational guidelines about the use of mpMRI in PCa management.

All recommendations have a level of evidence 2b unless otherwise noted.

TABLE 2.II-9 Framework and Fundamental Content of a Standardized Prostate mpMRI Report

Header	**Patient information**	Name
		Institution
		ID
		Date of birth
		Coordinates
	Study information	Study date, time
		Study description
		Study unique identifier in the institution (Accession number, etc.)
		MRI equipment (manufacturer, magnet strength, coil[s])
		Patient preparation (enema/spasmolytic/etc.)
		Protocol (list of series performed for the mpMRI), with potential changes or artifacts
	Patient history/ clinical indication	Age
		PSA in the last 3 months and, if available, previous PSA
		DRE findings
		Family history of PCa
		History and/or presence of functional signs, inflammatory or infectious signs
		History of functional prostate surgery (TURP, etc.)
		History of androgen deprivation or substitution therapy
		History of PCa with or without treatment, and initial PCa location
		History of previous biopsy series
		Prior films/studies reviewed (e.g. Comparison with study dd/mm/yyyy)

Reproduced with permission from Puech P, et al. How are we going to train a generation of radiologists (and urologists) to read prostate MRI? 2015;25(6):522-535.

Abbreviations: MRI: magnetic resonance imaging; mpMRI: multiparametric magnetic resonance imaging; PSA: prostate-specific antigen; DRE: digital rectal examination; PCa: prostate cancer; TURP: transurethral resection of the prostate; AS: active surveillance; RP: radical prostatectomy; HIFU: high-intensity focused ultrasound; VTP: vascular targeted photodynamic therapy; PZ: peripheral zone; TZ: transitional zone; AFMS: anterior fibromuscular stroma; PI-RADS: Prostate Imaging and Reporting and Data System; T2W: T2-weighted; DW: diffusion-weighted; DCE: dynamic contrast-enhanced; ECE: extracapsular extension; SV: seminal vesicle

continued on **page 185**

TABLE 2.II-9 Framework and Fundamental Content of a Standardized Prostate mpMRI Report, *Cont'd*

Header (cont'd)	**Context of current examination**	▪ Before a first series of biopsies (S1)
		▪ Before a second series of biopsies (S2) with previous negative, including date and institution where biopsies were performed (ideally report)
		▪ Before an nth series of biopsies (Sn) with previous negatives, including dates and institutions where biopsies were performed (ideally reports)
		▪ After a positive series of biopsies, with precision of date, positive cores, and significance of biopsies (report if available)
		  ▪ Patient with significant cancer requiring local staging
		  ▪ Patient with insignificant cancer requiring confirmation for AS inclusion
		  ▪ Patient under AS
		▪ Biological recurrence after RP
		▪ Biological recurrence after external radiotherapy
		▪ Biological recurrence after brachytherapy
		▪ Biological recurrence after focal therapy (HIFU, cryo, VTP, laser, etc.)

Findings	**Measurement of the gland**	Dimensions (x, y, z planes; volume in cc) Presence or not of a median lobe Surgical sequels (TURP)
	Background signal	Description of the global aspect of each of the 3 prostate compartments (PZ, TZ, AFMS), introducing signal changes and potential artifacts hampering the description of significant images (hemorrhagic changes, scars, atrophy, etc.) *(e.g. PZ shows bright high-intensity T2 signal, with no hemorrhagic artifact; PZ shows few non-hemorrhagic signal changes that do not hamper interpretation)* Presence of significant anatomical landmarks: cysts, calcifications, etc.
	Significant images	Clear enumeration of their count *(e.g. PZ analysis shows 2 significant images)* Separate description of each image, from the most suspicious (or biggest) lesion (index lesion) to the least, including: ▪ Appearance, as described in PI-RADS v2 lexicon (diffuse abnormality/ nodule/mass, etc.) ▪ Shape ▪ Margins ▪ Location (with reference to the standardized map sector, completed by explicit translation in reference to zonal anatomy). *(e.g. …in right mediolobar mid-gland PZ [z03p]…)* ▪ Additional information for locating the lesion on the MRI data, particularly series and slice number *(e.g. Series 0101; Slice 10-13, centre 12)* ▪ Size (in mm); ideally 3 planes, but x and y are fine

Reproduced with permission from Puech P, et al. How are we going to train a generation of radiologists (and urologists) to read prostate MRI? 2015;25(6):522-535.

Abbreviations: MRI: magnetic resonance imaging; mpMRI: multiparametric magnetic resonance imaging; PSA: prostate-specific antigen; DRE: digital rectal examination; PCa: prostate cancer; TURP: transurethral resection of the prostate; AS: active surveillance; RP: radical prostatectomy; HIFU: high-intensity focused ultrasound; VTP: vascular targeted photodynamic therapy; PZ: peripheral zone; TZ: transitional zone; AFMS: anterior fibromuscular stroma; PI-RADS: Prostate Imaging and Reporting and Data System; T2W: T2-weighted; DW: diffusion-weighted; DCE: dynamic contrast-enhanced; ECE: extracapsular extension; SV: seminal vesicle

continued on **page 186**

TABLE 2.II-9 Framework and Fundamental Content of a Standardized Prostate mpMRI Report, *Cont'd*

Findings (cont'd)	**Significant images (cont'd)**	▪ Signal description in each series (T2W imaging, DW imaging, DCE imaging, etc.) ▪ Suspicion score of malignancy (including objective and subjective score if [and only if] different from the objective one) *(e.g."…with a PI-RADS v2 score of 3/5, but more likely 4/5 based on our experience…")* ▪ Suspicion score of ECE (based on PI-RADS v1 classification or PI-RADS v2 staging terms), with supposed radial extension depth in mm ▪ Suspicion score of SV invasion for lesions involving prostate base ▪ Suspicion score of sphincter invasion for lesions involving prostate apex ▪ Reporting of ALL lesions previously described on a standardized 27- or 39-sector map. This reporting should be performed on a copy of a standardized map provided by current guidelines, including manual or electronic drawing of lesions, with position and size relative to the schematic gland. Lesions having a suspicion of ECE should have clear margins outside the contours of the schematic prostate slice ▪ Illustrative key image(s) can be included in the report, to facilitate recognition of significant images on the mpMRI series
	Locoregional staging	Report of pelvic nodes
	Metastatic staging	Report of potential bladder, periprostatic muscle, or rectal invasion Report of potential bone lesions
	Other findings	e.g. Hypertonic bladder with small diverticulitis; left iliac aneurysm
Overall impression/ conclusion	Conclusion should clearly state whether: ▪ the MRI is normal, showing no significant image in a gland with a completely normal background signal, or ▪ the MRI shows no significant image, with reserve of signal changes, that should be quantified (slight/important), or ▪ the MRI shows one or more significant images, with score either ≥ or > to 3/5, that require targeted biopsy. If so, count, laterality, and brief description (size, local, and locoregional staging) of the two most significant lesions should be repeated.	

Reproduced with permission from Puech P, et al. How are we going to train a generation of radiologists (and urologists) to read prostate MRI? 2015;25(6):522-535.

Abbreviations: MRI: magnetic resonance imaging; mpMRI: multiparametric magnetic resonance imaging; PSA: prostate-specific antigen; DRE: digital rectal examination; PCa: prostate cancer; TURP: transurethral resection of the prostate; AS: active surveillance; RP: radical prostatectomy; HIFU: high-intensity focused ultrasound; VTP: vascular targeted photodynamic therapy; PZ: peripheral zone; TZ: transitional zone; AFMS: anterior fibromuscular stroma; PI-RADS: Prostate Imaging and Reporting and Data System; T2W: T2-weighted; DW: diffusion-weighted; DCE: dynamic contrast-enhanced; ECE: extracapsular extension; SV: seminal vesicle

continued on **page 187**

TABLE 2.II-9 Framework and Fundamental Content of a Standardized Prostate mpMRI Report, *Cont'd*

Signature(s)	**Single reading**	Name, date, position, and signature
	Double reading (optional)	Additional physician information, completed by: ▪ Confirmation of primary reading without remark ▪ Remarks not changing primary reading ▪ Remarks having required consensus reading

Reproduced with permission from Puech P, et al. How are we going to train a generation of radiologists (and urologists) to read prostate MRI? 2015;25(6):522-535.

Abbreviations: MRI: magnetic resonance imaging; mpMRI: multiparametric magnetic resonance imaging; PSA: prostate-specific antigen; DRE: digital rectal examination; PCa: prostate cancer; TURP: transurethral resection of the prostate; AS: active surveillance; RP: radical prostatectomy; HIFU: high-intensity focused ultrasound; VTP: vascular targeted photodynamic therapy; PZ: peripheral zone; TZ: transitional zone; AFMS: anterior fibromuscular stroma; PI-RADS: Prostate Imaging and Reporting and Data System; T2W: T2-weighted; DW: diffusion-weighted; DCE: dynamic contrast-enhanced; ECE: extracapsular extension; SV: seminal vesicle

II-2.9 References

1. Barentsz J, Richenberg J, Clements R, *et al.* ESUR prostate MR guidelines 2012. *Eur Radiol.* 2012;22(4):746–757.
2. Leake JL, Hardman R, Ojili V, *et al.* Prostate MRI: access to and current practice of prostate MRI in the United States. *J Am Coll Radiol.* 2014;11(2):156–160.
3. Shah Z, Elias S, Abaza R, *et al.* Performance comparison of 1.5-T endorectal coil MRI with 3.0-T nonendorectal coil MRI in patients with prostate cancer. *Acad Radiol.* 2015;22(4):467–474.
4. Turkbey B, Merino M, Gallardo E, *et al.* Comparison of endorectal coil and nonendorectal coil T2W and diffusion-weighted MRI at 3 Tesla for localizing prostate cancer: correlation with whole-mount histopathology. *J Magn Reson Imaging.* 2014;39(6):1443–1448.
5. Lemaitre L, Puech P, Poncelet E, *et al.* Dynamic contrast-enhanced MRI of anterior prostate cancer: morphometric assessment and correlation with radical prostatectomy findings. *Eur Radiol.* 2009;19(2):470–480.
6. Rosenkrantz A, Mendrinos S, Babb J, *et al.* Prostate cancer foci detected on multiparametric magnetic resonance imaging are histologically distinct from those not detected. *J Urol.* 2012;187(6):2032–2038.
7. McDonald R, McDonald J, Kallmes D, *et al.* Intracranial gadolinium deposition after contrast-enhanced MR imaging. *Radiology.* 2015;275(3):772–782.
8. Somford D, Hamoen E, Fütterer J, *et al.* The predictive value of endorectal 3 Tesla multiparametric magnetic resonance imaging for extraprostatic extension in patients with low, intermediate and high risk prostate cancer. *J Urol.* 2013;190(5):1728–1734.
9. Feng T, Sharif-Afshar A, Smith S, *et al.* Multiparametric magnetic resonance imaging localizes established extracapsular extension of prostate cancer. *Urol Oncol.* 2015;33(3):109.e15–e22.
10. Johnston R, Wong L, Warren A, *et al.* The role of 1.5 Tesla magnetic resonance imaging in staging prostate cancer. *ANZ J Surg.* 2013;83(4):234–238.
11. Park B, Kim B, Kim C, *et al.* Comparison of phased-array 3.0-T and endorectal 1.5-T magnetic resonance imaging in the evaluation of local staging accuracy for prostate cancer. *J Comput Assist Tomogr.* 2007;31(4):534–538.
12. Heijmink S, Fütterer J, Hambrock T, *et al.* Prostate cancer: body-array versus endorectal coil MR imaging at 3 T--comparison of image quality, localization, and staging performance. *Radiology.* 2007;244(1):184–195.
13. Turkbey B, Mani H, Shah V, *et al.* Multiparametric 3T prostate magnetic resonance imaging to detect cancer: histopathological correlation using prostatectomy specimens processed in customized magnetic resonance imaging based molds. *J Urol.* 2011;186(5):1818–1824.
14. Renard-Penna R, Rouprêt M, Comperat E, *et al.* Accuracy of high resolution (1.5 tesla) pelvic phased array magnetic resonance imaging (MRI) in staging prostate cancer in candidates for radical prostatectomy: results from a prospective study. *Urol Oncol.* 2013;31(4):448–454.
15. Weinreb J, Blume J, Coakley F, *et al.* Prostate cancer: sextant localization at MR imaging and MR spectroscopic imaging before prostatectomy--results of ACRIN prospective multi-institutional clinicopathologic study. *Radiology.* 2009;251(1):122–133.
16. American College of Radiology. MR prostate imaging reporting and data system version 2.0. 2015. Available from: http://www.acr.org/Quality-Safety/Resources/PIRADS; Accessed: June 1, 2015.
17. Barentsz J, Villers A, Schouten M. Reply to letter to the editor re: ESUR prostate MR guidelines. *Eur Radiol.* 2013;23(8):2322–2323.
18. American College of Radiology. Prostate Imaging Reporting and Data System, 2015 version 2, Reston VA, USA; 2015. Available from: http://www.esur.org/fileadmin/content/user_upload/PIRADS_v2_20141223.pdf; Accessed: July 10, 2015.
19. Muller B, Fütterer J, Gupta R, *et al.* The role of magnetic resonance imaging (MRI) in focal therapy for prostate cancer: recommendations from a consensus panel. *BJU Int.* 2013;113(2):218–227.
20. Puech P, Villers A, Ouzzane A, *et al.* Prostate cancer: diagnosis, parametric imaging and standardized report. *Diagn Interv Imaging.* 2014;95(7–8):743–752.

21. Puech P, Ouzzane A, Gaillard V, *et al.* Multiparametric MRI-targeted TRUS prostate biopsies using visual registration. *BioMed Res Int.* 2014;2014:1–11.

22. Vaché T, Bratan F, Mège-Lechevallier F, *et al.* Characterization of prostate lesions as benign or malignant at multiparametric MR imaging: comparison of three scoring systems in patients treated with radical prostatectomy. *Radiology.* 2014;272(2):446–455.

23. Mueller-Lisse U, Scheidler J, Klein G, *et al.* Reproducibility of image interpretation in MRI of the prostate: application of the sextant framework by two different radiologists. *Eur Radiol.* 2005;15(9):1826–1833.

24. Dickinson L, Ahmed H, Allen C, *et al.* Clinical applications of multiparametric MRI within the prostate cancer diagnostic pathway. *Urol Oncol.* 2013;31(3):281–284.

25. Dickinson L, Ahmed H, Allen C, *et al.* Magnetic resonance imaging for the detection, localisation, and characterisation of prostate cancer: recommendations from a European consensus meeting. *Eur Urol.* 2011;59(4):477–494.

26. Haffner J, Lemaitre L, Puech P, *et al.* Role of magnetic resonance imaging before initial biopsy: comparison of magnetic resonance imaging-targeted and systematic biopsy for significant prostate cancer detection. *BJU Int.* 2011;108(8b):E171–E178.

27. Dickinson L, Ahmed H, Allen C, *et al.* Scoring systems used for the interpretation and reporting of multiparametric MRI for prostate cancer detection, localization, and characterization: could standardization lead to improved utilization of imaging within the diagnostic pathway? *J Magn Reson Imaging.* 2012;37(1):48–58.

28. Puech P, Sufana Iancu A, Renard B, *et al.* Detecting prostate cancer with MRI - why and how. *Diag Interv Imaging.* 2012;93(4):268–278.

29. Puech P, Rouvière O, Renard-Penna R, *et al.* Prostate cancer diagnosis: multiparametric MR-targeted biopsy with cognitive and transrectal US–MR fusion guidance versus systematic biopsy—prospective multicenter study. *Radiology.* 2013;268(2):461–469.

30. Hamoen E, de Rooij M, Witjes J, *et al.* Use of the Prostate Imaging Reporting and Data System (PI-RADS) for prostate cancer detection with multiparametric magnetic resonance imaging: a diagnostic meta-analysis. *Eur Urol.* 2015;67(6):1112–1121.

31. Muller B, Shih J, Sankineni S, *et al.* Prostate Cancer: Interobserver agreement and accuracy with the revised Prostate Imaging Reporting and Data System at multiparametric MR imaging. *Radiology.* 2015;277(3):741–750.

32. Renard-Penna R, Mozer P, Cornud F, *et al.* Prostate Imaging Reporting and Data System and Likert Scoring System: multiparametric MR imaging validation study to screen patients for initial biopsy. *Radiology.* 2015;275(2):458–468.

33. Rosenkrantz A, Kim S, Lim R, *et al.* Prostate cancer localization using multiparametric MR imaging: comparison of Prostate Imaging Reporting and Data System (PI-RADS) and Likert Scales. *Radiology.* 2013;269(2):482–492.

34. Rosenkrantz A, Lim R, Haghighi M, *et al.* Comparison of interreader reproducibility of the Prostate Imaging Reporting and Data System and Likert Scales for evaluation of multiparametric prostate MRI. *AJR Am J Roentgenol.* 2013;201(4):W612–W618.

35. Grey A, Chana M, Popert R, *et al.* Diagnostic accuracy of magnetic resonance imaging (MRI) prostate imaging reporting and data system (PI-RADS) scoring in a transperineal prostate biopsy setting. *BJU Int.* 2015;115(5):728–735.

36. Puech P, Betrouni N, Makni N, *et al.* Computer-assisted diagnosis of prostate cancer using DCE-MRI data: design, implementation and preliminary results. *Int J Comput Assist Radiol Surg.* 2009;4(1):1–10.

37. Niaf E, Rouvière O, Mège-Lechevallier F, *et al.* Computer-aided diagnosis of prostate cancer in the peripheral zone using multiparametric MRI. *Phys Med Biol.* 2012;57(12):3833–3851.

38. Regge D, Halligan S. CAD: How it works, how to use it, performance. *Eur J Radiol.* 2013;82(8):1171–1176.

39. Wang S, Burtt K, Turkbey B, *et al.* Computer aided-diagnosis of prostate cancer on multiparametric MRI: a technical review of current research. *Biomed Res Int.* 2014;2014:1–11.

40. Betrouni N, Makni N, Lakroum S, *et al.* Computer-aided analysis of prostate multiparametric MR images: an unsupervised fusion-based approach. *Int J Comput Assist Radiol Surg.* 2015;10(9):1515–1526.

41. Lemaitre G, Martí R, Freixenet J, *et al.* Computer-aided detection and diagnosis for prostate cancer based on mono and multi-parametric MRI: A review. *Comput Biol Med.* 2015;60:8–31.

42. Zhao K, Wang C, Hu J, *et al.* Prostate cancer identification: quantitative analysis of T2-weighted MR images based on a back propagation artificial neural network model. *Sci China Life Sci.* 2015;58(7):666–673.

43. Rakow-Penner R, White N, Parsons J, *et al.* Novel technique for characterizing prostate cancer utilizing MRI restriction spectrum imaging: proof of principle and initial clinical experience with extraprostatic extension. *Prostate Cancer Prostatic Dis.* 2015;18(1):81–85.

44. Rosenkrantz A, Geppert C, Grimm R, *et al.* Dynamic contrast-enhanced MRI of the prostate with high spatiotemporal resolution using compressed sensing, parallel imaging, and continuous golden-angle radial sampling: preliminary experience. *J Magn Reson Imaging.* 2015;41(5):1365–1373.

45. Dikaios N, Alkalbani J, Sidhu H, *et al.* Logistic regression model for diagnosis of transition zone prostate cancer on multi-parametric MRI. *Eur Radiol.* 2015;25(2):523–532.

46. Quentin M, Blondin D, Klasen J, *et al.* Evaluation of a structured report of functional prostate magnetic resonance imaging in patients with suspicion for prostate cancer or under active surveillance. *Urol Int.* 2012;89(1):25–29.

47. Kirkham A, Haslam P, Keanie J, *et al.* Prostate MRI: who, when, and how? Report from a UK consensus meeting. *Clin Radiol.* 2013;68(10):1016–1023.

48. Moore C, Kasivisvanathan V, Eggener S, *et al.* Standards of Reporting for MRI-targeted Biopsy Studies (START) of the prostate: recommendations from an International Working Group. *Eur Urol.* 2013;64(4):544–552.

49. Röthke M, Blondin D, Schlemmer H, *et al.* [PI-RADS classification: structured reporting for MRI of the prostate]. [Article in German] *Rofo.* 2013;185(3):253–261.

50. Westphalen A, Rosenkrantz A. Prostate Imaging Reporting and Data System (PI-RADS): reflections on early experience with a standardized interpretation scheme for multiparametric prostate MRI. *AJR Am J Roentgenol.* 2014;202(1):121–123.

51. Wibmer A, Vargas H, Sosa R, *et al.* Value of a standardized lexicon for reporting levels of diagnostic certainty in prostate MRI. *AJR Am J Roentgenol.* 2014;203(6):W651–W657.

52. Silveira P, Dunne R, Sainani N, *et al.* Impact of an information technology–enabled initiative on the quality of prostate multiparametric MRI reports. *Acad Radiol.* 2015;22(7):827–833.

53. Kahn C, Heilbrun M, Applegate K. From guidelines to practice: how reporting templates promote the use of radiology practice guidelines. *J Am Coll Radiol.* 2013;10(4):268–273.

54. Puech P, Randazzo M, Ouzzane A, *et al.* How are we going to train a generation of radiologists (and urologists) to read prostate MRI? *Curr Opin Urol.* 2015;25(6):522–536.

55. El-Shater Bosaily A, Parker C, Brown L, *et al.* PROMIS — Prostate MR imaging study: a paired validating cohort study evaluating the role of multi-parametric MRI in men with clinical suspicion of prostate cancer. *Contemp Clin Trials.* 2015;42:26–40.

56. Puech, P. Prostate MRI structured report wizard; v2 – December 22th, 2014. Available from: http://www.pcih.fr/mpmri; Accessed July 20, 2015.

57. Litjens G, Barentsz J, Karssemeijer N, *et al.* Clinical evaluation of a computer-aided diagnosis system for determining cancer aggressiveness in prostate MRI. *Eur Radiol.* 2015;25(11):3187–3199.

58. Mata C, Walker P, Oliver A, *et al.* ProstateAnalyzer: web-based medical application for the management of prostate cancer using multiparametric MR imaging. *Inform Health Soc Care.* 2015;24:1–21.

59. Plumb A, Grieve F, Khan S. Survey of hospital clinicians' preferences regarding the format of radiology reports. *Clin Radiol.* 2009;64(4):386–394.

60. Epstein JI. Diagnosis of limited adenocarcinoma of the prostate. *Histopathology.* 2012;60(1):28–40.

61. Wolters T, van der Kwast TH, Vissers CJ, *et al.* False-negative prostate needle biopsies: frequency, histopathologic features, and follow-up. *Am J Surg Pathol.* 2010;34(1):35–43.

62. Rosenkrantz AB, Scionti SM, Mendrinos S, *et al.* Role of MRI in minimally invasive focal ablative therapy for prostate cancer. *AJR Am J Roentgenol.* 2011;197(1):W90–W96.

63. Salami SS, Ben-Levi E, Yaskiv O, *et al.* In patients with a previous negative prostate biopsy and a suspicious lesion on magnetic resonance imaging, is a 12-core biopsy still necessary in addition to a targeted biopsy? *BJU Int.* 2015;115(4):562–570.

64. Ahmed HU, Kirkham A, Arya M, *et al.* Is it time to consider a role for MRI before prostate biopsy? *Nat Rev Clin Oncol.* 2009;6(4):197–206.

65. Pokorny MR, de Rooij M, Duncan E, *et al.* Prospective study of diagnostic accuracy comparing prostate cancer detection by transrectal ultrasound-guided biopsy versus magnetic resonance (MR) imaging with subsequent MR-guided biopsy in men without previous prostate biopsies. *Eur Urol.* 2014;66(1):22–29.

66. Lawrentschuk N, Haider MA, Daljeet N, *et al.* "Prostatic evasive anterior tumours": the role of magnetic resonance imaging. *BJU Int.* 2010;105(9):1231–1236.

67. Rastinehad AR, Baccala AA, Chung PH, *et al.* D'Amico risk stratification correlates with degree of suspicion of prostate cancer on multiparametric magnetic resonance imaging. *J Urol.* 2011;185(3):815–820.

68. Tavangar SM, Razi A, Mashayekhi R. Correlation between prostate needle biopsy and radical prostatectomy Gleason gradings of 111 cases with prostatic adenocarcinoma. *Urol J.* 2004;1(4):246–249.

69. Franiel T, Lüdermann L, Taupitz M, *et al.* Pharmacokinetic MRI of the prostate: parameters for differentiating low-grade and high-grade prostate cancer. *ROFO.* 2009;181(6):536–542.

70. Shukla-Dave A, Hricak H, Kattan MW, *et al.* The utility of magnetic resonance imaging and spectroscopy for predicting insignificant prostate cancer: an initial analysis. *BJU Int.* 2007;99(4):786–793.

71. Villeirs GM, De Meerleer GO, De Visschere, *et al.* Combined magnetic resonance imaging and spectroscopy in the assessment of high grade prostate carcinoma in patients with elevated PSA: A single-institution experience of 356 patients. *Eur J of Radiol.* 2011;77(2):340–345.

72. Turkbey B, Shah VP, Pang Y, *et al.* Is apparent diffusion coefficient associated with clinical risk scores for prostate cancers that are visible on 3-T MR images? *Radiology.* 2011;258(2):488–495.

73. Wang L, Hricak H, Kattan MW, *et al.* Prediction of organ-confined prostate cancer: incremental value of MR imaging and MR spectroscopic imaging to staging nomograms. *Radiology.* 2006;238(2):597–603.

74. Le Nobin J, Orczyk C, Deng F-M, *et al.* Prostate tumour volumes: evaluation of the agreement between magnetic resonance imaging and histology using novel co-registration software. *BJU Int.* 2014;114(6b):E105–E112.

75. Muller BG, van den Bos W, Brausi M, *et al.* Role of multiparametric magnetic resonance imaging (MRI) in focal therapy for prostate cancer: a Delphi consensus project. *BJU Int.* 2014;114(5):698–707.

76. Potter SR, Partin AW. Prostate biopsy schemes and the detection of prostate cancer. *Rev Urol.* 1999;1(4):207–208.

77. Baco E, Rud E, Eri LM, *et al.* A randomized controlled trial to assess and compare the outcomes of two-core prostate biopsy guided by fused magnetic resonance and transrectal ultrasound images and traditional 12-core systematic biopsy. *Eur Urol.* 2016;69(1):149–156.

78. Moore CM, Robertson NL, Arsanious N, *et al.* Image-guided prostate biopsy using magnetic resonance imaging-derived targets: a systematic review. *Eur Urol.* 2013;63(1):125–140.

79. Schoots IG, Roobol MJ, Nieboer D, *et al.* Magnetic resonance imaging-targeted biopsy may enhance the diagnostic accuracy of significant prostate cancer detection compared to standard transrectal ultrasound-guided biopsy: a systematic review and meta-analysis. *Eur Urol.* 2015;68(3):438–450.

80. Rosenkrantz AB, Taneja SS. Prostate MRI can reduce overdiagnosis and overtreatment of prostate cancer. *Acad Radiol.* 2015;22(8):1000–1006.

81. Panebianco V, Barchetti F, Sciarra A, *et al.* Multiparametric magnetic resonance imaging vs. standard care in men being evaluated for prostate cancer: a randomized study. *Urol Oncol.* 2015;33(1):17.e1–e7.

82. Zhang ZX, Yang J, Zhang CZ, *et al.* The value of magnetic resonance imaging in the detection of prostate cancer in patients with previous negative biopsies and elevated prostate-specific antigen levels: a meta-analysis. *Acad Radiol.* 2014;21(5):578–589.

83. Lawrentschuk N, Fleshner N. The role of magnetic resonance imaging in targeting prostate cancer in patients with previous negative biopsies and elevated prostate-specific antigen levels. *BJU Int.* 2009;103(6):730–733.

84. Sciarra A, Panebianco V, Ciccariello M, *et al.* Value of magnetic resonance spectroscopy imaging and dynamic contrast-enhanced imaging for detecting prostate cancer foci in men with prior negative biopsy. *Clin Cancer Res.* 2010;16:1875–1883.

85. Tonttila PP, Lantto J, Pääkkö E, *et al.* Prebiopsy multiparametric magnetic resonance imaging for prostate cancer diagnosis in biopsy-naive men with suspected prostate cancer based on elevated prostate-specific antigen values: results from a randomized prospective blinded controlled trial. *Eur Urol.* 2016;69(3):419–425.

86. Wysock JS, Rosenkrantz AB, Huang WC, *et al.* A prospective, blinded comparison of magnetic resonance (MR) imaging-ultrasound fusion and visual estimation in the performance of MR-targeted prostate biopsy: the PROFUS trial. *Eur Urol.* 2014;66(2):343–351.

87. Gayet M, van der Aa A, Beerlage HP, *et al.* The value of magnetic resonance imaging and ultrasonography (MRI/US)-fusion prostate biopsy platforms in prostate cancer detection: a systematic review. *BJU Int.* 2016;117(3)392–400.

88. Comet-Batlle J, Vilanova-Busquets JC, Saladié-Roig JM, *et al.* The value of endorectal MRI in the early diagnosis of prostate cancer. *Eur Urol.* 2003;44(2):201–207.

89. Rouse P, Shaw G, Ahmed HU, *et al.* Multi-parametric magnetic resonance imaging to rule-in and rule-out clinically important prostate cancer in men at risk: a cohort study. *Urol Int.* 2011;87(1):49–53.

90. Lane BR, Zippe CD, Abouassaly R, *et al.* Saturation technique does not decrease cancer detection during followup after initial prostate biopsy. *J Urol.* 2008;179(5):1746–1750.

91. Roehl KA, Antenor JAV, Catalona WJ. Serial biopsy results in prostate cancer screening study. *J Urol.* 2002;167(6):2435–2439.

92. de Rooij M, Crienen S, Witjes JA, *et al.* Cost-effectiveness of magnetic resonance (MR) imaging and MR-guided targeted biopsy versus systematic transrectal ultrasound-guided biopsy in diagnosing prostate cancer: a modelling study from a health care perspective. *Eur Urol.* 2014;66(3):430–436.

93. Giannarini G, Zazzara M, Rossanese M, *et al.* Will multi-parametric magnetic resonance imaging be the future tool to detect clinically significant prostate cancer? *Front Oncol.* 2014;4:294.

94. Lund L, Svolgaard N, Poulsen MH. Prostate cancer: a review of active surveillance. *Res Rep Urol.* 2014;6:107–112.

95. Dianat SS, Carter HB, Macura KJ. Performance of multiparametric magnetic resonance imaging in the evaluation and management of clinically low-risk prostate cancer. *Urol Oncol.* 2014;32(1):39.e1–39.e10.

96. Turkbey B, Mani H, Aras O, *et al.* Prostate cancer: can multiparametric MR imaging help identify patients who are candidates for active surveillance? *Radiology.* 2013;268(1):144–152.

97. Johnson LM, Choyke PL, Figg WD, *et al.* The role of MRI in prostate cancer active surveillance. *Biomed Res Int.* 2014;2014:203906.

98. Ehdaie B, Vertosick E, Spaliviero M, *et al.* The impact of repeat biopsies on infectious complications in men with prostate cancer on active surveillance. *J Urol.* 2014:191(3):660–664.

99. Wang Q, Li H, Yan X, *et al.* Histogram analysis of diffusion kurtosis magnetic resonance imaging in differentiation of pathologic Gleason grade of prostate cancer. *Urol Oncol.* 2015;33(8):337.e15–337.e24.

100. Boesen L, Chabanova E, Løgager V, *et al.* Apparent diffusion coefficient ratio correlates significantly with prostate cancer gleason score at final pathology. *J Magn Reson Imaging.* 2015;42(2):446–453.

101. Le JD, Tan N, Shkolyar E, *et al.* Multifocality and prostate cancer detection by multiparametric magnetic resonance imaging: correlation with whole-mount histopathology. *Eur Urol.* 2015;67(3):569–576.

102. Scheenen TW, Rosenkrantz AB, Haider MA, *et al.* Multiparametric magnetic resonance imaging in prostate cancer management: current status and future perspectives. *Invest Radiol.* 2015;50(9):594–600.

103. Fradet V, Kurhanewicz J, Cowan JE, *et al.* Prostate cancer managed with active surveillance: role of anatomic MR imaging and MR spectroscopic imaging. *Radiology.* 2010;256(1):176–183.

104. Margel D, Yap SA, Lawrentschuk N, *et al.* Impact of multiparametric endorectal coil prostate magnetic resonance imaging on disease reclassification among active surveillance candidates: a prospective cohort study. *J Urol.* 2012;187(4):1247–1252.

105. Vilanova JC, Luna-Alcalá A, Boada M, *et al.* Multiparametric MRI. [The role of MRI techniques in the diagnosis, staging and follow up of prostate cancer] [Article in Spanish]. *Arch Esp Urol.* 2015;68(3):316–333.

106. Somford DM, Hambrock T, Hulsbergen-van de Kaa CA, *et al.* Initial experience with identifying high-grade prostate cancer using diffusion-weighted MR imaging (DWI) in patients with a Gleason score ≤ 3 + 3 = 6 upon schematic TRUS-guided biopsy: a radical prostatectomy correlated series. *Invest Radiol.* 2012;47(3):153–158.

107. Marliere F, Puech P, Benkirane A, *et al.* The role of MRI-targeted and confirmatory biopsies for cancer upstaging at selection in patients considered for active surveillance for clinically low-risk prostate cancer. *World J Urol.* 2014;32(4):951–958.

108. Abdi H, Pourmalek F, Zargar H, *et al.* Multiparametric magnetic resonance imaging enhances detection of significant tumor in patients on active surveillance for prostate cancer. *Urology.* 2015;85(2):423–428.

109. Moore CM, Petrides N, Emberton M. Can MRI replace serial biopsies in men on active surveillance for prostate cancer? *Curr Opin Urol.* 2014;24(3):280–287.

110. Valerio M, Ahmed HU, Emberton M, *et al.* The role of focal therapy in the management of localised prostate cancer: a systematic review. *Eur Urol.* 2014;66(4):732–751.

111. Meiers I, Waters DJ, Bostwick DG. Preoperative prediction of multifocal prostate cancer and application of focal therapy: review 2007. *Urology.* 2007;70 Suppl 6:3–8.

112. Stamey TA, Freiha FS, McNeal JE, *et al.* Localized prostate cancer. Relationship of tumor volume to clinical significance for treatment of prostate cancer. *Cancer.* 1993;71 Suppl 3:933–938.

113. Muller BG, van den Bos W, Pinto PA, *et al.* Imaging modalities in focal therapy: patient selection, treatment guidance, and follow-up. *Curr Opin Urol.* 2014;24(3):218–224.

114. Tran M, Thompson J, Bohm M, *et al.* Combination of multiparametric MRI and transperineal template-guided mapping biopsy of the prostate to identify candidates for hemi-ablative focal therapy. *BJU Int.* 2016;117(1):48–54.

115. Lemaitre L, Puech P, Poncelet E, *et al.* Dynamic contrast-enhanced MRI of anterior prostate cancer: morphometric assessment and correlation with radical prostatectomy findings. *Eur Radiol.* 2009;19(2):470–480.

116. Bratan F, Melodelima C, Souchon R, *et al.* How accurate is multiparametric MR imaging in evaluation of prostate cancer volume? *Radiology.* 2015;275(1):144–154.

117. Lencioni R, Menchi I, Paolicchi A, *et al.* Prediction of pathological tumor volume in clinically localized prostate cancer: value of endorectal coil magnetic resonance imaging. *Magma.* 1997;5(2):117–121.

118. Anwar M, Westphalen AC, Jung AJ, *et al.* Role of endorectal MR imaging and MR spectroscopic imaging in defining treatable intraprostatic tumor foci in prostate cancer: quantitative analysis of imaging contour compared to whole-mount histopathology. *Radiother Oncol.* 2014;110(2):303–308.

119. Ouzzane A, Helfrich O, Le Nobin J, *et al.* Understanding the pathological implications of MRI: application to focal therapy planning. *Curr Opin Urol.* 2015;25(3):198–204.

120. Sciarra A, Barentsz J, Bjartell A, *et al.* Advances in magnetic resonance imaging: how they are changing the management of prostate cancer. *Europ Urol.* 2011;59(6):962–977.

121. Oto A, Sethi I, Karczmar G, *et al.* MR imaging-guided focal laser ablation for prostate cancer: phase I trial. *Radiology.* 2013;267(3):932–940.

122. Lepor H, Llukani E, Sperling D, *et al.* Complications, recovery, and early functional outcomes and oncologic control following in-bore focal laser ablation of prostate cancer. *Eur Urol.* 2015;68(6):924–926.

123. Bomers JG, Yakar D, Overduin CG, *et al.* MR imaging-guided focal cryoablation in patients with recurrent prostate cancer. *Radiology.* 2013;268(2):451–460.

124. Ghai S, Louis AS, Van Vliet M, *et al.* Real-time MRI-guided focused ultrasound for focal therapy of locally confined low-risk prostate cancer: feasibility and preliminary outcomes. *AJR Am J Roentgenol.* 2015;205(2):W177–W184.

125. D'Amico A, Cormack R, Kumar S, *et al.* Real-time magnetic resonance imaging-guided brachytherapy in the treatment of selected patients with clinically localized prostate cancer. *J Endourol.* 2000;14(4):367–370.

126. Van Gellekom MP, Moerland MA, Battermann JJ, *et al.* MRI-guided prostate brachytherapy with single needle method--a planning study. *Radiother Oncol.* 2004;71(3):327–332.

127. Ares C, Popowski Y, Pampallona S, *et al.* Hypofractionated boost with high-dose-rate brachytherapy and open magnetic resonance imaging-guided implants for locally aggressive prostate cancer: a sequential dose-escalation pilot study. *Int J Radiat Oncol Biol Phys.* 2009;75(3):656–663.

128. Badalament RA, Bahn DK, Kim H, *et al.* Patient-reported complications after cryoablation therapy for prostate cancer. *Urology.* 1999;54(2):295–300.

129. Woodrum DA, Gorny KR, Mynderse LA, *et al.* Feasibility of 3.0T magnetic resonance imaging-guided laser ablation of a cadaveric prostate. *Urology.* 2010;75(6):1514–1516.

130. Woodrum DA, Mynderse LA, Gorny KR, *et al.* 3.0T MR-guided laser ablation of a prostate cancer recurrence in the postsurgical prostate bed. *J Vasc Interv Radiol.* 2011;22(7):929–934.

131. Raz O, Haider MA, Davidson SR, *et al.* Real-time magnetic resonance imaging-guided focal laser therapy in patients with low-risk prostate cancer. *Eur Urol.* 2010;58(1):173–177.

132. Chopra R, Tang K, Burtnyk M, *et al.* Analysis of the spatial and temporal accuracy of heating in the prostate gland using transurethral ultrasound therapy and active MR temperature feedback. *Phys Med Biol.* 2009;54(9):2615–2633.

133. Daniel BL, Butts K, Block WF. Magnetic resonance imaging of frozen tissues: temperature-dependent MR signal characteristics and relevance for MR monitoring of cryosurgery. *Magn Reson Med.* 1999;41(3):627–630.

134. Tatli S, Acar M, Tuncali K, *et al.* Percutaneous cryoablation techniques and clinical applications. *Diagn Interv Radiol.* 2010;16(1):90–95.

135. Overduin CG, Bomers JGR, Jenniskens SFM, *et al.* T1-weighted MR image contrast around a cryoablation iceball: a phantom study and initial comparison with in vivo findings. *Med Phys.* 2014;41(11):112301.

136. van den Bosch MA, Josan S, Bouley DM, *et al.* MR imaging-guided percutaneous cryoablation of the prostate in an animal model: in vivo imaging of cryoablation-induced tissue necrosis with immediate histopathologic correlation. *J Vasc Interv Radiol.* 2009;20(2):252–258.

137. Morrison PR, Silverman SG, Tuncali K, *et al.* MRI-guided cryotherapy. *J Magn Reson Imaging.* 2008;27(2):410–420.

138. Butts K, Sinclair J, Daniel BL, *et al.* Temperature quantitation and mapping of frozen tissue. *J Magn Reson Imaging.* 2001;13(1):99–104.

139. Wansapura JP, Daniel BL, Vigen KK, *et al.* In vivo MR thermometry of frozen tissue using R2* and signal intensity. *Acad Radiol.* 2005;12(9):1080–1084.

140. Kaye EA, Josan S, Lu A, *et al.* Consistency of signal intensity and T2* in frozen ex vivo heart muscle, kidney, and liver tissue. *J Mag Reson Imaging.* 2010;31(3):719–724.

141. Schouten MG, Ansems J, Renema WK, *et al.* The accuracy and safety aspects of a novel robotic needle guide manipulator to perform transrectal prostate biopsies. *Med Phys.* 2010;37(9):4744–4750.

142. Tokuda J, Fischer GS, DiMaio SP, *et al.* Integrated navigation and control software system for MRI-guided robotic prostate interventions. *Comput Med Imaging Graph.* 2010;34(1):3–8.

143. Muntener M, Patriciu A, Petrisor D, *et al.* Transperineal prostate intervention: robot for fully automated MR imaging--system description and proof of principle in a canine model. *Radiology.* 2008;247(2):543–549.

144. van den Bosch MR, Moman MR, van Vulpen M, *et al.* MRI-guided robotic system for transperineal prostate interventions: proof of principle. *Phys Med Biol.* 2010;55(5):N133–N140.

145. Larson BT, Collins JM, Huidobro C, *et al.* Gadolinium-enhanced MRI in the evaluation of minimally invasive treatments of the prostate: correlation with histopathologic findings. *Urology.* 2003;62(5):900–904.

146. Lindner U, Lawrentschuk N, Weersink RA, *et al.* Focal laser ablation for prostate cancer followed by radical prostatectomy: validation of focal therapy and imaging accuracy. *Eur Urol.* 2010;57(6):1111–1114.

147. De Visschere PJ, De Meerleer GO, Futterer JJ, *et al.* Role of MRI in follow-up after focal therapy for prostate carcinoma. *AJR Am J Roentgenol.* 2010;194(6):1427–1433.

148. Coakley FV, Hricak H, Wefer AE, *et al.* Brachytherapy for prostate cancer: endorectal MR imaging of local treatment-related changes. *Radiology.* 2001;219(3):817–821.

149. Sheaff MT, Baithun SI. Effects of radiation on the normal prostate gland. *Histopathol.* 1997;30(4):341–348.

150. Pucar D, Shukla-Dave A, Hricak H, *et al.* Prostate cancer: correlation of MR imaging and MR spectroscopy with pathologic findings after radiation therapy-initial experience. *Radiology.* 2005;236(2):545–553.

151. Coakley FV, Teh HS, Qayyum A, *et al.* Endorectal MR imaging and MR spectroscopic imaging for locally recurrent prostate cancer after external beam radiation therapy: preliminary experience. *Radiology.* 2004;233(2):441–448.

152. Haider MA, Chung P, Sweet J, *et al.* Dynamic contrast-enhanced magnetic resonance imaging for localization of recurrent prostate cancer after external beam radiotherapy. *Int J Radiat Oncol Biol Phys.* 2008;70(2):425–430.

153. Rouviere O, Valette O, Grivolat S, *et al.* Recurrent prostate cancer after external beam radiotherapy: value of contrast-enhanced dynamic MRI in localizing intraprostatic tumor--correlation with biopsy findings. *Urology.* 2004;63(5):922–927.

154. Kim CK, Park BK, Park W, *et al.* Prostate MR imaging at 3T using a phased-arrayed coil in predicting locally recurrent prostate cancer after radiation therapy: preliminary experience. *Abdominal Imaging.* 2010;35(2):246–252.

155. Kim CK, Park BK, Lee HM, *et al.* MRI techniques for prediction of local tumor progression after high-intensity focused ultrasonic ablation of prostate cancer. *AJR Am J Roentgenol.* 2008;190(5):1180–1186.

156. Rouviere O, Girouin N, Glas L, *et al.* Prostate cancer transrectal HIFU ablation: detection of local recurrences using T2-weighted and dynamic contrast-enhanced MRI. *Eur Radiol.* 2010;20(1):48–55.

157. Lindner U, Lawrentschuk N, Trachtenberg J. Focal laser ablation for localized prostate cancer. *J Endourol.* 2010;24(5):791–797.

158. Rouviere O, Lyonnet D, Raudrant A, *et al.* MRI appearance of prostate following transrectal HIFU ablation of localized cancer. *Eur Urol.* 2001;40(3):265–274.

159. Kulik M, Nedelcu C, Martin F, *et al.* Post-treatment MRI aspects of photodynamic therapy for prostate cancer. *Insights Imaging.* 2014;5(6):697–713.

160. Ben Cheikh A, Girouin N, Ryon-Taponnier P, *et al.* [MR detection of local prostate cancer recurrence after transrectal high-intensity focused US treatment: preliminary results] [Article in French]. *J Radiol.* 2008;89(5 Pt 1):571–577.

161. Vellet AD, Saliken J, Donnelly B, *et al.* Prostatic cryosurgery: use of MR imaging in evaluation of success and technical modifications. *Radiology.* 1997;203(3):653–659.

162. Kalbhen CL, Hricak H, Shinohara K, *et al.* Prostate carcinoma: MR imaging findings after cryosurgery. *Radiology.* 1996;198(3):807–811.

163. Cirillo S, Petracchini M, D'Urso L, *et al.* Endorectal magnetic resonance imaging and magnetic resonance spectroscopy to monitor the prostate for residual disease or local cancer recurrence after transrectal high-intensity focused ultrasound. *BJU Int.* 2008;102(4):452–458.

164. Valerio M, Stricker PD, Ahmed HU, *et al.* Initial assessment of safety and clinical feasibility of irreversible electroporation in the focal treatment of prostate cancer. *Prostate Cancer Prostatic Dis.* 2014;17(4):343–347.

165. Punwani S, Emberton M, Walkden M, *et al.* Prostatic cancer surveillance following whole-gland high-intensity focused ultrasound: comparison of MRI and prostate-specific antigen for detection of residual or recurrent disease. *Br J Radiol.* 2012;85(1014):720–728.

166. Donnelly SE, Donnelly BJ, Saliken JC, *et al.* Prostate cancer: gadolinium-enhanced MR imaging at 3 weeks compared with needle biopsy at 6 months after cryoablation. *Radiology.* 2004;232(3):830–833.

167. Cirillo S, Petracchini M, Scotti L, *et al.* Endorectal magnetic resonance imaging at 1.5 Tesla to assess local recurrence following radical prostatectomy using T2-weighted and contrast-enhanced imaging. *Eur Radiol.* 2009;19(3):761–769.

168. Allen SD, Thompson A, Sohaib SA. The normal post-surgical anatomy of the male pelvis following radical prostatectomy as assessed by magnetic resonance imaging. *Eur Radiol.* 2008;18(6):1281–1291.

169. Sella T, Schwartz LH, Swindle PW, *et al.* Suspected local recurrence after radical prostatectomy: endorectal coil MR imaging. *Radiology.* 2004;231(2):379–385.

170. Boonsirikamchai P, Kaur H, Kuban DA, *et al.* Use of maximum slope images generated from dynamic contrast-enhanced MRI to detect locally recurrent prostate carcinoma after prostatectomy: a practical approach. *AJR Am J Roentgenol.* 2012;198(3):228–236.

171. Panebianco V, Barchetti F, Sciarra A, *et al.* Prostate cancer recurrence after radical prostatectomy: the role of 3T diffusion imaging in multiparametric magnetic resonance imaging. *Eur Radiol.* 2013;23(6):1745–1752.

172. Arrayeh E, Westphalen AC, Kurhanewicz J, *et al.* Does local recurrence of prostate cancer after radiation therapy occur at the site of primary tumor? Results of a longitudinal MRI and MRSI study. *Int J Radiat Oncol Biol Phys.* 2012;82(5):787–793.

173. Donati OF, Jung SI, Vargas HA, *et al.* Multiparametric prostate MR imaging with T2-weighted, diffusion-weighted, and dynamic contrast-enhanced sequences: are all pulse sequences necessary to detect locally recurrent prostate cancer after radiation therapy? *Radiology.* 2013;268(2):440–450.

174. Morgan VA, Riches SF, Giles S, *et al.* Diffusion-weighted MRI for locally recurrent prostate cancer after external beam radiotherapy. *AJR Am J Roentgenol.* 2012;198(3):596–602.

175. Kim CK, Park BK, Lee HM. Prediction of locally recurrent prostate cancer after radiation therapy: incremental value of 3T diffusion-weighted MRI. *J Magn Reson Imaging.* 2009;29(2):391–397.

176. Tamada T, Sone T, Jo Y, *et al.* Locally recurrent prostate cancer after high-dose-rate brachytherapy: the value of diffusion-weighted imaging, dynamic contrast-enhanced MRI, and T2-weighted imaging in localizing tumors. *AJR Am J Roentgenol.* 2011;197(2):408–414.

177. Chen M, Hricak H, Kalbhen CL, *et al.* Hormonal ablation of prostatic cancer: effects on prostate morphology, tumor detection, and staging by endorectal coil MR imaging. *AJR Am J Roentgenol.* 1996;166(5):1157–1163.

178. Kirkham AP, Emberton M, Hoh IM, *et al.* MR imaging of prostate after treatment with high-intensity focused ultrasound. *Radiology.* 2008;246(3):833–844.

179. Blana A, Walter B, Rogenhofer S, *et al.* High-intensity focused ultrasound for the treatment of localized prostate cancer: 5-year experience. *Urology.* 2004;63(2):297–300.

180. Jemal A, Siegel R, Xu J, *et al.* Cancer statistics, 2010. *CA Cancer J Clin.* 2010;60(5):277–300.

C2-III

Imaging in Localized Prostate Cancer:
III. Role of Molecular Imaging Techniques

CHAIR

Eric Barret, France

CO-CHAIR

Olivier Rouvière, France

MEMBERS

Hedvig Hricak, United States

Herbert Alberto Vargas, United States

Andreas Wibmer, United States

CONTENTS

Imaging in Localized Prostate Cancer:
III. Role of Molecular Imaging Techniques

III-2.1 Introduction

Prostate cancer (PCa) is confined to the prostate or peri-prostatic tissues in four out of five patients with newly diagnosed disease.[1] Accurate tumour localization and staging, as well as assessment of the tumour's aggressiveness, are crucial for implementing the most appropriate management strategy, and are particularly important in the context of image-guided therapies.

Multiparametric magnetic resonance imaging (mpMRI) is currently regarded as the imaging modality of choice for prostate tumour localization and local staging. The role of nuclear medicine techniques has traditionally been limited to the detection of skeletal metastases in patients with newly diagnosed high-risk PCa or the localization of recurrent disease after radical treatment, with bone scintigraphy being the most widely applied method in the field.

More recently, however, more than a dozen positron emission tomography (PET) radiotracers of potential relevance to PCa have been developed for which initial safety, biodistribution, and feasibility studies have been completed. Although most of the work with these imaging probes in PCa to date has focused on the localization and characterization of metastatic disease, there have also been studies specifically evaluating their use in the assessment of primary disease.[2] Their potential role as tools for image-guided therapy and disease monitoring, however, remains largely unexplored, and thus further research in this specific context is eagerly awaited. In this chapter, we summarize the evidence published thus far, and discuss the potential of novel radiotracers for the assessment of localized PCa.

III-2.2 Radiotracers for Potential Use in PCa

Radiotracers used for imaging of PCa can be categorized into those that localize to areas of increased metabolic needs of cancer cells and those that accumulate by binding to receptors or membrane proteins. The most important of the former group are radiolabelled analogues of choline, acetate, and glucose, while tracers in the latter group target the gastrin-releasing peptide receptor or the prostate-specific membrane antigen (PSMA). Several other PCa-specific imaging targets have been identified in pre-clinical experiments and preliminary clinical trials, but no clinical data are available on their potential for assessing localized PCa.

III-2.2.1 Choline

Choline is essential for the synthesis of cell membranes and, thus, for cell proliferation, as it constitutes the backbone of the hydrophilic head groups of phosphatidylcholine and sphingomyelin. It is also important for the synthesis of the essential proteinogenic amino acid methionine. Overexpression of

choline-specific membrane transporters and choline-processing enzymes has been found in several human cancers, including PCa.[3] The uptake of choline appears to be affected by the cell's sensitivity to and the presence of androgens and anti-androgenic drugs[4,5], as well as by tumour hypoxia.[6]

Two labelled analogues of choline, ^{11}C-choline and ^{18}F-choline, are available for use in PET. While ^{11}C-choline, which has a shorter half-life (20 minutes), is rapidly metabolized, ^{18}F-choline (half-life: 110 minutes) is excreted via the urine, which may affect the assessment of primary PCa in close proximity to the urinary bladder. Several studies on ^{18}F-choline PET/computed tomography (CT) found significant overlap between levels of tracer accumulation in benign and malignant prostate tissue, and thus raised doubts about the usefulness of ^{18}F-choline for tumour localization and staging of localized PCa.[7-12] Subsequent research revealed that the strong ^{18}F-choline uptake of adenomatous prostatic hyperplasia is one reason for the tracer's suboptimal diagnostic accuracy.[13] The presence of prostatic hyperplasia or prostatic intraepithelial neoplasia within tumours was also shown to be associated with ^{11}C-choline uptake of localized PCa.[14] In other studies, however, ^{18}F-choline PET/CT reliably detected PCa when results were analyzed by prostate sextant,[15,16] and regional ^{18}F-choline uptake correlated with the degree of tumour infiltration on histopathology.[17]

Studies on the assessment of PCa aggressiveness by radiolabelled choline analogues have yielded discrepant results. In one study, ^{11}C-choline uptake was significantly different between Gleason score (GS) ≤3+4 versus ≥4+3 tumours, and also correlated with the cancer proliferation rate as indicated by Ki-67 expression levels.[18] This observation was confirmed by another group, which found that the tumour-to-prostate ratio of ^{11}C-choline uptake was significantly higher in GS ≥3+4=7 cancer than in GS ≤3+3=6 cancer.[19] Others, however, found only weak or no correlation between uptake of ^{11}C-choline and GS on histopathology.[20-22] ^{11}C-choline was also tested as a potential marker for treatment response assessment, and its uptake in primary PCa was shown to significantly decrease after neoadjuvant androgen deprivation therapy, as well as after radical prostate radiotherapy.[23] Preliminary studies tested the potential of ^{11}C/^{18}F-choline PET/CT for radiotherapy planning,[24,25] but more data are needed to make a judgment about the utility of this approach.

Simultaneous PET/MRI is a novel imaging technique that, it is hoped, will improve the localizability of pathologic tracer uptake within the prostate. One group reported that the image quality of ^{18}F-choline PET/MRI was similar to that of PET/CT,[26] while other investigators found that the quality of PET/CT images was better than that of the PET scan acquired as part of PET/MRI.[27] These contrasting observations may be attributable to some initial technical difficulties with the technique, which has yet to be fully developed. In a preliminary study of ^{18}F-choline PET/MRI conducted in 15 PCa patients, there was a good correlation between cancer-suspicious areas on PET and MRI and, in three out of 15 patients, PET showed areas of focal uptake that were negative on diffusion-weighted MRI.[28] Wetter *et al.* also compared the quantity of ^{18}F-choline uptake and diffusion restriction on MRI and found no significant correlation, which indicates that these two parameters may depict different aspects of PCa biology.[29]

III-2.2.2 **Acetate**

Acetate is a central molecule of the cell's energy metabolism. It is an important compound for the synthesis of fatty acids and thus of phospholipids and glycolipids for cell membranes. Cholesterol, which is also essential for cell membrane structure, is another biochemical derivate of acetate. Increased uptake of acetate has been repeatedly observed in PCa cells, most likely due to the upregulation of fatty acid synthetase.[30,31] Two radiolabelled analogues of acetate are available for PET imaging, i.e. ^{11}C-acetate and ^{18}F-acetate, but the literature on the value of acetate PET for assessing localized PCa is relatively scarce and is limited to reports on ^{11}C-acetate.

Initial research reported an age-related accumulation of ^{11}C-acetate in non-cancerous prostatic tissue that posed an obstacle to the accurate detection and localization of organ-confined PCa.[32] Other investigators found that ^{11}C-acetate uptake was significantly higher in localized PCa than in normal prostate tissue, but similar to the uptake in benign prostate hyperplasia.[33] A subsequent study found that, in determining which of the two prostate lobes contained the dominant PCa focus, ^{11}C-acetate PET/CT had a sensitivity of 80% and specificity of 29%.[34] When a sextant-based approach was applied to the same data, the sensitivity decreased to 64%, while the specificity increased to 63%. Another study, in which the diagnostic accuracy of ^{11}C-acetate PET/CT was compared to that of prostate MRI, found that a combination of findings from both examinations yielded more accurate results than either individual examination alone.[35]

III-2.2.3 **Glucose**

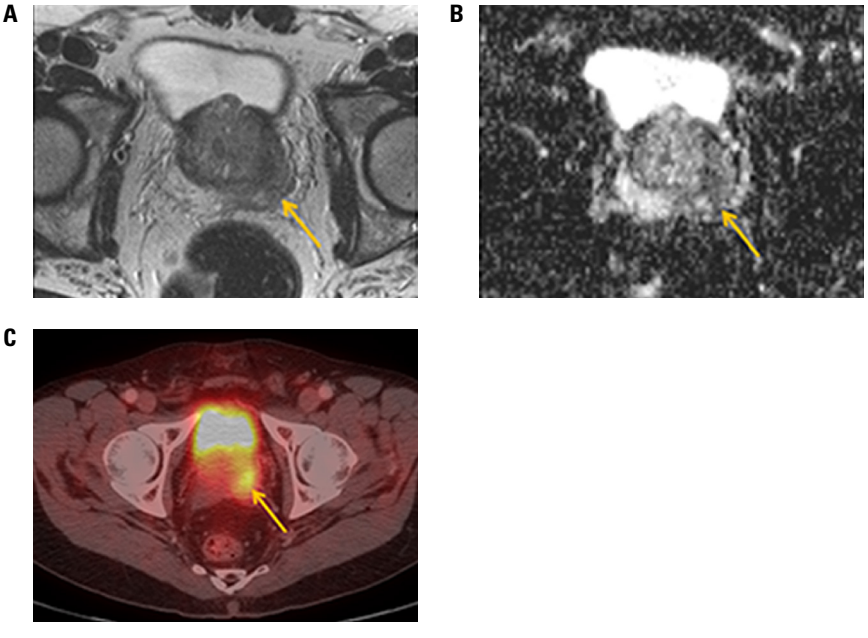

FIGURE 2.III-1
Gleason Score 4+4 PCa in the Left Basal Peripheral Zone

The tumour is clearly shown (arrows) on axial T2-weighted magnetic resonance image (**A**), apparent diffusion coefficient map (**B**), and fused ^{18}F-fluorodeoxyglucose (FDG) PET/CT image (**C**).

For many cancers, glucose represents the most important metabolic fuel. The overexpression of glucose transmembrane transporters is the major determinant of the cellular uptake of ^{18}F-FDG, a radiolabelled glucose analogue that is widely utilized in cancer imaging. In PCa cells, however,

the expression of these transport molecules and thus the uptake of ^{18}F-FDG is variable and can be affected by a number of biological factors, such as the degree of tissue differentiation,[36] androgen dependency,[37] anti-androgenic therapy,[38] expression of hexokinase II,[39] or tumour hypoxia.[6] While some prostate cancers demonstrate abnormal ^{18}F-FDG accumulation on PET (**Figure 2.III-1**), the multiple determinants of cellular ^{18}F-FDG uptake are reflected in the unpredictability of the degree of ^{18}F-FDG uptake in PCa foci on standard clinical imaging examinations. Furthermore, ^{18}F-FDG is excreted in the urine, and levels of tracer accumulation in normal and cancerous prostate tissue overlap significantly.[40] As a consequence, the performance of ^{18}F-FDG PET/CT in the detection and localization of primary PCa is relatively poor. One study that evaluated patients with elevated prostate-specific antigen levels found that ^{18}F-FDG PET/CT detected cancer in 52% of patients with positive biopsy results (positive predictive value: 43%).[41] Similar findings were reported by another study of patients with suspected PCa, in which ^{18}F-FDG PET/CT was reported to have an area under the receiver operating characteristic curve (ROC) of 0.54 for the detection of PCa.[42] ^{18}F-FDG PET/CT has also been evaluated for its capacity to estimate the histological grade of PCa and has been shown to differentiate GS ≤7 from GS ≥8 cancers with an accuracy of 71%.[43] However, another study did not find a significant correlation between GS and ^{18}F-FDG uptake in localized PCa (ρ=0.204, p=0.375).[20]

In the vast majority of cases, ^{18}F-FDG PET/CT is applied in patients with non-prostatic diseases. Incidental prostatic tracer uptake has been reported to occur in 0.6% to 2.8% of such patients, of whom 3.1% to 16% have ultimately been diagnosed with PCa.[44-49]

III-2.2.4 Gastrin-releasing peptide receptor (bombesin)

By binding the extracellular domain of its membrane receptor, mammalian bombesin (i.e. gastrin-releasing peptide) activates intracellular signalling pathways that lead to increased expression of transcription factors, activation of key elements of the cell cycle, and expression of growth factor receptors. In PCa cells, bombesin receptors have been found to be overexpressed on the mRNA as well as on the protein level;[50] their expression in benign prostate tissues, on the other hand, has been found to range from low to non-detectable.[51,52] Several radiolabelled bombesin analogues have been developed for PET imaging, including ^{18}F-, ^{68}Ga-, and ^{64}Cu-labelled substances.[53-58] However, the clinical experience with these radiopharmaceuticals in localized PCa is limited. In one preliminary clinical study, the ^{18}F-radiolabelled bombesin analogue BAY 864367 delineated localized PCa in three of five patients with positive biopsy results.[59] One of the two false-negative cases had multifocal PCa on prostatectomy, and the other was found to have a GS 4+4=8 cancer in the base of the prostate, which might have been obscured by the tracer excretion into the urinary bladder. In another study of four patients with newly diagnosed localized PCa, the bombesin receptor antagonist ^{64}Cu-CB-TE2A-AR06 depicted the primary cancer site with high contrast (tumour-to-prostate ratios: >4) in three patients and with low contrast in one patient, who was found to have fewer than 5% tumour cells in the biopsy specimen (tumour-to-prostate ratio: 1.9).[60]

III-2.2.5 Prostate-specific membrane antigen

Prostate-specific membrane antigen, a transmembrane protein with large extracellular enzymatic domains, is expressed at low levels on the surface of normal prostate epithelium, but at very high levels in PCa. The PSMA is internalized into the endosomal compartments of the cell, which increases its

potential value as an imaging and therapeutic target. It is more abundant on the surface of castration-resistant tumours, and its expression on PCa cells was found to be associated with the probability of tumour progression.[61,62] Positron emission tomography imaging of PSMA is based on radiolabelled monoclonal antibodies, antibody fragments, or small-molecule inhibitors of its enzymatic domains.

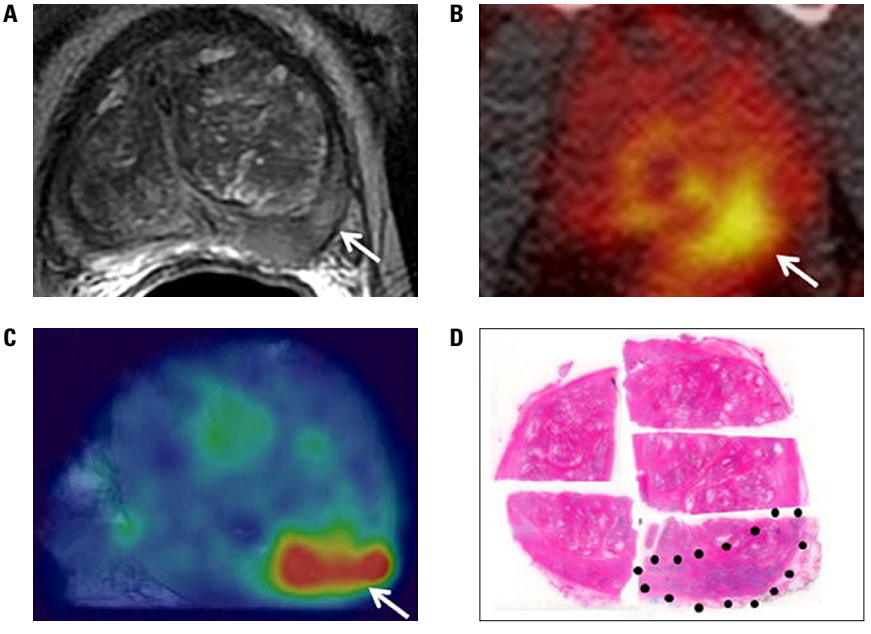

FIGURE 2.III-2
Gleason Score 4+5 PCa in the Left Mid-Gland Peripheral Zone

The tumour is shown (arrows) on axial T2-weighted magnetic resonance image (**A**), in vivo ^{89}Zr-J591 PET (**B**), ex vivo ^{89}Zr-J591 PET image (**C**), and histopathology section (**D**). Dotted area indicates cancer. Reduced from ×1.

Reprinted from: Osborne JR. J Urol. 2014;191(5):1439-1445, Copyright 2014, with permission from Elsevier.

In an early clinical report on the performance of single photon emission computed tomography (SPECT)/CT with two ^{123}I-labelled small-molecule inhibitors of PSMA, the prostates of healthy volunteers showed only low tracer accumulation, while the agents were able to detect focal lesions in patients with PCa.[63] In a case report of a patient with newly diagnosed PCa who underwent PET/MRI with a ^{68}Ga-labelled PSMA ligand, an area of intense tracer uptake in the peripheral zone matched with low signal intensity on T2-weighted MRI, restricted diffusion on diffusion-weighted MRI, and a GS 7 tumour on whole-mount histopathology.[64] In a prospective pilot study (n=11 patients), PET with a ^{89}Zr-labelled monoclonal antibody targeting the extracellular domain of PSMA correctly identified eight of 11 index lesions, as determined by post-prostatectomy histopathology (**Figure 2.III-2**).[65] The GS of the three PET-negative index lesions was 4+4=8, and their diameters were 4 mm, 5 mm, and 13 mm. Seven of 11 non-index lesions were negative on the PET images, six of which were GS 3+3 cancers. Immunohistochemistry proved PSMA expression by all index and non-index lesions. In this trial, the identification of localized PCa foci was dependent on tumour size and GS, and the intensity of tracer uptake was positively correlated with a lesion's GS.[65]

III-2.3 **Conclusion**

Currently, several PET tracers are available that accumulate in or on PCa cells and therefore have the potential to show not only metastatic disease but also localized cancer. These tracers might augment the work-up of newly diagnosed PCa by providing metabolic and/or molecular information that is not accessible with prostate MRI, which remains the standard imaging technique for local tumour staging. It is possible that imaging with these probes may complement mpMRI by providing information related to tumour biology that could aid PCa characterization and assessment of the risk of rapid disease progression and spread. The relatively low spatial resolution of PET and the low tissue contrast of prostate CT are the major obstacles to reliably allocating pathologic tracer accumulation to cancer foci within the gland. Combined PET/MRI may provide adequate tissue contrast and help to enhance the clinical value of these substances. [**Level of Evidence: 3**]

III-2.4 **References**

1. National Cancer Institute. SEER Stat Fact Sheets: Prostate Cancer. 2015. Surveillance, Epidemiology, and End Results Program. Available from: http://seer.cancer.gov/statfacts/html/prost.html. Accessed June 1, 2015.
2. National Comprehensive Cancer Network. Clinical Practice Guidelines in Oncology (NCCN Guidelines®) Prostate Cancer Version 1.2015. Available from: http://www.nccn.org/professionals/physician_gls/pdf/prostate.pdf. Accessed June 1, 2015.
3. Ramírez de Molina A, Rodríguez-González A, Gutiérrez R, *et al.* Overexpression of choline kinase is a frequent feature in human tumor-derived cell lines and in lung, prostate, and colorectal human cancers. *Biochem Biophys Res Commun.* 2002;296(3):580–583.
4. Emonds K, Swinnen J, van Weerden W, *et al.* Do androgens control the uptake of 18F-FDG, 11C-choline and 11C-acetate in human prostate cancer cell lines? *Eur J Nucl Med Mol Imaging.* 2011;38(10):1842–1853.
5. Emonds K, Swinnen J, Lerut E, *et al.* Evaluation of androgen-induced effects on the uptake of [18F]FDG, [11C]choline and [11C] acetate in an androgen-sensitive and androgen-independent prostate cancer xenograft model. *EJNMMI Res.* 2013;3(1):31.
6. Hara T, Bansal A, DeGrado T. Effect of hypoxia on the uptake of [methyl-3H]choline, [1-14C] acetate and [18F]FDG in cultured prostate cancer cells. *Nucl Med Biol.* 2006;33(8):977–984.
7. Igerc I, Kohlfürst S, Gallowitsch H, *et al.* The value of 18F-Choline PET/CT in patients with elevated PSA-level and negative prostate needle biopsy for localisation of prostate cancer. *Eur J Nucl Med Mol Imaging.* 2008;35(5):976–983.
8. Schmid D, John H, Zweifel R, *et al.* Fluorocholine PET/CT in patients with prostate cancer: initial experience. *Radiology.* 2005;235(2):623–628.
9. Souvatzoglou M, Weirich G, Schwarzenboeck S, *et al.* The sensitivity of [11C]choline PET/CT to localize prostate cancer depends on the tumor configuration. *Clin Cancer Res.* 2011;17(11):3751–3759.
10. Bundschuh R, Wendl C, Weirich G, *et al.* Tumour volume delineation in prostate cancer assessed by [11C]choline PET/CT: validation with surgical specimens. *Eur J Nucl Med Mol Imaging.* 2013;40(6):824–831.
11. Grosu A, Weirich G, Wendl C, *et al.* 11C-Choline PET/pathology image coregistration in primary localized prostate cancer. *Eur J Nucl Med Mol Imaging.* 2014;41(12):2242–2248.
12. Boychak O, Vos L, Makis W, *et al.* Role for 11C-choline PET in active surveillance of prostate cancer. *Can Urol Assoc J.* 2015;9(3–4):E98–E103.
13. de Perrot T, Rager O, Scheffler M, *et al.* Potential of hybrid 18F-fluorocholine PET/MRI for prostate cancer imaging. *Eur J Nucl Med Mol Imaging.* 2014;41(9):1744–1755.
14. Yoneyama T, Tateishi U, Terauchi T, *et al.* Correlation of metabolic tumor volume and 11C-choline uptake with the pathology of prostate cancer: evaluation by use of simultaneously recorded MR and PET images. *Jpn J Radiol.* 2014;32(3):155–163.
15. Kwee SA, Thibault GP, Stack RS, *et al.* Use of step-section histopathology to evaluate 18F-fluorocholine PET sextant localization of prostate cancer. *Mol Imaging.* 2008;7(1):12–20.
16. Kuang Y, Wu L, Hirata E, *et al.* Volumetric modulated arc therapy planning for primary prostate cancer with selective intraprostatic boost determined by 18F-choline PET/CT. *Int J Radiat Oncol Biol Phys.* 2015;91(5):1017–1025.
17. Beheshti M, Imamovic L, Broinger G, *et al.* 18F choline PET/CT in the preoperative staging of prostate cancer in patients with intermediate or high risk of extracapsular disease: a prospective study of 130 patients *Radiology.* 2010;254(3):925–933.
18. Chen J, Zhao Y, Li X, *et al.* Imaging primary prostate cancer with 11C-choline PET/CT: relation to tumour stage, Gleason score and biomarkers of biologic aggressiveness. *Radiol Oncol.* 2012;46(3):179–188.
19. Park H, Wood D, Hussain H, *et al.* Introducing parametric fusion PET/MRI of primary prostate cancer. *J Nucl Med.* 2012;53(4):546–551.
20. Chang J, Lim Joon D, Lee S, *et al.* Diffusion-weighted MRI, 11C-choline PET and 18F-fluorodeoxyglucose PET for predicting the Gleason score in prostate carcinoma. *Eur Radiol.* 2013;24(3):715–722.

21. Van den Bergh L, Koole M, Isebaert S, *et al.* Is there an additional value of 11C-choline PET-CT to T2-weighted MRI images in the localization of intraprostatic tumor nodules? *Int J Radiat Oncol Biol Phys.* 2012;83(5):1486–1492.

22. Testa C, Schiavina R, Lodi R, *et al.* Prostate cancer: sextant localization with MR imaging, MR spectroscopy, and 11C-choline PET/CT. *Radiology.* 2007;244(3):797–806.

23. Challapalli A, Barwick T, Tomasi G, *et al.* Exploring the potential of [11C]choline-PET/CT as a novel imaging biomarker for predicting early treatment response in prostate cancer. *Nucl Med Commun.* 2014;35(1):20–29.

24. López E, Lazo A, Gutiérrez A, *et al.* Influence of 11C-choline PET/CT on radiotherapy planning in prostate cancer. *Rep Pract Oncol Radiother.* 2015;20(2):104–112.

25. Fersino S, Giaj Levra N, Mazzola R, *et al.* Impact of 18F-choline PET/CT in the decision-making strategy of treatment volumes in definitive prostate cancer volumetric modulated radiation therapy. *Clin Nucl Med.* 2015;40(11):e496–e500.

26. Wetter A, Lipponer C, Nensa F, *et al.* Evaluation of the PET component of simultaneous [18F]choline PET/MRI in prostate cancer: comparison with [18F]choline PET/CT. *Eur J Nucl Med Mol Imaging.* 2013;41(1):79–88.

27. Souvatzoglou M, Eiber M, Takei T, *et al.* Comparison of integrated whole-body [11C]choline PET/MR with PET/CT in patients with prostate cancer. *Eur J Nucl Med Mol Imaging.* 2013;40(10):1486–1499.

28. Wetter A, Lipponer C, Nensa F, *et al.* Simultaneous 18F choline positron emission tomography/magnetic resonance imaging of the prostate. *Invest Radiol.* 2013;48(5):256–262.

29. Wetter A, Nensa F, Schenck M, *et al.* Combined PET imaging and diffusion-weighted imaging of intermediate and high-risk primary prostate carcinomas with simultaneous [18F] choline PET/MRI. *PLoS ONE.* 2014;9(7):e101571.

30. Vavere A, Kridel S, Wheeler F, *et al.* 1-11C-Acetate as a PET radiopharmaceutical for imaging fatty acid synthase expression in prostate cancer. *J Nucl Med.* 2008;49(2):327–334.

31. Pflug B, Pecher S, Brink A, *et al.* Increased fatty acid synthase expression and activity during progression of prostate cancer in the TRAMP model. *Prostate.* 2003;57(3):245–254.

32. Kato T, Tsukamoto E, Kuge Y, *et al.* Accumulation of [11C]acetate in normal prostate and benign prostatic hyperplasia: comparison with prostate cancer. *Eur J Nucl Med Mol Imaging.* 2002;29(11):1492–1495.

33. Mena E, Turkbey B, Mani H, *et al.* 11C-Acetate PET/CT in localized prostate cancer: a study with MRI and histopathologic correlation. *J Nucl Med.* 2012;53(4):538–545.

34. Jambor I, Borra R, Kemppainen J, *et al.* Functional imaging of localized prostate cancer aggressiveness using 11C-acetate PET/CT and 1H-MR spectroscopy. *J Nucl Med.* 2010;51(11):1676–1683.

35. Jambor I, Borra R, Kemppainen J, *et al.* Improved detection of localized prostate cancer using co-registered MRI and 11C-acetate PET/CT. *Eur J Radiol.* 2012;81(11):2966–2972.

36. Stewart GD, Gray K, Pennington CJ, *et al.* Analysis of hypoxia-associated gene expression in prostate cancer: lysyl oxidase and glucose transporter-1 expression correlate with Gleason score. *Oncol Rep.* 2008;20(6):1561–1567.

37. Price D, Coleman R, Liao R, *et al.* Comparison of [18F]fluorocholine and [18F]fluorodeoxyglucose for positron emission tomography of androgen dependent and androgen independent prostate cancer. *J Urol.* 2002;168(1):273–280.

38. Kukuk D, Reischl G, Raguin O, *et al.* Assessment of PET tracer uptake in hormone-independent and hormone-dependent xenograft prostate cancer mouse models. *J Nucl Med.* 2011;52(10):1654–1663.

39. Moon J, Jin W, Kwak J, *et al.* Androgen stimulates glycolysis for de novo lipid synthesis by increasing the activities of hexokinase 2 and 6-phosphofructo-2-kinase/fructose-2,6-bisphosphatase 2 in prostate cancer cells. *Biochem J.* 2010;433(1):225–233.

40. Salminen E, Hogg A, Binns D, *et al.* Investigations with FDG-PET scanning in prostate cancer show limited value for clinical practice. *Acta Oncol.* 2002;41(5):425–429.

41. Minamimoto R, Uemura H, Sano F, *et al.* The potential of FDG-PET/CT for detecting prostate cancer in patients with an elevated serum PSA level. *Ann Nucl Med.* 2010;25(1):21–27.

42. Watanabe H, Kanematsu M, Kondo H, *et al.* Preoperative detection of prostate cancer: A comparison with 11C-choline PET, 18F-fluorodeoxyglucose PET and MR imaging. *J Magn Reson Imaging.* 2010;31(5):1151–1156.

43. Shiiba M, Ishihara K, Kimura G, *et al.* Evaluation of primary prostate cancer using 11C-methionine-PET/CT and 18F-FDG-PET/CT. *Ann Nucl Med.* 2011;26(2):138–145.

44. Kang PM, Seo WI, Lee SS, *et al.* Incidental abnormal FDG uptake in the prostate on 18-fluoro-2-deoxyglucose positron emission tomography-computed tomography scans. *Asian Pac J Cancer Prev.* 2014;15(20):8699–8703.

45. Yang Z, Hu S, Cheng J, *et al.* Prevalence and risk of cancer of incidental uptake in prostate identified by fluorine-18 fluorodeoxyglucose positron emission tomography/computed tomography. *Clin Imaging.* 2014;38(4):470–474.

46. Seino H, Ono S, Miura H, *et al.* Incidental prostate 18F-FDG uptake without calcification indicates the possibility of prostate cancer. *Oncol Rep.* 2014;31(4):1517–1522.

47. Kwon T, Jeong I, You D, *et al.* Prevalence and clinical significance of incidental 18 F-fluoro-2-deoxyglucose uptake in prostate. *Korean J Urol.* 2015;56(4):288–294.

48. Hwang I, Chong A, Jung S, *et al.* Is further evaluation needed for incidental focal uptake in the prostate in 18-fluoro-2-deoxyglucose positron emission tomography–computed tomography images? *Ann Nucl Med.* 2013;27(2):140–145.

49. Han E, O JH, Choi W, *et al.* Significance of incidental focal uptake in prostate on 18-fluoro-2-deoxyglucose positron emission tomography CT images. *Br J Radiol.* 2010;83(995):915–920.

50. Mansi R, Fleischmann A, Mäcke H, *et al.* Targeting GRPR in urological cancers—from basic research to clinical application. *Nat Rev Urol.* 2013;10(4):235–244.

51. Bartholdi M, Wu J, Pu H, *et al.* In situ hybridization for gastrin-releasing peptide receptor (GRP receptor) expression in prostatic carcinoma. *Int J Cancer.* 1998;79(1):82–90.

52. Markwalder R, Reubi JC. Gastrin-releasing peptide receptors in the human prostate: relation to neoplastic transformation. *Cancer Res.* 1999;59(5):1152–1159.

53. Richter S, Wuest M, Krieger S, *et al.* Synthesis and radiopharmacological evaluation of a high-affinity and metabolically stabilized 18F-labeled bombesin analogue for molecular imaging of gastrin-releasing peptide receptor-expressing prostate cancer. *Nucl Med Biol.* 2013;40(8):1025–1034.

54. Varshney R, Hazari P, Fernandez P, *et al.* (68)Ga-Labeled bombesin analogs for receptor-mediated imaging. *Recent Results Cancer Res.* 2013;194:221–256.

55. Zhou Z, Wagh N, Ogbomo S, *et al.* Synthesis and in vitro and in vivo evaluation of hypoxia-enhanced 111In-bombesin conjugates for prostate cancer imaging. *J Nucl Med.* 2013;54(9):1605–1612.

56. Zhang H, Abiraj K, Thorek D, *et al.* Evolution of bombesin conjugates for targeted PET imaging of tumors. *PLoS ONE.* 2012;7(9):e44046.

57. Marsouvanidis P, Maina T, Sallegger W, *et al.* 99mTc Radiotracers based on human GRP(18-27): synthesis and comparative evaluation. *J Nucl Med.* 2013;54(10):1797–1803.

58. Jiang L, Miao Z, Liu H, *et al.* 177Lu-labeled RGD-BBN heterodimeric peptide for targeting prostate carcinoma. *Nucl Med Commun.* 2013;34(9):909–914.

59. Sah B, Burger I, Schibli R, *et al.* Dosimetry and first clinical evaluation of the new 18F-radiolabeled bombesin analogue BAY 864367 in patients with prostate cancer. *J Nucl Med.* 2015;56(3):372–378.

60. Wieser G, Mansi R, Grosu A, *et al.* Positron emission tomography (PET) imaging of prostate cancer with a gastrin releasing peptide receptor antagonist - from mice to men. *Theranostics.* 2014;4(4):412–419.

61. Sweat S, Pacelli A, Murphy G, *et al.* Prostate-specific membrane antigen expression is greatest in prostate adenocarcinoma and lymph node metastases. *Urology.* 1998;52(4):637–640.

62. Ross JS, Sheehan CE, Fisher HA, *et al.* Correlation of primary tumor prostate-specific membrane antigen expression with disease recurrence in prostate cancer. *Clin Cancer Res.* 2013;9(17):6357–6362.

63. Barrett J, Coleman R, Goldsmith S, *et al.* First-in-man evaluation of 2 high-affinity PSMA-avid small molecules for imaging prostate cancer. *J Nucl Med.* 2013;54(3):380–387.

64. Eiber M, Nekolla SG, Maurer T, *et al.* Ga-PSMA PET/MR with multimodality image analysis for primary prostate cancer. *Abdom Imaging.* 2015;40(6):1769–1771.

65. Osborne J, Green D, Spratt D, *et al.* A prospective pilot study of 89Zr-J591/prostate specific membrane antigen positron emission tomography in men with localized prostate cancer undergoing radical prostatectomy. *J Urol.* 2014;191(5):1439–1445.

C3

Prostatic Biopsies: Available Techniques and Approaches

CHAIRS

Badrinath R. Konety, United States
Osamu Ukimura, United States

MEMBERS

Ahmed El-Shater Bosaily, United Kingdom
Jurgen Fütterer, The Netherlands
Arvin K. George, United States
Mahir Maruf, United States
Neil Mendhiratta, United States
Caroline M. Moore, United Kingdom
Peter A. Pinto, United States
Ardeshir R. Rastinehad, United States
Samir S. Taneja, United States
Arnauld Villers, France
Christopher Warlick, United States

CONTENTS

Prostatic Biopsies: Available Techniques and Approaches

3.1 Introduction

The role of prostate biopsies has changed. Because of sampling error during systematic random prostate biopsy, the historical likelihood of missing clinically significant cancers has led to the introduction of new techniques. These techniques have evolved from pure cancer detection to assisting in clinical patient management, focusing on the localization of clinically significant cancer, and potentially reducing over-detection of clinically insignificant cancer. The major challenge for image-guided prostatic tissue preservation strategy in both active surveillance and focal therapy is the precise mapping of baseline cancer location and extent. The technical key to refining optimal biopsy protocols may include not only increasing the number of cores taken with template-based three-dimensional (3D) cancer mapping, but also improving the precision and quality of each biopsy by real-time image-guided targeting or robotic control, and documenting each individual biopsy location to revisit the exact location of the known cancer during possible future interventions.

In an effort to accurately diagnose all clinically significant cancers, several groups have proposed transperineal template-based 3D mapping ("saturation" biopsy) prior to focal therapy. A saturation biopsy method may yield maximum cancer detection, but can result in overdiagnosis of clinically insignificant cancer when one simply increases the number of biopsies to increase detection.

On the other hand, modern imaging potentially improves the process of clinically significant cancer detection through the ability to visualize and characterize lesions and to guide precise, targeted biopsy. A higher prevalence of image-detected, biopsy-proven cancers has been reported using evolving imaging modalities such as advanced multiparametric transrectal ultrasound (mpTRUS) technologies or multiparametric magnetic resonance imaging (mpMRI).

In-bore magnetic resonance imaging (MRI)–guided biopsy can be performed in order to achieve reliable targeting from the magnetic resonance (MR)–suspicious lesion in patients with prior negative systematic prostate biopsy. In-bore MRI-guided biopsy has the advantage of real-time feedback of sampling locations, resulting in the low likelihood of a sampling error. However, it also has the disadvantage of higher costs for long MR-gantry time and difficulty of sampling from the remaining prostatic field.

Other efforts have been focused on using computer-assisted technology, including the image capture of real-time transrectal ultrasound (TRUS) for assessing 3D volume of the prostate in computer reconstruction models in order to achieve image fusion with advanced mpMRI. This can be supported by either using the tracking technology of the two-dimensional (2D) TRUS probe, such as magnetic tracking or mechanical tracking, or by using the 3D TRUS image-based tracking of the prostate. These emerging technologies allow the novel opportunity for image fusion-guided prostate biopsy between real-time TRUS and any other imaging modality, such as mpMRI, acquired prior to the time of biopsy. This is because the image fusion of the preoperatively acquired MRI data with TRUS requires reliable registration between preoperative and intraoperative conditions. However, there are various challenges to achieve precise registration between the preoperative and the intraoperative reality of the prostate. The intraoperative reality of the prostate may change if the patient moves or

if the prostate is deformed or shifted during needle insertion. Real-time monitoring and adjustment of such intraoperative change in location or shape of the prostate compared with the preoperative condition are essential to achieve reliable image fusion.

Since the prostate is a mobile organ and prostate shape is deformable at the time of prostate biopsy between preoperative and intraoperative conditions, the use of a nonrigid (i.e. elastic) image-fusion technique is vital to achieve precise image fusion between them. An image-based tracking system using real-time 3D TRUS with elastic image fusion seems to be the most reliable registration and localization system for documenting biopsy trajectory overlaid onto the image-suspicious lesion.

On the other hand, in order to achieve precise real-time targeting of the suspected lesion, real-time simultaneous parallel display of the real-time TRUS and virtual MRI target is very helpful. Since the prostate is deformable at the time of needle insertion, real-time 2D TRUS monitoring of such deformation is vital.

An important and obvious limitation of the image-guided prostate biopsy technique is that it is operator dependent, requiring significant radiologic expertise or cooperation with the radiology team. For the further acceptance of image-guided prostate biopsy in general practice, it seems essential to require significant co-operation with radiologic experts and standardization of practical protocols.

This chapter is focused on outlining best practice guidelines based on expert opinions that apply to each of the commonly used novel techniques for prostate imaging and targeted biopsy.

3.2 Magnetic Resonance Imaging–Compatible Prostate Biopsy Platforms

Magnetic resonance imaging–guided biopsy capitalizes on the ability of mpMRI to detect the foci of prostate cancer (PCa). In-bore MRI-guided biopsies are conducted in 2 phases. The first phase is the diagnostic mpMRI (described elsewhere in this chapter) from which suspicious lesions are identified. The second phase is a separate MRI session in which T2-weighted (T2W) and diffusion-weighted (DW) images are obtained. The T2W MR images are obtained to establish the position of the needle guide relative to the patient's prostate to enable the software to calculate the targeting coordinates required to deliver the biopsy needle to the appropriate location. The DW MR images are used to target the most aggressive area within the lesion.[1] While multiple MRI-ultrasound (US) fusion systems have been introduced into the market, there are 2 direct MRI-guided systems commercially available: the DynaCAD/DynaTRIM system from Invivo Corporation (Florida, USA) and an MR-compatible robotic system from Soteria Medical (Arnhem, the Netherlands).

FIGURE 3-1
The DynaTRIM Device From Invivo Corporation (Florida, USA)

Image courtesy of Invivo Corporation.

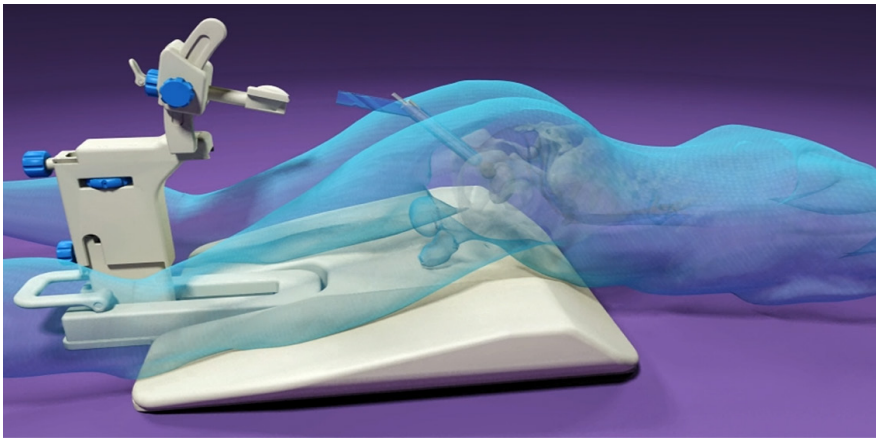

The DynaTRIM is a piece of hardware that facilitates the physical targeting of the biopsy needle to the correct location within the prostate. It consists of a padded, plastic baseplate and clamp stand, which are washable and reusable (**Figure 3-1**). A disposable plastic needle guide is attached to the system for each patient. The entire apparatus is MRI compatible and affixes to the MRI table for each use. The clamp stand contains the needle-guide control apparatus, which consists of 3 dials allowing for 3D adjustments to be made. The disposable needle guide also contains a small spacer at the needle insertion site that controls how deep the needle can be inserted into the needle guide. This spacer is either left in place or removed, depending on the location of the biopsy target.

A series of disposable tools are required for each patient. The needle guide is inserted into the rectum of each patient and attached to the clamp stand at the start of the procedure. Fully MRI-compatible 18-gauge spring-loaded biopsy devices with needle lengths of 150 mm and 175 mm are needed. One or both of the needles may be required for each patient, depending on the size of the prostate and the location of the biopsy target. Between the two different biopsy devices, and the presence or absence of the spacer on the needle guide, biopsies are performed in 1 of 4 different configurations: the 150-mm needle with or without the spacer, and the 175-mm needle with or without the spacer, as instructed by the DynaCAD software depending on the size of the prostate and the location of the biopsy target.

The Soteria transrectal robotic device is designed to interact with the patient in any standard clinical closed-bore MR system. The entire device is constructed of MR-compatible materials (i.e. nonmagnetic and nonconductive) to preclude artifacts of the MR images due to distortion of the magnetic field, and to assure patient safety. The robotic system consists of the robot itself and a controller unit located outside the MR cage of Faraday. Compressed air for the pneumatic motors, generated in a compressor outside the MR room, is delivered via plastic tubes to the robot. The robotic system is fitted with five computer-controlled degrees of freedom for delivering an interventional procedure. To assure patient safety and meet standard safety requirements for the use in a medical environment, the needle guide has a mechanical safety built in that allows only a maximum amount of force on the patient before being released.

In addition to transrectal biopsy approaches, MRI-guided transperineal systems have also been reported. Susil *et al.*[2] examined a system allowing for MRI-guided transperineal prostate biopsies to be performed as well as MRI-guided transperineal interventions such as high-dose brachytherapy. This system consists of a lockable positioning arm (Siemens Medical Systems, Erlangen, Germany), an endorectal coil (USA Instruments, Aurora, Ohio, USA), and a custom-built transperineal template that is MRI compatible and that is connected at a right angle to the endorectal imaging coil. Patients are placed in the left decubitus position in the MRI bore, and a localizing scan is performed to register the transperineal template with the imaging coil. The holes in the transperineal template are filled with water-soluble lubricant to enhance their visibility by MRI. Custom-made software was developed to allow the tracking of the biopsy (or interventional) needles on the prostate images. A complete description of the technique is described by Susil *et al.*[2] In addition, Tokuda *et al.*[3] have also developed an in-bore MRI-guided transperineal system for prostate biopsy. This system allows for the patient to be placed in stirrups in a low-lithotomy position, with a Z frame allowing access to the perineum, while still being inside the MRI bore. Open-source software (3D Slicer; http://www.slicer.org) was used to register the images to the transperineal template. MR-compatible needles are inserted by hand, though a motorized needle-guide template is under development.[4]

3.2.1 Prostate biopsy procedure

Given the commercial availability and relatively wide distribution of the near-in-bore systems, we will restrict our procedure description to this type of approach. Standard precautions for transrectal prostate biopsies should be considered prior to performing an MRI-guided prostate biopsy. This includes cessation of nonsteroidal anti-inflammatory drugs for at least 7 days prior to the procedure, performance of an enema prior to the procedure to remove gross stool from the rectum, and the inclusion of a prophylactic antibiotic such as a fluoroquinolone.[5] Since many patients receiving an MRI-guided prostate biopsy may have previously undergone a TRUS-guided biopsy using fluoroquinolone prophylaxis, use of an additional or different antibiotic to protect against inadvertent selection of fluoroquinolone-resistant bacteria may be considered. Infectious complications have been reported in 2% of patients.[6]

Patients who have claustrophobia or who are anxious may benefit from the administration of a pre-procedure anxiolytic, particularly since administration of a periprostatic block is difficult, and patients will be asked to remain motionless for a significant period of time. For patients who cannot tolerate the MRI or the biopsy procedure even after the administration of an anxiolytic, the procedure may be performed under conscious sedation with appropriate monitoring of blood pressure, heart rate, and oxygenation, or even under general anesthesia if required. This practice should be restricted to appropriately selected patients, and only performed in MRI centers equipped to handle a general anesthetic and where an anesthesiologist is available to administer the anesthesia.

3.2.2 Near-in-bore systems

Appropriate patient positioning for MRI-guided biopsies is critical to the success of the procedure. Patients will be asked to lay motionless for an extended period of time in a relatively uncomfortable position. Once the needle-guide position has been established using the DynaCAD software, any movement by the patient can negatively affect the accuracy of the targeting. Any significant movement may render the targeting unusable, requiring the procedure to be aborted or requiring it to be started over. Therefore, care should be taken to maximize patient comfort, increasing the likelihood that the patient will be able to remain compliant during the procedure.

After informed consent, patients undress from the waist down and are placed in a prone position on the MRI bore, with all pressure points carefully padded. Patients are given the option of having their arms placed over their head or placed down at their sides. Their head is placed on a pillow. Extra padding is provided to the patients' knees, and their lower legs are propped up on pillows to keep their toes suspended in air and off of the MRI bore. A digital rectal exam (DRE) is performed. The DynaTRIM device is then secured to the bore, and the lubricated needle guide is placed into the patient's rectum and secured to the baseplate. Care is taken to ensure the needle-guide adjustments are in their baseline positions, and the MRI surface coil is placed carefully over the patient's lower abdomen and pelvis, making sure to leave adequate room to be able to place the biopsy device in the needle guide without being obstructed by the coil. The patient is given protective earphones or earplugs and placed into the MRI scanner.

An initial localizing T2 sagittal scan is performed to ensure correct positioning of the needle guide relative to the patient's prostate. The needle guide should be abutting the rectal wall without deeply deforming the prostate. Ideally, the needle guide should be positioned against the mid-portion of the prostate to increase the likelihood of being able to reach all areas of the prostate from this initial position. The patient's body habitus can sometimes make this positioning difficult. Adjustments such as placing a pillow under the patient's lower abdomen to change the angle of the pelvis can be helpful in attaining the correct positioning of the needle guide. If the needle guide is not in an acceptable position, it will be necessary to pull the patient out of the MRI, reposition the needle guide, and re-scan the patient to ensure correct positioning of the needle guide, as this is critical for the conduct of the rest of the procedure.

FIGURE 3-2
MRI-Guided Biopsy Using DynaCAD/DynaTRIM System From Invivo (Florida, USA)

A: T2W image with anterior hypointense area suspicious for cancer.

B: Apparent diffusion coefficient image demonstrating restricted diffusion in same anterior location as T2 image.

C: Screen capture from DynaCAD system showing coordinates to set DynaTRIM device to target suspicious lesion.

D: T2W image with the biopsy device needle (linear hypointense signal) in the target lesion.

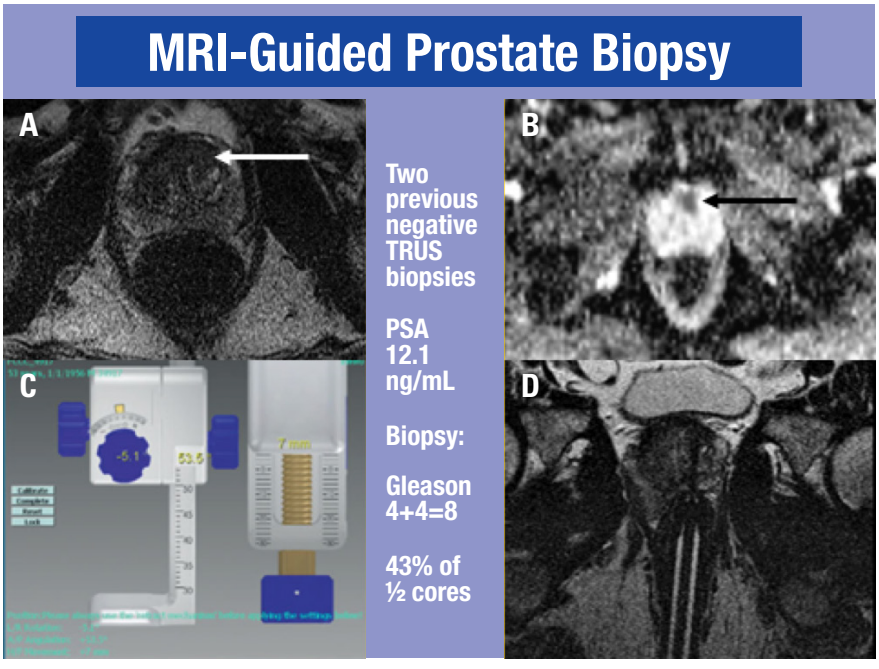

Following confirmation of the correct positioning of the needle guide, T2W axial and sagittal images are obtained through the prostate. The images are transferred to the DynaCAD workstation, where they are interpreted and used for biopsy planning. After calibrating the software based upon the imaged location of the needle guide, a biopsy target is selected. The software then determines how the adjustments on the needle guide should be made to allow biopsy of the target lesion. The software also indicates whether the 150-mm or the 175-mm biopsy device should be used, and whether the spacer on the end of the needle guide should or should not be used. The spacer determines how far into the needle guide the biopsy device is placed (and thus how far into the prostate). The patient is then pulled back out of the MRI tube in preparation for the biopsy.

The patient is reminded to remain still, as significant movements by the patient after the calibration of the software based on the relative position of the needle guide to the prostate will render the targeting inaccurate. The adjustments to the needle guide are made, including a left/right adjustment, a superior/inferior adjustment, and a proximal/distal adjustment. After the adjustments are made, including the removal or placement of the spacer, the biopsy device is inserted into the needle guide as far as it will go, which will place the needle into the target lesion. The 18-gauge biopsy device is then fired, resulting in a core of prostate tissue up to 1.5 cm in length. The biopsy device is then removed for core retrieval.

However, it is also possible to re-scan the patient with the biopsy device in place in the patient's prostate to confirm sampling of the biopsy target. An axial or sagittal view can be used for this purpose. The needle will appear as a linear hypointense signal on the MRI (**Figure 3-2**).

Once confirmation of correct targeting has been made, the biopsy device is removed and the core retrieved from the device. If the target was missed, then the biopsy device is removed, the core is retrieved, appropriate adjustments are made to the targeting controls, and the biopsy is repeated. Once the target has been hit and the core retrieved, the next target is selected on the DynaCAD platform, the appropriate adjustments made on the needle guide, and the next biopsy is taken. This process is repeated until all targets have been biopsied.

Upon completion of the biopsies, the needle guide is removed from the patient's rectum and he is removed from the prone position. Typical procedure times are approximately 30 to 45 minutes, depending on the number of targets and whether confirmation scans are obtained.

Complications of the procedure are similar to those for any transrectal prostate biopsy approach and include pain, bleeding, and infection. The risk of sepsis may theoretically be lower, since typically fewer needle passes are made during an MRI-guided biopsy compared to standard extended TRUS-guided biopsies, though there are no data to address this hypothesis. Some patients also experience musculoskeletal discomfort from having to lie still in a prone position for a significant period of time, or may be lightheaded upon first getting up.

3.2.3 Cognitive fusion

An alternative to the use of a near-in-bore system, as described above, is to perform cognitive fusion. This technique involves obtaining a diagnostic mpMRI and then using the information gained from the MRI to inform the selection of biopsy cores during a TRUS-guided biopsy. Thus, the fusion of MRI data onto the US image is performed in the mind of the operator. Correct selection of the appropriate area for biopsy can be facilitated by partitioning the prostate into multiple sectors (sextants or octants, for instance) and documenting the location of the MRI-suspicious regions according to this map. This approach has the obvious advantage of being less expensive and readily available to most practices. A disadvantage is that the success of the approach is extremely user dependent, and accurate targeting of the MRI-suspicious areas cannot be verified. This limitation may be lessened by oversampling of the suspicious region. In addition, sometimes a corresponding abnormality seen on MRI can be detected on US once particular attention is paid to a region.

3.2.4 Results of cognitive fusion-based magnetic resonance imaging–targeted biopsies

Early efforts to evaluate the performance of MRI-targeted biopsies focused on men with previous negative TRUS biopsies, but in whom there was persistent concern that they had PCa, primarily due to a rising prostate-specific antigen (PSA). Several studies evaluated the ability of MRI and, often, MRI spectroscopy to inform further TRUS-guided biopsies in these men, representing the early efforts at cognitive fusion.[7-12] This approach relies on the MRI to indicate where additional prostate biopsies should be obtained, typically oversampling these areas, but using only TRUS guidance for the actual biopsy.

Results from early reports of using MRI to direct TRUS biopsies were encouraging, though studies were limited by small patient numbers. Perrotti *et al.*[7] demonstrated promising PCa detection rates in their population, with 7/33 men (21.2%) on post-MRI and 5/7 (71.4%) men with high suspicion for carcinoma on MRI positive for carcinoma on biopsy. Beyersdorf *et al.*[8] detected PCa in 12/38 (32%) men with varying numbers of previous negative biopsies after undergoing MRI with an endorectal and surface coil using T1 and T2 images only. In this population, 10/20 (50%) of the men with the highest level of suspicious lesion were found to have PCa on repeat biopsy. However, site-by-site analysis failed to demonstrate a correlation between biopsy positivity and MRI findings. Yuen *et al.*[9] reported a sensitivity of 100%, a specificity of 70.6%, a positive predictive value (PPV) of 58.3%, a negative predictive value (NPV) of 100%, and an accuracy of 79.2% in a population of 24 men undergoing repeat 10 to 14 core biopsies (with oversampling of the suspicious regions) after evaluation with MRI using spectroscopy. Prando *et al.*[10] reported on the ability of primarily MRI spectroscopy to direct repeat TRUS biopsy in men with at least 2 previous negative biopsies. In these men, 17/31 (55%) of those with abnormal spectroscopy were found to have PCa on biopsy, resulting in a sensitivity of 100%, a specificity of 44%, a PPV of 55%, an NPV of 100%, and an accuracy of 67%. Similarly, Amsellem-Ouazana *et al.*[11] reported a sensitivity of 73.3%, a specificity of 96.3%, PPV of 91.6%, an NPV of 86.6%, and an accuracy of 88% in 42 men undergoing repeat TRUS guided biopsy following evaluation by MRI with spectroscopy. In a similar study, Cirillo *et al.*[12] reported on 54 men undergoing repeat biopsy after MRI with spectroscopy and reported a sensitivity of 100%, a specificity of 51.4%, PPV of 48.6%, an NPV of 100%, and an accuracy of 66.7%. Taken together, these early reports generated enthusiasm for the ability of MRI with or without spectroscopy to guide biopsies to increase the detection rate of cancer in men with previous negative biopsies. All of these early studies are limited by small numbers of patients, restricted ability to confirm that biopsies were actually obtained from the suspicious regions, varying repeat TRUS biopsy strategies, and lack of whole prostate specimens as a gold standard for determining the presence/absence of PCa. Furthermore, none of the above studies used current multiparametric methods, including diffusion-weighted imaging (DWI) and perfusion MRI.

More recent evaluations include a report by Lee *et al.*[13] demonstrating 46/82 (56%) men with suspicious lesions on MRI were found to have PCa on subsequent TRUS biopsy using cognitive fusion. Twenty-eight percent of targeted cores versus 3.6% of standard cores were found to have cancer. A majority of the lesions found were in the apex or anterior portion of the prostate. A study by Puech *et al.*[14] reported that while targeted biopsies revealed more cancer than systematic biopsies in their men with a suspicion of PCa, there was no significant difference in the cancer yield between men undergoing cognitive fusion, with 47% of the targets being positive for cancer versus 53% of the targets being positive in the men undergoing MRI/US fusion biopsies.

In addition to being useful for identifying cancer in patients with previous negative biopsies, MRI-targeted cognitive-fusion biopsies have been conducted for a variety of indications, including initial diagnosis (no previous prostate biopsy).[15-18] The studies by Panebianco *et al.*[18] and Haffner *et al.*[17] demonstrated improvements in the detection of clinically significant disease in the men undergoing MR-directed biopsy, and a reduction in the diagnosis of clinically insignificant disease, while the study by Acar *et al.*[16] failed to demonstrate a significant benefit, though the data suggest a trend toward benefit for men undergoing cognitive fusion and near-in-bore biopsies. Other examples of the use of cognitive fusion are in the diagnosis of recurrent PCa,[19] and in patients on active

surveillance.[20-22] Findings in the active surveillance population were consistent in showing that MRI and subsequent follow-up biopsy were helpful in predicting the presence of clinically significant cancer with subsequent upgrading, often with fewer cores of tissue required and with a reduction in the detection of clinically insignificant disease. Thus, overall, cognitive fusion may be beneficial in increasing cancer detection rates when MRI-suspicious lesions are present, compared to performing a systematic TRUS biopsy. However, the ultimate success of this approach will be variable and likely dependent upon the experience and skill of the person performing the biopsy, the size of the prostate, and the size and location of the suspicious area, as well as the biopsy strategy (degree of sampling in the suspicious region) utilized. Direct MRI guidance systems address some of these limitations, likely providing more consistent results, as discussed below.

3.2.5 Results of in-bore system magnetic resonance imaging–guided biopsy

The in-bore systems provide an advantage over cognitive fusion as well as over MRI/US fusion approaches by being better able to verify placement of the biopsy needle into the suspicious lesions. Images can be obtained with the needle in place, thus providing convincing evidence that the target was indeed sampled. In addition, because the targeting process does not require co-registration of MRI and US images, an additional variable and source of error is not involved in the in-bore systems, compared to MRI/US fusion platforms.

Results using the in-bore approach in patients who have had at least one previous negative TRUS biopsy provided some of the best early data demonstrating the utility of MRI-guided targeting approaches for PCa. Anastasiadis *et al.*[23] published an early report of 27 men with a previous negative TRUS biopsy and continued suspicion of cancer who underwent MR-guided biopsy in whom 15/27 (56%) were found to have cancer. Roethke *et al.*[24] reported similar results in a cohort of 100 patients undergoing MR-guided biopsy for a history of negative TRUS biopsy but persistent concern for cancer, with a cancer detection rate of 52% (52/100). Hambrock *et al.*[25] reported a cancer detection rate of 59% (40/68) in men with at least two previous negative TRUS biopsies, compared to historical cancer detection rates of approximately 22% (55/248) in men undergoing repeat systematic TRUS biopsies for similar indications. An update of this experience was subsequently published by Hoeks *et al.*,[6] reporting a cancer detection rate of 41% (108/265) in men with at least one previous negative TRUS biopsy, with approximately 90% being clinically significant cancers.

Success with detecting cancer in previously biopsied patients led to the testing of MR-guided biopsies in men during their initial biopsy setting, performed for elevated PSA or abnormal DRE. Pokorny *et al.*[26] reported detecting PCa in 126/223 (56%) men, 47 (37%) of whom were low risk. Conversely, MR-guided biopsy detected PCa in 99/142 (70%) men with equivocal or suspicious findings on mpMRI, only 6% of whom were considered low risk. Including mpMRI and MR-guided biopsy reduced the need for biopsy by 51% and decreased the diagnosis of low-risk disease by 89%, while increasing the diagnosis of intermediate and high-risk disease by 18%. This suggests an advantage to this approach compared to conventional pathways, including TRUS biopsies for all men with elevated PSAs or abnormal DREs.

In addition, it is apparent that an advantage of MR-guided biopsies (whether cognitive fusion, near-in-bore, or transperineal approaches) is in the detection of anterior tumours that may not be sampled routinely on TRUS-guided biopsies. Ouzanne *et al.*[27] reported that 46% of anterior tumours diagnosed by cognitive fusion were not diagnosed by systematic biopsy. Volkin *et al.*[28] reported that mpMRI and MRI/US fusion biopsy detected more anterior tumours than TRUS biopsy, and an average core length of cancer in this location 112% longer than those obtained by TRUS. Penzkofer *et al.*[29] showed the highest biopsy yield in their mixed indication cohort was for men with lesions in the anterior prostate, where 40/64 (63%) targets were found to be positive for cancer, higher than for any other part of the prostate.

3.2.6 Transperineal magnetic resonance–guided biopsy results

Limited data exist for biopsy results using MR-guided transperineal biopsy platforms. However, Penzkofer *et al.*[29] reported on a mixed cohort of 87 men who underwent MR-guided transperineal prostate biopsy for indications of concern for PCa but no previous biopsy, active surveillance, or for a suspicion of PCa recurrence after radiation therapy. The overall cancer detection rate was 57% (51/90). Gleason pattern of 4 or higher was diagnosed in 25/32 (78%) of men with no prior biopsy and the active surveillance groups combined. In addition, Menard *et al.*[30] published on the use of MR-guided transperineal prostate biopsy to improve determination of tumour boundaries to aid in the targeting of lesions for salvage focal therapy.

MR-guided biopsy represents the first large-scale interventional application to take advantage of mpMRI for PCa. Though first tested extensively in men with previous negative biopsies, MR-guided biopsies are now being used during the first biopsy for men with MRI-suspicious lesions. This approach may lead to fewer biopsies required to gain similar, if not better, information regarding the presence of clinically significant disease. The advent of MRI/US fusion technology has now surpassed MR-guided biopsy as the most common approach for performing biopsy of MRI-suspicious lesions. Most of the current data being generated today with regard to MR image–guided biopsy are through this platform. The convenience of being able to perform the procedure in the clinic, as well as the increased patient comfort, has catapulted this approach past traditional in-bore systems. However, there are still specific indications for the in-bore system, such as in patients with no rectum, as well as tiny lesions (<8 mm). Regardless of whether an MRI/US fusion system, in-bore system, or MR-guided transperineal biopsy platform is used, it is apparent that MR-guided biopsy in general is quickly evolving into what will likely be the standard of care in the very near future.

Guideline Statement	Level of Evidence [LOE]	Grade of Recommendation [GOR]
MRI-guided biopsy can lead to fewer biopsies	3	B
MRI-guided biopsy can detect tumours missed on systematic TRUS biopsy	3	B

Guideline Statement	Level of Evidence [LOE]	Grade of Recommendation [GOR]
MRI-guided biopsy can detect anterior tumours	3	B
There are no significant differences in detection rates between different platforms for MRI-guided biopsy	3	B

3.3 Robotic Prostate Biopsy With Magnetic Resonance Imaging–Ultrasound Fusion

In contemporary practice, men with elevated or rising serum PSA and suspicion for PCa undergo systematic transrectal prostate biopsy guided by TRUS visualization as the standard of care. However, this approach is subject to significant sampling bias, resulting in a limited sensitivity for detecting cancer.[31] In order to overcome this inherent limitation, mpMRI of the prostate, combining anatomical and functional imaging, allows for localization and characterization of prostate tissue suspicious for cancer.[32] Performing MRI prior to biopsy provides the potential to more accurately sample potential tumour foci in order to improve diagnostic yield and disease characterization.

Prostate MRI may be used to guide biopsy in two ways. First, MRI performed prior to biopsy allows targeted sampling of suspicious areas within the prostate during TRUS-guided biopsy. Targeted biopsy may be performed by viewing prebiopsy MRI and live US images side-by-side, an approach known as cognitive co-registration or visual estimation; alternatively, several biopsy systems have become available that incorporate software-based fusion algorithms to co-register MRI and US images.[33] Second, biopsies may be guided by MRI in real time using in-bore prostate biopsy systems.[34]

3.3.1 Magnetic resonance imaging–ultrasound fusion-targeted biopsy

Software-based fusion algorithms allow accurate co-registration of prebiopsy prostate MRI images to a TRUS model of the prostate obtained in the biopsy setting, thus avoiding limitations of cognitive fusion by providing a reproducible method to target MRI abnormalities on real-time TRUS, and facilitating more accurate sampling of suspicious areas in the prostate.[35,36] Use of a fusion biopsy platform first requires a prebiopsy diagnostic MRI to identify areas suspicious for cancer based on imaging characteristics. Suspicious areas are circumscribed on MRI prior to biopsy. The co-registration of the MRI to the TRUS images can be performed either by rigid or elastic registration, or both, depending on the platform. Rigid registration allows for translation and rotation, but not deformation, of images. Elastic fusion accounts for the addition of local deformation by stretching the image volumes

and targeted lesion(s), resulting in matched borders. Biopsy of the prostate is then performed with MRI and real-time TRUS images superimposed and displayed side-by-side, thus creating an easily navigable 3D prostate reconstruction.

In addition to accurate identification of abnormal areas within the prostate during biopsy, optimal sampling relies on accurate localization of the biopsy needle to suspicious targets. Robotic techniques for biopsy needle localization after MRI-US fusion have been implemented by two commercially available biopsy systems in order to improve sampling of MRI targets: the ei-Nav|Artemis (Eigen, California, USA) and BioXbot (Biobot Surgical, Singapore). While both are designed to improve sampling of MRI abnormalities, these systems differ in their approach to biopsy and implementation of robotic elements.

The ei-Nav|Artemis biopsy system, incorporating MRI-US fusion by ProFuse software (Eigen, California, USA), provides guidance for biopsy needles through a transrectal approach. The probe is placed in a fixed cradle contained within a robotic arm, navigated manually by the operator. Biopsy guidance is performed through mechanical registration/tracking of the needle guide relative to a fixed point in the robotic arm. After scanning the prostate using an endfire US probe, the system creates a 3D model of the prostate, which is fused to the previously obtained MRI sequence, allowing mapping of MRI abnormalities onto the live US images. The system then allows the operator to position the biopsy needle under US visualization. With a locking arm that acts as a fixed point in space, Artemis utilizes robotic spatial tracking to compute needle trajectory, core position, and depth with a high degree of accuracy, allowing the operator to adjust the needle in order to optimize sampling of the selected target.

Wysock *et al.* compared the clinical outcomes of Artemis biopsy using ProFuse image fusion to cognitive co-registration among 125 consecutive men presenting to a single center for biopsy in a randomized study design.[37] The authors detected slightly more Gleason sum ≥7 cancers than visual targeting (cancer detection rates of 20.3% versus 15.1%, p=0.0523). In comparison to cancers detected by 12-core standard biopsy in this cohort, cancers detected by targeted biopsy using either software fusion or visual estimation demonstrated greater overall and Gleason ≥7 cancer core length. Sonn *et al.* additionally reported clinical outcomes of MRI/US fusion targeted biopsy (MRF-TB) using the Artemis system, supporting the use of this platform as a means of conducting highly accurate MRI-targeted biopsies in clinical practice.[38]

The BioXbot robot is a transperineal biopsy system that implements a robotic arm to guide needle biopsies.[39,40] The system houses a movable platform with six degrees of rotational freedom. During the biopsy session, initial TRUS imaging of the prostate is obtained, which the system uses to construct a 3D model of the prostate. This system is distinct from the Artemis system in that it utilizes a motorized automated mechanism for needle alignment within the 3D model. The urologist selects biopsy targets on the image and the 3D prostate model, and the system simulates the needle trajectory through these sampling locations. Once approved by the urologist, the robotic platform then aligns the biopsy needle guide to target each selected biopsy location, with reported targeting accuracy within 2 mm.[39] The BioXbot guides needle biopsies through two puncture points in the perineal skin, one each for the left and right lobes of the prostate. All needle trajectories within one lobe pass through a single puncture in the skin, which serves as a pivot point.

Limited clinical outcomes data using the iSR'obot™ (Biobot Surgical, Singapore) system are available. A small pilot study of 20 patients demonstrated the safety and feasibility of the device for image-guided transperineal prostate biopsy using visual targeting.[39] In follow-up of the pilot study, the authors have performed several hundred transperineal saturation biopsies within their centre at Singapore General Hospital. With the more recent implementation of a software platform for MRI-US fusion, the system may provide the first opportunity for MRF-TB using a robotic transperineal approach. Pilot studies are underway in several centres. Outcomes of this biopsy system are eagerly awaited.

3.3.2 In-bore magnetic resonance imaging–guided biopsy

In addition to MRI-US fusion platforms guided by TRUS, robotic systems have been introduced to facilitate in-bore MRI-guided prostate biopsy.[41-43] Using MRI-compatible components, these systems allow precise needle localization, within 2 to 5 mm.[43,44] While certain systems require manual needle placement into the prostate, thus requiring the patient to be removed from the MRI scanner, others incorporate automated needle insertion, allowing for truly real-time MRI visualization.[45,46] Most trials investigating in-bore MRI-guided prostate biopsy in humans have used transrectal or transgluteal needle insertion approaches. Recently, Tilak *et al.* employed a transperineal approach among 99 men undergoing in-bore biopsy, and compared targeting accuracy between robotic and manual targeting templates.[47] The robotic template improved needle accuracy as compared to the manual template, yielding mean accuracies (distance of the needle from intended target) of 2.4 mm versus 3.7 mm, respectively. Several efforts are underway to commercialize applications for in-gantry robots capable of conducting targeted transperineal biopsy. Such applications would likely greatly reduce the time and inaccuracy associated with current handheld commercial platforms.

Both MRI-US fusion platforms and in-bore biopsy systems employ prostate MRI to more accurately identify PCa foci. The incorporation of robotic elements theoretically improves biopsy yield through improved sampling accuracy. Fusion systems appear to provide the advantage of less time spent in the MRI scanner, and therefore less cost, while in-bore techniques may avoid distortion artifacts, such as those introduced by the deformation of the prostate by the TRUS probe. The latter may be mitigated by improvements in registration techniques, either by developing more robust registration algorithms or by manipulating the prostate during prebiopsy MRI to mimic deformation by the TRUS probe, as proposed by Ukimura *et al.*[48] Ultimately, robotic elements may play a role in improving PCa detection and characterization by increasing the accuracy of biopsy needle localization. In conjunction with prebiopsy MRI and accurate MRI-US co-registration, robotic prostate biopsy may improve cancer detection and characterization through more efficient and accurate sampling, compared to traditional biopsy techniques. At this time, the data available are too preliminary to make concrete recommendations regarding the precise applications or relative efficacy of robotic prostate biopsy.

Guideline Statement	LOE	GOR
Robotic prostate biopsy is a feasible technique	3	C

3.4 Template Mapping Biopsies: An Accurate Method of Risk Stratification for Prostate Cancer

Prostate cancer is the most common male cancer in many developed countries, with a doubling in incidence over the last 15 years in the UK.[49] Recent results of randomized studies have suggested that the survival benefit associated with treatment is restricted to men with higher-risk disease only.[50,51] Although these data were based on standard TRUS-guided biopsy assessment, it makes sense that assessment of the prostate should be as accurate as possible in order to inform treatment options for men with localized disease. This is particularly true when these options range from active surveillance to radical treatment. As well as informing the decision of whether or not to treat, accurate assessment of the prostate can also inform the decision of whether a radical or focal approach to treatment should be adopted.

Unfortunately, the current standard diagnostic pathway of PSA followed by standard TRUS-guided biopsy is often unable to provide enough accurate information on its own to make such judgment. Standard TRUS biopsy is subject to systematic and random errors, which lead to:

- Missing significant cancers, particularly with anterior and apical lesions[52,53] with a false negative rate of 30% to 45%.[54,55]
- Misrepresentation of true disease burden, resulting in misclassification of risk, which may lead to over- or under-treatment.[56-59]
- Poor disease localization

The lack of accuracy of TRUS biopsy means that, in many centers, if a man is interested in active surveillance, he will be counselled to have a confirmatory TRUS biopsy. Whilst this will reduce the random error of missed or under-sampled lesions in the peripheral zone on an initial TRUS biopsy, it does not reduce the systematic error of missed lesions at areas commonly under-sampled with TRUS, such as the apical, midline, and anterior gland.

Trans-perineal template mapping biopsy (TMB) was developed to address these issues and provide accurate risk assessment and localization of PCa.[60] Template mapping biopsy is based on the trans-perineal approach used in brachytherapy, where a 5-mm template grid is used to guide the insertion of radioactive seeds through the perineum and into the prostate under US visualization.[57] This allows access to all areas of the prostate, including the apex and anterior aspects, provides excellent disease localization, and avoids the risk of infection associated with the transrectal route. The potential disadvantages include the use of a general anaesthetic, or sedoanalgesia, along with an increase in the risk of urinary retention compared to a standard TRUS approach.

3.4.1 Approaches to transperineal template mapping biopsy

There is considerable variation between clinicians in the details of the practice of TMB. When reviewing different protocols, it is important to keep two key points in mind:

- The diagnostic performance for detection of any cancer, and estimation of maximum, size, and grade is related to the sampling density (cores per mL of prostate).
- The accuracy of assigning a positive biopsy to a given location in the prostate will depend on the number of discrete areas that the gland is divided into for the purposes of identifying the biopsy specimens.

This chapter does not cover the use of transperineal biopsies targeted to lesions seen on MRI, as this is covered elsewhere. However, this can be a way to use the transperineal approach whilst reducing the biopsy intensity and maintaining accuracy.[58]

3.4.2 The 5-mm mapping approach

Barzell *et al.* divided the prostate into 26 separate zones, each sampled separately.[57] The prostate is divided craniocaudally into apical and basal potions and sampled every 5 mm. At University College London (UCL), we have amended this approach into a 20-zone approach, which we have compared against MRI-targeted biopsies.[61,62] In our clinical practice, we have also employed a more simplified 12-zone system, as we found this to be a good balance between localization accuracy and burden for the pathology team.

A 5-mm sampling density provides similar diagnostic performance for the detection of any cancer however the cores are obtained. The localization accuracy is inversely related to the number of zones into which the biopsies specimens are separated. The need for localization will be dependent on the therapeutic options available—if whole gland treatment is the only available option, then localization may inform nerve sparing or resection margins at radical prostatectomy (RP), whereas a focal ablation approach based on a suspicious MRI lesion rather than a hemi- or quadrantic ablation would require a more precise zonal localization strategy for biopsies.

3.4.3 Sector-based sampling

Many of the publications on TMB describe a more limited number of biopsies per gland, which is sometimes termed "saturation biopsies." Saturation biopsies tend to employ a set number of biopsies in prespecified regions of the prostate. For example, Symons[63] employed a 22-sample protocol from 14 zones in the prostate, irrespective of prostate volume, whilst Gershman *et al.*[64] concentrated their biopsies on the anterior aspect of the prostate in a cohort of men who had not shown any cancer on a previous standard transrectal biopsy.

One of the less intensive sampling methods that is being used at Guy's Hospital in the UK is the template sectoral approach described by Vyas.[65] This approach preferentially, but not exclusively, targets the peripheral zone by dividing the gland into anterior, mid, and posterior segments targeting additional basal sectors in glands above 50 cc. The rationale is to reduce biopsies of the transition

zone in an attempt to minimize bleeding and urinary retention. Others consider that, as around a quarter of PCa at RP is found in the anterior gland[66-70] and there is a relatively low incidence of side effects with either approach,[71] a more intense sampling of the transition zone is justified.

3.4.4 Complications and side effects of template mapping biopsy

When comparing the side effects of TMB, the most notable difference to TRUS biopsy is the incidence of urinary retention, which varies from 4% to 11%,[71-74] compared to 1% to 2% for a standard transrectal approach.[74] An advantage is the lower risk of hospital admission for sepsis, which is usually <1% for a transperineal approach, compared with 3% to 4% for a transrectal approach.[74] Some authors have reported a few men with transient difficulties with erectile function after an intensive transperineal biopsy sampling, but this is not rigorously reported.[71]

The additional morbidity of general anesthetic is a very small added risk to the patient, yet TMB can be performed in a limited manner under local and periprostatic anathesia.[60]

3.4.5 The diagnostic performance of template mapping biopsy in recent literature

When considering the diagnostic performance of any prostate biopsy approach, it is important to consider both the helpful diagnosis of clinically significant disease and the unwanted diagnosis of clinically insignificant disease. The threshold for true clinical significance will depend not only on the pathological features, but also on the age and health of the patient. Whilst TMB can significantly increase the diagnosis of clinically significant disease compared to a standard transrectal biopsy, it will also increase the diagnosis of clinically insignificant disease. When detection of any cancer is reported, the primary outcome detection rates of 56% to 73% have been shown.[63,75]

The diagnostic performance of TMB is demonstrated best on direct comparison with standard transrectal biopsy. Several authors have demonstrated this value in cohorts of patients who have had previous negative TRUS biopsy with continued suspicion of PCa, reporting detection rates in the order of 60%.[63,75,76] A significant proportion of these lesions were located anteriorly and in areas commonly under-sampled by standard transrectal biopsy.[77]

3.4.6 Interpreting the results of template mapping biopsy

Standard transrectal biopsy can lead to inaccurate risk stratification of patients, resulting in either under- or over-treatment. It is important, however, to be careful that the increase in the detection of any cancer by an intensive sampling strategy such as that used in TMB does not over-estimate the risk of the disease in a given individual and prompt unnecessary treatment. In order to assess risk in an intensive sampling approach, we cannot apply the same absolute measurements of numbers of cores involved to the prostate, as those approaches that are based on 10 to 12 core transrectal biopsies.

Ahmed *et al.* at UCL have developed a classification system[76] that attempts to address this, and is useful for both an intensive general sampling strategy and an MRI-directed approach. Ahmed used 3D computer models of 107 whole mound RP specimens to perform 500 TMB simulations

per prostate to evaluate the maximum and total cancer core lengths on TMB that are associated with pathological volumes of 0.2 cc and 0.5 cc at RP. They concluded that a maximum cancer core length ≥6 mm on a biopsy core represents a lesion with a volume of ≥0.5 cc. A cancer core length involvement ≥4 mm represents a cancer volume of ≥0.2 cc. These findings, when considered with the Gleason score detected, are the basis of the UCL risk stratification, with 3-mm Gleason 3+3 or less being low risk, any secondary Gleason pattern 4 or 4-mm disease being intermediate risk, and 6 mm of any grade of disease or any primary Gleason pattern 4 being highest risk. These parameters need to be correlated with long-term outcomes to assess their true utility.

3.4.7 Template mapping biopsy as a reference standard

Template mapping biopsy is currently considered an accurate reference standard ideal for research use. It has been employed in both large-scale therapeutic and diagnostic trials and research.[53,56,59] Its particular advantages include:

- Apart from RP, TMB is the most accurate method for mapping the grade and extent of disease in a given prostate. Yet, unlike RP, TMB can be employed prior to and/or after treatment, which is particularly useful in assessing focal therapy modalities.
- Most men recommended a prostate biopsy can undergo a TMB procedure, allowing assessment of a large spectrum of cases ranging from large-volume, high-risk disease to benign prostates. This eliminates the significant bias toward high-risk disease when RP is used as a reference standard.
- 5-mm TMB biopsies provide excellent spatial information on the location and extent of a given lesion in the prostate. If categorized accurately with detailed coordinate documentation, they can register a 3D representation of a histological lesion.

Template-guided prostate mapping biopsies are the most intensive method of diagnosing and characterizing PCa, short of RP specimens. They are not susceptible to the systematic errors of standard transrectal biopsy, and can detect disease not well detected by standard transrectal biopsy with an acceptable side effect profile.

Guideline Statement	LOE	GOR
TMB is the most accurate method of mapping extent and grade of cancer	4	C
5-mm TMB can provide very good spatial information on location and extent of cancer in a given prostate	3	B
TMB carries higher risk of side effects than transrectal biopsy	3	B

3.5 Magnetic Resonance Imaging–Ultrasound Fusion-Guided Prostate Biopsy

The ability of mpMRI to localize areas suspicious for PCa has now facilitated directed biopsies potentially outside of the standard systematic 12-core template. Targeted sampling has brought prostate biopsy in line with that of other solid organ malignancies, in that it no longer relies on indiscriminate systematic cores but rather targeting of specific areas via image-guidance. Intuitively, it would be expected that indications would include all those with suspicion for PCa; however, at the current time cost considerations would necessitate judicious use to maximize the potential benefit of imaging. Accepted indications include those with continued concern for occult malignancy despite a prior negative TRUS biopsy, and for the determination of candidacy for active surveillance through confirmatory biopsy.[78-82] The integration of mpMRI information with TRUS has occurred primarily through cognitive fusion or software-based registration platforms via either a transrectal or transperineal approach. Software-based platforms share some steps in workflow, but can differ in image registration, tracking, and hardware.

3.5.1 Cognitive biopsy

The cognitive fusion biopsy refers to the operator creating a mental registration of lesions using the prebiopsy mpMRI, and then performing the TRUS biopsy in an attempt to target the suspicious lesions. This biopsy method requires no additional hardware or software training or their associated costs, making it the easiest technique to implement in the outpatient setting. Comparative studies of cognitive fusion biopsy against a standard TRUS biopsy show targeting lesions increases the rate of cancer detection, as well as more accurately represents the disease burden and Gleason grade.[83-85] Transperineal fusion biopsy with mpMRI cognitive recognition was shown to detect equal rates of clinically significant PCa with fewer cores sampled when compared to a systemic template-guided transperineal biopsy.[86] These concepts have been discussed in greater detail in the first section of this chapter.

Despite improvement over the status quo, cognitive biopsy does require the user to be able to interpret MRI and observe US features not routinely given attention. The variability of operator experience may result in biopsy inaccuracy. A number of additional considerations are required. A particular challenge, even when anticipated, is that oblique fanning images acquired by TRUS versus true axial MRI slices can result in inaccuracies in comparative perception.

Multiparametric MRI–TRUS fusion prostate biopsy platforms, "fusion platforms," have appeared as a technique to address the shortcomings of cognitive registration. The addition of hardware and software to merge prebiopsy mpMRI with real-time TRUS images to identify biopsy targets guide the needle to the target, and archive the 3D location of the biopsy. A prospective comparison of MR-US fusion biopsy versus visual estimation targeted biopsy demonstrated no difference in overall cancer detection rate (32.0% versus 26.7%, respectively, p=0.0137) or detection of Gleason ≥7 cancers

(20.3% versus 15.1%, respectively, p=0.052) on a per-lesion analysis.[87] The study did, however, show that MR-US fusion biopsy improved the cancer detection rate in patients with smaller and anterior lesions. The PROFUS trial was likely underpowered and, given visual targeting was performed after fusion biopsy, this may have introduced bias, potentially increasing the accuracy of visual estimation.

3.5.2 Magnetic resonance imaging segmentation

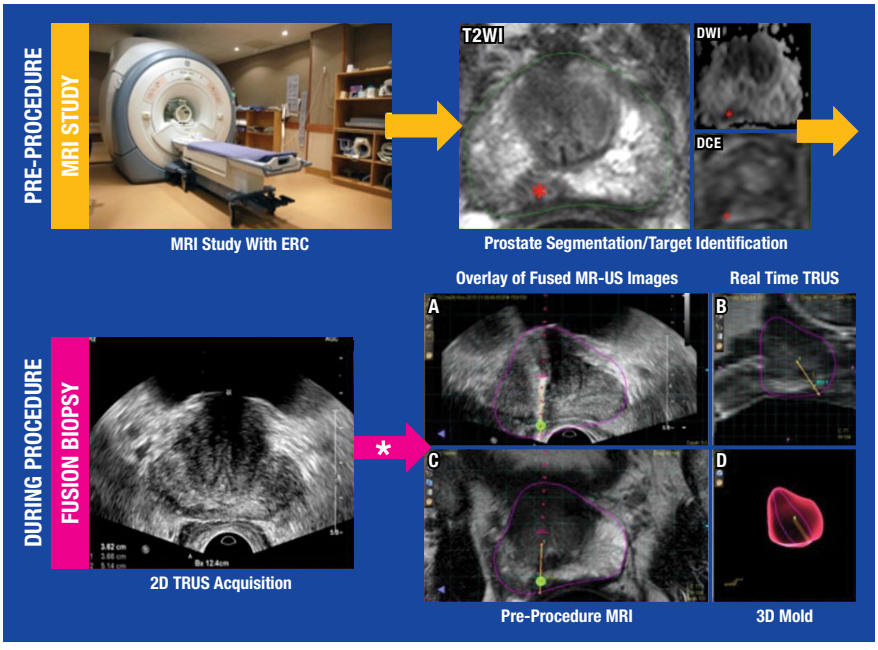

FIGURE 3-3
Multiparametric MRI Images Are Acquired

T2W imaging, DWI, and dynamic contrast-enhanced sequences are performed. The prostate and lesions identified on MRI are segmented. During the procedure, an 2D TRUS sweep of the prostate is performed, shown in the lower left. The images are semi-automatically registered. The image co-display can be side-by-side or superimposed.

Initial mpMRI is performed with or without endorectal coil. The inclusion of the coil improves signal-to-noise ratio and can be especially useful in providing detailed imaging for staging purposes. The images from the study are used to identify lesions suspicious of harbouring PCa based on anatomical and functional characteristics of the tissue, and assigned a suspicion score that correlates with the probability of harbouring clinically significant PCa. The complete workflow is outlined in **Figure 3-3**. Segmentation refers to the process by which the T2W MRI image is used to define the outline of the prostate and targets. Targets may be defined as a geometric center or contoured as a volume with a sub-region of interest, if desired. After the biopsy targets and prostate outline are identified, the MRI images are transferred to the biopsy workstation.

3.5.3 Magnetic resonance imaging–ultrasound registration

After the processed MRI is imported to the workstation, a 2D TRUS sweep of the prostate is completed to create a reconstructed 3D TRUS prostate volume. Semi-automated US segmentation of the prostate margins/contour is performed. Registration is the alignment of the MRI prostate volume with the TRUS volume. Two software registration algorithms, rigid and elastic, may be used to fuse the MR and US images, and differ in the extent of image distortion allowed for the alignment (**Figure 3-4**). Rigid registration permits rotational and translational manipulation of each image set. In this manner, the anatomy of the prostate and the location of the lesions remain preserved. Registration errors may occur when the MRI and US prostate shape differ, and are often due to organ or patient movement, or organ deformation from the endorectal coil. The operator can adjust the alignment with manual correction, adjustment of targeting, or altering the depth and pressure of the transrectal probe.[88] Elastic registration allows for correction of deformation, warping, and changes in scale. By manipulating the image outline, the correction may result in the distortion of the internal prostate architecture, which may be falsely reassuring. Currently, most platforms are capable of both rigid and elastic registration, allowing the operator to select the registration algorithm that produces an optimal alignment. An important concept is continuous re-registration of images. Confirmation of accurate registration includes review of the base, apex, and lateral edges in the axial and sagittal planes, in addition to rotational adjustment as needed. Prostatic hemorrhage, patient movement, and organ deformation can alter the registration and, as such, verifying registration after sampling each target is essential. Co-display of MRI and US facilitate this throughout the procedure (**Figure 3-5**).

3.5.4 Biopsy tracking

Fusion platforms allow the ability to track and record the position of the needle in 3D space. This allows the user to understand, on TRUS, the corresponding location on MRI and to guide the needle toward the target. Tracking is accomplished with three methods: 1) electromagnetic tracking, 2) position-encoded joints within smart robotic arms, and 3) image-based tracking.

Passive electromagnetic tracking is used by a number of commercially available platforms (UroNav, Invivo; Virtual Navigator, Esaote; and Real-time Virtual Sonography, Hitachi). This tracking method uses a magnetic field generator (attached to the table) and sensor (attached to the TRUS probe). The magnetic field generator introduces a continuously changing magnetic field, which produces variable electrical current in the sensor of the probe. The electrical signal is used to relate the sensor location to a 3D position within the field. Electromagnetic tracking maintains a freehand approach, offering a shallow learning curve since most urologists are familiar with operating a TRUS probe.[89]

Other fusion platforms (Artemis, Eigen; BiopSee, Pi Medical; and BioJet, BK Ultrasound) utilize smart robotic arms with position-encoded joints as a tracking approach. The probe of these platforms is mounted to a mechanical stepper with position sensors. The operator guides the robotic arm while the angle sensors within the arm relay the position of the probe and needle to the platform computer.[90] Though this approach may be unfamiliar to most urologists, adding to the learning curve, the steady arm of the robotic fixture diminishes mechanical error that may be introduced by the user.

FIGURE 3-4
The Two Registration Algorithms Are Rigid and Elastic Registration

The operator should be judicious as to not distort the internal architecture of the prostate.

Reproduced with permission from John Wiley and Sons. Source: Logan JK, Rais-Bahrami S, Turkbey B, et al. Current status of MRI and ultrasonography fusion software platforms for guidance of prostate biopsies. BJU Int 2014;114(5):641–652.

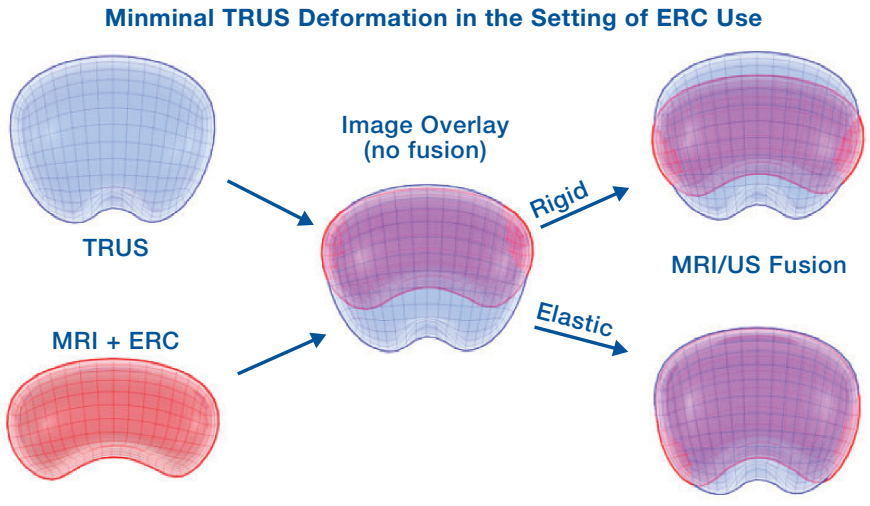

FIGURE 3-5
Co-Display Permits the Operator to View the Real Time US Images (**A**) With the MRI/US Overlay (**B**) in Order to Facilitate Proper Registration and Targeting

A right mid-peripheral zone lesion is identified on MRI and co-registered with the TRUS 3D volume.

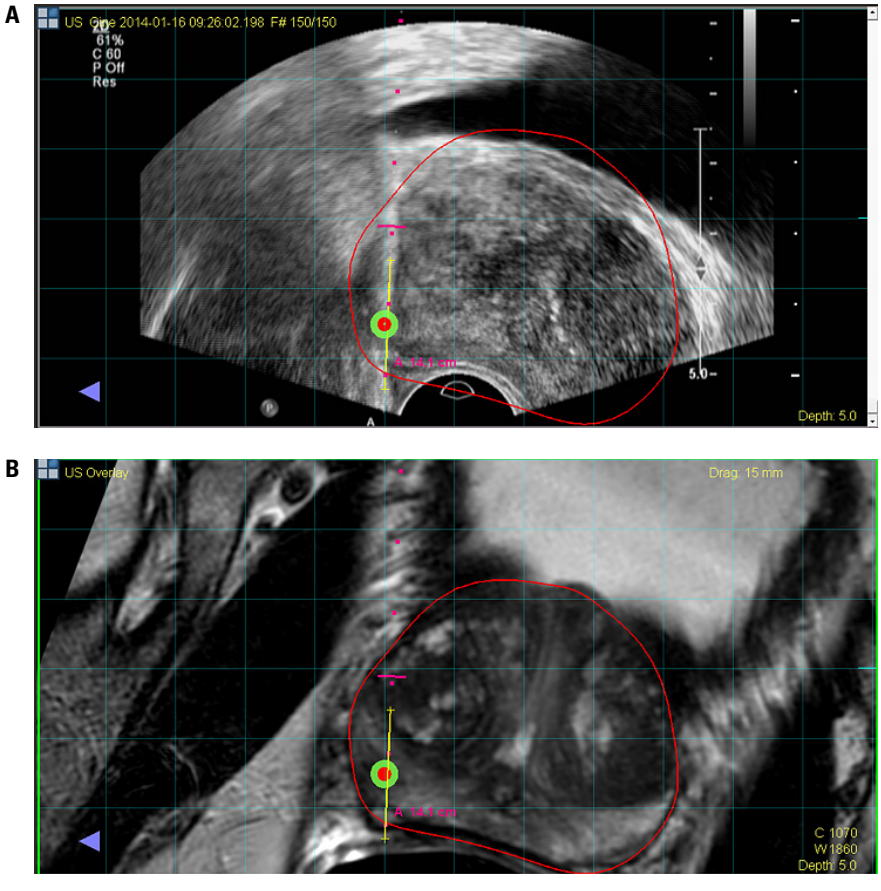

Image-based software registration (Urostation, Koelis) employs the TRUS images alone. This system acquires a real-time 3D TRUS image from each biopsy and registers it with the 3D TRUS sweep captured before biopsies are obtained in order to track the needle position. It allows acquisition of the 3D prostate volume data with digitalized location of each biopsy trajectory at every fire of the biopsy needle. This is a registration system of each 3D TRUS volume data of the prostate with 3D digitalized coordinates of each biopsy trajectory (i.e. from [x1, y1, z1] to [x2, y2, z2] within the real-time 3D TRUS volume data in each biopsy). Position tracking without additional hardware and the ability to use a freehand TRUS probe are both advantages to this approach. This biopsy-tracking system could provide an opportunity for the 3D TRUS documented biopsy mapping to precisely revisit geographically documented low-risk PCa and to perform serial analysis of cell-cycle progression gene panel.[91]

3.5.5 Fusion-guided prostate biopsy platforms

There are no available head-to-head comparisons evaluating different platforms and they are, to a certain degree, unnecessary. Selection of a platform is primarily based on user comfort, and the majority of those available have published data validating the advantage over systematic biopsy alone.

3.5.6 Electromagnetic tracking

The UroNav platform (Invivo, Gainesville, Florida, USA) has the capability of working with multiple TRUS vendors including the Philips, General Electric, and BK Ultrasound systems. Additionally, the UroNav can integrate with commonly used picture archiving and communication systems.

The patient is placed in a lateral decubitus position on the table, to which an electromagnetic field generator is fixed. Adequate analgesia is accomplished by applying lidocaine jelly in the rectum. The operator uses a TRUS probe attached to an electromagnetic tracking device to perform a sweep of the prostate, thus generating a 3D TRUS image that will be semi-automatically registered to the MRI data. Rigid and elastic registration adjustments can be made to enhance the alignment, and may be repeated as necessary for the duration of the procedure.

The US and MR images are displayed side-by-side or as overlays on the UroNav interface, with a blending slider for adjusting image transparency. The tip of the needle is in close proximity to the lesion of interest, and spring deployment of the needle acquires the cores in the axial and sagittal plane.[92] Once the needle biopsy is taken, mapping is used to archive the location of the biopsy.

The UroNav system requires conventional TRUS skill sets that would be familiar to many urologists and, as a result, the learning curve for this system is relatively low. After recent technical improvements, tracking error has been reported to be under 3 mm.[93] Initially developed with rigid registration, the UroNav now incorporates elastic registration and availability of a transperineal platform.

Siddiqui *et al.* demonstrated that fusion biopsy with the UroNav platform outperformed systematic biopsy in detecting high-risk PCa.[94] In this prospective study, patients underwent a fusion biopsy with the UroNav platform with a concomitant standard biopsy. Comparison of cancer detection rates revealed that fusion biopsy diagnosed 30% more high-risk PCa than systematic biopsy. Additionally,

fusion biopsy diagnosed 17% fewer low-risk cancers. These findings suggest that fusion biopsy with the UroNav platform may not only provide greater sensitivity for detecting PCa, but may also alter the distribution to favour the diagnoses of high-risk disease.

The Virtual Navigator (Esaote, Italy) and Real-time Virtual Sonography (Hitachi, Japan) are both fusion platforms originally designed to fuse real-time US data with other conventional imaging modalities such as computed tomography (CT), positron emission tomography (PET)-CT, or MRI for other procedures such as hepatobiliary interventions.[95] The platform was later adapted for use in prostate fusion biopsies. Like the UroNav platform previously described, the Virtual Navigator and Real-time Virtual Sonography utilize a freehand TRUS technique with an external electromagnetic field generator for tracking.[89] The Virtual Navigator semi-automatically registers the 3D TRUS image with the MRI data with rigid registration only, and consequently is prone to errors in local registration.[88] The Real-time Virtual Sonography platform may be applicable in transrectal as well as transperineal biopsies. Although the data on these two platforms are limited, both have shown higher cancer detection rates compared to a standard TRUS biopsy.[96] A study by Miyagawa *et al.* compared fusion biopsy using the Real-time Virtual Sonography against a standard TRUS biopsy in patients with an MRI lesion suspicious for cancer and elevated PSA after a prior negative prostate biopsy. With a combined approach, cancer was detected in 52/85 (61%) enrolled patients. Of these 52 patients, the targeted biopsy with Real-time Virtual Sonography alone detected cancer in 18 patients, whereas random biopsy alone detected cancer in 7 patients.

3.5.7 Mechanical position encoders

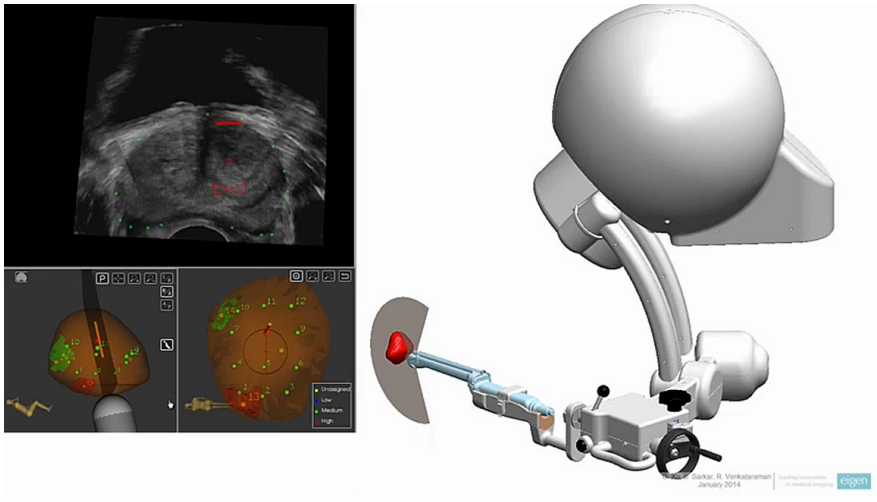

FIGURE 3-6
The Artemis System Comprises a Robotic Arm With Angle-Encoding Sensors

The software is able to present the segmented lesion, image plane, and prostate surface map with 12-core biopsy plan. This system incorporates navigation and mapping to archive core locations for future reference, including resampling if required.

Image courtesy of Eigen.

The Artemis platform (Eigen, California, USA) utilizes an endfire TRUS probe held by a robotic arm containing angle-sensing encoders within the arm's joint. Sensing encoders track the position of the probe in 3D space (**Figure 3-6**). The patient is positioned in the lateral decubitus position at the edge of the bed in order to align with the arm of the robot. The Artemis platform uses independent Eigen ProFuse software to build a 3D prostate model using the prebiopsy MRI, and the targets for biopsy are identified. These MRI data are semi-automatically aligned with the TRUS images obtained from

the initial sweep. Navigation capabilities aid in guiding the operator to the targets, and the system records the location of the biopsy site. With this, the operator can return to the site of biopsy within 2 to 3 mm of accuracy. A recent analysis of combined MR-US fusion/systematic versus MR-US fusion alone versus systematic biopsy alone revealed an improvement in the diagnosis Gleason ≥7 PCa, with a combined approach (35.0% versus 27.8% versus 24.1%, $p<0.01$). This study utilizing the Artemis device demonstrated the added value of fusion biopsy to systematic biopsy, but also revealed that targeted biopsy is not without shortcomings. Sixteen percent of patients without MR lesions harboured clinically significant PCa on systematic biopsy, which also identified 15 additional patients with high-risk disease (Gleason ≥8) that was missed with MR-US fusion alone.[97]

The BiopSee platform (Pi Medical, Greece) contains a TRUS probe on a mechanical stepper fixed to the operating table, and sampling is conducted via transperineal approach. The depth and rotational position of the probe is tracked with embedded encoders within the arm of the mechanical arm of the stepper. The hardware poses a limitation in the range of motion, increasing the learning curve for operating the platform.

The BioJet platform (BK Ultrasound, Peabody, Massachusetts, USA; DK Technologies, Barum, Germany) uses a TRUS probe attached to a mechanical arm containing angle-sensing encoders. Unlike the BiopSee platform, the BioJet platform is capable of both transrectal and transperineal biopsies. Rigid registration is employed; however, elastic registration has now been piloted.[98] Kuru *et al.* demonstrated the platform's superior ability to detect clinically significant PCa when compared to a standard TRUS biopsy (30% versus 8.2%, $p=0.01$) in a 347 biopsied patients using the BiopSee platform.[99] In this trial, both biopsy-naive and previously TRUS biopsy–negative patients underwent a standard biopsy and MRI-US fusion biopsy. The respective biopsy cores were pooled to determine the cancer detection rate. Targeted biopsy was positive in 386 of the 1,281 cores (30%), while systematic biopsy only yielded 523 positive cores of the 6,326 cores taken.

3.5.8 Image-based tracking

The Urostation platform (Koelis, France) is similar to the other platforms, as pre-procedure MRI data, freehand 3D probe manipulation, rigid registration, and elastic registration are all employed. However, unlike the other platforms, this system uses an image-based registration to track the position of the needle. A 3D panoramic volume is generated with the TRUS and registered with the prebiopsy MRI data with target information. As each biopsy is obtained, the operator acquires a 3D-TRUS image by holding the probe in place for a 3-second interval. This image is registered to the reference panoramic TRUS volume. Baco *et al.* demonstrated that MRI/TRUS fusion targeted biopsies using the system can reliably predict the location and primary Gleason pattern of an index tumour with 90% or greater accuracy.[100] A recent randomized controlled trial using the system revealed a similar rate of PCa detection between targeted biopsy guided by MRI/TRUS and 12-core random biopsy. The traditional 12-core random biopsy may be replaced by two-core MRI/TRUS targeted biopsy for detection of clinically significant PCa.[101]

The addition of mpMRI and targeted biopsy has undoubtedly improved the diagnosis and risk stratification of PCa. One systematic review reported an equivalent diagnosis of clinically significant cancer among targeted and systematic biopsies but with a lesser number of cores needed to obtain the same information (3.8 versus 12 cores) with targeted biopsies.[102] Targeted biopsy did, however, lead to a 10% reduction in the diagnosis of clinically insignificant cancers. In the future, the indications for fusion biopsy will expand as prospective trials build on our current knowledge. Image-guidance will enter and remain within the paradigm of PCa diagnosis, though its optimal role will continue to evolve and be defined.

Guideline Statements	LOE	GOR
MRI-TRUS guided fusion targeted biopsy can lead to increased detection of high-risk PCa	2	B
MRI-TRUS guided fusion biopsy can lead to decreased detection of low-risk PCa	2	B
MRI-TRUS guided fusion biopsy can detect anterior tumours	3	B

3.6 References

1. Hambrock T, Hoeks C, Hulsbergen-van de Kaa C, *et al.* Prospective assessment of prostate cancer aggressiveness using 3-T diffusion-weighted magnetic resonance imaging-guided biopsies versus a systematic 10-core transrectal ultrasound prostate biopsy cohort. *Eur Urol.* 2012;61:177–184.
2. Susil RC, Camphausen K, Choyke P, *et al.* System for prostate brachytherapy and biopsy in a standard 1.5 T MRI scanner. *Magn Reson Med.* 2004;52(3):683–687.
3. Tokuda J, Tuncali K, Iordachita I, *et al.* In-bore setup and software for 3T MRI-guided transperineal prostate biopsy. *Phys Med Biol.* 2012;57(18):5823–5840.
4. Song SE, Tokuda J, Tuncali K, *et al.* Development and preliminary evaluation of a motorized needle guide template for MRI-guided targeted prostate biopsy. *IEEE Trans Biomed Eng.* 2013;60(11):3019–3027.
5. Zani EL, Clark OA, Rodrigues Netto N Jr. Antibiotic prophylaxis for transrectal prostate biopsy. *Cochrane Database Syst Rev.* 2011;11(5):CD006576.
6. Hoeks CM, Schouten MG, Bomers JG, *et al.* Three-Tesla magnetic resonance-guided prostate biopsy in men with increased prostate-specific antigen and repeated, negative, random, systematic, transrectal ultrasound biopsies: detection of clinically significant prostate cancers. *Eur Urol.* 2012;62(2):902–909.
7. Perrotti M, Han KR, Epstein RE, *et al.* Prospective evaluation of endorectal magnetic resonance imaging to detect tumor foci in men with prior negative prostatic biopsy: A pilot study. *J Urol.* 1999;162(4):1314–1317.
8. Beyersdorff D, Taupitz M, Winkelmann B, *et al.* Patients with a history of elevated prostate-specific antigen levels and negative transrectal US-guided quadrant or sextant biopsy results: value of MR imaging. Radiology. 2002;224(3):701–706.
9. Yuen JS, Thng CH, Tan PH, *et al.* Endorectal magnetic resonance imaging and spectroscopy for the detection of tumor foci in men with prior negative transrectal ultrasound prostate biopsy. *J Urol.* 2004;171(4):1482–1486.
10. Prando A, Kurhanewicz J, Borges AP, *et al.* Prostatic biopsy directed with endorectal MR spectroscopic imaging findings in patients with elevated prostate specific antigen levels and prior negative biopsy findings: early experience. *Radiology.* 2005;236(3):903–910.
11. Amsellem-Ouazana D, Younes P, Conquy S *et al:* Negative prostatic biopsies in patients with a high risk of prostate cancer. Is the combination of endorectal MRI and magnetic resonance spectroscopy imaging (MRSI) a useful tool? A preliminary study. *Eur Urol.* 2005;47(5):582–586.
12. Cirillo S, Petracchini M, Della Monica P, *et al.* Value of endorectal MRI and MRS in patients with elevated prostate-specific antigen levels and previous negative biopsies to localize peripheral zone tumours. *Clin Radiol.* 2008;63(8):871–879.
13. Lee SH, Chung MS, Kim JH, *et al.* Magnetic resonance imaging targeted biopsy in men with previously negative prostate biopsy results. *J Endourol.* 2012;26(7):787–791.
14. Puech P, Rouvière O, Renard-Penna R, *et al.* Prostate cancer diagnosis: multiparametric MR-targeted biopsy with cognitive and transrectal US-MR fusion guidance versus systematic biopsy--prospective multicenter study. *Radiology.* 2013;268(2):461–469.
15. Panebianco V, Barchetti F, Sciarra A, *et al.* Multiparametric magnetic resonance imaging vs. standard care in men being evaluated for prostate cancer: a randomized study. *Urol Oncol.* 2015;33(1):17. e1–e7.
16. Acar Ö, Esen T, Çolakoğlu B, *et al.* Multiparametric MRI guidance in first-time prostate biopsies: what is the real benefit? *Diagn Interv Radiol.* 2015;21(4):271–276.
17. Haffner J, Lemaitre L, Puech P, *et al.* Role of magnetic resonance imaging before initial biopsy: comparison of magnetic resonance imaging-targeted and systematic biopsy for significant prostate cancer detection. *BJU Int.* 2011;108(8 Pt 2):E171–E178.
18. Panebianco V, Barchetti F, Manenti G, *et al.* MR imaging-guided prostate biopsy: technical features and preliminary results. *Radiol Med.* 2015;120(6):571–578.
19. Linder BJ, Kawashima A, Woodrum DA, *et al.* Early localization of recurrent prostate cancer after prostatectomy by endorectal coil magnetic resonance imaging. *Can J Urol.* 2014;21(3):7283–7289.

20. Vargas HA, Akin O, Afaq A, *et al.* Magnetic resonance imaging for predicting prostate biopsy findings in patients considered for active surveillance of clinically low risk prostate cancer. *J Urol.* 2012;188(5):1732–1738.

21. Margel D, Yap SA, Lawrentschuk N, *et al.* Impact of multiparametric endorectal coil prostate magnetic resonance imaging on disease reclassification among active surveillance candidates: a prospective cohort study. *J Urol.* 2012;187(4):1247–1252.

22. Kasivisvanathan V, Dufour R, Moore CM, *et al.* Transperineal magnetic resonance image targeted prostate biopsy versus transperineal template prostate biopsy in the detection of clinically significant prostate cancer. *J Urol.* 2013;189(3):860–866.

23. Anastasiadis AG, Lichy MP, Nagele U, *et al.* MRI-guided biopsy of the prostate increases diagnostic performance in men with elevated or increasing PSA levels after previous negative TRUS biopsies. *Eur Urol.* 2006;50(4):738–748.

24. Roethke M, Anastasiadis AG, Lichy M, *et al.* MRI-guided prostate biopsy detects clinically significant cancer: analysis of a cohort of 100 patients after previous negative TRUS biopsy. *World J Urol.* 2012;30(2):213–218.

25. Hambrock T, Somford DM, Hoeks C, *et al.* Magnetic resonance imaging guided prostate biopsy in men with repeat negative biopsies and increased prostate specific antigen. *J Urol.* 2010;183(2):520–527.

26. Pokorny MR, de Rooij M, Duncan E, *et al.* Prospective study of diagnostic accuracy comparing prostate cancer detection by transrectal ultrasound-guided biopsy versus magnetic resonance (MR) imaging with subsequent MR-guided biopsy in men without previous prostate biopsies. *Eur Urol.* 2014;66:22–29.

27. Ouzzane A, Puech P, Lemaitre L, *et al.* Combined multiparametric MRI and targeted biopsies improve anterior prostate cancer detection, staging, and grading. *Urology.* 2011;78(6):1356–1362.

28. Volkin D, Turkbey B, Hoang AN, *et al.* Multiparametric magnetic resonance imaging (MRI) and subsequent MRI/ultrasonography fusion-guided biopsy increase the detection of anteriorly located prostate cancers. *BJU Int.* 2014;114(6b):E43–E49.

29. Penzkofer T, Tuncali K, Fedorov A, *et al.* Transperineal in-bore 3-T MR imaging-guided prostate biopsy: a prospective clinical observational study. *Radiology.* 2015;274(1):170–180.

30. Ménard C, Iupati D, Publicover J, *et al.* MR-guided prostate biopsy for planning of focal salvage after radiation therapy. *Radiology.* 2015;274(1):181–191.

31. Djavan B, Ravery V, Zlotta A, *et al.* Prospective evaluation of prostate cancer detected on biopsies 1, 2, 3 and 4: when should we stop? *J Urol.* 2001;166(5):1679–1683.

32. Haffner J, Lemaitre L, Puech P, *et al.* Role of magnetic resonance imaging before initial biopsy: comparison of magnetic resonance imaging-targeted and systematic biopsy for significant prostate cancer detection. *BJU Int.* 2011;108(8 Pt 2):E171–E178.

33. Logan JK, Rais-Bahrami S, Turkbey B, *et al.* Current status of magnetic resonance imaging (MRI) and ultrasonography fusion software platforms for guidance of prostate biopsies. *BJU Int.* 2014;114(5):641–652.

34. Sridhar AN, Hughes-Hallett A, Mayer EK, *et al.* Image-guided robotic interventions for prostate cancer. *Nat Rev Urol.* 2013;10(8):452–462.

35. Cool DW, Zhang X, Romagnoli C, *et al.* Evaluation of MRI-TRUS fusion versus cognitive registration accuracy for MRI-targeted, TRUS-guided prostate biopsy. *AJR AM J Roentgenol.* 2014;204(1):83–91.

36. Delongchamps NB, Peyromaure M, Schull A, *et al.* Prebiopsy magnetic resonance imaging and prostate cancer detection: comparison of random and targeted biopsies. *J Urol.* 2013;189(2):493–499.

37. Wysock JS, Rosenkrantz AB, Huang WC, *et al.* A prospective, blinded comparison of magnetic resonance (MR) imaging-ultrasound fusion and visual estimation in the performance of MR-targeted prostate biopsy: the PROFUS trial. *Eur Urol.* 2014;66(2):343–351.

38. Sonn GA, Chang E, Natarajan S, *et al.* Value of targeted prostate biopsy using magnetic resonance-ultrasound fusion in men with prior negative biopsy and elevated prostate-specific antigen. *Eur Urol.* 2014;65(4):809–815.

39. Ho H, Yuen JS, Mohan P, *et al.* Robotic transperineal prostate biopsy: pilot clinical study. *Urology.* 2011;78(5):1203–1208.

40. Ho H, Yuen JSP, Cheng CWS. Robotic prostate biopsy and its relevance to focal therapy of prostate cancer. *Nat Rev Urol.* 2011;8(10):579–585.

41. Fütterer JJ, Barentsz JO. MRI-guided and robotic-assisted prostate biopsy. *Curr Opin Urol.* 2012;22(4):316–319.

42. Elhawary H, Zivanovic A, Rea M, *et al.* The feasibility of MR-image guided prostate biopsy using piezoceramic motors inside or near to the magnet isocentre. *Med Image Comput Comput Assist Interv.* 2006;9(Pt 1):519–526.

43. Schouten MG, Bomers JG, Yakar D, *et al.* Evaluation of a robotic technique for transrectal MRI-guided prostate biopsies. *Eur Radiol.* 2012;22(2):476–483.

44. Xu H, Lasso A, Guion P, *et al.* Accuracy analysis in MRI-guided robotic prostate biopsy. *Int J Comput Assist Radiol Surg.* 2013;8(6):937–944.

45. Elhawary H, Tse ZT, Rea M, *et al.* Robotic system for transrectal biopsy of the prostate: real-time guidance under MRI. *IEEE Eng Med Biol Mag.* 2010;29:78–86.

46. Zangos S, Melzer A, Eichler K, *et al.* MR-compatible assistance system for biopsy in a high-field-strength system: initial results in patients with suspicious prostate lesions. *Radiology.* 2011;259(3):903–910.

47. Tilak G, Tuncali K, Song SE, *et al.* 3T MR-guided in-bore transperineal prostate biopsy: A comparison of robotic and manual needle-guidance templates. *J Magn Reson Imaging.* 2015;42(1):63–71.

48. Ukimura O, Hirahara N, Fujihara A, *et al.* Technique for a hybrid system of real-time transrectal ultrasound with preoperative magnetic resonance imaging in the guidance of targeted prostate biopsy. *Int J Urol.* 2010;17(10):890–893.

49. National Institute for Health and Care Excellence (NICE). Prostate cancer diagnosis and management. 2014. p. 1–44. Available: https://www.nice.org.uk/guidance/cg175; Accessed: August 25, 2015.

50. Holmberg L, Bill-Axelson A, Steineck G, *et al.* Results from the Scandinavian Prostate Cancer Group Trial Number 4: a randomized controlled trial of radical prostatectomy versus watchful waiting. *J Natl Cancer Inst* Monogr. 2012;2012(45):230–233.

51. Wilt TJ. The Prostate Cancer Intervention Versus Observation Trial: VA/NCI/AHRQ Cooperative Studies Program #407 (PIVOT): design and baseline results of a randomized controlled trial comparing radical prostatectomy with watchful waiting for men with clinically localized prostate cancer. *J Natl Cancer Inst* Monogr. 2012;2012(45):184–190.

52. Lecornet E, Ahmed HU, Hu Y, *et al.* The accuracy of different biopsy strategies for the detection of clinically important prostate cancer: a computer simulation. *J Urol.* 2012;188(3):974–980.

53. Barzell WE, Melamed MR, Cathcart P, *et al.* Identifying candidates for active surveillance: an evaluation of the repeat biopsy strategy for men with favorable risk prostate cancer. *J Urol.* 2012;188(3):762–767.

54. Djavan B, Ravery V, Zlotta A, *et al.* Prospective evaluation of prostate cancer detected on biopsies 1, 2, 3 and 4: when should we stop? *J Urol.* 2001;166(5):1679–1683.

55. Scattoni V, Zlotta A, Montironi R, *et al.* Extended and saturation prostatic biopsy in the diagnosis and characterisation of prostate cancer: a critical analysis of the literature. *Eur Urol.* 2007;52(5):1309–1322.

56. Onik G, Miessau M, Bostwick DG. Three-dimensional prostate mapping biopsy has a potentially significant impact on prostate cancer management. *J Clin Oncol.* 2009;27(26):4321–4326.

57. Barzell WE, Melamed MR. Appropriate patient selection in the focal treatment of prostate cancer: the role of transperineal 3-dimensional pathologic mapping of the prostate--a 4-year experience. *Urology.* 2007;70(suppl 6):27–35.

58. Kasivisvanathan V, Dufour R, Moore CM, *et al.* Transperineal magnetic resonance image-targeted prostate biopsy versus transperineal template prostate biopsy in the detection of clinically significant prostate cancer. *J Urol.* 2013;189:860–866.

59. Onik G, Barzell W. Transperineal 3D mapping biopsy of the prostate: an essential tool in selecting patients for focal prostate cancer therapy. *Urol Oncol.* 2008;26(5):506–510.

60. Barzell WE, Whitmore WF, Andriole GL. How to perform transperineal saturation prostate biopsy: technique addresses diagnostic, therapeutic dilemmas that arise following TRUS biopsies. *Urology Times.* 2003;31:41.

61. El-Shater Bosaily A, Parker C, Brown LC, *et al.* PROMIS--Prostate MR imaging study: A paired validating cohort study evaluating the role of multi-parametric MRI in men with clinical suspicion of prostate cancer. *Contemp Clin Trials.* 2015;42:26–40.

62. Simmons LA, Ahmed HU, Moore CM, *et al.* The PICTURE study -- prostate imaging (multi-parametric MRI and Prostate HistoScanning™) compared to transperineal ultrasound guided biopsy for significant prostate cancer risk evaluation. *Contemp Clin Trials.* 2014;37(1):69–83.

63. Symons JL, Huo A, Yuen CL, *et al.* Outcomes of transperineal template-guided prostate biopsy in 409 patients. *BJU Int.* 2013;112(5):585–593.

64. Gershman B, Zietman AL, Feldman AS, *et al.* Transperineal template-guided prostate biopsy for patients with persistently elevated PSA and multiple prior negative biopsies. *Urol Oncol.* 2013;31(7):1093–1097.

65. Vyas L, Acher P, Kinsella J, *et al.* Indications, results and safety profile of transperineal sector biopsies (TPSB) of the prostate: a single centre experience of 634 cases. *BJU Int.* 2014;114(1):32–37.

66. Reissigl A, Pointner J, Strasser H, *et al.* Frequency and clinical significance of transition zone cancer in prostate cancer screening. *Prostate.* 1997;30(2):130–135.

67. Augustin H, Erbersdobler A, Graefen M, *et al.* Biochemical recurrence following radical prostatectomy: a comparison between prostate cancers located in different anatomical zones. *Prostate.* 2003;55(1):48–54.

68. Stamey TA, Donaldson AN, Yemoto CE, *et al.* Histological and clinical findings in 896 consecutive prostates treated only with radical retropubic prostatectomy: epidemiologic significance of annual changes. *J Urol.* 1998;160(6 Pt 2):2412–2417.

69. Noguchi M, Stamey TA, Neal JE, *et al.* An analysis of 148 consecutive transition zone cancers: clinical and histological characteristics. *J Urol.* 2000;163(6):1751–1755.

70. McNeal JE, Redwine EA, Freiha FS, *et al.* Zonal distribution of prostatic adenocarcinoma. Correlation with histologic pattern and direction of spread. *Am J Surg Pathol.* 1988;12(12):897–906.

71. Losa A, Gadda GM, Lazzeri M, *et al.* Complications and quality of life after template-assisted transperineal prostate biopsy in patients eligible for focal therapy. *Urology.* 2013;81(6):1291–1296.

72. Merrick GS, Taubenslag W, Andreini H, *et al.* The morbidity of transperineal template-guided prostate mapping biopsy. *BJU Int.* 2008;101(12):1524–1529.

73. Buskirk SJ, Pinkstaff DM, Petrou SP, *et al.* Acute urinary retention after transperineal template-guided prostate biopsy. *Int J Radiat Oncol Biol Phys.* 2004;59(5):1360–1366.

74. Miller J, Perumalla C, Heap G. Complications of transrectal versus transperineal prostate biopsy. *ANZ J Surg.* 2005;75(1-2):48–50.

75. Bittner N, Merrick GS, Bennett A, *et al.* Diagnostic Performance of Initial Transperineal Template-guided Mapping Biopsy of the Prostate Gland. *Am J Clin Oncol.* 2015;38(3):300–303.

76. Ahmed HU, Hu Y, Carter T, *et al.* Characterizing clinically significant prostate cancer using template prostate mapping biopsy. *J Urol.* 2011;186(2):458–464.

77. Mabjeesh NJ, Lidawi G, Chen J, *et al.* High detection rate of significant prostate tumours in anterior zones using transperineal ultrasound-guided template saturation biopsy. *BJU Int.* 2012;110(7):993–997.

78. Hu JC, Change E, Natarajan S, *et al.* Targeted prostate biopsy in select men for active surveillance: do the Epstein criteria still apply? *J Urol.* 2014;192(2):385–390.

79. Sonn GA, Chang E, Natarajan S, *et al.* Value of targeted prostate biopsy using magnetic resonance-ultrasound fusion in men with prior negative biopsy and elevated prostate-specific antigen. *Eur Urol.* 2014;65(4):809–815.

80. Vourganti S, Rastinehad A, Yerram NK, *et al.* Multiparametric magnetic resonance imaging and ultrasound fusion biopsy detect prostate cancer in patients with prior negative transrectal ultrasound biopsies. *J Urol.* 2012;188(6):2152–2157.

81. Abdi H, Zargar H, Goldenberg SL, *et al.* Multiparametric magnetic resonance imaging-targeted biopsy for the detection of prostate cancer in patients with prior negative biopsy results. *Urol Oncol.* 2015;33(4):165.e1–e7.

82. Manfredi M, Costa Moretti TB, Emberton M, *et al.* MRI/TRUS fusion software-based targeted biopsy: the new standard of care? *Minerva Urol Nefrol.* 2015;67(3):233–246.

83. Haffner J, Lemaitre L, Puech Pet, *et al.* Role of magnetic resonance imaging before initial biopsy: comparison of magnetic resonance imaging-targeted and systematic biopsy for significant prostate cancer detection. *BJU Int.* 2011;108(8 Pt 2):E171–E178.

84. Park BK, Park JW, Park SY, *et al.* Prospective evaluation of 3-T MRI performed before initial transrectal ultrasound-guided prostate biopsy in patients with high prostate-specific antigen and no previous biopsy. *AJR Am J Roentgenol.* 2011;197(5):W876–W881.

85. Cerantola Y, Haberer E, Torres J, *et al.* Accuracy of cognitive MRI-targeted biopsy in hitting prostate cancer-positive regions of interest. *World J Urol.* 2016;34(1):75–82.

86. Kasivisvanathan V, Dufour R, Moore CM, *et al.* Transperineal magnetic resonance image targeted prostate biopsy versus transperineal template prostate biopsy in the detection of clinically significant prostate cancer. *J Urol.* 2013;189(3):860–866.

87. Wysock JS, Rosenkrantz AB, Huang WC, *et al.* A prospective, blinded comparison of magnetic resonance (MR) imaging-ultrasound fusion and visual estimation in the performance of MR-targeted prostate biopsy: the PROFUS trial. *Eur Urol.* 2014;66(2):343–351.

88. Logan JK, Rais-Bahrami S, Turkbey B, *et al.* Current status of magnetic resonance imaging (MRI) and ultrasonography fusion software platforms for guidance of prostate biopsies. *BJU Int.* 2014;114(5):641–652.

89. Sonn GA, Margolis DJ, Marks LS. Target detection: magnetic resonance imaging-ultrasound fusion-guided prostate biopsy. *Urol Oncol.* 2014;32(6):903–911.

90. Hadaschik BA, Kuru TH, Tulea C, *et al.* A novel stereotactic prostate biopsy system integrating pre-interventional magnetic resonance imaging and live ultrasound fusion. *J Urol.* 2011;186(6):2214–2220.

91. Ukimura O, Gross ME, de Castro Abreu AL, *et al.* A novel technique using three-dimensionally documented biopsy mapping allows precise re-visiting of prostate cancer foci with serial surveillance of cell cycle progression gene panel. *Prostate.* 2015;75(8):863–871.

92. Hong CW, Rais-Bahrami S, Walton-Diaz A, *et al.* Comparison of magnetic resonance imaging and ultrasound (MRI-US) fusion-guided prostate biopsies obtained from axial and sagittal approaches. *BJU Int.* 2015;115(5):772–779.

93. Xu S, Kruecker J, Turkbey B, *et al.* Real-time MRI-TRUS fusion for guidance of targeted prostate biopsies. *Comput Aided Surg.* 2008;13(5):255–264.

94. Siddiqui MM, Rais-Bahrami S, Turkbey B, *et al.* Comparison of MR/ultrasound fusion-guided biopsy with ultrasound-guided biopsy for the diagnosis of prostate cancer. *JAMA.* 2015;313(4):390–397.

95. Di Mauro E, Solbiati M, De Beni S, *et al.* Virtual navigator real-time ultrasound fusion imaging with positron emission tomography for liver interventions. *Conf Proc IEEE Eng Med Biol Soc.* 2013;2013:1406–1409.

96. Miyagawa T, Ishikawa S, Kimura T, *et al.* Real-time Virtual Sonography for navigation during targeted prostate biopsy using magnetic resonance imaging data. *Int J Urol.* 2010;17(10):855–860.

97. Filson CP, Natarajan S, Margolis DJ, *et al.* Prostate cancer detection with magnetic resonance-ultrasound fusion biopsy: The role of systematic and targeted biopsies. *Cancer.* 2016;122(6):884–9.

98. Tewes S, Hueper K, Hartung D, *et al.* Targeted MRI/TRUS fusion-guided biopsy in men with previous prostate biopsies using a novel registration software and multiparametric MRI PI-RADS scores: first results. *World J Urol.* 2015;33(11):1707–1714.

99. Kuru TH, Roethke MC, Seidenader J, *et al.* Critical evaluation of magnetic resonance imaging targeted, transrectal ultrasound guided transperineal fusion biopsy for detection of prostate cancer. *J Urol.* 2013;190(4):1380–1386.

100. Baco E, Ukimura O, Rud E, *et al.* Magnetic resonance imaging-transrectal ultrasound image-fusion biopsies accurately characterize the index tumor: correlation with step-sectioned radical prostatectomy specimens in 135 patients. *Eur Urol.* 2015;67(4):787–794.

101. Baco E, Rud E, Eri LM, *et al.* A Randomized Controlled Trial To Assess and Compare the Outcomes of Two-core Prostate Biopsy Guided by Fused Magnetic Resonance and Transrectal Ultrasound Images and Traditional 12-core Systematic Biopsy. *Eur Urol.* 2016;69(1):149–156.

102. Moore CM, Robertson NL, Arsanious N, *et al.* Image-guided prostate biopsy using magnetic resonance imaging-derived targets: a systematic review. *Eur Urol.* 2013;63(1):125–140.

C4

Available Ablation Energies to Treat Prostate Cancer

CHAIR

Jean de la Rosette, The Netherlands

CO-CHAIR

Jonathan Coleman, United States

MEMBERS

Sébastien Crouzet, France
Martijn de Bruin, The Netherlands
Theo de Reijke, The Netherlands
José Luis Domínguez-Escrig, Spain
Scott Eggener, United States
Sangeet Ghai, Canada
Aaron Katz, United States
György Kovacs, Germany
Sascha Pahernik, Germany
Bradley Pieters, The Netherlands
John Varkarakis, Greece

Committee 4

CONTENTS

Available Ablation Energies to Treat Prostate Cancer

4.1 Energy Sources and Ablation

4.1.1 High-intensity focused ultrasound ablation

4.1.1.1 History

Treating tissue using high-intensity sound waves originated at the beginning of the 20th century. In 1927, the *London, Edinburgh, and Dublin Philosophical Magazine and Journal of Science* published a paper by Wood and Loomis entitled, "The Physical and Biological Effects of High-Frequency Sound-Waves of Great Intensity."[1] In this paper, Wood and Loomis described one of the first experimental setups designed to generate high-intensity sound waves by using a piezo-electric oscillator made of quartz running at 3.33 kHz immersed in an oil bath. With this setup, the experimenters raised a 150 g object approximately 7 cm by what they excitedly described as "a fountain of oil drops," with the additional result of burn wounds on their hands.

It was not until 1950 that the notion of an ultrasound (US) wave-induced temperature effect intended for medical use was extensively investigated by the Fry brothers.[2] Based on their efforts, the physical mechanism was translated into a neurosurgical device that allowed for high-intensity focused ultrasound (HIFU) treatment.

Sometime later in the mid-1990s, HIFU was used again and described as a device for ablative cancer therapy in a review paper by Vaughan, Hill, and ter Haar, with the potential for use in the liver, bladder, kidney, prostate, breast, and brain.[3,4] Soon after this review paper was published, the first applications of HIFU in prostate cancer (PCa) treatment emerged in medical literature, with descriptions of its use in treating 28 patients by Madersbacher *et al.*[5]

4.1.1.2 Principles and state-of-the-art techniques

High-intensity focused ultrasound

In the field of ablative techniques, HIFU is unique in that it is not necessary to insert a probe into the target tissue, making it the only truly non-invasive ablative technique. The physical principle behind state-of-the-art HIFU is based on the creation of a focus with the US waves. High-intensity beams can readily be achieved using lens, curbed transducer, or phased array–focusing procedures and, by choice of a suitable acoustic frequency, regions of tissue destruction can be induced (**Figure 4-1**). By focusing at more than one place or by scanning the focus, a volume of tissue can be ablated (**Figure 4-2**).

FIGURE 4-1
Tissue Attenuation Curves for Different Tissue Types

By choosing a specific frequency, different tissues can be ablated.

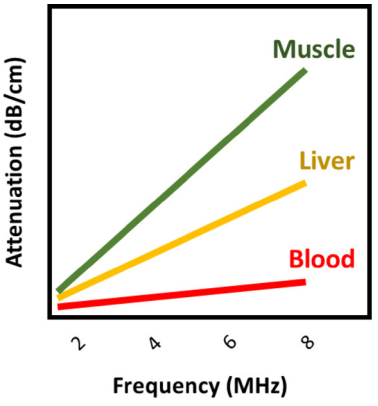

FIGURE 4-2
Different HIFU Intensity Settings

A A focus in US is either created by a curbed transducer or a phased array.

B Vessel disappearance and cellular destruction by thermal coagulation.

C Superficial vessel disappearance and cellular destruction by thermal coagulation, accompanied by small cavitational stress waves.

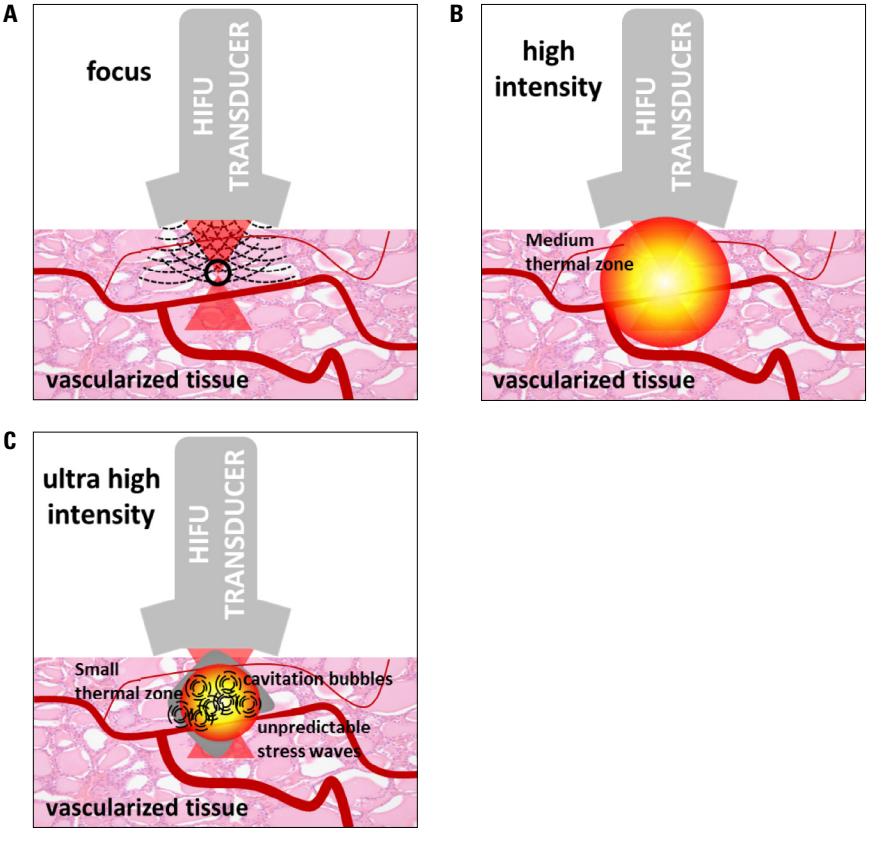

Hyperthermia versus cavitation

Using focus techniques, HIFU can destroy tissue via two methods: hyperthermia and cavitation. Hyperthermia, also called thermal ablation, uses high energy to produce heat, raising the local temperature above the denaturation temperature of proteins, thereby inducing cell death. Cavitation occurs when acoustic intensities are high enough to create microbubbles that interact with the acoustic field. As the microbubbles grow, they implode, resulting in the shockwaves and microjets that can mechanically damage tissue. This process can be rather unpredictable and is therefore usually

avoided in clinical applications.[6] The HIFU ablation zone is formed primarily at the focus location. As it travels through the tissue away from the focus location, the intensity of the generated HIFU field decreases exponentially. This is described by the US attenuation coefficient (**Figure 4-1**). For HIFU, frequencies in the range of 600 kHz to 7 MHz are used, depending on the application type and the penetration depth. Intensity and pressure values range from 1.000-25.000 watts per cm^2 and 3-100 MPa, respectively. During a single sonication, the temperature within the focal point should be between 60°C and 95°C to induce tissue coagulation and necrosis.[7]

4.1.1.3 Future

Novel ablation systems aim to ablate three-dimensional (3D) volumes of tissue, and special high-power output transducers are recently available to ensure ablation zones without gaps. Nonetheless, a single ablation of a lesion is still time consuming due to the small volume that is generated. Between each single sonication, there is a necessary defined cooling time in order to protect adjacent healthy tissue from heat accumulation and overheating. To overcome this obstacle several techniques have been developed. One possibility is to enlarge the US focus size, preserving the transducer's aperture and the focused characteristic of the sound field. Additionally, optimized scan algorithms or the use of exogenous cavitation microbubbles have been proposed.[8] The latter, however, is more critical with respect to unintended adverse effects such as overheating and uncontrolled ablation zones. Still, exogenous microbubbles are increasingly researched to localize PCa using US, and the combination might be the clear future for image-guided HIFU treatment.

4.1.2 Laser ablation

4.1.2.1 History

When Gordon, Zeiger, and Townes invented the first version of light amplification by stimulated emission of radiation—a laser, which they originally termed maser—in a laboratory of Columbia University, they may have envisioned a wide variety of medical applications.[9] Based on Einstein's predictions, they achieved the first amplification and generation of electromagnetic waves by stimulated emission, an accomplishment that earned Townes jointly a Nobel Prize in Physics in 1964.

Obviously, these ammonia-based systems were not very practical in use. In 1960, Theodore Maiman at Hughes Research Laboratories constructed the first operational laser. It was designed with a synthetic ruby rod of 1 cm by 2 cm with silver-coated endings which functioned as reflectors that allowed for the lasing process.[10] An industry of commercially available lasers was created, and their first applications in medicine began to emerge. In 1963, Goldman *et al.* demonstrated the use of experimental laser therapy in skin[11] and retinal surgery.[12] In 1964, the Nd:YAG (neodymium:yttrium-aluminum-garnet) laser and CO_2 (carbon dioxide) lasers were developed at Bell Laboratories. The CO_2 laser is a continuous-wave gas laser that emits infrared light at 1060 nm in an easily manipulated, focused beam that is well absorbed by water. Because soft tissue consists mostly of water, researchers found that a CO_2 laser beam could cut tissue like a scalpel, but with minimal blood loss.

Novel surgical applications emerged after the invention of fibre optics by Kao at the Standard Telecommunications Labs (jointly awarded Nobel Prize in Physics 2009). This new technology allowed for the delivery of light at the tip of a flexible glass fibre, enabling the use of lasers inside the

human body. Müssiggang and Katsaros demonstrated the first use of a laser in the prostate in 1971.[13] Nevertheless, it took until 1992 for Costello *et al.* to demonstrate the use of a laser as an ablative method in benign hypertrophic prostates.[14]

4.1.2.2 Principles and state-of-the-art techniques

Laser

Light amplification by stimulated emission of radiation can be achieved by pumping external energy into a gain medium. As light of a specific wavelength (colour) passes through the gain medium, it is amplified. If the medium is confined between two mirrors (one of which is typically more transparent than the other), the light is "trapped" and begins to travel back and forth through the gain medium. As a result, the light amplifies more and more energy by generating more light waves of the same nature (population inversion). When energy levels are high enough, called the lasing threshold, the laser beam is coupled out of the more transparent of the two mirrors, and lasing of coherent light occurs. Coherence is the creation of high-energy light of the same wavelength in a small area over a very long distance, hence the term "laser beam."

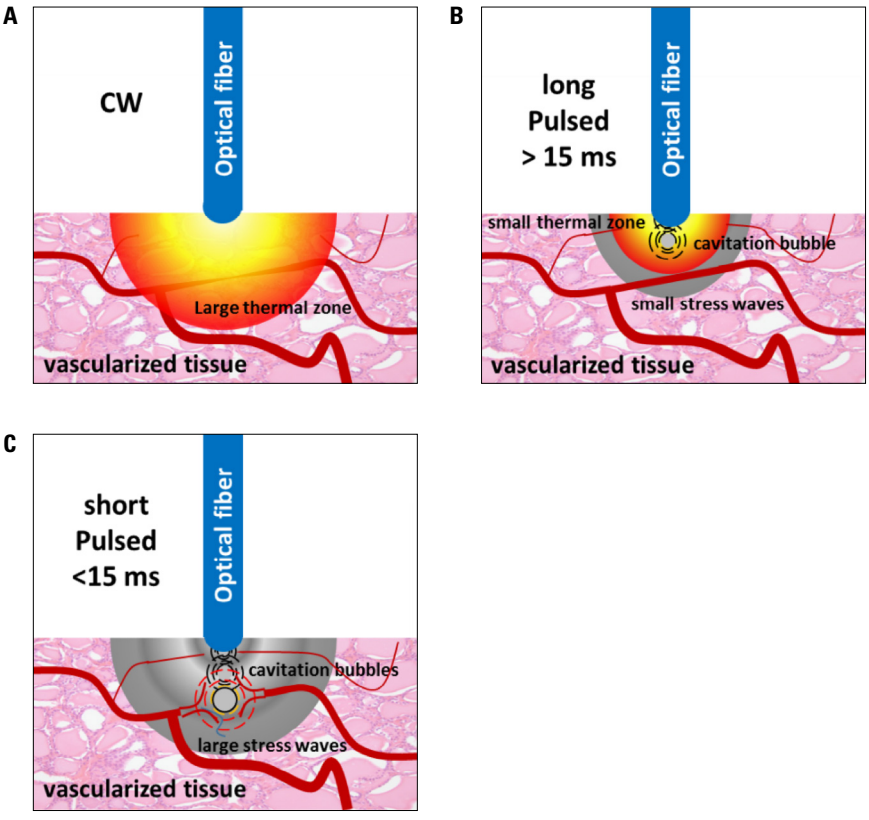

FIGURE 4-3
Short and Long Pulsed Thermal Coagulation

A Vessel disappearance and cellular destruction by thermal coagulation.

B Superficial vessel disappearance and cellular destruction by thermal coagulation, occasionally accompanied by small cavitational stress waves.

C Vessel wall rupture and cellular destruction by large cavitational stress waves.

Continuous wave versus pulsed

There are two main modes of operation of a laser emitter, continuous wave (CW) and pulsed. Using a CW laser usually leaves a thermal coagulum at the boundary of the treated area. This coagulum can impede the healing process or induce unwanted repair mechanisms and eschar formation. A CW

laser with relatively moderate irradiance can easily reach temperatures of 60°C to 100°C. A pulsed laser is able to reduce heat transfer to surrounding tissues by emitting a thermal energy shorter than the thermal relaxation time of tissue.

In general, pulsed ablation is a trade-off between thermal damage to surrounding tissue caused by relatively long pulses (>15 ms) and mechanical damage to surrounding tissue caused by relatively short pulses (<15 ms). A short laser pulse can create thermoelastic expansion and recoil of tissue, which in turn can lead to stress waves that propagate with the speed of sound or even faster, as in the case of shockwaves. If the laser pulse length is shorter than the time it takes for the stress wave to propagate out of the irradiated tissue volume, large stress peaks can be reached which, in turn, may inflict damage to the probed and surrounding area. In summary, a CW laser produces a large thermal response with less control over the treatment area or cutting intersection, whereas a pulsed laser produces a controlled thermal response with possible induction of mechanical damage by shockwaves.[15]

Wavelength-scattering and absorption

A laser beam that encounters the tissue surface may be completely reflected, transmitted (in the case of transparent tissue), scattered, or absorbed. Scattering and absorption are two main properties of light and tissue interaction that determine light propagation and subsequently the efficiency of ablation. A scattering event changes the direction of light propagation and is usually determined by the light scattering content of cells in tissue. Absorption occurs when a specific wavelength of light is absorbed by a chromophore, subsequently converting the light's energy into heat energy. Each tissue type has its own specific scattering properties and set of absorbing chromophores for which a laser system that operates at a certain wavelength is optimal. Known absorbers for prostate tissue are similar for most tissues and include water, hemoglobin, and proteins. **Figure 4-4** is a graph of wavelength versus absorption for different tissue absorbers and lasers that operate at these wavelength regimes.

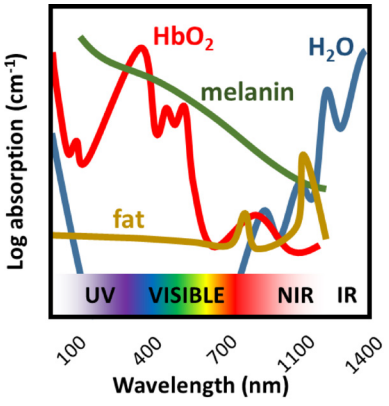

FIGURE 4-4
Tissue Absorption Spectrum With the Four Main Absorbers

Specific absorption peaks are found between 500 to 600 nm for hemoglobin, 1200 to 1220 nm for fat, and from upwards of 1200 nm for water.

Abbreviations: IR, infrared; NIR, near infrared; UV, ultraviolet.

The output geometry of the optics (i.e., the employed fibres) used to deliver the light will also influence ablation efficiency. The combination of optics, wavelength, and delivered energy determines the penetration depth into tissue.[16,17] Consequently, low scattering and absorption of water and hemoglobin can generate deeper tissue damage.

4.1.2.3 Future

With the development of diode lasers for the whole visible and nearly the whole infrared spectrum, a much more easily applicable range of laser systems has become available. These diodes are very energy efficient, permitting the minimization of their cooling system. Improvements in the design of high-power diode laser sources have made medical laser systems smaller, more portable, more powerful, and less expensive than those of previous generations. For PCa, quartz fibres with a diameter of 300 µm to 600 µm and a diffuser on the tip have replaced bare fibres.[18] In the future, smart fibre tip solutions might further increase ablation efficiency.

Combining novel solid-state diode lasers with another fibre design has resulted in currently available lasers that operate at 532 nm, hence the name the green laser. This laser operates at CW and pulsed modes, and gives more control due to the small penetration depth of green light. Active cooling of the fibre tip minimizes damage to the fibre that can result when the fibre overheats. However, because of their high power (≤180 W), careful use is necessary.

4.1.3 Photodynamic therapy

4.1.3.1 History

Although photodynamic therapy (PDT) was developed for clinical use only relatively recently, the foundations of the concept were laid as early as the beginning of the 20th century when Raab noted that certain wavelengths of light were lethal to paramecia exposed to acridine and certain other dyes.[19] By 1903, researchers had already translated this knowledge into the treatment of skin cancer and named this photodynamic action.[20,21]

From the beginning, a vast amount of research went into understanding photobiology and cancer biology. The most explored class of chemical compounds in PDT today, the porphyrins, were investigated by Meyer-Betz as early as 1913 for the accumulation of hematoporphyrin and its derivatives in rat tumours and PDT effects following systemic administration.[22] However, many years went by before Thomas Dougherty and coworkers at Roswell Park Cancer Institute in Buffalo, New York, clinically tested PDT again for its use in cancer therapy. In 1978, striking results were published in which 113 cutaneous or subcutaneous malignant skin tumours were treated and a total or partial resolution of 111 tumours was observed.[23]

Parallel to these developments, novel light sources were becoming available and lasers and optical fibres were readily implemented (see section on laser ablation), making the therapy a viable option for clinical research. In 1996, the first canine prostates were experimentally treated by Chang *et al.*,[24] quickly followed by the first human experimental tests using less toxic compounds.[25]

4.1.3.2 Principles and state-of-the-art techniques

Two-stage process

Photodynamic therapy is a two-stage process that involves a) the interaction between light with a photosensitive agent (administrated either orally or intravenously) and b) the interaction between the agent and oxygen present in tissue (**Figure 4-5**).[26] Interaction between laser and tissue was briefly described in the section on laser ablation. For most PDT treatments, infrared and near-infrared light is used for optimal tissue penetration and light distribution. When illumination is sufficient,

absorption of light by the photosensitive agent creates a chain reaction that induces the release of singlet oxygen and antioxidants. The singlet oxygen can directly kill tumour cells by the induction of necrosis and/or apoptosis. It can also cause destruction of tumour vasculature, and produces an acute inflammatory response that attracts leukocytes, such as dendritic cells and neutrophils. In summary, PDT is a two-stage process, the first stage involves light and is governed by the physics behind light-tissue interaction, and the second stage involves a photosensitive agent and is governed by cell biology and biochemistry.

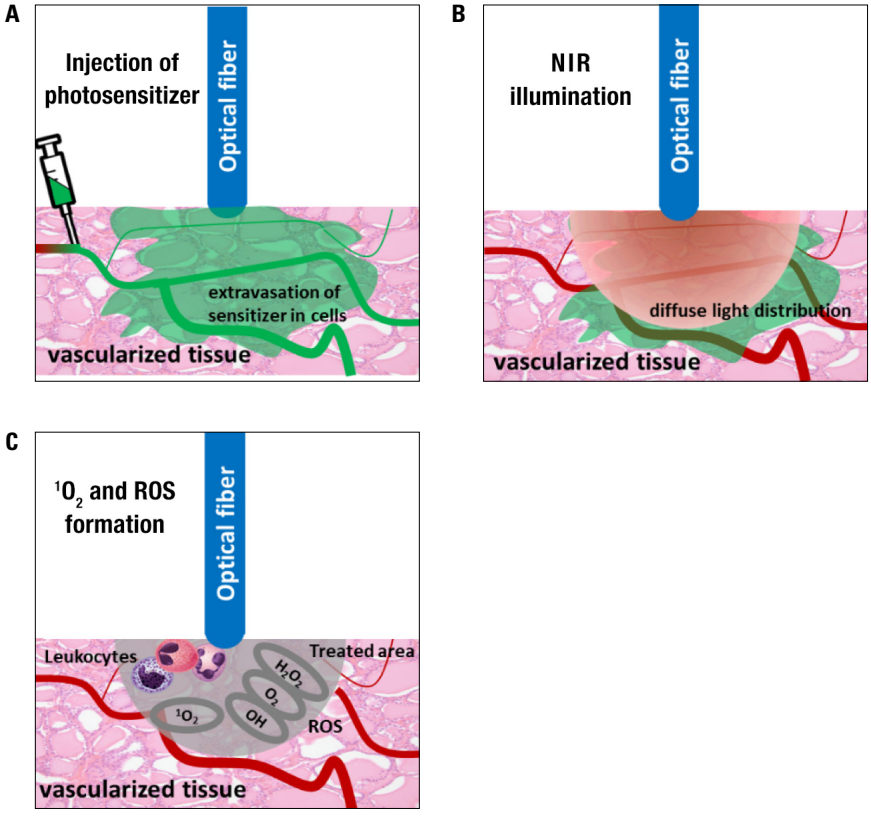

FIGURE 4-5
Photodynamic Therapy Procedure

A PDT employs a photosensitive agent, which is usually administrated intravenously. The photosensitizer accumulates in malignant tissue because of a preference for overexpressed tumour lipoproteins and leaky neovasculature.

B The photosensitizer is illuminated with a near-infrared (NIR) light source. Only the illuminated tissue is ablated by activation of free radicals, reactive oxygen species (ROS), and leukocyte infiltration.

Pharmacological uptake

The efficiency of pharmacological PDT uptake relies on two principles. First, the hydrophobic and lipophilic photosensitive agent has a higher affinity for malignant tissue. This is due to a preference for overexpressed lipoproteins in malignant cells, which is amplified even more by the increased acidic environment in a tumour. Second, neovascularization of tumours allows for the accumulation of the agent. Neoplastic angiogenesis usually results in the development of leaky vasculature, which increases the presence of the photosensitizer in the tumour cells.

Biochemistry and activation

In its basic state, the photosensitizer is biochemically inactive and stable. When illuminated, the drug goes into an excited state, and the excess energy is restored by (a) the release of heat and (b) emission of fluorescent photons, and is (c) transferred into the intermediate *triplet* state. It is in this triplet

state that the cytotoxic action of the photosensitizer appears. Simultaneously, the oxidoreduction reactions lead to the formation of radical intermediates (type 1 reaction), and energy transfer from the photoexcited sensitized reactions leads to the formation of the highly cytotoxic singlet oxygen (type 2 reaction). This type 2 reaction is usually dominating and leads to apoptosis and necrosis. Subsequently, the photosensitizer is destroyed by the singlet oxygen and the radical intermediates. This decrease of efficiency over time is called photobleaching (**Figure 4-6**).[27]

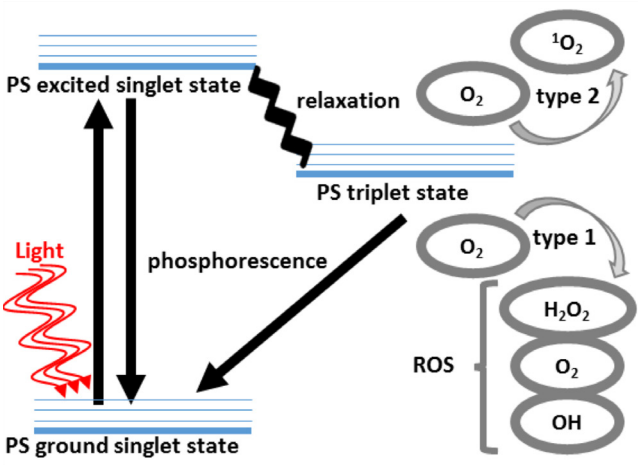

FIGURE 4-6
Photosensitizer Mode of Action

When illuminated, the photosensitizer goes into an excited state and the excess energy is restored by emission of fluorescent photons and transferred into the intermediate triplet state. Simultaneously, the oxidoreduction reactions lead to the formation of radical intermediates (type 1 reaction), and energy transfer from the photoexcited sensitized reactions leads to the formation of the highly cytotoxic singlet oxygen (type 2 reaction).

4.1.3.3 Future

Prostatic PDT will benefit from the same advances in light source developments as regular laser ablation. Novel, cheaper, and easier-to-use light sources are being developed with novel endoscopic light sources or needle-based probes for interstitial treatment. Additionally, PDT, which targets specific cells or tissue locations, is being developed and tested. A photosensitizer named WST11, which targets the vasculature of PCa, has been advanced from its dermatological predecessor, and its first trials in PCa are underway.[28] Moreover, Aguilar *et al.* are intensively researching improved delivery mechanisms. This latest research line focuses on liposomal drug delivery systems that will improve the efficacy and efficiency of photosensitizer distribution of PDT.[29]

4.1.4 Cryoablation

4.1.4.1 History

The process of destroying or damaging tissue by extreme cold was first described by James Arnott in 1845 using crushed ice and saline solutions to reach temperatures between –18°C and –24°C.[30] Arnott went as far as designing an apparatus for controlled delivery of cold temperatures for skin anesthesia, which was shown at the Great Exhibition in London. Well before it was used therapeutically, however, the Egyptians had already known about the pain-relieving and inflammation-reducing capabilities of cold temperatures as early as 2500 BC.[31] After the description by Arnott, medical developments for cryotechnology followed each other quickly. Progresses in cooling of gases resulted in the first clinical application of liquid air (–190°C) in 1899 by a New York City physician, Campbell

White, who used either a swab, a spray, or a brass roller device to treat skin cancer.[32] Following World War II, liquid nitrogen (–196°C) became commercially available. Irving Cooper and Arnold Lee built a cryosurgical probe that became the blueprint from which every subsequent liquid nitrogen cryosurgical probe has been designed.[33]

Prostate cryosurgery followed in the mid-1960s, when Gonder and colleagues were the first to develop a modified apparatus and probes suitable for the transurethral freezing of prostatic tissue.[34] This was extended by Flocks and colleagues to a perineal approach to the gland.[35] Between 1961 and 1970, other cryosurgical apparatuses were developed using liquid nitrogen and other cryogenic agents, including nitrous oxide, carbon dioxide, argon, ethyl chloride, and fluorinated hydrocarbons. Clinical applicability however was derived from the understanding of the Joule-Thomson effect, which is still the fundamental basis of modern cryoablation devices.[36]

4.1.4.2 Principles and state-of-the-art techniques

Joule-Thomson

The Joule-Thomson effect was named in honour of James Joule and William Thomson (better known as Lord Kelvin), who discovered that when a gas is expanded through a pinhole valve, its temperature decreases. They discovered that in gases such as argon, the gas atoms stick to each other, whereas in others, such as helium, they repel each other. A sticky gas packed into a small volume at high pressure is subject to numerous interactions with relatively low internal energy. After being released into a larger volume at a lower pressure, the molecules are subject to less interaction and have a larger internal energy. The conversion from a low-energy state to a high-energy state consumes energy, which is drained from the environment, resulting in a drop in temperature. Conversely, using a gas with repelling forces, a rise in temperature will occur, and the combined application of sticky and repelling gases will give control over freezing and thawing of tissue.[37]

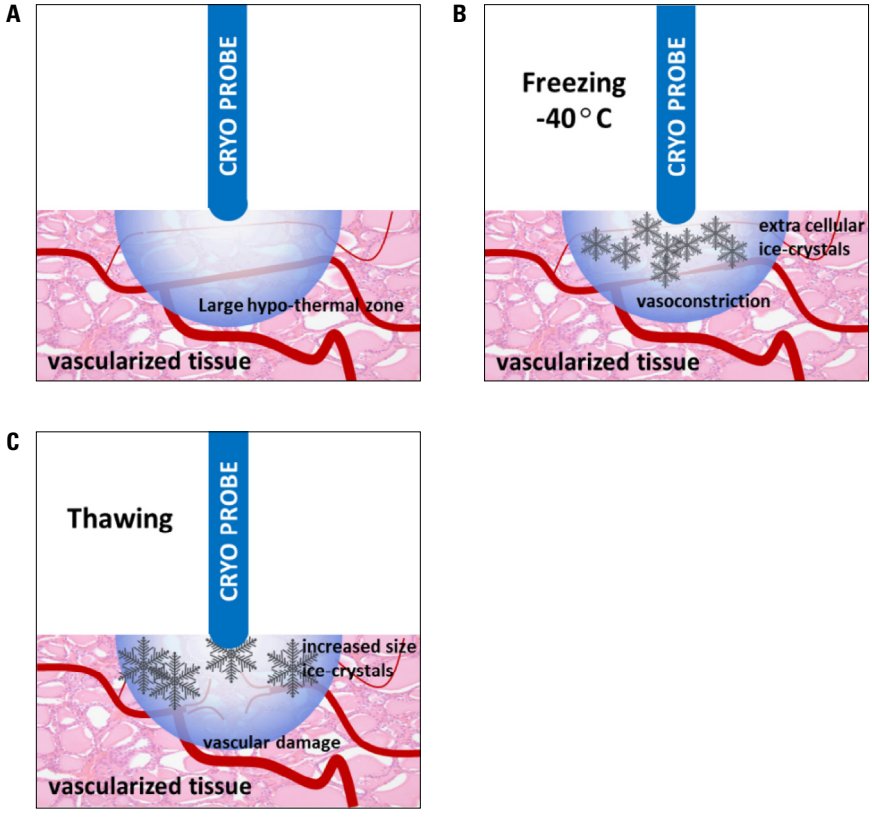

FIGURE 4-7
Photodynamic Therapy Procedure

A Using a probe that allows active freezing and thawing, a large frozen zone can be created.

B Freezing tissue to –40°C results in crystals that form primarily in the intracellular space.

C Subsequent thawing increases the crystal size, resulting in large cellular membrane rupture, followed by necrosis.

Vascular injury

Cryogenic methods for damaging tissue can be categorized by two different mechanisms of action: cellular injury and vascular injury. Cellular injury is mainly immediate, and vascular injury is largely delayed. Destruction of the vascular network and subsequent hypoxia of the probed tissue is considered to be the main mechanism of cell death in cryoablation. Vascular injury, which is slower to take effect, results from the progressive failure of the microcirculation, ultimately leading to vascular stasis and subsequent necrosis.[38] Freezing leads to vasoconstriction and a subsequent decrease in blood flow. Thawing will restore blood flow; however, damage to the endothelial layer leads to increased permeability of the capillary walls, edema, platelet aggregation, and microthrombus formation.[38]

Cellular injury

Cellular injury is induced by the formation of ice crystals, which in turn results in tissue desiccation. Crystallization occurs at –15°C; however, a temperature of –40°C ensures intracellular ice formation. When freezing cells slowly, crystal formation initially occurs in the extracellular spaces, which withdraws water from the system and creates a hyperosmotic extracellular environment. This, in turn, draws water from the cells. Freezing cells rapidly does not allow time for water to leave the cells and therefore keeps their solute freezing point higher. In this situation, the solution-effect injury is secondary to the results of intracellular ice crystal formation. The effect of thawing is that the ice crystals fuse and increase in size. As a result, cell membranes rupture, which causes additional damage.[38]

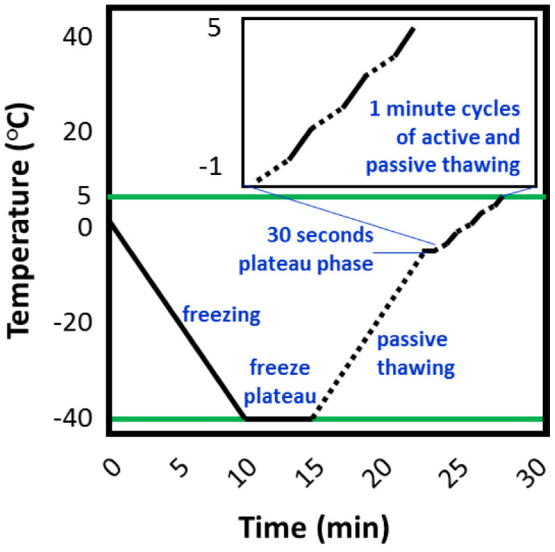

FIGURE 4-8
An Example of a Freezing-Thawing Cycle for Prostate Tissue

The overall freezing-thawing cycle takes about 25 to 30 minutes, starting with freezing until the –40°C point is reached. This temperature is held for 5 minutes, after which passive thawing reaches a plateau of about 30 seconds. After this plateau phase, a cycle of active thawing and freezing is initiated until a temperature of 5°C is reached. The complete cycle can be repeated if needed.

4.1.4.3 Future

Novel innovations in cryotherapy range from new freezing equipment that does not require gas as a cooling mechanism, to improved use of knowledge of freezing and thawing cycles. Recent equipment developments have led to systems that do not need a cryogenic gas or liquid, which presumably makes the system easier in use and transport. Additionally, cryoablation leaves behind a mass of dead cells, which the immune system can perceive as a threat. By adding immune-modulating drugs to a treatment protocol, the immune system can be altered and optimized for improved tumour cell removal.

4.1.5 Irreversible electroporation

4.1.5.1 History

One of the first descriptions of electroporation was mostly likely by J.A. Nollet in 1754. In his book, Nollet described a set of experiments in which red spots appeared on the skin after electric sparking.[39] This experiment was repeated by J.P. Reilly, who related the red spots to stratum corneum degradation.[40] Studies on the effects of electricity on biological materials intensified in the 18th century. J.W. Ritter studied the effects of direct currents and alternating currents on muscle tissue[324], previously described by Alessandro Volta[325]. Ritter observed that a contraction occurred when a strong current passed through a muscle nerve, an observation that was later called Ritter's opening tetanus.[324] G.W. Fuller reported the first work on irreversible electroporation (IRE) in 1898. In an experiment designed to purify the water of the Ohio River, he found that multiple high-voltage discharges applied to a sample of water had some bactericidal effects. Fuller's reported bactericidal effect is most likely due to IRE, based on the methods in which IRE is currently used for sterilization of fluids.[41] Because the formation of pores in cell walls had not yet been established, it is important to note that authors attributed such results to the thermal effects of electrical fields on biological materials.[42] It was not until the 20th century, in 1936, that McKinley concluded that damage caused to living tissues by high-frequency fields (10–100 MHz) cannot solely be from a thermal origin, particularly in the case of nervous tissue. This was confirmed by Doevenspeck in 1961, who described the use of electrical pulses to break apart cellular components for industrial food-related processing of animal meat

through non-thermal means. However he considered the effect to be non-thermal if the temperature increase was at most 30°C.[43] Towards the end of the 1960s, it was known that electrical pulses have a permeabilizing and thermal effect on the cell membrane. In the following years, most research was focused on the field of reversible electroporation. From 1990 to 2000, its mechanics, physics, and use to facilitate drug delivery were mainly studied, and in recent years interest turned to IRE as a tumour ablation modality.[44] In 2004 Davalos and Rubinsky filed a patent that proposed the use of IRE for tissue ablation.[45] In a subsequent paper, the technology was described as non-thermal with important implications in post-treatment healing,[46] and the first tests to treat cancer were reported in liver cells.[47] Ablative procedures with IRE in the prostate were first reported using canine prostates by Onik *et al.*,[48] and the first human applications were explored in 2007 by Rubinsky and colleagues.[49]

4.1.5.2 Principles and state-of-the-art techniques

Generator and electrodes

An IRE device consists of a low-energy direct current (LEDC) generator capable of connecting (16-gauge needle) electrodes. Various parameters to be adjusted in IRE ablation include voltage, pulse number, pulse length, electrode number, and electrode spacing. Irreversible electroporation procedures take place under general anesthesia with additional muscle relaxation in order to prevent severe muscle contractions that result from the electrical pulses. Irreversible electroporation pulses have the potential of causing cardiac arrhythmia, therefore synchronization of the IRE pulses with the cardiac rhythm is advised. This is performed by interfacing a synchronization device with the IRE console. The IRE electrodes are placed in a similar fashion to radiofrequency (RF) ablation or cryoablation probes. Parallel insertion of the probes is important to ensure an equal distribution of the electrical field. Generally practiced IRE settings for tumour ablation are: electrode spacing of 15 mm to 20 mm, electrode tip exposure of 15 mm to 20 mm, 70 to 90 pulses of 70 µs to 90 µs each, which are synchronized with an electrocardiogram, and a pulse intensity of 1500 V/cm. Due to fast repetition and microsecond pulse length, an IRE pulse cycle lasts only 5 to 10 minutes.

Electroporation effect

Electroporation or electropermeabilization uses an electrical pulse to create temporary pores in cell membranes. An electrical pulse at an optimized voltage that only lasts a few microseconds to a millisecond is discharged through the cell suspension. This disturbs the phospholipid bilayer of the membrane and results in the formation of temporary pores. These pores can remain open for a certain amount of time before they close again, and if the time is short enough the process is reversible. With the right voltage and pulse length, the pores can remain open long enough to make this process irreversible and result in apoptosis.[50]

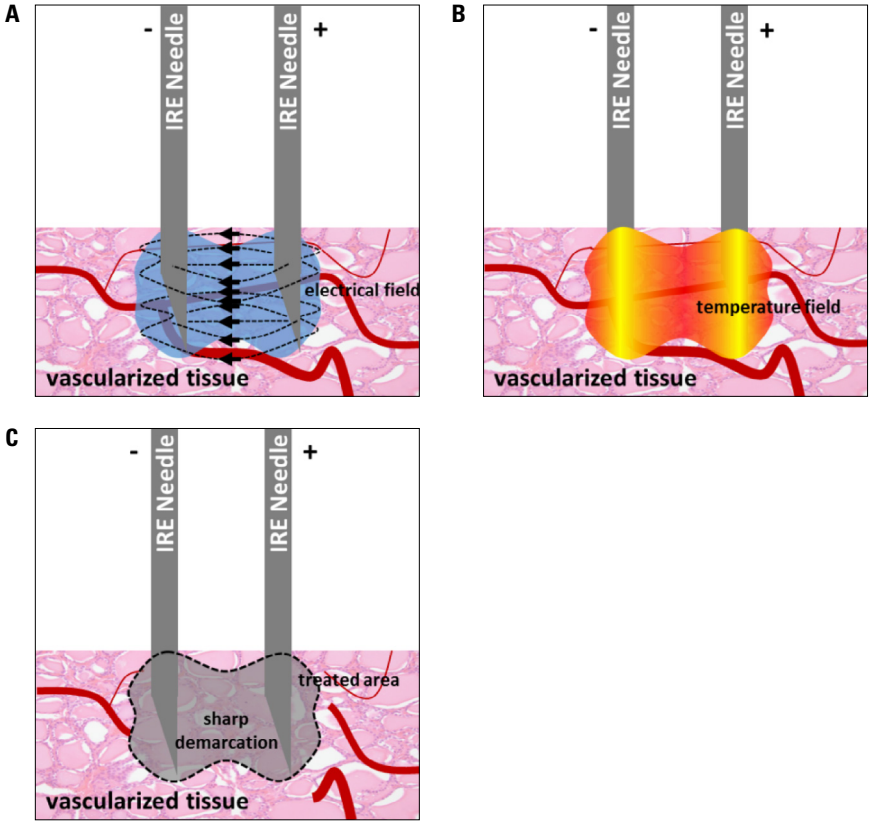

FIGURE 4-9
Irreversible Electroporation Procedure

A Ablation with electroporation is partially accomplished by the formation of pores in the phospholipid membrane of cells. With the right voltage and pulse length, the pores can remain open long enough to make this process irreversible and result in apoptosis.

B Simultaneously, theory and experiments have demonstrated a lethal thermal effect in tissue in clinically practiced settings.

C The resulting ablated area might be a combined result of the electrical and thermal field.

Thermal effect

It is known that the application of repetitive high-intensity electric pulses has the potential of substantially heating the targeted tissue and in effect causing thermal damage. Lethal cellular damage will occur within 4 to 6 minutes at temperatures above 50°C and almost instantaneously when temperatures exceed 60°C. van Gemert *et al.* performed a mathematical temperature simulation based on the electrical and thermal properties of prostate tissue in combination with clinically practiced IRE settings. Using an electrode spacing of 1 cm, the estimated temperatures reached between 92°C and 67°C at a distance 0.5 mm to 5 mm from the probes.[51] This was confirmed by *in vivo* experiments in porcine kidney by Wagstaff *et al.*[52] This temperature increase was not yet observed in prostate tissue. Although the presence of nanopores following the delivery of electrical pulses has been visualized using electron microscopy, it remains unclear whether these pores are the true mechanism of IRE-induced cell death.[53]

Advantages

Nevertheless, IRE appears to offer a number of advantages. First, it is not dependent on thermal energy and is therefore not influenced by "thermal sink." Second, IRE is confined to damage of the cell membrane, sparing tissue architecture and minimizing damage to blood vessels, nerves, and the renal collecting system. Irreversible electroporation lesions show a sharp demarcation between ablated and non-ablated tissue, whereas thermal ablation techniques show a transitional zone (TZ) of partially damaged tissue where insufficient temperatures were reached for definitive ablation.

FIGURE 4-10
Temperature Development Using Different Voltage Configurations

Temperature development during IRE over time for various voltages measured in a gel phantom with tissue mimicking electrical conduction properties using a thermal camera.

Adapted from van den Bos, et al. J Vas Interv Radiol. 2016;27:433-443.[326] *Printed with permission from authors.*

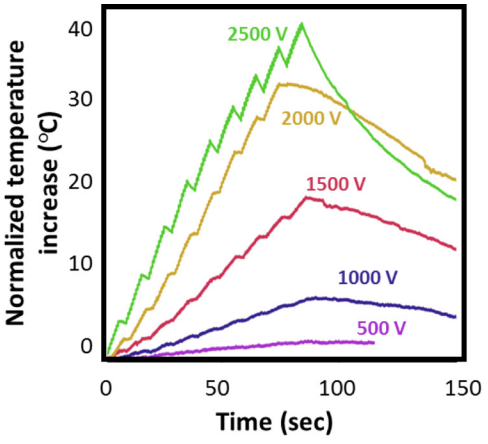

4.1.5.3 Future

Since the effects of IRE appear to be a both thermal and due to electroporation, ideas have been developed on the use of novel pulse trains that will reduce the thermal component. It has been hypothesized that adapting these intervals to longer time periods between the pulse trains allows the tissue to reduce heat. Additionally, the ability to treat large volumes is also under debate. Specifically, common lesion sizes with an IRE double-needle electrode system are only in the range of single centimetre. Larger lesion sizes can be created by introducing more needles. However, it was shown by Cannon *et al.* that this might hamper the precision needed to treat larger lesions and that eradication efficacy was lower for multiple-needle placements.[327] Recent research suggest that this is improved by optimized pulse timing.[54] Finally, thermal effect might also be reduced by the use of cooling during IRE. Future attempts to achieve truly cold IREs might restore all previously claimed benefits of the procedure.

4.1.6 Radiation oncology

4.1.6.1 History

The discovery of x-ray radiation by Wilhelm Röntgen in 1895 started an exciting era and field of physics and medicine.[328] However, several years before this invention, a medical student in Chicago named Emil Grubbe saw the peeling of his skin after radiation exposure and decided to treat a woman with locally advanced breast cancer.[328] One year after Röntgen's discovery, the first diagnostic x-ray was made, and Antoine-Henri Becquerel discovered that certain elements spontaneously emitted rays or subatomic particles from matter, a property that came to be known as radioactivity.[328] Pierre and Marie Curie extended this work when they discovered the radioactive elements polonium and radium.[328] During their experiments, they found that radium was able to kill diseased cells, the first observation of treatment capabilities by radiation.[328] This jump-started the field of radiation medicine and although the mechanism of action was unknown, cases of cancer regression were reported, as well as harmful effects when used inappropriately.[328] Most novel ablative technologies were not researched further during both world wars, with the exception of radiation, which was studied and used extensively as a diagnostic device.[328] Soldiers were trained to become radiation technologists, and in 1917, a brachy approach for the prostate was employed by Barringer *et al.* using a transperineal needle implant.[329] From 1910 to 1960, physicists and biologists continued to discover how radiation works and how to measure a dose accurately.[328] In 1953, the *rad* (1 rad = 100 ergs/g = 10 μJ/g)

was introduced as the unit of absorbed dose. In 1970, this was redefined to *gray* (joules absorbed per 100 kg). In the early days, external beam systems were developed, named linear accelerators.[328] Orthovoltage systems were used; however, they could penetrate only tissue to a depth of about 6 cm.[328] With the introduction of megavoltage systems in the 1960s, penetration depth was increased to 30 cm.[328]

In 1962, Malcolm Bagshaw demonstrated the curative potential of radiation therapy in PCa.[330] Parallel to external beam radiation, local or brachytherapy using radium for PCa was developed by Willet Whitmore.[331] Beginning in the 1970s, computers and novel imaging techniques were employed for treatment planning. This moved the external beam radiation field from 3D conformal radiotherapy (RT) using 3D computed tomography (CT) imaging to intensity-modulated radiotherapy (IMRT) and image-guided radiotherapy (IGRT), the standard of care for PCa nowadays (**Figure 4-11**).[328]

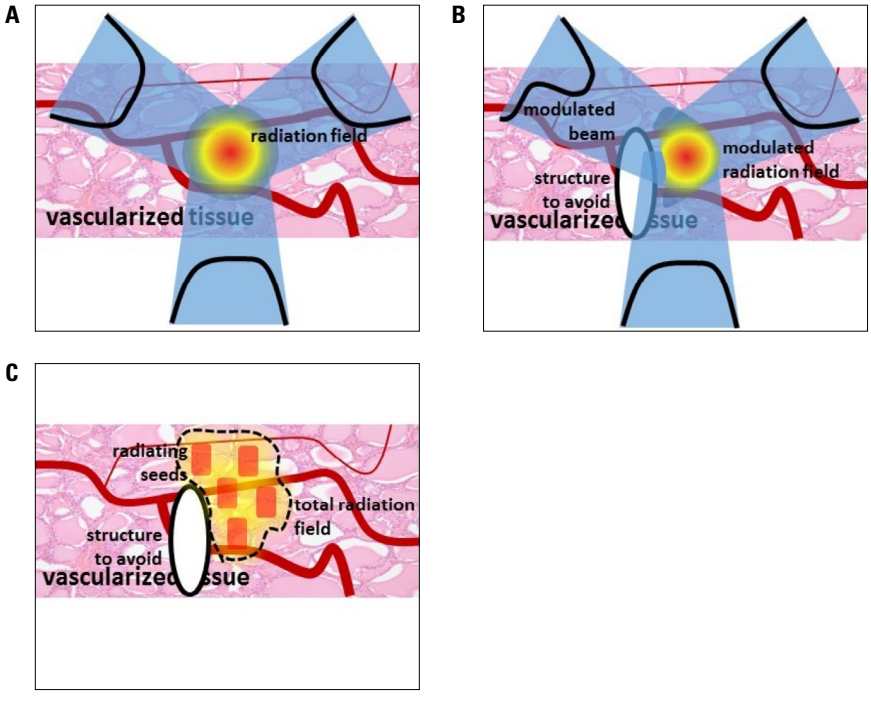

FIGURE 4-11
Radiation Therapy Procedure

Different aspects of radiation therapy, including

A dose fractionation,

B modulation of the radiation field, and

C brachytherapy.

4.1.6.2 Principles and state-of-the-art techniques

Radiation therapy

Radiation therapy uses ionizing radiation to kill cells directly, or indirectly via free-radical intermediaries formed from the radiolysis of cellular water. Ionizing radiation carries enough energy to free electrons from atoms or molecules, thereby ionizing them.

The most common type of radiation is high-energy photon radiation. The radiation is produced from a radioactive source such as cobalt or cesium, or with the use of a linear accelerator machine. The photon beam is then directed towards the location of the tumour in the body, passes through the cancerous cells and exits from the other side of the body. The high energy of the photons that pass through the body allows them to break the DNA bonds and inhibit the replication of cells. Particle

beams, generated by a linear accelerator, can also be used to irradiate tissue. Electron particle beams do not travel far into the human body and are therefore optimal to treat near-surface tissue. Proton particle beams experience less side scatter, as the proton beam does not widen much and the travel distance into tissue is controlled by the energy of the proton. Neutron beams are less frequently used and are an alternative to the other types of radiation therapy.

Dose fractionation

One of the most influential steps in the development of RT was dose fractionation. Most cancer cells replicate faster than normal cells. However, DNA can only be damaged when the cells are undergoing the replication process, also known as the radiosensitive phase of the cell cycle. Normal cells take longer to replicate and are therefore less affected than cancerous cells. If the total dose is delivered in small time–separated fractions, it will allow healthy tissue to repair sub-lethal damage and repopulate. It will also increase the damage to the tumour by reoxygenation of the tumour environment and reassortment of the probed cells into radiosensitive phases.

Intensity-modulated radiotherapy

As with dose fractionation, intensity modulation increased the efficacy of RT dramatically. Based on acquired 3D scans, the radiation beam is guided from many angles to the target. At each of these angles, the intensity of the radiation is varied (modulated) and the shape of the beam is adapted to match the shape of the tumour, which minimizes the impact on surrounding structures. In addition to intensity modulation, IMRT also uses inverse treatment planning with optimization by a computer.

Image-guided radiotherapy

Patient and organ movement poses a challenge in the treatment of PCa. As a result, prostate motion during RT can lead to underdosing the prostate and/or overdosing critical normal structures such as the rectum and bladder due to day-to-day variations. This is mostly circumvented by active image guidance. One method uses injected gold markers to visualize the prostate using CT before each treatment. Additional patient tracking by external cameras in the room could improve overall localization.

4.2 High-Intensity Focused Ultrasound Ablation: Transrectal

4.2.1 Description technology

The first description of HIFU was made in 1942, and its ability to destroy tissue was established in 1944.[55,56] In 1992 Chapelon *et al.* established the US parameters required to induce irreversible tissue lesions in animals. With the experimental adenocarcinoma of a prostate implanted in rats (R3327 AT2 Dunning tumour), they demonstrated that HIFU could be used to ablate the tumour and cure cancer without causing metastasis.[57] In 1993 Gelet *et al.* established that it was possible to induce irreversible coagulation necrosis lesions transrectally in the prostate of dogs without damaging the

rectal wall.[58] An ethics committee approved the evaluation of the use of HIFU for the treatment of localized PCa in humans. The results of a pilot study were published in 1996 and the preliminary results of the first 50 patients in 1999.[59,60]

HIFU produces US waves that are generated by a spherical transducer and the US energy is focused on a fixed point. The first experiments on the prostate were performed on dogs and on men with benign prostate hypertrophy.[58,61,62] Ultrasound waves deposit energy as they travel through tissues, however, for imaging purposes this deposited energy is insignificant. By increasing the intensity of the waves and focusing them on a single point, HIFU deposits a large amount of energy into the tissue, resulting in tissue destruction through cellular disruption and coagulative necrosis.[63]

There are two mechanisms involved in the destruction of the tissue: thermal effects and cavitation.[64] The thermal effect relies on the absorption of US energy by the tissue and its conversion into heat. Under the right conditions, the temperature within sonicated tissue will rise to a level sufficiently high enough to induce irreversible damage. Cavitation is the result of the interaction between US and microbubbles in the sonicated tissue. This interaction may lead to oscillations of these microbubbles, violent collapses, and dispersion of energy, all enhancing tissue ablation. The aim is to treat the entire gland by a juxtaposition of elementary lesions. The main sonication parameters are acoustic intensity, duration of exposure, the on/off ratio, the distance between two elementary lesions, and the displacement path when multiple lesions are made. This technique has the advantage of a transrectal treatment route with prostate destruction while sparing the rectum itself. By combining a precise control of the position of the transducer within the rectum and an active cooling of the rectal mucosa, the risk for rectal injury is minimized.

HIFU-induced lesions are visible using standard US as hyperechoic areas, but their extent is not always accurately defined. Magnetic resonance imaging (MRI) is the gold-standard technique used for HIFU treatment efficacy assessment. Gadolinium-enhanced T1-weighted (T1W) images can very clearly show the extent of necrosis.[65] Magnetic resonance imaging has also been used to guide HIFU treatment as well as to monitor temperature changes during HIFU, but it must be noted that this technology is experimental for transrectal PCa treatment.

4.2.1.1 Currently available HIFU devices

Three HIFU devices are currently available for the treatment of PCa: Sonablate® (SonaCare Medical, Indianapolis, United States), Ablatherm® (EDAP TMS S.A., Vaulx-en-Velin, France), and Focal One® (EDAP TMS S.A., Vaulx-en-Velin, France).

The Sonablate® 500 uses a single transducer (4 MHz) for imaging and treatment. Several probes are available with focal lengths from 25 mm to 45 mm. The size of the elementary lesion is 10 mm in length and 2 mm in diameter. The Sonablate procedure is conducted in a dorsal position with the patient lying on a conventional operating table. Sonablate uses a single treatment protocol, and the operator must manually adapt the power. The treatment is usually made in three consecutive coronal layers that start from the anterior prostate area and move to the posterior area, and at least one probe switch is made during the procedure.[66] The probe is chosen to match the prostate size, with larger glands requiring longer focal-length probes.

The latest generation of Sonablate (Sonablate 500) uses a Tissue Change Monitoring (TCM) system that allows visual confirmation of the treated prostate. The TCM's colour-coding feature highlights tissue that was not been adequately "heated", alerting the operator of the need to retreat that section of the prostate in real time for confirmation of adequate treatment of the entire prostate. An RF signal is sent to the treated prostate site before HIFU delivery, with another RF signal sent to the same site after HIFU delivery. Tissue change monitoring calculates and displays the change that occurred, with tissue change quantified through comparison of RF US pulse-echo signals at each treatment site.

The Ablatherm® Integrated Imaging incorporates both the imaging (7.5 MHz) and therapeutic (3 MHz) transducers into a single endorectal probe focused at 40 mm. A custom bed is required with the Ablatherm device, where the patient lies in a lateral position. The lateral treatment position permits gas bubbles produced through the heating of prostatic tissue to rise with gravity to a position lateral to the prostate, thus reducing the risk of acoustic interference with the HIFU waves.

The Ablatherm device includes four treatment protocols specifically designed for the treatment parameters required in different clinical indications. These include standard, HIFU re-treatment, post-external beam radiation therapy (EBRT), and post-brachytherapy. The size of the elementary lesion varies from 19 mm to 26 mm in length, and is 1.7 mm in diameter. Ablatherm Integrated Imaging offers real-time US monitoring of treatment. The HIFU probe is robotically adjusted, with a permanent control of the distance between the transducer and the rectal wall. Repeating the shots and moving the transducer, which is defined by the operator in the planning phase, treat a precise volume. Treatment is made in transversal layers. The device has many safety features, including control of the distance between the transducer and the rectal wall; a urethral cooling system; and a patient motion detector.

Treatment planning is slightly different between the two devices. With the Ablatherm, the prostate is divided into four- to six-volume boundaries and treated from the apex to the base slice-by-slice by an entirely computer-driven probe.[67] With the Sonablate, the treatment is usually made in three consecutive coronal layers, starting from the anterior part of the prostate and moving to the posterior part, with at least one probe switch during the procedure.[66]

The risk for urethrorectal fistulas (URFs), which was the only significant complication in the early stages of HIFU development, has been dramatically reduced (incidence between 0% and 0.5% for primary procedures in contemporary series).[68–71]

The Focal One is the latest and most advanced HIFU device for the treatment of PCa. With this device, the procedure is performed with the patient in the lateral position using a conventional operating table. Included in this device is the new dynamic-focusing transducer, made of 16 isocentric rings. Each ring is driven by a dedicated electronic system comprised of 16 different power lines. Adjustment of the respective phases of the 16 electrical signals supplying the transducer allows the operator to electronically steer the US beam and move the focal point of the transducer to a maximum of eight different points that are 32 mm to 67 mm away from the transducer.

Treatment with dynamic focusing involves unitary HIFU lesion stacking within the prostate along the transducer US beam axis. Each lesion size is as small as 5 mm, and by stacking two to eight unitary lesions it is possible to extend the necrotic lesion by 5 mm to 40 mm in order to adequately target either small or large prostate glands. Each US pulse lasts one second, and there is no interruption time between the different US pulses. Compared with HIFU treatment using fixed focusing, dynamic focusing allows the treatment of larger prostates because the maximum lesion height is 40 mm instead of 26 mm with previous-generation devices. The wide range in lesion height (5–40 mm) enables highly precise contouring of the prostate, and treatment duration of PCa is shortened with the continuous shooting process and lack of interruption between firings. Finally, HIFU using dynamic focusing is anticipated to provide a more homogeneous necrotic zone due to improved energy distribution within the prostate.

Focal One is the first HIFU device specifically designed for focal therapy of PCa, and combines all the necessary tools to visualize, target, treat, and confirm the focal treatment. The process is divided in four logical steps: treatment preparation using imported MRI images and fusion with real-time US volume; focal target definition; application of precise destructive energy; and confirmation of the devascularized target area.

Focal One is capable of importing standard Digital Imaging and Communications in Medicine (DICOM) magnetic resonance (MR) images. Using this MR volume image, the operator can define the contours of the prostate and one or several regions of interest (ROIs) that have been confirmed as prostate tumours. These contours can be performed on a desktop computer or on Focal One just before beginning the treatment. The operator on the live US volume feature of the Focal One transrectal probe executes the same prostate contouring. The software automatically registers the two volumes and proceeds to an "elastic fusion"; the live US volume is used as the reference volume, and the MR volume is smoothly deformed to every dimension, so that the 3D contour of the prostate on the MR volume matches perfectly in three dimensions to the contours of the prostate on the US volume. The same 3D elastic transformation is applied to the ROI initially indicated in the MR image so they appear at the adequate position on the live US image.

The application of HIFU energy is planned for transversal slices. On each slice, the operator defines the contour of the area to be treated. The section of the ROI initially defined on MR image and transformed in the previous elastic fusion step automatically appears on the live US image of the transversal view being planned, serving to guide the planning process by surrounding the tumour focus with the appropriate margin. The Focal One software automatically directs the focus of the HIFU shot to entirely destroy the defined area. Delivery of HIFU energy begins when all slices within the block are defined.

Focal One is equipped with the latest generation of HIFU probe (dynamic focusing) and is able to electronically vary the focal point along the acoustic axis using a HIFU-phased array transducer. The focal point can be steered from 32 mm to 67 mm away from the probe without any mechanical movement. A longer lesion is achieved by stacking unitary 5 mm HIFU lesions. At any point during the HIFU energy delivery process, the operator can observe a live US image of the treated area, and if necessary pause the treatment to readjust the treatment planning in the case of a shifting prostate or change in some other aspect, such as swelling.

At the end of the treatment process, while the probe remains in the patient's rectum, the integrated US probe is able to acquire a contrast-enhanced ultrasound (CEUS) volume after intravenous (IV) injection of microbubbles (SonoVue®, Bracco, Switzerland). The acquired volume clearly shows the devascularized area. This image volume can be superimposed with the treatment planning and the initial MR image showing the targeted lesions. The physician can choose to complete treatment by planning additional HIFU energy spots.

4.2.2 Clinical data

4.2.2.1 Indication and patient selection

Whole-gland ablation

The recommendations and updated guidelines on the use of HIFU for PCa as a primary treatment option concern patients with localized PCa (clinical T1–T2 stage Nx/0 M0 PCa) who are not suitable for a radical prostatectomy (RP) for reasons including age >70 years, life expectancy ≤10 years, and major comorbidities precluding surgery, or those who refuse to undergo surgery.[72,73]

Focal treatment

There is still no recommendation in the guidelines for focal treatment of PCa. Focal therapy is investigational, and should be performed in clinical trials.

Ideally, candidates for focal therapy should undergo transperineal template mapping biopsies or multiparametric MRI (mp-MRI) with transrectal ultrasound (TRUS) biopsy (Bx) with an MRI/US fusion system. Focal therapy should be limited to patients with a low to moderate risk.

The aim of focal HIFU is to treat the cancer foci inside the prostate gland by juxtaposition of elementary lesions. The transrectal route offers an excellent acoustic window to ablate the prostate. The combination of focused US sources and active cooling of the rectal mucosa minimizes the risk for rectal injury. HIFU-induced lesions are visible with standard US as hyper-echoic areas, but their extent is not always accurately defined visually.

Magnetic resonance imaging (MRI) is the gold standard technique for assessing HIFU treatment efficacy. Gadolinium-enhanced T1W images can effectively reveal the extent of necrosis.[74] Magnetic resonance imaging has also been used to guide and monitor temperature changes during HIFU treatment, but it should be noted that this technology remains in the early preclinical stage of evaluation for use in transrectal PCa treatment.

More recently, CEUS demonstrated that ablated (devascularized) and viable (enhancing) tissue could be distinguished immediately after HIFU treatment.[75] Pulse echo US backscattered signals have also been used to estimate changes in tissue properties induced by HIFU.[76] These less-expensive, US-based techniques are now incorporated into routine clinical use with different devices for assessing post-HIFU thermal injury to prostatic targets.

4.2.2.2 Contraindications

There is no definitive contraindication of HIFU. Nevertheless, intense prostate calcifications may block the US beam, resulting in an incomplete treatment and a risk for posterior accumulation of energy that may lead to rectal injury unless removed by transurethral resection of the prostate (TURP). Bowel pathology, such as inflammatory disease, is a potential contraindication because treatment is applied using a transrectal approach. Anatomical conditions that interfere with probe introduction or placement within the rectum are a potential contraindication.

Finally, rectal wall thickness >6 mm is a contraindication for the Sonablate and the Ablatherm devices. This drawback does not apply to the Focal One device because it is able to electronically vary the focal point along the acoustic axis to adjust to any rectal wall.

4.2.2.3 Outcome

Whole-gland ablation

Among publications on HIFU as a primary therapy for PCa, 16 studies report a series of at least 50 patients,[66,70,71,77–89] while the others report on fewer patients.[67,90–92] Follow-up varies significantly between series (range: 6 months to 6.4 years). In most cases, the prostate-specific antigen (PSA) nadir was reached 3 to 4 months after the HIFU treatment and was ≤0.05 ng/mL in 55% to 91% of the cases. Many studies have demonstrated that the PSA nadir was a significant predictor of HIFU failure. Patients with a PSA nadir over 0.5 ng/mL must be carefully monitored.[70,85] A PSA nadir >0.2 ng/mL after HIFU has been associated with a four times greater risk for treatment failure (as defined by cancer on Bx after HIFU).[93]

The 7-year disease-free survival (DFS) rate in the longest follow-up multicentre study was 75%, 63%, and 62% for low-, intermediate-, and high-risk patients, respectively, and the 8-year, cancer-specific survival rate was 99%.[77] Complication rates were low, with sloughing occurring in 0.3% to 8.6% of patients, impotence in 20% to 77% of patients, and bladder outlet obstruction in 12% to 22% of patients. The incontinence rate reported in a recent study was grade 1 in 4% to 17.5% and grade 2 and 3 in 0% to 5% of patients.[94,95] From a single centre, the 8-year biochemical DFS rates (Phoenix definition) were 76%, 63%, and 57% for low-, intermediate-, and high-risk patients, respectively ($p<0.001$) after whole-gland treatment. At 10 years, the PCa-specific survival rate and metastasis-free survival rate (MFSR) were 97% and 94%, respectively.[96]

In a study from a prospective database, Shoji *et al.* included 326 patients who filled out self-administered questionnaires on urinary function, quality of life (QOL), and sexual assessment.[97] The Functional Assessment of Cancer Therapy-General (FACT-G), Functional Assessment of Cancer Therapy-Prostate (FACT-P), and International Index of Erectile Function-5 (IIEF-5) were used. Maximum flow rate and residual urine volume were significantly impaired at 6 months ($p=0.010$) after HIFU, even if they returned to baseline values at 12 or 24 months after HIFU. The total FACT-G score significantly improved at 24 months ($p=0.027$) after HIFU. At 6, 12, and 24 months after HIFU, 52%, 63%, and 78% of the patients who had not received neoadjuvant hormonal therapy were potent, respectively.

In a prospective study, Li *et al.* compared the IIEF score, penile colour Doppler US, and penile length and circumference of patients treated for PCa with HIFU or cryoablation.[98] A total of 55 patients in the HIFU group and 47 in the cryoablation group were included. At 36 months, cryoablation patients experienced a lower erectile function recovery rate compared with HIFU patients (cryoablation=46.8%; HIFU=65.5%; p=0.021). No significant decreases in penile length and circumference were found in the two groups (all p values ≥0.05). Finally, HIFU treatment seems to be standardized with similar outcomes between centres.[72]

In the case of incomplete treatment or treatment failure, HIFU does not result in a therapeutic impasse. Unlike radiation, there is no dose limitation and no limited number of sessions. The re-treatment rate is estimated in the literature to be between 1.2% and 1.47%.[66,69,77,87] The morbidity related to repeat HIFU treatment for localized PCa has been studied on 223 patients with a re-treatment rate of 22%. While urinary infection, bladder outlet obstruction, and chronic pelvic pain did not significantly differ after one or more sessions, a significant increase was observed for urinary incontinence and impotence in the group which required retreatment.[69]

Salvage HIFU after external beam radiation therapy

There appears to be a role for salvage HIFU therapy with curative intent for patients with a locally proven recurrence after EBRT and without metastasis. Local control was achieved with negative biopsies in 73% of the cases with a median PSA nadir of 0.19 ng/mL.[99] With a mean follow-up of 18.1 (3–122) months, the overall actual 5-year specific survival rate was 84%. The actual 3-year progression-free survival (PFS) (PSA greater than nadir + 2 ng/mL, positive Bx, or salvage treatment requirement) was 53%, 43%, and 25%, respectively, for low-, intermediate- and high-risk patients according to D'Amico's risk groups. Disease progression was inversely related to the pre-HIFU PSA and the use of androgen deprivation therapy (ADT) during PCa management.

In a recent study, we examined the outcomes of salvage HIFU in 290 consecutive patients (non-published data). The mean PSA nadir post-HIFU was 1.54±3.38 ng/mL (median 0.14 ng/mL). The estimated cancer-specific and metastasis-free survival rates at 5 and 7 years were 80% (95% CI: 72.7–88.5) and 79.6% (95% CI: 73.5–86.2), respectively. In the multivariate analysis three factors were significantly linked to disease progression. The increase of the PFS rate (PFSR) with the pre-HIFU PSA level was statistically significant (p=0.0002). A previous AD treatment increased the PFSR by a factor of 1.3 (p=0.01) and a Gleason score (GS) ≥8 increased it by a factor of 1.2 (p=0.01) compared with a GS ≤6. While the technique offers promising results, it has to be weighed against the side effects.

Since 2002, the Ablatherm device included specific acoustic parameters for salvage HIFU. The acoustic dose was adapted to the low blood flow inside the gland fibrosis induced by radiation. For incontinence, 54% of the patients had no incontinence after salvage HIFU and 25% had a grade 1 incontinence (no pads + grade 1=79%). The risk for URF was only 0.4% with the introduction of a specific treatment algorithm designed for radiation failure. The impotence rate increased from 36.9% before salvage HIFU to 58.7% after treatment.[100] With the Sonablate, the biochemical survival rate was 71% at 9 months[101] and 52% at 5 years.[102]

Nevertheless, the risk-benefit ratio of salvage HIFU compares favourably with those of the other available techniques and with less morbidity and similar oncological outcomes. In this context, HIFU appears to be an effective curative treatment option for local recurrence after radiation failure.

Salvage HIFU after brachytherapy

Sylvester *et al.* reported 15-year biochemical relapse-free survival (BRFS) rate and cause-specific survival following iodine-125 prostate brachytherapy in 215 patients. Fifteen-year BRFS for the entire cohort was 80.4%, and the cancer-specific survival rate was 84%.[103] There was no significant difference between the low- and intermediate-risk groups. Salvage surgery is a challenging procedure after brachytherapy.[104]

A study with the Ablatherm device is currently being conducted in Lyon, France, and includes 26 patients with a mean age of 67 years with MRI- and Bx-proven recurrence after brachytherapy (non-published data). Nineteen patients underwent whole-gland ablation and seven underwent focal therapy (hemiablation). The mean follow-up was 19 months. The mean PSA before HIFU was 5.02±4.8 ng/mL, (median PSA=0.35 ng/mL). Nine patients have undetectable PSA with no hormonal deprivation treatment, eight needed hormonal deprivation treatment for a rising PSA, and nine are recent cases with a very short follow-up. The complication rate was high in the first nine cases with three urinary incontinences (grade 3) and one URF. For those first patients, we used the treatment acoustic parameters defined for radiation failure.

Because of the high rates of rectal injury and severe incontinence, new treatment parameters specifically designed for brachytherapy failure were developed with a decrease in the acoustic dose according to the intensity of prostate fibrosis. Since the introduction of these new parameters, no URFs occurred and no rectal lesions were seen on control MRI, and there was no reduction of treatment efficacy.

HIFU focal therapy as primary care treatment

In 2008, Muto *et al.* reported the outcomes of 29 patients treated with the Sonablate device.[105] In selected patients with cancer confined to a single lobe based on multi-regional Bx, the total peripheral zone and a half-portion of the TZ were ablated. The average prostate volume decreased from 35.8 cc to 30.3 cc, and mean PSA level decreased from 5.36±5.89 ng/mL to 1.52±0.92 ng/mL at 36 months. Of the 29 patients, 28 underwent control Bx 6 months after the procedure. Residual cancer foci were found in three patients (10.7%).

At 12 months post-HIFU, 17 patients underwent control Bx. Residual cancer foci were found in four patients (23.5%); only one patient had a urethral stricture. No significant differences were found in 2-year DFS rates between low- and intermediate-risk patients with whole-prostate treatment (90.9% vs. 49.9%, respectively) and focal therapy (83.3% vs. 53.6%, respectively). Indwelling urethral catheter following HIFU remained in place a mean of 15±4 days. The frequency of urethral stricture and urinary tract infection was 4% for each. No significant changes were found in International Prostate Symptom Score (IPSS) and maximal flow rate pre-HIFU and 12 months post-HIFU. No information was provided regarding erectile function.

Ahmed *et al.* presented the first published series of prostate hemi-ablation with HIFU.[106] Patients with low-moderate risk (GS ≤7, PSA ≤15 µg/mL), unilateral (≤T2bN0M0) PCa on TRUS Bx underwent multi-sequence MRI (T2-weighted [T2W], dynamic contrast-enhanced [DCE], diffusion) and 5 mm-spaced transperineal template Bx for disease localization. All patients received transrectal HIFU that involved ablation of the entire positive hemi-prostate up to the urethra. Of the 20 patients (mean age, 60.4 years), 25% had low-risk and 75% intermediate-risk PCa. Before HIFU, the mean PSA was 7.3 ng/mL, 95% were pad-free, and 95% could achieve an erection sufficient for penetration. At 12-month follow-up, mean PSA decreased to 1.5±1.3 ng/mL and 89% had no histological evidence of cancer. Two patients (11.1%) had a positive Bx at 6 months with residual 1 mm GS 3+3; one elected to have HIFU retreatment, and the other active surveillance (AS). Trifecta status was achieved by 89%.

The Association Française d'Urologie (AFU, French Urological Association) initiated a prospective multi-institutional study (2009–2015) to evaluate HIFU hemi-ablation as primary treatment for patients >50 years, stage T1 or T2, PSA <15 ng/mL, GS ≤7, with unilateral cancer. A total of 111 patients were treated, with a mean age of 64.8±6.2 years and mean PSA of 6.23±2.57 ng/mL. Gleason score was ≤6 in 74% and 7 in 26%. Clinically significant cancer (CSC) at follow-up (6–12 months) Bx was defined by presence of GS of 7 or maximum cancer core length >3 mm in the prostate. The primary outcome was the absence of CSC at Bx. The secondary outcomes were genitourinary side effects measured with validated questionnaires.

The patient selection was performed with pre-Bx MRI, and systematic and targeted transrectal biopsies to localize the cancer. Cancer was treated by HIFU template hemi-ablation of the gland. The PSA nadir value was 1.9±1.5 ng/mL and the PSA at 12 months was 2.5±2.10 ng/mL (mean decrease of PSA: 59.9%). Ninety patients of 101 (89%) had histological absence of significant disease (GS 7 or maximum cancer core length >3 mm); 5% had a treated side and 5.9% had an untreated side. However, 32.7% of men had persistent cancer of any threshold. Additional therapies included AS (*n*=16 [48.5%]), second-HIFU (*n*=8 [24.2%]), EBRT (*n*=3 [9%]), radical surgery (*n*=6 [18.2%]). The radical treatment-free survival rate at 2 years was 89%. At 12 months the continence (pad-free) rate was 97% and erectile function was preserved in 40 of 51 patients with pre-HIFU IIEF-5 ≥16 (78%).[107]

In 2012, Ahmed *et al.* published a prospective trial of focal therapy for localized unifocal and multifocal PCa.[108] Forty-two patients with localized PCa were included (stage T1/T2, PSA ≤15 ng/mL, GS ≤4+3: 7), 27% had low-risk, 63% intermediate-risk, and 10% had high-risk PCa. Patients received HIFU focal therapy using the Sonablate 500 device, delivered to all suspected tumour lesions that were localized using mp-MRI and transperineal template-mapping Bx. A maximum of 60% of the prostate was ablated. The edge of the ablation zone was ≥10 mm from a neurovascular bundle (NVB) in unilateral disease, and ≥5 mm from the NVBs in bilateral disease. Of 41 treated patients, 49% received unilateral single-area ablation, 37% received bilateral two-area ablation, and 15% received a midline one-area ablation. All patients were able to void through the urethra on the first postoperative day.

A significant decrease in PSA was reported at 12 months, with median baseline PSA of 6.6 ng/mL and 1.9 ng/mL at 12 months (p=0.0001). Histological evidence of tumour was negative in 30 of 39 (77%) patients biopsied at 6 months. Of the 39 men biopsied (transrectal route) at 6 months, nine (23%) had evidence of tumour, and three (8%) had evidence of clinically significant tumour (Epstein criteria:

GS >3+3, > 2 cores positives, >2 mm involvement). Of those with positive Bx, five were placed on AS and four received a second HIFU session. None of the four men undergoing a repeat focal therapy consented to further biopsies, but all received control MRI.

After retreatment in four patients, 39 of 41 (95%) had no evidence of disease on mp-MRI at 12 months. All 38 men were pad free at baseline and remained pad free at 12 months. IPSS score improved, with a decrease between baseline and 12 months (p=0.026). Of the 35 men with good baseline erectile function, 31 (89%) had erection sufficient for penetration 12 months after focal therapy. Finally, of the 31 men with good baseline erectile function, 26 (84%) achieved the trifecta status of being leak free and pad free, with erections sufficient for intercourse, and no evidence of clinically significant disease on mp-MRI at 12 months. One patient experienced acute urinary retention requiring a urethral catheter for 5 days. One patient received a partial rectal wall injury with extravasation of urine outside the prostate. The patient was successfully managed with suprapubic catheter and quinolone antibiotics. This patient required an endoscopic dilatation for a delayed urethral stricture. Two patients with large prostate size required a limited TURP because voiding did not return to normal.

This study supports the proposition that tissue preservation leads to functional preservation. The histological outcomes were slightly less than those achieved after hemi-ablation, likely due to reduction in margin around the tumour.

High-intensity focused ultrasound—focal therapy as primary care treatment

Focal salvage HIFU (FSH) represents a new therapeutic option. The aim of FSH is to destroy the recurrent tumour with minimal risk of severe side effects. The initial results of this new treatment approach were recently published.[109]

In this trial, 39 patients received FSH therapy for localized recurrence after EBRT (hemi-ablation, n=16; quadrant ablation, n=23). Patients with multifocal tumour foci underwent index lesion ablation if the untreated areas had ≤1 core with ≤3 mm 3+3 GS. A PSA response was observed in 87% of patients; 44% of treated patients achieved a PSA nadir <0.5 ng/mL. Of those who achieved a nadir <0.5, the 3-year biochemical-free survival rate (BFSR; Phoenix criteria) was 63%. Of those who achieved a nadir >0.5, the 3-year BFSR was 0%. Two patients developed metastasis and 40% required salvage androgen deprivation therapy. Twenty-five patients (64%) were continent (pad free, leak free) at last follow-up. The mean pre-salvage IIEF-15 score decreased from 18±16 to 13±21 after FSH.

More recently, Baco *et al.*[110] reported the short-term results of hemi-salvage HIFU ablation (HSH) for unilateral recurrent PCa following radiation therapy. Between 2009 and 2012, 48 patients were prospectively enrolled from two European centres. Inclusion criteria were positive MRI and at least one positive Bx in one lobe after primary radiation therapy. Mean age was 68.8±6 years and the mean pre-HIFU PSA was 5.2±5.2 ng/mL. With a median follow-up of 16.3 months, the mean PSA nadir after HSH was 0.69±0.83 ng/mL.

Disease progression occurred in 16 patients (35.5%). Local recurrence was found in the untreated lobe in four patients, and bilaterally in four patients. Six patients developed metastases and two had rising PSA without local recurrence or radiologically proven metastasis. Progression-free survival (Phoenix criteria) rates at 12, 18, and 24 months were 83%, 64%, and 52%, respectively. No rectal

fistula was observed. There were no significant changes in European Organisation for Research and Treatment of Cancer Quality of Life Questionnaire (EORTC-QLQ)-C30 and IPSS scores. Pad-free, leak-free urinary continence status after HSH was attained in 36 of 48 patients (75%). Four patients (8.3%) experienced severe post-HSH incontinence. All four had a post-EBRT local recurrence involving the apex, and HSH was voluntarily performed without a sphincter safety margin. Three of the four did not show disease progression; their PSA values at last follow-up were 0.12, 0.05, and 0.07 ng/mL. No URFs were observed. Two patients (4%) experienced a delayed pubic osteitis that was conservatively managed.

There were no statistically significant differences in IPSS and QOL (EORTC-QLQ-C30) scores between baseline and follow-up. A significant decrease in erectile function score was observed (IIEF-5 score), with a median of 5 to 7.5 at 24-month follow-up. One URF occurred and was resolved with urinary and bowel diversion. Sloughing occurred in 18% of patients and urinary tract infection or epididymitis in 8%. No osteitis was observed.

4.3 High-Intensity Focused Ultrasound Ablation: Transurethral

4.3.1 Description technology

For energy delivery of HIFU, the transducer can be applied to various locations: transrectal, which is the most commonly applied method,[111,112] transurethral,[113,114] and extracorporeal (placing the transducer against the perineum).[113] MRI commonly guides the transurethral application of HIFU.

MRI-guided transurethral US ablation is a novel technology that precisely ablates the prostate gland using real-time MRI monitoring and active temperature feedback control, which makes this technology suitable for focal treatment of PCa. High-energy US is delivered by the device once inserted into the urethra and is used to heat prostate tissue to the point of thermal coagulation (thermal ablation). The treatment is conducted entirely within an MRI, which enables real-time temperature images of the heated region to be acquired during treatment. Magnetic resonance imaging is used during treatment to measure the temperature distribution in the prostate in real time, enabling closed-loop feedback control of the heating pattern and precise ablation of the target lesion.

Measurement of tissue temperature is possible through a variety of techniques; however, MRI thermometry based on proton resonance frequency shift[115,116] is the most widely applicable because of its tissue-type independence and linearity over the range of temperatures relevant for thermal ablation. In addition, it has been demonstrated to be able to measure *in vivo* temperature precisely and control US ablation.[117–119] Therefore, targeting can be confirmed using MR thermometry overlapping temperature maps onto anatomic images. Coupling US ablation with MRI for real-time temperature feedback control could improve the accuracy of treatment, thereby reducing the risk for damage to important surrounding anatomy such as the rectum, urinary sphincters, NVBs, and pelvic bone.[120]

Moreover, MRI is used prior to treatment to guide device positioning and perform treatment planning. After treatment, contrast-enhanced MRI can be used to visualize the area not perfused and assess the extent of thermal ablation. Technically, the US applicator is inserted through the urethra, and delivers US energy directly into the prostate gland (**Figure 4-12**).

FIGURE 4-12
Illustration of the MRI-guided Transurethral Ultrasound Therapy (TULSA) Device

Image courtesy of Profound Medical Corp., Toronto, Canada.

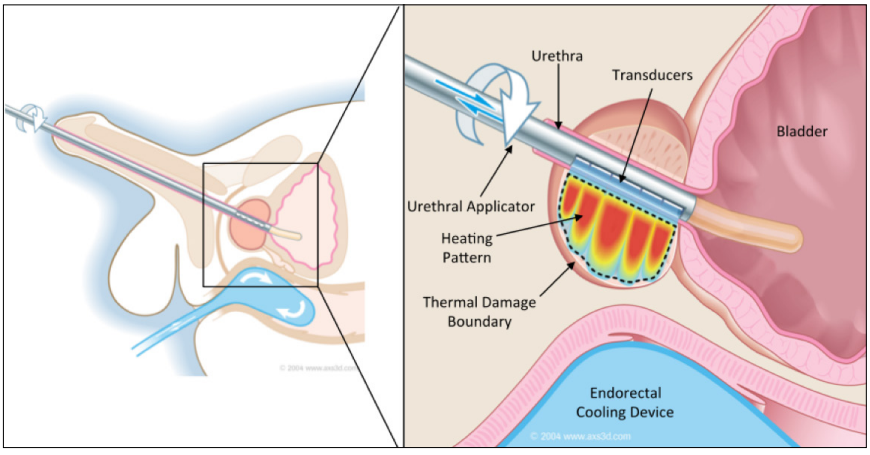

A linear array of 10 independent, rectangular transducer elements emits directional high-intensity US energy directly into the prostate, quickly raising tissue temperatures to thermal coagulation (**Figure 4-13**).

FIGURE 4-13
Representative Temperature Distribution Generated by the Ultrasound Applicator Along the Heating Direction

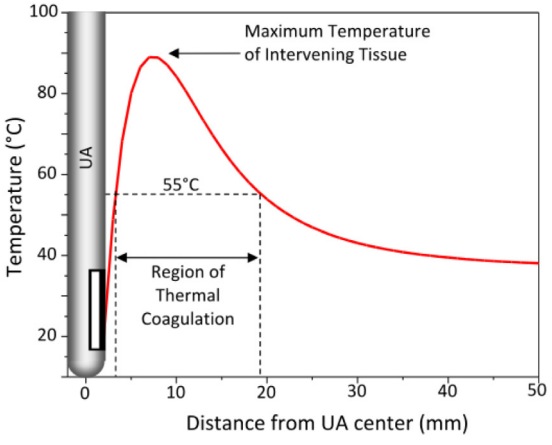

Water flows in the US applicator to cool the transducers and to couple the generated US to the tissue. A representative temperature gradient generated by the applicator in the direction of heating is shown in **Figure 4-13**. Maximum temperatures are maintained below 100°C to avoid tissue carbonization and boiling, both undesirable during US therapy. Using this technology, a reduction of treatment times can be achieved resulting in an ablation time of approximately less than 1 minute per 1 cc of prostate volume.[121,122]

There is one device for transurethral MR-guided HIFU ablation available, the MRI-guided transurethral ultrasound ablation (MRI-TULSA or TULSA-PRO™) from Profound Medical Corp. (Toronto, Canada), which was tested experimentally and in first human case series clinically. A similar prototype for transurethral MR-guided US therapy of the prostate was tested preclinically in dogs (Philips Healthcare, Vantaa, Finland).[123] Other systems have been developed to study the theory and feasibility of transurethral US ablation *in vitro* and *in vivo* in animal experiments.[124–129] In contrast to transurethral MR-guided systems, there are several transrectal MR-guided focused US ablation systems available, such as ExAblate® 2100 (InSightec, Haifa, Israel)[127,130–133] or various MR-compatible HIFU devices.[128,134,135]

The MRI-TULSA system (Profound Medical Corp., Toronto, Canada) has been developed and validated up to now experimentally by simulating theoretical treatments in computer models, verifying the performance in tissue-mimicking gel phantoms, validating the therapeutic approach in animal experiments, and showing safety and feasibility clinically in select patients.

Initial feasibility of using MRI-TULSA for prostate ablation has been evaluated extensively in computer simulations to optimize US device requirements, MRI thermometry specifications, as well as treatment delivery feedback control algorithms and treatment planning strategies.[120,121,136–139] Feasibility, accuracy, and precision of heating tissue to thermal ablation using a prototype transurethral US device under MRI guidance have been investigated in tissue-mimicking gel phantoms.[138,140,141] Apart from validation of this technology, tissue-mimicking gel phantom experiments were also used for refinement of the MRI protocols and thermometry sequences.[141]

The technique has been investigated *in vivo* in preclinical experiments using a canine prostate model.[133,142–145] These studies have shown the ability to accurately generate thermal damage *in vivo* that conform to target volumes within about 1 mm using closed-loop temperature feedback control. Histological analysis of the prostate tissue after treatment revealed a close relationship between necrosis and 55°C target temperature area on MRI thermometry. The boundary of thermal damage in histological analysis was very sharp, resulting in spatial distance of 3 mm between necrotic and viable tissue. The surrounding structures, such as urethra and sphincter, as well as the neighbouring organs were preserved. Importantly, the urethra could also be spared from damage due to temperature gradients generated by the transducer within a margin of approximately 1 mm to 2 mm.

Moreover, using the preclinical canine model, safety and feasibility were studied with a follow-up of 28 days.[122] The study showed that this technology is a safe and feasible procedure for the accurate and precise conformal ablation of prostate tissue.

Using a similar device, a prototype for transurethral MR-guided US ablation (Philips Healthcare, Vantaa, Finland), focal therapy of the prostate has been investigated in three dogs.[123] It was demonstrated that thermal dose estimates and ablation volumes on MRI correspond to the extent of necrosis and non-viability of cells found in histopathology. The device enabled multi-planar temperature monitoring, allowing for safe, targeted, and controlled ablation of prescribed prostatic lesions.

In clinical use, the procedure using the MRI-TULSA (Profound Medical Corp., Toronto, Canada) has been performed under general anesthesia.[119] The device is connected and used in conjunction with a 3 Tesla (3T) MRI, which is important for an appropriate spatial resolution. The presence of a cystostomy is important to drain urine, permanently ensuring a stable anatomical situation of the lower urinary tract. The treatment delivery control is a standard PC located in the MRI console room and is connected to the MRI host computer.

The fluid circuit hardware and system electronics are mounted to the system cart, typically located in the equipment room. The device requires two external grounded electrical outlets, one for the electronic system and one for the treatment delivery console. The general idea is to keep the high-power electronics outside of the MR suite in order to minimize the MR-compatible equipment and reduce imaging artifacts. Some electronics remain in the magnet room in a shielded enclosure to minimize the signals entering the room.

During treatment, the US applicator, the endorectal-cooling device, the positioning system interface box, and the positioning system are located inside the magnetic field environment. They are connected to the system cart via an electrical cable and fluid tubes. The cable passes through an electrically grounded filter box in the wall of the MRI suite, while the tubes pass through a waveguide. The US applicator and the endorectal-cooling device are inserted into the patient prior to treatment. Next, the US applicator is connected to the specially developed positioning system. Positioning of the US applicator and endorectal cooling device is verified by means of MRI and adjusted if necessary (**Figure 4-14**).

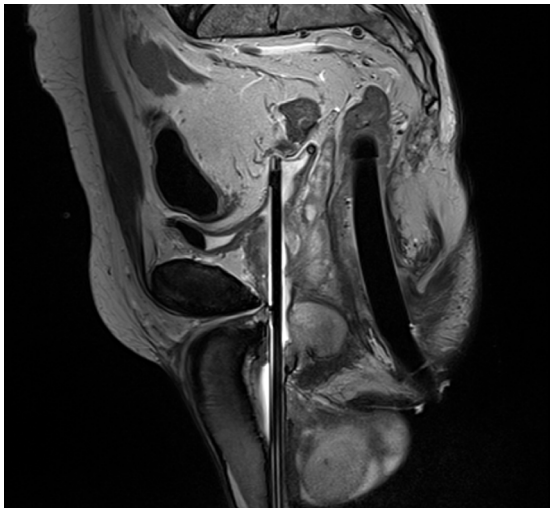

FIGURE 4-14
MRI-Guided Device (Ultrasound Applicator, Endorectal Cooling Device) Positioning

Image courtesy of Dr. Sascha Pahernik, Department of Urology, University of Heidelberg, Germany.

The endorectal cooling device is important for preventing thermal injury to the rectum. High-resolution treatment planning images of the patient's prostate and surrounding tissue are acquired by the MRI scanner and displayed on the treatment delivery console. The surgeon outlines the prostate boundary in multiple MRI planes using a custom treatment-planning interface within the software.

During treatment, real-time MR thermometry images are acquired, processed, and displayed on the user interface. The MR thermometry that is used (proton resonance frequency shift) is sensitive to tissue motions and changes in the local magnetic susceptibility that can be caused by the motion of an air bubble in the rectum. Therefore, air bubbles in the field of view should be avoided. Because of this, a spatiotemporal filtering of MR temperature artifacts has been developed to remove artifacts arising from bowel motions.[146] In addition, Buscopan® (hyoscine butylbromide) is usually administered intravenously prior to treatment to avoid peristalsis.

The control algorithm uses the temperature distribution information as feedback to control the US output power, frequency range, and US applicator rate of rotation to raise the temperature of the acute ablation boundary to the target temperature while keeping the temperature outside of the acute ablation volume below this value.

The operator can navigate through multiple MR images throughout the prostate and view the heating pattern in real time. The software monitors heat delivery in the prostate and takes appropriate action if excessive heating is detected.

The system has several advantages:

- Quantitative dosimetry *in situ*:
  - Using MR thermometry, the temperature pattern can be measured in real time during treatment.[115] The temperature information is given in 12 oblique-axial planes with a spatial resolution of 2 mm, a temporal resolution of six seconds, and a temperature uncertainty of 1°C .
- Adaptive temperature delivery:
  - The quantitative information about temperature distribution can be incorporated as feedback (**Figure 4-15**) into the energy delivery, allowing for modification of the treatment to the specific anatomical and pathophysiological requirements of the patient.[143]
- High spatial accuracy and precision:
  - The system allows a target boundary to be treated with an accuracy and precision of ±1 mm.[119,122]
- Treatment monitoring:
  - Contrast-enhanced MRI can be used to visualize the region of thermal damage immediately after treatment. Non-perfused areas have been shown to be in good agreement with histological findings as a marker for thermal coagulation.[117,147,148]

FIGURE 4-15
Magnetic Resonance-Thermometry Maps Overlaid on Corresponding T2-Weighted Pre-ablation Planning Magnetic Resonance Images

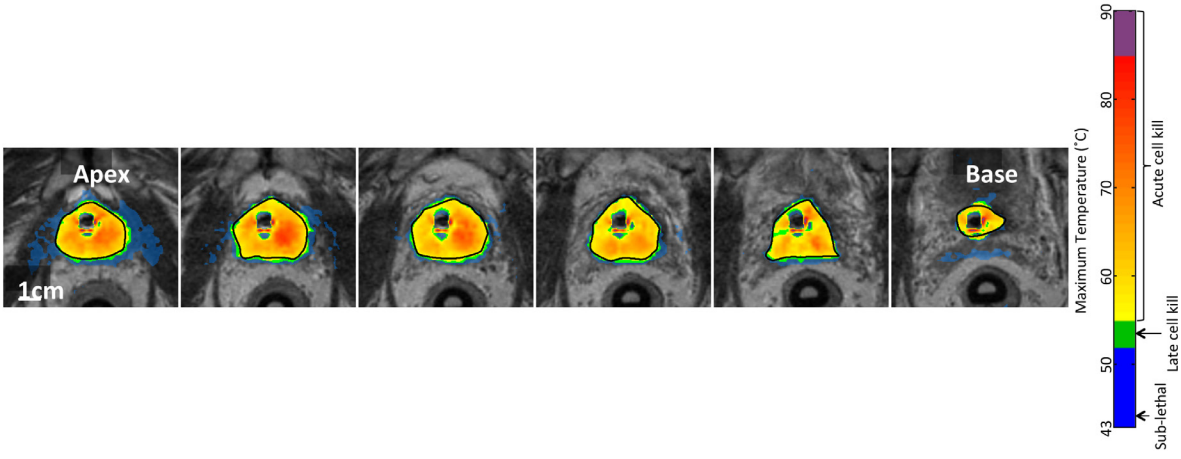

These requirements are important for focal treatment strategies. The transurethral approach for energy delivery overcomes some of the limitations associated with the transrectal approach, which requires pauses between sonication to avoid damage to the rectal wall, resulting in long treatment times.

The entire prostate gland can be treated in approximately 30 minutes by the transurethral approach. It also provides closer access to the anterior area of the prostate, which is especially important for large prostates. Fluid is required in the US applicator to couple the US to the surrounding tissue and to cool the US transducers. Cooling through the US applicator and the endorectal cooling device protects the urethra and the rectal wall from thermal damage. Therefore, the urethra can be spared, one of the functional advantages of the transurethral approach.

Disadvantages of the system include the complex infrastructure required for the procedure, such as the availability of an MRI suite, as well as the presence of different practitioners such as urologists, anesthesiologists, radiologists, and nurses. Moreover, a tumour adjacent to the urethra might not be treated efficiently due to the temperature gradients that are generated. Lesions in huge prostates located posteriorly to the peripheral zone might not be treated efficiently. The transurethral approach is limited to treatment of angular sectors.

4.3.2 Clinical data

Clinical data are available only for the MRI-TULSA (Profound Medical Corp., Toronto, Canada). Only one case-series study including a total of eight patients with organ-confined PCa (GS ≤7, PSA ≤15 ng/mL) has been reported.[119,145] Immediately after MR-guided transurethral US ablation, patients underwent RP. Ablation was performed focally around the urethra.

The study investigated the safety and feasibility with conservative aims to treat <30% of the prostate volume, far from any critical surrounding anatomy. Whole-mount histology sections confirmed the presence and extent of a continuous region of thermal ablation, correlating to the 55°C target

temperature maps. A clear demarcation between normal and ablated tissue with margins (≤3 mm) could be observed. There was an excellent agreement between the zone targeted for treatment and the zone of thermal injury. Clinical short-term and long-term outcomes as well as complications could not be assessed because patients underwent prostatectomy immediately after the procedure. The intraoperative period was uneventful. The authors concluded that the technology is safe and feasible for focal as well as for whole-organ treatment of the prostate. **[Level of Evidence (LOE) 3]**

A single-arm, prospective, phase 1 clinical trial has been performed investigating 30 patients to determine the safety and feasibility of the device (Clinical Protocol DOC-10246, Food and Drug Administration [FDA] IDE G130103, Health Canada ITA 199241, Eudamed No. CIV-13-04-010681).

Patients underwent prostate ablation as primary treatment for Bx-proven PCa (cT1c–cT2a; PSA ≤10 ng/mL; GS ≤7a). Under general anesthesia and cystostomy, the transurethral device was inserted and positioned in the prostatic urethra using MRI guidance. Conservative whole-gland treatment planning was performed under MRI prostate visualization, including a 3 mm safety margin at the prostate capsule, and 10% residual viable prostate tissue expected around the gland periphery.

Ultrasound treatment was delivered under continuous real-time MRI thermometry feedback control. Primary endpoints were safety (frequency and severity of adverse events) and feasibility (conformal thermal ablation on MRI thermometry and CE-MRI). Clinical follow-up included serial PSA, QOL questionnaires (IPSS, erectile function domain of the IIEF-15, and bowel habits domain of the University of California, Los Angeles Prostate Cancer Index Short Form [UCLA-PCI-SF]), 12-month prostate Bx, and MRI.

Specific technical contraindications for transurethral MR-guided US ablation of the prostate include:

- Suspected tumour on baseline MRI within 3 mm of the prostatic urethra, or in the prostate apex within 3 mm from the sphincter plane.
- Pathology (urethral stricture, bladder neck contracture, urethral fistula, urethral diverticulum) or prior interventions (TURP, urethral stenting, urethroplasty or chronic indwelling urethral catheter, brachytherapy, artificial urinary sphincter, or penile implant) of the lower urinary tract.
- Prostate calcifications >1 cm in diameter
- Median lobe of the prostate protruding significantly into the bladder resulting in an obstruction.

4.3.2.1 Summary

Novel transurethral MR-guided US ablation devices combined with real-time multi-planar MR thermometry is a safe and feasible technique in animal experiments and in first human case series, allowing for controlled ablation of the prostate. **[LOE 3]**

Recommendation

Clinical trials should be performed to investigate feasibility and safety of this technology and the oncological control and functional outcome of this treatment for PCa. **[Grade of Recommendation (GOR) C]**

4.4 Cryosurgery Ablation

4.4.1 Introduction

Prostate cryotherapy was first introduced in the early 1970s as a treatment for PCa, but never gained popularity due to high rates of recurrence and numerous complications associated with the procedure. The addition of a percutaneous approach, US monitoring allowing for cryotherapy probe placement to be accurately monitored in real time, and urethral warmers to prevent sphincter and urethral injury have made cryotherapy a more practical treatment option. Cryotherapy is not cancer specific and will kill all the cells in the ablated area. The process of cryotherapy occurs by lowering the temperature, resulting in intracellular dehydration, denaturation of cellular proteins, and metabolic failure, all of which cause apoptosis of the cells.[149] Complete cell death occurs at −40°C. The apoptotic cells are located on the peripheral region of the ablation area. As the ablated area thaws, further cell death occurs as the extracellular fluid shifts into the intracellular space causing the cells to burst. The freezing also results in loss of blood supply to the ablated area, further killing the cancerous cells and resulting in secondary necrosis of the targeted tissue.

For patients with localized, unilateral disease, focal cryotherapy is a viable treatment option. Unlike radical therapy that treats the entire prostate, focal cryotherapy treats cancer with targeted therapy, resulting in fewer complications. In this section of the chapter we shall discuss current findings on patient selection, procedure technique, treatment advantages and disadvantages, as well as possible adverse events.

4.4.2 Patient selection

Determining selection criteria for patients considering focal ablation is a controversial subject. Patients and practitioners would like to achieve a proper balance between achieving adequate treatment areas, avoiding undertreatment of multifocal cancer, and minimizing complications of overtreatment.

A recent study by Singh *et al.* investigated the role of transperineal prostate mapping biopsies to determine the best candidates for focal ablation.[150] The authors concluded that men with unifocal cancers or cancers with smaller ipsilateral lesions located far from the nerve bundle are ideal for cryoablation. In addition, multifocal diseases with aggressive lesions or lesions near the nerve bundle are unsuitable for treatment with cryotherapy. Furthermore, a recent study from the same group found that transperineal prostate mapping biopsies could correctly identify an index lesion in 44.4% to 59.2% of men having clinically significant disease. The authors concluded that the success of tissue-preserving focal therapy is dependent on appropriate patient selection.

This selection necessitates an accurate investigative tool that can exclude significant cancer outside the area to be ablated, while precisely localizing individual cancer lesions, which are to be selectively destroyed. Based on our experience at Winthrop University Hospital, the optimal patients for focal ablation have the following characteristics:

- PSA <10 ng/mL
- GS of <7 or GS of 7 with primary pattern 3
- Percentage core involvement (in each of the 12 cores): <50%
- Total cores sampled: minimum of 12
- 3T mp-MRI showing no contralateral cancer, no capsular bulge or involvement, and no seminal vesicle invasion
- Prostate size: <60 g

4.4.3 Focal cryotherapy

As a primary treatment option, patients can have either a total or focal cryoablation. Focal cryotherapy is defined as less-than-complete ablation of the prostate with ice. Probes (cryoneedles) are distributed in and around the tumour and the region is aggressively frozen. Typically, four needles are used during a focal ablation, depending on prostate size. The remaining regions of the prostate are spared in order to preserve sexual potency and urinary continence.

4.4.4 Equipment

A cryoablation system consists of multiple cryoprobes or cryoneedles, thermocouples, argon and helium inlets, and computer-monitoring software. Cryoprobes are filled with argon gas, which rapidly cools the probe, creating an ice ball that ablates the prostatic lesion under high pressure (**Figure 4-16**).

FIGURE 4-16
Unfrozen and Frozen 17-Gauge Cryoprobe

A 17-gauge cryoprobe with ice ball formation.

B Ruler for scale.

Image courtesy of Dr. Aaron Katz, Winthrop University, United States.

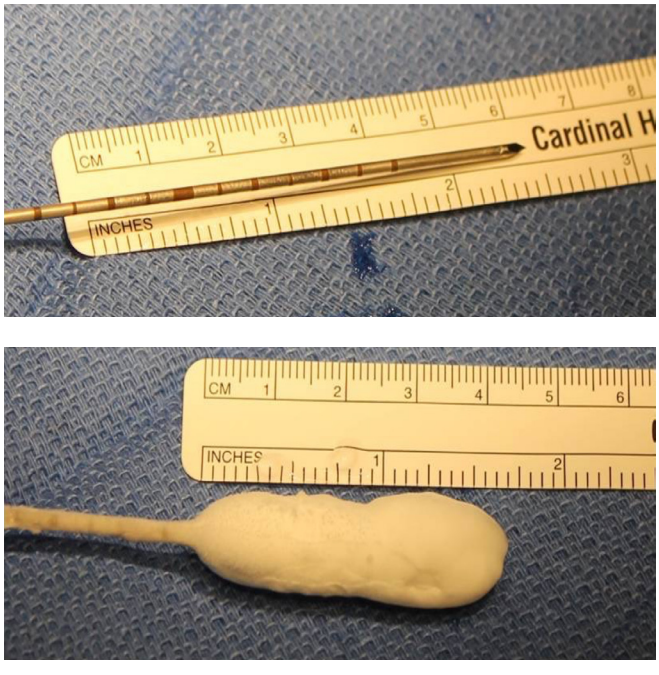

The argon gas is then utilized under low pressure to thaw the area. Cryoablation procedures consist of two freeze-thaw cycles. In addition, compared to the older liquid nitrogen probes that were 2.4 mm to 3 mm in size, argon gas probes are much smaller in diameter, at 1.5 mm for a 17-gauge probe. A mapping grid is used as a guide for targeting the lesion with the cryoprobe (**Figure 4-17**).

FIGURE 4-17
Intra-operative Setup With Placement of Cryoprobes Using Radiotherapy Template

Image courtesy of Dr. Aaron Katz, Winthrop University, United States.

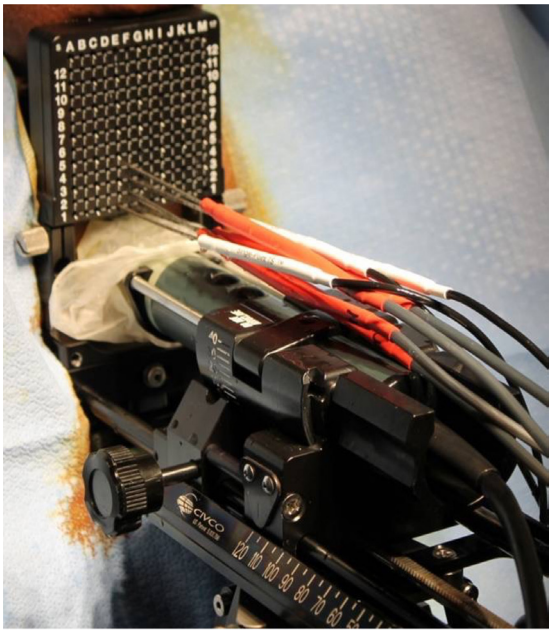

The use of a TRUS allows for real-time visualization of the freezing process. Thermocouples are placed strategically around the prostate to monitor the temperature throughout the procedure. A urethral warming device is used to prevent freeze injury by circulating heated saline through a double-lumen catheter.[151] In our experience as well as others that have reported on outcomes, the use of the urethral warmer has significantly reduced the overall side effects, and the urethral slough rate is almost nonexistent today.

4.4.5 Surgical technique

Prostate cryotherapy is an outpatient surgical procedure that is done under spinal anesthesia in the majority of cases. The patient is placed in the lithotomy position and a 7.5 MHz US probe is inserted into the rectum. A mapping grid is placed close to the perineum and 17-gauge cryoprobes are introduced percutaneously into the treatment area via US guidance. During a focal cryoablation, the freezing zone of the cryoprobes should be ≤20 mm apart from each other prior to initiation of the freeze-thaw cycles (**Figure 4-18**). The needles should be placed 10 mm away from the urethra and at least 10 mm from the posterior surface of the prostate capsule. Since the NVB on the treated side will be intentionally ablated, the cryoprobes should be positioned within 10 mm from the lateral capsule.

FIGURE 4-18
Transverse View of Prostate Showing Cryoneedle Configuration

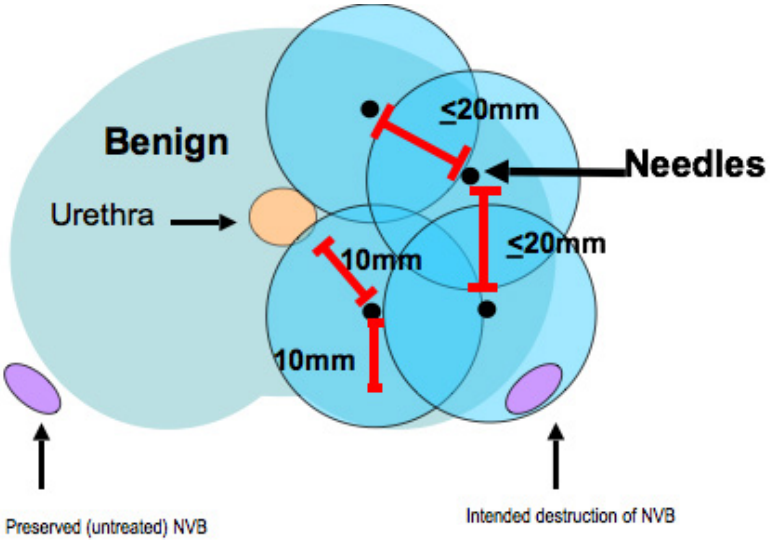

Temperature probes, placed in multiple areas of the prostate, allow for real-time temperature monitoring throughout the procedure. A urethral warming catheter is placed over a guide wire, which is inserted via flexible cystoscopy. Once the setup is completed, the procedure begins with the delivery of argon gas to focally freeze the area of interest. Transrectal US monitors the freeze cycle in relation to nearby organs (**Figure 4-19**). Once adequately frozen, hydrogen gas is administered to thaw the area. The argon-hydrogen gas administration is then repeated. Once completed, the cryoprobes, temperature probes, US probes, and urethral warming catheter are removed and an indwelling 18 Foley catheter is placed. The patient is discharged home the same day as the procedure and the Foley catheter is removed several days later. Antibiotics are prescribed to prevent postoperative infection. Typically, pain medication is not required.

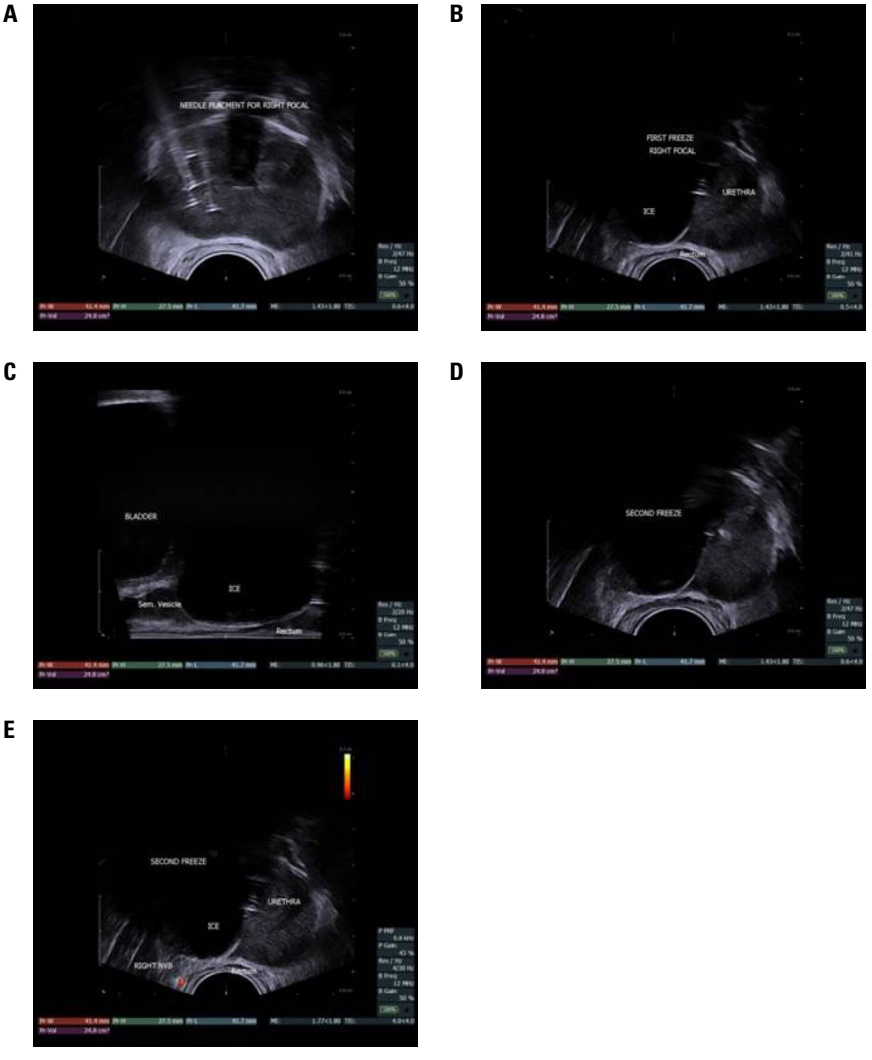

FIGURE 4-19
Needle Placement for Right-Focus Cryoablation

A Ice ball formation after first freeze cycle. Urethra and rectal mucosa are spared.

B Sagittal view of first freeze cycle showing ice ball relation to bladder, seminal vesicle, and rectum.

C Ice ball formation after second freeze cycle.

D Second freeze ice ball formation in relation to urethra, and rectum.

E Right NVB, visualized using coloured Doppler.

Image courtesy of Dr. Aaron Katz, Winthrop University, United States.

The greatest strengths of cryoablation are the ability to potentially tailor the procedure to the extent of the patient's disease and its unique ability to be repeated with no added morbidity. In addition, patients with recurrent cancer can still be treated with either RP or radiation therapy. The authors recently published an article on a series of men who were treated with stereotactic body radiosurgery after a recurrence from focal ablation.[152] These patients did very well with no evidence of recurrence and urethral or rectal toxicity. Recent articles discussing improved cryoablation techniques have shown excellent success rates, with multiple series showing better than 90% negative Bx rates and 87%, to 95% DFS rates.[153] Cryoablation appears to be equal for treatment of all Gleason grades, including GS >7. Furthermore, recent publications of 5- and 7-year biochemical DFS consistently report equivalent, if not superior, results to radiation and surgical treatments.[154]

4.4.6 Post-surgical follow-up period

As with any cancer treatment, focal cryoablation patients should follow up with their physician to monitor for the recurrence of disease. A few days post-surgery, patients will need to return for the removal of their catheter and for a trial of voiding. It is our practice to leave the catheter indwelling for four nights and then have an active trial of void. More than 98% of the patients void well, and do not need another catheter.

The patients are routinely placed on an alpha-blocker for 30 days as well as a 5-alpha-reductase inhibitor (5-ARI) for 90 days. The first visit after catheter removal is then at 3 months where a digital rectal examination is performed as well as a serum PSA test. Afterwards, patients routinely follow up every 3 months for the first year and then every 6 months thereafter. We have recently started to use MRI in follow-up, irrespective of the PSA. We believe that this can be a useful tool to not only detect an early recurrence but also allow us to ensure that ablation was performed adequately. The MRI characteristics of cryoablation are well known for renal cancers, and we have extrapolated the information for PCa therapy.

During these follow-ups, physicians often monitor men's postsurgical PSA values on a regular basis. A patient's PSA nadir is defined as his absolute lowest PSA level following treatment. While literature is still emerging on what constitutes a successful nadir value, nadir values are nonetheless utilized as a benchmark to measure a rise in PSA. A steady increase in serum PSA over time, typically three consecutive tests at least 2 weeks apart, is known as biochemical recurrence. Some doctors prefer to measure patient's PSA doubling time (PSADT) rather than strictly serum PSA. A shorter PSADT may be indicative of disease recurrence and warrant additional treatment. The purpose of closely monitoring post-cryoablation PSA is to detect and treat any recurrence while it is local, before it metastasizes into distant disease.

In the event of recurrence, patients may prefer alternate treatment to cryotherapy, such as radiation. However, the clinician and patient may find it best to repeat the procedure. Any form of cryotherapy following treatment of PCa is considered to be *salvage* therapy, and is noted in our database as such. While the technical aspects of the procedure for salvage and primary cryoablation are essentially the same, salvage patients may experience more urinary symptoms after treatment such as irritative voiding patterns. Thus, doctors take numerous factors into account when determining whether a man is eligible for salvage therapy. Ideal candidates for salvage procedures have no evidence of metastasis; PSA less than 10 ng/mL; PSADT less than 6 months; and a life expectancy greater than 10 years.

4.4.7 Adverse events, side effects, and complications

Immediately following cryoablation of the prostate, men may experience swelling of the genitals. Testicular swelling is caused by the entry of the needles via the perineum, causing irritation that can be treated with simple over-the-counter, anti-inflammatory medication. With the 17-gauge ice rods, we have seen this very rarely, currently in less than 1% of men. Due to the extensive vascularity of the prostate, another common side effect of cryotherapy is hematuria. This is usually transient and in more than 2,000 procedures that we have performed, the transfusion rate is 0%. Some patients

may have slight blood in the catheter immediately after the procedure. As all of the procedures are performed in our ambulatory centre, which is not near a hospital, it has been our practice to use a three-way catheter at the end of the procedure and use bladder irrigation for an hour in the recovery room. To date, we have not had to transfer any patient to the hospital after cryotherapy.

Neither swelling nor hematuria are considered serious side effects, as they typically subside within a week of the procedure. Very few men experience urinary incontinence after cryoablation (less than 1% ever use a pad). However, this is far more common in salvage cryoablation patients.

A serious but far less common complication of cryotherapy is URF. Fortunately, in the focal cryoablation setting, this complication has not yet been reported. In URFs, a channel forms between the urethra and the rectum, causing patients to void into their rectum. URFs are more common after RP, as they occur in less than 1% of present-day cryotherapy patients.[155] To date, we have not had a patient who developed any bowel complications after a focal ablation.

Many of the adverse events of cryoablation are related to sexual function. Cryoablation includes the destruction of periprostatic tissue and NVBs, similar to non-nerve-sparing RP. Neurovascular bundles are located on either side of the prostate gland. They consist of erectile nerves that play a significant role in a man's ability to obtain an erection.[156] As these nerves are localized on both sides of the prostate, only one side is typically damaged during focal cryoablation, a benefit that is not available for total cryotherapy patients. Cryoablation thus has a significant impact on postoperative sexual function and most patients can expect to experience at least some impotence.

However, the recent introduction of 17-gauge cryoneedles and coloured Doppler allows for better targeting and preservation of the NVB. This may improve the rates of erectile dysfunction (ED) and potency following cryoablation, and we have found that the majority of patients recover sexual function over time, usually back to baseline within 6 months. As with other forms of PCa therapy, it is important to take the patient's age, capability of sexual function prior to cryoablation, and the aggressiveness and location of the cancer into account when determining whether the procedure is the cause of ED. Even if a man can maintain an erection and reach orgasm after cryosurgery, many report the absence of ejaculate in a condition known as retrograde ejaculation.

In patients suffering from retrograde ejaculation, the urinary sphincter, which controls the opening from the bladder to the urethra, can no longer function properly. Rather than be discharged through the penis, the ejaculate is redirected into the bladder. In our experience, the majority of men who have had a focal ablation are able to maintain their ejaculation to the level that it was present before the procedure. This is clearly an advantage over radical surgery and radiation.

The greatest concern with focal cryoablation is leaving a significant cancer untreated on the side opposite the cryoablation. It is well known that 65% to 70% of PCa is multifocal, the recognition of which constitutes the major theoretical objection against performing focal cryoablation. However, many studies have noted that multifocal tumours might not be as clinically significant as once thought,[157] and with the use of genomics and MRI, we may be closer now than before to properly selecting those men with a need for treatment with curative intent.

4.4.8 Cryotherapy: a brief review of the literature

Since its introduction to the clinical world, cryotherapy has consistently grown as a treatment option for PCa. Literature supports cryotherapy as a treatment option for patients who are ineligible for radiation or RP as well as men who experience recurrence after radiation treatment.[158] Furthermore, the biochemical recurrence-free rate was 75.7% for 2 years after focal cryoablation.[159] In comparison to total cryoablation or radical treatment, focal cryotherapy has been proven to be less detrimental to the overall health-related QOL of patients. According to the Cryo On-Line Database (COLD) registry, of all cryotherapy procedures, focal cryotherapy rates have increased from 2.1% in 1999 to 38.2% in 2007.[159]

4.4.9 Conclusion

Advances in our understanding of the clinical features, natural history, and biology of PCa have evolved the landscape of PCa management. Patients and practitioners now have numerous options for less-invasive, localized treatment. The non-invasive nature of cryotherapy makes it an attractive treatment option for patients with localized PCa. Although much of the clinical data from cryotherapy results are retrospective, new clinical trials and prospective studies will expand our understanding of their efficacy and guide patient selection.

4.5 Vascular-Targeted Photodynamic Therapy

4.5.1 Introduction

The palladium-bacteriochlorophyll derivatives, TOOKAD® (WST09, padoporfin) and TOOKAD® Soluble (WST11, padeliporfin) represent a novel generation of radical oxygen species (ROS)-generating photosensitizers, also known as laser-activated vascular occluding agents (VOA).

Rather than targeting tumour cells, these compounds have the particularity of being rapidly cleared from the circulatory system. They remain confined to the vasculature and do not migrate to extravascular tissues. This allows for localized, predictable, and well-controlled vascular damage with resulting rapid vascular arrest within the illuminated area, as demonstrated by initial preclinical experiments.[160–162]

Upon illumination with a near-infrared laser light, the photosensitizer promotes the rapid release of ROS, leading to the occlusion of tumour-feeding arteries and veins, and resulting in permanent vascular arrest and subsequent tumour necrosis within 24 to 48 hours after vascular-targeted photodynamic therapy (VTP). The ROS involved are superoxide and hydroxyl radicals, as demonstrated experimentally with WST09 by Vakrat-Haglili *et al.*, using picosecond and nanosecond time-resolved spectroscopies, electron spin resonance (ESR) spectroscopy, time-resolved singlet oxygen phosphorescence, and chemical product analysis.[163] Similarly, Ashur *et al.*[164] confirmed that WST11 generates

only superoxide and hydroxyl radicals, with no induction of singlet oxygen species using time-resolved spectroscopy, ESR spectroscopy, electrochemistry, spectroelectrochemistry, oximetry, and protein mass spectroscopy. This mechanism has been further studied and comprehensively demonstrated in a series of experiments conducted at the Weizmann Institute of Science and recently published.

Plaks *et al.*[165] studied the effects of TOOKAD-induced VTP *in vivo* using a subcutaneous WISH-PC14 human PCa xenograft. The exact sequence of endothelial events induced by TOOKAD VTP therapy was described by Madar-Balakirski *et al.*, *in vivo* and in real time using a mouse earlobe MADB106 tumour model and state-of-the-art non-invasive online imaging techniques including dynamic light scattering imaging (DLSI), fluorescent intravital microscopy (fINM), angiography with fluorescein isothiocyanate-dextran (FITC-dextran), and photosensitized MRI. TOOKAD VTP induced rapid vasodilatation (mean volume increase of 70%) of tumour-feeding arteries and transient increase in blood-flow. This was followed by vasoconstriction, and blood clotting—particularly at precapillary bifurcations—was seen within 25 seconds, together with increased vessel permeability and decreased flow, resulting in an arterial occlusion at 63.2±1.5 seconds and an irreversible arrest after 10 minutes. A parallel venous occlusion was also demonstrated. More importantly, healthy tissue vessels appeared intact and functional after VTP, as demonstrated by FITC-dextran angiography and DLSI monitoring.[166]

A second paper from this institute has also elucidated the mechanisms involved in the propagation of the TOOKAD soluble-induced oxidative insult among endothelial cells. In a series of experiments using a highly sophisticated methodology, the authors demonstrated that while illumination of bEnd.3 cell cultures pretreated with WST11 induced the production of ROS in the illuminated cells, the propagation of the oxidative insult to non-illuminated cells was dependent on the following conditions:

a. Functional gap junctions
b. Direct result of *de novo* generation of ROS as well as radical nitrogen species (nitrous oxide and peroxynitrite),
c. Nuclear translocation of c-Jun N-terminal kinase
d. Apoptosis in all bystander cells adjacent to the initially injured endothelial cell

Thus, this led to the propagation of oxidative stress over hundreds of microns from the focal injury. The authors concluded that functional gap junction intercellular communications were mandatory for local oxidative stress expansion among endothelial cells.[167]

4.5.2 Description of the procedure

Analysis of data from phase 1/2 trials with TOOKAD Soluble VTP therapy by Betrouni *et al.*,[168] demonstrated that PDT planning is possible and reliable, allowing the design of a response model that was subsequently validated. Optimal response is achieved with a drug dose of 4 mg/kg WST11 and a light dose of 200 J/cm (NIR: 753 nm laser light wavelength). The model confirmed an optimal correlation between the illuminated tissue volume and the resulting volume of necrosis, assessed on day-7 MRI. This protocol is now implemented as the standard for TOOKAD Soluble VTP therapy of PCa in the clinical setting.

The technical aspects and standardization of the procedure for VTP therapy with TOOKAD Soluble in localized PCa have been described in an exquisitely detailed paper recently published.[169]

In preparation for surgery, patients received an alpha-blocker for 1 month starting the week before the procedure to ameliorate the symptoms derived from the prostatic VTP induced swelling.

The procedure is performed under general anesthesia, and curarization is recommended to avoid any slight movement of the patient that would require a complete repositioning of all fibre insertion catheters (FICs). The patient, protected from light at all times, is placed in lithotomy position with the hips flexed to expose the perineum and legs spread to facilitate the positioning of the FIC. Following antiseptic skin scrub, the patient is fully draped covering the Brachystepper™ and probe, to secure a sterile operative area.

The bladder is drained with a Foley catheter, which is then sealed with a spigot, pushed in the bladder, and fixed with tape to the glans penis, avoiding puncture during the procedure.

Using the transrectal US and aided by the guidance of the TOOGUIDE® software, we then proceed with the accurate placement of the FICs, which is facilitated by their metallic tips. As described by the author, "the best way to introduce the FIC was to do it swiftly." Once all the FICs are in place, the accurate measurement of each corresponding optical fibre is performed, always respecting the 5 mm safety margins to urethra, rectal wall, sphincter, and capsule. Each optical fibre is calibrated by inserting its illuminating diffusor into the integrating sphere in the laser generator in order to adjust the power with the planned values (within ±5 mW), and is then inserted into the corresponding FIC, fixed by an O-ring clamp and further secured to the plastic drape with steri-strips, as depicted by Azzouzi *et al.*[169]

At the end of this stage of the procedure, the surgeon has to verify that the light density index (LDI) is above 1, and a final safety check is performed using a light sensor in the lumen of the rectum and illuminating all fibres in a "test mode" to guarantee that the highest level of light intensity is kept below 13 mW/cm^2.

At this point, with the patient completely protected from light and wearing goggles, a 10-minute single bolus of 4 mg/kg of TOOKAD Soluble is infused intravenously, through an opaque syringe and an IV line set. The activation of TOOKAD Soluble is achieved by illumination with a near infrared 753 nm laser light at a power of 150 mW/cm and a light energy of 200 J/cm, delivered by a multichannel diode laser commencing at the end of the infusion and for a period of 22 minutes and 15 seconds and matching with the peak serum concentration of the photosensitizer.

Once the procedure is completed, which lasts between 1.5 and 2 hours, all fibres and FICs are removed. The urinary catheter is left on free drainage and the patient is kept protected from light exposure during the transfer to his bed.

Postoperatively, the patient is kept under dimmed light for at least 6 hours and may be discharged on the day of the procedure as a day-case surgery, as reported by Azzouzi *et al.*[169] In our institution, the patients were kept for observation in their room for 24 hours and discharged the following day.

They are informed of the need to avoid direct exposure to sunlight during the 48 hours following the injection. The urinary catheter can be removed 3 to 4 hours after the procedure or on the following day. An alpha-blocker is continued due to the increased risk of lower urinary tract symptoms (LUTS) during the first 4 weeks.

4.5.3 Preclinical data

4.5.3.1 WST09 Preclinical studies

The bacteriochlorophyll-derived photosensitizer TOOKAD (Pd-Bacteriopheophorbide, also known as WST09; Negma-Lerads, Toussus-le-Noble, France) was the initial compound assessed in both the preclinical and clinical settings. WST09 (TOOKAD) PDT effectively induced extensive hemorrhagic necrosis in preclinical *in vivo* models.

In a series of experiments, Koudinova *et al.*[170] assessed the *in vivo* response to TOOKAD (WST09) PDT. For this, male CD1-nude mice were grafted with the human SCCP (WISH-PC2) in the subcutaneous tissue, intraosseously, and orthotopically. TOOKAD was administered at a dose of 4 mg/kg and followed by immediate illumination (650–800 nm) from a xenon light source or a diode laser emitting at 770 nm. Endpoints of the study were: tumour volume, human plasma chromogranin A levels, animal well-being, and survival. Furthermore, tumour response to PDT was studied by histopathology and immunohistochemistry. With the animals followed for up to 90 days, complete tumour response was documented histologically in 69% of subcutaneous xenografts as well as in approximately 50% of intraosseous and orthotopic tumours.

In 2002, Chen *et al.*[171] evaluated the potential of TOOKAD-mediated PDT *in vivo* as an alternative treatment for PCa, using a normal canine prostate model. In these studies, after 5 or 15 minutes following administration of 2 mg/kg TOOKAD (WST09), the surgically exposed canine prostate was irradiated superficially or interstitially with a 763 nm light and at light doses from 50 J/cm^2 to 200 J/cm^2. In these studies, the adjacent bladder and rectum were also exposed to light.

During treatment, the temperature and light fluence were recorded. Histological assessment of harvested prostates demonstrated uniform hemorrhagic necrosis and atrophy, with lesions clearly delineated from the adjacent normal tissue. Optical dosimetry demonstrated that 20 J/cm^2 were required to produce prostatic necrosis, well below the dosimetry required to induce damage to adjacent tissues (40–80 J/cm^2), thus, the authors concluded that TOOKAD (WST09)-mediated PDT appeared to be a promising candidate for prostate ablation in patients with recurrent, or possibly even primary, PCa.

Later, this same group evaluated the effects of TOOKAD (WST09)-mediated PDT on a canine prostate model pretreated with ionizing radiation (54 Gy 5–6 months prior to PDT). After infusion of 2 mg/kg TOOKAD and employing light fluences of 50 J/cm to 200 J/cm, the interstitial tissue oxygen profile and light fluence rate were assessed. One week later, histology confirmed well-defined hemorrhagic necrosis, clearly delineated from the RT-induced preexisting fibrosis. The lesion size correlated with light fluence and it was comparable to that in non-irradiated prostates. Importantly, there was no noticeable damage to the urethra, bladder, or adjacent colon, suggesting that it could be an alternative for recurrent PCa after RT.[172]

Using spontaneous canine PCa and normal canine prostate models, Huang *et al.*[173] further investigated the effects of different drug doses and light doses for one- and two-session PDT. Pharmacokinetics assessment demonstrated a peak of plasma WST09 levels at the end of the infusion, in the order of 0.5, 4.6, and 5.9 μg/mL for administered doses of 0.25, 1.0, and 2.0 mg/kg, respectively, and followed by a rapid clearance. In this study, conventional CT scans did not show PDT-induced tissue damage, which was better identified by a blood perfusion scan performed at days 2 and 7 after VTP.

The investigators focused their attention on MRI imaging as an ideal tool for the assessment and follow-up after VTP therapy. In a preclinical study on dogs, the authors evaluated the optimal MRI methodology to assess PDT-induced response in the canine prostate. TOOKAD 1 mg/kg was infused and the exposed prostates illuminated via a cylindrical diffuser with a 763 nm light (50–300 J/cm). Comparing fast spin echo T2W, contrast-enhanced T1 (CE-T1), and diffusion weighted images (DWI) on days 2, 7, and 30 post-treatment. The authors concluded that on day 7 after PDT, gadolinium diethylenetriamine penta-acetic acid (DTPA) contrast-enhanced MRI was superior to DWI and T2W imaging at delineating the PDT-induced tissue necrosis.[174]

Subsequently, several preclinical and clinical studies have further evaluated and optimized the MRI imaging protocols for the assessment and follow-up after WST09 therapy. This methodology has later been implemented in the phase 1/2 and recent phase 3 trials with TOOKAD Soluble, and it now constitutes the mainstay in the post-VTP follow-up.

4.5.3.2 WST11 TOOKAD soluble preclinical studies

In 2011, Chevalier *et al.*[175] published their initial results with WST11 TOOKAD Soluble in a canine model and compared it with WST09 PDT. A single bolus infusion of 10 min using varying doses of WST11 was administered to 34 dogs and of 2 mg/kg WST09 to the other three animals, and the prostates were illuminated for 33.2 minutes. Circulating WST11 levels increased with drug infusion and decreased rapidly during 1 hour, being undetectable at 24 hours. Only transient mild urinary symptoms were recorded and they resolved within 48 hours. Hemorrhage was observed in all treated prostates in a drug-dose and fluence-dependent manner, and it translated into necrosis, which was associated with loss of the vessel endothelial layer. In this study, WST11 VTP demonstrated a superior tissue ablation than WST09 in the canine prostate model.

Using the dog model, this group further studied the safety and efficacy of WST11 TOOKAD Soluble VTP with transurethral illumination, in the context of benign prostatic hyperplasia (BPH). For this, a 753 nm laser light (200–300 J, 200 mW/cm fluence) was delivered through an urethrally placed laser fibre. Varying doses of WST11 (5–15 mg/kg) were infused intravenously starting 5 to 15 minutes before and during illumination, or as a single bolus 5 to 10 minutes before illumination.

Outcomes were measured by US, urodynamic assessment, cystourethrogram, and histopathology. Follow-up of the treated animals continued from 1 week to 1 year. WST11 TOOKAD Soluble VTP was well tolerated, with only one dog developing urinary retention. Hemorrhagic lesions were detected in all treated animals, demonstrating a periurethral necrosis with loss of endothelial layer, and a concentric outer layer of inflammation and atrophy, with normal blood vessels. During follow-up,

prostatic urethral width increased as early as week 6, accompanied by a reduction of prostate volume, reaching 25% by 26 weeks. Urodynamic assessment confirmed a parallel decrease in urethral pressure at 6 weeks, lasting up to 1 year.[176]

4.5.4 Clinical data

4.5.4.1 Indication and patient selection

Inclusion criteria for phase 1 and 2 studies with WST09 TOOKAD in patients with recurrent PCa following definitive radiation therapy:[177,178]

- Histologically proven PCa following definitive EBRT
- Life expectancy >5 years
- Organ-confined disease on staging CT (≤cT2c)
- PSA <20 ng/mL
- Prostate volume <50 mL on US scan
- GS >6

Exclusion criteria:[177,178]

- Previous hormonal therapy within 6 months
- Previous chemotherapy
- Previous transurethral resection of prostate
- Significant history of allergies, particularly to Chromophore®
- Hematological disorders
- Significant RT-induced cystitis or proctitis
- Renal or hepatic disorders

Inclusion criteria for phase 2 studies (PCM201, PCM202, and PCM203) with WST11, TOOKAD Soluble VTP in patients with localized PCa:[180,181]

- Patients with Bx-proven low-risk PCa suitable for AS
- Dynamic contrast MRI performed in all patients
- Organ-confined disease ≤cT2b-cN0/Nx-cTM0/Nx (radiological cT2c acceptable)
- PSA <10 ng/mL
- Prostate volume <50 mL on US scan
- GS 3+3 in patients diagnosed by US scan-guided transrectal Bx
- In PCM201 and PCM203 studies, Gleason pattern 4 was accepted in patients diagnosed by transperineal Bx if low burden (<3 cores affected and ≤3 mm maximum cancer core length)
- In PCM202 only ≤50% of cores could be affected and ≤5 mm maximum cancer core length
- Only patients with unilateral disease at entry were included

Exclusion criteria: [180,181]

- Previous or current treatment of the cancer, including: hormonal therapy (excluding 5-ARIs) or androgen supplements in the last 6 months, RT, chemotherapy, or TURP
- Use of any photosensitizing medication for 1 month before or 1 week after VTP

Inclusion criteria for the **European Randomized Phase 3 Study to Assess the Efficacy and Safety of TOOKAD Soluble for Localized Prostate Cancer Compared to Active Surveillance CLIN 1001 PCM301 (NCT01310894):**[182]

- Men with low-risk PCa

Low-risk PCa defined by (10–24 cores TRUS Bx):

- Clinical stage up to cT2a (rT2c and pT2c permitted)
- Absence of Gleason pattern 4 or 5
- 1 core positive (3–5 mm maximum cancer core length)
- 2–3 cores positive (1–5 mm maximum cancer core length)
- PSA ≤10 µg/L
- Prostate volume >25 cc and <70 cc
- Life expectancy ≥10 years
- Signed informed consent form by the patient

Inclusion criteria for the **Latin America- Phase 3 Study of the Efficacy, the Safety and Quality of Life after TOOKAD® Soluble PCM304 (NCT01875393):**[182]

- Prostate adenocarcinoma diagnosed using prostate Bx showing:
- Gleason 3+3 with Gleason 3+4 acceptable provided it is not present in >2 cores and no more than 50% cancer in any core
- Clinical stage up to cT2a – N0/Nx – M0/Mx.
- Prostate volume >25 cc and <70 cc
- Life expectancy ≥10 years
- Signed informed consent form by the patient

4.5.4.2 Oncological outcomes

WST09, TOOKAD oncological outcomes

In 2007, Trachtenberg *et al.*[177] published the results of the first phase 1 clinical trial assessing safety and efficacy of palladium bacteriopheophorbide (WST09) TOOKAD VTP in patients with Bx-proven recurrent PCa following definitive RT (Level 2). Twenty-four patients were enrolled in two consecutive arms: initial drug dose escalation (0.1, 0.25, 0.5, 1, and 2 mg/kg) evaluating drug tolerability and safety at a fixed light energy (100 J/cm), using only two fibres. Once the safety of the 2 mg/kg TOOKAD dose was demonstrated, the light dose was escalated to 230 J/cm and 360 J/cm. Treatment efficacy was assessed by 6-month standard 12-core systematic biopsy (SB), PSA readings at months 1, 2, 3, and 6, and MRI on day 7 and at 6 months post-VTP. Peak plasma concentration was reached at 20 minutes post-infusion. At a dose of 2 mg/kg, plasma levels were undetectable after 2 hours.

The first MRI-detected avascular lesion was achieved with 1 mg/kg TOOKAD at 100 J/cm, increasing with increasing doses, with response in six of six patients treated with the highest dose schedule (2 mg/kg at 360 J/cm). Data suggested that VTP threshold dose of 2 mg/kg TOOKAD and a light dose of 100 J/cm was required for a consistent induction of lesions, above which a dose dependence of the lesion size was observed.

In 2008, the same group reported on the outcomes of a second, light dose escalation study, further assessing the efficacy of TOOKAD (WST09) VTP as a method for whole-prostate ablation in patients with recurrent PCa after failure of EBRT. In this phase 2 clinical trial, 28 participants received a fixed dose of 2 mg/kg TOOKAD and patient-specific light dose as determined by computer-aided treatment planning and with up to six fibres for illumination (Level 2).

Treatment efficacy was evaluated by means of a 6-month 18-core systematic prostate Bx, MRI imaging at 1 week and 6 months, and PSA measurements at months 1, 2, 3, and 6 after VTP. As expected, light dose correlated with tissue response as measured by MRI. A complete response as defined by a negative 6-month Bx required a light dose of at least 23 J/cm in 90% of prostate volume. The finding was further supported by the PSA response in these patients. This study demonstrated that the day-7 MRI was a reliable surrogate for 6-month Bx. All participants with >60% of devascularized prostate on day-7 MRI were subsequently found to have a negative Bx.[178]

Haider *et al.*[179] published separate results from the 25 patients with a mean age of 73 years (58–83) included in the imaging analysis. Dynamic gadolinium-enhanced T1W and T2W MRI scans were performed with a mean 12.8 (4–36) days before and 7 days, 30 days, and 6 months after VTP, and results were correlated with PSA response. Contrast-enhanced T1W MRI on day-7 post-VTP confirmed intraprostatic necrosis in all 25 patients, with the percentage of necrosis ranging from 0.9% to 80% and irregular treatment margins in 21 of 25 cases. The non-enhanced T2W MRI showed unclear boundaries in all cases. The NVB appeared to be spared in all patients and urethral preservation was complete in 10 of 25 patients. Maximal MR-depicted necrosis was seen on the day-7 scan, being superior to the 30-day scan when assessing VTP response. Importantly, the MR-depicted intraprostatic necrosis correlated with the percentage decrease in PSA levels at 4 and 12 weeks.

WST11, TOOKAD soluble oncological outcomes

Results from the PCM201 phase 2 study, conducted across nine university hospitals in Europe and Canada, were published by Moore *et al.*[180] in 2014. A prospective, multicentre, open-label, single IV dose-escalation trial of TOOKAD Soluble VTP was designed to determine the optimal drug concentration and light dose parameters to achieve prostate ablation in men with early PCa (Level 2). The patients received 2, 4, or 6 mg/kg TOOKAD Soluble using a 753 nm laser light at a fixed power (150 mW/cm) and light energy (200 J/cm). Three patients received 2 mg/kg but the dose was considered insufficient. On the contrary, the 6 mg/kg dose was found excessive, and hence unsuitable for small prostates.

The primary efficacy criterion was the result of the 6-month Bx, which was negative in 53% of evaluable patients. Furthermore, in the group of patients with optimal conditions (4 mg/kg, 200 J/cm and LDI ≥1) the negative Bx rate increased to 83%. The secondary efficacy criterion was the volume of VTP effect, defined as the volume of hypoperfusion at 1 week MRI divided by the mean of the intended treatment volume at baseline and at 1 week post-VTP MRI. Overall, the mean percentage treatment effect was 38%, and it increased to 42% in the 4 mg/kg group.

In 2013, Azzouzi *et al.*[181] reported on the initial results from the PCM201 study in patients with localized PCa (NCT00975429), conducted within seven academic European centres**.** The phase 2, multicentre, open-label, multiple-arm, single IV dose-escalation, 6-month, non-randomized clinical trial was designed to determine the optimal treatment conditions needed to achieve PCa ablation and to assess the efficacy of TOOKAD Soluble VTP in patients with localized PCa (Level 2).

In part one of the study, patients were initially assigned to 4 mg/kg or 6 mg/kg TOOKAD Soluble depending on whether the prostate was <60 mL or ≥60 mL, respectively, and a light dose set at 200 J/cm. In part two of the study, patients were assigned to treatment groups with 4 mg/kg or 6 mg/kg

TOOKAD Soluble and activated with 200 J/cm or 300 J/cm. Patients were followed for 6 months after VTP, at which time they underwent a Bx. Magnetic resonance imaging was performed before treatment as well as at 1 week and at 6 months following VTP. PSA was checked at 1, 3, and 6 months.

At the 6-month follow-up, 74% of patients had negative biopsies. Overall, the mean necrosis percentage, assessed by MRI on day 7, was 78% (83 patients) with some evidence of extraprostatic necrosis reported in 76% of patients, although without sequelae. The mean percentage of necrosis reduced with time, with values of 8.5% and 7.3% at 3 and 6 months, respectively. Importantly, in the subset of patients treated with 4 mg/kg TOOKAD Soluble and 200 J/cm light (unilateral), 83% had negative biopsies and the mean necrosis percentage at 7 days after VTP was 88%.

The LDI was evaluated clinically, with the aim of optimizing the light delivery. The LDI is defined as the ratio between total light-emitting length of inserted VTP fibres (cm) and the baseline target volume by planimetry (cm^3). In the present study, overall, the mean percentage of necrosis at day-7 MRI after VTP was 88% and 58%, in patients treated with an LDI of ≥1 and an LDI of <1, respectively. And it increased to 91% in those patients treated with 4 mg/kg TOOKAD Soluble and 200 J/cm light (unilateral) and an LDI of ≥1. Overall, a higher percentage of patients treated with an LDI of ≥1 had negative biopsies at the 6-month follow-up when compared with those treated with an LDI of <1 (79% vs. 63%, respectively).

In 2015, Azzouzi *et al.*[182] published the pooled analysis of 117 men from the three phase 2 studies (PCM201, PCM202, and PCM203), and evaluated the 6-month effects of VTP TOOKAD Soluble administered at the recommended dose of 4 mg/kg in a 10-minute, single bolus IV infusion, and activated by a 753 nm laser light at 200 J/cm, considered the optimal combination in terms of safety and efficacy (Level 2).

The primary endpoint was the negative 12-core prostate Bx rate at 6 months after TOOKAD Soluble VTP. Secondary efficacy criteria included change in PSA (checked at months 1, 3, and 6) and MRI result on day 7 and at 6 months.

Pooled analysis demonstrated that focal VTP treatment with TOOKAD Soluble at 4 mg/kg and 200 J/cm resulted in an overall negative 6-month Bx rate of 68.4% which improved to 80.6% for those patients treated by hemiablation and with an LDI of ≥1.

Mean percentage of tissue necrosis on day 7 MRI was 76.5 % overall and 86.3% in the protocol population with and an LDI of ≥1. Extraprostatic necrosis was reported in 67.2 % of patients, and this was usually not associated with clinically significant disorders. Mean PSA level variations from baseline were –2.1 and –2.0 ng/mL, respectively, at 3 and 6-months. In the protocol population with an LDI of ≥1, PSA changes from baseline were in the order of –2.3 ng/mL at both 3 and 6 months.

Investigators at the Angers University Hospital reviewed the histological findings from 56 patients included in two phase 2 WST11 trials. In these series, the 6-month Bx was negative in 29 of 56 patients. Scarring, as a result of the TOOKAD Soluble VTP treatment was observed in 53 of 56 cases, affecting the treated lobe, being minimal or nonexistent in the untreated lobe, and characterized

by well-demarcated areas of fibrosis, always at least at 5 mm from the prostate capsule, which was either normal or moderately fibrotic. Coagulative necrosis was observed in 53% of cases. Importantly, residual tumour was never seen within the scar tissue.[183]

4.5.4.3 **Functional outcomes**

WST09, TOOKAD functional outcomes

Functional assessment (IPSS and QOL Patient-Orientated Prostate Utility Scale) performed during the phase 1 trial of WST09 TOOKAD VTP in patients with recurrent PCa following definitive RT demonstrated that bowel, urinary, and erectile functions were preserved in the long-term assessment (6 months) when compared with baseline. In responders, a worsening of urinary function was seen in the first month, returning to baseline at 6 months. Similarly, during the phase 2 clinical trial, most patients had an initial deterioration of their IPSS scores, particularly due to storage symptoms that were controlled with medication. At 6 months, the IPSS had reverted towards baseline levels in all patients.[177,178]

WST11, TOOKAD soluble functional outcomes

For all 34 evaluable men in the PCM201 phase 2 study WST11 TOOKAD Soluble VTP, the mean IPSS score decreased from 7.3 at baseline, to 6.6, 5.4, and 5.1 at 1, 3, and 6 months after VTP, respectively. Among men (n=29) in the optimal treatment group (4 mg/kg and 200 J/cm), the mean IPSS score decreased from 6.3 at baseline, to 5.6, 3.7, and 3.8 at 1, 3, and 6 months after VTP, respectively. For the health-related QOL domain of the IPSS score, there was a significant improvement from 2.1 to 1.3, from baseline to 6 months after VTP (p<0.013) and comparable between all patients and those receiving the optimal treatment.

Regarding erectile function, overall, the mean baseline IIEF-5 score was 17.7, falling to 13.8 at 1 month, then rising to 16.5 at 3 months and 16.6 at 6 months after VTP. There was no statistical difference between baseline and 3 or 6 months after VTP. Among men in the optimal treatment group, the mean baseline score was 18.0, falling to 13.3 at 1 month, rising to 16.4 at 3 months and 17.0 at 6 months after VTP. Over the 6-month follow-up period, four patients developed *de novo* erectile dysfunction, defined by a decrease of the IIEF score of ≥10 points.[180]

Reported functional outcomes from the phase 2 PCM203 trial also showed a decrease of the mean IPSS score from 6.0 at baseline to 4.8 and 4.7, at 3 and 6 months after VTP. Despite a transient increase to 8.5 at 1 month, the overall trend indicated an improvement in urinary symptoms, with a decrease of the health-related QOL domain of the IPSS score from 1.6 at baseline to 1.1 at 6 months after VTP.

In parallel to the previous study, the IIEF-5 questionnaire demonstrated a slight deterioration of erectile function, with a score reduction from 19.7 at baseline to 13.7 at 1 month, then rising to 15.7 at 3 months, and 15.3 at 6 months post-VTP. Over the 6-month period of the study, nine patients reported treatment-emergent adverse events (TEAEs) of erectile dysfunction.[181]

Pooled analysis, assessing functional outcomes in the cohort of patients treated with the optimal drug (4 mg/kg) and light (200 J/cm) doses, was consistent with the previously published data. The mean IIEF-5 scores were 19.4, 12.9, 15.1, and 15.3 at baseline and 1, 3, and 6 months, respectively.

There was a slight deterioration on erectile function (mean –3.0 score change from baseline). For the same time points, the mean IPSS scores were 6.0, 8.5, 5.1, and 4.7, respectively, representing a slight improvement in urinary symptoms (mean –1.8 score variation from baseline).[182]

4.5.4.4 Complications

The aforementioned preclinical studies using a canine model already demonstrated the feasibility, tolerability, and safety of TOOKAD and TOOKAD Soluble VTP therapy. Safety was further investigated *in vivo* in studies that evaluated the potential impact on nerve conduction[184] and skin photosensitivity.[185]

The safety profile has been extensively assessed in the already published phase 1/2 trials conducted with both WST09 (TOOKAD) and WST11 (TOOKAD Soluble), as well as in ongoing international, prospective, phase 3 trials.

No serious adverse effects (AEs) were reported by Trachtenberg *et al.* during the phase 1 trial of TOOKAD VTP in patients with recurrent PCa following definitive RT. Intra-operative hypotension was reported in 12 of 24 patients, with no adverse events related to it. No cutaneous photosensitivity was observed on skin testing at 3 hours after infusion.[177] During the light dose-escalation phase 2 trial, however, the authors reported two serious AEs due to rectal fistula, one of which resolved spontaneously.[178]

Importantly, the intraoperative hypotension observed following infusion of the original WST09 was related to the Cremophor® that was used as a vehicle for the non-soluble WST09. This issue was resolved with the newer and soluble compound WST11, TOOKAD Soluble, which replaced the original radiosensitizer and is currently undergoing full clinical testing.

Moore *et al.*[180] reported a total of 131 AEs in 34 patients, those that were related to treatment were mild to moderate. In all, 66.7% had at least one AE related to the technical procedure and 33.3% had at least one AE related to the study drug.

The most common AEs related to the technical procedure were dysuria (*n*=9), hematuria (*n*=8), hematospermia (*n*=5), erectile dysfunction (*n*=4), perineal pain (*n*=4), and transient urinary retention (*n*=2).

Three patients reported serious AEs related to the technical procedure, including pelvic pain (*n*=1) and extra-prostatic necrosis (*n*=2) caused by an excessive light dose due to a calibration error, with both patients recovering without sequelae.

Of the 40 patients who received the complete VTP procedure, none withdrew due to AEs. In all, 87% (75 of 86) of patients included in the phase 2 NCT00975429 study reported 228 TEAEs, most being mild or moderate. All 75 patients who had a TEAE reported at least one TEAE that was considered related to the technical procedures of the study (194 TEAEs in total). Overall, 61% (52 of 86) of patients reported a TEAE that was considered related to study drug, and 64% (55 of 86) of patients

reported at least one TEAE that was considered related to the study device, including dysuria (34%), UTI (86 [14%]), urinary retention (13%), constipation (86 [13%]), and perineal pain (86 [12%]), mostly considered related to the technical procedures of the study. No patients discontinued due to AEs.

Eight patients (9%) experienced nine serious TEAEs, of which five events were considered related to the study procedure (*n*=1 for each of prostatitis, hematuria, epididymo-orchitis, cystoprostatitis, and stricture). Study drug–related serious TEAEs were reported in two cases *(n*=1 for each of ischemic optic neuropathy and inflammatory prostatic cyst 193 days after therapy).

There were some minor changes in the biochemical parameters, including elevation of hepatic enzymes that could have been related to anesthesia. Renal toxicity was not reported.[181]

Safety analysis of the pooled data from the three phase 2 studies, including patients treated with the optimal drug and light doses, reported 386 TEAEs in 97 patients (82.9%), the majority of which were grades 1 or 2. Overall, 52.1% reported at least one TEAE that was considered related to study drug, 45.3% reported at least one TEAE related to the study device, and 76.9% reported at least one TEAE that was considered related to the technical procedure.

The most frequently reported TEAEs were dysuria (33.3%), erectile dysfunction (16.2%), perineal pain (15.4%), hematuria (13.7%), urinary retention (11.1%), and micturition urgency (9.4%). No TEAEs led to study discontinuation or premature withdrawal from the study. Serious TEAEs, related to the drug, device, or procedure were reported by either treatment groups including extraprostatic necrosis (*n*=2), prostatitis (*n*=2), pelvic pain (*n*=1), hematuria (*n*=1), urethral stricture (*n*=1), and orchiepididymitis (*n*=1).[182]

A question when considering the widespread implementation of any particular energy source in the context of focal therapy is the potential impact on a future rescue of these patients, should this be required. Indeed, the debate continues regarding the risk of impairing a latter treatment, particularly RP, due to the tissue changes induced by the primary focal approach. Responding to this issue, Lebdai *et al.*,[186] recently published the first series of salvage RP following TOOKAD Soluble VTP treatment and reported preliminary results from a cohort of 19 patients pooled from two phase 2 (NCT00707356 and NCT00975429) and one phase 3 (NCT01310894) European clinical trials. Patients underwent RP (open *n*=12, laparoscopic *n*=2, or robot assisted *n*=5), with a median delay from VTP of 17 months (8–48).

With a median operating time of 150 (90–210) minutes, median estimate blood loss was 400 (100–1,000) mL, the median catheterization time was 7 (5–18) days, and the median hospital stay was 7 (4–21) days. The authors reported preoperative complications in three patients: one pelvic hematoma (Clavien IIIa), one superficial wound infection (Clavien I), and one patient requiring blood transfusion (Clavien II).

When reporting on functional outcomes and with a median follow-up of 10 (1–46) months, 13 patients were completely continent (68%), five needed ≤1 pad/day, and one needed 3 pads/day (Clavien I). Eight and 18 patients reported severe erectile dysfunction, before and after RP, respectively.

From the oncological point of view, the median postoperative PSA was 0.02 ng/mL (<0.01–0.3 ng/mL), and remained undetectable in 84% of patients. Nine patients had positive margins, found to be significantly associated with bilateral VTP (HR, 4.3; 95% CI, 1.6–11.7; p=0.003) and six received complementary RT. The authors concluded that rescue RP following VTP therapy is feasible, safe, and efficient for most of the locally recurrent tumours.[186]

4.5.5 Conclusion

The increase in early, clinically low-risk PCa that has resulted from the widespread implementation of PSA testing and the implications of conventional therapies for these patients in terms of overtreatment has turned the field's attention to less-invasive techniques. As has been seen in many other tumours, a better understanding of the disease, together with improved energy sources and imaging technology, has resulted in the rapid development of focal therapy aimed to minimize side effects while preserving oncological safety. Vascular-targeted PDT is one such technology currently being evaluated in the clinical setting.

The novel TOOKAD Soluble VTP therapy represents a clear example of a bench-to-clinic technology. Created with a robust scientific basis and thoroughly tested in a series of preclinical animal model studies, it is currently undergoing a meticulous and well-designed clinical development plan. With its efficacy and tolerability demonstrated in several consecutive phase 1/2 trials, and following the optimization of the technical aspects of the procedure, TOOKAD Soluble VTP has now been tested in two large, international, multicentre, prospective, phase 3 trials **[LOE 1],** of which the results were expected at the end of 2015.

4.6 Irreversible Electroporation

4.6.1 Introduction

Electroporation or electropermeabilization is a technique in which short, micro- or millisecond electric pulses, travelling between two or more electrodes, are used to create nanopores in the cell membrane. These pores allow for molecules to pass into the cell. Depending on the field amplitude, duration, and number of electrical pulses, this process can be temporary (reversible electroporation), or permanent (irreversible electroporation [IRE]) when above a certain threshold. When permanent, cell death occurs due to cells' inability to maintain homeostasis, resulting in the irreversible loss of calcium ions and the constant disturbance of the sodium/potassium gradient.[187–189] The cell membrane breakdown and its ability to reseal when introduced in an electric field were first demonstrated at the cellular level in the 1970s.[190–195]

Over the last decade, reversible electroporation has been commonly used in medicine and biotechnology to introduce non-permeable chemical species across the cell membrane, ranging from small molecules such as fluorescent dyes, radioactive tracers, and cytotoxic drugs such as bleomycin or cisplatin (now known as electrochemotherapy) to high molecular-weight molecules such as

antibodies, enzymes, dextrans, nucleic acids, and DNA.[196–198] Currently, the primary therapeutic *in vivo* applications of reversible electroporation are transdermal drug delivery, electrochemotherapy, and electrogene therapy, a form of non-viral gene therapy.

The various applications of reversible electroporation require cells to survive the procedure, and therefore the occurrence of IRE, which leads to cell death, is obviously undesirable in such a setting. Consequently, during the last three decades, when the field of electroporation has become dominated by reversible electroporation applications, IRE was viewed as an undesirable side effect and was studied only to define the upper limit of electrical parameters that induce reversible electroporation. It was quickly noted that this side effect could be advantageous, causing irreversible damage and thus ablating tissue.

Surprisingly, the ability of electricity to kill cells has been known for centuries. Reports show that this effect may have been observed as early as 1754 when Nollet studied the discharge of a static electrical generator on the skin,[39] and Fuller in 1898 reported that multiple high-voltage discharges had a bactericidal effect on a water sample.[199] Pulsed electrical fields have also been studied extensively as a method to destroy prokaryotic and eukaryotic cells and amoebae with regards to water decontamination.[200,201] Due to the capability of this technology to kill microorganisms, electroporation has also been used in the food industry since 1961 for sterilization and preprocessing of food.[43]

Electrical fields causing IRE also gained momentum during the last decade as a method to kill normal[202] or cancerous mammalian cells *in vitro*. This ability was duplicated *in vivo* and confirmed during tumour ablation of the liver, pancreas, kidney, and lung,[203–206] leading to the development of commercially available IRE medical equipment used in minimally invasive surgery for tumour ablation.[207]

4.6.2 Device and procedure description

The AngioDynamics Inc HVP-01 Electroporation System (also registered as the NanoKnife® IRE System) has received FDA clearance for surgical ablation of soft tissue. It has also been approved by the European regulatory authorities (CE certificate).

The system is the first commercially available technological platform based on the principles of IRE, and is intended for applications that require the ablation of tissue that is primarily cellular. The NanoKnife System consists of two major components: an LEDC generator and needle-like electrode probes (**Figures 4-20** and **4-21**).

FIGURE 4-20
Low-Energy, Direct-Current Electroporation System (NanoKnife IRE System, AngioDynamics)

One is the activator probe and the other is a standard probe. Up to five standard needles can additionally be connected to the generator forming five pairs of IRE circuits with the activator probe.

Image courtesy of AngioDynamics.

FIGURE 4-21
A Couple of IRE Probes

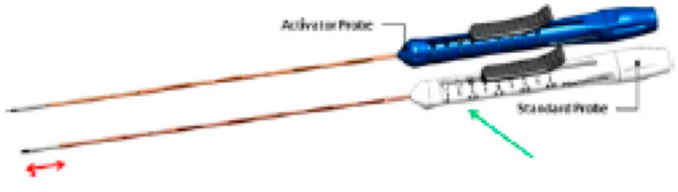

The NanoKnife Generator delivers LEDC energy to the NanoKnife electrode probes placed around a targeted area of soft tissue intended for ablation. The NanoKnife electrode probes work in a two-pole operating mode, where one is the positive supply and the other is the negative return. There is no need for a ground pad. Up to six NanoKnife electrode probes can be placed at a fixed distance apart in soft tissue to create several two-pole electrode configurations. It is important that the probes are placed in such a way that each one is parallel to the other. In addition, the inter-probe distance should not be less than 10 mm and not more than 20 mm. Therefore, LEDC is applied in cross pairs that have less than 2 cm distance apart. The active needle tip has a length of between 0.5 cm to 2 cm depending on the amount of retraction of the probe protective cap. This means that if the prostate length is more than 2 cm, the needles require a second treatment session after they have been pulled back (**Figure 4-22**).

FIGURE 4-22

A Three IRE probes placed in the prostate under biplanar TRUS guidance with the help of a 5-by-5 stepping grid.

B Two, three, and four NanoKnife IRE probe configurations. The inter-probe distance should be at least 1 cm and no more than 2 cm. The protective cap can be retracted in order to present the active tip, which has a maximum length of 2 cm. Probes should be parallel to each other.

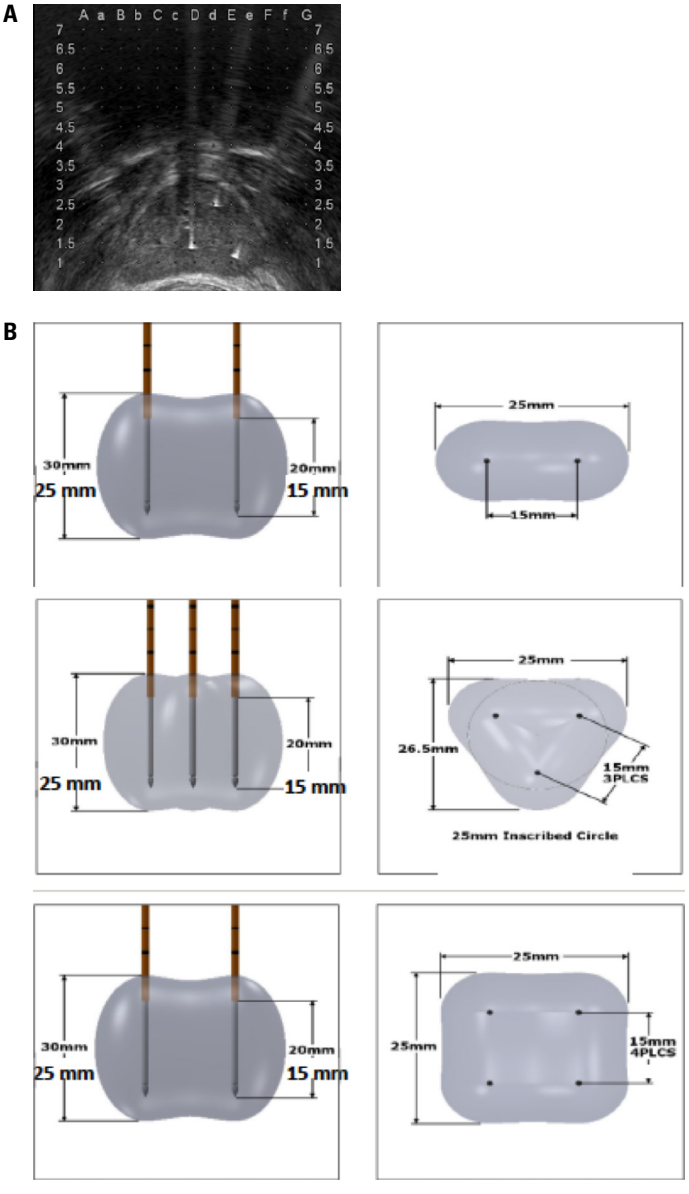

The number and configuration of electrode probes that are placed depends on the size and shape of the targeted area. During initial experience with IRE, care is taken so that the probes are distanced at least 5 mm from the urethra, the rectum, the bladder, the urethral sphincter, and the prostatic capsule (in the case of a nerve-sparing procedure).

Once the probes are properly in place, the user enters the appropriate parameters for voltage, number of pulses, and the pulse length into the LEDC generator user interface. Prior to the delivery of LEDC energy, the LEDC generator delivers a test pulse to characterize the electrical current dynamics between each probe pair during ablation. The unit then charges for approximately 30 to 40 seconds

and subsequently delivers a series of short electric pulses within seconds. Adjustments to maintain current within treatment range are made accordingly, and the final component consisting of a train of 70 pulses per probe pair is used to produce the tissue ablation. Voltages are chosen to attain effective electric field strength of >1,600 volts per cm between any probe pair. The delivery of LEDC energy can be monitored with real-time US.

The procedure is performed under general anesthesia with full muscle paralysis. This is required because whole-body muscle spasms can occur during the therapy, and muscle paralysis minimizes patient movements. Perioperative chemoprophylaxis is always provided. Apart from general medical history, elaborate cardiac history is advisable, as arrhythmia is always possible despite the fact that the prostate is relatively far from the heart and initial experience suggests the near absence of cardiac events. The patient is placed in the lithotomy position, catheterized, and prepped. The needle electrodes are placed transperineally under US guidance with biplane imaging using a 5-by-5 mm template (perineal grid) similar to that used for perineal mapping biopsies/brachytherapy (**Figure 4-23**).

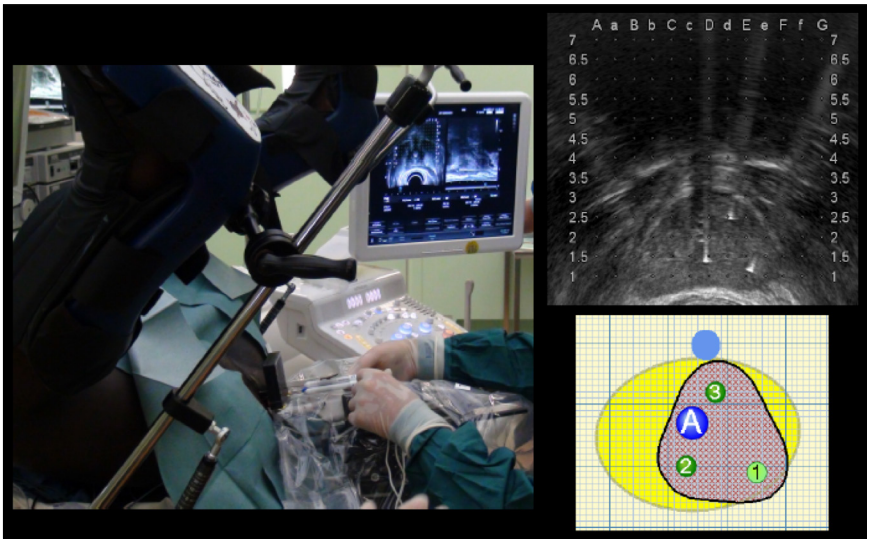

FIGURE 4-23
Patient placed in the lithotomy position and placement of three IRE probes in the lesion with the assistance of a brachytherapy stepping grid.

As previously mentioned, the number of electrodes required depends on the size of the lesion, with up to six IRE probes placed in a configuration that will allow encircling the area of interest. The lesion is seen using MRI/TRUS fusion imaging techniques, or if such elaborate software is not available, under TRUS imaging after cognitively knowing the area of interest from mp-MRI images. A technique similar to that used for brachytherapy allows for accurate placement of the probes around the lesion. After placing the needles, the procedure is performed and completed as described above. In some centres, cystoscopy is performed after needle placement to ensure proper placement.

After the procedure is concluded, the patient is awakened and returned to the floor with the catheter still in place. The catheter is usually removed on the next postoperative day, and the patient is discharged after usual postoperative recovery goals have been achieved.

4.6.3 Advantages and safety

As with any other new technology, small steps are taken initially, as safety issues are of major concern. After a number of bench research and preclinical animal studies showing the feasibility and potential advantages of this technology, limited human clinical testing has provided feasibility and safety data in order to proceed with more extended clinical trials.

4.6.3.1 Advantages

Sharp well-defined ablation margins and uniform lesion destruction

Initial studies indicate that due to the fact that IRE ablation is non-thermal in nature, no cold or heat sink phenomena are observed, as in other forms of energy such as cryoablation, HIFU, or radiofrequency ablation (RFA). As a consequence, a sharp demarcation between ablated and non-ablated tissue is seen, whereas thermal ablation techniques show a TZ of partially damaged tissue where insufficient temperatures were reached for definitive ablation. In fact, the IRE ablation area is primarily confined to between the electroporation probes, in contrast to RFA and cryosurgery, where the process of tissue ablation radiates from the RF or cryoprobe outward and is not bounded. With IRE, whatever tissue is within the electrical field is homogeneously "killed" with no skip lesions observed. This makes IRE very effective, provided targeting of the cancerous lesion is precise.

However, we still don't know how dynamic changes during treatment and tissue heterogeneity in structure and conductivity may affect the area of necrosis. For example, how would electric fields behave in the presence of radioactive seeds if IRE was used as a salvage procedure after failed brachytherapy? Therefore, the creation of an "electric" sink phenomenon that alters the predicted ablation zone in a similar fashion to what happens with the heat/cold sink event is possible and requires further research.[208]

Rapid ablation results and complete lesion resolution

In thermal ablation techniques, vascularity of the targeted organ may affect the size of the ablation zone due to the heat/cold sink phenomenon. As a consequence, ablation time with thermal energy sources may be prolonged, as repeated cycles of ablation may be required. In addition, the "kill" end-effect as observed during imaging follow-up requires time in such protocols. In fact, lesions treated by both heat- and cold-based sources take several months to show a decrease in size and years to show complete resolution. Thus, determination of treatment failure by imaging takes time and becomes elaborate, and is a matter of assessing continued tumour growth at the margins of the treated lesion or stability of the size of the lesion, signs that usually require experience to follow.

On the contrary, IRE ablation is independent of thermal diffusion. In fact, LEDC energy can be repeatedly delivered in a very short period of time at the targeted tissue. This results in a rapid lesion creation, making IRE a fast ablation modality. It was also noted that the treated area quickly resolved to a minimal scar in approximately 2 weeks, with disappearance of targeted cells, leaving no residual cavity or distortion.[209] It was postulated that the underlying basis for this phenomenon is the preservation of the microvasculature, down to the arteriolar level, throughout the LEDC lesion. Onik *et al.*[210] believe that LEDC lesions are therefore able to heal throughout their volume, whereas RFA and cryotherapy lesions are completely devascularized shortly after lesion creation, and are slowly resolved from the edges of the lesions inward.

The preservation of the microvasculature inside the lesion raises the possibility of tissue regeneration in that area. With correct targeting of the tumour for complete destruction, regeneration of the tumour should not be an issue. The possibility that normal tissue might regenerate within the previously made lesion in organs such as the liver, where normal tissue regeneration is a well-known phenomenon, is a possibility requiring research.

Rapid resolution of an IRE lesion in the prostate leads also to a fast decrease of total prostate volume. As a consequence, urinary symptoms may actually improve over both the short and the long term in patients with PCa and associated BPH. This makes IRE a potential therapeutic modality for BPH treatment requiring evaluation. Other energy sources like cryoablation have failed in this sense due to the thermal-based unfavourable characteristics of lesion resolution.

Sparing of sensitive structures such as nerves, vessels, and urethra

Preclinical data show that certain connective and neurological tissues such as blood vessels, ductal systems, urethra, and nerves may be spared when they are in high electric field zones during IRE ablation. This may also be correlated with the fact that no significant temperature changes occur during IRE, as happens with other heat-based forms of ablation.[211]

Because the IRE mechanism induces cell death by affecting the cellular membrane, it is able to kill cells in a targeted region without damaging the collagen and other interstitial constituents, thus preserving the integrity of the critical structures mentioned above. As seen histologically in the NVB areas, the vessels had variable loss of endothelium and were surrounded by scattered red blood cells, neutrophils, and edematous stroma. The lumen of affected vessels remained patent; however, without evidence of thrombosis. In addition, no heat sink effect was evident adjacent to vessels with complete necrosis adjacent to, and often surrounding, patent vasculature. Nerves within the NVBs appeared to be intact and unaffected. The margins of the lesions were very distinct, with a narrow zone of transition from normal to complete necrosis as discussed previously.[211]

Better imaging

Early data indicate that the conformational changes that tissue undergoes in the course of an LEDC ablation can be detected in real time with US and possibly CT and MRI imaging. Most importantly, these imaging modalities are not rendered useless during the procedure. Conversely, during cryoablation, physicians are "blinded" to all US image information beyond the proximal rim, due to the formation of a high echogenicity ice ball along that edge. Similarly, during RF procedures, tissue out-gassing obscures images to the point of losing all detail, rendering this imaging modality nearly useless.

Potential use in immunosuppressed patients

Al-Sakere *et al.* did not observe an increase in the number of immune cells after IRE ablation.[187] This suggests that the immune system is not needed to ablate tumours with LEDC, and therefore IRE via LEDC may be a viable option to consider within the choice of treatments for immunosuppressed cancer patients.[212]

Does not preclude subsequent radical surgery

Although initial clinical experience is limited, subsequent RP in patients one month after IRE ablation was no more difficult than with any other RP.

4.6.3.2 Safety

Current experience regarding safety and efficacy of IRE in humans shows no major adverse events during IRE.[213] This technology has been used in the liver,[214,215] pancreas,[216,217] kidney, lung,[218] and prostate.[219,220] Most complications were minor and associated with the puncture itself rather than with the technology. Reported complications in these studies are presented in **Table 4-1**. For the prostate in particular, Neal *et al.*[221] treated the first two patients with IRE of the prostate with no complications apart from mild hematuria, which was self-limiting. Both patients had a catheter for 10 days, which seems from more advanced experience not necessary. Larger series evaluating IRE of the prostate are presented in more detail in the next section.

TABLE 4-1 Complications Reported in Irreversible Electroporation of the Liver, Pancreas, Lung, Kidney, and Prostate

Hepatic IRE	6% (8/129)	Pneumothorax Hemothorax Pleural effusion Occlusion of major hepatic vein Portal vein thrombosis Bile duct obstruction Cholangitis Biliary stent occlusion
Pancreatic IRE	19% (8/42)	Pneumothorax (intubation related) Subcutaneous hematoma Portal vein thrombosis Bile leak Pancreatitis
Renal IRE		Arrhythmia Postural hypotension (accidental adrenal ablation) Transient hematuria
Lung IRE		Parenchymal hemorrhage Pneumothorax
Prostate IRE		Hematuria Dysuria Hemospermia UTI Epididymitis Urethral stricture Urinary retention Sepsis Arrhythmia

Abbreviations: IRE, irreversible electroporation; UTI, urinary tract infection.

4.6.4 Clinical data

Irreversible electroporation is a very new ablation modality, and therefore clinical data are scarce. Small clinical trials with fewer than 40 patients have been published showing the feasibility and safety profile of this procedure. An overview of data from all three major centres (Amsterdam-AMC/Athens-AMS, London-UCL/Sydney-St Vincent, New York-MSKCC[222]) is presented in **Table 4-2.**

TABLE 4-2 Clinical Data From Three Major Centres

Centre	Amsterdam-AMC/ Athens-AMS	London-UCL/ Sydney-St Vincent,	New York-MSKCC
Patient characteristics	**Prospective study**	**Retrospective study**	**Prospective study**
Number of prostate IRE patients	16	34	35
IRE as primary treatment	16 (100%)	34 (76%)	27 (77.1%)
IRE as salvage treatment	0	11 (25%)	8 (22.9%)
Mean age (range)	60 (44–75)	65 (59–71)	63.1 (59.3–67.6)
Mean PSA (range)	9 (3.6–25)	6.1 (4.3–7.7)	4.3 (3.3–5.6)
GS (range)	6–8	6–8	6–7
Prostate cancer stage or risk group	cT1-cT2c	Low/intermediate risk 97%	Low/intermediate risk 100%
Unilateral	11		
Bilateral	5		
Operative data			
Mean operative time (range)	104 (65–140) min		73 (56–87) min
Mean IRE time (range)	13 (2.5–27) min	27 (11–55) min	14 (6.9–27) min
Number of probes (range)	3.5 (2–4)	4 (2–6)	4.8 (3–6)
Intraoperative complications (if yes specify)	One additional dose of muscle relaxant	One self-limited tachycardia	
Perioperative data			
Mean hospital stay (range)	3.05 (3–4) days	1 (1–2) days	1 day
Postoperative complications			
Grade 1	15/16 (93.7%)	12 (35%)	6/27 (22.2%)
Grade 2	8/16 (50%)	10 (29%)	8/27 (29.6%)

Abbreviations: Bx, biopsy; EF, erectile function; IIEF, International Index of Erectile Function; IPSS, International Prostate Symptom Score; IRE, irreversible electroporation; RP, radical prostatectomy; UTI, urinary tract infection.

Centres: AMC, Amsterdam Medical Center; AMS, Athens Medical School; MSKCC, Memorial Sloan Kettering Cancer Center; UCL, University College London.

continued on **page 313**

TABLE 4-2 Clinical Data From Three Major Centres, *Cont'd*

Centre	Amsterdam-AMC/ Athens-AMS		London-UCL/ Sydney-St Vincent,	New York-MSKCC	
Patient characteristics	**Prospective study**		**Retrospective study**	**Prospective study**	
Grade 3 or 4	1/16 (6.25)		0 (0%)	2/27 (7.4%)	
Retention (%)	5/16 (31%)		2/34 (6%)	6/27 (22.2)	
Mean catheter duration (range)	7 (5–9)		3 (0–9)	(2–15)	
Hematuria (%)	10/16 (62.5%)		6/34 (18%)	4/27 (14.8%)	
Hemospermia (%)	2/16 (12.5%)			1/27 (3.7%)	
Hematohezia (%)	1/16 (6.25%)				
UTI (%)	2/16 (14%)		5/34 (15%)	2/27 (7.4%)	
Dysuria (%)	2/16 (14%)		5/34 (15%)	1/27 (3.7%)	
Urethral stricture (%)				1/8 salvage cases	
Other	1/16 (6.25%) sepsis			2/27 (7.4%) epididymitis	
Postoperative data					
Follow-up mean (range)	1		6 (1–24)	6	
Urinary bother at baseline	Mean IPSS	11		Urinary function ≥17	17/22 (77%)
Urinary bother at first follow-up	Mean IPSS (1 week)	12		Urinary function ≥17 (6 months)	13/16 (81%)
Urinary bother at last follow-up	Mean IPSS (4 weeks)	12		Urinary function ≥17 (12 months)	15/17 (88%)
Continent at baseline (%)	100%			27/27 (100%)	
Continent at first follow-up (%)	72%		24/24 (100%)	26/27 (96.3%)	
Continent at last follow-up (%)	Patient had RP			25/27 (92.6%)	
Potency at baseline (%)	Mean IIEF	17.3		EF ≥22	13/22 (59%)
Potency after first follow-up (%)	Mean IIEF (1 week)	15.7	19/20 (95%)	EF ≥22 (6 months)	7/16 (44%)
Potency after last follow-up (%)	Mean IIEF (4 weeks)	16.9		EF ≥22 (12 months)	11/17 (65%)

Abbreviations: Bx, biopsy; EF, erectile function; IIEF, International Index of Erectile Function; IPSS, International Prostate Symptom Score; IRE, irreversible electroporation; RP, radical prostatectomy; UTI, urinary tract infection.

Centres: AMC, Amsterdam Medical Center; AMS, Athens Medical School; MSKCC, Memorial Sloan Kettering Cancer Center; UCL, University College London.

continued on **page 314**

TABLE 4-2 Clinical Data From Three Major Centres, *Cont'd*

Centre	Amsterdam-AMC/ Athens-AMS	London-UCL/ Sydney-St Vincent,	New York-MSKCC
Patient characteristics	**Prospective study**	**Retrospective study**	**Prospective study**
Oncologic control	All patients had RP No viable tumour in ablation zone	4 patients (17%) second treatment 6 patients (25%) lesion on MRI	
(+) Bx overall (%)			7/25 (28%)
(+) Bx at ablated region (%)			4/25 (16%)
(+) Bx outside ablated area			3/25 (12%)

Abbreviations: Bx, biopsy; EF, erectile function; IIEF, International Index of Erectile Function; IPSS, International Prostate Symptom Score; IRE, irreversible electroporation; RP, radical prostatectomy; UTI, urinary tract infection.

Centres: AMC, Amsterdam Medical Center; AMS, Athens Medical School; MSKCC, Memorial Sloan Kettering Cancer Center; UCL, University College London.

4.6.4.1 Patient selection

All three series included a small number of patients (16, 34, and 35). The absolute majority (97–100%) of patients had low- to intermediate-risk PCa with only a couple of GS 8 patients included. Mean PSA values were <10 ng/mL with more patients having unilateral disease. Nevertheless, patients with bilateral cancer and PSA values >10 ng/mL were included occasionally.

Irreversible electroporation was predominantly used in the primary setting, although some patients underwent IRE as a salvage procedure. After initial diagnosis, patients usually underwent a confirmatory Bx under mp-MRI-TRUS fusion guidance for better identification/topography of the index lesion; however, this was not the rule. The patients recruited in Amsterdam and Athens were planned to have a RP and did not have a confirmatory Bx.

Patients were healthy with life expectancy >10 years. Patients with cardiac history were avoided because of the possibility of cardiac arrhythmia initiated during the IRE application. However, in one instance after the procedure, self-limiting tachycardia was encountered, requiring 24-hour inpatient cardiology surveillance. Inclusion and exclusion criteria are presented in **Tables 4-3** and **4-4**, as determined in the Amsterdam study.

TABLE 4-3 Inclusion Criteria for Irreversible Electroporation Ablation of the Prostate in the Amsterdam Medical Center/Athens Medical School Study

Inclusion Criteria	1. > 50 years 2. Histologically confirmed organ-confined PCa (clinical stage T1-T2) 3. GS ≤7 4. PSA <20 ng/mL 5. Able to visualize prostate gland adequately on transrectal US imaging 6. No prostate calcification greater than 5 mm 7. Ability of subject to stop anticoagulant and antiplatelet therapy for 7 days prior to and 7 days after the procedure

TABLE 4-4 Exclusion Criteria for Irreversible Electroporation of the Prostate in the Amsterdam Medical Center/Athens Medical School Study

Exclusion Criteria	1. Other Conditions/Status a. Bleeding disorder as determined by prothrombin time (PT) >14.5 seconds, partial thromboplastin time (PTT) >34 seconds, and platelet count <140/μL b. Active UTI c. History of bladder neck contracture d. Anesthesia Surgical Assignment, category IV or greater e. History of inflammatory bowel disease f. Concurrent major debilitating illness g. Prior or concurrent malignancy h. Cardiac history i. Implantable cardioverter defibrillator (ICD) or pacemaker 2. Prior or current therapies a. Biologic therapy for PCa b. Chemotherapy for PCa c. Hormonal therapy for PCa within 3 months of procedure d. RT for PCa e. TURP, urethral stent f. Prior major rectal surgery (except hemorrhoids) g. Inability or unwillingness to tolerate temporary cessation of concurrent anticoagulation therapy or antiplatelet drugs for a period of 7 days prior to and up to 7 days after the procedure

4.6.4.2 Perioperative outcomes

All patients underwent IRE under general anesthesia with full muscle paralysis. This is necessary, as small muscle contractions are evident during the application of LEDC energy. In one patient, an additional dose of muscle relaxant was required due to more intense muscle spasms. Operating time was around 1 to 2 hours depending on the experience each center had with focal therapy. Operating times less than an hour were recorded as well. Procedural time for the IRE ablation was much shorter, ranging from 2.5 to 55 minutes. Mean values ranged from 13 to 27 minutes in the three studies. Usually 3 to 4 (range, 2–6) probes were used. Hospital stay varied from 1 to 4 days depending on local administrative routines. All patients were ambulating on the first postoperative day. Patients did not complain for pain, as visual analogue scale (VAS) scores did not change significantly.

Most complications were grade 1 (18%–97%) and grade 2 (24%–29.6%), which were self-limiting and did not require hospitalization. Hematuria and hemospermia, as with prostatic biopsies, could take longer to clear (30 days). Only a couple of cases had serious UTIs requiring hospitalization, among

them one septic episode required a 6-day hospitalization and one epididymitis required subsequent orchiectomy. This last patient had a prostate of 61 g, and after the IRE procedure that required self-intermittent catheterizations for 2 weeks is when his epididymitis occurred. This was not responsive to antibiotics, and removal of the organ was necessary.

Most complications are similar to what could occur during a prostatic Bx. Urinary retention was not absent as one would expect due to the non-thermal ablation modality associated theoretically with less swelling of the prostate. This complication ranged from 6% to 31%. Most patients had the catheter successfully removed after a mean of 7 (5–9) days. Only a minority required longer catheterization or assistance with self-catheterization.

A deterioration of previous urethral stricture was reported in the MSKCC series in a patient who had failure after salvage cryotherapy for failed primary brachytherapy.

A rectal fistula was never reported. Nevertheless, most centres during this initial experience were very attentive to stay far away from the rectal wall.

4.6.4.3 Functional outcomes

Continence

Continence was temporarily affected in 18% of patients in the Amsterdam series although mature data of post-prostatectomy continence rates after the RP are awaited. In the UCL series, continence rates after 6 months were 100%. In the MSKCC, all but one patient were continent at 6 months (continence 96.3%) while one more patient was incontinent after 12 months of follow-up (continence of 92.6%).

Urinary function

In the MSKCC series, urinary function (UF), determined as UF ≥17, did not change significantly after the ablation procedure (77% at baseline, 81% at 6 months, 88% at 12 months). In fact, it seems that in some patients it was improved after the ablation procedure, indicating a potential improvement in BPH symptoms as well. Similarly, in the AMC study where urinary function was evaluated by IPSS, urinary function did not differ from baseline (mean IPSS=11 at baseline, mean IPSS=12 at 1 week, and mean IPSS=12 at 4 weeks).

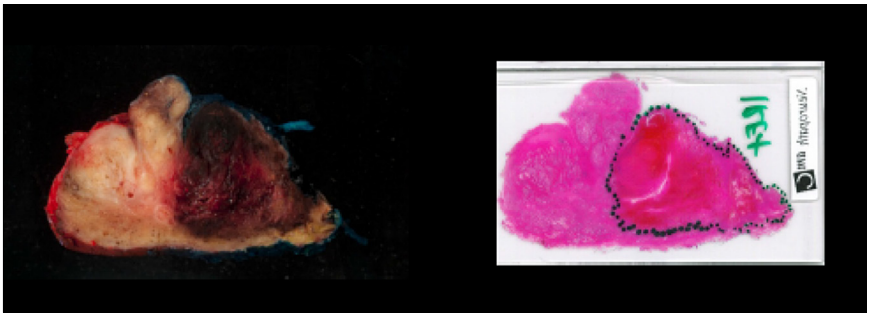

FIGURE 4-24
Macroscopic fixed 4 mm–thick prostate slice and whole-mount pathology slide with hematoxylin and eosin (H&E) staining after irreversible electroporation (IRE) ablation.

4.7 Intensity-Modulated Radiotherapy and Stereotactic Body Radiotherapy

4.7.1 Introduction

Radiotherapy has traditionally been administered to the entire gland by external beam or brachytherapy. Over the course of several decades, external beam radiation for PCa has evolved from a merely non-conformal to conformal radiation. Technological progress has allowed RT to be concentrated more selectively and recently to dose intensify predetermined regions of the prostate. The ability to dose escalate is notable, as the likelihood for long-term cancer control is directly associated with the radiation dose. The aim of conformal RT is to treat the target volume as tightly as possible with a minimal dose to neighboring critical structures and organs. The most advanced technique to achieve this goal with photon therapy is intensity-modulated radiotherapy (IMRT) and stereotactic body radiotherapy (SBRT).

Intensity-modulated radiotherapy limits the dose to critical surrounding structures, such as the bladder and rectum. Zelefsky *et al.* achieved excellent long-term biochemical control rates while improving the toxicity profile by sparing adjacent organs from treatment-related effects.[223] Image-guided RT for prostate is one of many methods for identifying the location of the prostate, followed by adjustment of the treatment fields to target the prostate. Methods for monitoring prostate position include identification of metal fiducials on kilovoltage imaging, integrated CT prior to each fraction, and the implantation of electromagnetic fiducials. With increased accuracy of prostate localization comes the prospect of reducing planning margins and reducing toxicity to surrounding organs.

In keeping with the trend of applying higher doses to more precise areas, investigators have used IMRT to treat a single lobe of the prostate, or more exactly a biological target volume consisting of a dominant intraprostatic lesion (DIL). In a feasibility study reported by van Lin *et al.* using MRI with magnetic resonance spectroscopic imaging (MRSI) to identify a DIL, the whole prostate was irradiated to 70 Gy with a DIL boost to 90 Gy.[224]

Brachytherapy seeds as permanent or removable high-dose rate (HDR) implants may represent the most promising and best studied of current techniques to be considered for focal therapy. Brachytherapy with MRSI or ProstaScint® guided dose escalation targeting intraprostatic lesions allow boost doses from 150% to 190% beyond the prescription dose.[225,226] To provide conformal application of a higher tumour radiation dose, HDR 192-Ir implants have been used to boost EBRT and less frequently as monotherapy on the whole gland.[227,228] Experience with HDR monotherapy has achieved acceptable biochemical recurrence-free rates,[228–230] and in combination with image guidance, it may be a promising technology for focal therapy.[231]

Radiotherapy appears to be particularly suitable to study as a focal treatment option. It has an established biological basis, known tumouricidal activity, and familiarity to radiotherapists and urologists. When applied as focal therapy, its use remains investigational, as the effects of radiation scatter, and the long-term tumour control rates and the ability to re-treat are unknown. However, SBRT for PCa is an emerging technique.

4.7.2 Intensity-modulated radiotherapy

With IMRT, subsegments of the target volume are treated to different intensity levels, shaping the isodose lines to the contour of the target volume.[232,233]

For the purpose of radiation, a treatment plan is calculated that determines the radiation intensity to the target volume subsegments. In addition to delineation of the target volume, organs at risk (OAR) are also delineated for treatment planning. Organs at risk and structures that have to be considered for prostate treatment are the bladder, rectum, anal canal, urethra, neurovascular penile plexus, and penile bulb. Because the urethra and neurovascular penile plexus are usually poorly visible on regular imaging, they are often not taken into account in the treatment planning. Dose and volume constraints are assigned to the delineated structures for treatment planning.

To design and calculate an IMRT plan, inverse treatment planning is used. Dose and volume constraints are assigned to the contoured organs and structures (target volume and OAR) in order to create an inverse treatment plan for IMRT. If the plan is not satisfactory, the dose-volume constraints are modified for a next iterative planning process. These steps are repeated until a satisfactorily and acceptable treatment plan is obtained.

Several techniques can be used to fulfill IMRT:

1. Static segment therapy (also called step-and-shoot). With this technique several beam directions are designed, each consisting of several segments. These segments are designed by the aperture of the multileaf collimator of the linear accelerator. Each segment is irradiated in sequence, leading to a non-homogeneous dose deposition from each beam direction.
2. Dynamic segment therapy (also called sliding-window). With this technique, the different intensity levels from each beam direction are designed by the continuously moving leaves.
3. Volumetric-modulated arc therapy. This technique does not use static beam directions, but a continuously moving gantry and also continuously moving leaves.
4. Helical tomotherapy. With this technique, IMRT is delivered by simultaneous movement of the couch, gantry, and binary collimator.

Until now there are no reported studies on IMRT for focal therapy of PCa. There are also no trials listed in the trial register of ClinicalTrials.gov.[332] On the contrary, several studies are performed or recruiting for brachytherapy. The evidence obtained for brachytherapy is discussed in the brachytherapy chapter. Obviously in the radiation community there is a preference to perform brachytherapy rather than IMRT. The planning margins (4–8 mm) needed to account for dosimetric uncertainties with IMRT, certainly if ablative doses of >90 Gy are used, prevent proper usage of IMRT due to the risk for normal tissue damage.

4.7.3 The CyberKnife

The CyberKnife® Robotic Radiosurgery System (Accuray Incorporated, Sunnyvale, CA) uses a robotically mounted linear accelerator to deliver a large number of small conformal beams. The CyberKnife robotic irradiation system is a unique radio-surgical system capable of treating tumours anywhere in the body non-invasively and with submillimeter accuracy. The CyberKnife delivers radiation using a precise targeting methodology allowing a focal treatment margin around the target, thus limiting the volume of adjacent tissue receiving high doses of radiation. This in turn allows for the delivery of high doses of radiation to the DIL in the prostate over a short series of treatments. It consists of a linear accelerator mounted on an industrial robot. The advantages of the CyberKnife include:

- Beam collimation/low penumbra with a sharper field edge
- Precise targeting (≤1 mm) of selected lesions
- A unique ability to provide real-time monitoring of the treated target throughout treatment using an advanced image-guidance system
- A unique ability to correct during treatment for limited target motion (e.g., due to small patient movements)
- A capacity to deliver higher doses of radiation to smaller volumes, reducing the amount of radiation to surrounding healthy tissue.
- The latter allows for a reduction of the number of sessions of RT (hypofractionation), which should be associated with an improved patient QOL.

These points justify the choice for the CyberKnife to be used as a means to treat DIL in the prostate as focal therapy. It has been used for more than 7 years in the United States and elsewhere to treat low- and intermediate-risk PCa with hypofractionated regimens typically consisting of four to six fractions. Biochemical DFS and toxicity compare favourably with standard fractionation regimens.[234–236]

4.7.4 Rationale of focal therapy with stereotactic body radiotherapy

Studies of patterns of failure following conventionally fractionated EBRT show that the area responsible for local recurrence is the dominant intraprostatic nodule in 89%[237] to 100%,[238,239] of cases. It is, therefore, logical that treatment of only the DIL may be able to keep the same biochemical control whilst avoiding the increase in side effects seen with whole-gland dose escalation. Stereotactic body RT planning techniques and software have an enhanced ability to dose paint, which enables heterogeneous doses within the prostate and can mimic the dose distributions seen with HDR brachytherapy.[240,241]

Prostate cancer has an unusual radiobiology. The biologically effective dose (BED) of a given dose and fractionation depends on the intrinsic radiosensitivity of a tumour expressed as a parameter called the alpha-beta ratio (α/β ratio). The value of this parameter is not precisely known, but is likely to be less than 2 Gy for PCa cells. This low α/β ratio is lower than that of the dose-limiting organ, the rectum.[242–244] This implies that hypofractionation has a proportionally larger effect on PCa cells than the normal surrounding tissues. Using large doses per fraction could potentially increase cure rates while minimizing damage to normal tissues.

These are logical reasons why HDR to only the DIL nodule may keep the same therapeutic ratio as whole-gland RT. However, this strategy relies on being able to delineate the dominant prostate disease nodule accurately. The most important factor to make this treatment possible and oncologically efficient is how to accurately detect the DIL in the prostate.

Newer MRI techniques have improved tumour delineation in PCa.[245,246] These include DCE-MRI, which assesses the ability of tissues to take up MRI-contrast agents, often gadolinium. Additional techniques such as diffusion-weighted MRI (DW-MRI), which assesses the diffusion of water molecules across barriers such as the vasculature, and MR spectroscopy, which measures the ratio of choline and citrate in tissues, can further increase accuracy and prostate nodule definition. The normal prostate gland has low levels of choline and high levels of citrate, whereas for PCa the reverse is true.[247]

4.7.5 Treatment delivery

CyberKnife prostate SBRT treatment times are much longer than conventional fractionation and often take 35 to 45 minutes to deliver. The prostate is partially mobile within the pelvis and exhibits a variety of patient-specific and idiosyncratic movements.[248,249] The margin likely to be needed to account for intrafraction motion, assuming interfraction motion is assessed and corrected, is likely

to be 2 mm to 3 mm.[250–252] Patients have to be tracked for intrafraction motion using gold fiducials and the CyberKnife prostate-tracking algorithm. A margin of 3 mm to 5 mm is probably needed around the DIL.

4.7.6 Conclusion

Intensity-modulated radiotherapy and SBRT are known effective treatments for PCa. However, clinically there is very limited experience in focal prostate therapy. One drawback for all external beam modalities is that because of geometric uncertainties, a larger area than the tumour volume itself needs to be treated, preventing ablative doses in certain cases. Therefore, there is still a preference for brachytherapy.

4.8 Interventional Radiotherapy (Brachytherapy)

4.8.1 Introduction

Prostate cancer brachytherapy is one of the most frequently used modern treatment techniques in localized PCa. Brachytherapy uses radioisotopes with short radii of activity to optimize effective treatment of small target volumes within the prostate as well for minimizing the risk to adjacent non-cancerous tissues.

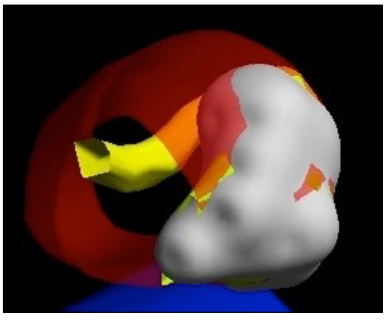

FIGURE 4-25
3D Dose Calculations of Low-Dose-Rate Implantation

3D dose calculation of a prostate focal low-dose-rate (LDR) implantation with I-125 seeds (based on dose calculation visualization with the use of sectional transrectal ultrasound [TRUS] images).

Legend: red:prostate shape; yellow: urethra shape; blue: ventral rectum; grey: reference isodose shape

FIGURE 4-26
3D Dose Calculations of High-Dose-Rate Implantation

3D dose calculation of a prostate focal high-dose-rate (HDR) implantation with Ir-192 stepping source (based on dose calculation visualization with the use of sectional transrectal ultrasound [TRUS] images). Grey: prostate shape; yellow: urethra shape; blue: ventral rectal wall; green: reference isodose shape with afterloading needles.

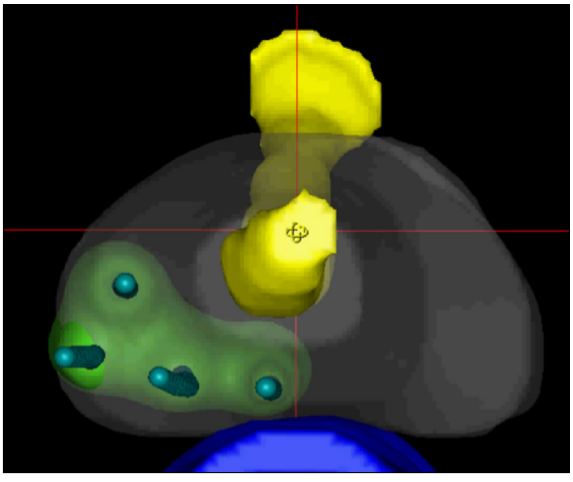

Brachytherapy offers the optimal technical performance for partial organ treatment in comparison with other modern RT techniques (**Table 4-5**). Both low-dose-rate (LDR, **Figure 4-25**) and high-dose-rate (HDR, **Figure 4-26**) brachytherapy are eligible for delivering partial organ treatments; however, the stepping source technology used in HDR implants has technological and economic advantages (**Table 4-6**). According to an international and interdisciplinary expert panel consensus report,[253] patients selected for focal prostate treatment should have unilateral low- to intermediate-risk disease with clinical stage ≤cT2a. Prostate size, tumour volume, and tumour topography are important selection criteria that may influence the choice of ablative technology used.

Currently, the optimum staging for men being considered for focal therapy is transperineal template mapping prostate biopsies. As an additional staging tool, MRI of the prostate using a multiparametric (MP) technique, including DCE and DWI, is increasingly being used to diagnose and stage primary PCa with excellent results. However, for general use, these newer imaging techniques require validation in longer-term prospective clinical trials. Until such studies are performed, MRI will in most centres continue to be an investigative tool in assessing eligibility of patients for focal therapy, but it should not be relied upon in the absence of Bx.

Additionally, Langley *et al.*[254] published selection criteria for focal therapy with LDR seed implants. They recommend:

a. Life expectancy >10 years
b. PSA ≤15 ng/mL
c. The use of a mp-MRI (T1W/T2W, DWI, DCE±spectroscopy) prior to Bx, (in order to avoid post-Bx hemorrhagic artifact)
d. Whole gland template-guided prostate mapping Bx with 5 mm sampling
e. Unilateral disease; lesion size ≤0.5 mL (approximately equates to maximum cancer length of 10 mm) with or without clinically insignificant disease on the contralateral side (cancer core length ≤3 mm)
f. GS of index lesion 6–7 (3 + 4)
g. Tumour stage ≤T2b (clinical)
h. Prostate size ≤60 mL

TABLE 4-5 Comparison of Technical Eligibility of Modern Radiotherapy Methods in Focal Treatments for Localized Prostate Cancer

	CyberKnife	IMRT	IGRT	Brachytherapy
Target definition	+ (with image fusion)	–	–	+
Interfraction movement	+	–	+	+
Intrafraction movement	+	+ (with 4D)*	+ (with 4D)	+
Target dose painting	+	+ (with 4D)	+ (with 4D)	+
Low-dose volumes	–	–	–	+
Dose on organs at risk	+	–	–	+
Smallest reasonable radiation field	0.5 cm^3	2.0 cm^3	2.0 cm^3	0.5 cm^3

Abbreviations: 4D, four dimensional; IGRT, image-guided radiotherapy; IMRT, intensity-modulated radiotherapy.
*Radiation field "follows" in real time the target.

TABLE 4-6 Comparison of Low-Dose-Rate and High-Dose-Rate Technology

	Source	Dose painting	Radiation protection	Economics	Fractionation
Low-dose-rate seeds	Linear	Not possible	Simple at procedure Complicated at post-transplant	Expensive 250k € per 100 patients	Single
High-dose-rate afterloading	Stepping	Possible	Needs an HDR unit No post-implant protection necessary	Economic 25k € per 100 patients	Single

Interventional RT in the form of LDR or HDR brachytherapy as sole treatment (monotherapy is without complementary external beam radiation) has been widely used for the treatment of localized PCa, with good long-term outcome results and acceptable toxicity rates.[229,255–265]

There are no prospective randomized clinical study results comparing LDR with HDR in PCa treatments, however, analysis of dosimetry,[266] retrospective patient cohorts,[230] as well post-treatment IPSS scores[267] underline the superior potential of the stepping-source-technology (HDR).

In fact, only a very few reports have been published so far on primary focal brachytherapy. The first large patient cohort in the literature with partial prostate treatment was published by Nguyen *et al.*, 2012, with 318 patients.[268] Selection criteria included GS <3+4, T1c, PSA <15 ng/mL, and eligibility for MRI-guided implantation. Target volume for implantation was only the peripheral zone of the gland. Following a median follow-up of 5.1 years, the overall survival (OS) for intermediate-risk cases was 73% at 5 years and 66% at 8 years, respectively. Of note, this type of partial (peripheral only) implantation is rather different from the various current proposals for focal brachytherapy.

Cosset *et al.* published a preliminary series of a highly selected cohort of patients who had primary focal brachytherapy.[269] In this group, the treatment volume corresponded to a mean value of 34% of the entire organ volume. After treatment with 145 Gy (average D90 of 183.2 Gy and a mean V100 of 99.3%), the PSA had reduced in all cases 1 year following the implantation. The follow-up was very short in this series; however, the average PSA of 6.9 ng/mL at diagnosis decreased to a mean value of 5.5 at 2 months and to 2.6 ng/mL after 1 year. In terms of toxicity, there was a borderline improvement in IPSS scores at 6 months and a significantly better IIEF score compared with comparative historical results for whole-gland prostate implants.

Regarding acute toxicity for partial prostate treatments, Barret *et al.* reported favourable results in a cohort of 106 patients with only 2% major complications. The authors did not report any toxicity related to focal brachytherapy treatments in their patient cohort.[270] In a recent review on focal RT, Kovács *et al.* highlighted the potential role for this type of treatment in localized PCa; however, they also underlined the current lack of and necessity for long-term results.[271]

Clinical trials such as the NCT01830166 (I-125 seeds), NCT02391051, NCT02290366 (HDR), and NCT01902680 (I-125 seeds) trials should offer more information in the future.

There are few ongoing trials—the NCT01354951 (I-125) as well the NCT02290366 (Cs-131)—that have already completed patient recruitment. The first publications from these trials are expected soon.[25]

TABLE 4-7 Registered Studies Using Interventional Radiotherapy for Focal Prostate Radiation

Study	Study level	Isotope	Starting date	Study completion	Enrolling estimation	Endpoint
NCT02290336	Phase 2	Cs-131	2014	2019	100	5 years bNED
NCT01354951	Phase 2	I-125	2011	2016	80	Late toxicity
NCT01830166	Phase 2	I-125	2013	2018	10	QOL
NCT02391051	Phase 2	Ir-192	2014	2027	50	Early toxicity
NCT01902680	Phase 1	I-125	2013	2015	17	Target definition
NCT01802307	Phase 2	I-125	2013	2018	50	Toxicity

Abbreviations: bNED, biochemical no evidence of disease; Cs, cesium.

4.8.2 NCT02290366 (Cs-131)

The study evaluates focal brachytherapy using the isotope cesium-131 (Cs-131) to treat patients with low-risk PCa. The goals of the study are to determine the biochemical DFS at 5 years in these patients, as well as to determine the acute and late urinary, bowel, and sexual toxicity associated with focal prostate brachytherapy using Cs-131.

Patients eligible for the study will be men with histologically confirmed adenocarcinoma of the prostate with clinical stage T1c-T2aN0M0, GS ≤3+3=6, PSA <10 ng/mL or a PSA density ≤0.15 ng/cc, and ≤2 cores positive out of a minimum of 12 cores sampled. Additionally, patients must have a single, dominant index lesion on MRI.

The study is a phase 2 study. Patients will be followed prospectively. Dosimetry will be evaluated post-procedure, and PSAs will be obtained every 3 months in year 1 and every 6 months from years 2 through year 5. Urinary, bowel, and sexual morbidity will be assessed by patient survey prior to treatment, at 2 weeks, after treatment, at 3-month intervals in year 1 and at 6-month intervals in years 2 through 5.

Further study details:

- Estimated enrollment: 100
- Study start date: November 2014
- Estimated study completion date: August 2015

4.8.3 NCT01354951 (I-125)

The purpose of this study is to identify the side effects of a radiation treatment called focal brachytherapy in treating early-stage PCa. The study is also looking at how useful focal brachytherapy will be in treating PCa. Additionally, the investigators would like to see how this type of treatment impacts QOL.

Further study details:

- Estimated enrollment: 80
- Study start date: May 2011
- Estimated study completion date: May 2016

4.8.4 NCT01830166 (I-125)

This investigation develops and evaluates a treatment plan for prostate focal therapy based on low-dose-rate brachytherapy. The participants entering this study are those suitable for AS. These participants will be monitored with various imaging methods and interventions such as MR elastography, TRUS elastography, positron emission tomography (PET)/CT, and transperineal mapping Bx to determine the extent of cancer and suitable treatments. Those suitable for focal therapy will be offered the option of low-dose-rate brachytherapy (LDRB) focal therapy in addition to AS or radical therapy.

This study will be used to evaluate the long-term use of multi-modal, MP PCa imaging, combining data from MRI, US, and 11C-choline PET/CT. Such methods can be used to eliminate the need for invasive methods such as mapping biopsies.

Further study details:

- Estimated enrollment: 10
- Study start date: May 2013
- Estimated study completion date: January 2018

4.8.5 NCT02391051 (Ir-192, HDR)

This trial examines the feasibility and toxicity of focal brachytherapy in patients with low-risk PCa.

Further study details:

- Estimated enrollment: 50
- Study start date: October 2014
- Estimated study completion date: July 2017

4.8.6 NCT01902680 (I-125)

This is a prospective, biomedical, pilot study of interventional type which includes 17 patients on 24 months (12 months of inclusion and 12 months of follow-up). The objective of the study is to verify that the focal therapy technique used (with the help of KOELIS® system) allows for obtaining optimal dosimetric coverage of the prostate target (i.e., dose of 160 Gy ± 5% delivered on the envelope isodose) evaluated by CT scan performed 30 days after implantation.

Further study details:

- Estimated enrollment: 17
- Study start date: August 2013
- Estimated study completion date: September 2015

4.8.7 NCT01802307 (I-125)

The purpose of this study is to investigate the use of focal, targeted treatment of PCa, that is, to treat only the small area of cancer instead of the entire prostate. The authors hope to show that this strategy will reduce the amount of side effects without compromising cancer cure.

Further study details:

- Estimated enrollment: 50
- Estimated study completion date: March 2018

4.8.8 Summary

Focal therapy for localized PCa is technically not different from whole-gland treatments. The principle challenges are appropriate patient selection and the definition of the optimal target treatment volumes. Therefore, close interdisciplinary cooperation between interventional RT, urology, and imaging experts is obligatory. At the present time, only a few Level D (expert opinion) reports are published in the literature. However, several ongoing controlled clinical trials are likely to deliver higher LOE on this topic in the next years.

4.9 Laser Ablation

4.9.1 Description technology

Focal laser ablation (FLA), alternatively known as laser interstitial thermotherapy (LITT), has only been evaluated utilizing one system, Visualase® (Houston, United States). In 2014, Visualase was purchased by Medtronic (Minnesota, United States).[272]

The Visualase platform was approved by the FDA in the United States in 2007 via the 510K pathway for prostate soft-tissue ablation, and represents a novel approach to PCa ablation. Therefore, clinical series are limited and relatively little data is available. Among the case-series from Canada, Europe, and the United States, patient selection, preparation, procedural specifications, and follow-up have varied.

4.9.2 Feasibility studies

A proof-of-principle animal study was performed to establish technical specifications, feasibility, and histologic outcomes. Stafford *et al.* placed the laser via laparotomy in five dogs and used 4 W to 14 W of power for mean treatment times of 2.5 minutes. The resulting treatment lesions were as large as 15-by-27 mm (ellipsoid-shaped), correlated well between MRI and histology, and led to non-viable regions with a rim of coagulative necrosis.[273]

A group from the University of Toronto performed FLA on four men who subsequently underwent RP 1 week later.[274] Using cytokeratin 8 staining, there was a distinct transition between vital glandular tissue and the ablation zone, without patches of vital tissue within the necrotic areas. Additionally, no viable cancer was visualized in the region of ablation between the two laser fibres that were used, and effective zones of treatment were taken all the way to the prostatic capsule. Interestingly, MRI-estimated ablation volume was 40% greater than histological-estimated volume (range, 0%–60%) and 10% greater than vital staining volume (range, 96%–129%).

4.9.3 Procedure

4.9.3.1 Preparation

All patients receive antibiotics, and some centres use a urethral catheter during the procedure. Anesthesia has ranged from conscious sedation with periprostatic nerve block[275] to regional (e.g., spinal) and general anesthesia.

When the ablation takes place in the MRI gantry, patients are positioned either supine or prone, depending on whether the prostate is accessed via the perineum or rectum, respectively. With MRI-informed ablation and laser placement guided by US, patients are positioned in dorsal lithotomy.[276] When the transperineal approach is employed, an endorectal coil is typically used to optimize image quality and stabilize the prostate.

4.9.3.2 Laser placement

A 980 nm, 15 W laser (30 W also available) is inserted into the intended region of the prostate. When placed transperineally, the laser typically traverses through an MRI-compatible brachytherapy template secured to the patient to minimize motion. When placed transrectally, multiple proprietary devices can be utilized to facilitate laser placement.

An MR-compatible, 14 G, 14 cm titanium trochar is placed into the intended lesion/region of treatment. Accurate placement of the trochar into the prostate can be time-consuming and involves multiple iterations of modifying its location based on MR images, often requiring multiple passes and repositioning.

When a brachytherapy template is used, it has three saline fiducials, which can be identified on a T2W turbo spin-echo sequence. Data is transferred to planning software on a workstation and a virtual map of the template and insertion paths are superimposed onto MR images. Based on this information, an entry portal on the brachytherapy template is selected, along with an estimated craniocaudal distance of insertion.

4.9.3.3 Treatment planning

A 1.6 mm cooling catheter with stylet is then passed through the trochar. The trochar is then pulled back to expose the tip of the cooling catheter. A laser with a 600 mm core and 10 mm to 15 mm tip is then passed through the cooling catheter, which has room-temperature sterile saline flowing through it. One group's MR sequences and parameters have been previously published.[275]

A workstation (**Figure 4-27**) is used to repetitively monitor the acquired MRI images. A high-temperature threshold (e.g., 90°C) can be set to minimize risk of excess damage within the ablation zone (e.g., char, vaporization, cavitation), and similar lower-threshold markers (e.g., 45°C) can be placed near adjacent structures (e.g., bladder, rectum, cavernosal nerves) to lower the risk of damage and automatically halt ablation if the preset measures are met. A low-energy, short-segment pulse is administered via the laser (e.g., approximately 5–7 W) to confirm positioning.

4.9.3.4 Ablation

Most commonly, the procedure takes place in the MRI, allowing for real-time monitoring via proton resonance frequency (PRF) shift MR thermometry. Other investigators have utilized MRI-informed, US-guided focal laser ablation.[276]

During ablation at 6 W to 15 W, multiple real-time MRI images are visualized on the workstation, including sagittal and axial views, along with an Arrhenius estimate of necrosis area. The duration of ablation is typically 1 to 2 minutes per lesion, depending on the intended volume of ablation. If necessary, multiple ablations can be performed with the same laser fibre, adjacent to the original zone or in a separate area. Additional laser fibres can also be used.

4.9.3.5 Postablation

Following ablation, gadolinium is administered and T1 images are obtained to visualize the prostate. Men are discharged from the office or hospital setting the same day, and nearly all are able to return to normal work-related activity the following day. Men are asked to limit physical and sexual activity for approximately 1 week.

4.9.4 Clinical data

4.9.4.1 Inclusion criteria

Among the reported studies, there are slight variations in patient eligibility, but inclusion criteria generally consist of men with PSA <10 ng/mL, clinical stage T1c-T2a, GS of 6 to 7, and cancers with visible lesions on MRI that are concordant with Bx findings (**Table 4-8**).

TABLE 4-8 Inclusion Criteria for Published Focal Laser Ablation Series

	Lindner *et al.*[276]	Oto *et al.*[275]	Lepor *et al.*[277]
Subjects	12	9	25
PSA	<10 ng/mL	<10 ng/mL	<10 ng/mL
GS	6	≤7	≤7
Bx	<33% of all cores no core >50% 1 sextant with cancer	≤3 cores no core >50%	N/A
Clinical stage	T1c-T2a	T1c-T2a	T1c-T2a
MRI	Concordant with Bx findings Lesion ≤1 cm^3	Concordant with Bx findings	≤2 suspicious lesions

Abbreviations: Bx, biopsy; GS, Gleason score; PSA, prostate-specific antigen; MRI, magnetic resonance imaging; N/A, not available.

4.9.4.2 Outcomes

Oncologic

At the University of Toronto, median volume of treatment among 12 patients, as measured by MRI 1 week following treatment was 2.2 cm^3. At 3 to 6 months following treatment, a positive Bx outside of the ablation zone was observed in 17%, and cancer within the treatment zone in 33%.[276]

The University of Chicago group reported a non-enhancing MRI defect identified in all patients, and on seven of nine (78%) patients without cancer on Bx of the ablation zone at 6 months following treatment. Both patients with residual cancer (22%) had a low-volume (1–2 mm) of Gleason 6. No significant change in PSA was noted, presumably due to the small lesions that were treated (4–12 mm).[275]

In a report from New York University and Sperling Prostate Center, mean PSA decreased from 5.3 ng/mL to 2.9 ng/mL. At 3 months following the procedure, residual cancer was identified within the ablation zone via MR-guided or MR-US fusion Bx in 4% (2 of 28 patients). Early SBs were not performed.[277]

Functional

At the University of Toronto, 25% of patients had acute urinary retention immediately following the procedure, and there was no significant change in mean urinary (IPSS) or sexual function (Sexual Health Inventory for Men [SHIM]) within 6 months.[276]

The University of Chicago group reported no significant change in urinary or sexual function within 6 months, as measured by mean IPSS and SHIM, respectively. No patient had more than a 5-point change in IPSS. At 6 months after the procedure, six (67%) had a SHIM score within 4 points of baseline, one (11%) had a 5-point decrease, one (11%) had an 8-point decrease, and one patient (11%) had a 12-point increase.[275]

In the patients reported by New York University and the Sperling Prostate Center, 28% had acute urinary retention, all resolving within 3 days. At 3 months following treatment, mean urinary bother and erectile function were unchanged, as measured by the American Urological Association (AUA) symptom score and SHIM, respectively.[277]

Complications

The University of Toronto group reported 25% of patients with perineal discomfort.[276] The University of Chicago group reported one (11%) patient with a perineal abrasion and one (11%) with penile paresthesia, both of which were self-resolving without further measures.[275]

4.9.4.3 Considerations

Relative contraindications include very large lesions, apical location, concern for established extracapsular extension or seminal vesicle invasion, or close proximity to adjacent structures such as cavernosal nerves, external urethral sphincter, or rectum.

Performing FLA is a time- and technology-intensive endeavour that requires coordination among a multidisciplinary team. Among experienced teams, it is generally recognized that there is a learning curve to determining the number and size of ablations, and locations, and efficiently placing the trochar (and ultimately the laser fibre) into the intended ablation zone.

4.9.4.4 Future

Focal laser ablation is a treatment strategy with a novel mechanism, unique technical considerations, and relatively sparse oncologic and functional outcomes. Among the data reported in the peer-reviewed literature, small series with short follow-up suggest a safe, minimally invasive approach with minimal morbidity. Ongoing follow-up of previously reported series coupled with completed or ongoing larger trials will ultimately determine the potential role of focal laser ablation in the treatment of select patients with PCa.

4.10 New Energy Sources

4.10.1 Introduction

From the ablation of a localized small tumour to experimental therapies, different energy sources have shown an increasing role in treatment of solid neoplasms in the body. Although most widely recognized in the treatment of hepatic and renal neoplasms, recent advances in imaging, particularly mp-MRI, and Bx techniques, have increased such opportunities in focal thermal ablation of PCa. Cryotherapy and HIFU as thermal energy sources for focal treatment of PCa have the most mature experience, and these along with newer techniques such as laser, photodynamic therapy, and irreversible electroporation have been discussed separately in this textbook. This section of the chapter examines the rapidly evolving further new ablation modalities in radiofrequency ablation and water vapour ablation for PCa treatment. Microwave (MW) energy ablation tested in the past for focal therapy in PCa is also discussed.

Thermal energy-based ablation of tumours causes irreversible cell injury and coagulative necrosis by application of extreme high or low temperatures. While in many other organs, percutaneous energy–based ablation techniques have been used for unresectable tumours or in patients who are not good surgical candidates, the primary goal of focal therapy in PCa is to find the fine balance between oncologic control and preservation of quality of life, the so–called trifecta of continence, potency, and oncologic effectiveness.[278,279]

At the same time, recent reports describing as yet unexplained regression of untreated distant metastases after thermal ablation of the primary tumour have generated interest in a possible systemic immunomodulation.[280–282] This phenomenon has also been observed following RT.[283,284] Though not yet tested for PCa, its implications for immune enhancement have generated a lot of interest among cancer researchers and may generate further interest in focal thermal therapy in PCa. At present, focal ablative therapy in PCa is being evaluated for control of primary cancer and also for salvage therapy.[285,286] Although PCa is often multifocal, there is evidence to support that the largest lesion with the highest grade of cancer in the gland, the index lesion, predominantly determines the natural history of the disease.[287,288] The index lesion is often visible on mp-MRI or detected at Bx, and therefore can be targeted for primary ablation.

While several academic expert centres are attempting to drive changes into how PCa is treated in the future to maintain trifecta of life, the level and degree of evidence available for widespread adoption of these new technologies is up for debate.[289,290] Though there is agreement across the board that there is lack of level 1 evidence in the field, and prospective, multicentre, randomized control trials (RCTs) are the need of the hour to reduce the risk for internal bias,[291] it is well known that performing RCTs in surgical science is challenging.[292] And therefore in the absence of high level 1 evidence, it is important that the prospective single-arm trials are of high quality, with a mechanism to assess the quality of evidence. This would take into account the study design, trial/cohort size, risk of bias, imprecision, and also publication bias.

Several energy modalities, namely, freezing effect of cryotherapy,[159,293–295] thermal effect of HIFU,[96,106,108,111,112,132,144,296–298] thermal effect of light in FLA,[274–277,299,300] activation of a photosensitizer by light for PDT,[181,182] non-thermal IRE[219,301] using short pulses of DC current to cause cell death, are being tested for focal therapy of PCa with a few high-quality prospective studies published in the literature.[302] This chapter will, however, discuss some of the other energy modalities in PCa therapy, including water vapour ablation, radiofrequency, and MW ablation. There is scant level 1 evidence with few ongoing prospective trials using these newer energy sources that will be discussed in the following paragraphs.

4.10.2 Radiofrequency ablation

Radiofrequency ablation uses imaging guidance to directly place the electrodes into the tumour tissue. Temperatures of 60°C to 100°C are generated by a high-frequency alternating current causing frictional heating when the ions within the tissue attempt to change directions with the alternating current. By heating tissue at this temperature, RFA denatures proteins, damages cell membranes, and is directly cytodestructive.[303] Interestingly, temperatures of over 100°C lead to tissue impedance for electric conduction within the tissue, and therefore make this form of thermal energy less effective. As with HIFU, the heat-sink effect is a commonly described limitation of RFA and occurs where flowing blood or air carries the heat away from the site of ablation, thereby decreasing its efficiency and making tissue adjacent to a vessel less susceptible to damage by hyperthermia.[304]

Radiofrequency ablation technology has been available since the early 1990s for soft-tissue ablation, and was first utilized in oncology practice for percutaneous treatment of primary and metastatic hepatic lesions.[305] Within the domain of urology, it has gained widespread use in the treatment of small renal masses with an approximate 90% clinical efficacy.[306] However, RFA for PCa is in its infancy, with only animal models, proof-of-concept, and small phase 1/2 trials published to date.

The first feasibility study on RFA for PCa was published almost 20 years ago.[307] In this seminal paper, the authors report their experience treating 13 patients with RFA immediately prior to planned RP for localized PCa, where whole-mount pathology was employed to assess the efficacy of the ablation comparing various probes and power settings. An additional patient was treated with primary full-gland RFA without RP.

The transperineal RFA was carried out under general or spinal anesthesia with TRUS guidance using monopolar probes, bipolar probes, or combination. No technical problems were encountered, and all patients recovered uneventfully from their radical prostatectomies. Maximum temperature at probe was 103°C, and mean energy delivered was 10.5 kJ. Rectal temperatures never reached above 38°C, even in patients with planned burn at posterior capsule, and no urethral sphincter injuries occurred. Unfortunately, the authors found that the size of the lesion induced by monopolar and bipolar probes poorly correlated with the expected burn based on the energy delivered. It was also found that RFA interfered with the TRUS image, so that US did not accurately predict the true thermal lesion. The authors suggest that, although RFA could create large necrotic lesions in the prostate, better imaging would be needed to advance the modality.

Interestingly, in another publication from the same group, post-RFA MR and pathology were compared, and when attempting to create a 2x2x2 cm RFA lesion, the MR-detected burn and pathology-detected burn were almost identical.[308]

Radiofrequency ablation has also been used in phase 1/2 trials for salvage therapy. In a 2005 publication, Shariat *et al.* used focal RFA for 11 patients with hormone-naïve, localized PCa who had failed EBRT or were not candidates for upfront radical therapy.[309] This salvage TRUS-guided RFA was confirmed with a post-RFA power Doppler and verified at 1 month with MRI. Using a monopolar device (RITA medical systems 500P generator with semicircular electrodes), focal areas were treated based on previously mapped transperineal biopsies under IV sedation in an outpatient cystoscopy suite. Temperatures of 100°C were maintained for 5 minutes, and patients received anywhere from one to four burns. More than 90% of the patients experienced a PSA decrease of >50%, and overall, PSADT slowed post-RFA from 14 months to 37 months. Long-term oncologic outcomes are not published for this cohort; however, 60% of patients were free of cancer at systematic TRUS Bx 12 months post-RFA.

This study reported no significant changes in LUTS and no major complications. Minor complications included transient hematuria, bladder spasms, and dysuria in four patients. The authors concluded that RFA may delay or prevent PCa progression, but the efficacy is limited by proper identification of lesions.

There are several ongoing trials evaluating the ENCAGE™ RFA device (Trod Medical, Leuven, Belgium), which was initially studied in bull[310] and canine[311] models. This technology uses a device with a coiled configuration creating a Faraday cage effect, where only tissue within the coil is burned by the bipolar RFA energy while surrounding tissue is completely spared. The transperineal treatment uses a specially designed driver mechanism intended to position the probe within 0.5 mm of its target, and is performed under TRUS guidance.[312] Study NCT01423006 finished accrual and treated five patients with very low-risk PCa from 2011 to 2013, but has yet to report its findings aside from a conference abstract. The abstract reports that 8 mm to 16 mm probes were used, and each ablation lasted 200 seconds. One patient suffered transient hematuria, and no other complications or oncologic outcomes were reported to date.[333]

There are now three ongoing ENCAGE trials recruiting patients with localized lesions. The FUSAblate study at NYU (NCT02303054—Samir Taneja, principal investigator) will treat 21 patients with GS 6 (3+3) or GS 7 (3+4) tumours of up to 1.2 cm on MRI. Primary outcome will be the rate of positive 3DUS fusion-targeted biopsies at 6 months post-treatment. Patient-reported QOL will also be assessed.[334] Two other trials with similar protocols are also ongoing (NCT02328807[335]—Julio Pow-Sang, principal investigator; Florida, United States; 30 patients; and the ProRAFT study NCT02294903[336]—Mark Emberton, principal investigator; United Kingdom; 40 patients).

The evidence supporting the use of RFA for focal therapy of PCa is sparse. Although it has been demonstrated to be safe, the oncologic outcomes are uncertain, as no long-term data have been published to date. Several phase 1/2 trials using the ENCAGE device should be reporting in the near future.

4.10.3 Water vapour ablation

Water vapour energy is a unique and natural thermal technique for prostate ablation. The technology involves heating sterile water, which is converted into vapor (steam) and then injected into target areas of tissue. When the injected vapour condenses back to a liquid state, the stored thermal energy is released into the tissue, causing the cell membranes in the target zone to rupture resulting in cell death. The Convective Water Vapor Energy (WAVE®) device is a handheld delivery device that uses radiofrequency power to heat a few drops of water to approximately 103°C. When water gets heated to steam or vapour, its volume expands almost 1700 times with 540 calories of thermal energy for every milliliter.[313–315]

The WAVE technology using the Rezūm® System uses very small amounts of sterile water (generally in the range of 0.5 mL) and has multiple holes to ensure uniform vapour dispersion throughout the target zone of ablation. The vapour delivery is at a slightly higher pressure to push the vapour through tissue as it condenses and releases the thermal energy into the target tissue. Because the vapour condenses into liquid state quickly, the energy does not travel further than intended, which therefore provides a safety factor.

The surgical capsule between the transition zone and peripheral zone also acts as a barrier for the vapour as it disperses through the tissue. The energy is released against the walls of the target cells and leads to denaturation of the cell membranes, causing instant cell death of tissue membranes including nerves and small blood vessels. The device is presently being studied in clinical trials under an investigational device exemption (IDE) granted by the FDA.

The Rezūm System has been used transurethrally as a treatment for LUTS from BPH. In this study, seven patients were treated with transurethral intraprostatic injections of sterile steam under endoscopic visualization followed by adenectomy. The extirpated adenomas were evaluated for tissue ablation using triphenyl-tetrazolium chloride (TTC) staining. Another set of 15 patients were treated similarly but followed by contrast-enhanced MRI performed 1 week after the procedure. The largest ablated volume in this cohort of patients was 35.1 cc. Ablation was confirmed in all patients and remained confined to the transition zone. In a separate prospective, randomized, multicentre Rezūm II trial using the WAVE technology, 136 patients treated using the Rezūm device showed rapid and sustained improvement in LUTS and flow, with minimal adverse events, which were typically mild and transient.[313–315]

Apart from the multicentre clinical trials for the treatment of LUTS from BPH (NCT01912339[337]—Claus Roehrborn and Kevin McVary, principal investigators; 195 patients), vapour thermal energy is also being assessed to treat focal PCa.

In a study recently presented at the annual European Association of Urology (EAU) meeting in March 2015, the authors described the feasibility of the Reviv™ System as a minimally invasive technique for treating localized PCa.[316] In this study across two centres, 14 patients underwent vapour thermal therapy using the Reviv System followed by RP. The vapor was prospectively targeted in peripheral zone and/or the transition zone of the prostate gland via a transrectal-guided transperineal approach using 18-gauge Francis™ needles.[316]

The aim was to simulate focal, zonal, hemi, or whole-gland ablation. Areas were also targeted at the apex and the capsule. Safety was assessed by real-time US visualization and temperature monitoring by placement of thermocouples at the posterolateral aspect of the gland.[316] Following the ablation, the patients underwent prostatectomy with whole mounts and TTC staining, which showed good correlation with the intended treatment, confirming that vapour energy could effectively ablate prostate tissue.[316] No thermal effects were seen outside the prostate gland and mild thermal effects were seen in the prostatic urethra when the transition zone was targeted. While this initial study using vapour as a source of thermal energy confirms its feasibility as a source of thermal energy for focal therapy of PCa, the published data on use of this technique is sparse.[316] Prospective trials with intermediate to long-term follow-up are needed to assess the trifecta of oncologic outcome, potency, and urinary continence.[316]

4.10.4 Microwave thermal therapy

Like radiofrequency ablation, microwave ablation (MWA) uses electromagnetic waves to generate heat apart from direct hyperthermic injury. An electromagnetic field, typically between 900 MHz and 2,500 MHz, is created through placement of an antenna within the tumour. The field forces intrinsic dipoles, mainly water, within the tissue to continuously realign, which increases their kinetic energy, leading to an increased temperature in the tissue and thermal effects. The advantages of MWA over RFA as a source of thermal energy include the ability to achieve higher temperatures and treat larger tumour volumes with a lower susceptibility to heat-sink effects when compared with RFA or HIFU. With MWA, multiple antennas can be used simultaneously to enhance the ablative effect. At the same time, MWA systems are more cumbersome to use and the antennas are prone to overheating, thereby requiring a cooling mechanism.

Thermal therapy with MW technology was first used in the 1980s and was found to improve local controls of several tumours when employed in the adjuvant setting at moderate temperatures (40–45°C , termed hyperthermia).[317] Hyperthermia was also used in the palliative setting. For example, Montorsi *et al.* utilized this in men with symptomatic, locally advanced PCa administered with specialized transurethral applicators to successfully palliate obstructive voiding symptoms.[318]

In PCa, MW thermal therapy can also be used as primary focal therapy with curative intent because at higher temperatures (>50°C) coagulative necrosis ensues.[319] Microwave antennas inserted through an introducer sheath can be organized in an array and treat lesions up to 3 cm using a transperineal approach with a brachytherapy-like grid. Microwave antennas launch small electromagnetic waves that heat lesions secondary to electrical resistance of tissues. Helical tip transducers have been used to decrease interference between probes, several of which are often required to ablate a single lesion. For areas outside the active zone, thermal conduction is relied on to spread heat to wider zones.

4.10.5 Published studies

Published studies have been carried out for salvage interstitial peripheral–gland ablation. In a stage 1/2 trial of 25 men with PSA recurrence post-EBRT, bilateral peripheral–gland MW therapy was performed.[320] This was done with transperineal placement of helical probes under TRUS guidance following creation of a hydrodissected space between the rectum and prostate to prevent rectal burn. The urethra, rectum, and hydrodissected space were also protected with cooling devices. Target temperatures >55°C were reached in the ablated zones while urethral and rectal temperatures were preserved <35°C . Median pre-treatment PSA was 6.5 ng/mL and half of the treated patients reached a post-treatment nadir of <0.5 ng/mL. However, up to 35% of patients had positive post-treatment biopsies. Although no major complications occurred, irritative and voiding urinary symptoms were common (approximately 35%). Although full-gland MW therapy is primarily designed as salvage treatment, the same group used it with success to treat a man localized PCa who refused all conventional treatments,[321] but no long-term functional or oncologic outcomes are available.

In smaller pilot studies, it was demonstrated that neoadjuvant androgen deprivation therapy (ADT) could be used to shrink the prostate to a size more amenable to treatment,[322] and that treatment could be performed under MRI guidance using MR thermometry.[323]

4.10.6 Conclusion

Advances in imaging have made image-guided focal ablation possible in PCa. While there is a dearth of prospective, randomized clinical trials in the field, significant progress has been made. In the last decade or so, some ablative technologies such as cryoablation, HIFU, and laser ablation have moved beyond the initial proof-of-principle, animal, or preclinical phase and are now being tested in humans in phase 1/2 and pivotal trials. However, there continue to be rapid changes in the field. The newer ablative technologies face an uphill challenge in not only providing high-quality evidence for their superiority over the available treatment options for PCa but also competing with the existing thermal ablation techniques in PCa. They need to be accurate, cost-effective, and found to be clinically beneficial to be widely disseminated. Tumour size and location have been important parameters in selecting the thermal energy source and perhaps an à *la carte* approach may be needed in this age of personalized medicine.

The transrectal HIFU approach may not be ideal for an anterior tumour. These anterior tumours may be ideally suited for transperineal laser ablation or RFA, if the tumour is visible on mp-MRI. Similarly, if the tumour is sparse and not visible on mp-MRI, a hemiablation approach using HIFU, or even MWA, rather than a targeted approach may be best suited to the individual. At the same time, there continue to be advances in modern imaging techniques and in the technology. From an initial stage of disbelief and denial, we physicians have moved to adoption of these new technologies in prostate ablation. It is up to us now to provide high-quality trials and a mechanism to assess the quality of evidence.

4.11 Recommendations

Recommendations	LOE/GOR
Cryoablation and HIFU can be offered as primary treatment in selected patients.	II/A
Cryoablation and HIFU can be considered as salvage treatment following recurrence from radiation.	II/A
To avoid major complications following (salvage) ablation treatments (including urinary incontinence, rectourethral fistula formation, and erectile dysfunction), specific protocols should be put in place.	II/A
Focal ablation may be considered for primary unifocal high-volume low-grade or moderate-grade local PCa.	III/C
Transurethral HIFU, IRE, RFA, water vapour ablation, MW thermal therapy, and histotripsy are investigational, and should only be offered within clinical trials.	IV/D
IMRT radiation therapy and brachytherapy may be explored for focal ablation.	IV/D
(Real-time) imaging should be used for patient selection, treatment guidance, and follow-up in ablative treatments.	II/A

4.12 Acknowledgements

David Habibian, Courtney Berg, Juan Casanova Ramón-Borja, Shafak Aluwini, and Nathan Perlis for their support to this work.

4.13 References

1. Wood RW, Loomis AL. The physical and biological effects of high-frequency sound-waves of great intensity. *The London, Edinburgh, and Dublin Philosophical Magazine and Journal of Science*. 1927;4(22):417–436.
2. Fry WJ, Wulff VJ, Tucker D, *et al.* Physical factors involved in ultrasonically induced changes in living systems: I. identification of non-temperature effects. *J Acoust Soc Am*. 1950;22(6):867.
3. Hill CR, ter Haar GR. Review article: high intensity focused ultrasound--potential for cancer treatment. *Br J Radiol*. 1995;68(816):1296–1303.
4. Vaughan MG, ter Haar GR, Hill CR, *et al.* Minimally invasive cancer surgery using focused ultrasound: a pre-clinical, normal tissue study. *Br J Radiol*. 1994;67:267–274.
5. Madersbacher S, Pedevilla M, Vingers L, *et al.* Effect of high-intensity focused ultrasound on human prostate cancer in vivo. *Cancer Res*. 1995;55(15):3346–3351.
6. ter Haar GT, Coussios C. High intensity focused ultrasound: physical principles and devices. *Int J Hyperthermia*. 2007;23(2):89–104.
7. Al-Bataineh O, Jenne J, Huber P. Clinical and future applications of high intensity focused ultrasound in cancer. *Cancer Treat Rev*. 2012;38(5):346–353.
8. Dubinsky TJ, Cuevas C, Dighe MK, *et al.* High-intensity focused ultrasound: current potential and oncologic applications. *AJR Am J Roentgenol*. 2008;190(1):191–199.
9. Gordon JP, Zeiger HJ, Townes CH. The maser—new type of microwave amplifier, frequency standard, and spectrometer. *Phys Rev*. 1955;99(4):1264–1274.
10. Maiman TH. Stimulated optical radiation in ruby. *Nature*. 1960;187:493–494.
11. Goldman L, Blaney DJ, Kindel DJ Jr. Pathology of the effect of the laser beam on the skin. *Nature*. 1963;197:912–914.
12. Goldman L. *Biomedical Aspects of the Laser: The Introduction of Laser Applications Into Biology and Medicine*. New York, Springer-Verlag, 1967, pp 1–222.
13. Müssiggang H, Katsaros W. A study of the possibilities of laser surgery. *Int Urol Nephrol*. 1971;3(3):229–243.
14. Costello AJ, Bowsher WG, Bolton DM, *et al.* Laser ablation of the prostate in patients with benign prostatic hypertrophy. *Br J Urol*. 1992;69(6):603–608.
15. Anderson RR, Parrish JA. Selective photothermolysis: precise microsurgery by selective absorption of pulsed radiation. *Science*. 1983;220(4596):524–527.
16. Te AE. The development of laser prostatectomy. *BJU Int*. 2004;93(3):262–265.
17. Welch AJ, van Gemert MJC. *Optical-Thermal Response of Laser-Irradiated Tissue*, 2nd ed. Springer, Dordrecht, 1995, pp 1–947.
18. Colin P, Mordon S, Nevoux P, *et al.* Focal laser ablation of prostate cancer: definition, needs, and future. *Adv Urol*. 2012;2012:589160.
19. Raab C. Über die Wirkung fluoreszierender Stoffe auf Infusoria. *Z Biol*. 1900;39:524–526. [Article in German]
20. von Tappeiner H, Jesionek A. Therapeutische Versuche mit fluoreszierenden Stoffen. *Munch Med Wochenschr*. 1903;47:2042–2044. [Article in German]
21. von Tappeiner H, Jodlbauer A. Die sensibilisierende wirkung fluoreszierender substanzer: gesamte Untersuchungen ber die photodynamische erscheinung. Leipzig: FCW Vogel; 1907. [Article in German]
22. Meyer-Betz F. Untersuchungen über die biologische (photodynamische) Wirkung des Hämatoporphyrins und anderer Derivate des Blut- und Gallenfarbstoffs. *Dtsch Arch Klin Med*. 1913;112:476–503. [Article in German]
23. Dougherty TJ, Kaufman JE, Goldfarb A, *et al.* Photoradiation therapy for the treatment of malignant tumors. *Cancer Res*. 1978;38(8):2628–2635.

24. Chang SC, Buonaccorsi G, MacRobert A, *et al*. Interstitial and transurethral photodynamic therapy of the canine prostate using meso-tetra-(m-hydroxyphenyl) chlorin. *Int J Cancer*. 1996;67(4):555–562.

25. Momma T, Hamblin MR, Wu HC, *et al*. Photodynamic therapy of orthotopic prostate cancer with benzoporphyrin derivative: local control and distant metastasis. *Cancer Res*. 1998;58:5425–5431.

26. Bozzini G, Colin P, Betrouni N, *et al*. Photodynamic therapy in urology: what can we do now and where are we heading? *Photodiagnosis Photodyn Ther*. 2012;9(3):261–273.

27. Moore CM, Pendse D, Emberton M. Photodynamic therapy for prostate cancer--a review of current status and future promise. *Nat Clin Pract Urol*. 2009;6(1):18–30.

28. Azzouzi AR, Lebdai S, Benzaghou F, *et al*. Vascular-targeted photodynamic therapy with TOOKAD® Soluble in localized prostate cancer: standardization of the procedure. *World J Urol*. 2015;33(7):937–944.

29. Aguilar G, Choi B, Broekgaarden M, *et al*. An overview of three promising mechanical, optical, and biochemical engineering approaches to improve selective photothermolysis of refractory port wine stains. *Ann Biomed Eng*. 2012;40(2):486–506.

30. Arnott J. Practical illustrations of the remedial efficacy of a very low or anesthetic temperature. I. In cancer. *Lancet*. 1850;56:257–259.

31. Freiman A, Bouganim N. History of cryotherapy. *Dermatol Online*. 2005;11(2):9.

32. White AC. Liquid air: its application in medicine and surgery. *Med Rec*. 1899;56:109–112.

33. Cooper IS, Lee AS. Cryostatic congelation: a system for producing a limited, controlled region of cooling or freezing of biologic tissues. *J Nerv Ment Dis*. 1961;133:259–263.

34. Gonder MJ, Soanes WA, Shulman S. Cryosurgical treatment of the prostate. *Invest Urol*. 1966;3(4):372–378.

35. Flocks RH, Nelson CM, Boatman DL. Perineal cryosurgery for prostatic carcinoma. *J Urol*. 1972;108(6):933–935.

36. Roebuck JR. The Joule-Thomson Effect in Air. *Proc Natl Acad Sci USA*. 1926;12(1):55–58.

37. Roy BN. *Fundamentals of Classical and Statistical Thermodynamics*. New York, John Wiley & Sons, 2002, pp 1–744.

38. Theodorescu D. Cancer cryotherapy: evolution and biology. *Rev Urol*. 2004;6(Suppl 4):S9–S19.

39. Nollet JA. *Recherches sur les causes particulieres des phénomenes électriques, et sur les effets nuisible ou avantageux qu'on peut en attendre*. Paris, Chez H.L. Guerin & L. F. Delatour, 1754. [Article in French]

40. Reilly JP. *Applied Bioelectricity: From Electrical Stimulation to Electropathology*. New York, Springer-Verlag, 2012, pp 1–563.

41. Fuller GW. *Report on the Investigations Into the Purification of the Ohio River Water at Louisville Kentucky Made to the President And Directors of the Louisville Water Company*. New York, D. Van Nostrand Company, 1898, pp 1–461.

42. McKinley GM. Short electric wave radiation in biology, in: Duggar BM (ed). *Biological Effects of Radiation*. New York, McGraw-Hill Book Company, 1936.

43. Doevenspeck H. Influencing cells and cell walls by electrostatic impulses. *Fleischwirtschaft*. 1961;13:986–987.

44. Prausnitz MR, Mitragotri S, Langer R. Current status and future potential of transdermal drug delivery. *Nat Rev Drug Discov*. 2004;3(2):115–124.

45. Davalos RV, Rubinsky B. Tissue ablation with irreversible electroporation. US patent application 0043345. Oakland, The Regents of the University of California, 2004.

46. Davalos RV, Mir IL, Rubinsky B. Tissue ablation with irreversible electroporation. *Ann Biomed Eng*. 2005;33(2):223–231.

47. Miller L, Leor J, Rubinsky B. Cancer cells ablation with irreversible electroporation. *Technol Cancer Res Treat*. 2005;4(6):699–705.

48. Onik G, Mikus P, Rubinsky B. Irreversible electroporation: implications for prostate ablation. *Technol Cancer Res Treat*. 2007;6(4):295–300.

49. Rubinsky J, Onik G, Mikus P, *et al*. Optimal parameters for the destruction of prostate cancer using irreversible electroporation. *J Urol*. 2008;180(6):2668–2674.

50. Gehl J. Electroporation: theory and methods, perspectives for drug delivery, gene therapy and research. *Acta Physiol Scand*. 2003;177(4):437–447.

51. van Gemert MJ, Wagstaff PG, de Bruin DM, *et al.* Irreversible electroporation: just another form of thermal therapy? *Prostate*. 2015;75(3):332–335.

52. Wagstaff PG, de Bruin DM, van den Bos W, *et al.* Irreversible electroporation of the porcine kidney: Temperature development and distribution. *Urol Oncol.* 2015;33(4):168.e1–7.

53. Chang DC, Reese TS. Changes in membrane structure induced by electroporation as revealed by rapid-freezing electron microscopy. *Biophys J*. 1990;58(1):1–12.

54. Jiang C, Shao Q, Bischof J. Pulse timing during irreversible electroporation achieves enhanced destruction in a hindlimb model of cancer. *Ann Biomed Eng.* 2015;43(4):887–895.

55. Lynn JG, Zwemer RL, Chick AJ. The biological application of focused ultrasonic waves. *Science*. 1942;96(2483):119–120.

56. Lynn JG, Putnam TJ. Histology of cerebral lesions produced by focused ultrasound. *Am J Pathol.* 1944;20(3):637–649.

57. Chapelon JY, Margonari J, Vernier F, *et al.* In vivo effects of high-intensity ultrasound on prostatic adenocarcinoma Dunning R3327. *Cancer Res.* 1992;52(22):6353–6357.

58. Gelet A, Chapelon JY, Margonari J, *et al.* Prostatic tissue destruction by high-intensity focused ultrasound: experimentation on canine prostate. *J Endourol*. 1993;7(3):249–253.

59. Gelet A, Chapelon JY, Bouvier R, *et al.* Treatment of prostate cancer with transrectal focused ultrasound: early clinical experience. *Eur Urol.* 1996;29(2):174–183.

60. Gelet A, Chapelon JY, Bouvier R, *et al.* Local control of prostate cancer by transrectal high intensity focused ultrasound therapy: preliminary results. *J Urol*. 1999;161(1):156–162.

61. Gelet A, Chapelon JY, Margonari J, *et al.* High-intensity focused ultrasound experimentation on human benign prostatic hypertrophy. *Eur Urol.* 1993;23(Suppl 1):44–47.

62. Madersbacher S, Kratzik C, Szabo N, *et al.* Tissue ablation in benign prostatic hyperplasia with high-intensity focused ultrasound. *Eur Urol.* 1993;23(Suppl 1):39–43.

63. Beerlage HP, van Leenders GJ, Oosterhof GO, *et al.* High-intensity focused ultrasound (HIFU) followed after one to two weeks by radical retropubic prostatectomy: results of a prospective study. *Prostate*. 1999;39(1):41–46.

64. Kennedy JE, Ter Haar GR, Cranston D. High intensity focused ultrasound: surgery of the future? *Br J Radiol.* 2003;76(909):590–599.

65. Rouvière O, Lyonnet D, Raudrant A, *et al.* MRI appearance of prostate following transrectal HIFU ablation of localized cancer. *Eur Urol.* 2001;40(3):265–274.

66. Uchida T, Ohkusa H, Nagata Y, *et al.* Treatment of localized prostate cancer using high-intensity focused ultrasound. *BJU Int.* 2006;97(1):56–61.

67. Ficarra V, Antoniolli SZ, Novara G, *et al.* Short-term outcome after high-intensity focused ultrasound in the treatment of patients with high-risk prostate cancer. *BJU Int.* 2006;98(6):1193–1198.

68. Vallancien G, Prapotnich D, Cathelineau X, *et al.* Transrectal focused ultrasound combined with transurethral resection of the prostate for the treatment of localized prostate cancer: feasibility study. *J Urol.* 2004;171(6 Pt 1):2265–2267.

69. Blana A, Rogenhofer S, Ganzer R, *et al.* Morbidity associated with repeated transrectal high-intensity focused ultrasound treatment of localized prostate cancer. *World J Urol.* 2006;24(6):585–590.

70. Lee HM, Hong JH, Choi HY. High-intensity focused ultrasound therapy for clinically localized prostate cancer. *Prostate Cancer Prostatic Dis.* 2006;9(4):439–443.

71. Poissonnier L, Chapelon JY, Rouvière O, *et al.* Control of prostate cancer by transrectal HIFU in 227 patients. *Eur Urol.* 2007;51(2):381–387.

72. Rébillard X, Davin JL, Soulie M. Treatment by HIFU of prostate cancer: survey of literature and treatment indications. *Prog Urol.* 2003;13(6):1428–1456. [Article in French]

73. Mottet N, Bellmunt J, Briers E, *et al.* European Association of *Urology* (EAU) Guidelines on Prostate Cancer 2016. Available: https://uroweb.org/guideline/prostate-cancer/. Accessed June 20, 2016.

74. Rouvière O, Souchon R, Salomir R, *et al.* Transrectal high-intensity focused ultrasound ablation of prostate cancer: effective treatment requiring accurate imaging. *Eur J Radiol.* 2007;63(3):317–327.

75. Rouvière O, Glas L, Girouin N, *et al.* Prostate cancer ablation with transrectal high-intensity focused ultrasound: assessment of tissue destruction with contrast-enhanced US. *Radiology.* 2011;259(2):583–591.

76. Chen WH, Sanghvi NT, Carlson R, *et al.* Real-time tissue change monitoring on the Sonablate® 500 during high intensity focused ultrasound (HIFU) treatment of prostate cancer. AIP Conference Proceedings. 2011;1359:391-6.

77. Crouzet S, Rebillard X, Chevallier D, *et al.* Multicentric oncologic outcomes of high-intensity focused ultrasound for localized prostate cancer in 803 patients. *Eur Urol.* 2010;58(4):559–566.

78. Uchida T, Nakano M, Shoji S, *et al.* Ten year biochemical disease free survival after high intensity focused ultrasound (HIFU) for localised prostate cancer: comparison with three different generation devices. *J Urol.* 2009;181(4):228.

79. Ahmed HU, Zacharakis E, Dudderidge T, *et al.* High-intensity-focused ultrasound in the treatment of primary prostate cancer: the first UK series. *Br J Cancer.* 2009;101(1):19–26.

80. Blana A, Brown SC, Chaussy C, *et al.* Primary prostate HIFU without pretreatment hormone therapy: Biochemical survival of 468 patients tracked with the @-registry. *J Urol.* 2009;181(4):227.

81. Mearini L, D'Urso L, Collura D, *et al.* Visually directed transrectal high intensity focused ultrasound for the treatment of prostate cancer: a preliminary report on the Italian experience. *J Urol.* 2009;181(1):105–111.

82. Blana A, Murat FJ, Walter B, *et al.* First analysis of the long-term results with transrectal HIFU in patients with localised prostate cancer. *Eur Urol.* 2008;53(6):1194–1201.

83. Misraï V, Rouprêt M, Chartier-Kastler E, *et al.* Oncologic control provided by HIFU therapy as single treatment in men with clinically localized prostate cancer. *World J Urol.* 2008;26(5):481–485.

84. Blana A, Rogenhofer S, Ganzer R, *et al.* Eight years' experience with high-intensity focused ultrasonography for treatment of localized prostate cancer. *Urology.* 2008;72(6):1329–1333.

85. Ganzer R, Rogenhofer S, Walter B, *et al.* PSA nadir is a significant predictor of treatment failure after high-intensity focused ultrasound (HIFU) treatment of localised prostate cancer. *Eur Urol.* 2008;53(3):547–553.

86. Uchida T, Ohkusa H, Yamashita H, *et al.* Five years experience of transrectal high-intensity focused ultrasound using the Sonablate device in the treatment of localized prostate cancer. *Int J Urol.* 2006;13(3):228–233.

87. Thüroff S, Chaussy C, Vallancien G, *et al.* High-intensity focused ultrasound and localized prostate cancer: efficacy results from the European multicentric study. *J Endourol* 2003;17(8):673–677.

88. Chaussy C, Thüroff S. Results and side effects of high-intensity focused ultrasound in localized prostate cancer. *J Endourol.* 2001;15(4):437–440;discussion 447–438.

89. Gelet A, Chapelon JY, Bouvier R, *et al.* Transrectal high-intensity focused ultrasound: minimally invasive therapy of localized prostate cancer. *J Endourol* 2000;14(6):519–528.

90. Challacombe BJ, Murphy DG, Zakri R, *et al.* High-intensity focused ultrasound for localized prostate cancer: initial experience with a 2-year follow-up. *BJU Int.* 2009;104(2):200–204.

91. Maestroni U, Ziveri M, Azzolini N, *et al.* High Intensity Focused Ultrasound (HIFU): a useful alternative choice in prostate cancer treatment. Preliminary results. *Acta Biomed.* 2008;79(3):211–216.

92. Koch MO, Gardner T, Cheng L, *et al.* Phase I/II trial of high intensity focused ultrasound for the treatment of previously untreated localized prostate cancer. *J Urol.* 2007;178(6):2366–2370.

93. Uchida T, Illing RO, Cathcart PJ, *et al.* To what extent does the prostate-specific antigen nadir predict subsequent treatment failure after transrectal high-intensity focused ultrasound therapy for presumed localized adenocarcinoma of the prostate? *BJU Int.* 2006;98(3):537–539.

94. Chaussy C, Thüroff S, Rebillard X, *et al.* Technology insight: High-intensity focused ultrasound for urologic cancers. *Nat Clin Pract Urol.* 2005;2(4):191–198.

95. Crouzet S, Poissonnier L, Murat FJ, *et al.* Outcomes of HIFU for localised prostate cancer using the Ablatherm Integrate Imaging® device. *Prog Urol.* 2011;21(3):191–197. [Article in French]

96. Crouzet S, Chapelon JY, Rouvière O, *et al.* Whole-gland ablation of localized prostate cancer with high-intensity focused ultrasound: oncologic outcomes and morbidity in 1002 patients. *Eur Urol.* 2014;65(5):907–914.

97. Shoji S, Nakano M, Nagata Y, *et al.* Quality of life following high-intensity focused ultrasound for the treatment of localized prostate cancer: a prospective study. *Int J Urol.* 2010;17(8):715–719.

98. Li LY, Lin Z, Yang M, *et al.* Comparison of penile size and erectile function after high-intensity focused ultrasound and targeted cryoablation for localized prostate cancer: a prospective pilot study. *J Sex Med.* 2010;7(9):3135–3142.

99. Murat FJ, Poissonnier L, Rabilloud M, *et al.* Mid-term results demonstrate salvage high-intensity focused ultrasound (HIFU) as an effective and acceptably morbid salvage treatment option for locally radiorecurrent prostate cancer. *Eur Urol.* 2009;55(3):640–647.

100. Berge V, Baco E, Karlsen SJ. A prospective study of salvage high-intensity focused ultrasound for locally radiorecurrent prostate cancer: early results. *Scand J Urol Nephro.* 2010;44(4):223–227.

101. Zacharakis E, Ahmed HU, Ishaq A, *et al.* The feasibility and safety of high-intensity focused ultrasound as salvage therapy for recurrent prostate cancer following external beam radiotherapy. *BJU Int.* 2008;102(7):786–792.

102. Uchida T, Shoji S, Nakano M, *et al.* High-intensity focused ultrasound as salvage therapy for patients with recurrent prostate cancer after external beam radiation, brachytherapy or proton therapy. *BJU Int.* 2010;107(3)378–382.

103. Sylvester JE, Grimm PD, Wong J, *et al.* Fifteen-year biochemical relapse-free survival, cause-specific survival, and overall survival following I(125) prostate brachytherapy in clinically localized prostate cancer: Seattle experience. *Int J Radiat Oncol Biol Phys.* 2011;81(2):376–381.

104. Heidenreich A, Richter S, Thuer D, *et al.* Prognostic parameters, complications, and oncologic and functional outcome of salvage radical prostatectomy for locally recurrent prostate cancer after 21st-century radiotherapy. *Eur Urol.* 2010;57(3):437–443.

105. Muto S, Yoshii T, Saito K, *et al.* Focal therapy with high-intensity-focused ultrasound in the treatment of localized prostate cancer. *Jpn J Clin Oncol.* 2008;38(3):192–199.

106. Ahmed HU, Freeman A, Kirkham A, *et al.* Focal therapy for localized prostate cancer: a phase I/II trial. *J Urol.* 2011;185(4):1246–1254.

107. Crouzet S, Villers A, Rischmann P, *et al.* Focal treatment of prostate cancer with HIFU. 5th International Symposium on Focal Therapy and Imaging in Prostate & Kidney Cancer. Duke, 2012.

108. Ahmed HU, Hindley RG, Dickinson L, *et al.* Focal therapy for localised unifocal and multifocal prostate cancer: a prospective development study. *Lancet Oncol.* 2012;13(6):622–632.

109. Ahmed HU, Cathcart P, McCartan N, *et al.* Focal salvage therapy for localized prostate cancer recurrence after external beam radiotherapy: a pilot study. *Cancer.* 2012;118(17):4148–4155.

110. Baco E, Gelet A, Crouzet S, *et al.* Hemi salvage high-intensity focused ultrasound (HIFU) in unilateral radiorecurrent prostate cancer: a prospective two-centre study. *BJU Int.* 2014;114(4):532–540.

111. Cordeiro ER, Cathelineau X, Thüroff S, *et al.* High-intensity focused ultrasound (HIFU) for definitive treatment of prostate cancer. *BJU Int.* 2012;110(9):1228–1242.

112. Crouzet S, Rouviere O, Martin X, *et al.* High-intensity focused ultrasound as focal therapy of prostate cancer. *Curr Opin Urol.* 2014;24(3):225–230.

113. Zini C, Hipp E, Thomas S, *et al.* Ultrasound- and MR-guided focused ultrasound surgery for prostate cancer. *World J Radiol.* 2012;4(6):247–252.

114. Bomers JG, Sedelaar JP, Barentsz JO, *et al.* MRI-guided interventions for the treatment of prostate cancer. *AJR Am J Roentgenol.* 2012;199(4):714–720.

115. Ishihara Y, Calderon A, Watanabe H, *et al.* A precise and fast temperature mapping using water proton chemical shift. *Magn Reson Med.* 1995;34(6):814–823.

116. Grissom WA, Kerr AB, Holbrook AB, *et al.* Maximum linear-phase spectral-spatial radiofrequency pulses for fat-suppressed proton resonance frequency-shift MR Thermometry. *Magn Reson Med.* 2009;62(5):1242–1250.

117. Vanne A, Hynynen K. MRI feedback temperature control for focused ultrasound surgery. *Phys Med Biol.* 2003;48(1):31–43.

118. Mougenot C, Quesson B, de Senneville BD, *et al.* Three-dimensional spatial and temporal temperature control with MR thermometry-guided focused ultrasound (MRgHIFU). *Magn Reson Med.* 2009;61(3):603–614.

119. Chopra R, Colquhoun A, Burtnyk M, *et al.* MR imaging-controlled transurethral ultrasound therapy for conformal treatment of prostate tissue: initial feasibility in humans. *Radiology*. 2012;265(1):303–313.

120. Burtnyk M, Chopra R, Bronskill M. Simulation study on the heating of the surrounding anatomy during transurethral ultrasound prostate therapy: a 3D theoretical analysis of patient safety. *Med Phys*. 2010;37(6):2862–2875.

121. Burtnyk M, Chopra R, Bronskill MJ. Quantitative analysis of 3-D conformal MRI-guided transurethral ultrasound therapy of the prostate: theoretical simulations. *Int J Hyperthermia*. 2009;25(2):116–131.

122. Burtnyk M, Hill T, Cadieux-Pitre H, *et al.* Magnetic resonance image guided transurethral ultrasound prostate ablation: a preclinical safety and feasibility study with 28-day followup. *J Urol*. 2015;193(5):1669–1675.

123. Partanen A, Yerram NK, Trivedi H, *et al.* Magnetic resonance imaging (MRI)-guided transurethral ultrasound therapy of the prostate: a preclinical study with radiological and pathological correlation using customised MRI-based moulds. *BJU Int*. 2013;112(4):508–516.

124. Diederich CJ. Ultrasound applicators with integrated catheter-cooling for interstitial hyperthermia: theory and preliminary experiments. *Int J Hyperthermia*. 1996;12(2):279–297.

125. Diederich CJ, Stafford RJ, Nau WH, *et al.* Transurethral ultrasound applicators with directional heating patterns for prostate thermal therapy: in vivo evaluation using magnetic resonance thermometry. *Med Phys*. 2004;31(2):405–413.

126. Kinsey AM, Diederich CJ, Rieke V, *et al.* Transurethral ultrasound applicators with dynamic multi-sector control for prostate thermal therapy: in vivo evaluation under MR guidance. *Med Phys*. 2008;35(5):2081–2093.

127. Salgaonkar VA, Prakash P, Rieke V, *et al.* Model-based feasibility assessment and evaluation of prostate hyperthermia with a commercial MR-guided endorectal HIFU ablation array. *Med Phys*. 2014;41(3):033301.

128. Sommer G, Pauly KB, Holbrook A, *et al.* Applicators for magnetic resonance-guided ultrasonic ablation of benign prostatic hyperplasia. *Invest Radiol*. 2013;48(6):387–394.

129. Lafon C, Koszek L, Chesnais S, *et al.* Feasibility of a transurethral ultrasound applicator for coagulation in prostate. *Ultrasound Med Biol*. 2004;30(1):113–122.

130. Napoli A, Anzidei M, Ciolina F, *et al.* MR-guided high-intensity focused ultrasound: current status of an emerging technology. *Cardiovasc Intervent Radiol*. 2013;36(5):1190–1203.

131. Napoli A, Anzidei M, De Nunzio C, *et al.* Real-time magnetic resonance-guided high-intensity focused ultrasound focal therapy for localised prostate cancer: preliminary experience. *Eur Urol*. 2013;63(2):395–398.

132. Ghai S, Louis AS, Van Vliet M, *et al.* Real-Time MRI-Guided Focused Ultrasound for Focal Therapy of Locally Confined Low-Risk Prostate Cancer: Feasibility and Preliminary Outcomes. *AJR Am J Roentgenol*. 2015;205(2):W177–184.

133. Boyes A, Tang K, Yaffe M, *et al.* Prostate tissue analysis immediately following magnetic resonance imaging guided transurethral ultrasound thermal therapy. *J Urol*. 2007;178(3 Pt 1):1080–1085.

134. Petrusca L, Ngo J, Brasset L, *et al.* Experimental investigation of MRgHIFU sonication with interleaved electronic and mechanical displacement of the focal point for transrectal prostate application. *Phys Med Biol*. 2012;57(15):4805–4825.

135. Yiallouras C, Ioannides K, Dadakova T, *et al.* Three-axis MR-conditional robot for high-intensity focused ultrasound for treating prostate diseases transrectally. *J Ther Ultrasound*. 2015;3:2.

136. Chopra R, Burtnyk M, Haider MA, *et al.* Method for MRI-guided conformal thermal therapy of prostate with planar transurethral ultrasound heating applicators. *Phys Med Biol*. 2005;50(21):4957–4975.

137. Chopra R, Wachsmuth J, Burtnyk M, *et al.* Analysis of factors important for transurethral ultrasound prostate heating using MR temperature feedback. *Phys Med Biol*. 2006;51(4):827–844.

138. Burtnyk M, N'Djin WA, Kobelevskiy I, *et al.* 3D conformal MRI-controlled transurethral ultrasound prostate therapy: validation of numerical simulations and demonstration in tissue-mimicking gel phantoms. *Phys Med Biol*. 2010;55(22):6817–6839.

139. N'djin WA, Burtnyk M, Bronskill M, *et al.* Investigation of power and frequency for 3D conformal MRI-controlled transurethral ultrasound therapy with a dual frequency multi-element transducer. *Int J Hyperthermia*. 2012;28(1):87–104.

140. Tang K, Choy V, Chopra R, *et al.* Conformal thermal therapy using planar ultrasound transducers and adaptive closed-loop MR temperature control: demonstration in gel phantoms and ex vivo tissues. *Phys Med Biol*. 2007;52(10):2905–2919.

141. N'Djin W A, Burtnyk M, Kobelevskiy I, *et al.* Coagulation of human prostate volumes with MRI-controlled transurethral ultrasound therapy: results in gel phantoms. *Med Phys*. 2012;39(7):4524–4536.

142. Chopra R, Baker N, Choy V, *et al.* MRI-compatible transurethral ultrasound system for the treatment of localized prostate cancer using rotational control. *Med Phys*. 2008;35(4):1346–1357.

143. Chopra R, Tang K, Burtnyk M, *et al.* Analysis of the spatial and temporal accuracy of heating in the prostate gland using transurethral ultrasound therapy and active MR temperature feedback. *Phys Med Biol.* 2009;54(9):2615–2633.

144. Chopra R, Burtnyk M, N'djin WA, *et al.* MRI-controlled transurethral ultrasound therapy for localised prostate cancer. *Int J Hyperthermia*. 2010;26(8):804–821.

145. Siddiqui K, Chopra R, Vedula S, *et al.* MRI-guided transurethral ultrasound therapy of the prostate gland using real-time thermal mapping: initial studies. *Urology.* 2010;76(6):1506–1511.

146. Schmitt A, Mougenot C, Chopra R. Spatiotemporal filtering of MR-temperature artifacts arising from bowel motion during transurethral MR-HIFU. *Med Phys*. 2014;41(11):113302.

147. McDannold, Hynynen K, Wolf D, *et al.* MRI evaluation of thermal ablation of tumors with focused ultrasound. *J Magn Reson Imaging*. 1998;8(1):91–100.

148. Breen MS, Lazebnik RS, Fitzmaurice M, *et al.* Radiofrequency thermal ablation: correlation of hyperacute MR lesion images with tissue response. *J Magn Reson Imaging.* 2004;20(3):475–486.

149. Nomura T, Mimata H. Focal therapy in the management of prostate cancer: an emerging approach for localized prostate cancer. *Adv Urol*. 2012;2012:391437.

150. Singh PB, Anele C, Dalton E, *et al.* Prostate cancer tumour features on template prostate-mapping biopsies: implications for focal therapy. *Eur Urol*. 2014;66(1):12–19.

151. Lau B, Shah TT, Valerio M, *et al.* Technological aspects of delivering cryotherapy for prostate cancer. *Expert Rev Med Devices*. 2015;12(2):183–190.

152. Quarrier S, Katz A, Haas J. Treatment of prostate cancer local recurrence after whole-gland cryosurgery with frameless robotic stereotactic body radiotherapy: initial experience. *Clin Genitourin Cancer.* 2013;11(2):89–93.

153. Bahn DK, Silverman P, Lee F Sr, *et al.* Focal prostate cryoablation: initial results show cancer control and potency preservation. *J Endourol*. 2006;20(9):688–692.

154. Ritch CR, Katz AE. Prostate cryotherapy: current status. *Curr Opin Urol.* 2009;19(2):177–181.

155. Polom W, Krajka K, Fudalewski T, *et al.* Treatment of urethrorectal fistulas caused by radical prostatectomy - two surgical techniques. *Cent European J Urol*. 2014;67(1):93–97.

156. Strebel RT, Muentener M, Fatzer M, *et al.* Neurovascular bundle block as predictor of postoperative erectile function after radical prostatectomy. *Int J Impot Res*. 2005;17(6):510–512.

157. Furusato B, Gao CL, Ravindranath L, *et al.* Mapping of TMPRSS2-ERG fusions in the context of multi-focal prostate cancer. *Mod Pathol*. 2008;21(2):67–75.

158. Al Ekish S, Nayeemuddin M, Maddox M, *et al.* The role of cryosurgery of the prostate for nonsurgical candidates. *JSLS*. 2013;17(3):423–428.

159. Ward JF, Jones JS. Focal cryotherapy for localized prostate cancer: a report from the national Cryo On-Line Database (COLD) Registry. *BJU Int.* 2012;109(11):1648–1654.

160. Berdugo M, Bejjani RA, Valamanesh F, *et al.* Evaluation of the new photosensitizer Stakel (WST-11) for photodynamic choroidal vessel occlusion in rabbit and rat eyes. *Invest Ophthalmol Vis Sci.* 2008;49(4):1633–1644.

161. Brandis A, Mazor O, Neumark E, *et al.* Novel water-soluble bacteriochlorophyll derivatives for vascular-targeted photodynamic therapy: synthesis, solubility, phototoxicity and the effect of serum proteins. *Photochem Photobiol*. 2005;81(4):983–993.

162. Mazor O, Brandis A, Plaks V, *et al.* WST11, a novel water-soluble bacteriochlorophyll derivative; cellular uptake, pharmacokinetics, biodistribution and vascular-targeted photodynamic activity using melanoma tumors as a model. *Photochem Photobiol*. 2005;81(2):342–351.

163. Vakrat-Haglili Y, Weiner L, Brumfeld V, *et al.* The microenvironment effect on the generation of reactive oxygen species by Pd-bacteriopheophorbide. *J Am Chem Soc*. 2005;127(17):6487–6497.

164. Ashur I, Goldschmidt R, Pinkas I, *et al.* Photocatalytic generation of oxygen radicals by the water-soluble bacteriochlorophyll derivative WST11, noncovalently bound to serum albumin. *J Phys Chem A*. 2009;113(28):8027–8037.

165. Plaks V, Koudinova N, Nevo U, *et al.* Photodynamic therapy of established prostatic adenocarcinoma with TOOKAD: a biphasic apparent diffusion coefficient change as potential early MRI response marker. *Neoplasia*. 2004;6(3):224–233.

166. Madar-Balakirski N, Tempel-Brami C, Kalchenko V, *et al.* Permanent occlusion of feeding arteries and draining veins in solid mouse tumors by vascular targeted photodynamic therapy (VTP) with Tookad. *PLoS One*. 2010;5(4):e10282.

167. Feine I, Pinkas I, Salomon Y, *et al.* Local oxidative stress expansion through endothelial cells--a key role for gap junction intercellular communication. *PLoS One*. 2012;7(7):e41633.

168. Betrouni N, Lopes R, Puech P, *et al.* A model to estimate the outcome of prostate cancer photodynamic therapy with TOOKAD Soluble WST11. *Phys Med Biol*. 2011;56(15):4771–4783.

169. Azzouzi AR, Lebdai S, Benzaghou F, *et al.* Vascular-targeted photodynamic therapy with TOOKAD® Soluble in localized prostate cancer: standardization of the procedure. *World J Urol*. 2015;33(7):937–944.

170. Koudinova NV, Pinthus JH, Brandis A, *et al.* Photodynamic therapy with Pd-Bacteriopheophorbide (TOOKAD): successful in vivo treatment of human prostatic small cell carcinoma xenografts. *Int J Cancer*. 2003;104(6):782–789.

171. Chen Q, Huang Z, Luck D, *et al.* Preclinical studies in normal canine prostate of a novel palladium-bacteriopheophorbide (WST09) photosensitizer for photodynamic therapy of prostate cancers. *Photochem Photobiol*. 2002;76(4):438–445.

172. Huang Z, Chen Q, Trncic N, *et al.* Effects of Pd-bacteriopheophorbide (TOOKAD)-mediated photodynamic therapy on canine prostate pretreated with ionizing radiation. *Radiat Res*. 2004;161(6):723–731.

173. Huang Z, Chen Q, Luck D, *et al.* Studies of a vascular-acting photosensitizer, Pd-bacteriopheophorbide (Tookad), in normal canine prostate and spontaneous canine prostate cancer. *Lasers Surg Med*. 2005;36(5):390–397.

174. Huang Z, Haider MA, Kraft S, *et al.* Magnetic resonance imaging correlated with the histopathological effect of Pd-bacteriopheophorbide (Tookad) photodynamic therapy on the normal canine prostate gland. *Lasers Surg Med*. 2006;38(7):672–681.

175. Chevalier S, Anidjar M, Scarlata E, *et al.* Preclinical study of the novel vascular occluding agent, WST11, for photodynamic therapy of the canine prostate. *J Urol*. 2011;186(1):302–309.

176. Chevalier S, Cury FL, Scarlata E, *et al.* Endoscopic vascular targeted photodynamic therapy with the photosensitizer WST11 for benign prostatic hyperplasia in the preclinical dog model. *J Urol*. 2013;190(5):1946–1953.

177. Trachtenberg J, Bogaards A, Weersink RA, *et al.* Vascular targeted photodynamic therapy with palladium-bacteriopheophorbide photosensitizer for recurrent prostate cancer following definitive radiation therapy: assessment of safety and treatment response. *J Urol*. 2007;178(5):1974–1979.

178. Trachtenberg J, Weersink RA, Davidson SR, *et al.* Vascular-targeted photodynamic therapy (padoporfin, WST09) for recurrent prostate cancer after failure of external beam radiotherapy: a study of escalating light doses. *BJU Int*. 2008;102(5):556–562.

179. Haider MA, Davidson SR, Kale AV, *et al.* Prostate gland: MR imaging appearance after vascular targeted photodynamic therapy with palladium-bacteriopheophorbide. *Radiology*. 2007;244(1):196–204.

180. Moore CM, Azzouzi AR, Barret E, *et al.* Determination of optimal drug dose and light dose index to achieve minimally invasive focal ablation of localised prostate cancer using WST11-vascular-targeted photodynamic (VTP) therapy. *BJU Int*. 2015;116(6):888–896.

181. Azzouzi AR, Barret E, Moore CM, *et al.* TOOKAD® Soluble vascular-targeted photodynamic (VTP) therapy: determination of optimal treatment conditions and assessment of effects in patients with localised prostate cancer. *BJU Int*. 2013;112(6):766–774.

182. Azzouzi AR, Barret E, Bennet J, *et al.* TOOKAD® Soluble focal therapy: pooled analysis of three phase II studies assessing the minimally invasive ablation of localized prostate cancer. *World J Urol*. 2015;33(7):945–953.

183. Eymerit-Morin C, Zidane M, Lebdai S, *et al.* Histopathology of prostate tissue after vascular-targeted photodynamic therapy for localized prostate cancer. *Virchows Arch*. 2013;463(4):547–552.

184. Dole KC, Chen Q, Hetzel FW, *et al.* Effects of photodynamic therapy on peripheral nerve: in situ compound-action potentials study in a canine model. *Photomed Laser Surg.* 2005;23(2):172–176.

185. Weersink RA, Forbes J, Bisland S, *et al.* Assessment of cutaneous photosensitivity of TOOKAD (WST09) in preclinical animal models and in patients. *Photochem Photobiol.* 2005;81(1):106–113.

186. Lebdai S, Villers A, Barret E, *et al.* Feasibility, safety, and efficacy of salvage radical prostatectomy after Tookad® Soluble focal treatment for localized prostate cancer. *World J Urol.* 2015;33(7):965–971.

187. Al-Sakere B, André F, Bernat C, *et al.* Tumor ablation with irreversible electroporation. *PLoS One.* 2007;2(11):e1135.

188. Olweny EO, Kapur P, Tan YK, *et al.* Irreversible electroporation: evaluation of nonthermal and thermal ablative capabilities in the porcine kidney. *Urology.* 2013;81(3):679–684.

189. Pech M, Janitzky A, Wendler JJ, *et al.* Irreversible electroporation of renal cell carcinoma: a first-in-man phase I clinical study. *Cardiovasc Intervent Radiol.* 2011;34(1):132–138.

190. Baker PF, Knight DE. Calcium-dependent exocytosis in bovine adrenal medullary cells with leaky plasma membranes. *Nature.* 1978;276(5688):620–622.

191. Crowley JM. Electrical breakdown of bimolecular lipid membranes as an electromechanical instability. *Biophys J.* 1973;13(7):711–724.

192. Gauger B, Bentrup FW. A study of dielectric membrane breakdown in the Fucus egg. *J Membr Biol.* 1979;48(3):249–264.

193. Kinosita K Jr, Tsong TT. Hemolysis of human erythrocytes by transient electric field. *Proc Natl Acad Sci USA.* 1977;74(5):1923–1927.

194. Neumann E, Rosenheck K. Permeability changes induced by electric impulses in vesicular membranes. *J Membr Biol.* 1972;10(3):279–290.

195. Zimmermann U, Pilwat G, Riemann F. Dielectric breakdown of cell membranes. *Biophys J.* 1974;14(11):881–899.

196. Chang DC, Chassy BM, Saunders JA, *et al. Guide to Electroporation and Electrofusion.* San Diego, Academic Press, 1992.

197. Neumann E, Schaefer-Ridder M, Wang Y, *et al.* Gene transfer into mouse lyoma cells by electroporation in high electric fields. *EMBO J.* 1982;1(7):841–845.

198. Neumann E, Sowers AE, Jordan CA. *Electroporation and Electrofusion in Cell Biology.* New York, Plenum Press, 1989, pp 1–431.

199. Fuller GW. *Report on the Investigations Into the Purification of the Ohio River Water at Louisville Kentucky Made to the President And Directors of the Louisville Water Company.* New York, D. Van Nostrand Company, 1898, pp 1–461.

200. Rowan NJ, MacGregor SJ, Anderson JG, *et al.* Pulsed electric field inactivation of diarrhoeagenic Bacillus cereus through irreversible electroporation. *Lett Appl Microbiol.* 2000;31(2):110–114.

201. Vernhes MC, Benichou A, Pernin P, *et al.* Elimination of free-living amoebae in fresh water with pulsed electric fields. *Water Res.* 2002;36(14):3429–3438.

202. Vernhes MC, Cabanes PA, Teissie J. Chinese hamster ovary cells sensitivity to localized electrical stresses. *Bioelectrochem Bioenerg.* 1999;48(1):17–25.

203. Ball C, Thomson KR, Kavnoudias H. Irreversible electroporation: a new challenge in "out of operating theater" anesthesia. *Anesth Analg.* 2010;110(5):1305–1309.

204. Garner AL, Chen G, Chen N, *et al.* Ultrashort electric pulse induced changes in cellular dielectric properties. *Biochem Biophys Res Commun.* 2007;362(1):139–144.

205. Miller L, Leor J, Rubinsky B. Cancer cells ablation with irreversible electroporation. *Technol Cancer Res Treat.* 2005;4(6):699–705.

206. Scheffer HJ, Nielsen K, de Jong MC, *et al.* Irreversible electroporation for nonthermal tumor ablation in the clinical setting: a systematic review of safety and efficacy. *J Vasc Interv Radiol.* 2014;25(7):997–1011.

207. Bertacchini C, Margotti PM, Bergamini E, *et al.* Design of an irreversible electroporation system for clinical use. *Technol Cancer Res Treat.* 2007;6(4):313–320.

208. Garcia PA, Davalos RV, Miklavcic D. A numerical investigation of the electric and thermal cell kill distributions in electroporation-based therapies in tissue. *PLoS One.* 2014;9(8):e103083.

209. Rubinsky B, Onik G, Mikus P. Irreversible electroporation: a new ablation modality--clinical implications. *Technol Cancer Res Treat*. 2007;6:37–48.

210. Onik G, Mikus P, Rubinsky B. Irreversible electroporation: implications for prostate ablation. *Technol Cancer Res Treat*. 2007;6(4):295–300.

211. Joshi RP, Schoenbach KH. Bioelectric effects of intense ultrashort pulses. *Crit Rev Biomed Eng*. 2010;38(3):255–304.

212. Al-Sakere B, Bernat C, Andre F, *et al*. A study of the immunological response to tumor ablation with irreversible electroporation. *Technol Cancer Res Treat*. 2007;6(4):301–306.

213. Thomson KR, Cheung W, Ellis SJ, *et al*. Investigation of the safety of irreversible electroporation in humans. *J Vasc Interv Radiol*. 2011;22(5):611–621.

214. Kingham TP, Karkar AM, D'Angelica MI, *et al*. Ablation of perivascular hepatic malignant tumors with irreversible electroporation. *J Am Coll Surg*. 2012;215(3):379–387.

215. Narayanan G, Froud T, Lo K, *et al*. Pain analysis in patients with hepatocellular carcinoma: irreversible electroporation versus radiofrequency ablation-initial observations. *Cardiovasc Intervent Radiol*. 2013;36(1):176–182.

216. Martin RC 2nd, McFarland K, Ellis S, *et al*. Irreversible electroporation therapy in the management of locally advanced pancreatic adenocarcinoma. *J Am Coll Surg*. 2012;215(3):361–369.

217. Narayanan G, Hosein PJ, Arora G, *et al*. Percutaneous irreversible electroporation for downstaging and control of unresectable pancreatic adenocarcinoma. *J Vasc Interv Radiol*. 2012;23(12):1613–1621.

218. Usman M, Moore W, Talati R, *et al*. Irreversible electroporation of lung neoplasm: a case series. *Med Sci Monit*. 2012;18(6):CS43–47.

219. Valerio M, Stricker PD, Ahmed HU, *et al*. Initial assessment of safety and clinical feasibility of irreversible electroporation in the focal treatment of prostate cancer. *Prostate Cancer Prostatic Dis*. 2014;17(4):343–347.

220. van den Bos W, de Bruin DM, Muller BG, *et al*. The safety and efficacy of irreversible electroporation for the ablation of prostate cancer: a multicentre prospective human in vivo pilot study protocol. *BMJ Open*. 2014;4(10):e006382.

221. Neal RE 2nd, Millar JL, Kavnoudias H, *et al*. In vivo characterization and numerical simulation of prostate properties for non-thermal irreversible electroporation ablation. *Prostate*. 2014;74(5):458–468.

222. Murray KS, Ehdaie B, Musser J, *et al*. Pilot Study to Assess Safety and Clinical Outcomes of Irreversible Electroporation for Partial Gland Ablation in Men with Prostate Cancer. *J Urol*. 2016. Apr 22 pii: S0022-5347 (16)30278-6. [Epub ahead of print]

223. Zelefsky MJ, Fuks Z, Hunt M, *et al*. High-dose intensity modulated radiation therapy for prostate cancer: early toxicity and biochemical outcome in 772 patients. *Int J Radiat Oncol Biol Phys*. 2002;53(5):1111–1116.

224. van Lin EN, Fütterer JJ, Heijmink SW, *et al*. IMRT boost dose planning on dominant intraprostatic lesions: gold marker-based three-dimensional fusion of CT with dynamic contrast-enhanced and 1H-spectroscopic MRI. *Int J Radiat Oncol Biol Phys*. 2006;65(1):291–303.

225. Ellis RJ, Vertocnik A, Kim E, *et al*. Four-year biochemical outcome after radioimmunoguided transperineal brachytherapy for patients with prostate adenocarcinoma. *Int J Radiat Oncol Biol Phys*. 2003;57(2):362–370.

226. Zelefsky MJ, Cohen G, Zakian KL, *et al*. Intraoperative conformal optimization for transperineal prostate implantation using magnetic resonance spectroscopic imaging. *Cancer J*. 2000;6(4):249–255.

227. Aluwini S, van Rooij PH, Kirkels WJ, *et al*. High-dose-rate brachytherapy and external-beam radiotherapy for hormone-naïve low- and intermediate-risk prostate cancer: a 7-year experience. *Int J Radiat Oncol Biol Phys*. 2012;83(5):1480–1485.

228. Demanes DJ, Rodriguez RR, Schour L, *et al*. High-dose-rate intensity-modulated brachytherapy with external beam radiotherapy for prostate cancer: California endocurietherapy's 10-year results. *Int J Radiat Oncol Biol Phys*. 2005;61(5):1306–1316.

229. Demanes DJ, Martinez AA, Ghilezan M, *et al*. High-dose-rate monotherapy: safe and effective brachytherapy for patients with localized prostate cancer. *Int J Radiat Oncol Biol Phys*. 2011;81(5):1286–1292.

230. Grills IS, Martinez AA, Hollander M, *et al*. High dose rate brachytherapy as prostate cancer monotherapy reduces toxicity compared to low dose rate palladium seeds. *J Urol*. 2004;171(3):1098–1104.

231. Moman MR, van den Berg CA, Boeken Kruger AE, *et al.* Focal salvage guided by T2-weighted and dynamic contrast-enhanced magnetic resonance imaging for prostate cancer recurrences. *Int J Radiat Oncol Biol Phys*. 2010;76(3):741–746.

232. Hartford AC, Galvin JM, Beyer DC, *et al.* American College of *Radiology* (ACR) and American Society for Radiation Oncology (ASTRO) Practice Guideline for Intensity-modulated Radiation Therapy (IMRT). *Am J Clin Oncol*. 2012;35(6):612–617.

233. Bauman G, Rumble RB, Chen J, *et al.* Intensity-modulated radiotherapy in the treatment of prostate cancer. *Clinical Oncol (R Coll Radiol)*. 2012;24(7):461–473.

234. Aluwini S, van Rooij P, Hoogeman M, *et al.* CyberKnife stereotactic radiotherapy as monotherapy for low- to intermediate-stage prostate cancer: early experience, feasibility, and tolerance. *J Endourol*. 2010;24(5):865–869.

235. Freeman DE, King CR. Stereotactic body radiotherapy for low-risk prostate cancer: five-year outcomes. *Radiat Oncol*. 2011;6:3.

236. King CR, Brooks JD, Gill H, *et al.* Long-term outcomes from a prospective trial of stereotactic body radiotherapy for low-risk prostate cancer. *Int J Radiat Oncol Biol Phys*. 2012;82(2):877–882.

237. Arrayeh E, Westphalen AC, Kurhanewicz J, *et al.* Does local recurrence of prostate cancer after radiation therapy occur at the site of primary tumor? Results of a longitudinal MRI and MRSI study. *Int J Radiat Oncol Biol Phys*. 2012;82(5):e787–793.

238. Cellini N, Morganti AG, Mattiucci GC, *et al.* Analysis of intraprostatic failures in patients treated with hormonal therapy and radiotherapy: implications for conformal therapy planning. *Int J Radiat Oncol Biol Phys*. 2002;53(3):595–599.

239. Pucar D, Hricak H, Shukla-Dave A, *et al.* Clinically significant prostate cancer local recurrence after radiation therapy occurs at the site of primary tumor: magnetic resonance imaging and step-section pathology evidence. *Int J Radiat Oncol Biol Phys*. 2007;69(1):62–69.

240. Fuller DB, Naitoh J, Lee C, *et al.* Virtual HDR CyberKnife treatment for localized prostatic carcinoma: dosimetry comparison with HDR brachytherapy and preliminary clinical observations. *Int J Radiat Oncol Biol Phys*. 2008;70(5):1588–1597.

241. Cengiz M, Dogan A, Ozyigit G, *et al.* Comparison of intracavitary brachytherapy and stereotactic body radiotherapy dose distribution for cervical cancer. *Brachytherapy*. 2012;11(2):125–129.

242. Brenner DJ, Martinez AA, Edmundson GK, *et al.* Direct evidence that prostate tumors show high sensitivity to fractionation (low alpha/beta ratio), similar to late-responding normal tissue. *Int J Radiat Oncol Biol Phys*. 2002;52(1):6–13.

243. Carlson DJ, Stewart RD, Li XA, *et al.* Comparison of in vitro and in vivo alpha/beta ratios for prostate cancer. *Phys Med Biol*. 2004;49(19):4477–4491.

244. Fowler JF. The radiobiology of prostate cancer including new aspects of fractionated radiotherapy. *Acta Oncol*. 2005;44(3):265–276.

245. Kirkham AP, Emberton M, Allen C. How good is MRI at detecting and characterising cancer within the prostate? *Eur Urol*. 2006;50(6):1163–1174.

246. Schmuecking M, Boltze C, Geyer H, *et al.* Dynamic MRI and CAD vs. choline MRS: where is the detection level for a lesion characterisation in prostate cancer? *Int J Radiat Biol*. 2009;85(9):814–824.

247. Turkbey B, Pinto PA, Choyke PL. Imaging techniques for prostate cancer: implications for focal therapy. *Nat Rev Urol*. 2009;6(4):191–203.

248. Noel C, Parikh PJ, Roy M, *et al.* Prediction of intrafraction prostate motion: accuracy of pre- and post-treatment imaging and intermittent imaging. *Int J Radiat Oncol Biol Phys*. 2009;73(3):692–698.

249. Xie Y, Djajaputra D, King CR, *et al.* Intrafractional motion of the prostate during hypofractionated radiotherapy. *Int J Radiat Oncol Biol Phys*. 2008;72(1):236–246.

250. McNair HA, Hansen VN, Parker CC, *et al.* A comparison of the use of bony anatomy and internal markers for offline verification and an evaluation of the potential benefit of online and offline verification protocols for prostate radiotherapy. *Int J Radiat Oncol Biol Phys*. 2008;71(1):41–50.

251. Adamson J, Wu Q. Inferences about prostate intrafraction motion from pre- and posttreatment volumetric imaging. *Int J Radiat Oncol Biol Phys*. 2009;75(1):260–267.

252. Beltran C, Herman MG, Davis BJ. Planning target margin calculations for prostate radiotherapy based on intrafraction and interfraction motion using four localization methods. *Int J Radiat Oncol Biol Phys*. 2008;70(1):289–295.

253. de la Rosette J, Ahmed H, Barentsz J, *et al.* Focal therapy in prostate cancer-report from a consensus panel. *J Endourol*. 2010;24(5):775–780.

254. Langley S, Ahmed HU, Al-Qaisieh B, *et al.* Report of a consensus meeting on focal low dose rate brachytherapy for prostate cancer. *BJU Int*. 2012;109(Suppl 1):7–16.

255. Barkati M, Williams SG, Foroudi F, *et al.* High-dose-rate brachytherapy as a monotherapy for favorable-risk prostate cancer: a Phase II trial. *Int J Radiat Oncol Biol Phys*. 2012;82(5):1889–1896.

256. Battermann JJ, Boon TA, Moerland MA. Results of permanent prostate brachytherapy, 13 years of experience at a single institution. *Radiother Oncol*. 2004;71(1):23–28.

257. Corner C, Rojas AM, Bryant L, *et al.* A Phase II study of high-dose-rate afterloading brachytherapy as monotherapy for the treatment of localized prostate cancer. *Int J Radiat Oncol Biol Phys*. 2008;72(2):441–446.

258. Cosset JM, Hannoun-Lévi JM, Peiffert D, *et al.* Permanent implant prostate cancer brachytherapy: 2013 state-of-the art. *Cancer Radiother*. 2013;17(2):111–117. [Article in French]

259. Ghilezan M, Martinez A, Gustason G, *et al.* High-dose-rate brachytherapy as monotherapy delivered in two fractions within one day for favorable/intermediate-risk prostate cancer: preliminary toxicity data. *Int J Radiat Oncol Biol Phys*. 2012;83(3):927–932.

260. Hoskin P, Rojas A, Lowe G, *et al.* High-dose-rate brachytherapy alone for localized prostate cancer in patients at moderate or high risk of biochemical recurrence. *Int J Radiat Oncol Biol Phys*. 2012;82(4):1376–1384.

261. Potters L, Morgenstern C, Calugaru E, *et al.* 12-year outcomes following permanent prostate brachytherapy in patients with clinically localized prostate cancer. *J Urol*. 2005;173(5):1562–1566.

262. Rogers CL, Alder SC, Rogers RL, *et al.* High dose brachytherapy as monotherapy for intermediate risk prostate cancer. *J Urol*. 2012;187(1):109–116.

263. Tselis N, Tunn UW, Chatzikonstantinou G, *et al.* High dose rate brachytherapy as monotherapy for localised prostate cancer: a hypofractionated two-implant approach in 351 consecutive patients. *Radiat Oncol*. 2013;8:115.

264. Yoshioka Y, Konishi K, Sumida I, *et al.* Monotherapeutic high-dose-rate brachytherapy for prostate cancer: five-year results of an extreme hypofractionation regimen with 54 Gy in nine fractions. *Int J Radiat Oncol Biol Phys*. 2011;80(2):469–475.

265. Zelefsky MJ, Kuban DA, Levy LB, *et al.* Multi-institutional analysis of long-term outcome for stages T1-T2 prostate cancer treated with permanent seed implantation. *Int J Radiat Oncol Biol Phys*. 2007;67(2):327–333.

266. Wang Y, Sankreacha R, Al-Hebshi A, *et al.* Comparative study of dosimetry between high-dose-rate and permanent prostate implant brachytherapies in patients with prostate adenocarcinoma. *Brachytherapy*. 2006;5(4):251–255.

267. Hoskin P. HDR versus LDR seeds, in Kovács G, Hoskin P (Ed): *Interstitial Prostate Brachytherapy LDR-PDR-HDR*. Heidelberg, Springer-Verlag, 2013, pp 179–186.

268. Nguyen PL, Chen MH, Zhang Y, *et al.* Updated results of magnetic resonance imaging guided partial prostate brachytherapy for favorable risk prostate cancer: implications for focal therapy. *J Urol*. 2012;188(4):1151–1156.

269. Cosset JM, Cathelineau X, Wakil G, *et al.* Focal brachytherapy for selected low-risk prostate cancers: a pilot study. *Brachytherapy*. 2013;12(4):331–337.

270. Barret E, Ahallal Y, Sanchez-Salas R, *et al.* Morbidity of focal therapy in the treatment of localized prostate cancer. *Eur Urol*. 2013;63(4):618–622.

271. Kovács G, Cosset JM, Carey B. Focal radiotherapy as focal therapy of prostate cancer. *Curr Opin Urol*. 2014;24(3):231–235.

272. Medtronic. MRI-guided laser ablation technology adds to surgical technologies product portfolio and broader neuroscience leadership position. 2014. Available: http://newsroom.medtronic.com/phoenix.zhtml?c=251324&p=irol-newsArticle&ID=1951904; Accessed: April 20, 2016.

273. Stafford RJ, Shetty A, Elliott AM, *et al.* Magnetic resonance guided, focal laser induced interstitial thermal therapy in a canine prostate model. *J Urol*. 2010;184(4):1514–1520.

274. Lindner U, Lawrentschuk N, Weersink RA, *et al.* Focal laser ablation for prostate cancer followed by radical prostatectomy: validation of focal therapy and imaging accuracy. *Eur Urol*. 2010;57(6):1111–1114.

275. Oto A, Sethi I, Karczmar G, *et al.* MR imaging-guided focal laser ablation for prostate cancer: phase I trial. *Radiology*. 2013;267(3):932–940.

276. Lindner U, Weersink RA, Haider MA, *et al.* Complications, Recovery, and Early Functional Outcomes and Oncologic Control Following In-bore Focal Laser Ablation of Prostate Cancer. *J Urol*. 2009;182(4):1371–1377.

277. Lepor H, Llukani E, Sperling D, *et al.* Complications, recovery, and early functional outcomes and oncologic control following in-bore focal laser ablation of prostate cancer. *Eur Urol*. 2015;68(6):924–926.

278. Lindner U, Trachtenberg J, Lawrentschuk N. Focal therapy in prostate cancer: modalities, findings and future considerations. *Nat Rev Urol*. 2010;7(10):562–571.

279. Lindner U, Trachtenberg J. Focal therapy for localized prostate cancer -choosing the middle ground. *Can Urol Assoc J*. 2009;3(4):333–335.

280. Sánchez-Ortiz RF, Tannir N, Ahrar K, *et al.* Spontaneous regression of pulmonary metastases from renal cell carcinoma after radio frequency ablation of primary tumor: an in situ tumor vaccine? *J Urol*. 2003;170(1):178–179.

281. Kim H, Park BK, Kim CK. Spontaneous regression of pulmonary and adrenal metastases following percutaneous radiofrequency ablation of a recurrent renal cell carcinoma. *Korean J Radiol*. 2008;9(5):470–472.

282. Soanes WA, Ablin RJ, Gonder MJ. Remission of metastatic lesions following cryosurgery in prostatic cancer: immunologic considerations. *J Urol*. 1970;104(1):154–159.

283. Formenti SC, Demaria S. Systemic effects of local radiotherapy. *Lancet Oncol*. 2009;10(7):718–726.

284. Formenti SC, Demaria S. Combining radiotherapy and cancer immunotherapy: a paradigm shift. *J Natl Cancer Inst*. 2013;105(4):256–265.

285. van den Bos W, Muller BG, de Bruin DM, *et al.* Salvage ablative therapy in prostate cancer: international multidisciplinary consensus on trial design. *Urol Oncol*. 2015;33(11):495.e1–7.

286. Pisters LL, Leibovici D, Blute M, *et al.* Locally recurrent prostate cancer after initial radiation therapy: a comparison of salvage radical prostatectomy versus cryotherapy. *J Urol*. 2009;182(2):517–525.

287. Karavitakis M, Winkler M, Abel P, *et al.* Histological characteristics of the index lesion in whole-mount radical prostatectomy specimens: implications for focal therapy. *Prostate Cancer Prostatic Dis*. 2011;14(1):46–52.

288. Wise AM, Stamey TA, McNeal JE, *et al.* Morphologic and clinical significance of multifocal prostate cancers in radical prostatectomy specimens. *Urology*. 2002;60(2):264–269.

289. Valerio M, El-Shater Bosaily A, Emberton M, *et al.* Defining the level of evidence for technology adoption in the localized prostate cancer pathway. *Urol Oncol*. 2014;32(6):924–930.

290. Ramsay CR, Adewuyi TE, Gray J, *et al.* Ablative therapy for people with localised prostate cancer: a systematic review and economic evaluation. *Health Technol Assess*. 2015;19(49):1–490.

291. Ahmed HU, Berge V, Bottomley D, *et al.* Can we deliver randomized trials of focal therapy in prostate cancer? *Nat Rev Clin Oncol*. 2014;11(8):482–491.

292. Cook JA. The challenges faced in the design, conduct and analysis of surgical randomised controlled trials. *Trials*. 2009;10:9.

293. Tsivian M, Polascik TJ. Focal cryotherapy for prostate cancer. *Curr Urol Rep*. 2010;11(3):147–151.

294. Polascik TJ, Mayes JM, Mouraviev V. Nerve-sparing focal cryoablation of prostate cancer. *Curr Opin Urol*. 2009;19(3):182–187.

295. Mendez MH, Passoni NM, Pow-Sang J, *et al.* Comparison of outcomes between preoperatively potent men treated with focal versus whole gland cryotherapy in a matched population. *J Endourol*. 2015;29(10):1193–1198.

296. Dickinson L, Ahmed HU, Kirkham AP, *et al.* A multi-centre prospective development study evaluating focal therapy using high intensity focused ultrasound for localised prostate cancer: The INDEX study. *Contemp Clin Trials*. 2013;36(1):68–80.

297. Rouvière O, Gelet A, Crouzet S, *et al.* Prostate focused ultrasound focal therapy--imaging for the future. *Nat Rev Clin Oncol*. 2012;9(12):721–727.

298. Crouzet S, Murat FJ, Pasticier G, *et al.* High intensity focused ultrasound (HIFU) for prostate cancer: current clinical status, outcomes and future perspectives. *Int J Hyperthermia*. 2010;26(8):796–803.

299. Atri M, Gertner MR, Haider MA, *et al.* Contrast-enhanced ultrasonography for real-time monitoring of interstitial laser thermal therapy in the focal treatment of prostate cancer. *Can Urol Assoc J.* 2009;3(2):125–130.

300. Raz O, Haider MA, Davidson SR, *et al.* Real-time magnetic resonance imaging-guided focal laser therapy in patients with low-risk prostate cancer. *Eur Urol.* 2010;58(1):173–177.

301. Valerio M, Dickinson L, Ali A, *et al.* A prospective development study investigating focal irreversible electroporation in men with localised prostate cancer: Nanoknife Electroporation Ablation Trial (NEAT). C*ontemp Clin Trials.* 2014;39:57–65.

302. Coleman JA, Scardino PT. Targeted prostate cancer ablation: energy options. *Curr Opin Urol.* 2013;23(2):123–128.

303. Health Policy Advisory Committee on Technology (HealthPACT). Technology brief: ablative techniques for the treatment of localised prostate cancer, November 2014. 2014. p. 1–20. Available: https://www.health.qld.gov.au/healthpact/docs/briefs/WP198.pdf. Accessed July 11, 2016.

304. Chu KF, Dupuy DE. Thermal ablation of tumours: biological mechanisms and advances in therapy. *Nat Rev Cancer.* 2014;14(3):199–208.

305. Curley SA, Izzo F, Delrio P, *et al.* Radiofrequency ablation of unresectable primary and metastatic hepatic malignancies: results in 123 patients. *Ann Surg.* 1999;230(1):1–8.

306. El Dib R, Touma NJ, Kapoor A. Cryoablation vs radiofrequency ablation for the treatment of renal cell carcinoma: a meta-analysis of case series studies. *BJU Int.* 2012;110(4):510–516.

307. Zlotta AR, Djavan B, Matos C, *et al.* Percutaneous transperineal radiofrequency ablation of prostate tumour: safety, feasibility and pathological effects on human prostate cancer. *Br J Urol.* 1998;81(2):265–275.

308. Djavan B, Zlotta AR, Susani M, *et al.* Transperineal radiofrequency interstitial tumor ablation of the prostate: correlation of magnetic resonance imaging with histopathologic examination. *Urology.* 1997;50(6):986–992.

309. Shariat SF, Raptidis G, Masatoschi M, *et al.* Pilot study of radiofrequency interstitial tumor ablation (RITA) for the treatment of radio-recurrent prostate cancer. *Prostate.* 2005;65(3):260–267.

310. Richstone L, Ziegelbaum M, Okeke Z, *et al.* Ablation of bull prostate using novel bipolar radiofrequency ablation probe. *J Endourol.* 2009;23(1):11–16.

311. Hu B, Hu B, Chen L, *et al.* Contrast-enhanced ultrasonography evaluation of radiofrequency ablation of the prostate: a canine model. *J Endourol.* 2010;24(1):89–93.

312. Marshall S, Taneja S. Focal therapy for prostate cancer: The current status. *Prostate Int.* 2015;3(2):35–41.

313. Dixon C, Cedano ER, Pacik D, *et al.* Efficacy and Safety of Rezūm System Water Vapor Treatment for Lower Urinary Tract Symptoms Secondary to Benign Prostatic Hyperplasia. *Urology.* 2015;86(5):1042–1047.

314. Dixon CM, Rijo Cedano E, Mynderse LA, *et al.* Transurethral convective water vapor as a treatment for lower urinary tract symptomatology due to benign prostatic hyperplasia using the Rezūm® system: evaluation of acute ablative capabilities in the human prostate. *Res Rep Urol.* 2015;7:13–18.

315. Mynderse LA, Hanson D, Robb RA, *et al.* Rezūm System Water Vapor Treatment for Lower Urinary Tract Symptoms/Benign Prostatic Hyperplasia: Validation of Convective Thermal Energy Transfer and Characterization With Magnetic Resonance Imaging and 3-Dimensional Renderings. *Urology.* 2015;86(1):122–127.

316. Dixon C, Cabanas C, Rijo E, *et al.* Development of convective water vapor therapy (steam) for focal therapy of prostate cancer. In vivo treatment and immediate radical prostatectomy. European Urology Supplements. 2015;14(2):e827-e827a.

317. Sherar MD, Trachtenberg J, Davidson SR, *et al.* Interstitial microwave thermal therapy for prostate cancer. *J Endourol.* 2003;17(8):617–625.

318. Montorsi F, Galli L, Guazzoni G, *et al.* Transrectal microwave hyperthermia for benign prostatic hyperplasia: long-term clinical, pathological and ultrastructural patterns. *J Urol.* 1992;148(2 Pt 1):321–325.

319. Khair AA, Pacelli A, Iczkowski KA, *et al.* Does transurethral microwave thermotherapy have a different effect on prostate cancer than on benign or hyperplastic tissue? *Urology.* 1999;54(1):67–72.

320. Sherar MD, Gertner MR, Yue CK, *et al.* Interstitial microwave thermal therapy for prostate cancer: method of treatment and results of a phase I/II trial. *J Urol.* 2001;166(5):1707–1714.

321. Lancaster C, Toi A, Trachtenberg J. Interstitial microwave thermoablation for localized prostate cancer. *Urology*. 1999;53(4):828–831.

322. Trachtenberg J, Chen J, Kucharczyk W, *et al*. Microwave Thermoablation for Localized Prostate Cancer After Failed Radiation Therapy: Role of Neoadjuvant Hormonal Therapy. *Mol Urol*. 1999;3(3):247–250.

323. Chen JC, Moriarty JA, Derbyshire JA, *et al*. Prostate cancer: MR imaging and thermometry during microwave thermal ablation-initial experience. *Radiology*. 2000;214(1):290–297.

324. Ritter, Johann Wilhelm. Complete Dictionary of Scientific Biography. 2008. Available: http://www.encyclopedia.com/doc/1G2-2830903689.html. Accessed July 11, 2016.

325. Pancaldi G. Volta: Science and Culture in the Age of Enlightenment. Princeton, United States: Princeton University Press; 2003.

326. van den Bos, Hester J, *et al*. Thermal Energy during Irreversible Electroporation and the Influence of Different Ablation Parameters. *J Vasc Interv Radiol*. 2016;27:433–443.

327. Cannon R, Ellis S, Hayes D, *et al*. Safety and early efficacy of irreversible electroporation for hepatic tumors in proximity to vital structures. *J Surg Oncol*. 2013;107(5):544–549.

328. Bernier J, Hall EJ, and Giaccia A. Radiation oncology: a century of achievements. *Nat Rev Cancer*. 2004;4(9):737–747.

329. Holm HH. The history of interstitial brachytherapy of prostatic cancer. *Semi Surg Oncol*. 1997;13(6):431–437.

330. Bagshaw, M.A., Kaplan, H.S. Radical external radiotherapy of localized prostate carcinoma. Presented at the Tenth International Congress of Radiology. Montreal, Canada; September 15–18, 1962.

331. Aronowitz JN. Whitmore, Henschke, and Hilaris: The reorientation of prostate brachytherapy (1970–1987). *Brachytherapy*. 2012;11(2):157–162.

332. U.S. National Institutes of Health. ClinicalTrials.gov. [Internet]. Available: https://clinicaltrials.gov/ct2/home. Accessed June 21, 2016.

333. Pilot Study on Focal Prostate Radio-Frequency Ablation. (NCT01423006). Available: https://clinicaltrials.gov/ct2/show/NCT01423006. Accessed June 21, 2016.

334. MRI-Targeted Focal Ablation of the Prostate in Men with Prostate Cancer (FUSAblate). (NCT02303054) Available: https://clinicaltrials.gov/ct2/show/NCT02303054. Accessed June 21, 2016.

335. Focal Prostate Radio-Frequency Ablation (NCT02328807). Available: https://clinicaltrials.gov/ct2/show/NCT02328807. Accessed June 21, 2016.

336. Focal Prostate Radiofrequency Ablation (ProRAFT). NCT2294903. Available: https://clinicaltrials.gov/ct2/show/NCT02294903. Accessed June 21, 2016.

337. Safety and Efficacy Study for the Treatment of BPH (Enlarged Prostate) (REZUM) (NCT01912339). Available: https://clinicaltrials.gov/ct2/show/NCT01912339. Accessed June 21, 2016.

C5

Surveillance After Focal Therapy

CHAIR

Thomas J. Polascik, United States

CO-CHAIR

Mahul Amin, United States

MEMBERS

Sangeet Ghai, Canada
Rafael E. Jimenez, United States
James Kench, Australia
Laurence Klotz, Canada
Rodolfo Montironi, Italy
Satoru Muto, Japan
Ardeshir R. Rastinehad, United States
Kae Jack Tay, United States
Ismail Baris Turkbey, United States
Arnauld Villers, France

CONTENTS

Surveillance After Focal Therapy

5.1 Introduction

Advancements in diagnostic tools such as prostate mapping biopsies and multiparametric magnetic resonance imaging (mpMRI) have provided clinicians with the ability to identify a specific cancer focus within the prostate. This improved diagnostic approach has created a clinical paradigm where one is able to treat that specific focus while sparing the remainder of the gland in order to preserve sexual and continence mechanisms. As active surveillance protocols modernize with the increased use of mpMRI and molecular markers, this new approach may better select men for treatment versus observation.[1] Utilizing these new technologies, and recognizing that low-risk prostate cancer is unlikely to cause mortality, has led to the paradigm shift of treating organ-confined intermediate- or high-grade tumours to "downgrade" the patient back to being an active surveillance candidate.

However, as we shift away from whole-gland treatment, traditional markers of therapeutic success are becoming less relevant. After a curative radical prostatectomy, one expects an undetectable level of prostate-specific antigen (PSA). After radiation therapy, a significant rise in PSA has been agreed upon as the defining mark of biochemical recurrence. After focal therapy, the PSA level may not significantly change from baseline pre-treatment levels, reflecting the amount of viable prostate epithelia that has been preserved. The assessment of oncological outcome then becomes more onerous, requiring the use of imaging modalities and tissue ascertainment.

Paralleling the development of active surveillance strategies as a management option for patients with prostate cancer, there has been a recent consensus by the World Health Organization (WHO), the International Society of Urological Pathologists (ISUP), and an international multidisciplinary grading group to develop a new prognostic grading scheme to be reported in parallel with the Gleason system. Among several other clinical advantages, this scheme potentially allows for better counseling of patients for non-whole-gland treatment approaches. Used in the current manuscript, the new prognostic grade grouping system, independently validated in over 20,000 patients treated at multiple international centres by surgery and radiation therapy, is categorized in five groups: prognostic grade group 1: Gleason score 3 + 3 = 6; prognostic grade group 2: Gleason score 3 + 4 = 7; prognostic grade group 3: Gleason Score 4 + 3 = 7; prognostic grade group 4: Gleason Score 4 + 4 = 8; prognostic grade group 5: Gleason Score 4 + 5, 5 + 4, and 5 + 5 = 9 or 10.[2]

As prostate focal therapy remains a nascent field, long-term outcomes from large cohorts are not yet available upon which to base recommended follow-up protocols. In this chapter, we review the best available current evidence, combined with the expert opinion of the panel members, to develop guidelines for follow-up after prostate focal therapy.

5.2 Definition of Success/Failure: Evaluating the Treated Zone vs. Untreated Area

Following the application of focal therapy, there will be one or more treated segments of the prostate, and the remainder of the gland will not have received any intervention. Therefore, to holistically/comprehensively evaluate oncological outcome, we need to divide the definitions of success or failure into two categories: the treated area(s) and the untreated zones that remain on surveillance. Success can be defined by radiological or biopsy criteria. A limitation is that these outcome measures are not as definitive as whole mount pathology. However, successful treatment ultimately is best defined from the patient's perspective, that is, eradication of all aggressive or clinically significant disease. In other words, the portion of the prostate undergoing treatment should have all aggressive disease eradicated, while the untreated portion should be thoroughly interrogated for aggressive disease, whether with imaging or biopsy, and monitored with active surveillance if low-grade disease is present.

In a consensus meeting (Donaldson 2015) the panel agreed that persistent or recurrent cancer in the treated zone of Gleason grade 3 + 3 (prognostic grade group 1) with a cancer core length ≤3 mm is an acceptable treatment outcome, as long as it represents a decrease from the original cancer burden.[3] The original cancer lesion should be of a higher grade or higher volume than the cancer that remains in the treatment field. The Donaldson consensus panel felt that remaining lesions of Gleason grade 3 + 4 or 4 + 3 (prognostic grade groups 2 and 3) in the treated zone should be considered failures, regardless of cancer core length [**Level of Evidence (LOE) 4**]. Additionally, the finding of a more substantial volume of Gleason 6 (>3 mm of core length) does not in itself indicate failure. Rather, it is important as a predictor of higher-grade cancer, and its presence should prompt an MRI and targeted biopsy if a target is identified [**LOE 3**].[4]

5.2.1 Assessing the treated zone

In the treated zone, the definition of success can be described in terms of immediate or technical ablative success versus intermediate to long-term oncological outcomes. Immediate or technical success depends on the operator's assessment that sufficient energy delivery has occurred to the target zone with a suitable margin around the target area, depending on the ablative technology used. For example, with cryotherapy at least two freeze-thaw cycles with an ideal nadir temperature of -40 degrees Celsius is often required to cause complete cell death within the freeze zone.[5] The posterior margin of ablation is usually visible to the operator as the edge of the ice ball. With thermal modalities such as high-intensity focused ultrasound (HIFU) or focal laser ablation (FLA), a temperature of 55°C for 5 seconds is lethal to almost all epithelial cells.[6,7] Using in-bore techniques allow for a more targeted ablation approach. Magnetic resonance thermometry may help in ascertaining that the target temperature has been reached, and an enhanced scan at the end of the procedure can assess treatment coverage while the patient is still on the table.[8] Similarly, immediate evaluation of the treated area with contrast-enhanced ultrasound (CEUS) microbubble agents can be performed to allow for additional focal ablation of any areas suspicious for residual disease. After irreversible

electroporation (IRE), treatment-related changes in the target zone are not apparent on greyscale ultrasound but may be visualized using CEUS or dynamic contrast-enhanced MRI techniques.[9] Before completing the therapy, the operator should have an assessment of whether the treatment coverage was adequate. If not, provisions for repeat or additional therapy may need to be made. All these refer to immediate technical success, which is just one part of treatment or cancer success.

In the intermediate- to long-term, oncological success is defined histologically with biopsy, and radiologically with mpMRI[a]. These criteria have their pitfalls. As small foci of significant cancer may persist at the margins of the treated zone, or exist as skip lesions, longitudinal follow-up with repeated assessments will be necessary to ensure that success is enduring. Based on the latest pathological data from ISUP, from an oncological point of view, we would consider small volume Gleason 3 + 3 (prognostic grade group 1) or very small volume (<0.2 cc or <7 mm in diameter) Gleason 3 + 4 (prognostic grade group 2) as acceptable within the treated zone at longitudinal follow-up. Significant volume (≥0.2 cc or ≥7 mm in diameter) of Gleason 3 + 4 (prognostic grade group 2) within the treated zone would be considered failure [**Grade of Recommendation (GOR) C**].

5.2.2 Appraising the untreated area

The untreated area may be monitored for *de novo* disease alongside the treated area with radiological means. If there is low-risk disease in the untreated area, it should be monitored with standard of care active surveillance protocols. The majority of protocols stipulate a systematic re-biopsy within 12 to 18 months, and thereafter using predefined PSA, PSA-derivative, or radiological triggers.[10] The definition of focal therapy failure in the untreated area would be the development of any foci of clinically significant cancer requiring further therapy [**GOR C**]. Those who develop such foci early on (within 12–18 months) likely represent selection failure.

5.3 Role of Prostate-Specific Antigen, Derivatives, and Other Molecular Markers

5.3.1 PSA

Prostate-specific antigen (PSA) being produced by normal prostatic cells does not usually reduce to undetectable levels after non-extirpative therapies. Despite this, robust criteria have been developed to define biochemical recurrence after radiation therapy, and in this setting PSA nadir levels, times to nadir, and subsequent doubling times (PSADT) have been found to be of prognostic value.[11–15] Consequently, these criteria have also been adopted for other non-radiation-based, non-extirpative treatments such as cryotherapy or HIFU.[16,17] After partial gland ablation or true focal therapy with

a By today's standards, mpMRI is the best imaging technique, but radiological assessment may entail other imaging modalities to supplement or complement mpMRI in the future.

treatment of the index lesion alone, serum PSA levels have been noted to decrease.[18] However, the remaining volume of viable prostate epithelium impairs accurate interpretation of serum PSA levels. Furthermore, the post-treatment serum PSA trend may be affected by age, benign prostatic hypertrophy, and other non-malignant entities.[19,20] There is currently not enough data describing the course of serum PSA post-focal therapy with long-term prognosis, but expert consensus has been to record post-treatment PSA levels including density, nadir, and other kinetics for future research purposes [**GOR C, LOE 4**].[21]

5.3.2 Prostate-specific antigen derivatives

Derivatives of PSA have been developed in order to control for factors affecting serum PSA besides prostate cancer. In cases where focal therapy was applied to disease exclusively located to one or two foci, could PSA derivatives potentially aid in the monitoring of both the treated and untreated zone(s) after focal therapy by improving cancer detection?

Adjustment of PSA to account for prostate volume using PSA density (PSAD) has been investigated in the pre-diagnosis setting.[22] PSA density is particularly pertinent to the post-focal therapy setting as a marked reduction of the treated portion of the gland is routinely observed at follow-up transrectal ultrasound (TRUS) and MRI. However, the critique of PSAD is its user-dependence as a result of ultrasound-based prostate volume assessment. While this may be less of an issue with the increased use of MRI for follow-up post-focal therapy, threshold PSADs based on MRI prostate volume are still being developed.[23] The doubling time of PSA (PSADT) is an estimation of the trajectory of the increase of PSA. It is based on the hypothesis that cancer cells multiply more quickly than benign prostatic cells and thus cause a rapid increase in serum PSA. The PSA doubling time has been investigated extensively in the active surveillance setting as a trigger for intervention and has been found to be prognostic after radiation and in the metastatic prostate cancer setting.[24–26] However, the lack of specificity of rapid PSA rise (which often occurs due to prostatitis or other non-malignant causes) limits its use.[27]

While PSA derivatives are a promising refinement to serum PSA alone, they have generally been developed and studied in the pre-biopsy PSA 4 to 10 ng/ml setting, and even here they have not gained widespread acceptance and use. There is currently no published evidence defining their use in the post-focal therapy setting [**GOR D, LOE 4**].

5.3.3 Other molecular markers

Biomarkers beyond PSA have been the subject of intense interest and investigation, particularly in pre-diagnosis or active surveillance applications. Markers such as urinary PCA3, serum [-2] pre-pro-PSA, tissue genome prostatic scores, or cell cycle progression scores show some efficacy in predicting high-grade disease and may hold some value in detecting treatment zone recurrences or *de novo* disease/disease progression in the non-treated zone under surveillance. However, there is currently little evidence to incorporate these into a post-focal therapy protocol [**GOR D, LOE 4**]. They may be collected for research purposes.

5.4 Role of Multiparametric MRI in the Post-focal Therapy Setting

5.4.1 Introduction

Prostate focal therapy was initially pursued as a hemi-ablation technique, based on biopsy findings of laterality. Multiparametric MRI, which is gaining widespread acceptance in prostate cancer diagnosis, staging, and surveillance, has revolutionized the identification of prostate cancer index lesions, their subsequent targeting for confirmatory biopsy, and ensuing targeted focal ablation. After focal ablation of an mpMRI-detected lesion, the use of mpMRI for post-treatment surveillance provides the advantage of comparison between the follow-up and pre-ablation treatment zone. Targets can then be assigned for use as in-bore MRI or a TRUS-MRI fusion confirmatory biopsy of the treated area and/or suspicious lesion. Furthermore, mpMRI is known to detect higher-grade significant prostate cancers, and it may play a role in the monitoring of the untreated zone if determined to contain low-grade, low-risk disease initially [**LOE 3**].[28,29] At recent expert consensus group meetings, MRI has been recommended at 6- to 12-month intervals after focal treatment of the prostate, with one group advising a yearly scan for the first five years [**LOE 4**].[21,30]

5.4.2 Technical requirements of multiparametric MRI

Multiparametric MRI typically comprises, in addition to the anatomical T1 and T2 sequences, functional imaging such as diffusion-weighted imaging (DWI) and dynamic contrast-enhanced (DCE) imaging. DWI is widely regarded as the most useful functional imaging sequence for detecting prostate cancer in the untreated prostate, especially for detecting cancer in the peripheral zone with an inverse relationship between quantitative apparent diffusion coefficient (ADC) values and Gleason score.[31] The main drawback of DWI is that technical expertise and specific equipment are required to overcome spatial distortion and signal loss due to magnetic susceptibility effects, especially at higher b values. DWI may also be limited in assessment post-focal therapy because of the fibrosis at the treated site.[32] DCE is a function of vascular flow patterns, and a type 3 curve with rapid uptake and washout of gadolinium contrast is typical of high-grade cancer.[33] Though highly sensitive, its sensitivity is limited when there is prostatitis and benign enlargement, which also display high vascular flow, especially in the transition zone.[34] However, it is generally believed that early nodular enhancement on DCE post-focal therapy is a pattern which suggests residual or recurrent disease at the site of treatment.[35] Magnetic resonance spectroscopic imaging (MRSI) is sometimes performed to examine metabolic activity of the prostate with cancer cells exhibiting a high choline/citrate ratio. While MRSI suffers from poor spatial resolution and needs more time and expertise to perform, it has been used in the post-radiation setting to detect prostate cancer recurrence.[36] As a combination modality, mpMRI has high sensitivity and specificity for the detection of clinically significant prostate cancer, and a high negative predictive value with a modest positive predictive value [**LOE 3**].[37] Thus, a negative mpMRI may be informative, but when there is a suspicious area in the treated zone on mpMRI, histological confirmation is necessary.

5.4.3 Evidence for multiparametric MRI in active surveillance and translation to the focal therapy setting

In the active surveillance setting, mpMRI has been found to predict tumours that would be reclassified at a future re-biopsy session whereby both Gleason score and volume progression may occur [**LOE 3**].[38–40] Furthermore, in a cohort of 72 men on active surveillance undergoing MRI fusion biopsy of all suspicious lesions, mpMRI was found to have a perfect negative predictive value.[41] These findings are applicable to the untreated zone after focal therapy of prostate cancer. A negative mpMRI finding in this area confers a very low risk of significant disease in the untreated zone. A caveat is that many of the studies were conducted in academic or highly specialized centres with radiologists who have a special interest in prostate MRI. Generalizability to the broad academic or community setting remains to be demonstrated.

The evidence for mpMRI in the post-focal treatment arena is sparse. Multiparametric MRI changes after prostate ablation with HIFU have been described in a whole-gland series reporting the sensitivity of DCE-MRI between 73% and 87% and a specificity between 73% and 82%.[42] It is not known whether the performance characteristics of mpMRI will be similar in the treated zone after focal therapy with HIFU. In a more recent study, Ahmed *et al.* reported on a series of 52 men receiving focal HIFU where mpMRI was negative in the treatment zone in 10% of men at 6-month follow-up.[18] Notably, two men had suspicious mpMRI findings in the untreated zone and both were positive for significant disease at biopsy. In a longitudinal study using MRSI, it was also reported that local recurrence of prostate cancer after radiation occurred at the same site in eight of nine men, as detected by MRSI.[43] Multiparametric MRI has otherwise not been reported in the follow-up surveillance after focal cryotherapy or other focal therapy modalities. Long-term imaging, and in particular mpMRI follow-up data following focal therapy, need to be collected to both study its performance characteristics and interrogate if focal ablation of a segment of the prostate does not lead to any adverse changes in the untreated portions of the gland.

5.4.4 Summary and recommendations

Multiparametric MRI is a useful tool in follow-up after focal therapy of the prostate for purposes of monitoring the treated zone as well as the untreated zone. Three-Tesla mpMRI, or 1.5 Tesla with endorectal coil, should be the minimum standards [**GOR C**].[21] Until further evidence suggests otherwise, given the developmental nature of focal therapy, mpMRI is recommended at least once, 6 to 12 months after initial treatment [**GOR C**]. Subsequent serial MR imaging should be performed periodically. The optimal frequency of imaging is not known, and should be determined by patient factors and resource availability [**GOR D**]. Given the long natural history of prostate cancer and the low rate of progression of well-characterized Gleason 6 (prognostic grade group 1) cancer (about 1% per year), it is likely that repeat imaging in low risk patients can be infrequent [**GOR D**]. A negative mpMRI suggests a low risk of disease recurrence or progression [**GOR C**]. A positive mpMRI should lead to a targeted biopsy for histologic confirmation [**GOR C**].

5.5 Role of Biopsy

5.5.1 Types of biopsy available

Periodic follow-up biopsies are considered to be essential for monitoring after focal therapy. Options available include extended sextant 12-core TRUS biopsy, saturation TRUS biopsy (>20 cores), transperineal mapping biopsy, in-bore MRI targeted biopsy, or MRI-TRUS fusion biopsy. These modalities have been investigated in the diagnosis and active surveillance settings, and in general, have shown that an increasing yield for clinically significant disease is seen with an increasing number of biopsies performed [**LOE 3**].[44–47] While MRI-fusion biopsy has a higher detection rate for clinically significant disease, it has not detected all clinically significant disease in cohorts undergoing simultaneous systematic biopsy [**LOE 3**].[48] By today's standards, targeted biopsy implies either the utilization of MRI-TRUS fusion technology or in-bore MRI guidance.

5.5.2 Timing of biopsy

One expert panel (van den Bos *et al.* 2014) had a consensus that TRUS-guided systematic whole-prostate biopsies and additional targeted (software or cognitive fusion) biopsies should be performed between 6 and 12 months after treatment [**LOE 4**].[49] This interval was recommended to account for the time taken for resolution of inflammatory effects and formation of scar tissue. It must also be remembered that ablation of a segment of the prostate followed by the reparative process will not only cause scarring and contraction of the ablation site, but also distortion and settling of the untreated area to "fill in" the space created by that tissue contraction. Thus, targeting of the treated zone post-therapy, depending on when it is assessed, poses its own unique set of challenges. Stromal fibrosis persists at up to 16 months follow-up but does not impair pathologists' ability to grade recurrences.[50] This method would account for surveying the portion of the untreated gland on surveillance while assessing oncological outcome of the treated zone. Another expert panel (Muller 2015) recommended a biopsy of the treated zone in addition to a systematic 12-core TRUS biopsy of the whole prostate (including the untreated zone) at 1 year after treatment and thereafter only when there is suspicion on imaging [**LOE 4**].[21] A third panel (Donaldson 2015) agreed that the optimal time for the first prostate biopsy after focal treatment is at 1 year and that the biopsy should be performed in a targeted manner, as otherwise, previously untreated tissue could easily be inadvertently sampled [**LOE 4**].[3] This panel remained uncertain about whether post-treatment biopsy should also routinely sample the untreated gland.

5.5.3 Triggers for biopsy

Traditional triggers for biopsy in active surveillance settings have been based on time since the diagnostic biopsy and on PSA changes. As mentioned, PSA kinetics are difficult to interpret in the post-focal therapy setting. An expert panel (Muller 2015) has recommended mpMRI as the only trigger for biopsy of both the treated and untreated zone after a first negative 12-month biopsy [**LOE 4**].[21] If biopsy is required, this group recommends a 4- to 6-core targeted biopsy of the ablation zone in order to account for fibrosis-related gland deformity and possible misregistration when using software or cognitive fusion.

Donaldson's consensus group agreed that a suspicious area on mpMRI was a trigger for biopsy but also felt that a rising PSA was a valid trigger [**LOE 4**].[3] However, given the effect of the remnant prostate on fluctuations in serum PSA, using this as trigger may generate more unnecessary biopsies and thus clinical discretion is advised.

5.5.4 Summary and recommendations

There is currently little longitudinal data in focal therapy series to inform the optimal follow-up biopsy regimen. While a transperineal mapping saturation biopsy may be informative, it often necessitates general anesthesia and a trip to the operating room. Multiparametric MRI may detect large and clinically significant lesions in both treated and untreated areas. It should be a part of any focal therapy program and should trigger a targeted biopsy if a suspicious lesion is detected. By today's standards, targeted biopsy implies either the utilization of MRI-TRUS fusion technology or in-bore MRI guidance. In general we would recommend 4 to 6 cores from the treated zone alone, depending on volume/size of treated area, at 3 to 6 months and 12-core systematic plus targeted biopsy of the ablation zone at 12 to 24 months [**GOR C**]. Following 24 months, the gland should be biopsied only if there is a suspicious change in MRI or PSA/clinical findings [**GOR C**]. If clinical parameters/PSA are stable, we would also recommend repeat mpMRI at the 5-year mark with possible biopsies of abnormal areas [**GOR D**]. Biopsy may also be triggered by heightened clinical suspicion based on PSA kinetics, rising PSA, or new mpMRI suspicious findings.

TABLE 5-1: Consensus Recommendations on Follow-up Strategy

	MRI with Possible Fusion Biopsy	Systematic Biopsy
Treated Area	Mandatory biopsy at 3–6 months, 12–24 months, and again at 5 years	-
Untreated Area	12–24 months and again at 5 years	12–24 months and again at 5 years

5.6 Histological Interpretation of Post-treatment Biopsy

5.6.1 Post-radiation treatment changes

Longstanding data for post-treatment histological changes following non-extirpative prostate cancer treatment has largely come from post-irradiation series using external beam or brachytherapy. After radiation, typical histologic changes include a decreased ratio of tumour glands to stroma; atrophy and squamous-like metaplasia of non-neoplastic glands, with or without atypia; stromal fibrosis; arterial luminal narrowing due to myo-intimal proliferation; foam cells within vessel walls; and fibrosis and atrophy of seminal vesicles.[51] After 3D conformal radiation, benign prostatic glands show profound histologic changes that may be confused with prostate cancer.[52] In one cohort, routine biopsy after seed implant brachytherapy found that up to 17% of men have a biopsy reported as indeterminate.[53] In another cohort, after external beam irradiation, 17% of men with positive post-treatment biopsy

remained clinically disease free at 10 years.[54] In yet another cohort, even among those receiving high-dose rate (HDR) brachytherapy boost for intermediate-risk prostate cancer, persistent cancer cells on routine 2-year biopsy did not predict which patients would ultimately fail biochemically.[55] These observations have contributed to uncertainty regarding the adoption of post-radiation prostate biopsies as a gold standard for treatment efficacy.[56] Immunohistochemical studies for basal-cell-associated markers (p63, high molecular weight cytokeratin [CK] 5/6), cancer-associated markers (racemase and ERG), and/or cytokeratin stains to detect subtle infiltrating cancer cells play an important role in indeterminate cases and must be employed before an indeterminate diagnosis is rendered. If cancer is present and it shows no recognizable treatment changes, it should be assigned a Gleason grade and a corresponding prognostic grade group. In cancers with treatment effect, a grading of treatment effect has been proposed to provide an estimate of the extent of treatment effect. Methods of assessing viability of cancer by using MIB-1 (Ki-67) proliferation etc. remain experimental at this time.

5.6.2 Treatment changes after high-intensity focused ultrasound

Early reports of the effects of HIFU on canine prostates were of a subtotal hemorrhagic liquefactive necrosis in 90% of the gland.[57] In human prostates, radical prostatectomy specimens at 2 weeks after HIFU treatment showed a spectrum of morphological changes, from necrosis to subtle ultrastructural cell damage with all lesions demonstrating loss of cytokeratin 8, signifying severe cellular damage.[58] In a 65-year-old man treated with radical cysto-prostatectomy for a prostate-rectal fistula from post-radiation salvage HIFU, histological changes of dense fibrosis consisting of fibroblast proliferation, neuronal proliferation, and chronic inflammation were noted where the prostate should have been located, with no evidence of residual cancer.[59] In an examination of needle biopsies taken 6 months after HIFU treatment, necrosis, often accompanied by acute, chronic, or granulomatous inflammation, was noted in 72% of the cases, with mild to moderate fibrosis in all biopsies.[60] Interestingly, in the 11 patients with residual prostate cancer detected, few to no treatment changes were seen among the glands, raising the possibility of insufficient delivery of thermal energy.

5.6.3 Post-cryotherapy treatment changes

Cryotherapy induces tumour ablation through multiple pathways, including mechanical cell destruction by the formation of ice crystals, necrosis, and the induction of apoptosis through metabolic, vascular, and immune pathways.[61] The evolution of the cryogenic lesion has been described as that of a central coagulative necrosis, surrounded by a relatively thin peripheral zone (freeze margin, where cell destruction may be initially incomplete), that progresses to edema and necrosis of the central zone, and apoptosis and secondary necrosis in the marginal area in a few days.[62] In the following weeks to months, the necrotic tissue is then removed by inflammatory cells and replaced by a fibrous scar. The most frequently described histopathological changes at 1- to 2-year post-cryotherapy biopsy are chronic inflammation, myxoid stromal change, stromal hemosiderin, and stromal fibrosis.[63] As is found in post-HIFU series, patients with positive post-treatment biopsy have been found to have glands with little or no typical post-therapeutic histological changes, suggesting under-treatment as a cause of disease persistence.[63,64]

5.6.4 Changes associated with other treatment modalities

There are a limited number of published studies on the histopathological changes associated with newer partial therapy modalities, most encompassing only a small number of cases.

Laser ablation induces tissue necrosis by thermal injury, and thus the findings are similar to those of HIFU. Lindner *et al.* described four patients that underwent radical prostatectomy after laser ablation therapy.[65] The ablation zone was characterized by homogeneous areas of coagulation necrosis surrounded by a small hemorrhagic rim and devoid of vital glandular tissue. Vitality of the residual glands was assessed by the use of cytokeratin 8, which demonstrated an abrupt transition of positive (vital) glandular tissue and negative (ablated) glands. The points of insertion of the laser fibres were easily identified in the whole mount sections of the radical prostatectomy specimen, and the absence of residual tumour in between the two fibres was evident. The ablation zone extended all the way to the prostate capsule. Also, there was a good correlation between MRI and whole mount hematoxylin and eosin (H&E) histological examination, and an even better correlation with the loss of cytokeratin 8 immunohistochemical staining. Oto *et al.* published results on 6-month post-procedure biopsy on nine patients that underwent laser ablation.[66] Seven patients had no evidence of residual/recurrent disease, while two showed Gleason 3 + 3 adenocarcinoma. Retrospective review of the ablation images revealed incomplete coverage of the lesion site by the ablation zone for the two patients with positive follow-up biopsies. Similarly, Lee *et al.* reported that 12 of their 13 patients who had laser ablation therapy had no residual cancer on follow-up biopsy.[67] The remaining patient had Gleason 3 + 4 = 7 adenocarcinoma. An additional patient developed a new mpMRI abnormality away from the treated area that, upon biopsy, revealed Gleason 3 + 3 adenocarcinoma. Both cases were subsequently re-ablated.

Histopathologic changes associated with photodynamic therapy include hemorrhagic necrosis with inflammation, gland destruction, atrophy, and vascular thrombosis in the treated area, ultimately followed by dense fibrosis.[68,69] Early changes include hemorrhage and coagulative necrosis. Later to late changes include stromal edema, acute and chronic inflammation, focal coagulative necrosis, hemorrhage, hemosiderin deposition, reactive fibroblasts, stromal fibrosis, glandular atrophy, and hyaline scars. Eymerit-Morin *et al.* described the histopathologic findings in 6-month follow-up biopsies of 53 patients that underwent focal photodynamic therapy.[70] These included sharply demarcated hyaline scars, rare atrophic glands, mild chronic inflammatory infiltrate, hemosiderin deposition, and coagulative necrosis. Vascular lesions such as intimal hyaline fibrosis or organized thrombi were not prominent. Seventeen of the 53 patients had residual carcinoma in the treated lobe, all located outside the scarred area, usually close to the capsule. The viable carcinoma glands did not display any therapy-related changes and were easily recognized in most cases with routine histology.

Although a multicentre pilot study is currently underway to evaluate the effects of IRE, including the assessment of histopathologic changes, a small study by Neal *et al.* describes the findings in two patients that underwent radical prostatectomy after IRE.[71,72] The treatment areas showed extensive necrosis with inflammatory neutrophilic infiltrate, surrounded by an area of reactive fibroblasts and hemorrhage. The adjacent viable ducts displayed squamous metaplasia. Irreversible electroporation is

believed to show a sharp demarcation between ablated and non-ablated tissue, in contrast to thermal ablation techniques, which show a transitional zone with partially damaged tissue between ablated and healthy tissue.[71]

5.6.5 Reporting recommendations for post-focal therapy treatment biopsies

In biopsies from the treatment area, it is important for the pathologist to report findings that confirm that the treatment area has been biopsied (necrosis, hemorrhage, acute and chronic inflammation, stromal edema, glandular atrophy, hemosiderin deposition, reactive fibroblasts, stromal fibrosis).

In the treatment area, a diagnostic menu for biopsy findings may include:

1. Post-treatment changes and benign prostatic epithelium, no residual carcinoma;
2. High-grade prostatic intraepithelial neoplasia (HGPIN);
3. Atypical small acinar proliferation, suspicious for carcinoma (a diagnosis usually rendered after examination of multiple levels and/or immunohistochemical studies);
4. Prostatic adenocarcinoma

If no treatment-induced changes are apparent, which is usually the case with focal therapy, a Gleason score should be assigned to the finding of prostatic carcinoma in the treatment area. A finding of HGPIN in the treated area following focal therapy is uncertain, but an isolated focus of HGPIN in this setting is of little clinical significance. As outlined in the introduction, the recently WHO- and ISUP-recommended prognostic grade groups should be reported in parallel with the Gleason grade.

In core and systematic biopsies outside of the treatment areas, handling and reporting should occur in conjunction with established practices.

5.6.6 Molecular markers to help interpret post-treatment histological changes

Immunohistochemistry markers are useful in the microscopic interpretation of treated glands in biopsy specimens.[68,69] Basal cell markers such as cytokeratin 34BE12, p63, or cytokeratin 5/6 selectively label basal cells in prostatic glands. These cells are present only in benign glands, thus their detection is reassuring when the benignity of a group of atypical glands is questioned. The presence of alpha-methylacyl coenzyme A racemase (AMACR), a well-known marker overexpressed in prostate cancer, has been found to facilitate or support decision making in differentiating cancer from benign glands with atypia, such as those seen after radiation therapy. Indeed, the use of a p63/high-molecular weight cytokeratin/AMACR immune-histochemical stain cocktail is a common practice in modern pathology laboratories dealing with prostate biopsy, and its utility has been demonstrated in the setting of treated prostates, including post-radiation and post-HIFU.[50,73,74] Cytokeratin 8 has been suggested as a marker of gland viability after HIFU and laser ablation therapy.[58,65]

In a quest for better prognostication after non-extirpative treatment, several molecular biomarkers have been identified to predict disease progression in the post-irradiation setting. In addition to Gleason score, the presence of DNA-ploidy has been identified as a significant predictor of distant

metastasis-free survival and cancer-specific survival.[75] The cellular proliferation index derived from MIB-1 labeling is another significant predictor of post-radiation recurrence.[76] In an effort to distinguish between biologically active and inactive "residual tumours" following prostate irradiation, Crook *et al.* studied the presence or absence of proliferative cell nuclear antigen (PCNA), finding that a negative PCNA in a positive biopsy predicts an 83% to 97% chance for eventual resolution of tumour.[77]

5.6.7 Summary and recommendations

Characteristic changes occur in the prostate following treatment with various energy modalities. Indeterminate situations can sometimes be resolved with the use of various immuno-histochemical molecular markers, though these should be further evaluated prior to use in routine practice. Our recommendation is to treat definitive cancer on biopsy as a positive finding. Indeterminate findings should be communicated to the patient, and whether to proceed with further treatment should be a shared decision.

5.7 Clinical Management of Cancer Recurrence or Persistence

5.7.1 Introduction

There have thus far been no guidelines defined for the management of patients with failure or recurrence after focal therapy. Further treatment should logically be determined by the new disease status—clinically, biochemically, histologically, and radiologically—coupled with the patient's comorbidities and quality of life considerations, just as one would for any newly presenting prostate cancer.

In general, findings of high-grade prostate intraepithelial neoplasia and atypical small acinar proliferation are acceptable. We would recommend that a finding of Gleason 3 + 3 (prognostic grade group 1) at a significantly lower volume than pre-treatment is considered acceptable and likely can be monitored. Small volume Gleason score 3 + 4 (prognostic grade group 2) lesions at a lower volume than pre-treatment may be cautiously monitored depending on the clinical situation, or offered further treatment. A Gleason score 3 + 4 (prognostic grade group 2) lesion of 0.2 cc (or 7 mm in diameter) or greater should be treated. Any Gleason score ≥4 + 3 (prognostic grade group 3–5) should be treated.

5.7.2 Role of repeat focal therapy

The use of repeat focal therapy remains investigational at this point and we would recommend caution in its application. Failure in the treated zone may be due to various factors, including potential problems with disease localization, targeting, and energy delivery. Unless one has clearly identified a reversible or correctable factor that encumbered the initial attempt at focal therapy, persisting anatomical or other difficulties may continue to affect the efficacy of a repeat focal therapy. For example, if the treatment failure was due to incomplete coverage, then re-treatment may be offered.

However, if the issue was failure to attain the required temperature because of a heat sink effect, then re-treatment using that particular device would not be recommended. In another example, HIFU may be less effective at the prostatic apex and a recurrence or persistence there could be better salvaged with focal cryotherapy or another ablative technique.[78] In a consensus meeting report (Donaldson 2015) the panel agreed that retreatment rates of <20% with focal therapy were clinically acceptable [**LOE 4**].[3] There was agreement that any subsequent whole-gland therapy reflects a failure of focal therapy. A retreatment rate of <10% with whole-gland therapy was considered to be clinically acceptable.

5.7.3 Choosing the modality of treatment

Following prostate irradiation, re-irradiation with brachytherapy and/or image-guided radiotherapy has been found to render up to 50% of patients biochemical relapse-free.[79] Re-irradiation following radiation-based focal therapies might be a reasonable extrapolation of these findings, if not limited by dose.

Post-radiation salvage radical prostatectomy has traditionally been observed to have much higher rates of complications, incontinence, and erectile dysfunction.[80] There is little data regarding these outcomes following focal therapy with lesion-ablation, quadrant-ablation, hemi-ablation, etc., but one might expect complication rates to potentially be higher, and functional outcomes poorer, depending on the location of the target tissue. The degree of technical difficulty may be dependent on the volume and location of the lesion within the prostate that had been ablated in the focal setting. If additional focal therapy is undertaken, it may be reasonable to switch to a different device or mechanism of action based on the location of the lesion and the goal of treatment (e.g. to preserve continence/potency when re-treating an apical lesion).

5.7.4 Summary and recommendations

The cause of cancer persistence or recurrence in the treated zone may be multifactorial. Patients should not be precluded from any of the standard prostate cancer treatment options, including additional focal therapy if clinically appropriate. We generally would only recommend salvage focal therapy where the reasons for initial failure can be clearly identified and corrected, and both the physician and patient believe this option is reasonable [**GOR D**].

5.8 Management of the Untreated Portion of the Gland on Active Surveillance

5.8.1 Role and method of active surveillance

Prostate cancer is a multifocal disease in 60% to 80% of men.[81,82] In men with prostate cancer, morphologically normal prostate tissues contain high levels of mutations even though they are distant from the prostate cancer foci.[83] Furthermore, focal therapy series treating the index lesion only have reported detection of clinically significant disease arising in the untreated area at 6-month biopsy.[84] It remains unclear at present whether occurrence of cancer in the untreated area is due to disease progression as a result of field change, or previously undetected small foci of cancer. Nonetheless, the data provides evidence supporting active surveillance of the untreated area.

Multiple active surveillance protocols have been published. The majority of series include clinical assessment with digital rectal examination, PSA/ PSA kinetics, and re-biopsy at 12 to 18 months, followed by time or for cause trigger-based biopsies.[10] Modern protocols have started to include mpMRI and there may be a role for other potential molecular markers.[1] Since patients treated with focal therapy also have areas of untreated tissue, patients will be under a monitoring program likely encompassing the utilization of both mpMRI and prostate biopsy, which goes hand in hand with contemporary active surveillance practices.

5.8.2 Summary and recommendations

Detection of significant cancer in the untreated zone following focal therapy should be handled in the same way as any *de novo* prostate cancer. Patients should be counseled regarding whole-gland and focal approaches to treating these new foci where appropriate. One or two well-delineated foci of significant cancer can be ablated to keep the patient in the "active surveillance pool" [**GOR D**]. More extensive disease should be treated with traditional whole-gland techniques.

5.9 References

1. Tay KJ, Mendez M, Moul JW, *et al.* Active surveillance for prostate cancer: can we modernize contemporary protocols to improve patient selection and outcomes in the focal therapy era? *Curr Opin Urol.* 2015;25(3):185–90.
2. Epstein JI, Zelefsky MJ, Sjoberg DD, *et al.* A Contemporary Prostate Cancer Grading System: A Validated Alternative to the Gleason Score. *Eur Urol.* 2016;69(3):428-35.
3. Donaldson IA, Alonzi R, Barratt D, *et al.* Focal therapy: patients, interventions, and outcomes—a report from a consensus meeting. *Eur Urol.* 2015;67(4):771–7.
4. Bratt O, Folkvaljon Y, Loeb S, *et al.* Upper limit of cancer extent on biopsy defining very low-risk prostate cancer. *BJU Int.* 2015;116(2):213–9.
5. Babaian RJ, Donnelly B, Bahn D, *et al.* Best practice statement on cryosurgery for the treatment of localized prostate cancer. *J Urol.* 2008;180(5):1993–2004.
6. Napoli A, Anzidei M, De Nunzio C, *et al.* Real-time Magnetic Resonance–guided High-intensity Focused Ultrasound Focal Therapy for Localised Prostate Cancer: Preliminary Experience. *Eur Urol.* 2013;63(2):395–8.
7. Hildebrandt B, Wust P, Ahlers O, *et al.* The cellular and molecular basis of hyperthermia. *Crit Rev Oncol Hematol.* 2002;43(1):33–56.
8. Tay KJ, Cheng CW, Kwek JW, *et al.* Initial experience with MRgFUS focal therapy for low-risk prostate cancer. *J Endourol.* 2011;25:A99–A100.
9. Van Den Bos W, De Bruin DM, Van Randen A, *et al.* Imaging of the ablation zone after focal irreversible electroporation treatment in prostate cancer. *Eur Urol.* 2015;14(2):e828–828a.
10. Dall'Era MA, Albertsen PC, Bangma C, *et al.* Active surveillance for prostate cancer: a systematic review of the literature. *Eur Urol.* 2012;62(6):976–83.
11. Consensus statement: guidelines for PSA following radiation therapy. American Society for Therapeutic *Radiology* and Oncology Consensus Panel. *Int J Radiat Oncol Biol Phys.* 1997;37(5):1035–41.
12. Roach M, Hanks G, Thames Jr H, *et al.* Defining biochemical failure following radiotherapy with or without hormonal therapy in men with clinically localized prostate cancer: Recommendations of the RTOG-ASTRO Phoenix Consensus Conference. *Int J Radiat Oncol Biol Phys.* 2006;65(4):965–74.
13. Zietman AL, Tibbs MK, Dallow KC, *et al.* Use of PSA nadir to predict subsequent biochemical outcome following external beam radiation therapy for T1-2 adenocarcinoma of the prostate. *Radiother Oncol.* 1996;40(2):159–62.
14. Ray ME, Thames HD, Levy LB, *et al.* PSA nadir predicts biochemical and distant failures after external beam radiotherapy for prostate cancer: a multi-institutional analysis. *Int J Radiat Oncol Biol Phys.* 2006;64(4):1140–50.
15. Lee WR, Hanks GE, Hanlon A. Increasing prostate-specific antigen profile following definitive radiation therapy for localized prostate cancer: clinical observations. *J Clin Oncol.* 1997;15(1):230–8.
16. Levy DA, Ross AE, ElShafei A, *et al.* Definition of Biochemical Success Following Primary Whole Gland Prostate Cryoablation. *J Urol.* 2014;192(5):1380–4.
17. Cordeiro ER, Cathelineau X, Thuroff S, *et al.* High-intensity focused ultrasound (HIFU) for definitive treatment of prostate cancer. *BJU Int.* 2012;110(9):1228–42.
18. Ahmed HU, Dickinson L, Charman S, *et al.* Focal Ablation Targeted to the Index Lesion in Multifocal Localised Prostate Cancer: a Prospective Development Study. *Eur Urol.* 2015;68(6):927-36.
19. Roehrborn CG, Boyle P, Gould AL, *et al.* Serum prostate-specific antigen as a predictor of prostate volume in men with benign prostatic hyperplasia. *Urology.* 1999;53(3):581–9.
20. Bohnen AM, Groeneveld FP, Bosch JL. Serum prostate-specific antigen as a predictor of prostate volume in the community: the Krimpen study. *Eur Urol.* 2007;51(6):1645–52; discussion 52–3.
21. Muller BG, van den Bos W, Brausi M, *et al.* Follow-up modalities in focal therapy for prostate cancer: results from a Delphi consensus project. *World J Urol.* 2015;33(10):1503-9.

22. Bazinet M, Meshref AW, Trudel C, *et al.* Prospective evaluation of prostate-specific antigen density and systematic biopsies for early detection of prostatic carcinoma. *Urology.* 1994;43(1):44–51; discussion –2.

23. Turkbey B, Fotin SV, Huang RJ, *et al.* Fully automated prostate segmentation on MRI: comparison with manual segmentation methods and specimen volumes. *AJR Am J Roentgenol.* 2013;201(5):W720–9.

24. Zumsteg ZS, Spratt DE, Romesser PB, *et al.* The Natural History and Predictors of Outcome Following Biochemical Relapse in the Dose Escalation Era for Prostate Cancer Patients Undergoing Definitive External Beam Radiotherapy. *Eur Urol.* 2015;67(6):1009-16

25. Klotz L, Vesprini D, Sethukavalan P, *et al.* Long-term follow-up of a large active surveillance cohort of patients with prostate cancer. *J Clin Oncol.* 2015;33(3):272–7.

26. Studer UE, Collette L, Whelan P, *et al.* Using PSA to guide timing of androgen deprivation in patients with T0-4 N0-2 M0 prostate cancer not suitable for local curative treatment (EORTC 30891). *Eur Urol.* 2008;53(5):941–9.

27. Loblaw A, Zhang L, Lam A, *et al.* Comparing prostate specific antigen triggers for intervention in men with stable prostate cancer on active surveillance. *J Urol.* 2010;184(5):1942–6.

28. Arumainayagam N, Ahmed HU, Moore CM, *et al.* Multiparametric MR imaging for detection of clinically significant prostate cancer: a validation cohort study with transperineal template prostate mapping as the reference standard. *Radiology.* 2013;268(3):761–9.

29. Rosenkrantz AB, Mendrinos S, Babb JS, *et al.* Prostate cancer foci detected on multiparametric magnetic resonance imaging are histologically distinct from those not detected. *J Urol.* 2012;187(6):2032–8.

30. Muller BG, Futterer JJ, Gupta RT, *et al.* The role of magnetic resonance imaging (MRI) in focal therapy for prostate cancer: recommendations from a consensus panel. *BJU Int.* 2014;113(2):218–27.

31. Gupta RT, Kauffman CR, Polascik TJ, *et al.* The state of prostate MRI in 2013. *Oncology* (Williston Park). 2013;27(4):262–70.

32. Haider MA, van der Kwast TH, Tanguay J, *et al.* Combined T2-weighted and diffusion-weighted MRI for localization of prostate cancer. *AJR Am J Roentgenol.* 2007;189(2):323–8.

33. Hara N, Okuizumi M, Koike H, *et al.* Dynamic contrast-enhanced magnetic resonance imaging (DCE-MRI) is a useful modality for the precise detection and staging of early prostate cancer. *Prostate.* 2005;62(2):140–7.

34. Barentsz JO, Richenberg J, Clements R, *et al.* ESUR prostate MR guidelines 2012. *Eur Radiol.* 2012;22(4):746–57.

35. Ghai S, Trachtenberg J. Prostate cancer: a consensus on trial design for focal therapy. *Nat Rev Urol.* 2014;11(4):190–2.

36. Pickett B, Kurhanewicz J, Coakley F, *et al.* Use of MRI and spectroscopy in evaluation of external beam radiotherapy for prostate cancer. *Int J Radiat Oncol Biol Phys.* 2004;60(4):1047–55.

37. Thompson JE, Moses D, Shnier R, *et al.* Multiparametric Magnetic Resonance Imaging Guided Diagnostic Biopsy Detects Significant Prostate Cancer and Could Reduce Unnecessary Biopsies and Over Detection: A Prospective Study. *J Urol.* 2014;192(1):67–74.

38. Mullins JK, Bonekamp D, Landis P, *et al.* Multiparametric magnetic resonance imaging findings in men with low-risk prostate cancer followed using active surveillance. *BJU Int.* 2013;111(7):1037–45.

39. Vargas HA, Akin O, Afaq A, *et al.* Magnetic resonance imaging for predicting prostate biopsy findings in patients considered for active surveillance of clinically low risk prostate cancer. *J Urol.* 2012;188(5):1732–8.

40. Margel D, Yap SA, Lawrentschuk N, *et al.* Impact of multiparametric endorectal coil prostate magnetic resonance imaging on disease reclassification among active surveillance candidates: a prospective cohort study. *J Urol.* 2012;187(4):1247–52.

41. Da Rosa MR, Milot L, Sugar L, *et al.* A prospective comparison of MRI-US fused targeted biopsy versus systematic ultrasound-guided biopsy for detecting clinically significant prostate cancer in patients on active surveillance. *J Magn Reson Imaging.* 2015;41(1):220–5.

42. Punwani S, Emberton M, Walkden M, *et al.* Prostatic cancer surveillance following whole-gland high-intensity focused ultrasound: comparison of MRI and prostate-specific antigen for detection of residual or recurrent disease. *Br J Radiol.* 2012;85(1014):720–8.

43. Arrayeh E, Westphalen AC, Kurhanewicz J, *et al.* Does local recurrence of prostate cancer after radiation therapy occur at the site of primary tumor? Results of a longitudinal MRI and MRSI study. *Int J Radiat Oncol Biol Phys.* 2012;82(5):e787–93.

44. Abouassaly R, Lane BR, Jones JS. Staging saturation biopsy in patients with prostate cancer on active surveillance protocol. *Urology.* 2008;71(4):573–7.

45. Crawford ED, Rove KO, Barqawi AB, *et al.* Clinical-pathologic correlation between transperineal mapping biopsies of the prostate and three-dimensional reconstruction of prostatectomy specimens. *Prostate.* 2013;73(7):778–87.

46. Chang JJ, Shinohara K, Bhargava V, *et al.* Prospective evaluation of lateral biopsies of the peripheral zone for prostate cancer detection. *J Urol.* 1998;160(6 Pt 1):2111–4.

47. Tsivian M, Hruza M, Mouraviev V, *et al.* Prostate biopsy in selecting candidates for hemiablative focal therapy. *J Endourol.* 2010;24(5):849–53.

48. Siddiqui MM, Rais-Bahrami S, Turkbey B, *et al.* Comparison of MR/ultrasound fusion-guided biopsy with ultrasound-guided biopsy for the diagnosis of prostate cancer. *JAMA.* 2015;313(4):390–7.

49. van den Bos W, Muller BG, Ahmed H, *et al.* Focal therapy in prostate cancer: international multidisciplinary consensus on trial design. *Eur Urol.* 2014;65(6):1078–83.

50. Ryan P, Finelli A, Lawrentschuk N, *et al.* Prostatic needle biopsies following primary high intensity focused ultrasound (HIFU) therapy for prostatic adenocarcinoma: histopathological features in tumour and non-tumour tissue. *J Clin Pathol.* 2012;65(8):729–34.

51. Bostwick DG, Egbert BM, Fajardo LF. Radiation injury of the normal and neoplastic prostate. *Am J Surg Pathol.* 1982;6(6):541–51.

52. Gaudin PB, Zelefsky MJ, Leibel SA, *et al.* Histopathologic effects of three-dimensional conformal external beam radiation therapy on benign and malignant prostate tissues. *Am J Surg Pathol.* 1999;23(9):1021–31.

53. Prestidge BR, Hoak DC, Grimm PD, *et al.* Posttreatment biopsy results following interstitial brachytherapy in early-stage prostate cancer. *Int J Radiat Oncol Biol Phys.* 1997;37(1):31–9.

54. Miller EB, Ladaga LE, el-Mahdi AM, *et al.* Reevaluation of prostate biopsy after definitive radiation therapy. *Urology.* 1993;41(4):311–6.

55. D'Alimonte L, Helou J, Sherman C, *et al.* The clinical significance of persistent cancer cells on prostate biopsy after high dose-rate brachytherapy boost for intermediate-risk prostate cancer. *Brachytherapy.* 2015;14(3):309-14.

56. Crook J, Malone S, Perry G, *et al.* Postradiotherapy prostate biopsies: What do they really mean? Results for 498 patients. *Int J Radiat Oncol Biol Phys.* 2000;48(2):355–67.

57. Kincaide LF, Sanghvi NT, Cummings O, *et al.* Noninvasive ultrasonic subtotal ablation of the prostate in dogs. *Am J Vet Res.* 1996;57(8):1225–7.

58. Van Leenders GJLH, Beerlage HP, Ruijter ET, *et al.* Histopathological changes associated with high intensity focused ultrasound (HIFU) treatment for localised adenocarcinoma of the prostate. *J Clin Pathol.* 2000;53(5):391–4.

59. Chalasani V, Martinez CH, Williams AK, *et al.* Histological changes in the human prostate after radiotherapy and salvage high intensity focused ultrasound. *Can Urol Assoc J.* 2010;4(4):E100–2.

60. Biermann K, Montironi R, Lopez-Beltran A, *et al.* Histopathological findings after treatment of prostate cancer using high-intensity focused ultrasound (HIFU). *Prostate.* 2010;70(11):1196–200.

61. Baust JG, Bischof JC, Jiang-Hughes S, *et al.* Re-purposing cryoablation: a combinatorial 'therapy' for the destruction of tissue. *Prostate Cancer Prostatic Dis.* 2015;18(2):87-95.

62. Baust JG, Gage AA, Bjerklund Johansen TE, *et al.* Mechanisms of cryoablation: clinical consequences on malignant tumors. *Cryobiology.* 2014;68(1):1–11.

63. Gooden C, Nieh PT, Osunkoya AO. Histologic findings on prostate needle core biopsies following cryotherapy as monotherapy for prostatic adenocarcinoma. *Hum Pathol.* 2013;44(5):867–72.

64. El-Shafei A, Abd El Latif A, Hatem A, *et al.* 1816 RECURRENCE DESCRIPTIVE PATTERN ON POST CRYOABLATION PROSTATE BIOPSY. *J Urol.* 187(4):e733-e734.

65. Lindner U, Lawrentschuk N, Weersink RA, *et al.* Focal laser ablation for prostate cancer followed by radical prostatectomy: validation of focal therapy and imaging accuracy. *Eur Urol.* 2010;57(6):1111–4.

66. Oto A, Sethi I, Karczmar G, *et al.* MR imaging-guided focal laser ablation for prostate cancer: phase I trial. *Radiology.* 2013;267(3):932–40.

67. Lee T, Mendhiratta N, Sperling D, *et al.* Focal laser ablation for localized prostate cancer: principles, clinical trials, and our initial experience. *Rev Urol.* 2014;16(2):55–66.

68. Srigley JR, Delahunt B, Evans AJ. Therapy-associated effects in the prostate gland. *Histopathology.* 2012;60(1):153–65.

69. Evans AJ, Ryan P, Van derKwast T. Treatment effects in the prostate including those associated with traditional and emerging therapies. *Adv Anat Pathol.* 2011;18(4):281–93.

70. Eymerit-Morin C, Zidane M, Lebdai S, *et al.* Histopathology of prostate tissue after vascular-targeted photodynamic therapy for localized prostate cancer. *Virchows Arch.* 2013;463(4):547–52.

71. van den Bos W, de Bruin DM, Muller BG, *et al.* The safety and efficacy of irreversible electroporation for the ablation of prostate cancer: a multicentre prospective human in vivo pilot study protocol. *BMJ Open.* 2014;4(10):e006382.

72. Neal RE, 2nd, Millar JL, Kavnoudias H, *et al.* In vivo characterization and numerical simulation of prostate properties for non-thermal irreversible electroporation ablation. *Prostate.* 2014;74(5):458–68.

73. Yang XJ, Laven B, Tretiakova M, *et al.* Detection of alpha-methylacyl-coenzyme A racemase in postradiation prostatic adenocarcinoma. *Urology.* 2003;62(2):282–6.

74. Martens MB, Keller JH. Routine immunohistochemical staining for high-molecular weight cytokeratin 34-[beta] and [alpha]-methylacyl CoA racemase (P504S) in postirradiation prostate biopsies. *Mod Pathol.* 2005;19(2):287–90.

75. Cheng L, Sebo TJ, Slezak J, *et al.* Predictors of survival for prostate carcinoma patients treated with salvage radical prostatectomy after radiation therapy. *Cancer.* 1998;83(10):2164–71.

76. Scalzo DA, Kallakury BV, Gaddipati RV, *et al.* Cell proliferation rate by MIB-1 immunohistochemistry predicts postradiation recurrence in prostatic adenocarcinomas. *Am J Clin Pathol.* 1998;109(2):163–8.

77. Crook J, Robertson S, Esche B. Proliferative cell nuclear antigen in postradiotherapy prostate biopsies. *Int J Radiat Oncol Biol Phys.* 1994;30(2):303–8.

78. Barret E, Harvey-Bryan KA, Sanchez-Salas R, *et al.* How to diagnose and treat focal therapy failure and recurrence? *Curr Opin Urol.* 2014;24(3):241–6.

79. Crehange G, Roach M, 3rd, Martin E, *et al.* Salvage reirradiation for locoregional failure after radiation therapy for prostate cancer: who, when, where and how? *Cancer Radiother.* 2014;18(5-6):524–34.

80. Stephenson AJ, Eastham JA. Role of salvage radical prostatectomy for recurrent prostate cancer after radiation therapy. *J Clin Oncol.* 2005;23(32):8198–203.

81. Le JD, Tan N, Shkolyar E, *et al.* Multifocality and Prostate Cancer Detection by Multiparametric Magnetic Resonance Imaging: Correlation with Whole-mount Histopathology. *Eur Urol.* 2015;67(3):569–76.

82. Hollmann BG, van Triest B, Ghobadi G, *et al.* Gross tumor volume and clinical target volume in prostate cancer: How do satellites relate to the index lesion. *Radiother Oncol.* 2015;115(1):96-100.

83. Cooper CS, Eeles R, Wedge DC, *et al.* Analysis of the genetic phylogeny of multifocal prostate cancer identifies multiple independent clonal expansions in neoplastic and morphologically normal prostate tissue. *Nat Genet.* 2015;47(4):367–72.

84. Ahmed HU, Dickinson L, Charman S, *et al.* Focal Ablation Targeted to the Index Lesion in Multifocal Localised Prostate Cancer: a Prospective Development Study. *Eur Urol.* 2015;68(6):927-36.

C6

Goals for Evaluation and Diagnosis of the Small Renal Mass

CHAIR

Fernando P. Secin, Argentina

CO-CHAIR

Robert Uzzo, United States

MEMBERS

Paul Cairns, United States
Paul Crispen, United States
Ithaar Derweesh, United States
Chaitanya Divgi, United States
Darrel Drachenberg, Canada
Vinay Duddalwar, United States
John Eisenbrey, United States
Ethan Halpern, United States
William Huang, United States
Stella Kang, United States
Brian Lane, United States
Marc Smaldone, United States
Edouard Trabulsi, United States

CONTENTS

Goals for Evaluation and Diagnosis of the Small Renal Mass

Committee 6

6.1 Introduction

The incidental renal mass is a relatively common finding in an era of increased imaging for unrelated symptomatology. Today, a primary indication for abdominal imaging is to exclude diagnoses that, if missed, could compromise care and convalescence. In so doing, an era of *incidental radiology* has taken shape and, with it, anecdotes and analyses of the benefits and detriments of incidental diagnoses.

The benefits of early detection of many types of malignancies are widely cited. The proof exists in our current ability to frequently eradicate localized disease (*cure*) coupled with our inability to adequately control more advanced disease. Initial management of incidental renal masses was often *radical*, meaning full excision (usually by nephrectomy), with acceptance of the associated perioperative, functional, and quality of life risks. As surgical technologies have developed and minimally invasive surgery (MIS) has become more common, treatment of the incidental renal mass has become widely accepted, while recovery and perhaps risks have lessened. Concurrently, data have emerged demonstrating that many incidental renal tumours are more indolent than previously believed, and a body of literature evaluating judicious active surveillance (AS) with calculated intervention has taken shape. Indeed, even the lexicon of the incidental renal mass now reflects the growing recognition that small renal masses (SRMs) may not pose an imminent threat, and prior assumptions should be cautiously challenged.

Here, we evaluate and summarize the current data on the biological, radiographic, anatomical, and functional risks of the SRM in the context of patient risk and operative indications for intervention. The decision to intervene with a diagnosis of SRM should move beyond a "find it–fix it" mentality and be nuanced, keeping in mind that the goal of treatment (cure with minimal morbidity) must be traded off against our ability to quantify the biological risk of the tumour and the implications to the patient sitting in front of us.

6.2 Evaluating the Biological Risk of the SRM

6.2.1 Introduction

The incidence of renal cell carcinoma (RCC) is rising largely from incidental detection of SRMs.[1,2,3] Small renal masses can be solid or complex cystic lesions that are <4 cm with demonstrable contrast enhancement on radiologic imaging.[4] The inherent malignant potential of an SRM increases as the size increases.[5,6]

Studies have demonstrated that for solid-enhancing T1 (<7 cm) renal masses, 20% are benign, 60% are indolent RCCs, and 20% have the potential to be aggressive (i.e. high nuclear grade).[7–10]

Thus, resection of all SRMs is an overtreatment for the many patients who are expected to have a benign histopathology. The largest increase in incidentally detected SRMs occurred in patients aged 70 to 89 years, in whom comorbidities are more frequent and represent competing risks for mortality.[7,9]

While surgical resection remains the only known cure for RCC, such treatment predisposes patients to significant perioperative morbidities and the potential for chronic renal insufficiency and its sequelae. Decisions on the optimal management strategy, such as AS, ablative therapy, nephron-sparing surgery (NSS), and radical nephrectomy (RN), could be guided by a clearer understanding of the patient's specific biological risk, particularly as we approach an era of personalized medicine. This section will focus on assessment of the biological risk of SRMs, using renal mass biopsies (RMBs), clinical risk factors, hereditary syndromes, and unusual histopathology.

6.2.2 Renal mass biopsy

Renal mass biopsy (RMB) has emerged as a useful tool to aid in clinical decision-making. The goals of RMBs in SRMs are several-fold:[11]

1. Rule out metastatic renal disease (8%–13% of all SRMs).
2. Rule out pyogenic abscesses.
3. Rule out renal lymphomas.
4. Avoid unnecessary invasive procedures in the elderly and frail.
5. Avoid treatment of patients with benign SRMs.
6. Avoid unnecessary operations in those with compromised renal function and/or a solitary kidney.
7. Distinguish lipid-poor angiomyolipoma from RCC.
8. Obtain tissue samples for pathological analysis prior to ablative therapy.
9. Obtain tissue samples for genetic and other molecular analyses, such as next-generation sequencing, that could be used for future prognostic and therapeutic benefit in the era of personalized targeted molecular therapy (TMT).

Renal mass biopsy is considered a relatively safe procedure with an overall complication rate of 1.4% to 4.7%; major complications occur in just 0.46% of the cases.[1,7,12–26]

Complications include bleeding, infection, pneumothorax, tumour seeding, arteriovenous fistula, renal parenchymal injury, and damage to the collecting system.[1,7,23,27]

Bleeding, the most common complication, and pneumothorax, usually from posterior upper pole biopsies, are generally self-limiting and managed conservatively.[1,16] Gelfoam or a procoagulant pledget along the needle tract promotes hemostasis and helps reduce the risk of bleeding.[7] However, continued bleeding should prompt suspicion for arteriovenous fistulas.[23]

Tumour seeding has been reported in a handful of cases, and the evidence is anecdotal. Risk of tumour seeding decreases with the use of coaxial techniques, and the overall risks are considered very low.[1,28,29]

Urothelial carcinomas are associated with a higher risk of seeding than RCC, and thus, if suspected, caution should be taken when performing biopsy, particularly for centrally located infiltrative masses.[30] Renal mass biopsy sampling is performed through either fine-needle aspiration (FNA) or core biopsy, and often, both are used simultaneously. Fine-needle aspiration has a reported accuracy of up to 100% and 92% for malignancy and histopathological subtypes, respectively.[31,32]

When compared with core biopsy, however, FNA is associated with a higher rate of non-informative samples, as well as lower diagnostic yields for histological subtypes and grading.[7,15,33]

Combining both FNA and core biopsy results in a reported 93% sensitivity and 95% accuracy for malignancy, as well as improvement in assessment of tumour subtype and grade.[15,34] Diagnostic yields from subsequent biopsies are independent from previous biopsies. The diagnostic yield for re-biopsy of initial non-diagnostic biopsies was 75% to 100%, similar to the 78% to 100% diagnostic yield of first biopsies.[1,15–19,24,25,29,34–40]

Inaccuracy of RMB is thought to be due to sampling error, tumour necrosis, and tumour heterogeneity. Specifically, tumour size plays an important role because small masses may be difficult to target, whereas larger masses could potentially harbor more necrosis.[1]

In addition, there are concerns that RMB may detect only the benign portion of hybrid histology, leaving the malignant portion undetected. The largest study to date (n=1,829) found that only 2.7% (n=4) of patients had hybrid malignant pathology, all of which were chromophobe RCC in the setting of oncocytomas, and importantly, no benign tumour coexisted with high-grade malignancy.[1,40]

For additional information, see **Chapter 7: Renal Tumour Biopsy: Indications, Technique, Safety, Accuracy/Results, Pathologic Reporting, and Impact on Treatment Decision-Making**.

6.2.3 Clinical risk factors

Recently, a multi-institutional study (n=1,009) reported male sex, tumour diameter ≥3 cm, and a R.E.N.A.L. nephrometry score (NS) ≥8 points were independently predictive of both malignancy and unfavorable pathology (defined as RCC with Fuhrman grade III-IV and/or lesions postoperatively upstaged to pT3a).[41] Neither age nor institution was predictive. Those with all three variables had nearly a 90% chance of malignancy and would likely not benefit from RMB, whereas those with the lowest risk strata had only a 64% risk of malignancy and would likely benefit from RMB.[41]

The contribution of gender to malignancy risk of SRMs has been examined extensively. In one study with SRM patients aged 18 to 45 years, benign pathology was discovered in 36% and 9.5% of women and men, respectively.[6,10]

Moreover, the relative risk of benign pathology in women was 1.8 when compared with men.[6,42] Similarly, another study found that male gender was a strong predictor of malignancy, but was a weak predictor of indolent versus aggressive cancer.[6]

Others have found gender is the only clinical variable associated with benign pathology.[29,41,43,44]

Tumour size and anatomical complexity may also contribute to intrinsic biological risk of malignancy and/or aggressiveness. An increasing NS was identified as a predictor of malignancy, but not high-grade disease, among patients with SRMs.[29,41]

Others have demonstrated that tumour location correlates with biological potentiation, with exophytic tumours exhibiting less malignant lesions and less clear cell histopathology.[7,43,44]

Moreover, another study identified tumour volume, degree of endophytic component, and symptoms at diagnosis as significant predictors of benign disease. The likelihood of benign disease was 52.6% if the renal mass was <45% endophytic and had a volume <5.67 cm^3. Conversely, patients had only a 5.3% possibility of benign disease if the renal mass had a volume ≥5.67 cm^3 and was ≥35% endophytic; interestingly, the chance falls to 0% if the patients presented with symptoms (flank pain, hematuria, and/or palpable mass).[45] **(See Chapter 7: Renal Tumour Biopsy: Indications, Technique, Safety, Accuracy/Results, Pathologic Reporting, and Impact on Treatment Decision-Making)**

6.2.4 SRM in hereditary renal cell carcinoma syndromes

Less than 5% of RCCs occur in hereditary syndromes. Among the many renal cell carcinoma hereditary syndromes (HRCCSs), von Hippel-Lindau disease (VHLD), hereditary papillary renal cell carcinoma (HPRCC), hereditary leiomyomatosis and renal cell carcinoma (HLRCC), and Birt-Hogg-Dubé (BHD) are the most studied. These HRCCSs share many common features:

1. Are autosomal dominant
2. Involve tumour suppressor genes (TSGs)
3. Have earlier age of onset compared to sporadic RCC
4. Are bilateral
5. Are multifocal
6. Are less aggressive than sporadic

Exceptions apply to HLRCC and HPRCC, where the former presents as unilateral, solitary, and very aggressive, while the latter involves a proto-oncogene rather than a TSG. Tumour gene products are pVHL, cMET, fumarate hydratase, and folliculin, respectively. The penetrance of RCC in these syndromes ranges from 20% to 70%, with VHL carrying the highest percentage. Because of its aggressive nature, HLRCC-suspected patients must be treated immediately and aggressively, regardless of size of lesions present. Meanwhile, more conservative means could be appropriate with other syndromes. With the exception of HLRCC, other HRCCSs present as multifocal and bilateral. Such patients that have a family pedigree of syndromic pathology and syndromic manifestations and/or positive germline genetic testing may not require an RMB, as biological behavior can be anticipated by the expected histopathology of the individual syndromes, and should be managed by delaying surgical treatment as late as possible because of the increased chance of recurrence. A 3-cm intervention rule has been established, especially for VHLD patients.[46]

Although not hereditary, medullary renal cell carcinoma (medRCC) should be suspected in younger black patients with sickle cell trait (SCT) and a renal mass. Since medRCC is a poorly differentiated anaplastic tumour with an extremely aggressive course, these patients may benefit from biopsy to rule out medRCC. Immediate surgical intervention is perhaps beneficial, though most patients have metastasis upon presentation, and many die within months of diagnosis.[47]

6.2.5 Unusual pathological risks of SRMs

Tubulocystic carcinoma

This newly described subtype of RCC—tubulocystic carcinoma (TC)—typically has a favorable prognosis. Mean reported age is 58 years, with male (7:1) predominance. Grossly, it is a well-circumscribed tumour, typically a solitary mass involving mainly the renal cortex, and ranges in size from 0.5 cm to 17 cm, with a left to right (65% vs. 35%) and a subcapsular to corticomedullary (61.5% vs. 38.5%) predilection.[48–51] Most cases are pT1, with nearly 40% <2 cm.[51–56]

The cut surface reveals multilocular small cystic spaces with a spongy "Swiss cheese" or "bubble wrap" appearance.[48] Histologically, it has well-differentiated tubules and cysts separated by thin fibrous septae, with nuclei equivalent to Fuhrman grade III. The Fuhrman grade does not seem to have any prognostic value in TC, as all tumour sizes have similar nuclear grades.[48] Tubulocystic carcinoma is closely related to papillary renal cell carcinoma (pRCC), and both have been shown to coexist and share numerous cytogenic and chromosomal abnormalities. Both are characterized by the overexpression of alpha-methylacyl coenzyme A racemase (AMACR). Pathologically, TC could mimic pRCC, cystic nephroma, and multilocular cystic RCC. Most TCs are low grade (pT1) and are cured following surgery, with a reported 9% chance of distant metastasis.[48–51,53]

In one study, metastases were attributed to an associated high-grade pRCC component.[51]

Xp11.2 Translocation renal cell carcinomas with TFE3 gene fusion

Several translocations involve the transcription factor 3 (TFE3) gene that is located on chromosome Xp11.2 (i.e. Xp11.2 translocation RCC [Xp11.2 TRCC]).[54–65]

Many genetic fusions have been identified, such as ASPL-TFE3 (Xp11.2, 17q25), known as alveolar soft part sarcoma (ASPS); PRCC-TFE3; CLTC-TFE3; NONO-TFE3; and PSF (SFPQ)-TFE3.[53,54]

Numerous chromosomal translocation foci have been observed, including t(X;17)(p11.2;q25), t(X;1)(p11.2;p34), and t(X;1)(p11.2;q21), which lead to gene fusions of TFE3 with ASPL, PSF, and PRCC, respectively.[55,57,62,66] Xp11.2 Translocation renal cell carcinoma primarily affects children and young adults, with a strong female predominance.[55,57,58,59]

Transcription factor 3–related translocations are found in 35% and 1.6% to 5% of patients with pediatric and adult RCC, respectively. Although TRCC usually presents as an asymptomatic, painless mass, there have been associations with prior childhood exposure (10%–15%) to cytotoxic chemotherapy, with an estimated post-chemotherapy interval ranging from 4 to 13 years. Other studies (n=6) did not have a history of prior chemotherapy in their patients.[55–61]

Grossly, this tumour mimics clear cell renal cell carcinoma (ccRCC). Because microscopically Xp11.2 TRCC mimics ccRCC, pRCC type 2, and clear cell papillary renal cell carcinoma (ccpRCC), immunohistochemical and cytogenic molecular features play an integral part in the diagnosis. Expression of TFE3 fusion proteins is aberrantly high, perhaps because the fusion partners of TFE3 are ubiquitously expressed, and their promoters regulate the fusion protein. The TFE3 immunohistochemistry for neoplasms bearing the TFE3 gene has a sensitivity of 97.5% and a specificity of 99.6%.[60,67,68]

One retrospective study found that all tumours were cortically located and demonstrated intratumour hemorrhage, infiltrative growth, and invasion of the perirenal fat/renal sinus, but without any form of vascular invasion. Tumours always had calcifications on computed tomography (CT) and were mildly hyperintense on T1-weighted magnetic resonance imaging (MRI). In adults, they were much more aggressive and carried the potential for distant metastasis.[54,67,69,70]

In children and young adults, Xp11.2 TRCCs seem rather indolent, even when diagnosed at advanced stages. Poor prognostic indicators for this population subset include the ASPL-TFE3 gene fusion RCCs, which are more likely to present at advanced stages than any other TRCC.[55,65] Xp11.2 Translocation renal cell carcinomas have been shown to have a similar response rate and progression-free survival to ccRCC when treated with TMTs. Vascular endothelial growth factor receptor (VEGFR)-targeted therapies and mechanistic target of rapamycin (mTOR) inhibitors have been shown to be active against Xp11.2, with sunitinib being more effective than cytokines.[55,65]

Thyroid-like follicular carcinoma of the kidney

This unusual renal tumour characteristically shows similar histology to thyroid follicular carcinoma, with frequency seen in women that do not have any thyroid lesions. Numerous chromosomal losses and gains have been detected. A recent report on six cases failed to demonstrate chromosomal alterations on comparative genomic hybridization (CGH) analyses, and thus, suggested thyroid-like follicular RCC should be considered as a unique histological subtype.[10]

Sarcomatoid differentiation

Although about 5% of RCCs have sarcomatoid differentiation, it is only found in 15% of stage IV tumours (at presentation or post progression).[71,72]

The volume of sarcomatoid features within a tumour is highly variable (1%–100%), so an RMB may easily miss it. Therefore, dependence on preoperative identification via RMB is unreliable, with a sensitivity of only 10%.[73,74]

One study identified male sex (74%), symptomatic presentation (90%), M1 (69.2%), and median presenting size of 10 cm as predictors of sarcomatoid differentiation.[71]

Sarcomatoid histology responds poorly to immunotherapy, even though data suggest that its coexistence with ccRCC shows it to retain mutations in the hypoxia-inducible factor (HIF) pathways.[73,75,76]

Presently, the degree of sarcomatoid differentiation plays a critical role in defining the treatment options because those with large volume sarcomatoid pathology may benefit the most from cytotoxic chemotherapy (doxorubicin and gemcitabine). Patients with ccRCC and minimal sarcomatoid features were found to have a 20% response rate to TMTs (sunitinib, sorafenib, and bevacizumab).[71]

Currently, combination treatments of TMTs concurrently with cytotoxic agents are being investigated for the treatment of masses with sarcomatoid pathologies.

6.2.6 The course of the SRM

Retrospective and meta-analyses have demonstrated that the risk of metastatic progression while on AS is <2%, with one study (n=82) reporting only one patient developing metastasis after a 3-year follow-up.[77–80]

In a non-inferiority trial, the overall survival for primary intervention (PI) and AS was 98% and 96% at 2 years, and 92% and 75% at 5 years, respectively (p=0.06). Additionally, cancer-specific survival was 99% and 100% at 5 years, respectively (p=0.03). Neither tumour size, Eastern Cooperative Oncology Group (ECOG) score, nor R.E.N.A.L. NS were predictive of overall survival. However, age and an ECOG score <2 were predictive of progression, with a median growth rate of 0.11 cm/year. The study supported earlier findings from the Renal Cell Consortium of Canada, which found a growth rate of 0.13 cm/year, progression of 14% (n=25), and development of metastasis in 1% (n=2) while on AS.[81]

They concluded that AS with delayed intervention appears to be non-inferior in regard to oncologic outcomes for well-selected patients with SRMs (older, smaller average tumour size, and multiple comorbidities).[77] Currently, the "3-cm rule," which was extrapolated from clinical data on VHLD patients, is thought to be the threshold for initiating intervention. Masses <3 cm have a risk of synchronous metastases (<5%).[80]

It remains questionable whether such data may be appropriately applied to SRMs (<4 cm), especially knowing that the risk of metastasis increases with increasing growth rate on sequential imaging.

6.2.7 Recommendations of renal mass biopsy for those with SRMs

Currently, the American Urological Association (AUA) identifies renal mass biopsy (RMB) as an option for the management of SRM. The European Association of Urology (EAU) recommends evidence [**GOR C**] for RMB in those with SRM and on AS. However, given that the non-diagnostic yield is 20%, and its ability to distinguish high- from low-grade tumours is poor (50%), it is perhaps more beneficial to incorporate RMB only if pathological diagnosis is expected to either benefit patients (who are on AS for SRM) or change the management. Healthy, younger patients who could easily tolerate NSS should not undergo RMB because of the additive complications as well as the risk of misclassifying an RCC as an eosinophilic neoplasm. Elderly and comorbid patients with SRMs may benefit from RMB.[77]

Ultimately, the decision relies on balancing tumour progression/metastasis with the risks of intervention, including risk of progressive renal insufficiency. Currently, renal biopsy has limited capability for detection of high-risk features. Therefore, the urologist will have to rely on the entire clinical picture, combining the mass characteristics (size, location, complexity, growth rate) with the patient's age, comorbidities, and desires.

6.2.8 Future directions

Much progress has occurred over the past 2 decades in understanding the biology of kidney cancer. It is now well recognized that substantial genetic and histological heterogeneity in RCC exists, and this has been documented in many studies.[82]

Often, epigenetic modifications accompany the genetic changes that occur with RCC. Kidney cancer is primarily thought to be a metabolic disease, and targeting metabolic abnormalities, such as autophagy, glucose transport, and energy sensing, is an area of promising research.[47]

Advances in the understanding of inactivation of histone-modifying genes, DNA methylation, copy number alterations, and gene mutation and/or expression patterns will aid in further therapeutic interventions.[83]

While there is much research on drug therapy for locally advanced disease,[84] the role of genomics in the SRM realm remains an area of investigation and development.

Biomarkers offer several potential advantages, including providing additional information in predicting therapeutic response and in prognostication. Some tissue biomarkers under investigation include VHL alterations, hypoxia-inducible factor 1-alpha (HIF-1α), vascular endothelial growth factor A (VEGF-A), and carbonic anhydrase IX (CAIX), among others.[85,86]

Many markers have been used in prognostic models with some success; however, most biomarkers still require prospective validation. Tissue array microanalysis has also been used with success to differentiate the expression of Akt signaling parameters in oncocytoma and ccRCC.[87]

A major limitation of most biomarkers, with respect to SRM surveillance, is that they require tumour tissue. As aforementioned, the diagnostic yield can be relatively high (20%), with poor differentiation between high- and low-grade disease (50%). Nonetheless, core needle biopsy has been used, both for genomic and proteomic analyses, and has been utilized as a comparator for newer technologies such as laser capture microdissection.[87]

Blood-based biomarkers have been investigated as well, such as neutrophil gelatinase-associated lipocalin (NGAL) and human serum amyloid A. Similarly, others have investigated immunologic markers and urine markers such as B7-H1 and NMP-22, respectively. Currently, however, there are no circulating biomarkers to guide ccRCC management.[88]

In summary, evaluation of the biological risk of an SRM is still in its nascency. Around 80% of SRMs are benign or low risk. Individual risk is multifactorial, and should include clinical factors (sex, comorbidities, age) in addition to mass-related factors (size, growth rate, appearance, location). Most biological information of the mass can be determined by RMB, which has shown increasing popularity over the years. The emergence of genomics, biomarker development, and prognostic models will aid in the future risk stratification of SRMs, but still require validation. (**Level of Evidence [LOE] 2, Grade of Recommendation [GOR] B**)

6.3 Evaluating Tumour Size and Growth Kinetics as a Surrogate for Biological Risk of an SRM

Cross-sectional imaging provides valuable information, helping to guide treatment selection in patients presenting with solid renal tumours. Of the radiographic features available at the time of initial diagnosis, tumour size provides insight into the malignant potential of the mass.[6,89,90] Additional information on tumour histology and future clinical progression of a renal mass may be provided by the observed growth rate of the mass in patients selected to undergo AS.

6.3.1 Determination of renal tumour size and growth rate

When considering renal tumour size and growth rate as potential surrogates with biological potential, the majority of studies have evaluated maximal tumour diameter, determined by CT and MRI. However, a potential limitation of utilizing maximal tumour diameter is that it assumes the tumour is spherical, and may not provide an accurate reflection of tumour cell number. Tumour volume may be determined with three-dimensional (3D) reconstructions and provide a more accurate measure of tumour cell number; however, this is not routinely reported at most centres. In series reporting tumour volumetric growth, volume is often calculated based on the maximum diameter, width, and/or height of the tumour.

Tumour growth can be evaluated in several different ways. Linear tumour growth is the most common reported measure and is based upon changes in maximal tumour diameter. A potential drawback of reporting linear tumour growth is that it is not reflective of overall change in tumour volume. For example, a change in maximal diameter for a renal tumour from 1 cm (0.52 cm^3) to 2 cm (4.19 cm^3) does not represent a doubling of the volume, but rather a 700% increase in tumour volume. However, a 1-cm change in diameter from 4 cm (33 cm^3) to 5 cm (65 cm^3) only represents a 97% change in tumour volume.[91] Despite the potential limitations of evaluating linear tumour growth, it is simple to perform and provides a relatively reproducible means of assessing growth.

6.3.2 Impact of tumour size and complexity on observed growth rate

The association between renal tumour size at time of diagnosis and observed growth has been evaluated in multiple series. **Table 6-1** presents selected AS series evaluating the impact of tumour size and observed growth. Despite most series having a similar average tumour size at the time of presentation, the impact of tumour size on the observed growth rates is inconsistent. Two series have noted a direct relationship between tumour size and future growth. In the series by Mason *et al.*, tumours <2.45 cm at presentation grew at an average of 0.13 cm/year, compared to 0.40 cm/year in tumours that were >2.45 cm at presentation.[92] The second series by Beisland *et al.* noted increased growth rates in patients with tumours >4 cm, a size threshold where most patients would not be advised to undergo AS.[93] In contrast to these findings, two series noted an indirect relationship between tumour

size at presentation and observed growth. In the series by Crispen *et al.*, linear growth was not associated with tumour size at presentation; an indirect relationship was only noted when evaluating volumetric and proportional changes in tumour growth.[91] This indirect relationship is supported by the findings of increased presumed tumour growth compared to observed tumour growth in patients with prior normal imaging.[94]

TABLE 6-1 Active Surveillance Series Evaluating the Impact of Tumour Size on Observed Growth

Reference	Number of tumours	Average tumour size at presentation (cm)	Association between tumour size at presentation and observed growth rate
Crispen *et al.*[91]	172	2.0	Smaller tumours grew faster than larger tumours, based on volumetric and proportional growth
Rosales *et al.*[100]	223	2.8	No association
Schiavina *et al.*[101]	72	2.1	No association
Mason *et al.*[92]	84	2.3	Tumours >2.45 cm grew faster than tumours <2.45 cm
Matsumoto *et al.*[96]	47	1.7	No association
Dorin *et al.*[102]	131	2.1	Smaller tumours grew faster than larger tumours
Beisland *et al.*[93]	63	4.3	Tumours >4.0 cm grew faster than tumours <4.0 cm

While tumour size at presentation alone does not consistently foretell future tumour growth, assessment of tumour complexity may provide improved prediction. Several methods of assessing tumour complexity have been proposed, based upon a tumour's anatomical relationship with normal components of the kidney.[95] To date, the only complexity scoring system to be associated with tumour growth has been the R.E.N.A.L. nephrometry scoring system. In this system, a significant association was noted between increased tumour complexity and observed growth in both available series.[96,97] Additional investigation of this relationship in other AS series and evaluation of other tumour complexity scoring systems appear warranted. (**See Chapter 7: Renal Tumour Biopsy: Indications, Technique, Safety, Accuracy/Results, Pathologic Reporting, and Impact on Treatment Decision-Making**)

6.3.3 Growth rate of benign and malignant tumours

Renal oncocytomas represent the majority of benign solid renal tumours and are difficult to distinguish from malignant tumours based on cross-sectional imaging and percutaneous needle biopsy. Several series have reported observed growth rates of oncocytomas on needle biopsy and following surgical excision (**Table 6-2**). To date, no series have noted a significant difference between benign and malignant tumours. Furthermore, the percentage of tumours not exhibiting growth during observation appears to be similar between benign and malignant tumours. In a pooled analysis of several AS series, the percentage of benign tumours was noted to be similar between groups of tumours that did and did not demonstrate growth during observation.[98] Based on the available data, observed growth rate cannot be used to distinguish benign from malignant renal tumours.

TABLE 6-2 Growth Rates of Benign Versus Malignant Renal Lesions Under Active Surveillance

Reference	Number of tumours	Growth rate of benign tumours	Growth rate of malignant tumours
Kurup *et al.*[103]	33	0.29 cm/yr	NA
Neuzillet *et al.*[21]	15	Continued surveillance: 0.07 cm/yr; surgical treatment: 0.24 cm/yr	NA
Kawaguchi *et al.*[104]	69	0.20 cm/yr	NA
Crispen *et al.*[91]	61	0.34 cm/yr	Low grade: 0.34 cm/yr; high grade: 0.53 cm/yr
Jewett *et al.*[98]	46	0.17 cm/yr	0.14 cm/yr

6.3.4 Influence of tumour histology of malignant tumours on observed growth

There are limited data on the association between observed tumour growth, nuclear grade, and histological subtype of RCCs. Observed tumour growth was not associated with nuclear grade in 48 malignant tumours from the Jewett *et al.* series.[98] However, the majority of tumours within this series were low grade, 41 of 46. Similar findings were noted by Crispen *et al.*, with an observed growth rate of 0.34 cm/year in 40 low-grade tumours, compared to 0.53 cm/year in 12 high-grade tumours.[91] The lack of statistical significance in both series may be influenced by the small sample size. With the limited number of patients undergoing nephrectomy combined with the majority of tumours noted to be ccRCC in AS series, comparing the growth rates of different histological subtypes has not been possible.[91,98,99] Additional data are required before conclusions can be made regarding the association between observed tumour growth, nuclear grade, and histological subtype.

6.3.5 Association between observed tumour growth and metastatic progression

Metastatic progression is the greatest risk when observing renal tumours in patients who are candidates for definitive therapy. Thankfully, the number of patients progressing to metastatic disease has remained consistently low in AS series (<2%).[77] This may be attributed to several factors, including biased patient selection, indolent nature of most small renal tumours, short duration of follow-up in available series, or increased rate of definitive intervention for tumours demonstrating accelerated growth during observation. Given the reported low rate of metastatic progression in AS series, a pooled analysis was performed to identify potential predictors of disease progression.[80] Of the clinical features evaluated, patient age, tumour size at presentation (diameter and volume), and observed tumour growth (linear and volumetric) were significantly associated with metastatic progression. Average tumour growth was 0.8 cm/year in tumours progressing to metastatic disease, compared to 0.3 cm/year in tumours that did not progress to metastatic disease. Although these findings are based on a small number of patients, definitive therapy should be considered for tumours demonstrating increased growth during AS.

6.3.6 Conclusion

The use of AS for small renal tumours is gaining acceptance as an alternative to definitive therapy in select patients. To date, observed tumour growth has not proven to be a useful surrogate for differentiating benign from malignant disease. However, accelerated growth has been associated with the low number of patients who have demonstrated metastatic progression during observation. Prospective trials are needed to establish clinical thresholds to commence definitive therapy in patients initially treated with AS and to further evaluate the association between observed growth rate and tumour histology. [**LOE 3, GOR C**]

6.4 Blood, Urinary, and Needle Biopsy Biomarkers of the SRM

The potential role of biomarkers in SRMs lies in detection, differential diagnosis of RCC versus benign tumours, differential diagnosis of the histological cell type of RCC, and prognosis for stratification of potential aggressiveness. Currently, there is no proven biomarker for SRMs. The molecular alterations that underlie the initiation and development of SRMs are all candidate biomarkers. These include DNA sequence mutation, chromosome copy number, DNA methylation, histone modifications, messenger ribonucleic acid (mRNA) and microribonucleic acid (miRNA) expression, protein expression, and protein modifications. The increasing availability, ease of use, and lower cost of genome-wide or proteome-wide technologies are leading to the identification of candidate biomarkers for SRMs. The Cancer Genome Atlas has completed separate studies of ccRCC,[105] pRCC, and chromophobe RCC,[106] which represent a source of state-of-the-art, genome-wide DNA and RNA data.

While, to date, biomarker discovery studies typically have used resected RCC and benign renal tumour tissue specimens, the use of surveillance of SRMs dictates that needle biopsy or bodily fluid (blood or urine) will be the specimen available for the proposed biomarker assay. Blood is known to contain circulating tumour cells, circulating cell-free tumour DNA, and tumour DNA in exosomes. Urine also contains tumour DNA, but the source is less clear. The quantity or quality of specimen must provide a sufficient amount and quality of DNA, RNA, or protein for biomarker analysis. The different progenitor cells and molecular biology of each type of RCC and benign renal tumour mean that it is likely that panels of markers or signatures will be used, possibly a hybrid of biomarker types.[107,108]

Table 6-3 summarizes the main biomarker studies. The vast majority of studies have examined all pathological stages of RCC (and oncocytoma, angiomyolipoma, renal cysts), rather than exclusively SRMs, and compared them to normal renal tissue. In **Table 6-3**, biomarker studies where pT1a RCC was included are noted together with the occasional study of interest that included pT1 or stage I. Studies of resected RCC only and studies that looked at fluids or biopsies are indicated. Of note, Morrissey *et al.*[109] appear to be the only group to have examined a biomarker in the population to be

screened—a large series of patients undergoing routine abdominal CT. Ibragimova *et al.*[123] studied the promoter methylation profile in a specimen set of resected SRMs exclusively. The intended use of the biomarker (i.e. early detection, differential diagnosis, or prognosis) was given.

TABLE 6-3 Biomarkers in Renal Cell Carcinoma

Biomarker	Specimen source, type	Intended use	LOE	GOR	Reference
Circulating tumour cells	RCC T1a, onco, blood	Diagnosis	3	C	El-Heliebi *et al.*[107]
Circulating tumour cells	RCC pT1, blood	Diagnosis, prognosis	3	C	Bluemke *et al.*[108]
Protein expression AQP and PLIN2	CT scan, RCC, urine	Diagnosis	3	C	Morrissey *et al.*[109]
AQP and PLIN2	RCC, onco, PCa UC, urine	Differential diagnosis	3	C	Morrissey *et al.*[109]
CAIX	RCC, onco, stage T1, blood	Prognosis	3	C	Gilbert *et al.*[110]
Protein expression CAIX	RCC stage I-II	Prognosis	3	C	Bui *et al.*[111]
IMP3	ccRCC pT1a	Prognosis	3	C	Hoffmann *et al.*[112]
IMP3	RCC stage I	Prognosis	3	C	Jiang *et al.*[113]
Protein expression Hsp27	RCC, serum, urine	Diagnosis	3	C	White *et al.*[114]
B7-H1, survivin, Ki-67	ccRCC	Prognosis	3	C	Parker *et al.*[115]
Survivin, B7-H1	ccRCC pT1a	Prognosis	3	C	Krambeck *et al.*[116]
Survivin	RCC pT1	Prognosis	3	C	Byun *et al.*[117]
Survivin	ccRCC pT1a	Prognosis	3	C	Parker *et al.*[118]
Metabolites – acylcarnitines	RCC, urine	Diagnosis, prognosis	3	C	Ganti *et al.*[119]
Amino acid levels	RCC, serum	Diagnosis, prognosis	3	C	Mustafa *et al.*[120]
DNA methylation	RCC, urine, serum	Diagnosis	3	C	Hoque *et al.*[121]
DNA methylation	RCC, urine	Diagnosis	3	C	Battagli *et al.*[122]
DNA methylation	SRMs	Differential diagnosis	3	C	Ibragimova *et al.*[123]
DNA methylation	RCC, onco	Differential diagnosis	3	C	Slater *et al.*[124]
DNA methylation	RCC	Diagnosis	3	C	Lasseigne *et al.*[125]
DNA methylation	RCC, onco	Differential diagnosis	3	C	Costa *et al.*[126]

Abbreviations: aCGH, array comparative genomic hybridization; AQP, aquaporin; CAIX, carbonic anhydrase IX; ccRCC, clear cell renal cell carcinoma; CT, computed tomography; FISH, fluorescent in situ hybridization; FNA, fine-needle aspiration; GOR, Grade of Recommendation; Hsp27, heat shock protein 27; LOE, Level of Evidence; miRNA, microribonucleic acid; mtDNA, mitochondrial deoxyribonucleic acid; PLIN2, perilipin 2; RCC, renal cell carcinoma; SRM, small renal mass; UC, ulcerative colitis; VHL, von Hippel-Lindau.

continued on **page 396**

TABLE 6-3 Biomarkers in Renal Cell Carcinoma, *Cont'd*

Biomarker	Specimen source, type	Intended use	LOE	GOR	Reference
mRNA expression	ccRCC	Prognosis	3	C	Brooks *et al.*[127]
miRNA expression	ccRCC	Diagnosis	3	C	White *et al.*[128]
miRNA expression	RCC	Differential diagnosis	3	C	Youssef *et al.*[129]
miRNA expression	RCC	Diagnosis, prognosis	3	C	Osanto *et al.*[130]
miRNA expression	RCC, some pT1, miR-378 and miR-451	Diagnosis	3	C	Redova *et al.*[131]
miRNA expression	Serum only, 5-panel, some stage I	Diagnosis	3	C	Wang *et al.*[132]
Point mutation – mtDNA	RCC stage I, urine	Diagnosis	4	C	Jakupciak *et al.*[133]
Point mutation – VHL	ccRCC pT1a, serum	Diagnosis	3	C	Ashida *et al.*[134]
Chromosome copy number	RCC, onco (no stage info), FNA aCGH	Differential diagnosis	3	C	Vieira *et al.*[135]
Chromosome copy number	RCC pT1a, onco, FNA FISH	Differential diagnosis	3	C	Barocas *et al.*[136]

Abbreviations: aCGH, array comparative genomic hybridization; AQP, aquaporin; CAIX, carbonic anhydrase IX; ccRCC, clear cell renal cell carcinoma; CT, computed tomography; FISH, fluorescent in situ hybridization; FNA, fine-needle aspiration; GOR, Grade of Recommendation; Hsp27, heat shock protein 27; LOE, Level of Evidence; miRNA, microribonucleic acid; mtDNA, mitochondrial deoxyribonucleic acid; PLIN2, perilipin 2; RCC, renal cell carcinoma; SRM, small renal mass; UC, ulcerative colitis; VHL, von Hippel-Lindau.

6.4.1 Conclusion

To date, biomarkers for SRMs have mostly been examined only as part of a wider specimen set of all stages of RCC. Relatively few studies of candidate biomarkers have been performed, beyond a discovery set usually of resected tissue specimens. [**LOE 4, GOR D**]

Advances in technology will facilitate future biomarker discovery studies, which should focus on SRMs and aim for validation in a different set of SRMs, as well as in needle biopsies and bodily fluids. [**LOE 3, GOR C**]

6.5 Cross-sectional Radiologic Evaluation of the SRM

The biggest single change in the diagnosis of renal masses has been the increase in the number of incidental SRMs that have been identified. This is related not only to the increased resolution and the increased frequency of cross-sectional imaging in recent years, but also to a true increase in the incidence of renal masses, including RCCs. Today, over 80% of all renal masses are detected incidentally.[137,138]

While the sensitivity of current day imaging in identifying these SRMs is high, the challenge of being specific enough to confidently differentiate benign from malignant lesions remains.[139] Another goal for current imaging techniques is to noninvasively predict the types of renal tumours while providing the treating physicians with an idea of the biological behavior of the tumour.[140] This includes identifying the type and grade of RCCs. In addition, imaging provides supplementary information such as nephrometry and surgical anatomy, which are critical in deciding management.

The three mainstays of imaging include ultrasound (US), CT, and MRI. While US is discussed elsewhere, this section will focus on contemporary CT and MRI.

Computed tomography is currently the modality of choice for characterization and staging of renal masses.[140] In addition, it is the most common imaging technique used to identify the renal mass. Technical advances such as dual energy or spectral energy scanning have also helped to increase the tissue resolution, obviate the need for a non-contrast phase, and allow techniques such as iodine mapping.

Commonly used multidetector computed tomography (MDCT) protocols for evaluation of renal masses include a non-contrast phase followed by post-contrast phases at multiple points, including corticomedullary, nephrographic, and excretory phase imaging. While the nephrographic phase is the best for identifying lesions, the other phases help in surgical planning as well as specifying the type of renal tumours. Examples of this include the differentiation of clear cell carcinomas from papillary carcinomas based on enhancement characteristics through the various phases.[141–143] The demonstration of macroscopic fat is well recognized on CT and is critical in identifying angiomyolipomas.[144,145] Computed tomography is also good at classifying cystic renal lesions using the Bosniak classification system.

The demonstration of enhancement is the most critical factor in determining the likelihood of malignancy in a renal mass. In addition, quantification of enhancement in the different phases of CT as well as visual qualification of the pattern of enhancement are used to differentiate clear cell carcinomas from pRCCs. There have been multiple studies looking to further characterize tumours such as lipid-poor angiomyolipomas and oncocytomas, which are the two most common benign tumours that are surgically resected due to the nonspecificity of a preoperative diagnosis.[145–150]

The main drawback of CT is the issue of ionizing radiation. Numerous technical advances such as multidetector technology and the development of iterative image reconstruction techniques have helped in significantly reducing the radiation dose levels. Dual energy scanning may obviate the need for a non-contrast phase, thus helping to reduce the radiation dose further.[151]

Magnetic resonance imaging is often used as a supplementary problem-solving tool in clinical practice in the evaluation and characterization of renal masses.[140] Its strength lies in its ability to provide contrast resolution without using ionizing radiation. Magnetic resonance imaging is usually performed on 1.5 T and 3 T units using clinical breath-hold techniques. Examinations consist of multiple sequences, including T2-weighted imaging, T1-weighted opposed-phase imaging for identification of fat, and fat-suppressed T1-weighted gradient-echo acquisitions before and after gadolinium contrast injection. As on CT, post-contrast phases on MRI include corticomedullary, nephrographic, and excretory phase imaging. The opposed-phase imaging allows for detection of microscopic fat.

Advanced MRI techniques such as diffusion-weighted imaging (DWI) are now being widely used clinically. Diffusion-weighted imaging can potentially augment characterization of renal mass lesions, with differentiation of subtypes of RCC tumours now being reported in multiple studies. It is also sensitive to Brownian motion of water molecules in tissue. In cellular tissues such as tumours, there is restricted diffusion, whereas simple cysts have free mobility. The latter manifests as low-signal intensity on DWI sequences. This can also be quantified using apparent diffusion coefficient (ADC) values, which are used to characterize renal masses. Currently, the limitation of diffusion techniques is a poor signal-to-noise ratio.[152–155]

An additional MRI technique that has not yet translated to routine clinical practice includes dynamic perfusion MRI, which would allow quantitative analysis of enhancement and washout of renal masses following gadolinium contrast administration,[156] adding to the techniques used to characterize types of renal masses. For example, pRCCs tend to have a homogenous low-level enhancement compared to clear cell carcinomas.

An occasional clinical scenario is the evaluation of a patient with poor renal function who has an SRM. In non-emergent patients with glomerular filtration rate (GFR) <30 mL/min/1.73 m^2, iodinated contrast agents are generally not used due to problems of increasing nephrotoxicity. In these patients undergoing magnetic resonance (MR) examinations, there is an association with nephrogenic systemic fibrosis, and the current guidelines recommend against using gadolinium in this scenario.[157,158] A combination of non-contrast-enhanced imaging along with US and contrast-enhanced ultrasound (CEUS) is often used in this clinical scenario. [**LOE 3, GOR C**]

6.6 Ultrasound Evaluation of Solid Renal Masses

As an imaging modality, US is relatively inexpensive and uses no ionizing radiation, and thus, is an important tool for the evaluation of renal masses. Contrast-enhanced computed tomography (CECT) represents the gold standard for characterizing solid renal masses. Although US is less sensitive in detecting RCCs <3 cm that do not deform the contours of the kidney, up to 83% of asymptotic tumours are detected by US.[159,160] Ultrasound imaging for characterization of solid renal masses is often appropriate. The American College of Radiology identifies US with duplex Doppler as usually appropriate (tied with contrast-enhanced MRI), 1 point behind CECT for the evaluation of indeterminate renal masses in patients with normal renal function, and the single most appropriate imaging technique for the evaluation of indeterminate renal masses in patients with renal insufficiency.[161]

Grayscale US is effective in definitive characterization of category I renal cysts, which demonstrate sonolucent interiors and enhanced transmission of the sound wave through the posterior cyst wall.[162–164] Category II simple cysts are also relatively well characterized using B-mode US.[165] Characterization of solid renal masses using grayscale US is more difficult, as a great deal of echogenicity overlap exists between groups of renal tumours.[166,167] Common appearances of solid benign and malignant renal masses are presented in **Table 6-4** and **Table 6-5**, respectively.[163,164] While angiomyolipomas generally demonstrate hyperechogenicity and oncocytomas generally demonstrate hypoechogenicity, RCCs can mimic the appearance of both these masses, reducing the accuracy of solid tumour characterization by grayscale US.[166]

TABLE 6-4 Traditional Ultrasound Appearance of Benign Small Renal Masses

Tumour type	Appearance
Angiomyolipoma	▪ Predominantly hyperechoic ▪ Well defined ▪ May or may not demonstrate posterior shadowing ▪ May or may not demonstrate vascular components ▪ May or may not have cystic areas
Adenoma	▪ <3 cm ▪ Can be solitary/multiple in number ▪ Can be unilateral/bilateral ▪ Typically located below renal capsule ▪ Can demonstrate calcifications, hemorrhage, and/or necrosis
Oncocytoma	▪ Large range in size (can grow to ≤20 cm) ▪ Well defined ▪ May contain a central scar ▪ May be hyper-, hypo-, or isoechoic to renal parenchyma
Leiomyoma	▪ Indistinguishable from RCC ▪ Located peripherally, centrally, or parapelvic ▪ Can be solid, solid/cystic, or cystic ▪ Well defined ▪ Can have retroperitoneal extension ▪ Can have mass effect on the collecting system
Reninoma (juxtaglomerular)	▪ Hypo- or hyperechoic ▪ Well defined ▪ Solid mass ▪ Can be hypervascular
Hemangiopericytoma	▪ No distinguishable features from other benign lesions or RCC
Hemangioma	▪ Commonly located in the renal pyramids or pelvis ▪ Predominantly <1 cm ▪ Solid mass ▪ Hypo- or hypervascular ▪ May cause mass effect on collecting system or vasculature

Abbreviation: RCC, renal cell carcinoma.

TABLE 6-5 Traditional Ultrasound Appearance of Malignant Small Renal Masses

Tumour type		Appearance
Renal cell		▪ Hyper-, hypo-, or isoechoic to parenchyma ▪ Solid, solid/cystic, or cystic ▪ Hyper- or hypovascular ▪ May contain hypoechoic rim
Renal cell subtypes	Clear cell	▪ Multilocular cystic
	Papillary	▪ Frequently bilateral, hypervascular
	Chromophobic	▪ Large, generally no areas of necrosis and/or calcifications
Metastases		▪ Most commonly hypoechoic cortical lesions ▪ Most commonly bilateral ▪ Most commonly presenting with multiple lesions ▪ Well defined ▪ Infiltrative capabilities
Lymphoma		▪ Unilateral or bilateral ▪ Solitary mass, diffuse infiltrative involvement, and/or retroperitoneal invasion ▪ Enlarged kidney(s) ▪ Homogeneous hypoechoic
Squamous cell and adenocarcinoma		▪ Infiltrative mass affecting/involving the collecting system, renal sinus fat, and renal parenchyma ▪ Associated with chronic hydronephrosis, obstructing calculi, and chronic inflammation
Transitional cell		▪ Solitary intraluminal mass, mural thickening with lumen narrowing, and/or infiltrating renal sinus mass ▪ Poorly defined ▪ Hypo- or hyperechoic ▪ May cause pelvicaliectasis

Schmidt *et al.*[168] used both B-mode and tissue harmonic imaging to characterize focal renal masses with CECT, contrast-enhanced MRI, or pathology as a reference standard; they found that harmonic imaging significantly improved US sensitivity (88%) and accuracy (83%) due to the improved visualization of lesion conspicuity and fluid-solid differentiation, but a large proportion (80%) of the masses in their study were simple cysts. Aside from mass characterization, B-mode US may be useful in AS of the solid renal mass. The overall accuracy of US for estimating tumour size has been well documented, and B-mode US, therefore, may be a useful and cost-effective tool for serial imaging. Finally, grayscale US has also been shown useful for guidance of fine-needle or core biopsy, or ablation of solid renal masses.[19,24,169–172]

As can be seen in **Table 6-4** and **Table 6-5**, an understanding of mass blood flow may be useful in differentiating solid renal masses, although a great deal of overlap exists between subtypes. As a consequence of this overlap in Doppler patterns, Doppler US has had limited success in improving the accuracy of characterization of solid renal masses identified by cross-sectional imaging. One study evaluated colour Doppler US for renal tumours of all sizes prior to surgical excision.[173] This study was initiated retrospectively and continued in a prospective cohort. The retrospective analysis indicated a sensitivity of 92% for detecting ccRCC, which declined to 82% in the prospective cohort.

Specificity in distinguishing between benign and malignant lesions was poor, with 59% of oncocytomas demonstrating increased flow. Jinzaki and colleagues[167] evaluated the combined use of grayscale imaging and power Doppler in small (1.5–3.0 cm), solid renal masses to evaluate the distribution of flow within the mass. Their group found that peripheral flow (solely or mixed with penetrating flow) was an indicator of RCC, and improved the accuracy of characterization from 42% with grayscale imaging alone to 78% with both modes.

The recent commercial availability of acoustic radiation force impulse imaging packages allows investigators to noninvasively visualize and measure tissue elasticity. One such quantitative method, shear wave elastography, allows tissue characterization based upon the speed of a shear wave propagating away from a region of excitation.[174] Shear wave elastography has been used most extensively in the quantification of liver fibrosis,[175–177] but less so in the kidney to date. Tissue elasticity imaging has been used to study renal fibrosis or dysfunction,[178–180] but little work has been done that focuses on renal masses. Acoustic radiation force impulse imaging has been used to improve the depiction of renal masses.[181,182] Recently, shear wave speed has been investigated as a means for characterizing solid renal masses. A pilot study of 28 angiomyolipomas and 19 RCCs demonstrated a significant difference ($p<0.001$) in elasticity-based strain patterns between angiomyolipomas and RCC.[183] Guo *et al.*[180] showed significantly higher shear wave velocities in pseudotumours, compared with clear cell carcinomas or angiomyolipomas (but no significant difference between clear cells and angiomyolipomas) in 42 patients; shear wave velocities of ≥3.03 m/sec were indicative of pseudotumours. In an attempt to overcome inherent biovariability with this technique, Keskin at al.[184] used the ratio of shear wave velocity between renal masses and the renal cortex in 65 patients, and found that the ratio was 1.1 ± 0.1 for angiomyolipomas ($n=24$) and 3.4 ± 0.3 for RCCs ($n=41$). While the field of renal elastography is still in its infancy, preliminary results suggest that elastography may eventually be a clinically useful tool for characterizing solid renal tumours.

Contrast-enhanced ultrasound involves the intravenous injection of gas microbubbles stabilized by an outer shell for stability. Differences in impedance and compressibility of the gas relative to the surrounding blood provide US enhancement of up to 30 dB.[185] Contrast-enhanced ultrasound is Food and Drug Administration (FDA)-approved for echocardiography, but can also be used off-label within the United States for renal applications,[186] and represents the primary imaging modality for numerous vascular applications worldwide.[187,188] Due to the size of these agents (1–8 μm in diameter), they remain within the intravascular blood pool and permeate the tumour angiovasculature.[189] Additionally, US contrast agents have no renal contraindications and have demonstrated an exceptional safety record (severe reaction rates <0.01%) in retrospective studies,[190,191] making them ideal for renal imaging.

Studies using CEUS for renal masses have primarily focused on differentiating solid from cystic masses.[192] In a recent study, results were reported from 721 individuals referred for CEUS following an indeterminate MRI or CT exam, with or without contrast based on patient contraindications. The authors showed CEUS had a sensitivity of 100% and specificity of 95% when using heterogeneous enhancement equal to or greater than the surrounding parenchyma and early washout of contrast relative to the surrounding kidney as predictors of malignancy. Over half of the benign masses were

avascular, including congenital fusion abnormalities, scar tissue, or benign cystic masses. This study demonstrates the usefulness of CEUS for renal mass characterization when MRI/CT contrast is contraindicated.[193]

Similar to MR/CT imaging, the specificity of CEUS still suffers when characterizing only solid renal masses. Tamai *et al.*[194] completed a study of 29 patients with solid renal masses scheduled for surgical resection, comparing CEUS and CECT peak enhancement levels to histopathological findings. The group showed CEUS was superior in detecting flow in hypovascular lesions relative to CECT, but suffered from a poor overall specificity (45.5%). Using early contrast washout relative to the surrounding kidney, our group observed sensitivities of 67% to 89% and specificities of 75% to 100% while using either a commercially available harmonic contrast imaging package or investigational subharmonic imaging software.[195] An example of this washout process is provided in **Figure 6-1**, showing a papillary renal cell carcinoma (pRCC) at baseline with grayscale US on the left and with nonlinear harmonic imaging mode on the right. Heterogeneous enhancement of both the mass and the surrounding kidney is observed approximately 13 seconds after injection of 1 mL of Optison™ (GE Healthcare, New Jersey, United States). Early contrast washout from the mass relative to the surrounding tissue is observed approximately 30 seconds post injection (indicative of mass malignancy). Gerst *et al.*[196] used CEUS to monitor lesion enhancement, contrast washout, and heterogeneity in 34 patients scheduled for surgical resection. They found 83% specificity for predicting whether a lesion was cancerous and 82% specificity for predicting whether a lesion was conventional clear cell carcinoma or another tumour. These findings were consistent with other investigations in which less enhancement of lower-grade malignant tumours (non–clear cell subtypes) was seen on CEUS.[197,198]

FIGURE 6-1
Typical Appearance of a Contrast-Enhanced Ultrasound Exam of RCC

Baseline imaging of a biopsy-proven pRCC shows a 3.1-cm mass on the right upper pole in grayscale (left) and nonlinear contrast imaging mode (right). Contrast enhancement shows heterogeneous enhancement levels with similar overall intensity to the surrounding kidney, followed by early contrast washout relative to the surrounding renal parenchyma (an indicator of malignancy).

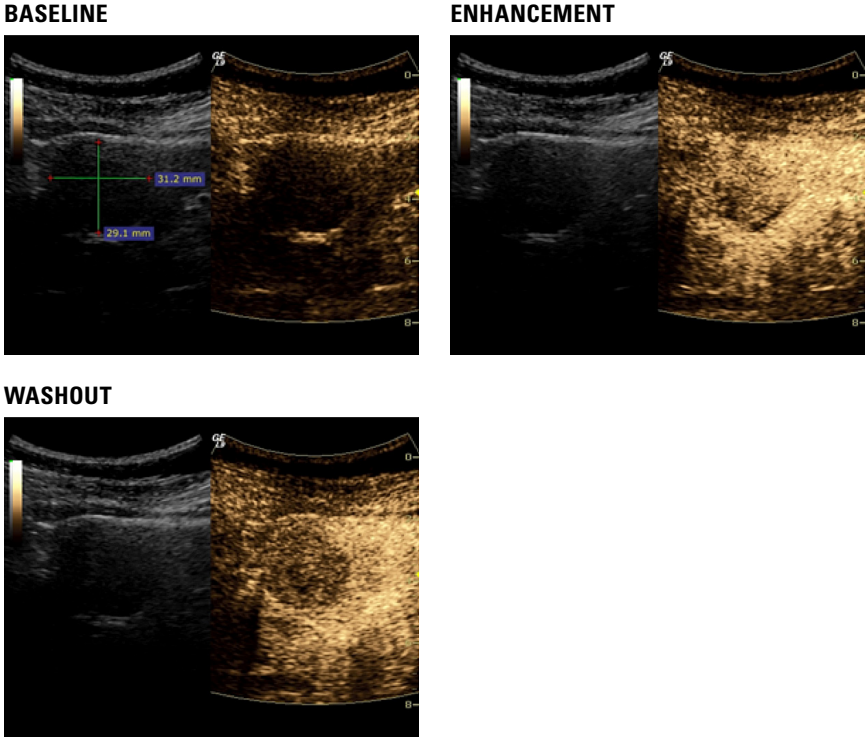

Looking beyond the initial characterization of solid renal masses, US may also be helpful in evaluating the treatment response of malignant renal masses to therapy. As previously discussed, tumour size measurements are readily obtained using grayscale US and may be used to monitor tumour progression/regression. Contrast-enhanced ultrasound can be used to monitor tumour vascularity as well as blood flow kinetics; these parameters have been useful for predicting treatment response of metastatic RCC (with most cases presenting in the liver).[199] Most importantly, the benefits of CEUS for monitoring treatment response to locoregional therapies have been demonstrated. A lack of contrast enhancement has been shown to confirm complete avascularity after radiofrequency ablation (RFA) or microwave ablation (MWA), with sensitivities of 64% to 100% and specificities of 96.6% to 98.7%.[200–203] Studies of CEUS following laparoscopic or percutaneous cryotherapy have demonstrated very high concordance with contrast-enhanced MRI and the extent of residual viable tumour.[195,204–206] Given the lack of contraindications to CEUS in patients with renal insufficiency, the role of CEUS in monitoring renal ablation is expected to grow.

Ultrasound is a safe, readily available, cost-effective, and portable tool for radiographic evaluation of solid renal masses. Mass size and the presence of cystic components are readily identified with grayscale US. Emerging applications of tissue elastography and CEUS are expected to improve on the current limitations of Doppler US, and will play an important role in monitoring response to locoregional therapies when other contrast media are contraindicated. [**LOE 3, GOR C**]

6.7 Molecular Imaging for Renal Masses

6.7.1 Introduction

The size of renal masses has decreased over the past decade,[137,207,208] and correspondingly, the incidence of benign masses has increased.[209] Imaging of renal masses, therefore, now needs to include not merely the presence of a mass in the kidney, but also the identification, as best as possible, of its phenotype, so the appropriate surgical management may be predetermined.

Advances in cross-sectional imaging—CT, MRI, and US—have contributed considerably to our understanding of the relationship between perfusion and other functional characteristics of renal masses, and are covered elsewhere in this chapter. This overview will, therefore, focus on advances in molecular imaging that have enabled phenotypic characterization of renal masses.

Positron emission tomography with computed tomography (PET/CT) has revolutionized imaging in general[210] by providing real-time and *in vivo* insight into the metabolic and phenotypic features of a variety of solid tumours, and this overview will, accordingly, focus on this modality. Positron emission tomography is a nuclear medicine technique that relies on the detection of energy emitted from radiotracers exogenously administered to patients.

Tracers are subpharmacologic quantities of substances that can evaluate biological processes without disturbing the milieu. Hevesy pioneered the tracer principle in 1935,[211] and it has been used for over 6 decades to understand a variety of biological processes.

Positron emission tomography images are created by the detection of coincident 511-keV gamma rays originating from the annihilation of positrons emitted by (positron-emitting) radionuclides, of which the most common is fluorine-18.[212] Positron emission tomography is currently the most sensitive clinical imaging tool, capable of detecting picomolar tracer concentrations; anatomical correlates provided by CT further enhance the ability of PET/CT to interrogate numerous features of the cancer phenotype, including cellular metabolism and proliferation, tumour-associated cell surface markers, and features of the tumour milieu (e.g. hypoxia and stromal/vascular characteristics).[213]

Imaging of the Warburg effect[214] and of glycolysis, in particular, has been made possible by a surrogate of glucose, [18F]-fludeoxyglucose (FDG), which enters the cell through glucose transporter pathways, and is then phosphorylated by hexokinase.[215] FDG-6-phosphate does not undergo subsequent enzymatic degradation, and thus, accumulates in the cell to an extent determined by these enzymes.[215] Most cancers utilize glucose as the preferred energy substrate,[214,216] appearing as foci of increased radioactivity concentration; FDG PET/CT has, consequently, become the most widely used oncologic molecular imaging modality today.

Other agents that assess metabolic features are also being explored, though none specifically for renal cancer. Uptake of [18F]-fluorothymidine (FLT) has been shown[217] to be directly proportional to cellular proliferation (as assayed *in vitro* by the Ki-67 proliferation index). Most metastatic renal cancers utilize glucose as an energy substrate; studies with other metabolic agents such as choline[218] and amino acids, including methionine[219] and glutamine,[220] are accordingly uncommon in renal cancer.

On the other hand, identification of a molecular phenotype that characterizes a cancer phenotype using PET/CT was pioneered[221,222] in clear cell renal cell carcinoma (ccRCC). This was accomplished through the use of a positron-labeled antibody (iodine-124 [124I]-labeled girentuximab, Redectane®) specific to carbonic anhydrase IX (CAIX), an antigen expressed consequent to von Hippel-Lindau (VHL) oncogene mutations.[223] Carbonic anhydrase IX is also overexpressed as a consequence of unfavorable tumour characteristics, particularly hypoxia.[224]

The ability of PET/CT to characterize features of the cancer phenotype will be further described with particular reference to the molecular characterization of renal masses.

6.7.2 Metabolism

[18F]-fludeoxyglucose

As outlined previously, [18F]-fludeoxyglucose (FDG) PET/CT has revolutionized molecular imaging *in vivo*. Its ability to identify renal neoplasms, however, is putatively limited by its renal excretion, with tracer in the collecting system obscuring tumour uptake. However, studies continue to show the ability of FDG PET/CT to identify renal neoplasms. A few studies will be briefly described.

Bachor *et al.*[225] identified 20 of 26 primary renal neoplasms using FDG PET. Uptake was greater in the less differentiated neoplasms, and nodal involvement was accurately identified in all patients. Goldberg *et al.*[226] had a sensitivity of 90% for malignant renal neoplasms, with a high specificity for benign lesions as well. Ramdave and colleagues[227] found comparable accuracy for FDG PET/CT and contrast-enhanced computed tomography (CECT) in identifying renal neoplasia, with greater accuracy for FDG PET/CT in identifying recurrent disease in the renal bed. On the other hand, studies by Aide *et al.*[228] and Kang *et al.*[229] showed less accuracy for FDG PET compared to CECT. Differences in image acquisition and processing may have contributed to their relatively discouraging results; these issues were well described in a review of the literature by Aras *et al.*[230]

In summary, FDG PET/CT is not currently used for identification of primary renal malignancy, but is increasingly used for detecting metastatic disease in patients with RCC (**Figure 6-2**).

FIGURE 6-2
FDG PET/CT of a Patient With Metastatic Right RCC

The bone and liver metastases are clearly visualized (solid arrows), although the primary lesion (dashed arrow) is not.

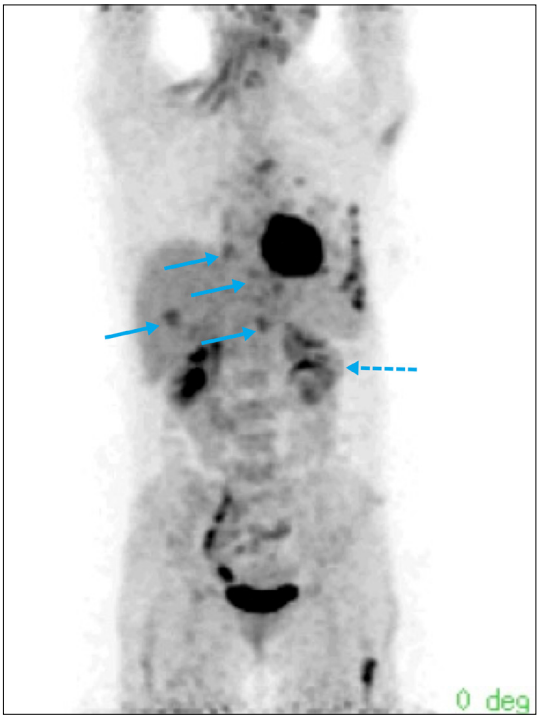

Other metabolic tracers

Relatively few studies in renal cancer have explored tracers that interrogate other metabolic processes. The advent of targeted therapy creates a need for imaging that can identify a therapeutic response, and in many cases, this would entail characterization of the primary neoplasm as well. One study[231] reported accumulation of [11C]-acetate in renal oncocytoma, while another[232] reported, as expected given its biology, no uptake of this fatty acid in renal carcinoma. Fluorothymidine is a radiotracer with the ability to image cellular proliferation,[233] and may have considerable utility in determining tumour aggressiveness; there have, as yet, been no published studies on renal cancer.

6.7.3 Imaging the cancer phenotype

Carbonic anhydrase IX

The identification of carbonic anhydrase IX (CAIX) as an antigen specifically associated with ccRCC[234] spurred interest in imaging this cancer phenotype to stratify patients with this most aggressive variant of renal neoplasms. Early imaging studies with an antibody against CAIX revealed targeting to both primary and metastatic lesions in patients with metastatic ccRCC.[235] This led to exploration of the utility of this antibody, labeled with a positron emitter (iodine-124 [124I]), to characterize this aggressive phenotype in renal masses.

Two studies were carried out with the [124I]-labeled antibody, cG250 (girentuximab). Both studies were carried out per FDA Guidance documents for carefully conducted clinical trials.[236] Both studied patients who were candidates for resection of a renal mass. In each case, the histology of the mass was not known prior to imaging and surgery. The first, the verification trial, was conducted in 26 subjects at a single centre (Memorial Sloan Kettering Cancer Center), while the second, the validation trial, was a multicentre trial in 228 subjects across 14 centres in the United States.

The accuracy of [124I]-cG250 in the preoperative characterization of the clear cell phenotype in patients with renal masses was very high in the verification trial,[221] with a specificity of 100% and a sensitivity of 94%. The validation trial[222] also compared the ability of CECT to characterize renal masses. Although the accuracy was lower, as would be expected in a multicentre trial, sensitivity and specificity were both around 86%, significantly higher than CECT, with a specificity of 47% (**Figure 6-3**).

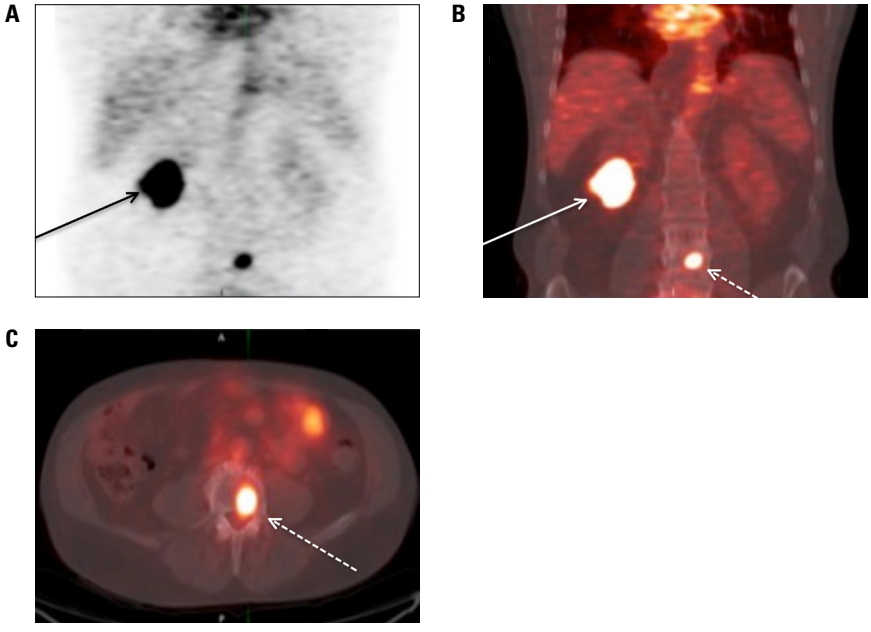

FIGURE 6-3
ImmunoPET With 124I-Girentuximab

The primary metastasis is visualized (solid arrow), as is a vertebral metastasis (dashed arrow).

Currently, preoperative histological characterization of the renal neoplasm is possible only by biopsy, with widely varying success rates.[7,21,34,169] Moreover, there are risks inherent in this invasive procedure, making its utilization less frequent in patients with comorbidities.[9,30] Biopsy is problematic in patients with multiple renal masses, confounding resection choice and surgical management. The incremental utility of preoperative RMB remains controversial, and perhaps, as a consequence, its actual clinical use is estimated at <10%.[30] For PET/CT to noninvasively identify an aggressive phenotype with comparable accuracy, it ought, therefore, to significantly influence the preoperative investigation of patients with renal masses.

6.7.4 Conclusion

Molecular imaging for delineation of tumour characteristics, particularly metabolism and phenotype, has made considerable progress in the last several decades, though its utilization is still far from routine clinical practice. Better understanding of the role of noninvasive imaging should enable greater understanding of the pathophysiology and course of diverse renal masses, as well as improve patient management. [**LOE 3, GOR C**]

6.8 Evaluating the Anatomical Risk of the SRM Using Radiographic Studies

6.8.1 Background

Small renal masses have variable biology and oncologic risk. Imaging characteristics of an SRM can suggest the tumour's biology, including subtype and grade, although histopathological evaluation has proven superior for distinguishing benign from malignant tumours. Although tumour size has been widely considered an essential predictor of tumour type and risk of metastases, it is inadequate to describe other characteristics of SRMs that appear to be important predictors of tumour biology and very relevant when considering between multiple treatment options. Evaluation of tumour features such as centrality and exophycity may help to predict oncologic and functional outcomes in patients with SRMs. Subsequently, more objective assessments of *nephrometry,* the various anatomical features of a given renal mass, can provide information regarding its depth, location, and proximity to the hilum or collecting system. Determination of the complexity of an SRM has significant implications on the management of the lesion and the outcomes expected after such management. Three types of assessments of the radiographic features of SRMs, in particular, deserve attention: nephrometry scoring systems to assess tumour complexity, assessment of tumour and parenchymal volumes, and 3D imaging for treatment planning.

6.8.2 Nephrometry

Although developed within the last 10 years, a great deal of literature has been generated regarding multiple measures of renal tumour complexity (**Table 6-6**). In 2008, the first system to measure tumour complexity was presented and subsequently published. The R.E.N.A.L. nephrometry scoring system is a point-based system that objectifies differences in the anatomical variations of a renal mass for the purpose of improving risk stratification, standardizing reporting, and allowing meaningful comparisons between published reports. Subsequently, the preoperative aspects and dimensions used for an anatomic (PADUA) classification (PC) and C-index (CI) nephrometry systems were developed. Similar to NS, PC is a point-based system to calculate tumour complexity. C-index calculates the centrality of a tumour from tumour radius and distance from the centre of the kidney. Each of the three first-generation scoring systems—R.E.N.A.L. scoring system, PC, and CI—is a strong predictor of surgery type, and perioperative and postoperative outcomes of treatments for SRMs. Although direct comparisons of the systems have been made, the overall conclusion from the published literature is that no clear winner has been identified. There is a wealth of literature regarding nephrometry as a predictor of clinical outcomes in retrospective studies, largely from single centres. Despite the significant enthusiasm in the use of these systems for clinical research, uptake of nephrometry as a standard component of clinical practice appears rather limited, in part, because of the multiplicity of systems and lack of higher quality evidence supporting their use. Second-generation nephrometry systems, including diameter-axial-polar (DAP), surgical approach renal ranking (SARR), and NePhRO, have been reported more recently, but they do not appear to significantly improve upon the first-generation systems and have even lesser quality evidence available.

TABLE 6-6 Number of Publications Utilizing Nephrometric Scoring Systems, Parenchymal Volume Calculation, Preoperative 3D-Imaging Assessment, or a Combination of Multiple Radiographic Assessments of Renal Tumour Anatomy

Reference	Nephrometry Systems				Volume Calculation			3D imaging
	R.E.N.A.L.	PADUA	C-index	Second generation	PFVP	SAVP	3DVP (volumetric)	
Matsumoto[96], Simhan[237], Gorin[238], Satasivam[239], Khalifeh[240], Kopp[242], Bruner[256], Hayn[257], Weight[258], Mufarrij[259], Liu[260], Simhan[261], Kutikov[262], Wang[263], Rosevear[264], Broughton[265], Stroup[266], Tobert[267], Tomaszewski[268], Mayer[269], Altunrende[270], Sisul[271], Okhunov[272], Schmit[273], Chang[274], Reyes[275], Jung[276], Canter[277], Ellison[278], Lane[279]	X							
Porpiglia[241], Tyritzis[280], Minervini[281], Greco[282], Desai[283]		X						
Samplaski[284], Simmons[285]			X					
Simmons[254], Leslie[286], Tannus[287], Wang[288], Maeda[289], Yoon[290], Hakky[291]				X				
Simmons[251], Simmons[292]					X			
Tobert[255]						X		

Abbreviations: 3D, three-dimensional; 3DVP, 3-dimensional assessment of volume preservation; PADUA, preoperative aspects and dimensions used for an anatomical score; PFVP, percent functional volume preservation; R.E.N.A.L., (R)adius (tumour size as maximal diameter), (E)xophytic/endophytic properties of the tumour, (N)earness of tumour deepest portion to the collecting system or sinus, (A)nterior (a)/posterior (p) descriptor, and the (L)ocation relative to the polar line; SAVP, surgeon assessment of volume preservation.

Methodology: We conducted multiple PubMed searches using a variety of terms and term combinations in order to identify the relevant publications for this chapter. For example, the term *nephrometry* generated 245 results, *R.E.N.A.L. nephrometry* generated 231 results, *PADUA score renal* generated 77 results, *renal volume preservation* resulted in 303 results, and *parenchymal volume preservation* generated 39 results. Additional references were collected from the references lists of several of the most pertinent publications and from recent journals' table of contents.

continued on **page 411**

TABLE 6-6 Number of Publications Utilizing Nephrometric Scoring Systems, Parenchymal Volume Calculation, Preoperative 3D-Imaging Assessment, or a Combination of Multiple Radiographic Assessments of Renal Tumour Anatomy, *Cont'd*

Reference	Nephrometry Systems				Volume Calculation			3D imaging
	R.E.N.A.L.	PADUA	C-index	Second generation	PFVP	SAVP	3DVP (volumetric)	
Sharma[249], Mir[253], Tobert[255], Woldu[293]							X	
Azhar[294], Coll[295], Derweesh[296], Gill[297], Ukimura[298], Shao[299], Silberstein[300]								X
Lagerveld[301], Kruck[302], Kobayashi[303], Yeon[304]	X	X						
Esen[305]		X	X					
Okhunov[272], Bylund[306], Lavallée[307], Spaliviero[308], Desantis[309], Moreno-Alarcón[310], Nisen[311]	X	X	X					
Wang[312]	X		X					
Simmons[252]	X		X	X				
Tobert[313]	X	X	X	X				
Simmons[314]	X				X			
Rini[315]	X						X	
Durso[316]					X		X	
Tobert[255]					X	X	X	
Tobert[326]						X	X	
Total Identified References	≥47	≥18	6	9	4	4	5	5

Abbreviations: 3D, three-dimensional; 3DVP, 3-dimensional assessment of volume preservation; PADUA, preoperative aspects and dimensions used for an anatomical score; PFVP, percent functional volume preservation; R.E.N.A.L., (R)adius (tumour size as maximal diameter), (E)xophytic/endophytic properties of the tumour, (N)earness of tumour deepest portion to the collecting system or sinus, (A)nterior (a)/posterior (p) descriptor, and the (L)ocation relative to the polar line; SAVP, surgeon assessment of volume preservation.

Methodology: We conducted multiple PubMed searches using a variety of terms and term combinations in order to identify the relevant publications for this chapter. For example, the term *nephrometry* generated 245 results, *R.E.N.A.L. nephrometry* generated 231 results, *PADUA score renal* generated 77 results, *renal volume preservation* resulted in 303 results, and *parenchymal volume preservation* generated 39 results. Additional references were collected from the references lists of several of the most pertinent publications and from recent journals' table of contents.

There are multiple measures of risk that must be considered in the management of SRMs. These include the risk of the tumour, such as its potential for metastasis; the risks associated with excision or ablation of the tumour, such as bleeding and urinary leakage; and the risks associated with the loss of functioning parenchyma that occurs from excision, ablation, or surveillance of a particular SRM. Each of the various nephrometry systems seeks to quantify the complexity of a renal tumour's anatomy by measuring similar aspects, including size, exophytic versus endophytic position, proximity to hilar structures and the collecting system, and location (medial/lateral and polar/interpolar). The anticipated result of nephrometry is to provide more meaningful comparisons of treatment choices, complications, pathology, and outcomes (both functional and survival).

Since their advent, investigators have evaluated the nephrometry scoring systems independently, collaboratively, and comparatively (**Table 6-6**), assessing their ability to provide insight into multiple descriptive and predictive outcome variables (**Table 6-7**). The initial intention of tumour complexity (nephrometry) measures was to describe clinically relevant treatment-specific parameters, such as treatment selection (NSS vs. RN), operative approach (open vs. minimally invasive surgery [MIS]), operative time, and warm ischemia time (**Table 6-7**). Specifically, investigators have found that NS, PC, and CI are each associated with surgical approach, including the use of NSS versus RN and MIS versus open techniques for partial nephrectomy (PN). Additionally, multiple investigations have used these systems to describe variations in operative complexity; in general, increasing complexity is associated with likelihood to perform RN (vs. NSS) and open surgery (vs. MIS), and longer operative and ischemic times.

TABLE 6-7 Level of Evidence and Grade of Recommendation for Descriptive and Predictive Uses of Anatomical Tumour Complexity (Nephrometry) Systems

	LOE	GOR	Reference
Nephrometry can predict			
Treatment type or approach	3	C	Weight[258], Kutikov[262], Rosevear[264], Broughton[265], Stroup[266], Tobert[267], Canter[277], Samplaski[284], Esen[305], Bylund[306], Simmons[314], Hew[317], Kolla[318], Okhunov[319]
Operative and ischemic times	3	C	Porpiglia[241], Tomaszewski[268], Mayer[269], Altunrende[270], Okhunov[272], Kruck[302], Bylund[306], Lavallée[307]
Complications:	3	C	Kutikov[262], Rosevear[264], Bylund[306]
After NSS (MIS or open):	3	C	Porpiglia[241], Hayn[257], Weight[258], Mufarrij[259], Liu[260], Ellison[278], Tyritzis[280], Minervini[281]
Urine leak focus	3	C	Bruner[256]
Hemorrhage focus	3	C	Jung[276], Kruck[302]
Conversion to RN	3	C	Kobayashi[303]
After RFA	3	C	Schmit[273], Chang[274], Reyes[275]

Abbreviations: 3D, three-dimensional; GOR, Grade of Recommendation; LOE, Level of Evidence; MIS, minimally invasive surgery; NSS, nephron-sparing surgery; RFA, radiofrequency ablation; RN, radical nephrectomy.

continued on **page 413**

TABLE 6-7 Level of Evidence and Grade of Recommendation for Descriptive and Predictive Uses of Anatomical Tumour Complexity (Nephrometry) Systems, *Cont'd*

	LOE	GOR	Reference
After cryoablation	3	C	Sisul[271], Okhunov[272], Schmit[273], Lagerveld[301]
Prolonged hospital stay	3	C	Kruck[302]
Pathology:	3	C	Gorin[238], Satasivam[239], Kutikov[262], Wang[312]
Histological subtype	3	C	Gorin[238], Satasivam[239], Kutikov[262], Wang[312]
Surgical margin status	3	C	Khalifeh[240], Porpiglia[241]
Survival	3	C	Kopp[242]
Tumour growth rate	3	C	Matsumoto[96]
Renal function	3	C	Okhunov[272], Samplaski[284], Kruck[302], Bylund[306]
Assessment of volume preservation can predict			
Renal function	3	C	Simmons[251], Mir[253], Tobert[255], Woldu[293], Rini[315], Golan[320], Kotamarti[321], Isotani[322]
Precision of excision and reconstruction	3	C	Takagi[323]
Parenchymal atrophy	3	C	Simmons[254], Mir[324], Choi[325]
Contralateral renal hypertrophy	3	C	Mir[324], Choi[325]
Preoperative 3D modeling can facilitate			
Partial nephrectomy	3	D	Coll[295], Derweesh[296]
Superselective clamping of renal vasculature	3	D	Azhar[294], Gill[297], Ukimura[298]

Abbreviations: 3D, three-dimensional; GOR, Grade of Recommendation; LOE, Level of Evidence; MIS, minimally invasive surgery; NSS, nephron-sparing surgery; RFA, radiofrequency ablation; RN, radical nephrectomy.

The most robust descriptive uses of nephrometry measures have been to correlate tumour complexity with the likelihood of complications with tumour excision or ablation (**Table 6-7**). Numerous retrospective investigations have demonstrated that surgical complications, including bleeding, urinary leak, and conversion to RN, are associated with tumour complexity. Among these publications, Simhan *et al.* offer perhaps the most robust assessment of risks characterized by NS, detailing complications by organ system, as well as clinical diagnosis in 390 patients undergoing open or MIS NSS.[237] Taken together, the published data [**GOR C**] uniformly demonstrate a positive correlation, primarily between urinary leak/perioperative blood loss/transfusion risk and tumour complexity, with less evidence in support of less commonly reported surgical and medical complications. Despite the multitude of reports, most remain single or limited, multi-institutional, retrospective assessments of the uncontrolled results of multiple surgeons with varied skill sets and levels of experience. Currently, there exists no level 1 data assessing the descriptive role of nephrometry systems leading to homogenously low LOE and GOR (**Table 6-7**). Whereas the collective experience with nephrometry systems is still growing and interobserver variability appears reasonable, the systems are only now being incorporated into prospectively designed clinical trials.

In addition to the ability to describe and predict the treatment outcomes for SRMs, nephrometry also appears to predict oncologic and functional outcomes. Multiple investigators have published primarily single-institutional, retrospective series using nephrometry to predict histological subtype according to complexity. Taken together, these data suggest that more complex lesions tend to be more biologically aggressive, as measured by stage, grade, and type. Moreover, one multi-institutional study found a correlation between NS and risk of upstaging after robotic PN.[238] Conversely, less complex lesions have been correlated with more indolent pathology, including a greater likelihood of benign histology.[239] At least two studies have used NS to predict postoperative margin status following MIS PN.[240,241] In patients under AS, tumour complexity has been shown to predict radiographic growth rates.[96] If tumour complexity predicts indolent versus aggressive disease, it would follow that it may be able to predict survival outcomes as well. At least one group has used their data to contend that a relationship between tumour complexity and survival outcomes exists following RN or PN for *c*T2 tumours.[242] Similarly, if complexity predicts ischemic time or amount of parenchyma resected, then it follows that it may also predict overall renal function following PN. Several investigators have published their experience with nephrometry scores predicting renal function. Taken together, they note a correlation between decline in renal function and higher complexity indices. However, measures that account for the volume of resected tumour and parenchyma, and the volume of preserved parenchyma appear to be more strongly associated with renal functional outcomes. One recent publication indicates that a hybrid measure of tumour complexity and volume, the tumour contact surface area with adjacent renal parenchyma, may predict both surgical outcomes and renal functional outcomes, although validation will be required in subsequent studies.

6.8.3 Assessment of volume preservation

Although the oncologic benefit of PN for SRMs has not been completely resolved, PN is clearly associated with improved renal functional outcomes due to preservation of kidney parenchyma.[243–248] Studies assessing the objective measurement of volume preservation have shown that preserved parenchyma is a strong predictor of function following PN.[249–251] The methodology to determine tumour volume and parenchymal volume preservation varies across studies, ranging from sophisticated analysis of 3D images obtained during thin-slice cross-sectional imaging to surgeon assessment of volume preservation (SAVP) in the operating room after PN has been completed. Despite the differences in methodology employed at different institutions, the findings of multiple studies validate the concept that volume preservation is the most important determining factor of renal function following PN, even when considering ischemia type and time.[249–253] When ascertained following surgery, the estimated volume of vascularized parenchymal mass is an excellent surrogate for preservation of renal function. Therefore, while assessment of tumour complexity may serve to predict tumour type and surgical outcomes, the amount and quality of preserved parenchyma appears to be a better predictor of renal functional outcomes, based on available evidence. [**GOR C**]

There is very limited evidence to indicate the best manner to assess parenchymal volume preservation. Objective 3D assessment of volume preservation (3DVP) is the most accurate, and can even quantify atrophy in the adjacent parenchyma and hypertrophy in the contralateral kidney when obtained >4 months after surgery.[254] Nevertheless, formal image review has not been adopted in practice, largely because it requires significant time and effort to obtain the volumetric calculations. In contrast, SAVP can be readily recorded prior to and following PN, and appears to provide

comparable information to 3DVP.[255] The surgeon simply records the proportion of functioning kidney estimated to have been preserved during NSS. Surgeon assessment of volume preservation has been validated in a multicentre study involving relatively low-and high-volume surgeons, but caution should be exercised in the use of SAVP in the research setting, as the values were not found to be interchangeable with 3DVP within a 5% level of difference.[326] Measures of tumour and kidney volumes that are less rigorous than 3DVP, but more complicated than SAVP, such as percent functional volume preservation (PFVP), have also been used in single-centre studies and require further validation before recommendation. With level 1 evidence indicating greater preservation of renal function with PN than with RN, but only level 3 evidence to support any of the volume assessment tools, a recommendation for any tool can be graded C at best. More evaluation of volume preservation in prospective trials is needed and underway.

6.8.4 Three-dimensional imaging for treatment planning

PN was first used in patients with absolute contraindications to RN. The need to excise the tumour completely with preservation of a functioning renal remnant is the central premise of the operation. Urologic surgeons have used every tool at their disposal to prepare for and optimize conditions for a successful surgery. Beginning with the availability of cross-sectional imaging and continuing to present day virtual surgical simulation with 3D models, renal imaging has improved from the multitude of technological advances. In the late 1990s, 3D renderings of axial imaging enabled a more detailed view of the renal vasculature and tumour-parenchyma interfaces. Individualized videos were recorded for surgeon review immediately prior to each operation and reported to facilitate the operation. More recently, similar approaches have been undertaken to enable surgeons to perform superselective clamping of the third and fourth order renal vessels, enabling an anatomical *zero-ischemia approach* to PN. Virtual surgical planning has even progressed from the computer screen to the physical with constructions of 3D models of the tumour-bearing kidney. For all of these advances, however, the LOE is low, with a corresponding GOR of C/D. Nevertheless, each such advance provides even greater detail and information to the surgeon, and efforts should continue to be made to use technology to its full extent.

6.8.5 Conclusion

Predictive markers of various outcome measures are the focus of intensive research in the field of localized kidney cancer. During the last decade, objective measures of the radiographic characteristics of SRMs have been developed and investigated, largely as descriptive and predictive tools. Nephrometry scoring systems, including the R.E.N.A.L. nephrometry scoring system, have been used in retrospective studies published by a relatively large number of centres. However, the data all remain fundamentally limited in that there are no prospective clinical trials to evaluate the clinical utility of this (or any other) measure of tumour complexity. Instead, they represent lower-level case-controlled series that relate tumour complexity to surgical complexity and related outcomes. Several reports do indicate that higher tumour complexity is correlated with more aggressive biology, faster growth rates, and lower survival, but these data again are low level. Three-dimensional analysis of tumour and renal volumes before and after PN can quantify the amount of volume preserved with PN. Similarly, sophisticated analysis of thin-slice cross-sectional imaging can facilitate virtual surgical planning, particularly when superselective clamping or non-clamped PN is to be performed.

Only low-level data exist to support either of these practices. Finally, retrospective analysis of SAVP is of growing interest, as preservation of renal parenchyma with NSS is a major predictor of renal functional outcomes. This straightforward assessment can be performed in the office and the operating room, and prospective evaluations are underway. Taken together, available data provide a provocative look at the value of objectifying the anatomical features of the SRM radiographically in order to predict tumour biology, surgical results, and functional outcomes. [**LOE 3, GOR C**]

6.9 Evaluating Patient Risk With SRMs

6.9.1 Introduction

Clinical intuition suggests that the well-documented rise in detection of SRMs due to increased use of cross-sectional abdominal imaging, and concurrent increase in the number of surgical procedures performed, should decrease cancer-specific and overall mortality for patients diagnosed with RCC. However, while the rates of renal surgery have risen simultaneously with increased tumour detection, mortality rates remain largely unchanged, suggesting that the absolute number of detectable lethal lesions has not diminished.[211] The implications from these emerging data suggest that a significant proportion of small, localized renal masses may be indolent tumours with little chance of tumour progression or cancer-related death. As a result, clinicians have begun to reassess contemporary management algorithms for incidentally diagnosed renal tumours in an effort to reduce overtreatment of patients in which the risks of surgical resection may outweigh a marginal survival benefit.

6.9.2 Quantitating competing risks

When counseling a patient regarding the need for definitive intervention, a number of factors must be considered, including the natural history of the lesion (if not treated), the patient's competing mortality risks, and assessment if procedural risks outweigh any potential survival benefit.

Contemporary best practice guidelines dictate that in most cases immediate intervention is appropriate for enhancing localized tumours. While surgical resection of SRMs in young, healthy patients is the accepted standard of care,[327] management of localized SRMs in elderly or infirm patients in whom comorbid medical conditions compete with RCC malignant potential as primary causes of death represents a unique set of challenges. Until recently, it has been difficult to dichotomize a patient's risk of cancer-specific death, which for localized low-stage kidney cancer is quite low, versus competing risks of death from comorbidities, such as cardiovascular or pulmonary disease. There are currently few randomized controlled trials for localized urologic malignancies that provide a long-term perspective regarding the effectiveness of surgical interventions.[328] However, results from the well-publicized European Organisation for Research and Treatment of Cancer (EORTC) trial 30904 do provide important insight on this phenomenon. While designed to compare the efficacy of RN and PN for localized tumours ≤5 cm, 117 deaths were documented over a median follow-up of 9.3 years. Of these, 10.3% were attributable to RCC versus 89.7% from comorbid conditions.[247]

A number of other reports quantitating the competing risks of death in patients with RCC have demonstrated similar results. In a series of 537 patients older than 75 years with renal masses (<7 cm) and a median follow-up of 3.9 years, Lane *et al.* reported the most common cause of death was cardiovascular (29%), compared to cancer progression (4%).[329] Using the Charlson Comorbidity Index (CCI) to stratify 192 patients with clinically localized RCC, Arrontes *et al.*[330] reported that patients with clinically localized RCC and a CCI >2 had significantly reduced overall survival versus patients with a CCI ≤2. From Surveillance, Epidemiology, and End Results (SEER) data involving more than 26,000 patients surgically treated for RCC, Hollingsworth *et al.*[331] presented 5-year mortality rates for cancer-specific and competing cause mortality (stratified by tumour size and age at presentation). The smallest tumours were associated with the lowest cancer-specific mortality, and competing cause mortality rose with age (28% 5-year competing cause mortality rate in patients ≥70 years).

These findings have raised the question whether such data can be used to objectively and quantitatively estimate competing risks for patient counseling purposes in the preoperative setting. An ensuing report proposed a nomogram estimating the risk of kidney cancer death, death from other malignancy, and non-cancer death utilizing select preoperative clinical and demographic variables, including age, race, gender, and tumour size in a large cohort of patients with RCC identified from the SEER database.[332] However, specific comorbidity information was not available for inclusion in the analysis, thereby limiting the clinical utility.

To improve on their initial effort, Kutikov *et al.*[333] used linked SEER-Medicare data, adjusting for patient severity using a claims-derived CCI score, to identify 6,655 individuals aged 66 years or older with localized RCC. Patients with localized node-negative kidney cancer had a lower 3-year (4.7%), 5-year (7.5%), and 10-year (11.9%) probability of cancer-specific death, but a significantly higher overall risk of death from competing causes with 3-year (10.9%), 5-year (20.1%), and 10-year (44.4%) mortality. Although caution must be used when extrapolating outcomes of patients treated surgically to counsel patients in the preoperative setting, these nomograms are useful tools in the clinical setting.

The elderly population presents a unique set of challenges in urologic oncology. In addition to the known natural history of disease, providers must also consider patient factors such as functional and nutritional status, comorbidities, and social support when determining the treatment plan.[334] The development of frailty measures and biomarkers to estimate surgical risk shows promise, with several assessment tools being predictive of surgical complications. Decreased dependence on chronologic age is important when assessing surgical fitness, as age cut-offs prevent the appropriate treatment of many elderly patients who would potentially benefit from active treatment.

Historically, decisions regarding operative candidacy have been subjectively determined by the evaluating surgeon. This is limited by interphysician variation in estimates of 10-year life expectancy, and there is evidence to suggest that elderly patients are less likely to receive guideline-concordant care.[335,336] Traditional risk assessment tools, such as the Charlson Comorbidity Index (CCI),[337] the ECOG performance status,[338] and the American Society of Anesthesiologists (ASA) physical status classification system,[339] were developed for accurate data collection, but not specifically to quantify risk, and all suffer from a lack of prospective validation. While each described classification system documents the burden of comorbidity to some degree, they do not capture nutritional status, cognitive

disability, or subclinical physiologic deficits. The Comprehensive Geriatric Assessment (CGA)[340] and the Preoperative Assessment of Cancer in the Elderly (PACE),[341] while labour-intensive to perform in the clinical setting, are tools (or multidisciplinary assessments) that incorporate comorbidities, physical activity, psychological state, social support, and other metrics. In comparison, the Fried Frailty criteria,[342] which assess weight loss, decreased grip strength, exhaustion, low activity, and slowed walking speed, can be performed in 10 minutes and are quantitated with a score from 0 (*not frail*) to 5 (*frail*). Recent retrospective series of patients undergoing elective and abdominal surgery have demonstrated that patients meeting *intermediately frail* (2–3) or *frail* (4–5) were more likely to experience complications, have a prolonged length of stay, or be discharged to skilled nursing facilities.[343,344] While a lack of objective trade-offs and guidance often contributes to physician reluctance to estimate competing risks,[345] our hope is that as cumulative experience with geriatric assessment tools increases, shared decision-making in the clinical setting will become more informed.

6.9.3 Malignant and metastatic potential of the SRM

There is growing concern that increasing incidental detection may result in the overdiagnosis (and overtreatment) of tumours never destined to progress or metastasize. As a result, there is considerable interest in quantifying the malignant and metastatic potential of SRMs, of which approximately 15% to 20% of tumours <4 cm are benign, based on pretreatment radiographic characteristics.[346] The most well-defined prognostic indicator is tumour size. A number of institutional reports demonstrate that as maximal linear tumour diameter increases, there is increased risk of malignancy,[6,92] high-grade disease, clear cell histology, and presence of synchronous metastases.[347,348] Rothman *et al.* used SEER data to explore the relationship between primary tumour size at presentation and histopathological features in 19,932 patients with localized renal tumours, and found that for each 1-cm increase in size, the probability of a high-grade tumour increased by 13%.[349]

However, the same authors found that while almost 85% of RCCs <4 cm were low grade, a substantial proportion of lesions >7 cm (70%) were also low-grade lesions. Thus, it appears that localized renal tumours can grow quite large without acquiring a biologically aggressive phenotype. Although available data clearly suggest that a significant proportion of SRMs tend to be indolent and only a small minority present with an aggressive phenotype, size at presentation is also associated with synchronous metastatic disease. Kunkle *et al.*[347] compared 110 patients with biopsy-proven synchronous metastatic disease at presentation to 250 controls with classically localized RCC. As expected, tumours associated with synchronous metastases were significantly larger than localized lesions, without evidence of distant or regional disease (8.0 cm vs. 4.5 cm), and with each 1-cm increase in tumour size, the odds of finding synchronous metastases rose by 22%. While this does provide evidence that tumour size at presentation does matter, it is also important to consider that all aggressive, as well as benign or indolent, lesions start off as SRMs. In the above study, while no patients with tumours ≤2 cm presented with biopsy-proven metastatic disease, close to 5% of patients with distant metastases presented with tumours <3 cm. A similar study using SEER data confirmed that the risk of synchronous metastasis for lesions <3 cm appears to be approximately 5%.[348] These findings highlight that the malignant potential of most small lesions is likely low, but illustrate that improved methods of identifying those with increased oncologic risk are essential to best counsel patients presenting with a newly diagnosed SRM who are considering AS versus definitive surgery or ablation.

6.9.4 Pretreatment prediction of malignant potential

One of the great challenges in managing the SRM remains achieving the ability to match specific tumour biology with an individualized treatment strategy. Currently, use of radiographic characteristics to determine malignant potential is limited, and alternative non-extirpative diagnostic strategies, including predictive statistical models and percutaneous biopsy, have shortcomings.

Percutaneous biopsy

Procedural risk, sampling error, and skepticism regarding the clinical relevance of the data gained for clinical decision-making, until recently, have largely obviated the utility of percutaneous biopsy, except in specific circumstances, such as suspicion of lymphoma, renal abscess, or metastatic disease from another primary malignancy. However, with advances in technique, most notably the use of 18-G core needles and improved immunohistochemical characterization, contemporary studies have reported more than 90% accuracy in differentiating malignant from benign histologies, as well as low-risk, minor complications (5%). Despite these improvements, percutaneous biopsy is often insufficient to determine, or tends to underestimate, tumour grade, which is arguably the most important prognostic indicator for clinical decision-making.[350] Although the role of biopsy in the treatment algorithm for the SRM is evolving and has been incorporated in a number of AS protocols,[98,351] it has not yet been accepted as standard practice in the treatment of young or otherwise healthy candidates for excision. In our practice, RMB is preferred in patients with absolute or relative indications for AS (such as significant comorbidity, poor underlying renal function, secondary malignancy) or specific circumstances, such as synchronous bilateral lesions or a solitary kidney.[352] The elusive goal remains the identification of molecular biomarkers, obtained from percutaneous biopsy specimens, predictive of an aggressive RCC phenotype. While biomarker discovery remains an area of intense interest, which is beyond the scope of this review, until these markers are available, alternative prognostic tools are required for risk stratification in patients with SRMs. **(See 6.4 Blood, Urinary, and Needle Biopsy Biomarkers of the SRM; see Chapter 7: Renal Tumour Biopsy: Indications, Technique, Safety, Accuracy/Results, Pathologic Reporting, and Impact on Treatment Decision-Making)**

6.9.5 Imaging techniques

Contrast-based abdominal imaging (either CT or MRI) remains the gold standard for evaluation of a renal mass to assess characteristics, bilateral renal flow and function, and radiographic staging data. These imaging techniques can differentiate most renal cystic lesions from solid masses, but cannot reliably distinguish between benign and malignant solid tumours, histological subtypes, or indolent versus aggressive disease.[346] Although also beyond the scope of this review, there are emerging histology-specific imaging modalities currently under evaluation that may play a more definitive role in the future.[224] **(See 6.5 Cross-sectional Radiologic Evaluation of the SRM)**

6.9.6 Clinical nomograms

Models to predict disease recurrence following definitive therapy are useful for patient reassurance and to help guide surveillance imaging intensity, but they currently have limited application for counseling in the preoperative setting. Unfortunately, early algorithms designed to predict the malignant or biological potential of SRMs using pretreatment characteristics also fall short due to

poor predictive accuracy. For example, a nomogram published by Lane *et al.*[10] incorporating gender, tumour size, and smoking history to predict malignant versus benign disease had only modest accuracy (concordance index of 0.64). Similarly, Jeldres *et al.* developed a nomogram to estimate risk of high-grade disease based on age at diagnosis, gender, tumour size, and symptom classification, but their predictive model was only accurate in 58.3% of cases.[8]

More encouraging data have emerged from recent reports suggesting a relationship may exist between renal mass anatomical characteristics and pathological features. The nephrometry score was recently introduced as a means of quantifying tumour anatomy to provide a reliably reproducible renal mass nomenclature and facilitate meaningful comparison of case mix.[95] In 2011, Kutikov *et al.* evaluated the relationship between nephrometric characteristics and pathological characteristics at the time of surgical excision, finding that total nephrectomy score and all individual anatomical descriptors significantly differed between tumour histology groups, except for anterior/posterior(A) designation.[262] Using institutional data, the authors developed a clinical nomogram integrating nephrometric variables with patient age and gender, developing the highest predictive accuracy for malignant histology (area under the curve [AUC] 0.76) and high-grade features (AUC 0.73) to date. Further, these accuracy rates, particularly for tumour grade, compare favourably with percutaneous core biopsy results, providing a valuable tool when counseling patients who are poor surgical candidates. This has since been externally validated in a number of institutional cohorts.[263,353] [**LOE 3, GOR C**] **(See Chapter 7: Renal Tumour Biopsy: Indications, Technique, Safety, Accuracy/Results, Pathologic Reporting, and Impact on Treatment Decision-Making)**

6.10 Evaluating Functional Risk in Patients With SRMs

6.10.1 Introduction

It has been recognized that kidney function is a critical outcome in the management of SRMs. Therefore, it is paramount for clinicians to understand the significance of kidney function and to appropriately assess kidney function as well the renal functional risk a patient may have following treatment of an SRM.

A major concern in patients undergoing treatment of renal masses is the development of chronic kidney disease (CKD). Chronic kidney disease has been shown to have implications on overall health since it is an independent predictor of all-cause mortality, cardiovascular mortality, and kidney failure in a wide range of populations.[354] The significance of CKD, however, secondary to the treatment of a renal mass remains unclear. Several studies have suggested that new-onset CKD from surgical loss of renal functional volume may not have the same implications as CKD that occurs secondary to advanced age or chronic medical conditions, such as diabetes mellitus, hypertension, and cardiovascular disease.[245,355] Despite the controversy, the prevention of CKD remains a critical endpoint, as progressive worsening of kidney function, regardless of the etiology, can have a significant impact on all-cause mortality and morbidity.

6.10.2 Defining kidney function and chronic kidney disease

Glomerular filtration rate (GFR) is accepted as the best overall measure of kidney function, and is essential for the detection, evaluation, and management of CKD. A normal GFR depends on age, sex, and body size, and is approximately 130 mL/min/1.73 m^2 and 120 mL/min/1.73 m^2 for men and women, respectively, with considerable variation even among normal individuals.[356] Chronic kidney disease is defined by either a GFR <60 mL/min/1.73 m^2 of body surface area or the presence of kidney damage, regardless of cause, for ≥3 months. Thus, patients with markers of kidney damage, such as albuminuria or abnormalities on imaging studies or on kidney biopsy, have the disease, even if GFR estimates are ≥60 mL/min/1.73m^2.[357]

Glomerular filtration rate, however, cannot be directly measured. Therefore, the best method of determining GFR is by measuring the urinary or plasma clearance of a filtration marker.[356] An ideal filtration marker is defined as a solute that is freely filtered at the glomerulus, nontoxic, neither secreted nor absorbed by the kidney tubules, and unchanged during its excretion by the kidney. The gold standard of exogenous filtration markers is inulin. Other exogenous markers such as iothalamate, ethylenediaminetetraacetic acid (EDTA), diethylenetriaminepentaacetic acid (DTPA), and iohexol are also used to measure GFR.[356] The classic protocol for measuring inulin clearance is cumbersome, as it requires a continuous intravenous infusion, multiple blood samples, and bladder catheterization. Measurement of GFR, however, is impractical for routine clinical use. It is associated with a measurement error of 5% to 20%, with variation greater for higher ranges of GFR.[358] Subsequently, GFR is more commonly estimated as opposed to measured.

6.10.3 Measurement versus estimation of glomerular filtration rate

Estimation of GFR is an essential part of the preoperative work-up for patients with kidney tumours. The most common methods utilized to estimate the GFR are measurement of creatinine clearance rate (Ccr) and estimation equations based upon serum creatinine. Creatinine is derived from the metabolism of skeletal muscle and from dietary meat intake. It is released into the circulation at a relatively constant rate, freely filtered across the glomerulus, and neither reabsorbed nor metabolized by the kidney. Creatinine is, however, secreted by proximal tubular cells. As a result, Ccr exceeds the GFR. Measuring Ccr, which involves 24-hour urine collection, is crude, cumbersome, and susceptible to error, making it impractical for routine use.[356]

On the contrary, equations estimating GFR are simple and easy to use. Serum creatinine-based equations such as the Cockcroft-Gault (CG) equation, the Modification of Diet in Renal Disease (MDRD) study equation, and, more recently, the Chronic Kidney Disease Epidemiology Collaboration (CKD-EPI) equation are commonly used to estimate GFR.[356] Estimating equations include variables such as age, sex, race, and body size, in addition to serum creatinine, as surrogates for muscle mass. Such equations, however, have been found to be less reliable in patients with unusual body habitus or diet (i.e. muscle wasting) and GFR >60 mL/min/1.73 m^2, as well as those patients being evaluated for kidney donation.[359,360]

An alternative to creatinine-based formulas are GFR formulas utilizing cystatin C (CysC), which is a member of the family of proteins that plays an important role in intracellular catabolism of various peptides and proteins. Cystatin C is considered to be a good biomarker of decreased renal function because it is produced at a relatively constant rate and released into plasma, >99% is filtered by glomeruli, and there is no significant protein binding.[361] Since CysC is less affected by muscle mass and diet than creatinine, it has been considered a potential replacement for serum creatinine. Currently, CysC is not recommended as an initial test to screen patients for CKD. It may serve, however, as a confirmatory test to ensure patients with verified CKD receive the appropriate resources for management. In addition, the utilization of CysC may be beneficial in patients with muscle wasting and chronic illnesses.[362]

6.10.4 Functional imaging

Imaging provides another method of evaluating kidney function, with the advantage of providing morphologic information, as well as functional data and kidney volume in the same examination. Functional imaging also overcomes a major limitation of serum marker-based formulas, which is the inability to provide individual kidney function. Knowledge of individual kidney function may be extremely useful when assessing the risk of kidney disease in patients who are considering renal surgery for a kidney tumour.

Nuclear scintigraphy has been utilized for decades to assess renal obstruction and individual kidney function. The radiopharmaceuticals available for assessing renal function and anatomy include technetium-99m (99mTc)-diethylenetriaminepentaacetic acid (DTPA), cleared by glomeruli; 99mTc-mercaptoacetyltriglycine (MAG3), cleared by proximal tubules; and 99mTc-dimercaptosuccinic acid (DMSA), retained in the tubules.[363,364] DTPA, which is the least expensive renal pharmaceutical, can be used to measure GFR. MAG3 provides scintigraphy images superior to DTPA, particularly in patients with impaired renal function. DMSA is an excellent cortical imaging agent and is used when high-resolution anatomical images are required, as in the detection of pyelonephritis or parenchymal scarring. Plasma sampling of these agents along with imaging can also provide individual kidney GFR, which serum creatinine and estimated glomerular filtration rate (eGFR) cannot provide.

Although nuclear scintigraphy is useful for providing important information, such as split function and renal obstruction, it is clinically impractical for routine use, given the radiotracer injections, blood sampling, extended acquisition time, and nearly no available anatomical information. Thus, these examinations are more commonly used in assessing split renal function, presence of obstruction, and renal cortical scarring, and occasionally, used to distinguish true solid renal masses from pseudotumours.

6.10.5 Magnetic resonance imaging

Magnetic resonance imaging (MRI) provides an excellent depiction of the anatomy and has shown promise in noninvasive assessment of renal function. Dynamic contrast-enhanced magnetic resonance (DCE-MR) renography was developed over the last decade, and involves monitoring a gadolinium-containing agent as it passes through the kidneys, with high temporal resolution in the range of seconds. As mentioned previously, ideal markers for renal function are freely filtered without

reabsorption or secretion; gadolinium-containing contrast media are exclusively excreted by glomerular filtration. This enables the measurement of dynamic parameters of renal function, such as renal blood flow, GFR, and urinary drainage, at a single kidney level.[365] Thus, MR renography can be used to evaluate the impact of kidney cancer surgery on kidney function.[366] In addition, the baseline function and compensatory response of the contralateral kidney can also be evaluated.[367] In the future, MRI may be useful not only for evaluating tumours and tumour recurrences, but also for assessing novel renoprotective agents and for preoperatively selecting patients for appropriate surgical treatment of kidney tumours.

6.10.6 Volume correlations with renal function

The use of cross-sectional imaging—CT and MRI—has also been evaluated as a means of calculating renal volume, and subsequently, preoperative and postoperative renal function. Studies of kidney donors have demonstrated a correlation between renal volume and function on imaging measurements.[368,369] Although US and CT may provide adequate assessment of kidney volume in patients with acute kidney injury (AKI), such as acute tubular necrosis, or in patients with interstitial kidney disease, the volume of viable renal parenchyma may not accurately correlate with kidney function. In this setting, MR renography may prove to be a better measure of function and renal volume since it not only offers quantitative kidney parenchymal volume, but also delivers a qualitative assessment of the filtering capacity of the kidney tissue.[368]

6.10.7 Predicting risk of chronic kidney disease following treatment of surgery for kidney cancer

It has been recognized that patients with SRMs have a higher incidence of CKD at time of diagnosis. The prevalence of CKD in the US population is noted to be 11%, but is on the rise.[370] Glomerular filtration rate declines over time with increased age and with comorbidities, such as hypertension, diabetes mellitus, and glomerular disease.[371,372] The prevalence of baseline CKD in patients with renal tumours has been noted in several institutional series to be greater than that of the general population at roughly 25%.[373,374]

The risk factors for kidney cancer are often thought to be the same as the risk factors for CKD, including smoking, obesity, and hypertension.[375] Furthermore, it is speculated that CKD itself may be associated with the development of malignancies.[376] The pretreatment assessment of renal function is frequently rudimentary, depending on the number of kidneys and tumours, and the baseline kidney function. For most patients with a solitary small renal mass and two normally functioning kidneys, the assessment of baseline renal function frequently does not go beyond measuring serum creatinine, estimating GFR through a creatinine-based formula, and evaluating proteinuria on urinalysis. For patients with multiple tumours, a solitary kidney, or pre-existing kidney dysfunction, more advanced methods of assessing kidney function, including single kidney function, may be indicated.

The development of CKD following treatment for small kidney tumours is frequently multifactorial and can be broken down into both modifiable and non-modifiable risk factors. The most significant non-modifiable risk factors are patient-related and include baseline kidney function, age, and gender. The impact of comorbid conditions such as diabetes mellitus and hypertension on the development

of postoperative CKD remains unclear, as several studies have failed to demonstrate an independent risk of these conditions on developing postoperative CKD.[374,377] Tumour-related characteristics can also be considered non-modifiable risk factors for the development of postoperative CKD. Large tumours, endophytic tumours, and tumours with a high NS have also been shown to be predictive of a greater loss of kidney function and renal volume.[378,379] For patients with known pre-existing CKD, particularly those in advanced stages of CKD (3b, 4, 5), surgical treatment of any kind may result in an increased risk of AKI and/or hemodialysis, and every effort should be made to not only identify such patients, but also to select the most appropriate treatment for their SRM.

The most significant modifiable risk factor is the treatment type. Although the impact of surgical treatment on kidney function is discussed in detail in a different chapter, it must be briefly discussed here since treatment selection for an SRM is an independent predictor of loss of kidney function.[373,380]

6.10.8 Radical nephrectomy

Radical nephrectomy (RN) has long been considered the treatment of choice for localized renal masses. Currently, RN remains the treatment standard for larger tumours (>7 cm) and locally advanced tumours. Despite superior oncologic control, both retrospective cohort studies and prospective studies have demonstrated that loss of the entire renal unit (i.e. RN) is an independent predictor of new-onset CKD.[373,381]

A decrease in GFR is not exactly correlated with kidney mass loss or nephron loss because the kidney adapts to the loss of some nephrons by compensatory hyperfiltration and/or increasing solute and water reabsorption in the remaining nephrons. Thus, an individual who has lost one-half of total kidney mass will not necessarily have one-half the normal amount of GFR. As a result, in patients with mild kidney disease, a small rise in serum creatinine usually reflects a marked fall in GFR, whereas a marked rise in serum creatinine in patients with advanced disease reflects a small reduction in GFR. Furthermore, a stable GFR does not necessarily imply stable disease. Signs of disease progression, other than a change in GFR, must be investigated, including an increase in activity of the urine sediment, a rise in protein excretion, or an elevation in blood pressure.[382] Removal of an entire kidney in patients with kidney tumours is associated with a median loss of 35% of renal function.[373,383] Such a loss is unlikely to be clinically meaningful in patients with adequate renal functional reserve. However, as demonstrated, up to 25% of patients with a solitary kidney tumour will have CKD at baseline, making the loss of an entire kidney a significant risk factor for CKD, and subsequently, for morbidity and mortality down the road. The risk of stage 3a CKD is nearly four times greater following RN than PN for patients with a solitary tumour and two normally functioning kidneys. When looking at a considerably more important endpoint of stage 3b CKD (GFR <45 mL/min/1.73m^2), the risk is nearly 12-fold. Based on these outcomes, RN is no longer the treatment of choice for patients with SRMs, and for patients with compromised renal function and a tumour amenable to alternative treatment options.[384]

6.10.9 Partial nephrectomy

Once considered a surgical alternative reserved for patients with significant CKD at baseline, multiple tumours, or a solitary kidney, elective partial nephrectomy (PN) has become the treatment of choice for most SRMs. The impact of PN on postoperative kidney disease may be influenced by a variety of factors, including ischemia time and type. The significance of ischemia time and type can vary widely, as reflected by studies examining the impact of renal ischemia on postoperative kidney function.[385] Review of the data suggest that a shorter ischemia time and the use of cold ischemia can have measurable benefits in patients with limited renal reserve (pre-existing CKD or solitary kidney). In fact, studies on solitary kidneys demonstrate an increased risk of AKI or CKD per additional minute of warm ischemia time.[386]

In order to mitigate the impact of ischemia time, hypothermia is commonly employed during PN. The benefit of cold ischemia appears to be most apparent in patients with low functional reserve (such as solitary kidney) or those undergoing PN with prolonged ischemia time.[374,385]

Other methods of minimizing or eliminating ischemic injury include more technically challenging procedures such as clampless PN, selective clamping, and zero-ischemia PN. At this time, these approaches can only be advocated for patients deemed at risk for poor renal functional outcomes due to inadequate renal reserve.

There do not appear to be significant differences in renal functional outcomes based on the various surgical approaches to PN, such as open versus laparoscopic or robotic techniques. One would assume that any perceivable differences between the approaches would be ultimately related to ischemia time and type, as opposed to differences among the surgical techniques.

Ultimately, when assessing functional risk following the various approaches to PN, the most important factors to take into account are baseline kidney function and tumour characteristics. Careful preoperative assessment of the patient and the tumour will allow for the optimal approach for excision of the tumour and reconstruction of the kidney, thus maximizing renal functional outcomes and minimizing renal functional risks.

6.10.10 Ablation

Ablative techniques, such as cryoablation (CA) and radiofrequency ablation (RFA), are alternative, minimally invasive, nephron-sparing approaches for the management of SRMs. Ablative therapy, particularly percutaneous, is considered a nephron-sparing alternative to PN in patients with significant comorbid conditions or who are poor surgical candidates.[327] Several clinical series indicate that ablation may offer the potential for reduced morbidity and recovery compared with extirpative surgical approaches.[387,388] Furthermore, ablation does not require renal hilar clamping, thus minimizing ischemic damage to the remaining renal parenchyma. Despite these perceived benefits, concerns of oncologic control remain when compared with PN or RN.

Studies examining renal functional outcomes in patients undergoing ablation are limited by selection bias and short follow-up. Nonetheless, most series demonstrate either equivalent or superior kidney functional outcomes.[387,388] Thus, ablative therapy may be considered a better treatment option compared with extirpative surgery in patients with SRMs where the renal functional outcomes are more important than the oncologic outcomes.

6.10.11 Controversies

Although kidney function is recognized as an important treatment outcome in patients with SRMs, the significance of postoperative CKD remains controversial. Over the past several years, the definition and staging of CKD have undergone important refinements. The duration and etiology of CKD have become important components in evaluating the risks and outcomes of patients with CKD. Even the staging system has undergone modifications, recognizing differences in outcomes for patients with stage 3 CKD and stratifying these patients in stage 3a and stage 3b CKD.[5]

The significance of new-onset CKD following surgery, particularly moderate CKD (stage 3a) remains uncertain. Numerous studies (mainly retrospective cohort studies) have demonstrated non-oncologic and overall survival benefits in patients treated with PN.[247,389] The findings have been criticized since the only randomized trial comparing RN with PN failed to demonstrate an overall survival advantage in those undergoing PN, despite a substantial reduction in the incidence of moderate renal dysfunction (eGFR <60 mL/min/1.73m^2).[3] Furthermore, very few patients went on to develop stage 4 or 5 CKD, underscoring the fact that baseline kidney function may be more important than treatment type in many circumstances.

Kidney Disease: Improving Global Outcomes (KDIGO) guidelines acknowledge that the implications of CKD are dependent not only on the GFR (stage of CKD), but also on the cause of CKD (renal damage vs. volume loss) and the existing comorbid conditions.[5] In patients with SRMs, the development of new-onset CKD following treatment is likely multifactorial, with causes including intrinsic renal parenchymal damage, surgical loss of renal volume, as well as comorbid conditions. In such patients, the consequences of kidney disease can be expected to be greater than kidney donors, for instance, who have healthy renal parenchyma, have few comorbid conditions, and have a lower eGFR due to loss of an entire renal unit. For patients with poor renal reserve, extirpative surgery will likely further reduce their GFR postoperatively, and subsequently, increase their risk of end-stage renal disease and mortality. One must keep in mind that decline in kidney function over time is frequently nonlinear, and may not be apparent without extended longitudinal follow-up. Therefore, it may take years before the impact of surgical treatment is recognized.

6.10.12 Conclusion

Proper treatment selection for SRMs is dependent on assessing oncologic risk along with renal functional risk. In some patients, the consequences from renal functional decline following treatment may be worse than the malignant potential of the tumour. Baseline renal function and tumour characteristics, such as nephrometry, should be carefully assessed prior to treatment in all patients with SRMs, as they have a significant role in the development of CKD following treatment. For patients

with low renal reserve, additional tests beyond serum creatinine or creatinine-based formulas may be required in order to allow for an appropriate treatment that maximizes kidney functional outcomes and minimizes the risk of complications from CKD. [**LOE 3, GOR C**]

6.11 Absolute, Relative, and Elective Indications for Nephron-Sparing Management of the SRM

6.11.1 Introduction/evolution of definitions

Over the last 3 to 4 decades, increasing utilization of nephron-sparing surgery (NSS) has been spurred by a combination of factors: increased understanding of the biology of RCC and the deleterious consequences of renal insufficiency, improvements in techniques and outcomes,[390,391] as well as an increase in the proportion of smaller renal masses discovered incidentally.[392,393] As outcomes have improved, and our understanding of physiologic and oncologic processes has increased, there has been a refinement in the indications for NSS.[242] The purpose of this section is to describe these evolving indications in a historical context, focusing on expanding utilization and the changing definitions of indications over time, which have resulted from our increased understanding of the biological processes involved.

6.11.2 Historical background

The reintroduction of PN for cortical lesions in the late 1970s and early 1980s with reproducible outcomes and decreased morbidity was pioneered by Puigvert,[394] Novick,[395] Schiff,[396] Zincke,[397] and Srinivas,[398] among others. They applied knowledge from renal ischemia studies, renovascular reconstruction techniques, and oncologic principles to initially treat patients with *imperative indications,* defined as tumour in a solitary kidney, bilateral synchronous renal masses, or patients with known *renal insufficiency,* defined as an elevated serum creatinine.[394–398]

The reproducibility of these early outcomes, in addition to increasing the proportion of incidentally discovered SRMs due to the expanding application of ultrasonography and cross-sectional imaging modalities (MRI and CT), ultimately spurred the utilization of NSS for smaller renal masses in an elective setting, first in the setting of clinical T1 tumours,[327,399,400] and now, increasingly for larger-sized masses.[242,401–405]

Initially, indications for NSS were classified as *imperative/mandatory,* defined as tumour in a solitary kidney, synchronous renal masses, and pre-existing chronic kidney insufficiency, and *elective,* defined as having a normal contralateral kidney and/or renal function.[394–398] With increasing experience in and application of NSS, an intermediate class of indications, termed *relative,* was coined in the early 1990s.[406] Initially, this category was composed of patients who, while having normal renal function overall, were at increased risk due to the contralateral kidney having a history of recurrent infection,

stone burden, and/or obstruction.[407,408] Over time, this latter category has broadened as refinement of our understanding of the risk factors, and progression and sequelae of CKD has developed,[373,387,409,410] thus adding a component of medical risk to pre-existing criteria[411–414] while also broadening the scope of what would be considered a relative and imperative indication.[415–417]

6.11.3 Broadening the definition of relative criteria

In 2005, Go *et al.* published their seminal study, which correlated progressively increasing risk with declining kidney function.[354] Further works in the urologic literature demonstrate that a significant proportion of patients presenting for renal surgery with a cortical tumour and with normal creatinine actually fit into the pre-existing CKD stage 3 category, expanding the proportion of patients with imperative indications for NSS.[373,417]

The realm of relative indications has expanded as our understanding of the risk factors and drivers for chronic renal insufficiency has increased. It now encompasses patients with normal renal function (eGFR >60), but with risk factors for renal degeneration, including, but not limited to, morbid obesity (body mass index [BMI] ≥40 kg/m^2), diabetes mellitus with sequelae (proteinuria, neuropathy), and morbid/severe hypertension (requiring ≥3 antihypertensive agents for stable blood pressure control).[392,414,415] In addition, the traditional anatomical/surgical criteria of a morphologically abnormal kidney (significant stone burden, history of prior infarcts/recurrent pyelonephritis, abscess, multiple access procedures) may be augmented by quantitative renal functional findings, whereby the contralateral kidney had <40% overall function or GFR of 30 on the preoperative renal scan.[418]

6.11.4 Moving forward: impact of surgically induced nephron loss on prognosis and a new synthesis

The publication of EORTC 30904, which revealed no difference in overall survival between RN and PN for RCC patients,[245] even in the setting of significantly improved renal function in the PN arm,[419] has raised questions about the impact of surgically induced nephron loss.[418] Indeed, despite the several valid criticisms of this study, this randomized clinical trial has called into question the emerging paradigms of NSS and called into question evolving assumptions about the salutary impact of nephron preservation at all costs, especially in the setting of larger tumours.[418]

Lane *et al.* examined the impact of surgically induced stage 3 CKD (eGFR <60) and medically induced stage 3 CKD in a cohort of over 4,000 patients. They found a significantly greater decrement in eGFR/year in the medical cohort.[420] Subsequent work from Lane *et al.*, and other groups with longer follow-ups, confirms the durability of these findings, yet suggests a subgroup of patients who nonetheless develop further functional decline after surgically induced CKD—with a postoperative eGFR value of 45 being the threshold at which surgically induced nephron loss significantly decreases overall survival, and with pre-existing medical risk factors and decreasing preoperative eGFR being independently associated with worsened overall survival.[421,422]

This work points to a further refining of the elective, relative, imperative criteria and to a subtle, yet important, shift in what may be considered relative criteria in particular. In the evolving paradigm, the relative criteria may be considered to be the anatomical factors—compromised contralateral

kidney (whether anatomically or by renal flow scan criteria)—in addition to the patients with medical risk factors for CKD and those who are at risk for development of postoperative eGFR after RN, but not PN. In this emerging paradigm, predictive models of renal function that rely on predicting the volume of spared parenchyma and incorporating the influence of pre-existing medical risk factors may play an increasingly important role.[423,424]

6.11.5 Conclusion

The definitions and criteria for utilization of NSS have undergone development, which has mirrored the evolving understanding of the biology of SRMs, as well as the consequences of renal insufficiency and the impact of surgically induced nephron loss. Further refinement of the criteria for nephron-sparing intervention is requisite, and will likely involve the incorporation of predictive models of volume of renal parenchymal preservation in different circumstances and algorithms that incorporate preserved volume and pre-existing factors that may drive renal insufficiency. [**LOE 4, GOR D**]

6.12 Summary of Consensus Statements

Proper treatment selection for small renal masses (SRMs) is dependent on assessing oncologic risk along with renal functional risk. In some patients, the consequences from renal functional decline following treatment may be worse than the malignant potential of the tumour.

Renal cell carcinoma (RCC) is both genetically and histologically heterogeneous; thus, establishing the biological risk of RCC upfront may spare surgical treatment and its potential complications.

The biological risk is multifactorial, including clinical factors (sex, comorbidities, age) and tumour-related factors (size, growth rate, appearance, location). While tumour size provides insight into the malignant potential of the SRM, the use of tumour growth kinetics as a surrogate for biological risk is more questionable, simply, because absence of growth does not rule out inherent aggressive features.

Assessment of tumour complexity, like the R.E.N.A.L. nephrometry scoring system and/or clinical nomograms integrating nephrometric variables with patient age and gender, may provide improved prediction.

In the last several decades, considerable progress has been made in the ability to characterize features of the cancer phenotype using PET/CT, though its utilization is still far from routine clinical practice.

With biopsy of the SRM becoming more popular, the emergence of genomics, biomarkers, and prognostic models will aid in the future risk stratification of the SRM, but still require validation.

Better understanding of the biological risk of the SRM will impact on the definitions and criteria for utilization of active surveillance, nephron-sparing surgery, or radical nephrectomy in the treatment of kidney cancer.

6.13 References

1. Tomaszewski JJ, Uzzo RG, Smaldone MC. Heterogeneity and renal mass biopsy: a review of its role and reliability. *Cancer Biol Med.* 2014;11(3):162–172.
2. Ljungberg B, Campbell SC, Choi HY, *et al.* The epidemiology of renal cell carcinoma. *Eur Urol.* 2011;60:615–621.
3. Kane CJ, Mallin K, Ritchey J, *et al.* Renal cell cancer stage migration: analysis of the National Cancer Data Base. *Cancer.* 2008;113:78–83.
4. Volpe A, Panzarella T, Rendon RA, *et al.* The natural history of incidentally detected small renal masses. *Cancer.* 2004;100:738–745.
5. Stakhovskyi O, Yap SA, Leveridge M, *et al.* Small renal mass: what the urologist needs to know for treatment planning and assessment of treatment results. *AJR Am J Roentgenol.* 2011;196(6):1267–1273.
6. Frank I, Blute ML, Cheville JC, *et al.* Solid renal tumors: an analysis of pathological features related to tumor size. *J Urol.* 2003;170:2217–2220.
7. Samplaski MK, Zhou M, Lane BR, *et al.* Renal mass sampling: an enlightened perspective. *Int J Urol.* 2011;18(1):5–19.
8. Jeldres C, Sun M, Liberman D, *et al.* Can renal mass biopsy assessment of tumor grade be safely substituted for by a predictive model? *J Urol.* 2009;182:2585–2589.
9. Lane BR, Samplaski MK, Herts BR, *et al.* Renal mass biopsy – a renaissance? *J Urol.* 2008;179:20–27.
10. Lane BR, Babineau D, Kattan MW, *et al.* A preoperative prognostic nomogram for solid enhancing renal tumors 7 cm or less amenable to partial nephrectomy. *J Urol.* 2007;178:429–434.
11. Gattuso P, Ramzy I, Truong LD, *et al.* Utilization of fine-needle aspiration in the diagnosis of metastatic tumors to the kidney. *Diagn Cytopathol.* 1999;21:35–38.
12. Rybicki FJ, Shu KM, Cibas ES, *et al.* Percutaneous biopsy of renal masses: sensitivity and negative predictive value stratified by clinical setting and size of masses. *AJR Am J Roentgenol.* 2003;180:1281–1287.
13. Reichelt O, Gajda M, Chyhrai A, *et al.* Ultrasound-guided biopsy of homogenous solid renal masses. *Eur Urol.* 2007;52:1421–1426.
14. Somani BK, Nabi G, Thorpe P, *et al.* Image-guided biopsy-diagnosed renal cell carcinoma: critical appraisal of technique and long-term follow-up. *Eur Urol.* 2007;51:1289–1295.
15. Schmidbauer J, Remzi M, Memarsadeghi M, *et al.* Diagnostic accuracy of computed tomography-guided percutaneous biopsy of renal masses. *Eur Urol.* 2008;53:1003–1011.
16. Volpe A, Mattar K, Finelli A, *et al.* Contemporary results of percutaneous biopsy of 100 small renal masses: a single center experience. *J Urol.* 2008;180:2333–2337.
17. Masoom S, Venkataraman G, Jensen J, *et al.* Renal FNA-based typing of renal masses remains a useful adjunctive modality: evaluation of 31 renal masses with correlative histology. *Cytopathology.* 2009;20:50–55.
18. Wang R, Wolf JS Jr, Wood DP Jr, *et al.* Accuracy of percutaneous core biopsy in management of small renal masses. *Urology.* 2009;73:586–590.
19. Johnson PT, Nazarian LN, Feld RI, *et al.* Sonographically guided renal mass biopsy: indications and efficacy. *J Ultrasound Med.* 2001;20:749–753.
20. Eshed I, Elias S, Sidi AA. Diagnostic value of CT-guided biopsy of indeterminate renal masses. *Clin Radiol.* 2004;59:262–267.
21. Neuzillet Y, Lechevallier E, Andre M, *et al.* Accuracy and clinical role of fine needle percutaneous biopsy with computerized tomography guidance of small (less than 4.0 cm) renal masses. *J Urol.* 2004;171:1802–1805.
22. Hara I, Miyake H, Hara S, *et al.* Role of percutaneous image-guided biopsy in the evaluation of renal masses. *Urol Int.* 2001;67:199–202.
23. Volpe A, Kachura JR, Geddie WR, *et al.* Techniques, safety and accuracy of sampling of renal tumors by fine needle aspiration and core biopsy. *J Urol.* 2007;178:379–386.

24. Caoili EM, Bude RO, Higgins EJ, *et al.* Evaluation of sonographically guided percutaneous core biopsy of renal masses. *AJR Am J Roentgenol*. 2002;179:373–378.

25. Vasudevan A, Davies RJ, Shannon BA, *et al.* Incidental renal tumours: the frequency of benign lesions and the role of preoperative core biopsy. *BJU Int.* 2006;97:946–949.

26. Lebret T, Poulain JE, Molinie V, *et al.* Percutaneous core biopsy for renal masses: indications, accuracy and results. *J Urol*. 2007;178:1184–1188.

27. Volpe A, Finelli A, Gill IS, *et al.* Rationale for percutaneous biopsy and histologic characterisation of renal tumours. *Eur Urol*. 2012;62:491–504.

28. Silverman SG, Gan YU, Mortele KJ, *et al.* Renal masses in the adult patient: the role of percutaneous biopsy. *Radiology*. 2006;240:6–22.

29. Mullins JK, Rodriguez R. Renal cell carcinoma seeding of a percutaneous biopsy tract. *Can Urol Assoc J.* 2013;7:E176–179.

30. Herts BR, Baker ME. The current role of percutaneous biopsy in the evaluation of renal masses. *Semin Urol Oncol*. 1995;13:254–261.

31. Garcia-Solano J, Acosta-Ortega J, Perez-Guillermo M, *et al.* Solid renal masses in adults: image-guided fine-needle aspiration cytology and imaging techniques – "two heads better than one?". *Diagn Cytopathol.* 2008;36:8–12.

32. Kümmerlin IP, ten Kate FJ, Wijkstra H, *et al.* Changes in the stage and surgical management of renal tumours during 1995-2005: an analysis of the Dutch national histopathology registry. *BJU Int.* 2008;102(8):946–951.

33. Breda A, Treat EG, Haft-Candell L, *et al.* Comparison of accuracy of 14-, 18- and 20-G needles in ex-vivo renal mass biopsy: a prospective, blinded study. *BJU Int.* 2010;105:940–945.

34. Wood BJ, Khan MA, McGovern F, *et al.* Imaging guided biopsy of renal masses: indications, accuracy and impact on clinical management. *J Urol*. 1999;161:1470–1474.

35. Veltri A, Garetto I, Tosetti I, *et al.* Diagnostic accuracy and clinical impact of imaging-guided needle biopsy of renal masses. Retrospective analysis on 150 cases. *Eur Radiol.* 2011;21:393–401.

36. Dechet CB, Zincke H, Sebo TJ, *et al.* Prospective analysis of computerized tomography and needle biopsy with permanent sectioning to determine the nature of solid renal masses in adults. *J Urol.* 2003;169:71–74.

37. Richter F, Kasabian NG, Irwin RJ Jr, *et al.* Accuracy of diagnosis by guided biopsy of renal mass lesions classified indeterminate by imaging studies. *Urology.* 2000;55:348–352.

38. Lechevallier E, André M, Barriol D, *et al.* Fine-needle percutaneous biopsy of renal masses with helical CT guidance. *Radiology*. 2000;216:506–510.

39. Waldert M, Klatte T, Haitel A, *et al.* Hybrid renal cell carcinomas containing histopathologic features of chromophobe renal cell carcinomas and oncocytomas have excellent oncologic outcomes. *Eur Urol.* 2010;57:661–665.

40. Ginzburg S, Uzzo R, Al-Saleem T, *et al.* Coexisting hybrid malignancy in a solitary sporadic solid benign renal mass: implications for treating patients following renal biopsy. *J Urol*. 2014;191:296–300.

41. Ball MW, Gorin MA, Bhayani SB, *et al.* Preoperative predictors of malignancy and unfavorable pathology for clinical T1a tumors treated with partial nephrectomy: a multi-institutional analysis. *Urol Oncol.* 2015;33:112.e9–14.

42. Eggener SE, Rubenstein JN, Smith ND, *et al.* Renal tumors in young adults. *J Urol.* 2004;171:106–110.

43. Schachter LR, Bach AM, Snyder ME, *et al.* The impact of tumour location on the histological subtype of renal cortical tumours. *BJU Int.* 2006;98:63–66.

44. Venkatesh R, Weld K, Ames CD, *et al.* Laparoscopic partial nephrectomy for renal masses: effect of tumor location. *Urology.* 2006;67:1169–1174.

45. Rendon RA, Mason RJ, Kirkland S, *et al.* A classification tree for the prediction of benign versus malignant disease in patients with small renal masses. *Can J Urol*. 2014;21(4):7379–7384.

46. Walther MM, Choyke PL, Glenn G, *et al.* Renal cancer in families with hereditary renal cancer: prospective analysis of a tumor size threshold for renal parenchymal sparing surgery. *J Urol.* 1999;161(5):1475–1479.

47. Linehan WM, Srinivasan R, Schmidt LS. The genetic basis of kidney cancer: a metabolic disease. *Nat Rev Urol.* 2010;7(5):277–285.

48. Al-Hussain TO, Cheng L, Zhang S, *et al.* Tubulocystic carcinoma of the kidney with poorly differentiated foci: a series of 3 cases with fluorescence in situ hybridization analysis. *Hum Pathol.* 2013;44:1406–1411.

49. Yang XJ, Zhou M, Hes O, *et al.* Tubulocystic carcinoma of the kidney: clinicopathologic and molecular characterization. *Am J Surg Pathol.* 2008;32:177–187.

50. Zhou M, Yang XJ, Lopez JI, *et al.* Renal tubulocystic carcinoma is closely related to papillary renal cell carcinoma: implications for pathologic classification. *Am J Surg Pathol.* 2009;33:1840–1849.

51. Amin MB, MacLennan GT, Gupta R, *et al.* Tubulocystic carcinoma of the kidney: clinicopathologic analysis of 31 cases of a distinctive rare subtype of renal cell carcinoma. *Am J Surg Pathol.* 2009;33(3):384–392.

52. Azoulay S, Vieillefond A, Paraf F, *et al.* Tubulocystic carcinoma of the kidney: a new entity among renal tumors. *Virchows Arch.* 2007;451:905–909.

53. Zhan HQ, Chen H, Wang CF, *et al.* A case of PSF-TFE3 gene fusion in Xp11.2 renal cell carcinoma with melanotic features. *Hum Pathol.* 2015;46(3):476–481.

54. Ross H, Argani P. Xp11 translocation renal cell carcinoma. *Pathology.* 2010;42:369–373.

55. Alexiev BA. Renal cell carcinoma associated with Xp11.2 translocation/transcription factor E3 (TFE3) fusion. *J Cytol Histol.* 2013;4:173.

56. Tomlinson GE, Nisen PD, Timmons CF, *et al.* Cytogenetics of a renal cell carcinoma in a 17-month-old child. Evidence for Xp11.2 as a recurring breakpoint. *Cancer Genet Cytogenet.* 1991;57:11–17.

57. Armah HB, Parwani AV. Xp11.2 translocation renal cell carcinoma. *Arch Pathol Lab Med.* 2010;134:124–129.

58. Argani P, Antonescu CR, Illei PB, *et al.* Primary renal neoplasms with the ASPL-TFE3 gene fusion of alveolar soft part sarcoma: a distinctive tumor entity previously included among renal cell carcinomas of children and adolescents. *Am J Pathol.* 2001;159:179–192.

59. Argani P, Antonescu CR, Couturier J, *et al.* PRCC- TFE3 renal carcinomas: morphologic, immunohistochemical, ultrastructural, and molecular analysis of an entity associated with the t(X;1)(p11.2;q21). *Am J Surg Pathol.* 2002;26:1553–1566.

60. Argani P, Lal P, Hutchinson B, *et al.* Aberrant nuclear immunoreactivity for TFE3 in neoplasms with TFE3 gene fusions: a sensitive and specific immunohistochemical assay. *Am J Surg Pathol.* 2003;27:750–761.

61. Argani P, Ladanyi M. Translocation carcinomas of the kidney. *Clin Lab Med.* 2005;25:363–378.

62. Kuroda N, Mikami S, Pan CC, *et al.* Review of renal carcinoma associated with Xp11.2 translocations/TFE3 gene fusions with focus on pathobiological aspect. *Histol Histopathol.* 2012;27:133–140.

63. Martignoni G, Pea M, Gobbo S, *et al.* Cathepsin-K immunoreactivity distinguishes MiTF/TFE family renal translocation carcinomas from other renal carcinomas. *Mod Pathol.* 2009:22:1016–1022.

64. Zhong M, De Angelo P, Osborne L, *et al.* Translocation renal cell carcinomas in adults: a single-institution experience. *Am J Surg Pathol.* 2012;36:654–662.

65. Malouf GG, Camparo P, Oudard S, *et al.* Targeted agents in metastatic Xp11 translocation/TFE3 gene fusion renal cell carcinoma (RCC): a report from the Juvenile RCC Network. *Ann Oncol.* 2010;21:1834–1838.

66. Klatte T, Streubel B, Wrba F, *et al.* Renal cell carcinoma associated with transcription factor E3 expression and Xp11.2 translocation: incidence, characteristics, and prognosis. *Am J Clin Pathol.* 2012;137:761–768.

67. Liu K, Xie P, Peng W, *et al.* Renal carcinomas associated with Xp11.2 translocations/TFE3 gene fusions: findings on MRI and computed tomography imaging. *J Magn Reson Imaging.* 2014;40:440–447.

68. Eble JN, Sauter G, Epstein JI, *et al.* Pathology and genetics of tumours of the urinary system and male genital organs. Lyon, IARC Press, 2004, pp 37–38.

69. Lopez-Beltran A, Scarpelli M, Montironi R, *et al.* 2004 WHO classification of the renal tumors of the adults. *Eur Urol.* 2006;49:798–805.

70. Moch H. An overview of renal cell cancer: pathology and genetics. *Semin Cancer Biol.* 2012;23:3–9.

71. Shuch B, Amin A, Armstrong AJ, *et al.* Understanding pathologic variants of renal cell carcinoma: distilling therapeutic opportunities from biologic complexity. *Eur Urol.* 2015;67:85–97.

72. Shuch B, Said J, La Rochelle JC, *et al.* Cytoreductive nephrectomy for kidney cancer with sarcomatoid histology—is up-front resection indicated and, if not, is it avoidable? *J Urol.* 2009;182:2164–2171.

73. Shuch B, Bratslavsky G, Shih J, *et al.* Impact of pathological tumour characteristics in patients with sarcomatoid renal cell carcinoma. *BJU Int.* 2012;109:1600–1606.

74. Abel EJ, Culp SH, Matin SF, *et al.* Percutaneous biopsy of primary tumor in metastatic renal cell carcinoma to predict high risk pathological features: comparison with nephrectomy assessment. *J Urol.* 2010;184(5):1877–1881.

75. Tomic D, Wood LS, Gallager E, *et al.* Metastatic Sarcomatoid Renal Cell Carcinoma Treated With mTOR-Targeted Therapy. Kidney Cancer Symposium; 2010; Chicago, IL.

76. De Peralta-Venturina M, Moch H, Amin M, *et al.* Sarcomatoid differentiation in renal cell carcinoma: a study of 101 cases. *Am J Surg Pathol.* 2001;25:275–284.

77. Pierorazio PM, Johnson MH, Ball MW, *et al.* Five-year analysis of a multi-institutional prospective clinical trial of delayed intervention and surveillance for small renal masses: the DISSRM registry. *Eur Urol.* 2015;68(3):408–415.

78. Kunkle DA, Egleston BL, Uzzo RG. Excise, ablate or observe: the small renal mass dilemma—a meta-analysis and review. *J Urol.* 2008;179:1227–1233.

79. Chawla SN, Crispen PL, Hanlon AL, *et al.* The natural history of observed enhancing renal masses: meta-analysis and review of the world literature. *J Urol.* 2006;175:425–431.

80. Smaldone MC, Kutikov A, Egleston BL, *et al.* Small renal masses progressing to metastases under active surveillance: a systematic review and pooled analysis. *Cancer.* 2012;118:997–1006.

81. Heng DY, Xie W, Regan MM, *et al.* Prognostic factors for overall survival in patients with metastatic renal cell carcinoma treated with vascular endothelial growth factor-targeted agents: results from a large, multicenter study. *J Clin Oncol.* 2009;27:5794–5799.

82. Dalgliesh GL , Furge K , Greenman C, *et al.* Systematic sequencing of renal carcinoma reveals inactivation of histone modifying genes. *Nature.* 2010;463(7279):360–363.

83. Ramakrishnan S, Ellis L, Pili R. Histone modifications: implications in renal cell carcinoma. *Epigenomics.* 2013;5:453–462.

84. Srinivasan R, Ricketts CJ, Sourbier C, *et al.* New strategies in renal cell carcinoma: targeting the genetic and metabolic basis of disease. *Clin Cancer Res.* 2015;1:21:10–17.

85. Sun M, Shariat SF, Cheng C, *et al.* Prognostic factors and predictive models in renal cell carcinoma: a contemporary review. *Eur Urol.* 2011;60:644–661.

86. Tang PA, Vickers MM, Heng DY. Clinical and molecular prognostic factors in renal cell carcinoma: what we know so far. *Hematol Oncol Clin North Am.* 2011;25:871–891.

87. Amend B, Hennenlotter J, Scharpf M, *et al.* Akt signalling parameters are different in oncocytomas compared to renal cell carcinoma. *World J Urol.* 2012;30:353–359.

88. Audenet F, Yates DR, Cancel-Tassin G, *et al.* Genetic pathways involved in carcinogenesis of clear cell renal cell carcinoma: genomics towards personalized medicine. *BJU Int.* 2012;109:1864–1870.

89. Crispen PL, Boorjian SA, Lohse CM, *et al.* Outcomes following partial nephrectomy by tumor size. *J Urol.* 2008;180(5):1912–1917.

90. Thompson RH, Kurta JM, Kaag M, *et al.* Tumor size is associated with malignant potential in renal cell carcinoma cases. *J Urol.* 2009;181(5):2033–2036.

91. Crispen PL, Viterbo R, Boorjian SA, *et al.* Natural history, growth kinetics, and outcomes of untreated clinically localized renal tumors under active surveillance. *Cancer.* 2009;115(13):2844–2852.

92. Mason RJ, Abdolell M, Trottier G, *et al.* Growth kinetics of renal masses: analysis of a prospective cohort of patients undergoing active surveillance. *Eur Urol.* 2011;59:863–867.

93. Beisland C, Hjelle KM, Reisaeter LA, *et al.* Observation should be considered as an alternative in management of renal masses in older and comorbid patients. *Eur Urol.* 2009;55:1419–1427.

94. Crispen PL, Soljic A, Stewart G, *et al.* Enhancing renal tumors in patients with prior normal abdominal imaging: further insight into the natural history of renal cell carcinoma. *J Urol.* 2012;188(4):1089–1093.

95. Kutikov A, Uzzo RG. The R.E.N.A.L. nephrometry score: a comprehensive standardized system for quantitating renal tumor size, location and depth. *J Urol.* 2009;182(3):844–853.

96. Matsumoto R, Abe T, Shinohara N, *et al.* RENAL nephrometry score is a predictive factor for the annual growth rate of renal mass. *Int J Urol.* 2014;21(6):549–552.

97. Mehrazin R, Smaldone MC, Egleston B, *et al.* Is anatomic complexity associated with renal tumor growth kinetics under active surveillance? *Urol Oncol.* 2015;33(4):167.e7–12.

98. Jewett MA, Mattar K, Basiuk J, *et al.* Active surveillance of small renal masses: progression patterns of early stage kidney cancer. *Eur Urol* 2011;60(1):39–44.

99. Crispen PL, Wong YN, Greenberg RE, *et al.* Predicting growth of solid renal masses under active surveillance. *Urol Oncol.* 2008;26(5):555–559.

100. Rosales JC, Haramis G, Moreno J, *et al.* Active surveillance for renal cortical neoplasms. *J Urol.* 2010;183(5):1698–1702.

101. Schiavina R, Borghesi M, Dababneh H, *et al.* Small renal masses managed with active surveillance: predictors of tumor growth rate after long-term follow-up. *Clin Genitourin Cancer.* 2015;13(2):e87–92.

102. Dorin R, Jackson M, Cusano A, *et al.* Active surveillance of renal masses: an analysis of growth kinetics and clinical outcomes stratified by radiological characteristics at diagnosis. *Int Braz J Urol.* 2014;40(5):627–636.

103. Kurup AN, Thompson RH, Leibovich BC, *et al.* Renal oncocytoma growth rates before intervention. *BJU Int.* 2012;110(10):1444–1448.

104. Kawaguchi S, Fernandes KA, Finelli A, *et al.* Most renal oncocytomas appear to grow: observations of tumor kinetics with active surveillance. *J Urol.* 2011;186(4):1218–1222.

105. Cancer Genome Atlas Research N. Comprehensive molecular characterization of clear cell renal cell carcinoma. *Nature.* 2013;499:43–49.

106. Davis CF, Ricketts CJ, Wang M, *et al.* The somatic genomic landscape of chromophobe renal cell carcinoma. *Cancer Cell.* 2014;26:319–330.

107. El-Heliebi A, Kroneis T, Zohrer E, *et al.* Are morphological criteria sufficient for the identification of circulating tumor cells in renal cancer? *J Transl Med.* 2013;11:214.

108. Bluemke K, Bilkenroth U, Meye A, *et al.* Detection of circulating tumor cells in peripheral blood of patients with renal cell carcinoma correlates with prognosis. *Cancer Epidemiol Biomarkers Prev.* 2009;18:2190–2194.

109. Morrissey JJ, Mobley J, Figenshau RS, *et al.* Urine aquaporin 1 and perilipin 2 differentiate renal carcinomas from other imaged renal masses and bladder and prostate cancer. *Mayo Clin Proc.* 2015;90:35–42.

110. Gilbert SM, Whitson JM, Mansukhani M, *et al.* Detection of carbonic anhydrase-9 gene expression in peripheral blood cells predicts risk of disease recurrence in patients with renal cortical tumors. *Urology.* 2006;67:942–945.

111. Bui MH, Seligson D, Han KR, *et al.* Carbonic anhydrase IX is an independent predictor of survival in advanced renal clear cell carcinoma: implications for prognosis and therapy. *Clin Cancer Res.* 2003;9:802–811.

112. Hoffmann NE, Sheinin Y, Lohse CM, *et al.* External validation of IMP3 expression as an independent prognostic marker for metastatic progression and death for patients with clear cell renal cell carcinoma. *Cancer.* 2008;112:1471–1479.

113. Jiang Z, Chu PG, Woda BA, *et al.* Analysis of RNA-binding protein IMP3 to predict metastasis and prognosis of renal-cell carcinoma: a retrospective study. *Lancet Oncol.* 2006;7:556–564.

114. White NM, Masui O, Desouza LV, *et al.* Quantitative proteomic analysis reveals potential diagnostic markers and pathways involved in pathogenesis of renal cell carcinoma. *Oncotarget.* 2014;5:506–518.

115. Parker AS, Leibovich BC, Lohse CM, *et al.* Development and evaluation of BioScore: a biomarker panel to enhance prognostic algorithms for clear cell renal cell carcinoma. *Cancer.* 2009;115:2092–2103.

116. Krambeck AE, Dong H, Thompson RH, *et al.* Survivin and b7-h1 are collaborative predictors of survival and represent potential therapeutic targets for patients with renal cell carcinoma. *Clin Cancer Res.* 2007;13:1749–1756.

117. Byun SS, Yeo WG, Lee SE, *et al.* Expression of survivin in renal cell carcinomas: association with pathologic features and clinical outcome. *Urology.* 2007;69:34–37.

118. Parker AS, Kosari F, Lohse CM, *et al.* High expression levels of survivin protein independently predict a poor outcome for patients who undergo surgery for clear cell renal cell carcinoma. *Cancer.* 2006;107:37–45.

119. Ganti S, Taylor SL, Kim K, *et al.* Urinary acylcarnitines are altered in human kidney cancer. *Int J Cancer.* 2012;130:2791–2800.

120. Mustafa A, Gupta S, Hudes GR, *et al.* Serum amino acid levels as a biomarker for renal cell carcinoma. *J Urol.* 2011;186:1206–1212.

121. Hoque MO, Begum S, Topaloglu O, *et al.* Quantitative detection of promoter hypermethylation of multiple genes in the tumor, urine, and serum DNA of patients with renal cancer. *Cancer Res.* 2004;64:5511–5517.

122. Battagli C, Uzzo RG, Dulaimi E, *et al.* Promoter hypermethylation of tumor suppressor genes in urine from kidney cancer patients. *Cancer Res.* 2003;63:8695–8699.

123. Ibragimova I, Slifker MJ, Maradeo ME, *et al.* Genome-wide promoter methylome of small renal masses. *PLoS One.* 2013;8:e77309.

124. Slater AA, Alokail M, Gentle D, *et al.* DNA methylation profiling distinguishes histological subtypes of renal cell carcinoma. *Epigenetics.* 2013;8:252–267.

125. Lasseigne BN, Burwell TC, Patil MA, *et al.* DNA methylation profiling reveals novel diagnostic biomarkers in renal cell carcinoma. *BMC Med.* 2014;12:235.

126. Costa VL, Henrique R, Ribeiro FR, *et al.* Quantitative promoter methylation analysis of multiple cancer-related genes in renal cell tumors. *BMC Cancer.* 2007;7:133.

127. Brooks SA, Brannon AR, Parker JS, *et al.* ClearCode34: A prognostic risk predictor for localized clear cell renal cell carcinoma. *Eur Urol.* 2014;66:77–84.

128. White NM, Bao TT, Grigull J, *et al.* miRNA profiling for clear cell renal cell carcinoma: biomarker discovery and identification of potential controls and consequences of miRNA dysregulation. *J Urol.* 2011;186:1077–1083.

129. Youssef YM, White NM, Grigull J, *et al.* Accurate molecular classification of kidney cancer subtypes using microRNA signature. *Eur Urol.* 2011;59:721–730.

130. Osanto S, Qin Y, Buermans HP, *et al.* Genome-wide microRNA expression analysis of clear cell renal cell carcinoma by next generation deep sequencing. *PLoS One.* 2012;7:e38298.

131. Redova M, Poprach A, Nekvindova J, *et al.* Circulating miR-378 and miR-451 in serum are potential biomarkers for renal cell carcinoma. *J Transl Med.* 2012;10:55.

132. Wang C, Hu J, Lu M, *et al.* A panel of five serum miRNAs as a potential diagnostic tool for early-stage renal cell carcinoma. *Sci Rep.* 2015;5:7610.

133. Jakupciak JP, Maragh S, Markowitz ME, *et al.* Performance of mitochondrial DNA mutations detecting early stage cancer. *BMC Cancer.* 2008;8:285.

134. Ashida S, Okuda H, Chikazawa M, *et al.* Detection of circulating cancer cells with von Hippel-Lindau gene mutation in peripheral blood of patients with renal cell carcinoma. *Clin Cancer Res.* 2000;6(10):3817–3822.

135. Vieira J, Henrique R, Ribeiro FR, *et al.* Feasibility of differential diagnosis of kidney tumors by comparative genomic hybridization of fine needle aspiration biopsies. *Genes Chromosomes Cancer.* 2010;49(10):935–947.

136. Barocas DA, Mathew S, DelPizzo JJ, *et al.* Renal cell carcinoma sub-typing by histopathology and fluorescence in situ hybridization on a needle-biopsy specimen. *BJU Int.* 2007;99(2):290–295.

137. Gill IS, Aron M, Gervais DA, *et al.* Clinical practice. Small renal mass. *N Engl J Med.* 2010;362(7):624–634.

138. Jayson M, Sanders H. Increased incidence of serendipitously discovered renal cell carcinoma. *Urology.* 1998;51(2):203–205.

139. Kang SK, Huang WC, Pandharipande PV, *et al.* Solid renal masses: what the numbers tell us. *AJR Am J Roentgenol.* 2014;202(6):1196–1206.

140. American College of Radiology. ACR Appropriateness Criteria®: indeterminate renal mass. 2014. p. 1–11. Available: http://www.acr.org/~/media/ACR/Documents/Appcriteria/Diagnostic/IndeterminateRenalMasses.pdf; Accessed: July 7, 2015.

141. Young JR, Margolis D, Sauk S, *et al.* Clear cell renal cell carcinoma: discrimination from other renal cell carcinoma subtypes and oncocytoma at multiphasic multidetector CT. *Radiology.* 2013;267(2):444–453.

142. Zhang J, Lefkowitz RA, Ishill NM, *et al.* Solid renal cortical tumors: differentiation with CT. *Radiology.* 2007;244(2):494–504.

143. Kim JK, Kim TK, Ahn HJ, *et al.* Differentiation of subtypes of renal cell carcinoma on helical CT scans. *AJR Am J Roentgenol*. 2002;178(6):1499–1506.

144. Simpson E, Patel U. Diagnosis of angiomyolipoma using computed tomography-region of interest < or =-10 HU or 4 adjacent pixels < or =-10 HU are recommended as the diagnostic thresholds. *Clin Radiol.* 2006;61(5):410–416.

145. Yang CW, Shen SH, Chang YH, *et al.* Are there useful CT features to differentiate renal cell carcinoma from lipid-poor renal angiomyolipoma? *AJR Am J Roentgenol*. 2013;201(5):1017–1028.

146. Bird VG, Kanagarajah P, Morillo G, *et al.* Differentiation of oncocytoma and renal cell carcinoma in small renal masses (<4 cm): the role of 4-phase computerized tomography. *World J Urol.* 2011;29(6):787–792.

147. Woo S, Cho JY, Kim SH, *et al.* Comparison of segmental enhancement inversion on biphasic MDCT between small renal oncocytomas and chromophobe renal cell carcinomas. *AJR Am J Roentgenol*. 2013;201(3):598–604.

148. McGahan JP, Lamba R, Fisher J, *et al.* Is segmental enhancement inversion on enhanced biphasic MDCT a reliable sign for the noninvasive diagnosis of renal oncocytomas? *AJR Am J Roentgenol*. 2011;197(4):W674–679.

149. O'Malley ME, Tran P, Hanbidge A, *et al.* Small renal oncocytomas: is segmental enhancement inversion a characteristic finding at biphasic MDCT? *AJR Am J Roentgenol*. 2012;199(6):1312–1315.

150. Choudhary S, Rajesh A, Mayer NJ, *et al.* Renal oncocytoma: CT features cannot reliably distinguish oncocytoma from other renal neoplasms. *Clin Radiol.* 2009;64(5):517–522.

151. Graser A, Johnson TR, Hecht EM, *et al.* Dual-energy CT in patients suspected of having renal masses: can virtual nonenhanced images replace true nonenhanced images? *Radiology.* 2009;252(2):433–440.

152. Kim S, Jain M, Harris AB, *et al.* T1 hyperintense renal lesions: characterization with diffusion-weighted MR imaging versus contrast-enhanced MR imaging. *Radiology.* 2009;251(3):796–807.

153. Zhang J, Tehrani YM, Wang L, *et al.* Renal masses: characterization with diffusion-weighted MR imaging–a preliminary experience. *Radiology.* 2008;247(2):458–464.

154. Yu X, Lin M, Ouyang H, *et al.* Application of ADC measurement in characterization of renal cell carcinomas with different pathological types and grades by 3.0T diffusion-weighted MRI. *Eur J Radiol.* 2012;81(11):3061–3066.

155. Rosenkrantz AB, Niver BE, Fitzgerald EF, *et al.* Utility of the apparent diffusion coefficient for distinguishing clear cell renal cell carcinoma of low and high nuclear grade. *AJR Am J Roentgenol.* 2010;195(5):W344–351.

156. Notohamiprodjo M, Sourbron S, Staehler M, *et al.* Measuring perfusion and permeability in renal cell carcinoma with dynamic contrast-enhanced MRI: a pilot study. *J Magn Reson Imaging.* 2010;31(2):490–501.

157. Sadowski EA, Bennett LK, Chan MR, *et al.* Nephrogenic systemic fibrosis: risk factors and incidence estimation. *Radiology* 2007;243(1):148–157.

158. American College of Radiology. ACR manual on contrast media: version 10.1. 2015. p. 1–129. Available: http://www.acr.org/quality-safety/resources/~/media/37D84428BF1D4E1B9A3A2918DA9E27A3.pdf/; Accessed: July 9, 2015.

159. Amendola MA, Bree RL, Pollack HM, *et al.* Small renal cell carcinomas: resolving a diagnostic dilemma. *Radiology.* 1988;166(3):637–641.

160. Siemer S, Uder M, Humke U, *et al.* Value of ultrasound in early diagnosis of renal cell carcinoma. *Urologe A.* 2000;39(2):149–153.

161. American College of Radiology. ACR Appropriateness Criteria®: indeterminate renal mass. 2014. p. 1–11. Available: https://acsearch.acr.org/docs/69367/Narrative. Accessed: March 30, 2015.

162. Silverman SG, Israel GM, Herts BR, *et al.* Management of the incidental renal mass. *Radiology.* 2008;249(1):16–31.

163. Paspulati RM, Bhatt S. Sonography in Benign and Malignant Renal Masses. *Ultrasound Clinics.* 2006;1(1):25–41.

164. Middleton W, Kurtz A, and Hertzberg B. Ultrasound: The Requisites, 2nd ed. St. Louis, Mosby, 2004;244-252.

165. Hélénon O, Correas JM, Balleyguier C, *et al.* Ultrasound of renal tumors. *Eur Radiol.* 2001;11(10):1890–1901.

166. Yamashita Y, Takahashi M, Watanabe O, *et al.* Small renal cell carcinoma: pathologic and radiologic correlation. *Radiology.* 1992;184(2):493–498.

167. Jinzaki M, Tanimoto A, Narimatsu Y, *et al.* Angiomyolipoma: imaging findings in lesions with minimal fat. *Radiology.* 1997;205(2):497–502.

168. Schmidt T, Hohl C, Haage P, *et al.* Diagnostic accuracy of phase-inversion tissue harmonic imaging versus fundamental B-mode sonography in the evaluation of focal lesions of the kidney. *AJR Am J Roentgenol.* 2003;180(6):1639–1647.

169. Maturen KE, Nghiem HV, Caoili EM, *et al.* Renal mass core biopsy: accuracy and impact on clinical management. *AJR Am J Roentgenol.* 2007;188(2):563–570.

170. Machi J, Oishi AJ, Furumoto NL, *et al.* Sonographically guided radio frequency thermal ablation for unresectable recurrent tumors in the retroperitoneum and the pelvis. *J Ultrasound Med.* 2003;22(5):507–512.

171. Yu J, Liang P, Yu XL, *et al.* US-guided percutaneous microwave ablation of renal cell carcinoma: intermediate-term results. *Radiology.* 2012;263(3):900–908.

172. Davis K, Kielar A, Jafari K. Effectiveness of ultrasound-guided radiofrequency ablation in the treatment of 36 renal cell carcinoma tumours compared with published results of using computed tomography guidance. *Can Assoc Radiol J.* 2012;63:S23–32.

173. Raj GV, Back AM, Iasonos A, *et al.* Predicting the histology of renal masses using preoperative Doppler ultrasonography. *J Urol.* 2007;177(1):53–58.

174. Nightingale K. Acoustic radiation force impulse (ARFI) imaging: a review. *Curr Med Imaging Rev.* 2011;7(4):328–339.

175. Garra BS. Elastography: current status, future prospects, and making it work for you. *Ultrasound Q.* 2011;27(3):177–186.

176. Sporea I, Sirli RL. Hepatic elastography for the assessment of liver fibrosis—present and future. *Ultraschall Med.* 2012;33(6):550–558.

177. Chen S, Sanchez W, Callstrom MR, *et al.* Assessment of liver viscoelasticity by using shear waves induced by ultrasound radiation force. *Radiology.* 2013;266(3):964–970.

178. Syversveen T, Brabrand K, Midtvedt K, *et al.* Assessment of renal allograft fibrosis by acoustic radiation force impulse quantification—a pilot study. *Transpl Int.* 2011;24(1):100–105.

179. Asano K, Ogata A, Tanaka K, *et al.* Acoustic radiation force impulse elastography of the kidneys: is shear wave velocity affected by tissue fibrosis or renal blood flow? *J Ultrasound Med.* 2014;33(5):793–801.

180. Guo LH, Xu HX, Fu HJ, *et al.* Acoustic radiation force impulse imaging for noninvasive evaluation of renal parenchyma elasticity: preliminary findings. *PLoS One.* 2013;8(7):e68925.

181. Fahey BJ, Nelson RC, Bradway DP, *et al.* In vivo visualization of abdominal malignancies with acoustic radiation force elastography. *Phys Med Biol.* 2008;53(1):279–293.

182. Clevert DA, Stock K, Klein B, *et al.* Evaluation of acoustic radiation force impulse (ARFI) imaging and contrast-enhanced ultrasound in renal tumors of unknown etiology in comparison to histological findings. *Clin Hemorheol Microcirc.* 2009;43:95–107.

183. Tan S, Özcan MF, Tezcan F, *et al.* Real-time elastography for distinguishing angiomyolipoma from renal cell carcinoma: preliminary observations. *AJR AM J Roentgenol.* 2013;200(4):W369-375.

184. Keskin S, Güven S, Keskin Z, *et al.* Strain elastography in the characterization of renal cell carcinoma and angiomyolipoma. *Can Urol Assoc J.* 2015;9:e67–71.

185. Goldberg BB, Schultz SM, Baltarowich O, *et al.* Effectiveness of the "teaching the teachers" diagnostic US training program. *Acad Radiol.* 2001;8(11):1159–1167.

186. Barr RG. Off-label use of ultrasound contrast agents for abdominal imaging in the United States. *J Ultrasound Med.* 2013;32(1):7–12.

187. Bouakaz A, de Jong N. WFUMB safety symposium on echo-contrast agents: nature and types of ultrasound contrast agents. *Ultrasound Med Biol.* 2007;33(2):187–196.

188. Claudon M, Dietrich CF, Choi BI, *et al.* Guidelines and good clinical practice recommendations for contrast enhanced ultrasound (CEUS) in the liver - update 2012: a WFUMB-EFSUMB initiative in cooperation with representatives of AFSUMB, AIUM, ASUM, FLAUS and ICUS. *Ultrasound Med Biol.* 2013;39(2):187–210.

189. Eisenbrey JR, Forsberg F. Contrast-enhanced ultrasound for molecular imaging of angiogenesis. *Eur J Nucl Med Mol Imaging.* 2010;37:S138–146.

190. Wei K, Mulvagh SL, Carson L, *et al.* The safety of Definity and Optison for ultrasound image enhancement: a retrospective analysis of 78,383 administered contrast doses. *J Am Soc Echocardiogr.* 2008;21(11):1202–1206.

191. Main ML. Ultrasound contrast agent safety: from anecdote to evidence. *JACC Cardiovasc Imaging.* 2009;2(9):1057–1059.

192. Siracusano S, Bertolotto M, Cicilato S, *et al.* The current role of contrast-enhanced ultrasound (CEUS) imaging in the evaluation of renal pathology. *World J Urol.* 2011;29(5):633–638.

193. Barr R, Peterson C, Hindi A. Evaluation of indeterminate renal masses with contrast-enhanced US: a diagnostic performance study. *Radiology.* 2014;271(1):133–142.

194. Tamai H, Takiguchi Y, Oka M, *et al.* Contrast-enhanced ultrasonography in the diagnosis of solid renal tumors. *J Ultrasound Med.* 2005;24(12):1635–1640.

195. Eisenbrey JR, Shaw CM, Lyshchik A, *et al.* Contrast-enhanced subharmonic and harmonic ultrasound of renal masses undergoing percutaneous cryoablation. *Acad Radiol.* 2015;22(7):820–826.

196. Gerst S, Hann LE, Duan L, *et al.* Evaluation of renal masses with contrast-enhanced ultrasound: initial experience. *AJR Am J Roentgenol.* 2011;197(4):897–906.

197. Roy C, Gengler L, Sauer B, *et al.* Role of contrast enhanced US in the evaluation of renal tumors. *J Radiol.* 2008;89:1735–1744.

198. Xu ZF, Xu HX, Xie XY, *et al.* Renal cell carcinoma and renal angiomyolipoma: differential diagnosis with real-time contrast-enhanced ultrasonography. *J Ultrasound Med.* 2010;29(5):709–717.

199. Lassau N, Koscienlny S, Albiges L, *et al.* Metastatic renal cell carcinoma treated with sunitinib: early evaluation of treatment response using dynamic contrast-enhanced ultrasonography. *Clin Cancer Res.* 2010;16(4):1216–1225.

200. Johnson DB, Duchene DA, Taylor GD, *et al.* Contrast-enhanced ultrasound evaluation of radiofrequency ablation of the kidney: reliable imaging of the thermolesion. *J Endourol.* 2005;19(2):248–252.

201. Hoeffel C, Pousset M, Timsit MO, *et al.* Radiofrequency ablation of renal tumours: diagnostic accuracy of contrast-enhanced ultrasound for early detection of residual tumour. *Eur Radiol.* 2010;20(8):1812–1821.

202. Kong WT, Zhang WW, Guo HQ, *et al.* Application of contrast-enhanced ultrasonography after radiofrequency ablation for renal cell carcinoma: is it sufficient for assessment of therapeutic response? *Abdom Imaging.* 2011;36(3):342–347.

203. Li X, Liang P, Yu J, *et al.* Role of contrast-enhanced ultrasound in evaluating the efficiency of ultrasound guided percutaneous microwave ablation in patients with renal cell carcinoma. *Radiol Oncol.* 2013;47(4):398–404.

204. Wink MH, Laguna MP, Lagerveld BW, *et al.* Contrast-enhanced ultrasonography in the follow-up of cryoablation of renal tumours: a feasibility study. *BJU Int.* 2007;99(6):1371–1375.

205. Zhu Q, Shimizu T, Endo H, *et al.* Assessment of renal cell carcinoma after cryoablation using contrast-enhanced gray scale ultrasound: a case series. *Clin Imaging.* 2005;29(2):102–108.

206. Zeccolini G, Del Biondo D, Cicero C, *et al.* Comparison of contrast-enhanced ultrasound scan (CEUS) and MRI in the follow-up of cryoablation for small renal tumors. Experience on 25 cases. *Urologia.* 2014;81:1–8.

207. Israel GM, Bosniak MA. How I do it: evaluating renal masses. *Radiology.* 2005;236(2):441–450.

208. Bosniak MA, Rofsky NM. Problems in the detection and characterization of small renal masses. *Radiology.* 1996;198(3):638–641.

209. Hollingsworth JM, Miller DC, Daignault S, *et al.* Rising incidence of small renal masses: a need to reassess treatment effect. *J Natl Cancer Inst.* 2006;98(18):1331–1334.

210. Juweid ME, Cheson BD. Positron-emission tomography and assessment of cancer therapy. *N Engl J Med.* 2006;354(5):496–507.

211. Hevesy G. Some applications of isotopic indicators, in: Les Prix Nobel en 1940–44. Stockholm, Norstedt & Söner, 1946.

212. Bailey DL, Townsend DW, Valk PE, *et al.* Positron Emission Tomography: Basic Sciences. Secaucus, Springer-Verlag, 2005.

213. Bouchelouche K, Choyke PL. PET/computed tomography in renal, bladder, and testicular cancer. *PET Clin.* 2015;10(3):361–374.

214. Warburg O, Posener K, Negelein E. Ueber den stoffwechsel der tumoren. *Biochem Z.* 1924;152:319–344. [Article in German]

215. Weber WA, Schwaiger M, Avril N. Quantitative assessment of tumor metabolism using FDG-PET imaging. *Nucl Med Biol.* 2000;27(7):683–687.

216. Cox BL, Mackie TR, Eliceiri KW. The sweet spot: FDG and other 2-carbon glucose analogs for multi-modal metabolic imaging of tumor metabolism. *Am J Nucl Med Mol Imaging.* 2014;5(1):1–13.

217. Shields AF. Positron emission tomography measurement of tumor metabolism and growth: its expanding role in oncology. *Mol Imaging Biol.* 2006;8(3):141–150.

218. Glunde K, Jacobs MA, Bhujwalla ZM. Choline metabolism in cancer: implications for diagnosis and therapy. *Expert Rev Mol Diagn.* 2006;6(6):821–829.

219. Juhász C, Dwivedi S, Kamson DO, *et al.* Comparison of amino acid positron emission tomographic radiotracers for molecular imaging of primary and metastatic brain tumors. *Mol Imaging.* 2014;13.

220. Huang C, McConathy J. Radiolabeled amino acids for oncologic imaging. *J Nucl Med.* 2013;54(7):1007–1010.

221. Divgi CR, Pandit-Taskar N, Jungbluth AA, *et al.* Preoperative characterisation of clear-cell renal carcinoma using iodine-124-labelled antibody chimeric G250 (124I-cG250) and PET in patients with renal masses: a phase I trial. *Lancet Oncol.* 2007;8(4):304–310.

222. Divgi CR, Uzzo RG, Gatsonis C, *et al.* Positron emission tomography/computed tomography identification of clear cell renal cell carcinoma: results from the REDECT trial. *J Clin Oncol.* 2013;31(2):187–194.

223. Nyhan MJ, El Mashad SM, O'Donovan TR, *et al.* VHL genetic alteration in CCRCC does not determine de-regulation of HIF, CAIX, hnRNP A2/B1 and osteopontin. *Cell Oncol (Dordr).* 2011;34(3):225–234.

224. Jiang J, Zhao JH, Wang XL, *et al.* Correlation between carbonic anhydrase IX (CA-9), XII (CA-12) and hypoxia inducible factor-2α (HIF-2α) in breast cancer. *Neoplasma.* 2015;62(3):456–463.

225. Bachor R, Kotzerke J, Gottfried HW, *et al.* Positron emission tomography in diagnosis of renal cell carcinoma. *Urologe A.* 1996;35(2):146–150.

226. Goldberg MA, Mayo-Smith WW, Papanicolaou N, *et al.* FDG PET characterization of renal masses: preliminary experience. *Clin Radiol.* 1997;52(7):510–515.

227. Ramdave S, Thomas GW, Berlangieri SU, *et al.* Clinical role of F-18 fluorodeoxyglucose positron emission tomography for detection and management of renal cell carcinoma. *J Urol.* 2001;166(3):825–830.

228. Aide N, Cappele O, Bottet P, *et al.* Efficiency of [(18)F]FDG PET in characterising renal cancer and detecting distant metastases: a comparison with CT. *Eur J Nucl Med Mol Imaging.* 2003;30(9):1236–1245.

229. Kang DE, White RL, Zuger JH, *et al.* Clinical use of fluorodeoxyglucose F 18 positron emission tomography for detection of renal cell carcinoma. *J Urol.* 2004;171(5):1806–1809.

230. Aras M, Dede F, Ones T, *et al.* Is the value of FDG PET/CT in evaluating renal metastasis underestimated? A case report and review of the literature. *Mol Imaging Radionucl Ther.* 2013;22(3):109–112.

231. Shriki J, Murthy V, Brown J. Renal oncocytoma on 1-11C acetate positron emission tomography: case report and literature review. *Mol Imaging Biol.* 2006;8(4):208–211.

232. Kotzerke J, Linné C, Meinhardt M, *et al.* [1-(11)C]acetate uptake is not increased in renal cell carcinoma. *Eur J Nucl Med Mol Imaging.* 2007;34(6):884–888.

233. Buck AK, Bommer M, Stilgenbauer S, *et al.* Molecular imaging of proliferation in malignant lymphoma. *Cancer Res.* 2006;66(22):11055–11061.

234. Lam JS, Pantuck AJ, Belldegrun AS, *et al.* G250: a carbonic anhydrase IX monoclonal antibody. *Curr Oncol Rep.* 2005;7(2):109–115.

235. Divgi CR, O'Donoghue JA, Welt S, *et al.* Phase I clinical trial with fractionated radioimmunotherapy using 131I-labeled chimeric G250 in metastatic renal cancer. *J Nucl Med.* 2004;45(8):1412–1421.

236. Woodcock J. Assessing the clinical utility of diagnostics used in drug therapy. *Clin Pharmacol Ther.* 2010;88(6):765–773.

237. Simhan J, Smaldone MC, Tsai KJ, *et al.* Perioperative outcomes of robotic and open partial nephrectomy for moderately and highly complex renal lesions. *J Urol.* 2012;187(6):2000–2004.

238. Gorin MA, Ball MW, Pierorazio PM, *et al.* Outcomes and predictors of clinical T1 to pathological T3a tumor up-staging after robotic partial nephrectomy: a multi-institutional analysis. *J Urol.* 2013;190(5):1907–1911.

239. Satasivam P, Sengupta S, Rajarubendra N, *et al.* Renal lesions with low R.E.N.A.L nephrometry score are associated with more indolent renal cell carcinomas (RCCs) or benign histology: findings in an Australian cohort. *BJU Int.* 2012;109:44–47.

240. Khalifeh A, Autorino R, Hillyer SP, *et al.* Comparative outcomes and assessment of trifecta in 500 robotic and laparoscopic partial nephrectomy cases: a single surgeon experience. *J Urol.* 2013;189(4):1236–1242.

241. Porpiglia F, Bertolo R, Amparore D, *et al.* Margins, ischaemia and complications rate after laparoscopic partial nephrectomy: impact of learning curve and tumour anatomical characteristics. *BJU Int.* 2013;112(8):1125–1132.

242. Kopp RP, Mehrazin R, Palazzi KL, *et al.* Survival outcomes after radical and partial nephrectomy for clinical T2 renal tumours categorised by R.E.N.A.L. nephrometry score. *BJU Int.* 2014;114(5):708–718.

243. Thompson RH, Boorjian SA, Lohse CM, *et al.* Radical nephrectomy for pT1a renal masses may be associated with decreased overall survival compared with partial nephrectomy. *J Urol.* 2008;179(2):468–471.

244. Weight CJ, Larson BT, Fergany AF, *et al.* Nephrectomy induced chronic renal insufficiency is associated with increased risk of cardiovascular death and death from any cause in patients with localized cT1b renal masses. *J Urol.* 2010;183(4):1317–1323.

245. Van Poppel H, Da Pozzo L, Albrecht W, *et al.* A prospective, randomised EORTC intergroup phase 3 study comparing the oncologic outcome of elective nephron-sparing surgery and radical nephrectomy for low-stage renal cell carcinoma. *Eur Urol.* 2011;59(4):543–552.

246. Kim SP, Thompson RH, Boorjian SA, *et al.* Comparative effectiveness for survival and renal function of partial and radical nephrectomy for localized renal tumors: a systematic review and meta-analysis. *J Urol.* 2012;188(1):51–57.

247. Tan HJ, Norton EC, Ye Z, *et al.* Long-term survival following partial vs radical nephrectomy among older patients with early-stage kidney cancer. *JAMA.* 2012;307(15):1629–1635.

248. Tobert CM, Riedinger CB, Lane BR. Do we know (or just believe) that partial nephrectomy leads to better survival than radical nephrectomy for renal cancer? *World J Urol.* 2014;32(3):573–579.

249. Sharma N, O'Hara J, Novick AC, *et al.* Correlation between loss of renal function and loss of renal volume after partial nephrectomy for tumor in a solitary kidney. *J Urol.* 2008;179(4):1284–1288.

250. Lane BR, Babineau DC, Poggio ED, *et al.* Factors predicting renal functional outcome after partial nephrectomy. *J Urol.* 2008;180(6):2363–2368.

251. Simmons MN, Fergany AF, Campbell SC. Effect of parenchymal volume preservation on kidney function after partial nephrectomy. *J Urol.* 2011;186(2):405–410.

252. Simmons MN, Hillyer SP, Lee BH, *et al.* Diameter-axial-polar nephrometry: integration and optimization of R.E.N.A.L. and centrality index scoring systems. *J Urol.* 2012;188(2):384–390.

253. Mir MC, Campbell RA, Sharma N, *et al.* Parenchymal volume preservation and ischemia during partial nephrectomy: functional and volumetric analysis. *Urology.* 2013;82(2):263–268.

254. Simmons MN, Lieser GC, Fergany AF, *et al.* Association between warm ischemia time and renal parenchymal atrophy after partial nephrectomy. *J Urol.* 2013;189(5):1638–1642.

255. Tobert CM, Boelkins B, Culver S, *et al.* Surgeon assessment of renal preservation with partial nephrectomy provides information comparable to measurement of volume preservation with 3-dimensional image analysis. *J Urol.* 2014;191(5):1218–1224.

256. Bruner B, Breau RH, Lohse CM, *et al.* Renal nephrometry score is associated with urine leak after partial nephrectomy. *BJU Int.* 2011;108(1):67–72.

257. Hayn MH, Schwaab T, Underwood W, *et al.* RENAL nephrometry score predicts surgical outcomes of laparoscopic partial nephrectomy. *BJU Int.* 2011;108(6):876–881.

258. Weight CJ, Atwell TD, Fazzio RT, *et al.* A multidisciplinary evaluation of inter-reviewer agreement of the nephrometry score and the prediction of long-term outcomes. *J Urol.* 2011;186(4):1223–1228.

259. Mufarrij PW, Krane LS, Rajamahanty S, *et al.* Does nephrometry scoring of renal tumors predict outcomes in patients selected for robot-assisted partial nephrectomy? *J Endourol.* 2011;25(10):1649–1653.

260. Liu ZW, Olweny EO, Yin G, *et al.* Prediction of perioperative outcomes following minimally invasive partial nephrectomy: role of the R.E.N.A.L nephrometry score. *World J Urol.* 2013;31(5):1183–1189.

261. Simhan J, Smaldone MC, Tsai KJ, *et al.* Objective measures of renal mass anatomic complexity predict rates of major complications following partial nephrectomy. *Eur Urol.* 2011;60(4):724–730.

262. Kutikov A, Smaldone MC, Egleston BL, *et al.* Anatomic features of enhancing renal masses predict malignant and high-grade pathology: a preoperative nomogram using the RENAL nephrometry score. *Eur Urol.* 2011;60(2):241–248.

263. Wang HK, Zhu Y, Yao XD, *et al.* External validation of a nomogram using RENAL nephrometry score to predict high grade renal cell carcinoma. *J Urol.* 2012;187(5):1555–1560.

264. Rosevear HM, Gellhaus PT, Lightfoot AJ, *et al.* Utility of the RENAL nephrometry scoring system in the real world: predicting surgeon operative preference and complication risk. *BJU Int.* 2012;109(5):700–705.

265. Broughton GJ, Clark PE, Barocas DA, *et al.* Tumour size, tumour complexity, and surgical approach are associated with nephrectomy type in small renal cortical tumours treated electively. *BJU Int.* 2012;109(11):1607–1613.

266. Stroup SP, Palazzi K, Kopp RP, *et al.* RENAL nephrometry score is associated with operative approach for partial nephrectomy and urine leak. *Urology.* 2012;80(1):151–156.

267. Tobert CM, Kahnoski RJ, Thompson DE, *et al.* RENAL nephrometry score predicts surgery type independent of individual surgeon's use of nephron-sparing surgery. *Urology.* 2012;80(1):157–161.

268. Tomaszewski JJ, Smaldone MC, Mehrazin R, *et al.* Anatomic complexity quantitated by nephrometry score is associated with prolonged warm ischemia time during robotic partial nephrectomy. *Urology.* 2014;84(2):340–344.

269. Mayer WA, Godoy G, Choi JM, *et al.* Higher RENAL nephrometry score is predictive of longer warm ischemia time and collecting system entry during laparoscopic and robotic-assisted partial nephrectomy. *Urology.* 2012;79(5):1052–1056.

270. Altunrende F, Laydner H, Hernandez AV, *et al.* Correlation of the RENAL nephrometry score with warm ischemia time after robotic partial nephrectomy. *World J Urol.* 2013;31(5):1165–1169.

271. Sisul DM, Liss MA, Palazzi KL, *et al.* RENAL nephrometry score is associated with complications after renal cryoablation: a multicenter analysis. *Urology.* 2013;81(4):775–780.

272. Okhunov Z, Shapiro EY, Moreira DM, *et al.* R.E.N.A.L. nephrometry score accurately predicts complications following laparoscopic renal cryoablation. *J Urol.* 2012;188(5):1796–1800.

273. Schmit GD, Thompson RH, Kurup AN, *et al.* Usefulness of R.E.N.A.L. nephrometry scoring system for predicting outcomes and complications of percutaneous ablation of 751 renal tumors. *J Urol.* 2013;189(1):30–35.

274. Chang X, Liu T, Zhang F. *et al.* The comparison of R.E.N.A.L., PADUA and centrality index score in predicting perioperative outcomes and complications following laparoscopic radio frequency ablation of renal tumors. *J Urol.* 2015;194(4):897-902.

275. Reyes J, Canter D, Putnam S, *et al.* Thermal ablation of the small renal mass: case selection using the R.E.N.A.L.-nephrometry score. *Urol Oncol.* 2013;31(7):1292–1297.

276. Jung S, Min GE, Chung BI, *et al.* Risk factors for postoperative hemorrhage after partial nephrectomy. *Korean J Urol.* 2014;55(1):17–22.

277. Canter D, Kutikov A, Manley B, *et al.* Utility of the R.E.N.A.L. nephrometry scoring system in objectifying treatment decision-making of the enhancing renal mass. *Urology.* 2011;78(5):1089–1094.

278. Ellison JS, Montgomery JS, Hafez KS, *et al.* Association of RENAL nephrometry score with outcomes of minimally invasive partial nephrectomy. *Int J Urol.* 2013;20(6):564–570.

279. Lane BR, Golan S, Eggener S, *et al.* Differential use of partial nephrectomy for intermediate and high complexity tumors may explain variability in reported utilization rates. *J Urol.* 2013;189(6):2047–2053.

280. Tyritzis SI, Papadoukakis S, Katafigiotis I, *et al.* Implementation and external validation of preoperative aspects and dimensions used for an anatomical (PADUA) score for predicting complications in 74 consecutive partial nephrectomies. *BJU Int.* 2012;109(12):1813–1818.

281. Minervini A, Vittori G, Salvi M, *et al.* Analysis of surgical complications of renal tumor enucleation with standardized instruments and external validation of PADUA classification. *Ann Surg Oncol.* 2013;20(5):1729–1736.

282. Greco F. Implementation and external validation of preoperative aspects and dimensions used for an anatomical (padua) score for predicting complications in 74 consecutive partial nephrectomies. *BJU Int.* 2012;109(12):1818.

283. Desai MM, de Castro Abreu AL, Leslie S, *et al.* Robotic partial nephrectomy with superselective versus main artery clamping: a retrospective comparison. *Eur Urol.* 2014;66(4):713–719.

284. Samplaski MK, Hernandez A, Gill IS, *et al.* C-index is associated with functional outcomes after laparoscopic partial nephrectomy. *J Urol.* 2010;184(6):2259–2263.

285. Simmons MN, Ching CB, Samplaski MK, *et al.* Kidney tumor location measurement using the C index method. *J Urol.* 2010;183(5):1708–1713.

286. Leslie S, Gill IS, de Castro Abreu AL, *et al.* Renal tumor contact surface area: a novel parameter for predicting complexity and outcomes of partial nephrectomy. *Eur Urol.* 2014;66(14):884-893.

287. Tannus M, Goldman SM, and Andreoni C. Practical and intuitive surgical approach renal ranking to predict outcomes in the management of renal tumors: a novel score tool. *J Endourol.* 2014;28(4):487–492.

288. Wang L, Li M, Chen W, *et al.* Is diameter-axial-polar scoring predictive of renal functional damage in patients undergoing partial nephrectomy? An evaluation using technetium Tc 99m (^{99}Tcm) diethylene-triamine-penta-acetic acid (DTPA) glomerular filtration rate. *BJU Int.* 2013;111(8):1191–1198.

289. Maeda M, Funahashi Y, Sassa N, *et al.* Prediction of partial nephrectomy outcomes by using the diameter-axis-polar nephrometry score. *Int J Urol.* 2014;21(5):442–446.

290. Yoon YE, Choi KH, Lee KS, *et al.* Usefulness of the diameter-axial-polar nephrometry score for predicting perioperative parameters in robotic partial nephrectomy. *World J Urol.* 2015;33(6):841–845.

291. Hakky TS, Baumgarten AS, Allen B, *et al.* Zonal NePhRO scoring system: a superior renal tumor complexity classification model. *Clin Genitourin Cancer.* 2014;12(1):e13–18.

292. Simmons MN, Hillyer SP, Lee BH, *et al.* Functional recovery after partial nephrectomy: effects of volume loss and ischemic injury. *J Urol.* 2012;187(5):1667–1673.

293. Woldu SL, Thoreson GR, Okhunov Z, *et al.* Comparison of renal parenchymal volume preservation between partial nephrectomy, cryoablation, and radiofrequency ablation using 3D volume measurements. *J Endourol.* 2015;29(8):948-955.

294. Azhar RA, Metcalfe C, Gill IS. Anatomic partial nephrectomy: technique evolution. *Curr Opin Urol.* 2015;25(2):95–99.

295. Coll DM, Uzzo RG, Herts BR, *et al.* 3-dimensional volume rendered computerized tomography for preoperative evaluation and intraoperative treatment of patients undergoing nephron sparing surgery. *J Urol.* 1999;161(4):1097–1102.

296. Derweesh IH, Herts B, Novick AC. Three-dimensional image reconstruction for preplanning of renal surgery. *Urol Clin North Am.* 2003;30(3):515–528.

297. Gill IS, Patil MB, Abreu AL, *et al.* Zero ischemia anatomical partial nephrectomy: a novel approach. *J Urol.* 2012;187(3):807–814.

298. Ukimura O, Nakamoto M, Gill IS, *et al.* Three-dimensional reconstruction of renovascular-tumor anatomy to facilitate zero-ischemia partial nephrectomy. *Eur Urol.* 2012;61(1):211–217.

299. Shao P, Li P, Xu Y, *et al.* Application of combined computed tomography arteriography, venography, and urography in laparoscopic partial nephrectomy with segmental artery clamping. *Urology.* 2014;84(6):1361–1365.

300. Silberstein JL, Maddox MM, Dorsey P, *et al.* Physical models of renal malignancies using standard cross-sectional imaging and 3-dimensional printers: a pilot study. *Urology.* 2014;84(2):268–272.

301. Lagerveld BW, Brenninkmeijer M, van der Zee JA, *et al.* Can RENAL and PADUA nephrometry indices predict complications of laparoscopic cryoablation for clinical stage T1 renal tumors? *J Endourol.* 2014;28(4):464–471.

302. Kruck S, Anastasiadis AG, Walcher U, *et al.* Laparoscopic partial nephrectomy: risk stratification according to patient and tumor characteristics. *World J Urol.* 2012;30(5):639–646.

303. Kobayashi K, Saito T, Kitamura Y, *et al.* The RENAL nephrometry score and the PADUA classification for the prediction of perioperative outcomes in patients receiving nephron-sparing surgery: feasible tools to predict intraoperative conversion to nephrectomy. *Urol Int.* 2013;91(3):261–268.

304. Yeon JS, Son SJ, Lee YJ, *et al.* The nephrometry score: is it effective for predicting perioperative outcome during robot-assisted partial nephrectomy? *Korean J Urol.* 2014;55(4):254–259.

305. Esen T, Acar Ö, Musaog˘lu A, *et al.* Morphometric profile of the localised renal tumors managed either by open or robot-assisted nephron-sparing surgery: the impact of scoring systems on the decision making process. *BMC Urol.* 2013;13:63.

306. Bylund JR, Gayheart D, Fleming T, *et al.* Association of tumor size, location, R.E.N.A.L., PADUA and centrality index score with perioperative outcomes and postoperative renal function. *J Urol.* 2012;188(5):1684–1689.

307. Lavallée LT, Desantis D, Kamal F, *et al.* The association between renal tumour scoring systems and ischemia time during open partial nephrectomy. *Can Urol Assoc J.* 2013;7(3-4):E207-214.

308. Spaliviero M, Poon BY, Aras O, *et al.* Interobserver variability of R.E.N.A.L., PADUA, and centrality index nephrometry score systems. *World J Urol.* 2015;33(6):853–858.

309. Desantis D, Lavallée LT, Witiuk K, *et al.* The association between renal tumour scoring system components and complications of partial nephrectomy. *Can Urol Assoc J.* 2015;9:39–45.

310. Moreno-Alarcón C, Ramírez-Backhaus M, Pelechano-Gómez P, *et al.* Nephrometry scores: interobserver reproducibility and perioperative factors prediction. *Actas Urol Esp.* 2014;38(8):523–529.

311. Nisen H, Ruutu M, Glücker E, *et al.* Renal tumour invasion index as a novel anatomical classification predicting urological complications after partial nephrectomy. *Scand J Urol.* 2014;48(1):41–51.

312. Wang L, Wu Z, Ye H, *et al.* Correlations of tumor size, RENAL, centrality index, preoperative aspects and dimensions used for anatomical, and diameter-axial-polar scoring with warm ischemia time in a single surgeon's series of robotic partial nephrectomy. *Urology.* 2014;83(5):1075–1079.

313. Tobert CM, Shoemaker A, Kahnoski RJ, *et al.* Critical appraisal of first-generation renal tumor complexity scoring systems: creation of a second-generation model of tumor complexity. *Urol Oncol.* 2015;33(4):167.

314. Simmons MN, Hillyer SP, Lee BH, *et al.* Nephrometry score is associated with volume loss and functional recovery after partial nephrectomy. *J Urol.* 2012;188(1):39–44.

315. Rini BI, Plimack ER, Takagi T, *et al.* A phase II study of pazopanib in patients with localized renal cell carcinoma to optimize preservation of renal parenchyma. *J Urol.* 2015;194(2)297-303.

316. Durso TA, Carnell J, Turk TT, *et al.* Three-dimensional reconstruction volume: a novel method for volume measurement in kidney cancer. *J Endourol.* 2014;28(6):745–750.

317. Hew MN, Baseskioglu B, Barwari K, *et al.* Critical appraisal of the PADUA classification and assessment of the R.E.N.A.L. nephrometry score in patients undergoing partial nephrectomy. *J Urol.* 2011;186(1):42–46.

318. Kolla SB, Spiess PE, Sexton WJ. Interobserver reliability of the RENAL nephrometry scoring system. *Urology.* 2011;78(3):592–594.

319. Okhunov Z, Rais-Bahrami S, George AK, *et al.* The comparison of three renal tumor scoring systems: C-index, P.A.D.U.A., and R.E.N.A.L. nephrometry scores. *J Endourol.* 2011;25(12):1921–1924.

320. Golan S, Patel AR, Eggener SE, *et al.* The volume of nonneoplastic parenchyma in a minimally invasive partial nephrectomy specimen: predictive factors and impact on renal function. *J Endourol.* 2014;28(2):196–200.

321. Kotamarti S, Rothberg MB, Danzig MR, *et al.* Increasing volume of non-neoplastic parenchyma in partial nephrectomy specimens is associated with chronic kidney disease upstaging. *Clin Genitourin Cancer.* 2015;13(3):239–243.

322. Isotani S, Shimoyama H, Yokota I, *et al.* Novel prediction model of renal function after nephrectomy from automated renal volumetry with preoperative multidetector computed tomography (MDCT). *Clin Exp Nephrol.* 2015;19(5):974–981.

323. Takagi T, Mir MC, Campbell RA, *et al.* Predictors of precision of excision and reconstruction in partial nephrectomy. *J Urol.* 2014;192(1):30–35.

324. Mir MC, Ercole C, Takagi T, *et al.* Decline in renal function after partial nephrectomy: etiology and prevention. *J Urol.* 2015;193:1889–1898.

325. Choi KH, Yoon YE, Kim KH, *et al.* Contralateral kidney volume change as a consequence of ipsilateral parenchymal atrophy promotes overall renal function recovery after partial nephrectomy. *Int Urol Nephrol.* 2015;47(1):25–32.

326. Tobert CM, Takagi T, Liss MA, *et al.* Multicenter validation of surgeon assessment of renal preservation in comparison to measurement with 3D image analysis. *Urology.* 2015;85(3):534–538.

327. Campbell SC, Novick AC, Belldegrun A, *et al.* Guideline for management of the clinical T1 renal mass. *J Urol*. 2009;182(4):1271–1279.

328. Corcoran A, Smaldone MC, Kutikov A, *et al.* Addressing the evidence gap: randomized controlled trials for the surgical management of localized genitourinary malignancies. *Urol Oncol.* 2013;31(4):393–397.

329. Lane BR, Abouassaly R, Gao T, *et al.* Active treatment of localized renal tumors may not impact overall survival in patients aged 75 years or older. *Cancer.* 2010;116(13):3119–3126.

330. Arrontes DS, Aceñero MJF, González JIG, *et al.* Survival analysis of clear cell renal carcinoma according to the Charlson comorbidity index. *J Urol*. 2008;179(3):857–861.

331. Hollingsworth JM, Miller DC, Daignault S, *et al.* Five-year survival after surgical treatment for kidney cancer: a population-based competing risk analysis. *Cancer.* 2007;109(9):1763–1768.

332. Kutikov A, Egleston BL, Wong YN, *et al.* Evaluating overall survival and competing risks of death in patients with localized renal cell carcinoma using a comprehensive nomogram. *J Clin Oncol.* 2010;28(2):311–317.

333. Kutikov A, Egleston BL, Canter D, *et al.* Competing risks of death in patients with localized renal cell carcinoma: a comorbidity based model. *J Urol*. 2012;188(6):2077–2083.

334. Chow WB, Rosenthal RA, Merkow RP, *et al.* Optimal preoperative assessment of the geriatric surgical patient: a best practices guideline from the American College of Surgeons National Quality Improvement Program and the American Geriatrics Society. *J Am Coll Surg*. 2012;215(4):453–466.

335. McKibben MJ, Smith AB. Evaluation and management of the geriatric urologic oncology patient. *Curr Geriatr Rep*. 2015;4(1):7–15.

336. Wilson JR, Clarke MG, Ewings P, *et al.* The assessment of patient life-expectancy: how accurate are urologists and oncologists? *BJU Int.* 2005;95(6):794–798.

337. Charlson ME, Pompei P, Ales KL, *et al.* A new method of classifying comorbidity in longitudinal studies: development and validation. *J Chronic Dis*. 1987;40(5):373–383.

338. Oken MM, Creech RH, Tormey DC, *et al.* Toxity and response criteria of the Eastern Cooperative Oncology Group. Am *J Clin Oncol.* 1982;5(6):649–655.

339. Keats AS. The ASA classification of physical status—a recapitulation. *Anesthesiology.* 1978;49(4):233–236.

340. Stuck AE, Siu AL, Wieland GD, *et al.* Comprehensive geriatric assessment: a meta-analysis of controlled trials. *Lancet.* 1993;342(8878):1032–1036.

341. Audisio RA, Pope D, Ramesh HS, *et al.* Shall we operate? Preoperative assessment in elderly cancer patients (PACE) can help. A SIOG surgical task force prospective study. *Crit Rev Oncol Hematol.* 2008;65(2):156–163.

342. Fried LP, Tangen CM, Walston J, *et al.* Frailty in older adults: evidence for a phenotype. *J Gerontol A Biol Sci Med Sci*. 2001;56(3):M146–M156.

343. Makary MA, Segev DL, Pronovost PJ, *et al.* Frailty as a predictor of surgical outcomes in older patients. *J Am Coll Surg.* 2010;210(6):901–908.

344. Feng MA, McMillan DT, Crowell K, *et al.* Geriatric assessment in surgical oncology: a systematic review. *J Surg Res*. 2015;193(1):265–272.

345. Lamont EB, Christakis NA. Complexities in prognostication in advanced cancer: "to help them live their lives the way they want to". *JAMA.* 2003;290(1):98–104.

346. Kutikov A, Fossett LK, Ramchandani P, *et al.* Incidence of benign pathologic findings at partial nephrectomy for solitary renal mass presumed to be renal cell carcinoma on preoperative imaging. *Urology.* 2006;68(4):737–740.

347. Kunkle DA, Crispen PL, Li T, *et al.* Tumor size predicts synchronous metastatic renal cell carcinoma: implications for surveillance of small renal masses. *J Urol*. 2007;177(5):1692–1696.

348. Nguyen MM, Gill IS. Effect of renal cancer size on the prevalence of metastasis at diagnosis and mortality. *J Urol*. 2009;181(3):1020–1027.

349. Rothman J, Egleston B, Wong YN, *et al.* Histopathological characteristics of localized renal cell carcinoma correlate with tumor size: a SEER analysis. *J Urol*. 2009;181(1):29–33.

350. Blumenfeld AJ, Guru K, Fuchs GJ, *et al.* Percutaneous biopsy of renal cell carcinoma underestimates nuclear grade. *Urology.* 2010;76(3):610–613.

351. Halverson SJ, Kunju LP, Bhalla R. Accuracy of determining small renal mass management with risk stratified biopsies: confirmation by final pathology. *J Urol*. 2013;189(2):441–446.

352. Rothman J, Crispen PL, Wong YN, *et al.* Pathologic concordance of sporadic synchronous bilateral renal masses. *Urology.* 2008;72(1):138–142.

353. Bagrodia A, Harrow B, Liu ZW, *et al.* Evaluation of anatomic and morphologic nomogram to predict malignant and high-grade disease in a cohort of patients with small renal masses. *Urol Oncol.* 2014;32(1):37.e17–23.

354. Go AS, Chertow GM, Fan D, *et al.* Chronic kidney disease and the risks of death, cardiovascular events, and hospitalization. *N Engl J Med.* 2004;351(13):1296–1305.

355. Demirjian S, Lane BR, Derweesh IH, *et al*. Chronic kidney disease due to surgical removal of nephrons: relative rates of progression and survival. *J Urol*. 2014;192(4):1057–1062.

356. Stevens LA, Coresh J, Greene T, *et al.* Assessing kidney function—measured and estimated glomerular filtration rate. *N Engl J Med.* 2006;354(23):2473–2483.

357. The Kidney Disease: Improving Global Outcomes (KDIGO) 2012 Clinical Practice Guideline for the Evaluation and Management of Chronic Kidney Disease. *Kidney Int.* 2013;3:1–150.

358. Levey AS, Greene T, Schluchter MD, *et al.* Glomerular filtration rate measurements in clinical trials. Modification of Diet in Renal Disease Study Group and the Diabetes Control and Complications Trial Research Group. *J Am Soc Nephrol.* 1993;4(5):1159–1171.

359. Poggio ED, Wang X, Greene T, *et al*. Performance of the modification of diet in renal disease and Cockcroft-Gault equations in the estimation of GFR in health and in chronic kidney disease. *J Am Soc Nephrol.* 2005;16(2):459–466.

360. Rule AD, Larson TS, Bergstralh EJ, *et al.* Using serum creatinine to estimate glomerular filtration rate: accuracy in good health and in chronic kidney disease. *Ann Intern Med.* 2004;141(12):929–937.

361. Zhang Z, Lu B, Sheng X, *et al.* Cystatin C in prediction of acute kidney injury: a systemic review and meta-analysis. *Am J Kidney Dis.* 2011;58(3):356–365.

362. Inker LA, Schmid CH, Tighiouart H, *et al.* Estimating glomerular filtration rate from serum creatinine and cystatin C. *N Engl J Med.* 2012;367(1):20–29.

363. Taylor A Jr, Ziffer JA, Eshima D. Comparison of Tc-99m MAG3 and Tc-99m DTPA in renal transplant patients with impaired renal function. *Clin Nucl Me.* 1990;15(6):371–378.

364. Al-Nahhas AA, Jafri RA, Britton KE, *et al.* Clinical experience with 99mTc-MAG3, mercaptoacetyltriglycine, and a comparison with 99mTc-DTPA. *Eur J Nucl Med.* 1988;14(9):453–462.

365. Prasad PV. Functional MRI of the kidney: tools for translational studies of pathophysiology of renal disease. *Am J Physiol Renal Physiol.* 2006;290(5):F958–F974.

366. Kang SK, Huang WC, Lee VS, *et al.* MR renographic measurement of renal function in patients undergoing partial nephrectomy. *AJR Am J Roentgenol*. 2013;200(6):1204–1209.

367. Kang SK, Huang WC, Wong S, *et al.* Dynamic contrast-enhanced magnetic resonance imaging measurement of renal function in patients undergoing partial nephrectomy: preliminary experience. *Invest Radiol.* 2013;48(10):687–692.

368. van den Dool SW, Wasser MN, de Fijter JW, *et al.* Functional renal volume: quantitative analysis at gadolinium-enhanced MR angiography—feasibility study in healthy potential kidney donors. *Radiology.* 2005;236(1):189–195.

369. Herts BR, Sharma N, Lieber M, *et al.* Estimating glomerular filtration rate in kidney donors: a model constructed with renal volume measurements from donor CT scans. *Radiology.* 2009;252(1):109–116.

370. Coresh J, Astor BC, Greene T, *et al.* Prevalence of chronic kidney disease and decreased kidney function in the adult US population: Third National Health and Nutrition Examination Survey. *Am J Kidney Dis.* 2003;41(1):1–12.

371. Glassock RJ, Winearls C. Ageing and the glomerular filtration rate: truths and consequences. *Trans Am Clin Climatol Assoc.* 2009;120:419–428.

372. Baba M, Shimbo T, Horio M, *et al.* Longitudinal study of the decline in renal function in healthy subjects. *PLoS One.* 2015;10(6):e0129036.

373. Huang WC, Levey AS, Serio AM, *et al.* Chronic kidney disease after nephrectomy in patients with renal cortical tumours: a retrospective cohort study. *Lancet Oncol.* 2006;7(9):735–740.

374. Clark MA, Shikanov S, Raman JD, *et al.* Chronic kidney disease before and after partial nephrectomy. *J Urol.* 2011;185(1):43–48.

375. Sanfilippo KM, McTigue KM, Fidler CJ, *et al.* Hypertension and obesity and the risk of kidney cancer in 2 large cohorts of US men and women. *Hypertension.* 2014;63(5):934–941.

376. Lowrance WT, Ordoñez J, Udaltsova N, *et al.* CKD and the risk of incident cancer. *J Am Soc Nephrol.* 2014;25(10):2327–2334.

377. Donin NM, Suh LK, Barlow L, *et al.* Tumour diameter and decreased preoperative estimated glomerular filtration rate are independently correlated in patients with renal cell carcinoma. *BJU Int.* 2012;109(3):379–383.

378. Meyer A, Woldu SL, Weinberg AC, *et al.* Predicting renal parenchymal loss after nephron sparing surgery. *J Urol.* 2015;194(3):658–663.

379. Mehrazin R, Palazzi KL, Kopp RP, *et al.* Impact of tumour morphology on renal function decline after partial nephrectomy. *BJU Int.* 2013;111(8):E374–382.

380. Barlow LJ, Korets R, Laudano M, *et al.* Predicting renal functional outcomes after surgery for renal cortical tumours: a multifactorial analysis. *BJU Int.* 2010;106(4):489–492.

381. Scosyrev E, Messing EM, Sylvester R, *et al.* Renal function after nephron-sparing surgery versus radical nephrectomy: results from EORTC randomized trial 30904. *Eur Urol.* 2014;65(2):372–377.

382. National Kidney Foundation. K/DOQI clinical practice guidelines for chronic kidney disease: evaluation, classification, and stratification. *Am J Kidney Dis.* 2002;39(2 Suppl 1):S1–266.

383. Lane BR, Fergany AF, Weight CJ, *et al.* Renal functional outcomes after partial nephrectomy with extended ischemic intervals are better than after radical nephrectomy. *J Urol.* 2010;184(4):1286–1290.

384. Huang WC, Atoria CL, Bjurlin M, *et al.* Management of small kidney cancers in the new millennium: contemporary trends and outcomes in a population-based cohort. *JAMA Surg.* 2015;150(7):664–672.

385. Lane BR, Russo P, Uzzo RG, *et al.* Comparison of cold and warm ischemia during partial nephrectomy in 660 solitary kidneys reveals predominant role of nonmodifiable factors in determining ultimate renal function. *J Urol.* 2011;185(2):421–427.

386. Thompson RH, Lane BR, Lohse CM, *et al.* Every minute counts when the renal hilum is clamped during partial nephrectomy. *Eur Urol.* 2010;58(3):340–345.

387. Lucas SM, Stern JM, Adibi M, *et al.* Renal function outcomes in patients treated for renal masses smaller than 4 cm by ablative and extirpative techniques. *J Urol.* 2008;179(1):75–79.

388. Mitchell CR, Atwell TD, Weisbrod AJ, *et al.* Renal function outcomes in patients treated with partial nephrectomy versus percutaneous ablation for renal tumors in a solitary kidney. *J Urol.* 2011;186(5):1786–1790.

389. Huang WC, Elkin EB, Levey AS, *et al.* Partial nephrectomy versus radical nephrectomy in patients with small renal tumors—is there a difference in mortality and cardiovascular outcomes? *J Urol.* 2009;181(1):55–61.

390. Herr HW. A history of partial nephrectomy for renal tumors. *J Urol.* 2005;173(3):705–708.

391. Uzzo RG, Novick AC. Nephron sparing surgery for renal tumors: indications, techniques and outcomes. *J Urol.* 2001;166(1):6–18.

392. Kane CJ, Mallin K, Ritchey J, *et al.* Renal cell cancer stage migration: analysis of the National Cancer Data Base. *Cancer.* 2008;113(1):78–83.

393. Woldrich JM, Palazzi K, Stroup SP, *et al.* Trends in the surgical management of localized renal masses: thermal ablation, partial and radical nephrectomy in the USA, 1998-2008. *BJU Int.* 2013;111(8):1261–1268.

394. Puigvert A. Partial nephrectomy for renal tumour: 21 cases. *Eur Urol.* 1976;2(2):70–78.

395. Novick AC, Stewart BH, Straffon RA, *et al.* Partial nephrectomy in the treatment of renal adenocarcinoma. *J Urol.* 1977;118(6):932–936.

396. Schiff M Jr, Bagley DH, Lytton B. Treatment of solitary and bilateral renal carcinomas. *J Urol.* 1979;121(5):581–586.

397. Zincke H, Swanson SK. Bilateral renal cell carcinoma: influence of synchronous and asynchronous occurrence on patient survival. *J Urol.* 1982;128(5):913–915.

398. Srinivas V, Herr HW, Hajdu EO. Partial nephrectomy for a renal oncocytoma associated with tuberous sclerosis. *J Urol.* 1985;133(2):263–265.

399. Hafez KS, Fergany AF, Novick AC. Nephron sparing surgery for localized renal cell carcinoma: impact of tumor size on patient survival, tumor recurrence and TNM staging. *J Urol.* 1999;162(6):1930–1933.

400. Ljungberg B, Bensalah K, Canfield S, *et al.* EAU guidelines on renal cell carcinoma: 2014 update. *Eur Urol.* 2015;67(5):913–924.

401. Becker F, Roos FC, Janssen M, *et al.* Short-term functional and oncologic outcomes of nephron-sparing surgery for renal tumours ≥ 7 cm. *Eur Urol.* 2011;59(6):931–937.

402. Breau RH, Crispen PL, Jimenez RE, *et al.* Outcome of stage T2 or greater renal cell cancer treated with partial nephrectomy. *J Urol.* 2010;183(3):903–908.

403. Karellas ME, O'Brien MF, Jang TL, *et al.* Partial nephrectomy for selected renal cortical tumours of ≥ 7 cm. *BJU Int.* 2010;106(10):1484–1487.

404. Long CJ, Canter DJ, Kutikov A, *et al.* Partial nephrectomy for renal masses ≥ 7 cm: technical, oncological and functional outcomes. *BJU Int.* 2012;109(10):1450–1456.

405. Alanee S, Nutt M, Moore A, *et al.* Partial nephrectomy for T2 renal masses: contemporary trends and oncologic efficacy. *Int Urol Nephrol.* 2015;47(6):945–950.

406. Provet J, Tessler A, Brown J, *et al.* Partial nephrectomy for renal cell carcinoma: indications, results and implications. *J Urol.* 1991;145(3):472–476.

407. Joniau S, Vander Eeckt K, Van Poppel H. The indications for partial nephrectomy in the treatment of renal cell carcinoma. *Nat Clin Pract Urol.* 2006;3(4):198–205.

408. Méjean A. How far should partial nephrectomy be extended for renal cell carcinoma? *Ann Urol (Paris).* 2006;40(Suppl 3):S68–71.

409. McKiernan J, Simmons R, Katz J, *et al.* Natural history of chronic renal insufficiency after partial and radical nephrectomy. *Urology.* 2002;59(6):816–820.

410. Malcolm JB, Bagrodia A, Derweesh IH, *et al.* Comparison of rates and risk factors for developing chronic renal insufficiency, proteinuria and metabolic acidosis after radical or partial nephrectomy. *BJU Int.* 2009;104(4):476–481.

411. Joniau S, Vander Eeckt K, Srirangam SJ, *et al.* Outcome of nephron-sparing surgery for T1b renal cell carcinoma. *BJU Int.* 2009;103(10):1344–1348.

412. Bagrodia A, Mehrazin R, Bazzi WM, *et al.* Comparison of rates and risk factors for development of osteoporosis and fractures after radical or partial nephrectomy. *Urology.* 2011;78(3):614–619.

413. Woldrich J, Mehrazin R, Bazzi WM, *et al.* Comparison of rates and risk factors for development of anaemia and erythropoiesis-stimulating agent utilization after radical or partial nephrectomy. *BJU Int.* 2012;109(7):1019–1025.

414. Sun M, Bianchi M, Hansen J, *et al.* Chronic kidney disease after nephrectomy in patients with small renal masses: a retrospective observational analysis. *Eur Urol.* 2012;62(4):696–703.

415. Filson CP, Schwartz K, Colt JS, *et al.* Use of nephron-sparing surgery among renal cell carcinoma patients with diabetes and hypertension. *Urol Oncol.* 2014;32(1):27.e15–21.

416. Longo N, Minervini A, Antonelli A, *et al.* Simple enucleation versus standard partial nephrectomy for clinical T1 renal masses: perioperative outcomes based on a matched-pair comparison of 396 patients (RECORd project). *Eur J Surg Oncol.* 2014;40(6):762–768.

417. Russo P. End stage and chronic kidney disease: associations with renal cancer. *Front Oncol.* 2012;2:28.

418. Weight CJ, Miller DC, Campbell SC, *et al.* The management of a clinical t1b renal tumor in the presence of a normal contralateral kidney. *J Urol.* 2013;189(4):1198–1202.

419. Scosyrev E, Messing EM, Sylvester R, *et al.* Renal function after nephron-sparing surgery versus radical nephrectomy: results from EORTC randomized trial 30904. *Eur Urol.* 2014;65(2):372–377.

420. Lane BR, Campbell SC, Demirjian S, *et al.* Surgically induced chronic kidney disease may be associated with a lower risk of progression and mortality than medical chronic kidney disease. *J Urol.* 2013;189(5):1649–1655.

421. Chung JS, Son NH, Byun SS, *et al.* Trends in renal function after radical nephrectomy: a multicentre analysis. *BJU Int.* 2014;113(3):408–415.

422. Lane BR, Demirjian S, Derweesh IH, *et al.* Survival and functional stability in chronic kidney disease due to surgical removal of nephrons: importance of the new baseline glomerular filtration rate. *Eur Urol.* 2015;68(6):996–1003.

423. Sorbellini M, Kattan MW, Snyder ME, *et al.* Prognostic nomogram for renal insufficiency after radical or partial nephrectomy. *J Urol.* 2006;176(2):472–476.

424. Lane BR, Demirjian S, Weight CJ, *et al.* Performance of the chronic kidney disease-epidemiology study equations for estimating glomerular filtration rate before and after nephrectomy. *J Urol.* 2010;183(3):896–901.

C7

Renal Tumour Biopsy: Indications, Technique, Safety, Accuracy/Results, Pathologic Reporting, and Impact on Treatment Decision Making

CHAIR

Michael A.S. Jewett, Canada

CO-CHAIR

Mahul B. Amin, United States

MEMBERS

Antonio Finelli, Canada
Xuesong Li, China
Mesut Remzi, Austria
Otto Van Delden, The Netherlands
Alessandro Volpe, Italy

Pathology Section

Maurizio Colecchia, Italy
Andrew J. Evans, Canada
David Grignon, United States
Ondrej Hes, Czech Republic
Naoto Kuroda, Japan
Victor E. Reuter, United States
Isabela Werneck da Cunha, Brazil

CONTENTS

Renal Tumour Biopsy: Indications, Technique, Safety, Accuracy/Results, Pathologic Reporting, and Impact on Treatment Decision Making

7.1 Abstract

The use of renal tumour biopsy (RTB) is increasing as indications expand. Case selection and modern techniques with image guidance have resulted in high success rates for obtaining diagnostic biopsy material. Pathological handling and interpretation of needle cores, which are preferred to fine-needle aspiration (FNA) specimens, are now sophisticated, and experienced pathologists can provide very useful information to guide the clinician in making better treatment decisions. Although there continues to be controversy regarding the impact of biopsy results on clinical management, there is increasing evidence that a diagnostic biopsy can reduce unnecessary treatment of benign tumours. A diagnostic biopsy can also enable initial active surveillance (AS), as opposed to surgical treatment or ablation in some early-stage malignant tumours in select patients. Systemic treatment options are increasingly being selected with RTB of the primary tumour in advanced stages of renal cell carcinoma (RCC). There are promising future directions for the interpretation of biopsy material.

7.2 Introduction

Renal tumour biopsy is slowly gaining in popularity. In many institutions, it is not performed except with tumours that are suspected of being secondary metastases or non-neoplastic. This could be considered a urological oncology disparity in the management of small renal masses (SRMs) when compared to the use of biopsy for prostate and bladder neoplasms. Many patients, often older and infirm, are being subjected to arguably unnecessary treatment of benign renal tumours or renal cell carcinomas (RCCs) with low risk for progression or metastatic potential, because the treatment decision is not based on pathological sampling. The future of individualizing treatment by risk assessment is moving slowly using biopsy material. The disparity is that we generally perform major urological surgery for the other common genitourinary malignancies without biopsy. For example, radical prostatectomy is virtually never performed without multiple biopsies that sample the prostate cancer as well as the benign-appearing gland. Radical cystectomy is not performed without a transurethral or other biopsy of the tumour, as well as adjacent normal bladder if possible. Orchiectomy for suspected testicular cancer and nephroureterectomy for upper tract urothelial cancer are the only other scenarios that have a high rate of extirpative surgery that is not routinely planned with a preoperative biopsy.

More advanced RCCs are now being biopsied, and we have addressed the reasons and indications. This practice will undoubtedly continue and probably expand. There is now an extensive and growing body of evidence that RTB is safe and useful in planning treatment. Although there are internet postings or literature reports about the hazards of biopsy, most are outdated and no longer valid. The adopters of biopsy will tell you that they rarely encounter serious complications, and that they perform biopsies on an outpatient basis with rare admissions and virtually unheard-of tumour complications. This information and experience needs to be taught in order to change practice.

Renal tumour biopsy is a "team sport" and requires imagers experienced with image guidance and biopsy technique. We have described what we believe to be the optimal technique. More than 90% of RTBs should be diagnostic after one attempt. Similarly, pathologists have not always been comfortable with RTBs but, where there is experience, the results are accurate and representative.

The clinical impact of RTB on treatment decision making has been limited by the relatively small series reported and expert centre-only experiences to date. This is a challenge to those of us encouraging adoption. We hope that this will be rectified with contributions like this, presentations, and other knowledge transfer (KT) initiatives.

Finally, we are on the cusp of personalizing medicine through a better understanding of genomics, epigenomics, transcriptomics, metabolomics, and much more, which will open new possibilities for treatment decision making with tissue obtained by renal biopsy.

7.3 Indications for Biopsy

Percutaneous RTB has historically been used with limited indications including: 1) differential diagnosis of lymphoma and renal abscess, 2) diagnosis of renal metastatic disease in the presence of a known extra-renal malignancy, and, 3) histological diagnosis of primary renal tumours in the setting of disseminated metastases or surgically unresectable retroperitoneal tumours. Beyond these indications, biopsies of renal tumours have not been used until recently because of a number of uncertainties regarding safety (risk of tumour seeding along the needle tract and hemorrhagic complications), diagnostic yield, accuracy, impact on clinical decision making, and, most importantly, the perception that all solid renal masses have malignant potential and should be treated after imaging only.

Most of these uncertainties have now been addressed by the growing experience of urologists and interventional radiologists performing biopsies, by pathologists interpreting biopsy specimens, and by the growing number of urologists who now believe that biopsy information is useful in clinical decision making.

The increasing incidence of SRMs, the development and increasing use of alternative treatments for localized renal tumours in selected patients, and the discovery of effective biological therapies for metastatic disease have increased the awareness that the histological characterization of renal masses is important to personalize treatment for each patient.[1]

Percutaneous biopsy can provide important information that has the potential for a significant impact on clinical practice, including:

7.3.1 Reduction of unnecessary treatment of benign conditions

Small renal tumours are frequently benign, with the likelihood significantly increasing with decreasing tumour size.[2-4] For example, current abdominal imaging techniques (computed tomography [CT], multiparametric magnetic resonance imaging [mpMRI], and contrast enhanced ultrasound

[US]) do not allow a reliable diagnosis of oncocytoma. The typical presentation of this tumour as a hypervascular homogeneous mass with a starry central scar was only reported in a limited number of cases. No other radiological feature was found to be sufficiently reliable for the diagnosis of this benign renal tumour, although it must be noted that chromophobe RCC and some clear cell RCC may also have a central scar.[5,6] Furthermore, although most angiomyolipomas (AMLs) are easily diagnosed at CT scan for their characteristic fat component, fat-poor AMLs (leiomyoma-like and epithelioid variants) cannot be adequately diagnosed with current imaging.[7] Overall, Remzi *et al.* reported that only 17% of benign tumours are correctly identified by preoperative imaging.[8]

Performing a percutaneous biopsy prior to a treatment decision can decrease the number of unnecessary surgeries and ablations for benign tumours, especially in the elderly population with frequent comorbidities and an increased risk of non-RCC–related mortality.[9,10]

7.3.2 Support for treatment decision making for localized renal tumours

While a large proportion of SRMs are benign, many are also low-grade RCCs, which appear to have a relatively indolent biological and clinical behaviour.[11,12]

Surgical resection is the gold standard treatment for localized RCC. Renal tumour biopsy is useful to select patients with SRMs who are suitable for nonsurgical treatment with focal ablative therapies and AS, especially in elderly patients with reduced life expectancy and higher surgical risk. [10,13,14]

Pre-ablation RTB can avoid unnecessary treatment of benign tumours, as well as individualize follow-up. Active surveillance is a valuable option for patients with low-grade RCC. The presence of high-grade histology at biopsy prompts consideration of surgical treatment, although the evidence for this stratification is weak. If a biopsy is nondiagnostic but there are radiological findings suspicious for malignancy, a second biopsy or surgical exploration should always be considered.[10]

A biopsy may also help to tailor the intensity of follow-up of patients based on tumour histology. Benign tumours can be followed with less stringent follow-up protocols, thereby reducing radiation exposure and costs. For AS patients or those who have had ablation therapy for RCC, chest imaging may be performed annually or more frequently based on clinical behaviour for biopsy-proven high-grade RCC and/or neoplasms displaying rapid interval growth patterns.[13,14]

Tumour size significantly correlates with diagnostic yield of biopsies. Hence, urologists should be aware of the higher risk of biopsy failure when biopsies of very small tumours (<1 cm) are performed, and should inform patients accordingly.

A recent meta-analysis showed a significantly lower specificity and, more importantly, lower sensitivity of RTB of cystic renal masses.[15] The new classification of cystic RCC with the introduction of the term multilocular cystic clear cell RCC of low malignant potential, plus the difficulty biopsying cystic masses where the solid components are very small, limits the application of RTB in cystic lesions.[16] Percutaneous sampling can be indicated for Bosniak category IV cysts, where clear enhancing solid nodules are visible within the lesion. Cyst fluid rarely demonstrates positive cytology even if

low-grade RCC is present in the walls, so this is not an indication for FNA of fluid. Certain histologic subtypes of RCC, particularly small and organ-confined RCC, appear not to metastasize or progress in the short term. These include clear cell papillary RCC and mucinous tubular and spindle cell carcinoma (MTSCC).

Biopsy can also be considered if a central lesion or a homogeneous infiltration of renal parenchyma is observed on scans to rule out urothelial carcinoma or lymphoma, respectively.[14] However, when a urothelial tumour is suspected, the higher risk of tumour seeding should be considered, and patients should be informed accordingly.

Percutaneous biopsy is increasingly being considered for larger, localized renal masses (T1b–T2). Although the choice to perform radical nephrectomy versus partial nephrectomy (PN) depends essentially on the patient's characteristics and the tumour's radiological features, histological information from percutaneous biopsy may be helpful for treatment decision in cases with high surgical complexity, e.g. radical treatment may be favoured in the presence of aggressive, high-grade disease, and nephron-sparing surgery may be favoured in the presence of benign or low-grade disease with indolent clinical behaviour.

7.3.3 Support for the definition of treatment success for ablative focal therapies

Although the outcomes of cryoablation and radiofrequency ablation for SRMs are encouraging, the risk of residual viable tumour after these procedures is not negligible.[17] The major urological guidelines recommend that a percutaneous biopsy be performed after tumour ablation when a suspicious recurrence or persistence of disease is detected at follow-up imaging.[10,13,18] Routine postablation biopsy may allow a better understanding of the oncological outcomes of minimally invasive ablative therapies. Preablation biopsy is essential to correlate with the outcomes and plan follow-up.[19]

7.3.4 Support for treatment decision making for metastatic renal tumours

The histological diagnosis of RCC with sarcomatoid differentiation predicts a poor prognosis, with limited response to systemic therapy and less benefit of cytoreductive nephrectomy. Surgical treatment can therefore be avoided in these patients to prevent unnecessary morbidity.[20,21] Moreover, the several available targeted agents for metastatic RCC (mRCC) have different response rates, depending on tumour histotype. For instance, mechanistic target of rapamycin (mTOR) inhibitors demonstrated a better activity compared to tyrosine-kinase inhibitors for metastatic chromophobe RCC. Likewise, foretinib is an active drug for treatment of papillary RCC, particularly in cases with germline mutations of the MET gene.[22,23]

Currently, percutaneous biopsy of the primary renal tumour is recommended before starting systemic therapy for metastatic disease when a cytoreductive nephrectomy is not indicated or when neoadjuvant systemic therapy is planned.[10,14]

Recommended indications for renal tumour biopsy

As the field continues to evolve with further evidence becoming available, routine RTB of all incidentally detected SRMs (including cystic renal lesions, Bosniak IV) is recommended in patients for whom AS or ablative therapy is being considered to avoid unnecessary treatment of benign tumours and to individualize therapy **[Grade of recommendation (GOR) D, Level of evidence (LOE) 4].**

Based on these considerations, percutaneous biopsy of renal tumours maybe useful in several clinical settings, and is currently recommended for the histological diagnosis of:

- Homogeneous infiltration of renal parenchyma to rule out lymphoma **[GOR C, LOE 2]**.
- Radiological suspicion of recurrence or disease persistence after renal tumour ablation **[GOR C, LOE 2]**.
- Suspicion of renal metastases in the presence of a known extrarenal malignancy **[GOR C, LOE 2]**.
- Retroperitoneal tumours involving the kidney when initial surgery is not feasible or indicated **[GOR C, LOE 2]**.
- Primary renal tumours with metastatic disease before systemic therapy (RTB is increasingly recommended to select systemic agents), when cytoreductive nephrectomy is not indicated, or when neoadjuvant systemic therapy is planned **[GOR D, LOE 4]**.
- Small renal masses <1 cm are difficult to biopsy, and may be followed until they reach this size **[GOR D, LOE 4]**.

7.4 Technique

7.4.1 Image guidance systems

Renal tumour biopsy is usually performed using US or CT guidance. To our knowledge, there are no data supporting which of these methods yields the best results. Magnetic resonance imaging is rarely used.

Ultrasound is a useful technique for visualizing the tumour, and has the advantages of real-time needle placement, multi-planar imaging, low cost, visualization of vascular structures, and no harmful side effects of radiation.[24] Also, with experience, biopsy with US guidance is relatively fast and takes less time than CT or MRI-guided biopsies. To further improve the reflectivity and visualization of the needle, the surface of the needle can be coated or scored.[25] Another major benefit of US is that the machines are portable, and examinations can be performed at the bedside when necessary. The

main disadvantage of US is that not all renal masses can be visualized, particularly in patients with small and/or endophytic renal lesions and in very obese patients. Some of these problems can be overcome by using intravenous contrast enhancement with microbubbles. However, as the microbubbles wash out in just a few minutes, this only gives the operator a short window of time to perform the biopsy. Ultrasound is a very operator-dependent technique and there is a significant learning curve, which may affect the final imaging results.[26] In many centres with extensive US experience, biopsies are primarily performed with US guidance, and CT is reserved for patients in whom US guidance is not feasible.

Other centres use CT guidance as the primary technique for RTB.[27] Computed tomography has a higher sensitivity for SRMs than US, particularly when lesions are endophytic. The technique of CT-guided biopsy is less operator-dependent than US-guided biopsy, although considerable skill is required for adequate biopsy.[26] The detection of lesions is improved by using intravenous contrast medium. Similar to contrast-enhanced US, CT contrast medium can only provide images during a limited window of time. However, as renal lesions often show a hypodense appearance compared to normal renal parenchyma on delayed phase CT imaging, the window of time for needle placement is often sufficient. Moreover, when the renal lesion shows a contour change on CT, the use of contrast medium is not always required for visualization of the lesion. Many of the newer-generation CT scanners are equipped with CT fluoroscopy technology, which enables real-time or almost real-time imaging during needle placement. Otherwise, the patient has to be moved in and out of the bore. With fluoroscopy, the procedure time is decreased and may increase the yield of CT-guided biopsies by more accurate needle placement, as well as a better use of the relatively short window of time after contrast injection in which the tumour shows optimal visibility. Laser guidance may also be of benefit to decrease procedure time and increase the accuracy of needle placement.[28,29] There are also some disadvantages associated with the use of CT, such as impaired accuracy of needle placement due to the patient's respiratory motion, or the patient's difficulties maintaining a fixed position while prone during the procedure.

When choosing an imaging guidance method for RTB, one should consider the tumour accessibility, availability of imaging modality, personal expertise, and individual case characteristics. A urology panel recently recommended using US for RTB, citing the benefits of no radiation, low cost, and high accessibility.[30] Computed tomography guidance should be considered when US is not feasible and such a strategy may be most cost-effective.

7.4.2 Needle core versus fine-needle aspiration biopsy

Core biopsy and FNA are the two most common methods of obtaining renal tumour issue. Some centres routinely use a combination of FNA and core biopsies where the two are used in a complementary manner.[26,31] Core biopsy systems are available with needle diameters ranging from 14 to 20 gauge (G). Most commonly, biopsies are performed using 16- or 18-G needles; these are preferred over FNA because of superior accuracy. Core biopsy samples may be obtained with needles ranging in size from 14 to 25 G,[32] although 18-G needles are most commonly used.[33-38] Data obtained from *ex vivo* sampling suggests 18-G needles are superior to 20-G needles for core biopsies;[39] however, 20-G needles may be preferred when patients have preexisting coagulation issues or the biopsy tract will pass through adjacent organs before reaching the kidney lesion.[40] Needles of 18 to 22 G are typically

used for FNA samples.[26,31] If only one modality is used, core biopsy is superior in terms of diagnostic yield for malignant lesions, as well as establishing histologic type and grade.[26,33,41,42] If biopsy is indicated, 90% of the clinicians choose core biopsy rather than FNA.[43] The tissue obtained from core biopsy allows for the assessment of tissue architecture and histologic subtype. Furthermore, there is likely more material for ancillary studies such as immunohistochemistry (IHC) and molecular studies, if needed.

7.4.3 Submitting and labelling core biopsy specimens

Core biopsy samples should be placed in containers labelled with appropriate patient identifiers, the kidney biopsied (left, right, or horseshoe), and further specification such as intrarenal location (upper, mid, or lower pole) from which cores were obtained. In the setting of multiple masses in the same kidney, one cannot assume they will all be of the same histologic type or that all will be benign or malignant.[44] Core biopsies obtained from multiple lesions should be submitted to the pathology laboratory in separate, appropriately labelled containers indicating the specific sites in the kidney from which the various core biopsies were obtained. The accompanying requisition form should include the number of lesions in the kidney (if more than one), the number of lesions biopsied (if more than one), the size and location of each lesion biopsied, and the number of cores obtained from each. Any known history of previous renal neoplasm(s), tumour-related syndrome, or previous nonrenal malignancy should also be included, as well as information on whether the lesion has been treated by chemo-/targeted or ablative therapy prior to biopsy.

7.4.4 Number of needle cores for single and multiple tumours

Currently, no consensus has been reached with regard to the optimal number of biopsies that should be performed for renal tumours. Renal tumours are heterogeneous, so multiple biopsy cores should be obtained to prevent sampling errors. In an *ex vivo* investigation, investigators showed that adding core numbers improved the diagnostic yield, with a similar rate for two-core (63%) and three-core (67%) RTB.[45] Neuzillet *et al.* reported that 88 RTBs with at least two core samplings resulted in a 90.9% diagnostic yield.[46] Similarly, Wang *et al.* analyzed 110 RTBs and demonstrated that biopsy with at least two cores resulted in 91% diagnostic yield.[47]

Although increasing the number of cores is associated with improved diagnostic yield, and biopsy with at least two cores can result in a considerably higher diagnostic yield, ultimately it is the quality of the core that defines the success of RTB. Currently, a minimum of two good-quality cores for a single renal tumour is generally accepted.

For multiple tumours, regardless of whether they are unilateral or bilateral lesions, a single RTB is insufficient because the histological characteristics may be different among the tumours.[8] Hence, biopsy for each of the visible lesions is recommended, and such a procedure could be completed in a single- or multiple-stage procedure.

7.4.5 Use of coaxial technique

Most operators perform core biopsy through a coaxial needle or cannula. The use of a coaxial guide appears to increase the diagnostic yield of biopsy and improve the standardization of sampling.[48] Appelbaum *et al.* reported a 15% increase of the biopsy success rate without increasing the complication rate.[49] However, the effect of coaxial technique on biopsy success rate is yet to be confirmed by large studies. Due to the large size and rigidity of the coaxial guiding needle, locating and positioning the needle is facilitated with both US and CT. The coaxial needle allows for multiple needle biopsies with only one access through the skin and underlying tissues, thereby minimizing the risk of needle-track seeding.[50] Moreover, with the use of a coaxial needle, there is no need for needle repositioning after one pass, which may reduce the procedure time and decrease patient discomfort. Finally, the reduction in reported tumour seeding has been attributed to the use of a coaxial sheath.[33]

7.4.6 Location of biopsy

There is no standard pattern for the biopsy location, but, in general, necrotic and cystic areas should be avoided. Hobbs *et al.*[45] investigated the impact of sampling location on the diagnostic accuracy of renal mass biopsy in an *ex vivo* study, and found the cancer identification rate could be increased by an additional central or peripheral core. They recommend at least two peripheral cores for RTB.

It is generally accepted that selecting the location of biopsy should depend on the tumour size. For large tumours (>4 cm), the incidence of central necrosis is higher, and a proper sampling pattern will be of greater importance when compared with smaller tumours.[51] An international multidisciplinary panel recommended sampling different regions, including central and peripheral biopsies for large tumours.[30] Jason *et al.* reported 122 biopsies in 117 ≥cT2 renal tumours and recommended a multi-quadrant biopsy technique for large renal tumours, which is defined as sampling from at least four separate solid-enhancing areas within the tumour.[52] Both US and contrast-enhanced CT may show central areas of hypo-echogenicity or non-enhancement in renal tumours, and these findings should be taken into account when planning image-guided biopsy.

Recommended technique for RTB

Based on these considerations, percutaneous biopsy of renal tumours should:

- Be performed with image guidance, usually US where feasible **[GOR C, LOE 4]**
- Be the preferred sampling method for a renal mass or density. Fine-needle aspiration, if used, should be used as a complementary method and should only exceptionally be the sole sampling method **[GOR C, LOE 4]**.
- Be done with a coaxial sheath to improve sampling and safety **[GOR D, LOE 5]**.
- Include at least two cores from SRMs **[GOR D, LOE 5]**.
- Be done for each SRM if there is more than one tumour **[GOR D, LOE 4]**.
- Be done from the peripheral area of the tumour if there are necrotic areas on imaging or from the enhancing areas if cystic **[GOR D, LOE 4]**.
- Sample the tumour as widely as possible **[GOR D, LOE 4]**.

7.5 Safety

7.5.1 Risk of tumour seeding

Although needle-track seeding remains a concern, all six reports dealing with needle-track seeding after RTB of renal tumours were published prior to 1993 and are anecdotal.[53] In 2,474 RTBs reported up to the year 2000 [54] and in all recent reports,[1,33] no case of tumour seeding has been reported. This is most likely related to the use of a sheath or coaxial technique, which reduces needle contact with the surrounding tissue and allows multiple biopsies to be performed through a cannula.[1] The use of a coaxial technique may not only decrease the chance for inadvertent tumour seeding, but also facilitates the accuracy and speed of the procedure, and is therefore recommended by most operators. For more information, see the Technique section of this chapter. Somani *et al.*[55] reported no specific survival difference after nephrectomy among patients with and without preoperative biopsy. Renal tumour biopsy should be performed with care when urothelial carcinoma of the upper urinary tract is suspected, due to the increased risk of needle-track seeding. It is therefore of the utmost importance to critically review the available imaging prior to each biopsy procedure, and to do urinary cytology when there is uncertainty about RCC versus urothelial disease.

7.5.2 Complications

In general, complications due to RTB are self-limiting and minor; however, reporting on complications and the grade of complications have not been standardized in the urology and radiology literature.

Although initial reports suggested substantial morbidity associated with RTB, contemporary series report infrequent minor complications (4.7%), exceedingly rare severe complications (0.3%), and no cases of mortality.[54] A recent collaborative review of complications reported significant complications requiring active treatment or hospital admission after 0% to 2% of biopsies.[1]

There are several major complications associated with RTB. Bleeding is the most common. Of 200 biopsies, a number of mild hematomas were identified on CT scans performed immediately after the biopsy.[56] However, clinically significant renal hemorrhages resulting in hospitalization or blood transfusion were extremely rare (0%–1.3%). A recent study evaluating the experience over the last 13 years confirms the safety of RTBs, with significant complications occurring in less than 1% of cases.[33] Of 24 (4.7%) perirenal hematomas, only one needed transcatheter arterial embolization.[33] This group also reported venous bleeding through coaxial sheath (*n*=12, 2.4%) treated by using hemostatic agents in 7 of the 12 (58.3%) cases. However, the impact of the use of these hemostatic agents on further bleeding problems remains unclear. Gross hematuria that may or may not be related to arteriovenous fistula was reported in 1% (*n*=5), all of them self-limiting. Additionally, 1 skin hematoma was reported.

The risk of bleeding is believed to be greater with larger (≥18-G) needles, but no study has directly compared complication rates of biopsies performed with needles of different sizes. Similarly, no study has clearly assessed the correlation among the number of cores obtained, tumour location, operator expertise, and rates of post-biopsy bleeding and other complications.[1] It is also unclear whether the above-mentioned coaxial technique decreases the chance for bleeding complications, as it decreases the number of needle passes through the skin and subcutaneous tissues but not the number of needle passes into the renal tumour itself. In the prospective study from Vienna[41] that included routine US control 6 hours after RTB, there were no serious adverse events, and 4 of 78 (5.1%) patients showed a clinically insignificant subcapsular hematoma. Lechevallier reported that, of 565 RTBs, only two cases of symptomatic perirenal hematoma necessitated hospitalization for surveillance; however, no intervention was needed.[27] It is important to distinguish reports of medical renal disease biopsy from RTB.

Other nonbleeding complications are extremely rare. Richard *et al.* reported nausea/vomiting in one (0.2%), persistent pain in three (0.6%), and dizziness in two (0.4%) of 509 patients.[33] The risk of clinically significant pneumothorax is reported to be <1%[41] and might be virtually absent when a subcostal needle approach is chosen. The occurrence of pneumothorax can be predicted when the lesion is located in the upper pole and when a transpleural biopsy route is chosen. A small pneumothorax can usually be treated by needle aspiration of the pneumothorax, followed by observation. Catheter drainage is only very rarely required. Procedure-related pain is usually transient and can be treated with oral analgesics with no need for hospitalization.

Recommendations regarding safety of RTB

- Renal tumour biopsy is safe **[GOR C, LOE 3]**.
- Needle-track seeding is extremely rare **[GOR C, LOE 3]**.
- Renal tumour biopsy should be performed with care when urothelial carcinoma of the upper urinary tract is suspected **[GOR C, LOE 4]**.
- Complications due to RTB are generally minor and self-limiting **[GOR C, LOE 3]**.

7.6 Pathology Perspectives With Recommendations and Handling of Renal Tumour Biopsies

7.6.1 Handling and preparation of needle core biopsies

1. Types of Specimens

Biopsy specimens submitted for histologic and/or cytopathologic assessment from renal masses include needle core biopsies and FNA samples. Needle core biopsies are preferred. This has been addressed in the Technique section (section 7.4) of this chapter.

2. Role of Rapid Evaluation, Including Specimen Adequacy

Issues pertaining to the definition of specimen adequacy are discussed later in this section (See **7.6.3 Histologic scope of needle biopsy**). Here, we discuss aspects that impact rapid evaluation. Most institutions do not consistently employ a protocol for rapid evaluation. It has been recommended that at least two cores of tissue be obtained and immediately examined grossly for adequacy (see section 7.4). Cores less than 10 mm in length or those that are fragmented, necrotic, or hemorrhagic should be considered inadequate. The biopsy procedure would ideally be repeated until two suitable cores have been obtained.[32,40,41,57,58] While there is obvious merit in considering grossly necrotic or hemorrhagic cores insufficient, using core length as a determinant of adequacy is debatable. An 18-G core biopsy may obtain two 1- to 2-cm nonfragmented cores, but consist only of renal parenchyma with no lesional tissue. Conversely, several 5-mm core fragments may consist entirely of lesional tissue (**Figure 7-1**).

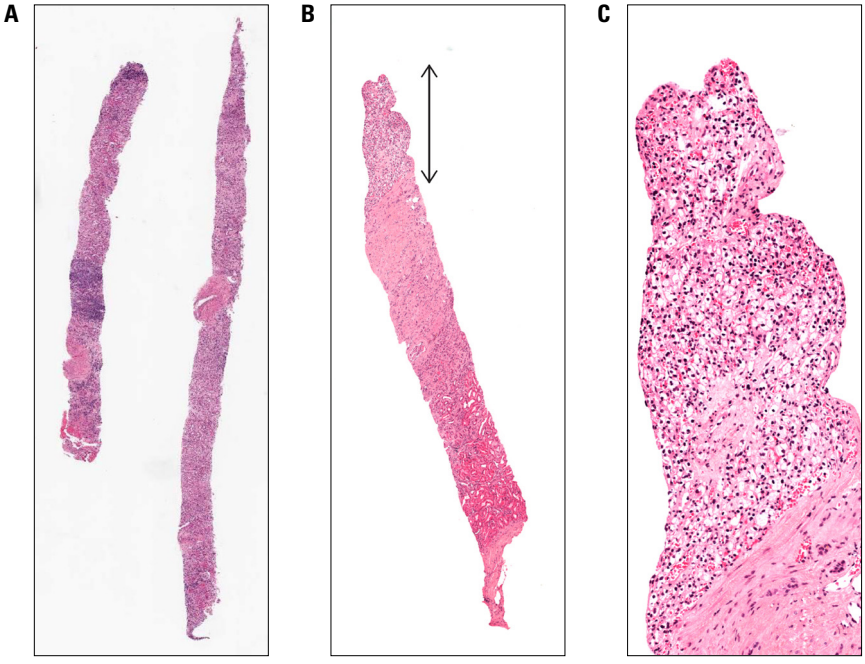

FIGURE 7-1

A Needle biopsy intending to sample a renal mass consisting a 15-cm core of renal parenchyma with no diagnostic abnormality. Such a core would be considered adequate by length criteria; however, it does not contain lesional tissue.

B Needle core biopsy of a renal mass measuring only 7 mm, yet consisting entirely of clear cell–type RCC.

C Higher power view of upper end of core illustrated in (**B**).

It therefore follows that core length and/or fragmentation are not reliable predictors of adequacy. The inclusion of non-tumour renal parenchyma in the core biopsy may be helpful in terms of determining whether a tumour is well demarcated or has an infiltrative pattern, which can be important for establishing a histologic differential diagnosis.[59]

Generally speaking, renal cortex immediately adjacent to a mass tends to be atrophic and not representative of the background kidney, and is of limited value in terms of assessing glomerular and/or tubular morphology.

When core biopsy and FNA are used in combination, FNA can be performed first to confirm proper positioning of the biopsy needle and/or guiding cannula (if a coaxial technique is used). The FNA samples are smeared directly onto several slides, air-dried or alcohol-fixed, and rapidly stained with Diff-Quik Romanowsky-Giemsa (for air-dried preparations) or with hematoxylin and eosin (H&E) or modified Papanicolaou stain (for fixed samples).[26] The resulting slides can be rapidly assessed for the presence of lesional cells by a cytopathologist or experienced cytotechnologist. This approach may be of particular value in situations where the diagnostic yield on core biopsy alone could be lower, such as a completely intraparenchymal (non-exophytic) mass that is smaller than 2 to 3 cm in dimension.[33,35] If a sufficient sample has been obtained, FNA material can also be fixed in 10% formalin, centrifuged, and embedded in paraffin, generating cell blocks for additional cytoarchitectural assessment, immunohistochemical staining, and molecular or cytogenetic analyses.[26,60]

As an alternative to using FNAs to assess adequacy, some centres have used touch preparations on core biopsy samples.[34] Damaging or air drying of the core biopsy and compromising the histology are possible risks associated with this method if care is not taken to perform the imprint cytology in a rapid and gentle fashion. Adequacy assessments of this nature are routinely performed in some institutions; however, this is not a consistent practice. See Section 7.6.2 Recommendations.

Performing frozen sections on freshly obtained core biopsy samples is yet another possible approach for establishing the presence of diagnostic tissue or obtaining a rapid diagnosis. Assessing frozen sections will not be as rapid as FNA assessment, nor will it be practical unless a cryostat is located close to the location where the core biopsy is performed. Frozen sections are typically thicker than the 3 to 5 μm obtained with paraffin sections, therefore potentially wasting valuable tissue that may be needed for immunohistochemical workup. Frozen section morphology may be suboptimal and insufficient for establishing a confident, rapid diagnosis. Finally, freezing the tissue may compromise the tumour morphology, as well as the ability to perform immunohistochemical staining once the tissue has been properly fixed and embedded in paraffin. The use of frozen sections for assessment of core biopsy should be discouraged for all of these reasons.

3. Submitting and Labelling Core Biopsy Specimens

As discussed in the Technique section, core biopsy samples should be placed in containers that are clearly labelled with patient identifiers, and the kidney-biopsied tumour location.

4. Fixation and Processing

All cores designated for routine processing should be placed in 10% formalin and may be fixed for 12 to 24 hours; however, it is possible to fix the samples for shorter periods without compromising histologic quality if rapid processing with same-day reporting is required.[61] As has been found for prostate biopsies, placing fresh cores between nylon mesh or sponges in a cassette at the time of formalin fixation can increase the chances of getting straight, flat cores that are easily embedded, providing the greatest amount of tissue for histologic examination.[62] Depending on the number of cores submitted, to further maximize the amount of tissue available for assessment, it is advisable to submit individual cores from the same mass in more than one block, enabling conservation of tissue for ancillary studies. Another approach to conserve tissue for further studies is to obtain numerous (at least 6) serial sections from each block, staining various levels with H&E, and saving intervening sections on charged slides for possible use for IHC. These approaches are not consistently practiced (see **section 7.6.2 Recommendations**). Immunohistochemical staining panels for most renal tumours are typically in the order of 2 to 5 different stains, depending on the differential diagnosis, and rarely exceed 10.[63,64] The need for prospective serial sectioning should be determined by individual institutions, and factors such as the experience of histotechnologists and the amount of lesional tissue should be considered (**Figure 7-2**).

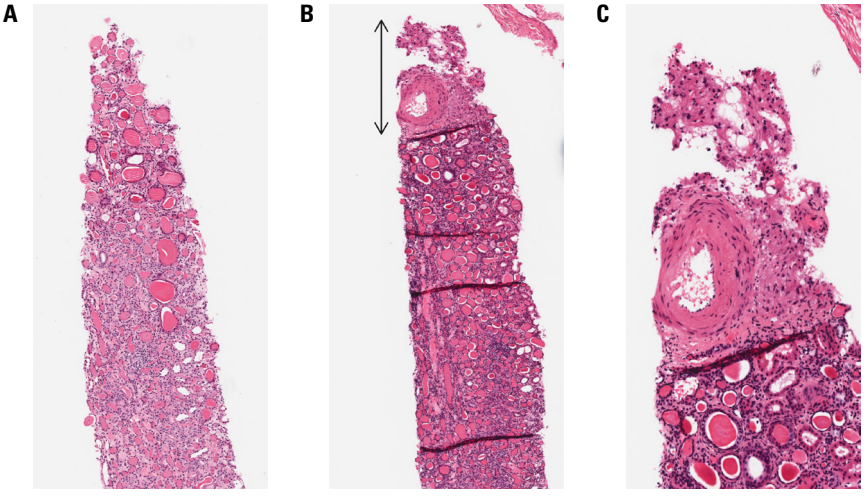

FIGURE 7-2
A Initial H&E section from a needle core biopsy of a SRM showing predominantly renal parenchyma, with a tiny fragment of tissue suspicious for a neoplasm on one end of the core.
B Deeper level from the biopsy revealing more lesional tissue sufficient in amount to establish a diagnosis of AML.
C Higher-power view of upper end of core illustrated in (**B**).

5. Snap Freezing of Samples for Cytogenetic and Molecular Analyses

Core biopsy samples have been found to be suitable for a variety of genomic, molecular, and cytogenetic assessments.[65-68] If this is required for patient care, clinical trials, or tissue banking for translational research, additional cores of fresh tissue can be placed in cryomolds containing optimal cutting temperature (OCT) frozen section medium or nunc tubes, snap frozen, and stored in liquid nitrogen. These cores can subsequently be thawed and used as required for histopathologic review or a variety of molecular analyses.

In terms of patient care, it is important that snap frozen core(s) not be used for any research purpose until a morphologic diagnosis has been established using diagnostic cores processed in the standard way. The core(s) designated for diagnosis at the time of core biopsy can be nondiagnostic, creating the need to examine the research core in the hope of establishing a tissue diagnosis.

Studies demonstrating the feasibility of performing fluorescence *in situ* hybridization (FISH) and molecular diagnostics on core biopsy samples are based on *ex vivo* core biopsy and FNA sampling[65-67] of nephrectomy specimens, as well as percutaneous core biopsy.[69] These techniques may be of particular benefit in sub-classifying renal tumours when IHC is inconclusive; however, they are only available in selected institutions at this time. Fluorescence *in situ* hybridization using commercially available probes[69] can be performed on core biopsy, FNA samples, and touch preps made from core biopsy, as well as formalin-fixed paraffin-embedded cell blocks made from FNA samples.

Molecular studies requiring DNA and/or RNA for profiling and genetic sequencing can also be carried out on biopsy material, as sufficient amounts of these analytes can be obtained from a single core biopsy,[65] the proviso being that the core biopsy contains lesional tissue. The use of these techniques to more precisely characterize tumour subtypes and identify potential therapeutic targets is expected to grow significantly as we move further into the era of personalized medicine.[60] See sections on **Role of Molecular Studies** and **Future Directions**, later in this chapter.

7.6.2 Recommendations for handling and preparation of needle core biopsies

- Rapid evaluation with a determination of specimen adequacy is very valuable, and pathologists should consider providing this service. The need for such an approach should be determined institutionally because of the importance of rapid evaluation as the best practical opportunity to receive adequate material for appropriate diagnosis. **[GOR D, LOE 4]**

- It is optional to procure additional tissue cores and snap freeze them for cytogenetic and molecular analyses. This determination should be made based on patient care needs, as well as research and tissue banking protocols in place at an institutional level **[GOR D, LOE 4]**

Specimen handling:

- If multiple cores from a single lesion are submitted in one container, we recommend submission of individual cores in more than one block to enhance the ability to perform additional studies, if necessary **[GOR C, LOE 4]**
- We recommend multiple prospective serial sections for renal core biopsies, up to six blanks with the first and last levels stained with H&E, and the remaining levels saved on charged slides for prospective IHC **[GOR C, LOE 4]**

7.6.3 Histologic scope of needle biopsy

Defining the pathologic process

The accuracy of determining the nature of a mass-forming lesion in the kidney has been excellent for biopsies determined to be diagnostic. The nomenclature promulgated in the WHO classification of urogenital tumours 2016 (WHO "blue book") (**Table 7-1**) should be used.[70] A systematic and algorithmic approach is recommended (**Figure 7-3**). This includes the identification of both benign and malignant processes. Benign processes that are reliably diagnosed on needle biopsies are largely restricted to benign neoplasms, including oncocytoma, AMLs, and others. In those series, making a specific diagnosis of oncocytoma or considering a diagnosis of oncocytic neoplasm as benign was the most commonly rendered benign diagnosis (39%–81% of benign diagnoses).[28,33,35,41,47,71-73]

The identification on non-neoplastic mass-forming lesions is much more problematic. Gellert *et al.*[34] reported that 2 of 218 biopsies (0.9%) yielded non-neoplastic tissue diagnostic of an inflammatory process (xanthogranulomatous pyelonephritis and abscess). Similarly, Lebret *et al.*[28] considered 5 of 94 diagnostic biopsies (5.3%) to be diagnostic of xanthogranulomatous pyelonephritis or abscess. In another report, Shah *et al.*[74] found 2 of 52 adequate biopsies to represent inflammatory processes (xanthogranulomatous pyelonephritis and granulomatous lesion). Volpe *et al.*[58] reported 4 of 84 diagnostic biopsies as "inflammatory lesion"[75] or "fibrotic lesion,"[75] and Veltri *et al.*[76] considered 8 cases (6%) to be diagnostic of "fibrous tissue/complicated cyst." Given the difficulty of excluding inflammation and/or fibrosis representing a response to a tumour, a definitive diagnosis of an inflammatory process is best made in conjunction with the clinical and radiological findings.

TABLE 7-1 World Health Organization (WHO) (2016) Classification of Tumours of the Kidney[70]

Clear cell RCC
Multilocular cystic renal neoplasm of low malignant potential
Papillary RCC
Hereditary leiomyomatosis and RCC (HLRCC)–associated RCC
Chromophobe RCC
Collecting duct carcinoma of the kidney
Renal medullary carcinoma
Microphthalmia transcription factor (MiT) family translocation carcinomas
Succinate dehydrogenase (SDH)–deficient RCC
MTSCC
Tubulocystic carcinoma
Acquired cystic disease–associated RCC
Clear cell papillary RCC
RCC unclassified
Papillary adenoma*
Renal oncocytoma
Metanephric tumours
Nephroblastic and cystic tumours occurring mainly in children
Mesenchymal tumours
Mixed epithelial stromal tumour family
Renal hematopoietic neoplasms
Neuroendocrine tumours
Germ cell tumours
Metastatic tumours

* A diagnosis of papillary adenoma in needle biopsies should be made with extreme caution because the presence of capsule or grade heterogeneity issues may not be visualized in biopsies.

FIGURE 7-3
Diagnostic Approach to Needle Core Renal Biopsies

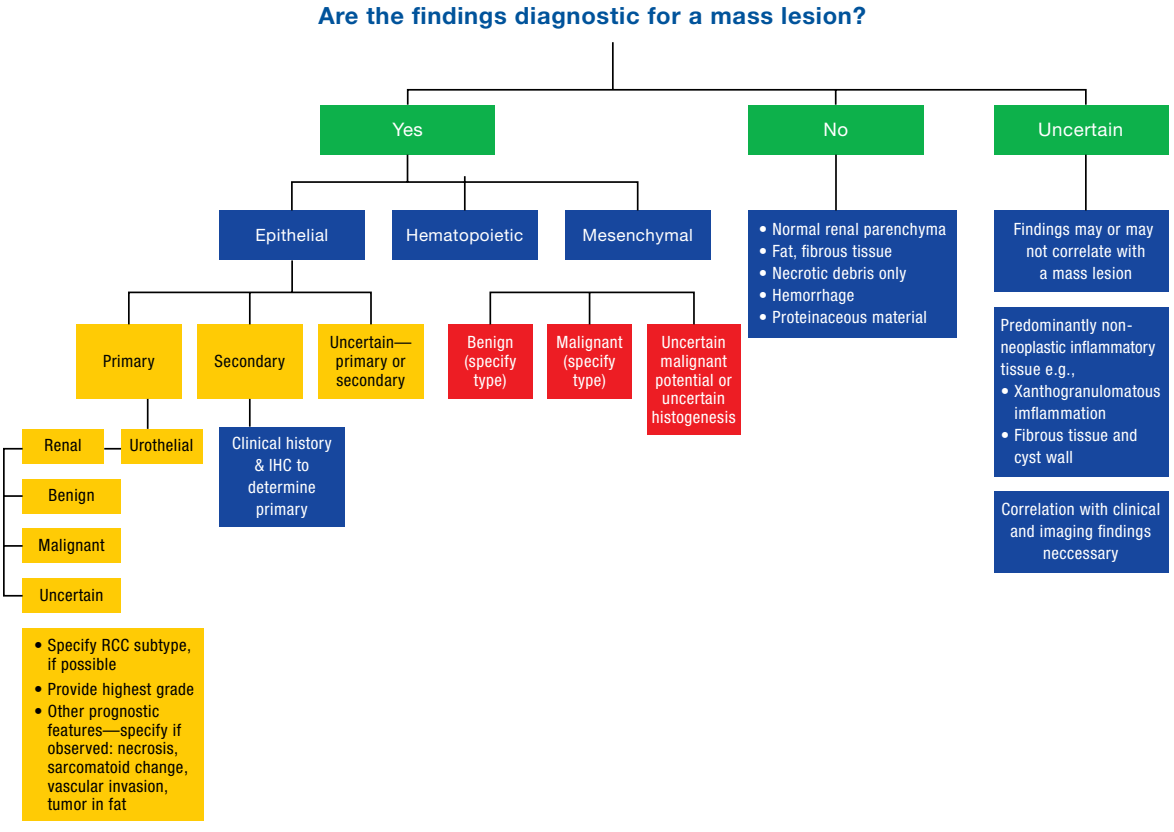

Oncocytoma

Renal oncocytoma is the most frequent benign lesion diagnosed on biopsies of renal masses, accounting for 50% to 81% of cases.[28,33,35,72,74,76] Renal oncocytoma is made up of cells with moderate to abundant granular eosinophilic cytoplasm (**Figure 7-4**).[77,78] The cells have uniform round nuclei with visible nucleoli. Mitoses are absent or, at most, vanishingly rare. In about a third of cases, pronounced degenerative nuclear atypia is present. Architecturally, the tumour has variably sized solid nests, tubules, and small cysts. The nests can be closely packed but, in almost all cases, areas with a loose hypocellular stroma are present. Observation of necrosis, mitotic activity, solid growth, and nondegenerative atypia (pleomorphism with nuclear chromatin alternations) is inconsistent with the diagnosis of renal oncocytoma. The list of renal epithelial tumours that can have eosinophilic cytoplasm is long and includes chromophobe RCC (particularly the eosinophilic type), papillary RCC, clear cell RCC, MiTF family translocation carcinomas, acquired cystic disease–associated RCC, SDH-deficiency–associated RCC, HLRCC-associated RCC, collecting duct carcinoma, and unclassified RCC. The major problems, however, are chromophobe RCC, so-called hybrid tumours, and tubular patterns of papillary RCC. Immunohistochemistry and histochemistry may or may not be helpful in the diagnosis (see following section).[63,64]

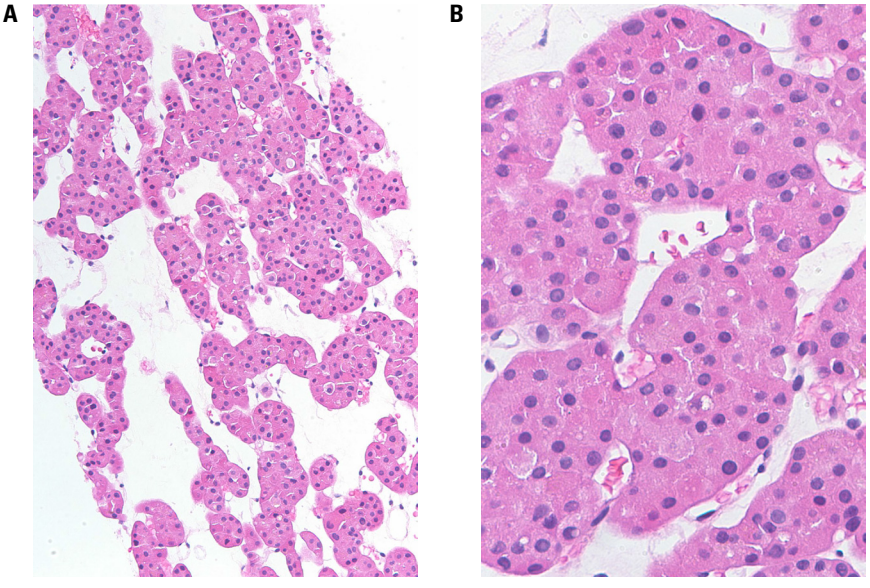

FIGURE 7-4
Renal Oncocytoma
A Low power
B High power

Rendering a specific diagnosis of oncocytoma on a biopsy specimen remains a controversial issue among specialized urologic pathologists. Oncocytoma has been included as a diagnostic category in most of the published biopsy series.[28,35,38,41,47,52,64,72,74,76,79,80] Other authors have used terms such as "renal neoplasm consistent with oncocytoma," "low grade oncocytic renal cortical neoplasm, favour oncocytoma," "oncocytic neoplasm suggestive of oncocytoma," "oncocytic renal neoplasm with features most consistent with oncocytoma," or simply "oncocytic neoplasm."[33,34,58,59,73] If typical diagnostic features of renal oncocytoma are observed in a needle biopsy, the diagnostic term "renal oncocytic neoplasm with features consistent of renal oncocytoma, see comment" may be used (**Figure 7-5**). Even in cases where morphology of chromophobe RCC may be additionally encountered, the prognosis for small organ-confined tumours is extremely favourable. Those authors using such qualified terminology have nonetheless placed these lesions in the benign diagnosis category while reporting their studies.

The concern regarding making a specific diagnosis of oncocytoma has largely revolved around the differentiation from so-called hybrid tumours that have areas mimicking both oncocytoma and chromophobe carcinoma. These tumours have been referred to as hybrid oncocytic/chromophobe tumour.[70] These tumours are most often reported in the setting of renal oncocytosis[81,82] and Birt-Hogg-Dubé syndrome[83,84] although rare *de novo* cases also occur.[85-87] In Birt-Hogg-Dubé syndrome, these tumours have FLCN gene mutations and fall within the range of renal tumours found in that clinical syndrome.[88] In renal oncocytosis, it has been shown that these tumours lack the cytogenetic features of chromophobe RCC, and have been considered in that setting to represent a type of renal epithelial neoplasm specific to that entity.[82] *De novo* hybrid tumours have also been shown to lack the genetic features of chromophobe RCC.[86,87] The concern about misdiagnosis is somewhat allayed by the excellent prognosis these tumours (sporadic and in renal oncocytosis) have had, with no examples of metastases in the reports to date in small organ-confined tumours lacking sarcomatoid change.[80-82,86,87,89]

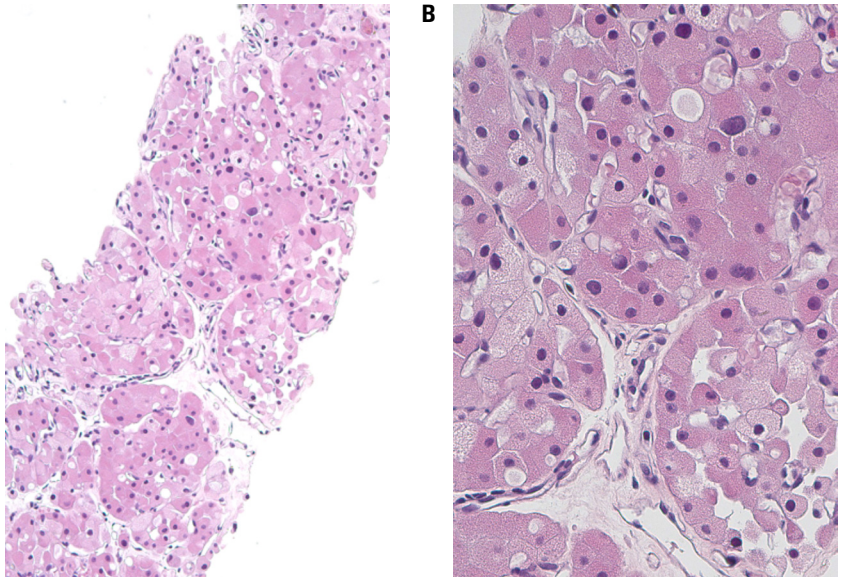

FIGURE 7-5
Renal Oncocytic Neoplasm
In this example, a definitive diagnosis between an oncocytoma and a chromophobe RCC cannot be made.

A Low power

B High power

Based on the review of needle biopsy series, it is evident that many authors are comfortable with making a specific diagnosis of oncocytoma, while other authors have recommended a noncommittal approach, as outlined above. For the authors making the diagnosis of oncocytoma, most recommend restricting the diagnosis to those cases with typical morphologic features and supportive ancillary studies, including Hale colloidal iron staining and IHC.[5-7,13,21,28,58,72,74,80] The antibody uniformly included in these recommendations is cytokeratin 7, with selected others such as vimentin, S100A1, CD117, alpha-methylacyl coenzyme A racemase (AMACR), CD10, and E-cadherin included in some panels.[28,58,64,72,74,80] Regardless of the approach, in virtually all series these tumours are placed in the benign category. Either approach to diagnosis is reasonable, and we would not specifically advocate for either.

Angiomyolipoma

Renal AML is the second most frequent benign diagnosis on needle biopsies of renal mases, accounting for 9% to 28% in larger series.[28,35,47,58,72,73,76] Most cases of renal AML can be diagnosed by imaging based on the presence of adipose tissue within the lesion. Some AMLs are smooth muscle predominant and have minimal fat, and these are the tumours most likely to be biopsied and/or resected.[90] In most cases, these are readily recognized by the presence of smooth muscle bundles and thick-walled, malformed blood vessels. Smooth muscle cells can be spindle shaped to more epithelioid. Nuclear atypia can be present, but mitoses are distinctly uncommon. Perivascular sclerosis can produce a trabecular architecture. Fat can be minimal or absent.

In pure smooth muscle lesions, the possibility of a smooth muscle neoplasm (leiomyoma/leiomyosarcoma) could be considered. In such cases, the diagnosis is readily confirmed by IHC. The presence of large ganglion cell–like cells with or without mitoses or necrosis should prompt consideration of an epithelioid AML. These tumours can have pure histology or can be mixed with more typical AML. In patients with tuberous sclerosis, rapid change in size or an atypical radiological appearance in a lesion can prompt a needle biopsy. In some instances, this can be due to development of an

epithelioid AML[91,92] or RCC.[93,94] The possibility of a sarcomatoid carcinoma can be considered when the sample is limited and nuclear atypia is present; however, the degree of pleomorphism and mitotic activity associated with this are absent in AML. The spindle cell component of MTSCC can closely resemble smooth muscle, and the presence of tubules or mucin in the background should suggest the possibility.

Other

A number of other benign neoplasms have been reported in needle biopsy specimens, including metanephric adenoma (**Figure 7-6**),[33,35,47,76] leiomyoma,[33,76,95] mixed epithelial and stromal tumours,[47] and benign cysts.[47,76] Metanephric adenoma is distinctive with small, bland cells with scant cytoplasm arranged in tiny nests or tubules, often in a dense fibrotic stroma (**Figure 7-5**). The tubules can be branching, and intratubular proliferations forming glomeruloid structures can be seen. Mitoses are absent or, at most, rare. Psammomatous calcifications are common and can be numerous. Major differential diagnostic considerations are epithelial-predominant Wilms' tumour and pure tubular patterns of papillary RCC. In challenging cases, IHC can usually resolve the diagnosis.

The 2016 WHO classification of renal tumours includes a revised definition for papillary adenoma.[96] The revised criteria include increasing the size allowed from 5 mm to 15 mm. Additional criteria include a nuclear grade of 1 or 2, and the absence of a pseudocapsule. The new size criteria will therefore include lesions that are likely to undergo needle biopsy. Because of the grade and capsule criteria, a definitive diagnosis probably should not be rendered on needle biopsy, although if the size of the mass is known, the possibility of papillary adenoma could be suggested.

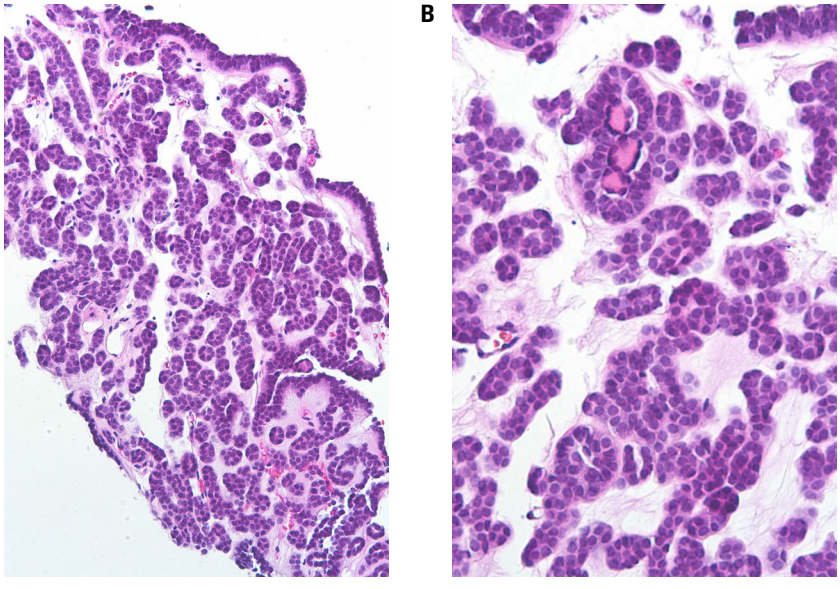

FIGURE 7-6
Metanephric Adenoma
A Low power
B High power

2) Histologic characterization of the neoplastic process

The vast majority of malignant renal masses subjected to biopsy are RCCs. In most series, these account for more than 95% of cases.[28,33,34,38,41,58,72,73] Less frequently, urothelial carcinoma presents as a mass lesion and is diagnosed by percutaneous needle biopsy.[28,34,41,58,72,73] In some cases, it is not

possible to specifically classify the origin of the carcinoma.[58,72] Occasional examples of metastatic carcinoma involving the kidney are included in published series (**Figure 7-7**).[28,33,34,47,58,72] Finally, other tumours, such as sarcoma and lymphoma, can be recognized.[28,34,47,74,76] The accuracy of properly classifying the nature of the neoplastic process has been very high, with most series reporting between 95% and 100% agreement between biopsy and resection specimens.[34,35,41,47,58,72,73,76]

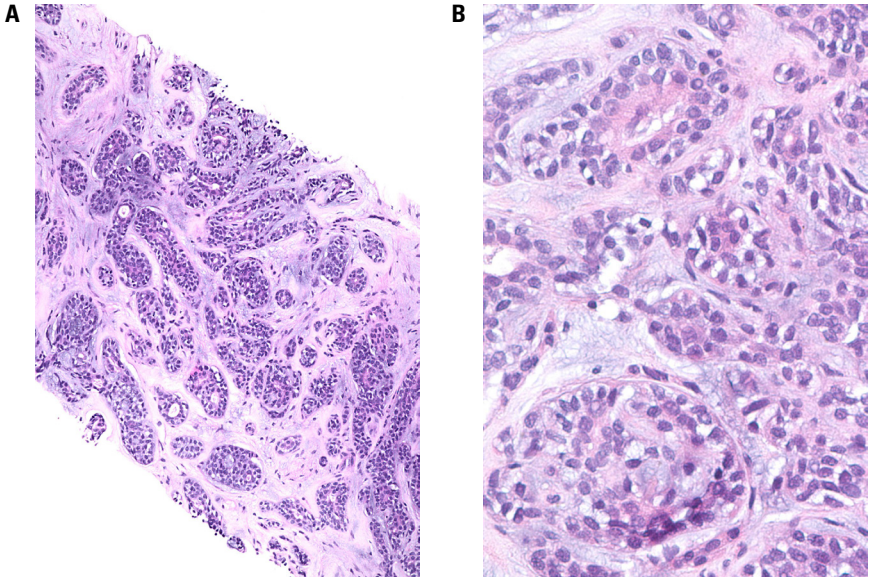

FIGURE 7-7
Metastatic Adenoid Cystic Carcinoma From the Parotid Gland to the Kidney

The possibility of urothelial carcinoma should be considered when the tumour demonstrates an infiltrative growth pattern with associated stromal desmoplasia. These tumours can have an intratubular growth, and this can be recognized in some cases. The presence of squamous differentiation in a high-grade tumour would also strongly suggest urothelial origin (**Figure 7-8**). When urothelial carcinoma invades renal parenchyma, it can closely mimic collecting duct carcinoma, and that is the major differential diagnosis. Other considerations would include renal medullary carcinoma, HLRCC-associated RCC, and metastatic carcinoma. In most problematic cases, the distinction of urothelial carcinoma from RCC can be made with selected immunohistochemical stains (see discussion below).

In very rare cases, especially if adequate tissue is not available for immunohistochemical studies, the diagnostic term "unclassified carcinoma, differential diagnosis includes renal versus urothelial versus metastatic" may be used.

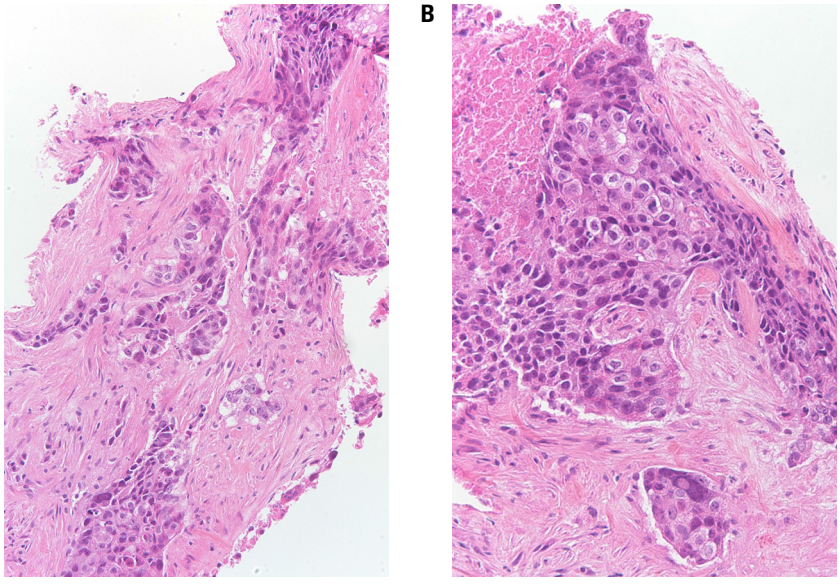

FIGURE 7-8
Urothelial Carcinoma of the Pelvicalyceal System Secondarily Involving the Renal Parenchyma

A Low power

B High power

3) Histologic subtyping of RCC

The current classification of RCC is complex and includes a large number of recognized entities (**Table 7-1**).[70] Fortunately, over 95% of cases are accounted for by the four most common types of RCC: clear cell RCC, papillary RCC, chromophobe RCC, and clear cell papillary RCC. Not surprisingly, then, the literature has repeatedly reported a high degree of accuracy in subtyping RCC on needle biopsy. In a review published in 2014, Gellert *et al.*[34] found that the accuracy of subtyping RCC ranged from 78% to 100% in contemporary series (2007–2013). The overall accuracy was 93%, based on the 547 cases summarized.[28,41,47,58,72,75,79,95] In their experience, the accuracy was 97%, but this was based on only a small percentage (22%) with biopsy/resection correlation. In a recent large series, Richard *et al.*[33] reported on their experience with RTB of 529 patients with tumours ≤4 cm, where paired biopsy and resection specimens were available for 166 of the cases diagnosed as RCC. Subtyping was accurate in 155 of the 166 cases (93.4%). It is beyond the scope of this section to provide a detailed review of the histology of all the types of RCC; however, the most common types of RCC with selected comments are provided below. The IHC of the tumours is detailed in a later section.

Clear cell RCC

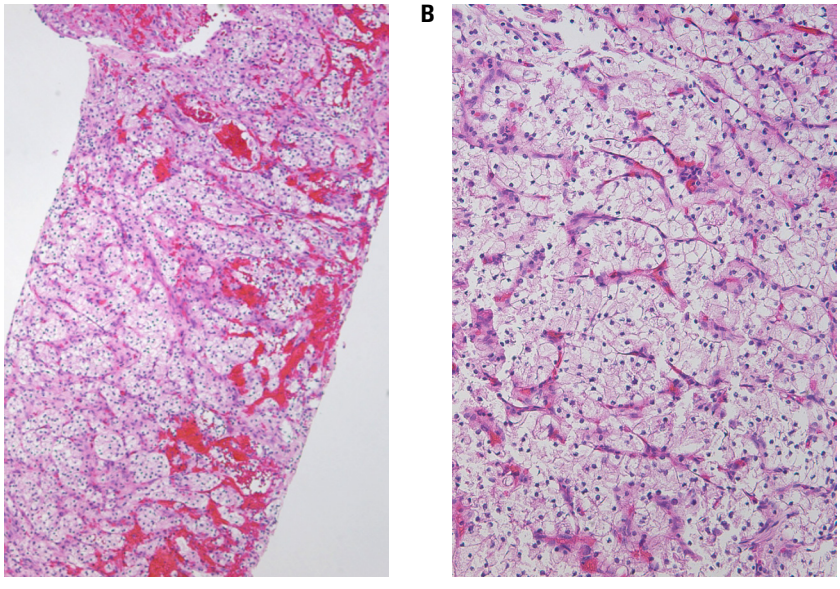

FIGURE 7-9
Clear Cell RCC
A Low power
B High power

Clear cell RCC is the most common type of RCC diagnosed on needle biopsy. Morphologically, the tumour consists of cells with moderate to abundant clear cytoplasm arranged in nests, tubules, and alveolar structures. A fine sinusoidal vascular network is characteristic (**Figure 7-9**). In some cases, the cells have granular eosinophilic cytoplasm, usually associated with higher-grade tumours, but retain the architectural features. Areas of cyst formation, fibrosis, and necrosis can be present.[59,97-99]

Well-defined papillary architecture and/or psammomatous calcifications should indicate an alternate diagnosis such as a papillary RCC, with cells having clear cytoplasm or an MiTF family translocation carcinoma. Growth in broad trabeculae or prominence of the cell membrane raises the possibility of a chromophobe RCC. The presence of branching tubular structures, particularly with short, stubby papillary infoldings, raises the possibility of clear cell papillary RCC, as does the presence of prominent stroma with a smooth muscle or smooth muscle–like appearance. The latter also can be present in RCC with angioleiomyoma-like stroma. In any case where a tumour at first glance suggests clear cell RCC but unusual features are present, confirmation of the diagnosis by IHC is recommended.

Papillary RCC

Papillary RCC is the second most frequent type of RCC encountered. These tumours are characterized by the presence of well-formed papillary structures, although tubular and solid architectures can be seen (**Figure 7-10**).[100-102] Tumour cells range from small and cuboidal with scant or basophilic cytoplasm to large and columnar with eosinophilic cytoplasm. Nuclei tend to be uniform and round. The tumour cells can be arranged as a single layer or with pseudostratification. In many cases, foamy macrophages are present in the papillary stalks and hemosiderin deposition can be prominent, including in the cytoplasm of tumour cells. Psammomatous calcifications can be present. Type 1 tumours characteristically have a single cell layer with most being low nuclear grade and composed of cells with scant to basophilic cytoplasm. In contrast, type 2 tumours have pseudostratification, with most made up of cells with high nuclear grade and abundant eosinophilic cytoplasm. Papillary

RCC with voluminous, finely granular, evenly distributed eosinophilic cytoplasm and oncocytoma-like nuclei have been called "oncocytic papillary RCCs." The nuclei are typically single layered and linearly arranged. Oncocytic papillary RCC has not been formally accepted as a subtype of papillary RCC in the new WHO classification.[70]

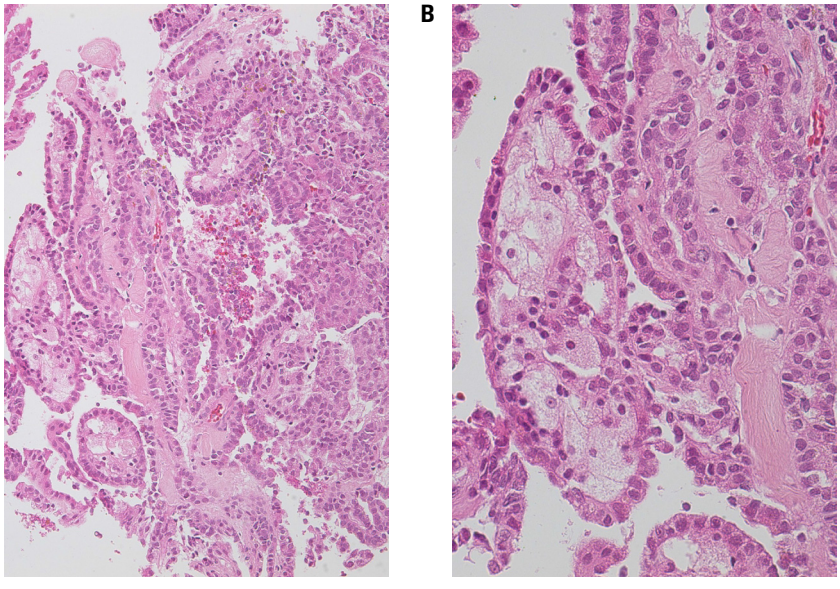

FIGURE 7-10
Papillary RCC
A Low power
B High power

When well defined, papillary structures are present with solid areas mimicking clear cell RCC, an MiTF family translocation carcinoma should be considered. If there is an associated high-grade infiltrative component and cells having macronucleoli ("viral inclusion-like"), an HLRCC-associated RCC should be entertained. Similar tumours with the papillae less well defined should also suggest the possibilities of collecting duct and medullary carcinomas. Short, blunt papillae within branching ducts or cystic spaces and composed of clear cells would indicate a clear cell papillary RCC. When tubular architecture predominates and there is mucinous material in the background, MTSCC is a possibility. The tubular pattern when composed of cells with eosinophilic cytoplasm can mimic renal oncocytoma. The message is that, for tumours with papillary and/or tubular architecture where the appearance is not typical, alternate diagnoses must be considered.

Chromophobe RCC

Chromophobe carcinoma is the third most common type of RCC.[103-105] Morphologically, there are two patterns that are characteristic. The typical or classic type is composed of variably sized but mostly large cells with pale eosinophilic to clear cytoplasm (**Figure 7-11**). Concentration of cell organelles at the periphery results in prominent eosinophilia resembling a thick cell membrane producing the plant cell–like appearance. Nuclei are often large and can have a striking wrinkled or "raisinoid" appearance. Binucleation is common. The cells are arranged in broad trabeculae or sheets with prominent vessels. The eosinophilic variant has small polygonal cells arranged in closely packed and relatively uniform nests. Individual cells have eosinophilic cytoplasm and often have a zone of

prominent perinuclear clearing. The nuclei tend to be round and uniform, with small or inconspicuous nucleoli. The nests are separated by a prominent vascular network. Edematous areas can result in the nests being pulled apart in cords and variable cell clusters.

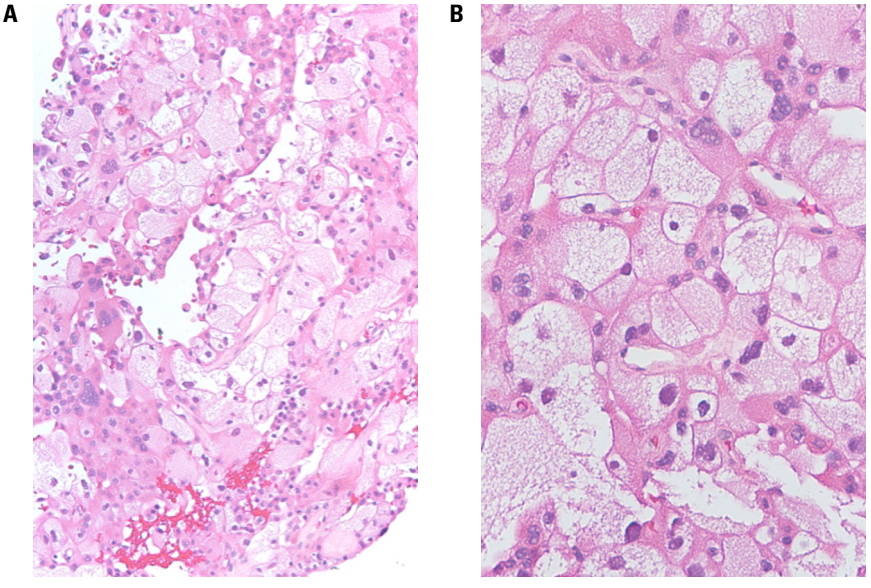

FIGURE 7-11
Chromophobe RCC in a Needle Biopsy
A Low power
B High power

When the classic type of chromophobe RCC is considered, the presence of a more nested or alveolar architecture raises the possibility of clear cell RCC. Similarly, somewhat smaller cells with more optically clear cytoplasm also would suggest clear cell RCC, or even an MiTF family translocation–associated carcinoma. For the eosinophilic variant, the presence of more variability in the size of the nests, prominent tubular differentiation, or a separation of the nests in a loose hypocellular stroma would make renal oncocytoma a strong consideration. Prominent cytoplasmic vacuoles should prompt consideration of a SDH-deficiency–associated RCC. Any papillary architecture, the presence of foamy histiocytes, or hemosiderin deposition would bring papillary RCC into the differential diagnosis. Immunohistochemistry, as detailed below, can be helpful in these various differential diagnosis considerations. In some cases of oncocytic renal tumours where the nuclear and/or cytoplastic features are not diagnostic for chromophobe RCC, and depending on how suggestive the diagnosis is, in needle biopsy settings descriptive diagnoses such as "renal oncocytic neoplasm, cannot rule out chromophobe RCC" or "renal oncocytic neoplasm favour chromophobe RCC" may be used.

Clear cell papillary RCC

Although only recently added as a distinct tumour to the classification of RCC, clear cell papillary RCC is now generally acknowledged to be the fourth most common type of RCC.[106,107] These tumours are almost always partially solid and partially cystic, are composed of cells with clear cytoplasm, and are of low nuclear grade (1 or 2) (**Figure 7-12**). Other characteristic features are a tubular architecture with branching tubules, short blunt papillae within tubules or cysts, nuclei located toward the apical end of the cells, and a prominent stroma that can have smooth muscle features.

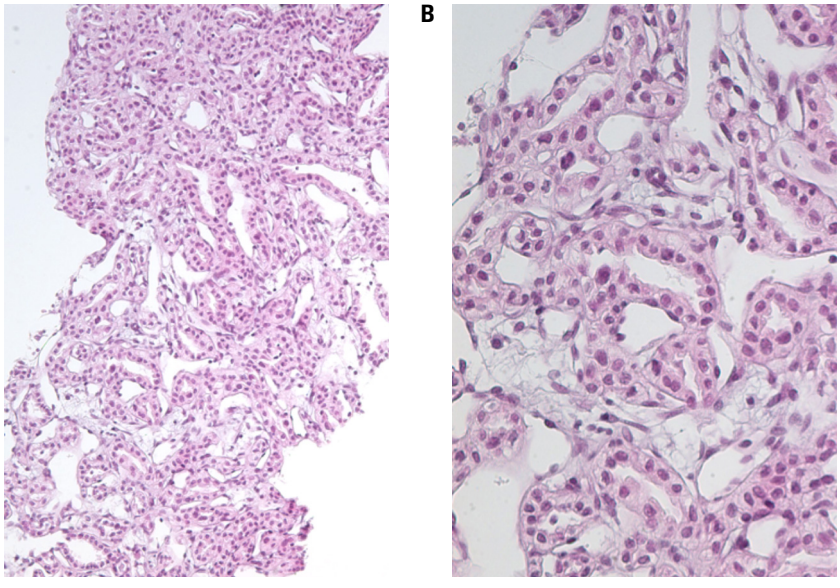

FIGURE 7-12
Clear Cell Papillary RCC
A Low power
B High power

This tumour can have areas that are virtually indistinguishable from clear cell RCC, with small nests and a prominent sinusoidal vascular network. In the absence of the characteristic features described above, clear cell RCC should be excluded by IHC. When the smooth muscle stroma is prominent or hemangioma-like areas are present, the possibility of RCC with angioleiomyoma-like stroma is considered. It is currently debated whether this tumour falls within the spectrum of clear cell papillary RCC or represents a distinct tumour type.[108-110] If papillae are well developed, the possibilities of MiTF family translocation–associated carcinoma and papillary RCC should be considered.

RCC, Unclassified

Renal cell carcinoma, unclassified is not a distinctive type of RCC but a diagnostic category of tumours that do not fit any of the subtypes of RCC. Some tumours may be low grade, including tumours with extensive cytoplasmic eosinophilia in which the differential diagnosis includes oncocytoma, although most cases are high grade (**Figure 7-13**). Although there are no formal studies, a higher number of cases in needle biopsies may be unclassified compared to in resection specimens where there is the possibility of having multiple sections to appreciate the architectural and cytological features, as well as adequate material to perform immunohistochemical studies for more appropriate classification. In needle biopsy specimens, due to inherent limitation of amount of tissue, "RCC, not otherwise specified, further histologic subtyping not possible in needle biopsy material" may be used.

FIGURE 7-13
Unclassified RCC

This high-grade carcinoma does not have histologic features specific or diagnostic for any of the subtypes of RCC.

A H&E;

B PAX 8 IHC supporting a renal histogenesis for this carcinoma.

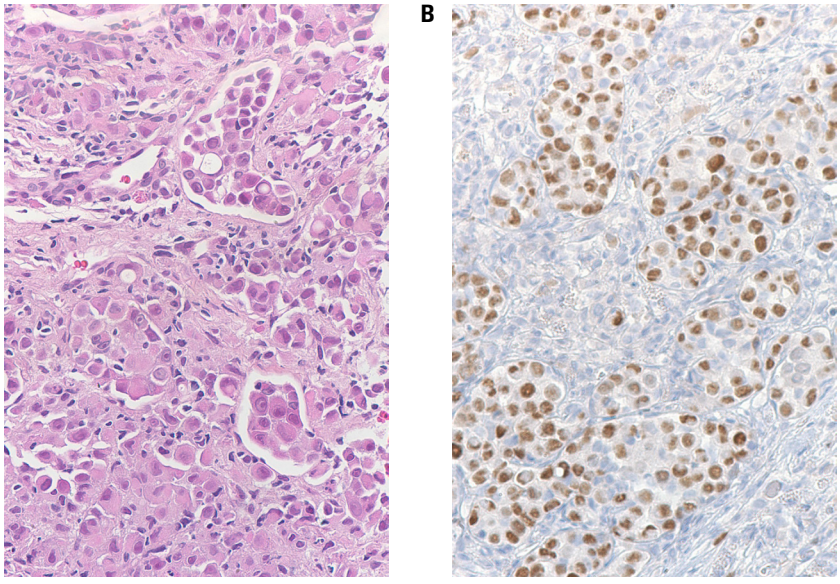

4) Histologic grade of RCC

Nuclear or nucleolar grading has been shown to be a significant prognostic indicator for clear cell RCC and papillary RCC.[111,112] Its significance in chromophobe RCC has been the subject of debate for many years and, in general, it is not considered to be a proven prognostic parameter in these tumours.[113,114] For the most part, there are insufficient data on the role of nuclear or nucleolar grading in other types of RCC. Nuclear grading using the system of Fuhrman *et al.*[115] has been the standard for over three decades, with substantial supporting data in the literature. It has, however, been recognized that most urologic pathologists have focused primarily on nucleolar size and, to a lesser degree, on nuclear shape and pleomorphism in assigning Fuhrman grade.[116-118] For that reason, this generally accepted application has been codified by the International Society of Urological Pathology (ISUP) as the ISUP grading system, and has been subsequently adopted by the WHO in 2016.[70,118] The current ISUP/WHO grading system is recommended, and the Fuhrman grade should also be reported until there is more widespread understanding about the former (in reality, in most urologic pathologists' hands the ISUP/WHO and Fuhrman grade will be identical in practically all clear cell and papillary RCCs). There are, at the present, few studies that have used the ISUP grading system as defined in 2012. It should also be noted that all of the needle biopsy series to date have utilized Fuhrman grading alone.

Grade heterogeneity in RCC is well recognized, and data in the literature support the assignment of the highest grade present as the most prognostically relevant. Grade heterogeneity has been shown to be significant even in SRMs.[71] This heterogeneity and the likelihood of under-grading on needle biopsy is well recognized and has been addressed in several reports. Overall concordance between biopsy and resection grade has ranged from 38% to 76%.[28,33,34,38,41,52,75,79,119-121] Regarding the frequency of upgrading from low (grades 1 and 2) to high (grades 3 and 4) nuclear grade, results have ranged from 6% to 50%.[28,33,34,38,41,52,79,119,121] Over-grading is also described but is much less frequent. Given the limitations on grading in needle biopsies, it has been recommended that grade be assigned using the phrase "at lease grade X" to highlight this uncertainty.

5) Reporting of other prognostic parameters

There are a number of other morphologic parameters beyond histologic type and nuclear grade that have been demonstrated to be of prognostic significance. Sarcomatoid change in any type of RCC is associated with a poor prognosis. This can be seen in needle biopsy specimens and, when present, should be reported.[52,120] In a series of biopsies of large (≥cT2) renal masses, Abel *et al.*[52] identified sarcomatoid change in 87% of tumours where it was present in the resection specimen using a technique with 4 cores taken from different areas of the tumour, compared to 25% when a standard approach was utilized. Microscopic tumour necrosis is also known to be significant prognostic feature for clear cell RCC and is included in the Mayo Clinic SSIGN score.[122,123] This has also been found in papillary RCC, though with more limited data.[124] More recently, the presence of microscopic necrosis has been used in conjunction with ISUP grading to create a new grading system that uses both parameters.[118] Bernhard *et al.*[38] identified microscopic tumour necrosis in 10% of needle biopsies in a group of tumours that, on resection, had necrosis present in 28% of cases. Microscopic lymph-vascular invasion has been studied in resection specimens and correlates with increased tumour recurrence and decreased cancer-specific survival.[112] Identification has not been described in biopsy series but could be reported if present. Finally, the biopsy could demonstrate tumour invasion beyond the renal parenchyma and, if this is present, it should be reported. There have been no studies that have reported on the frequency of this observation in needle biopsy specimens.

Recommendations for histologic scope of the needle core biopsies

- The diagnostic nomenclature recommended for use in renal core biopsies is the WHO 2016 Classification System **(Table 7-1) [GOR B, LOE 3]**.

- The diagnosis of renal oncocytoma should be made with caution in needle core biopsies. If a definitive diagnosis of renal oncocytoma is made, it requires rigid morphologic criteria combined with supportive histochemical and immunohistochemical studies. In cases with classic diagnostic features, we recommend the diagnostic terms "renal oncocytoma" or "renal oncocytic neoplasm with features consistent of renal oncocytoma." In other circumstances, the term "renal oncocytic neoplasm" may be used with an explanation in the comments explaining which features are unusual for an outright diagnosis of renal oncocytoma **[GOR C, LOE 4]**.

- An attempt to further subclassify RCCs should be made in every case. Before a diagnosis of "RCC, unclassified type" or "RCC, not otherwise specified, further histologic subtyping not possible in needle biopsy material" is rendered, metastasis and urothelial carcinoma should be ruled out based on morphologic and/or immunohistochemical criteria **[GOR B , LOE 3]**.

- The highest (majority of cells in a single high power field) histologic grade observed in a carcinoma should be provided. Due to grade heterogeneity in RCC, the recommended diagnostic term should include "at least grade X" to acknowledge the uncertainty that a higher grade may be present **[GOR B, LOE 3]**.

- For the common subtypes of RCC, specifically clear cell and papillary RCC, the ISUP/WHO grading system is recommended for use.[70] There is no accepted grading system for chromophobe RCC and rarer subtypes of RCC **[GOR B, LOE 3]**.

- In needle biopsies, other adverse prognostic parameters should be reported only if observed. These include sarcomatoid change, cells with rhabdoid features, necrosis, vascular-lymphatic invasion, and tumour infiltration of adipose tissue (suggesting pT3 disease) **[GOR B, LOE 3]**.

7.6.4 Role of Immunohistochemistry

Renal neoplasms are a heterogeneous group of lesions that span the spectrum from primary epithelial-derived tumours to mesenchymal and metastatic tumours. While most primary neoplasms have characteristic morphological features, some share histological features, at least focally, while others can express significant morphological heterogeneity within different areas of the same tumour mass. High grade and poorly differentiated tumours can present a significant diagnostic challenge, an issue that is magnified in needle biopsy samples. Because tumours commonly harbour a characteristic antigenic phenotype, IHC can be a valuable adjunct in establishing a precise diagnosis.[34,63,64,125]

Several guiding principles should always be followed when using IHC assays to evaluate a lesion:

a. Antibodies should be applied in panels rather than singly, and the panel should be tailored to the differential diagnosis being considered.
b. Qualitative and quantitative characteristics of the stain should be taken into consideration.
c. Antibody panels should be modified over time, as novel markers are clinically validated and found to be superior in sensitivity and specificity.

The ISUP has recently provided several best practice recommendations in the application of IHC in urologic pathology in general, and kidney tumours in particular.[126]

1) Determination of primary site and cell of origin

Both primary and metastatic tumours may involve the kidney. Apparent primary tumours may be of epithelial, mesenchymal, or even hematolymphoid origin. A proper clinical history is critical in the pathological evaluation of needle biopsy material and should be provided by the submitting clinician. If a patient with a renal mass is known to have a primary tumour elsewhere, knowing this information will direct the pathologist on how to work up the case. For example, in the case of adenocarcinoma of the lung, not only is the antigenic make-up of this tumour distinct from virtually all renal epithelial neoplasms (thyroid transcription factor 1 [TTF-1] and napsin positive while PAX8 negative), but the pathologist will be sure to preserve tissue for mutational profiling, which could inform subsequent systemic therapy. Other examples include melanoma (cytokeratin negative while S-100 and HMB-45 positive), which may require BRAF testing, and lymphoma (cytokeratin negative while positive for various lymphoid markers, depending on cell lineage), which may be critical for establishing proper therapy.

PAX8 is the most useful IHC marker for establishing a diagnosis of a primary renal neoplasm, as it is expressed in all RCC subtypes with a sensitivity of 95%.[63,127,128] The monoclonal antibody to this transcription factor (PAX8R1) exhibits a greater degree of specificity in staining virtually all RCC, as well as Müllerian and thyroid neoplasms. However, it is important to recognize that up to 20% of upper tract urothelial tumours can be PAX8 positive, an important potential pitfall. Urothelial tumours are usually immunoreactive for GATA3, as well as p63 (clone 4A4) and high molecular weight cytokeratin 34ßE12, a combination of antigens rarely, if ever, expressed in renal cortical neoplasms.[129-131]

Given its poor specificity, the RCC marker antigen is of limited utility, as it is expressed in a significant percentage of other primary carcinomas such as breast, lung, colon, and adrenal. As such, usage should be limited to very specific circumstances and never outside of a panel.[132-134] It is important to

keep in mind that several IHC markers, such as TTF-1, the intestinal marker CDX2, prostate-specific antigen (PSA), and estrogen receptor, are almost always negative in renal neoplasms. As such, positive staining for any of these analytes is strong evidence against a primary RCC.

The diagnosis of AML is usually made radiographically, given its trilineage differentiation and presence of fat density. However, its cellular components can be quite variable, with some cases being predominantly composed of smooth muscle, epithelioid cells, or, less frequently, fat. It is the smooth-muscle–predominant and epithelioid variants that lack fat density that are mistaken as solid renal masses and consequently more likely to be biopsied or resected. Angiomyolipoma, irrespective of its cellular components, will lack expression of PAX8 and epithelial markers, while variably expressing smooth muscle actin, HMB-45, Mart-1, and cathepsin K.[91,135,136] These markers are shared among tumours derived from perivascular epithelioid cells and classified under the term PEComas. The epithelioid variant of AML can be easily confused with RCC, while a smooth muscle predominant AML can be confused with sarcomatoid carcinoma or leiomyosarcoma. Dedifferentiated liposarcoma arising in the retroperitoneum may present as a renal mass and be mistaken for a sarcomatoid carcinoma. These tumours classically lack PAX8 and epithelial markers, but are more likely to coexpress S-100 protein, CDK-1, and MDM2.

2) The histological subtyping of RCC

Although the histological features of many renal neoplasms are well defined and classification rarely requires ancillary studies, this is not the case when confronted with the limited material provided by needle biopsy, in which between 30% and 50% of the cases will require these assays.[33,34,99]

Factors that contribute to this problem include sampling adequacy, tumour heterogeneity, cellular preservation, and tumour grade (degree of differentiation), including sarcomatoid features. Cystic neoplasms can be particularly challenging. The inclusion of antibody panels in the work-up of selected cases increases the diagnostic rate to over 90% in cases with adequate sampling. Another confounding factor is that multiple novel entities have recently been described and accepted by the ISUP and will soon be incorporated into the next edition of the WHO classification of renal tumours.[16] While some of these novel entities have well-defined morphology and immunophenotype, in others the entire spectrum of morphologies and antigen expression is still evolving. Good examples include the expanding spectrum of translocation-associated carcinomas, tumours associated with specific germline mutations, tumours with oncocytic features, clear cell carcinomas associated with a prominent myoid stroma, so-called type 2 papillary RCC, and unclassified RCC. The latter two categories are unquestionably non-entities representing a heterogeneous group of tumours that will certainly evolve over the years. In these situations, it is unlikely that a needle core biopsy will provide sufficient material to allow a pathologist to render a precise diagnosis. Despite these challenges, we have found that selecting among 5 well-characterized antibodies will resolve most cases that require IHC for proper classification of the more common tumours, depending on the differential diagnosis.[64,137] These include carbonic anhydrase IX (CAIX), AMACR, CK7, CD10, and CD117. Other antibodies should be applied if the differential diagnosis includes less common tumours.

Differential diagnosis of tumours with clear cell features:

While clear cell RCC is the most common type of renal tumour, many other renal tumours may exhibit a variable percentage of clear cells.[98,137] Importantly it is common for high-grade areas of clear cell RCC to not show cytoplasmic clearing. Clear cell RCCs are characteristically immunoreactive for CAIX in a diffuse and circumferential membranous distribution. This pattern of staining is not seen in any other type of renal carcinoma. Carbonic anhydrase IX is under the control of hypoxia inducible factor (HIF), which is invariably dysregulated in clear cell RCC. Expression can be focal in up to 25% of cases and can be negative in poorly differentiated areas.[138] Other markers positive in clear cell RCC but of lower specificity include epithelial membrane antigen (EMA) and wide spectrum cytokeratins (CK-Pan), vimentin, and CD10. They are usually negative or only focally positive for CK7, AMACR, and CD-117.[125,139-141] Other renal tumours that can mimic clear cell RCC include clear cell papillary RCC, chromophobe carcinoma, translocation-associated RCC, and epithelioid AML. **Table 7-2** summarizes the antibodies that can be used when considering this differential diagnosis.

TABLE 7-2 Immunoprofile of Renal Tumours Composed of Clear Cells

Tumour type	Usually positive	Usually negative
Clear cell RCC	CAIX*, CD10, EMA AE1/AE3, Vimentin	AMACR, CK7, CD117
Clear cell papillary RCC	CAIX*, CK7†	AMACR, CD10, CD117
Chromophobe RCC	CD117, CK7†	CAIX, AMACR, CD10, vimentin
TFE3 translocation–associated carcinoma	TFE3‡, cathepsin K§	CAIX, AE1/AE3, CK7, CD117
TFEB translocation–associated carcinoma	TFEB‡, cathepsin K§, HMB45	CAIX, AE1/AE3, CK7, CD117
Epithelioid AML	HMB45, cathepsin K§	AE1/AE3, TFE3/TFEB, PAX8

* CAIX is characteristically diffuse and membranous (box like) in clear cell RCC, diffuse but sparing the luminal border (cup like) in clear cell papillary RCC.

† CK7 is diffuse and strong in clear cell papillary RCC. In chromophobe RCC, it is diffuse cytoplasmic, but eosinophilic variants can have patchy or focal expression only.

‡ Antibodies for TFE3 and TFEB are difficult to perform on automated platforms, and most laboratories have found them to be unreliable. FISH break-apart probes are more useful.

§ Cathepsin K is expressed in only a subset of TFE3 RCC but in virtually all TFEB RCC and epithelioid AML.

Differential diagnosis of tumours with papillary architecture:

The prototypic example and most common type of papillary renal tumour is papillary RCC, type 1, which will rarely cause a diagnostic dilemma, even on needle biopsy. These tumours are commonly immunoreactive for CK7 and AMACR.[34,63] CD10 is variable, while CAIX is negative or only expressed at the tips of the papillae.[64] Type 1 papillary RCC can exhibit some cytological heterogeneity characterized by larger nuclei, prominent nucleoli, and more abundant eosinophilic cytoplasm.[142] These areas can mimic so-called type 2 papillary RCC and have a more variable immunophenotype. These features could lead to misdiagnosis at the time of needle biopsy. Other renal tumours that can mimic papillary RCC include clear cell papillary RCC, metanephric adenoma, translocation-associated RCC, type 2 papillary RCC, and some tumours with distal nephron morphology. Type 2 papillary RCC remains in the ISUP and WHO classification of renal tumours, even though it has been shown to be a heterogeneous category of tumours that includes tumours associated with HLRCC syndrome.[16,143]

These tumours can have a variable immunophenotype, but commonly express AMACR and, less frequently, CK7. (**Figure 7-14**). Equally challenging to diagnose on needle biopsy are the rare tuberous sclerosis complex (TSC)–associated RCC, some of which contain a prominent papillary architecture lined by cells with voluminous clear-to-granular cytoplasm.[93,94,144] **Table 7-3** summarizes antibodies that can be used when considering the differential diagnosis of renal tumours with a papillary architecture.

TABLE 7-3 Immunoprofile of Tumours With a Papillary Architecture

Tumour type	Usually positive	Usually negative
Papillary RCC, type 1	CK7^, AMACR	CAIX+
Papillary RCC, type 2	AMACR, CAIX	CAIX+, CK7^
Clear cell papillary RCC	CAIX*, CK7^	AMACR, CD10, CD117
Metanephric adenoma	WT-1, CD57	AMACR, CK7
TFE3 translocation–associated carcinoma	TFE3†, cathepsin K‡	CAIX, AE1/AE3, CK7, CD117
HLRCC	AMACR	CK7, FH (loss)

^ CK7 is diffuse and strong in type 1 papillary RCC and clear cell papillary RCC. In type 2 papillary RCC, CK7 can vary from negative to variably positive.

+ CAIX may have a cytoplasmic staining pattern, particularly adjacent to areas of necrosis.

* CAIX is characteristically diffuse but sparing the luminal border (cup like) in clear cell papillary RCC.

† Antibodies for TFE3 are difficult to perform on automated platforms, and most laboratories have found to be unreliable. FISH break-apart probes are more useful.

‡ Cathepsin K is expressed in only a subset of TFE3 RCC, correlating with the type of rearrangement.

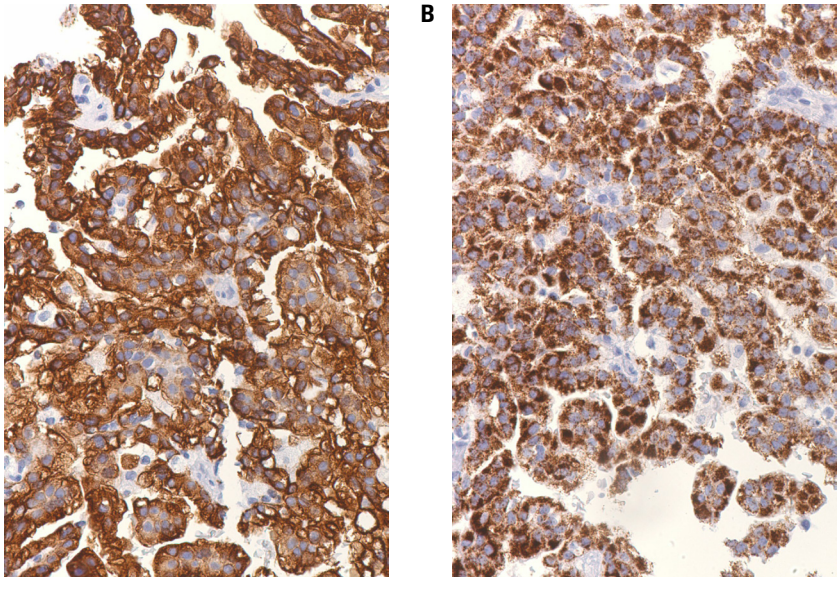

FIGURE 7-14 Immunohistochemistry in the Diagnosis of Papillary RCC

A CK7;

B AMACR/racemase; both positive. In the right morphologic context, this IHC profile is highly supportive of the diagnosis of papillary RCC.

Differential diagnosis of tumours with oncocytic features (cytoplasmic eosinophilia):
Oncocytomas comprise less than 10% of resected primary renal masses, but are more prevalent in series that look at SRMs.[34,145,146] As such, they can be readily encountered on needle biopsy material, but very challenging to classify. It is one of the few variants of renal epithelial neoplasms that is, by definition, benign. Classic examples are immunoreactive for CD-117 in a membranous distribution and typically show strong positive reactivity for CK7 in a small percentage of cells (<5%), or are completely negative. The main differential diagnosis is with the eosinophilic variant of chromophobe RCC, which can focally mimic oncocytoma morphologically. While classic examples of chromophobe RCC express not only CD-117 and CK7 diffusely, the eosinophilic variant can have variable expression of CK7.[63] Thus, lack of expression of this antigen on needle biopsy does not rule it out. Other antibodies, such as S-100A, claudin, and kidney-specific cadherin, have been advocated to address this differential diagnosis, but these are either unproven in large series or rarely used in diagnostic laboratories.[147-150] Other rarer entities enter into this differential diagnosis, such as the oncocytic variant of AML, tumours associated with the Birt-Hogg-Dubé syndrome, tumours with germline mutations of SDH, or tumours with TSC genes.[82,144,151,152]

The concept of hybrid oncocytic/chromophobe tumours (HOCT) is now in common usage in the renal pathology literature.[16] Traditionally, we and others limited this term to tumours encountered in a syndromic setting, particularly Birt-Hogg-Dubé Syndrome or in cases of renal oncocytosis where tumours with oncocytoma and chromophobe-like areas could be seen. The term is now being applied to unifocal sporadic cases with similar histology.[81,153] Without the proper clinical history, it would be impossible to make these diagnoses on needle biopsy. **Table 7-4** summarizes antibodies that can be used when considering the differential diagnosis of renal tumours with oncocytic features.

TABLE 7-4 Immunoprofile of Tumour With Oncocytic Features

Tumour type	Usually positive	Usually negative
Oncocytoma	CD117, S100A1	CK7, HMB-45, cathepsin K
Chromophobe carcinoma, eosinophilic variant	CD117, CK7 +/-*	HMB-45, cathepsin K, S100A1
Papillary RCC, oncocytic	AMACR, CK7 +/-*	HMB-45,
AML, oncocytic	HMB-45, cathepsin K	CK7, EMA, CD117

* CK7 can exhibit variable or absent staining in tumour with strong cytoplasmic eosinophilia, irrespective of cell of origin.

Differential diagnosis of tumours with spindle cell (sarcomatoid) features:
Most tumours with spindle cell morphology are high grade by definition, with the exception of the rare MTSCC of the kidney. Unless the needle biopsy contains other morphological components, it is very likely that a precise diagnosis is not achievable, and the pathologist should be content in establishing that the tumour is of epithelial and renal origin. Toward this goal, CK-Pan, EMA, and PAX8 may be useful.[137,140] Statistically, most cases of RCC with sarcomatoid differentiation are clear cell RCC. Up to 75% of cases have some membranous staining of CAIX, but this fact is unlikely to be diagnostic on needle biopsy, since similar staining can be seen in any tumour adjacent to necrosis. Mucinous tubular and spindle cell carcinomas have bland-appearing spindle cells and are likely to express both CK7 and AMACR.[154]

Other renal tumours that would enter into the differential diagnosis include variants that are high grade and exhibit sarcomatoid differentiation, including papillary RCC, chromophobe RCC, and distal nephron–type carcinomas. Other tumours to consider include smooth-muscle–predominant AML, sarcoma, and sarcomatoid urothelial carcinoma. In the case of AML, lack of expression of epithelial markers in combination with expression of cathepsin K and HMB45 are diagnostic.[63,125,137] The immunophenotype of sarcomas will depend on the cell of origin.

Differential diagnosis of tumours with distal nephron morphology:

This category includes tumours associated with high nuclear grade, solid, tubular, or papillary growth, and a fibro-inflammatory stromal reaction.[137,155,156] These nonspecific findings are more commonly associated with tumours thought to be associated with the distal nephron, such as collecting duct carcinoma, medullary carcinoma (**Figure 7-15**), and urothelial carcinoma of the renal pelvis. Some papillary RCC can exhibit similar features.[143] The age of the patient and clinical history of sickle cell trait are critical factors to take into consideration when considering this differential diagnosis. While all are likely to be immunoreactive for CK7, sickle cell trait and INI-1 loss are preferentially encountered in medullary carcinoma, while urothelial carcinoma is more likely to express GATA3 and coexpress p63 and 34ßE12.[155-157] **Table 7-5** summarizes antibodies that can be used when considering this differential diagnosis.

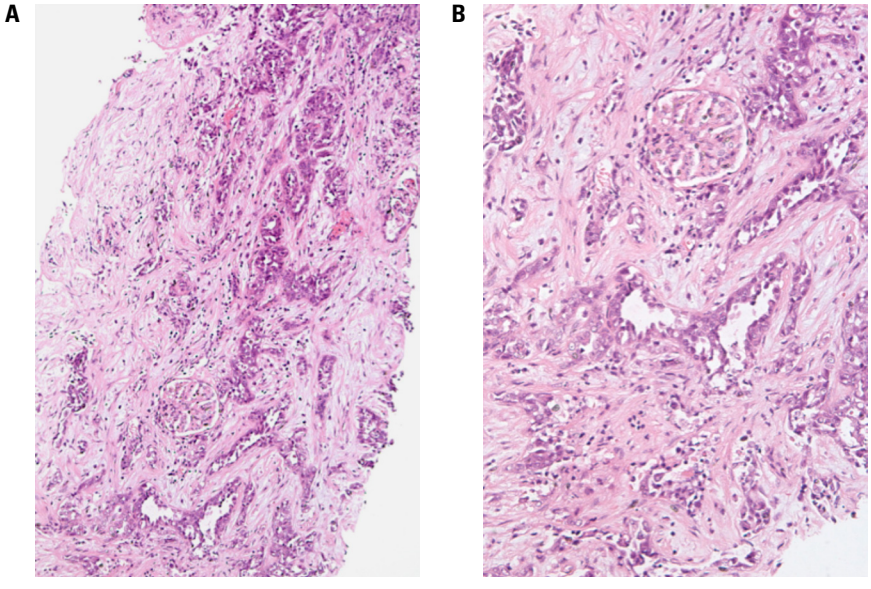

FIGURE 7-15
Renal Medullary Carcinoma
A Low power
B High power

Renal cell carcinoma, type unclassified:

This category of renal epithelial neoplasm is included in both the ISUP and WHO classification.[16,70,158] By definition, it includes any renal tumour that does not fit into any of the other well-defined categories. In essence, it constitutes a diagnosis of uncertainty. In large series, it represents 3% to 5% of resected neoplasms.[16,159] If used in association with a needle biopsy, the pathologist should try to give some type of estimation as to the degree of malignancy or, if appropriate, the favoured diagnosis. Many pathologists have used the term only in reference to high-grade, poorly differentiated tumours, although this is not how it is defined. For example, renal tumours with oncocytic features may be difficult to classify and fall into this category of tumours, with the stated caveat that they are "at worst of low malignant potential." Others use the term "renal oncocytic tumour" (RON) (**Figure 7-5**) or hybrid oncocytic/chromophobe tumours (HOCT) to describe such lesions. These designations in no way suggest a more precise diagnosis, although invariably at worst they suggest a low malignant potential.[34]

TABLE 7-5 Immunoprofile of Distal Nephron–Like Carcinomas*

Tumour type	Usually positive	Usually negative
Urothelial carcinoma	GATA3, p63 (4A4), CK7, FH (retained)	INI-1 (retained), OCT 3/4, PAX8†
Collecting duct carcinoma	CK7, FH (retained), INI-1 (retained)‡	OCT 3/4, p63
Medullary carcinoma	CK7, OCT 3/4, FH	INI-1 (loss)
HLRCC	AMACR	CK7, FH (loss)

* These tumours commonly share morphological features, including high-grade nuclei and stromal fibrosis.

† PAX8 may be positive in urothelial carcinomas.

‡ Up to 15% of collecting duct carcinomas have been reported to have INI-1 loss.

AMACR, alpha-methylacyl coenzyme A racemase; FH, fumarate hydratase.

HLRCC: hereditary leiomyomatosis and RCC.

Recommendation for IHC in renal needle core biopsies

- A judicious panel approach of using immunohistochemical stains with attention to qualitative and quantitative characteristics may be required in needle core biopsies, especially in cases of limited tissue **[GOR C, LOE 4]**.

- Panels should be constructed based on the specific differential diagnostic situation created by the needle biopsy findings on H&E sections and/or clinical history of previous malignancy, i.e. determination of primary site and cell of origin versus histologic subtyping; in the latter, a pattern-based approach (with clear cell features, with papillary architecture, with spindle cell features, with distal-nephron morphology) is necessary **[GOR C, LOE 4]**.

7.6.5 Role of cytogenetic/molecular studies, predominantly fluorescent *in situ* hybridization

TABLE 7-6 Summary of Common Cytogenetic Alterations and Related Commercial FISH Probes That May Play a Role in Confirming Histologic Subtyping of Renal Tumours

Tumour type	Cytogenetic alteration	Related FISH probe	Comments/ Reference(s)
Clear cell RCC	Loss of chromosome 3p25 (*VHL* gene) locus	3p25 (VHL)	9 of 20 cases were available[66]
Papillary RCC	Trisomy of chromosomes 7 and 17 Loss of chromosome Y	CEP 7, 17, Y	6 of 7 cases were available[66]
Chromophobe RCC	Multiple losses involving chromosomes 1, 2, 6, 10, 13, 17, and 21	CEP 1, 2, 6, 10, and 17; LSI 13 and 21	2 of 3 cases were available[66,167]
Oncocytoma	Loss of chromosome 1,14 and Y Rearrangement of *CCND1* gene (chromosome 11q13)	CEP 1, 14, Y; break apart probe CCND1	2 of 3 cases were available[66]
MTSCC	Multiple chromosome losses including chromosomes 1, 4, 6, 8, 13, 14, and 15	CEP 1, 4, 6, 8, 14, and 15; LSI 13	1 of 1 case was available[66]
Xp11.2 RCC	Translocation between *TFE3* and *ASPL, PRCC, SFPQ(PSF), CLTC,* or *NONO* genes	Break apart probe for *TFE3* gene	[171,172]
RCC with t(6;11)(p21;q12)	Translocation between *TFEB* and *MALAT1* (Alpha) genes	Break apart probe for *TFEB* gene	[173]
RCC with ALK rearrangement	Translocation between *ALK* and *VCL, EML4,* or *TMP3* genes	Break apart probe for *ALK* gene	Data limited[174]
Ewing sarcoma/primitive neuroectodermal tumour (PNET)	Translocation between *EWSR1* and *FLI1* or *ERG* genes	Break apart probe for *EWSR1* gene	Most cases were available[197]
Malignant rhabdoid tumour	Alteration of SMARCB1 *(INI-1)* gene (mutation or loss of gene locus)	SMARCB1/LSI 22q dual probe	[164]
Synovial sarcoma	Translocation between *SS18 (SYT)* and *SSX1* or *SSX2* genes	Break apart probe for *SS18* gene	1 of 1 case was available[163]

The combination of histology and FISH can improve the diagnostic accuracy in RTB, compared to histology alone.[1] Barocas *et al.* reported that histology alone was 87% accurate for the decision of tumour subtyping, whereas the combined procedure was 94% accurate, using 14-G needle biopsy specimens.[66] Chyhrai *et al.* performed three US-guided percutaneous biopsies in 25 patients with indeterminate renal masses using 18-G needles. The combination of histology and FISH resulted in higher accuracy (95.5% vs. 90.5%) in tumour-subtyping diagnosis than histology alone.[69] As FISH studies are generally performed in formalin-fixed and paraffin-embedded tissue and there are many commercially available probes to aid in renal tumour diagnosis, FISH can be a powerful adjunct for the definite diagnosis of renal tumour masses in select situations (**Table 7-6**). However, intratumoural heterogeneity of chromosomal abnormalities or inappropriate sampling may contribute to false-negative rates.

Ewing sarcoma/primitive neuroectodermal tumour, sarcoma, malignant rhabdoid tumour

Ewing sarcoma/PNET of the kidney generally affects young adults and should be histologically differentiated from the small round cell group, such as blastemal Wilms' tumour, synovial sarcoma, desmoplastic round-cell tumour, rhabdomyosarcoma, small cell carcinoma, and malignant lymphoma. The translocation between chromosomes 11q24 and 22q12 causes the production of the *EWS-FLI1* fusion gene. The partners of variant fusions include *ERG, ETV1, E1AF, FEV*, and *ZSG*. Fluorescence *in situ* hybridization study of *EWSR1* gene can detect the *EWSR1* translocation (**Figure 7-16**).[160,161] Synovial sarcoma needs to be morphologically distinguished from primary renal sarcoma, metastatic sarcoma, or sarcomatoid RCC. Monophasic synovial sarcoma often shows *SS18-SSX2* fusion, whereas biphasic synovial sarcoma demonstrates *SS18-SSX1*. In both types, translocation involving *SS18* gene locus can be detected using a SS18 dual colour break-apart probe (**Figure 7-17**).[162,163]

In some cases of malignant rhabdoid tumour, FISH analysis may show the loss of *INI* gene locus,[164] although this determination can be made by immunohistochemical analyses also.

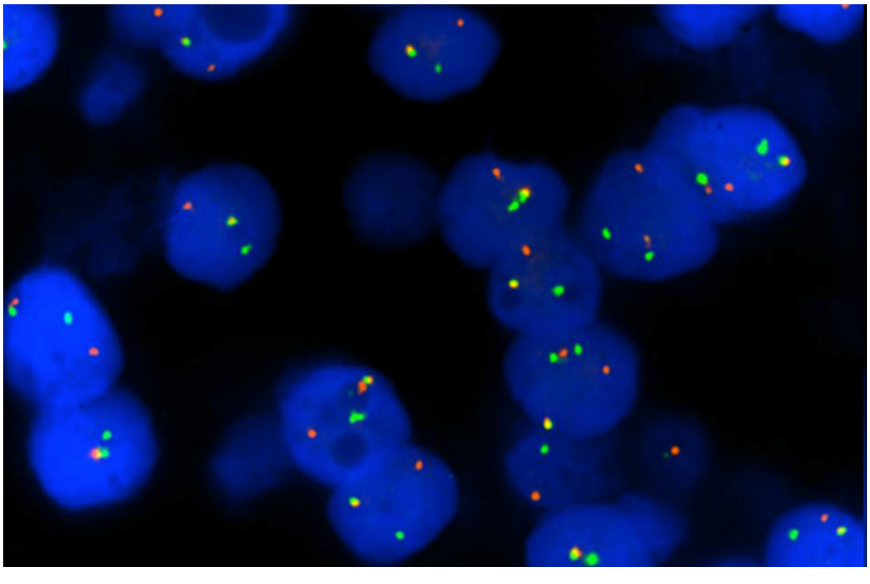

FIGURE 7-16
FISH analysis of break of EWSR1 gene (22q12) using break-apart rearrangement probe (Vysis EWSR1 Break Apart FISH Probe Kit, Abbott Molecular/Vysis) in formalin-fixed paraffin-embedded tissue.

Nuclei with one fusion (yellow), one orange, and one green (split) signal pattern indicative of a rearrangement of one copy of the EWSR1 gene region.

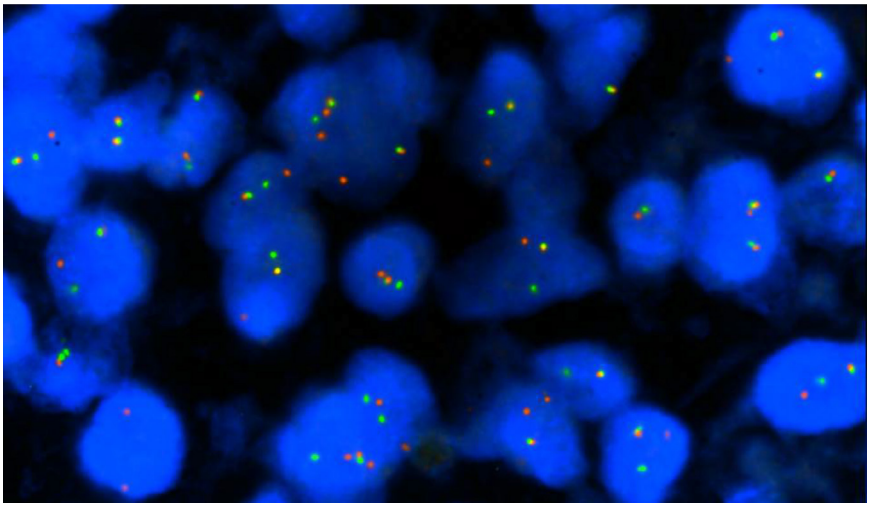

FIGURE 7-17
FISH analysis of break of SYT (≈SS18) gene (18q11.2) using break-apart rearrangement probe (Vysis SS18 Break Apart FISH Probe Kit, Abbott Molecular/Vysis) in formalin-fixed paraffin-embedded tissue.

Nuclei with one fusion (yellow), one orange, and one green (split) signal pattern indicative of a rearrangement of one copy of the SYT gene region.

7.6.6 RCC subtypes, including translocation-associated carcinoma

Histology alone seems to be more sensitive in the classification of the more common subtypes of RCC, including clear cell RCC, papillary RCC, and chromophobe RCC, than FISH alone.[67] The cytogenetic profiles that have potential diagnostic utility are outlined here. Clear cell RCCs frequently show the loss of chromosome 3p25 involving *VHL* gene locus or chromosome 3p21, mutations, or hypermethylation of *VHL* gene.[66,67,69,163] Additionally, some chromosomal alterations in clear cell RCC may have prognostic implications: gain of chromosome is linked with favourable prognosis, whereas losses of chromosomes 4q, 9p, and 14q are associated with poor prognosis.[67] In papillary RCCs, gains of chromosomes 7 and 17 are frequently observed,[66,67,69,163] more frequently in type 1 than type 2.

Chromophobe RCCs often demonstrate multiple losses involving chromosomes 1, 2, 6, 10, 13, and 17.[66,67] Gains of chromosomes are reported recently in several papers.[165-167] In renal oncocytoma, losses of chromosomes 1, 14, and Y may be observed.[1,67] Normal chromosome or rearrangement of *CCND1* gene at chromosome 11q13 may be seen in renal oncocytoma.[66,67,69] This information may be useful in separating renal oncocytomas from chromophobe RCC, although the utility of FISH studies in the renal biopsy setting has not been extensively studied, nor are these studies routinely employed.[67] Tubulocystic carcinomas show gains of chromosomes 7 and 17. These findings suggest that tubulocystic carcinomas may be closely related to papillary RCCs.[168,169] In cases with MTSCC, multiple chromosomal losses including chromosomes 1, 2, 13, and 17 are identified.[66, 170] Morphology alone, or appropriate and judicious IHC is sufficient for most tumours discussed in this paragraph.

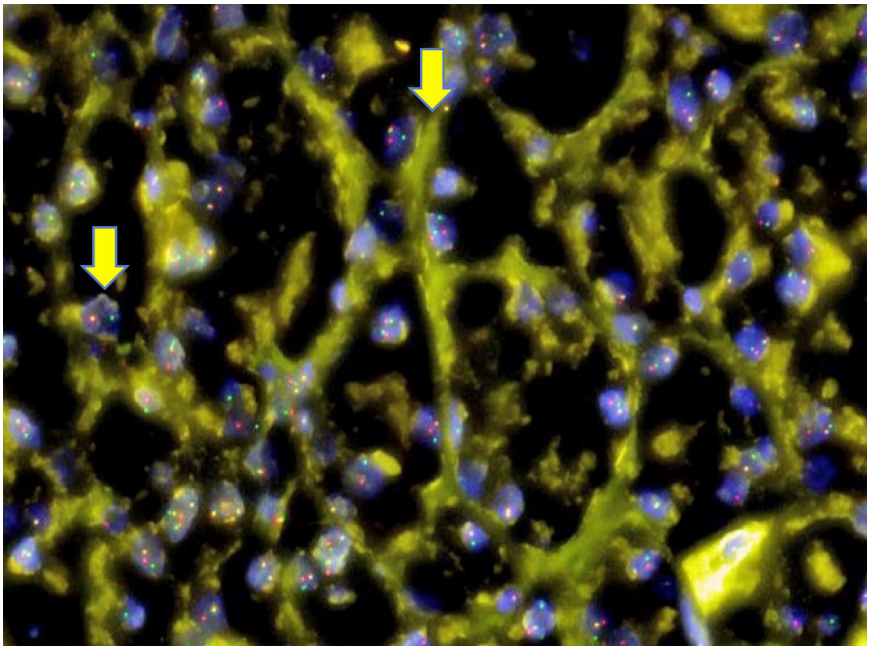

FIGURE 7-18
FISH analysis of break of TFEB gene using TFEB break-apart FISH probe (Empire Genomics) in formalin-fixed paraffin-embedded tissue. Split signals of TFEB gene (arrow) are observed.

FISH may play a vital and confirmatory role in the appropriate classification of tumours of the MiT family translocation carcinomas (Xp11.2 and t(6;11) RCC. Xp11.2 RCCs generally affect children and young adults, but adult Xp11.2 RCCs have been reported and account for approximately 1% of all renal neoplasms. The *TFE3* gene located at the chromosome Xp11.2 can fuse one of the partner genes, including *ASPL* at chromosome 17q25.3, *PRCC* at chromosome 1q21.2, *NonO* at chromosome Xq12, *PSF* at chromosome 11p34, and *CLTC* at chromosome 17q23. The formation of these chimeric transcripts gives rise to the up-regulation of TFE3 protein expression. The FISH analysis using *TFE3* gene break-apart probe can detect the rearrangement of *TFE3* gene in Xp11.2 RCCs.[171] However, possibility of *TFE3* gene amplification, which may cause the up-regulation of TFE3 protein expression, should be always considered.[172] RCCs with t(6;11)(p21;q12) commonly occurs in children and young adults, but adult-onset cases have also been reported. The frequency of this tumour comprises less than 1% of all adult renal tumours, and *Alpha-TFEB* gene fusion is observed. The *TFEB* gene split FISH assay can demonstrate the rearrangement of *TFEB* gene (**Figure 7-18**).[173] Recently, RCCs with *ALK* gene rearrangement have been identified. The fusion partners include *VCL*, *EML4*, or *TMP3*. Renal cell carcinomas with *VCL-ALK* gene fusion seem to be closely related to carcinoma. The *ALK* gene split FISH assay can find the *ALK* gene rearrangement.[174] Finally, FISH analysis in needle renal tumour specimens may be applicable to the diagnosis of mRCC, as well as primary RCC.[68]

Recommendation for FISH in renal needle core biopsies

In the context of morphology and differential diagnosis, FISH testing plays an important role in the diagnosis of certain tumour types in renal core biopsies; these include Xp11.2 RCC, t(6:11) RCC, RCC with ALK rearrangements, Ewing Sarcoma, and synovial sarcoma **[GOR C, LOE 4]**.

FISH testing is resource intensive and expensive. FISH probes should be appropriately chosen to confirm a diagnosis based on morphologic and immunohistochemical studies **[GOR C, LOE 4]**.

FISH studies add limited value if the light microscopic findings and IHC are diagnostic **[GOR C, LOE 4]**.

7.7 Results of Biopsy

7.7.1 Adequacy of renal tumour biopsy

There is presently no agreed-upon pathologic definition of the adequacy of an RTB specimen, but clinicians use the term "diagnostic" to indicate that the biopsy yielded tissue adequate for a definitive diagnosis.[33] This could include determination of the nature of the mass (e.g., inflammatory, neoplastic); for neoplastic diagnoses, the ability to determine the type of tumour (e.g., epithelial, mesenchymal, etc.); the ability to more specifically classify the tumour (e.g., if epithelial: RCC, urothelial carcinoma, etc.); whether the specimen is sufficient for further subtyping (e.g., if RCC: clear cell, papillary, etc.); and, finally, accurate definition of other important parameters (e.g., for clear cell RCC: grade of the tumour). Each of these levels of refinement will likely require increasing amounts of tumour tissue to allow for the utilization of ancillary techniques such as IHC, as well as multiple samples from different areas of the tumour to address the problem of tumour heterogeneity.

In one recent report, sample adequacy was defined as "the presence of representative lesional tissue in the biopsy sufficient for diagnosis."[34] Biopsies can be inadequate if they contain only normal tissue (renal parenchyma, perinephric fat), fibrous tissue (with or without inflammation), necrotic debris, or only minute fragments of tumour. Given that the vast majority of mass-forming lesions in the kidney are neoplastic, biopsies containing non-neoplastic tissue have a high likelihood of being false-negative samples. In the study from Gellert *et al.*,[34] of 25 specimens containing non-neoplastic tissue (excluding ablation site cases), 23 (92%) were false negatives. In another series, 24 of 26 patients with initial nondiagnostic biopsies were found to have a malignant tumour on repeat biopsy or resection.[75] A recent meta-analysis reported that the accuracy of core biopsy in distinguishing benign from malignant tumours was 88.9% in series published before 2001, but was vastly improved to 96% between 2001 and 2009.[54] A recent published paper with a large series demonstrated that the accuracy rate of core biopsy is up to 94%.[33]

Sampling different areas of a tumour compared with multiple biopsies from a single part of the tumour has been demonstrated to significantly improve the obtaining of diagnostic material.[52] The importance of sampling different areas of a tumour to identify aggressive pathologic features has also been studied.[52] Abel *et al.*[52] identified sarcomatoid change in 87% of tumours where it was present in the resection specimen using a technique with 4 cores taken from different areas of the tumour, compared to 25% using a standard approach. It has been recommended that, for larger tumours, different tumour regions, including central and peripheral, be sampled.[30]

Most large series have defined "inadequacy" as biopsies consisting of non-neoplastic or necrotic tissue. Adequacy has not been based on a quantitative evaluation of the number or size of the biopsy cores.[34,75] Menogue *et al.*[75] found that independent predictors of a diagnostic biopsy were tumour size, size (mm) of tissue submitted, and year of diagnosis. It is noteworthy that it was the cumulative length of the tissue submitted rather than the number of cores taken that was most significant. Volpe *et al.*[58] reported that length of the biopsy core trended (p=0.07) toward predicting biopsy adequacy. A recent International Consensus panel recommended that a minimum of 2 needle cores be obtained using an 18-G or larger needle.[30] Based on the available data, it would appear that adequacy cannot be based specifically on the number or size of cores, but rather on the presence or absence of diagnostic material. An International Consensus panel defined nondiagnostic biopsies as "those with insufficient tissue for analysis, as well as biopsies that, on pathological analysis, do not yield a diagnosis that explains the aetiology of the renal mass."[30]

The use of RTB appears to be increasing, and most contemporary series report a diagnostic rate in excess of 80%, with a median of 92% (interquartile range: 80.6%–96.8%) recently reported in a systematic review.[175] Nondiagnostic rates ranged from 0% to 36% and, in the series from the Princess Margaret Cancer Centre, it was recently reported at 10%.[33] It is well known that the diagnostic rate with cystic lesions is lower; this will not be covered in this chapter. Variables associated with a diagnostic biopsy include tumour size and exophytic location.[33] In instances where a nondiagnostic biopsy is followed by repeat biopsy, the success rate exceeds 80% for a diagnosis.[73]

In order to truly appreciate the accuracy of RTB, one must measure the concordance with a surgical specimen. To date, 14 studies have reported histologic concordance, with a median rate of 90% and a kappa of 0.683, a good degree of agreement.[175] The concordance rates ranged from 84% to 94%.[175] Histologic subtyping of RTB can be challenging and is obviously limited by the adequacy of the sample and how representative it is of the entire tumour. Small renal masses tend to be lower-grade tumours with less heterogeneity and, thus, overall histologic subtyping accuracy is excellent. However, mixed tumours can exist.[115] "Hybrid tumour" is a term that specifically refers to tumours that contain both chromophobe and oncocytoma.[176] Furthermore, the ability to further differentiate between different subtypes of a particular histology has been particularly challenging. For example, in the Princess Margaret experience, distinguishing between papillary types 1 and 2 was accurate in approximately 50% of cases.[31] In particular, biopsies originally classified as papillary type 2 were, on final pathology, reclassified as type 1 67% of the time. The converse was rare.[177]

Fuhrman grade is a powerful prognostic variable for clear cell RCC,[178] and grade in general is relevant to RCC outcomes. Currently, the ISUP/WHO grading system is recommended for use, although there are no published data using this system with needle biopsies. Since the ISUP/WHO system is

based largely off of the Fuhrman system, the application in needle biopsy specimens is likely to be valid (see discussion above). The ability of RTB to accurately grade a tumour is less robust than has been reported for histologic subtyping. Several studies have reported on Fuhrman grade concordance and the median kappa was 0.34 (range: 0.13–0.52), which indicates a fair agreement.[175] The accuracy varied and was dependent on whether a four-tier system or two-tier system was used to grade the tumours. The median concordance rate between RTB and the surgical specimen was 62.5% and 87%, for a four-tier and two-tier system, respectively.[175]

The literature contains multiple reports related to the diagnosis of oncocytoma on needle biopsy. In one series, 2 of 13 cases diagnosed as oncocytoma were considered to be hybrid tumours in the surgical specimens.[41] In both cases, the final diagnosis included the utilization of IHC, but whether IHC was applied to the needle biopsy specimens was not reported. Neuzillet *et al.*[80] reported 15 renal oncocytomas diagnosed by needle biopsy; the diagnosis was confirmed in 6 cases surgically resected, and 9 patients were followed without incident (mean: 50 months). Shannon *et al.*[72] followed 26 cases diagnosed as oncocytoma, with 24 remaining stable in size and 2 increasing in size (one by 1 cm after 6 years and the other by 0.6 cm after 1 year). Follow-up of 7 cases of oncocytoma diagnosed by needle biopsy in the study of Wang *et al.*[47] revealed no tumour growth with limited follow-up; one resected case had the diagnosis confirmed. Volpe *et al.*[58] followed 7 cases of oncocytoma without significant progression in size (length of follow-up not provided). Lebret *et al.*[28] reported confirmation of the diagnosis in 6 of 7 resected oncocytomas (one case considered to be uncertain on biopsy was revealed to be a chromophobe carcinoma) and followed 8 additional patients without progression.

7.7.2 Predictors of successful biopsy

An adequate biopsy with appropriate morphologic and immunohistochemical workup (if necessary) should provide adequate information regarding the nature of the lesion, i.e., benign or malignant, epithelial, mesenchymal, or other, and primary or metastatic. If it is a primary tumour, it is important to attempt to establish the histological subtype and provide information on grade and other prognostic parameters in the tumour, as specified in the sections above.

Factors influencing the success of the biopsy in terms of providing this information include tumour size, solid versus cystic nature, and location. Some clinical aspects are also:

1) Size of the tumour

The size of a tumour by itself is not a contraindication for biopsy. For tumours ≤4 cm, also referred as SRMs, the rate of nondiagnostic biopsy seems to be higher than that of larger renal masses. Wunderlich *et al.* reported on 250 fine-needle RTBs and demonstrated that, for tumours smaller than 4 cm, the individual accuracy of a central and peripheral biopsy is 83.3% and 75%, respectively.[51] The accuracy rate could go up to 96.7% when both peripheral and central biopsies are used concurrently. However, it should be noted that peripheral biopsy for SRMs may not obtain enough tissue because of the small lesion size. Hence, a high-quality biopsy core might be more important to a specific sampling pattern for SRMs. Recently, a meta-analysis demonstrated that percutaneous biopsy for SRM (<4 cm) is a very accurate method to detect malignancy, with sensitivity of 94% and specificity of 100%.[36] Even small renal tumours (as small as 1.0 cm) may be successfully biopsied, providing an opportunity for accurate diagnosis.[73,119] Wang,[47] in a series of 106 patients with tumours smaller than

4 cm, reported a success rate of 90.9%. Among the 10%, the indeterminate group, the median size was 1.9 cm. A review by Gellert *et al.*[34] demonstrated that the diagnostic accuracy has improved over the last few years, with the correct histological subtyping being achieved in the range of 77.5% to 100%.

There is a different situation pertaining to biopsies performed in large tumours (e.g., planning neoadjuvant treatment for advanced tumours). Larger tumours may show more heterogeneity and have hemorrhagic and necrotic areas. Thus, the radiologist should avoid these potential areas in order to maximize viable tissue for analysis.

2) Solid versus cystic nature

Usually the accuracy of core biopsies for cystic tumours is less than for solid tumours, as diagnostic areas may not be represented in a biopsy.[58,73] The potential for negative results or inadequate biopsy is higher, as are complications such as cyst rupture. Some studies have shown that, in some situations, especially in a context of solid-cystic tumours, a complementary FNA may improve diagnosis accuracy. Li showed that the success rate of using both FNA and core biopsy was superior (92.9%) to that of the FNA group alone (62.5%) and core biopsy group alone (76.7%).[31]

3) Location

The location of the tumour can impact on the success of a biopsy. There is no known association between histological subtype and location of tumour, although some tumour types are more likely to occur in the medulla/hilum of the kidney, e.g., renal medullary, collecting duct carcinoma, or urothelial carcinoma.

Usually, the best success rates are with exophytic tumours located in the lower pole and posterior locations. Tumours located in the superior pole are more difficult to biopsy due to their spatial relationship to the liver. For some rare cases, a transhepatic biopsy may be needed to access the tumour.

4) Patient characteristics

There are no reports pertaining to patient body characteristics and successful biopsy rates, although body mass index may have some influence in biopsy access.[1]

Overall, a multidisciplinary team approach is crucial for the success of the biopsy. Close interaction between the urologists, interventional radiologists, and pathologists is helpful.

Observations based on current results of RTB

- There is no agreement among pathologists as to what constitutes an adequate biopsy, but clinicians use the term "diagnostic" for biopsy tissue that provides a definitive diagnosis, and this can be achieved in approximately 92% of biopsies. Cystic lesions need to have a solid, enhancing component that can be targeted.

- Accuracy in terms of concordance with subsequent surgical specimens is approximately 90%, including grade **[GOR C, LOE 4]**.

- Certain pathological conditions, such as oncocytoma, present difficulties for interpretation **[GOR D, LOE 5]**.

7.8 Impact on Decision Making

The essence of the controversy regarding the utility of RTB in SRMs is whether the results will change management. If not, the additional risks, costs, and patient discomfort are not justified. The outcome of an RTB performed for an SRM is either diagnostic or nondiagnostic, as discussed previously and represented in **Figure 7-19**. In cases where a biopsy will not change management, such as when a biopsy reveals cancer in a very elderly or frail patient, watchful waiting or no follow-up at all is the management of choice. Generally, very small tumours ≤1 cm are observed until they are >1 cm, at which time the diagnostic rate of an RTB increases.[14,33] If re-biopsy will change management, it has the same chance of being diagnostic as the first one.[33] The diagnostic biopsy will usually demonstrate that the SRM is a primary renal tumour, but it may be benign, in which case a clinical decision can be made to observe.

The potential change in management from immediate treatment for a presumed malignancy to initial AS for a proven benign tumour is the most immediate benefit from RTB, and is clinically underappreciated at present based on the lack of widespread use of biopsy. In part, this is related to concerns about accuracy, which is also an underappreciation of the recent literature's results, which we discussed previously. If treatment is recommended, the type of treatment may be determined by the tumour type. For example, large and growing oncocytomas may be managed by PN, but margins can be so thin that they are really enucleated with minimal renal damage or need to control bleeding. Angiomyolipomas will frequently be embolized if symptomatic, if growing, or for other indications. Growth rates and the actual risk of hemorrhage have not been well defined.

FIGURE 7-19
SRM Biopsy Strategy

AML, angiomyolipomas; AS, active surveillance; cc, clear cell; p, papillary; RCC, renal cell carcinoma; RTB, renal tumour biopsy; SRM, small renal mass; WW, watchful waiting.

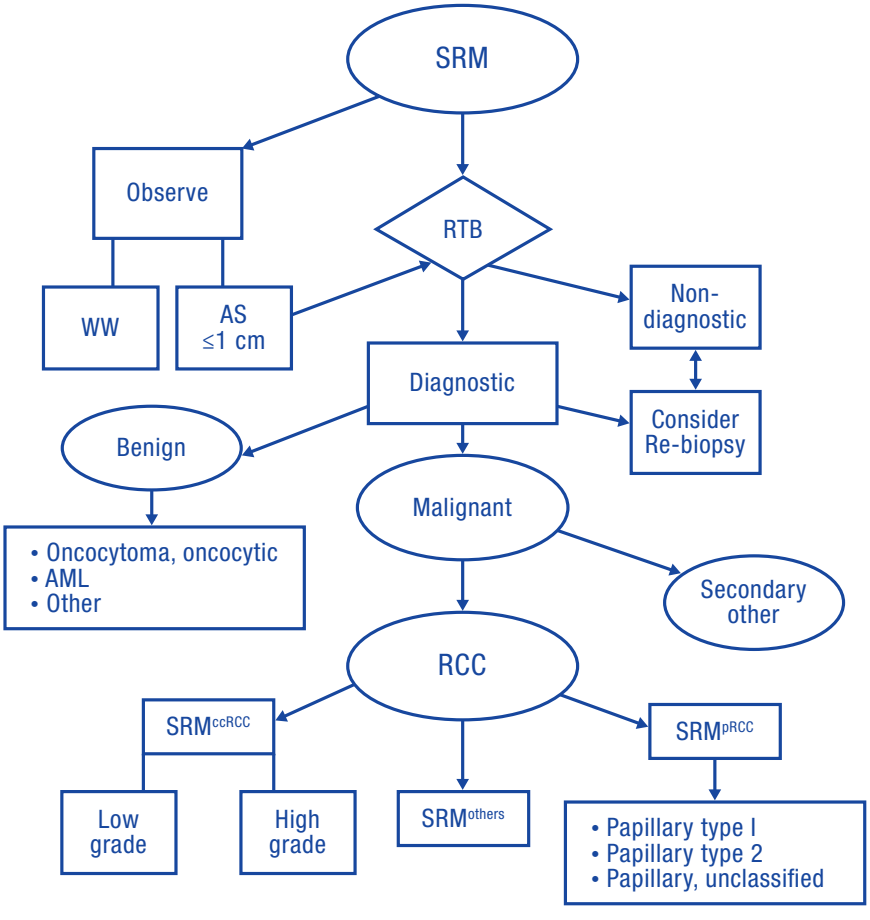

Malignant primary tumours are usually RCC and, as we learn more about the risk and natural history by RCC subtype and grade or other characteristics, it may be possible to stratify treatment by tumour type. Alternatives may include partial versus radical nephrectomy, ablation versus surgery, and, possibly, an increase use of initial AS.

FIGURE 7-20
Algorithm for Management of Biopsy-Characterized SRMs by Patient Characteristics

	Young/Fit	Elderly/Infirm
AS	SRM^{AML}	$SRM^{ccRCC(LG)}$
	SRM^{Onco}	SRM^{AML}
		SRM^{Onco}
Treatment	SRM^{ccRCC}	$SRM^{ccRCC(LG)}$

AML, angiomyolipomas; AS, active surveillance; cc, clear cell; HG, high grade; LG, low grade; Onco, oncocytoma; RCC, renal cell carcinoma; SRM, small renal mass.

Current management options that incorporate the patient's age and health are illustrated in **Figure 7-20**. Currently, young and fit patients with RCC, regardless of type and grade, are generally managed by surgery or, occasionally, ablation. However, AS is a reasonable option for the elderly and/or infirm. The number of high-grade SRMs is low, so we do not know if initial management is indicated when the risk of treatment is very high. In general, in centres that do RTB, there is a sense that treatment should be more aggressive in high-grade tumours.

Although the focus of this chapter has been SRM RTB, there is interest in biopsy in larger but localized tumours, as well as in mRCC. Indications are not well defined, but possible roles include decision making about the partial versus radical nephrectomy in very high–grade RCC and systemic agent selection for the treatment of mRCC.

7.9 Summary of Recommendations, Special Situations, and Future Directions

We have reviewed the relevant literature and practice of RTB, and hope to see increased study of what we believe is a safe and impactful tool for the management of kidney tumours, benign and malignant, small and large, localized and metastatic. We believe that RTB should be considered in the management of most patients with early-stage localized RCC, as well as metastatic disease; maybe we will even see the day of repeated biopsy through the trajectory of care. Not only do we want to see efforts in KT at meetings of all involved clinicians from imagers to pathologists and medical oncologists, but we hope that the explosion of knowledge in basic and translational science will open doors for new applications of biopsy that will allow full personalization of care for those afflicted by any type of renal mass.

7.9.1 Recommended indications for RTB

As the field continues to evolve with further evidence becoming available, routine RTB of all incidentally detected SRMs (including cystic renal lesions, Bosniak IV) in patients for whom AS or ablative therapy is being considered to avoid unnecessary treatment of benign tumours and to individualize therapy **[GOR D, LOE 4]**.

Based on these considerations, percutaneous biopsy of renal tumours maybe useful in several clinical settings, and is currently recommended for the histological diagnosis of:

- Homogeneous infiltration of renal parenchyma to rule out lymphoma **[GOR C, LOE 2]**.
- Radiological suspicion of recurrence or disease persistence after renal tumour ablation **[GOR C, LOE 2]**.
- Suspicion of renal metastases in the presence of a known extrarenal malignancy **[GOR C, LOE 2]**.
- Retroperitoneal tumours involving the kidney when initial surgery is not feasible or indicated **[GOR C, LOE 2]**.
- Primary renal tumours with metastatic disease before systemic therapy (RTB is increasingly recommended to select systemic agents), when cytoreductive nephrectomy is not indicated, or when neoadjuvant systemic therapy is planned **[GOR D, LOE 4]**.
- Small renal masses <1 cm are difficult to biopsy, and may be followed until they reach this size **[GOR D, LOE 4]**.

7.9.2 Recommended technique for RTB

Based on these considerations, percutaneous biopsy of renal tumours should:

- Be performed with image guidance, usually US where feasible **[GOR C, LOE 4]**.
- Provide needle core tissue +/- FNA, which may be complementary but will not provide as high a diagnostic yield **[GOR C, LOE 4]**.
- Be done with a coaxial sheath to improve sampling and safety **[GOR D, LOE 5]**.
- Include at least two cores from SRMs **[GOR D, LOE 5]**.
- Be done for each SRM if there is more than 1 tumour **[GOR D, LOE 4]**.
- Be done from the peripheral area of the tumour if there are necrotic areas on imaging or from the enhancing areas if cystic **[GOR D, LOE 4]**.
- Sample the tumour as widely as possible **[GOR D, LOE 4]**.

7.9.3 Recommendations regarding safety of RTB

- Renal tumour biopsy is safe **[GOR C, LOE 3]**.
- Needle-track seeding is extremely rare **[GOR C, LOE 3]**.
- Renal tumour biopsy should be performed with care when TCC of the upper urinary tract is suspected **[GOR C, LOE 4]**.
- Complications due to RTB are generally minor and self-limiting **[GOR C, LOE 3]**.

7.9.4 Recommendations for handling and preparation of needle core biopsies

- Rapid evaluation and determination of specimen adequacy is not routinely performed. The panel is of the opinion that rapid evaluation with a determination of specimen adequacy is very valuable, and pathologists should consider providing this service. The need for such an approach should be determined institutionally because of the importance of rapid evaluation as the best practical opportunity to receive adequate material for appropriate diagnosis. **[GOR D, LOE 4]**

- It is optional to procure additional tissue cores and snap freeze them for cytogenetic and molecular analyses. This determination should be made based on patient care needs, as well as research and tissue banking protocols in place at an institutional level **[GOR D, LOE 4]**.

- If multiple cores from a single lesion are submitted in one container, we recommend submission of individual cores in more than one block to enhance the ability to perform additional studies, if necessary **[GOR C, LOE 4]**.

- We recommend multiple prospective serial sections for renal core biopsies, up to six blanks with the first and last levels stained with H&E, and the remaining levels saved on charged slides for prospective IHC **[GOR C, LOE 4]**.

7.9.5 Specimen sampling

- Core biopsies from multiple lesions should be submitted separately **[GOR C, LOE 3]**.

- Specimen requisitions should optimally specify information such as the number of lesions in the kidney (if more than one), number of lesions biopsied (if more than one), location of each biopsy, and number of cores obtained from each lesion **[GOR C, LOE 4]**.

- It is optional to procure additional tissue cores and snap freeze them for cytogenetic and molecular analyses. This determination should be made based on patient care needs, as well as research and tissue banking protocols in place at an institutional level **[GOR D, LOE 4]**.

7.9.6 Recommendations for histologic scope of the needle core biopsies

- The diagnostic nomenclature recommended for use in renal core biopsies is the WHO 2016 Classification System **(Table 7-1) [GOR B, LOE 3]**.

- The diagnosis of renal oncocytoma should be made with caution in needle core biopsies. If a definitive diagnosis of renal oncocytoma is made, it requires rigid morphologic criteria combined with supportive histochemical and immunohistochemical studies. In cases with classic diagnostic features, we recommend the diagnostic terms "renal oncocytoma" or "renal oncocytic neoplasm with features consistent of renal oncocytoma." In other circumstances, the term "renal oncocytic neoplasm" may be used with an explanation in the comments explaining which features are unusual for an outright diagnosis of renal oncocytoma **[GOR C, LOE 4]**.

- An attempt to further subclassify RCCs should be made in every case. Before a diagnosis of "RCC, unclassified type" or "RCC, not otherwise specified, further histologic subtyping not possible in needle biopsy material" is rendered, metastasis and urothelial carcinoma should be ruled out based on morphologic and/or immunohistochemical criteria **[GOR B, LOE 3]**.

- The highest (majority of cells in a single high power field) histologic grade observed in a carcinoma should be provided. Due to grade heterogeneity in RCC, the recommended diagnostic term should include "at least grade X" to acknowledge the uncertainty that a higher grade may be present **[GOR B, LOE 3]**.

- For the common subtypes of RCC, specifically clear cell and papillary RCC, the ISUP/WHO grading system is recommended for use.[70] There is no accepted grading system for chromophobe RCC and rarer subtypes of RCC **[GOR B, LOE 3]**.

- In needle biopsies, other adverse prognostic parameters should be reported only if observed. These include sarcomatoid change, cells with rhabdoid features, necrosis, vascular-lymphatic invasion, and tumour infiltrating of adipose tissue (suggesting pT3 disease) **[GOR B, LOE 3]**.

7.9.7 Recommendation for IHC in renal needle core biopsies

- A judicious panel approach of using immunohistochemical stains with attention to qualitative and quantitative characteristics may be required in needle core biopsies, especially in view of the fact that there is limited tissue **[GOR C, LOE 4]**.

- Panels should be constructed based on the specific differential diagnostic situation created by the needle biopsy findings on H&E sections and/or clinical history of previous malignancy, i.e. determination of primary site and cell of origin versus histologic subtyping; in the latter, a pattern-based approach (with clear cell features, with papillary architecture, with spindle cell features, with distal-nephron morphology) is necessary **[GOR C, LOE 4]**.

7.9.8 Recommendation for FISH in renal needle core biopsies

- In the context of morphology and differential diagnosis, FISH testing plays an important role in the diagnosis of certain tumour types in renal core biopsies; these include Xp11.2 RCC, t(6:11) RCC, RCC with ALK rearrangements, Ewing sarcoma, and synovial sarcoma **[GOR C, LOE 4]**.

- FISH testing is resource intensive and expensive. FISH probes should be appropriately chosen to confirm a diagnosis based on morphologic and immunohistochemical studies **[GOR C, LOE 4]**.

- FISH studies add limited value if the light microscopic findings and IHC are diagnostic **[GOR C, LOE 4]**.

7.9.9 Observations based on current results of RTB

- There is no agreement among pathologists as to what constitutes an adequate biopsy, but clinicians use the term "diagnostic" for biopsy tissue that provides a definitive diagnosis, and this can be achieved in approximately 92% of biopsies. Cystic lesions need to have a solid, enhancing component that can be targeted.

- Accuracy in terms of concordance with subsequent surgical specimens is approximately 90%, including grade **[GOR C, LOE 4]**.

- Certain pathological conditions, such as oncocytoma, present difficulties for interpretation **[GOR D, LOE 5]**.

- Core biopsies and FNA samples are typically used to diagnose renal tumours and help in treatment decision making. In general, core biopsy is superior to fine-needle aspirates, although indications for performing the two techniques may vary based on the clinical situation **[GOR B, LOE 2]**.

7.9.10 Special situations and limitations (e.g., bone metastases)

Previous studies have confirmed the prognostic value of molecular and genetic markers in RCC, such as Ki-67, p53, vascular endothelial growth factor (VEGF) receptor, loss of 9p, etc.[179,180] Biopsy could help attain tissue samples suitable for molecular or genetic tests. By virtue of these tests, we may better differentiate renal tumours with more metastatic potential, and can use the information to optimize individual patient management of RCC. Hence, further studies investigating the molecular and genetic information from RTB are warranted.

There are still some limitations of RTB at present. The heterogeneity of renal tumours consistently hinders the accuracy of RTB, and a common biopsy cannot reflect the complex nature of such tumours. Grade heterogeneity in the same renal tumour exists in up to 25% of cases,[181] which contributes to the suboptimal accuracy of grade assessment. For hybrid tumours, such as ones that include the oncocytoma area in a chromophobe RCC or a hybrid oncocytic/chromophobe tumour, conventional renal biopsy method could correctly provide diagnostic information only when the biopsy samples the hybrid area by chance. The multi-quadrant method proposed by E. Jason may be a promising way to solve the problem of renal tumour heterogeneity;[52] however, this method still needs to be replicated in further studies. In addition, oncocytoma diagnoses continue to be a challenge in the clinical practice. The special case of such challenge is the differential diagnosis: oncocytoma, low-grade chromophobe RCC, a hybrid oncocytic/chromophobe tumour, and papillary type 2 (eosinophilic) RCC.[54] More accurate methods that could resolve this diagnostic problem are required.

7.9.11 Future directions

In the era of personalized molecular pathway-based therapies for mRCC, the importance of obtaining renal biopsies in the primary or metastatic settings is increasing. This may not only assist in accurate subtyping of renal tumours to select appropriate therapy, but also to obtain additional material for prognostic and predictive biomarkers. While IHC is the most widely used technique, a variety of molecular tests are already being utilized at major academic centres or at cancer institutes around the world. These include next-generation sequencing, microribonucleic acid (miRNA) profiling, methylation analysis, and comparative genomic hybridization (CGH) assays.

1) MicroRNA profiling

MicroRNAs are non-coding, single-strand small RNA molecules that can bind to messenger RNAs and act as post-transcriptional regulators. MicroRNA panels predicting recurrence and unfavourable prognosis have been identified,[182] and a unique pattern of expression in the miRNA profile has been shown to discriminate between the most common types of kidney tumours.[183] The reported upregulation of miR-210 and miR-122 in clear cell RCC has been proposed as a potential regulator of VHL genes, modulating HIF and miR-210, correlating with CAIX expression.[184] Other miRNAs (e.g., miR-34 and miR-18a) are upregulated in clear cell RCC, papillary RCC, and clear cell papillary RCC, but miRNA downregulation is more common in clear cell RCC. Stepwise downregulation of miRNA expression has been observed in the transition from normal kidney to primary RCC and mRCC.[185]

MicroRNAs have both advantages and disadvantages as potential biomarkers. Much work is necessary in terms of standardization of methods and cutoff values, as even minute amounts of paraffin-embedded tissue can provide profiling of a large number of miRNAs even from small tumour biopsy fragments. An increasing number of studies are exploring miRNAs quantified by RT-PCR to evaluate their use as predictive factors of response. In mRCC, high levels of miR-942, a regulator of platelet-derived growth factor receptor (PDGFR), have been reported to upregulate VEGF secretion, enhance endothelial migration, and confer resistance to sunitinib.[186]

2) Immunohistochemical biomarkers

Immunohistochemical biomarkers are currently not used for prognostication in biopsy and partial or radical nephrectomy samples,[125] but there have been promising results from recent studies using tissue microarrays. For example, inactivated BRCA-1 associated protein-1 (BAP1), a molecular mutation reported in 15% of RCCs,[187] is associated with poor survival.[188] RCC patients with BAP1 loss have a 2- to 3-fold increased risk of death with respect to BAP1-positive patients. Immunohistochemical assaying has similar predictive power to mutation analysis with exome sequencing or Sanger sequencing.[189]

Other promising biomarkers are beta-catenin expression (dysregulated in 17% of RCCs), which is an independent predictor of recurrence-free and cancer-specific survival,[190] and MUC-1 immunoreactivity, which is associated with poor prognosis when a circumferential staining pattern is observed.[191] These immunoassays, together with markers of proliferation, need to be tested to evaluate their usefulness in biopsy samples.

3) Next-generation sequencing technologies

Each analytic technique has minimum quantity requirements. Kurban reported the following amounts of tumour tissue from needle biopsy cores to be adequate:[65] 300 ng/sample for CGH analysis, 5 µg/sample for exome and whole genome sequencing, 200 ng/sample for RNA studies, and 200 ng/sample for microarray and whole transcriptome sequencing. A single biopsy sample may not contain adequate tumour tissue in some cases; hence, several cores may be required for complete analysis. This limit to a better understanding of the molecular alterations in RCC has not stopped the application of next-generation sequencing technologies to characterize exomes, transcriptomes, and single nucleotide polymorphism–based genome-wide copy number alterations in RCC. For example, detection of MET alterations may play a role not only in molecular profiling of papillary RCC, but also in the selection of appropriate targeted therapies (i.e., trials involving MET inhibitors).[22]

The establishment of the Von Hippel-Lindau (VHL) mutation as a poor prognostic biomarker makes the study of other mutations in the chromatin-modulating genes polybromo 1 (PBRM1),[192] SET domain containing 2 (SET D2),[193] BAP1,[187] and lysine (K)-specific demethylase 5C (KDM5C),[193] probably more useful for the assessment of tumour aggressiveness and clinical outcome.[194,195]

4) Reverse-phase protein arrays

There have been promising preliminary results from recent studies using laser capture microdissection and reverse-phase protein arrays (RPPAs) in liquid nitrogen–frozen sections to determine the signalling pathway status in tumour cells. Laser capture microdissection enables the separation of

tumour cells from their complex microenvironment, and RPPA can quantitatively measure protein expression and activation in a minimal sample, measuring the states of key signalling protein that span many signalling pathways.[196]

In summary, while there are several emerging prognostic and predictive biomarkers that have potential clinical value in RCC, their optimal detection methodology, sensitivity, specificity, and reporting issues need to be addressed and studied before they can be applied in routine clinical practice.

Recommendations for emerging tests discussed in this section

Novel markers and technologies that are helpful in the diagnosis, prognostication, and therapy selection in RCC have been recently described. While many of these studies show promise, there is currently no evidence to suggest that these tests should be routinely used in clinical practice. Tests may be used based on institutional multidisciplinary best practice recommendations **[GOR C, LOE 4].**

7.10 References

1. Volpe A, Finelli A, Gill IS, *et al.* Rationale for percutaneous biopsy and histologic characterisation of renal tumours. *Eur Urol.* 2012;62(3):491–504.
2. Sahni VA, Ly A, Silverman SG. Usefulness of percutaneous biopsy in diagnosing benign renal masses that mimic malignancy. *Abdom Imaging.* 2011;36(1):91–101.
3. Tsivian M, Mouraviev V, Albala DM, *et al.* Clinical predictors of renal mass pathological features. *BJU Int.* 2011;107(5):735–740.
4. Frank I, Blute ML, Cheville JC, *et al.* Solid renal tumors: an analysis of pathological features related to tumor size. *J Urol.* 2003;170(6 Pt 1):2217–2220.
5. Choudhary S, Rajesh A, Mayer NJ, *et al.* Renal oncocytoma: CT features cannot reliably distinguish oncocytoma from other renal neoplasms. *Clin Radiol.* 2009;64(5):517–522.
6. Rosenkrantz AB, Hindman N, Fitzgerald EF, *et al.* MRI features of renal oncocytoma and chromophobe renal cell carcinoma. *AJR Am J Roentgenol.* 2010;195(6):W421–W427.
7. Kim JK, Park SY, Shon JH, *et al.* Angiomyolipoma with minimal fat: differentiation from renal cell carcinoma at biphasic helical CT. *Radiology.* 2004;230(3):677–684.
8. Remzi M, Katzenbeisser D, Waldert M, *et al.* Renal tumour size measured radiologically before surgery is an unreliable variable for predicting histopathological features: benign tumours are not necessarily small. *BJU Int.* 2007;99(5):1002–1006.
9. Hollingsworth JM, Miller DC, Daignault S, *et al.* Five-year survival after surgical treatment for kidney cancer: a population-based competing risk analysis. *Cancer.* 2007;109(9):1763–1768.
10. Ljungberg B, Bensalah K, Canfield S, *et al.* EAU guidelines on renal cell carcinoma: 2014 Update. *Eur Urol,* 2015.
11. Jewett MA, Mattar K, Basiuk J, *et al.* Active surveillance of small renal masses: progression patterns of early stage kidney cancer. *Eur Urol.* 2011;60(1):39–44.
12. Smaldone MC, Kutikov A, Egleston BL, *et al.* Small renal masses progressing to metastases under active surveillance: a systematic review and pooled analysis. *Cancer.* 2012;118(4):997–1006.
13. Donat SM, Diaz M, Bishoff JT, *et al.* Follow-up for clinically localized renal neoplasms: AUA guideline. *J Urol.* 2013;190(2):407–416.
14. National Comprehensive Cancer Network. NCCN Guidelines Version 3.2015. Available: https://www.nccn.org/professionals/physician_gls/recently_updated.asp.
15. Marconi L, Dabestani S, Lam TB, *et al.* Systematic review and meta-analysis of diagnostic accuracy of percutaneous renal tumour biopsy. *Eur Urol.* 2016;69(4):660-673.
16. Srigley JR, Delahunt B, Eble JN, *et al.* The International Society of Urological Pathology (ISUP) Vancouver classification of renal neoplasia. *Am J Surg Pathol.* 2013;37(10):1469–1489.
17. Klingler HC, Marberger M, Mauermann J, *et al.* 'Skipping' is still a problem with radiofrequency ablation of small renal tumours. *BJU Int.* 2007;99(5):998–1001.
18. Campbell SC, Novick AC, Belldegrun A, *et al.* Guideline for management of the clinical T1 renal mass. *J Urol.* 2009;182(4):1271–1279.
19. Rendon RA, Kapoor A, Breau R, *et al.* Surgical management of renal cell carcinoma: Canadian Kidney Cancer Forum Consensus. *Can Urol Assoc J.* 2014;8:5–6.
20. Shuch B, Said J, La Rochelle JC, *et al.* Cytoreductive nephrectomy for kidney cancer with sarcomatoid histology--is up-front resection indicated and, if not, is it avoidable? *J Urol.* 2009;182(5):2164–2171.
21. Abel EJ, Culp SH, Matin SF, *et al.* Percutaneous biopsy of primary tumor in metastatic renal cell carcinoma to predict high risk pathological features: comparison with nephrectomy assessment. *J Urol.* 2010;184(5):1877–1881.
22. Choueiri TK, Vaishampayan U, Rosenberg JE, *et al.* Phase II and biomarker study of the dual MET/VEGFR2 inhibitor foretinib in patients with papillary renal cell carcinoma. *J Clin Oncol.* 2013;31(2):181–186.

23. Koh Y, Lim HY, Ahn JH, *et al.* Phase II trial of everolimus for the treatment of nonclear-cell renal cell carcinoma. *Ann Oncol.* 2013;24(4):1026–1031.

24. Uppot RN, Harisinghani MG, Gervais DA. Imaging-guided percutaneous renal biopsy: rationale and approach. *AJR Am J Roentgenol*. 2010;194(6):1443–1449.

25. Charboneau JW, Reading CC, Welch TJ. CT and sonographically guided needle biopsy: current techniques and new innovations. *AJR Am J Roentgenol*. 1990;154(1):1–10.

26. Volpe A, Kachura JR, Geddie WR, *et al.* Techniques, safety and accuracy of sampling of renal tumors by fine needle aspiration and core biopsy. *J Urol*. 2007;178(2):379–386.

27. Lechevallier E. Core biopsy of solid renal masses under CT guidance. *European Urology Supplement*. 2007;6(8):540–543.

28. Lebret T, Poulain JE, Molinie V, *et al.* Percutaneous core biopsy for renal masses: indications, accuracy and results. *J Urol*. 2007;178(4 Pt 1):1184-1188; discussion 1188.

29. Herts BR. Imaging guided biopsies of renal masses. *Curr Opin Urol*. 2000;10(2):105–109.

30. Tsivian M, Rampersaud EN Jr, del Pilar Laguna Pes M, *et al.* Small renal mass biopsy--how, what and when: report from an international consensus panel. *BJU Int.* 2014;113(6):854–863.

31. Li G, Cuilleron M, Zhao A, *et al.* Combination of core biopsy and fine-needle aspiration increases diagnostic rate for small solid renal tumors. *Anticancer Res*. 2012;32(8):3463–3466.

32. Delahunt B, Samaratunga H, Martignoni G, *et al.* Percutaneous renal tumour biopsy. *Histopathology*. 2014;65(3):295–308.

33. Richard PO, Jewett MA, Bhatt JR, *et al.* Renal tumor biopsy for small renal masses: a single-center 13-year experience. *Eur Urol.* 2015;68(6):1007–1013.

34. Gellert LL, Mehra R, Chen YB, *et al.* The diagnostic accuracy of percutaneous renal needle core biopsy and its potential impact on the clinical management of renal cortical neoplasms. *Arch Pathol Lab Med.* 2014;138(12):1673–1679.

35. Hu R, Montemayor-Garcia C, Das K. Role of percutaneous needle core biopsy in diagnosis and clinical management of renal masses. *Hum Pathol.* 2015;46(4):570–576.

36. He Q, Wang H, Kenyon J, *et al.* Accuracy of percutaneous core biopsy in the diagnosis of small renal masses (≤ 4.0 cm): a meta-analysis. *Int Braz J Urol*. 2015;41(1):15–25.

37. Lee SW, Lee MH, Yang HJ, *et al.* Experience of ultrasonography-guided percutaneous core biopsy for renal masses. *Korean J Urol.* 2013;54(10):660–665.

38. Bernhard, JC, Bigot P, Pignot G, *et al.* The accuracy of renal tumor biopsy: analysis from a national prospective study. *World J Urol.* 2015;33(8):1205–1211.

39. Breda A, Treat EG, Haft-Candell L, *et al.* Comparison of accuracy of 14-, 18- and 20-G needles in ex-vivo renal mass biopsy: a prospective, blinded study. *BJU Int.* 2010;105(7):940–945.

40. Volpe A, Jewett MA. Current role, techniques and outcomes of percutaneous biopsy of renal tumors. *Expert Rev Anticancer Ther.* 2009;9(6):773–783.

41. Schmidbauer J, Remzi M, Memarsadeghi M, *et al.* Diagnostic accuracy of computed tomography-guided percutaneous biopsy of renal masses. *Eur Urol.* 2008;53(5):1003–1011.

42. Garcia-Solano J, Acosta-Ortega J, Pérez-Guillermo M, *et al.* Solid renal masses in adults: image-guided fine-needle aspiration cytology and imaging techniques--"two heads better than one?". *Diagn Cytopathol.* 2008;36(1):8–12.

43. Kummerlin IP, Borrego J, Wink MH, *et al.* Nephron-sparing surgery and percutaneous biopsies in renal-cell carcinoma: a global impression among endourologists. *J Endourol*. 2007;21(7):709–713.

44. Simhan J, Canter DJ, Sterious SN, *et al.* Pathological concordance and surgical outcomes of sporadic synchronous unilateral multifocal renal masses treated with partial nephrectomy. *J Urol*. 2013;189(1):43–47.

45. Hobbs DJ, Zhou M, Campbell SC, *et al.* The impact of location and number of cores on the diagnostic accuracy of renal mass biopsy: an ex vivo study. *World J Urol.* 2013;31(5):1159–1164.

46. Neuzillet Y, Lechevallier E, Andre M, *et al.* Accuracy and clinical role of fine needle percutaneous biopsy with computerized tomography guidance of small (less than 4.0 cm) renal masses. *J Urol*. 2004;171(5):1802–1805.

47. Wang R, Wolf JS Jr, Wood DP Jr, *et al.* Accuracy of percutaneous core biopsy in management of small renal masses. *Urology.* 2009;73(3):586-590; discussion 590–591.

48. Rapp DE, Orvieto M, Sokoloff MH, *et al.* Use of biopsy sheath to improve standardization of renal mass biopsy in tissue-ablative procedures. *J Endourol.* 2004;18(5):453–454.

49. Appelbaum AH, Kamba TT, Cohen AS, *et al.* Effectiveness and safety of image-directed biopsies: coaxial technique versus conventional fine-needle aspiration. *South Med J.* 2002;95(2):212–217.

50. Silverman SG, Gan YU, Mortele KJ, *et al.* Renal masses in the adult patient: the role of percutaneous biopsy. *Radiology.* 2006;240(1):6–22.

51. Wunderlich H, Hindermann W, Al Mustafa AM, *et al.* The accuracy of 250 fine needle biopsies of renal tumors. *J Urol.* 2005;174(1):44–46.

52. Abel EJ, Heckman JE, Hinshaw L, *et al.* Multi-quadrant biopsy technique improves diagnostic ability in large heterogeneous renal masses. *J Urol.* 2015;194(4):886–891.

53. Remzi M, Marberger M. Renal tumor biopsies for evaluation of small renal tumors: why, in whom, and how? *Eur Urol.* 2009;55(2):359–367.

54. Lane BR, Samplaski MK, Herts BR, *et al.* Renal mass biopsy--a renaissance? *J Urol.* 2008;179(1):20–27.

55. Somani BK, Nabi G, Thorpe P, *et al.* Image-guided biopsy-diagnosed renal cell carcinoma: critical appraisal of technique and long-term follow-up. *Eur Urol.* 2007;51(5):1289–1295; discussion 1296–1297.

56. Ralls PW, Barakos JA, Kaptein EM, *et al.* Renal biopsy-related hemorrhage: frequency and comparison of CT and sonography. *J Comput Assist Tomogr.* 1987;11(6):1031–1034.

57. Klingler HC, Susani M. Focal therapy and imaging in prostate and kidney cancer: renal biopsy protocols before and after focal therapy. *J Endourol.* 2010;24(5):701–705.

58. Volpe A, Mattar K, Finelli A, *et al.* Contemporary results of percutaneous biopsy of 100 small renal masses: a single center experience. *J Urol.* 2008;180(6):2333–2337.

59. Evans AJ, Delahunt B, Srigley JR. Issues and challenges associated with classifying neoplasms in percutaneous needle biopsies of incidentally found small renal masses. *Semin Diagn Pathol.* 2015;32(2):184–195.

60. Marshall D, Laberge JM, Firetag B, *et al.* The changing face of percutaneous image-guided biopsy: molecular profiling and genomic analysis in current practice. *J Vasc Interv Radiol.* 2013;24(8):1094–1103.

61. Morales AR, Nassiri M, Kanhoush R, *et al.* Experience with an automated microwave-assisted rapid tissue processing method: validation of histologic quality and impact on the timeliness of diagnostic surgical pathology. *Am J Clin Pathol.* 2004;121(4):528–536.

62. Rogatsch H, Mairinger T, Horninger W, *et al.* Optimized preembedding method improves the histologic yield of prostatic core needle biopsies. *Prostate.* 2000;42(2):124–129.

63. Reuter VE, Argani P, Zhou M, *et al.* Best practices recommendations in the application of immunohistochemistry in the kidney tumors: report from the International Society of Urologic Pathology consensus conference. *Am J Surg Pathol.* 2014;38(8):e35–e49.

64. Al-Ahmadie HA, Alden D, Fine SW, *et al.* Role of immunohistochemistry in the evaluation of needle core biopsies in adult renal cortical tumors: an ex vivo study. *Am J Surg Pathol.* 2011;35(7):949–961.

65. Kurban G, Gallie BL, Leveridge M, *et al.* Needle core biopsies provide ample material for genomic and proteomic studies of kidney cancer: observations on DNA, RNA, protein extractions and VHL mutation detection. *Pathol Res Pract.* 2012;208(1):22–31.

66. Barocas DA, Mathew S, DelPizzo JJ, *et al.* Renal cell carcinoma sub-typing by histopathology and fluorescence in situ hybridization on a needle-biopsy specimen. *BJU Int.* 2007;99(2):290–295.

67. Gowrishankar B, Cahill L, Arndt AE, *et al.* Subtyping of renal cortical neoplasms in fine needle aspiration biopsies using a decision tree based on genomic alterations detected by fluorescence in situ hybridization. *BJU Int.* 2014;114(6):881–890.

68. Kos Z, Williams PA, Belanger EC, *et al.* Fluorescence in situ hybridization as an adjunct tool in the diagnosis of primary and metastatic renal cell carcinoma in fine needle aspiration specimens. *Diagn Cytopathol.* 2014;42(12):1013–1023.

69. Chyhrai A, Sanjmyatav J, Gajda M, *et al.* Multi-colour FISH on preoperative renal tumour biopsies to confirm the diagnosis of uncertain renal masses. *World J Urol.* 2010;28(3):269–274.

70. Moch H, A.M., Argani P, Cheville J, Delahunt B, Martignoni G, Srigley JR, Tan P, Tickoo S. Renal Cell Tumours Introduction. World Health Organization Classification of Tumours of the Urinary System and Male Genital Organs. Moch H, Humphrey P, Ulbright T and Reuter V [eds.] Lyon, France: IARC Press; 2016.

71. Ball MW, Bezerra SM, Gorin MA, *et al.* Grade heterogeneity in small renal masses: potential implications for renal mass biopsy. *J Urol.* 2015;193(1):36–40.

72. Shannon BA, Cohen RJ, de Bruto H, *et al.* The value of preoperative needle core biopsy for diagnosing benign lesions among small, incidentally detected renal masses. *J Urol.* 2008;180(4):1257–1261; discussion 1261.

73. Leveridge MJ, Finelli A, Kachura JR, *et al.* Outcomes of small renal mass needle core biopsy, nondiagnostic percutaneous biopsy, and the role of repeat biopsy. *Eur Urol.* 2011;60(3):578–584.

74. Shah RB, Bakshi N, Hafez KS, *et al.* Image-guided biopsy in the evaluation of renal mass lesions in contemporary urological practice: indications, adequacy, clinical impact, and limitations of the pathological diagnosis. *Hum Pathol.* 2005;36(12):1309–1315.

75. Menogue SR, O'Brien BA, Brown AL, *et al.* Percutaneous core biopsy of small renal mass lesions: a diagnostic tool to better stratify patients for surgical intervention. *BJU Int.* 2013;111(4 Pt B):E146–E151.

76. Veltri A, Garetto I, Tosetti I, *et al.* Diagnostic accuracy and clinical impact of imaging-guided needle biopsy of renal masses. Retrospective analysis on 150 cases. *Eur Radiol.* 2011;21(2):393–401.

77. Amin MB, Crotty TB, Tickoo SK, *et al.* Renal oncocytoma: a reappraisal of morphologic features with clinicopathologic findings in 80 cases. *Am J Surg Pathol.* 1997;21(1):1–12.

78. Trpkov K, Yilmaz A, Uzer D, *et al.* Renal oncocytoma revisited: a clinicopathological study of 109 cases with emphasis on problematic diagnostic features. *Histopathology.* 2010;57(6):893–906.

79. Blumenfeld AJ, Guru K, Fuchs GJ, *et al.* Percutaneous biopsy of renal cell carcinoma underestimates nuclear grade. *Urology.* 2010;76(3):610–613.

80. Neuzillet Y, Lechevallier E, Andre M, *et al.* Follow-up of renal oncocytoma diagnosed by percutaneous tumor biopsy. *Urology.* 2005;66(6):1181–1185.

81. Tickoo SK, Reuter VE, Amin MB, *et al.* Renal oncocytosis: a morphologic study of fourteen cases. *Am J Surg Pathol.* 1999;23(9):1094–1101.

82. Gobbo S, Eble JN, Delahunt B, *et al.* Renal cell neoplasms of oncocytosis have distinct morphologic, immunohistochemical, and cytogenetic profiles. *Am J Surg Pathol.* 2010;34(5):620–626.

83. Pavlovich CP, Grubb RL 3rd, Hurley K, *et al.* Evaluation and management of renal tumors in the Birt-Hogg-Dube syndrome. *J Urol.* 2005;173(5):1482–1486.

84. Adley BP, Smith ND, Nayar R, *et al.* Birt-Hogg-Dube syndrome: clinicopathologic findings and genetic alterations. *Arch Pathol Lab Med.* 2006;130(12):1865–1870.

85. Delongchamps NB, Galmiche L, Eiss D, *et al.* Hybrid tumour 'oncocytoma-chromophobe renal cell carcinoma' of the kidney: a report of seven sporadic cases. *BJU Int.* 2009;103(10):1381–1384.

86. Petersson F, Gatalica Z, Grossmann P, *et al.* Sporadic hybrid oncocytic/chromophobe tumor of the kidney: a clinicopathologic, histomorphologic, immunohistochemical, ultrastructural, and molecular cytogenetic study of 14 cases. *Virchows Arch.* 2010;456(4):355–365.

87. Pote N, Vieillefond A, Couturier J, *et al.* Hybrid oncocytic/chromophobe renal cell tumours do not display genomic features of chromophobe renal cell carcinomas. *Virchows Arch.* 2013;462(6):633–638.

88. Furuya M, Hong SB, Tanaka R, *et al.* Distinctive expression patterns of glycoprotein non-metastatic B and folliculin in renal tumors in patients with Birt-Hogg-Dube syndrome. *Cancer Sci.* 2015;106(3):315–323.

89. Waldert M, Klatte T, Haitel A, *et al.* Hybrid renal cell carcinomas containing histopathologic features of chromophobe renal cell carcinomas and oncocytomas have excellent oncologic outcomes. *Eur Urol.* 2010;57(4):661–665.

90. Mehta V, Venkataraman G, Antic T, *et al.* Renal angiomyolipoma, fat-poor variant--a clinicopathologic mimicker of malignancy. *Virchows Arch.* 2013;463(1):41–46.

91. Nese N, Martignoni G, Fletcher CD, *et al.* Pure epithelioid PEComas (so-called epithelioid angiomyolipoma) of the kidney: A clinicopathologic study of 41 cases: detailed assessment of morphology and risk stratification. *Am J Surg Pathol.* 2011;35(2):161–176.

92. Froemming AT, Boland J, Cheville J, *et al.* Renal epithelioid angiomyolipoma: imaging characteristics in nine cases with radiologic-pathologic correlation and review of the literature. *AJR Am J Roentgenol.* 2013;200(2):W178–W186.

93. Guo J, Tretiakova MS, Troxell ML, *et al.* Tuberous sclerosis-associated renal cell carcinoma: a clinicopathologic study of 57 separate carcinomas in 18 patients. *Am J Surg Pathol.* 2014;38(11):1457–1467.

94. Yang P, Cornejo KM, Sadow PM, *et al.* Renal cell carcinoma in tuberous sclerosis complex. *Am J Surg Pathol.* 2014;38(7):895–909.

95. Sofikerim M, Tatlisen A, Canoz O, *et al.* What is the role of percutaneous needle core biopsy in diagnosis of renal masses? *Urology.* 2010;76(3):614–618.

96. Moch H, Amin MB, Argani P, *et al.* Renal Cell Tumours Introduction. In: World Health Organization Classification of Tumours. Pathology and Genetic Tumors of the Urinary System and Male Genital Organs. Moch H, Humphrey P, Ulbright T, Reuter V. [eds.] Lyon, France: IARC Press; 2016:14-17.

97. Grignon DJ, Che M. Clear cell renal cell carcinoma. *Clin Lab Med.* 2005;25(2):305–316.

98. Reuter VE, Tickoo SK. Differential diagnosis of renal tumours with clear cell histology. *Pathology.* 2010;42(4):374–383.

99. Lhermitte B, de Leval L. Interpretation of needle biopsies of the kidney for investigation of renal masses. *Virchows Arch.* 2012;461(1):13–26.

100. Delahunt B, Eble JN. Papillary renal cell carcinoma: a clinicopathologic and immunohistochemical study of 105 tumors. *Mod Pathol.* 1997;10(6):537–544.

101. Chevarie-Davis M, Riazalhosseini Y, Arseneault M, *et al.* The morphologic and immunohistochemical spectrum of papillary renal cell carcinoma: study including 132 cases with pure type 1 and type 2 morphology as well as tumors with overlapping features. *Am J Surg Pathol.* 2014;38(7):887–894.

102. Warrick JI, Tsodikov A, Kunju LP, *et al.* Papillary renal cell carcinoma revisited: a comprehensive histomorphologic study with outcome correlations. *Hum Pathol.* 2014;45(6):1139–1146.

103. Amin MB, Paner GP, Alvarado-Cabrero I, *et al.* Chromophobe renal cell carcinoma: histomorphologic characteristics and evaluation of conventional pathologic prognostic parameters in 145 cases. *Am J Surg Pathol.* 2008;32(12):1822–1834.

104. Przybycin CG, Cronin AM, Darvishian F, *et al.* Chromophobe renal cell carcinoma: a clinicopathologic study of 203 tumors in 200 patients with primary resection at a single institution. *Am J Surg Pathol.* 2011;35(7):962–970.

105. Cheville JC, Lohse CM, Sukov WR, *et al.* Chromophobe renal cell carcinoma: the impact of tumor grade on outcome. *Am J Surg Pathol.* 2012;36(6):851–856.

106. Williamson SR, Eble JN, Cheng L, *et al.* Clear cell papillary renal cell carcinoma: differential diagnosis and extended immunohistochemical profile. *Mod Pathol.* 2013;26(5):697–708.

107. Zhou H, Zheng S, Truong LD, *et al.* Clear cell papillary renal cell carcinoma is the fourth most common histologic type of renal cell carcinoma in 290 consecutive nephrectomies for renal cell carcinoma. *Hum Pathol.* 2014;45(1):59–64.

108. Williamson SR, Cheng L, Eble JN, *et al.* Renal cell carcinoma with angioleiomyoma-like stroma: clinicopathological, immunohistochemical, and molecular features supporting classification as a distinct entity. *Mod Pathol.* 2015;28(2):279–294.

109. Aron M, Chang E, Herrera L, *et al.* Clear cell-papillary renal cell carcinoma of the kidney not associated with end-stage renal disease: clinicopathologic correlation with expanded immunophenotypic and molecular characterization of a large cohort with emphasis on relationship with renal angiomyoadenomatous tumor. *Am J Surg Pathol.* 2015;39(7):873–888.

110. Deml KF, Schildhaus HU, Compérat E, *et al.* Clear cell papillary renal cell carcinoma and renal angiomyoadenomatous tumor: two variants of a morphologic, immunohistochemical, and genetic distinct entity of renal cell carcinoma. *Am J Surg Pathol.* 2015;39(7):889–901.

111. Lohse CM, Blute ML, Zincke H, *et al.* Comparison of standardized and nonstandardized nuclear grade of renal cell carcinoma to predict outcome among 2,042 patients. *Am J Clin Pathol.* 2002;118(6):877–886.

112. Brookman-May S, May M, Shariat SF, *et al.* Features associated with recurrence beyond 5 years after nephrectomy and nephron-sparing surgery for renal cell carcinoma: development and internal validation of a risk model (PRELANE score) to predict late recurrence based on a large multicenter database (CORONA/SATURN Project). *Eur Urol.* 2013;64(3):472–477.

113. Delahunt B, Sika-Paotonu D, Bethwaite PB, *et al.* Fuhrman grading is not appropriate for chromophobe renal cell carcinoma. *Am J Surg Pathol.* 2007;31(6):957–960.

114. Steffens S, Janssen M, Roos FC, *et al.* The Fuhrman grading system has no prognostic value in patients with nonsarcomatoid chromophobe renal cell carcinoma. *Hum Pathol.* 2014;45(12):2411–2416.

115. Fuhrman SA, Lasky LC, Limas C. Prognostic significance of morphologic parameters in renal cell carcinoma. *Am J Surg Pathol.* 1982;6(7):655–663.

116. Sika-Paotonu D, Bethwaite PB, McCredie MR, *et al.* Nucleolar grade but not Fuhrman grade is applicable to papillary renal cell carcinoma. *Am J Surg Pathol.* 2006;30(9):1091–1096.

117. Delahunt B, Sika-Paotonu D, Bethwaite PB, *et al.* Grading of clear cell renal cell carcinoma should be based on nucleolar prominence. *Am J Surg Pathol.* 2011;35(8):1134–1139.

118. Delahunt B, McKenney JK, Lohse CM, *et al.* A novel grading system for clear cell renal cell carcinoma incorporating tumor necrosis. *Am J Surg Pathol.* 2013;37(3):311–322.

119. Abel EJ, Carrasco A, Culp SH, *et al.* Limitations of preoperative biopsy in patients with metastatic renal cell carcinoma: comparison to surgical pathology in 405 cases. *BJU Int.* 2012;110(11):1742–1746.

120. Halverson SJ, Kunju LP, Bhalla R, *et al.* Accuracy of determining small renal mass management with risk stratified biopsies: confirmation by final pathology. *J Urol.* 2013;189(2):441–446.

121. Millet I, Curros F, Serre I, *et al.* Can renal biopsy accurately predict histological subtype and Fuhrman grade of renal cell carcinoma? *J Urol.* 2012;188(5):1690–1694.

122. Frank I, Blute ML, Cheville JC, *et al.* An outcome prediction model for patients with clear cell renal cell carcinoma treated with radical nephrectomy based on tumor stage, size, grade and necrosis: the SSIGN score. *J Urol.* 2002;168(6):2395–2400.

123. Zigeuner R, Hutterer G, Chromecki T, *et al.* External validation of the Mayo Clinic stage, size, grade, and necrosis (SSIGN) score for clear-cell renal cell carcinoma in a single European centre applying routine pathology. *Eur Urol.* 2010;57(1):102–109.

124. Pichler M, Hutterer GC, Chromecki TF, *et al.* Presence and extent of histological tumour necrosis is an adverse prognostic factor in papillary type 1 but not in papillary type 2 renal cell carcinoma. *Histopathology.* 2013;62(2):219–228.

125. Tan PH, Cheng L, Rioux-Leclercq N, *et al.* Renal tumors: diagnostic and prognostic biomarkers. *Am J Surg Pathol.* 2013;37(10):1518–1531.

126. Amin MB, Epstein JI, Ulbright TM, *et al.* Best practices recommendations in the application of immunohistochemistry in urologic pathology: report from the International Society of Urological Pathology consensus conference. *Am J Surg Pathol.* 2014;38(8):1017–1022.

127. Sangoi AR, Karamchandani J, Kim J, *et al.* The use of immunohistochemistry in the diagnosis of metastatic clear cell renal cell carcinoma: a review of PAX-8, PAX-2, hKIM-1, RCCma, and CD10. *Adv Anat Pathol.* 2010;17(6):377–393.

128. Ordonez NG. Value of PAX 8 immunostaining in tumor diagnosis: a review and update. *Adv Anat Pathol.* 2012;19(3):140–151.

129. Amin MB, Trpkov K, Lopez-Beltran A, *et al.* Best practices recommendations in the application of immunohistochemistry in the bladder lesions: report from the International Society of Urologic Pathology consensus conference. *Am J Surg Pathol.* 2014;38(8):e20–e34.

130. Miettinen M, McCue PA, Sarlomo-Rikala M, *et al.* GATA3: a multispecific but potentially useful marker in surgical pathology: a systematic analysis of 2500 epithelial and nonepithelial tumors. *Am J Surg Pathol.* 2014;38(1):13–22.

131. Gonzalez-Roibon N, Faraj SF, Munari E, *et al.* Comprehensive profile of GATA binding protein 3 immunohistochemical expression in primary and metastatic renal neoplasms. *Hum Pathol.* 2014;45(2):244–248.

132. Sangoi AR, Fujiwara M, West RB, *et al.* Immunohistochemical distinction of primary adrenal cortical lesions from metastatic clear cell renal cell carcinoma: a study of 248 cases. *Am J Surg Pathol.* 2011;35(5):678–686.

133. McGregor DK, Khurana KK, Cao C, *et al.* Diagnosing primary and metastatic renal cell carcinoma: the use of the monoclonal antibody 'Renal Cell Carcinoma Marker'. *Am J Surg Pathol.* 2001;25(12):1485–1492.

134. Clayton EF, Ziober A, Yao Y, *et al.* Malignant tumors with clear cell morphology: a comparative immunohistochemical study with renal cell carcinoma antibody, Pax8, steroidogenic factor 1, and brachyury. *Ann Diagn Pathol.* 2013;17(2):192–197.

135. Martignoni G, Pea M, Gobbo S, *et al.* Cathepsin-K immunoreactivity distinguishes MiTF/TFE family renal translocation carcinomas from other renal carcinomas. *Mod Pathol.* 2009;22(8):1016–1022.

136. Pea M, Bonetti F, Zamboni G, *et al.* Melanocyte-marker-HMB-45 is regularly expressed in angiomyolipoma of the kidney. *Pathology.* 1991;23(3):185–188.

137. Reuter VE, Argani P, Zhou M, *et al.* Best practices recommendations in the application of immunohistochemistry in the kidney tumors: report from the international society of urologic pathology consensus conference. *Am J Surg Pathol.* 2014;38(8):e35–e49.

138. Genega EM, Ghebremichael M, Najarian R, *et al.* Carbonic anhydrase IX expression in renal neoplasms: correlation with tumor type and grade. *Am J Clin Pathol.* 2010;134(6):873–879.

139. Truong LD, Shen SS. Immunohistochemical diagnosis of renal neoplasms. *Arch Pathol Lab Med.* 2011;135(1):92–109.

140. Shen SS, Truong LD, Scarpelli M, *et al.* Role of immunohistochemistry in diagnosing renal neoplasms: when is it really useful? *Arch Pathol Lab Med.* 2012;136(4):410–417.

141. Zhou M, Roma A, Magi-Galluzzi C. The usefulness of immunohistochemical markers in the differential diagnosis of renal neoplasms. *Clin Lab Med.* 2005;25(2):247–257.

142. Tickoo SK, Reuter VE. Differential diagnosis of renal tumors with papillary architecture. *Adv Anat Pathol.* 2011;18(2):120–132.

143. Chen YB, Brannon AR, Toubaji A, *et al.* Hereditary leiomyomatosis and renal cell carcinoma syndrome-associated renal cancer: recognition of the syndrome by pathologic features and the utility of detecting aberrant succination by immunohistochemistry. *Am J Surg Pathol.* 2014;38(5):627–637.

144. Gill AJ, Hes O, Papathomas, *et al.* Succinate dehydrogenase (SDH)-deficient renal carcinoma: a morphologically distinct entity: a clinicopathologic series of 36 tumors from 27 patients. *Am J Surg Pathol.* 2014;38(12):1588–1602.

145. Thompson RH, Kurta JM, Kaag M, *et al.* Tumor size is associated with malignant potential in renal cell carcinoma cases. *J Urol.* 2009;181(5):2033–2036.

146. Snyder ME, Bach A, Kattan MW, *et al.* Incidence of benign lesions for clinically localized renal masses smaller than 7 cm in radiological diameter: influence of sex. *J Urol.* 2006;176(6 Pt 1):2391-2395; discussion 2395–2396.

147. Li G, Barthelemy A, Feng G, *et al.* S100A1: a powerful marker to differentiate chromophobe renal cell carcinoma from renal oncocytoma. *Histopathology.* 2007;50(5):642–647.

148. Kuehn A, Paner GP, Skinnider BF, *et al.* Expression analysis of kidney-specific cadherin in a wide spectrum of traditional and newly recognized renal epithelial neoplasms: diagnostic and histogenetic implications. *Am J Surg Pathol.* 2007;31(10):1528–1533.

149. Skinnider BF, Amin MB. An immunohistochemical approach to the differential diagnosis of renal tumors. *Semin Diagn Pathol.* 2005;22(1):51–68.

150. Osunkoya AO, Cohen C, Lawson D, *et al.* Claudin-7 and claudin-8: immunohistochemical markers for the differential diagnosis of chromophobe renal cell carcinoma and renal oncocytoma. *Hum Pathol.* 2009;40(2):206–210.

151. Martignoni G, Pea M, Bonetti F, *et al.* Oncocytoma-like angiomyolipoma. A clinicopathologic and immunohistochemical study of 2 cases. *Arch Pathol Lab Med.* 2002;126(5):610-612.

152. Martignoni G, Pea M, Bonetti F. Renal epithelioid oxyphilic neoplasms (REON): a pleomorphic variant of renal angiomyolipoma. *Int J Surg Pathol.* 1995;2 Suppl:539.

153. Hes O, Petersson F, Kuroda N, *et al.* Renal hybrid oncocytic/chromophobe tumors - a review. *Histol Histopathol.* 2013;28(10):1257–1264.

154. Tickoo SK, Alden D, Olgac S, *et al.* Immunohistochemical expression of hypoxia inducible factor-1alpha and its downstream molecules in sarcomatoid renal cell carcinoma. *J Urol.* 2007;177(4):1258–1263.

155. Amin MB, Smith SC, Agaimy A, *et al.* Collecting duct carcinoma versus renal medullary carcinoma: an appeal for nosologic and biological clarity. *Am J Surg Pathol.* 2014;38(7):871–874.

156. Liu Q, Galli S, Srinivasan R, *et al.* Renal medullary carcinoma: molecular, immunohistochemistry, and morphologic correlation. *Am J Surg Pathol.* 2013;37(3):368–374.

157. Ordonez NG. Value of GATA3 immunostaining in tumor diagnosis: a review. *Adv Anat Pathol*. 2013;20(5):352–360.

158. Eble J, Sauter G, Epstein J, Sesterhenn I. eds. Pathology and Genetics of Tumours of the Urinary System and Male Genital Organs. Lyon, France: IARC Press; 2004.

159. Crispen PL, Tabidian MR, Allmer C, *et al*. Unclassified renal cell carcinoma: impact on survival following nephrectomy. *Urology*. 2010;76(3):580–586.

160. Zhong J, Chen N, Chen X, *et al*. Peripheral primitive neuroectodermal tumor of the kidney in a 51-year-old female following breast cancer: a case report and review of the literature. *Oncol Lett*. 2015;9(1):108–112.

161. Castro EC, Parwani AV. Ewing sarcoma/primitive neuroectodermal tumor of the kidney: two unusual presentations of a rare tumor. *Case Rep Med*. 2012;2012:190581.

162. Markovic-Lipkovski J, Sopta J, Vjestica J, *et al*. Rapidly progressive course of primary renal synovial sarcoma--case report. *Srp Arh Celok Lek*. 2013;141(11–12):814–818.

163. Roh MH, Dal Cin P, Silverman SG, *et al*. The application of cytogenetics and fluorescence in situ hybridization to fine-needle aspiration in the diagnosis and subclassification of renal neoplasms. *Cancer Cytopathol*. 2010;118(3):137–145.

164. Thomson TA, Klijanienko J, Couturier J, *et al*. Fine-needle aspiration of renal and extrarenal rhabdoid tumors: the experience of the Institut Curie regarding 20 tumors in 13 patients. *Cancer Cytopathol*. 2011;119(1):49–57.

165. Vieira J, Henrique R, Ribeiro FR, *et al*. Feasibility of differential diagnosis of kidney tumors by comparative genomic hybridization of fine needle aspiration biopsies. *Genes Chromosomes Cancer*. 2010;49(10):935–947.

166. Tan MH, Wong CF, Tan HL, *et al*. Genomic expression and single-nucleotide polymorphism profiling discriminates chromophobe renal cell carcinoma and oncocytoma. *BMC Cancer*. 2010;10:196.

167. Sperga M, Martinek P, Vanecek T, *et al*. Chromophobe renal cell carcinoma--chromosomal aberration variability and its relation to Paner grading system: an array CGH and FISH analysis of 37 cases. *Virchows Arch*. 2013;463(4):563–573.

168. Herrera GA, Turbat-Herrera EA. Ancillary diagnostic techniques in the evaluation of adult epithelial renal neoplasms: indications, caveats, and pitfalls. *Appl Immunohistochem Mol Morphol*. 2014;22(2):77–98.

169. Chen N, Nie L, Gong J, *et al*. Gains of chromosomes 7 and 17 in tubulocystic carcinoma of kidney: two cases with fluorescence in situ hybridisation analysis. *J Clin Pathol*. 2014;67(11):1006–1009.

170. Marks-Jones DA, Zynger DL, Parwani AV, *et al*. Fine needle aspiration biopsy of renal mucinous tubular and spindle cell carcinoma: report of two cases. *Diagn Cytopathol*. 2010;38(1):51–55.

171. Green WM, Yonescu R, Morsberger L, *et al*. Utilization of a TFE3 break-apart FISH assay in a renal tumor consultation service. *Am J Surg Pathol*. 2013;37(8):1150–1163.

172. Macher-Goeppinger S, Roth W, Wagener N, *et al*. Molecular heterogeneity of TFE3 activation in renal cell carcinomas. *Mod Pathol*. 2012;25(2):308–315.

173. Rao Q, Zhang XM, Tu P, *et al*. Renal cell carcinomas with t(6;11)(p21;q12) presenting with tubulocystic renal cell carcinoma-like features. *Int J Clin Exp Pathol*. 2013;6(7):1452–1457.

174. Sugawara E, Togashi Y, Kuroda N, *et al*. Identification of anaplastic lymphoma kinase fusions in renal cancer: large-scale immunohistochemical screening by the intercalated antibody-enhanced polymer method. *Cancer*. 2012;118(18):4427–4436.

175. Marconi L, Dabestani S, Lam TB, *et al*. Systematic review and meta-analysis of diagnostic accuracy of percutaneous renal tumour biopsy. *Eur Urol*. 2016;69(4):660–673.

176. Merino MJ, Torres-Cabala C, Pinto P, *et al*. The morphologic spectrum of kidney tumors in hereditary leiomyomatosis and renal cell carcinoma (HLRCC) syndrome. *Am J Surg Pathol*. 2007;31(10):1578–1585.

177. Ginzburg S, Uzzo R, Al-Saleem T, *et al*. Coexisting hybrid malignancy in a solitary sporadic solid benign renal mass: implications for managing patients following renal biopsy. *J Urol*. 2014;191(2):296–300.

178. Sorbellini M, Kattan MW, Snyder ME, *et al*. A postoperative prognostic nomogram predicting recurrence for patients with conventional clear cell renal cell carcinoma. *J Urol*. 2005;173(1):48–51.

179. Klatte T, Seligson DB, LaRochelle J, *et al*. Molecular signatures of localized clear cell renal cell carcinoma to predict disease-free survival after nephrectomy. *Cancer Epidemiol Biomarkers Prev*. 2009;18(3):894–900.

180. Brunelli M, Eccher A, Gobbo S, *et al.* Loss of chromosome 9p is an independent prognostic factor in patients with clear cell renal cell carcinoma. *Mod Pathol.* 2008;21(1):1–6.

181. Herts BR, Baker ME. The current role of percutaneous biopsy in the evaluation of renal masses. *Semin Urol Oncol.* 1995;13(4):254–261.

182. Slaby O, Redova M, Poprach A, *et al.* Identification of MicroRNAs associated with early relapse after nephrectomy in renal cell carcinoma patients. *Genes Chromosomes Cancer.* 2012;51(7):707–716.

183. Youssef YM, White NM, Grigull J, *et al.* Accurate molecular classification of kidney cancer subtypes using microRNA signature. *Eur Urol.* 2011;59(5):721–730.

184. White NM, Bao TT, Grigull J, *et al.* miRNA profiling for clear cell renal cell carcinoma: biomarker discovery and identification of potential controls and consequences of miRNA dysregulation. *J Urol.* 2011;186(3):1077–1083.

185. Wotschofsky Z, Liep J, Meyer HA, *et al.* Identification of metastamirs as metastasis-associated microRNAs in clear cell renal cell carcinomas. *Int J Biol Sci.* 2012;8(10):1363–1374.

186. Prior C, Perez-Gracia JL, Garcia-Donas J, *et al.* Identification of tissue microRNAs predictive of sunitinib activity in patients with metastatic renal cell carcinoma. *PLoS One.* 2014;9(1):e86263.

187. Pena-Llopis S, Vega-Rubín-de-Celis S, Liao A, *et al.* BAP1 loss defines a new class of renal cell carcinoma. *Nat Genet.* 2012;44(7):751–759.

188. Kapur P, Peña-Llopis S, Christie A, *et al.* Effects on survival of BAP1 and PBRM1 mutations in sporadic clear-cell renal-cell carcinoma: a retrospective analysis with independent validation. *Lancet Oncol.* 2013;14(2):159–167.

189. Kapur P, Christie A, Raman JD, *et al.* BAP1 immunohistochemistry predicts outcomes in a multi-institutional cohort with clear cell renal cell carcinoma. *J Urol.* 2014;191(3):603–610.

190. Krabbe LM, Westerman ME, Bagrodia A, *et al.* Dysregulation of beta-catenin is an independent predictor of oncologic outcomes in patients with clear cell renal cell carcinoma. *J Urol.* 2014;191(6):1671–1677.

191. Langner C, Ratschek M, Rehak P, *et al.* Expression of MUC1 (EMA) and E-cadherin in renal cell carcinoma: a systematic immunohistochemical analysis of 188 cases. *Mod Pathol.* 2004;17(2):180–188.

192. Varela I, Tarpey P, Raine K, *et al.* Exome sequencing identifies frequent mutation of the SWI/SNF complex gene PBRM1 in renal carcinoma. *Nature.* 2011;469(7331):539–542.

193. Dalgliesh GL, Furge K, Greenman C, *et al.* Systematic sequencing of renal carcinoma reveals inactivation of histone modifying genes. *Nature.* 2010;463(7279):360–363.

194. Hakimi AA, Ostrovnaya I, Reva B, *et al.* Adverse outcomes in clear cell renal cell carcinoma with mutations of 3p21 epigenetic regulators BAP1 and SETD2: a report by MSKCC and the KIRC TCGA research network. *Clin Cancer Res.* 2013;19(12):3259–3267.

195. Sankin A, Hakimi AA, Mikkilineni N, *et al.* The impact of genetic heterogeneity on biomarker development in kidney cancer assessed by multiregional sampling. *Cancer Med.* 2014;3(6):1485–1492.

196. Cremona M, Espina V, Caccia D, *et al.* Stratification of clear cell renal cell carcinoma by signaling pathway analysis. *Expert Rev Proteomics.* 2014;11(2):237–249.

197. Bartholow T, Parwani A. Renal primitive neuroectodermal tumors. *Arch Pathol Lab Med.* 2012;136(6):686–690.

C8

Available Ablation Energies to Treat Small Renal Masses

CHAIR

Maria Pilar Laguna, The Netherlands

CO-CHAIR

Jochen Walz, France

MEMBERS

Thomas Atwell, United States
Riccardo Autorino, United States
Andrea Cestari, Italy
Jeffrey Gahan, United States
Tobias Klatte, Austria
Krijn van Lienden, The Netherlands
Dogu Teber, Germany
Peter GK Wagstaff, The Netherlands
Patricia J Zondervan, The Netherlands

CONTENTS

Available Ablation Energies to Treat Small Renal Masses

8.1 Introduction

Over the past decades, the annual incidence of kidney cancer has been rising, with the greatest increase observed for cases with localized tumours. This rise is due mostly to the increasing detection of small (≤4 cm) tumours through better diagnostic capabilities.[1] Widespread diffusion of abdominal imaging has driven the identification of a distinct population of small renal cortical tumours (cT1a No Mo), comprising roughly 70% of all renal tumours incidentally detected.[2] However, 15% to 20% of patients undergoing an operation for suspected renal cell carcinoma (RCC) have had a benign lesion at final histopathological evaluation (including angiomyolipomas and oncocytomas).[3] Furthermore, most of the small RCCs are either indolent or have low aggressiveness features, neither of which are identifiable by computed tomography (CT) scan or magnetic resonance imaging (MRI). Biopsy of this small renal tumour is not devoid of limitations, especially in determining grade accurately.[4]

Small renal tumours, followed expectantly by active surveillance (AS) programs, can remain stable for years or grow at slow rate (0.49 cm/year). Metastasis is also rare for masses less than 4 cm in size.[5] Radical nephrectomy is an excessive treatment for such small renal tumours, and nephron-sparing surgery (NSS), whenever technically feasible, is the first surgical choice in cT1 renal tumours, with excellent oncologic outcomes.[6,7]

In an attempt to minimize perioperative complications and preserve kidney function, ablation therapy emerged in the past decade as a reasonable treatment option for select patients, namely the elderly and patients with comorbidities or with high surgical risk.[8,9] Ablation therapy obviates the need for renal vascular pedicle manipulation, and parenchyma excision and reconstruction. Thus, hypothetically, such therapy lessens the likelihood for surgically induced renal function impairment and perioperative complications. Among all the ablation technologies, cryoablation (CA) and radiofrequency ablation (RFA) have been truly incorporated as real treatment options for kidney tumours, especially for small renal masses (SRMs).[8,9] Selection criteria have been explored in the past years, and their value and limitations are explained elsewhere.[10,11] In this chapter, we will review the mechanism of action and results of CA and RFA of renal tumours, as well as emerging ablation technologies. Last, a comparison between ablation outcomes and other treatment option outcomes for SRMs will be presented.

8.2 Methodology

A systematic literature review was performed using PubMed, Embase®, Scopus, Science Citation Index, and Cochrane Reviews from January 2006 to September 2015 to identify eligible studies (e.g. those reporting a comparative analysis of different ablative procedures for kidney cancer, or those comparing kidney ablation to partial nephrectomy [PN] or AS).

Only studies in English and in a clinical setting were included. Electronic searches were performed by applying a "free-text protocol" for a variety of search terms, including *kidney ablation, renal cryoablation, renal radiofrequency ablation*, and *renal focal therapy*. Article selection proceeded according to the search strategy based on Preferred Reporting Items for Systematic Reviews and Meta-Analyses (PRISMA) criteria (www.prisma-statement.org). In addition, cited references from select articles and from review articles retrieved in the search were assessed, and if relevant, they were included.

The standard, recognized ablation technology exclusion criteria included the following:

- Publications not written in English
- Conference abstracts
- Studies with 30 or fewer patients
- Studies lacking outcomes specific to complications and tumour control
- Studies lacking methodology or specifics of treatment necessary for critical appraisal

Additionally, for studies published from the same institution with overlapping patient populations, the most recent or most complete publication was prioritized for review, unless the publication included a unique comparison cohort. Meta-analyses and review articles were reviewed for original publications that may have been omitted in the original search process.

Experimental studies were manually retrieved and included when judged relevant. When enough evidence was available, a systematic review of the clinical outcomes was performed. For these clinical studies, attention was specifically directed to publications including original treatment outcomes. Given the inclusion of both procedural- and tumour-specific outcomes, proven malignant pathology was not required, thus allowing one to capture a greater breadth of the potential limitations of treatment.

The Level of Evidence (LOE) of included studies was rated according to the criteria by the Centre for Evidence-Based Medicine.[12] Whenever available, the most recently published meta-analysis was considered. The section "Ablation in Perspective" contains the results of the meta-analysis of comparative studies for relevant outcomes that was performed, as none was available, using Review Manager (RevMan) software statistical package (The Cochrane Collaboration, Oxford, United Kingdom). In the case of multiple series from the same authors/institutions, the one with the largest number of cases or more complete data was considered for the purpose of the meta-analysis. Total numbers, proportions, means, and standard deviations (SDs) were extracted from each study. The weighted mean differences (WMDs) and the odds ratios (ORs) were used to compare continuous and dichotomous variables, respectively. All outcomes were reported with 95% confidence intervals (CIs). For continuous variables, the difference in mean values and the 95% CI were calculated. This method requires that a study report the standard errors of the mean, the SDs, or the CIs. However, some studies did not report any of these parameters, but presented continuous data using median and range; under this circumstance, an approximate transformation was made using the technique described by Hozo *et al.*[13] Heterogeneity was evaluated with I^2 statistics and the chi-square test for heterogeneity. In the case of heterogeneity among studies ($p<0.05$), a random effects model was applied, otherwise a fixed effects model was used.

8.3 Established Ablation Technology

8.3.1 Cryoablation

8.3.1.1 Technology and mechanisms of action

Cryoablation uses extreme cold (*cryo*) to destroy or damage tissue (*ablation*). Briefly, CA is performed using dedicated hollow needles (*cryoprobes*) through which cooled, thermally conductive fluids are circulated following the Joule-Thomson effect, using argon to freeze and helium to thaw.[14] Cryoprobes are inserted into or placed adjacent to the oncologic tissue. When the probes are in place, the cryogenic freezing unit removes heat, or "cools," from the tip of the probe, and by extension, from the surrounding tissue, leading to tissue death (*devitalization*).

In summary, the mechanism of action of CA can be synthesized into three steps:

1. Formation of ice crystals within cells, thereby disrupting membranes, and interrupting cellular metabolism and other processes
2. Coagulation of blood, thereby interrupting blood flow to the tissue, causing ischemia and cell death
3. Induction of apoptosis, the so-called programmed cell death cascade

8.3.1.1.1 The freezing-thawing cycle

Proper cryosurgical technique requires, ideally, that the tissue be frozen rapidly, thawed slowly and completely, and then, exposed to a second freeze cycle. Optimal technique accomplishes the goal of achieving a lethal temperature in the target tissue while assuring a safe margin around the tumour. Every phase of the freezing-thawing cycle—the cooling rate, nadir tissue temperature, duration of freezing, and thawing rate—is considered to be injurious, cooperating together to lead to tumoural death.[15]

Rapid cooling increases the probability of lethal intracellular ice crystal formation and should be induced as fast as possible.[16,17] However, the maximum cooling rates are a function of the cryogen type, the cryoprobe design, and the applied technology. Moreover, the repetition of the freezing-thawing cycle allows for the repeat and amplification of the injurious events. This double freezing-thawing cycle is often considered to be important for ensuring proper destruction of malignant tumours.

The concept of nadir temperature is of pivotal importance in the cryosurgical technique. It rests upon the fact that as tissues experience deeper freezing, cells progressively die. Cancer cell viability sharply decreases with declining temperatures, and most cells (both tumoural and normal) die as temperatures approach −40°C. However, as some cancer cells have been shown to survive at lower temperatures, there is a need for a double freezing-thawing cycle to −40°C.[18]

The thawing rate also affects cancer cell survival, and proper thawing is as lethal as proper freezing. Rapid thawing rates are less damaging and are to be avoided. Slow thawing affords a longer interval of exposure to subfreezing temperatures after the damage induced by the freezing phase of the procedure. In clinical practice, the slow thawing of the frozen lesion is passive, simply performed by switching off or using the standby mode of the cryogenic system. It relies upon body heat as the source of heat energy for the thaw. Cryosurgical devices with thaw mechanisms can provide heat only to the freeze zone adjacent to the cryoprobe, which serves to loosen the cryoprobes for removal at the end of the procedure and/or for eventual repositioning. This focused, rapid thawing occurring adjacent to the cryoprobe does not impact cell survival in that region.

Regarding the freezing duration, physician instinct (anecdotal evidence) guides toward longer durations. Few basic research studies have been conducted to provide laboratory-based evidence pertinent to duration, except to note that a significant increase in cell death occurs when freeze duration is increased from 5 minutes to 10 minutes.[19] In this study, it was further noted that exposure intervals of less than 1 minute for a given temperature often yielded significantly lower cell death compared with freeze durations of greater than 1 minute. Moreover, it must be considered that with modern cryosystems, the steady state of the ice ball is typically achieved within an interval of 10 to 20 minutes, and prolonged freezing duration will not further increase the diameter of the covered area.

8.3.1.1.2 Cryogenic injury

The mechanisms of cell death following CA are a complex cascade of events, including direct injury to the cells by ice crystal formation, failure of the microcirculation following thawing, and induction of apoptosis and necrosis. During the rapid freezing phase, extracellular ice crystal formation removes water from the cells. This, in turn, creates deleterious metabolic disturbances related to the freeze concentration of solutes, a process referred to as the "solution effects." Ice crystals cause mechanical damage due to the shearing forces affecting cell membrane integrity, especially in highly organized tissues.[16] Intracellular ice crystal formation occurs secondarily in the freeze zone and is lethal. Moreover, during the passive (slow) thawing phase, the ice microcrystals that were formed during the rapid freezing phase, instead of melting, recrystallize into macrocrystals, thus leading to further mechanical destruction of the cell membranes.

The loss of blood supply due to vascular stasis in the volume of previously frozen tissue occurs soon after thawing, increasing the probability that the cells will not survive. While the relative contribution of these two mechanisms of injury can be debated, they are clearly synergistic in cryoinjury.[19-22]

Both intrinsic (*mitochondrial-related*) and extrinsic (*membrane-related*) apoptosis have been shown to affect cell death in a cryogenic lesion.[23-26] Disruption of the normal function of mitochondria through the influence of the Bcl2 family of proteins is critical to the intrinsic apoptotic pathways. Levels of Bax, a pro-apoptotic protein found in the cytoplasm, increase immediately after thawing. Analysis of Bcl2, a prosurvival protein, and Bax reveals that immediately post-thaw, a mitochondrial-based signal promotes cell death. An extension of the apoptotic cell death cascade occurs with activation of the extrinsic pathway at lower temperatures.[25] In this regard, exposure to ultracold, freezing temperatures (below –30°C) was recently reported to result in the rapid initiation and progression of

the extrinsic, membrane-mediated apoptotic pathway.[25] This recent discovery has shown there is a molecular component to cancer cell death in the core of a cryogenic lesion, where historically intracellular ice formation was believed to be the predominant mechanism of cell death.

Following the initial freeze rupture of all cell types, the release of cytokines leads to the recruitment of circulating immune cells and local inflammation. The *cryoimmunologic response* occurs later,[26] and may overcome the local immunosuppressive actions of tumour-associated immune cells. With destruction of the tumour microenvironment, any surviving cancer cells are deprived of essential support, losing proliferative and, therefore, mutagenic capabilities. As a result, any surviving cells within the freeze target are likely to undergo delayed or secondary necrosis for a period of days to weeks, which is observed histologically as a region of coagulative necrosis. It is the sequence and consequences of the three ablative processes (i.e. freeze rupture, apoptosis, and necrosis)[25] that uniquely support an outcome of prolonged tissue destruction.

8.3.1.2 Technique and approach

Renal CA was initially performed via an open approach in the early 1990s as a nephron-sparing option for very select cases. Nowadays, the open approach should be considered anecdotal, as nearly all CA procedures are performed laparoscopically or percutaneously.

Laparoscopic renal CA was performed with encouraging, short-term and midterm results, both in the United States and Europe, at the end of the 20th century and beginning of the 21st century.[28,29] The next years were followed by the widespread diffusion of percutaneous CA procedures, performed both under CT or MRI guidance,[30,31] due mainly to the technological evolution of the various cryosystems available on the market, specifically small-diameter probes (17–18 G).

Long and coworkers[32] recently performed a literature review to clarify the differences between a surgical (laparoscopic) approach and a percutaneous approach to renal CA. Their analysis evidenced how surgical CA facilitates direct tumour visualization via tissue mobilization and subsequent probe insertion, while percutaneous CA obviates the need for general anesthesia. Currently, use of each approach depends largely on institutional traditions and surgeon preference. Some institutions use a purely laparoscopic approach, modified only by treating anterior lesions using a transperitoneal laparoscopic approach and posterior lesions using a retroperitoneoscopic approach. In other centres, anterior lesions are treated laparoscopically and posterior lesions percutaneously. A third philosophy is to largely avoid laparoscopy, and perform only percutaneous CA.

8.3.1.3 Procedural and perioperative outcomes

Perhaps related to techniques where imaging can act as a surrogate for pathology, specific definitions for CA procedural and oncologic outcomes have been suggested. Such standardized terminology and reporting criteria were developed by the International Working Group on Image-Guided Tumor Ablation and updated in 2014.[33] The term *technical success* addresses whether a tumour was ablated according to protocol and covered entirely by the ablation zone, analogous to margin status following resection. Such a definition may be applied to any renal mass, irrespective of histology. In contrast to technical success, the term *technique success* is used to describe efficacy of the ablative treatment over time. Such a term is best applied to those masses shown to be malignant. While controversial, *secondary efficacy* has been used to describe successful re-treatment of locally recurrent tumours.

Finally, local tumour *progression* has been proposed as an alternative to local *tumour recurrence*. This is based on the premise that a tumour at the ablation margin represents progression of the residual tumour following a presumed initially successful treatment.

Such terminology has led to confusion when assessing renal tumour ablation outcomes, with heterogeneous application of the definitions to treatment success, thereby compromising formal comparison of surgical standards. In contrast, the National Cancer Institute defines locally recurrent cancer as, "cancer that has recurred (come back) at or near the same place as the original (primary) tumor, usually after a period of time during which the cancer could not be detected."[34]

The modified Clavien criteria are commonly used in reporting ablation complications, with grading based on degree of deviation from normal clinical recovery.[35-38] Reporting standards for renal ablation have been proposed by the Society of Interventional Radiology (SIR), with endorsement of previously published grading of complications.[39,40] Such criteria are generalized, with emphasis on deviation from normal level of care and limitations in the classification of those patients routinely hospitalized after treatment.

Of the initial 199 publications included in the original search, 46 met the criteria detailed in the methodology. All were observational case series [LOE 3] detailing CA complications and/or efficacy in renal mass treatment. Nine of the 46 publications included a non-randomized comparison cohort consisting of patients treated with either surgical resection or RFA. When not specified in the methods of the series, previously described outcome definitions were applied.

Additional studies were included separately in this review when they illustrated specific attributes of ablation outside of the primary inclusion criteria, notably when published as a unique cohort of a larger published patient population.

The ability to visualize the ice ball generated during the CA process, either directly or with imaging, gives the operator a high level of confidence in complete tumour treatment, secondarily yielding a high *technical success* rate for most tumours. The leading edge of the ice ball, as visualized by CT, is 0°C.[41] This simple fact allows extrapolation of lethal isotherms for the tumour treatment process. Overall technical success rates, not including re-treatments, range from 86% to 100%.[42-44] Such outcomes are similar between laparoscopic cryoablation (LCA) and percutaneous cryoablation (PCA). Additionally, the synergy of multiple cryoprobes allows for technically successful treatment of large tumours, including cT1b and cT2 masses, although staged treatments may be needed.[45-48] However, there may be limitations with intraoperative monitoring during the ablation of endophytic tumours; a single study found that such tumours have a higher risk for treatment failure.[49] Otherwise, treatment of centrally located tumours can be successfully performed.[50]

Perhaps because the term *technical success* was derived from the percutaneous ablation literature or because the procedural term has questionable relevance to oncologic efficacy, the reporting of such an outcome has been inconsistent. In addition, particularly when one considers tumour re-treatments and subtotal ablations, discriminating between technical and technique failure in manuscripts can be difficult.[51]

8.3.1.4 Complications

The complications following CA have been thoroughly characterized in several publications. Overall complication rates range from 0% to 40%.[49,52] Summarizing the incidence of major complications is more difficult due to variable Clavien grades assigned as "major." If one assumes a complication of Clavien grade II or greater to be a major complication (to allow for a broader inclusion of published experience), the reported major complication rates published since 2006 range up to 40%, although conversions to open technique and intraoperative blood transfusion confound the reporting of such complications.[52,53] When one considers two large, published experiences detailing the complications of LCA[54] and PCA,[35] the rate of major complications (Clavien grade ≥II) was similar (7.7%–10.1%). Specific to PCA, complications may be greater in those centres with less procedural experience.[55]

When one considers complications related to CA, it is important to recognize the level of comorbidity in the selected patient population, as directed by the American Urological Association (AUA) guidelines.[8] In fact, the average Charlson Comorbidity Index (CCI) scores reported by many publications range from 5 to 7.[43-45,52,56] Many studies also report the mean/median body mass index (BMI) of the patient population to be 30 or greater.[48,56-60]

Some studies have shown that the R.E.N.A.L. nephrometry score may be associated with complications following percutaneous thermal ablation.[37,42,61-63] The R.E.N.A.L. nephrometry score consists of (R)adius (tumour size as maximal diameter), (E)xophytic/endophytic properties of the tumour, (N)earness of tumour deepest portion to the collecting system or sinus, (A)nterior (a)/posterior (p) descriptor, and the (L)ocation relative to the polar line. When considering both LCA and PCA, Sisul *et al.* showed that the R.E.N.A.L. score was significantly associated with complications due to CA, with the nearness (N) to the collecting system being the most predictive component.[62] Schmit *et al.* showed that the tumour nephrometry score for patients with a complication following thermal ablation was 8.1 compared with 6.8 for those without a complication ($p<0.001$). A subsequent publication by the same group showed that certain tumour-related factors were significantly associated with major complications using their reported "(MC)2" scoring system. Factors evaluated included the maximum diameter of the tumour (M), prior myocardial infarction (M), central tumour location (C), and complicated diabetes mellitus (C).[64] Recognizing the derivation of the nephrometry scoring systems in predicting extirpative outcomes, it is intuitive that more specific predictive measures of tumour characteristics can be applied to thermal ablation techniques.

Of the complications related to CA, hemorrhage is the most common. Reported hemorrhagic complication rates vary, but most experiences quote a range from 1% to 10%.[45,65] Major hemorrhage following CA has been shown to be related to tumour size, number of cryoprobes, and central location.[35,66] Such hemorrhage may result in the conversion of LCA to an extirpative technique.[67,68]

Higher transfusion rates are reported for LCA compared with PCA. This may be because of the clearly visible and dynamic bleeding present at the time of surgery that warrants real-time management. Such bleeding is typically only appreciated on static imaging obtained following PCA, often similar to the bleeding known to occur after other renal interventions.[69] Additionally, the closed retroperitoneal space created by the percutaneous approach may provide a tamponade effect, limiting the amount of blood loss.

As more commonly seen with PCA, nerve injuries may result in either sensory or motor deficits. Such complications occur in 10% to 16% of patients, and are typically related to injury to the intercostal nerves or the nerves coursing along the psoas muscle adjacent to the tumour. [38,56]

Hematuria is not uncommon following CA, although a significant obstructing ureteral clot warranting ureteral stent placement may occur in up to 2% of patients.[35,70] Collecting system injuries resulting in urine leakage may occur and are typically self-limited, although events requiring percutaneous drainage, ureteral stenting, and nephrectomy have been reported.[42,44,56,71]

While difficult to quantify, medical events are relatively common following CA. Such events include myocardial ischemia, cardiac arrhythmia, hypertension, pulmonary edema, pneumonia, and bronchospasm. Deep venous thrombosis, pulmonary embolus, and cerebrovascular events may also occur. It has been suggested that CA may induce a hypercoagulable state, predisposing patients to such thromboembolic events.[72] Additional complications following CA include injury to adjacent viscera (bowel, diaphragm, spleen, and liver), pneumothorax, and ileus, port site hernia, and infection.

8.3.1.5 Tumour-specific treatment outcomes

Following the initial description of renal CA in 1995, the durability of the technique in the management of renal masses has been demonstrated.[73] Treatment outcomes reporting has evolved over the past 10 years, migrating from describing generalized tumour control outcomes to RCC-specific outcomes. This reflects an early practice of both inconsistent performance of biopsy prior to treatment and added emphasis to reflect feasibility and safety of the treatment, with secondary justification to include all tumour pathology when publishing one's experience. As long-term oncologic outcomes evolve, specific cancer-related outcomes become evident, allowing for more prudent validation of the technique in RCC management.

8.3.1.5.1 Limitations

When considering outcomes, some limitations should be kept in mind. It is worth noting potential variances in reporting. In particular, given the recognized triage of select patients to ablation, a preexisting history of RCC may confound assessment of oncologic outcomes. In addition to RCC-specific outcomes, the reported tumour control rates following technically unsuccessful ablation are occasionally dubious. Specifically, it is occasionally unclear whether such patients were included in the long-term outcome analysis. Cancer control rates may also be difficult to report for patients with multifocal or metachronous tumours. In contrast to some prior surgical reports including ipsilateral metachronous tumours,[74] all 45 publications considered in this review since 2006 defined local recurrence as new tumour specifically at the ablation site, based on imaging. While imaging is often used to diagnose locally recurrent tumours, one needs to consider the role of a negative result following biopsy of a suspicious finding.[70]

Within one's clinical practice, there is a selection bias that is introduced the moment a patient is triaged to a primary treatment option for a renal mass. While selection criteria are often generalized, they do specify those patients with comorbid illness or other relative contraindications to surgery. However, the feasibility of ablation is often a poorly defined impression on behalf of the operator, and based on the expectation of a favourable outcome. Specifically, some patients may be appropriately excluded from ablative treatment based on tumour size or location, thus creating a bias compared with those without such exclusion criteria or compared with other definitive treatment methods (e.g. nephrectomy). The increasing application of nephrometry scores in renal mass management will allow such selection criteria to be better appreciated.

It is also important to consider the heterogeneity of treatment techniques and operator experience in performing PCA or LCA. Breen *et al.* demonstrated a trend toward improved tumour control outcomes with longer duration of operator experience.[45] Variances in the performance of CA applicators are also recognized. Appreciating the strengths and weaknesses of such specific applicators may be a challenge, particularly, as demonstrated, with the use of a single cryoprobes.[60,75,76]

Of the 46 reviewed publications since 2006, 39 included outcomes specific to treatment efficacy or oncologic outcomes. Of these 39, 24 included tumours shown pathologically to be RCC, although only 18 reported outcomes specific to RCC, either technique success or recurrence-free survival (**Table 8-1**). Six of the 18 studies included patients treated with both LCA and PCA. Otherwise, LCA was performed in seven studies and PCA in five. Five of the studies reporting LCA outcomes included a small minority of patients treated with open CA in the outcome analysis.

TABLE 8-1 Patients and Tumour Characteristics, and Oncologic Outcomes of Cryoablation Series

Reference	Year	LCA (no. tumours)	PCA (no. tumours)	% RCC	Patients (N)	Mean patient age	
Atwell *et al.*[82]	2013	–	189	56	163	68	
Bandi *et al.*[57]	2007	68	20	55	78	68	
Beemster *et al.*[79]	2010	100	–	54	92	69	
Breen *et al.*[45]	2013	–	171	–	147	67	
Finley *et al.*[52]	2008	24 –	– 19	67	19 18	– –	
Georgiades *et al.*[46]	2014	–	134	100	134	68	
Goyal *et al.*[43]	2012	54* –	– 154	52 73	53 141	68 70	
Johnson *et al.*[67]	2014	112	–	76	92	60	
Kim *et al.*[59]	2014	167 –	– 123	52 63	145 118	69 73	
Kim *et al.*[77]	2015	68*	–	66	68	62	
Klatte *et al.*[44]	2011	41	–	85	41	75	
Larcher *et al.*[68]	2015	174	–	63	174	66	
Littrup *et al.*[70]	2007	–	49	73	48	67	
Schwartz *et al.*[53]	2006	85*	–	59	84	67	
Strom *et al.*[48]	2011	84* –	– 61	58 76	84 61	66 68	
Yoost *et al.*[84]	2010	47	–	58	45	68	

Abbreviations: CSS: cancer-specific survival; DFS: disease-free survival; f/u: follow-up; LCA: laparoscopic cryoablation; PCA: percutaneous cryoablation; OS: overall survival; RCC: renal cell carcinoma; RFS: recurrence-free survival.
*Small number of open cryoablations included in published experience.

continued on **page 535**

TABLE 8-1 Patients and Tumour Characteristics, and Oncologic Outcomes of Cryoablation Series, *Cont'd*

	Mean/ median size	Size details	Mean/ median f/u (yr)	RFS, % all tumours	RFS, % RCC	DFS, %	CSS, %	OS, %
	2.3	≤3 cm	1.8	95.6 (at 5 yr)	90.6 (at 3 yr)	–	–	–
	2.6	LCA: 2.7; PCA: 2.2	1.6	98.7	100	–	100	88.5
	2.5	–	–	94 (at 3 yr)	92 (at 3 yr)	100	100	90 (at 3 yr)
	3.3	T1a: 48; T1b: 14	1.7	99.2	98.4	–	–	–
	3.0 2.7	– –	1.1	95.8 94.7	96.6	–	–	–
	2.8	T1a: 115; T1b: 19	–	97.0 (at 5 yr)	97.0 (at 5 yr)	–	100	97.8
	2.1 2.4	– –	3.7 3.0	94.4 98.0	85.2 (at 5 yr) 95.6 (at 5 yr)	– –	100 98 (5 yr)	78.8 (at 5 yr) 77.7 (at 5 yr)
	2.3	–	–	–	86.5 (at 10 yr)	–	98.2 (at 10 yr)	70.7 (at 10 yr)
	2.4 2.7	20% ≥3 cm; 34% ≥3 cm	5.9 3.2	85.5 (at 5 yr); 86.3 (at 5 yr)	84.3 (at 5 yr)	–	98.8 (at 5 yr)	98.8 (at 5 yr)
	2.3	0.3–5.7	5.0	83	84.6	–	–	100
	2.5	all T1a	2.8	–	83 (at 3 yr)	–	100	–
	2.0	T1a	–	97.1	95 (at 10 yr)	81 (at 10 yr)	100	61 (at 10 yr)
	3.3	1.7–7.2	1.1	93.8	91.7	–	–	–
	2.6	≤5.0 cm	0.8	98.2	100	–	–	–
	2.5 2.7	T1b: 4 (4.8%); T1b: 6 (9.1%)	3.5 2.6	94.0 83.6	89.8 82.6	91.7 93.7	– –	89.3 88.9
	2.7	1.2–5.4	1.1	83.0	87	–	–	–

Abbreviations: CSS: cancer-specific survival; DFS: disease-free survival; f/u: follow-up; LCA: laparoscopic cryoablation; PCA: percutaneous cryoablation; OS: overall survival; RCC: renal cell carcinoma; RFS: recurrence-free survival.
*Small number of open cryoablations included in published experience.

When one considers the available sum experiences reflected in **Table 8-1** and the outcomes specific to RCC, a total of 740 of 791 (94%) RCCs were effectively controlled using either LCA or PCA, although there is considerable variation in the duration of mean follow-up among patients as a whole, ranging from 0.8 to 5.0 years.[53,77] Longer-term follow-up is reflected in recurrence-free survival (RFS), where 3-year, 5-year, and 10-year RFS rates range from 83% to 96%, 84% to 97%, and 87% to 95%, respectively.

As one might expect, patients with SRMs treated with ablation have favourable cancer-specific survival (CSS) rates, although such outcomes are complicated by those patients with prior history of RCC. Published experience reports CSS rates ranging from 98% to 100%. Including a clearly defined cohort of 116 patients with isolated, sporadic RCC, Schmit *et al.* demonstrated 100% CSS at 3 years.[78] Overall survival (OS) rates are less favourable, likely reflecting the selection bias toward those patients with advanced medical comorbidities.[74]

Disease-free survival (DFS) has been more difficult to elucidate, perhaps, in part, due to the inclusion of patients with prior RCC in the outcome analysis. Published DFS rates following CA range from 81% to 100%.[65,66,68,79]

When one considers the ablation of renal masses as a whole, important observations can be made that will help shape patient/tumour triage processes in the future. As previously stated, it is technically feasible to treat larger renal masses using CA. While the treatment of such tumours carries added procedural risk, the oncologic outcomes may remain favourable compared with other treatment alternatives. In one study detailing the treatment of 46 patients with cT1b RCC, imaging follow-up showed a 3-year RFS rate of 96%.[31] For the treatment of tumours measuring up to 6.5 cm in diameter, Blute *et al.* showed that size was not associated with tumour recurrence.[63] Following PCA of 38 tumours measuring 1.2 to 7.0 cm, Spreafico *et al.* reported only two treatment failures in tumours measuring 2.8 cm and 3.0 cm.[66] This finding led the authors to suspect that a learning curve, rather than tumour size, may be a limiting factor in achieving treatment success.[66]

Others have reported less than favourable outcomes with CA of larger tumours. With CA of 26 tumours, using conscious sedation, Derweesh *et al.* found local recurrence in three (11.5%), all measuring over 4 cm in size.[58] Local recurrence also developed in all four patients with T1b RCC treated with LCA in the Kim *et al.* series.[77]

While heat-based thermal ablation may have limitations in the management of central/endophytic renal masses due to thermal sink effects,[80,81] such tumours may be successfully treated with aggressive CA.[45,50,82] In one study comparing PCA with RFA of renal masses measuring 3 cm or smaller, central location was not associated with PCA failure.[82] Similarly, Breen *et al.* found no association between local recurrence and central tumour location following PCA.[45]

Others have demonstrated potential limitations in successful CA of centrally located renal masses.[49,58,83,84] In the treatment of 47 tumours with LCA, Yoost *et al.* showed a treatment success rate of only 53% for tumours with broad-based interface with the renal sinus, compared with 97% for

tumours without such contact.[84] Wright *et al.* also demonstrated considerable difficulty with successful LCA of centrally located renal masses, suggesting that there may be technical limitations with intraoperative ultrasound (US) in the treatment such tumours.[49]

8.3.1.6 Renal functional outcomes

Published studies detailing renal functional outcomes following both LCA and PCA show little, if any, change in renal function following treatment. Beemster *et al.* found a mean decrease of 7 mL/min/1.73 m^2 in estimated glomerular filtration rate (eGFR) following LCA.[79] This was felt to be of questionable significance in a patient population where most patients presented with a preoperative eGFR ≥60 mL/min/1.73 m^2. In this group, 15% of patients progressed to moderate chronic kidney disease (CKD), and of those with preexisting moderate CKD, only 13% progressed to severe CKD.

In a comparison study including patients with solitary kidneys undergoing minimally invasive nephron-sparing surgery, a significantly greater drop in eGFR was seen following laparoscopic partial nephrectomy (LPN) compared with CA at 6 months.[85] Tanagho *et al.* also demonstrated the advantage of CA (both LCA and PCA) in the preservation of renal function compared with robotic partial nephrectomy (RPN), with a 6% decrease at last follow-up in patients treated with ablation compared with 13% in those treated with RPN.[86]

In comparing LCA with PCA, both Derweesh *et al.* and Kim *et al.* have shown no significant difference in renal function changes.[58,83]

8.3.1.7 Conclusion

Cryoablation has been shown to be an effective treatment option in select patients with SRMs. Selection criteria for triage to nephron-sparing tumour management strategies preclude formal comparison and will make future randomized studies difficult. Nevertheless, CA warrants consideration in renal mass treatment algorithms. **(LOE 2c, Grade of Recommendation [GOR] B)**

8.3.2 Radiofrequency ablation

8.3.2.1 Technology and mechanism of action

Radiofrequency ablation involves the delivery of alternating currents between 375 and 500 kHz to a target tissue. Heating occurs when the tissue surrounding the probe impedes the electric current, which results in a transfer of heat energy.[87,88] Two basic systems are available for the delivery of radiofrequency (RF) energy: the temperature-based system and the impedance-based system. Temperature-based systems determine the treatment endpoint by monitoring the temperature of the probe and terminate the procedure once a set temperature is reached. A target temperature of 60°C is often cited as adequate to achieve cell death, although higher temperatures are often used.[89] Impedance-based systems determine the treatment endpoint by monitoring the tissue impedance to the RF current. Impedance is measured in ohms (Ω), in accordance with Ohm's law, and increases as the tissue desiccates. Radiofrequency current can be delivered via monopolar or bipolar probes. When monopolar probes are used, the current flows through the probe, into the patient, and then to a grounding pad. The grounding pad is generally placed on the thighs or back, and away from metal implants to eliminate internal heating. Monopolar probes are used to a much greater extent than bipolar probes.

Several devices are commonly used to perform RFA. The StarBurst® Radiofrequency Ablation System (AngioDynamics, New York, United States) for radiofrequency interstitial tissue ablation (RITA) is a temperature feedback–based system. The probe averages the temperature of the tines deployed, and once a preset temperature is reached, the generator maintains the RF current for a specified duration, which is largely dependent on the tumour size. Multiple treatment algorithms have been published for temperature-based systems.[90-92] The Cool-tip™ RF ablation system (Covidien, Dublin, Ireland [Covidien was acquired by Medtronic in 2015]) is an impedance-based system that emits up to 200 W at 480 Hz. Current is emitted from the probes until the surrounding tissue reaches 30 Ω above baseline. The power is then briefly switched off, or if using multiple probes, transferred to another probe. This is repeated throughout the duration of the treatment cycle. Multiple treatment techniques have also been reported using the Cool-tip system.[93-95] The RF3000™ system (Boston Scientific, Minnesota, United States) is an impedance-based system that uses tines deployed in an umbrella-shaped pattern. In this system, the power is steadily increased until there is a loss of current due to the surrounding tissue impedance. To date, there is no evidence to suggest one type of ablation system is superior to another. In a study pooling 27 series, Modabber *et al.* showed clinical efficacy was similar for both temperature- and impedance-based systems (91.0% for temperature-based RFA systems vs. 91.5 % for impedance-based RFA systems; p=0.73).[96]

8.3.2.2 Technique and approach

Radiofrequency ablation of renal tumours can be performed either percutaneously using CT guidance or laparoscopically using US guidance. This section will focus on percutaneous RFA (PRFA). Although many of the studies reported combined laparoscopic radiofrequency ablation (LRFA) and PRFA,[90,97-99] attempts were made to separate the results. However, this is likely not critical, as several studies have demonstrated no differences between PRFA and LRFA in terms of oncologic outcomes.[98,100] A more in-depth discussion on imaging modalities used for targeting renal tumours (CT, MRI, and US) will be discussed in subsequent sections.

Radiofrequency ablation has been reported to be successful when performed under both general anesthesia and conscious sedation. There are no reported series directly comparing the outcomes between anesthesia types, although there are theoretical advantages to each. General anesthesia allows for more precise respiratory control, which may lead to more accurate probe placement and greater ablation success.[101] General anesthesia may also allow for greater patient tolerance and a higher chance of completing the planned procedure.[101] Conscious or intravenous sedation allows for RFA to be performed as an outpatient procedure, and has been used successfully at several institutions.[102,103] Intravenous sedation in PRFA has further been shown to be effective in patients who are at high surgical risk, and who may not otherwise tolerate general anesthesia.[104]

8.3.2.3 Procedural and perioperative outcomes

Radiofrequency ablation success is often defined as lack of enhancement in a targeted region based on contrast-enhanced imaging, most commonly CT scan and less commonly contrast-enhanced MRI. Published series have typically used 10 to 20 Hounsfield units (HU) as the upper limit of acceptable enhancement in the targeted region for RFA to be considered successful. Other studies have used only the subjective finding of enhancement.[74,93,98,105] Still, several studies include lack of tumour involution or tumour growth in their definition of failure.[99] When using MRI, most series report any enhancement in the targeted region as a failure, although several studies have reported an objective

15% increase in enhancement as a failure.[93,94] Weight *et al.* questioned the use of enhancement as a surrogate for RFA success by performing post-RFA biopsies. In this study, 6 of 25 patients (24%) without evidence of enhancement demonstrated viable tumour at 6 months. The study concluded that there is a poor correlation between post-RFA radiographic findings and biopsy results.[106] Another study reported that post-RFA biopsies of targeted tumours failed to involute, but did demonstrate enhancement. Of the 43 tumours biopsied, 5 were positive, 3 of these in non-enhancing regions of ablation.[99] Conversely, Raman *et al.* demonstrated the absence of viable tumour by performing biopsies of non-enhancing areas 1 year after RFA (n=20 tumours). They showed no viable tumour in any biopsy specimen. The authors maintained that the tissue architecture continues to change up to 6 months post-RFA, and cell viability should not be assessed by biopsy earlier.[107] Currently, there is not a consistently used definition of RFA success, and there remain conflicting studies regarding the correlation between post-RFA radiographic findings and tumour viability. Therefore, the need for a consistent definition of RFA success remains.

Technical success refers to the initial success of RFA treatment at the time of the first imaging follow-up (typically 4 weeks to 3 months). This is often reported based on the enhancement patterns on cross-sectional imaging and is rarely confirmed by biopsy. Early in the RFA experience, studies reported technical success based on two or three RFA attempts.[103] The practice has been replaced by a more strict definition, allowing for only a single RFA attempt. In reported series, technical success after one RFA attempt ranged from 87% to 99.6%.[90,95,105,108,109] It must be noted that these studies were heterogeneous, specifically in terms of average tumour size (1.9–3.0 cm), with several studies identifying different size cut-offs that stratify RFA success. Best *et al.* showed a significant difference in technical success for tumours less than 3 cm compared with tumours 3 cm or greater (96.6% vs. 80%, respectively).[90] Atwell *et al.* reported their technical success for all tumours less than 3 cm to be 99.6%, with an average tumour size of 1.9 cm.[82] Using the TNM staging system, Pstuka *et al.* also showed that technical success was dependent on size, with 94.6% of T1a and 80.9% of T1b tumours successfully treated.[105] Finally, Zagoria *et al.* reported no technical failures for tumours less than 3.5 cm, noting those that failed ablation had a median size of 5.2 cm.[93] Tumour location has also been examined as a factor influencing technical success. Gervais *et al.* showed on multivariate analysis that both small size (p<0.001) and non-central location (p=0.005) were independent predictors of success after the first ablation.[103] Gahan *et al.* examined the use of the R.E.N.A.L. nephrometry score in predicting RFA success. They found that the combined location components of the R.E.N.A.L. score (endophytic properties of the tumour, nearness to sinus, and the location relative to the polar lines) correlated significantly with technical success (p=0.033).[110]

8.3.2.4 Complications

Identifying factors contributing to complications following RFA is difficult, as a standardized classification system has not been consistently used throughout the ablation literature. The two systems most commonly used are the Clavien-Dindo classification to objectively report surgical complications, and the Society of International Radiology criteria, a standardized way to classify complications after radiographic procedures.[35,111] Although several studies report complications based on these systems,[34,108,112,113] the majority of studies either do not address complications or report them in a non-standardized manner. **Table 8-2** shows RFA series reporting complications based on the Clavien-Dindo classification or those describing the complications in detail. The rate of overall complications in RFA is generally low, ranging from 7% to 13.1%, with the majority of complications

described as minor (Clavien-Dindo grade <III).[34,98,112,113] The most common minor complication reported was nerve injury or pain, seen in up to 3.9% of patients (**Table 8-2**).[34,114] The vast majority of nerve injuries reported were self-limited.[34,114] Other minor complications are described, but these occurred sporadically and in small numbers.

TABLE 8-2 Selected RFA Series Reporting the Two Most Common Major and Minor Complications

Reference	Year	N	Overall	Minor complications (Clavien <III)	Most common minor complications	Major complications (Clavien ≥III)	Most common major complications
Johnson *et al.*[114]	2004	133	8.3%	6.0%	Nerve injury: 3.0%; pneumonia: 0.7%	2.3%	Urinary tract: 1.5%; death: 0.4%
Gervais *et al.*[103]	2005	85	10.6%	5.9%	Hemorrhage: 3.5%; nerve injury: 1.2%	4.8%	Hemorrhage: 2.4%; urinary tract: 2.4%
Atwell *et al.*[82]	2012	254	9.8%	Grade I: 5.1%; grade II: 1.2%	Nerve injury: 3.9%	Grade III: 3.5%; grade IV: 0%	Urinary tract: 2.4%; hemorrhage: 0.8%
Leveillee *et al.*[95]	2013	274	27.3%	Grade I: 26.2%; grade II: 5.8%	NR	Grade III: 3.3%; grade IV: 1.5%	NR
Seideman *et al.*[112]	2013	199	7.0%	Grade I–II: 5.0%	NR	Grade III: 2.0%; grade IV: 3–4%	Hemorrhage: 1.0%; pneumothorax: 0.5%
Chang *et al.*[97]	2014	170	12.4%	Grade I–II: 8.8%	Nerve injury: 2.9%; fever: 2.4%	Grade III: 3.6%; grade IV: 0%	Urinary tract: 2.9%; hemorrhage: 0.6%
Lorber *et al.*[98]	2014	53	26.4%	Grade I: 18.9%; grade II: 7.5%	NR	0%	NR
Wah *et al.*[108]	2014	165	13.9%	7.3%	Nerve injury: 3.0%; hemorrhage: 2.4%	6.7%	Urinary tract: 3.5%; abscess: 1.2%

Abbreviation: NR: not reported.
Urinary tract injury includes ureteral stricture (and ureteropelvic junction obstruction), urine leak, or urinoma.
Nerve injury includes sensory deficits (pain or paresthesia) or flank laxity.

Major complications (Clavien-Dindo classification ≥III) following RFA are reported in up to 6.7% of patients. Of the major complications, injury to the urinary system (ureteral stricture or leak) and significant hemorrhage were the most common, occurring in up to 2.9% and 3.5% of patients, respectively. In an attempt to mitigate urinary system injuries, retrograde cold perfusion has been used during ablation of tumours near the ureter or collecting system.[108,115] Wah *et al.* found this technique effective, although strictures still developed when the tumour was within 1 cm of the ureter.[108] Hydrodissection has also been shown to be effective in minimizing RFA-associated complications. Several studies report being able to achieve more than 1 cm of separation from critical structures (colon), ensuring safe ablation.[103,116] Leveillee *et al.* reported safe and effective treatment of tumours less than 5 mm from the collecting system could be performed using real-time temperature monitoring. However, this study did not report specific complications in higher-risk tumours.[95] It should be noted that several series state that major complications occurred early in their experience (specifically urinary system injuries), altering patient selection. In a study by Johnson *et al,* greater than 50% of the complications occurred in the first one-third of patients treated.[114]

In the largest series looking at factors contributing to complications, Atwell *et al.* showed that increased size and central location were associated with complication grade ($p<0.01$); however, this series combined both CA and PRFA, thus limiting conclusions specific to PRFA.[82] Chang *et al.* showed that RFA complications correlate with tumour complexity based on the R.E.N.A.L. nephrometry score, with all patients in the highest complexity tertile experiencing some form of complication, although LRFA was the only modality used.[113] A recent study in which PRFA was the primary modality (85%) did not find the R.E.N.A.L. score to be predictive of RFA complications.[112] In this study, complications did not correlate to tumour size or any of the individual components of the R.E.N.A.L. score. It is not clear whether the R.E.N.A.L. score has a role in predicting PRFA complications, as it was originally designed to assess tumours undergoing extirpative treatment.[117] Overall, RFA has been demonstrated to be safe, having a low rate of complications, with the majority of these being reported as minor. Limited conclusions can be drawn concerning factors contributing to RFA complications due to significant selection bias in many series and non-standardized reporting. However, it is generally accepted that tumours in close proximity to the ureter or collecting system pose a greater risk, and advanced PRFA techniques or treatment modalities other than PRFA may be reserved for these tumours.

8.3.2.5 Tumour-specific outcomes

Radiofrequency ablation oncologic outcomes are now being reported using standard oncologic measures. These include RFS, metastasis-free survival (MFS), DFS, CSS, and OS. **Table 8-3** shows the oncologic outcomes for select RFA series. Of note, all series are retrospective case series and demonstrate significant heterogeneity in terms of patient and tumour characteristics.

TABLE 8-3 Selected RFA Series Showing Tumour Characteristics and Oncologic Outcomes

Reference	N*	Approach (no. tumours)	Size (cm)	Follow-up (months)	RCC, %	Definition of recurrence	Technical success, %	DFS, %	CSS, %	OS, %
McDougal *et al.*[119]	23	PRFA	3.1	55	87	>10–15 HU	69	NR	100 (5 yr)	55 (5 yr)
Tracy *et al.*[109]	208	PRFA: 172; LRFA: 68	2.4	27	79	Subjective	97	NR	99	NR
Best *et al.*[90]	159	PRFA: 102; LRFA: 57	2.4	62	72	>10 HU	95	91 (5 yr)	98 (5 yr)	75 (5 yr)
Pstuka *et al.*[105]	185	PRFA	3.0	77.2	97	10–15 HU	87	88 (5 yr)	>99 (5 yr)	73 (5 yr)
Leveillee *et al.*[95]	274	PRFA: 174; LRFA: 112	2.5	26	67	>20 HU	96	NR	99 (5 yr)	74 (5 yr)
Atwell *et al.*[82]	222	PRFA	1.9	34.8	54	>20 HU	>99	93 (5 yr)	NR	NR

Abbreviations: DFS: disease-free survival; CSS: cancer-specific survival; HU: Hounsfield units; LRFA: laparoscopic radiofrequency ablation; NR: not reported; OS: overall survival; PRFA: percutaneous radiofrequency ablation.
*Number of patients undergoing ablation.

continued on **page 542**

TABLE 8-3 Selected RFA Series Showing Tumour Characteristics and Oncologic Outcomes, *Cont'd*

Reference	N*	Approach (no. tumours)	Size (cm)	Follow-up (months)	RCC, %	Definition of recurrence	Technical success, %	DFS, %	CSS, %	OS, %
Wah *et al.*[108]	200	PRFA	2.9	46.1	92	>20 HU	96	94 (5 yr)	98 (5 yr)	76 (5 yr)
Thompson *et al.*[74]	180	PRFA	2.1	34.8	41	Subjective	NR	98 (3 yr)	NR	82 (3 yr)
Lorber *et al.*[98]	53	PRFA: 29; LRFA: 24	2.3	65.6	100	>20 HU	NR	91 (10 yr)	100 (10 yr)	93 (10 yr)
Chang *et al.*[97]	45	PRFA: 9; LRFA: 36	3.0	66	98	>10 HU	NR	87 (5 yr)	96 (5 yr)	90 (5 yr)

Abbreviations: DFS: disease-free survival; CSS: cancer-specific survival; HU: Hounsfield units; LRFA: laparoscopic radiofrequency ablation; NR: not reported; OS: overall survival; PRFA: percutaneous radiofrequency ablation.
*Number of patients undergoing ablation.

Recurrence-free survival was defined as the proportion of patients without local disease recurrence, and included technical failures along with local recurrences. The estimated 5-year RFS in the reported series ranged from 92% to 95%.[98,100,105,109] Disease-free survival was also reported (in some cases in place of RFS), and included local as well as distant recurrences. The estimated 5-year DFS ranged from 87% to 94%.[82,90,94,105,108] These series also included a heterogeneous patient and tumour population. As with technical success, RFS and DFS were shown to be dependent on tumour size. As multiple series have demonstrated, larger tumours are more likely to recur, even after achieving complete ablation.[82,90,93] Pstuka *et al.* showed local recurrence following successful ablation was significantly less in T1a tumours compared to T1b tumours (4.2% vs. 14.4%, respectively; p=0.020).[105] Gahan *et al.* examined the role of the R.E.N.A.L. score in predicting RFS. They found that when the R variable was modified to include a 3-cm cutoff, rather than a 4-cm cutoff, the R.E.N.A.L. score was predictive of RFS based on tertile stratification (p=0.003). This suggests that tumour size is the primary predictor of RFS, with tumour location being less important.[110] Atwell *et al.* reported a somewhat different result, showing tumour location was more significant. This study noted the 3-year RFS for central tumours was 77.9% compared to 97.8% for exophytic tumours.[82] It has been theorized that tumour histology (as a surrogate for tumour biology) may have a role in RFA outcomes. In a study involving two institutions, Lay *et al.* demonstrated that patients with clear cell RCC are more likely to develop local disease recurrence compared to patients with papillary RCC, independent of tumour size (89.7% vs. 100% for 5-year DFS, respectively; p=0.04).[118] This study suggests the vascular nature of clear cell tumours makes clear cell RCC more susceptible to recurrence following RFA.

A standardized reporting system for tumour location is not yet widely used. As such, there are inconsistent and conflicting data as to the effect of tumour location on RFA outcomes. There are also limited data to support that tumour subtype is a factor in RFA outcomes, and more studies are needed before drawing any conclusions. However, there are now a significant number of well-performed case

series with sufficient follow-up, which means that RFA can be recommended as a treatment option for small renal tumours. Given the higher rate of technical failures and local recurrence in larger tumours, RFA is best reserved for tumours less than 3 cm (grade C).

The number of metastases occurring in any single series is small, ranging from 0.4% to 2% of patients.[61,74,82,95,97,98,105,118] This finding remains consistent when evaluating series with longer follow-up (65–77 months), with the majority of metastases reported in the first 3 years.[98,105] The low incidence of metastasis limits the ability to assess risk factors associated with the development of systemic disease in the post-RFA setting. Cancer-specific survival following RFA is high, ranging from 94% to 100%, and is a reflection of the low rates of metastasis observed.[74,95,97,98,105,108] Overall survival varies significantly across series, ranging from 63% to 93%.[74,95,97,98,100,105,108] This is likely related to the age and comorbidities of the treated population. Lorber *et al.*[98] reported an average CCI score of 3.8, with an OS of 98%, while Psutka *et al.*[105] reported an average CCI score of 5, with an OS of 64%. Thompson *et al,* on multivariate analysis comparing RFA and PN, found the only significant factors predicting patient death were CCI score and age ($p<0.001$), not treatment approach ($p=0.08$).[74] There are significant differences in average age and degree of comorbidities across published case series, in addition to inconsistent use of an objective reporting system for comorbidities. Therefore, a comparison of OS rates between RFA series or other treatment modalities is often not possible.

When considering RFA failures, the majority of RFA recurrences occur locally and relatively soon after treatment.[119] Atwell *et al.* showed overall that 3.2% of patients experienced recurrence, with a median time to recurrence of 2.8 years.[82] Tracy *et al.* reported nine recurrences, all occurring within 3 years of ablation.[109]

In general, the majority of local recurrences happen within 3 years of ablation, although there are long-term failures. For those patients who experience recurrence, options include repeat ablation (RFA or CA), extirpative treatment (radical or PN) or, AS. In a pooled analysis of seven institutions, 63 patients were identified who experienced technical failure or recurrence after ablation.[120] The majority (59%) underwent repeat ablation, with 37 (80.4%) of those patients having successful treatment. This study was limited in that it included CA failures, although this represented a minority (6.2%) of the population. Lorber *et al.* reported four local recurrences in their series of 53 patients.[98] Three patients were treated with repeat ablation (PRFA or LRFA) and one with radical nephrectomy. All patients remained recurrence-free after salvage treatment. Nguyen *et al.* analyzed 22 patients undergoing salvage treatment after PRFA. Four patients progressed, needing radical or PN. Specifically, they reported no significant increased difficulty of the extirpative procedures following RFA, although the numbers were small, and conclusions were based on operative reports and lack of complications.[121] In a series of healthy patients, Ma *et al.* reported three failures (5.8%).[100] All patients underwent repeat ablation; however, all progressed to radical nephrectomy as repeat ablation was not successful. Although more aggressive treatment was likely pursued given the young and healthy patient population, this is not explicitly stated. As detailed here, there is significant variation in the number of patients undergoing repeat ablation and extirpative therapy, thus limiting any general conclusions regarding treatment of RFA failures.

8.3.2.6 Functional outcomes

The majority of studies report minimal or no impairment in renal function following RFA.[108,122-124] The best evidence for this comes from several studies examining renal functional outcomes in a solitary kidney population.[121,123,124] In a multi-institutional study, Raman *et al.* (*n*=47) showed that 92.9% of patients experienced no decline of renal function at 3 months, with 89.6% maintaining renal function at greater than 12 months.[125] Krokidis *et al.* (*n*=23) showed no significant change from baseline renal function (eGFR: 47.0 mL/min/1.73 m^2) compared with renal function at 3 months (eGFR: 38.0 mL/min/1.73 m^2) or at 1 year (eGFR: 41.0 mL/min/1.73 m^2).[122] Similarly, Pieper *et al.* (*n*=38) reported no patients with an eGFR >60 had a significant decline in renal function, and that patients with an eGFR <60 had a minimal decline in renal function (mean decline: 1.68 mL/min/1.73 m^2).[124] Wah *et al,* in contrast, reported a mean decrease in eGFR of 3.1%, which was significantly different from pre-RFA measurements ($p<0.001$), although only four (2.4%) patients had a decline in eGFR >25%.[108] Maintenance of parenchymal volume has recently been shown to be an independent predictor of renal function following nephron-sparing treatment.[126] Woldu *et al.* showed PRFA resulted in favourable parenchymal preservation. They also showed that, on average, 92.4% of the parenchymal volume was preserved, which was significantly higher than extirpative techniques.[127] Based on a number of case series, renal function appears to be minimally impacted following RFA, and is thus considered a favourable nephron-sparing approach for the treatment of SRMs.

8.3.2.7 Patient selection

The average patient age in RFA series ranges from roughly 55 to 75 years, with the majority of series reporting an average age >65 years. Overall patient health using objective measures, such as CCI score or American Society of Anesthesiologists (ASA) score, is infrequently reported, although most series state that the treated patient population was unfit for surgery or was in relatively poor health.[108] The few series that did utilize objective measures reported significant morbidity, with CCI scores ranging from 2.1 to 5.[74,98,105] In contrast, several recent studies have published results with younger and healthier patients. A study by Ma *et al.* examined long-term RFA oncologic outcomes in a healthy patient population (ASA: 1 or 2; mean age: 57).[100] This study demonstrated an estimated 10-year RFS of 94.2%, with no patients developing metastases or dying of RCC (MFS and CSS: 100%). Chang *et al.* also reported favourable RFA outcomes in a younger patient population (mean age: 52.9).[113] In this study, 5-year RFS and CSS were 86.7% and 95.6%, respectively. This study was limited by sample size (*n*=44), and did not report patient comorbidities, but did show durable oncologic outcomes over a median follow-up of 66 months.

There remain limited data demonstrating durable RFA outcomes in younger or healthy patients. The majority of case series represent an older and unhealthy patient population. Therefore, RFA remains preferentially reserved for patients who are older or have significant comorbidities. **[GOR C]**

8.3.2.8 Conclusion

There are now a sufficient number of larger series with sufficient follow-up to support RFA as a safe and effective treatment option for SRMs, with optimal results for tumours up to 3 cm. The patient population best suited for RFA is older and with significant comorbidities, although newer studies are questioning this doctrine. Going forwards, new publications should make every effort to report data in a standardized manner, using accepted definitions for oncologic outcomes, complications, and comorbidities. **[LOE 2c; GOR B]**

8.3.3 Targeting the lesion

Compared with other urologic tumours (e.g. prostate), kidney tumours are amendable to cross-sectional imaging (CT/MRI). Focal therapy requires exact planning with high-quality imaging preoperatively, and transferring of obtained data to the intraoperative setting for targeting and navigation. However, the intraoperative application of imaging in soft tissue surgery is limited because of considerable organ shift and tissue deformation caused by breathing, heartbeat, patient movement, and manipulation by the surgeon. Systems currently available are not able to predict organ motion, which reduces the predictive value of the preoperative imaging data.

The problem of "targeting the lesion" during any procedure is being approached with different intraoperative imaging devices, such as US, fluoroscopy, CT, or MRI.[128] Intraoperative US is widely used for laparoscopic surgery as well as for percutaneous approaches due to its real-time imaging and easy use. Furthermore, it is a noninvasive and inexpensive procedure. However, these benefits come at the cost of low image quality and validity. To enhance the image quality of US, different developments have been made, including contrast-enhanced ultrasound (CEUS) and fusion of US with cross-sectional imaging.[129] Fluoroscopy is also a commonly used method of intraoperative imaging. Especially in urology, we experience difficulties in accessing the kidney in our daily work.[130] Based on their success in vascular and cardiac surgery, intraoperative CT systems are also becoming a focus of urology. The *syngo* DynaCT (Siemens Healthcare, Erlangen, Germany), for example, is an isocentric C-arm system, equipped with a large, flat-panel detector for intraoperative imaging. It has the ability to acquire a small three-dimensional (3D) volume in cone-beam CT image quality within 32 seconds by rotating around the patient. It, therefore, enables the surgeon to visualize the entire abdominal area at the current position of the patient. Apart from these commonly used methods, some efforts have been made to integrate open MRI intraoperatively, which showed successful image guidance with near real-time magnetic resonance (MR) images and 3D visualization in some experimental settings. However, due to cost and time, standardized integration in clinical settings has not been achieved yet.[129]

8.3.3.1 Ultrasound

Ultrasound imaging features low costs and high availability. It is easy and quick to apply, acquires images in real-time, and does not expose the patient or physician to radiation.[131] However, correct interpretation of US images is not trivial, especially when image quality is low. Furthermore, some lesions are not visible at all on US images because their echogenicity is similar to that of the surrounding tissue.

To address these issues, US imaging can be enhanced using preoperative data of higher quality. Referred to as *fusion imaging* or *real-time virtual sonography (RVS)*, this technique involves the fusion of real-time US and preoperative CT or MR images, as illustrated in **Figure 8-1**. Fusion of the images is often achieved by localizing the US probe in 3D space (*tracking*) and transferring the preoperative image to the tracking space (*registration*). Most commercial US systems that feature image fusion are based on electromagnetic (EM) tracking.[132] With EM tracking, no line of sight is required to localize the US probe, which is beneficial for integration of such systems into clinical workflows. However, an awareness of the lack of robustness against sources of distortion is necessary, as EM tracking accuracy can be compromised by magnetic field distortion due to nearby medical diagnostic devices

or other ferromagnetic objects.[133] Image registration can be achieved manually, by using tracked markers attached to the patient, or by selecting anatomical landmarks such as vessel bifurcations in both images. In practice, the registration procedure is sometimes separated into two steps: (1) rough registration (e.g. performed with external markers) and (2) fine-tuning adjustment (e.g. based on anatomical landmarks).[134] Robust automatic approaches for image registration are a subject of ongoing research.[135,136]

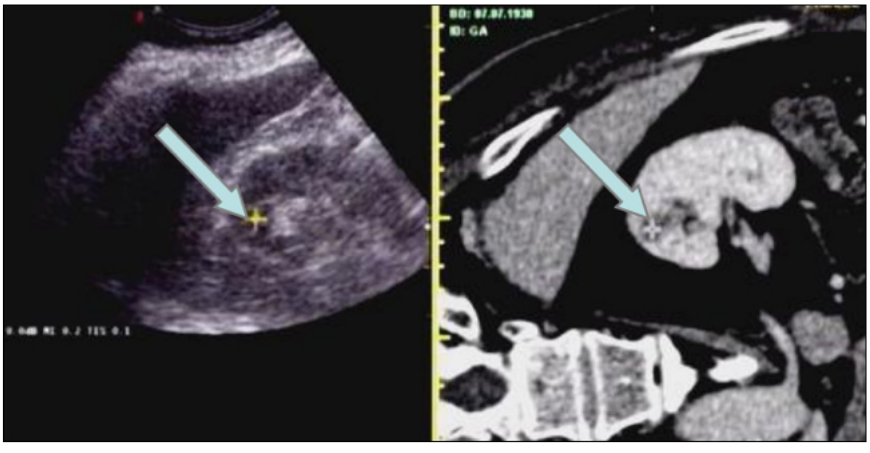

FIGURE 8-1
Fusion Imaging of a Renal Cyst

Real-time US data (left) is fused with preoperative CT data (right). The image was taken with an Esaote Virtual Navigator US machine.

Ultrasound fusion can be used for not only noninvasive diagnosis, but also invasive procedures. For example, using a conventional needle guide allows for accurate needle placement during percutaneous interventions. This includes targeting of lesions during renal CA[137] and RFA.[138–140]

Technically, tracked US, as used in US fusion, requires accurate calibration of the tracking system and US probe. Such calibration methods have been the focus of research for many years.[141,142] However, commercial tracked US systems are usually calibrated by the manufacturer. With a tracking system available, several other methods of computer assistance are enabled in addition to image fusion. By taking advantage of a tracked two dimensional (2D) US probe, a 3D US image can be acquired.[141] In addition, it is possible to localize instruments in 3D space, which allows for performing enhanced 3D navigation techniques. This includes path projections from a needle to the US plane, making needle guides obsolete and allowing for out-of-plane needle trajectories.[143–145]

With tracked US, new technical components, such as the EM field generator and EM sensors, have been introduced that have to be placed near to the patient. This results in higher complexity procedures, and can possibly hamper integration of such systems into clinical routine. To address this issue, new concepts to integrate tracking systems with US probes into a single combined device were proposed recently. It was shown that it is possible to integrate EM field generators[145] as well as optical tracking systems[146] with US probes, thus simplifying the setup of tracked US systems. However, these systems have not yet been used for image fusion.

8.3.3.2 Computed tomography

In contrast to US, CT imaging features high image quality and is less operator dependent.[131] For some lesions that are difficult to see on US (e.g. due to the patient's body habitus or intervening structures, such as air or bone), CT guidance might be preferable for accurate targeting. However, many CT scans are only taken for diagnostic purposes, before the actual intervention. As mentioned previously, the intraoperative application of these images in soft tissue surgery is limited because organ shift and tissue deformation are usually not taken into account, and may lead to a high localization error of the lesion that needs to be targeted.

To enable accurate conventional CT guidance, minimally invasive interventions such as percutaneous needle insertions are performed in an interventional CT suite.[147] Here, CT is used during the intervention to provide updated images whenever required. For CT guidance in more complex intraoperative settings, the patient is sometimes transferred from the CT suite to the operating room, which is time-consuming and bears several risks to the patient. Intraoperative CT scanners, such as C-arms, enable the acquisition of CT images inside the operating room during an intervention.

A robotic C-arm features extended options for targeting a lesion under CT guidance in the intraoperative setting.[148] The *syngo* DynaCT is such a device and is available from Siemens Healthcare (Erlangen, Germany). The C-arm can be moved automatically by a robotic arm, and is able to acquire 3D cone-beam CT scans and 2D real-time fluoroscopic images by means of a flat-panel detector.[149] As the position of the C-arm in relation to the patient stretcher is always determined by the angles of the robotic arm's joints, 3D-CT data can be merged with fluoroscopic 2D images automatically. An insertion trajectory planned on the 3D data set can then be visualized as overlay in the 2D fluoroscopic image and used to insert a needle under fluoroscopic control. In addition, a laser system is integrated into the device to mark a planned insertion point on the patient's body and to align the needle to the correct angle, as shown in **Figure 8-2**.

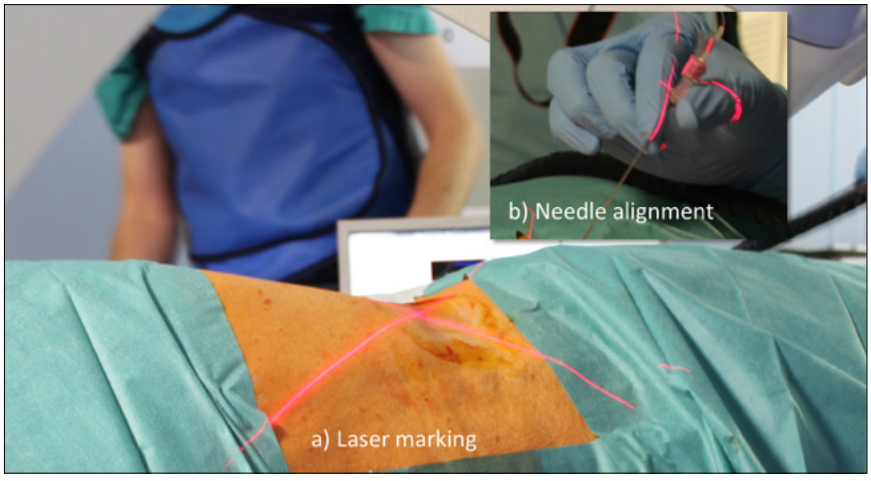

FIGURE 8-2
Targeting a Lesion with the Laser Marking of a Robotic C-arm System

Figure provided by Dr. Dogu Teber, University of Heidelberg, Heidelberg, Germany.

A common application of this principle in urology is to gain the percutaneous kidney access, first shown by Ritter *et al.* in an ex vivo model.[150] After performing a Uro DynaCT with 3D rendering and post-image processing, the 3D reconstruction is used to plan the puncture of the renal pelvis.

From there, the urologist will mark the target point and the possible point of needle insertion in one plane of the reconstructed images, taking into consideration the surrounding structures. After cross-checking the insertion pathway of the needle in all planes of reconstruction, the puncture is best started in the bull's eye view—the insertion point of the needle that was marked with the previously mentioned laser alignment (**Figure 8-2**). During insertion of the needle, the laser cross needs to be kept in an inline position to the needle; needle position can be checked using the indicated roadmap on the fluoroscopy monitor. With this principle, the authors could show that a laser-guided Uro DynaCT allows for fast and successful percutaneous access to the kidney in 9 of 10 cases with a median puncture time of 3.2 minutes.[150] A limitation of this ex vivo model is that the complete static setting must be mentioned. Transferring this system to patients, organ shifting and deformation need to be considered as complicating factors. This problem was addressed by the same authors in a more recent study, where percutaneous kidney access was established successfully in 9 of 12 patients using the described system. With a short median planning and puncture, the Uro DynaCT–based puncture technique also shows promising results in the clinical setting.[151]

Recently, an intraoperative CT-supported approach to gaining kidney access has assumed importance in the treatment of SRMs due to the exact planning demanded by focal therapy. Due to the known heterogeneity of renal masses, multiple and precise tumour biopsies are required before planning ablation therapy.[152] A renal tumour biopsy may be further complicated by cystic tumours, which makes targeting even harder. Therefore, a reliable, exact planning, and guiding tool is needed, such as the dynamic CT-guided puncture technique for gaining access to the renal pelvis that was recently proposed.[153]

Current developments tend toward intraoperative computer-assisted use of CT modalities: the principle consists of a combination of augmented reality tools, which have been presented by different research groups,[140,154,155] as well as fluoroscopy and CT image fusion. However, all groups faced the problem of intraoperative organ shifting, observed especially in renal surgery. Furthermore, changing the patient's position from supine to flank leads to ventral and caudal movement of the kidney. This might impair the surgeon's orientation compared with standard preoperative CT scans.

Intraoperative CT imaging and fluoroscopy fusion enable imaging at any time during surgery to facilitate during difficult steps. For image fusion, a known spatial relation between the imaging device and the patient (c.f. DynaCT) or a landmark-based transformation can be used. For the latter, radiopaque skin markers,[156] specially designed needle-shaped markers applied to the organ[154] or anatomical landmarks, were proposed. With these methods, the authors were able to gain experience in PN, and found the application to be feasible and helpful. In particular, small and total endophytic tumours could be located faster and more securely, which may not only prevent tissue trauma and positive margins, but also spare renal function. Additionally, this application allows for realizing laparoscopic approaches in complex cases where open surgery is usually preferred. Another application of intraoperative CT was demonstrated by Nozaki *et al.* Those authors performed lymph node dissection with the support of intraoperative CT. Using surgical clips as markers, they were able to identify the dissection template more precisely.[157] As virtual guidance by means of merged 3D data sets remains challenging, a method of using mobile displays, such as the iPad, for intuitive visualization was recently proposed.[156] However, these systems are still experimental and currently reserved for complex cases due to cost and time.

8.3.3.3 Conclusion

Although progress is being made to optimize puncture and targeting of renal lesions, at the present, there is no integrated system applicable in clinical practice. **[LOE 4; GOR D, as no recommendation is possible]**

8.4 Emerging Ablation Technology

New ablation technology aims to overcome the limitations of RFA and CA. When considering emerging ablation technologies, increasing the volume of the ablated zone and overcoming the downsides of RFA and CA are of capital importance. The latter includes possible damage to vital structures in the vicinity of the ablation zone (e.g. the collecting system or intestine), and unpredictable results due to difficulty in monitoring the ablation zone and "thermal sink" effect. Novel ablation technologies such as microwave (MW) and irreversible electroporation (IRE) are not susceptible, or are less susceptible, to the thermal sink. They have the potential to spare tissue architecture and minimize damage to the blood vessels, nerves, and collecting system. Nonetheless, the main question remains whether there is enough evidence in the literature to recommend MW and IRE as standard ablation methods, or whether a higher level of evidence is needed before they overcome the label of "emerging technologies."

The mechanism of action and physical process of the different ablation technologies, as well as the tissue characteristics that can modify their effects, remain important considerations when a range of technology is available. Similarly to standard ablation technologies, these emerging technologies exhibit a broad variation of published outcomes. These outcomes are frequently difficult to interpret due to the absence of standardized reporting criteria, and the preliminary or investigational nature of the reports.

8.4.1 Microwave ablation

8.4.1.1 Technology and devices

Microwave ablation (MWA) is a heat-based needle ablation, and has already used in breast, liver, and lung. Alternating electrical currents are used to generate electromagnetic MWs in frequencies ranging from 900 to 2,450 MHz. Microwaves agitate water molecules and cause friction. These polarized molecules are then forced to continuously realign with the oscillating MW field, resulting in increasing kinetic energy and tissue temperature.[158]

Similarly to radiofrequency, the high temperature of MWA induces cellular death by coagulative necrosis. However, MWs do not need ground pads, and are not limited by tissue impedance. Because they are able to radiate through desiccated tissue, more consistent and larger ablation volumes are reached in a shorter time than with RF.[159-161] The minimal thermal dispersion reduces thermal sinking, and the MW effect seems to be less sensitive to tissue type.[159,162-166]

The electromagnetic field induced depends on the antenna design, and drives the size and shape of the ablated zone. Currently, three different types of MW systems are available. The first generation of MW systems, without active antenna cooling and limited to low power and short duration, was likely unpowered to reach high temperatures.[167] The second generation included antenna cooling, but still had limited generator power. The third generation of MW systems integrated shaft antenna cooling (with water, saline, or CO_2) and high generator power, delivering increased energy to the target tumour and minimizing injury to surrounding tissue.[158,166] Overall, fluid-based cooling systems require a larger antenna diameter, while gas-cooled systems work with a smaller antenna diameter (17-G).

The new antenna designs aim for more rounded and forward-weighted heating that, at least theoretically, allows for the safe treatment of smaller tumours. In general, the higher temperature is reached within 1 cm of the antenna tip, and the effect of multiple antennas is synergistic.[168] CO_2-cooled systems permit the creation of an early, small ice ball to stabilize the position of the antenna. Both frequencies, 915 MHz and 2.45 GHz, create large ablation zones, although the longer wavelength at 915 MHz seems to result in larger ones.[169-171]

Performance of the different systems varies depending on the antenna diameters, number of antennas, power generated, frequency, and power lost between the generator and the tip of the antenna. Understanding the characteristics of the system being used is critical for properly selecting patients and evaluating outcomes.[162,172] As for other ablation methods, the expected ex vivo ablation diameters are provided by the manufacturer.

8.4.1.2 Animal ex vivo and in vivo trials

A considerable number of studies have assessed MWA in the liver, lung, and kidney. Different ablation protocols in terms of generator power (watts; W), number of antennas, and ablation time have shown in pig livers consistent ablation zones between 3 cm and 6.4 cm using a single antenna.

The first generation of MW systems showed inconsistent and asymmetric ablation zones, denuded urothelium, antenna charring, and damage to the collecting system in in vivo porcine kidneys.[173] More advanced systems have assessed the effect of different MWA powers (60–180 W) and times of application (2–6 minutes), using a 1.8-mm antenna and 2.45-GHz system, in bovine liver and porcine muscle and kidney. Increased power settings and time significantly increased ablation volume in the three tissues by up to 140 W. Optimal efficiency for this novel probe and system was found at settings of ≤140 W for 6 minutes.[174] He *et al.* tested 50 W at 10 minutes in in vitro, and acute and chronic in vivo porcine kidneys, showing the predictability of thermal tissue injury.[175]

Ex vivo studies show variable degrees of contraction of the ablation lesion, depending on the tissue tested. The degree of contraction in liver (30%–38%) or lung (47%–52%) is superior to that in kidney (4%–7%), and proportional to tissue vascularization and desiccation.[176,177]

A porcine kidney ex vivo study using 90-W MWA showed significant variations in differential post-intervention volumes (–3.8% to –7.2%), depending on application time, but similar dehydration rates (62.6%–64.2%). The authors concluded that the coagulation zone is underestimated by visualization, and the effective coagulation volume is significantly greater with higher deployed energy.[178]

The use of double antennas enlarges considerably the coagulation zone. A single MW antenna results in a significantly larger ablation zone than a single RF electrode. High-power triaxial MW antennas also produce larger ablation zones in porcine kidneys than RF with similar-sized and number of applicators.[166] Furthermore, the 32 ablated areas produced by a novel, refrigerated, 17-G antenna (Amica™, Mermaid Medical, Stenløse, Denmark) showed a mean diameter of 1.2 cm to 4.2 cm, depending on power time and exposure.[179] In this study, 50-W power offered the optimal necrotic lesion size and spherical index. Pathological evaluation with nicotinamide adenine dinucleotide (NADH) staining did not show skipped lesions in any of the ablated tissues.[179]

So far, animal kidney studies have failed to show that antegrade pyeloperfusion with cooled 5% glucose protects the collecting system during MWA. Consequently, MWA of central lesions abutting the collecting systems should be carefully considered or avoided.[180]

Lastly, when comparing temperature- and power-controlled MW systems on porcine kidneys, no significant differences were found in ablation zone geometry. However, system failures occurred less frequently with temperature-controlled systems (0% vs. 13%).[178] Attempts to establish treatment guidelines in terms of power and time have been made based on the in vivo porcine kidney. Hope *et al.* proved that the diameter of the ablated tissue (n=308) varies significantly by time and power applied, and their interaction. With their system, the optimal setting to perform kidney MWA was settled at 45 W for 10 minutes.[181]

In summary, animal kidney studies show that the optimal MWA protocol is highly dependent on the system characteristics, and the whole technical procedure should be adapted to the desired targeted ablation zone.

8.4.1.3 Human trials

Three phase 1 studies have focused on the feasibility and safety of MWA for kidney tumours, prior to nephrectomy or tumour enucleation. In spite of the different protocols and probes used, all of the studies showed the presence of coagulative necrosis with uniform and reproducible ablation lesions, and absence of vital tumour cells inside the induced lesion. Up to three probes were used in one study, resulting in a large mean ablated lesion size of 5.7 x 4.7 x 3.8 cm. Most importantly, the surrounding healthy tissue was preserved. Complications were negligible in these studies.[182-184]

Besides a number of retrospective studies, one structured report on CA versus MWA and one randomized controlled trial (RCT) comparing MWA with open partial nephrectomy (OPN) in kidney tumours have been conducted so far.

A meta-analysis comparing CA with MWA for SRMs was published in 2013.[185] Overall, there were seven studies included, and a total of 164 patients treated by MWA. Patients with familial/hereditary syndromes were excluded,[167,183,186-190] and one of the studies included only hamartomas.[186] Half of the patients received laparoscopically assisted MWA and 37.2% received percutaneously assisted MWA. Mean tumour size was 3.13 cm (SD: 0.8). At a mean follow-up of 18 months (SD: 8), primary effectiveness was 91.3%, and CSS was 96.8%. Local tumour progression was observed in 2.54% of patients, without any metastatic progression. A total of 11 complications were observed in the MWA group. The reported complication rate (detailed within the reported raw number) was 61%.

The most recent results of four series published after the meta-analysis are depicted in **Table 8-4**.[191-194] These retrospective series support the previously reported outcomes. Of note, all the systems delivered high power through cooled antennas, and most SRMs included were of low or intermediate complexity.[191] Treatment was performed percutaneously and under general anesthesia in most of the patients. Hydrodisplacement with a 5% dextrose sterile water solution was necessary in 38% of the cases in the Moreland *et al.* series.[191] Carrafiello *et al.* followed seven patients with MWA-treated Bosniak III–IV cysts radiologically for 24 months, observing minimal reduction in diameter, and even increase in diameter in some cases (range: −4 mm to +3.3 mm), although the differential Hounsfield unit was below 10 in all cases during follow-up.[193]

TABLE 8-4 Most Recent Studies on Human Microwave Ablation

Reference	No pat /tumours	Methodology	MW system/ approach	Age, yr (mean)	
Moreland *et al.*[191]	53 RCC (biopsy proven)	Retrospective	2.45 GHz; CO_2 cooled; percutaneous	66	
Horn *et al.*[192]	14/15 (suspect small RCCs)	Retrospective	2.45 GHz; CO_2 cooled; percutaneous	62	
Lin *et al.*[194]	14/16 Functional monokidney*	Retrospective	KY-2000; double cooled; percutaneous	51.2	
Carrafiello *et al.*[193]	6/7 Bosniak III–IV	Retrospective	915 MHz; saline cooled; percutaneous	74	

Abbreviations: MV: microwave; RCC: renal cell carcinoma; CSM: cancer-specific mortality; RFS: recurrence-free survival (local and metastatic).
* Three cases already M+.
† Three cases >4 cm, including RCCs and one von Hippel-Lindau.
‡ Pseudoaneurysm renal artery branch.
§ By means of two sessions in six cases.

continued on **page 553**

Besides these observational studies, the RCT by Guan *et al.* deserves special mention. Those authors compared PN with MWA (open or laparoscopically assisted) in SRMs.[187] During the minimum follow-up of 2 years (median: 32 and 36 months for MW and PN, respectively), surgical and hospitalization times were similar for both arms. Estimated blood loss (p=0.0002) and complication rate (p=0.0187) were significantly lower in the MWA group (12.5% vs. 33% for the MWA and PN arms, respectively). Of note, one MWA patient developed urinary leak. Decline in postoperative renal function (p=0.0092) was also significantly lower in the MWA group; although at last follow-up, the decrease in eGFR was similar (p=1.0). Kaplan-Meier estimation of the RFS rate at 3 years was 91.3% for MWA and 96% for PN (p=0.054). For RCC, the 3-year RFS rate was 90.4% for MWA and 96.6% for PN (p=0.46). Accordingly, MWA was proved to be even safer and as equally efficient as PN in this trial. However, the sample size of this RCT was very small, and selection bias cannot be ruled out. In spite of the highest evidence, currently, it seems prudent to await confirmation of the data.

8.4.1.4 Conclusion

Preclinical animal studies and phase 2 human trials support the emerging utility of MWA in kidney tumours. There is evidence on procedural safety and short-term efficacy. Early differences in terms of efficacy and complications may reflect variations among MW systems and settings. However, with the new high-powered cooling devices, the rate of complication has decreased to a low level.

There is still a lack of large prospective trials and long-term outcomes reports. A unique **[LOE 2b]** comparing MWA with PN (laparoscopic or open) shows a lower perioperative complication rate for MWA and similar 3-year outcomes for both techniques. While there is agreement that third-generation

TABLE 8-4 Most Recent Studies on Human Microwave Ablation, *Cont'd*

	Mean tumour size, cm (range)	Complications	Follow-up, months	Outcomes
	2.6 (0.8–4)	11% (Clavien I: 5; Clavien II: 1)	Median: 8 (in 38 patients)	RFS: 100%
	2.2 (1.0– 3.9)	6.7%‡	Mean: 3	Complete necrosis: 93.3%; enhancement at 3 months: 6.7%
	3.2 (1.0–8.4)†	Minor: 4.5%; mild pain at puncture site: 14.5%; gross hematuria: 7.1%	Median: 9	Complete ablation: 93.8%§; CSM: 14.3%
	1.7 (1.4–2.7)	No major complications	All 24	Technical effectiveness: 100%; RFS: 100%

Abbreviations: MV: microwave; RCC: renal cell carcinoma; CSM: cancer-specific mortality; RFS: recurrence-free survival (local and metastatic).
* Three cases already M+.
† Three cases >4 cm, including RCCs and one von Hippel-Lindau.
‡ Pseudoaneurysm renal artery branch.
§ By means of two sessions in six cases.

MWA is safe and feasible for SRMs, caution is still recommended regarding long-term outcomes, as, so far, follow-up is clearly insufficient for pronouncing sustained efficacy. **[LOE 3; GOR C]**

8.4.2 Irreversible electroporation

8.4.2.1 Technology

Electroporation or electropermeabilization is a technology in which electric pulses traveling between electrodes are used to create nanoscale defects (*nanopores*) in the cell membrane.[195-197] The process can be temporary—reversible electroporation (RE). However, above a certain electrical threshold, the nanopores become permanent, causing cell death due to the inability to maintain homeostasis—in a process called irreversible electroporation (IRE).[198-200] In recent years, interest has turned to IRE as a tumour ablation modality, leading to the development of commercially available medical equipment.[197,201]

Although the presence of nanopores following the delivery of electrical pulses has been visualized using electron microscopy,[195,196] it remains unclear whether these pores are the true mechanism of IRE-induced cell death.[202,203] Nevertheless, IRE appears to offer a number of advantages. First, it is not dependent on thermal energy, and therefore, is not influenced by thermal sink. Second, IRE should confine damage to the cell membrane, sparing tissue architecture and minimizing damage to blood vessels, nerves, and renal collecting system.[204]

8.4.2.2 Device and procedure

At the time of this writing, only one IRE platform had specific clearance for the ablation of soft tissue, namely the NanoKnife® IRE System, also registered as the HVP-01 Electroporation System (AngioDynamics, New York, United States). This platform consists of a low-energy direct current (LEDC) generator, capable of connecting up to six monopolar needle electrodes (16 G). Parameters to be adjusted in IRE ablation are voltage, pulse number, pulse length, electrode number, and electrode spacing. Irreversible electroporation procedures take place under general anaesthesia with additional muscle relaxation in order to prevent severe muscle contractions as a result of the electrical pulses.[205] Irreversible electroporation pulses have the potential to cause cardiac arrhythmia. Therefore, synchronization of the IRE pulses with the cardiac rhythm is advised—performed by interfacing a synchronization device to the IRE console. The IRE electrodes are placed in a similar fashion to RFA or CA probes. Parallel insertion of the probes is important to guarantee equal distribution of the electrical field. Generally practiced IRE settings for tumour ablation are electrode spacing of 15 to 20 mm, electrode tip exposure of 15 to 20 mm, 70 to 90 pulses of 70 to 90 µs (synchronized with electrocardiogram [ECG]), and a pulse intensity of 1,500 V/cm. Due to the fast repetition and microsecond pulse length, an IRE pulse cycle will take only 5 to 10 minutes.

8.4.2.3 Animal trials

Early in vivo experiments of IRE in rat livers showed that ablation of the parenchyma produced a sharp boundary between treated and untreated tissue. Furthermore, preservation of blood vessels and ductal structures was observed.[206] Kidney-specific animal testing, using a porcine model, has confirmed acute, short-term and midterm safety of IRE.[199,207-209] Monopolar and bipolar IRE ablation were both tested. Bipolar IRE was found to result in smaller ablation volumes, and was more likely to cause urothelial erosion and necrosis.[207] Following this, the focus turned to monopolar IRE. Irreversible electroporation of the porcine kidney, including the renal collecting system, can result in damage to the urothelium. However, histological evaluation at 14 days post-IRE shows the onset of cellular repair and repopulation.[199,207,210] Furthermore, it was noted that the basement membrane, collagen, and fibroblasts remained unaffected.[210] These results support the theory that IRE could spare vital structures within the ablation zone. On the contrary, repetitive high-intensity electric pulses, as used in IRE, have the potential to cause joule heating. A study measuring temperature development and distribution during IRE of the porcine kidney, using generally practiced settings, showed a peak temperature increase of 47°C in the heart of the ablation zone.[211] Such temperatures lead to thermal damage, warranting the consideration of safety measures such as temperature monitoring. On CT imaging, acute and subacute lesions showed cortical necrosis and pelvic urothelial necrosis with preservation of pelvic extracellular matrix. Midterm follow-up showed cortical fibrosis and urothelial regeneration.[208] Dynamic contrast-enhanced MRI showed inhomogeneous necrosis with small perifocal edema at short-term follow-up and sharp delimitable scars at midterm follow-up.[209]

8.4.2.4 Human trials

The feasibility and safety of IRE ablation of RCC in humans was first tested by Pech *et al.* in an "ablate and resect" pilot study performed during anesthesia in six patients directly before kidney resection.[200] Patients were monitored by ECG and basic laboratory sampling. Blood gas analysis and laboratory blood testing showed no abnormal changes. In one patient, one intraoperative supraventricular extrasystole was encountered; this was not followed by any further ECG abnormalities. Histopathological examination of the resected tumours showed swelling of the ablated cells, but no actual dead cells were observed. These histopathology results are in line with the supposed mechanism of IRE. As the induced cell death involves predominantly apoptosis, the IRE effects need more time to become visible.[200] This pilot study addressed, in particular, the possible risks associated with the need for general anesthesia (to induce muscle relaxation) and with the need to synchronize IRE pulses with the refractory period of the cardiac rhythm (to avoid rhythm disorders).

Thomson *et al.*[212] investigated the safety of IRE in humans by ablating tumours in 38 volunteers with advanced liver, lung, or kidney malignancies. This was a single-centre, prospective, non-randomized cohort study in which IRE of the kidney was performed in 10 cases in 7 patients. Safety analysis consisted of clinical examination, basic laboratory sampling, and CT scans performed before, directly after the procedure, and at 1 month and 3 months post-ablation. One patient developed obstruction of the ureter, which was previously damaged by RFA ablation. The other six patients showed no signs of stricture while the ureter or collecting system was within the ablation zone. Transient hematuria was observed in two patients who had IRE treatment extending into the central portion of the kidney. Two patients required a second IRE treatment after 3 months of follow-up.[212] Recently, Trimmer *et al.* reported on 20 cases of IRE in SRMs, with 1 year of imaging follow-up. Two of the 20 cases presented with residual tumour at 6-week follow-up imaging, which were treated with salvage RFA. Six-month follow-up was available for the 15 cases showing no signs of recurrence. One-year follow-up was available for the six cases, of which one showed recurrence, treated by PN. No major complications were observed.[213]

A phase 2a trial is underway aimed at confirming the efficacy of IRE for the ablation of SRMs, by performing PN 28 days after ablation. Short-term follow-up, between IRE and resection, will be performed using MRI. When completed, this trial will provide data on the histopathology of (partially) resolved IRE lesions and valuable insights into post-ablation MRI.[214] When these short-term efficacy results become available, the next step will be the first phase 3 follow-up trial of this new ablation modality.

Based on the studies of Pech *et al.* and Thompson *et al.*, it seems that, besides the need for general anesthesia with additional muscle relaxation and the need to synchronize IRE pulses with the refractory period of the cardiac rhythm, IRE is a feasible and safe procedure.[200,212] This can give further body for the second step in investigating the efficacy of IRE. A study has to be performed to investigate the effect of IRE after days or even weeks, with pathology as the reference standard, to confirm the early ablation effect. The trial by Wendler *et al.* is underway, and will, hopefully, shed light on this matter.[214] After pathological confirmation of the IRE ablation effect, research can progress to follow-up trials addressing intermediate-term and long-term ablation success. **Table 8-5** displays the main findings of animal and human studies in kidney IRE.

TABLE 8-5 Main Findings for Animal and Human Studies on Irreversible Electroporation of the Kidney

Reference	Tissue type	Number of IRE ablations	Follow-up method	Follow-up	Conclusions	Type of study
Trimmer *et al.*[213]	Human kidney tumour	20	▪ CT ▪ MRI	▪ 1 year	Renal IRE appears safe for the treatment of small renal tumours. CT and MRI are feasible imaging techniques for follow-up after IRE.	Case series
Pech *et al.*[200]	Human kidney tumour	6	▪ Pathology	▪ Ablation/ resection	IRE of human kidney tumours is feasible and safe.	Prospective cohort
Thomson *et al.*[212]	Human kidney tumour	11	▪ CT	▪ Directly ▪ 1 month ▪ 3 months	IRE of human kidney tumours is safe if pulses are synchronized with ECG.	Prospective cohort
Olweny *et al.*[199]	Porcine kidney	24	▪ Retrograde pyelogram ▪ Histology	▪ 24 hours ▪ 7 days ▪ 21 days	IRE of porcine kidney is safe and effective. High-intensity IRE protocols showed significant collecting system injury.	In-vivo animal study
Tracy *et al.*[207]	Porcine kidney	24	▪ Histology	▪ 10 minutes ▪ 1 hour ▪ 7 days ▪ 14 days	IRE of porcine kidney leads to histological changes characteristic of cellular death within 1 hour after ablation, with relative urothelial sparing.	In vivo animal study
Deodhar *et al.*[208]	Porcine kidney	29	▪ CT ▪ Histology	▪ <24 hours ▪ 36 hours ▪ 3 weeks	IRE of porcine kidney showed sparing of connective tissue, and relatively early resolution of ablation defect on axial imaging. No evidence of early collecting system damage observed. Good correlation between histopathology and imaging.	In vivo animal study
Wendler *et al.*[209]	Porcine kidney	8	▪ MRI ▪ Histology	▪ 30 minutes ▪ 7 days ▪ 28 days	IRE of porcine kidney showed preservation of adjacent renal parenchyma, connective tissue, and urinary system. MRI is a suitable imaging technique for follow-up after IRE, providing higher soft tissue contrast compared to CT.	In vivo animal study

Abbreviations: IRE: irreversible electroporation; CT: computed tomography; MRI: magnetic resonance imaging; ECG: electrocardiogram

continued on **page 557**

TABLE 8-5 Main Findings for Animal and Human Studies on Irreversible Electroporation of the Kidney, *Cont'd*

Reference	Tissue type	Number of IRE ablations	Follow-up method	Follow-up	Conclusions	Type of study
Sommer *et al.*[210]	Porcine kidney	10	▪ CT ▪ Histology	▪ Ablation/ resection	IRE of porcine kidney with involvement of the renal pelvis is feasible and safe. Size, but not shape, of the treatment zone is significantly affected by applicator configuration.	In vivo animal study
Wagstaff *et al.*[211]	Porcine kidney	8	▪ Temperature monitoring, ▪ Gross histology	▪ Ablation/ resection	IRE ablation of porcine kidney, using clinically practised settings, causes a lethal rise in temperature within the ablation zone.	In vivo animal study

Abbreviations: IRE: irreversible electroporation; CT: computed tomography; MRI: magnetic resonance imaging; ECG: electrocardiogram

8.4.2.5 Conclusion

Irreversible electroporation is an experimental technology for the treatment of renal masses that is offered as an alternative to already existing focal therapies such as RFA and CA. The literature is scarce in evidence, with only five porcine studies evaluating IRE effects, and only three human studies on the feasibility and safety of IRE. Furthermore, as the three human studies are case series or poor-quality prospective cohort studies, they should be considered level 4 evidence, according to the University of Oxford's Centre for Evidence-Based Medicine. Therefore, at this stage in the development of the technology, we do not recommend routine clinical use of IRE for renal masses. Irreversible electroporation of renal masses should be performed only in the setting of a well-designed study protocol. **[LOE 4; GOR C]**

8.5 Investigation Ablation Technology

This section summarizes the current evidence on investigational ablation methods for the treatment of primary renal tumours, including the CyberKnife®, high-intensity focused ultrasound (HIFU), and photodynamic therapy (PDT).

8.5.1 CyberKnife

Although radiotherapy is an accepted palliative treatment for bone and brain metastases in RCC, historical randomized trials testing preoperative and postoperative radiation of primary tumours or renal fossa have been unsuccessful.[215-217] These studies had several limitations, including patient selection, study power, dose, and dose delivery. With laboratory data showing RCC to be the least radiosensitive tumour among 76 cell types,[218] RCC has been considered radio-resistant, limiting the possible role of radiation therapy to unresectable primary tumours.

In general, radiation therapy can be delivered as a single-treatment session (radiosurgery), or over a course of 3 to 5 treatment sessions (hypofractionated) or 2 to 6 weeks (fractionated). The term *radiosurgery* is misleading, as it does not involve surgery and is fully noninvasive. Stereotactic radiosurgery (SRS) and stereotactic body radiotherapy (SBRT), also known as stereotactic ablative radiation therapy (SABR), use an external coordinate system to deliver a safe, high, single hypofractionated dose of radiation of up to 25 Gy.[219] These techniques have gained recent attention as potentially curative treatments for primary renal tumours. Compared with cryotherapy or RFA, they are capable of treating larger tumours, and those close to major vessels and the collecting system. Procedures are usually performed on an outpatient basis without anesthesia. A wide range of devices, doses, and dose fractionation schedules have been used in the past two decades, and have been reviewed recently.[220]

A specific challenge in the treatment of the kidney is synchronous, respiration-induced organ movement. The CyberKnife® Robotic Radiosurgery System (Accuray Incorporated, California, United States) uses a true robotic manipulator, which can correct for kidney and tumour movement throughout the respiratory cycle. In vivo studies showed that the effect of the CyberKnife is focal, and surrounding renal parenchyma remains unaffected.[221] Percutaneous insertion of gold fiducials in renal parenchyma or tumour is usually necessary to facilitate tumour tracking.

Several noncontrolled, prospective case series of CyberKnife for primary renal tumours have been published (**Table 8-6**). Kaplan *et al.*[222] reported a phase 1 dose-escalation trial in medically inoperable patients with renal tumours of up to 5 cm (clinical trial registration number: NCT00807339). Stereotactic body radiosurgery (SBRS) dose levels were 21 Gy, 28 Gy, 32 Gy, or 39 Gy delivered in three fractions. Three patients were treated per dose cohort. One patient treated with 21 Gy had local progression. There was no relevant acute or chronic toxicity. Two patients with preexisting CKD had worsening renal function during follow-up, while all other creatinine levels remained stable. A phase 2 trial (NCT01890590) is currently recruiting patients at the same institution, but results are not expected until 2019.

TABLE 8-6 Treatment Details and Oncologic Outcomes of Recent CyberKnife Studies

Reference	Country	Year	n	Treatment	Follow-up, months	Local control, %	Complete response, n (%)	Partial response/ minor, n (%)	SD, n (%)
Kaplan *et al.*[222]	United States	2010	12	21–39 Gy, 3 fractions	NA	92	NA	NA	NA
Nair *et al.*[223]	Canada	2013	3	39 Gy, 3 fractions	13	100	0	1 (33%)	2 (67%)
Lo *et al.*[224]	Taiwan	2014	3	40 Gy, 5 fractions	12–40	100	NA	NA	NA
Staehler *et al.*[225]	Germany	2015	45	25 Gy, 1 fraction	28	98	19 (42%)	19 (42%)	7 (16%)

Nair *et al.*[223] published an initial Canadian series of three patients with inoperable renal tumours, including two with a solitary kidney and one with local recurrence after RFA. Median tumour volume was 21 cm^3. Patients were treated with 39 Gy in three fractions. There were no acute or chronic treatment-related toxicities. Renal function remained unchanged. After a mean follow-up of 13 months, local tumour control was achieved in all patients, with two having stable disease and one showing a partial response.

Lo and colleagues[224] treated three patients with CKD and stage I RCC. A total of 40 Gy was delivered in five fractions. Local control was achieved in all patients. One patient developed lung metastases 9 months after the procedure. Toxicity was generally mild and self-limiting.

Staehler *et al.*[225] published the largest series to date, reporting outcomes for 40 patients with 45 tumours who had an indication for nephrectomy, and would have subsequently been on hemodialysis. Tumours were treated with a 25-Gy dose in a single fraction (SRS). Of the 45 lesions, 30 were RCC and 15 were transitional cell carcinoma (TCC). The median follow-up was 28 months. The 9-month local control rate was 98%. A complete response was achieved in 42% of patients. The complete response rate was higher in patients with TCC (13/15; 87%) than RCC (6/30; 20%). No significant changes in renal function were noted, and the authors observed only minor early toxicities, including erythroderma (n=1), fatigue (n=3), and nausea (n=2).

8.5.2 High-intensity focused ultrasound

High-intensity focused ultrasound has the advantage of not needing to puncture the tumour, precluding the possible risk for hemorrhage and tumour spillage.[226] There are two possible approaches: extracorporeal/percutaneous or intracorporeal/laparoscopic.

Häcker *et al.*[227] reported outcomes of 19 patients with renal tumours treated with extracorporeal HIFU who underwent nephrectomy after HIFU lesions were placed. Histology showed limited signs of tissue ablation in about 80% of kidneys, although the ablated volume never reached the targeted volume. Marberger *et al.*[228] published on 16 patients with small renal tumours. Fourteen tumours were removed following ablation, showing again that the ablated volume comprised only 15% to 35% of the targeted volume. Ritchie *et al.*[229] presented 3-year follow-up data of 17 renal tumours with a mean size of 2.5 cm. After 12 days, radiologic evidence of a treatment effect was seen in 7 of 15 tumours (47%). Fourteen patients were evaluated after 6 months, of which 6 (43%) showed a mean decrease in the tumour area of 12%. Four patients had irregular enhancement on imaging and underwent alternative therapies. Ten patients continued follow-up after a mean interval of 3 years; thus, percutaneous HIFU achieved stable lesions in only two-thirds of patients.

Problems with respiratory movement and interphases are avoided when an intracorporeal probe is brought directly to the target through a 12-mm or 18-mm laparoscopic port.[230] Klingler *et al.*[231] performed a clinical phase 1 trial, and ablated eight small renal tumours with curative intent. Of the seven tumours that were removed directly after HIFU, four showed complete ablation of the entire tumour, two showed a 1- to 3-mm rim of viable tissue at the surface of the tumour, and one showed a central area with vital tissue (skipping). Ritchie *et al.*[232] published comparable results with his series of 12 patients. The ablated zones were within the targeted area in all patients, and about 90% to 100% of the target zones were ablated. No intralesional skipping was seen, but small areas of subcapsular skipping at the tumour surface were observed in two patients. At present, there are no data regarding the oncologic efficacy of laparoscopic HIFU for tumours left in situ after ablation.

8.5.3 Photodynamic therapy

Photodynamic therapy is another investigational ablation method for primary renal tumours. In general, a photosensitizer is administered intravenously and accumulates in the target tissue, which is illuminated percutaneously or interstitially, leading to subsequent necrosis. In a mouse model using the photosensitizer m-tetrahydroxyphenylchlorin (mTHPC) to target tissue and vessels, Kroeze *et al.*[233] observed complete loss of cell viability at a drug-light interval of 4 hours. Vascular-targeted PDT with the novel water-soluble photosensitizer WST-11 has been tested recently. Kimm *et al.*[234] performed 30 percutaneous, image-guided ablations in 16 pigs. In contrast to other focal therapies, the normal renal tissue, blood vessels, and collecting system were completely spared, supporting the photosensitizer's clinical evaluation for tumours close to sensitive structures, such as the renal hilum or renal pelvis. A clinical phase 1/2 trial is currently ongoing (NCT01573156).

8.5.4 Conclusion

CyberKnife is an investigative ablation method in the early stage of clinical development. It is technically feasible and has shown encouraging results regarding short-term local tumour control, treatment-related toxicity, and maintenance of renal function. However, as inclusion criteria, treatment schemes, and outcome measures were not standardized between studies, the studies are difficult to compare. There was no histological assessment of the tumour prior to ablation in many cases. Furthermore, these results have to be interpreted in the context of AS, where renal tumours have shown a mean annual growth rate of 0.3 cm, and about 23% have exhibited zero net growth.[235] Finally, CA and RFA ablation have set a high bar for the safety and oncologic efficacy of new ablation methods.[236] Extracorporeal HIFU of renal tumours showed poor outcomes, and results appear to be inferior compared with established ablation methods. Intracorporeal HIFU and PDT are still early clinically and require in-patient data. **[LOE 4; GOR D]**

8.6 Ablation in Perspective

In this chapter, kidney ablation techniques are put into perspective by summarizing and analyzing the best available evidence of studies, comparing these techniques with other treatment options (PN or AS), and looking at comparative outcomes of different ablative procedures. Studies comparing kidney ablation with radical nephrectomy, those in which thermal ablation was used in conjunction with PN, or those in which CA and RFA were pooled together were not considered.

8.6.1 Comparative analysis: kidney ablation versus partial nephrectomy

8.6.1.1 Cryoablation versus partial nephrectomy

As partial nephrectomy remains the standard of care in the management of SRMs, it is of foremost importance to compare kidney ablation techniques with this procedure. Since the first study reported in 2005 by Desai *et al*,[237] several others have reported on comparative cohorts of CA versus extirpation, although a true randomized trial has not been performed.

Using a matched-pair analysis to include age-adjusted Charlson Comorbidity Index (CCI) and preoperative aspects and dimensions used for an anatomical score (PADUA) scores, Klatte *et al.* compared the outcomes of 41 patients who underwent LCA with 82 patients who underwent OPN.[44] The 3-year RFS rate was significantly (p=0.015) better for those patients who underwent OPN (100%) vs. LCA (83%). Complication rates and renal functional outcomes after surgery were similar.

Haramis *et al.* published a retrospective analysis of patients treated with LPN and LCA.[238] At the relatively short follow-up in each treatment arm (median: 22 months for LPN and 14 months for LCA), recurrences were found in 2.2% of tumours treated with LCA and 1.1% of those treated with LPN (p=0.588). Complications were significantly less common following LCA (8.0% vs. 11.9%; p<0.001).

In a study reflecting very early outcomes (median follow-up: 5 months) following RPN, the Cleveland Clinic showed promising oncologic outcomes for RPN compared with LCA. There were no local recurrences in the robotic PN group, and there was an 11% local recurrence rate in the LCA group (although positive surgical margins were found in 2% of RPN patients).[239] A greater decrease in eGFR was reported the day after RPN, although there was no significant difference in eGFR between the two groups at 1 and 6 months after ablation. Complications were more common in patients treated with RPN (23% vs. 12%).

A similar comparison study but with longer follow-up in the robotic PN cohort was conducted.[240] Although positive surgical margins were found in 6% of patients treated with RPN, there were no local recurrences at a mean follow-up of 17 months. Local recurrences were found in 2 of 56 (4%) patients treated with LCA at a mean follow-up of 31 months, both of whom were successfully re-treated with CA. Complication rates were similar between the two groups.

Thompson *et al.* recently published a large retrospective review comparing treatment of T1 renal masses using PN, PCA, or RFA.[74] Although selection bias could not be ruled out, there was no significant difference in RFS between the three treatment methods in the management of cT1a renal masses. However, duration of median follow-up was much greater in the PN cohort. Perhaps more surprising was that there was no significant difference in RFS among patients with a cT1b renal mass treated with PN versus those treated with PCA.

A recent structured report and meta-analysis compared outcomes of LCA (*n*=564) with robot-assisted, laparoscopic, invasive PN (*n*=627).[241] Thirteen retrospective, observational studies were included, of which seven (53%) were of high quality according to the modified Newcastle-Ottawa Scale. Patients undergoing CA were older (WMD: 6.1 years), had a higher ASA score (OR: 2.65), and presented with smaller tumours (WMD: 0.25 cm). Laparoscopic cryoablation was associated with significantly shorter operative times (WMD: 35.4 minutes), lower estimated blood loss (WMD: 130.1 mL), shorter length of stay (WMD: 1.2 days), and lower risk of complications (relative risk [RR]: 1.82). Patients undergoing LCA had a significantly increased risk of local (RR: 9.39) and metastatic tumour progression (RR 4.68). Overall, this meta-analysis suggests that oncologic outcomes are substantially worse for LCA than for minimally invasive PN, although LCA is associated with improved perioperative outcomes. Similar conclusions were drawn in another recent meta-analysis by Tang *et al.* of a smaller number of studies.[242]

8.6.1.2 Radiofrequency ablation versus partial nephrectomy

Eleven retrospective case-controlled studies were identified where a direct comparison of outcomes between RFA and PN was performed (**Table 8-7**).[74,85,97,125,243-249] For two of them, a propensity score analysis was applied.[97,246] Radiofrequency ablation (*n*=547) was performed by either percutaneous (*n*=346; 63.2%) or laparoscopic approach (*n*=201; 36.7%), whereas PN (*n*=1,407) was performed by either open (*n*=1,176; 83.5%) or laparoscopic approach (*n*=204; 14.5%). In one more recent study, robot-assisted LPN (*n*=27) was performed.[249]

TABLE 8-7 Radiofrequency Ablation Versus Partial Nephrectomy—Published Comparative Series (All Retrospective Case-Controlled Studies [LOE 3])

Reference	Approach (N of cases)		Age, years		ASA score		Baseline eGFR, mL/min		Tumour size, cm		Follow-up, months		DFS, %	
	PN	RFA	PN	RFA	PN	RFA	PN	RFA	PN	RFA	PN	RFA	PN	RFA
Bensalah *et al.*[244]	LPN: 50	LRFA:38	56.5	62	NA	NA	NA	NA	2.6	2.3	15	25.2	NA	NA
Stern *et al.*[243]	LPN: 7; open: 30	LRFA: 14; PRFA: 26	56.4	60.5	NA	NA	NA	NA	2.4	2.4	46.7	29.8	95.8	93.4
Turna *et al.**[85]	LPN: 36	PRFA: 29	60.3	60.7	NA	NA	65	53.2	2.5	2.6	42.5†	14†	100	33.2
Raman *et al.**[125]	OPN: 42	LRFA: 9; PRFA: 38	59.6	65.9	2†	3†	55.9†	46.5†	3.5†	2.7†	30†	18.1†	NA	NA
Bird *et al.*[245]	LPN: 33	LRFA: 36	57.8	75.2	2.2	2.8	82.3	62.7	3.1	2.8	27	12	NA	NA
Olweny *et al.*[246]	LPN: 28; open: 9	LRFA: 12; PRFA: 25	54.1	63.2	1.9	2.3	NA	NA	2.5†	2.1†	74.7	77.7	89.2	89.2
Youn *et al.*‡[247]	OPN: 14	LRFA: 41	59.1	53.9	1.7	1.7	72.9	73.7	2.4	2.3	50	50	NA	NA
Chang *et al.*‡[97]	LPN: 35; open: 10	LRFA: 36; PRFA: 9	56.9	64	1.7	1.7	104.8	99.1	4	3.6	69	67.6	89	81
Chang *et al.*[248]	LPN: 15; open: 14	LRFA: 15; PRFA: 12	52.8	52.9	1.5	2.1	86.4	78.8	5.2	4.7	70.2	65.9	88.5	86.7
Thompson *et al.*[74]	OPN: 1,057	PRFA: 180	60.1	70.7	NA	NA	NA	NA	2.5	2.1	36	36	NA	NA
Kim *et al.*[249]	RPN: 27	PRFA: 27	60.3	58.6	1	1.6	86.7	84	1.7	1.8	10.9	16.7	NA	NA

Abbreviations: ASA: American Society of Anesthesiologists; DFS: disease-free survival; eGFR: estimated glomerular filtration rate; LPN: laparoscopic partial nephrectomy; LRFA: laparoscopic radiofrequency ablation; PRFA: percutaneous radiofrequency ablation; NA: not available (or calculable); OPN: open partial nephrectomy; PN: partial nephrectomy; RFA: radiofrequency ablation; RPN: robotic partial nephrectomy.
Values expressed as means (unless otherwise specified) and percentages.
* Only patients with solitary kidney.
† Median values.
‡ Propensity score analysis used.

Meta-analysis of extractable data showed that patients treated with RFA presented with significantly smaller tumour size (WMD: –0.37 cm; 95% CI: –0.4 to –0.3; $p<0.001$). They were also older (WMD: 6.7 years; 95% CI: 4.2–9.1; $p<0.001$), and had higher ASA scores (WMD: 0.44; 95% CI: 0.18–0.69; $p<0.001$), and worse baseline estimated renal function (WMD eGFR: –7.33 mL/min/1.73 m^2; 95% CI: –13.8 to –0.8; $p=0.03$). Moreover, they tended to have a shorter length of follow-up (WMD: –5.89 months; 95% CI: –12.53 to 0.74; $p=0.08$). Radiofrequency ablation exhibited significantly shorter hospital stay (WMD: 1.88 days; 95% CI: 2.54–1.22; $p<0.001$), and there was no significant difference in terms of complications (OR: 0.66; 95% CI: 0.39–1.12; $p=0.12$). Moreover, there was no statistically significant difference in terms of tumour recurrence (OR: 1.6; 95% CI: 0.7–53.9; $p=0.25$), and the use of RFA allowed for a less significant decline in terms of estimated renal function (WMD eGFR: –4.4 mL/min/1.73 m^2; 95% CI: –6.93 to –1.88; $p<0.001$) (**Figure 8-3**). Given the recognized limitations of a meta-analysis of case-controlled studies, the data hereby confirm that patients undergoing RFA are usually sicker and at higher surgical risk, representing a "per se" selection bias. Radiofrequency

ablation can be regarded as an effective treatment option for select patients with localized kidney cancer, as it allows for the achievement of comparable oncologic outcomes to the "gold standard" PN, with the advantage of a better preservation of renal function.

FIGURE 8-3
Forest Plots of Meta-analysis Outcomes of Comparative Series: Radiofrequency Ablation Versus Partial Nephrectomy

A Hospital Stay: Radiofrequency Ablation Versus Partial Nephrectomy

B Major Complication Rate: Radiofrequency Ablation Versus Partial Nephrectomy

C Tumour Recurrence: Radiofrequency Ablation Versus Partial Nephrectomy

D Decline in Estimated Glomerular Filtration Rate: Radiofrequency Ablation Versus Partial Nephrectomy

A

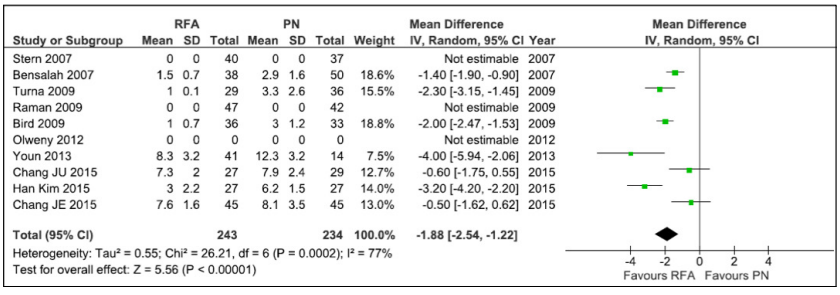

B

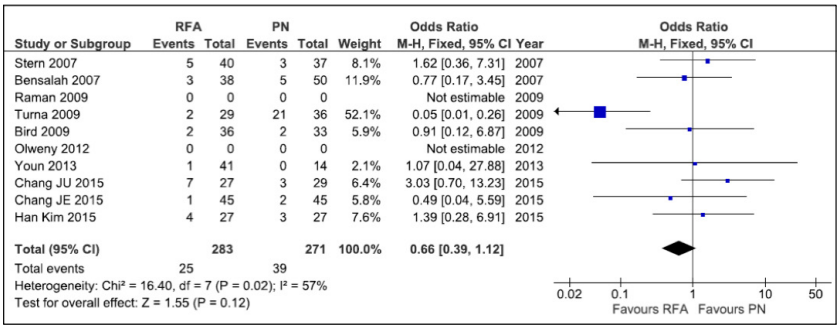

C

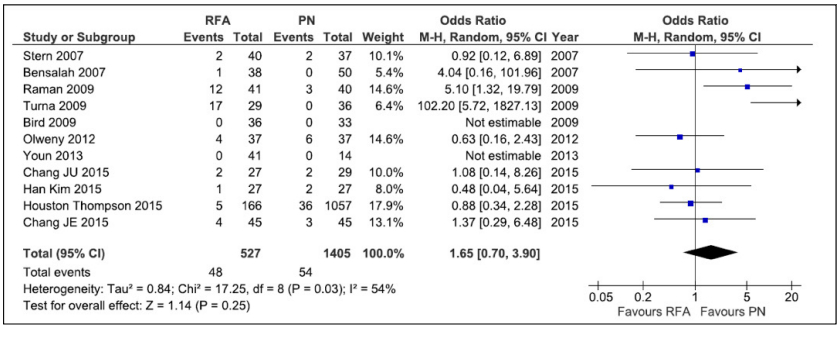

D

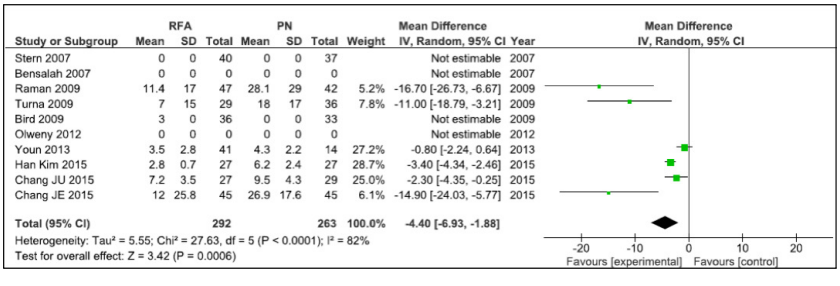

With maturing data, there are now series available that are reporting long-term (5-year) oncologic outcomes. Olweny *et al.* first reported such outcomes in a single-institutional study involving consecutive patients with a single histologically confirmed T1a RCC treated by RFA (n=37) or PN (n=37).[246] The 5-year OS rate was 97.2% versus 100% (p=0.31), CSS was 97.2% versus 100% (p=0.31), and DFS was 89.2% versus 89.2% (p=0.78). Based on these findings, the authors suggested that indication for RFA may be extended to selected younger and healthier patients looking for a minimally invasive therapeutic option. These findings were recently corroborated by a comparative propensity score match analysis from China, where 90 patients with T1a renal tumours (RFA: 45; PN: 45) were studied.[97] In this series as well, no differences in relevant oncologic outcomes at 5 years, including OS (90.2% vs. 93.2%), CSS (95.6% vs. 97.7%), and DFS (86.7% vs. 88.5%), were found. On the other hand, in the largest comparative study reported to date, including 1,424 cT1a patients (PN: 1,057; RFA: 180; CA: 187), local RFS was found to be similar among the three treatments (98% for all treatments; p=0.49), but metastases-free survival was significantly lower for RFA (93%) compared with PN (99%; p=0.005) and CA (100%; p=0.021). However, the authors recognized that this finding should be interpreted with caution given the small number of patients.[74]

Chang *et al.* also reported the long-term outcomes of 56 patients (RFA: 27; PN: 29) with T1b tumours.[248] In this study, RFA patients were older, with higher ASA scores, and smaller tumour size, accounting for an obvious selection bias. No significant difference was found between the two techniques in terms of overall CSS and DFS.

In regard to the functional outcomes, it is worth looking at the two studies that included only patients with a solitary kidney, as estimate of renal function in this subset of patients is more reliable. Turna *et al.* found that LPN was associated with the greatest decrease of renal function at 6 months, with a higher likelihood for temporary or permanent dialysis.[85] Conversely, the authors found a much lower DFS rate for RFA compared with LPN (33.2% vs. 100%; p<0.001). In the second study looking at this same subset of kidney cancer patients (RFA: 47; OPN: 42), those treated with OPN had a greater decline in glomerular filtration rate (GFR) at all time points, including early after the procedure (15.8% vs. 7.1%; p<0.001), 12 months after surgery (24.5% vs. 10.4%; p<0.001), and at last follow-up (28.6% vs. 11.4%; p<0.001).[125]

8.6.1.3 Microwave ablation versus partial nephrectomy

The only study comparing MWA with PN was reported in 2012 by Guan *et al.*[187] The authors conducted a prospective randomized study including 102 patients (PN [open or laparoscopic]: 54; MWA [open or laparoscopic]: 48). Surgical and hospitalization times were comparable between both groups. The MWA group had a significantly lower mean estimated blood loss (PN: 466 mL; MWA: 138 mL; p<0.001) and complication rate (PN: 33.3%; MWA: 12.5%; p=0.01). Decrease in renal function at the last available follow-up was similar in both groups. Kaplan-Meier estimates of the local RFS rate at 3 years were 96.0% for PN and 91.3% for MWA (p=0.54).

8.6.1.4 Ablation versus partial nephrectomy in solitary kidney

A kidney tumour in a solitary kidney represents a challenging scenario, yet it provides a unique investigational opportunity, as it allows for a more reliable evaluation of the effect of treatment on the loss of renal function. So far, seven studies have been reported comparing the outcomes of thermal ablation (either cryotherapy or RF) with PN in this specific subset of patients.[85,125,250-254] Yang *et al.*

recently reported a meta-analysis including all these studies.[255] They found that changes in eGFR in the ablation arm were significantly less than those in the PN arm (p<0.0001). Moreover, significantly less onset of CKD was observed in the thermal ablation group (p=0.04). In regard to perioperative outcomes, patients who underwent ablation had significantly shorter operation times (p=0.002), less blood loss (p<0.0001), shorter length of stay (p<0.00001), and lower transfusion rate (p=0.01). In addition, they suffered less intra- and postoperative complications (p=0.007 vs. p<0.00001, respectively). On the other hand, DFS (p<0.00001) and CSS (p=0.01) were significantly better in the PN arm. Among available studies, Panumatrassamee *et al.* was the only one to report functional outcomes in relation to tumour complexity.[254] Interestingly, those authors found that CA provided better perioperative outcomes (operative time, estimated blood loss, transfusion, hospital stay, and complications), and change in renal function was slightly greater in the PN group; however, statistical significance was not reached for any of the tumour complexities.

8.6.1.5 Laparoscopic cryoablation versus robotic partial nephrectomy

Given its recognized advantages, robot-assisted partial nephrectomy (RAPN) is rapidly gaining popularity as the preferred technique for minimally invasive PN.[256] In three single-institutional studies, the outcomes of CA (mostly laparoscopic) were compared with those of RAPN (**Table 8-8**).[86,239,240]

TABLE 8-8 Cryoablation Versus Robotic Partial Nephrectomy—Published Comparative Series (All Retrospective Case-Controlled Studies [LOE 3])

Reference	CA technique	N of cases		Age, years		Baseline eGFR, mL/min		Tumour size, cm		Follow-up, months	
		RAPN	CA	RAPN	CA	RAPN	CA	RAPN	CA	RAPN	CA
Guillotreau *et al.*[239]	Laparoscopic	210	226	57.8	67.4	86.3	65.8	2.4	2.2	4.8*	44.5*
Tanagho *et al.*[86]	Percutaneous and laparoscopic	233	267	57.4	69.3	84.5	66.3	2.9	2.5	21.9	39.8
Emara *et al.*[240]	Laparascopic	47	56	60.5	69.7	NR	NR	32.8	25.6	16.5	31.3

Abbreviations: CA: cryoablation; eGFR: estimated glomerular filtration rate; RAPN: robotic-assisted partial nephrectomy; NR: not reported.
Values expressed as means unless otherwise specified.
*Median values.

Meta-analysis of extractable data from these comparative studies suggests that patients undergoing RAPN were younger (WMD: –10.7 years; 95% CI: –12.12 to –9.29; p<0.001), had a better baseline renal function (WMD: 18.89 mL/min; 95% CI: 15.5–22.2; p<0.001), and had larger tumours (WMD: 0.46 cm; 95% CI: 0.11–0.8; p=0.009). In terms of surgical outcomes, RAPN was associated with higher estimated blood loss (WMD: 78.3; 95% CI: 22.4–134.2; p=0.006). No difference was found for the hospital stay (p=0.55). Cryoablation carried a lower odds for postoperative complications (OR: 2; 95% CI: 1.3–3.1; p=0.001). There was less decline in eGFR in patients undergoing CA (WMD: 5; 95% CI: 1.7–8.3; p=0.003). In terms of tumour recurrence, this was more likely to happen in the CA group (OR: 0.03; 95% CI: 0.01–0.16; p<0.001) (**Figure 8-4**).

FIGURE 8-4
Forest Plots for Different Outcomes Meta-analysis: Cryoablation Versus Robotic-Assisted Partial Nephrectomy

A Estimated Blood Loss: Cryoablation Versus Robotic-Assisted Partial Nephrectomy

B Postoperative Complication Rate: Cryoablation Versus Robotic-Assisted Partial Nephrectomy

C Decline in Estimated Glomerular Filtration Rate: Cryoablation Versus Robotic-Assisted Partial Nephrectomy

D Tumour Recurrence Rate: Cryoablation Versus Robotic-Assisted Partial Nephrectomy

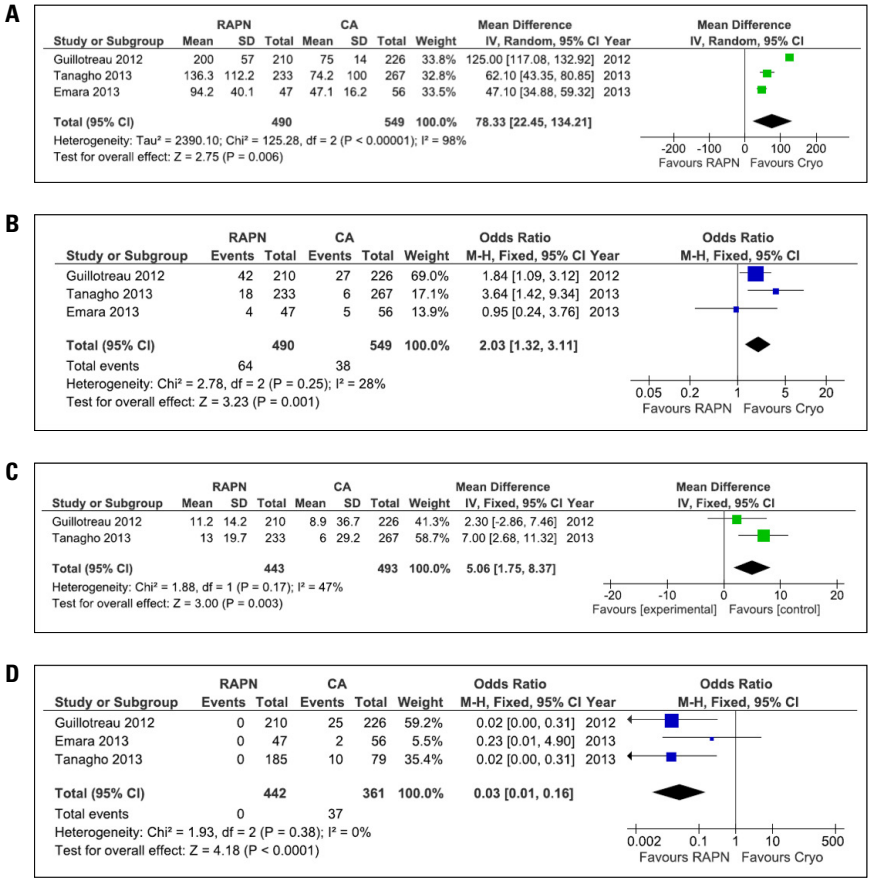

Recently, Weinberg *et al.*[257] reported an analysis of the Nationwide Inpatient Sample, looking at patients undergoing RAPN (n=10,034) or laparoscopic CA (n=4,241). No differences were identified in terms of perioperative complications, transfusion, length of stay, or median cost between the two procedures. On multivariate analysis, sicker patients were more likely to have LCA (OR: 1.34; p=0.048), and they had greater postoperative complications (OR: 3.30; p<0.001).

8.6.2 Comparative analysis between different ablation technologies

8.6.2.1 Cryoablation versus radiofrequency ablation

Two meta-analyses of studies evaluating either CA or RFA for SRMs have been published to date (**Table 8-9**).

TABLE 8-9 Cryoablation Versus Radiofrequency Ablation for Small Renal Masses—Overview of Published Cumulative Analyses

	Kunkle and Uzzo[258]	El Dib *et al.*[259]
No. of studies CA RFA	47 22 25	31 20 11
No. of kidney lesions CA RFA	1,375 600 775	1,007 500 507
Mean patient age, years CA RFA	67.2 66.3 67.8	NR 64 64
Mean tumour size, cm CA RFA	2.6 2.6 2.7	NR 2.5 2.7
Preferred approach, % CA RFA	 Laparoscopic (65) Percutaneous (94)	 Laparoscopic (65)* Percutaneous (71)*
Preablation biopsy rate, % CA RFA	71 82 62	NR
Known RCC pathology, % CA RFA	81 72 90	
Mean follow-up, months CA RFA	18.7 22.5 15.8	NR 17.9 18.1
Repeat ablation rate, % CA RFA	5.3 1.3 8.5	NR
Local progression, % CA RFA	9.5 5.2 12.9	
Metastatic progression, % CA RFA	1.8 1 2.5	

Abbreviations: CA: cryoablation; NR: not reported; RCC: renal cell carcinoma; RFA: radiofrequency ablation.
* Percentage of published studies.
† Clinical efficacy defined as the percentage of tumours treated successfully by the procedure. Successfully treated tumour was defined as no growth or no evidence of recurrence on CT scan or MRI. The following outcomes were considered as clinical efficacy measurements: CSS rate, radiographic success, and no evidence of local tumour progression or distant metastases.

continued on **page 569**

TABLE 8-9 Cryoablation Versus Radiofrequency Ablation for Small Renal Masses—Overview of Published Cumulative Analyses, *Cont'd*

	Kunkle and Uzzo[258]	El Dib *et al.*[259]
Clinical efficacy†, % CA RFA	NR	 89 90
Complication rate, % CA RFA		 19.9 19

Abbreviations: CA: cryoablation; NR: not reported; RCC: renal cell carcinoma; RFA: radiofrequency ablation.
* Percentage of published studies.
† Clinical efficacy defined as the percentage of tumours treated successfully by the procedure. Successfully treated tumour was defined as no growth or no evidence of recurrence on CT scan or MRI. The following outcomes were considered as clinical efficacy measurements: CSS rate, radiographic success, and no evidence of local tumour progression or distant metastases.

Kunkle and Uzzo retrieved and analyzed 47 studies representing 1,375 kidney lesions treated by CA or RFA.[258] No differences were detected between the two modalities in terms of mean patient age, tumour size, or duration of follow-up. Pretreatment biopsy was performed more often for cryoablated lesions (82.3% vs. 62.2%; $p<0.0001$). Repeat ablation was performed more often after RFA (8.5% vs. 1.3%; $p<0.0001$), and local tumour progression was significantly higher for RFA (12.9% vs. 5.2%; $p<0.0001$). Treatment by RFA was found to be correlated with a higher incidence of local tumour progression on both univariate and on multivariate regression analyses. Cryoablation was mostly performed laparoscopically (65%), whereas a percutaneous approach was adopted for the great majority (94%) of RFA treatments. This finding may reflect the fact that urologists have used CA preferentially, whereas RFA has been primarily adopted in interventional radiology suites. Cryoablation results in fewer re-treatments and improved local tumour control, although no significant difference could be detected in terms of progression to metastatic disease.

More recently, El Dib *et al.* reported another proportional meta-analysis with a comprehensive systematic review of 31 uncontrolled studies (case series), including 1,007 treated lesions.[259] Interestingly, those authors used a quite broad definition of *clinical efficacy,* intended as the percentage of tumours treated successfully by the procedure. A *successfully treated tumour* was defined as having no growth or no evidence of recurrence on CT scan or MRI. Thus, the following "traditional" outcomes were considered as measures of clinical efficacy and pooled in the same outcome parameter (specifically created for the purpose of the meta-analysis): CSS rate, radiographic success, and no evidence of local tumour progression or distant metastases. Overall, regardless of reported outcomes, no significant differences in efficacy were found between the two ablation techniques (pooled proportion of clinical efficacy: 89% for cryotherapy vs. 90% for RFA). This finding is in contrast to the previously mentioned meta-analysis by Kunkle and Uzzo.[258] Of note, El Dib *et al.* found significant heterogeneity in the reported oncologic outcomes of the cryotherapy series.[259] The studies differed considerably in their patient selection, baseline disease severity, techniques, management of outcomes, and duration of follow-up. Moreover, the funnel plot for the cryotherapy series suggested the possibility of publication bias. As for the RFA series, there was far less heterogeneity in terms of the clinical efficacy

outcome, which might suggest that the RFA series were far more consistent in patient selection and treatment protocol. The two techniques performed similarly in terms of complication rate (cryotherapy: 19.9%; RFA: 19%). In this case, however, some heterogeneity was found for both techniques.

Our literature search identified four publications comparing CA with RFA—all of them retrospective case-controlled studies—and providing extractable data for meta-analysis (**Table 8-10**).[74,82,260,261] In terms of tumour recurrence/persistence, cryotherapy had a significantly lower rate compared with RFA (OR: 0.48; 95% CI: 0.25–0.93; p=0.03). On the other hand, there seems to be no significant difference in terms of rate of major complications between the two techniques (OR: 1.22; 95% CI: 0.52–2.86; p=0.65).

TABLE 8-10 Cryoablation Versus Radiofrequency Ablation—Published Comparative Series (All Retrospective Case-Control Studies [LOE 3])

Reference	N of cases		Approach		Tumour size, cm		Tumour recurrence/ persistence, %		Major complication rate, %	
	CA	RFA	CA	RFA	CA	RFA	CA	RFA	CA	RFA
Hegarty *et al.*[260]	161	72	LCA	PRFA	2.5	2.5	1.8	11.1	1.8	1.4
Pirasteh *et al.*[261]	70	41	PCA	PRFA	2.2	2.2	7	11	0	0
Atwell *et al.*[82]	189	256	PCA	PRFA	2.3	1.9	2.8*	3.2*	5.1†	4.3†
Thompson *et al.*[74]	187	180	PCA	PRFA	2.9	2.1	1.6	2.7	NR	NR

Abbreviations: CA: cryoablation; LCA: laparoscopic cryoablation; NR: not reported; PCA: percutaneous cryoablation; PRFA: percutaneous radiofrequency ablation; RFA: radiofrequency ablation.
Values expressed as means (unless otherwise specified).
* Calculated based on the cases with minimum 3 months of follow-up.
† Calculated based on the number of procedures.

During extirpative surgery, the pathological specimen can be examined to confirm treatment success. Ablation techniques have relied mostly on radiographic imaging to determine treatment success. Successful tumour ablation has been defined as the absence of contrast enhancement on post-treatment imaging. This is based on the idea that a renal lesion no longer enhances after ablation. As mentioned, Weight *et al.* studied the correlation between post-ablation imaging and post-ablation biopsy findings by studying 109 renal lesion ablated with PRFA and 192 lesions treated with laparoscopic CA.[106] Patients were followed with radiographic imaging and post-ablation biopsy at 6 months. Radiographic success at 6 months was 85% and 90% for RFA and CA, respectively. The rate of pathological success, defined as the lack of malignant/atypical cells on post-ablation biopsy or radical nephrectomy, for RFA and CA was 65% and 94%, respectively (p<0.001). Six of 13 (46.2%) patients with a 6-month positive biopsy after RFA demonstrated no enhancement on post-treatment imaging. For patients treated with CA, all positive biopsies revealed post-treatment enhancement on imaging just before biopsy. The authors concluded that there might be a poor correlation between post-RFA radiographic imaging and post-RFA pathological analysis, considering radiographic images of renal lesions treated with cryotherapy appeared to correlate adequately with corresponding biopsy findings.

The amount of medication used for sedation during percutaneous kidney ablation can be regarded as an important clinical parameter, given that patients undergoing these procedures are generally elderly and at high surgical risk. Allaf *et al.* reported the first study comparing analgesic requirements in a small series of patients undergoing CA (10 patients) or RFA (14 patients) for renal tumours.[262] Cryoablation was associated with a significantly lower dose of fentanyl (75.0 μg vs. 165.0 μg; $p<0.001$) and midazolam (1.6 mg vs. 2.9 mg; $p=0.026$). Moreover, in the RFA group, one patient required general anesthesia, and one patient required supplemental narcotics and sedatives. None of the patients in the CA group required any additional or alternate anesthetics. The authors concluded that percutaneous CA appears to require less analgesia than RFA. Similar findings were more recently reported by Truesdale *et al.* Those authors conducted another retrospective analysis, but on a larger set of patients (PRFA: 71 patients; cryotherapy: 65 patients).[263] They also found RFA to be associated with a significantly higher mean dose of fentanyl (236.43 μg vs. 172.27 μg; $p<0.001$) and higher mean dose of midazolam (4.5 mg vs. 3.27 mg; $p<0.001$). Thus, in their experience, CA was performed with less medication, suggesting that it might be less painful. No further studies have been reported addressing this issue. Therefore, these findings require further investigation.

8.6.2.2 Cryoablation versus microwave ablation

No studies are available where MWA was directly compared with either CA or RFA.

A recent meta-analysis of 51 studies comprising 3,950 kidney lesions treated with either CA or MWA was considered (**Table 8-11**).[185] The mean tumour size was significantly larger in the MWA group than in the CA group (2.58 vs. 3.13 cm, respectively; $p=0.04$). In the MWA studies, a laparoscopic approach was used more often over a percutaneous one, whereas both approaches were adopted to a similar extent in the CA studies. A higher use of pretreatment biopsy was found in the MWA studies. There were no differences in any of the oncologic outcomes, including proportion of tumours without enhancement after a single session, local tumour progression, and CSS. These findings must be interpreted with caution, given the differences in average tumour size, histology, and length of follow-up between groups. Another limitation of this analysis was the difference in the sample size between the two techniques, as the literature on MWA remains limited. Nevertheless, these data suggest no difference in cancer control between the two techniques.

TABLE 8-11 Cryoablation Versus Microwave Ablation for Small Renal Masses—Cumulative Analysis

	Cryoablation	Microwave ablation	*p* values
No. of series	44	7	–
No. of lesions	3,786	164	–
Mean patient age, years	66.9	58.8	0.15
Biopsy rate, %	37.5	85.9	<0.0001
Mean tumour size, cm	2.5	3.1	0.04
Histology, %			
Clear cell	34.9	84.4	<0.001
Papillary	34.9	4.9	<0.001
Chromophobe	13.7	1.4	<0.001
Oncocytoma	13.7	2.8	<0.001
Angiomyolipoma	2.7	6.4	0.03
Type of approach, %			
Laparoscopic	49.2	50.6	0.77
Percutaneous	49.8	37.2	0.002
Open	1	12.2	<0.001
Mean follow-up, months	30.2	17.8	0.07
Primary effectiveness, %	93.7	91.2	0.41
CSS, %	98.2	96.8	0.48
Local progression, %	4	2.5	0.46

Abbreviations: CSS: cancer-specific survival

Adapted from Martin J, Athreya S. Meta-analysis of cryoablation versus microwave ablation for small renal masses: is there a difference in outcome? Diagn Interv Radiol. 2013;19(6):501–507.[185]

8.6.3 Cost analysis

We identified eight studies addressing the timely issue of cost related to the different nephron-sparing treatment options for patients with SRMs by using different methodologies (**Table 8-12**).

TABLE 8-12 Ablation Versus Partial Nephrectomy for Renal Masses—An Overview of Cost Analysis Studies

Reference	Treatments	Methodology	Findings
Lotan *et al.*[266]	OPN vs. LPN vs. PRFA	Direct cost analysis based on actual hospital billing	▪ PRFA is significantly less costly than LPN and OPN. ▪ Cost advantage of >$2,500 is directly related to savings garnered by a short hospital stay (0.5 days) and lower operative costs.
Link *et al.*[264]	OPN vs. LPN vs. LCA vs. PCA	Sensitivity analysis	▪ PCA is 2.2–2.7 times less costly than the other options (cost savings of $3,625–$5,155 per case). ▪ Cryoprobe consumables are responsible for >70% of total cost of PCA. ▪ LCA is more costly than all forms of extirpative surgery if more than two cryoprobes are used. ▪ LCA is no longer cost advantageous over OPN if >4 CT scans are obtained during the first postoperative year or if local recurrence rate >23%.
Bensalah *et al.*[244]	LRFA vs. LPN	Direct cost analysis based on actual hospital billing	▪ No statistically significant difference in terms of cost between LRFA and LPN ($6,103 vs. $6,808; p=0.3). ▪ Main cost component of LRFA is the probe ($1,525). Other related costs (anesthesia, laboratory, operating room, room and board, pharmacy), except radiology, are lower for LRFA.
Pandharipande *et al.*[268]	RFA vs. PN	Cost-effectiveness analysis (Markov model)	▪ PN yields a minimal greater average quality-adjusted life expectancy than RFA (2.5 days), but it is more expensive. ▪ RFA is preferred, and it remains so if the annual probability of post-RFA local recurrence is up to 48% higher than post-PN.
Chang *et al.*[270]	OPN vs. LPN vs. PA vs. LA vs. AS	Cost-effectiveness analysis (Markov model)	▪ Immediate LPN is the preferred nephron-sparing option for healthy patients younger than 74 years old with a SRM. ▪ AS with possible delayed percutaneous ablation is a cost-effective alternative for patients with advanced age or significant comorbidities.
Castle *et al.*[267]	OPN vs. RLPN vs. PRFA vs. LRFA	Cost data analysis	▪ Mean costs of PRFA are 35% of RAPN, 40% of OPN, and 48% of LRFA. ▪ Except for imaging fees, all associated costs are lowest for PRFA.
Bhan *et al.*[271]	AS vs. PRFA vs. PCA	Cost-effectiveness analysis (Markov model)	▪ Dominant (most effective and least costly) strategy is AS with subsequent PCA if needed. ▪ Immediate PCA has a similar life expectancy (3 days fewer), but costs $3,010 more. ▪ Strategies employing PRFA have decreased quality-adjusted life expectancies (82–87 days fewer than the dominant strategy) and higher costs ($3,231–$6,398 more).
Chehab *et al.*[265]	PCA vs. OPN vs. RAPN	Direct cost analysis based on actual hospital billing	▪ PCA can be performed for approximately $5,000 less than OPN, and over $6,400 less than RAPN for tumours of similar size, complexity, and malignancy.

Abbreviations: AS: active surveillance; CT: computed tomography; LA: laparoscopic ablation; LCA: laparoscopic cryoablation; LPN: laparoscopic partial nephrectomy; LRFA: laparoscopic radiofrequency ablation; OPN: open partial nephrectomy; PA: percutaneous ablation; PCA: percutaneous cryoablation; PN: partial nephrectomy; PRFA: percutaneous radiofrequency ablation; RAPN: robot-assisted partial nephrectomy; RFA: radiofrequency ablation; RLPN: robotic-assisted partial nephrectomy; SRM: small renal mass.

Link *et al.* created a mathematical model incorporating procedure-related costs, which were derived from a retrospective review of 317 patients treated at the Johns Hopkins Medical Institutions with different nephron-sparing procedures.[264] Sensitivity analysis showed PCA to be over 2.2 times cheaper than other options (OPN, LPN, LCA), with cryoprobe consumption playing an important role in driving the total cost of the procedure. The authors also explored the issue of cost related to postoperative imaging by extending their model to include 1-year postoperative CT scanning. Interestingly, they found that for percutaneous CA to lose its cost advantage over LPN, more than nine CT scans must be performed during postoperative year 1, which would be an unrealistic scenario. More recently, Chehab *et al.* compared the cost of percutaneous CA to that of open and robotic PN.[265] Total cost was calculated by including the direct costs of procedural and periprocedural variables (operating room, supplies and devices, imaging, anesthesia, recovery room, routine room and board, intensive care unit [ICU] room and board, respiratory care, laboratory and pathology fees, pharmacy, and other costs) as well as additional indirect costs (those coming from non-patient care departments, such as human resources, housekeeping, utilities, etc.). Overall, the mean total cost was lower for percutaneous CA than for open or RAPN ($6,067 vs. $11,392 or $11,830, respectively; $p<.0001$).

Lotan and Cadeddu were the first to report a comparative cost analysis of OPN ($n=16$), LPN ($n=14$), and PRFA ($n=16$).[266] They reviewed detailed cost information of 46 nephron-sparing procedures, and found that, overall, RFA was statistically less costly than LPN and OPN. For the same institution, Bensalah *et al.* compared LPN cases ($n=40$) with LRFA cases ($n=14$) by analyzing direct procedure-related costs, as provided by their hospital billing department.[244] They could not find a statistically significant difference between the procedures. Not surprisingly, the main cost component for RFA was the probe, whereas all other related costs (anesthesia, laboratory, operating room, room and board, pharmacy), except radiology, were lower for RFA. Of note, they did not consider any indirect costs, such as the radiographic follow-up required for LRFA, or the financial effects of the loss of work. More recently, Castle *et al.* analyzed data related to the surgical costs, the associated hospital stay, and the 6-month postoperative period of different nephron-sparing procedures offered at their institution.[267] Multivariable linear regression showed surgical approach ($p=0.007$), length of stay ($p<0.001$), and operating room time ($p<0.001$) to be significant predictors of total cost. Overall, they found the 6-month cost to be the lowest with RFA (either approach) compared with both RLPN and OPN. In another study using a decision-analytic Markov model, Pandharipande *et al.* evaluated the relative cost-effectiveness of PRFA versus PN in patients with small RCC.[268] Using base-case assumptions, PN yielded a minimal greater than average, quality-adjusted life expectancy than RFA (2.5 days), but was more expensive. Therefore, RFA was considered preferred, and remained so if the annual probability of post-RFA local recurrence was up to 48% higher relative to that post-PN.

Active surveillance has become part of the standard discussion for management options of SRMs.[269] Given its recent adoption and clinical implementation, comparative outcome analyses of this conservative approach versus ablation techniques are very limited. Chang *et al.* developed a decision-analytic Markov model estimating the costs and health outcomes of treating a healthy 65-year-old patient with an asymptomatic, unilateral SRM using competing nephron-sparing options (i.e. OPN, LPN, ablation), AS with possible delayed intervention, and nonsurgical management with observation.[270] In this case scenario, the least costly option was observation, and the optimal option was immediate LPN, which had an incremental cost-effectiveness ratio of $36,645 per quality-adjusted life-year gained compared with surveillance with possible delayed percutaneous ablation.

Using the same methodology, Bhan *et al.* also reported a cost-utility analysis to determine the optimal management strategy for an average 67-year-old, poor surgical candidate (i.e. non-amenable to PN) with an SRM.[271] A decision-analytic Markov model was developed from the perspective of a third-party payer to compare quality-adjusted life expectancy and lifetime costs. The dominant strategy (most effective and least costly) was AS with subsequent CA if needed. Strategies that employed RFA decreased quality-adjusted life expectancies (82–87 days fewer than the dominant strategy) and resulted in higher costs ($3,231–$6,398 more).

8.7 Recommendations and Statements

	LOE	GOR
CA is an effective treatment in selected patients with cT1a kidney tumours.	2c	B
RFA is an effective treatment in selected patients with SRMs, with the best efficacy in tumours of up to 3 cm.	2c	B
There is level 2b evidence that MWA is as effective as PN at midterm in cT1a kidney tumours. However, in view of this evidence being based solely on an RCT and the lack of long-term efficacy outcomes, the panel considers MWA for kidney tumours to be indicated only when CA or RFA are dismissed.	3	C
IRE cannot be recommended currently as standard ablation technology for cT1a kidney tumours outside of clinical investigational protocols.	4	C
CyberKnife, HIFU, and PDT cannot be recommended as standard ablation technology for cT1a kidney tumours outside of clinical investigational protocols.	4	D
Currently, there is no integrated system applicable in practice to better target the lesion than CT or US.	4	NA
In cT1a kidney tumours, no differences exist for perioperative complications or midterm/long-term clinical efficacy between CA and RFA.	2	NA
CA and RFA preserve post-procedural renal function better than PN. However, there are no differences in renal function preservation at midterm/long term.	3	NA
There is evidence that local recurrence is higher after CA or RFA than after PN.	2a	NA
There is evidence that the perioperative complication rate is lower after CA or RFA than after PN.	2a	NA
Cost-efficacy studies and artificial neural models estimate the cost of CA and RFA to be lower than PN.	3	NA

Abbreviations: CA: cryoablation; CT: computed tomography; GOR: Grade of Recommendation; HIFU: high-intensity focused ultrasound; IRE: irreversible electroporation; LOE: Level of Evidence; MWA: microwave ablation; NA: not applicable; PDT: photodynamic therapy; PN: partial nephrectomy; RCT: randomized controlled trial; RFA: radiofrequency ablation; SRM: small renal mass; US: ultrasound.

8.8 Acknowledgements

Claudia Gasch, Alfred Franz and Tobias Simpfendorfer of the University of Heidelberg for their contribution to the section “Targeting the lesion.”

8.9 References

1. Hollingsworth JM, Miller DC, Daignault S, *et al.* Rising incidence of small renal masses: a need to reassess treatment effect. *J Natl Cancer Inst.* 2006;98(18):1331–1334.
2. Russo P. Renal cell carcinoma: presentation, staging, and surgical treatment. *Semin Oncol.* 2000;27(2):160–176.
3. McKiernan JM, Yossepowitch O, Kattan MW, *et al.* Partial nephrectomy for renal cortical tumors: pathologic findings and impact on outcome. *Urology.* 2002;60(6):1003–1009.
4. Dechet CB, Zincke H, Sebo TJ, *et al.* Prospective analysis of computerized tomography and needle biopsy with permanent sectioning to determine the nature of solid renal masses in adults. *J Urol.* 2003;169(1):71–74.
5. Kassouf W, Aprikian AG, Laplante M, *et al.* Natural history of renal masses followed expectantly. *J Urol.* 2004;171(1):111–113.
6. McKiernan J, Simmons R, Katz J, *et al.* Natural history of chronic renal insufficiency after partial and radical nephrectomy. *Urology.* 2002;59(6):816–820.
7. Leibovich BC, Blute M, Cheville JC, *et al.* Nephron sparing surgery for appropriately selected renal cell carcinoma between 4 and 7 cm results in outcome similar to radical nephrectomy. *J Urol.* 2004;171(3):1066–1070.
8. Campbell SC, Novick AC, Belldegrun A, *et al.* Guideline for management of the clinical T1 renal mass. *J Urol.* 2009;182(4):1271–1279.
9. European Association of Urology. Oncology guidelines: renal cell carcinoma. 2016. http://uroweb.org/guideline/renal-cell-carcinoma/; Accessed: March 1, 2016.
10. Breau RH, Crispen PL, Jenkins SM, *et al.* Treatment of patients with small renal masses: a survey of the American Urological Association. *J Urol.* 2011;185(2):407–413.
11. Millman AL, Pace KT, Ordon M, *et al.* Surgeon-specific factors affecting treatment decisions among Canadian urologists in the management of pT1a renal tumours. *Can Urol Assoc J.* 2014;8(5-6):183–189.
12. Abrams P, Khoury S. International Consultation on Urological Diseases: Evidence-based medicine overview of the main steps for developing and grading guideline recommendations. *Neurol Urodyn.* 2010;29(1):116–118.
13. Hozo SP, Djulbegovic B, Hozo I. Estimating the mean and variance from the median, range, and the size of a sample. *BMC Med Res Methodol.* 2005;5:13.
14. Gage AA, Baust JM, Baust JG. Experimental cryosurgery investigations in vivo. *Cryobiology.* 2009;59(3):229–243.
15. Clarke DM, Robilotto AT, Rhee E, *et al.* Cryoablation of renal cancer: variables involved in freezing-induced cell death. *Technol Cancer Res Treat.* 2007;6(2):69–79.
16. Gage AA, Baust J. Mechanisms of tissue injury in cryosurgery. *Cryobiology.* 1998;37(3):171–186.
17. Hong JS, Rubinsky B. Patterns of ice formation in normal and malignant breast tissue. *Cryobiology.* 1994;31(2):109–120.
18. Klossner DP, Robilotto AT, Clarke DM, *et al.* Cryosurgical technique: assessment of the fundamental variables using human prostate cancer model systems. *Cryobiology.* 2007;55(3):189–199.
19. Baust JG, Gage AA. Progress toward optimization of cryosurgery. *Technol Cancer Res Treat.* 2004;3(2):95–101.
20. Baust JG, Gage AA, Clarke D, *et al.* Cryosurgery--a putative approach to molecular-based optimization. *Cryobiology.* 2004;48(2):190–204.
21. Hoffmann NE, Bischof JC. The cryobiology of cryosurgical injury. *Urology.* 2002;60(2 Suppl 1):40–49.
22. Hollister WR, Mathew AJ, Baust JG, *et al.* Effects of freezing on cell viability and mechanisms of cell death in a human prostate cell line. *Mol Urol.* 1998;2:13–18.
23. Clarke DM, Baust JM, Van Buskirk RG, *et al.* Chemo-cryo combination therapy: an adjunctive model for the treatment of prostate cancer. *Cryobiology.* 2001;42(4):274–285.
24. Clarke DM, Baust JM, Van Buskirk RG, *et al.* Addition of anticancer agents enhances freezing-induced prostate cancer cell death: implications of mitochondrial involvement. *Cryobiology.* 2004;49(1):45–61.

25. Robilotto AT, Baust JM, Van Buskirk RG, *et al.* Temperature-dependent activation of differential apoptotic pathways during cryoablation in a human prostate cancer model. *Prostate Cancer Prostatic Dis.* 2013;16(1):41–49.

26. Yang WL, Addona T, Nair DG, *et al.* Apoptosis induced by cryo-injury in human colorectal cancer cells is associated with mitochondrial dysfunction. *Int J Cancer.* 2003;103(3):360–369.

27. Sabel MS, Su G, Griffith KA, *et al.* Rate of freeze alters the immunologic response after cryoablation of breast cancer. *Ann Surg Oncol.* 2010;17(4):1187–1193.

28. Gill IS, Novick AC, Meraney AM, *et al.* Laparoscopic renal cryoablation in 32 patients. *Urology.* 2000;56(5):748–753.

29. Cestari A, Guazzoni G, dell'Acqua V, *et al.* Laparoscopic cryoablation of solid renal masses: intermediate term followup. *J Urol.* 2004;172(4 Pt 1):1267–1270.

30. Shingleton WB, Sewell PE Jr. Percutaneous renal tumor cryoablation with magnetic resonance imaging guidance. *J Urol.* 2001;165(3):773–776.

31. Atwell TD, Farrell MA, Leibovich BC, *et al.* Percutaneous renal cryoablation: experience treating 115 tumors. *J Urol.* 2008;179(6):2136–2140.

32. Long CJ, Canter DJ, Smaldone MC, *et al.* Role of tumor location in selecting patients for percutaneous versus surgical cryoablation of renal masses. *Can J Urol.* 2012;19(5):6417–6422.

33. Ahmed M, Solbiati L, Brace CL, *et al.* Image-guided tumor ablation: standardization of terminology and reporting criteria--a 10-year update. *Radiology.* 2014;273(1):241–260.

34. National Cancer Institute. *NCI Dictionary of Cancer Terms.* 2015. http://www.cancer.gov/publications/dictionaries/cancer-terms?cdrid=559442; Accessed: January 5, 2016.

35. Atwell TD, Carter RE, Schmit GD, *et al.* Complications following 573 percutaneous renal radiofrequency and cryoablation procedures. *J Vasc Interv Radiol.* 2012;23(1):48–54.

36. Dindo D, Demartines N, Clavien PA. Classification of surgical complications: a new proposal with evaluation in a cohort of 6336 patients and results of a survey. *Ann Surg.* 2004;240(2):205–213.

37. Okhunov Z, Shapiro EY, Moreira DM, *et al.* R.E.N.A.L. nephrometry score accurately predicts complications following laparoscopic renal cryoablation. *J Urol.* 2012;188(5):1796–1800.

38. Sidana A, Aggarwal P, Feng Z, *et al.* Complications of renal cryoablation: a single center experience. *J Urol.* 2010;184(1):42–47.

39. Burke DR, Lewis CA, Cardella JF, *et al.* Quality improvement guidelines for percutaneous transhepatic cholangiography and biliary drainage. *J Vasc Interv Radiol.* 2003;14(9 Pt 2):S243–246.

40. Clark TW, Millward SF, Gervais DA, *et al.* Reporting standards for percutaneous thermal ablation of renal cell carcinoma. *J Vasc Interv Radiol.* 2009;20(7 Suppl):S409–416.

41. Saliken JC, McKinnon JG, Gray R. CT for monitoring cryotherapy. *AJR Am J Roentgenol.* 1996;166(4):853–855.

42. Camacho JC, Kokabi N, Xing M, *et al.* R.E.N.A.L. (Radius, exophytic/endophytic, nearness to collecting system or sinus, anterior/posterior, and location relative to polar lines) nephrometry score predicts early tumor recurrence and complications after percutaneous ablative therapies for renal cell carcinoma: a 5-year experience. *J Vasc Interv Radiol.* 2015;26(5):686–693.

43. Goyal J, Verma P, Sidana A, *et al.* Single-center comparative oncologic outcomes of surgical and percutaneous cryoablation for treatment of renal tumors. *J Endourol.* 2012;26(11):1413–1419.

44. Klatte T, Mauermann J, Heinz-Peer G, *et al.* Perioperative, oncologic, and functional outcomes of laparoscopic renal cryoablation and open partial nephrectomy: a matched pair analysis. *J Endourol.* 2011;25(6):991–997.

45. Breen DJ, Bryant TJ, Abbas A, *et al.* Percutaneous cryoablation of renal tumours: outcomes from 171 tumours in 147 patients. *BJU Int.* 2013;112(6):758–765.

46. Georgiades CS, Rodriguez R. Efficacy and safety of percutaneous cryoablation for stage 1A/B renal cell carcinoma: results of a prospective, single-arm, 5-year study. *Cardiovasc Intervent Radiol.* 2014;37(6):1494–1499.

47. Moynagh MR, Schmit GD, Thompson RH, *et al.* Percutaneous Cryoablation of Clinical T2 (> 7 cm) Renal Masses: Technical Considerations, Complications, and Short-Term Outcomes. *J Vasc Interv Radiol.* 2015;26(6):800–806.

48. Strom KH, Derweesh I, Stroup SP, *et al.* Second prize: Recurrence rates after percutaneous and laparoscopic renal cryoablation of small renal masses: does the approach make a difference? *J Endourol*. 2011;25(3):371–375.

49. Wright AD, Turk TM, Nagar MS, *et al.* Endophytic lesions: a predictor of failure in laparoscopic renal cryoablation. *J Endourol*. 2007;21(12):1493–1496.

50. Rosenberg MD, Kim CY, Tsivian M, *et al.* Percutaneous cryoablation of renal lesions with radiographic ice ball involvement of the renal sinus: analysis of hemorrhagic and collecting system complications. *AJR Am J Roentgenol*. 2011;196(4):935–939.

51. Buy X, Lang H, Garnon J, *et al.* Percutaneous renal cryoablation: prospective experience treating 120 consecutive tumors. *AJR Am J Roentgenol*. 2013;201(6):1353–1361.

52. Finley DS, Beck S, Box G, *et al.* Percutaneous and laparoscopic cryoablation of small renal masses. *J Urol*. 2008;180(2):492–498.

53. Schwartz BF, Rewcastle JC, Powell T, *et al.* Cryoablation of small peripheral renal masses: a retrospective analysis. *Urology.* 2006;68(1 Suppl):14–18.

54. Laguna MP, Beemster P, Kumar V, *et al.* Perioperative morbidity of laparoscopic cryoablation of small renal masses with ultrathin probes: a European multicentre experience. *Eur Urol.* 2009;56(2):355–361.

55. Welch BT, Brinjikji W, Schmit GD, *et al.* Evaluation of the charges, safety, and mortality of percutaneous renal thermal ablation using the nationwide inpatient sample. *J Vasc Interv Radiol.* 2015;26(3):342–347.

56. Tsivian M, Chen VH, Kim CY, *et al.* Complications of laparoscopic and percutaneous renal cryoablation in a single tertiary referral center. *Eur Urol.* 2010;58(1):142–147.

57. Bandi G, Wen CC, Hedican SP, *et al.* Cryoablation of small renal masses: assessment of the outcome at one institution. *BJU Int.* 2007;100(4):798–801.

58. Derweesh IH, Malcolm JB, Diblasio CJ, *et al.* Single center comparison of laparoscopic cryoablation and CT-guided percutaneous cryoablation for renal tumors. *J Endourol*. 2008;22(11):2461–2467.

59. Kim EH, Tanagho YS, Bhayani SB, *et al.* Percutaneous cryoablation of renal masses: Washington University experience of treating 129 tumours. *BJU Int.* 2013;111(6):872–879.

60. Malcolm JB, Berry TT, Williams MB, *et al.* Single center experience with percutaneous and laparoscopic cryoablation of small renal masses. *J Endourol.* 2009;23(6):907–911.

61. Schmit GD, Thompson RH, Kurup AN, *et al.* Usefulness of R.E.N.A.L. nephrometry scoring system for predicting outcomes and complications of percutaneous ablation of 751 renal tumors. *J Urol.* 2013;189(1):30–35.

62. Sisul DM, Liss MA, Palazzi KL, *et al.* RENAL nephrometry score is associated with complications after renal cryoablation: a multicenter analysis. *Urology.* 2013;81(4):775–780.

63. Blute ML Jr, Okhunov Z, Moreira DM, *et al.* Image-guided percutaneous renal cryoablation: preoperative risk factors for recurrence and complications. *BJU Int.* 2013;111(4 Pt B):E181–185.

64. Schmit GD, Schenck LA, Thompson RH, *et al.* Predicting renal cryoablation complications: new risk score based on tumor size and location and patient history. *Radiology.* 2014;272(3):903–910.

65. Lai WJ, Chung HJ, Chen CK, *et al.* Percutaneous computed tomography-guided cryoablation for renal tumor: Experience in 30 cases. *J Chin Med Assoc.* 2015;78(5):308–315.

66. Spreafico C, Nicolai N, Lanocita R, *et al.* CT-guided percutaneous cryoablation of renal masses in selected patients. *Radiol Med.* 2012;117(4):593–605.

67. Johnson S, Pham KN, See W, *et al.* Laparoscopic cryoablation for clinical stage T1 renal masses: long-term oncologic outcomes at the Medical College of Wisconsin. *Urology.* 2014;84(3):613–618.

68. Larcher A, Fossati N, Mistretta F, *et al.* Long-term oncologic outcomes of laparoscopic renal cryoablation as primary treatment for small renal masses. *Urol Oncol.* 2015;33(1):22.e1–9.

69. Ralls PW, Barakos JA, Kaptein EM, *et al.* Renal biopsy-related hemorrhage: frequency and comparison of CT and sonography. *J Comput Assist Tomogr.* 1987;11(6):1031–1034.

70. Littrup PJ, Ahmed A, Aoun HD, *et al.* CT-guided percutaneous cryotherapy of renal masses. *J Vasc Interv Radiol.* 2007;18(3):383–392.

71. Hinshaw JL, Shadid AM, Nakada SY, *et al.* Comparison of percutaneous and laparoscopic cryoablation for the treatment of solid renal masses. *AJR Am J Roentgenol*. 2008;191(4):1159–1168.

72. Hartman JB, Bhojwani N, Corn DJ, *et al.* Incidence of hypercoagulable events after image-guided percutaneous cryoablation of renal tumors: a single-center experience. *J Vasc Interv Radiol*. 2014;25(5):776–779.

73. Uchida M, Imaide Y, Sugimoto K, *et al.* Percutaneous cryosurgery for renal tumours. *Br J Urol*. 1995;75(2):132–137.

74. Thompson RH, Atwell T, Schmit G, *et al.* Comparison of partial nephrectomy and percutaneous ablation for cT1 renal masses. *Eur Urol*. 2015;67(2):252–259.

75. Park SH, Kang SH, Ko YH, *et al.* Cryoablation for endophytic renal cell carcinoma: intermediate-term oncologic efficacy and safety. *Korean J Urol*. 2010;51(8):518–524.

76. Littrup PJ, Jallad B, Vorugu V, *et al.* Lethal isotherms of cryoablation in a phantom study: effects of heat load, probe size, and number. *J Vasc Interv Radiol*. 2009;20(10):1343–1351.

77. Kim HK, Pyun JH, Kim JY, *et al.* Renal cryoablation of small renal masses: a Korea University experience. *Korean J Urol*. 2015;56(2):117–124.

78. Schmit GD, Thompson RH, Kurup AN, *et al.* Percutaneous cryoablation of solitary sporadic renal cell carcinomas. *BJU Int*. 2012;110(11 Pt B):E526–531.

79. Beemster PW, Barwari K, Mamoulakis C, *et al.* Laparoscopic renal cryoablation using ultrathin 17-gauge cryoprobes: mid-term oncological and functional results. *BJU Int*. 2011;108(4):577–582.

80. Veltri A, Gazzera C, Busso M, *et al.* T1a as the sole selection criterion for RFA of renal masses: randomized controlled trials versus surgery should not be postponed. *Cardiovasc Intervent Radiol*. 2014;37(5):1292–1298.

81. Wah TM, Irving HC, Gregory W, *et al.* Radiofrequency ablation (RFA) of renal cell carcinoma (RCC): experience in 200 tumours. *BJU Int*. 2014;113(3):416–428.

82. Atwell TD, Schmit GD, Boorjian SA, *et al.* Percutaneous ablation of renal masses measuring 3.0 cm and smaller: comparative local control and complications after radiofrequency ablation and cryoablation. *AJR Am J Roentgenol*. 2013;200(2):461–466.

83. Kim EH, Tanagho YS, Saad NE, *et al.* Comparison of laparoscopic and percutaneous cryoablation for treatment of renal masses. *Urology*. 2014;83(5):1081–1087.

84. Yoost TR, Clarke HS, Savage SJ. Laparoscopic cryoablation of renal masses: which lesions fail? *Urology*. 2010;75(2):311–314.

85. Turna B, Kaouk JH, Frota R, *et al.* Minimally invasive nephron sparing management for renal tumors in solitary kidneys. *J Urol*. 2009;182(5):2150–2157.

86. Tanagho YS, Bhayani SB, Kim EH, *et al.* Renal cryoablation versus robot-assisted partial nephrectomy: Washington University long-term experience. *J Endourol*. 2013;27(12):1477–1486.

87. Salas N, Castle SM, Leveillee RJ. Radiofrequency ablation for treatment of renal tumors: technological principles and outcomes. *Expert Rev Med Devices*. 2011;8(6):695–707.

88. Nahum Goldberg S, Dupuy DE. Image-guided radiofrequency tumor ablation: challenges and opportunities--part I. *J Vasc Interv Radiol*. 2001;12(9):1021–1032.

89. Goldberg SN, Gazelle GS, Mueller PR. Thermal ablation therapy for focal malignancy: a unified approach to underlying principles, techniques, and diagnostic imaging guidance. *AJR Am J Roentgenol*. 2000;174(2):323–331.

90. Best SL, Park SK, Youssef RF, *et al.* Long-term outcomes of renal tumor radio frequency ablation stratified by tumor diameter: size matters. *J Urol*. 2012;187(4):1183–1189.

91. Levinson AW, Su LM, Agarwal D, *et al.* Long-term oncological and overall outcomes of percutaneous radio frequency ablation in high risk surgical patients with a solitary small renal mass. *J Urol*. 2008;180(2):499–504.

92. Ferakis N, Bouropoulos C, Granitsas T, *et al.* Long-term results after computed-tomography-guided percutaneous radiofrequency ablation for small renal tumors. *J Endourol*. 2010;24(12):1909–1913.

93. Zagoria RJ, Traver MA, Werle DM, *et al.* Oncologic efficacy of CT-guided percutaneous radiofrequency ablation of renal cell carcinomas. *AJR Am J Roentgenol*. 2007;189(2):429–436.

94. Takaki H, Soga N, Kanda H, *et al.* Radiofrequency ablation versus radical nephrectomy: clinical outcomes for stage T1b renal cell carcinoma. *Radiology.* 2014;270(1):292–299.

95. Leveillee RJ, Castle SM, Gorbatiy V, *et al.* Oncologic outcomes using real-time peripheral thermometry-guided radiofrequency ablation of small renal masses. *J Endourol.* 2013;27(4):480–489.

96. Modabber M, Martin J, Athreya S. Thermal versus impedance-based ablation of renal cell carcinoma: a meta-analysis. *Cardiovasc Intervent Radiol.* 2014;37(1):176–185.

97. Chang X, Liu T, Zhang F, J *et al.* Radiofrequency ablation versus partial nephrectomy for clinical T1a renal-cell carcinoma: long-term clinical and oncologic outcomes based on a propensity score analysis. *J Endourol.* 2015;29(5):518–525.

98. Lorber G, Glamore M, Doshi M, *et al.* Long-term oncologic outcomes following radiofrequency ablation with real-time temperature monitoring for T1a renal cell cancer. *Urol Oncol.* 2014;32(7):1017–1023.

99. Karam JA, Ahrar K, Vikram R, *et al.* Radiofrequency ablation of renal tumours with clinical, radiographical and pathological results. *BJU Int.* 2013;111(6):997–1005.

100. Ma Y, Bedir S, Cadeddu JA, *et al.* Long-term outcomes in healthy adults after radiofrequency ablation of T1a renal tumours. *BJU Int.* 2014;113(1):51–55.

101. Gupta A, Raman JD, Leveillee RJ, *et al.* General anesthesia and contrast-enhanced computed tomography to optimize renal percutaneous radiofrequency ablation: multi-institutional intermediate-term results. *J Endourol.* 2009;23(7):1099–1105.

102. Carrafiello G, Laganà D, Ianniello A, *et al.* Percutaneous radiofrequency thermal ablation of renal cell carcinoma: is it possible a day-hospital treatment? *Inter J Surg.* 2008;(6 Suppl 1):S31–35.

103. Gervais DA, McGovern FJ, Arellano RS, *et al.* Radiofrequency ablation of renal cell carcinoma: part 1, Indications, results, and role in patient management over a 6-year period and ablation of 100 tumors. *AJR Am J Roentgenol.* 2005;185(1):64–71.

104. Su Li, Jarrett TW, Chan DY, *et al.* Percutaneous computed tomography-guided radiofrequency ablation of renal masses in high surgical risk patients: preliminary results. *Urology.* 2003;61(4 Suppl 1):26–33.

105. Psutka SP, Feldman AS, McDougal WS, *et al.* Long-term oncologic outcomes after radiofrequency ablation for T1 renal cell carcinoma. *Eur Urol.* 2013;63(3):486–492.

106. Weight CJ, Kaouk JH, Hegarty NJ, *et al.* Correlation of radiographic imaging and histopathology following cryoablation and radio frequency ablation for renal tumors. *J Urol.* 2008;179(4):1277–1281.

107. Raman JD, Stern JM, Zeltser I, *et al.* Absence of viable renal carcinoma in biopsies performed more than 1 year following radio frequency ablation confirms reliability of axial imaging. *J Urol.* 2008;179(6):2142–2145.

108. Wah TM, Irving HC, Gregory W, *et al.* Radiofrequency ablation (RFA) of renal cell carcinoma (RCC): experience in 200 tumours. *BJU Int.* 2014;113(3):416–428.

109. Tracy CR, Raman JD, Donnally C, *et al.* Durable oncologic outcomes after radiofrequency ablation: experience from treating 243 small renal masses over 7.5 years. *Cancer.* 2010;116(13):3135–3142.

110. Gahan JC, Richter MD, Seideman CA, *et al.* The performance of a modified RENAL nephrometry score in predicting renal mass radiofrequency ablation success. *Urology.* 2015;85(1):125–129.

111. Omary RA, Bettmann MA, Cardella JF, *et al.* Quality improvement guidelines for the reporting and archiving of interventional radiology procedures. *J Vasc Interv Radiol.* 2003;14(9 Pt 2):S293–295.

112. Seideman CA, Gahan J, Weaver M, *et al.* Renal tumour nephrometry score does not correlate with the risk of radiofrequency ablation complications. *BJU Int.* 2013;112(8):1121–1124.

113. Chang X, Ji C, Zhao X, *et al.* The application of R.E.N.A.L. nephrometry scoring system in predicting the complications after laparoscopic renal radiofrequency ablation. *J Endourol.* 2014;28(4):424–429.

114. Johnson DB, Solomon SB, Su LM, *et al.* Defining the complications of cryoablation and radio frequency ablation of small renal tumors: a multi-institutional review. *J Urol.* 2004;172(3):874–877.

115. Cantwell CP, Wah TM, Gervais DA, *et al.* Protecting the ureter during radiofrequency ablation of renal cell cancer: a pilot study of retrograde pyeloperfusion with cooled dextrose 5% in water. *J Vasc Interv Radiol.* 2008;19(7):1034–1040.

116. Farrell MA, Charboneau JW, Callstrom MR, *et al.* Paranephric water instillation: a technique to prevent bowel injury during percutaneous renal radiofrequency ablation. *AJR Am J Roentgenol.* 2003;181(5):1315–1317.

117. Kutikov A, Uzzo RG. The R.E.N.A.L. nephrometry score: a comprehensive standardized system for quantitating renal tumor size, location and depth. *J Urol.* 2009;182(3):844–853.

118. Lay AH, Faddegon S, Olweny EO, *et al.* Oncologic Efficacy of Radio Frequency Ablation for Small Renal Masses: Clear Cell vs Papillary Subtype. *J Urol.* 2015; 194(3):653–657.

119. McDougal WS, Gervais DA, McGovern FJ, *et al.* Long-term followup of patients with renal cell carcinoma treated with radio frequency ablation with curative intent. *J Urol.* 2005;174(1):61–63.

120. Matin SF, Ahrar K, Cadeddu JA, *et al.* Residual and recurrent disease following renal energy ablative therapy: a multi-institutional study. *J Urol.* 2006;176(5):1973–1977.

121. Nguyen CT, Lane BR, Kaouk JH, *et al.* Surgical salvage of renal cell carcinoma recurrence after thermal ablative therapy. *J Urol.* 2008;180(1):104–109.

122. Krokidis M, Spiliopoulos S, Jarzabek M, *et al.* Percutaneous radiofrequency ablation of small renal tumours in patients with a single functioning kidney: long-term results. *Eur Radiol.* 2013;23(7):1933–1939.

123. Ofude M, Kitagawa Y, Koda W, *et al.* Preserved renal function after percutaneous radiofrequency ablation for renal tumors: experience of a single institution. *Anticancer Res.* 2013;33(10):4669–4673.

124. Pieper CC, Fischer S, Strunk H, *et al.* Percutaneous CT-Guided Radiofrequency Ablation of Solitary Small Renal Masses: A Single Center Experience. *Rofo.* 2015;187(7):577–583.

125. Raman JD, Raj GV, Lucas SM, *et al.* Renal functional outcomes for tumours in a solitary kidney managed by ablative or extirpative techniques. *BJU Int.* 2010;105(4):496–500.

126. Simmons MN, Fergany AF, Campbell SC. Effect of parenchymal volume preservation on kidney function after partial nephrectomy. *J Urol.* 2011;186(2):405–410.

127. Woldu SL, Thoreson GR, Okhunov Z, *et al.* Comparison of Renal Parenchymal Volume Preservation Between Partial Nephrectomy, Cryoablation, and Radiofrequency Ablation Using 3D Volume Measurements. *J Endourol.* 2015;29(8):948–955.

128. Delahunt B, Samaratunga H, Martignoni G, *et al.* Percutaneous renal tumour biopsy. *Histopathology.* 2014;65(3):295–308.

129. Baumhauer M, Feuerstein M, Meinzer HP, *et al.* Navigation in endoscopic soft tissue surgery: perspectives and limitations. *J Endourol.* 2008;22(4):751–766.

130. de la Rosette J, Assimos D, Desai M, *et al.* The Clinical Research Office of the Endourological Society Percutaneous Nephrolithotomy Global Study: indications, complications, and outcomes in 5803 patients. *J Endourol.* 2011;25(1):11–17.

131. Khati NJ, Gorodenker J, Hill MC. Ultrasound-guided biopsies of the abdomen. *Ultrasound Q.* 2011;27(4):255–268.

132. Minami Y, Kitai S, Kudo M. Treatment response assessment of radiofrequency ablation for hepatocellular carcinoma: usefulness of virtual CT sonography with magnetic navigation. *Eur J Radiol.* 2012;81(3):e277–280.

133. Franz AM, Haidegger T, Birkfellner W, *et al.* Electromagnetic tracking in medicine--a review of technology, validation, and applications. *IEEE Trans Med Imaging.* 2014;33(8):1702–1725.

134. Di Mauro E, Solbiati M, De Beni S, *et al.* Virtual navigator real-time ultrasound fusion imaging with positron emission tomography for liver interventions. *Conf Proc IEEE Eng Med Biol Soc.* 2013;2013:1406–1409.

135. Mauri G, De Beni S, Forzoni L, *et al.* Virtual navigator automatic registration technology in abdominal application. *Conf Proc IEEE Eng Med Biol Soc.* 2014;2014:5570–5574.

136. Nouranian S, Mahdavi SS, Spadinger I, *et al.* An automatic multi-atlas segmentation of the prostate in transrectal ultrasound images using pairwise atlas shape similarity. *Med Image Comput Comput Assist Interv.* 2013;16(Pt 2):173–180.

137. Haber GP, Colombo JR, Remer E, *et al.* Synchronized real-time ultrasonography and three-dimensional computed tomography scan navigation during percutaneous renal cryoablation in a porcine model. *J Endourol.* 2010;24(3):333–337.

138. Hung AJ, Ma Y, Zehnder P, *et al.* Percutaneous radiofrequency ablation of virtual tumours in canine kidney using Global Positioning System-like technology. *BJU Int.* 2012;109(9):1398–1403.

139. Slabaugh TK, Machaidze Z, Hennigar R, *et al.* Monitoring radiofrequency renal lesions in real time using contrast-enhanced ultrasonography: a porcine model. *J Endourol.* 2005;19(5):579–583.

140. Ukimura O, Mitterberger M, Okihara K, *et al.* Real-time virtual ultrasonographic radiofrequency ablation of renal cell carcinoma. *BJU Int.* 2008;101(6):707–711.

141. Mercier L, Langø T, Lindseth F, *et al.* A review of calibration techniques for freehand 3-D ultrasound systems. *Ultrasound Med Biol.* 2005;31(4):449–471.

142. Hsu PW, Prager RW, Gee AH, *et al.* Freehand 3D ultrasound calibration: a review, in Sensen CW, Hallgrimsson B (Ed): *Advanced Imaging in Biology and Medicine: Technology, Software Environments, Applications*. Berlin, Springer-Verlag, 2009, pp 47–84.

143. Birth M, Iblher P, Hildebrand P, *et al.* Ultrasound-guided interventions using magnetic field navigation. First experiences with Ultra-Guide 2000 under operative conditions. *Ultraschall Med.* 2003;24(2):90–95. [Article in German]

144. Sindram D, Swan RZ, Lau KN, *et al.* Real-time three-dimensional guided ultrasound targeting system for microwave ablation of liver tumours: a human pilot study. *HPB (Oxford).* 2011;13(3):185–191.

145. März K, Franz AM, Seitel A, *et al.* Interventional real-time ultrasound imaging with an integrated electromagnetic field generator. *Int J Comput Assist Radiol Surg.* 2014;9(5):759–768.

146. Stolka PJ, Foroughi P, Rendina M, *et al.* Needle guidance using handheld stereo vision and projection for ultrasound-based interventions. *Med Image Comput Comput Assist Interv.* 2014;17(Pt 2):684–691.

147. Nöldge G, Richter GM, Grenacher L, *et al.* CT-guided puncture. *Radiologe.* 1996;36(9):683–691. [Article in German]

148. Binder N, Matthäus L, Burgkart R, *et al.* A robotic C-arm fluoroscope. *Int J Med Robot.* 2005;1(3):108–116.

149. Akpek S, Brunner T, Benndorf G, *et al.* Three-dimensional imaging and cone beam volume CT in C-arm angiography with flat panel detector. *Diagn Interv Radiol.* 2005;11(1):10–13.

150. Ritter M, Rassweiler MC, Häcker A, *et al.* Laser-guided percutaneous kidney access with the Uro Dyna-CT: first experience of three-dimensional puncture planning with an ex vivo model. *World J Urol.* 2013;31(5):1147–1151.

151. Ritter M, Rassweiler MC, Michel MS. The Uro Dyna-CT Enables Three-dimensional Planned Laser-guided Complex Punctures. *Eur Urol.* 2015;68:880–884.

152. Ball MW, Bezerra SM, Gorin MA, *et al.* Grade heterogeneity in small renal masses: potential implications for renal mass biopsy. *J Urol.* 2015;193(1):36–40.

153. Jewett MA, Finelli A. Kidney cancer: Routine small renal mass needle biopsy should be adopted. *Nat Rev Urol.* 2014;11(10):548–549.

154. Teber D, Guven S, Simpfendörfer T, *et al.* Augmented reality: a new tool to improve surgical accuracy during laparoscopic partial nephrectomy? Preliminary in vitro and in vivo results. *Eur Urol.* 2009;56(2):332–338.

155. Teber D, Simpfendörfer T, Guven S, *et al.* In-vitro evaluation of a soft-tissue navigation system for laparoscopic prostatectomy. *J Endourol.* 2010;24(9):1487–1491.

156. Müeller M, Rassweiler MC, Klein J, *et al.* Mobile augmented reality for computer-assisted percutaneous nephrolithotomy. *Int J Comput Assist Radiol Surg.* 2013;8(4):663–675.

157. Nozaki T, Iida Y, Morii A, *et al.* Laparoscopic radical nephrectomy under near real-time three-dimensional surgical navigation with C-arm cone beam computed tomography. *Surg Innov.* 2012;19(3):263–267.

158. Hinshaw JL, Lubner MG, Ziemlewicz TJ, *et al.* Percutaneous tumor ablation tools: microwave, radiofrequency, or cryoablation--what should you use and why? *Radiographics.* 2014;34(5):1344–1362.

159. Brace CL. Radiofrequency and microwave ablation of the liver, lung, kidney, and bone: what are the differences?. *Curr Probl Diagn Radiol.* 2009;38(3):135–143.

160. Andreano A, Brace CL. A comparison of direct heating during radiofrequency and microwave ablation in ex vivo liver. *Cardiovasc Intervent Radiol.* 2013;36(2):505–511.

161. Duffey BG, Kyle Anderson J. Current and future technology for minimally invasive ablation of renal cell carcinoma. *Indian J Urol.* 2010;26(3):410–417.

162. Brace CL. Microwave tissue ablation: biophysics, technology, and applications. *Crit Rev Biomed Eng.* 2010;38(1):65–78.

163. Lubner MG, Brace CL, Hinshaw JL, *et al.* Microwave tumor ablation: mechanism of action, clinical results, and devices. *J Vasc Interv Radiol.* 2010;21(8 Suppl):S192–203.

164. Knavel EM, Hinshaw JL, Lubner MG, *et al.* High-powered gas-cooled microwave ablation: shaft cooling creates an effective stick function without altering the ablation zone. *AJR Am J Roentgenol.* 2012;198(3):W260–265.

165. Li X, Zhang L, Fan W, *et al.* Comparison of microwave ablation and multipolar radiofrequency ablation, both using a pair of internally cooled interstitial applicators: results in ex vivo porcine livers. *Int J Hyperthermia.* 2011;27(3):240–248.

166. Laeseke PF, Lee FT Jr, Sampson LA, *et al.* Microwave ablation versus radiofrequency ablation in the kidney: high-power triaxial antennas create larger ablation zones than similarly sized internally cooled electrodes. *J Vasc Interv Radiol.* 2009;20(9):1224–1229.

167. Castle SM, Salas N, Leveillee RJ. Initial experience using microwave ablation therapy for renal tumor treatment: 18-month follow-up. *Urology.* 2011;77(4):792–797.

168. Oshima F, Yamakado K, Nakatsuka A, *et al.* Simultaneous microwave ablation using multiple antennas in explanted bovine livers: relationship between ablative zone and antenna. *Radiat Med.* 2008;26(7):408–414.

169. Durick NA, Laeseke PF, Broderick LS, *et al.* Microwave ablation with triaxial antennas tuned for lung: results in an in vivo porcine model. *Radiology.* 2008;247(1):80–87.

170. Sun Y, Wang Y, Ni X, *et al.* Comparison of ablation zone between 915- and 2,450-MHz cooled shaft microwave antenna: results in in vivo porcine livers. *AJR Am J Roentgenol.* 2009;192(2):511–514.

171. Strickland AD, Clegg PJ, Cronin NJ, *et al.* Experimental study of large-volume microwave ablation in the liver. *Br J Surg.* 2002;89(8):1003–1007.

172. Bertram JM, Yang D, Converse MC, *et al.* A review of coaxial-based interstitial antennas for hepatic microwave ablation. *Crit Rev Biomed Eng.* 2006;34(3):187–213.

173. Moore C, Salas N, Zaias J, *et al.* Effects of microwave ablation of the kidney. *J Endourol.* 2010;24(3):439–444.

174. Niemeyer DJ, Simo KA, McMillan MT, *et al.* Optimal ablation volumes are achieved at submaximal power settings in a 2.45-GHz microwave ablation system. *Surg Innov.* 2015;22(1):41–45.

175. He X, McGee S, Coad JE, *et al.* Investigation of the thermal and tissue injury behaviour in microwave thermal therapy using a porcine kidney model. *Int J Hyperthermia.* 2004;20(6):567–593.

176. Brace CL, Diaz TA, Hinshaw JL, *et al.* Tissue contraction caused by radiofrequency and microwave ablation: a laboratory study in liver rand lung. *J Vasc Interv Radiol.* 2010;21(8):1280–1286.

177. Sommer CM, Sommer SA, Mokry T, *et al.* Quantification of tissue shrinkage and dehydration caused by microwave ablation: experimental study in kidneys for the estimation of effective coagulation volume. *J Vasc Interv Radiol.* 2013;24(8):1241–1248.

178. Sommer CM, Arnegger F, Koch V, *et al.* Microwave ablation of porcine kidneys in vivo: effect of two different ablation modes ("temperature control" and "power control") on procedural outcome. *Cardiovasc Intervent Radiol.* 2012;35(3):653–660.

179. Bartoletti R, Cai T, Tosoratti N, *et al.* In vivo microwave-induced porcine kidney thermoablation: results and perspectives from a pilot study of a new probe. *BJU Int.* 2010;106(11):1817–1821.

180. Isfort P, Penzkofer T, Tanaka T, *et al.* Efficacy of antegrade pyeloperfusion to protect the renal pelvis in kidney microwave ablation using an in vivo swine model. *Invest Radiol.* 2013;48(12):863–868.

181. Hope WW, Schmelzer TM, Newcomb WL, *et al.* Guidelines for power and time variables for microwave ablation in an in vivo porcine kidney. *J Surg Res.* 2009;153(2):263–267.

182. Clark PE, Woodruff RD, Zagoria RJ. Microwave ablation of renal parenchymal tumors before nephrectomy: phase I study. *AJR Am J Roentgenol.* 2007;188(5):1212–1214.

183. Muto G, Castelli E, Migliari R, *et al.* Laparoscopic microwave ablation and enucleation of small renal masses: preliminary experience. *Eur Urol.* 2011;60(1):173–176.

184. Bartoletti R, Meliani E, Simonato A, *et al.* Microwave-induced thermoablation with Amica-probe is a safe and reproducible method to treat solid renal masses: results from a phase I study. *Oncol Rep.* 2012;28(4):1243–1248.

185. Martin J, Athreya S. Meta-analysis of cryoablation versus microwave ablation for small renal masses: is there a difference in outcome? Diagn Interv Radiol. 2013;19(6):501–507.

186. Yu J, Liang P, Xu XL, *et al.* US-guided percutaneous microwave ablation of renal cell carcinoma: intermediate-term results. *Radiology*. 2012;263(3):900–908.

187. Guan W, Bai J, Liu J, *et al.* Microwave ablation versus partial nephrectomy for small renal tumors: intermediate-term results. *J Surg Oncol*. 2012;106(3):316–321.

188. Bai J, Hu Z, Guan W, *et al.* Initial experience with retroperitoneoscopic microwave ablation of clinical T(1a) renal tumors. *J Endourol*. 2010;24(12):2017–2022.

189. Guan W, Bai J, Hu Z, *et al.* Retroperitoneoscopic microwave ablation of renal hamartoma: middle-term results. *J Huazhong Univ Sci Technolog Med Sci*. 2010;30(5):669–671.

190. Carafiello G, Mangini M, Fontana F, *et al.* Single-antenna microwave ablation under contrast-enhanced ultrasound guidance for treatment of small renal cell carcinoma: preliminary experience. *Cardiovasc Intervent Radiol.* 2009;33(2):367–374.

191. Moreland AJ, Ziemlewicz TJ, Best SL, *et al.* High-powered microwave ablation of t1a renal cell carcinoma: safety and initial clinical evaluation. *J Endourol*. 2014;28(9):1046–1052.

192. Horn JC, Patel RS, Kim E, *et al.* Percutaneous microwave ablation of renal tumors using a gas-cooled 2.4-GHz probe: technique and initial results. *J Vasc Interv Radiol.* 2014;25(3):448–453.

193. Carrafiello G, Dionigi G, Ierardi AM, *et al.* Efficacy, safety and effectiveness of image-guided percutaneous microwave ablation in cystic renal lesions Bosniak III or IV after 24 months follow up. *Int J Surg.* 2013;(11 Suppl 1):S30–35.

194. Lin Y, Liang P, Yu XL, *et al.* Percutaneous microwave ablation of renal cell carcinoma is safe in patients with a solitary kidney. *Urology.* 2014;83(2):357–363.

195. Lee EW, Wong D, Prikhodko SV, *et al.* Electron microscopic demonstration and evaluation of irreversible electroporation-induced nanopores on hepatocyte membranes. *J Vasc Interv Radiol.* 2012;23(1):107–113.

196. Chang DC, Reese TS. Changes in membrane-structure induced by electroporation as revealed by rapid-freezing electron microscopy. *Biophys J.* 1990;58(1):1–12.

197. Wagstaff PG, de Bruin DM, Zondervan PJ, *et al.* The efficacy and safety of irreversible electroporation for the ablation of renal masses: a prospective, human, in-vivo study protocol. *BMC Cancer.* 2015;15:165.

198. Al-Sakere B, Andre F, Bernat C, *et al.* Tumor ablation with irreversible electroporation. *PLoS One.* 2007;2(11):e1135.

199. Olweny EO, Kapur P, Tan YK, *et al.* Irreversible electroporation: evaluation of nonthermal and thermal ablative capabilities in the porcine kidney. *Urology* 2013;81(3):679–684.

200. Pech M, Janitzky A, Wendler JJ, *et al.* Irreversible electroporation of renal cell carcinoma: a first-in-man phase I clinical study. *Cardiovasc Intervent Radiol.* 2011;34(1):132–138.

201. Bertacchini C, Margotti PM, Bergamini E, *et al.* Design of an irreversible electroporation system for clinical use. *Technol Cancer Res Treat.* 2007;6(4):313–320.

202. van Gemert MJ, Wagstaff PG, de Bruin DM, *et al.* Irreversible electroporation: just another form of thermal therapy? *Prostate.* 2015;75(3):332–335.

203. Davalos RV, Bhonsle S, Neal RE 2nd. Implications and considerations of thermal effects when applying irreversible electroporation tissue ablation therapy. *Prostate.* 2015;75(10):1114–1118.

204. Golberg A, Yarmush ML. Nonthermal irreversible electroporation: fundamentals, applications, and challenges. *IEEE Trans Biomed Eng.* 2013;60(3):707–714.

205. Nielsen K, Scheffer HJ, Vieveen JM, *et al.* Anaesthetic management during open and percutaneous irreversible electroporation. *Br J Anaesth.* 2014;113(6):985–992.

206. Edd JF, Horowitz L, Davalos RV, *et al.* In vivo results of a new focal tissue ablation technique: irreversible electroporation. *IEEE Trans Biomed Eng.* 2006;53(7):1409–1415.

207. Tracy CR, Kabbani W, Cadeddu JA. Irreversible electroporation (IRE): a novel method for renal tissue ablation. *BJU Int.* 2011;107(12):1982–1987.

208. Deodhar A, Monette S, Single GW Jr, *et al.* Renal tissue ablation with irreversible electroporation: preliminary results in a porcine model. *Urology.* 2011;77(3):754–760.

209. Wendler JJ, Porsch M, Huhne S, *et al.* Short- and mid-term effects of irreversible electroporation on normal renal tissue: an animal model. *Cardiovasc Intervent Radiol.* 2013;36(2):512–520.

210. Sommer CM, Fritz S, Wachter MF, *et al.* Irreversible electroporation of the pig kidney with involvement of the renal pelvis: technical aspects, clinical outcome, and three-dimensional CT rendering for assessment of the treatment zone. *J Vasc Interv Radiol.* 2013;24(12):1888–1897.

211. Wagstaff PG, de Bruin DM, van den Bos W, *et al.* Irreversible electroporation of the porcine kidney: Temperature development and distribution. *Urol Oncol.* 2015;33(4):168.e1–7.

212. Thomson KR, Cheung W, Ellis SJ, *et al.* Investigation of the safety of irreversible electroporation in humans. *J Vasc Interv Radiol.* 2011;22(5):611–621.

213. Trimmer CK, Khosla A, Morgan M, *et al.* Minimally Invasive Percutaneous Treatment of Small Renal Tumors with Irreversible Electroporation: A Single-Center Experience. *J Vasc Interv Radiol.* 2015;26(10):1465–1471.

214. Wendler JJ, Porsch M, Nitschke S, *et al.* A prospective Phase 2a pilot study investigating focal percutaneous irreversible electroporation (IRE) ablation by NanoKnife in patients with localised renal cell carcinoma (RCC) with delayed interval tumour resection (IRENE trial). *Contemp Clin Trials.* 2015;43:10–19.

215. Juusela H, Malmio K, Alfthan O, *et al.* Preoperative irradiation in the treatment of renal adenocarcinoma. *Scand J Urol Nephrol.* 1977;11(3):277–281.

216. Kjaer M, Frederiksen PL, Engelholm SA. Postoperative radiotherapy in stage II and III renal adenocarcinoma. A randomized trial by the Copenhagen Renal Cancer Study Group. *Int J Radiat Oncol Biol Phys.* 1987;13(5):665–672.

217. Kjaer M, Iversen P, Hvidt V, *et al.* A randomized trial of postoperative radiotherapy versus observation in stage II and III renal adenocarcinoma. A study by the Copenhagen Renal Cancer Study Group. *Scand J Urol Nephrol.* 1987;21(4):285–289.

218. Deschavanne PJ, Fertil B. A review of human cell radiosensitivity in vitro. *Int J Radiat Oncol Biol Phys.* 1996;34(1):251–266.

219. Brown JM, Carlson DJ, Brenner DJ. The tumor radiobiology of SRS and SBRT: are more than the 5 Rs involved? *Int J Radiat Oncol Biol Phys.* 2014;88(2):254–262.

220. Siva S, Pham D, Gill S, *et al.* A systematic review of stereotactic radiotherapy ablation for primary renal cell carcinoma. *BJU Int.* 2012;110(11 Pt B):E737–743.

221. Ponsky LE, Crownover RL, Rosen MJ, *et al.* Initial evaluation of Cyberknife technology for extracorporeal renal tissue ablation. *Urology.* 2003;61(3):498–501.

222. Kaplan ID, Redrosa I, Martin C, *et al.* Results of a phase I dose escalation study of stereotactic radiosurgery for primary renal tumors. *Int J Radiat Oncol Biol Phys.* 2010;78(3):S191.

223. Nair VJ, Szanto J, Vandervoort E, *et al.* CyberKnife for inoperable renal tumors: Canadian pioneering experience. *Can J Urol.* 2013;20(5):6944–6949.

224. Lo CH, Huang WY, Chao HL, *et al.* Novel application of stereotactic ablative radiotherapy using CyberKnife® for early-stage renal cell carcinoma in patients with pre-existing chronic kidney disease: Initial clinical experiences. *Oncol Lett.* 2014;8(1):355–360.

225. Staehler M, Bader M, Schlenker B, *et al.* Single fraction radiosurgery for the treatment of renal tumors. *J Urol.* 2015;193(3):771–775.

226. Klatte T, Marberger M. High-intensity focused ultrasound for the treatment of renal masses: current status and future potential. *Curr Opin Urol.* 2009;19(2):188–191.

227. Häcker A, Michel MS, Marlinghaus E, *et al.* Extracorporeally induced ablation of renal tissue by high-intensity focused ultrasound. *BJU Int.* 2006;97(4):779–785.

228. Marberger M, Schatzl G, Cranston D, *et al.* Extracorporeal ablation of renal tumours with high-intensity focused ultrasound. *BJU Int.* 2005;(95 Suppl 2):52–55.

229. Ritchie RW, Leslie T, Phillips R, *et al.* Extracorporeal high intensity focused ultrasound for renal tumours: a 3-year follow-up. *BJU Int.* 2010;106(7):1004–1009.

230. Sea JC, Bahler CD, Ring JD, *et al.* Calibration of a novel, laparoscopic, 12-mm, ultrasound, image-guided, high-intensity focused ultrasound probe for ablation of renal neoplasms. *Urology.* 2015;85(4):953–958.

231. Klingler HC, Susani M, Seip R, *et al.* A novel approach to energy ablative therapy of small renal tumours: laparoscopic high-intensity focused ultrasound. *Eur Urol.* 2008;53(4):810–818.

232. Ritchie RW, Leslie TA, Turner GD, *et al.* Laparoscopic high-intensity focused ultrasound for renal tumours: a proof of concept study. *BJU Int.* 2011;107:1290–1296.

233. Kroeze SG, Grimbergen MC, Rehmann H, *et al.* Photodynamic therapy as novel nephron sparing treatment option for small renal masses. *J Urol.* 2012;187(1):289–295.

234. Kimm S, Tarin T, Wimmer T, *et al.* Renal tissue ablation produced with WST-11 vascular targeted photodynamic therapy: safety assessment, histopathologic and radiographic analysis. *J Urol.* 2014;191(4):e650–651.

235. Smaldone MC, Kutikov A, Egleston BL, *et al.* Small renal masses progressing to metastases under active surveillance: a systematic review and pooled analysis. *Cancer.* 2012;118(4):997–1006.

236. Klatte T, Kroeger N, Zimmermann U, *et al.* The contemporary role of ablative treatment approaches in the management of renal cell carcinoma (RCC): focus on radiofrequency ablation (RFA), high-intensity focused ultrasound (HIFU) and cryoablation. *Worl J Urol.* 2014;32(3):597–605.

237. Desai MM, Aron M, Gill IS. Laparoscopic partial nephrectomy versus laparoscopic cryoablation for the small renal tumor. *Urology.* 2005;66(5 Suppl):23–28.

238. Haramis G, Graversen JA, Mues AC, *et al.* Retrospective comparison of laparoscopic partial nephrectomy versus laparoscopic renal cryoablation for small (<3.5 cm) cortical renal masses. *J Laparoendosc Adv Surg Tech A.* 2012;22(2):152–157.

239. Guillotreau J, Haber GP, Autorino R, *et al.* Robotic partial nephrectomy versus laparoscopic cryoablation for the small renal mass. *Eur Urol.* 2012;61(5):899–904.

240. Emara AM, Kommu SS, Hindley RG, *et al.* Robot-assisted partial nephrectomy vs laparoscopic cryoablation for the small renal mass: redefining the minimally invasive 'gold standard'. *BJU Int.* 2014;113(1):92–99.

241. Klatte T, Shariat SF, Remzi M. Systematic review and meta-analysis of perioperative and oncologic outcomes of laparoscopic cryoablation versus laparoscopic partial nephrectomy for the treatment of small renal tumors. *J Urol.* 2014;191(5):1209–1217.

242. Tang K, Yao W, Li H, *et al.* Laparoscopic renal cryoablation versus laparoscopic partial nephrectomy for the treatment of small renal masses: a systematic review and meta-analysis of comparative studies. *J Laparoendosc Adv Surg Tech A.* 2014;24(6):403–410.

243. Stern JM, Svatek R, Park S, *et al.* Intermediate comparison of partial nephrectomy and radiofrequency ablation for clinical T1a renal tumours. *BJU Int.* 2007;100(2):287–290.

244. Bensalah K, Zeltser I, Tuncel A, *et al.* Evaluation of costs and morbidity associated with laparoscopic radiofrequency ablation and laparoscopic partial nephrectomy for treating small renal tumours. *BJU Int.* 2008;101(4):467–471.

245. Bird VG, Carey RI, Ayyathurai R, *et al.* Management of renal masses with laparoscopic-guided radiofrequency ablation versus laparoscopic partial nephrectomy. *J Endourol.* 2009;23(1):81–88.

246. Olweny EO, Park SK, Tan YK, *et al.* Radiofrequency ablation versus partial nephrectomy in patients with solitary clinical T1a renal cell carcinoma: comparable oncologic outcomes at a minimum of 5 years of follow-up. *Eur Urol.* 2012;61(6):1156–1161.

247. Youn CS, Park JM, Lee JY, *et al.* Comparison of laparoscopic radiofrequency ablation and open partial nephrectomy in patients with a small renal mass. *Korean J Urol.* 2013;54(9):603–608.

248. Chang X, Zhang F, Liu T, *et al.* Radio frequency ablation versus partial nephrectomy for clinical T1b renal cell carcinoma: long-term clinical and oncologic outcomes. *J Urol.* 2015;193(2):430–435.

249. Kim SH, Lee ES, Kim HH, *et al.* A propensity-matched comparison of perioperative complications and of chronic kidney disease between robot-assisted laparoscopic partial nephrectomy and radiofrequency ablative therapy. *Asian J Surg.* 2015;38(3):126–133.

250. Mitchell CR, Atwell TD, Weisbrod AJ, *et al.* Renal function outcomes in patients treated with partial nephrectomy versus percutaneous ablation for renal tumors in a solitary kidney. *J Urol.* 2011;186(5):1786–1790.

251. Mues AC, Korets R, Graversen JA, *et al.* Clinical, pathologic, and functional outcomes after nephron-sparing surgery in patients with a solitary kidney: a multicenter experience. *J Endourol*. 2012;26(10):1361–1366.

252. Goyal J, Sidana A, Georgiades CS, *et al.* Renal function and oncologic outcomes after cryoablation or partial nephrectomy for tumors in solitary kidneys. *Korean J Urol*. 2011;52(6):384–389.

253. Haber GP, Lee MC, Crouzet S, *et al.* Tumour in solitary kidney: laparoscopic partial nephrectomy vs laparoscopic cryoablation. *BJU Int*. 2012;109(1):118–124.

254. Panumatrassamee K, Kaouk JH, Autorino R, *et al.* Cryoablation versus minimally invasive partial nephrectomy for small renal masses in the solitary kidney: impact of approach on functional outcomes. *J Urol*. 2013;189(3):818–822.

255. Yang Q, Meng F, Li K, *et al.* Safety and Efficacy of Thermal Ablation for Small Renal Masses in Solitary Kidney: Evidence from Meta-Analysis of Comparative Studies. *PLoS One*. 2015;10(6):e0131290.

256. Khalifeh A, Autorino R, Hillyer SP, *et al.* Comparative outcomes and assessment of trifecta in 500 robotic and laparoscopic partial nephrectomy cases: a single surgeon experience. *J Urol*. 2013;189(4):1236–1242.

257. Weinberg AC, Woldu SL, Wen T, *et al.* Utilization and perioperative complications of laparoscopic cryoablation vs. robotic partial nephrectomy for localized renal tumors. *Int Braz J Urol*. 2015;41(3):473–485.

258. Kunkle DA, Uzzo RG. Cryoablation or radiofrequency ablation of the small renal mass: a meta-analysis. *Cancer*. 2008;113(10):2671–2680.

259. El Dib R, Touma NJ, Kapoor A. Cryoablation vs radiofrequency ablation for the treatment of renal cell carcinoma: a meta-analysis of case series studies. *BJU Int*. 2012;110(4):510–516.

260. Hegarty NJ, Gill IS, Desai MM, *et al.* Probe-ablative nephron-sparing surgery: cryoablation versus radiofrequency ablation. *Urology*. 2006;68(1 Suppl):7–13.

261. Pirasteh A, Snyder L, Boncher N, *et al.* Cryoablation vs. radiofrequency ablation for small renal masses. *Acad Radiol*. 2011;18(1):97–100.

262. Allaf ME, Varkarakis IM, Bhayani SB, *et al.* Pain control requirements for percutaneous ablation of renal tumors: cryoablation versus radiofrequency ablation--initial observations. *Radiology*. 2005;237(1):366–370.

263. Truesdale CM, Soulen MC, Clark TW, *et al.* Percutaneous computed tomography-guided renal mass radiofrequency ablation versus cryoablation: doses of sedation medication used. *J Vasc Interv Radiol*. 2013;24(3):347–350.

264. Link RE, Permpongkosol S, Gupta A, *et al.* Cost analysis of open, laparoscopic, and percutaneous treatment options for nephron-sparing surgery. *J Endourol*. 2006;20(10):782–789.

265. Chehab M, Friedlander J, Handel J, *et al.* Percutaneous Cryoablation vs Partial Nephrectomy: Cost Comparison of T1a Tumors. *J Endourol*. 2016;30(2):170–176.

266. Lotan Y, Cadeddu JA. A cost comparison of nephron-sparing surgical techniques for renal tumor. *BJU Int*. 2005;95(7):1039–1042.

267. Castle SM, Gorbatiy V, Avallone MA, *et al.* Cost comparison of nephron-sparing treatments for cT1a renal masses. *Urol Oncol*. 2013;31(7):1327–1323.

268. Pandharipande PV, Gervais DA, Mueller PR, *et al.* Radiofrequency ablation versus nephron-sparing surgery for small unilateral renal cell carcinoma: cost-effectiveness analysis. *Radiology*. 2008;248(1):169–178.

269. Pierorazio PM, Johnson MH, Ball MW, *et al.* Five-year analysis of a multi-institutional prospective clinical trial of delayed intervention and surveillance for small renal masses: the DISSRM registry. *Eur Urol*. 2015;68(3):408–415.

270. Chang SL, Cipriano LE, Harshman LC, *et al.* Cost-effectiveness analysis of nephron sparing options for the management of small renal masses. *J Urol*. 2011;185(5):1591–1597.

271. Bhan SN, Pautler SE, Shayegan B, *et al.* Active surveillance, radiofrequency ablation, or cryoablation for the nonsurgical management of a small renal mass: a cost-utility analysis. *Ann Surg Oncol*. 2013;20(11):3675–3684.

C9

Follow-up Evaluation After Focal Ablation of Renal Masses

CHAIR

Jaime Landman, United States

CO-CHAIR

Vinay Duddalwar, United States

MEMBERS

Mahul B. Amin, United States
Manju Aron, United States
Jeffrey Cadeddu, United States
Heidi Coy, United States
Chandana Lall, United States
Kari Nelson, United States
Zhamshid Okhunov, United States
Steve Raman, United States
Pheroze Tamboli, United States

CONTENTS

Follow-up Evaluation After Focal Ablation of Renal Masses

9.1 Introduction

With the wide usage of cross-sectional imaging, there is an increasing detection rate and subsequent treatment of small renal masses (SRM).[1] Concomitantly, with the advancement of minimally invasive technology, the spectrum of treatment modalities available for SRM has expanded to include laparoscopic and robot-assisted extirpative procedures, ablative modalities, and active surveillance. Partial or radical nephrectomy, however, remains the gold-standard treatment, with a 97% 5-year disease-specific survival rate.[2] However, advanced age and comorbidities may make a large number of patients suboptimal candidates for surgical intervention. As such, ablative options have become increasingly important management strategies. In addition, extirpative modalities are associated with greater renal functional loss compared to ablation, and the negative effects of renal functional deterioration on cardiovascular health and longevity continue to be elucidated.

Documentation of the successful oncologic outcomes with ablative therapies in the treatment of SRM has led to the broader use of ablation in younger patients and those without comorbidities.[3-5] According to American Urological Association and European Urological Association guidelines, focal ablative therapies, specifically cryoablation (CA) and radiofrequency ablation (RFA), are now considered viable treatment options for renal cortical neoplasms.[6,7]

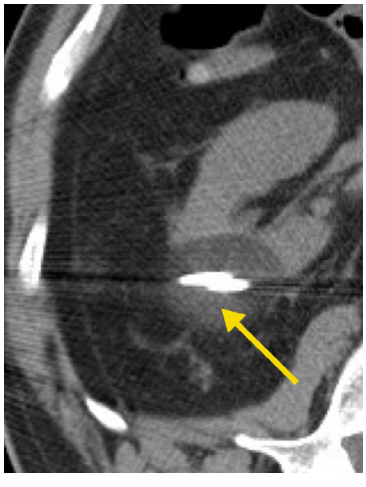

FIGURE 9-1
Cryoablation Under Image Guidance
Intra-procedural computed tomography (CT) during CA demonstrates 2 cryoprobes with well-demarcated hypodense surrounding ice ball (arrow)

Cryoablation for SRM was first performed in 1995 by Uchida and colleagues.[8] The CA procedure involves rapid freeze followed by thaw cycles to produce cell destruction.[9] Extracellular ice formation during the freezing cycles causes the movement of intracellular water, alterations in intracellular pH, and protein denaturation.[10] Ice formation also results in the mechanical disruption of cell membranes.[10] Local death and necrosis of microvasculature several hours and days after the ablation cause a decrease in tissue perfusion and delayed cell death.[11] Cryoablation can be deployed either laparoscopically or percutaneously with image-guidance (CT or magnetic resonance imaging [MRI]) (**Figure 9-1**).[12-16] Intra-operative ultrasound (US) can be used to confirm extension of the ice ball beyond the tumour margins for optimal efficacy during laparoscopic procedures, and CT or MRI can be utilized to monitor percutaneous CA procedures.[17]

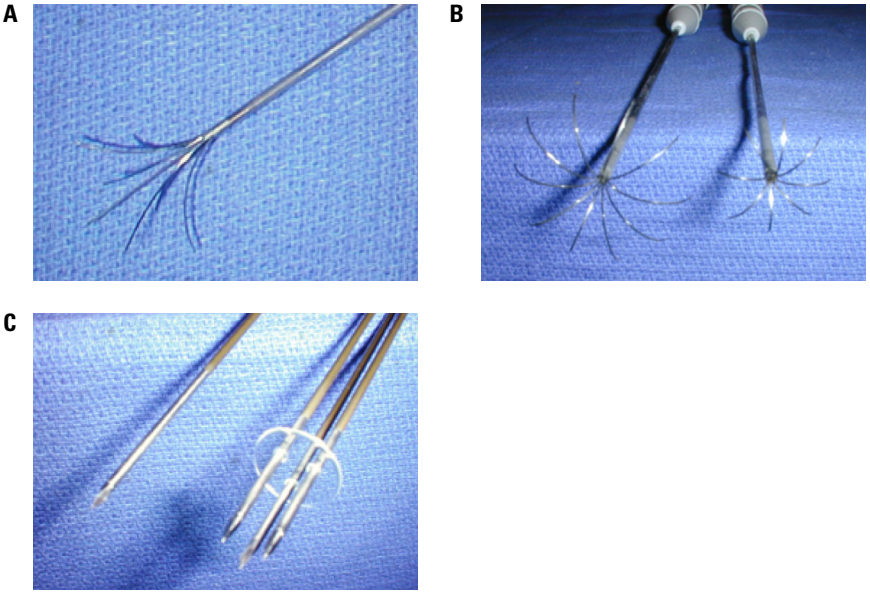

FIGURE 9-2
Examples of Internally Cooled Electrodes (**A**) and Expandable Tine Type Electrodes (**B** and **C**)

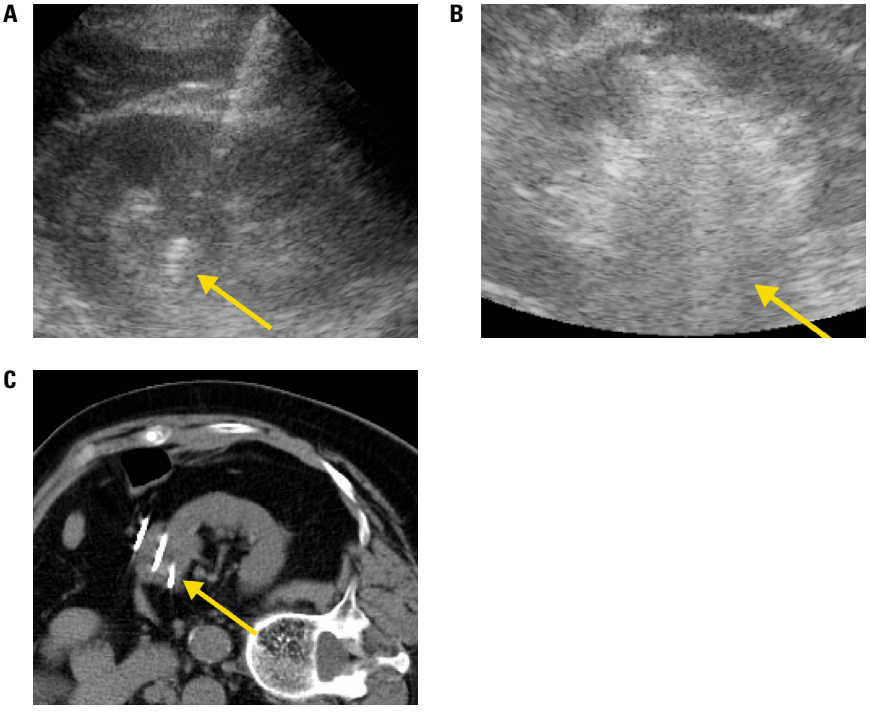

FIGURE 9-3
Use of RFA Probes in Procedures Under Imaging Guidance

A Intraprocedural US with internally cooled RFA electrode in a 58-year-old man with central renal cell carcinoma (RCC).

B During ablation, a large echogenic cloud completely encompassing lesion during RFA in a 58-year-old man with central RCC.

C Intraprocedural CT in a 73-year-old woman with an anterior clear cell RCC demonstrates three internally cooled intralesional RFA electrodes.

The first clinical application of RFA was reported in 1997 for an exophytic renal mass before open radical nephrectomy.[18] McGovern and colleagues subsequently reported their series of RFA as the only treatment for a renal tumour.[19] RFA probes can similarly be deployed via open, laparoscopic, or percutaneous approach under US, CT, or MRI guidance (**Figures 9-2** and **9-3**).[20] Radiofrequency (RF)

energy converted to heat in the tissue, causing thermal tissue damage.[20,21] High-frequency current applied to target tissues results in ionic agitation, thereby heating the tissues and resulting in the denaturation of proteins and disintegration of cell membranes.[22] This process occurs over 4 to 6 minutes at temperatures above 50°C and almost immediately at temperatures above 60°C.[22] Since temperatures greater than 105°C result in tissue vaporization and ineffective ablation, optimal RFA is performed at temperatures of 50°C to 100°C throughout the tumour.[22,23]

As the number of patients with SRM undergoing ablation increases, developing a standardized follow-up protocol for these patients is increasingly important. In the current chapter, we will review and suggest definitions of residual and recurrent tumour after ablation of SRM, define the role of imaging, define the role of pre-operative, intra-operative, and post-procedure biopsies, and examine patient outcomes with different histopathological subtypes.

9.2 Definition of Recurrence After Ablation for Small Renal Masses

The ultimate goal of tumour ablation is to achieve complete necrosis of the targeted neoplasm with minimal damage to surrounding normal tissue. Unlike surgical extirpation, efficacy of ablation cannot be assessed histologically due to absence of excised tumour. Thus, imaging characteristics of the post-ablation zone remain the most important parameter for the assessment of treatment outcomes. In this regard, accurate assessment and definition of radiological characteristics of successfully ablated tumours is critical.[24] Successful renal tumour ablation is characterized by the absence of contrast enhancement on postoperative follow-up imaging. However, there is a significant variability in the manner by which residual or recurrent tumours are defined.

Imaging findings following tumour ablation differ based on the type of ablation performed and the imaging modality used, as well as the location and type of tumour ablated.[24] Immediate post-ablation CT or MRI usually demonstrates an ablation zone larger than the actual tumour and diffuse non-enhancement of the ablated zone. Typically, the ablation zone is hyperintense on T1WI with a peritumoural rim of different signal intensity.[25] Ablated tissue presents as a heterogeneous and hyperintense to normal parenchyma on T1-weighted sequences, and as hypointense on T2-weighted sequences due to the presence of hemorrhage and coagulative necrosis.

Similarly, on CT imaging, the ablated tissue on early post-CA imaging may appear hyperdense. An enhancing peritumoural rim is secondary to acute reaction of the surrounding tumour tissue to ablation. In addition, it is recommended that the ice ball during CA extend at least 5 mm to 10 mm beyond the tumour margin, in order to reduce the likelihood of residual tumour at the margin of tumour and healthy tissue.[9,26] The initial apparent increase in tumour size gradually decreases as acute reaction resolves and ablated tissue shrinks. Gill and colleagues monitored 56 patients who underwent a laparoscopic CA using MRI, and all ablated tumours presented with an initial apparent increase in size and demonstrated a 75% size reduction. Almost 40% of tumours were undetectable by the end of 3-year follow-up.[27]

9.3 Role of Imaging

Radiological imaging remains the most important tool in the follow-up of patients following renal tumour ablation.[28] Imaging must be performed as per standardized protocols and, currently, contrast-enhanced CT and MRI are the most commonly utilized imaging modalities for SRM follow-up after ablation.[28]

Guidelines for optimal follow-up imaging frequency are not well established.[29] The timing of the initial imaging evaluation varies among different operators and institutions, ranging from 1 week and 3 months after the procedure.[30,31] Some institutions and authors recommend immediate imaging after ablation to identify efficacy and capture baseline characteristics of the treatment area.[30] But, in general, it is recommended to delay the imaging until the local tissue reaction to ablation has resolved.[29] For defining the optimal imaging frequency post-ablation, multiples factors should be considered. These include type of ablation performed, tumour location, radiation dosage from imaging, and cost of the procedure.

Matin and colleagues performed a retrospective multi-institutional review of more than 600 patients who underwent energy-based ablative therapies.[32] Of these, 63 patients were found to have residual or recurrent disease. Seventy percent of incomplete treatments were detected within the first 3 months, with most of them identified within the first 12 months. However, residual tumours and ablation site recurrences have been reported up to 2.5 years after ablation.[30-35] This supports the fact that patients with SRM who undergo ablative therapies require long-term follow-up imaging to identify potential recurrences. Based on review of the existing literature, we recommend initial imaging 3 to 6 months after the procedure and annually thereafter.

Computed tomography is the most commonly performed follow-up imaging modality. MRI is traditionally reserved for patients in whom the use of contrast-enhanced CT is contraindicated. MRI has several advantages. Although it requires more patient cooperation during the procedure, there is no ionizing radiation associated with MRI, and it has been shown to have a superior tissue resolution compared to CT.[36] MRI should be used with caution in patients with chronic kidney disease who have a glomerular filtration rate less than 30, due to the risk of developing nephrogenic systemic fibrosis.[37]

9.3.1 Post-procedural imaging protocols

9.3.1.1 Modalities and immediate post-procedural image findings

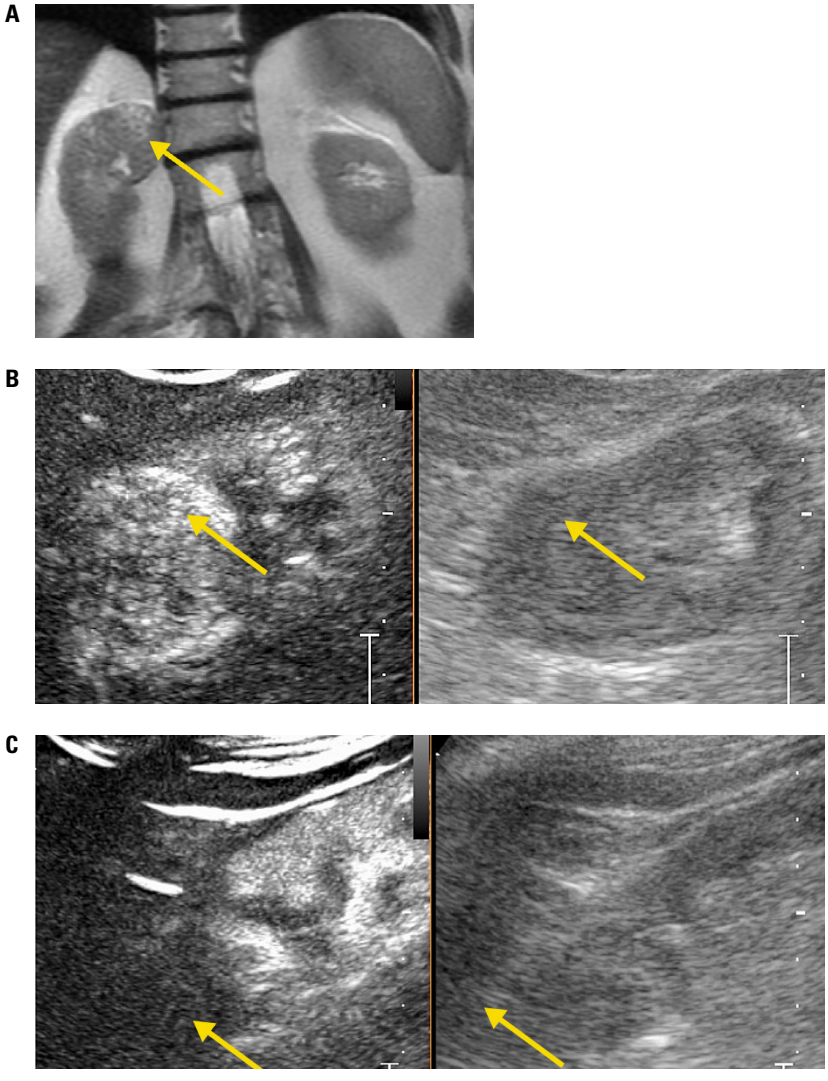

FIGURE 9-4
A 77-Year-Old Woman With a Superior Right Kidney Mass and Renal Insufficiency

This patient had a T2 hyperintense lesion on diagnostic MRI (**A**) and demonstrated lesion enhancement on contrast-enhanced ultrasound (CEUS) (**B**). Immediately following microwave ablation (MWA), no residual enhancement can be seen on CEUS (**C**), indicating ablative success.

Post-ablation imaging is typically performed with either contrast-enhanced CT or MRI. Magnetic resonance imaging is preferred for most patients due to its superior tissue contrast, lack of ionizing radiation, and minimal contrast requirement relative to CT. However, either modality is preferable to performing an unenhanced US, which is inadequate for detection of early recurrences. Intravascular microbubble US contrast agents have been approved for diagnostic US imaging outside the United States. However, many centres in the United States use these agents off label. They consist of <8 micron intravenously injected bubbles that are nonlinearly compressed by US beam and, in turn, generate higher harmonic frequencies that are visualized as bright reflectors. This enables much higher renal mass contrast relative to renal parenchymal background in real time over multiple contrast phases.

The entire kidney and target renal mass may be evaluated before and after RFA, MW, and CA. This is particularly advantageous for young patients, patients with traditional contrast allergies, or patients with renal impairment (**Figure 9-4**).[38-44]

9.3.1.2 Conventional ultrasound

On conventional US, the kidneys are evaluated with curved phased array 3 MHz to 5 MHz transducers, and kidneys appear as bean-shaped ovals measuring 9 to 12 cm in length. The renal parenchyma is typically hypoechoic and the renal medullary fat is hyperechoic. The medullary pyramids are typically slightly hypoechoic to cortex. Most renal masses, including RCC, are well circumscribed, centred in the cortex, and variable in echotexture, although they are generally hypoechoic to renal cortex. Fat-containing renal lesions such as angiomyolipomas may be hyperechoic. All solid lesions typically have some degree of colour and power Doppler signal. Both arterial and venous waveforms may be obtained in larger hypervascular lesions, although this does not characterize lesions.[45,46]

9.3.1.3 Contrast-enhanced ultrasound

Contrast agents can be administered intravenously by hand microbolus followed by a normal saline flush. Several boluses of contrast can be given for each lesion, and multiple lesions can be evaluated during a single CEUS examination. The contrast is activated with brief (<1 minute) and rapid agitation in an automated device provided by the manufacturer. Real-time cine images are obtained by holding the transducer over the renal mass while each microbolus is injected intravenously, and cine capture clips of approximately 2-minute duration are obtained for diagnostic evaluation. This can be performed multiple times to assess the relative enhancement of renal lesions relative to renal parenchyma over the renal cortical and medullary enhancement phases.[47-60]

9.3.1.4 Computed tomography

Patients in whom iodinated contrast material is not contraindicated usually undergo intravenous (IV) iodinated contrast-enhanced CT, typically using 64-detector or dual-source scanners. Scans are obtained at a collimation of 2.5 mm to allow detection of small renal lesions and to facilitate multiplanar reformation. A baseline unenhanced low-dose scan should be obtained, and then multiphasic contrast-enhanced CT scans in the corticomedullary, nephrographic, and excretory phases should be obtained to assess contrast enhancement within the ablation zone. In general, CT is more widely available with widespread expertise, is less prone to artifact, and requires less patient cooperation than does MRI.[46,61,62]

9.3.1.5 Magnetic resonance imaging

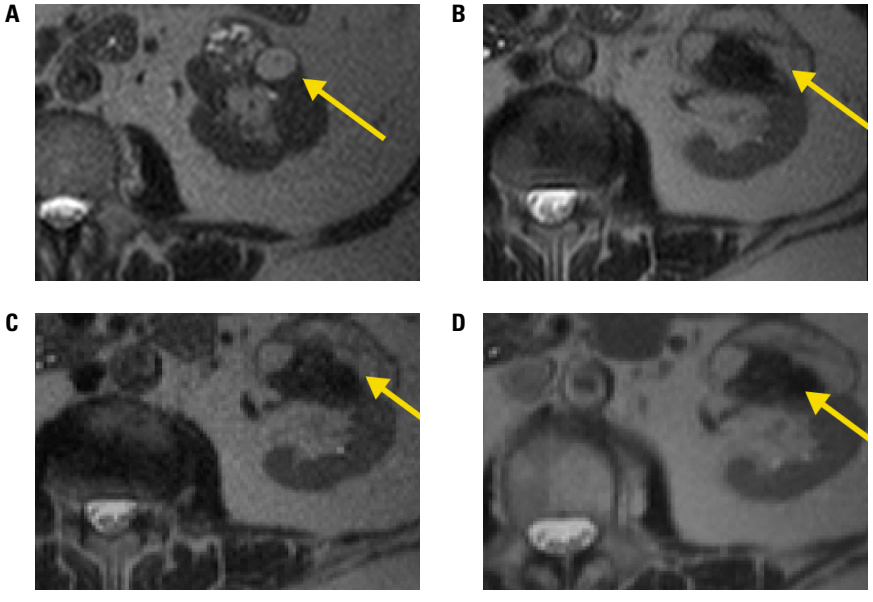

FIGURE 9-5
Longitudinal Follow-up Imaging of a 73-Year-Old Woman With Clear Cell RCC Treated With RFA

A Axial T2-weighted pre-treatment MRI scan.

B-D 3-, 6-, and 12-month post-RFA treatment showing a persistent post-ablation defect with peri-ablation halo without a change in size.

For MRI, T1- and T2-weighted images, as well as gradient-echo (GRE) T1-weighted images, should be obtained before and after the administration of IV gadolinium-based contrast. Most sequences are performed with parallel imaging to image the liver and kidneys during a single breath-hold. A T2-weighted single-shot fast-spin-echo (FSE) sequence in the axial and coronal planes is helpful because of its speed and resistance to artifacts, including motion artifact. For axial T1-weighted images, a breath-hold dual-echo spoiled GRE sequence with both in-phase and opposed-phase echo times should be acquired. Fat-suppressed T2-weighted images can be acquired using either a breath-hold or respiratory-triggered fast SE sequence, with fat suppression to improve the conspicuity of fluid on T2-weighted images. For gadolinium-enhanced images, a 3D breath-hold fat-suppressed GRE sequence and unenhanced scans followed by power injection of 0.01 mmol/kg of IV gadolinium, with multiphasic enhanced scans in the corticomedullary, nephrographic, and excretory phases are usually performed. The multiple contrast-enhanced data sets can be subtracted from the unenhanced scan to improve detection of recurrences (**Figure 9-5**).[46,61-64]

9.3.2 Surveillance imaging

9.3.2.1 Frequency

Patients who undergo renal ablation for RCC should undergo post-ablation surveillance imaging (CT or MRI) with unenhanced and multiphasic scans at 3 and 6 months following ablation to assess treatment success, followed by annual abdominal scans thereafter for 5 years. Beyond 5 years, there is no defined indication for imaging, but patients may undergo further scanning based on individual patient risk factors. Patients undergoing ablative procedures who have either biopsy-proven low-risk RCC, benign lesions such as oncocytoma, nondiagnostic biopsies, or no prior biopsy should undergo annual chest x-ray to assess for pulmonary metastases for 5 years.[61,62,65,66]

9.3.3 Image findings immediately after ablation and up to 1 year: longitudinal follow-up

9.3.3.1 Cryoablation

FIGURE 9-6
RCC in a 63-Year-Old Man Treated With CA

Diagnostic CT (**A**) demonstrates endophytic lesion. Immediately following CA (**B**), there is a hypodense ablated lesion with stranding and enhancement within the perinephric fat.

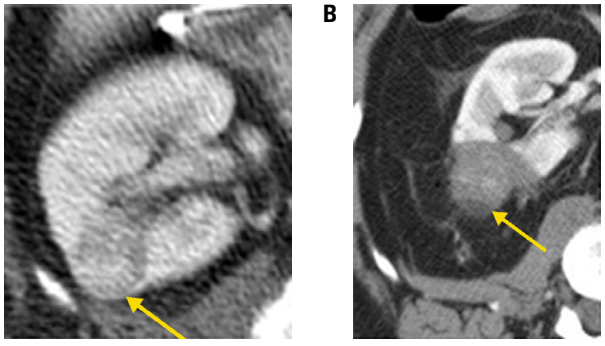

On post-contrast CT imaging during the acute period immediately following ablation, the treatment zone appears larger than the original tumour, and infiltration in the fat surrounding the ablation zone may show enhancement (**Figure 9-6**). The ablation zone has low attenuation, and emergence of the peripheral halo in perinephric fat surrounding the smaller high-density ablated lesion can be seen the first few months following CA. On post-contrast MRI, cryo-treated lesions appear variably T1 hyperintense and/or T2 hypointense relative to the renal parenchyma. The peripheral halo of the ablation zone border can be seen after contrast administration, and surrounding fat retains signal on all sequences.[63]

9.3.3.2 Radiofrequency and MWA

Some of the immediate perilesional changes seen on contrast-enhanced CT following RFA include:[67-69]

- Blood products (compare pre- with postcontrast to differentiate degraded blood products from residual tumour enhancement)
- A post-ablation halo (a thin, organized, incomplete spherical rim of soft tissue attenuation or signal within the perinephric fat surrounding the ablation site)
- A cortical wedge-shaped infarct associated with or adjacent to the treated lesion, and as a result of segmental arterial thrombosis in the treatment zone
- The presence of perinephric stranding (amorphous or incomplete curvilinear soft tissue attenuation or signal within the perinephric fat adjacent to the ablation site)

Immediately following treatment (24 hours to 1 week), a circumferential high-attenuating region corresponding to a marginal hyperemic inflammatory reaction to the damaged cells has been demonstrated in the surrounding renal parenchyma, causing the lesion to appear larger than primary.[64,70]

In general, findings for MW-ablated lesions are similar to RF-ablated lesions. Lesions tend to shrink more when treated with MW. The hypodense non-enhancing core with surrounding curvilinear halo is typically present and stable over time. Inflammatory hemorrhage and fluid resolves by 3 months.

9.3.3.3 Definition of successful outcomes

Immediate post-procedural imaging of the ablated tumour generally shows the tumour to be perceived as larger than its pretreatment size, for RFA due to ablation of a peripheral margin of normal tissue, and for CA due to extension of the ice ball beyond the original tumour margin. Successful outcomes of cryoablated tumours are characterized on imaging by significant shrinkage and loss of contrast enhancement on CT. Tumours successfully treated with RFA demonstrate no contrast enhancement, but with minimal shrinkage on CT.[69] On MRI, the imaging hallmark of successful renal tumour ablation is lack of tumour enhancement at gadolinium-enhanced imaging. Rim enhancement, believed to represent reactive change, may occasionally be seen at early post-procedural MR scanning after RFA or CA, and later resolves.

9.3.3.4 Late follow-up appearances following CA

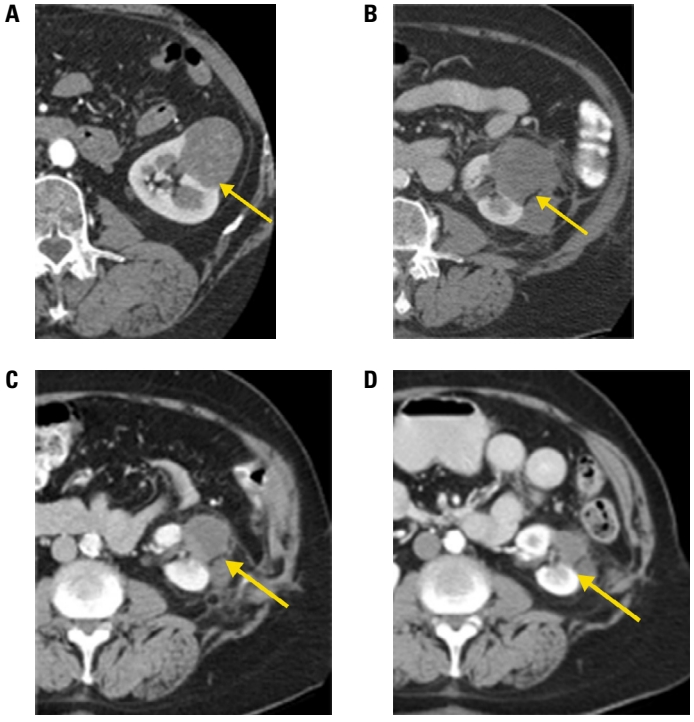

FIGURE 9-7
Involution of a Cryoablated Lesion Over Time

A In a 63-year-old man, diagnostic CT demonstrates an exophytic papillary RCC.

B One month post-cyroablation, CT imaging demonstrates stranding and a hypodense ablation zone.

C One year post-CA, significant decrease in ablation zone and lesion size, with residual curvilinear enhancement and stranding in the perinephric fat.

D Two years post-CA, significant decrease in ablation zone and lesion size, with reduced curvilinear enhancement and persistent stranding.

The size of the lesion and the ablation zone should progressively decrease, and up to a third of cryoablated lesions may become undetectable over time (**Figure 9-7**). In addition, decreased stranding, hematomas, and perinephric fluid should be observed. Over time on MRI, the size of the lesion, stranding, and hematomas should progressively decrease.[71,72]

9.3.3.5 Late follow-up appearances following RFA and MWA

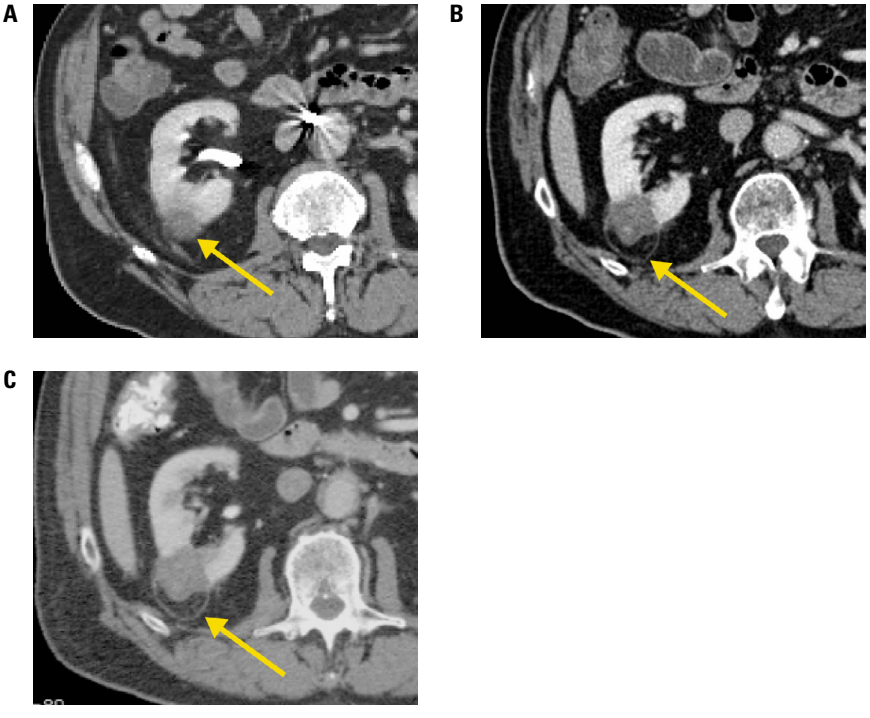

FIGURE 9-8
A 70-Year-Old Man With an Exophytic Posterior Papillary RCC Lesion Treated With RFA

Longitudinal surveillance CT imaging acquired at 3, 6, and 12 months.

A Three months post-RFA, demonstrating stranding within the perinephric fat.

B Six months post-RFA, demonstrating no significant decrease in size, no residual enhancement, and emergence of the perinephric halo.

C Twelve months post-RFA, demonstrating no significant decrease in size and no residual enhancement.

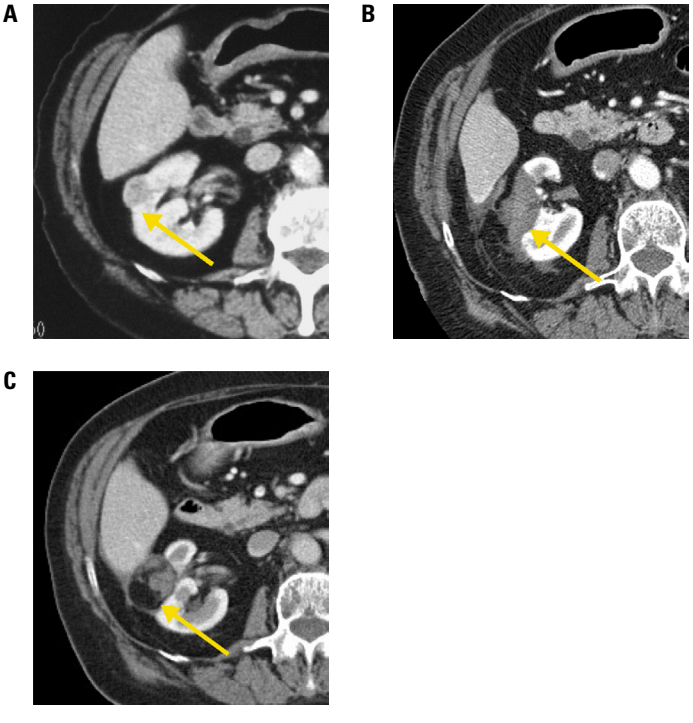

FIGURE 9-9
Follow-Up CT Imaging After RFA: Indicators of Ablative Success

A 72-year-old man with a diagnostic CT demonstrating an exophytic anterior lesion (**A**). CT scan obtained immediately following RFA (**B**) demonstrates perinephric stranding and an ablation zone larger than the original lesion. At 6-month follow-up (**C**), lesion remodeling can be seen without nodular enhancement, indicating ablative success.

FIGURE 9-10
Follow-Up MRI After MWA: Indicators of Ablative Success

A 68-year-old man with an exophytic anterior lesion (**A**) treated with MWA (**B**). At 1-month follow-up MRI, the lesion appears hypointense on T2 (**C**), with no residual enhancement seen on T1 post-contrast corticomedullary (**D**) or nephrographic (**E**) images.

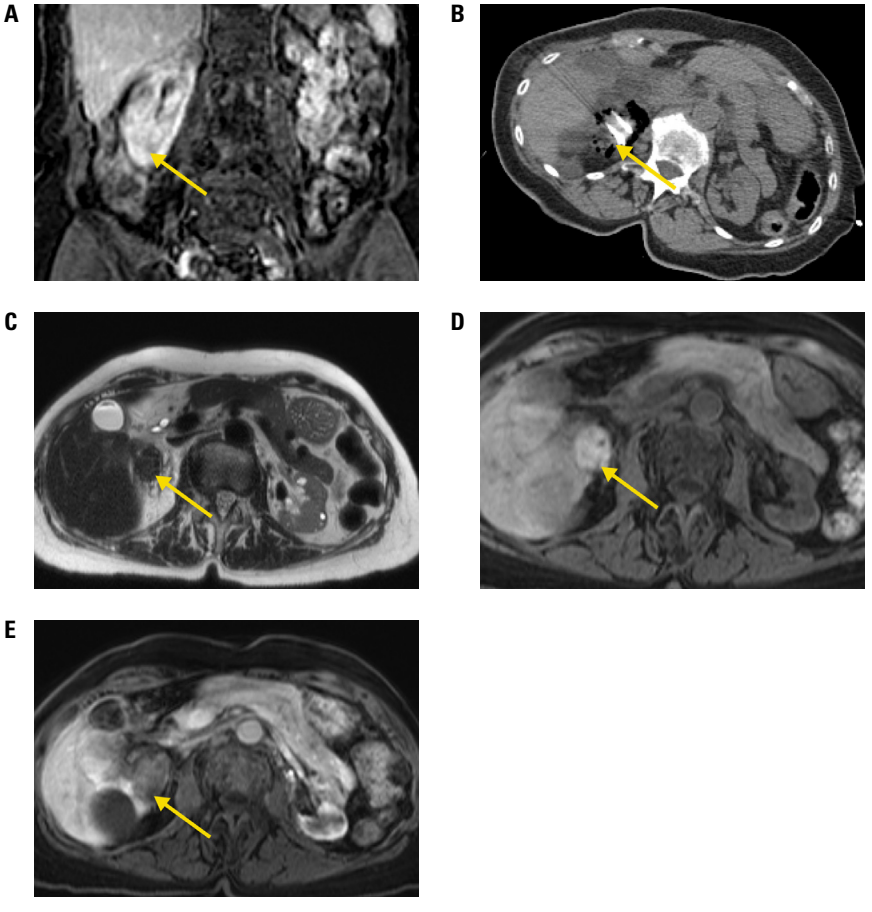

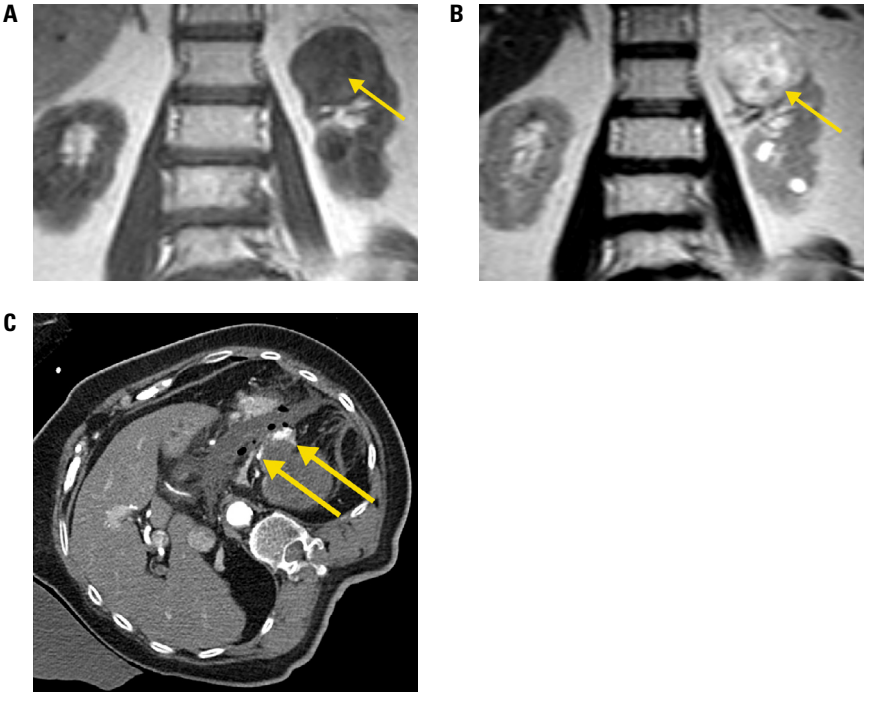

FIGURE 9-11
A 73-Year-Old Woman With a Large Exophytic Posterior RCC Treated With RFA

The diagnostic MRI demonstrates a T1 hypointense (**A**) and T2 hyperintense (**B**) lesion. Immediately following RFA, a contrast-enhanced CT scan in the corticomedullary phase (**C**) demonstrates nodular enhancement >10 Hounsfield unit (HU), indicating an incomplete ablation.

At longitudinal post-treatment follow-up imaging, decreased stranding, hematomas, and perinephric fluid should be observed (**Figure 9-8**). A decrease in lesion size will not be as pronounced as with cryo-ablated tumours, and the primary indicator of ablative success is a lack of linear or nodular tumour enhancement (<10 HU) (**Figure 9-9**). On post-contrast MRI, RF-treated lesions appear T1 hyperintense and T2 hypointense relative to the renal parenchyma. At longitudinal follow-up scans, the emergence of the peripheral halo in the perinephric fat surrounding the ablated lesion can be seen. Stranding and hematomas should progressively decrease; however, lesion size will not decrease significantly. On post-contrast CT imaging, residual lesion enhancement <10 HU is considered to be successful ablation, and no recurrence of tumour and complete necrosis, in addition to a well-defined non-enhancing zone, indicates ablative success (**Figures 9-10** and **9-11**).[64,67,70,73-79]

9.3.3.6 Irreversible electroporation

To date, there is insufficient evidence as to how long it takes for complete tumour involution to occur after successful irreversible electroporation (IRE) ablation, or how long after IRE one may expect to observe residual tumour cells if the ablation was incomplete. On post-contrast CT imaging up to 1 week after IRE, the lesion is hypodense and non-enhancing. After 3 weeks, the lesion can disappear completely with no residual enhancement. On post-treatment MRI up to 1 week after IRE, the lesion appears hypointense and necrotic. MRI after 1 month shows a sharply demarcated scar-like lesion with cortical shrinkage and no contrast enhancement.[80-87]

9.3.4 Signs of recurrence

FIGURE 9-12
A 67-Year-Old Man With an Endophytic Lesion Treated With CA

Longitudinal follow-up scans obtained on T1 gadolinium enhanced coronal images at 1, 3, and 6 months.

A One-month post-CA surveillance MRI demonstrating curvilinear enhancement within the ablated lesion.

B Three-month post-CA surveillance MRI demonstrating persistent curvilinear enhancement and a subtle increase in lesion size.

C Six-month post-CA surveillance MRI demonstrating increased nodular enhancement and an increase in lesion size.

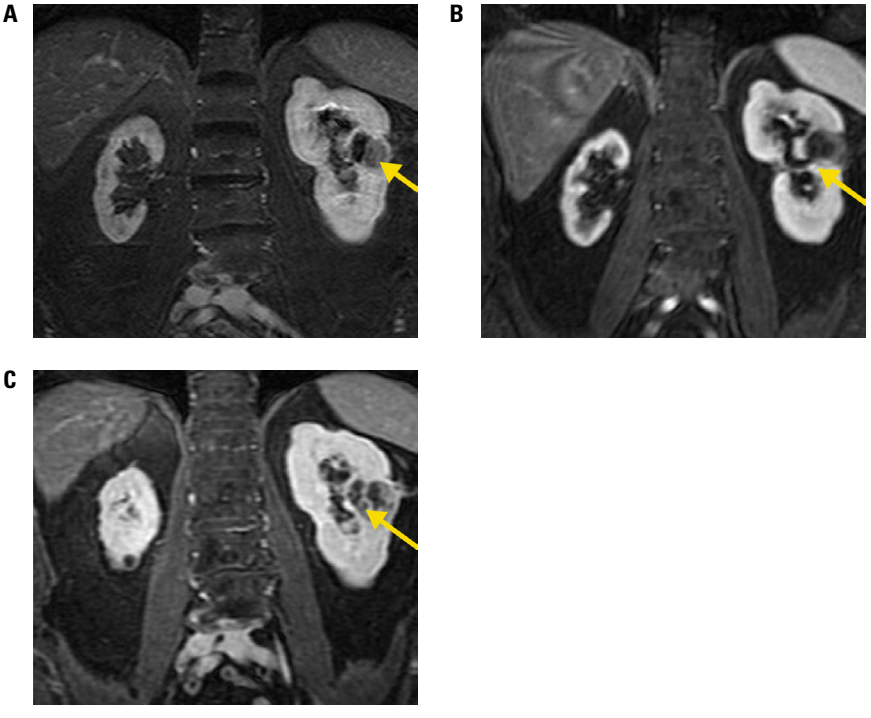

FIGURE 9-13
Identification of Tumour Recurrence on MRI

A 57-year-old man with a large posterior endophytic clear cell RCC (**A**) treated with RFA (**B**). At 3-month MRI follow-up, the lesion appears dark on T2 FSE (**C**), appears bright on T1 pre-contrast (**D**), and does not demonstrate any enhancement on the T1 post-contrast corticomedullary (**E**) or T1 post-contrast nephrographic (**F**) gadolinium-enhanced images.

Continued next page.

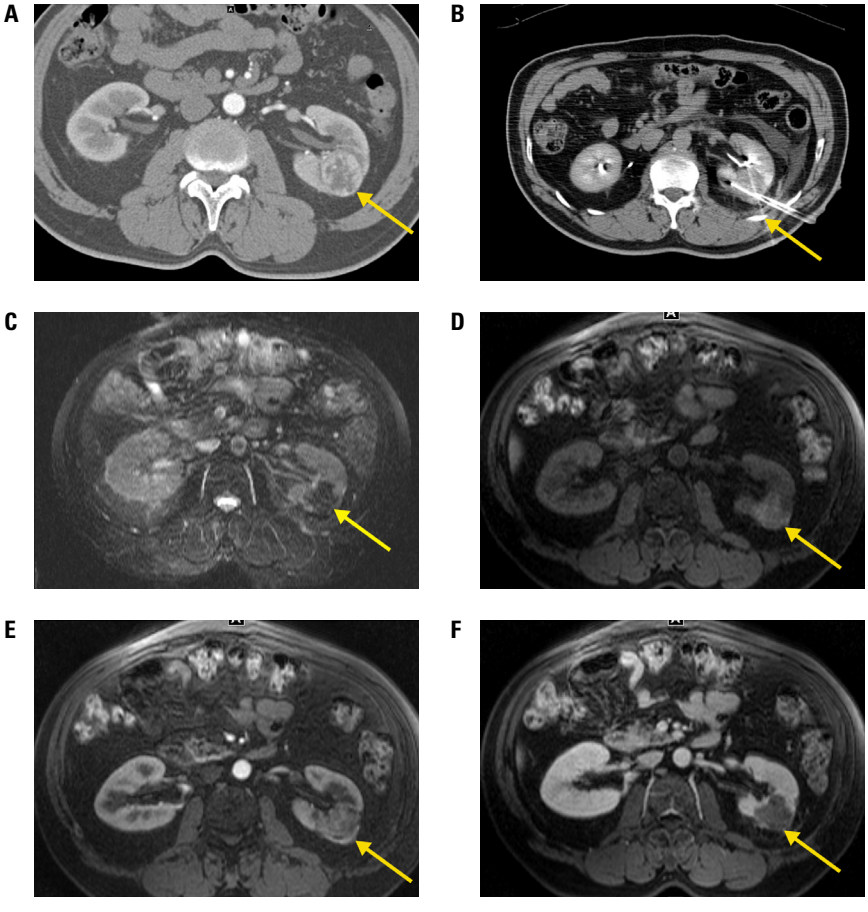

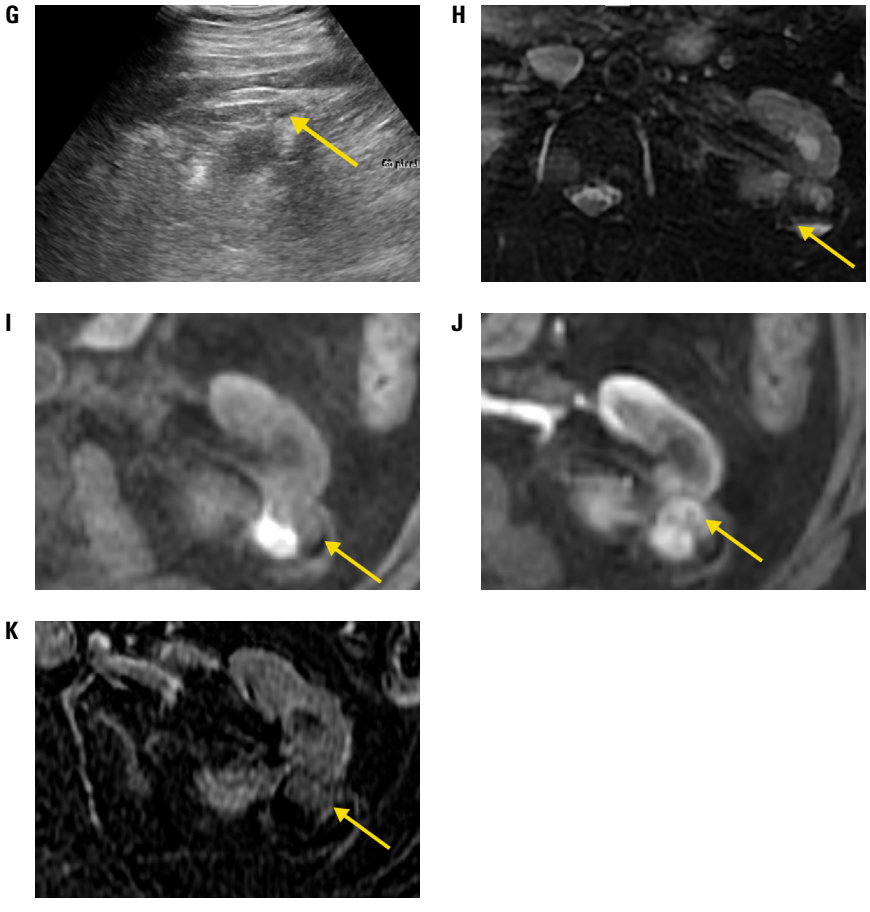

FIGURE 9-13, CONT'D
However, at 2-year longitudinal follow-up imaging, the echogenic ablated lesion became partially hypoechoic on US (**G**). The hypoechoic region appeared T2 hyperintense (**H**), hypointense relative to the ablation zone on pre-contrast T1 (**I**), and enhanced on T1-post contrast corticomedullary imaging (**J**). MR subtraction imaging (**K**) confirmed tumour recurrence.

With both post-contrast CT and MRI, findings of concern include the appearance of uniform circular enhancement around the necrosis zone, indicating inflammatory congestion, lesion, and/or the presence of irregular peripheral enhancement in scattered, nodular, or eccentric pattern, which indicate local tumour progression and failure of regression in size of the treated lesion over time.[74-79] On CT imaging, recurrences typically enhance avidly (>10 HU) in the corticomedullary phase and wash out in the subsequent nephrographic and excretory phases. Signs of tumour recurrence on MRI include any qualitative level of linear or nodular MRI enhancement (change in signal intensity) and an enlarging ablation zone (**Figure 9-12**). On MR subtraction imaging, small, nodular, or curvilinear regions that enhance strongly generally indicate tumour recurrence (**Figure 9-13**).[63,71,72,88-90]

9.3.4.1 Biopsy after ablation

Repeat biopsy should be performed if there is radiographic evidence of treatment failure within 6 months if the patient is a candidate for further treatment. Radiographic evidence includes progressive increase in size of an ablated neoplasm with or without contrast enhancement, new nodularity in or around the ablation zone, failure of the treated lesion to regress in size over time, and satellite lesions. Biopsy can help to rule out whether additional treatment is necessary.

However, the disadvantages include the potential for false-negative results and the small risk of biopsy track seeding. Patients who experience track seeding are likely to have a subsequent course of treatment similar to patients with metastatic disease.[91,92] It is particularly important for the biopsy to be taken from an enhancing area of the lesion, avoiding the fibrotic regions. It is possible there will be a small number of tumour cells present, and the residual tumour growth pattern can be distorted by the initial ablative procedure. It is also helpful to compare to the pathology of the biopsy material obtained prior to the initial ablation.[93-95]

In conclusion, imaging is critical during ablation and in the assessment and management of RCC at longitudinal post-ablation follow-up. In the United States, US is mainly reserved for intraprocedural guidance of probe placement, while CT and MRI are used for diagnosis and characterization at follow-up. Thermal ablative techniques have predictable imaging characteristics during and following ablation. These are well established for heat-based techniques, including RFA and MWA, and for CA, and are being investigated for IRE. Immediately following thermal ablative techniques, the ablation zone should not contain regions of central or nodular peripheral enhancement; however, peripheral curvilinear enhancement may be characterized up to 6 months following ablation. Areas of linear or nodular enhancement at the site of the original lesion are suggestive of incomplete ablation and residual disease. A decrease in lesion size is more pronounced over time with lesions treated with CA versus lesions treated with RFA or MWA. Surveillance imaging should be evaluated not only for tumour recurrence in the ablation zone, but also for evidence of metastatic disease and possible delayed complications.

9.4 Biopsy and Pathological Review

The numerous issues surrounding the pathological features related to renal mass biopsy (RMB), such as adequacy of specimen, role of rapid evaluation, timing of the biopsy in relation to ablation, tumour types, diagnostic definitions, the use of core needle biopsy (CNB) versus fine needle aspiration biopsies (FNAB), sampling techniques, role of immunohistochemical and molecular studies, etc., are reviewed in Chapter 7. In this section, we discuss the issues relating to pathological evaluation during the post-ablation follow-up period.

Within the past 20 years, since the first reports of renal mass ablations, there have been improvements in our ability to accurately characterize the pathological features of renal masses by utilizing image-guided CNB and FNAB. Although a body of work has been amassed on the topic of RMB in the management of the SRM, there is a paucity of information regarding the utility of RMB in the evaluation of post-ablation recurrence. Most studies of post-ablation follow-up and management are retrospective case reviews, where the focus of the study has been to compare either differences between two ablation modalities (RFA versus CA) or techniques (percutaneous versus laparoscopic). These studies generally provide limited data regarding post-ablation RMB and the pathology of the post-ablated tumour. We could not find any higher levels of evidence for the role of RMB in the post-ablation management of an SRM. Further confounding the problem of limited information is the fact that both RFA and CA generally have a less than 10% rate of recurrence.[96] Keeping the

above limitations in mind, we address which patients to biopsy, the timing of the biopsy, pathological features reported on post-ablation biopsies, the tumour types reported, and questions regarding evaluation of tumour viability.

9.4.1 Which patients to biopsy

The question of which patients should undergo RMB during post-ablation follow-up has been not been directly addressed in the literature; however, it has been briefly reported in retrospective case series studying post-ablation outcomes or therapy for a post-ablation recurrence. As it stands today, the general practice amongst urologists is to perform RMB only in the presence of radiological evidence of residual/recurrent tumour.[96-98]

In 2008, in one of the early large studies correlating radiographic imaging and histopathological changes following CA and RFA, Weight and colleagues reported routinely performing RMB in less than half of the tumours (129 out of 285), with the biopsy performed after evaluation of the 6-month post-ablation imaging results.[99] Moreover, since there is no consensus regarding the added benefit of RMB to radiographic imaging alone in evaluation of the post-ablation mass, it is important to keep in mind that all patients with a radiographically visible recurrence may not necessarily require RMB. For example, in 2015 Karam and colleagues reported their experience of 14 patients undergoing salvage nephrectomy following local recurrence of ablated renal tumours.[100] Of these 14 patients, only 7 were biopsied. Zargar and colleagues, reporting long-term follow-up data on 436 patients who underwent ablation over a 15-year period (these include some of the same cases reported by Weight and colleagues in 2008), acknowledge the lack of pathological confirmation by biopsy for all the recurrent tumours.[99,100] These studies highlight the absence of any strong evidence indicating the role of routine biopsies in the evaluation of the post-ablation mass.[96-98] **(Level of Evidence [LOE] 3)**

9.4.2 Timing of the biopsy

As with the question of who to biopsy, the issue of when to biopsy an ablated mass has not been directly addressed either. During the first few months after ablation, the tumour undergoes involution and the pathophysiologic responses to the injury may result in radiographic enhancement and even enlargement of the ablated area. Furthermore, data from a large multi-institutional study reported that 92% of recurrent tumours were detected by imaging within the first 12 months after ablation, with 70% of residual tumours detected within the first 3 months.[32]

From reviewing the literature, it appears that post-ablation RMB is not performed earlier than 6 months after ablation. Karam and colleagues reported post-ablation biopsy no earlier than 7 months (range: 7–76 months; median: 21 months; mean: 24.3 months), and only for tumours that did not involute and still showed enhancement.[97] Zargar and colleagues used the criterion of a positive biopsy at 6 months post-ablation to consider the tumour as a recurrence.[98] However, they did not present any data on the temporal relationship between ablation and the post-ablation biopsy and, as mentioned before, not all of their patients underwent a post-ablation biopsy. **[LOE 3]**

9.4.3 Pathological features reported on post-ablation RMB and nephrectomy

Pathological features of the post-ablation tumour have not been systematically reported, except in some animal models or small series. The histopathological features seen in post-ablation RMB or nephrectomy include one or more of the following: reactive/reparative changes, necrotic tumour (**Figure 9-14**), and viable tumour (**Figure 9-15**). The proportion of these 3 components varies depending on the elapsed time between ablation and post-ablation pathological examination. After about 3 months post-ablation, almost all ablated tumours will have necrotic debris and reactive/reparative changes.

Finding the viable tumour is highly dependent on the sampling method, and CNBs are the preferred methodology for a post-ablation RMB. Due to the inherent sampling bias of RMB, and the high probability of a false negative, it may take multiple cores from different sites within the post-ablation mass to detect viable tumour. In 2013, Karam *et al.* reported performing multiple post-ablation biopsies, sampling all 4 quadrants and the central portion of the ablation zone for tumours larger than 3 cm, and a minimum of 3 cores from smaller tumours.[97] The post-ablation nephrectomy specimen is usually composed of necrotic tumour in the ablation zone, which should be sampled extensively to rule out the presence of viable tumour, since it is usually admixed with the necrotic tumour.

It is important to note that some post-ablation zones that show radiographic evidence of recurrence may not have viable tumour in them. For example, Karam and colleagues showed viable tumour in only 13 of the 14 tumours that underwent nephrectomy after ablation for local recurrence.[100] Kowalczyk and colleagues reported recurrent RCC in only 7 of the 13 nephrectomies performed due to suspicion of post-RFA recurrence.[101] Conversely, some post-ablation zones without radiographic evidence of recurrence may have viable tumour in them.[99] **[LOE 4]**

FIGURE 9-14
Needle Core Biopsy Showing Necrotic Tumour Without Any Visible Intact Tumour Cells

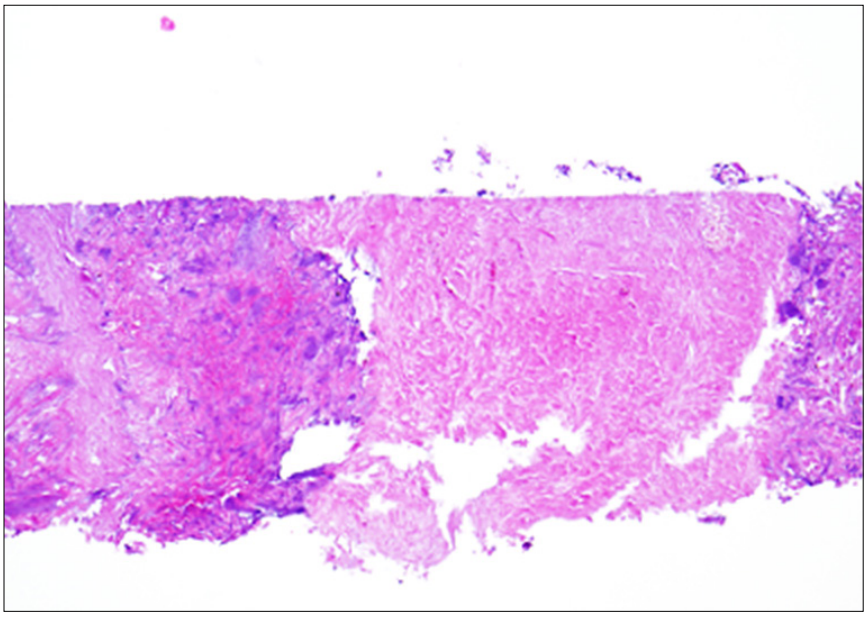

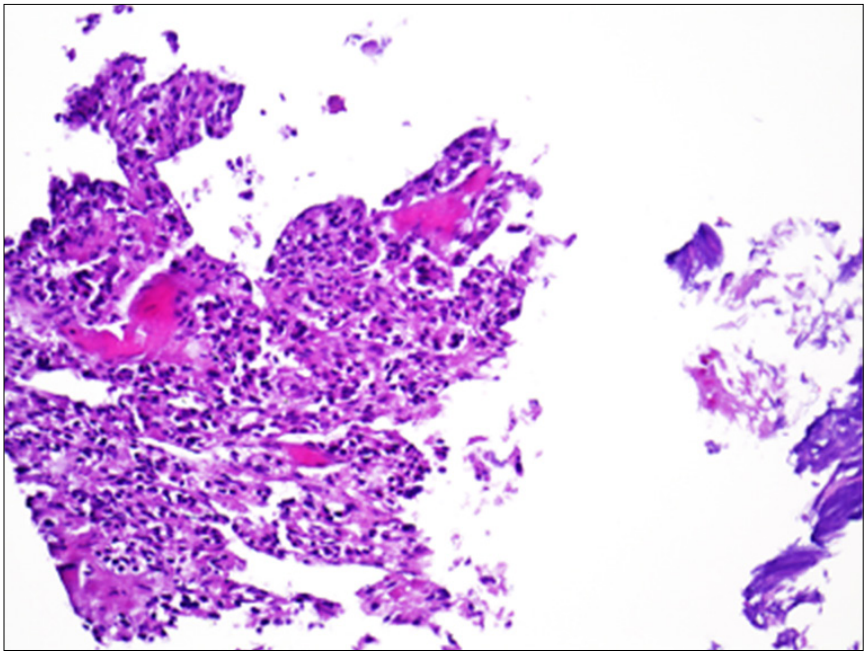

FIGURE 9-15
Needle Core Biopsy From Same Tumour as in **Figure 9-14**, With a Minute Focus of Viable Clear RCC

9.4.4 Tumour types in post-ablation recurrences

Only RCCs have been reported to recur following ablation; however, there is limited information on the RCC subtypes. Schmit and colleagues reported 17 local tumour recurrences out of 751 tumours that were ablated over a 12-year period (2000–2012).[96] Of these 17 recurrent tumours, 14 were reported as RCC; however, the pathology of the other 3 tumours was not reported. Psutka and colleagues retrospectively reviewed long-term outcomes data on 185 patients with sporadic TNM stage T1 RCC who underwent RFA, where they had 12 patients with local recurrence, but they did not report the RCC types of the recurrent tumour.[102] They also reported new renal tumours (ipsilateral and contralateral) in 5 patients and distant metastases in 4 patients. Of the 243 patients who underwent RFA, as reported by Tracy and colleagues, 9 patients developed a recurrence, all of which were clear cell RCC.[103] Four of these 9 patients underwent nephrectomy, which also showed clear cell RCC. However, Tracy and colleagues do not mention whether any of these patients underwent biopsy of the post-ablation mass or not.

Based on these relatively limited data, it is difficult to opine if any particular subtype of RCC is more likely to recur post-ablation. From a diagnostic perspective, the purpose of the post-ablation biopsy is to diagnose the presence or absence of residual/recurrent tumour (based on timing of biopsy) and to determine its viability. The diagnosis of the histologic subtype of RCC is only important if the recurrent tumour is not the same subtype as reported in the pre-ablation RMB. **[LOE 4]**

9.4.5 Evaluation of tumour viability

Finding recurrent RCC during the pathological evaluation of the post-ablation mass always raises the question of whether the tumour that is seen on hematoxylin and eosin (H&E) sections is viable or not. Use of the nicotinamide adenine dinucleotide (NADH) vital stain for detecting the reduced form of NADH has been reported in earlier studies for assessing tumour viability in the post-ablation pathology specimen.[104]

The routine use of NADH stain is not feasible due to the need for immediate snap freezing of the tumour tissue, use of frozen sections for staining, and, finally, the finicky nature of this stain itself. Further, using NADH stain for RMB is even more difficult due to the tissue distortion caused by the snap-freezing process, which may not allow accurate pathological evaluation of such a limited sample. In addition, false positive NADH staining has been reported if it is performed within 2 hours of RFA.[104] In the cases the authors have had experience with, the diagnosis of recurrent/residual tumour, if present, is relatively straightforward, and this panel does not see any value in doing special studies to evaluate post-ablation tumour viability. Therefore, while NADH may be used as an investigational tool, its use in the routine evaluation of post-ablation RMB is not recommended. **[LOE 4]**

9.5 Conclusions

Pathological features of post-ablation biopsies performed for SRM have not been well documented. The most common observation is the presence of reactive/reparative changes, and we have seen rare examples of both necrotic (non-viable) and viable tumour.

We recommend the following reporting approach to pathologists who may encounter such specimens:

- Provide histologic description of a) reactive changes such as hemorrhage, granulation tissue, xanthomatous cells, etc., b) viable tumour in specimen, whether residual or recurrent tumour based on the timing of the biopsy, and c) necrotic tumour in specimen.
- Cytokeratin stains may be of value to identify neoplastic cells and distinguish them from xanthomatous cells.
- An attempt should be made to histologically subclassify the RCC if there is adequate viable tissue.
- If the tumour has been previously histologically characterized, the histology of the post-ablation biopsy should be compared with the pre-ablation sample.

TABLE 9-1 Level of Evidence Summary

	Level of Evidence	Grade of Recommendation	References
Ablative techniques and intraprocedral image findings			
CA	3	C	
RFA and MWA	3	C	
IRE	3	C	Hoeffel[39], Johnson[38], Kong[40], Li[41], Wink[43], Wink[44], Zhu[42]
Post-procedural imaging protocols			
Conventional US	3	C	Dunmire[45], Krajewski[46]
CEUS	3	C	Allard[52], Amalou[59], Chen[57], Eisenbrey[51], Gerst[50], Houtzager[58], King[49], Lackey[60], Li[55], Piscaglia[47], McArthur[48], Meloni[53], Wah[56], Zeccolini[54]
CT	3	C	Davenport[61], Wile[62]
MRI	3	C	Allen[63], Davenport[61], Kawamoto[64], Krajewski[46], Wile[62]
Surveillance imaging			
Frequency	3	C	Davenport[61], Iannuccilli[65], Lang[66], Wile[62]
Image findings post-ablation			
CA	3	C	Allen[63]
RFA and MWA	3	C	Boss[68], Gervais[70], Kawamoto[64], Matsumoto[69], Merkle[67]
Definition of successful outcomes			
CA	3	C	Beemster[71], Porter[72]
RFA and MWA	3	C	Boss[68], Carrafiello[74], Castle[77], Gervais[70], Kawamoto[64], Laeseke[76], Li[78], Matsumoto[69], Merkle[67], Oshima[75], Sommer[79], Tracy[73]
IRE	3	C	Davalos[85], Golberg[80], Hjouj[81], Maor[86], Sommer[87], Wendler[82], Wendler[83], Wendler[84]
Signs of recurrence	3	C	Allen[63], Beemster[71], Carrafiello[74], Castle[77], Laeseke[76], Li[78], Porter[72], Purohit[88], Oshima[75], Sommer[79]
Biopsy after ablation	4	C	Frank[93], Lam[94], Slywotzky[92], Smith[91], Sorbellini[95]

Level of Evidence using the modified version of the Oxford Centre for Evidence-Based Medicine system, as adopted by the ICUD for follow-up evaluation after focal ablation of renal masses

9.6 References

1. Hollingsworth JM, Miller DC, Daignault S, *et al.* Rising incidence of small renal masses: a need to reassess treatment effect. *J Natl Cancer Inst.* 2006;98(18):1331–1334.
2. Kutikov A, Kunkle DA, and Uzzo RG. Focal therapy for kidney cancer: a systematic review. *Curr Opin Urol.* 2009;19(2):148–153.
3. Klatte T, Shariat SF, Remzi M. Systematic review and meta-analysis of perioperative and oncologic outcomes of laparoscopic cryoablation versus laparoscopic partial nephrectomy for the treatment of small renal tumors. *J Urol.* 2014;191(5):1209–1217.
4. Thompson RH, Atwell T, Schmit G, *et al.* Comparison of partial nephrectomy and percutaneous ablation for cT1 renal masses. *Eur Urol.* 2015;67(2):252–259.
5. Olweny EO, Park SK, Tan YK, *et al.* Radiofrequency ablation versus partial nephrectomy in patients with solitary clinical T1a renal cell carcinoma: comparable oncologic outcomes at a minimum of 5 years of follow-up. *Eur Urol.* 2012;61(6):1156–1161.
6. Ljungberg B, Bensalah B, Canfield S, *et al.* EAU Guidelines on renal cell carcinoma: 2014 update. *Eur Urol.* 2015;67(5):913–924.
7. Campbell SC, Novick AC, Belldegrun A, *et al.* Guideline for management of the clinical T1 renal mass. *J Urol.* 2009;182(4):1271–1279.
8. Uchida M, Imaide Y, Sugimoto K, *et al.* Percutaneous cryosurgery for renal tumours. *Br J Urol.* 1995;75(2):132-6; discussion 136–137.
9. Weld KJ, Hruby G, Humphrey PA, *et al.* Precise characterization of renal parenchymal response to single and multiple cryoablation probes. *J Urol.* 2006;176(2):784–786.
10. Hoffmann NE, Bischof JC. The cryobiology of cryosurgical injury. *Urology.* 2002;60(2 Suppl 1):40–49.
11. Gemery JM, Hoffer EK. Re: Correlation of radiographic imaging and histopathology following cryoablation and radio frequency ablation for renal tumors: C. J. Weight, J. H. Kaouk, N. J. Hegarty, E. M. Remer, C. M. O'Malley, B. R. Lane, I. S. Gill and A. C. Novick, *J Urol* 2008; 179: 1277-1283. *J Urol.* 2009;181(2):918–919.
12. Okhunov Z, Juncal S, Ordon M, *et al.* Comparison of outcomes in patients undergoing percutaneous renal cryoablation with sedation vs general anesthesia. *Urology.* 2015;85(1):130–134.
13. Blute ML Jr, Okhunov Z, Moreira DM, *et al.* Image-guided percutaneous renal cryoablation: preoperative risk factors for recurrence and complications. *BJU Int.* 2013;111(4 Pt B):E181–E185.
14. Okhunov Z, Shapiro EY, Moreira DM, *et al.* R.E.N.A.L. nephrometry score accurately predicts complications following laparoscopic renal cryoablation. *J Urol.* 2012;188(5):1796–1800.
15. Lay AH, Faddedon, S, Olweny EO, *et al.* Oncologic efficacy of radiofrequency ablation for small renal masses: clear cell versus papillary subtype. *J Urol.* 2015;194(3)653-657.
16. Ramirez D, Ma YB, Bedir S, *et al.* Laparoscopic radiofrequency ablation of small renal tumors: long-term oncologic outcomes. *J Endourol.* 2014;28(3):330–334.
17. Ames CD, Vanlangendonck R, Venkatesh R, *et al.* Enhanced renal parenchymal cryoablation with novel 17-gauge cryoprobes. *Urology.* 2004. 64(1):173–175.
18. Zlotta AR, Wildschutz T, Raviv G, *et al.* Radiofrequency interstitial tumor ablation (RITA) is a possible new modality for treatment of renal cancer: ex vivo and in vivo experience. *J Endourol.* 1997;11(4):251–258.
19. McGovern FJ, Wood BJ, Goldberg N, *et al.* Radio frequency ablation of renal cell carcinoma via image guided needle electrodes. *J Urol.* 1999;161(2):599–600.
20. Aron M and Gill IS. Minimally invasive nephron-sparing surgery (MINSS) for renal tumours. Part II: probe ablative therapy. *Eur Urol.* 2007;51(2):348–357.
21. Tracy CR, Raman JD, Donnally C, *et al.* Durable oncologic outcomes after radiofrequency ablation: experience from treating 243 small renal masses over 7.5 years. *Cancer.* 2010;116(13):3135–3142.
22. Goldberg SN, Gazelle GS, and Mueller PR. Thermal ablation therapy for focal malignancy: a unified approach to underlying principles, techniques, and diagnostic imaging guidance. *AJR Am J Roentgenol.* 2000;174(2):323–331.

23. Zagoria RJ, Hawkins AD, Clark PE, *et al.* Percutaneous CT-guided radiofrequency ablation of renal neoplasms: factors influencing success. *AJR Am J Roentgenol*. 2004;183(1):201–207.

24. Ahmed M, Solbiati L, Brace CL, *et al.* Image-guided tumor ablation: standardization of terminology and reporting criteria—a 10-year update. *J Vasc Interv Radiol.* 2014;25(11):1691–1705 e4.

25. Davenport MS, Caoili E, Cohan R, *et al.* MRI and CT characteristics of successfully ablated renal masses: imaging surveillance after radiofrequency ablation. *AJR Am J Roentgenol*. 2009;192(6):1571–1578.

26. Weld KJ, Figenshau RS, Venkatesh R, *et al.* Laparoscopic cryoablation for small renal masses: three-year follow-up. *Urology.* 2007;69(3):448–451.

27. Gill IS, Remer EM, Hasan WA, *et al.* Renal cryoablation: outcome at 3 years. *J Urol*. 2005;173(6):1903-1907.

28. Donat, SM, Remer EM, Hasan WA, *et al.* Follow-up for clinically localized renal neoplasms: AUA Guideline. *J Urol*. 2013;190(2):407–416.

29. Goldberg SN, Grassi CJ, Cardella JF, *et al.* Image-guided tumor ablation: standardization of terminology and reporting criteria. *Radiology*. 2005;235(3):728–739.

30. Ganguli S, Brennan DD, Faintuch S, *et al.* Immediate renal tumor involution after radiofrequency thermal ablation. *J Vasc Interv Radiol.* 2008;19(3):412–418.

31. Rutherford EE, Cast JE, and Breen DJ. Immediate and long-term CT appearances following radiofrequency ablation of renal tumours. *Clin Radiol.* 2008;63(2):220–230.

32. Matin SF, Ahrar K, Cadeddu JA, *et al.* Residual and recurrent disease following renal energy ablative therapy: a multi-institutional study. *J Urol*. 2006;176(5):1973–1977.

33. Levinson AW, Su LM, Agarwal D, *et al.* Long-term oncological and overall outcomes of percutaneous radio frequency ablation in high risk surgical patients with a solitary small renal mass. *J Urol*. 2008;180(2):499–504; discussion 504.

34. Ferakis N, Bouropoulos C, Granitsas T, *et al.* Long-term results after computed-tomography–guided percutaneous radiofrequency ablation for small renal tumors. *J Endourol*. 2010;24(12):1909–1913.

35. Varkarakis IM, Allaf ME, Inagaki T, *et al.* Percutaneous radio frequency ablation of renal masses: results at a 2-year mean followup. *J Urol*. 2005;174(2):456–460; discussion 460.43.

36. Natalin RA, Prince MR, Grossman ME, *et al.* Contemporary applications and limitations of magnetic resonance imaging contrast materials. *J Urol*. 2010;183(1):27–33.

37. Sheth S, Scatarige JC, Horton KM, *et al.* Current concepts in the diagnosis and management of renal cell carcinoma: role of multidetector CT and three-dimensional CT. *Radiographics*. 2001;21 Suppl 1:S237–S254.

38. Johnson DB, Duchene DA, Taylor GD, *et al.* Contrast-enhanced ultrasound evaluation of radiofrequency ablation of the kidney: reliable imaging of the thermolesion. *J Endourol*. 2005;19(2):248–252.

39. Hoeffel C, Pousset M, Timsit MO, *et al.* Radiofrequency ablation of renal tumours: diagnostic accuracy of contrast-enhanced ultrasound for early detection of residual tumour. *Eur Radiol.* 2012;20(8):1812–1821.

40. Kong WT, Zhang WW, Guo WW, *et al.* Application of contrast-enhanced ultrasonography after radiofrequency ablation for renal cell carcinoma: is it sufficient for assessment of therapeutic response? *Abdom Imaging.* 2011;36(3):342–347.

41. Li X, Liang P, Yu J, *et al.* Role of contrast-enhanced ultrasound in evaluating the efficiency of ultrasound guided percutaneous microwave ablation in patients with renal cell carcinoma. *Radiol Oncol.* 2013;47(4):398–404.

42. Zhu Q, Shimizu T, Endo H, *et al.* Assessment of renal cell carcinoma after cryoablation using contrast-enhanced gray scale ultrasound: a case series. *Clin Imaging.* 2005;29(2):102–108.

43. Wink MH, Laguna MP, Lagerveld BW, *et al.* Contrast-enhanced ultrasonography in the follow-up of cryoablation of renal tumours: a feasibility study. *BJU Int.* 2007;99(6):1371–1375.

44. Wink MH, Lagerveld BW, Laguna MP, *et al.* Cryotherapy for renal cell cancer: diagnosis, treatment, and contrast-enhanced ultrasonography for follow-up. *J Endourol*. 2006;20(7):456–458.

45. Dunmire B, Harper JD, Cunitz BW, *et al.* Use of the acoustic shadow width to determine kidney stone size with ultrasound. *J Urol*. 2016;195(1):171–177.

46. Krajewski KM, Giardino AA, Zukotynski K, *et al.* Imaging in renal cell carcinoma. *Hematol Oncol Clin North Am.* 2011;25(4):687–715.

47. Piscaglia F, Nolsøe C, Dietrich CF, *et al.* The EFSUMB Guidelines and Recommendations on the Clinical Practice of Contrast Enhanced Ultrasound (CEUS): update 2011 on non-hepatic applications. *Ultraschall Med.* 2012;33(1):33–59.

48. McArthur C, Baxter GM. Current and potential renal applications of contrast-enhanced ultrasound. *Clin Radiol.* 2012;67(9): 909–922.

49. King KG, Gulati M, Malhi H, *et al.* Quantitative assessment of solid renal masses by contrast-enhanced ultrasound with time-intensity curves: how we do it. *Abdom Imaging.* 2015;40(7):2461–2471.

50. Gerst S, Hann LE, Li D, *et al.* Evaluation of renal masses with contrast-enhanced ultrasound: initial experience. *AJR Am J Roentgenol.* 2011;197(4):897–906.

51. Eisenbrey JR, Shaw CM, Lyshchik A, *et al.* Contrast-enhanced subharmonic and harmonic ultrasound of renal masses undergoing percutaneous cryoablation. *Acad Radiol.* 2015;22(7):820–826.

52. Allard CB, Coret A, Dason S, *et al.* Contrast-enhanced ultrasound for surveillance of radiofrequency-ablated renal tumors: a prospective, radiologist-blinded pilot study. *Urology.* 2015;86(6)1174–1178.

53. Meloni MF, Smolock A, Cantisani V, *et al.* Contrast enhanced ultrasound in the evaluation and percutaneous treatment of hepatic and renal tumors. *Eur J Radiol.* 2015;84(9):1666–1574.

54. Zeccolini G, Del Biondo D, Cicero C, *et al.* Comparison of Contrast-Enhanced Ultrasound Scan (CEUS) and MRI in the follow-up of cryoablation for small renal tumors. Experience on 25 cases. *Urologia.* 2014;81 Suppl 23:1–8.

55. Li X, Liang P, Yu J, *et al.* Role of contrast-enhanced ultrasound in evaluating the efficiency of ultrasound guided percutaneous microwave ablation in patients with renal cell carcinoma. *Radiol Oncol.* 2013;47(4):398–404.

56. Wah TM, Irving HC, Gregory W, *et al.* Radiofrequency ablation (RFA) of renal cell carcinoma (RCC): experience in 200 tumours. *BJU Int.* 2014;113(3):416–428.

57. Chen Y, Huang J, Xia L, *et al.* Monitoring laparoscopic radiofrequency renal lesions in real time using contrast-enhanced ultrasonography: an open-label, randomized, comparative pilot trial. *J Endourol.* 2013;27(6):697–704.

58. Houtzager S, Wijkstra H, de la Rosette JJ, *et al.* Evaluation of renal masses with contrast-enhanced ultrasound. *Curr Urol Rep.* 2013;14(2):116–123.

59. Amalou H, Wood BJ. Multimodality fusion with MRI, CT, and ultrasound contrast for ablation of renal cell carcinoma. *Case Rep Urol.* 2012;2012:390912.

60. Lackey L II, Peterson C, Barr RG. Contrast-enhanced ultrasound-guided radiofrequency ablation of renal tumors. *Ultrasound Q.* 2012;28(4):269–274.

61. Davenport MS, Caoili EM, Cohan RH, *et al.* MRI and CT characteristics of successfully ablated renal masses: Imaging surveillance after radiofrequency ablation. *AJR Am J Roentgenol.* 2009;192(6):1571–1578.

62. Wile GE, Leyendecker JR, Krehbiel KA, *et al.* CT and MR imaging after imaging-guided thermal ablation of renal neoplasms. *Radiographics.* 2007;27:325–340.

63. Allen BC, Remer EM. Percutaneous cryoablation of renal tumors: patient selection, technique, and postprocedural imaging. *Radiographics.* 2010;30(4):887–900.

64. Kawamoto S, Permpongkosol S, Bluemke DA, *et al.* Sequential changes after radiofrequency ablation and cryoablation of renal neoplasms: role of CT and MR imaging. *Radiographics.* 2007(2);27:343–355.

65. Iannuccilli JD, Grand DJ, Dupuy DE, *et al.* Percutaneous ablation for small renal masses-imaging follow-up. *Semin Intervent Radiol.* 2014;31(1):50–63.

66. Lang EK, Zhang KK, Nguyen Q, *et al.* Efficacy of percutaneous cryoablation of renal cell carcinoma in older patients with medical comorbidities: outcome study in 70 patients. *Can Urol Assoc J.* 2015;9(5–6):256–261.

67. Merkle EM, Nour SG, Lewin JS. MR imaging follow-up after percutaneous radiofrequency ablation of renal cell carcinoma: findings in 18 patients during first 6 months. *Radiology.* 2005;235(3):1065–1071.

68. Boss A, Martirosian P, Schraml C, *et al.* Morphological, contrast-enhanced and spin labelling perfusion imaging for monitoring of relapse after RF ablation of renal cell carcinomas. *Eur Radiol.* 2006;16(6):1226–1236.

69. Matsumoto ED, Watumull L, Johnson DB, *et al.* The radiographic evolution of radio frequency ablated renal tumours. *J Urol.* 2004;172(1):45–48.

70. Gervais DA, McGovern FJ, Arellano RS, *et al.* Renal cell carcinoma: clinical experience and technical success with radiofrequency ablation of 42 tumours. *Radiology.* 2003;226(2):417–424.

71. Beemster P, Phoa S, Wijkstra H, *et al.* Follow-up of renal masses after cryosurgery using computed tomography; enhancement patterns and cryolesion size. *BJU Int.* 2008;101(10):1237–1242.

72. Porter CA IV, Woodrum DA, Callstrom MR, *et al.* MRI after technically successful renal cryoablation: early contrast enhancement as a common finding. *AJR Am J Roentgenol.* 2010;194(3):790–793.

73. Tracy CR, Raman JD, Donnally C, *et al.* Durable oncologic outcomes following radiofrequency ablation (RFA): experience from treating 243 small renal masses over 7.5 years. *Cancer.* 2010;116(13):3135–3142.

74. Carrafiello G, Laganà D, Mangini M, *et al.* Microwave tumors ablation: principles, clinical applications and review of preliminary experiences. *Int J Surg.* 2008;6 Suppl 1:S65–S69.

75. Oshima F, Yamakado K, Nakatsuka A, *et al.* Simultaneous microwave ablation using multiple antennas in explanted bovine livers: relationship between ablative zone and antenna. *Radiat Med.* 2008;26(7):408–414.

76. Laeseke PF, Lee FT Jr, Sampson LA, *et al.* Microwave ablation versus radiofrequency ablation in the kidney: high-power triaxial antennas create larger ablation zones than similarly sized internally cooled electrodes. *J Vasc Interv Radiol.* 2009;20(9):1224–1229.

77. Castle SM, Salas N, Leveillee RJ. Initial experience using microwave ablation therapy for renal tumor treatment: 18-month follow-up. *Urology.* 2011;77(4):792–797.

78. Li X, Liang P, Yu J, *et al.* Role of contrast-enhanced ultrasound in evaluating the efficiency of ultrasound guided percutaneous microwave ablation in patients with renal cell carcinoma. *Radiol Oncol.* 2013;47(4):398–404.

79. Sommer CM, Sommer SA, Mokry T, *et al.* Quantification of tissue shrinkage and dehydration caused by microwave ablation: experimental study in kidneys for the estimation of effective coagulation volume. *J Vasc Interv Radiol.* 2013;24(8):1241–1248.

80. Golberg A, Yarmush ML. Nonthermal irreversible electroporation: fundamentals, applications, and challenges. *IEEE Trans Biomed Eng Mar.* 2013;60(3):707–714.

81. Hjouj M, Lavee J, Last D, *et al.* The effect of blood flow on magnetic resonance imaging of non-thermal irreversible electroporation. *Sci Rep.* 2013;3:3088.

82. Wendler JJ, Porsch M, Hühne S, *et al.* Short- and mid-term effects of irreversible electroporation on normal renal tissue: an animal model. *Cardiovasc Intervent Radiol.* 2013;36(2):512–520.

83. Wendler JJ, Pech M, Porsch M, *et al.* Urinary tract effects after multifocal nonthermal irreversible electroporation of the kidney: acute and chronic monitoring by magnetic resonance imaging, intravenous urography and urinary cytology. *Cardiovasc Intervent Radiol.* 2012;35(4):921–926.

84. Wendler JJ, Pech M, Blaschke S, *et al.* Angiography in the isolated perfused kidney: radiological evaluation of vascular protection in tissue ablation by nonthermal irreversible electroporation. *Cardiovasc Intervent Radiol.* 2012;35(2):383–390.

85. Davalos RV, Mir IL, Rubinsky B. Tissue ablation with irreversible electroporation. *Ann Biomed Eng.* 2005;33(2):223–231.

86. Maor E, Ivorra A, Leor J, *et al.* The effect of irreversible electroporation on blood vessels. *Technol Cancer Res Treat.* 2007;6(4):307–312.

87. Sommer CM, Fritz S, Wachter MF, *et al.* Irreversible electroporation of the pig kidney with involvement of the renal pelvis: technical aspects, clinical outcome, and three-dimensional CT rendering for assessment of the treatment zone. *J Vasc Interv Radiol.* 2013;24(12):1888–1897.

88. Purohit NB, Theaker J, Breen DJ. Unusual radiological behaviour after cryoablation of renal cell carcinoma. *Cardiovasc Intervent Radiol.* 2014;37(6):1631–1634.

89. Khoder WY, Siegert S, Stief CG, *et al.* Results of a prospective study comparing the clinical efficacy of cryoablation of renal cell cancer followed by immediate partial nephrectomy. *Eur J Surg Oncol.* 2014;40(1):96–102.

90. Jansen MC, van Hillegersberg R, Schoots IG, *et al.* Cryoablation induces greater inflammatory and coagulative responses than radiofrequency ablation or laser induced thermotherapy in a rat liver model. *Surgery.* 2010;147(5):686–695.

91. Smith EH. Complications of percutaneous abdominal fine-needle biopsy: review. *Radiology.* 1991;178(1):253–258.

92. Slywotzky C, Maya M. Needle tract seeding of transitional cell carcinoma following fine needle aspiration of a renal mass. *Abdom Imaging.* 1994;19(2):174–176.

93. Frank I, Blute ML, Cheville JC, *et al:* An outcome prediction model for patients with clear cell renal cell carcinoma treated with radical nephrectomy based on tumor stage, size, grade and necrosis: the SSIGN score. *J Urol.* 2002;168(6):2395–2400.

94. Lam JS, Shvarts O, Leppert JT, *et al.* Postoperative surveillance protocol for patients with localized and locally advanced renal cell carcinoma based on a validated prognostic nomogram and risk group stratification system. *J Urol.* 2005;174(2):466–472.

95. Sorbellini M, Kattan MW, Snyder ME, *et al.* A postoperative prognostic nomogram predicting recurrence for patients with conventional clear cell renal cell carcinoma. *J Urol.* 2005;173(1):48–51.

96. Schmit, GD, Thompson RH, Kurup AN, *et al.* Usefulness of R.E.N.A.L. nephrometry scoring system for predicting outcomes and complications of percutaneous ablation of 751 renal tumors. *J Urol.* 2013;189(1):30–35.

97. Karam, JA, Ahrar K, Vikram R, *et al.* Radiofrequency ablation of renal tumours with clinical, radiographical and pathological results. *BJU Int.* 2013;111(6):997–1005.

98. Zargar, H, Samarasekera S, Khalifeh A, *et al.* Laparoscopic vs percutaneous cryoablation for the small renal mass: 15-year experience at a single center. *Urology.* 2015;85(4):850–855.

99. Weight, CJ, Kaouk JH, Hegarty NJ, *et al.* Correlation of radiographic imaging and histopathology following cryoablation and radio frequency ablation for renal tumors. *J Urol.* 2008;179(4):1277–1281.

100. Karam, JA, Wood CG, Compton ZR, *et al.* Salvage surgery after energy ablation for renal masses. *BJU Int.* 2015;115(1):74–80.

101. Kowalczyk, KJ, Hooper HB, Linehan WM, *et al.* Partial nephrectomy after previous radio frequency ablation: the National Cancer Institute experience. *J Urol.* 2009;182(5):2158–2163.

102. Psutka, SP, Feldman AS, McDougal WS, *et al.* Long-term oncologic outcomes after radiofrequency ablation for T1 renal cell carcinoma. *Eur Urol.* 2013;63(3):486–492.

103. Tracy, CR, Raman JD, Donnally C, *et al.* Durable oncologic outcomes after radiofrequency ablation: experience from treating 243 small renal masses over 7.5 years. *Cancer.* 2010. 116(13):3135–3142.

104. Stern, JM, Anderson JK, Lotan Y, *et al.* Nicotinamide adenine dinucleotide staining immediately following radio frequency ablation of renal tumors—is a positive stain synonymous with ablative failure? *J Urol.* 2006;176(5):1969–1972; discussion 1972.

WHAT BEING AN **SIU MEMBER MEANS**

SIU members span over 100 countries and represent the full spectrum of clinicians and investigators from all the urological sub-specialties, including established academic and non-academic urologists, as well as physicians undergoing full-time training in urology.

SIU membership gives you an **equal voice** in this influential organization. We believe that each member can contribute the knowledge and experience needed to forge valuable links between urologists, and between developed and developing nations. By **working together**, our members carry on the tradition of creating positive change in a changing world. As a new member, you will be a partner in **the one urological association** dedicated to creating sustainable educational projects and providing and improving urological resources worldwide.

Members are able to vote for SIU leadership, organize SIU-endorsed educational activities, become involved in the congress scientific programme, as well as contribute to various SIU Academy programmes. We strive to make each member feel **valued**, **respected**, and **supported**.

The SIU network, both virtual and live, is an unparalleled pool of global contacts. **SIU brings urologists together**.

JOIN TODAY

SIU membership fees are based on World Bank data. Physicians undergoing full-time training in urology may apply for a trainee membership, absolutely free.

Fill out your application form today at: **www.siu-urology.org**

COUNTRY	A - $150 US	B - $75 US	C - $50 US

SIU Central Office
1155 Robert-Bourassa Blvd.
Suite 1012
Montreal, Quebec
Canada H3B 3A7

T +1 514 875 5665
F +1 514 875 0205
central.office@siu-urology.org
www.siu-urology.org

Benefits for SIU Members Include:

Education

Exclusive access to the SIU's eLearning platform, the SIU Academy, featuring:

- Clinical case studies, electronic annotated publications and eSeries
- Live surgery broadcasts and Congress webcasts
- Continuing medical education credits on selected courses

Publications

- Annual online subscription to the *World Journal of Urology*, the official monthly journal of the SIU
- Access to the most recent joint SIU-ICUD (International Consultation on Urological Diseases) publications
- Quarterly SIU newsletter (included in the *World Journal of Urology*)

SIU Congress

- Significantly reduced registration fees at SIU Congresses
- Fast-track Congress check-in for members

Philanthropy

Your dues contribute toward the development of ongoing SIU philanthropic activities such as:

- Sponsoring professional membership and journal subscriptions for urologists from developing nations
- Supporting SIU symposia and lectureships at annual national and international meetings
- Providing complimentary registration and housing at SIU Congresses for up to 10 young urologists from developing countries

SIU 2016 BUENOS AIRES Argentina

SIU ACADEMY
e-learning and more

FSIU
Foundation of the Société Internationale d'Urologie

www.siu-urology.org

SIU ACADEMY REACHES OVER 46,000 USERS.

ARE YOU AMONG THEM?

Did you know? SIU Academy...

Brings you content from SIU-endorsed events

The endorsed event programme allows approved webcasts from high-quality meetings around the world to be presented and shared on the portal.

Offers a **wide range of content** eligible for self-learning CME credits

Non-accredited content is eligible for self-learning credits. Contact your national accreditation body to find out how.

Has the **best search engine**

Navigate the portal to its full potential by using the top and bottom panels. This allows you to narrow down your search by selecting the type of content, topic, sub-topics and labels to find exactly what you are looking for.

Shows you what's trending

The What's Trending page gives you an overview of featured content and the most recent material at a glance.

Allows you to **weigh in** on content

The "Rate & Comment" feature allows you to comment on every piece of material available on the portal.

Lets **you share**

Share exciting new content with colleagues through Facebook and Twitter at the click of a button.

Register today!
www.siu-urology.org

SIU ACADEMY
e-learning and more

SOCIÉTÉ INTERNATIONALE D'UROLOGIE SIU


ACCESS TO
BASIC UROLOGICAL
CARE CAN MEAN
THE DIFFERENCE
BETWEEN
LIFE AND
DEATH
In many countries, lack of adequate care means that many treatable conditions can lead to life-threatening complications or death.
FSIU puts 100% of all donations towards surgical training—no exceptions.
Donate today at:
www.fsiu.org
FSIU
Foundation of the
Société Internationale
d'Urologie

IMAGE-GUIDED THERAPIES FOR PROSTATE AND KIDNEY CANCERS

Technological breakthroughs in recent years have expanded the use of image-guided therapy in urology. Advances in the fields of urology, imaging, radiology, and minimally invasive surgery have led to innovations in the application of image-guided modalities for different urological conditions.

This book represents a huge effort from a large international faculty, working in nine committees as part of the Société Internationale d'Urologie (SIU)-International Consultation on Urological Diseases (ICUD) joint consultation on Image-Guided Therapies for Prostate and Kidney Cancers, held in Melbourne, Australia and chaired by Rafael Sánchez-Salas and Mihir Desai.

This ICUD publication details the consensus statements on the use of image-guided therapies for prostate and renal cancers. On the subject of prostate cancer, the committees provide their recommendations on diagnosis, selection for and surveillance after focal therapy, imaging and biopsies, and available ablation energies for treatment. On the subject of renal cancer, the recommendations focus on the goals for evaluation and diagnosis, renal tumour biopsy, treatment strategies, as well as follow-up evaluation after focal ablation of renal masses.

We hope that you enjoy reading the book, and that you find it an important and timely reference on image-guided therapy for prostate and renal cancers.

For information and orders:
SIU Central Office
1155 Robert-Bourassa Blvd.
Suite 1012
Montreal, Quebec
Canada H3B 3A7

T: +1 514 875-5665
F: +1 514 875-0205
E: communications@siu-urology.org
W: www.siu-urology.org

ISBN 978-0-9877465-9-7